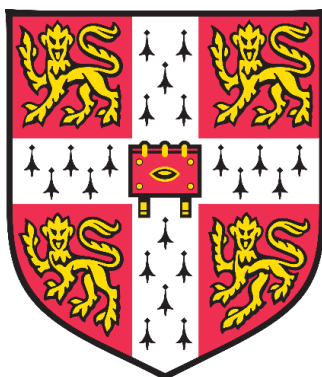


Tertiary alkylamines as effective directing groups for palladium-catalysed C(sp³)-H activation strategies

Jesus Rodrigalvarez Garcia

Christ's College
University of Cambridge



This thesis is submitted for the Degree of Doctor of Philosophy

May 2021

Department of Chemistry

Lensfield Road

Cambridge

CB2 1EW

United Kingdom

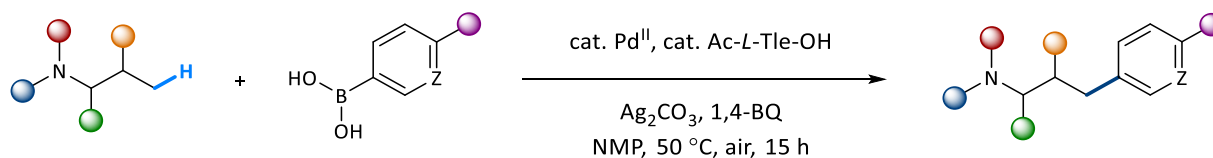
Declaration and Statement of length

This thesis is submitted in fulfilment of the requirements for the degree of Doctor of Philosophy and describes the work conducted in the Department of Chemistry from October 2017 to April 2021. It is the result of my own work and includes nothing which is the outcome of work done in collaboration except as declared in the Preface and specified in the text. I further state that no substantial part of my thesis has already been submitted, or, is being concurrently submitted for any such degree, diploma or other qualification at the University of Cambridge or any other University or similar institution except as declared in the Preface and specified in the text. It does not exceed the prescribed word limit of 60,000 as set by the Degree Committee for the faculty of Physics and Chemistry.

Jesus Rodrialvarez Garcia

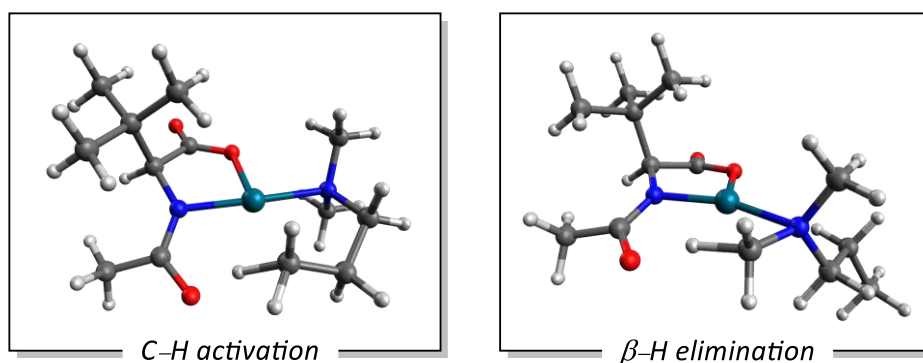
Abstract

Tertiary alkylamines as effective directing groups for palladium-catalysed C(sp³)-H activation strategies



C-H activation has emerged as a powerful strategy to streamline organic synthesis by exploiting the ubiquitous nature of C-H bonds in any synthetic precursor. Within the last decade, primary and secondary alkylamines have been reported to direct C-H cleavage on a series of palladium-catalysed reactions. The work reported in this dissertation describes the development of a new palladium-catalysed strategy towards the functionalisation of aliphatic tertiary amines. Methyl, methylene, and methine C-H cleavage have been disclosed by exploiting direct coordination of the amine substrate to the palladium metal centre. Subsequent cross-coupling with aryl boron reagents delivered a series of C(sp³)-C(sp²) bond forming transformations. In an attempt to shape a greener, cheaper, and more atom economical reaction, studies towards the replacement of silver additives as terminal oxidants by a combination of oxygen and alkene derivatives, and the reduction of palladium catalyst loadings were explored.

Pivotal to the success of these discoveries was the use of mono-protected amino acid ligands. Combined experimental and computational analysis revealed that these readily available ligands can prevent amine decomposition by avoiding the geometrical coplanarity needed for β-H elimination processes. The inherent chirality of amino acids enabled the development of asymmetric C-H activation reactions, targeting both methyl and methylene C-H bonds to construct diastereo- and enantioselective aryl-amine motifs.



Jesus Rodrigalvarez Garcia

Acknowledgements

I would like to start by thanking Matt for giving me the opportunity to work in his research group. Throughout these years you have given me the freedom to explore and investigate the complicated world of C–H activation, and I hope to have contributed within this time in fulfilling the overarching goals of the Gaunt group in facilitating amine synthesis. This journey would not have been possible without my funding bodies, La Caixa Foundation and Cambridge Trust, to whom I am deeply grateful.

Working at University of Cambridge provided a fantastic environment to do research while being surrounded by exceptional chemists. I am particularly thankful to Manuel for his guidance during my first stages within the group and for his passionate arguments about any possible topic of discussion; and to Nils for being incredibly patient in teaching me how to get started in the world of *in silico* reactions. This thesis will not be the same without their contribution. I am also very grateful to Hiro, Luke, Javi, and Matt Burns, who were wild enough to join me in exploring the scope and limitations of amine functionalisation. I also need to cite Will, whose fascination and interest in palladium and C–H activation excelled my ones; and two undergraduate students, Sam and Edward, whose efforts have also contributed in the results obtained throughout these years. A particular acknowledgement also goes to Luke, Roopender, and Georgia for proofreading this thesis, and to all the university staff who contributed in running all facilities as smoothly as possible. Duncan and Andrew, thank you for constantly dealing with the 700 MHz autosampler; and Stuart, thank you for answering emails late at night about dummy operating system questions.

John, Roopender, Yuki, Sarah, Sanesh, Elena, Javi, Hiro, Nils, Manuel, Jaime, Jorge, Ali, in no particular order, it was a pleasure to have shared this experience with you. Thank you for your support, advice, jokes and humour sense in either *latin* lunches, coffee breaks or Yim-Wah dinners. You are all great individuals with very successful pathways ahead of you. Nonetheless, a particular mention goes to Elena, who offered us a home in rather one of the most chaotic moments of my life; and to Javi, a truly Apple fanboy who made this experience much more cracking and enjoyable.

I cannot finish these lines without thanking my parents for teaching me the values of integrity, confidence and perseverance, all of which have contributed to the development of this work. Most importantly, I am extremely grateful to my partner. Lorena, thank you for your willingness to share this challenging and crazy journey with me, and thank you for your help, guidance and for relentlessly listening to my complains. You helped me in becoming a more free, modern and better person and I am extremely happy to share this life with you.

Abbreviations

Ac	Acetyl
Ala	Alanine
app	Apparent
aq	Aqueous
Ar	Aryl
Ar _F	Perfluoroaryl
ax	axial
B3LYP	Becke, 3-parameter, Lee-Yang-Parr
Bn	Benzyl
Boc	<i>tert</i> -Butyloxycarbonyl
BQ	1,4-Benzoquinone
BSSE	Basis-set superposition error
Bz	Benzoyl
cat	Catalytic
Cbz	Carboxybenzyl
CMD	Concerted metalation-deprotonation
Cy	Cyclohexane
D3BJ	Dispersion-3 with Becke-Johnson damping
dba	Dibenzylideneacetone
DCE	1,2-Dichloroethane
DCM	Dichloromethane
DEA	Diethylamine
decomp	Decomposition
DG	Directing group
DFT	Density functional theory
DMA	Dimethylacetamide
DMAP	4-(Dimethylamino)pyridine
DMF	Dimethylformamide
DMSO	Dimethyl sulfoxide
dr	diastereomeric ratio
E	Electrophile
ee	Enantiomeric excess
eq	Equatorial

equiv	Equivalent
ESI	Electrospray ionisation
Et	Ethyl
EDG	Electron-donating group
EWG	Electron-withdrawing group
FID	Flame ionisation detector
Fmoc	Fluorenylmethyloxycarbonyl
GC	Gas Chromatography
Gly	Glycine
HetAr	Heteroaryl
HFIP	Hexafluoro-2-propanol
HRMS	High resolution mass spectra
<i>i</i> Bu	Isobutyl
IEF	Integral Equation Formalism
<i>i</i> Pr	Isopropyl
IR	Infrared spectroscopy
IRC	Intrinsic reaction coordinate
KIE	Kinetic isotopic effect
L	Generic ligand
LDA	Lithium diisopropylamide
LANL2DZ	Los Alamos National Laboratory 2-double Z
M	Metal
Me	Methyl
Mes	Mesitylene
mp	Melting point
MPAA	Mono-protected amino acid
MS	Mass spectrometry
NBE	Norbornene
<i>n</i> Bu	Butyl
NFSI	<i>N</i> -Fluorobenzenesulfonimide
NMP	<i>N</i> -Methyl-2-pyrrolidone
NMR	Nuclear Magnetic Resonance
Nu	Nucleophile
PCM	Polarizable continuum model

PE	Petroleum ether
PG	Protecting group
Ph	Phenyl
Phe	Phenylalanine
phen	Phenanthroline
Phth	Phthalimide
PIDA	(Diacetoxyiodo)benzene
Pin	Pinacolato
Piv	Pivaloyl
R	Generic organic group
RE	Reductive elimination
rpm	Revolutions per minute
rt	Room temperature
sat	Saturated
tamylOH	2-Methylbutan-2-ol
tBu	<i>tert</i> -Butyl
T	Temperature
t	Time
Tf	Triflyl, Trifluoromethanesulfonyl
TBS	<i>tert</i> -Butyldimethylsilyl
TFA	Trifluoroacetic acid
TFAA	Trifluoroacetic anhydride
TFE	2,2,2-Trifluoroethanol
THF	Tetrahydrofuran
TIPS	Triisopropylsilyl
TLC	Thin layer chromatography
Tle	<i>tert</i> -Leucine
TMP	2,2,6,6-Tetramethylpiperidine
TON	Turnover number
Ts	Tosyl, 4-Toluenesulfonyl
TS	Transition state
Val	Valine
X	Unspecified group (typically heteroatom or halogen)
Xantphos	4,5-Bis(diphenylphosphino)-9,9-dimethylxanthene

Table of contents

1. Introduction to palladium-mediated C–H activation	1
1.1. C–H activation and palladium: Concept, mechanism and reactivity	3
1.2. Engineered directing groups in C(sp ³)–H palladium catalysis	9
1.3. Transient directing groups for amine substrates in C(sp ³)–H palladium catalysis	14
1.4. Native amine-directed palladium catalysis of C–H bonds	20
1.4.1. Primary alkylamines in C(sp ³)–H activation	22
1.4.2. Secondary alkylamines in C(sp ³)–H activation	24
1.4.3. Benzylic tertiary amines in C(sp ²)–H activation	31
1.5. Ligands in palladium-catalysed C(sp ³)–H activation reactions	33
1.6. Alternative C(sp ³)–H functionalisation strategies for tertiary amines	37
1.7. Summary and outlook	41
2. Methyl C(sp³)–H activation of tertiary alkylamines via palladium catalysis	43
2.1. Background & Previous work	45
2.2. Project aims	50
2.3. Results & Discussion	50
2.4. Computational findings	65
2.5. Summary	81
3. Enantioselective methylene C(sp³)–H activation of tertiary alkylamines via palladium catalysis	83
3.1. Background & Previous work	85
3.2. Project aims	89
3.3. Results & Discussion	89
3.4. Computational findings	101
3.5. Summary	106
4. Conclusion and outlook	109
5. Experimental procedures	115
5.1. General information	117
5.2. Methyl C(sp ³)–H activation of tertiary alkylamines	119
5.3. Enantioselective methylene C(sp ³)–H activation of tertiary alkylamines	132
6. References	151

Appendix	165
I. Synthesis and characterisation of starting materials	167
II. Supplementary Data	194
II.I. X-Ray Crystallography	194
II.II. Asymmetric Analysis	196
II.III. NMR Spectra	226
III. Computational complexes	355
III.I. Nuclear coordinates for complexes containing <i>N,N</i> -dimethylpropan-1-amine	358
III.II. Nuclear coordinates for complexes containing 1-propylpiperidine	382
III.III. Nuclear coordinates for complexes containing 1-propylpyrrolidine	394
III.IV. Nuclear coordinates for complexes containing 1-propylazepane	406
III.V. Nuclear coordinates for complexes containing <i>tert</i> -butyl 4-propyl-1,4-diazepane-1-carboxylate	416
III.VI. Nuclear coordinates for complexes containing 1-cyclopropyl- <i>N,N</i> -dimethylmethanamine	421
III.VII. Nuclear coordinates for complexes containing 1-cyclobutyl- <i>N,N</i> -dimethylmethanamine	430
IV. Published work	443

Chapter 1

Introduction to palladium-mediated C–H activation

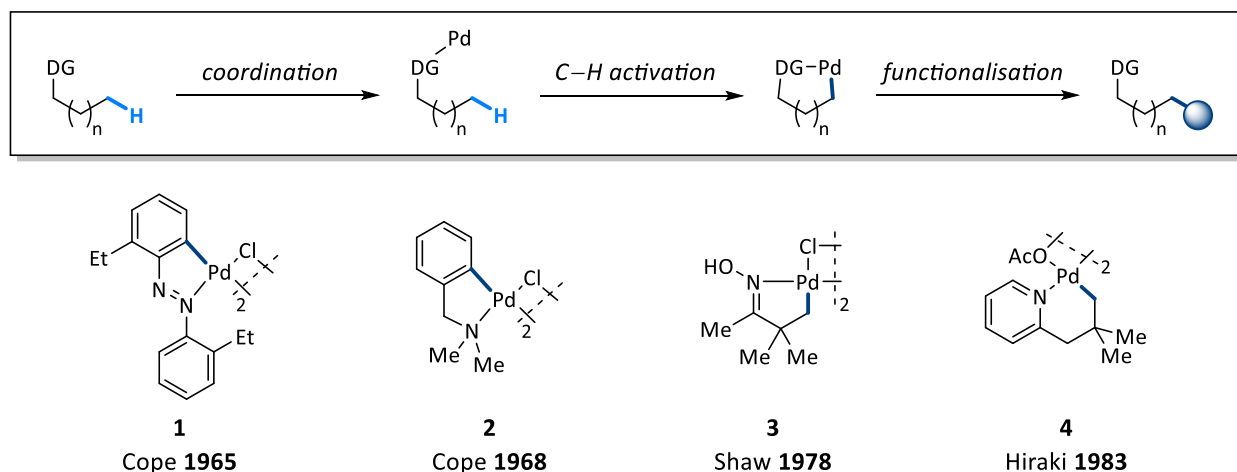
1.1. C–H activation and palladium: Concept, mechanism and reactivity

Carbon and hydrogen are among the smallest atoms of the Universe. Their marginal difference in electronegativity (2.55 vs 2.20 on the Pauling scale, respectively) delivers a short, strong, covalent, and non-polar bond of 1.09 Å with a bond energy of 104 kcal·mol⁻¹ (for a methane molecule). Combined with their relatively abundance on the Earth's crust, these synergistical properties have established C–H bonds as the chemical foundations of nature and life. The different hybridisation modes of a carbon atom have unlocked rich and versatile synthetic transformations, such as the formation of enols, elimination reactions in saturated carbon backbones, or the generation of conjugated and aromatic systems with delocalised electrons in the *p* orbitals; unarguably key reactions and functional groups for any living organism. However, the ability of nature to modify C–H bonds typically relies on the presence of proximal heteroatoms (N, O, S, etc). These more electronegative elements acidify vicinal C–H bonds in an aliphatic backbone making them susceptible to base-mediated cleavage. This not only ensures reactivity, but most importantly, grants the ability to distinguish between neighbouring C–H bonds by their different chemical properties. Therefore, the selective breaking of C–H bonds lacking of nearby functionalities is a challenging task rarely achieved by enzymes.^{1,2}

Synthetic chemists define C–H activation as a metal-mediated process which enables the selective cleavage of a typically inert carbon hydrogen bond, *i.e.* whose chemical environment precludes a precise and selective reactivity through metal-free polar or radical pathways, generating an organometallic complex where the hydrocarbon is coordinated to the inner-sphere of the metal forming a M–C bond. Multiple late-transition metals exhibit this reactivity.^{3–6} Alternatively, C–H cleavage can occur through an outer-sphere process where functionalisation occurs in the absence of a metal-carbon intermediate. Examples of this reactivity are metal carbene chemistry and biochemical P450 mediated processes, but they are not classified as C–H activation reactions.^{7–9} Nevertheless, both pathways ultimately aim to replace the abstracted hydrogen atom by a non-metallic heteroatom leading to a C–H functionalised product.

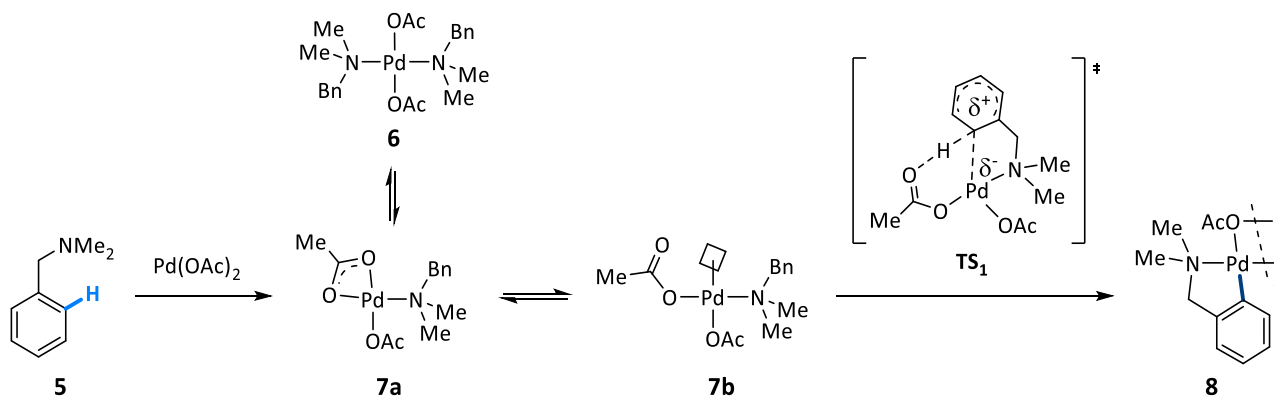
Palladium is unarguably the most widely exploited transition-metal in C–H activation reactions.^{10–14} Its electronegativity of 2.20, identical to an hydrogen atom generates a covalent Pd–C bond susceptible to both nucleophilic and electrophilic reactivity; and its compatibility with air or moisture facilitates the isolation of reaction intermediates, enabling its detailed study in elementary steps such as oxidative addition, reductive elimination, and transmetalation. This, combined with the vast existent literature precedents around palladium chemistry prior to the study of C–H activation reactions, might have biased the synthetic community towards the study of this particular metal. In particular, the development of chiral bidentate ligands during the last decade for alkyl C–H cleavage have dramatically expanded the range of synthetic transformations which palladium can perform,^{15–18} leaving other metals at the infancy of their possibilities.^{19–26}

During the 60s, 70s and 80s, the inner-sphere pathway by which palladium performs C–H activation generated multiple examples of isolated organometallic complexes, both activating aryl and alkyl systems (Scheme 1). Cope reported the first example of a well-defined palladacycle arising from C–H activation by using aromatic azo compounds (**1**),²⁷ and tertiary benzyl amines (**2**).²⁸ Shaw observed that this strategy was also applicable to C(sp³)–H bonds, isolating complex **3** by using an oxime functional group,²⁹ while Hiraki found pyridine substrates also to be amenable to C(sp³)–H cleavage (**4**).³⁰ A common feature of these examples, which is still applicable to the field nowadays, is the presence of a good σ -donating functional group. This directing functionality is a common feature in C–H activation because not only it accelerates the kinetics of the reaction by positioning the metal centre in close proximity to a C–H bond, but it also enhances the thermodynamic stability of the resultant generated palladacycle. Another interesting observation was the strong preference for the isolation of 5-membered ring organometallic complexes, whereas higher ring sizes are only accessible when no γ -H with respect to the *N*-directing group were present (**4**).³¹



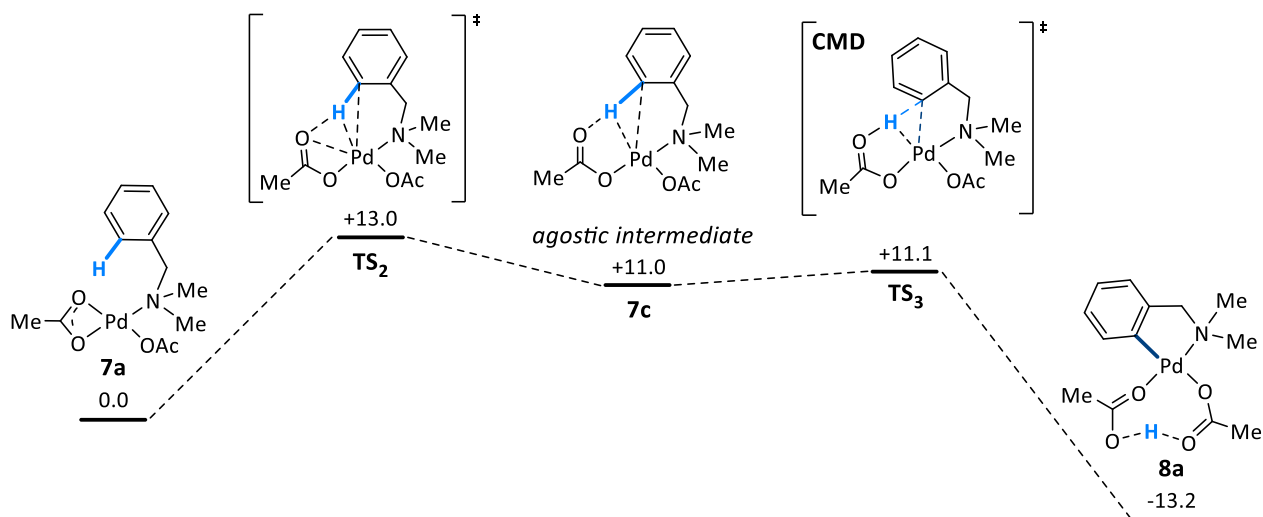
Scheme 1: C–H activation via inner-sphere cyclopalladation

Despite the established reactivity and selectivity of palladium complexes, little experimental work was conducted to elucidate the mechanism by which palladium C–H activation occurred, and what accounts for its selectivity. In 1985, Ryabov studied the cyclopalladation reaction of amine **5** with Pd(OAc)₂ (Scheme 2).³² An equilibrium between bisamine complex **6** and monoamine complex **7a** was observed, being the later an unsaturated intermediate where an acetate ligand switches between η^1 - and κ^2 - binding modes. The generated vacant site in **7b** allows for C–H activation to happen. Based on a kinetic isotope effect (KIE) K_H/K_D of 2.2 and a large negative activation entropy of $-250 \text{ J}\cdot\text{K}^{-1}\cdot\text{mol}^{-1}$, *ortho*-palladation was proposed to occur via a highly ordered transition state, similar to a Wheland-type intermediate, in which an internal acetate acts as a base to abstract the leaving hydrogen (**TS**₁). However, this proposal is not compatible with the activation of aliphatic hydrocarbons due to the absence of conjugation capable of allocating the partial positive charge generated.



Scheme 2: Electrophilic *ortho*-palladation proposed by Ryabov

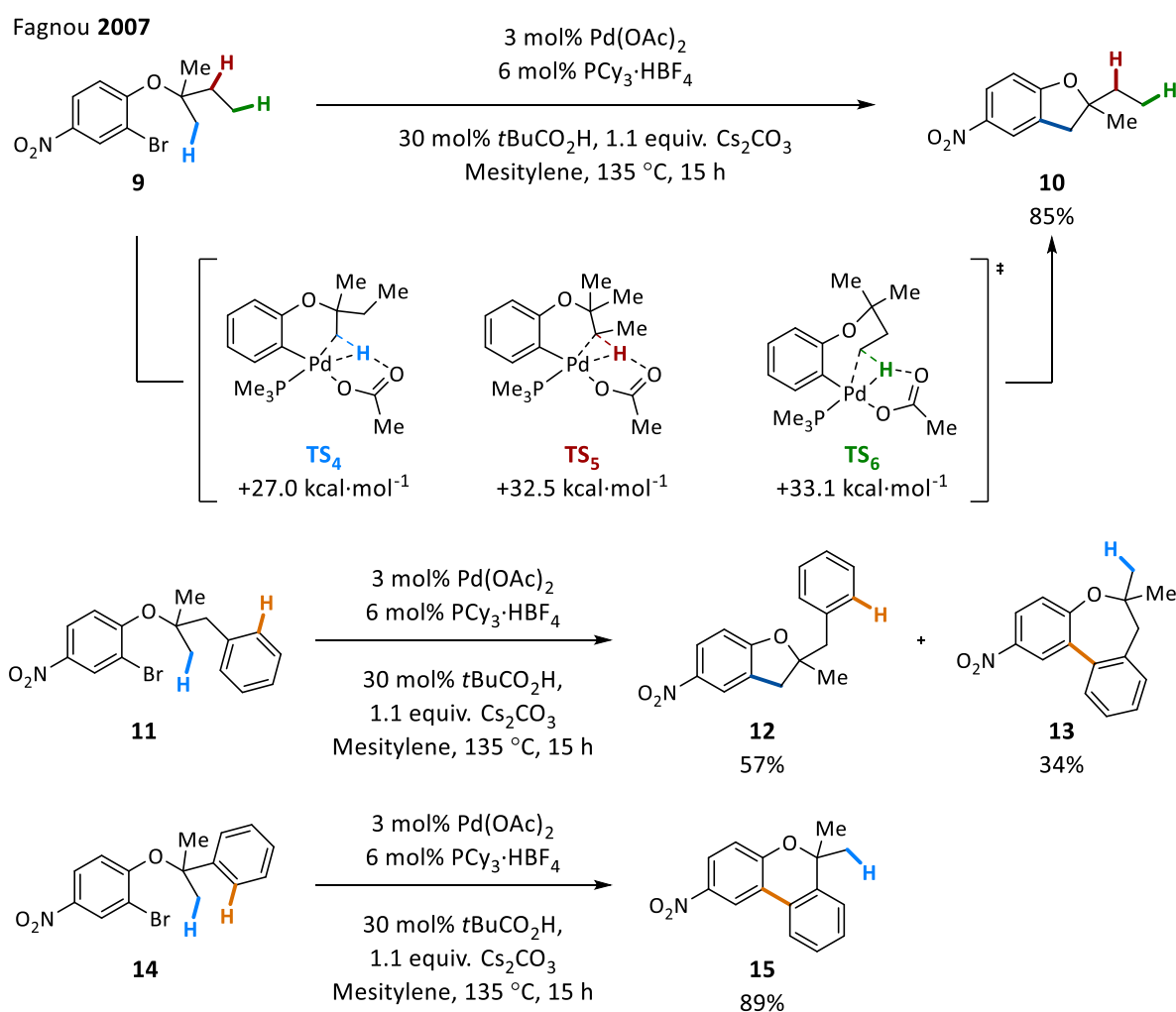
In 2005, a computational study by Davies and Macgregor established the most accepted mechanism for the palladium-mediated C–H activation step.³³ As proposed by Ryabov, C–H activation starts from monoamine complex **7a** (Scheme 3). Displacement of the κ^2 -binded acetate by the *ortho*-C(sp^2)–H bond leads to the agostic intermediate **7c**, where a short Pd–H interaction of 1.91 Å is exhibited. The absence of a partial positive charge in any of the aryl ring carbons and the negligible decrease in positive charge from palladium disproved a putative Wheland-type intermediate. From intermediate **7c**, proton-transfer from the aromatic ring to the acetate occurs through a barrierless six-membered ring transition state to form 5-membered palladacycle **8a**. Although other mechanistic pathways were considered, this redox neutral acetate-assisted proton-transfer process was found to be the lowest energetic pathway and it was later termed concerted metalation-deprotonation (CMD).^{34,35}



Scheme 3: Proposed base-mediated C–H cleavage by Davies and Macgregor

Shortly after these mechanistic investigations, Fagnou reported the first computational study of alkyl C–H activation (Scheme 4).³⁶ Oxidative addition of Pd⁰ into aryl bromide **9** positioned the transition metal in close proximity to multiple C(sp^3)–H bonds from where intramolecular C–H activation can take place. The exclusive formation of dihydrobenzofuran products (**10**) was observed, forged after reductive elimination of

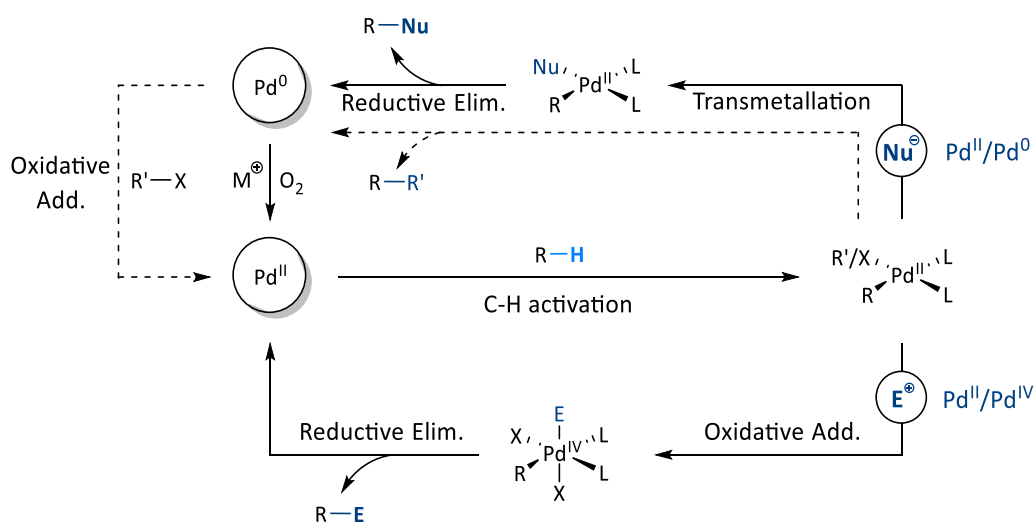
the desired C(sp³)–C(sp²) bond. In agreement with previous studies, DFT investigations in a simpler system concluded that the lowest energetic barrier for C–H cleavage proceeded through a CMD three-centre two-electron transition state where a bidentate carboxylate group acts as an internal base after generating a vacant site in the organometallic complex (**TS₄**). Other alternative pathways, such as oxidative addition into the C–H bond of interest, were disproved as they possessed much higher energy barriers. Interestingly, this research work also studied the selectivity for different types of C–H bonds. As illustrated in Scheme 1, the formation of 5-membered ring palladacycles is always preferred as it arises from a 6-membered ring transition state. Nevertheless, there were no C–H bonds in substrate **9** capable of accessing these ideal arrangement, and the only available C(sp³)–H cleavage occurred through a 7-membered ring transition state to generate a 6-membered ring palladacycle (**TS₄**, +27.0 kcal·mol⁻¹, Scheme 4). In agreement with experimental findings, methylene (**TS₅**, +32.5 kcal·mol⁻¹) or more distal methyl C–H activation (**TS₆**, +33.1 kcal·mol⁻¹) were computationally observed to possess higher transition states. Competition between C(sp²)–H and C(sp³)–H activation was also studied, which revealed that aryl C–H activation is more facile, even when proceeding through less favourable 8- or 9-membered ring transition states (**15** and **13**, respectively).



Scheme 4: Experimental and computational comparison between aryl and alkyl C–H activation

Within the field of C–H activation, it is essential to differentiate between aromatic C(sp²)–H bonds and aliphatic C(sp³)–H bonds, with the prior being more facile to cleave due to the favourable metal-substrate interaction with the ring π -system. As demonstrated by Fagnou's calculations, even sharp differences are encountered when comparing alkyl C–H bonds. Terminal methyl groups are more readily activated than methylene units based primarily on sterics, and methine activation being very rare to occur.^{37–39} Reactions capable of overcoming this intrinsic selectivity are scarce and often require biased substrates.^{40–42}

Once it has been established how palladium imparts reactivity and selectivity in C–H activation reactions, it is also important to describe how palladacycles can be functionalised through the rich and versatile reactivity which palladium exhibits. After C–H cleavage from a Pd^{II} oxidation state, one can exploit a low-valent manifold with nucleophiles (Suzuki cross-coupling) or alkenes (Heck cross-coupling) among others, to obtain the desired product after reductive elimination (Scheme 5). To close the catalytic cycle, the resultant Pd⁰ is oxidised to Pd^{II} with other transition metals (Cu^{II}, Ag^I), organic additives (1,4-benzoquinone),^{43–47} or atmospheric O₂ in the best case scenario.⁴⁸ An alternative approach is to begin with a Pd⁰ precatalyst where oxidative addition into an organohalide occurs prior to the C–H activation step (see Scheme 4 as an example). These types of transformations are useful to generate intramolecular C–C bonds without the need of Lewis basic functionalities, as the palladium-aryl intermediate acts effectively as a directing group. On the other hand, high-valent Pd^{II}/Pd^{IV} catalysis is accessible when using electrophilic coupling partners (organohalides or hypervalent iodine(III) compounds) capable of oxidising the generated Pd^{II} palladacycle. Control in the final reductive elimination step can deliver a diverse range of functionalised products, both in the form of C–C bonds or C–X bonds (X = N, O, F).^{49,50} It is worth mentioning that Scheme 5 summarises the most commonly used mechanistic manifolds in C–H activation reactions, but it does not intend to summarise all possible transformations. Other mechanistic manifolds involving double C–H activation reactions,^{51,52} oxidation of Pd^{II} to Pd^{III} dimers,^{53,54} or C–H activation through Pd^{IV} intermediates have all been proposed.⁵⁵

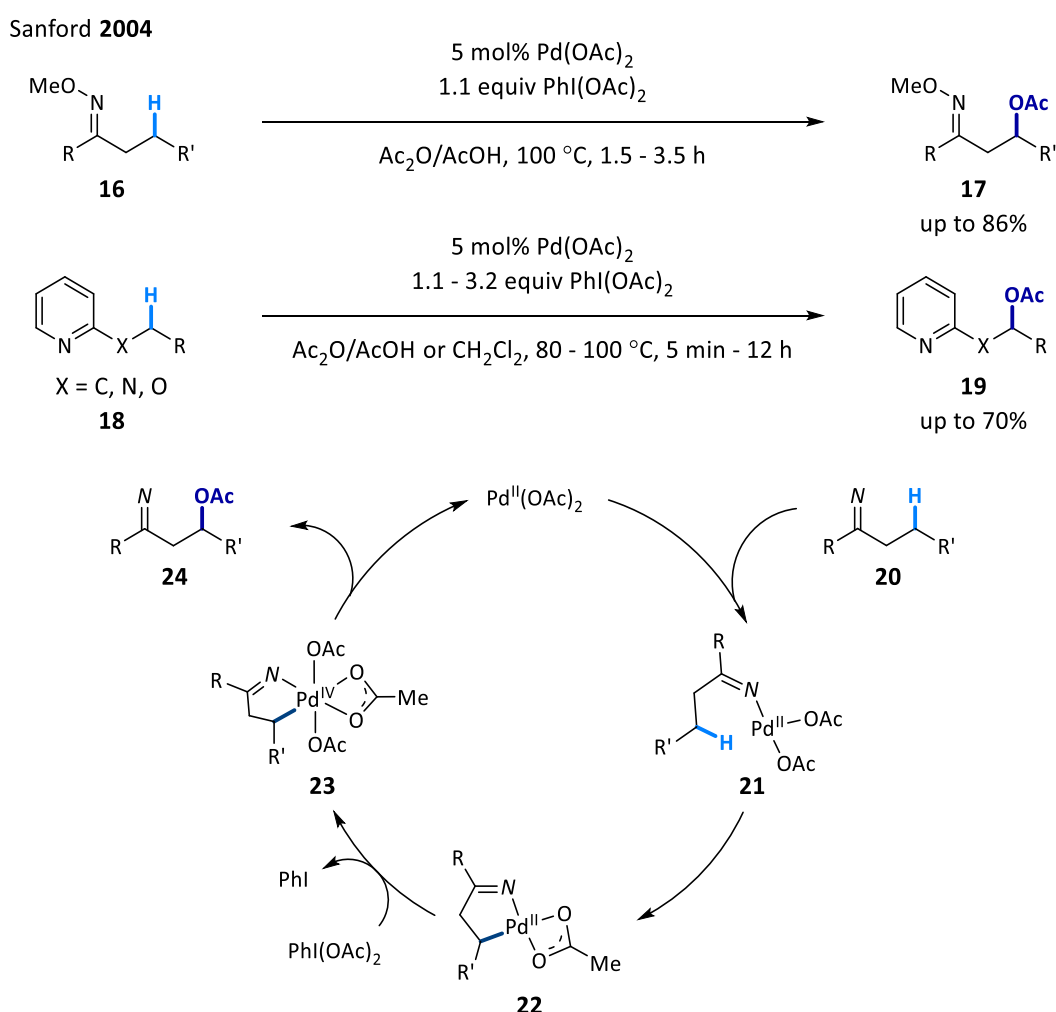


Scheme 5: General mechanistic manifolds in palladium-catalysed C–H activation reactions

The last crucial point worthy of discussion is the prevalent use of Ag^I additives when performing C–H activation reactions under palladium catalysis. These usually are important or essential components in alkyl C–H activation reactions, despite their relative high cost and their use in superstoichiometric amounts. It was initially proposed that Ag^I additives were simply involved in the oxidation of Pd⁰, or that they could act as halide scavengers when aryl iodides or hypervalent iodine reagents were employed to access Pd^{IV} intermediates. However, more recent computational and mechanistic studies suggest that the energy barriers leading to C–H cleavage can be lowered when forming bimetallic Ag-Pd complexes, if compared with monomeric or dimeric palladium complexes.^{56–58} Even more remarkable is the use of silver as the only metal for C–H cleavage, although this has only been achieved to date in C(sp²)-H bonds.^{59–63} Unfortunately, not every reported C–H activation reaction in the literature assessed the role of the Ag^I additive used, which remains a topic of discussion and speculation in the field.

1.2. Engineered directing groups in C(sp³)–H palladium catalysis

It has been previously illustrated that substrates bearing aryl halides can effectively direct C–H activation via oxidative addition to Pd⁰, which yields an intramolecular C–C bond forming reaction upon reductive elimination (Scheme 4). Nevertheless, intermolecular C–H functionalisation reactions remained more elusive. The presence of strongly coordinating directing groups facilitates C–H activation, but the resultant palladacycles are unable to deliver functionalised products under well-known low-valent palladium chemistry due to their enhanced stability.^{64,65} In 2004, a seminal paper by Sanford reported the intermolecular C(sp³)–H functionalisation of oximes (**16**) and pyridines (**18**) by exploiting high-valent palladium pathways, accessed using hypervalent iodonium salts as stoichiometric oxidants (Scheme 6).⁶⁶



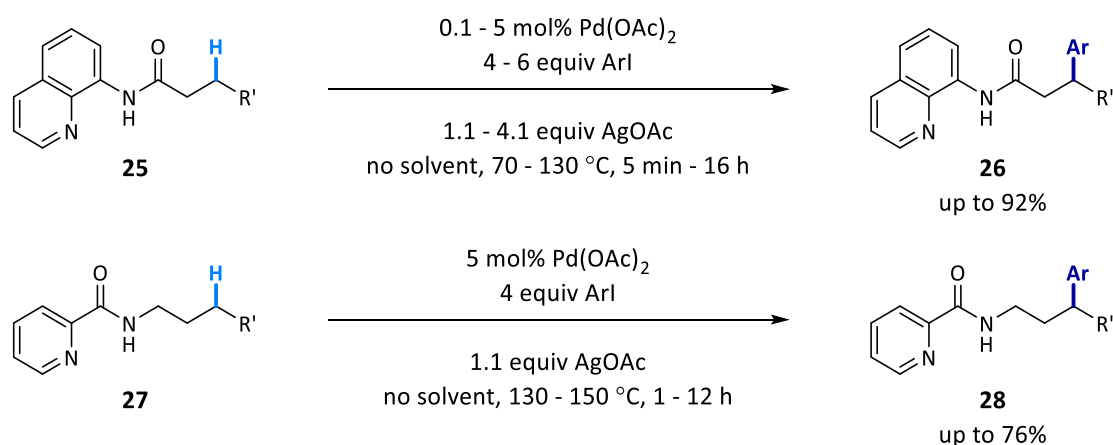
Scheme 6: First intermolecular palladium-catalysed C(sp³)–H activation

Coordination of the sp² hybridised nitrogen effectively directs the palladium atom towards C–H cleavage (**21**). The resulting Pd^{II} palladacycle (**22**) can then be oxidised by the highly electrophilic iodonium (III) reagent to form octahedral intermediate **23**, from which a more facile reductive elimination is possible to generate the resultant C–O bond (**24**). Of note is that consideration into the selectivity of the reductive elimination step

was not required because acetates are the only anions available within the reaction media, making acetoxylation the only possible functionalisation. Reactivity was observed in both methyl and cyclic methylene positions where the C–H bond is capable of forming 5-membered ring palladacycles, including C–H bonds next to heteroatoms.

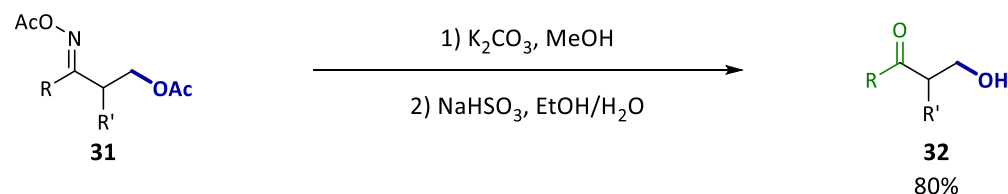
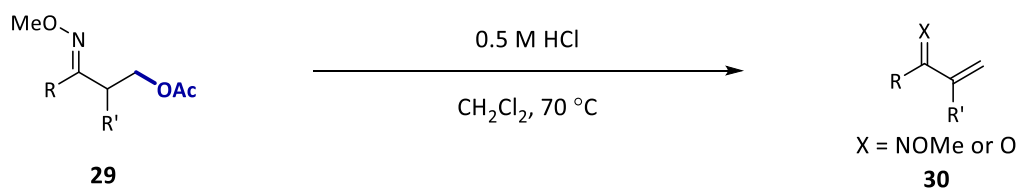
The following year, Daugulis reported the successful arylation of 8-aminoquinoline amides (**25**) and picolinamides (**27**) using aryl iodides as the electrophilic coupling partner.⁶⁷ Once again, a high-valent mechanistic manifold is exploited to oxidise the Pd^{II} palladacycle to a Pd^{IV} complex, but this time a selective reductive elimination furnished a resultant C–C bond with no acetoxyated products observed. Remarkably, this bidentate directing group could target any methyl or methylene unit leading to 5-membered ring palladacycles, including arylation at benzylic positions, which granted access to poly-arylated products. This highly efficient reaction reached TON values of 650, although stoichiometric silver additives and high reaction temperatures were required.

Daugulis 2005

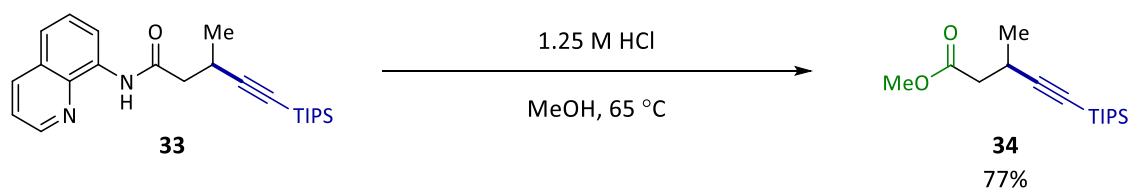
**Scheme 7:** First intermolecular C–C bond formation through C(sp³)–H activation

These two landmark publications exemplified the challenges of aliphatic C–H activation. Ignoring the high reaction temperatures needed, any successful functionalisation requires the prior modification of common functional groups, such as ketones, amines and carboxylic acids, into oximes, picolinamides, and 8-aminoquinoline amides, respectively. Not only is manipulation of the starting material required, but also the removal of these exogenous directing groups after C–H activation. Scheme 8 illustrates the challenges associated with this simple premise. Substrate decomposition or undesired deprotections can occur under the harsh reaction conditions required to liberate the desired functionalised substrate.^{68–71} For the interest of the present work, this introduction is only focused on the C–H activation of amine substrates, while extensive reviews for other types of organic functional groups can be found elsewhere.^{11–13}

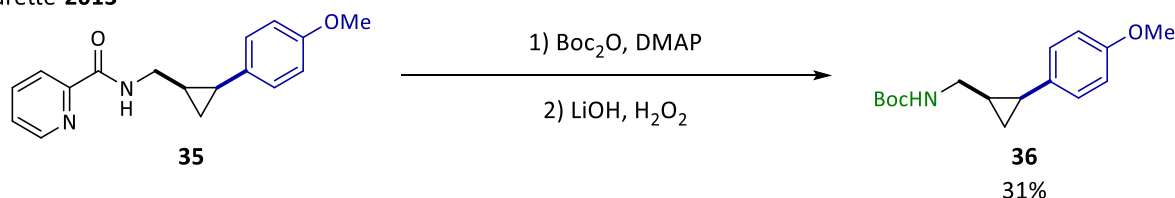
Sanford 2010



Chatani 2011

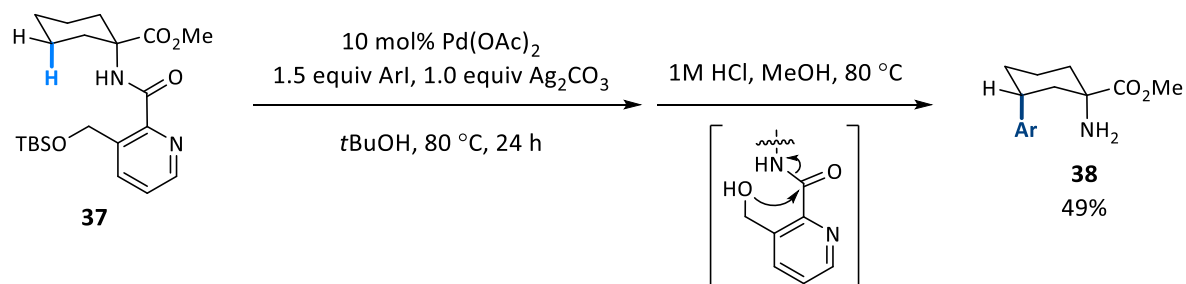


Charette 2013

**Scheme 8:** Challenges of removing exogenous directing groups after C(sp³)-H activation

Picolinamide derivatives (**27**) have been extensively used as directing groups in the field of C–H activation as their bidentate character greatly facilitates γ -C(sp³)-H bond cleavage. The resultant palladacycles can react with a vast range of reagents enabling C–C bond formation (arylation, alkylation, carbonylation, etc),^{71–74} C–N ring closing reactions,^{75,76} or C–X bond formation (alkoxylation, borylation, etc).^{77,78} To facilitate the removal of this privileged directing motif, Chen developed a modified picolinamide group bearing a silyl protected alcohol on the pyridine directing moiety (**37**, Scheme 9).⁷⁹ After successful C–H arylation using aryl iodides, deprotection of the alcohol released the γ -arylated amine substrate upon intramolecular attack of the amide bond, along with the cyclised picolinate ester which could be recovered for subsequent use. Since then, multiple procedures have been developed to liberate the functionalised primary amine from this scaffold after successful C–H activation, usually involving the presence of a Lewis acid (BF₃ or AlCl₃) under heating conditions,^{80,81} or a reductive acidic media.⁸² More recently, Maes exploited the ability of Ni(cod)₂ to insert into amide C–N bonds to develop neutral deprotection conditions which delivered the functionalised product as a *-Boc* protected amine.⁸³

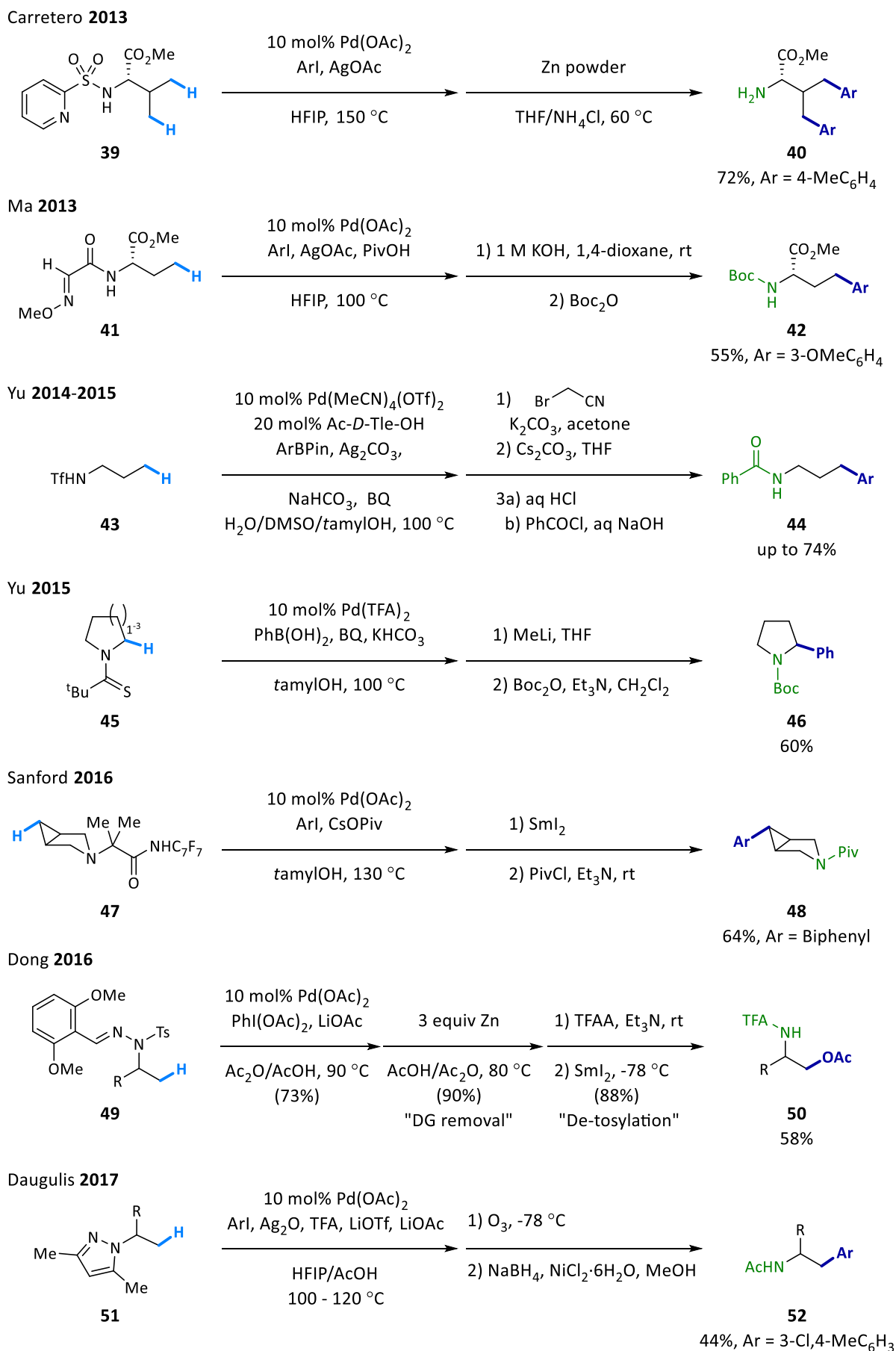
Chen 2011



Scheme 9: A picolinamide derivative to remove under milder reactions conditions the directing group after C–H activation

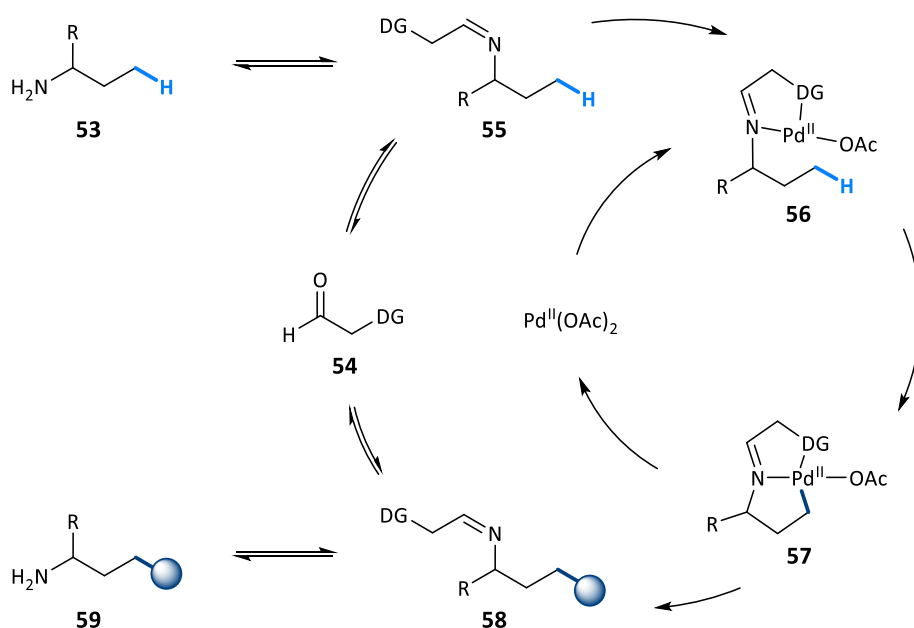
During the last decade, multiple research groups attempted the development of alternative amine-derived directing groups to access other C–H bonds apart from γ -C–H activation, or to release the functionalised amine with milder and/or orthogonal deprotection reactions (Scheme 10).^{39,84–91} When using high-valent palladium catalysis, all these examples rely on the same reaction mechanisms outlined in the seminal reports of Sanford (Scheme 6) and Daugulis (Scheme 7). Nevertheless, two depicted examples from the Yu group achieved functionalisation via a low-valent manifold using boron reagents as viable coupling partners. The resemblance between some of the tailored directing groups depicted in Scheme 10 and the previously reported picolinamide derivatives are clear. The use of bidentate auxiliaries provides a second binding point with modular and tuneable properties susceptible of optimisation to maximise yield and reactivity. Depending on the nature of the installed auxiliary, its removal after C–H activation can lead to a α - or β -functionalised product, despite all palladacycles possessing well-defined 5-membered ring structures.

Exogenous directing groups provided proof of concept that palladium-catalysed C(sp³)–H activation is possible under a diverse range of catalytic conditions. However, the incorporation and subsequent removal of these auxiliaries can present incompatibilities with other functional groups on the molecule, and the process ultimately results in a multi-step synthesis which can diminish the overall efficiency of the transformation. Therefore, research in the field of C–H activation transitioned to the development of more straightforward strategies through either the use of native organic functional groups or the generation of transient species within the reaction mixture capable of effectively undergoing C–H activation.

Scheme 10: Amine-derived directing groups in C(sp³)–H activation reactions

1.3. Transient directing groups for amine substrates in C(sp³)-H palladium catalysis

The use of transient directing groups in palladium-catalysed C–H activation reactions arose from the need to streamline amine functionalisation by developing a one-pot procedure capable of incorporating and removing the engineered directing group needed for successful C(sp³)-H cleavage. Instead of using a stable amide bond, such as the picolinamide derivative, to incorporate the needed auxiliary, it was envisaged that the condensation of a primary amine substrate (**53**) with an aldehyde (**54**) could form an *in situ* transient bidentate imine directing group (**55**), capable of chelating to palladium to greatly enhance C–H cleavage (**56**, Scheme 11). Once the functionalised product is obtained (**58**), hydrolysis of the resultant imine intermediate generates the desired amine product (**59**) while recovering the aldehyde additive, which is typically used in substoichiometric amounts. In an analogous strategy, this concept has also been effectively applied to the functionalisation of aldehyde and ketone substrates with primary amines behaving as the transient directing motifs.^{92–96} These examples stand outside the topic of discussion, but the mechanism, reagents and reaction conditions employed do not differ significantly from the ones which will be discussed hereafter.

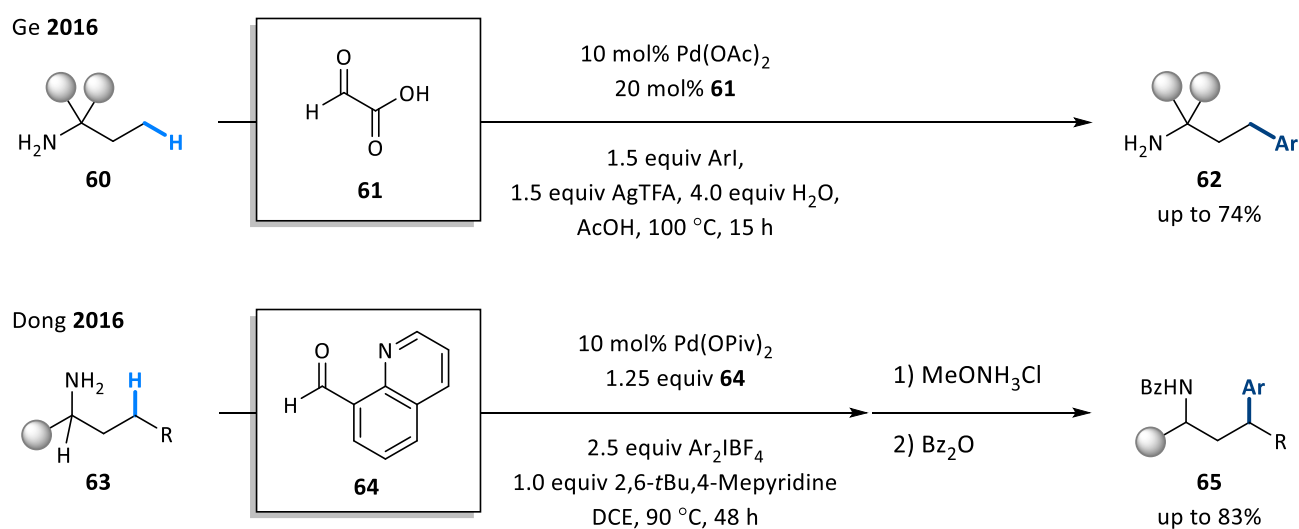


Scheme 11: Transient directing group strategy for the C(sp³)-H activation of amine substrates

It is worth highlighting two features common to all of the reactions that will be presented in this section. Firstly, the use of a strongly coordinating bidentate ligand generates palladacycle (**57**), whose tridentate nature has to date only made possible its functionalisation through high-valent Pd^{II}/Pd^{IV} chemistry. Secondly, these transformations typically occur in acidic media to favour amine condensation, but most importantly, to disfavour direct amine-palladium coordination by substrate protonation. Of note to the reader is that the subsequent schemes of this introduction will illustrate amines with unspecified grey substituents where the presence of alkyl groups in these positions are required to achieve reactivity or significant product formation.

Seminal papers using the aforementioned strategy were published simultaneously by Ge and Dong.^{97,98} The Ge group used glyoxylic acid in catalytic amounts to enhance palladium coordination with a carboxylate group acting as the second intramolecular binding point (**61**, Scheme 12). After C–H activation, functionalisation with aryl iodides led to the formation of the desired product in up to 74% yield. Silver(I) additives were found to be crucial to yield any reactivity, and it was later elucidated by DFT calculations that the lowest barrier for C–H cleavage proceeded via a dimeric Pd–Ag complex.⁵⁸ Unfortunately, primary amines with α -H were not tolerated, with only methyl C–H activation being reported. This exemplifies the difficulty of achieving reactivity in substrates whose directing groups aren't robust and stable amide functionalities.

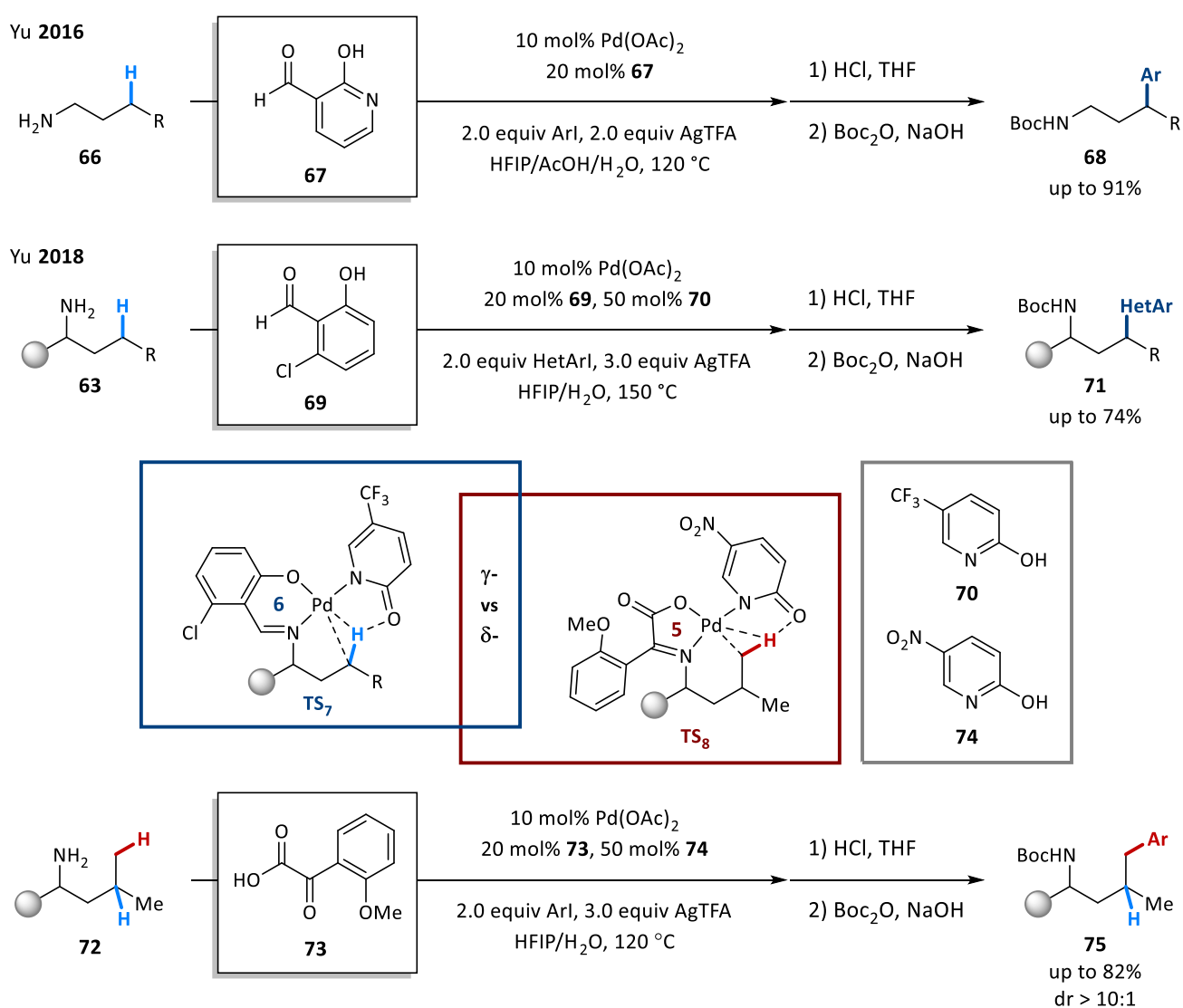
The Dong group chose quinoline-8-carbaldehyde (**64**) as the transient directing group in an attempt to mimic the excellent reactivity of Daugulis' pyridine-type directing groups (see Scheme 8). The resultant reaction used high-valent iodonium salts to achieve a silver-free arylation reaction where substrates bearing α -H were successfully tolerated this time, and both methyl and methylene γ -C–H bonds could be functionalised. Interestingly, aniline-type substrates, which are difficult to functionalise due to their lack of coordination with the metal atom, were reported to perform δ -arylation at the methyl group of an *ortho*-*tert*-butyl substituent. Of note is that 10% of remaining starting material was usually observed by ¹H-NMR after C–H activation. This can be attributed to the multiple equilibria present in the reaction, hampering reaction completion by product inhibition, as observed by others.⁹⁹



Scheme 12: First seminal palladium-mediated C–H activation reactions using aldehydes as transient directing groups

Within the same year, Yu reported another arylating methodology using aryl iodides as the coupling partner and 2-hydroxynicotinaldehyde as the transient additive for C–H cleavage (**67**, Scheme 13).¹⁰⁰ This set of reaction conditions exhibited the widest substrate scope as it targeted methyl and methylene bonds, both in cyclic systems of different ring-sizes as well as linear alkyl chains (**68**). It could deliver good yields of arylated

amines containing two α -Hs, and it was compatible with heteroaryl coupling partners, albeit only when targeting methyl C–H bonds. Further optimisation in a later publication revealed that the addition of pyridone additives (**70**), previously used for C(sp²)–H bonds,^{101,102} facilitated arylation at methylene positions with a broad range of heteroaryl iodides and bromides.⁴¹ The same report explored the ability to selectively target methyl δ -C–H bonds (**TS₈**) over methylene γ -C–H bonds (**TS₇**) by relying on a 5-membered ring bidentate transient directing group, rather than a 6-membered one. To achieve this, the chosen transient directing group did not consist of an aldehyde, but rather a conjugated α -keto carboxylic acid (**73**). Unfortunately, the work lacked true selectivity as direct comparison of γ - versus δ -methyl positions was not reported, and substituents at the γ -position were needed to transform this preferred reactive site in a much more elusive methine unit.

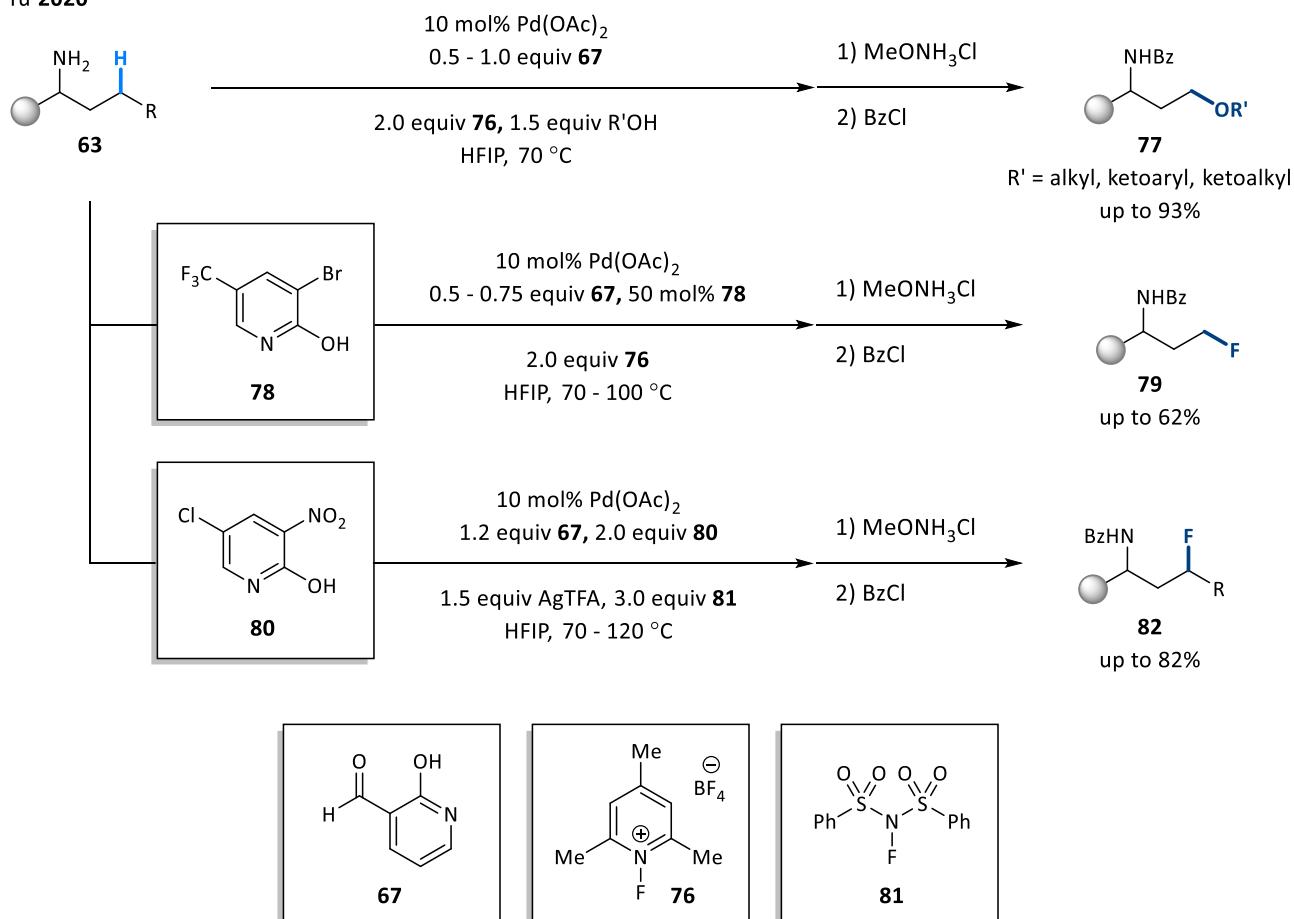


Scheme 13: Development of new transient directing groups to incorporate heteroaryl functionalities at γ - and δ - positions

The Yu group continued exploring the reactivity of these transient directing groups, testing novel transformations in the context of γ -carbon-heteroatom bond formation. By exploring a range of oxidants,

including iodonium (III) salts and peroxides, it was found that 1-fluoro-2,4,6-trimethylpyridinium tetrafluoroborate (**76**) effectively oxidised the Pd^{II} palladacycle intermediate to the high-valent Pd^{IV}, which showed exclusive selectivity for a C–O reductive elimination (Scheme 14).¹⁰³ Both aliphatic and aromatic carboxylic acids performed well under the reaction conditions to deliver exclusive formation of the desired carboxylated product (**77**). Aliphatic alcohols could also be incorporated into the functionalised amine product, albeit with diminished yields, and with pyridone additives needed in certain cases. In comparison with previous work from the group, the resulting primary amines were isolated in the less tractable form of benzamides. Unfortunately, the amine substrate scope proved to be capricious, requiring substitutions in either the α - or β - positions to the nitrogen in order to achieve good conversions, while a very moderate yield of 30% was obtained for the simplest *n*-propylamine substrate.

Yu 2020

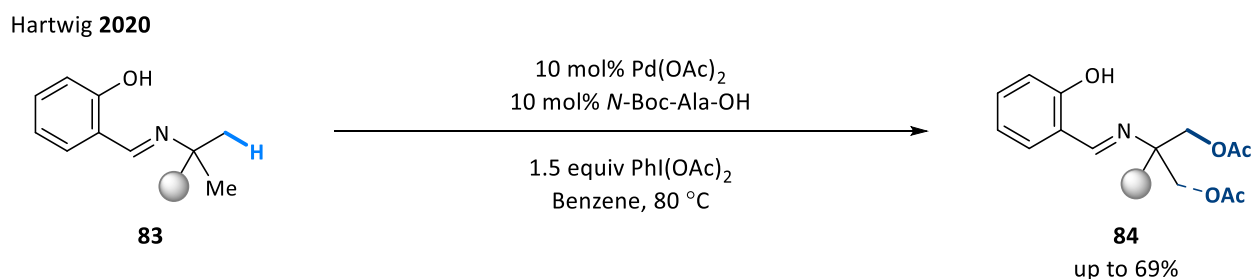


Scheme 14: Oxygenation and fluorination of primary amines

Very shortly after, Yu reported that the addition of pyridone ligand (**78**) to the same reaction conditions switched the selectivity for C–F reductive elimination (note that 20 mol% of acetate is available for C–O reductive elimination), albeit in modest yields (only one example was isolated above 50% yield).¹⁰⁴ No hypothesis was given to rationalise this observation, although similar investigations by the same research

group in benzaldehyde substrates with the same “F⁺” oxidant concluded that C–O bond formation proceeded through a S_N2 attack into the C–Pd bond, rather than a metal-mediated reductive elimination, applicable only to the construction of the C–F bond.⁵⁰ Within the same publication, it was also described that the use of NFSI (**81**) as the stoichiometric oxidant in combination with AgTFA achieved methylene C–H fluorination mediated by the super-stoichiometric use of a transient directing group and another electron-deficient pyridone ligand (**80**). This time, DFT calculations hypothesised that the key silver(I) additive aid oxidative addition of the palladacycle into the N–F bond while also lowering the reductive elimination barrier leading to C–F bond formation.

The Hartwig group demonstrated that the transient directing group can be tuned to access a highly challenging β-C–H activation.¹⁰⁵ By pre-condensing the desired primary amine with salicylic aldehyde, the resultant imine (**83**, Scheme 15) effectively directed cyclopalladation to form a putative strained 4-membered ring intermediate, which after oxidation with PIDA gave access a range of β-acetoxyated amine products in modest yields. Despite the unusual site-selectivity observed, it is worth highlighting that γ-acetoxylation is preferentially obtained when methyl or methylene γ-C–H bonds were available; and the amine scope proved to be narrow as no α-H were tolerated and *gem*-dimethyl substituents proved key for reactivity, introducing issues of mono-selectivity. Unfortunately, this method did not report a one-pot procedure to achieve incorporation and removal of the aldehyde directing group motif, but it has been included in this section as it exemplifies how weakly bonded bidentate directing groups can effectively enhance C–H activation at other less-classical alkyl positions, and there is little difference if the isolation of the resultant functionalised amine occurs as an imine, carbamate or amide protecting group.

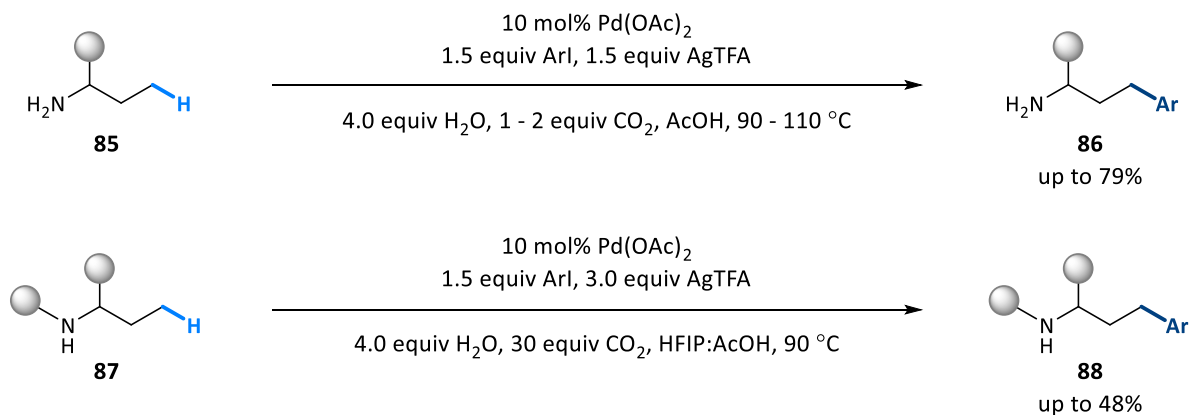


Scheme 15: β-Acetoxylation of α-tertiary amines

In 2018, Young published an alternative approach to the aldehyde mediated transient directing group strategy by using CO₂ in the form of dry ice (Scheme 16).¹⁰⁶ The authors proposed that CO₂ reacts *in situ* with the amine substrate to form a carbamate intermediate. This species is then capable of directing C–H activation, despite this happening through an unlikely 9-membered ring transition state. The method enabled arylation of not only primary amines, but also secondary amines, albeit in lower yields (**88**). Interestingly, when both γ-C(sp³)–H and γ-C(sp²)–H bonds are present in the same molecule, an unprecedented exclusive selectivity for

arylation at the alkyl position was observed. The specific use of AgTFA as a silver(I) additive proved key for reactivity, generating even more questions about the reaction mechanism and its CMD transition state.

Young 2018



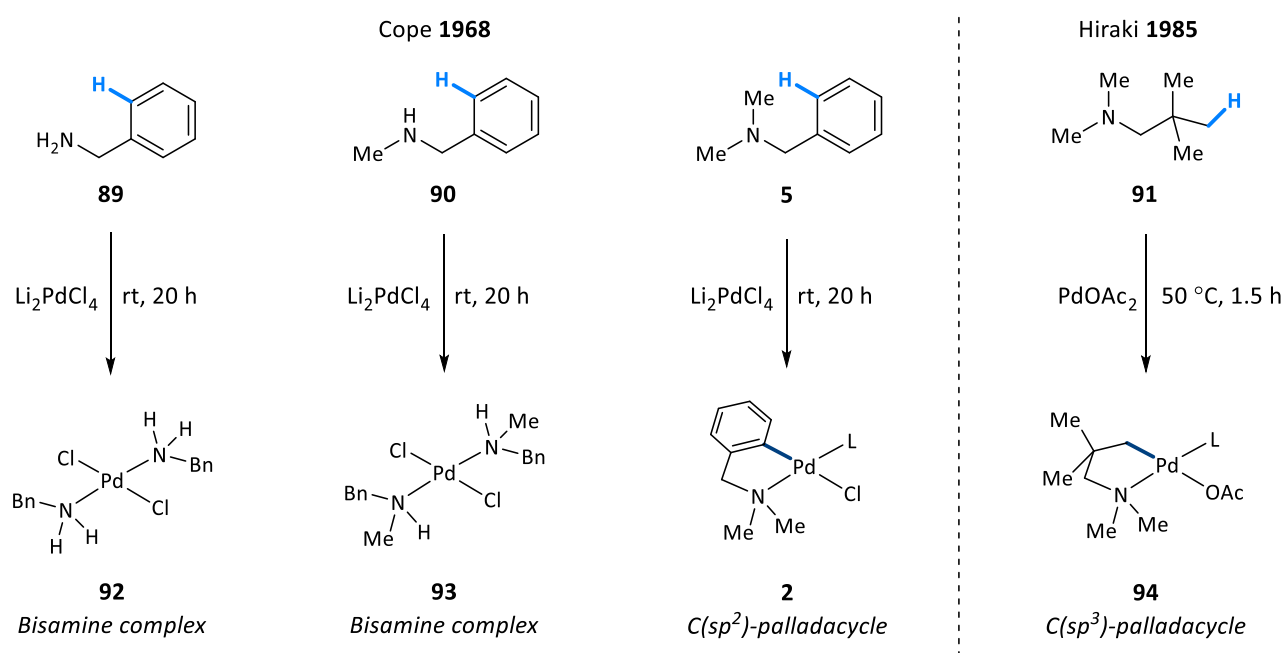
Scheme 16: CO₂ as a transient directing group for the C–H arylation of primary and secondary amines

The transient directing group strategy is a very vibrant area within C–H activation, as has been clearly exemplified by the recent publications discussed. Both C–C and C–X bond forming reactions have been developed targeting C–H bonds in both methyl and methylene positions. Despite these significant advances, the idea of incorporating an engineered directing group, either transient or not, is mainly limited to primary amine substrates, which stimulated the development of new strategies capable of expanding the range of amines susceptible to C(sp³)–H activation processes.

1.4. Native amine-directed palladium catalysis of C–H bonds

In previous sections it has been explained how palladium-catalysed C–H activation reactions can be directed by a nitrogen motif masked in the form of imines, amides, or sulfonamides. This preparative step, either *in situ* or not, prior to C–H cleavage greatly simplifies any transformation as it prevents amine decomposition through β -H elimination processes (note that some transient directing group methods are unable to tolerate α -H to the nitrogen), but perhaps equally important is the introduction of a modular second coordination point which can be tuned and modified to maximise the potential of each individual substrate and transformation. Unfortunately, the nature of those strategies is, most of the time, restricted to primary amine substrates, thus limiting the wider synthetic possibilities of the field.

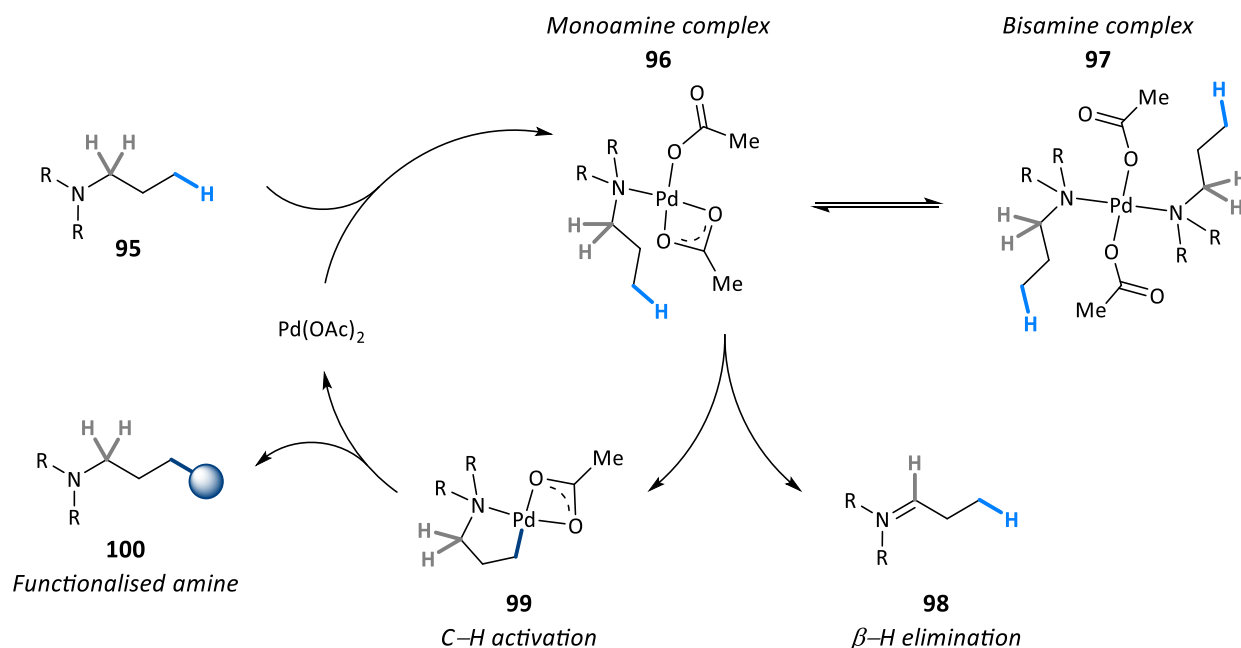
The use of a native directing group within an organic molecule to direct C–H cleavage is one of the long-standing goals in the field of C–H activation, as this straightforward approach avoids unnecessary protection and deprotections, or the use of bespoke organic additives. As early as 1968, Cope reported that amines effectively directed $C(sp^2)$ -H activation (**2**),²⁸ and Hiraki demonstrated that this was even possible in alkyl $C(sp^3)$ -H systems (**94**, Scheme 17).¹⁰⁷ Interestingly, Cope described how C–H activation was only accessible when using tertiary amine substrates (**5**), while primary and secondary amines exclusively afforded bisamine complexes **92** and **93**, respectively.



Scheme 17: First isolated complexes using alkyl amines for palladium-directed C–H activation

This simple observation summarises one of the main challenges of free amine C–H activation. Upon coordination of the amine substrate to the palladium metal centre, an equilibrium is established between its monoamine (**96**) and bisamine complexes (**97**), the latter usually being more energetically stable (Scheme 18).

The high stability of these complexes is further enhanced under catalytic conditions, where an excess of the amine substrate with respect to the transition metal is used. Bisamine complexes cannot generate the required vacant site for C–H activation, thus becoming detrimental off-cycle species. Presumably, the superior steric hindrance of tertiary amines weakens the stability of their bisamine complex, achieving enough population of the desired monoamine complex within the reaction media to enter the catalytic cycle.^{3,108}

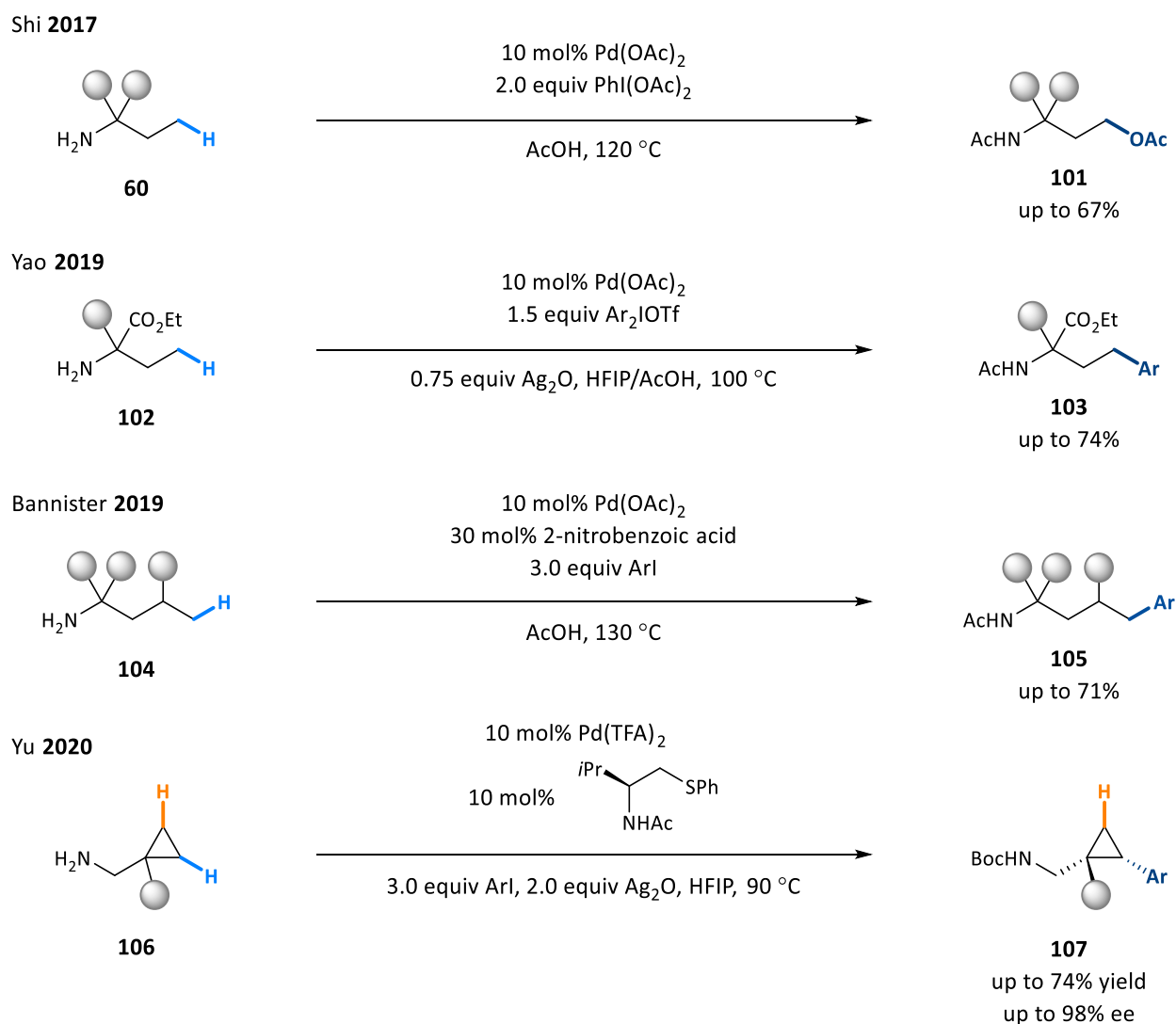


Scheme 18: General catalytic cycle for amine directed C–H activation

The vacant site fundamentally needed in complex **96** to access C–H activation comes along with the second inherent problem of palladium-mediated amine reactions: the propensity of amine substrates to undergo β -H elimination. The palladium metal centre can either abstract an α -H or a γ -H, generating imine **98**, or the desired cyclopalladated product **99**, respectively. Any method attempting the functionalisation of free amines must circumvent these two fundamental issues to deliver any functionalised product.

1.4.1. Primary alkylamines in C(sp³)-H activation

Primary amine substrates display the strongest affinity towards palladium binding and the formation of the monomeric amine complexes required for C-H activation is highly disfavoured. Nevertheless, a few reports have successfully accomplished the functionalisation of aliphatic primary amines without the aid of transient directing groups. A common feature of these reactions is the use of an acidic solvent, key at sequestering free amine from the reaction media, and thus precluding the formation of off-cycle bisamine palladium complexes which would arise under neutral conditions. The first example was developed by Shi, reporting the straightforward acetoxylation of substrate **60** using hypervalent iodine reagents without any further additives (Scheme 19).¹⁰⁹ Unfortunately, the reaction showed moderate yields and poor functional group compatibility, likely due to the acidic media and the strong oxidant needed to access Pd^{IV} intermediates, and no substrates with α -C-H to the amine were tolerated.



Scheme 19: C-H acetoxylation and arylation of primary amines

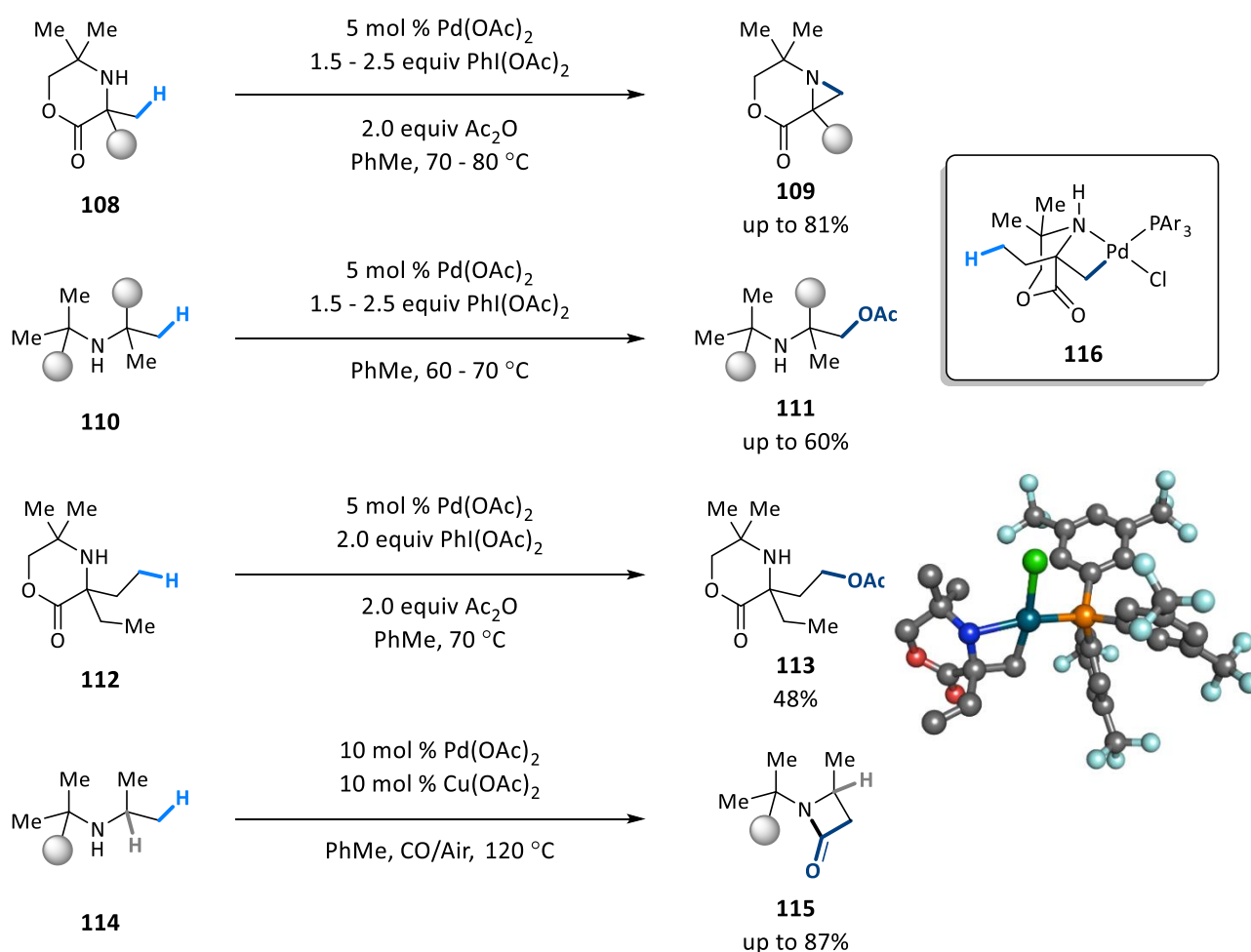
Subsequent publications from the Yao and Bannister group attempted to develop C–H arylation reactions using hypervalent iodine reagents and aryl iodides, respectively. Yao reported the γ -arylation of esterified amino acids lacking α -H (**103**), which was later applied to the functionalisation of *tert*-leucine with no apparent racemisation in the products obtained (not shown).^{110,111} Bannister reported that, when reactivity at γ -C–H bonds is disfavoured by sterics, it is possible to functionalise the more distal δ -C–H bond of an alkyl chain (**105**).¹¹² 2-Nitrobenzoic acid was employed as a sub-stoichiometric additive, but the reaction did perform well without it. Both reactions suffered from the same problems encountered by Shi, affording reactivity on very simple amine substrates with fully substituted α -carbons.

Very recently, the Yu group published another high valent palladium manifold in acidic conditions to arylate primary amines with appendant cyclopropanes (**107**).¹¹³ Interestingly, a chiral β -aminothiol ligand was key to ensure reactivity, but also delivered excellent asymmetric induction. Amine substrates were limited to β -substituted cyclopropanes and only alkyl, aryl or ether functional groups were tolerated within the amine backbone. Noteworthy are the more modest enantioselective values observed when testing different palladium precatalysts, but also silver additives, which opens the path for putative bimetallic intermediates, and raises questions about the real nature of the C–H cleavage step. Other low-valent functionalisations, such as a carbonylation reaction with $\text{Mo}(\text{CO})_6$, or an olefination with a perfluorinated alkene were attempted, but significantly lower yields were obtained.

These reports provide proof of concept that primary amines can also deliver C–H functionalised in the absence of transient directing groups. Nevertheless, the acidic media and the lack of a second binding point which transient directing groups provide to enhance stability and reactivity limits the amine substrates amenable to these transformations.

1.4.2. Secondary alkylamines in C(sp³)-H activation

In 2014, our research group reported the pioneering β -C-H functionalisation of unprotected aliphatic secondary amines without the use of any directing additive apart from the sole amine-nitrogen motif.¹¹⁴ In the first reported transformation, the typical Pd^{II}/Pd^{IV} catalytic cycle was exploited with high-valent iodonium salts as oxidants (Scheme 20). Interestingly, ring-closing C-N reductive elimination was the only observed product when β -methyl substituents are activated in morpholinone substrates (**108**), while TMP derivatives or acyclic amines delivered β -acetylated products (**111**). In line with these results, morpholinone substrates bearing *gem*-diethyl substituents (**112**) yielded the more typical γ -acetylated products (**113**), which was further optimised in a later publication.¹¹⁵ The aziridine products obtained (**109**) were shown to react with a range of nucleophiles, such as chloride, water, or basic heterocycles, among others, to generate complex hindered amine scaffolds.



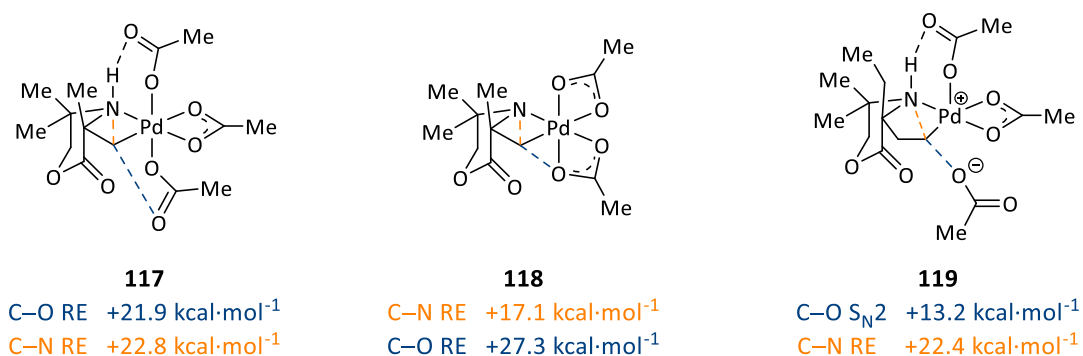
Scheme 20: First C-H activation of aliphatic secondary amines

Further transformations were reported by exploring a more unusual low-valent manifold within C(sp³)-H activation to obtain β -lactam products (**115**) using atmospheric carbon monoxide. In this case, all amine classes, including morpholinones, TMP derivatives, and acyclic amines, delivered the same ring-strained

amide, with no γ -carbonylated products observed. With regards to the reaction conditions used, a catalytic amount of Cu^{II} is required in combination with atmospheric oxygen to oxidise the generated Pd^0 after C–C reductive elimination, thereby closing the catalytic cycle.

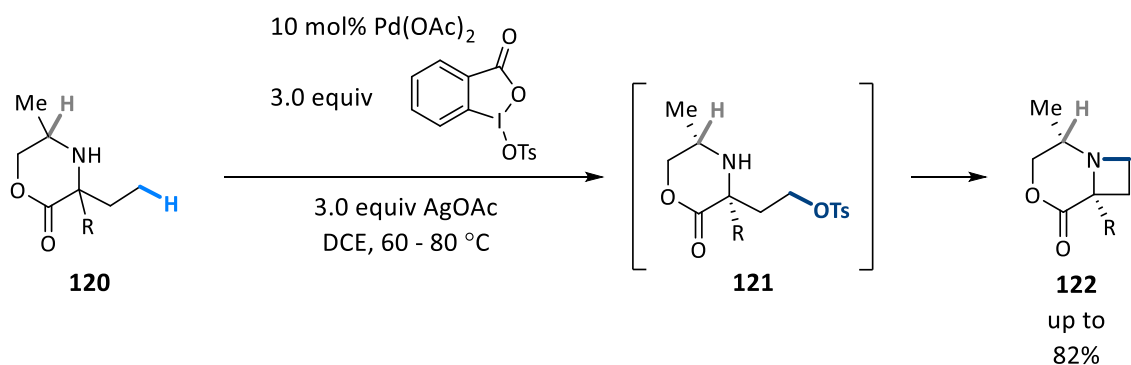
The use of substrates with fully substituted α -carbons to the nitrogen helped in overcoming both of the essential problems of amine-directed C–H activation. This not only disfavours the formation of undesired bisamine complexes by steric hindrance, but also avoids amine decomposition by β -hydride elimination pathways due to the lack of α -C–H bonds. Amine substrates with α -H failed to deliver any functionalised product using high-valent palladium manifolds, due to the likely incompatibility between the iodonium(III) oxidant and the amine substrate. However, the low-valent $\text{Pd}^{\text{II}}/\text{Pd}^0$ catalytic cycle could effectively tolerate up to two α -H, albeit delivering lower reaction yields. Stoichiometric studies exhibited the rare preference of morpholinone substrates to form 4-membered ring over 5-membered ring palladacycles, which led to the isolation of the crystalline palladacycle **116**. A later publication revealed that the addition of 20 equivalents of acetic acid accelerated this transformation, suggesting that amine protonation effectively disfavoured the formation of the off-cycle bisamine complex by exploiting an acid-base equilibria.¹¹⁶

Detailed computational and kinetic studies have been published to understand the capricious selectivity for C–X bond formation.^{115,116} To make the reported energies of Scheme 21 comparable, the energy barriers were normalised taking intermediate **117** as the resting state, being this obtained after oxidation of the 4-membered ring palladacycle with PIDA. Octahedral complex **117** displayed little selectivity between C–N or C–O reductive elimination, being inconsistent with experimental results. C–O reductive elimination followed by nucleophilic attack of the unbounded secondary amine was discarded because β -chloride substituents, a functional group also amenable to nucleophilic displacement, was tolerated in the reported substrate scope. After exploring alternative pathways, DFT calculations determined that a more facile C–N reductive elimination (**118**) is obtained after amine deprotonation in intermediate **117**. On the other hand, 5-membered ring complexes exhibited the lowest reaction barrier for C–O bond formation through the $\text{S}_{\text{N}}2$ attack of one of the acetate ligands (**119**). Unfortunately, acetate-nucleophilic displacement at intermediate **117** was not studied, which might be the lowest energetic pathway for substrates other than morpholinones.



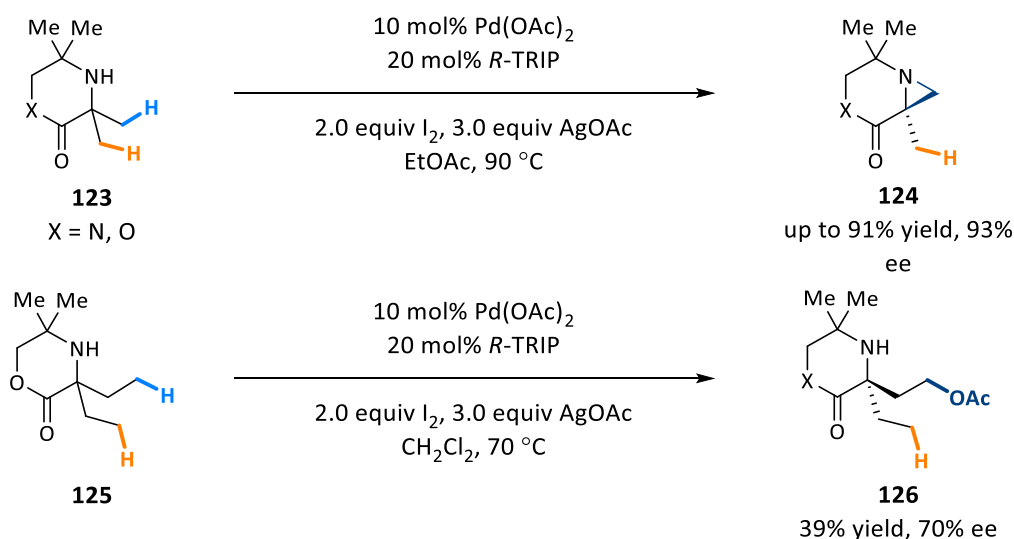
Scheme 21: Computational studies for reductive elimination at Pd^{IV} intermediates

These trends at reductive elimination from Pd^{IV} complexes were exploited to form azetidines products by modifying the iodine(III) oxidant used (Scheme 22).¹¹⁷ The use of a cyclic oxidant with a tosylate group presumably delivered a tosylated amine intermediate (**121**) through the same S_N2-type reactivity, which intramolecularly cyclises upon amine dissociation from palladium to yield the final ring-strained product (**122**). Note that an α -H to the nitrogen was tolerated, even in oxidative reaction conditions.



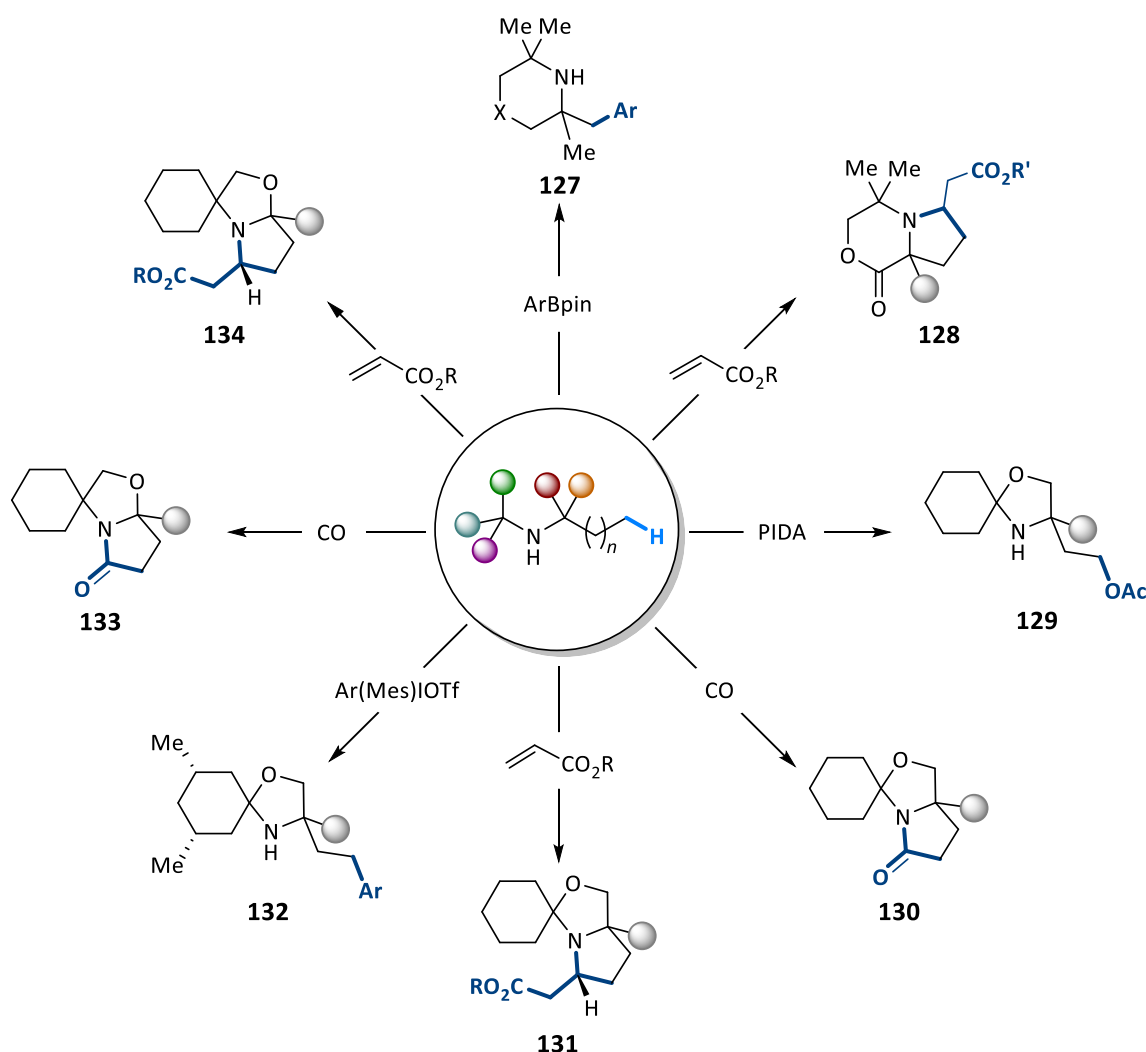
Scheme 22: Synthesis of azetidines via palladium-catalysed C–H tosylation

In the diverse range of reactions described, computational and kinetic experiments determined that C–H activation proceeded through a rate-limiting CMD transition state, based on kinetic isotopic effects (KIE), and C–H cleavage was favoured at the alkyl groups nearest to the carbonyl, presumably due to electronic effects. In an attempt to induce enantioselectivity, it was investigated whether chiral additives could be effectively used as the ligated base needed for proton abstraction. The recurrent BINOL derivatives were employed as phosphate ligands to deliver good to excellent enantioselectivity when used in polar non-protic solvents, and in the absence of acetic acid, which can compete as another base for proton abstraction (**124**, Scheme 23).¹¹⁸ Interestingly, replacement of PIDA with a combination of iodine and AgOAc delivered slightly better yields and enantioselectivities, in particular when developing a desymmetrising acetoxylation reaction.¹¹⁵



Scheme 23: Morpholine-directed enantioselective C–H activation reactions

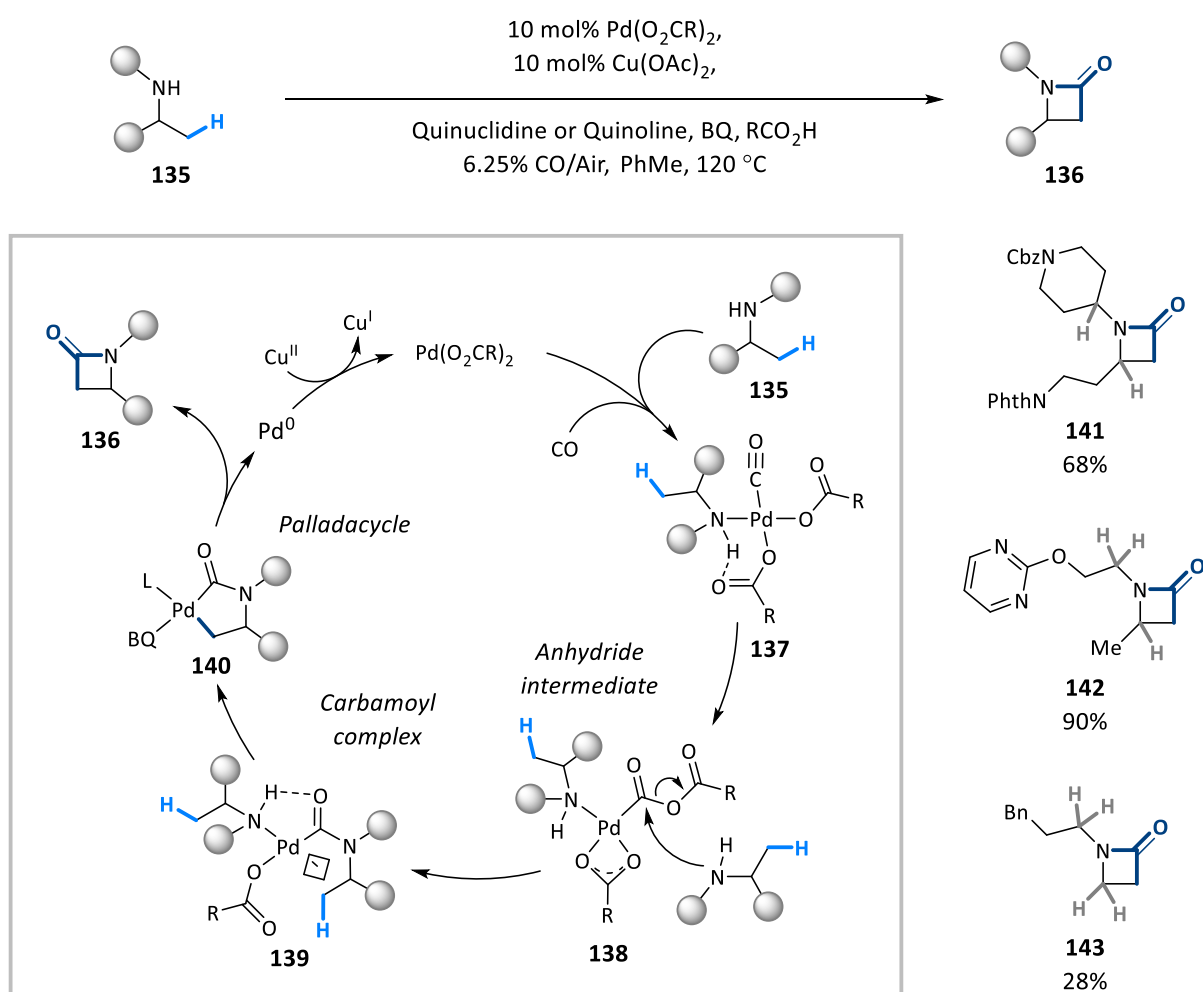
This class of hindered amines have been further utilised in low-valent palladium catalysis to perform arylation¹¹⁹ and alkenylation¹²⁰ reactions, mediated by the use of a mono-protected amino acid ligands (see section 1.5 for a detailed explanation on the use of ligands in palladium-catalysed C–H activation reactions), which surprisingly made C–H cleavage reversible (**127** and **128**, Scheme 24). To expand the class of substrates amenable to this strategy, our research group explored the protection of amino alcohols¹²¹ and keto acids¹²² to construct fully α -substituted secondary amines capable of directing a diverse range of high-valent (acetoxylation (**129**), arylation (**132**)) and low-valent (carbonylation (**130**, **133**), alkenylation (**131**, **134**)), palladium-catalysed reactions.



Scheme 24: Secondary amine-directed C–H activation reactions

Despite proving that aliphatic amines can direct alkyl C–H activation reactions, the need for highly substituted α -carbons greatly limits the applicability of the previously described methodologies. In 2016, our group uncovered a novel mechanistic pathway by which non-sterically hindered secondary amines (**135**) were converted into β -lactams (**136**) through a Pd^{II}/Pd⁰ carbonylation process.¹²³ Scheme 25 illustrates the proposed catalytic cycle, which was supported by computational and stoichiometric studies. The strong σ -donating

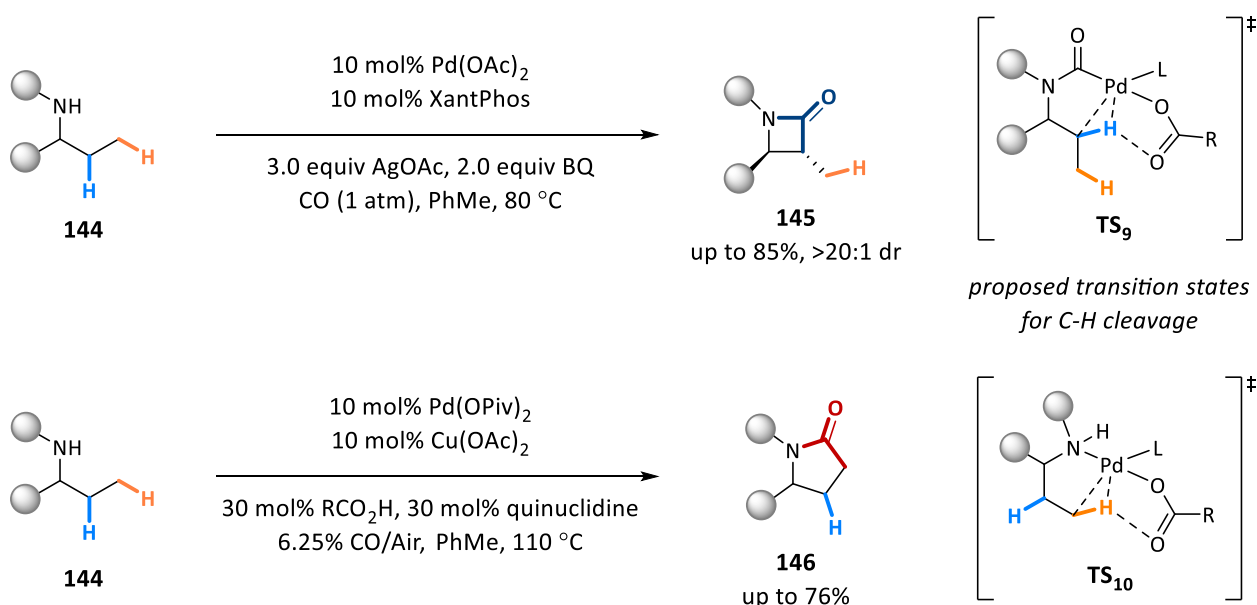
coordination of carbon monoxide to palladium competes with amine binding, making monoamine complex **137** with a bound carbon monoxide unit just slightly higher in energy than the resting-state bisamine complex (not shown for clarity). From monoamine complex **137**, the coordination of a second amine substrate triggers the rearrangement of a carboxylate ligand to form the putative anhydride intermediate **138**.¹²⁴ Amine dissociation favoured by a κ^2 -carboxylate binding prompted a nucleophilic amine attack to the carbonyl closer to the metal centre, forming carbamoyl complex **139**. Unproductive nucleophilic attack to the other anhydride carbonyl is disfavoured by the use of bulky carboxylate ligands. From here, an unusual β -C–H activation can occur through the typically preferred 6-membered ring CMD transition state to generate a 5-membered ring palladacycle intermediate (**140**). A benzoquinone additive aided the final C–C reductive elimination event to generate the desired β -lactam products (**136**). To close the catalytic cycle, a catalytic amount of $\text{Cu}(\text{OAc})_2$ is needed to oxidise the generated Pd^0 . An extensive substrate scope of amines possessing multiple α -C–H to nitrogen was reported, and only the simplest amine substrates consisting of two linear alkyl chains (**143**) displayed poor reactivity, likely due to the high stability of their resultant bisamine complexes.



Scheme 25: β -Carbonylation of non-hindered aliphatic amines

The reaction possessed interesting details worth of further discussion. The fact that C–H activation occurred through carbamoyl complex **139** implies that palladium cannot abstract an α -H to the nitrogen to undergo β -H elimination, even when the vacant site needed for C–H cleavage is available. Presumably, the strong coordination of carbon monoxide disfavours the formation of vacant sites before the formation of intermediate **139**, which avoids amine decomposition. The typically more reactive γ -methyl substituents were completely inert, thus indicating that the more classical N–Pd palladacycle is inaccessible under the reaction conditions. The reaction exhibited a reversible C–H activation, based on proton/deuterium scrambling, with a KIE value of 1.1, suggesting that other transition states rather than C–H cleavage are rate-limiting. In fact, the reported DFT calculations suggested that the rate-limiting step of this catalytic cycle occurred in the amine nucleophilic attack to anhydride **138** to generate the key carbamoyl intermediate for β -C–H activation. This evidence also disproves the direct formation of a 4-membered ring palladacycle before carbon monoxide insertion, which is observed computationally to possess a very high energetic barrier.

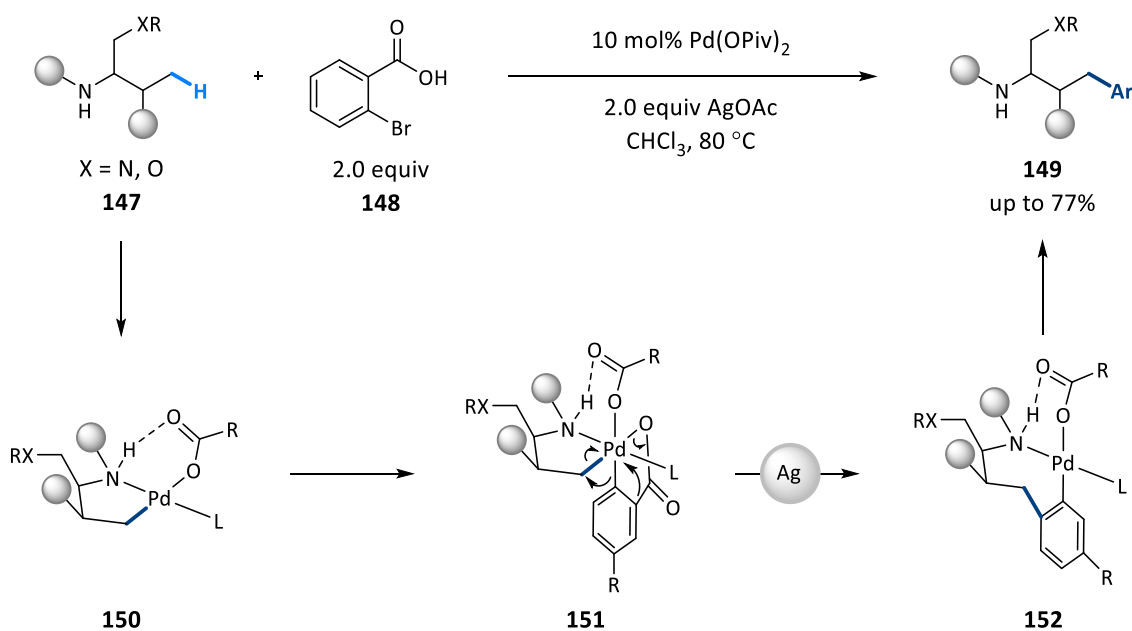
In subsequent publications, the carbonylation platform was further optimised to target methylene C–H bonds in good yields and diastereoselectivities by using a key XantPhos ligand in combination with silver(I) additives (**145**, Scheme 26).¹²⁵ Once again, only β -H, rather than γ -H, delivered the expected lactam products, strongly suggesting the formation of a carbamoyl intermediate, capable of accessing C–H cleavage through the preferred 6-membered ring transition state (**TS₉**). The use of secondary amines with a fully substituted α -carbon delivered an unusual selectivity for methylene C–H cleavage over other typically more preferred positions, such as methyl or even aryl C(sp²)-H bonds.⁴⁰



Scheme 26: Site selective carbonylation of aliphatic secondary amines

A third set of reaction conditions was later reported to this time target γ -methyl C–H activation (**146**, Scheme 26).¹²⁶ The optimisation process resulted in the removal of bulky carboxylic acids and benzoquinone additives essential for β -methyl C–H activation, while finding that electron-deficient benzoic acids favoured the formation of γ -lactam products (**146**) over the previously obtained ring-strained β -amides (**145**). Equally important is to use a non-saturated atmosphere of carbon monoxide. Stoichiometric studies elucidated a switch in the reaction mechanism, as a high concentration of carbon monoxide within the reaction media precludes direct amine binding to palladium, needed for γ -C–H activation (note the difference between **TS₉** and **TS₁₀**).

In an attempt to develop alternative functionalisations tolerant with amines containing α -C–H bonds, our group explored the feasibility of 2-halobenzoic acids (**148**) as viable coupling partners for arylation reactions (Scheme 27).¹²⁷ Extensive stoichiometric studies demonstrated that these novel reagents can react with the palladacycles obtained after C–H cleavage (**150**) to generate C(sp²)-7-membered ring intermediates (**152**). The aryl substitution pattern on the resultant arylated products (**149**) determined that C–C bond formation occurred at the halogenated aryl position, while the carboxylate moiety underwent a concerted decarboxylation-reductive elimination step enabled by a once again non-innocent silver(I) additive. Upon proto-demetalation, an arylated amine product is obtained with none of the 1,2-halocarboxylic acid functionalities, making the carboxylate motif a traceless directing group to aid oxidative addition. Remarkably, stoichiometric studies proved that this assisted oxidative addition could be achieved at room temperature, while the more traditional aryl iodides were unreactive. Unfortunately, the reported amine scope was quite narrow, as reactivity was only observed in γ -C–H bonds with a very precise substitution pattern along the reactive carbon backbone.

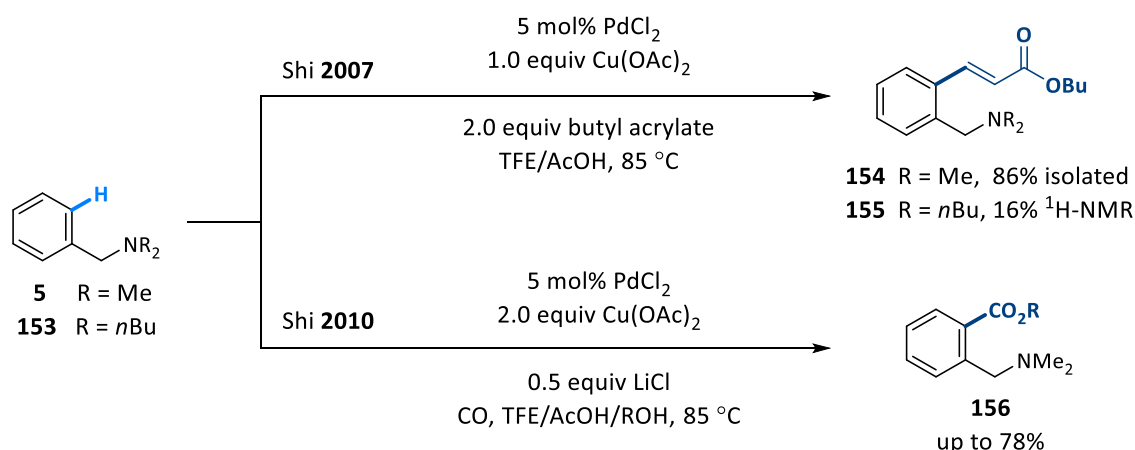


Scheme 27: Carboxylate-directed γ -arylation of less hindered secondary amines

1.4.3. Benzylic tertiary amines in C(sp²)–H activation

At the beginning of the present section, it was illustrated how tertiary amines inherently disfavour the formation of off-cycle bisamine complexes, thus accessing C–H cleavage with more ease (see Scheme 17). Despite this, the development of a catalytic C(sp³)–H functionalisation reaction using these amines as substrates has been elusive. Tertiary amine additives have been historically used in cross-coupling reactions as sacrificial oxidants to reduce a Pd^{II} pre-catalyst to the desired Pd⁰ active species.¹²⁸ The propensity of alkyl amines for oxidative decomposition, likely by β–H elimination pathways, have precluded their use in alkyl C–H activation reactions.¹²⁹ In fact, their decomposition has recently been exploited to synthesize aryl ketones,¹³⁰ functionalised pyrazoles,¹³¹ or aryl amides.¹³² Nevertheless, remarkable success has been found in activating more facile C(sp²)–H bonds.

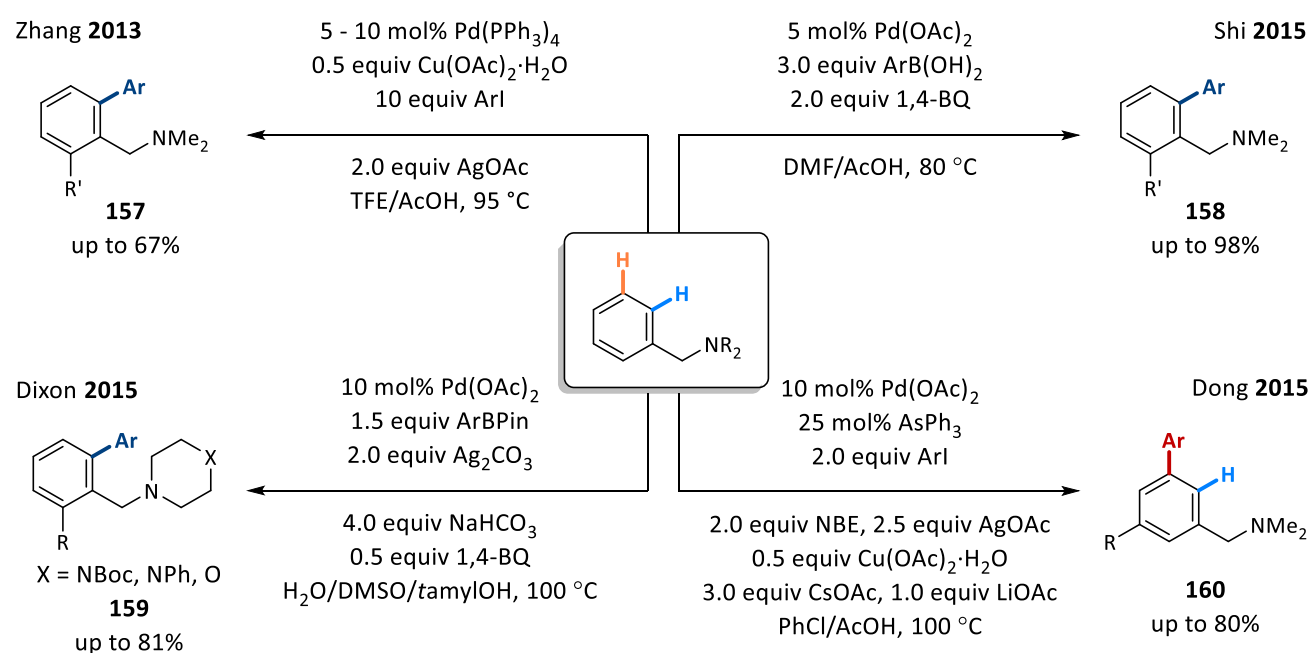
In 2007, Shi and co-workers reported the olefination of *ortho*-aromatic C–H bonds in benzylamine substrates through an oxidative Heck coupling with acrylates and acrylamides in good yields (Scheme 28).¹³³ The reported substrate scope exhibited sharp contrasts, as a diverse range of functional groups, both electron-donating and electron-withdrawing were tolerated in the amine aryl ring, while the amine core, key in directing palladation, only delivered good reactivity when having two methyl substituents (compare **154** and **155**). As previously reported by others,²⁸ it was observed that no secondary or primary amine derivatives delivered any reactivity. The same group also accomplished the introduction of ester functionalities by using carbon monoxide in combination with nucleophilic alcohols (**156**).¹³⁴ This time, the reaction suffered from low yields when carbonylation was attempted on electron-poor aryl rings. Both transformations exploited low-valent catalytic manifolds which do not require strong oxidants typically incompatible with the amine substrate. Lastly, the recurrent silver(I) additives were not needed in these transformations as copper and oxygen could efficiently oxidise the resultant Pd⁰ to close the catalytic cycle.



Scheme 28: Seminal tertiary amine-directed palladium-catalysed C(sp²)–H activation reactions

Unarguably, the most exploited transformation in these amine substrates is the formation of biaryl systems through a C(sp²)–C(sp²) bond forming arylation reaction (Scheme 29). Aryl iodides¹³⁵ and aryl boron

reagents^{136,137} were shown to be viable coupling partners in both high-valent and low-valent catalytic manifolds, respectively. As previously observed by Shi, electron-poor aromatic rings displayed lower reaction yields in all these reactions, due to the less electron-rich C–H bond. Double *ortho*-arylated products were commonly observed, with monofunctionalised products only being isolated in biased starting materials with 1,2- or 1,3- substitution patterns. Among all three reported reactions, Shi's delivered the highest reaction yields, used ubiquitous aryl boronic acids and provided the cheapest and most environmentally friendly reaction conditions, as no other metal additives were needed to oxidise Pd⁰. The Shi group also noted that diminished yields were obtained at longer reaction times, indicative of the reactive nature of tertiary amines towards oxidative decomposition when using transition metals.



Scheme 29: Tertiary amine-directed C(sp²)-H arylation reactions

To access a more unusual *meta*-C–H arylation, the Dong group exploited norbornene-mediated catalysis to form biaryl systems using aryl iodides as coupling partners (**160**).¹³⁸ The addition of multiple additives, including high silver loadings and the catalytic amount of an arsenate ligand, is required for high reaction yields. Interestingly, a α -methyl to the nitrogen in the benzylic methylene unit was successfully tolerated, obtaining a 64% yield of mono- and diarylated products; and arylation was successfully reported in heterocyclic pyridine and pyrrole amine substrates. As observed for *ortho*-functionalisation reactions, diarylated products were mainly obtained when both *meta*-C–H bonds were accessible, and only aryl iodides with *ortho*-EWG groups, such as esters, amides, or nitro functionalities delivered the desired reactivity. It was hypothesised that the presence of electron-withdrawing groups could accelerate oxidative addition of the aryl iodide through a combined electronic and weakly-directing effect.

1.5. Ligands in palladium-catalysed C(sp³)–H activation reactions

The last decade has seen the discovery and development of multiple ligands capable of dramatically enhancing C–H activation reactions. Most of these ligands enabled C–H activation in substrates displaying very electron-deficient directing functional groups, such as perfluorinated arylamides,^{15,16,139,140} triflyl-protected amides,⁸⁶ or free carboxylic acids,^{141,142} among others.^{17,113} Nevertheless, these ligands not only enabled reactivity, but also exploited their chirality to deliver enantioenriched C–H functionalised products. Detailed analysis of each of these ligands is out of the scope of this introduction, and this section will mainly focus on the discovery and reactivity of mono-protected amino acid (MPAA) ligands.¹⁴³

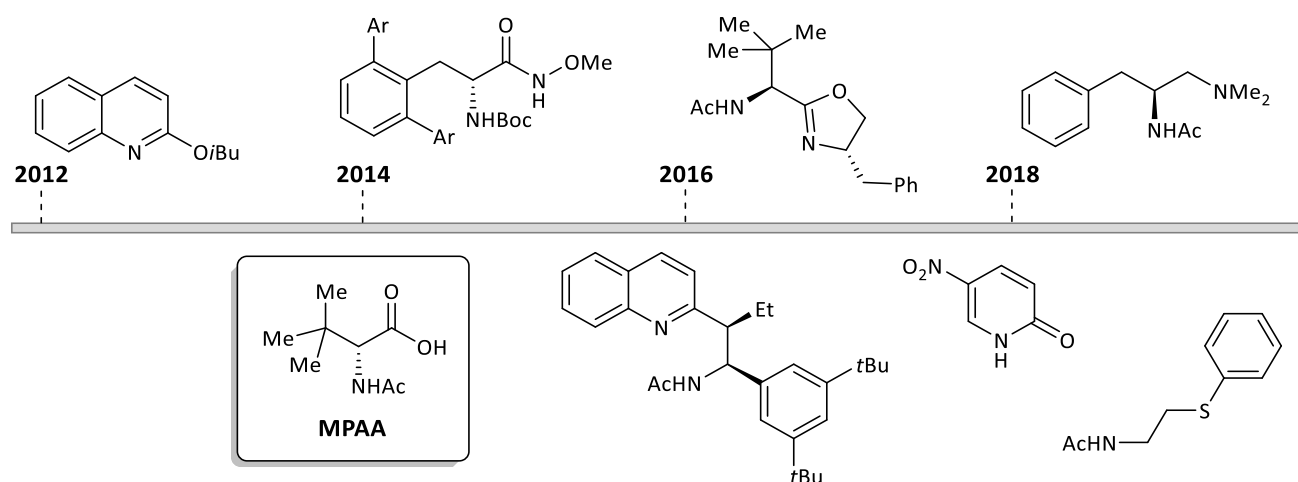
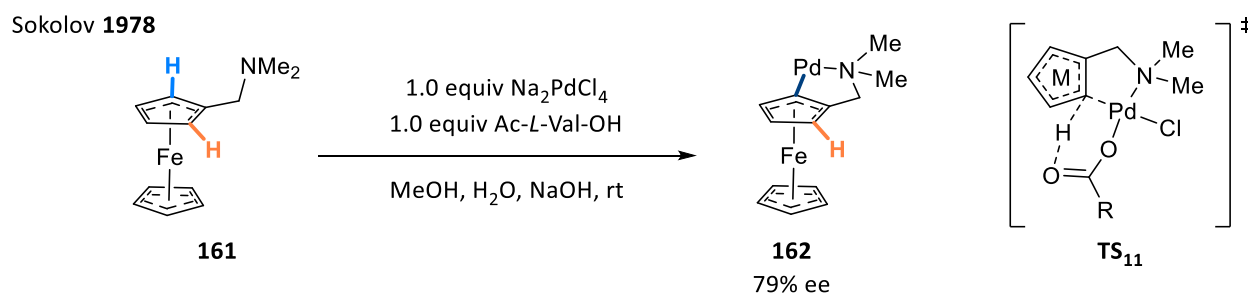


Figure 1: Ligands in palladium-catalysed C(sp³)–H activation reaction

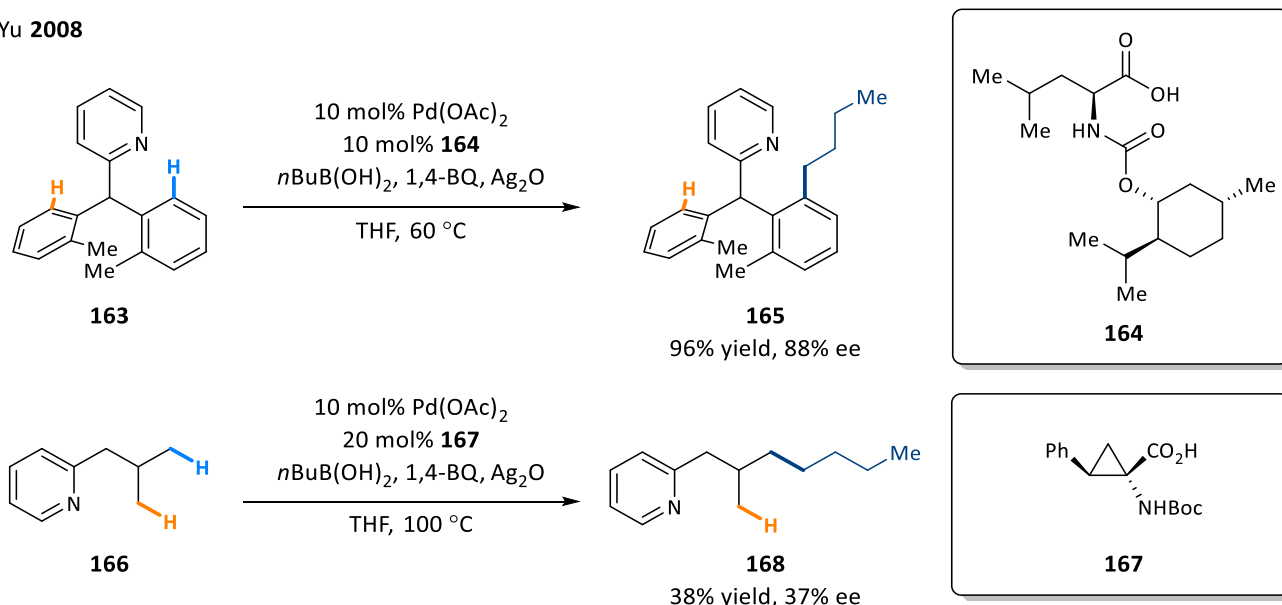
The first use of MPAA ligands in palladium C–H activation was reported by Sokolov in 1978 when performing an asymmetric C(sp²)–H activation of ferrocene **161** (Scheme 30).^{144,145} Based on previous findings,¹⁴⁶ it was thought that the carboxylate ions were involved in the C–H activation transition state, leading to the hypothesis that asymmetric palladacycles could be generated in an enantioselective manner by using optically active carboxylate salts. Although little enantioselectivity was observed when using α -hydroxy acids, *N*-acetyl-*S*-valine generated palladacycle **162** in a notable 79% ee. Sokolov proposed a CMD transition state where the carboxylate acts as the hydrogen abstractor while coordinated to the palladium centre (**TS₁₁**).



Scheme 30: Asymmetric cyclopalladation of (dimethylaminomethyl)ferrocene

Despite this early precedent, it was not until 2008 when Yu and co-workers utilised MPAA ligands to catalytically desymmetrise pyridine **163**.¹⁴⁷ The same reaction was applied to C(sp³)–H bonds but poor yields and low enantioselectivities were observed (**168**). Since then, other substrates, such as carboxylic acids,^{148,149} and protected amines,^{150,151} have found remarkable success at directing the desymmetrisation of C(sp²)–H bonds through both high- and low-valent palladium manifolds. Moreover, the excellent chiral relay of these ligands has even been successfully applied in the development of kinetic resolution reactions.^{152,153} Computational investigations have proposed that, depending on the nature of the substrate, enantioselectivity is induced by exploiting detrimental substrate-ligand interactions, or the conformational restrictions of the substrate.^{154,155}

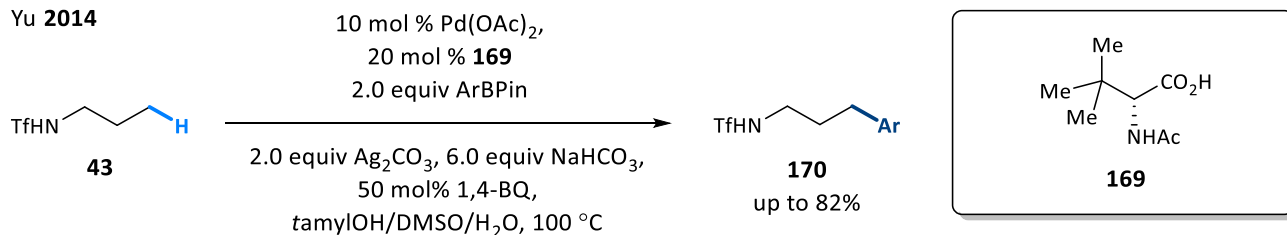
Yu 2008



Scheme 31: Enantioselective C–H activation of pyridine substrates

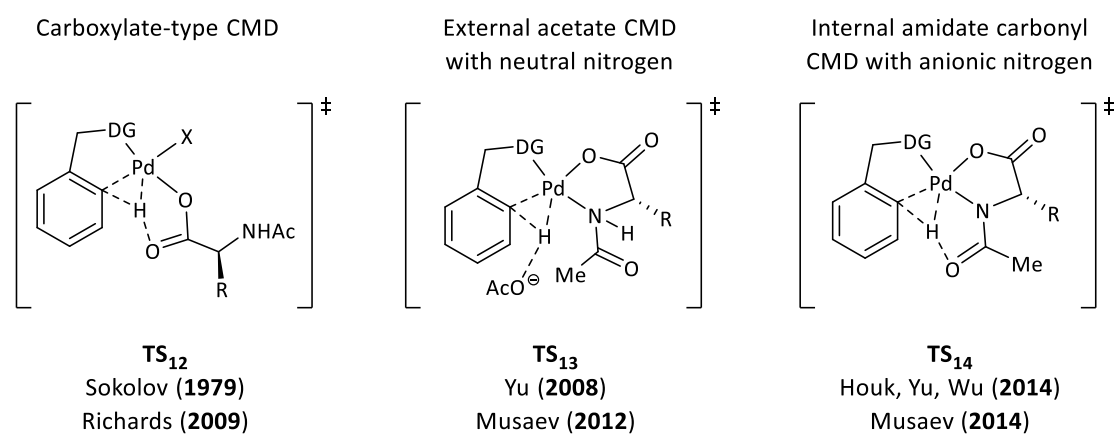
In 2014, Yu and co-workers reported a major breakthrough with these ligands being successfully involved in the catalytic γ -arylation of C(sp³)–H bonds in triflyl-protected amines (**43**, Scheme 32).⁸⁶ The *N*-acetyl protecting group of the ligand proved to be essential, as other protecting groups (Boc-, Fmoc-, Cbz-) delivered product **170** in significantly lower yields. No product formation was observed in the absence of ligand, evidencing that, rather than just a source of chirality, MPAA ligands can be used to enhance reactivity in alkyl C–H activation reactions.

Yu 2014



Scheme 32: First C(sp³)–H arylation on triflyl amides enabled by MPAA ligands

This finding triggered the detailed study of how MPAA ligands perform C–H bond cleavage. Although different models have been proposed over the last decade,^{145,147,154,156} the generally accepted hypothesis, supported by computational studies, relies on the bidentate ability of MPAA ligands to coordinate to palladium in a κ^2 -(N,O) coordination mode (**TS**₁₄, Scheme 33).^{155,157,158} Deprotonation of the *N*-protected amide triggers C–H activation through an inner-sphere CMD transition state, where the carbonyl of the *N*-protecting group acts as the internal base. The facile deprotonation of the amide when coordinated to palladium generates an inner-sphere strong base, accelerating C–H cleavage when compared with a weaker acetate anion. Nevertheless, the actual catalytic nature of these palladium complexes is still a subject of debate, as NMR and kinetic studies have suggested the formation in solution of dimeric palladacycles from where functionalisation favourably takes place.¹⁵⁹

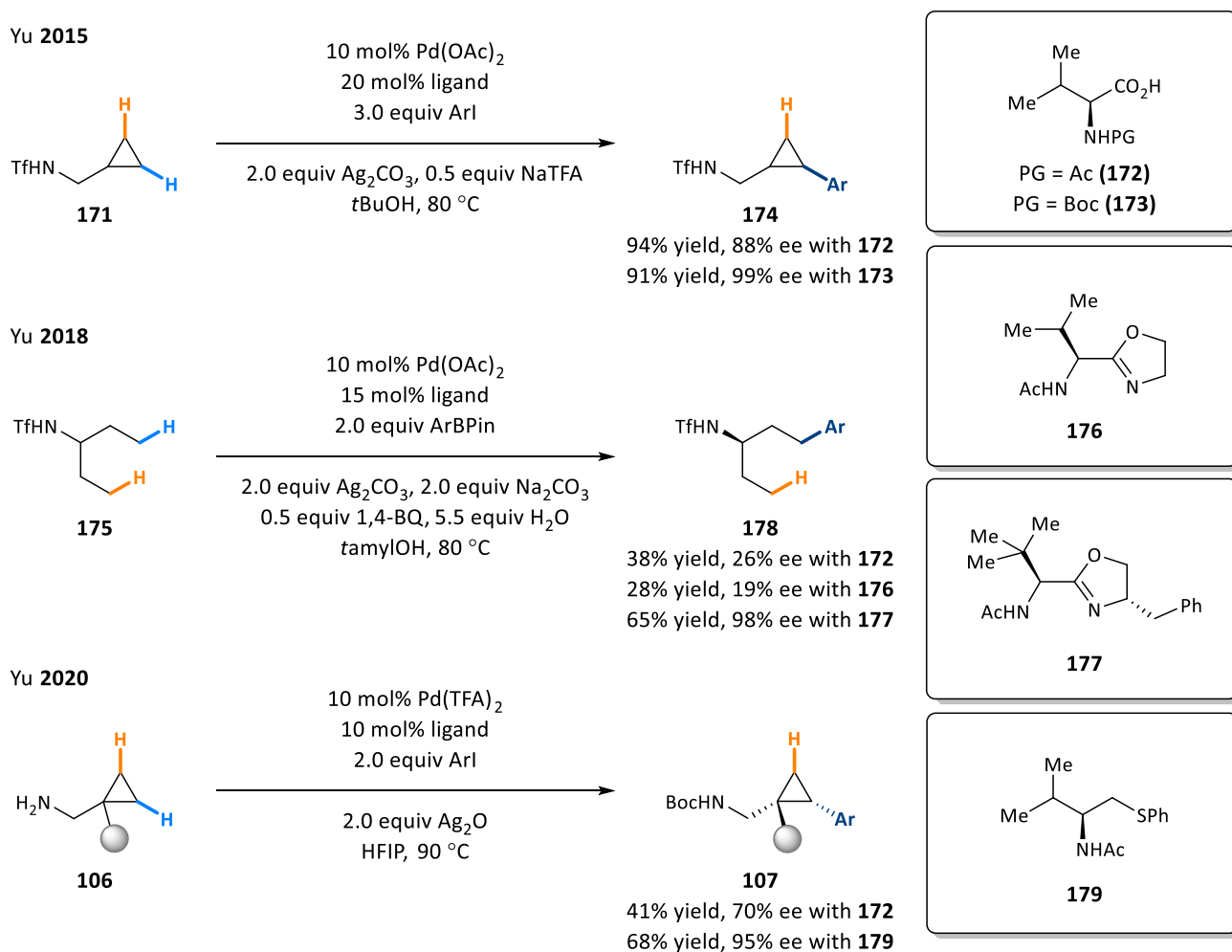


Scheme 33: Proposed mechanisms for C–H cleavage involving mono-protected amino acid ligands

These computational findings rationalised why ligands containing acetamide moieties can enhance C(sp³)–H activation reactions, thus becoming common features in all ligand classes (see Figure 1). On the other hand, the anionic carboxylate unit of MPAA ligands is a tuneable handle which can be transformed into oxazolines,¹⁶ amines,¹⁴¹ or thiols,¹⁴² among others,¹⁵ to match the coordinating properties of substrate and ligand to the palladium centre, thus maximising catalytic efficiency and asymmetric induction.

Following the success of triflyl-protected amines with MPAA ligands, the Yu group explored the enantioselective C–H activation of cyclopropane units (Scheme 34). Directed by the *N*-protected motif, the nature of the bicyclic palladacycle intermediate led to exclusive *cis* arylated products, while functionalisation was this time achieved with aryl iodides via a high-valent palladium manifold (**174**).⁸⁷ The ligand protecting group had little influence in reactivity, and higher enantioselective values were obtained with the less common *-Boc* protecting group (**173**). Interestingly, no reactivity was observed in the absence of silver. While its role can be at first attributed as being a halide scavenger, it arises questions about its putative role during C–H cleavage. The desymmetrisation of more flexible alkyl chains proved to be challenging, and poor asymmetric induction was obtained when using acetyl-ligand **172** with the prochiral protected amine **175**.¹⁶⁰ Taking

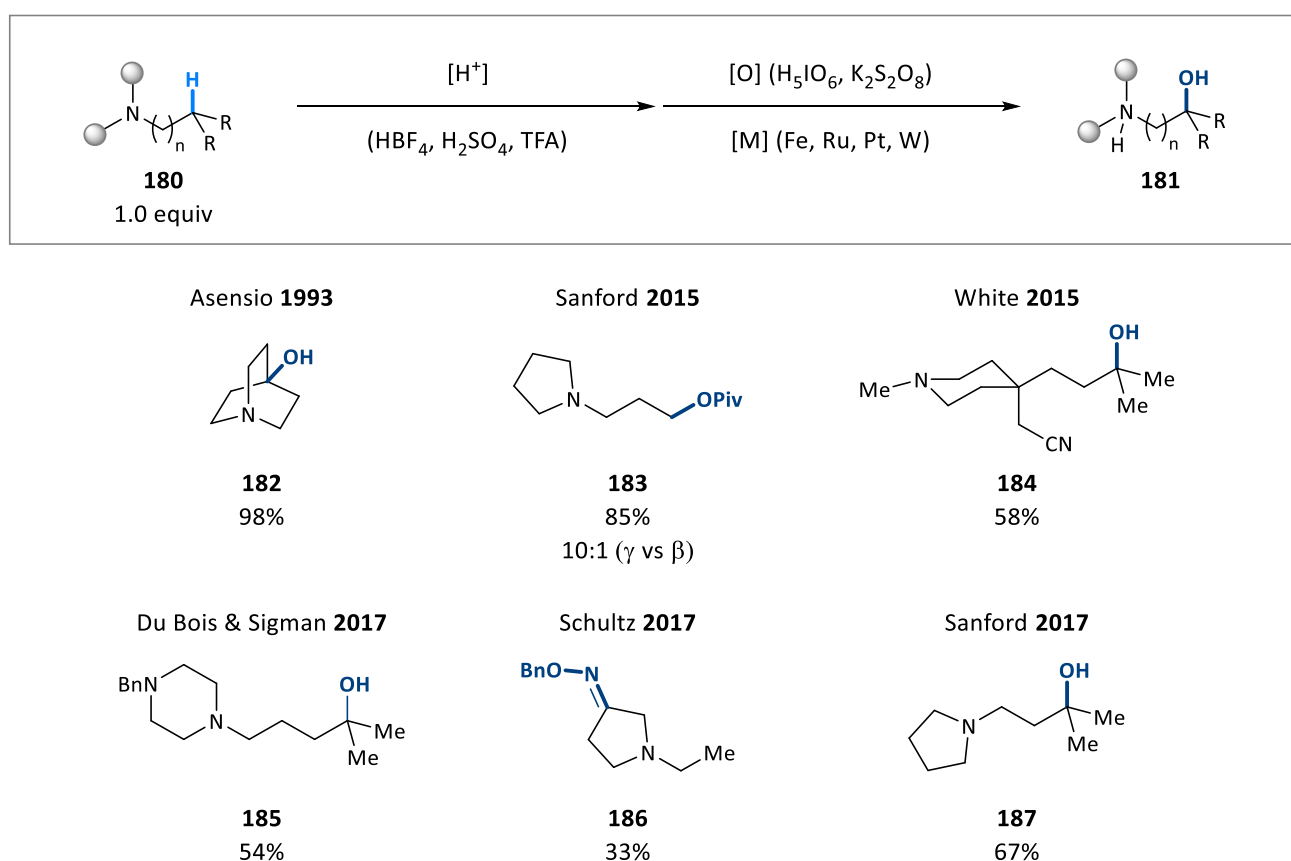
advantage of the previously discovered oxazoline ligands,¹⁶ which possess two modular chiral centres, it was possible to further optimise this transformation to afford an excellent enantioselectivity with moderate yields (**178**). The recently discovered desymmetrisation of unprotected primary amines has been previously discussed in section 1.4.1. Nevertheless, this reaction has been reincluded here to illustrate how MPAA ligand **172** only afforded moderate yields and enantioenrichment of arylated amine **107**.¹¹³ This time, transformation of the ligand carboxylic acid handle into a thiophenol functionality delivered a better reactivity and enantioselectivity. More modest enantioselective values were observed when testing different palladium precatalysts, but also silver additives, which opens once again the path for putative bimetallic intermediates, and raises questions about the real nature of the C–H cleavage step. Other low-valent functionalisations, such as a carbonylation reaction with Mo(CO)₆, or an olefination with a perfluorinated alkene were attempted, but significantly lower yields were obtained.



Scheme 34: Enantioselective C(sp³)–H activation reactions of primary amines

1.6. Alternative C(sp³)–H functionalisation strategies for aliphatic tertiary amines

Previous sections have established the advances and current limitations of performing palladium-catalysed C(sp³)–H activation reactions, with particular emphasis on the amine-directed approach. Taking into account the topic of the present PhD thesis, it is also worth considering what other strategies have been developed to functionalise aliphatic C–H bonds in molecules containing tertiary amines. The most straightforward approach, developed in the 90s, relied on strong oxidants, either as a metal catalyst or an inorganic salt, to cleave the most accessible or most reactive C–H bond to access a range of oxygenated products (**181**, Scheme 35).^{161–166} To avoid oxidation of the amine functionality, acidic conditions were needed to mask the amine lone pair, which also disfavoured reactivity at the closest α - and β -C–H bonds.

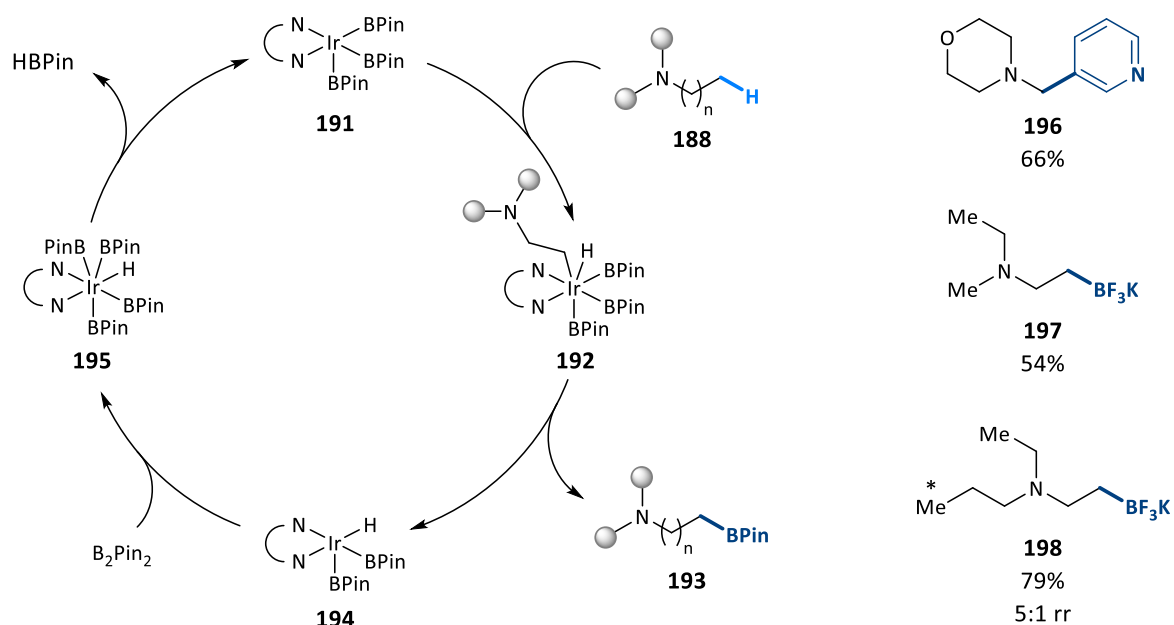
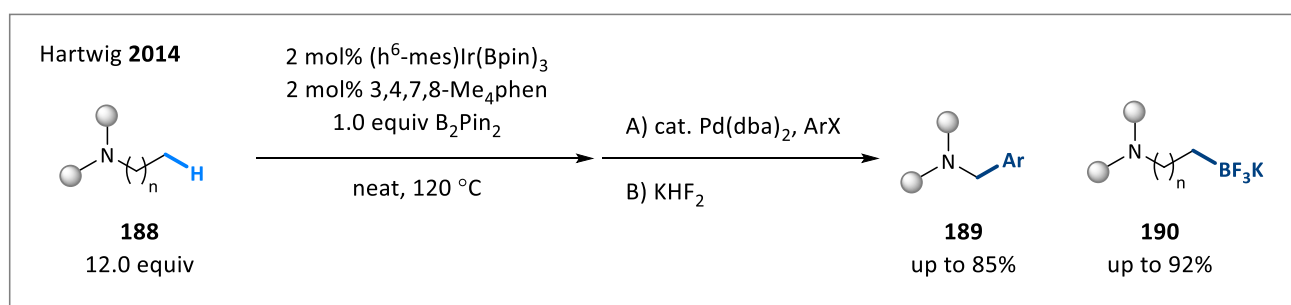


Scheme 35: Amine-masked C(sp³)–H functionalisation of aliphatic tertiary amines

Unfortunately, this strategy implies a few clear limitations. Firstly, the aqueous media and the nature of the oxidants has restricted functionalisation to oxygenated products only; being ketones if a methylene position is functionalised, or an alcohol, if the reactive site is a methine or methyl unit. Secondly, the reported substrate scope is significantly narrow as many functional groups are incompatible with the harsh oxidants and strong acidic conditions. Lastly, the lack of amine coordination in these systems generates little selectivity when two or more similar C–H bonds are present in the molecule, which can result in complex product mixtures and difficult isolation processes. Nevertheless, these methods can be applied to all amine classes,

not only tertiary alkylamines, providing an opportunity to rapidly functionalise alternative C–H bonds which are further away than the typically targeted γ -C–H bond of palladium catalysis.

A second more elaborated strategy was developed by Hartwig using reductive borylation conditions with rhodium,¹⁹ ruthenium,²⁰ and iridium²³ (Scheme 36). The reaction does not involve coordination of the nitrogen lone pair to the metal centre, and reactivity is driven by sterics. Therefore, functionalisation is not only possible in alkylamines, but also in ethers and simple alkanes. The transition metal ligated to phenanthroline is surrounded by boronate ligands except for an empty vacant site which undergoes oxidative addition into the most accessible C–H bond of the substrate (**191**), hence the exclusive selectivity for methyl C–H bonds. Reductive elimination from this intermediate readily generates the functionalised borylated amine **193**. To close the catalytic cycle, B_2Pin_2 regenerates the active catalyst by eliminating HBPIn from the iridium hydride complex **194**.



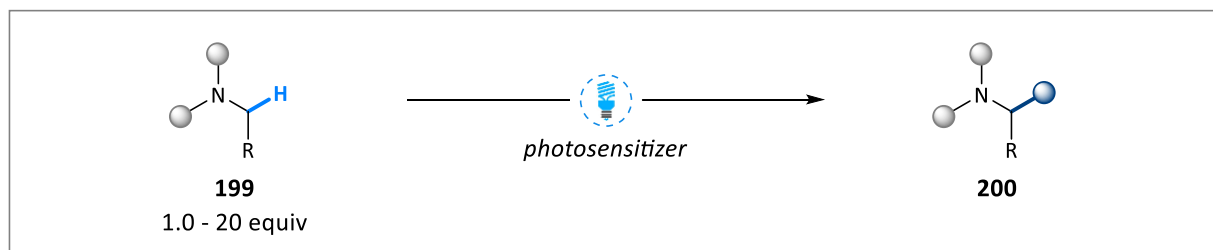
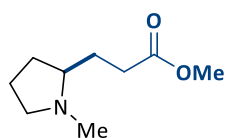
Scheme 36: Iridium-catalysed borylation of tertiary amines at methyl C–H bonds

A detailed mechanistic study of the iridium-catalysed borylation reaction displayed a preferential selectivity in competition experiments for β -methyl functionalisation. Computational studies on the transition

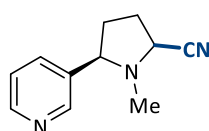
state elucidated that a weak Lewis acid-base interaction occurs between the nitrogen substrate motif and the boron coordinated ligand which preferentially places a β -methyl C–H bond in close proximity for oxidative addition. Nevertheless, borylation in α -, β -, γ -, and δ -methyls were all possible, and the obtained borylated products were shown either to undergo *in situ* cross-coupling reactivity (**196**), or to be isolated in the form of trifluoroborate salts (**197–198**). Unfortunately, the reported substrate scope is limited to the simplest alkyl amines with no appendant functional groups, as they are needed in a large excess and at high temperatures presumably to avoid polyfunctionalised products.

A third, and last approach, relies on exploiting the electron-rich nature of tertiary amines to undergo oxidation via radical pathways to furnish α -functionalised products (**200**, Scheme 37).^{167–176} When photosensitisers are introduced in the reaction, these can absorb a photon upon light irradiation, exciting them to an energetic state from where abstraction of an electron from the amine lone pair is possible. The generated amine radical cation typically reacts through an α -amino radical with electrophilic species, or it is further oxidised to an imine intermediate to react with nucleophiles. Nevertheless, each individual reaction may occur through alternative reaction mechanisms, in particular when exploiting photoredox catalytic cycles with iridium or ruthenium complexes. One of the main challenges of this approach is to achieve site selectivity by distinguishing between the three alkyl substituents of the amine substrate. Scheme 37 illustrates how some methods have found remarkable regioselectivity at functionalising heterocycles or methyl substituents depending on the reaction conditions used, offering complementary and orthogonal reactivity. Nevertheless, the amine substrate is typically used in excess to achieve monofunctionalised products.

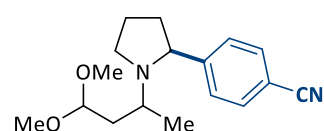
The three aforementioned strategies offer complementary reactivity to forge C–O, C–B, or C–C bonds at different positions of the amine backbone. Acid-mediated oxidation and metal-catalysed borylation processes offer reactivity at multiple C–H bonds of the amine substrate, although the functional group compatibility has been to date very limited. On the other hand, photo-mediated reactions have succeeded in offering a wide range of C–C bond forming reactions to forge more complex amine structures. However, the challenge of distinguishing between three different alkyl backbones limits the applicability of this strategy to simple amine coupling partners. Taken together, the functionalisation of tertiary alkylamines is an underdeveloped area of research which is in need of milder reaction conditions and lower amine loadings in order to expand its functional group compatibility and to use more elaborated amine substrates.

Pete **2000****201**

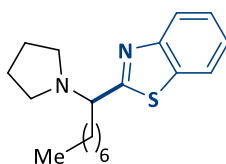
87%

Tan **2011****202**

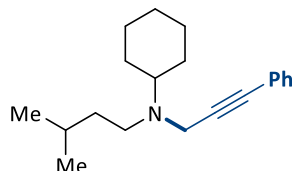
85%

MacMillan **2011****203**

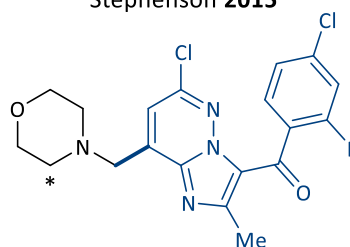
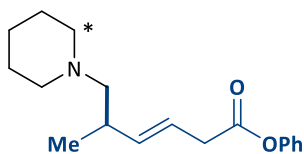
78%

Weaver **2013****204**

92%

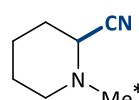
Hashmi **2015****205**

78%

Stephenson **2015****206**56%
>10:1 rrRovis **2017****207**

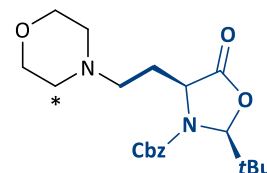
62%

2.5:1 rr

Oderinde & Emmert **2018****208**

85%

4:1 rr

Jui **2018****209**

82%

1:1 rr

Scheme 37: α -Functionalisation of aliphatic tertiary amines through radical pathways

1.7. Summary and outlook

Over the last 15 years, palladium-catalysed C(sp³)–H activation has established itself as a young and vibrant area of research, receiving considerable attention from the synthetic chemistry community. It started with the development of biased directing groups with an extreme binding affinity for palladium, which afforded robust catalytic cycles, in particular through Pd^{II}/Pd^{IV} manifolds aided by the enhanced stability of the resultant Pd^{IV} octahedral intermediates.^{66,67} It was soon noticed that these directing scaffolds afforded little synthetic applicability because of the harsh reactions conditions required in liberating the functionalised product from them.^{68–71} Therefore, multiple research groups attempted to find alternative directing groups with milder or orthogonal deprotection conditions, while delivering other C–C or C–X bond forming reactions.^{39,84–91} More recently, much more appealing methods have disclosed the use of native functional groups to direct C–H activation reactions. Primary amines,¹⁰⁹ secondary amines,^{114,123} carboxylic acids,^{177,178} and amides,^{179,180} are all now suitable directing groups in palladium-catalysed C(sp³)–H activation reactions, greatly enlarging the scope and applicability of this new reaction paradigm.

While the field steadily advanced towards the use of ubiquitous directing groups in C–H activation reactions, formidable efforts were also invested in the development of new ligands capable of facilitating C–H cleavage.⁸⁶ The fortuitous replacement of an acetate ion by an acetamide functional group as the intramolecular base⁸⁶ required for C–H cleavage has dramatically expanded the range of C–H bonds susceptible of functionalisation.¹⁵⁷ Most importantly, an acetamide functional group provides a new modular binding point for the development of bidentate ligands, which can induce an asymmetric C–H cleavage.^{15,16,141}

Despite these significant advances, palladium-mediated C–H reactions have great challenges remaining to be solved. The costs associated with using high catalyst loadings, often accompanied by stoichiometric silver additives, have limited the applicability of these reactions to milligram-scale synthesis in the context of medicinal chemistry. While there is a plethora of reactions affording C–C bond formation, particularly at incorporating aromatic rings by using aryl iodides or aryl boron reagents, C–X (being X an heteroatom) bond formation is more scarce and restricted to high-valent manifolds. The use of strong oxidants and the difficulty at predicting selectivity in the reductive elimination step must be addressed to enlarge to synthetic applicability of these transformations.^{50,103,104} Perhaps the most fundamental problem is the inherent formation of 5-membered ring palladacycles. Reaction capable of accessing other ring sizes without using biased substrates are to date very scarce.^{40,123}

Palladium-mediated C–H activation aims to use any native functional group to direct a selective C–H cleavage in any position of the molecule of interest. While very impressive breakthroughs have been reported, this premise is far from being solved. Only the future will tell if this area of research will mature to become a reliable and useful tool for synthetic chemistry and, as the ultimate consequence, for society.

Chapter 2

Methyl C(sp³)-H activation of tertiary alkylamines
via palladium catalysis

2.1. Background & Previous work

Tertiary alkylamines are prominent motifs in medicinal chemistry.¹⁸¹ The nucleophilicity, polarity and basic character of the nitrogen core atom provides an excellent way to modulate the lipophilicity, solubility and hydrogen-bonding properties of a drug candidate, which are essential parameters to achieve high potency and bioavailability.^{182,183} In particular, 6-membered heterocycles such as piperidine and piperazine provide a polar and rigid 3D structure with well-defined exit vectors amenable for further synthetic iterations in order to improve drug binding and potency. Consequently, 1 out of 4 marketed pharmaceuticals displays a tertiary alkylamine, either in the drug core structure or as an appendant hydrophilic functional group (Figure 2).^{184,185}

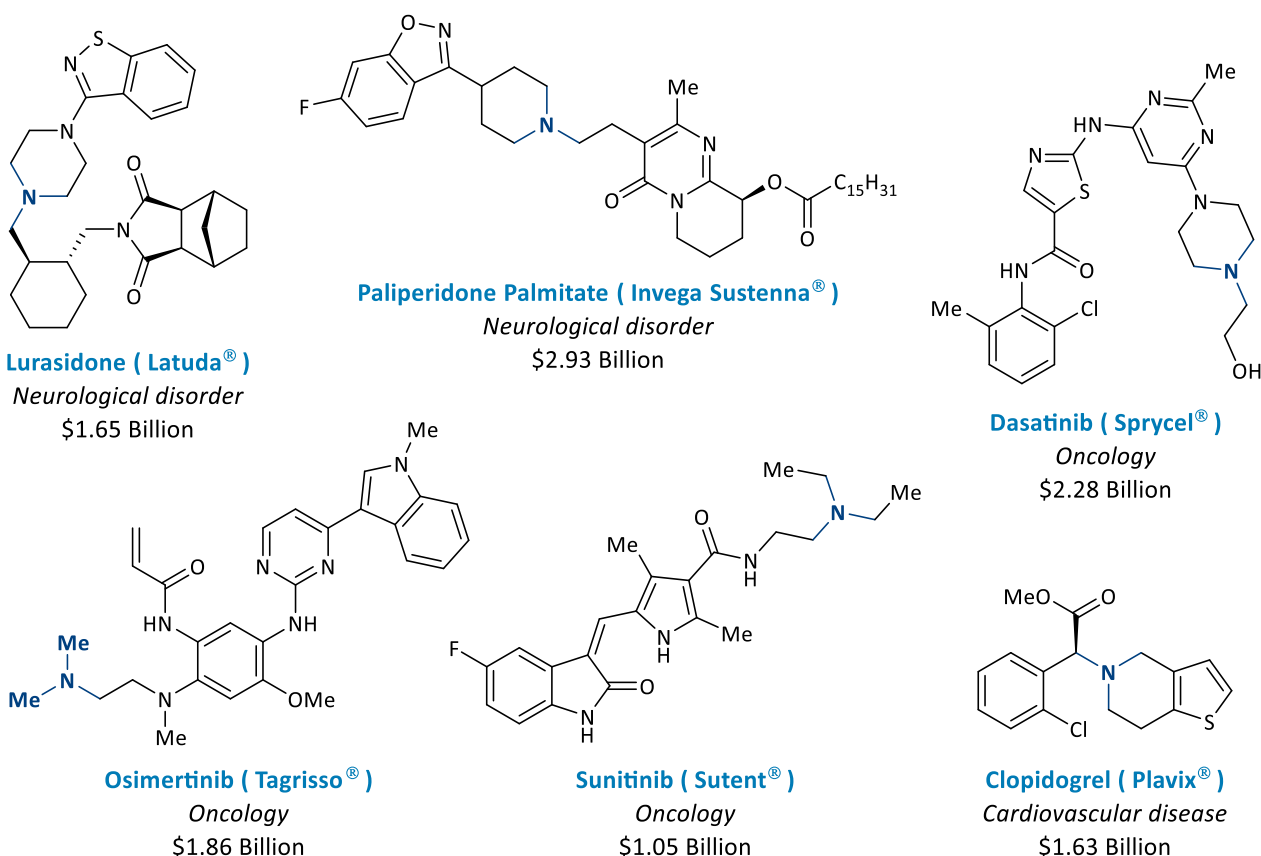
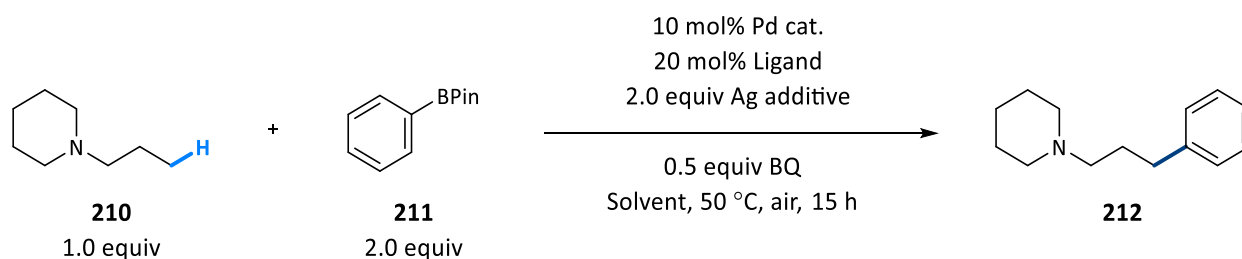


Figure 2: Selected top 100 commercial drugs by sales in 2018 containing an aliphatic tertiary amine functional group.

The prevalent use of tertiary amines in medicinal chemistry contrasts with the lack of C–H activation reactions applicable to this type of substrates. A few methods have successfully achieved catalytic C(sp²)-H activation with palladium (see Section 1.4.3), while alternative strategies have targeted C(sp³)-H bond by masking the amine moiety with strong acidic conditions, or by using a steric-controlled approach with other transition metals (see Section 1.6.). This deficiency of palladium-mediated strategies is certainly influenced by the inability of tertiary amines to incorporate and remove exogenous directing groups which typically provide a second modular binding point to facilitate C–H cleavage (see Section 1.2.). Therefore, the potential use of tertiary amines in palladium-catalysed C–H reactions is strictly limited to the binding affinity of each particular substrate to the metal centre. This section summarises previous efforts of the author to develop a palladium-

catalysed C(sp³)–H activation in tertiary alkylamines, these being conducted during his master's degree studies.¹⁸⁶

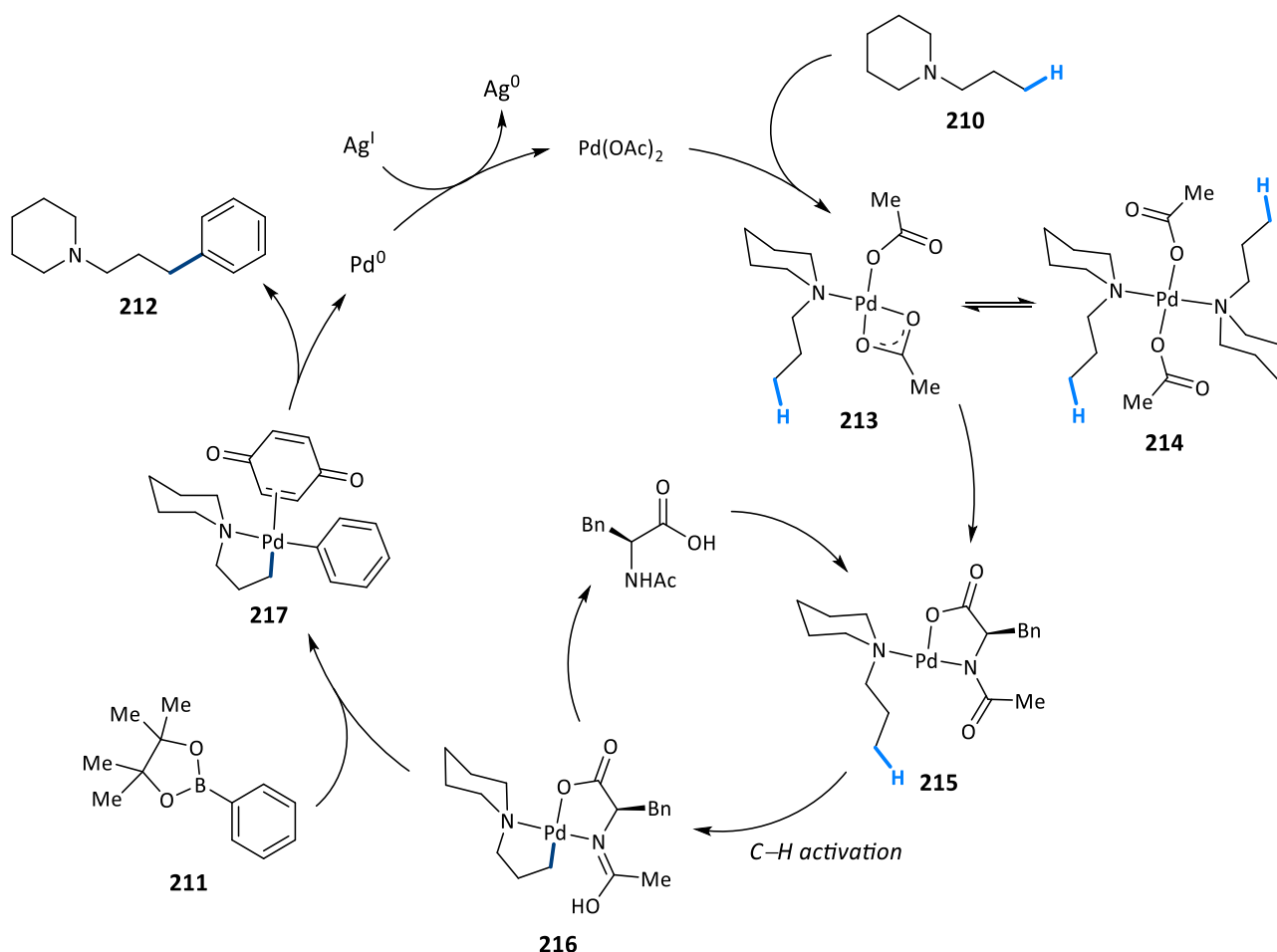
Amine **210** was chosen as the model substrate targeting C–H activation at the more facile γ -methyl unit. After C–H cleavage, a transmetalation step using aryl boron reagents (**211**) would lead to the formation of a C–H arylated product (**212**). Table 1 summarises the following key results: (a) the addition of water was crucial to enhance transmetalation (entries 1-3); (b) *t*amylOH proved to be the best solvent system, working best in more diluted conditions (entries 4-7); (c) other protecting groups in the *N*-terminus apart from an acetyl unit were ineffective, as well as the use of any other amino acid residue (entries 8-10); (d) other palladium precatalysts or silver additives delivered lower reactions yields (entries 11-14); and (e) the reaction reached a plateau at 48 h with an observed 48% yield of arylated amine **212** and a remaining 20% of starting amine **210**, evidencing some amine decomposition at prolonged reaction times (entry 15).



Entry	Pd cat.	Ligand	Ag additive	Solvent [M]	H ₂ O (equiv)	Yield 212 (%)
1	Pd(OAc) ₂	Ac-Phe-OH	Ag ₂ CO ₃	<i>t</i> amylOH [0.1]	0	9
2	Pd(OAc) ₂	Ac-Phe-OH	Ag ₂ CO ₃	<i>t</i> amylOH [0.1]	5	22
3	Pd(OAc) ₂	Ac-Phe-OH	Ag ₂ CO ₃	<i>t</i> amylOH [0.1]	10	19
4	Pd(OAc) ₂	Ac-Phe-OH	Ag ₂ CO ₃	<i>t</i>amylOH [0.05]	5	34
5	Pd(OAc) ₂	Ac-Phe-OH	Ag ₂ CO ₃	THF [0.05]	5	12
6	Pd(OAc) ₂	Ac-Phe-OH	Ag ₂ CO ₃	HFIP [0.05]	5	0
7	Pd(OAc) ₂	Ac-Phe-OH	Ag ₂ CO ₃	DMF [0.05]	5	18
8	Pd(OAc) ₂	Boc-Phe-OH	Ag ₂ CO ₃	<i>t</i> amylOH [0.05]	5	0
9	Pd(OAc) ₂	Ac-Ala-OH	Ag ₂ CO ₃	<i>t</i> amylOH [0.05]	5	9
10	Pd(OAc) ₂	Ac-Val-OH	Ag ₂ CO ₃	<i>t</i> amylOH [0.05]	5	13
11	Pd(OPiv) ₂	Ac-Phe-OH	Ag ₂ CO ₃	<i>t</i> amylOH [0.05]	5	25
12	Pd(PhCN) ₂ Cl ₂	Ac-Phe-OH	Ag ₂ CO ₃	<i>t</i> amylOH [0.05]	5	25
13	Pd(OAc) ₂	Ac-Phe-OH	AgOAc	<i>t</i> amylOH [0.05]	5	19
14	Pd(OAc) ₂	Ac-Phe-OH	AgTFA	<i>t</i> amylOH [0.05]	5	0
15 ^a	Pd(OAc)₂	Ac-Phe-OH	Ag₂CO₃	<i>t</i> amylOH [0.05]	5	48

Table 1: Initial studies towards the C–H arylation of tertiary alkylamines. ^a48 h. Yield determined by GC-FID analysis.

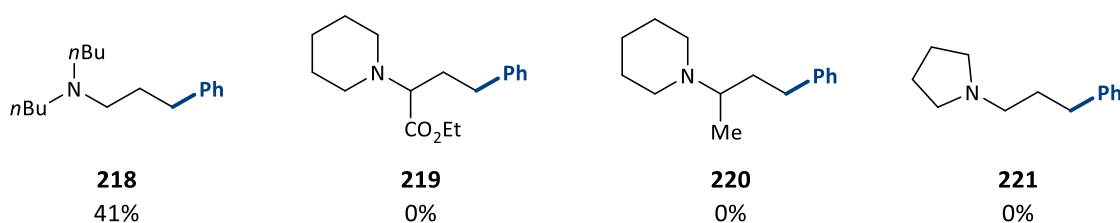
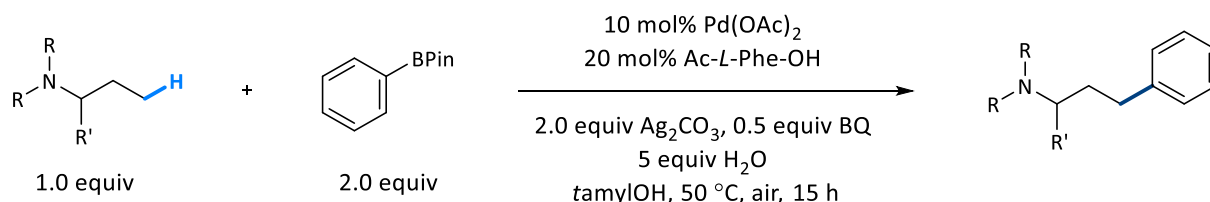
All reaction components were essential for product formation except silver, affording 12% yield of amine **212** in its absence. This indicated that C-H activation could be accessed without silver additives and attributes to this additive the role of oxidising Pd⁰, thereby closing the catalytic cycle. Taken altogether, Scheme 38 illustrates the most likely catalytic cycle under this set of reactions conditions. Amine binding to palladium establishes an equilibrium between monoamine (**213**) and bisamine (**214**) complexes. Based on the seminal reports of Cope and Ryabov,^{3,28,32} the hindrance around the nitrogen core disfavours the formation of bisamine complexes, hence leading to palladacycle **216** with the aid of mono-protected amino acid ligands.⁸⁶ After C-H cleavage, transmetalation with pinacol boronic esters affords complex **217**, which requires the binding of 1,4-benzoquinone to promote the C(sp³)-C(sp²) reductive elimination step leading to arylated product **212** and Pd⁰. This is oxidised by stoichiometric silver additives to close the catalytic cycle.



Scheme 38: Proposed catalytic cycle for the palladium-catalysed C-H activation of tertiary alkylamines

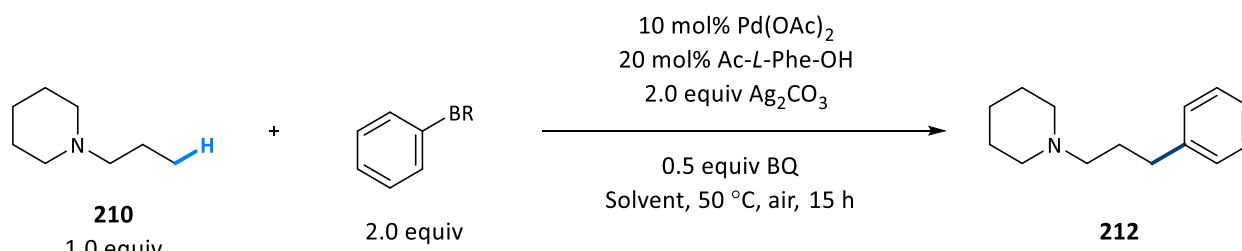
The subtle amine decomposition observed under the reaction conditions prompted the study of other amine starting materials to understand if the piperidine heterocycle was a viable substrate. Product **218** displaying an acyclic amine was obtained in 41% yield, being very similar to the yields afforded by the model piperidine substrate under the same reaction conditions (Scheme 39). It was hypothesised that the putative bisamine complexes generated during the reaction were too stable, thus hampering an efficient catalytic cycle.

Amine substrates displaying appendant α -functionalities were synthesised and subjected to the reaction conditions to observe if the presence of electron-withdrawing groups (**219**) or if a more sterically hindered nitrogen motif (**220**) could deliver a better reactivity. Unfortunately, no arylated product was obtained, indicative that the nitrogen core of these substrates was too hindered to bind effectively to palladium. Surprisingly, a one carbon contraction within the amine heterocycle did not result in product formation (**221**), triggering questions about the capricious reactivity of tertiary alkylamines.



Scheme 39: Exploratory work on different tertiary amine substrates

With these new results in hand, the piperidine model substrate **210** was considered a viable starting material to further explore this reaction. With no success in finding better ligands for C–H cleavage, efforts were focused on improving the transmetalation and reductive elimination step. Higher reaction temperatures delivered lower mass balances without a significant increase in reaction yield, and different organic and inorganic bases were screened without success. The use of less hindered boronic esters delivered similar yields and reaction rates when compared with pinacol phenyl boronic ester **211** (entries 1-3, Table 2). Aryl trifluoroborate salts proved also to be suitable coupling partners, although accurate control of the amount of water present in the reaction mixture was crucial to observe significant reactivity. On the one hand, slow hydrolysis of these reagents led to poor yields of γ -arylated amine **212** (entry 5). On the other hand, when hydrolysis occurred too fast, biphenyl formation was observed, arising from the *homo* cross-coupling of two aryl boron units (entry 6). Other typical arylating reagents such as aryl iodides were unreactive, suggesting the difficulty in accessing high valent mechanistic manifolds. Lastly, the simple phenyl boronic acid proved to be more reactive, achieving significant product formation in the absence of water and accompanied with significant amounts of biphenyl (entry 7). When the reaction stoichiometry was reversed (entry 12), an encouraging 47% yield of amine **212** was observed in much shorter reaction times and using NMP as solvent, which was appealing for further studies.



Entry	R	Solvent [M]	H ₂ O (equiv)	Yield 212 (%)
1	1,3-propanediol	<i>t</i> amyOH [0.05]	5	30
2	2,2-dimethyl-1,3-propanediol	<i>t</i> amyOH [0.05]	5	36
3 ^a	2,3-butanediol	<i>t</i> amyOH [0.05]	5	38
4	F ₃ K	<i>t</i> amyOH [0.05]	5	41
5	F ₃ K	<i>t</i> amyOH [0.05]	0	11
6 ^a	F ₃ K	<i>t</i> amyOH [0.05]	50	31
7	(OH) ₂	<i>t</i> amyOH [0.05]	0	24
8	(OH) ₂	DMF [0.05]	0	27
9	(OH) ₂	DMA [0.05]	0	34
10	(OH) ₂	NMP [0.05]	0	36
11 ^b	(OH) ₂	NMP [0.05]	0	39
12 ^{b,c}	(OH)₂	NMP [0.05]	0	47

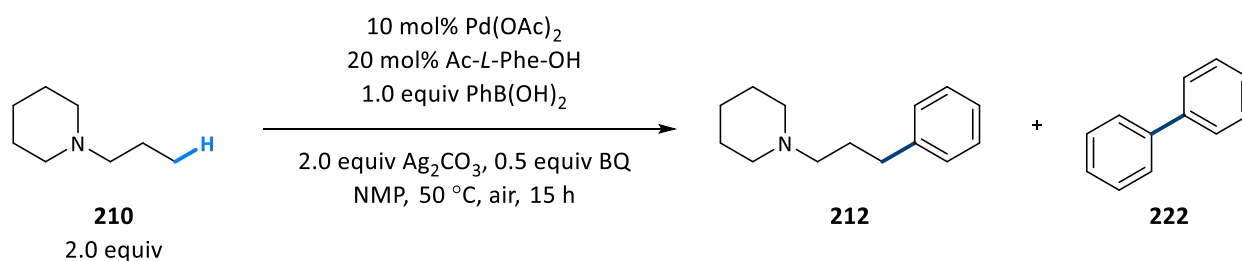
Table 2: Screening of boron reagents for a C–H arylation of tertiary alkylamines. ^aFormation of biphenyl observed. ^b1.0 equiv of PhB(OH)₂. ^c2.0 equiv of amine **210**. Yield determined by GC-FID analysis.

2.2. Project Aims

This research aims to develop better reaction conditions to enhance the formation of γ -arylated amines through a palladium-catalysed C–H activation strategy. To do so, and taking into account the insufficient reactivity of aryl boronic esters, aryl boronic acids will be explored as viable coupling partners by trying to disfavour the formation of undesired *homo* cross-coupling products. Depending on the nature of the transmetalation step, the presence of electron-withdrawing or electron-donating substituents on the aryl ring should impact the rate of transmetalation, favouring either an oxopalladium or boronate pathway, respectively.^{187–189} As well as this, other benzoquinone or alkene derivatives should be explored due to their essential role in the reductive elimination step. Lastly, alternative amine heterocycles and acyclic substrates must be tested to assess the scope of this important component of the reaction.

2.3. Results & Discussion

The focus of initial studies was to achieve good conversion to product **212** by preventing detrimental *homo* cross-coupling of phenyl boronic acid. Slightly lower biphenyl formation was observed when the reaction was conducted in more diluted conditions, which had a positive effect on arylated amine **212** (entries 1-3, Table 3), whereas no significant differences with the addition of water as an additive were observed (entry 4).



Entry	Concentration [M]	H ₂ O (equiv)	Yield 212 (%)	Yield 222 (%)
1	0.050	0	47	36
2	0.040	0	55	34
3	0.033	0	51	32
4	0.040	5	54	28

Table 3: Concentration screening. Reactions conducted at 0.1 mmol. Yield determined by GC-FID analysis using dodecane as internal standard.

To gain a better understanding of the reactivity of phenyl boronic acid, the reaction was monitored over time (Figure 2). Unexpectedly, the initial stages of the reaction delivered a fast and exclusive formation of biphenyl, being this rate then rapidly decreased in favour of productive C–H activation. The initial formation of biphenyl could be attributed to the reaction set-up, as amine **210** was typically added as the last reagent to

the reaction mixture at room temperature, before placing the reaction at 50 °C in a pre-heated oil bath. A second reaction was monitored by pre-stirring all reaction components except for PhB(OH)₂ for 10 minutes at 50 °C. Unfortunately, the same reaction behaviour was observed and similar yields of **212** and **222** were obtained. Even the slow addition of PhB(OH)₂ over 3 hours using a syringe pump was attempted, but same results were obtained. If the data represented in Figure 2 is critically analysed, one can observe that the initial amount of biphenyl (15%) is comparable to that of catalyst loading (e.g. 5 catalytic cycles leading to exclusive biphenyl formation would consume all phenyl boronic acid available). It is worth to emphasize that Pd(OAc)₂ exists as a trimeric complex, both in solid state and in solution.^{190,191} This data suggests that the palladium precatalyst is unable to perform the desired C–H activation reaction, or its rate is outperformed by *homo* cross-coupling. After reductive elimination, the generated Pd⁰ can lead to the formation of palladium nanoparticles,^{192,193} or its oxidation to Pd^{II} can deliver monomeric palladium, or bimetallic palladium-silver species,^{56–58} from where C–H activation is accessible and preferred. Unfortunately, the use of Pd⁰ precatalysts such as Pd₂(dba)₃, Pd(PPh₃)₄, or Pd(PtBu)₂ only afforded similar or worse yields of amine **212**.

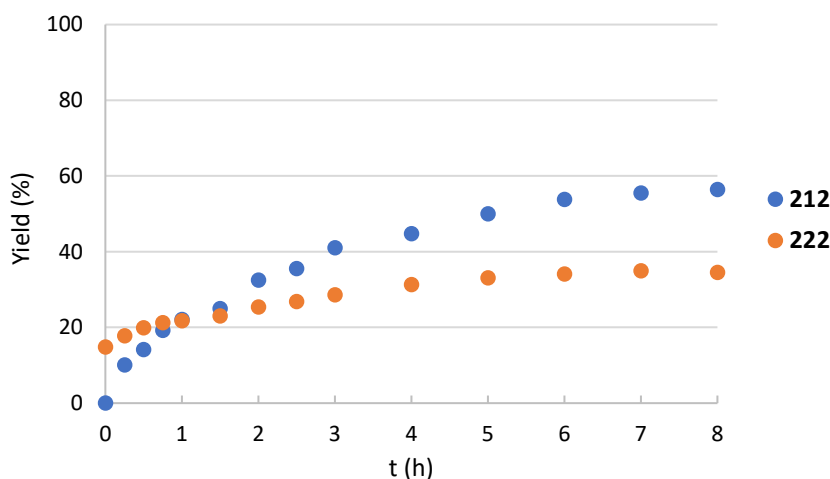
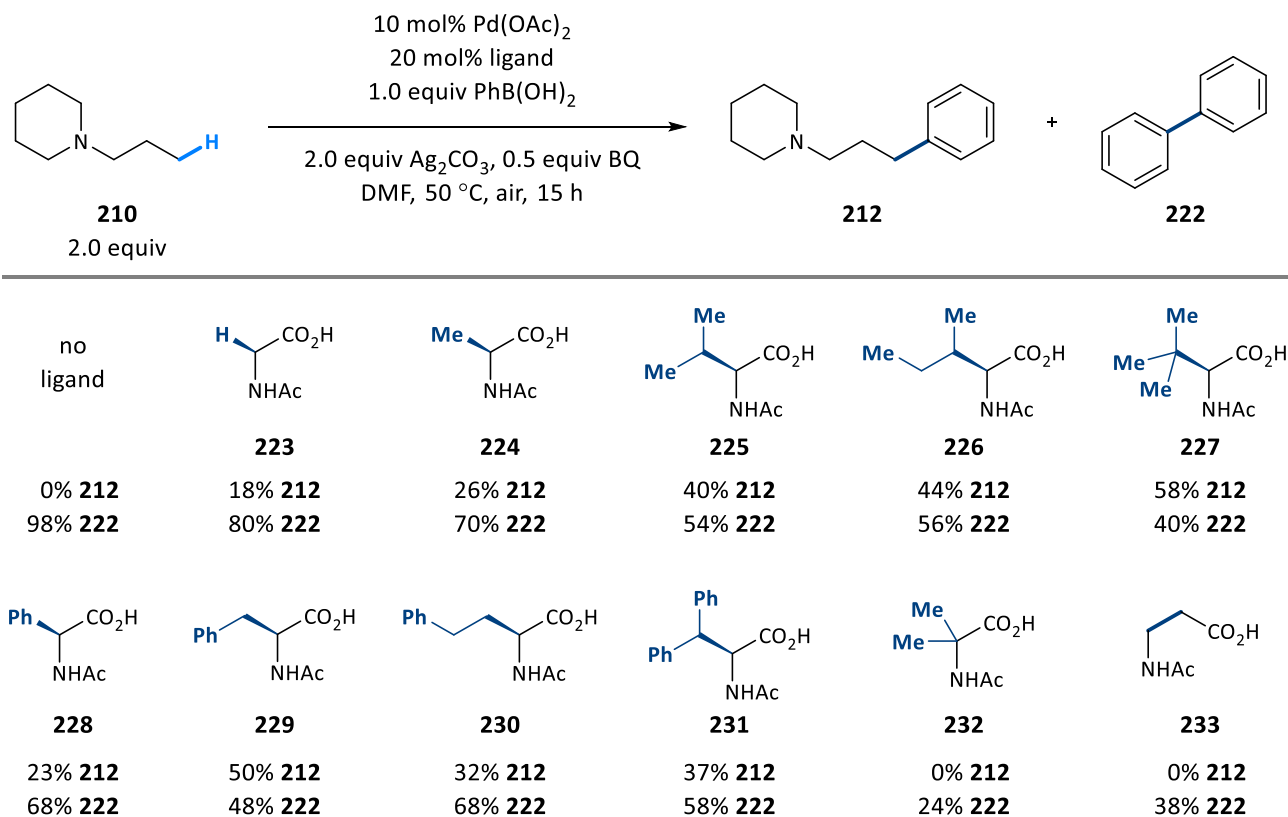


Figure 2: Time study of the arylation reaction using phenyl boronic acid and reaction conditions described in entry 2, Table 3. Data determined by GC-FID using dodecane as internal standard.

If this reactivity profile is compared with that of PhBPin, the reaction is now completed in 8 h, rather than 48 h, offering wider possibilities for further reaction optimisation. Having identified the side reactivity problem of this reaction, a set of acetyl-protected amino acid ligands were revisited to understand the influence of this key component in the rate of C–H activation versus *homo* cross-coupling (Scheme 40). Taking acetyl phenylalanine as a reference (**229**), this ligand delivered 50% of arylamine **212** and 48% of biphenyl, which slightly differs from the previous data obtained due to the use of DMF instead of NMP as solvent. Among all the ligands tested, there is a clear trend towards the formation of arylated amine when using bulkier amino acid ligands (compare from **223** to **227**), perhaps indicative that the increase in sterics slows down transmetalation by preventing the approach of the boron reagent to palladium. Interestingly, acetylated *tert*-leucine (**227**), a non-natural but affordable and commercial amino acid, delivered significantly better yields of

the desired amine than acetyl phenylalanine (**229**). Of note is that bulky ligands with α -quaternary centres (**232**), or β -amino acids (**233**) did not deliver any desired product formation.

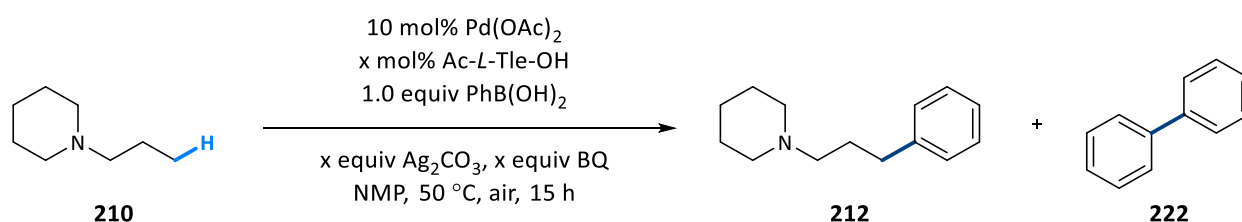


Scheme 40: Ligand screening. Reactions conducted at 0.1 mmol. Yield determined by GC-FID analysis using dodecane as internal standard.

The use of polar aprotic solvents like DMF, NMP, or DMSO is concerning as it implies an experimental challenge when trying to extract the amine products from the reaction media. While DMF can be evaporated by using a nitrogen or air flow, solvents with higher boiling points like NMP cannot be efficiently removed. Basic aqueous work-up with 10% aqueous NaOH and dichloromethane failed in extracting these solvents into the aqueous phase, and large amounts of DMF and NMP were observed by ¹H-NMR analysis of the reaction crude upon evaporation of the organic chlorinated phase. After testing different organic solvents such as ethyl acetate or chloroform, treatment of the reaction mixture with 10% NaOH and Et₂O considerably diminished the presence of any amide solvent into the ether organic phase. Further optimisation afforded complete removal of DMF or NMP by washing an ether organic layer three times with aqueous NaOH (1%). The resultant reaction crudes could be easily analysed by ¹H-NMR using 1,1,2,2-tetrachloroethane as an internal standard to deliver statistically identical yields to those previously observed by GC-FID.

Having found a viable procedure for the isolation of the resultant γ -arylated amines, reaction optimisation was resumed using acetyl *tert*-leucine (**227**) as the ligand and NMP as the reaction solvent. Fine tuning of the ligand loading (entries 1-5, Table 4) in NMP greatly diminished the formation of biphenyl to

deliver a highly appealing 71% yield of amine **212**, this being further enhanced to 76% yield when using 2 equivalents of the 1,4-benzoquinone additive (entries 6-8). Nevertheless, when the conditions of entry 7 were scaled to 0.3 mmol scale, a more modest 56% yield of amine **212** was obtained (entry 9). After reproducibility errors were discarded, attention was focused on the different reaction set up. Reactions on a 0.1 mmol scale were conducted in a 2–5 mL microwave round bottom vial, while 0.3 mmol scale reactions were assembled in a 10–20 mL microwave round bottom vial. The use of insoluble Ag₂CO₃ as oxidant generated an heterogeneous solution susceptible to irreproducibility problems and mass-transfer limitations.⁵⁵ Systematic analysis of the reaction flask, size of stirring bar, and speed of the reaction stirring, led to a reproducible and enhanced yield of 84% when increasing the loading of starting amine and Ag₂CO₃ (entry 11). At this point, the reaction was considered to be optimised and this set of reaction conditions was used to assess the scope of the reaction.

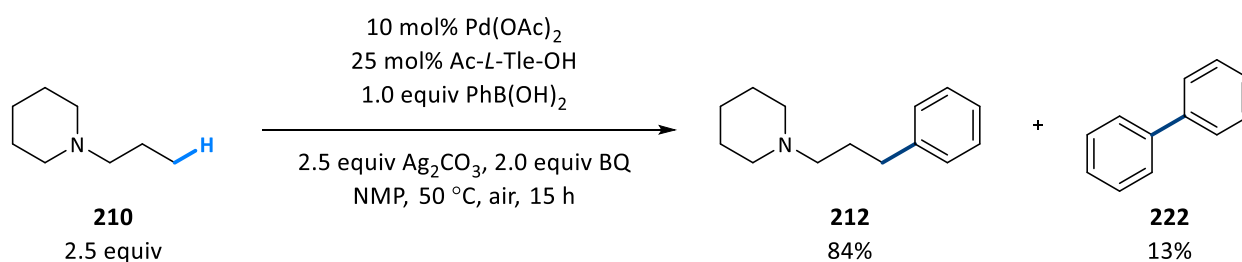


Entry	Ligand (mol%)	210 (equiv)	BQ (equiv)	Ag ₂ CO ₃ (equiv)	Yield 212 (%)	Yield 222 (%)
1	10	2.0	1.0	2.0	63	28
2	20	2.0	1.0	2.0	66	20
3	25	2.0	1.0	2.0	71	15
4	30	2.0	1.0	2.0	71	15
5	40	2.0	1.0	2.0	61	16
6	25	2.0	0.5	2.0	51	15
7	25	2.0	2.0	2.0	76	15
8	25	2.0	5.0	2.0	77	12
9 ^a	25	2.0	2.0	2.0	56	10
10 ^a	25	2.0	2.0	2.5	74	12
11 ^a	25	2.5	2.0	2.5	84 (81)	13

Table 4: Optimisation of reaction parameters using ligand **227**. Reactions conducted at 0.1 mmol. ^aReactions conducted at 0.3 mmol. Yield determined by ¹H-NMR using 1,1,2,2-tetrachloroethane as internal standard.

Control experiments determined that palladium (entry 1, Table 5), ligand (entry 2) and 1,4-benzoquinone (entry 3) were essential components of the reaction. Benzoquinone is a common additive in low valent palladium C–H activation reactions as it is known to facilitate reductive elimination from palladium(II),^{194–197} hence the lack of product or even biphenyl formation. The absence of silver additives did afford product conversion comparable to that of catalyst loading (entry 4), suggesting that C–H cleavage can be accessed

without silver, and its role is limited to the oxidation of palladium(0). Nevertheless, further experiments were conducted to better elucidate the role of silver and benzoquinone in the reaction, as this later additive is also known to oxidise palladium(0) in the presence of O₂.^{198,199} Reactions with 10 mol% of benzoquinone afforded significant catalyst turnover, even in a N₂ atmosphere, proving that benzoquinone is not consumed within the reaction and its role as the terminal oxidant is unlikely (entries 5-6). Nevertheless, a superstoichiometric amount of this additive can replace Ag₂CO₃ when using an O₂ atmosphere (entry 7). A remarkable 40% yield was obtained in the absence of silver(I), which evidenced that bimetallic silver-palladium species are not required for C–H cleavage, and it opens the path to the development of a cheaper, greener and more atom-economical C–H activation reaction.



Entry	Ligand (mol%)	BQ (equiv)	Ag ₂ CO ₃ (equiv)	atmosphere	Yield 212 (%)	Yield 222 (%)
1 ^a	25	2.0	2.5	air	0	0
2	0	2.0	2.5	air	0	95
3	25	0	2.5	air	0	6
4	25	2.0	0	air	22	7
5	25	0.1	2.5	air	39	18
6	25	0.1	2.5	N ₂	37	19
7	25	2.0	0	O ₂	40	20

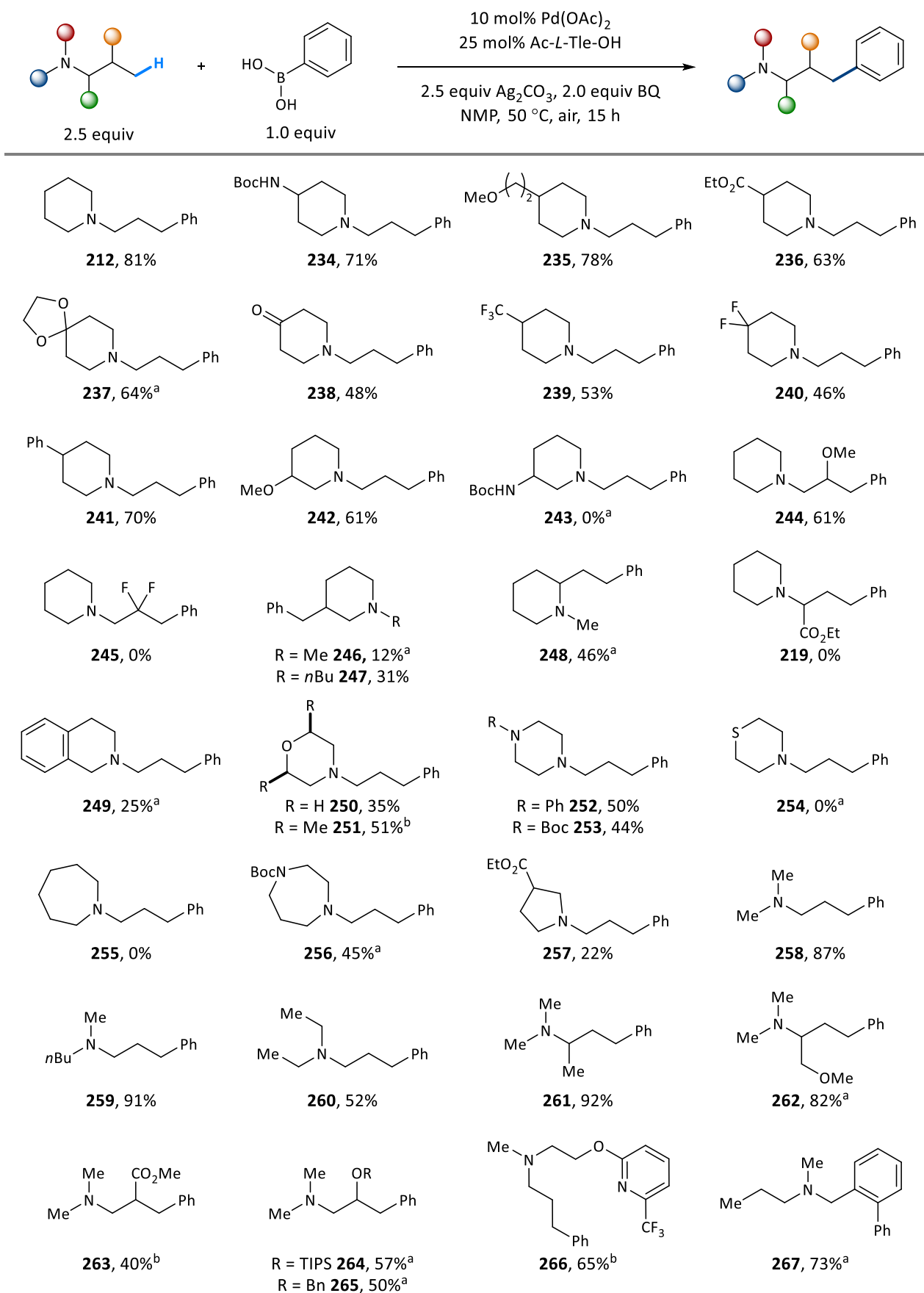
Table 5: Control experiments. Reactions conducted at 0.1 mmol. ^aAbsence of Pd(OAc)₂. Yield determined by ¹H-NMR using 1,1,2,2-tetrachloroethane as internal standard.

Having established optimal conditions for γ -C–H arylation, attention was focused towards the scope of the amine component (Scheme 41). *N*-propyl piperidine scaffolds bearing different functionalities on the heterocycle underwent efficient C(sp³)-H arylation to the desired products (**234–242**) in generally good yields. It was noticeable that the yields of product were slightly reduced in the presence of electron-withdrawing substituents on the heterocycle (compare from **234** to **240**), which may reflect attenuated binding of the amine to the Pd^{II} catalyst brought about by the inductive effect of the remote functionality. The use of native functionalities to direct C–H activation makes this strategy highly substrate dependant. For instance, altering the substitution pattern of an *N*-protected nitrogen in the piperidine ring can deliver good yields of the arylated amine (**234**), or become a completely unreactive substrate (**243**), likely due to bidentate binding of

substrate to palladium when the 3-substituted functional group is in the axial conformation. β -Substituents in the propyl chain were also tolerated (**244**) if these are not strong electron-withdrawing groups (**245**), which hampers amine binding to palladium and removes electron density from the cleavable C-H bond. Interestingly, a substrate with the targeted C(sp³)-H bond in a 3-methyl substituent on the heterocycle underwent arylation to the 3-benzyl-piperidine derivative **247**. This challenging cyclopalladation must have involved metal binding to the axial lone pair of the piperidine nitrogen and with the reacting methyl group also projected in the axial position, hence the better reactivity when having larger *N*-alkyl substituents (**246**). The reacting C-H bond can also be located in a 2-ethyl substituent on the piperidine ring, producing amine **248** in more synthetically useful yields. Unfortunately, substrates bearing α -substituents in the *N*-propyl chain did not deliver any reactivity (**219**).

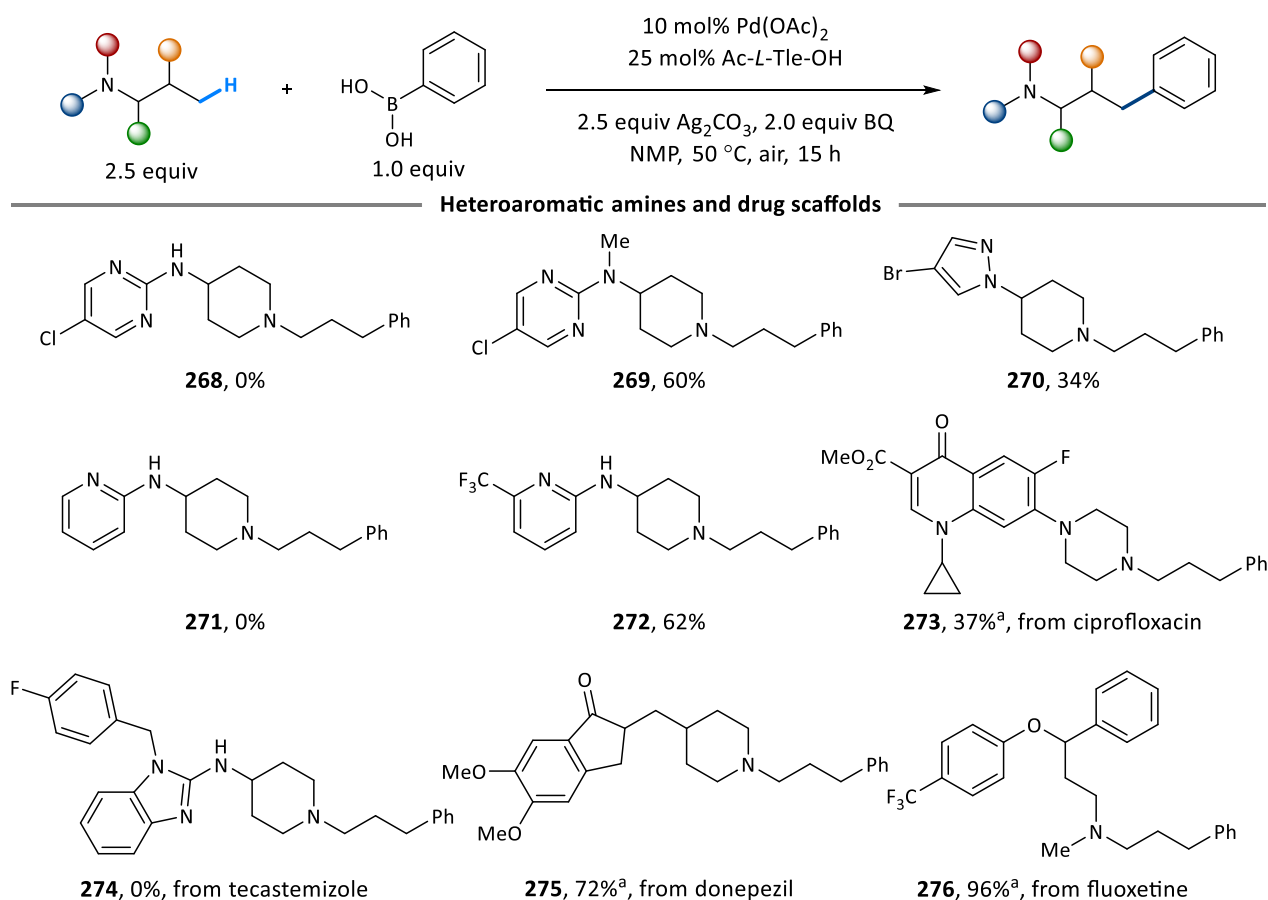
Other heterocyclic amine scaffolds were tested to understand their reactivity profile (**249–257**). *N*-Propyl tetrahydroisoquinoline delivered poor yields due to substrate decomposition (**249**), as it is known that the benzylic C-H bonds of this bicyclic amine are highly susceptible to oxidation.²⁰⁰ Heterocycles containing other heteroatoms, such as morpholines (**250–251**) or protected piperazines (**252–253**), afforded synthetically useful yields of their corresponding γ -arylated amines. The significant decrease in yield can be attributed to the deleterious bidentate binding of substrate to palladium, in combination with the presence of electronegative atoms close to the metal-directing nitrogen. Thiomorpholine (**254**) was unreactive due to the superior affinity of sulphur atoms for palladium binding, leaving no empty vacant sites for C-H cleavage. Products **255** and **256** exemplify once again the sharp difference in reactivity between *a priori* similar amine substrates. While an azepane ring did not deliver any product formation, *Boc*-protected diazepane led to its corresponding γ -arylated amine **256** in 45% yield. Lastly, pyrrolidine scaffolds delivered poor reactivity due to competing β -H elimination (**257**).

Acyclic scaffolds can contain up to eight C-H bonds adjacent to nitrogen, which means they are especially prone to β -hydride elimination on complexation with Pd(II) salts. Gratifyingly, a range of *N,N*-dialkylamine derivatives smoothly reacted to form amines **258–267** in good yield, without observing any deleterious amine decomposition. Amines possessing a *N*-methyl substituent delivered excellent product formation (**258–259**), while diethylpropylamine, a substrate having extended alkyl substituents with a high degree of freedom, delivered significantly lower yields (**260**). This can be attributed to unfavourable binding to palladium due to its bulkiness and multiple conformations, hindering the amine lone pair. This time, acyclic amines containing α -substituents performed well to deliver the expected aryated amine in excellent yields (**261–262**). As well as this, tertiary alkylamines with β -substituents, such as esters (**263**) or protected alcohols (**264–265**), were also converted to their corresponding functionalised products. Finally, a competition experiment was conducted to assess C(sp²)-H versus C(sp³)-H activation. As expected, amine **267**, arising from aromatic C-H activation, was exclusively obtained.



Scheme 41: Palladium-catalysed γ -C-H activation of tertiary alkylamines. Scope of the amine component. Reactions conducted at 0.3 mmol. ^aConducted by Dr. Azuma. ^bConducted by Dr. Nappi

The scope outlined in Scheme 41 evidenced the capricious reactivity of some amine substrates, affording little or no reactivity mainly due to substrate decomposition via β -H elimination, or deleterious bidentate binding of substrate to palladium. Heteroaromatic functionalities are pivotal in medicinal chemistry.¹⁸¹ However, the strong binding affinity of these structures to palladium can override amine coordination to the same metal.²⁰¹ To study this effect more in detail, a range of tertiary alkylamines with appendant heteroaromatic functionalities were synthesised and tested in the reaction conditions (Scheme 42). Product **268**, displaying a functionalised pyrimidine, was not accessible despite the presence of the moderately electron-withdrawing effect of a chlorine substituent. Nevertheless, methylation of the secondary amine disfavoured palladium coordination by steric hindrance, affording a more promising 60% yield of amine **269**. Noteworthy was the 34% yield obtained for piperidine **270**, displaying an appendant *N*-substituted pyrazole with a typically reactive bromine functionality. The low yields obtained were attributed to competing binding to palladium, rather than side reactivity at the C-Br bond. An analogue amine substrate to **268** was synthesised containing a 2-substituted pyridine. Again, no reactivity was observed due to the favourable binding of the heteroaromatic motif to palladium (**271**). This time, the introduction of a strongly electron-withdrawing group removed enough electron-density of the heteroaromatic ring to deliver a productive C-H arylation reaction directed by the tertiary amine functionality (**272**).

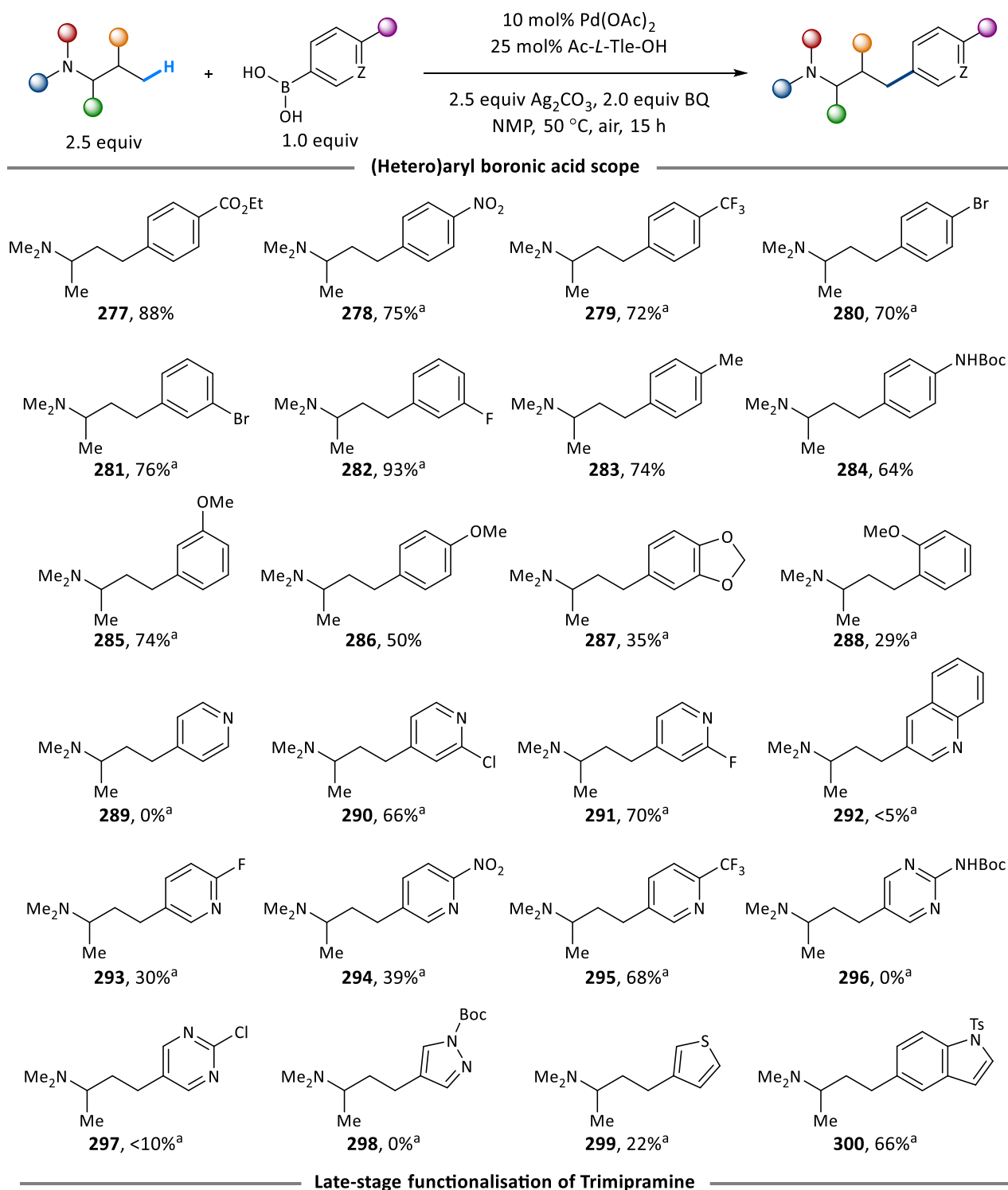


Scheme 42: Scope of tertiary amines displaying heteroaromatic substituents or drug scaffolds. Reactions conducted at 0.3 mmol. ^aConducted by Dr. Azuma.

To finish with the amine scope, a series of *N*-propyl derivatives of pharmaceuticals were submitted to the reaction conditions. *N*-Propyl ciprofloxacin delivered moderate reactivity, in line with previous piperazine substrates, and despite the presence of Michael acceptors and cyclopropane rings (**273**). *N*-Propyl tecastemizole was unreactive (**274**), in line with the previously observed heteroaromatic trends. On the other hand, donepezil and fluoxetine derivatives both afforded good conversion to the expected γ -arylated products (**275–276**).

Next, the scope of the aryl-boronic acid coupling partner was evaluated. Aryl groups displaying electron-withdrawing substituents in *meta*- and *para*- positions delivered good yields to form the corresponding γ -aryl alkylamine products (**277–282**, Scheme 43). Again, palladium-sensitive functionalities such as aryl bromides (**280–281**) were successfully tolerated with no observed reactivity at these positions. Arenes with electron-donating substituents could be also incorporated into the amine backbone, although it was noticeable the subtle loss in yield when trying to couple highly electron-rich aromatic rings due to competing *homo* cross-coupling to form biaryl side products (**283–287**). On the other hand, *ortho*-substituents afforded little to no reactivity (**288**). In pursuit of making this reaction amenable to the incorporation of heteroaromatic rings, a wide range of commercially available heteroaromatic boronic acids were tested as potential coupling partners. As predicted, electron-rich pyridine-type substrates were found to be unreactive (**289** and **292**). However, 2-substituted pyridines with electron-withdrawing groups afforded product formation in moderate to good yields (**290–291**, **293–295**). Subtle differences were encountered using boronic acids with different substitution pattern. Pyridines with 4-substituted boron motifs delivered higher yields and in the presence of more moderate electron-withdrawing groups. Other heteroaromatic rings such as pyrimidines (**296–297**) or *N*-protected pyrazoles (**298**) failed to deliver any reactivity. The more electron-rich thiophene ring afforded product formation (**299**), accompanied with protodeboronation and *homo* cross-coupling. Indoles with the boron functionality at the 3-position delivered no reactivity, but product **300** could be obtained in a 66% yield starting from the 5-substituted analogue.

The tricyclic antidepressant trimipramine, which is used to treat major depressive disorders, was also an excellent substrate for the arylation process, affording γ -(hetero)aryl tertiary alkylamine derivatives in excellent yield (**301–303**); 90% of the unreacted excess amine starting material can be recovered, further demonstrating the controlling in selectivity between C–H activation and other potentially competing pathways. The success of this transformation demonstrates the potential of its application as a tool for late-stage functionalisation of pharmaceutical agents; many different aryl groups could be transferred to already biologically active molecules, producing previously unexplored candidates that would require multistep syntheses to prepare by traditional means.

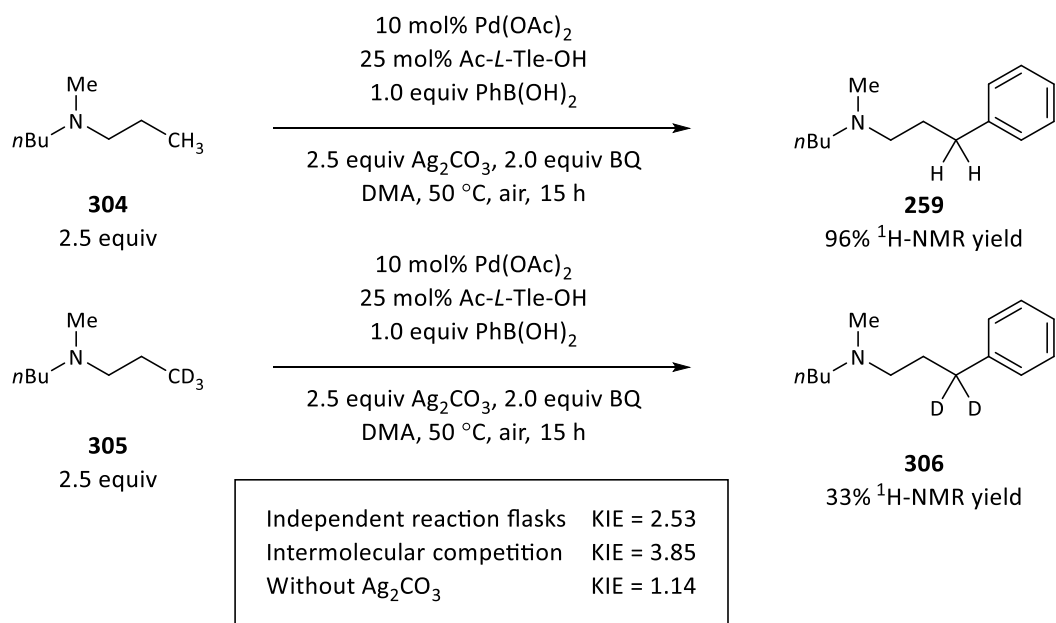


Scheme 43: Scope of the (hetero)aryl boronic acid component and late-stage functionalisation of trimipramine. Reactions conducted at 0.3 mmol. ^aConducted by Dr. Azuma.

After an extensive scope of the amine and boronic acid components of the reaction, the following conclusions can be made: i) acyclic amines and 6-membered ring heterocycles, including piperidine, piperazine, and morpholine, can efficiently direct cyclopalladation to access their corresponding γ -arylated products; ii) the presence of strong electron-withdrawing groups in close proximity to the directing nitrogen can have a detrimental effect in reactivity; iii) pyrrolidine substrates delivered poor reactivity, while 7-membered ring heterocycles can afford moderate reactivity depending on the substitution pattern; iv) electron-poor heteroaromatic structures can be tolerated both in the amine backbone and as coupling partners; v) aromatic boronic acids displaying *meta*- or *para*- substituents are viable coupling partners, with yields being more moderate when the *ipso*- carbon to boron is highly electron-rich. These findings were encapsulated in a scientific publication at the beginning of 2020.²⁰²

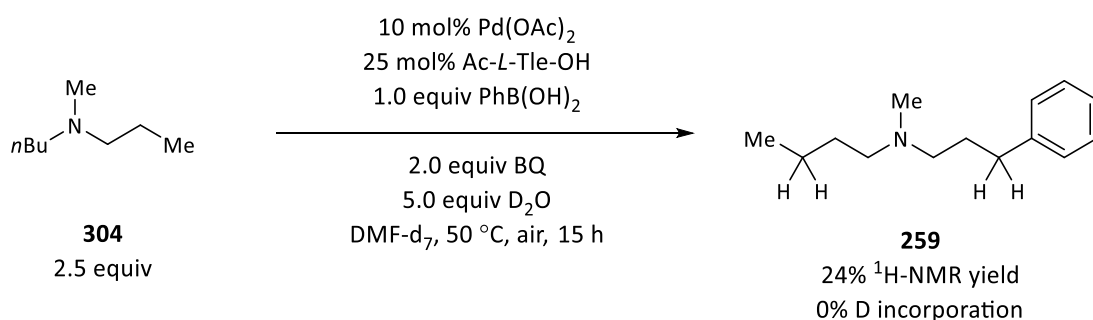
In an attempt to better understand the fundamental steps of this new reaction, acyclic amine **305** was synthesised with the reacting γ -methyl deuterated. Using the hydrogenated and deuterated analogues of this amine, the kinetic rates in the initial stages of the reaction were measured by taking aliquots over time. Reactions were followed by $^1\text{H-NMR}$ using 1,4-dimethoxybenzene as an internal standard, an additive which showed no difference in reactivity. DMA was used as the reaction solvent to facilitate interpretation of the $^1\text{H-NMR}$ spectra, performing with no significant difference in yield compared with NMP. The monitoring of independent reactions flasks led to an observed KIE of 2.53, thus indicating that C–H cleavage is the rate-determining step of the reaction (Scheme 44). KIE arising from the rate measurement of independent reaction flasks can imply errors in the reaction set up, variable induction periods, catalyst decomposition, or the presence of impurities in one of the amine substrates.²⁰³ To further validate these findings, a new large KIE of 3.85 was obtained by measuring the rate constants of both amines in the same reaction flask, thus evidencing the clear inferior reactivity of the isotopic amine variant. In fact, submitting amine **305** to the standard reaction conditions could only deliver a very modest 33% $^1\text{H-NMR}$ yield of the γ -deuterated arylated amine after 15 h.

Previous control experiments indicated that silver(I) additives were not involved during C–H cleavage because significant product formation was observed in their absence. To further corroborate this hypothesis, and to gain a better insight into the C–H cleaving step, KIE experiments were conducted without Ag_2CO_3 . If silver is not involved during C–H activation, an observed KIE with very similar values of 2.53 and 3.85 would be expected. However, the reaction rate without Ag_2CO_3 displayed a KIE of 1.14, indicating a strong switch in mechanism, and suggesting that C–H cleavage is now likely not involved in the rate-limiting step. Taking into account the ability of 1,4-benzoquinone to catalyse the oxidation of palladium(0) with oxygen,¹⁹⁹ seems reasonable to hypothesise that this stage of the catalytic cycle, not aided now by silver(I) additives, has become the rate-limiting step of the reaction.



Scheme 44: Kinetic isotopic experiments of the palladium-catalysed C(sp³)-H arylation of tertiary alkylamines. Reactions conducted at 0.3 mmol. Yield determined by ¹H-NMR using 1,1,2,2-tetrachloroethane analysis using dodecane as internal standard.

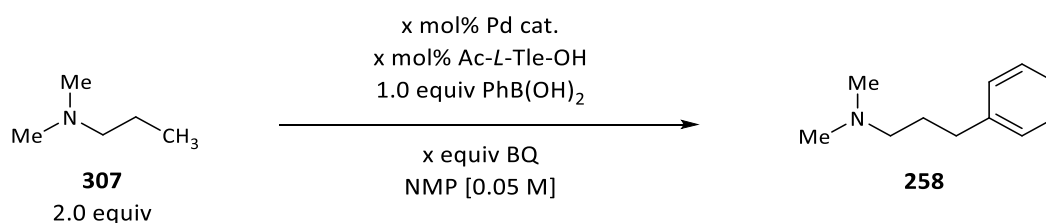
To gain insight into the irreversibility of C-H cleavage, amine **304** was submitted to the reaction conditions using DMF-d₇ in combination with 5 equiv of D₂O and in the absence of Ag₂CO₃. Although a low yield was obtained, no deuterium incorporation was observed in any of the γ-positions available, thus suggesting the irreversible nature of C-H cleavage even under conditions where this is not a rate-determining step.¹²⁰



Scheme 45: Isotopic labelling experiments of the palladium-catalysed C(sp³)-H arylation of tertiary alkylamines. Reaction conducted at 0.05 mmol. Yield determined by ¹H-NMR using 1,1,2,2-tetrachloroethane as internal standard.

In parallel with these findings, and inspired by the recent discovery of bulky benzoquinones as enhanced ligands for high palladium turnovers in C(sp²)-H activation reactions,¹⁹⁹ dimethylpropylamine **307** was chosen as the new model substrate to optimise a greener set of reaction conditions with lower palladium loadings and in the absence of other metal additives. Removal of Ag₂CO₃ from the previously reported standard reaction conditions delivered a 52% ¹H-NMR yield of the expected arylated amine **258** (entry 1, Table 6), comparable to the 40% yield observed during control experiments for arylated piperidine **212** (Table 5).

Counterintuitively, the use of half catalyst loading with its corresponding reduction in the amount of ligand delivered the same reaction yield, accounting for 11 catalyst turnovers (entry 2). The use of slightly higher reaction temperatures in combination with longer reaction times increased the yield to 74% (entry 3), a value not so different to the previously reported in Scheme 41, but achieved with 5 mol% Pd(OAc)₂ and without silver additives. It was attempted to maximise catalyst turnover by assessing the most suitable amount of ligand loading with 1 mol% of Pd catalyst (entries 6–9). Little differences in yield were observed, with values between 13% to 17%, which directly correlates to 13 to 17 catalyst turnovers. Nevertheless, a reaction conducted on a 0.3 mmol scale and in a 10–20 mL microwave round bottom vial afforded 27 catalyst turnovers, perhaps indicative of a better solvent oxygenation over the prolonged reaction times (entry 10). The use of catalytic amounts of 1,4-benzoquinone afforded greater product formation compared to the loading of this additive, proving that it is not consumed within the reaction conditions and oxygen acts as the terminal oxidant of the reaction (entries 11–12).



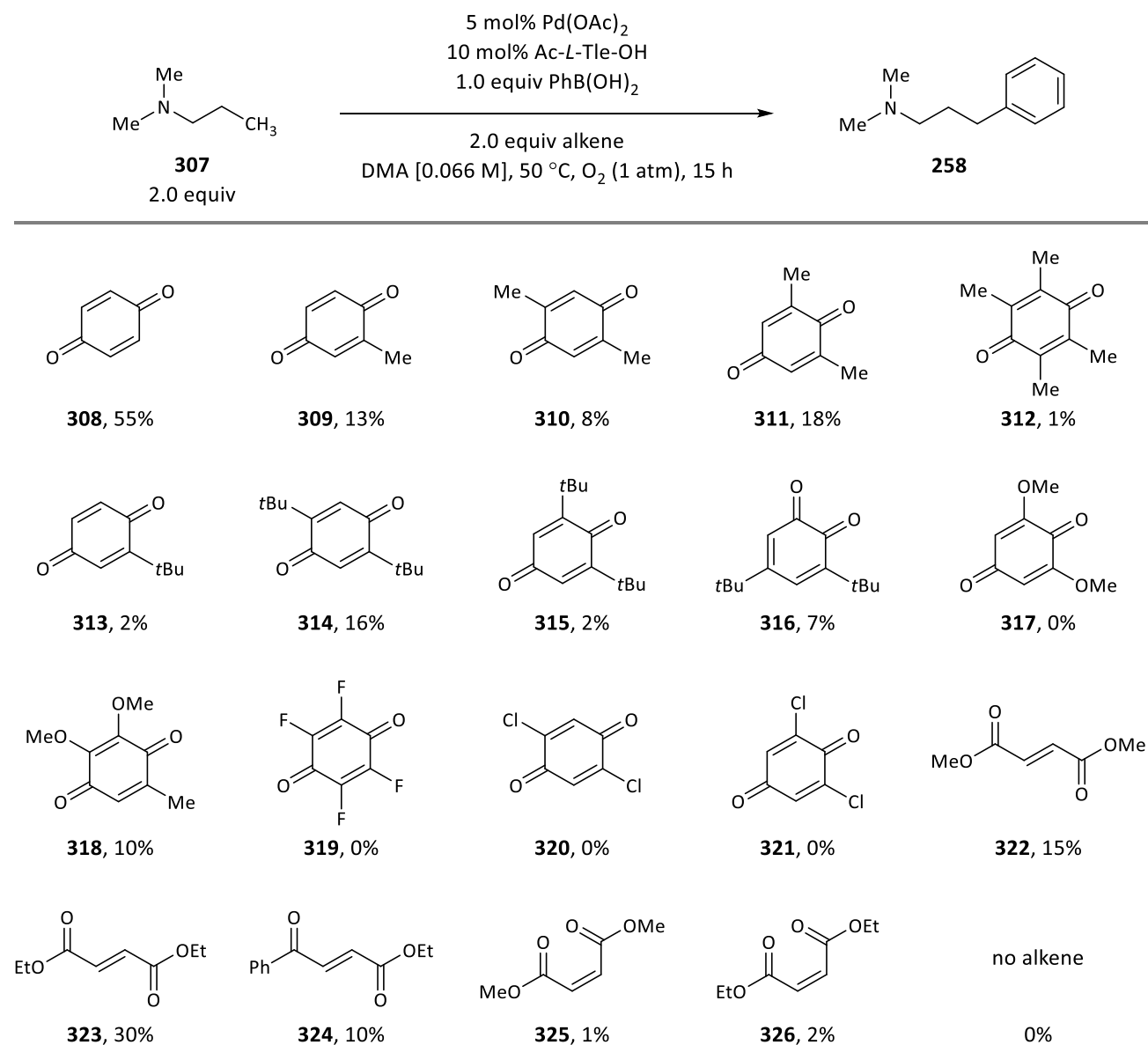
Entry	Pd (mol%)	ligand (mol%)	T (°C)	BQ (equiv)	t (h)	atmosphere	Yield 258 (%)
1	10	25	50	2.0	15	O ₂	52
2	5	10	50	2.0	15	O ₂	55
3	5	10	60	2.0	15	O ₂	68
4	5	10	60	2.0	24	O ₂	74
5	2	5	60	2.0	48	O ₂	32
6	1	1	60	2.0	48	O ₂	13
7	1	2	60	2.0	48	O ₂	15
8	1	5	60	2.0	48	O ₂	17
9	1	10	60	2.0	48	O ₂	15
10 ^a	1	5	60	2.0	48	O ₂	27
11	5	10	60	0.1	24	O ₂	25
12	5	10	60	0.5	24	O ₂	60
13	5	10	60	2.0	24	air	72
14	5	10	60	2.0	24	N ₂	71
15	10	20	60	2.0	15	N ₂	82

Table 6: Discovery of 1,4-benzoquinone as an effective terminal oxidant for tertiary amine C–H activation reactions. Reactions conducted at 0.2 mmol. ^a Reaction conducted at 0.3 mmol in a 10–20 mL microwave round bottom vial. Yield determined by ¹H-NMR using 1,1,2,2-tetrachloroethane as internal standard.

Control experiments obtained under these new reaction conditions were particularly noteworthy, delivering the same reaction performance in a N₂ atmosphere, and with degassed solvents (entries 14–15). This is a rare example of a palladium-mediated C(sp³)-H activation reaction using 1,4-benzoquinone as the sole and terminal oxidant. Basic electron-rich and σ -donating amine substrates may favour direct reduction of 1,4-benzoquinone by the palladium metal centre, a proposal which must be explored in the near future.²⁰⁴ To further corroborate this result, acyclic amine **304** was submitted to the reaction conditions of entry 15, delivering a comparable 75% yield of arylated amine **259**.

Deprotonation of the acetamide functional group of the ligand is key to generate the intramolecular base needed for C-H cleavage. Hence, replacement of silver carbonate by other cheaper inorganic bases may favour product formation. Two equivalents of Na₂CO₃, KHCO₃, K₂HPO₄, and CsHCO₃ were added to independent reactions using conditions of entry 8, but lower yields were obtained in all cases. Future studies should explore alternative palladium precatalysts, amino acid ligands, solvents and higher reaction temperatures to further optimise this highly appealing transformation.

In an attempt to find a better oxidant, a diverse range of functionalised quinones and alkenes were tested in the presence of an oxygen atmosphere at 50 °C, as it is unsure that other quinones can benefit from the same unique reactivity of 1,4-benzoquinone under N₂. A range of 1,4-quinones with alkyl substituents differing in bulkiness and substitution pattern were tested under the silver-free reaction conditions, but inferior yields were obtained in all cases with no particular trend among the different additives (**309–315**, Scheme 46). Electron-rich quinones did not show any significant improvement, and their results are comparable to their alkyl quinone analogues (**317–318**). On the other hand, electron-deficient halogenated quinones failed to deliver any arylated product, causing the reaction to turn black within seconds (**319–321**). Lastly, a range of simple electron-poor alkenes were tested. While *cis* isomers did not deliver any reactivity (**325–326**), the corresponding *trans* derivatives afforded some success: 6 turnovers were observed when using diethyl fumarate (**323**). It is worth mentioning that *trans* alkenes presumably require oxygen as the terminal oxidant, and reactions conducted at higher reaction pressures and temperature may benefit from a higher turnover.¹⁹⁹



Scheme 46: Alkene screening for a silver-free palladium-catalysed C(sp³)-H arylation of tertiary alkylamines. Reaction conducted at 0.2 mmol. Yield determined by ¹H-NMR using 1,1,2,2-tetrachloroethane as internal standard.

The ability of fumarate derivatives to impact on the palladium oxidation step opens the possibility to modulate the alkene binding properties by sequentially modifying both of the esters groups to access a range of electronically diverse conjugated alkenes displaying esters, amides, or ketones derivatives. The combined use of 1,4-benzoquinones with fumarate derivatives cannot be discarded, while no other palladium precatalysts, amino acids ligands, solvents or temperatures were screened. Overall, these preliminary results provide a solid foundation that a greener, cheaper, and more atom-economical native amine-directed C(sp³)-H activation reaction is possible and appealing for further studies.

2.4. Computational findings

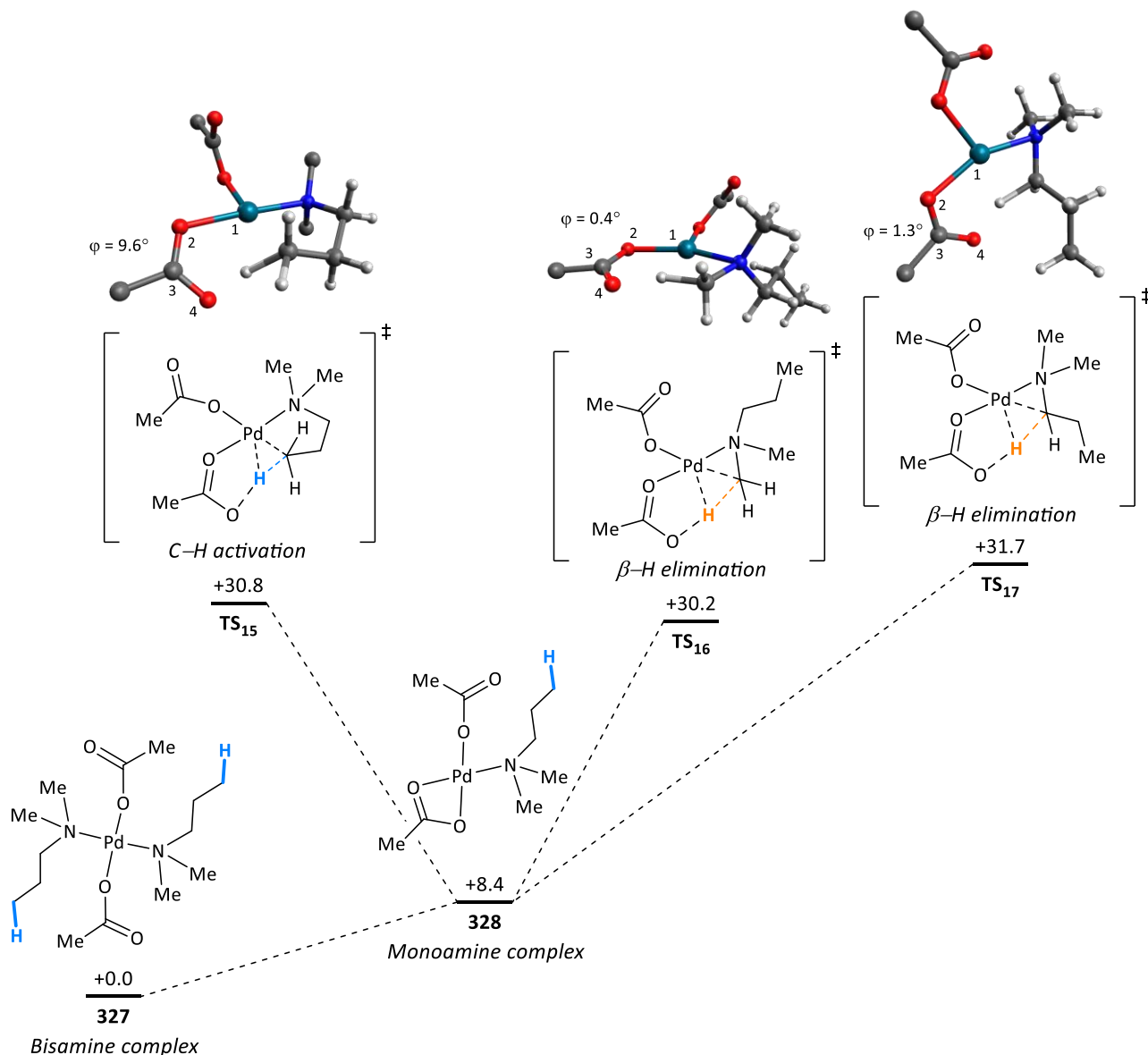
The previous section exemplified the reactivity encountered among different tertiary alkylamine substrates. Acyclic amines and piperidines delivered excellent conversions, but other 6-membered ring heterocycles afforded more modest results; pyrrolidine scaffolds displayed little conversion, an azepane units showed no conversion to the desired arylated amine. Taking into account that C–H activation is the rate-limiting step of the reaction under the conditions employed for the amine scope of Scheme 41, computational studies were conducted to understand what differences in binding and reactivity are encountered between all these heterocyclic amines in the transition state leading to C–H cleavage.

All calculations were made using the Gaussian 16 (Revision A.03) program.²⁰⁵ All geometries were optimised at the B3LYP-D3BJ/[6-31G(d,p)/LanI2dz(Pd)] level of theory at 323.15 K and accounting for solvation effects using the self-consistent reaction field polarizable continuum model (IEF-PCM) in DMF. Single-point energies of the optimised structures were calculated at the B3LYP-D3BJ/[6-311+G(2d,p)/SDD(Pd)] level of theory, accounting for solvation as above. These functionals and basis sets have been employed in Pd-catalysed C–H activation previously.^{155,157,206} Dispersion was accounted for using Grimme's DFT-D3 scheme²⁰⁷ with Becke-Johnson damping.²⁰⁸ To confirm that the obtained transition states reside along a relevant reaction coordinate, IRC-calculations were undertaken for selected transition states.²⁰⁹ Basis-set superposition error (BSSE) was assumed to be negligible for the large basis sets employed as indicated by previous studies.²¹⁰

For its simplicity, acyclic amine **307** was chosen as the model substrate. Surprisingly, tertiary alkylamines still display a strong affinity for the formation of a bisamine complex (**327**) against their corresponding monoamine analogue (**328**), and this energy difference is comparable to hindered secondary amines (Scheme 47).^{116,123} From the unsaturated monoamine complex, an agostic complex with a resting energy of +18.8 kcal·mol⁻¹ (not shown) precedes the transition state leading to γ -C–H activation through the widely accepted concerted-metalation deprotonation (CMD) mechanism (**TS₁₅**).^{33–35} This transition state displays a conformation similar to a chair-like structure between palladium, nitrogen, the 3-carbon backbone, and hydrogen to minimise steric interactions between the hydrogens of the *N*-propyl chain. According to the Eyring equation, an overall energy barrier of 30.8 kcal·mol⁻¹ should be typically possible to overcome at temperatures around 100 °C, delivering significant product formation in 15 h. Nevertheless, the corresponding arylated amine product was never observed in the absence of ligand. Assuming that C–H activation is also the rate-limiting step of the reaction in the absence of an amino acid ligand, it was hypothesised that another reaction proceeding through a lower transition state was hampering C–H activation.

Tertiary alkylamines were used by Heck in the 70s as sacrificial reductants for the *in situ* reduction of Pd(OAc)₂ to Pd⁰, stating that the finely divided metal obtained from this process outperformed Pd⁰ precatalysts.¹²⁸ This redox process was expected to proceed through a β -H elimination pathway upon binding

of the amine additive to the palladium metal centre, resulting in the generation of an imine intermediate. In fact, this by-product has been exploited by others to achieve alternative palladium-catalysed transformations.^{130–132,211} It was considered that the decomposition of amine **307** through β -H elimination could also arise from monoamine complex **328**, becoming a deleterious competing pathway.



Scheme 47: Ligandless pathway for the C(sp³)-H activation of acyclic amine **307**. Energy values in kcal·mol⁻¹.

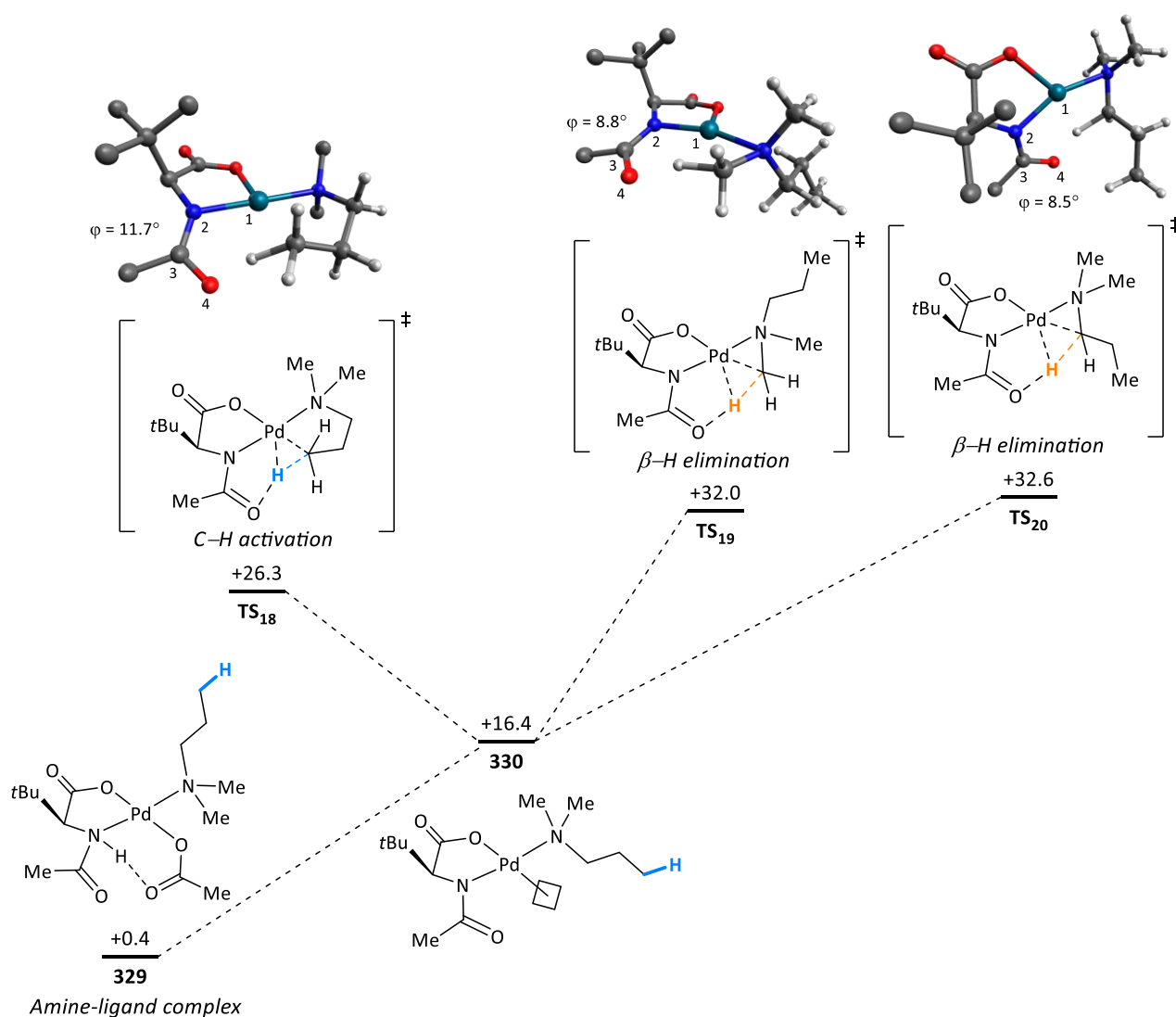
It was found that an acetate-mediated CMD transition state is also operative during β -H elimination, where a concerted redox process reduces the metal centre without the formation of a Pd-H intermediate (**TS₁₆**). Amine decomposition was assessed with both alkyl substituents, finding that formation of the *a priori* more stable imine product, arising from α -C-H cleavage at the *N*-propyl chain, proceeded through a higher transition state (**TS₁₇**). This is the case because α -C-H cleavage occurs through a flat 4-membered ring TS between palladium, nitrogen, carbon and hydrogen, causing the amine backbone to adopt an eclipsed conformation through the reacting C-N bond with greater torsional strain in **TS₁₇** than in the abstraction of

the α -C-H bond in a *N*-methyl substituent (**TS₁₆**). The dihedral angle between palladium, nitrogen, carbon and the cleavable hydrogen is an excellent descriptor of this effect (not shown in Scheme 47 to avoid confusion with the reported dihedral angle for acetate and palladium). While **TS₁₆** displays an angle of 0.8°, **TS₁₇** occurs through a less favourable 12.5°, indicative of a poorer orbital overlap in the arising imine π -bond, and resulting in a difference of +1.5 kcal·mol⁻¹ between both transition states. The lack of reactivity in the absence of ligand can therefore be attributed to β -H elimination possessing a lower transition state than C-H activation, thus leading to substrate decomposition rather than to the formation of the desired palladacycle.

The same reaction pathway and transition states were calculated replacing both acetate anions by the acetyl-*tert*-leucine ligand, to study if the ligand can differentiate between these two base-mediated processes. As previously observed by others, the use of mono-protected amino acid (MPAA) ligands in C-H activation is believed to occur through a bidentate coordination mode (see Section 1.5.).^{155,157,158} Addition of this ligand to monoamine complex **328** resulted in a significantly enhanced stability where one of the acetates remains bound to palladium while displaying hydrogen-bonding to the N-H bond of the acetamide (**329**, Scheme 48). Interestingly, this monoamine-ligand complex can compete with the stability of bisamine complexes, displaying an energy difference of only +0.4 kcal·mol⁻¹ between them. Intramolecular ligand deprotonation leads to complex **330** while releasing acetic acid and generating a vacant site. This can form an agostic complex with a γ -C-H bond and with an energy resting state of +18.3 kcal·mol⁻¹ (not shown) leading to C-H activation (**TS₁₈**), or it can be used to access the same concerted transition state of β -H elimination, thus leading to amine decomposition (**TS₁₉** and **TS₂₀**).

As it could be anticipated, the replacement of an acetate anion by a stronger acetamide base facilitates C-H cleavage, decreasing the barrier for C-H activation by -4.5 kcal·mol⁻¹. However, the same strong base through the same CMD pathway resulted in a subtle increase of the energy barrier for transition states leading to β -H elimination (**TS₁₉** and **TS₂₀**). The amine conformations in the transition states of Scheme 48 are identical to those of Scheme 47, and puts the spotlight on the geometrical constraints of the ligand. After careful analysis of the atomic distances between Pd-H, the cleaved C-H, and the formed O-H and Pd-C from **TS₁₅** to **TS₂₀**, only absolute differences below 0.05 Å were observed, which cannot be the origin of such divergent behaviour in the energy barriers. On the other hand, a difference was noted in the dihedral angle between acetate and/or acetamide with palladium. These are significantly similar for transition states leading to γ -C-H activation (9.6° for **TS₁₅** compared to 11.7° for **TS₁₈**), but differ in transition states leading to β -H elimination (0.4° for **TS₁₆** compared to 8.8° for **TS₁₉**). Acetate anions possess a high degree of freedom, adapting themselves to the most favourable amine conformation in order to maximise orbital overlap between hydrogen, oxygen, and palladium, but the acetamide motif is dependant of the amino acid backbone. The bulky *tert*-butyl substituent of the ligand is favourably positioned above the palladium complex to minimise steric interactions, which displaces the acetamide moiety below the palladium complex due to the planar

geometry of the deprotonated nitrogen. In fact, complex **330**, arising after acetamide deprotonation, displays a dihedral angle of 17.4° . This restriction in mobility is scarcely noticeable during C–H activation, where the liberated acetate base performs γ -C–H cleavage from an angle of 9.6° . However, α -C–H cleavage occurs through a coplanar 4-membered ring TS between palladium, nitrogen, carbon and hydrogen, which positions the acetate base in a negligible angle of 0.4° (**TS₁₆**). This optimal geometry for β -H elimination is now inaccessible for the acetamide of the ligand, occurring through a more distorted angle of 8.8° , and causing the energy barrier to be increased by $+1.8$ kcal·mol⁻¹ from **TS₁₆** to **TS₁₉** despite using a stronger base for C–H cleavage. Overall, the transition state leading to ligand-assisted C–H activation (**TS₁₈**) possesses the lowest energy barrier and a difference of -5.7 kcal·mol⁻¹ compared with its β -H elimination analogue (**TS₁₉**), hence leading to product formation.



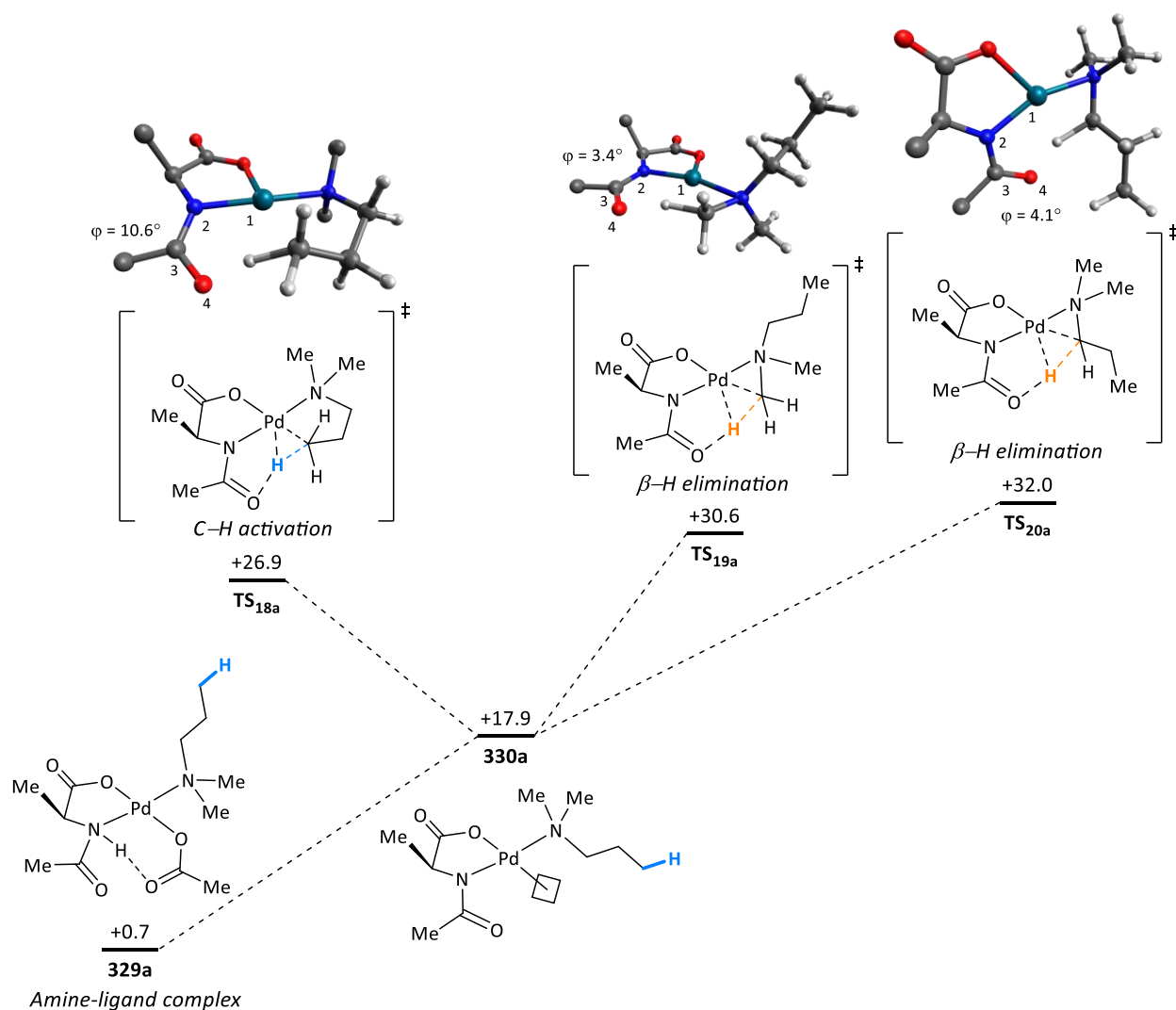
Scheme 48: Ligand-enabled C(sp³)-H activation of acyclic amine **307**. Energy values in kcal·mol⁻¹.

Table 7 summarises all the aforementioned angle and energy differences to facilitate direct comparison between them.

		Base	Dihedral angle (φ) Pd-O-C-O for acetate Pd-N-C-O for acetamide	Dihedral angle (φ) Pd-N-C-H	ΔG (kcal·mol ⁻¹)
C-H act.	TS ₁₅	OAc	9.6°	-	+30.8
	TS ₁₈	-NHAc	11.7°	-	+26.3
β -H elim.	TS ₁₆	OAc	0.4°	0.8°	+30.2
	TS ₁₇	OAc	1.3°	12.5°	+31.7
	TS ₁₉	-NHAc	8.8°	10.4°	+32.0
	TS ₂₀	-NHAc	8.5°	18.2°	+32.6

Table 7: Comparison of the transition states of acyclic amine **307** using acetyl-*tert*-leucine as a ligand.

To corroborate the influence of the *tert*-butyl substituent of the ligand in β -H elimination through the detrimental positioning of the acetamide base, the same intermediates and transition states were calculated for acetyl-alanine as a ligand, expecting that the less bulky methyl substituent of this residue would lower the energy barriers for β -H elimination.



Scheme 49: Acetyl-alanine as a ligand for C(sp³)-H activation of acyclic amine **307**. Energy values in kcal·mol⁻¹.

Indeed, it was found that the less restrictive methyl substituent favours a better coplanarity of the acetamide base with the palladium complex, resulting in lower dihedral angles and lower energy barriers for the analogue transition states leading to β -H elimination (**TS**_{19a} and **TS**_{20a}). The already favourable dihedral angle for C-H activation exhibits no significant differences (**TS**_{18a}), thus leading to a decrease in the energy difference between C-H activation and β -H elimination from -5.7 kcal·mol⁻¹ (for acetyl-*tert*-leucine ligand) to -3.7 kcal·mol⁻¹ (for acetyl-alanine ligand). To facilitate direct comparison between both ligands, Table 8 summarises all the aforementioned angle and energy differences for acetyl-alanine as the ligand of choice.

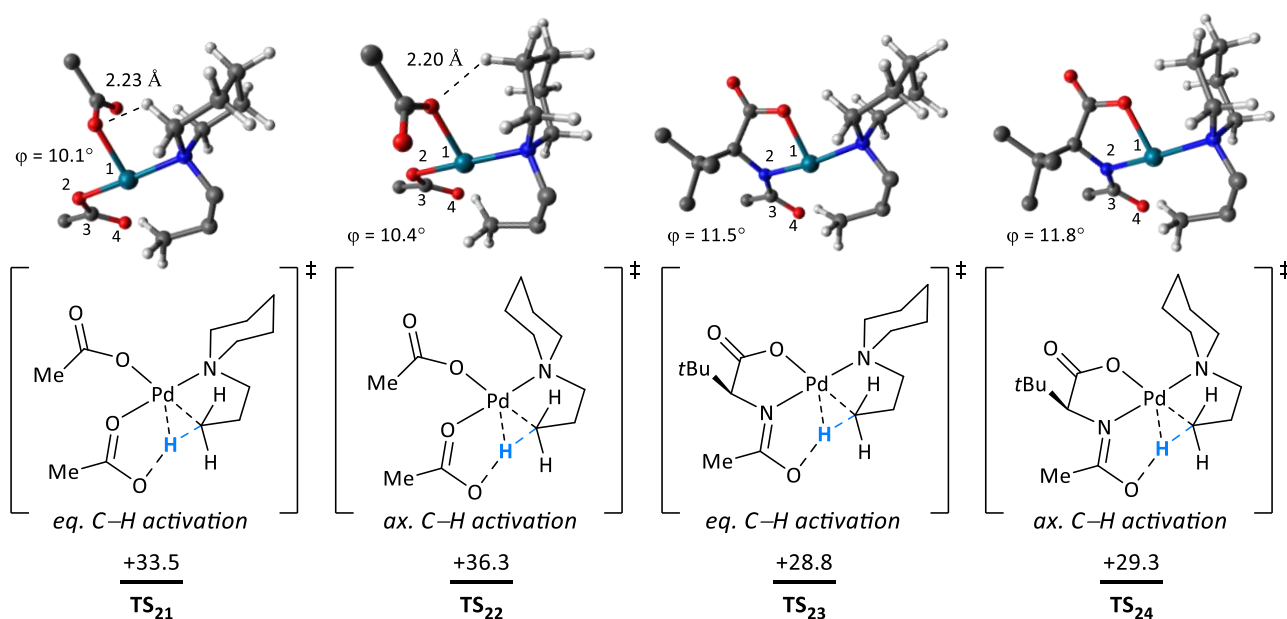
		Base	Dihedral angle (φ)	Dihedral angle (φ)	ΔG (kcal·mol ⁻¹)
			Pd-O-C-O for acetate Pd-N-C-O for acetamide	Pd-N-C-H	
C-H act.	TS ₁₅	OAc	9.6°	-	+30.8
	TS _{18a}	-NHAc	10.6°	-	+26.9
β -H elim.	TS ₁₆	OAc	0.4°	0.8°	+30.2
	TS ₁₇	OAc	1.3°	12.5°	+31.7
	TS _{19a}	-NHAc	3.4°	4.5°	+30.6
	TS _{20a}	-NHAc	4.1°	12.8°	+32.0

Table 8: Comparison of the transition states of acyclic amine **307** using acetyl-alanine as a ligand.

Overall, these findings provide a solid hypothesis of how β -H elimination can be disfavoured when using acetylated amino acid ligands. The proposed model supports that (a) C-H activation of tertiary alkylamines occurs through a concerted-metalation deprotonation (CMD) transition state in the presence of acetates or the acetamide of the ligand, as observed by others for alternative substrates;^{33-35,155,157,158} (b) β -H elimination is a competing reaction pathway which also occurs through a CMD transition state when using intramolecular bases such as acetate or acetamide, without any evidence for the formation of a Pd-H intermediate;²¹² (c) the ligand α -side chain restricts the mobility of the acetamide base and it positions it out of the plane of geometry of the palladium complex. This has a positive impact in γ -C-H activation, benefiting from the use of a stronger intramolecular base, but impedes the abstraction of α -C-H bonds through a β -H elimination process; (d) from the multiple α -C-H bonds susceptible to amine decomposition, β -H elimination occurs more readily through transition states where an excellent orbital overlap between Pd-N and the broken C-H bond can be achieved without torsional strain in the amine backbone.

To further validate this model, and to assess if these conclusions are valid for other amine substrates, the same transition states were calculated for the experimental model substrate *N*-propyl piperidine (**210**). The use of piperidine as the coordinating nitrogen incorporates another variable to the calculations because palladium can coordinate to the nitrogen lone pair through an axial or equatorial binding. Scheme 50 displays the most relevant transition states obtained for C-H activation through acetate and ligand mediated pathways. It is quickly noticeable that the energy barriers for C-H activation using an acetate base are

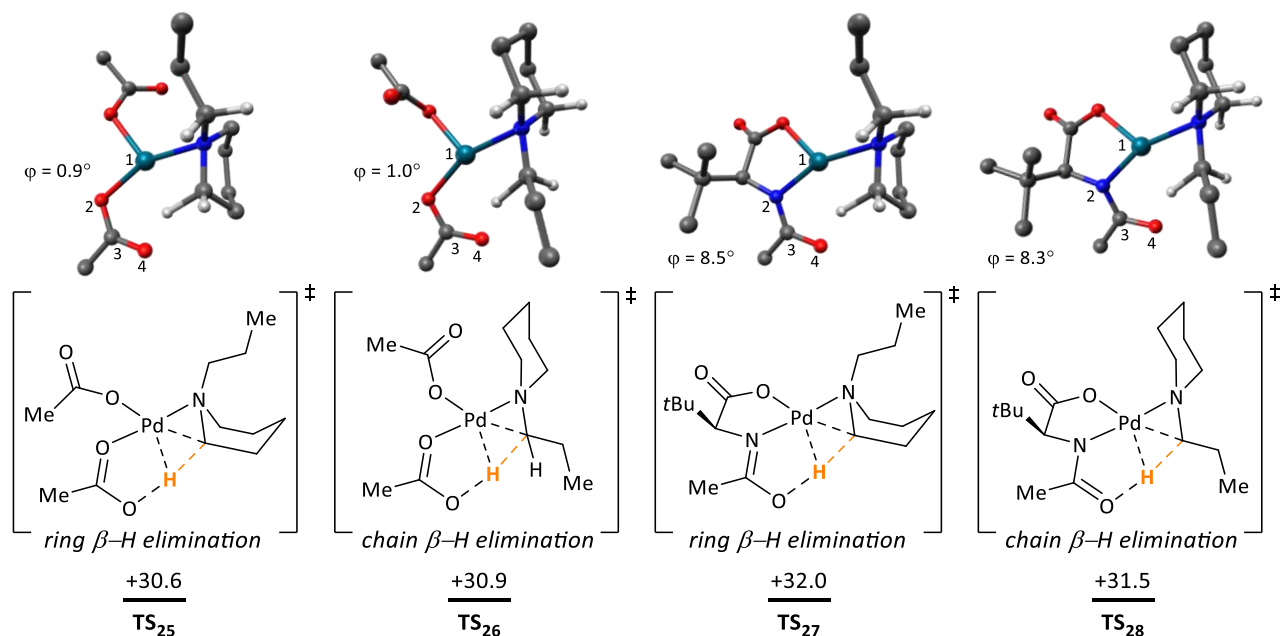
significantly higher in energy than for acyclic amine **307**. With C–H cleavage proceeding through a chair-like conformation, the nitrogen atom of the amine is briefly forming a highly restricted spirocycle with no room to minimise detrimental interactions. Comparison between ligandless **TS₁₅**, **TS₂₁**, and **TS₂₂** delivers a distance of 2.44 Å, 2.23 Å, and 2.20 Å respectively, between the oxygen atom of the acetate bounded to palladium and the closest α- or β-C–H bond of the amine substrate. The latter distances fall below the sum of Van der Waals radius for both atoms, thus indicating a steric interaction. This is more profound when palladium is bounded through an axial conformation, with the piperidine displaying staggered angles of 51° in order to minimise this repulsion, hence the difference of 2.8 kcal·mol⁻¹ between **TS₂₁** and **TS₂₂**. The amino acid ligand has a bite angle of 79° in comparison with a value of 88° for the free acetates. For this reason, a ligand-enabled C–H activation proceeds through **TS₂₃** or **TS₂₄** with a marginal difference of 0.5 kcal·mol⁻¹. Analogously to amine **307**, piperidine **210** benefits from a decrease of -4.7 kcal·mol⁻¹ (**TS₂₁** vs **TS₂₃**) in the C–H activation barrier when using the amino acid ligand as it occurs through a very similar base-palladium dihedral angle, but it uses a stronger intramolecular base.



Scheme 50: Transition states leading to C(sp³)-H activation for piperidine **210**. Energy values in kcal·mol⁻¹.

When considering the different transition states leading to β–H elimination, these can target an α–C–H bond of the piperidine ring (**TS₂₅**) or the propyl chain (**TS₂₆**, Scheme 51). Interestingly, C–H cleavage at the piperidine ring displayed the lowest energy barrier despite occurring through an unfavourable boat conformation (**TS₂₅**). The energy penalty of this conformation is apparently recovered by the excellent orbital overlap between the electrons of the Pd–N bond and the broken C–H bond (φ = 2.5°, Table 9). As previously observed for acyclic substrates, proton abstraction from the propyl chain in **TS₂₆** implies significant torsional strain and poorer orbital overlap (φ = 11.3°, Table 9), making this transition state less favourable. When attempting β–H elimination using acetyl-*tert*-leucine ligand (**TS₂₇** and **TS₂₈**), the restricted mobility of the

acetamide base difficulties C–H cleavage ($\varphi = 8.3\text{--}8.5^\circ$), resulting in higher energy barriers despite using a stronger intramolecular base. Direct comparison of ligand-assisted C–H activation in **TS**₂₃ and β –H elimination in **TS**₂₈ delivers an energy gap of $-2.7\text{ kcal}\cdot\text{mol}^{-1}$, sufficient to largely avoid amine decomposition.



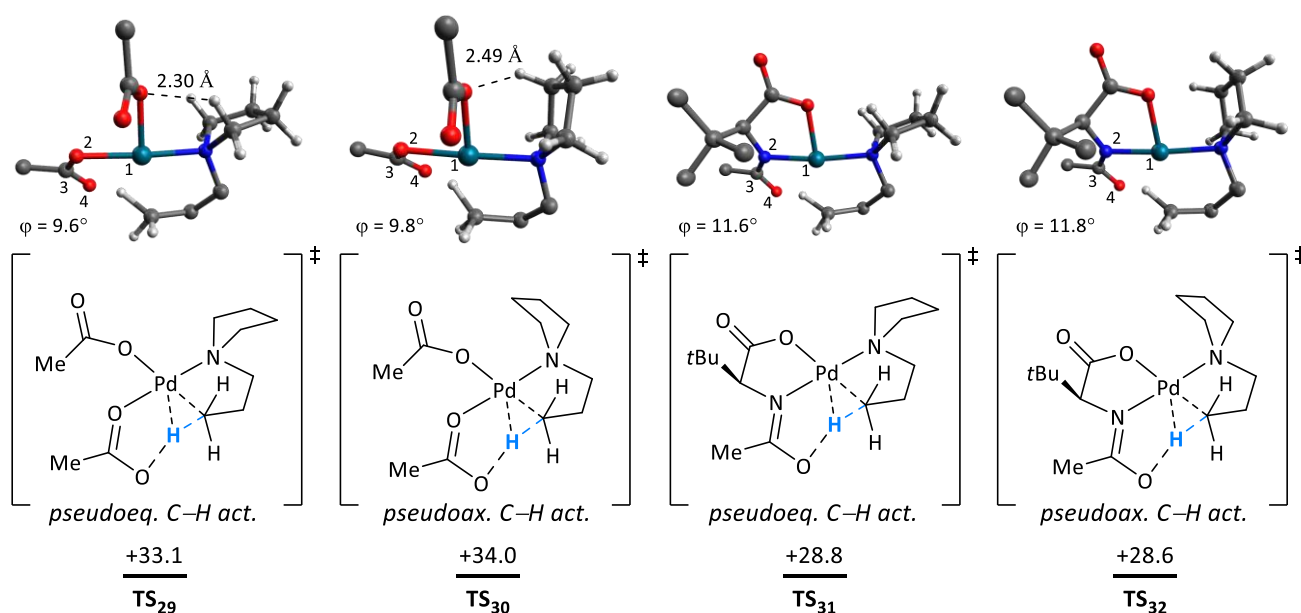
Scheme 51: Transition states leading to β –H elimination for piperidine **210**. Energy values in $\text{kcal}\cdot\text{mol}^{-1}$.

Among the 8 most representative transition states found for piperidine **210**, the lowest energy barrier belongs to ligand-assisted γ –C–H activation, hence rationalising the high yields observed experimentally for this amine heterocycle. Most importantly, the findings and conclusions obtained for acyclic amine **307** are still valid for this class of heterocycle, thus reinforcing the robustness of this mechanistic model. Table 9 summarises all the aforementioned angle and energy differences between transition states using piperidine **210** to facilitate direct comparison between them.

		Base	Dihedral angle (φ) Pd–O–C–O for acetate Pd–N–C–O for acetamide	Dihedral angle (φ) Pd–N–C–H	ΔG ($\text{kcal}\cdot\text{mol}^{-1}$)
C–H act.	TS ₂₁	OAc	10.1°	-	+33.5
	TS ₂₂	OAc	10.4°	-	+36.3
	TS ₂₃	-NHAc	11.5°	-	+28.8
	TS ₂₄	-NHAc	11.8°	-	+29.3
β –H elim.	TS ₂₅	OAc	0.9°	2.5°	+30.6
	TS ₂₆	OAc	1.0°	11.3°	+30.9
	TS ₂₇	-NHAc	8.5°	6.2°	+32.0
	TS ₂₈	-NHAc	8.3°	16.2°	+31.5

Table 9: Comparison of the transition states of piperidine **210** using acetyl-*tert*-leucine as a ligand.

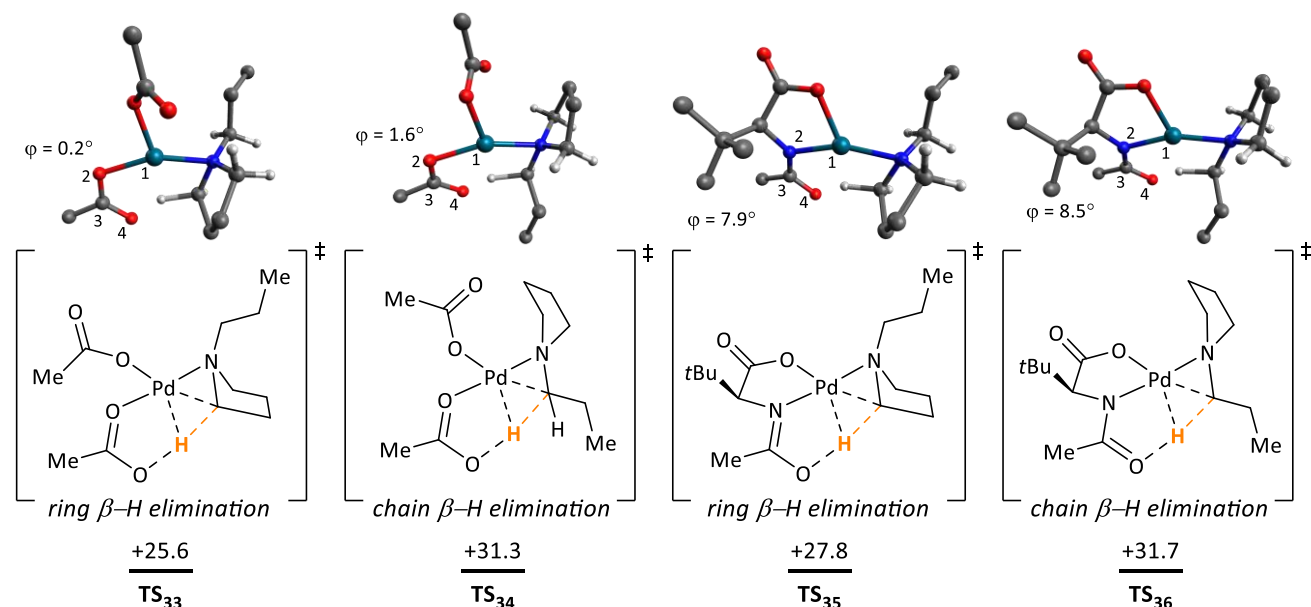
The *in silico* competition between γ -C-H activation and β -H elimination has been found to be favourable for product formation in acyclic amines and piperidine substrates, in line with experimental results. Equally important is also to assess if unreactive heterocycles can also be predicted by this model. Pyrrolidine substrates afforded very poor conversions to the desired arylated product with significant loss in the recovered amine reagent (**257**, Scheme 41). The transition states leading to C-H activation in *N*-propyl pyrrolidine (**331**) display extremely similar energy barriers and dihedral angles compared to those previously obtained for piperidine **210** (**TS₂₉**–**TS₃₂**), notable factor being the significant reduction in sterics between acetate and the C-H bonds of the heterocycle. A reduction of -4.3 kcal·mol⁻¹ when using the amino acid ligand (**TS₂₉** vs **TS₃₂**) is in line with all previous amine substrates and doesn't explain the lack of reactivity in 5-membered ring scaffolds. Of note, the lower ligand bite angle reverses the stability between pseudo-axial and pseudo-equatorial palladium binding (**TS₃₁** vs **TS₃₂**).



Scheme 52: Transition states leading to C(sp³)-H activation for pyrrolidine **331**. Energy values in kcal·mol⁻¹.

Interestingly, transition states leading to β -H elimination were found to be lower in energy than **TS₃₂**, explaining the decomposition and lack of reactivity of this substrate (Scheme 53). The pyrrolidine backbone does not possess well-defined chair-like conformations like piperidine, and it is actually forced to adopt eclipsed conformations in envelope or half-chair conformations. This is unfortunately the ideal conformation from where β -H elimination takes place, as it permanently positions the reacting α -C-H bond in close proximity to the nitrogen lone pair. As a result, β -H elimination occurs through the very facile and ligandless **TS₃₃** with an ideal dihedral angle of 0.2° for the acetate base and 1.8° between the reacting C-H bond and the nitrogen lone pair. The distorted β -H elimination induced by the ligand is unable to compete with this heterocycle conformation (**TS₃₅**), leaving the barrier for C-H activation $+0.8$ kcal·mol⁻¹ higher than for amine

decomposition (**TS**₃₂). Nevertheless, this difference is not enough to completely avoid the formation of the desired palladacycle, thus leading to small amounts of γ -arylated product.



Scheme 53: Transition states leading to β -H elimination for pyrrolidine **331**. Energy values in kcal·mol⁻¹.

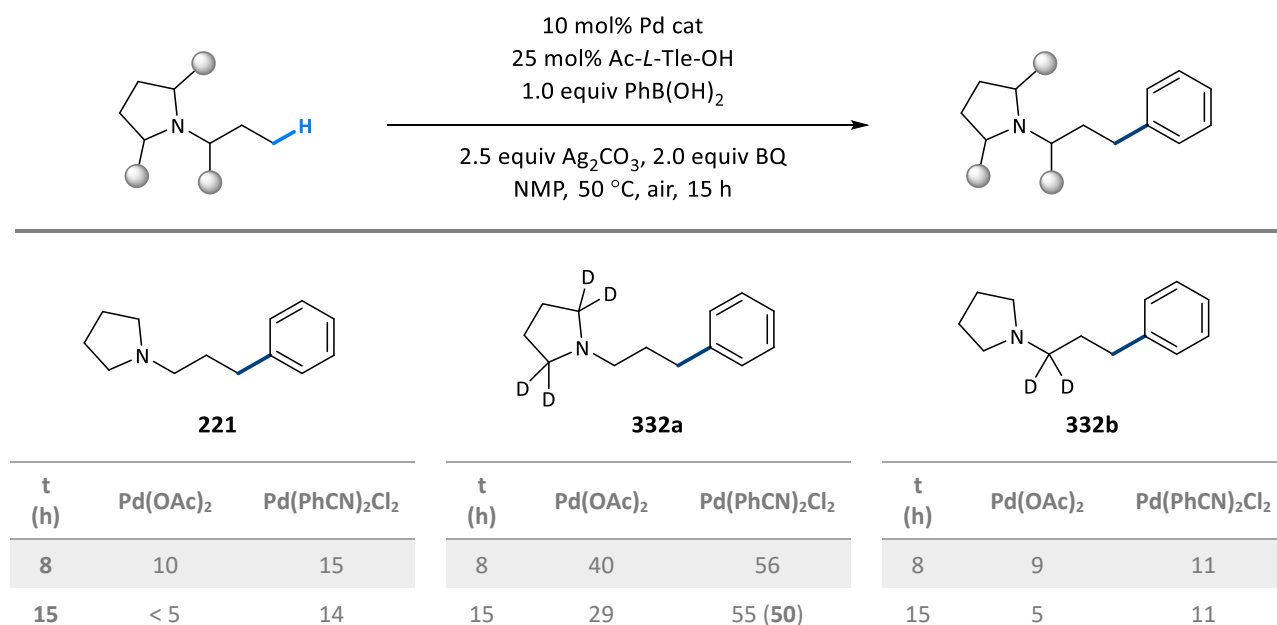
For consistency with the previously studied amines, Table 10 summarises all the aforementioned angle and energy differences when using *N*-propyl pyrrolidine (**331**) to facilitate direct comparison between them.

		Base	Dihedral angle (φ) Pd-O-C-O for acetate Pd-N-C-O for acetamide	Dihedral angle (φ) Pd-N-C-H	ΔG (kcal·mol ⁻¹)
C-H act.	331				
	TS ₂₉	OAc	9.6°	-	+33.1
	TS ₃₀	OAc	9.8°	-	+34.0
	TS ₃₁	-NHAc	11.6°	-	+28.8
	TS ₃₂	-NHAc	11.8°	-	+28.6
β -H elim.	TS ₃₃	OAc	0.2°	1.8°	+25.6
	TS ₃₄	OAc	1.6°	10.5°	+31.3
	TS ₃₅	-NHAc	7.9°	9.5°	+27.8
	TS ₃₆	-NHAc	8.5°	15.6°	+31.7

Table 10: Comparison of the transition states of pyrrolidine **331** using acetyl-*tert*-leucine as a ligand.

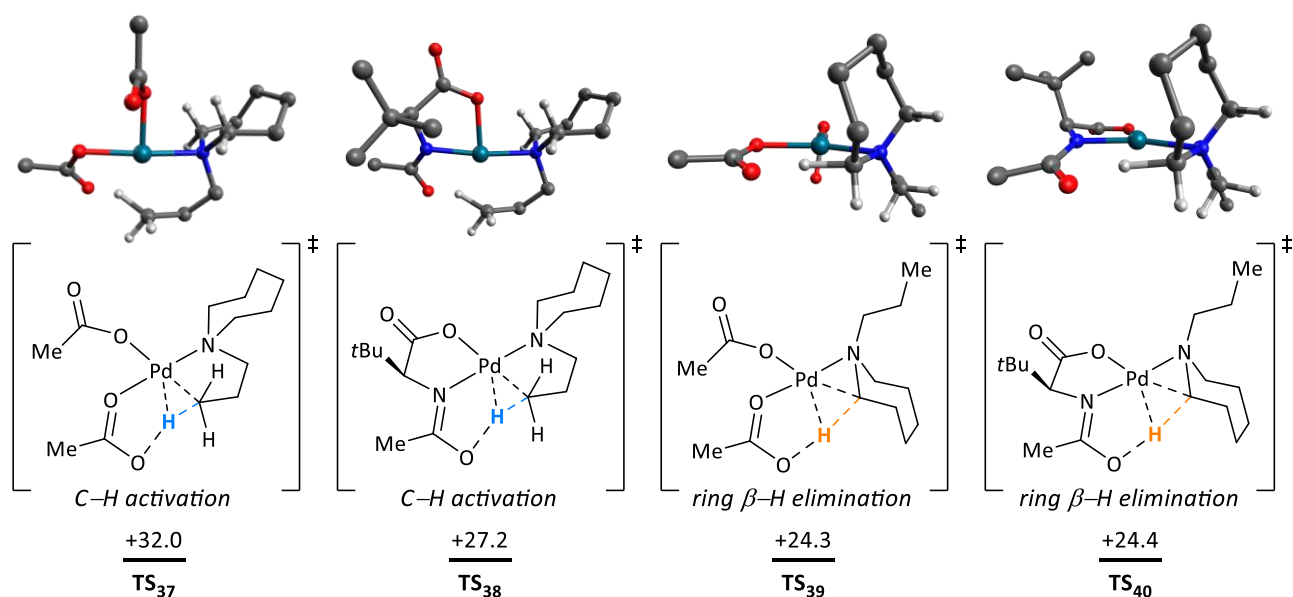
The little difference in energy between γ -C-H activation and β -H elimination in pyrrolidine substrates was exploited for further experimental studies. It was hypothesised that, if both processes occur through a CMD-type mechanism, the transition state of β -H elimination must be affected by isotope experiments in a similar manner to C-H activation, where a large KIE of 2.53 was observed. The use of *N*-propyl pyrrolidine (**331**) in combination with Pd(OAc)₂ delivered little product formation under standard reaction conditions, and

evidenced the decomposition over time of arylated product **221** (Scheme 54). Replacement of the pervasive Pd(OAc)₂ by Pd(PhCN)₂Cl₂, a precatalyst with no bidentate anions capable of performing C–H cleavage, led to a significant increase of product formation without observable erosion over time. It was hypothesised that the absence of acetate anions disfavoured TS₃₃ as a viable reaction pathway, hence relying in the small difference of 0.8 kcal·mol⁻¹ between a ligand-assisted C–H activation (TS₃₂) and β–H elimination (TS₃₅). Remarkably, a α-deuterated pyrrolidine analogue afforded better reactivity to achieve 40% ¹H-NMR yield of arylated amine **332a**. This substrate also exhibited product decomposition when using Pd(OAc)₂, something not observed for the Pd(PhCN)₂Cl₂ precatalyst. Overall, this new palladium source facilitated the isolation of γ-arylated pyrrolidine **332a** in a 50% yield and provided an experimental evidence for the competition between C–H activation and β–H elimination in palladium-catalysed reactions using tertiary alkylamines. For consistency, deuteration of the α-C–H bonds of the propyl substituent had no impact in product formation (**332b**), thus pointing to the conclusion that β–H elimination is occurring preferentially at the pyrrolidine ring, as predicted by the computational model.



Scheme 54: Use of α-deuterated pyrrolidine heterocycles to study β–H elimination. Reactions conducted at 0.3 mmol. Yield determined by ¹H-NMR using 1,1,2,2-tetrachloroethane as internal standard. Isolated yield in bold.

The use of azepane as the directing heterocycle failed in delivering any arylated product for this palladium reaction (**255**, Scheme 41). As expected, C–H activation proceeds through a pseudo-equatorial palladium binding and the use of acetyl-*tert*-leucine diminishes the energy barrier for this pathway by –4.8 kcal·mol⁻¹ (TS₃₇ vs TS₃₈, Scheme 55). Nevertheless, this reduction in energy is once again unable to compete with amine decomposition.



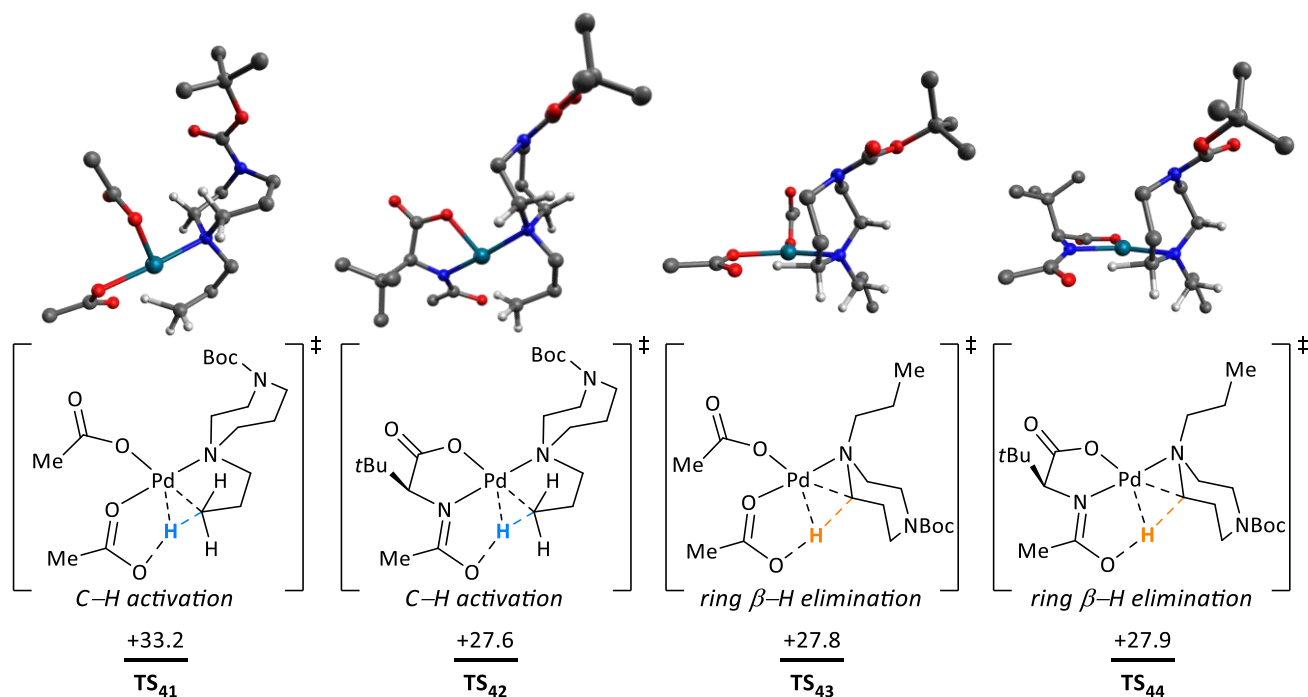
Scheme 55: Transition states leading to C–H activation or β –H elimination in azepane (**333**). Energy values in kcal·mol⁻¹.

The flexible azepane possesses multiple interconvertible chair or twist-chair conformations which can adapt its shape in each transition state to disfavour steric interactions. Unfortunately, this heterocycle can find multiple stable conformations where the reacting α -C–H bond and the nitrogen lone pair are placed in an eclipsed conformation, resulting in a very facile β –H elimination process (**TS**₃₉) and in an energy difference of +2.8 kcal·mol⁻¹ in favour of amine decomposition (**TS**₃₈ vs **TS**₄₀). This gap is significantly larger than for a pyrrolidine ring (**331**) and avoids any product formation. Table 10 summarises all the relevant dihedral angles and energy differences for azepane (**333**).

		Base	Dihedral angle (φ) Pd–O–C–O for acetate Pd–N–C–O for acetamide	Dihedral angle (φ) Pd–N–C–H	ΔG (kcal·mol ⁻¹)
C–H act.	TS ₃₇	OAc	9.1°	-	+32.0
	TS ₃₈	-NHAc	11.0°	-	+27.2
β –H elim.	TS ₃₉	OAc	0.2°	3.6°	+24.3
	TS ₄₀	-NHAc	7.8°	9.7°	+24.4

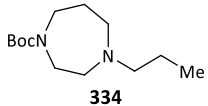
Table 10: Comparison of the transition states of azepane **333** using acetyl-*tert*-leucine as a ligand.

This computational model has successfully predicted the reason why different amine heterocycles can access or not product formation in this palladium-catalysed arylation reaction. To assess its limitations, it was questioned why a protected diazepane (**334**) delivered the expected γ -arylated product (**256**, Scheme 41), while its azepane analogue (**333**) did not (**255**, Scheme 41). Scheme 56 compares the most stable transition states for C–H activation and β –H elimination with and without the acetyl-*tert*-leucine ligand.



Scheme 56: Transition states leading to C–H activation or β –H elimination in diazepane **334**. Energy values in kcal·mol⁻¹.

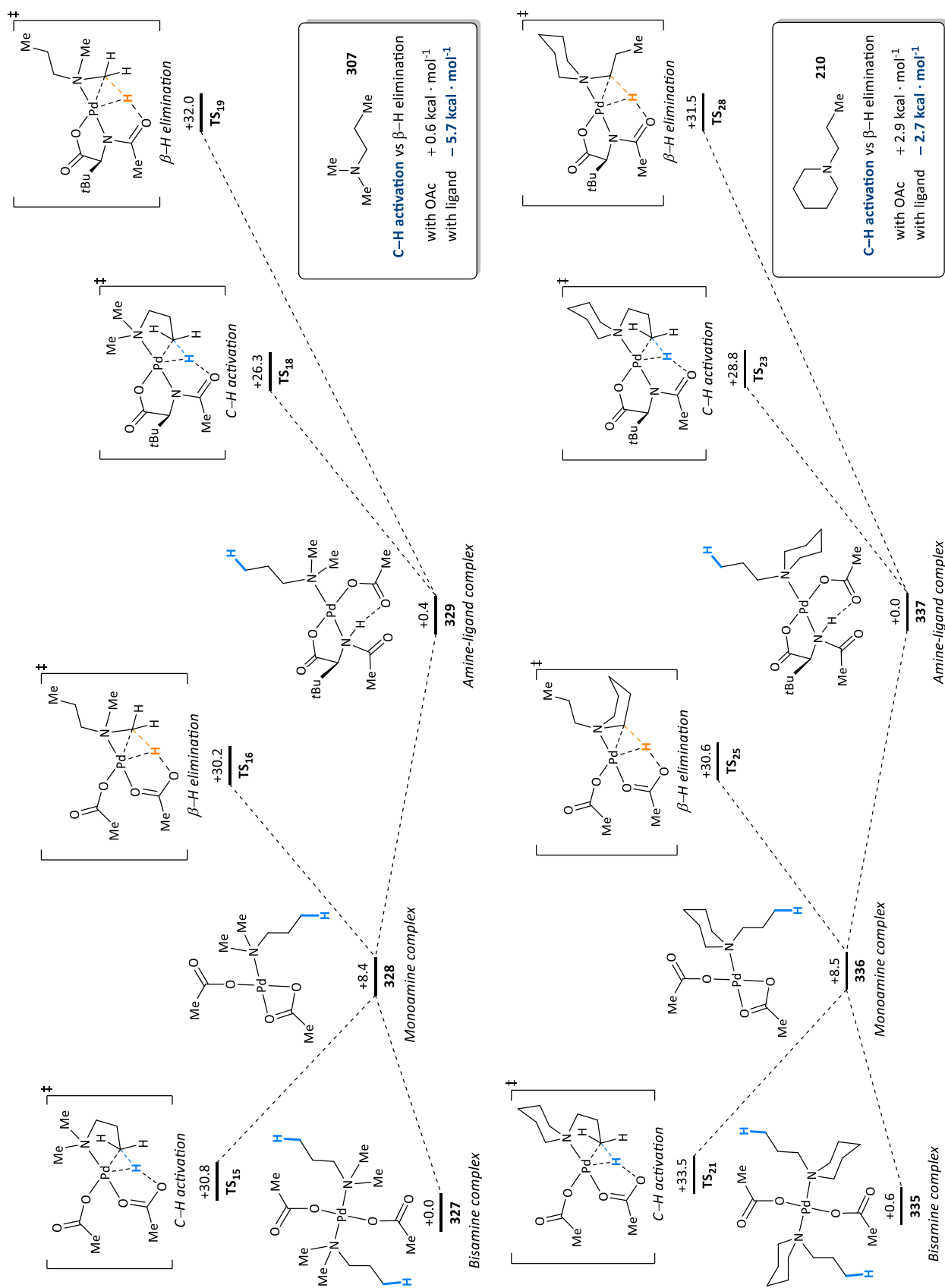
In agreement with experimental findings, a marginal difference of -0.3 kcal·mol⁻¹ is observed in favour of C–H activation (**TS**₄₂ vs **TS**₄₄) when using amino acid ligands, which can lead to significant amounts of product formation when considering the excess of 2.5 equivalents of amine starting material used. However, no significant differences are observed when comparing the dihedral angles in the transition state leading to β –H elimination in azepane (**TS**₄₀, Table 10) and diazepane (**TS**₄₄, Table 11) substrates. The increase in the energy barrier for β –H elimination in diazepane substrates is explained with the more subtle restricted conformation of the amine heterocycle. The *-Boc* protected nitrogen forces an inherent coplanarity between both of its *sp*³ carbon substituents and the oxygens of this protecting group. Due to the cyclic nature of these carbon substituents, a steric interaction arises between some of its hydrogens and the vicinal oxygens. During C–H activation, the diazepane heterocycle can adopt multiple conformations in both pseudoaxial or pseudoequatorial binding modes to minimise this interaction (**TS**₄₂). However, the more restricted amine conformation in β –H elimination reactions is less capable of accommodating its shape (**TS**₄₄), resulting in an increase in its energy barrier when compared with **TS**₄₀ of azepane. The steric interactions arising from the more restricted conformation of diazepane are noticeable in the propyl substituent of this amine, which displays unusual staggered conformations of 51° (**TS**₄₃ and **TS**₄₄).



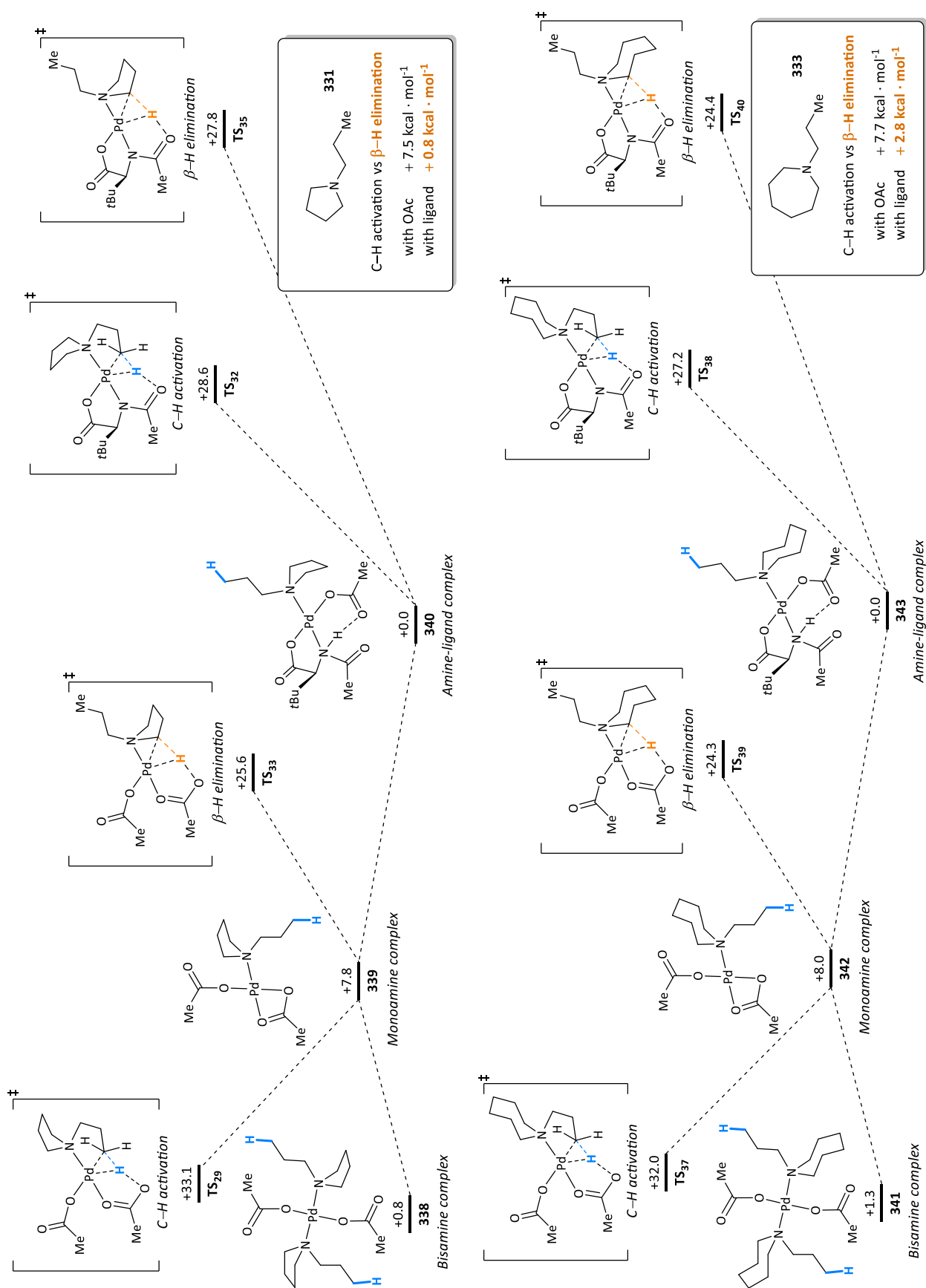
		Base	Dihedral angle (φ) Pd–O–C–O for acetate Pd–N–C–O for acetamide	Dihedral angle (φ) Pd–N–C–H	ΔG (kcal·mol ⁻¹)
C–H act.	TS ₄₁	OAc	10.1°	-	+33.2
	TS ₄₂	-NHAc	11.8°	-	+27.6
β -H elim.	TS ₄₃	OAc	1.2°	1.7°	+27.8
	TS ₄₄	-NHAc	8.0°	9.1°	+27.9

Table 11: Comparison of the transition states of diazepane **334** using acetyl-*tert*-leucine as a ligand.

Overall, this section has developed and successfully validated a model where a competition between γ -C–H activation and β -H elimination is constantly established for each tertiary alkylamine substrate. Acetylated amino acids have been found as suitable ligands, not only to enhance C–H activation by using a stronger acetamide base, but also to disfavour β -H elimination by distorting its highly planar transition state. Each particular amine heterocycle can accommodate its conformation with more or less success to favour one pathway or the other. This study has focused on 4 tertiary alkylamine classes, acyclic amines (**307**), piperidines (**210**), pyrrolidines (**331**), and azepanes (**333**). Nevertheless, the introduction of other heteroatoms or substituents in the heterocycle can have a big impact in the amine conformations and, as a result, in the whole selectivity of the reaction, as clearly exemplified by diazepane **334**. This model can be therefore used as a preliminary step to assess if a tertiary alkylamine substrate can override amine decomposition to access fruitful C–H activation reactions. To conclude, Schemes 57 and 58 display and summarise the lowest transition states found for the aforementioned tertiary alkylamines to encapsulate the key content of this section.



Scheme 57: Computational pathway for C-H activation or β -H elimination in acyclic amines and piperidines using acetyl-*tert*-leucine as ligand. Energy values in kcal · mol⁻¹.



Scheme 58: Computational pathway for C-H activation or β -H elimination in *N*-alkyl pyrrolidines and azepanes using acetyl-*tert*-leucine as ligand. Energy values in kcal · mol⁻¹.

2.5. Summary

This chapter has demonstrated the viability of tertiary alkylamines to act as native directing substrates for palladium-catalysed C-H activation reactions. The use of aryl boronic acids as coupling partners exploits a low-valent catalytic cycle to deliver a wide range of γ -arylated products in piperidines, piperazines, morpholines, diazepanes and acyclic amines. Electron-donating and electron-withdrawing groups can be tolerated in the reacting aromatic ring, as well as electron-deficient heteroaromatic coupling partners, thus expanding the scope and synthetic applicability of this transformation. A detailed study of the reaction components determined that Ag₂CO₃ is not needed at higher reaction temperatures to access efficient product formation, with the multifaceted 1,4-benzoquinone in control of both the C(sp²)-C(sp³) reductive elimination step and the subsequent oxidation of Pd⁰ to close the catalytic cycle. Noteworthy is that this oxidation step can be performed in the absence of oxygen and becomes a rare example of 1,4-benzoquinone acting as the terminal oxidant. Overall, these findings open new possibilities for the optimisation of a greener C-H activation reaction with lower catalyst loadings and in the absence of expensive superstoichiometric silver additives.

The systematic study through computational studies of a variety of tertiary alkylamines established a constant competition between the desired γ -C-H activation reaction and a detrimental β -H elimination pathway which leads to substrate decomposition. Acetylated amino acids have been found as suitable ligands, not only to enhance C-H activation by using a stronger acetamide base, but also to disfavour β -H elimination. Interestingly, this deleterious pathway was found to proceed through the same concerted metalation-deprotonation (CMD) mechanism of γ -C-H activation, rather than through the formation of a more classical metal-hydride intermediate. The bulkiness of the ligand α -side chain proved to be crucial in positioning the key acetamide moiety out of the plane of geometry of the complex, thus distorting the highly planar 4-membered ring transition state of β -H elimination. The ability of each amine heterocycle to successfully adapt its conformation during this now more restrictive transition state will favour one pathway or the other. In an excellent agreement with experimental findings, the developed computational model accurately predicted the viability of five different classes of tertiary amine substrates to access γ -C-H activation. Among those, cyclic amines displaying stable eclipsed conformations (pyrrolidine and azepane derivatives) tend to favour a β -H elimination process, hence delivering little product formation.

Overall, these findings become the cornerstone of tertiary alkylamines as native substrates for palladium-catalysed C(sp³)-H activation reactions, and it is hoped that this knowledge will inspire future breakthroughs in the context of substrate compatibility, alternative functionalisations, or more environmentally friendly reaction conditions.

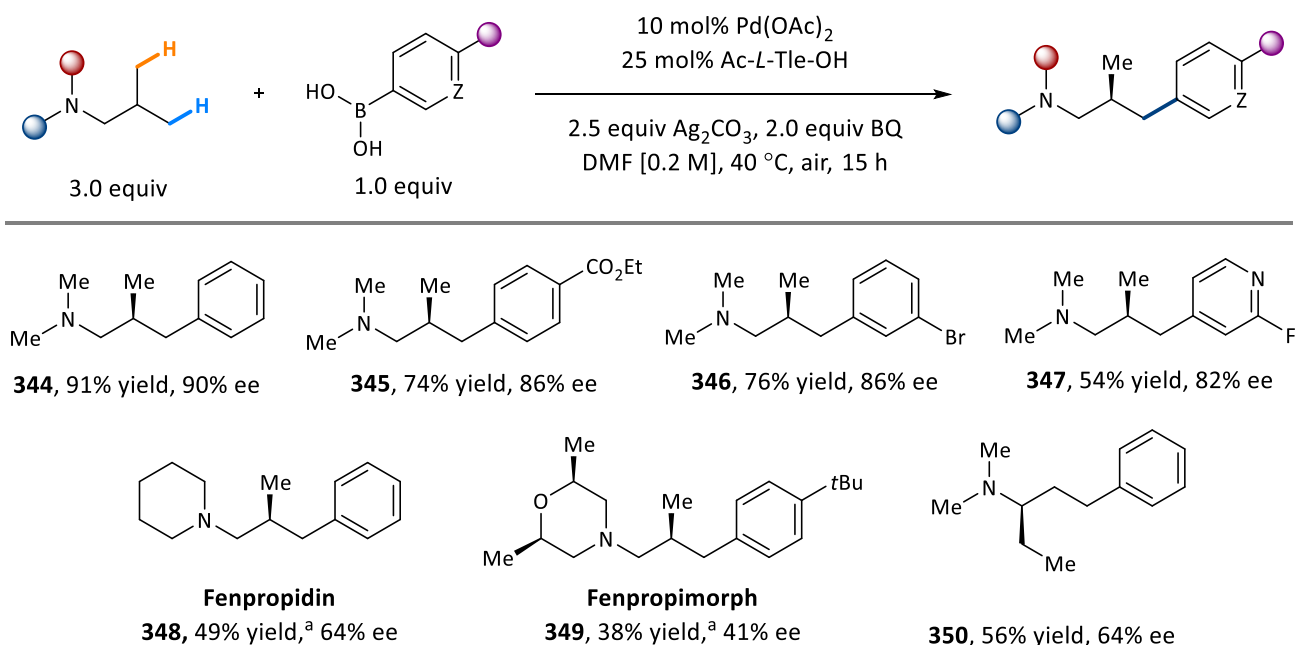
Chapter 3

Enantioselective methylene C(sp³)-H activation of tertiary
alkylamines via palladium catalysis

3.1. Background & Previous work

The previous chapter disclosed the ability of tertiary alkylamines to direct a palladium-catalysed C–H activation reaction targeting γ -methyl C–H bonds and functionalising them with aryl boronic acids as coupling partners. Key for the success of this transformation was the use of mono-protected amino acid (MPAA) ligands, which not only enhances C(sp³)-H activation by using a stronger acetamide base,^{155,157,158} but also disfavoured deleterious β -H elimination pathways. The crucial role of this ligand during C–H cleavage and its inherent chirality prompted the study of an asymmetric variant of the previously reported γ -methyl C–H activation reaction. The ability of this class of ligand to induce enantioselective C–H activation reactions is well-known in C(sp²)-H bonds,^{147–151} and their C(sp³)-H analogues.^{87,213,214} However, the relatively small size of the ligand and the large distance between its chiral centre and the cleavable C–H bond usually delivers poor asymmetry (see Scheme 34, Section 1.5.), or requires the synthesis of bespoke amino acids to achieve good enantioselectivity.

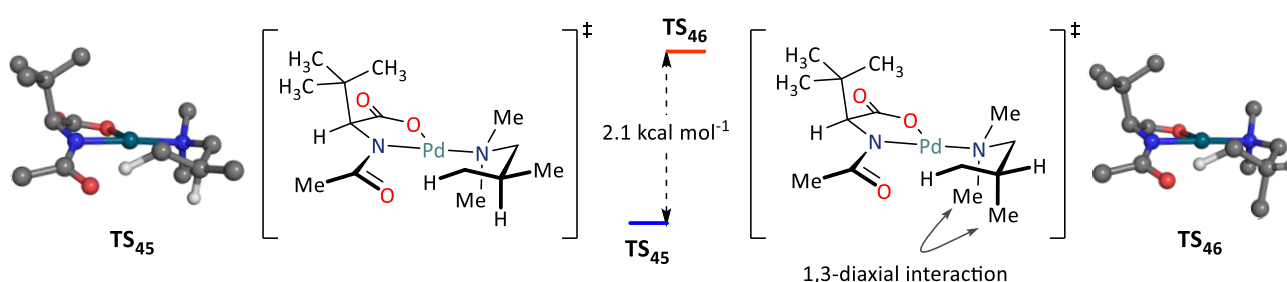
In our group, Dr. Nappi attempted to desymmetrise amines bearing geminal dimethyl substituents (Scheme 59). Taking the standard reactions conditions of the previous chapter as a starting point, and after a short optimisation, the use of DMF as the reaction solvent at lower reaction temperatures delivered an excellent 91% yield and 90% ee of arylated amine **344** using the ubiquitous *N*-acetyl-*tert*-leucine as the chiral ligand. Unexpectedly, enantiomeric excesses were slightly dependant of the boronic acid used (**345–347**), and other amine heterocycles (**348–349**) or the desymmetrisation of alternative alkyl chains (**350**) afforded more modest asymmetric inductions, thus limiting the applicability of this transformation.



Scheme 59: Desymmetrisation of γ -methyl groups in tertiary alkylamines through a palladium-catalysed C–H activation strategy. Reactions conducted at 0.3 mmol by Dr. Nappi. ^a 50 °C in NMP.

Interestingly, comparable enantioselectivity was observed when using the less bulky acetyl-alanine as ligand (86% ee), suggesting that steric parameters alone are not responsible for the observed asymmetric induction. Computational studies conducted by Dr. Flodén determined that C–H activation is occurring through a chair-like transition state, being crucial the positioning of the non-reacting methyl group during C–H cleavage (Scheme 60). The β -methyl substituent of the amine backbone can be placed in a pseudo-equatorial (**TS₄₅**) or pseudo-axial (**TS₄₆**) position, the latter being more destabilised by a pseudo-1,3-diaxial interaction between one of the *N*-methyl substituents and the non-reacting β -methyl group. This carries an energetic penalty of 2.1 kcal·mol⁻¹, which is in agreement with the observed experimental asymmetry based on the Boltzmann populations at the given temperature (calculated 88% ee for acetyl-*tert*-leucine and 83% ee for acetyl-alanine).²⁰⁶ As a control experiment, the computational model did not deliver any asymmetric induction when using acetyl-glycine.

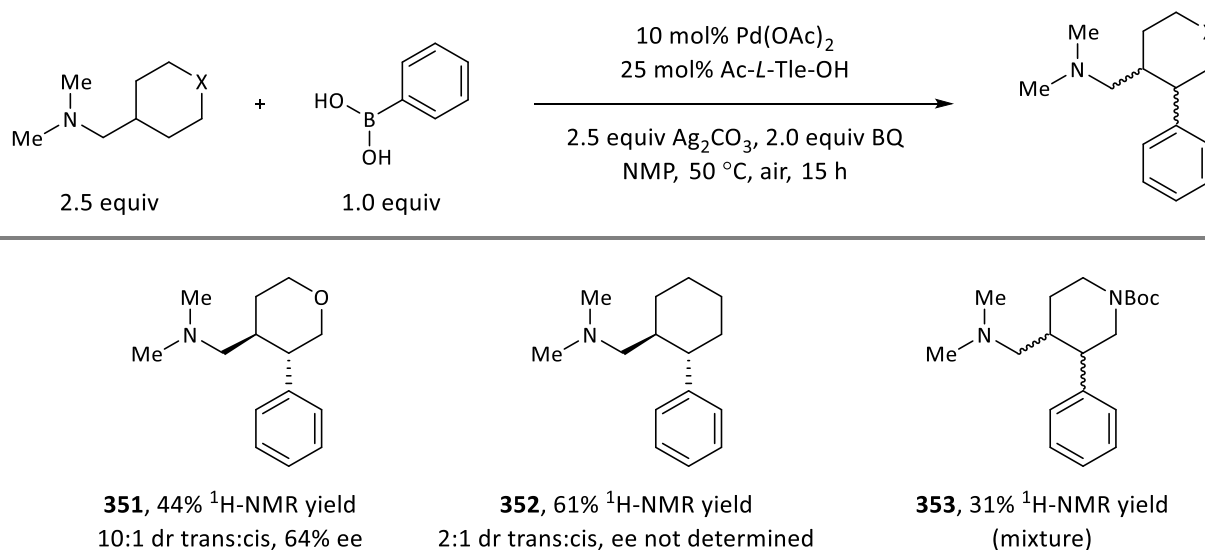
The study concluded that enantioselectivity is not achieved by a direct ligand-substrate interaction. Instead, chirality transfer relies on the projection of the acetamide moiety below the square-planar palladium complex, which limits and controls the amine conformation during C–H cleavage. This grants the simple α -methyl substituent of acetyl-alanine the rare strength to induce high levels of enantioselectivity during C–H cleavage, potentially converting this cheap and commercial chiral ligand into one of the most atom economical transformations within enantioselective catalysis. Nevertheless, this indirect mode of enantioinduction is highly dependent on the steric interactions arising in each amine substrate during C–H activation. It explains, for example, the moderate asymmetry observed for other tertiary alkylamines such as piperidine or morpholine heterocycles, or the minor enantioselectivity obtained in the *gem*-diethyl substituents of amine **350**.



Scheme 60: Computational insight into the desymmetrisation of γ -methyl groups in tertiary alkylamines through C–H activation. Energy values in kcal·mol⁻¹. Conducted by Dr. Flodén.

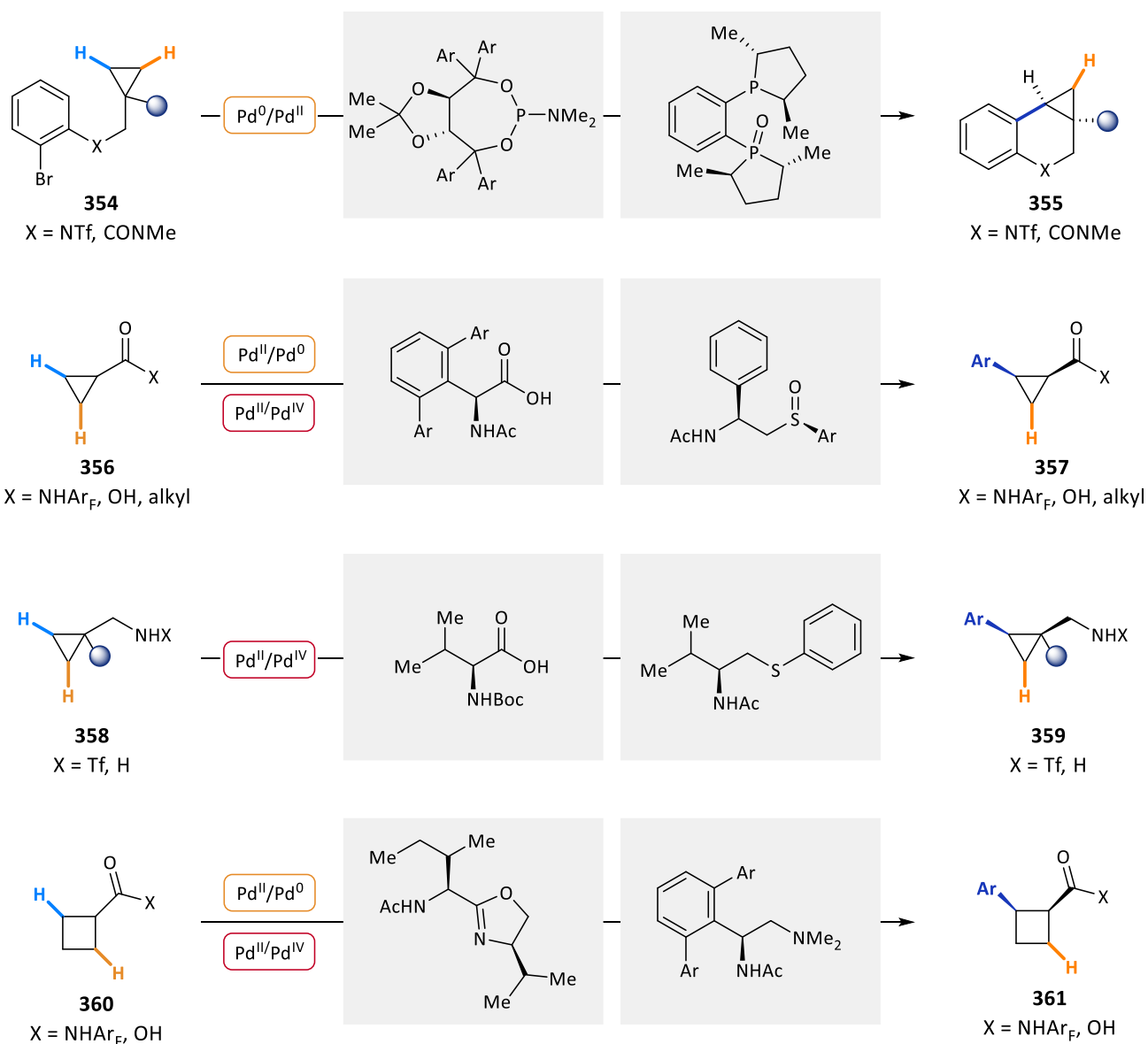
In an attempt to expand this desymmetrisation process to other acyclic amines, Dr. Azuma discovered that cyclic methylene C–H bonds were also amenable to palladium-mediated C–H cleavage, isolating arylated amine **351** in 34% yield (Scheme 61). Out of the four potential stereoisomers, acetyl-*tert*-leucine delivered notable selectivity to obtain a 10:1 diastereomeric ratio in favour of the *trans* cyclic product and a 64%

enantiomeric excess. Unfortunately, other 6-membered ring substrates afforded poor diastereoselectivity (**352–353**) and evidenced the limitations of this transformation.



Scheme 61: Enantioselective methylene C–H activation of tertiary alkylamines. Reactions conducted at 0.3 mmol by Dr. Azuma.

Enantioselective methylene C–H activation is a challenging area of research due to the increased sterics surrounding the C–H bond of this carbon unit. A recurrent way to circumvent this problem is to target the activated C–H bonds of ring-strained alkanes. The distorted angles of cyclopropane and cyclobutane and the partial hybridised character of their C–H bonds makes it easier to achieve reactivity in these substrates. One of the first enantioselective palladium-catalysed C–H activation reactions involving cyclopropanes was reported by Cramer, who used triflyl protected bromoaryl amides to achieve an intramolecular C–H cleavage after oxidative addition of Pd⁰ into aryl bromide bonds (**354**, Scheme 62).²¹⁵ This approach, later applied in similar substrates,^{216–218} provided excellent diastereoselectivity due to the bicyclic nature of the resultant product, while enantioselectivity was induced using a Taddol-derived phosphoramidite ligand. To deliver intermolecular C–H activation, a range of engineered directing groups, such as fluorinated arylamides (**356**, **360**)^{140,219–221} or triflyl amides (**358**),⁸⁷ and, more recently, simpler carboxylic acids,^{141,214} ketones,²²² and primary amines,¹¹³ have been all found as effective directing groups at promoting C–H cleavage by exploiting their coordination to the palladium metal centre. The restricted geometry of the resultant bicyclic palladacycles grants exclusive access to *cis* functionalised products, while asymmetry is typically governed by bulky bidentate ligands with an appendant key acetamide unit in the concerted metalation deprotonation (CMD) transition state. In comparison, the second ligand binding point is a recurrent tuneable handle which can be converted into a carboxylic acid, a sulfoxide, a thiophenol, an oxazoline, or an amine functional group to match the binding properties of the ligand with those of the substrate. Interestingly, an iridium-catalysed borylation has also been reported using α -substituted cyclopropylamides as directing motifs, expanding the selection of metals and functional groups amenable to C–H activation processes.²²³



Scheme 62: Literature precedents for enantioselective palladium C–H arylation reactions using alternative directing groups.

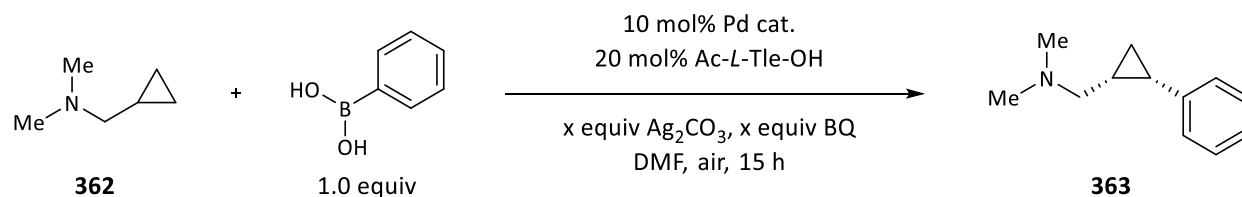
3.2. Project aims

This research aims to develop a palladium-catalysed C–H arylation reaction targeting ring-strained systems in tertiary alkylamines substrates. Preliminary results provide proof of concept that the chiral amino acid ligand is capable of inducing an asymmetric C–H cleavage in amine substrates displaying *gem*-dimethyl, *gem*-diethyl, and in tetrahydropyran substituents. To date, only one literature example is capable of using unprotected amines to perform C–H activation in ring-strained alkanes, achieving this on cyclopropane rings displaying β -substituents, and using primary amines as substrates in combination with thiophenol amine derivatives as ligands.¹¹³ Taking into account the relevance of tertiary amines in medicinal chemistry, a reaction building diastereo- and enantiopure ring-strained motifs with this appendant functional group and with the aid of readily available chiral ligands can expedite the synthesis and study of this class of compounds as viable drug candidates.

3.3. Results & Discussion

Taking the standard reaction conditions of the previous chapter as a starting point, amine **362**, containing a cyclopropylmethyl substituent, afforded an excellent reactivity to deliver the corresponding *cis* arylated product as the only diastereoisomer in 94% yield and with an enantiomeric excess of 98% (entry 1, Table 12). Upon variation of the reaction conditions, two significant problems were detected. Firstly, the reaction was highly dependent on temperature, obtaining a more moderate 52% yield at 40 °C (entry 2). Secondly, the absence of chiral ligand delivered a modest 12% yield of racemic **363**, hence evidencing an operative background C–H activation reaction mediated by acetate anions (entry 3). This had little impact in the excellent enantiomeric excess observed in entry 1, providing direct evidence for the ability of mono-protected amino acid ligands to outperform acetate ions during C–H cleavage, as observed computationally in section 2.4. Nevertheless, this background and racemic C–H activation reaction could deliver diminished levels of enantioselectivity depending on the directing amine substrates employed.

Among the different palladium sources tested, Pd(PhCN)₂Cl₂, a palladium precatalyst with no bidentate anions capable of performing C–H cleavage, exhibited the same reactivity as Pd(OAc)₂ (entry 4) with no observable product formation in the absence of the amino acid ligand (entry 5). Interestingly, the lack of acetate ions further improved the enantiomeric excess of arylated amine **363** above 99% ee. Excellent yield above 90% were achieved at lower temperatures, exhibiting the superior reactivity of this new palladium precatalyst (entry 6). Overall, this enabled reduction in the amounts of amine reagent, 1,4-benzoquinone (BQ), and silver carbonate used with minimal erosion in yield, obtaining 82% isolated yield of amine **363** and finishing with the optimisation process.



Entry	Pd cat.	362 (equiv)	BQ (equiv)	Ag_2CO_3 (equiv)	T (°C)	Yield 363 (%)	ee (%)
1	$\text{Pd}(\text{OAc})_2$	3.0	2.0	2.5	50	94	98
2	$\text{Pd}(\text{OAc})_2$	3.0	2.0	2.5	40	52	98
3 ^a	$\text{Pd}(\text{OAc})_2$	3.0	2.0	2.5	50	12	0
4	$\text{Pd}(\text{PhCN})_2\text{Cl}_2$	3.0	2.0	2.5	50	93	>99
5 ^a	$\text{Pd}(\text{PhCN})_2\text{Cl}_2$	3.0	2.0	2.5	50	0	-
6	$\text{Pd}(\text{PhCN})_2\text{Cl}_2$	3.0	2.0	2.5	40	94	>99
7	$\text{Pd}(\text{PhCN})_2\text{Cl}_2$	1.5	1.0	1.5	40	88 (82)	>99
8	-	1.5	1.0	1.5	40	0	-
9	$\text{Pd}(\text{PhCN})_2\text{Cl}_2$	1.5	0	1.5	40	0	-
10	$\text{Pd}(\text{PhCN})_2\text{Cl}_2$	1.5	1.0	0	40	0	-
11	$\text{Pd}(\text{OAc})_2$	1.5	2.0	0	60	89	98

Table 12: Optimisation of the enantioselective γ -C–H arylation of cyclopropylmethylamine **362** through palladium-catalysis. Reactions conducted at 0.1 mmol. Yield determined by $^1\text{H-NMR}$ using 1,1,2,2-tetrachloroethane as internal standard. Isolated yield in bold. ^a Absence of acetyl-*tert*-leucine

Control experiments determined that palladium (entry 8) and benzoquinone (entry 9) were essential to achieve product formation, but the presence of silver carbonate was also essential (entry 10). The absence of this additive delivered significant amounts of product formation when targeting the C–H bonds of a γ -methyl substituent (see Section 2.3.), and it was initially hypothesised that silver could now have an intimate role during C–H cleavage of the more challenging methylene C–H bonds. However, the study of 1,4-benzoquinone as an effective terminal oxidant in Section 2.3. disclosed the authentic role of silver as a halide scavenger. Return to the ubiquitous $\text{Pd}(\text{OAc})_2$ as the precatalyst of choice delivered an excellent conversion to arylated amine **363** at 60°C and in the absence of silver additives (entry 11). The same value of 98% ee obtained in the absence of Ag_2CO_3 discarded once again any putative role of this additive during C–H cleavage. Unfortunately, this finding occurred towards the end of the present dissertation, and the scope of this asymmetric transformation was conducted using the reaction conditions reported in entry 7.

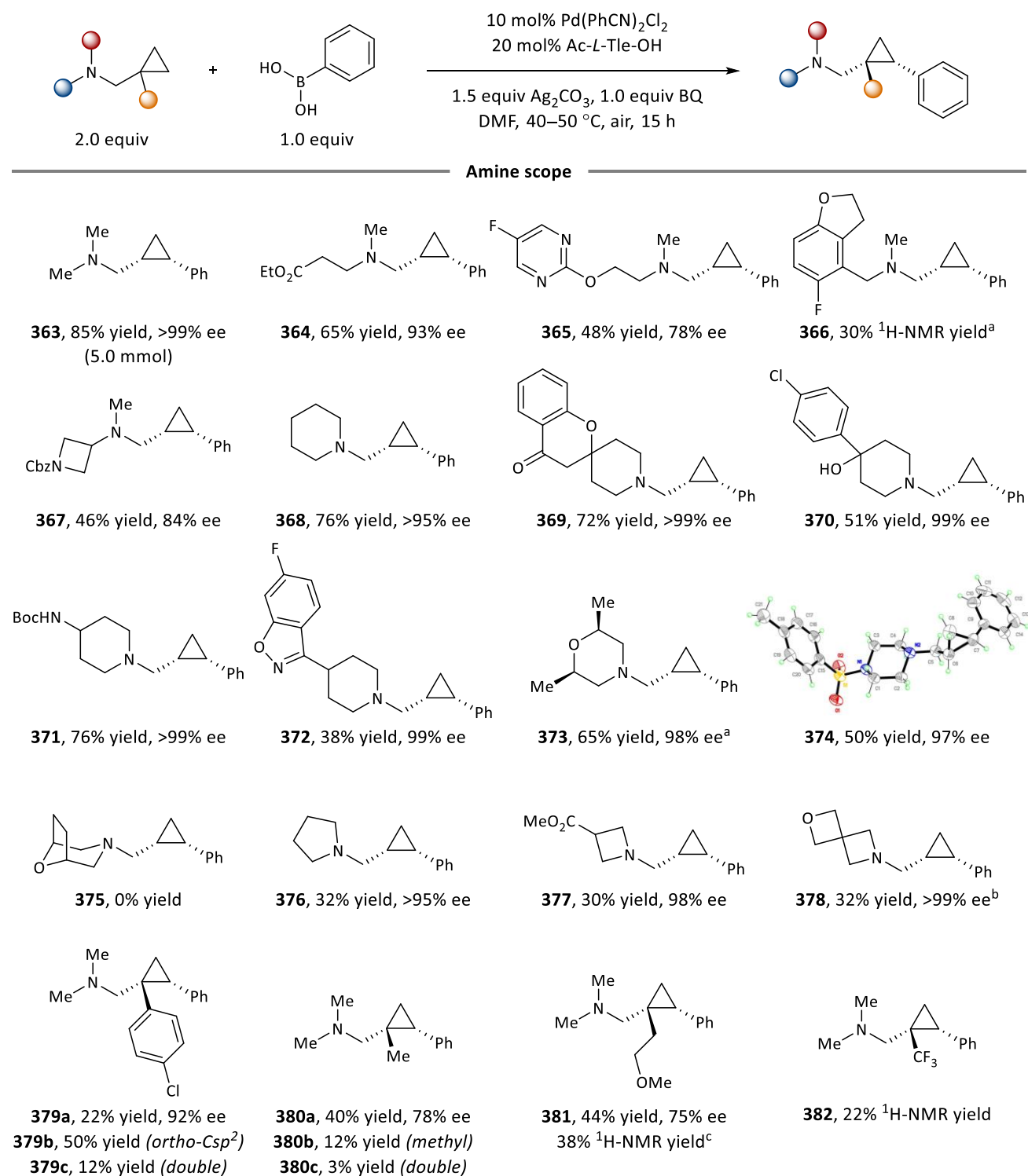
It is important to discuss the analytical methods available to assess the enantioselectivity of this transformation. The enantioenriched tertiary amine products obtained were found to be difficult to separate by simple HPLC analysis in a chiral stationary phase. The use of a hexane mobile phase with 0.1% of diethylamine dramatically increased the separation of both enantiomers by preventing peak tailing in a

CHIRALPAK®AD-H column. Nevertheless, this solution was not effective for all isolated products and it could not become a general analysis method. GC-FID analysis was found to be a viable method in some specific volatile compounds, but the physical foundations of this instrument made it unsuitable for larger organic molecules. A third alternative analysis was a ¹H-NMR analysis procedure developed by Lacour,²²⁴ which consists in the methylation of the arylated tertiary amine to generate a quaternary ammonium salt, followed by anion exchange with a chiral hexacoordinated phosphate. The resulting diastereoisomers displayed distinguishable ¹H-NMR signals suitable for quantitative analysis except for highly enantioenriched products, where integration of the minor diastereoisomer proved to be difficult. In those cases, enantiomeric excesses have been reported as greater than 95%. These three analytical techniques have made possible the analysis of all products obtained. On the one hand, simple amine products with no polar functional groups presented a scarce separation by HPLC analysis, but were amenable for GC-FID or ¹H-NMR analysis. On the other hand, complex amine scaffolds, unsuitable for GC-FID or ¹H-NMR analysis due to their high boiling point or the numerous overlapped NMR signals, presented other functional groups which aided in the interaction with the stationary phase and separation by HPLC analysis.

To assess the scope of the amine component, a range of acyclic amines displaying various substituents in place of one of the *N*-methyl substituents were synthesised and subjected to the optimised reaction conditions (Scheme 63). The presence of coordinating substituents such as an ester group (**364**) or a pyrimidine (**365**) delivered more moderate enantiomeric excesses along with diminished yields. A benzylamine derivative with no available *ortho*-C(sp²)-H bonds delivered surprisingly low yields of the corresponding γ -arylated product (**366**); and α -substituted amine **367** afforded a more moderate reactivity with an 84% ee. Overall, it was concluded that the flexibility of acyclic amines offered undesired substrate chelation modes, and that the substitution pattern of the amine backbone had a direct impact in the amine conformation during C-H cleavage.

Taking into account the previous results obtained in the group when trying to desymmetrise *gem*-dimethyl substituents (see Section 3.1.), it was imperative to know if other amine heterocycles could maintain the same levels of enantioselectivity observed for amine **363**. Gratifyingly, piperidines with a diverse range of functional groups, including free alcohols (**370**), *N*-protecting groups (**371**), oximes (**372**) and chlorinated aromatic rings (**370**), all exhibited excellent enantioselectivities, reaching values of >99% ee. Isolated yields were good except for substrates displaying strong coordinating groups (**372**). Other ubiquitous heterocyclic amines, such as morpholine (**373**), *N*-tosyl piperazine (**374**), pyrrolidine (**376**), and azetidine derivatives (**377**–**378**), were all found to access C-H activation to deliver their corresponding γ -arylated product with moderate to good yields, but all with excellent enantioselectivity. Piperazine **374** was successfully crystallised in a mixture of hexane and isopropanol to reveal the absolute configuration of the generated chiral cyclopropane. Product **378** exemplifies the strength of this transformation, opening new synthetic routes to the expeditious synthesis

of a diastereo- and enantiopure amines with ring-strained heterocycles and a spirocycle. Unfortunately, bicyclic amine **375** was found to be unreactive likely due to the steric interaction between the axially-bound palladium metal centre and the bridged azepane ring.

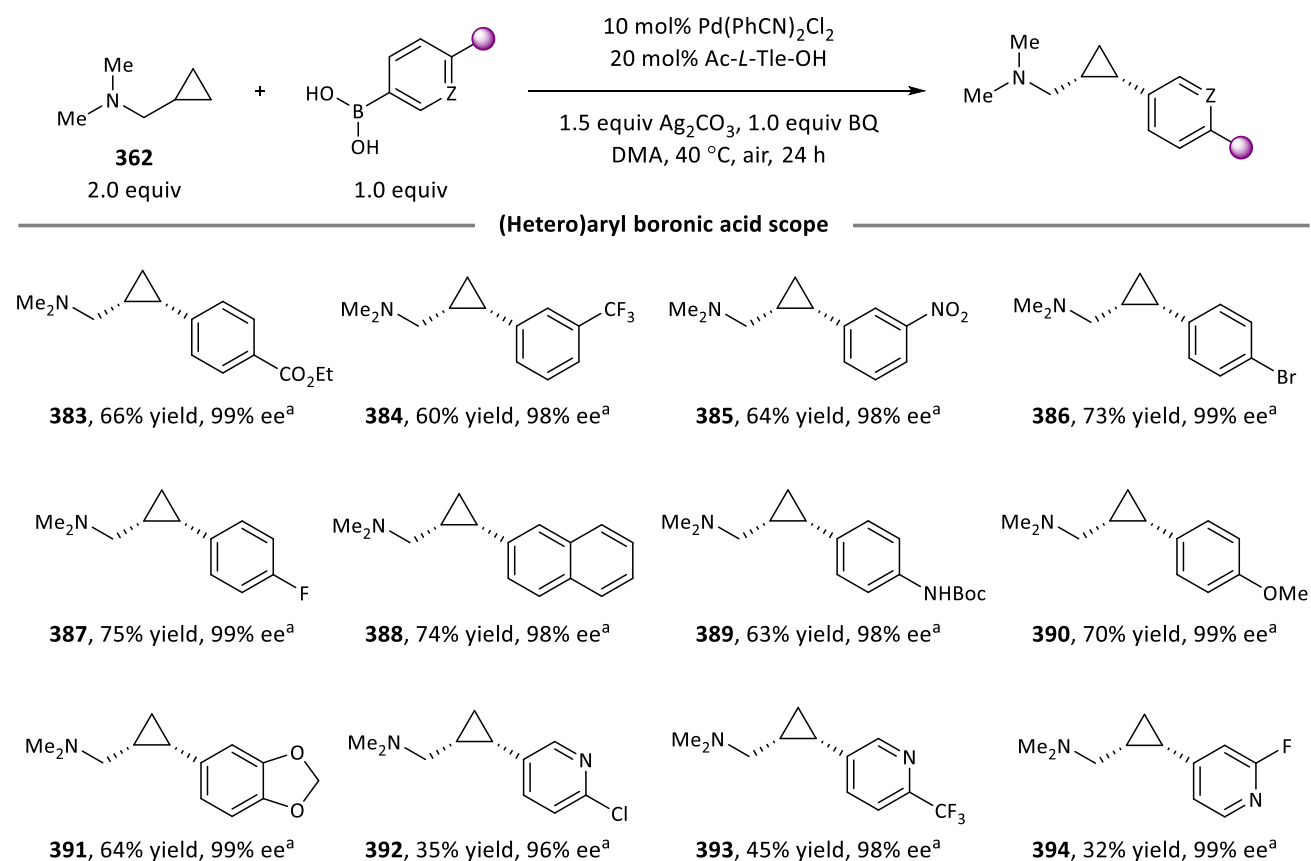


Scheme 63: Scope of the amine component in the palladium-catalysed C–H activation of cyclopropanes in tertiary alkylamines. Reactions conducted at 0.3 mmol. ^a Conducted by Dr. Miró. ^b PhBPIN instead of PhB(OH)₂. ^c Pd(OAc)₂, no ligand.

In an attempt to further expand the amine scope, it was questioned whether quaternary centres at the β -position of the amine backbone could be tolerated. Such a profound change in the cyclopropane ring, and in so close proximity to the targeted C-H bond can drastically alter the enantiodetermining transition state. Nevertheless, reactivity could be accessed in these substrates to deliver excellent asymmetric induction when displaying C(sp²) centres (**379**), and more moderate values when possessing C(sp³) substituents (**380–381**). Interestingly, these amines enabled the direct comparison in reactivity between C-H bonds of different nature. When comparing methyl vs. methylene C-H activation of cyclopropane rings, a ratio of nearly 4:1 was observed in favour of arylation in the strained 3-membered ring (**380a–380b**). In palladium catalysis, multiple reports exemplify the ease by which C(sp²)-H bonds react preferentially over alkyl C-H bonds. Therefore, it is noteworthy that arylation could still be achieved on the targeted methylene C-H bond in the presence of an aromatic substituent, albeit C(sp³)-H arylation giving the minor regioisomer (**379a–379b**). Unfortunately, the presence of strong electron-withdrawing groups delivered poor reactivity due to diminished binding of the amine substrate to palladium and the less electron-rich C-H bond of the cyclopropane (**382**).

The significant reduction of enantioselectivity in products **380** and **381** prompted further studies to investigate this loss of asymmetry. Unexpectedly, racemic product **380** could be obtained in 38% yield in the absence of ligand when replacing the Pd(PhCN)₂Cl₂ precatalyst by Pd(OAc)₂. One plausible explanation for this outcome is that the β -substituent of amine backbone induces a Thorpe-Ingold effect, accelerating C-H activation in the absence of ligand, and this being operative when an acetate base is available in the reaction media. When using Pd(PhCN)₂Cl₂, it is likely that an erosion in enantiomeric excess is observed due to the release of carbonate ions from the silver additive.

Shifting the attention towards the other component of the reaction, a range of both electron withdrawing and electron donating aryl boronic acids were tested in the reaction conditions with amine **362**. Aryl boron reagents with electron withdrawing groups initially delivered lower reactions yields, due to the significant formation of biaryl species due to its *homo* cross-coupling. Luke Reeve conducted a short optimisation finding a better conversion to the desired product when carrying the reaction at 40 °C for longer reaction times and in DMA as solvent. With this subtle improvement of the reaction conditions, any substituent on the *meta*- or *para*- positions delivered good yields, including typically incompatible halogenated aromatic rings (**386**). Esters (**383**), fluorinated substituents (**384**, **387**), nitro groups (**385**), protected anilines (**389**), and alkoxy substituents (**390**, **391**) all performed well under the reaction conditions. Unfortunately, boronic acids displaying *ortho*-substituents failed to deliver any product. All arylated amines displayed excellent levels of enantioselectivity, indicative that the boronic acid component is not involved in the enantiodetermining step. With more moderate isolated yields, heterocyclic pyridines can be also incorporated into the amine structure while retaining the excellent asymmetric induction observed throughout the scope (**392–394**).

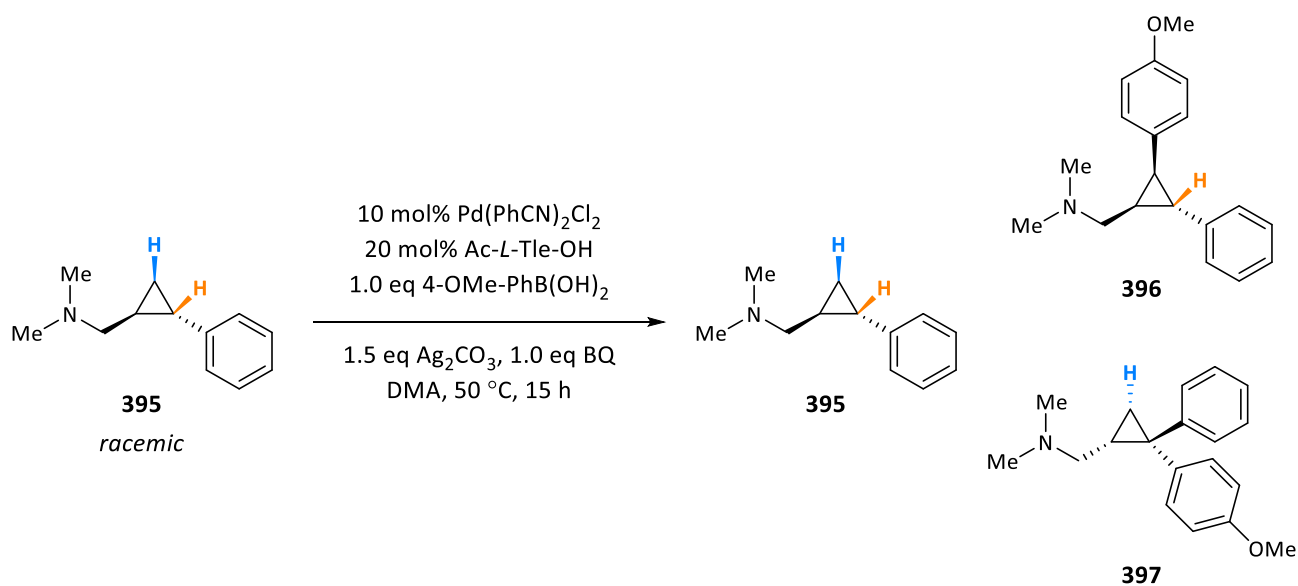


Scheme 64: Scope of the boronic acid component in the palladium-catalysed C–H activation of cyclopropanes in tertiary alkylamines. Reactions conducted at 0.3 mmol. ^a Conducted by Luke Reeve.

This extensive scope has demonstrated that the desymmetrisation of tertiary alkylamines containing cyclopropanes can be achieved using mono-protected amino acid ligands. Gratifyingly, multiple amine heterocycles can direct and impart high levels of asymmetric induction delivering an enantiomeric excess greater than 99% in some cases. It was envisaged that this exquisite selectivity for the formation of one single enantiomer could be exploited in a kinetic resolution event. Kinetic resolution processes are of extreme difficulty because the ligand must clearly differentiate between both enantiomers of a racemic mixture. If a large difference in rate can be achieved for the formation of one of the enantiomers, up to half of the starting material can be recovered in an enantioenriched form along with the expected chiral product. Due to the relevance of *trans* cyclopropane derivatives in the field of medicinal chemistry, amine **395** was chosen as the initial substrate (Table 13). Taking into account that only *cis* C–H bonds with regards to the amine substituent are amenable to C–H cleavage, this kinetic resolution reaction had an extra degree of difficulty in trying to differentiate between the γ -C–H bond of the cyclopropane methylene unit (highlighted in blue), and the γ -C–H bond at the methine benzylic position (highlighted in orange).

Taking the same conditions used in Scheme 63, the first kinetic resolution attempt delivered a remarkable 61% yield of *trans* diaryl amine **396**, with an excellent enantiomeric excess of 96% (entry 1).

Surprisingly, small amounts of product **397**, arising from methine C–H activation, were also isolated with excellent asymmetry (>99% ee), offering the possibility to synthesise distinct ring-strained 3D structures in a diastereo- and enantiopure form. The two equivalents of amine starting material used delivered a more modest asymmetric induction for the recovered amine **395** (51% ee). When the same reaction was conducted with 1.0 equivalent of amine, more modest yields were obtained, but an excellent 93% ee was observed for the recovered amine substrate (entry 2). Depending on the synthetic needs, it is possible to access all 3 arylated amines with excellent enantioselectivities, proving that this amine-directed C–H activation strategy is amenable to kinetic resolution reactions. Unfortunately, the conversion of amine **395** to two different arylated products made highly challenging to establish a selectivity value (s) for this transformation.

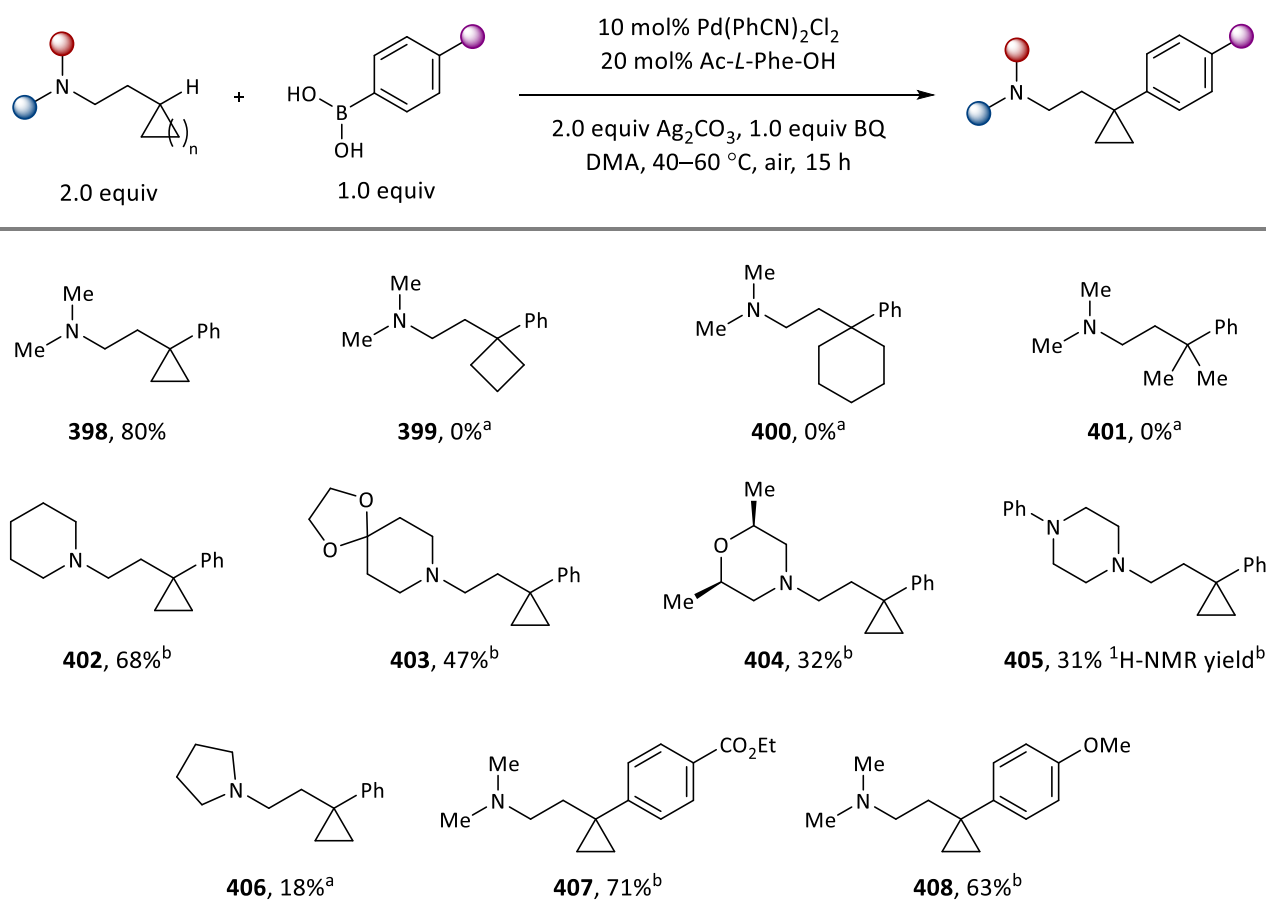


Entry	395 (equiv)	395 (%)	396 (%)	397 (%)
1	2.0	82% yield; 51% ee	61% yield; 96% ee	6% yield; >99% ee
2	1.0	16% yield; 93% ee	38% yield; 86% ee	5% yield; >99% ee

Table 13: Kinetic resolution of *trans*-cyclopropane **395**. Reaction conducted at 0.3 mmol.

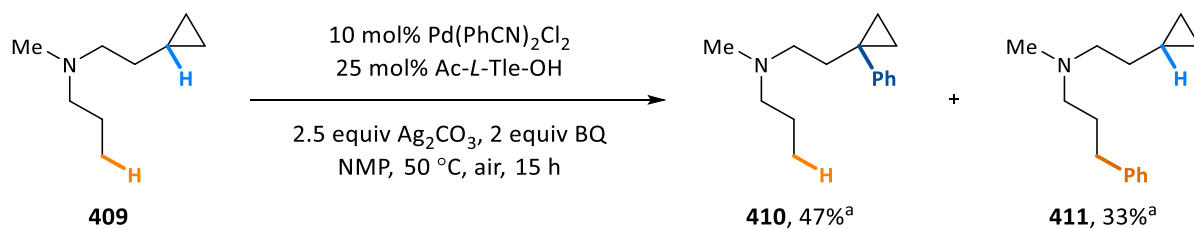
There are very few literature examples reporting palladium-mediated C–H activation reactions at methine C–H bonds.^{38,122,215,225–231} The hindered nature of this bond makes C–H cleavage and its subsequent functionalisation a great challenge only achieved so far in ring-strained systems or bridgehead positions to typically deliver intramolecular cyclisations. The isolation of compound **397** offered a unique opportunity to explore the ability of tertiary amines to access the rare methine C–H activation. Gratifyingly, the benzylic nature of the methine C–H bond in **397** was not a requirement for reactivity. Arylated amine **398** exclusively forged the expected quaternary centre in an excellent 80% yield and with no other detectable side-products arising at the more distal methylene δ -C–H activation (Scheme 65). This research was then further explored by two undergraduate students of the group. Samuel McKee observed that, in line with previous reports,²³²

the methine C–H bond encountered in a cyclobutane (**399**), cyclohexane (**400**), or a non-cyclic substituent (**401**) proved to be unreactive, likely due to the congested environment of this bond during C–H cleavage, but also due to the difficult transmetalation step in the resulting bulky palladacycle. Amine heterocycles were also amenable to direct this transformation, and Edward Shellard optimised the formation of arylated piperidine **402** to find that acetyl-phenylalanine performed better than the widely used acetyl-*tert*-leucine. This new set of reaction conditions was applied to morpholines (**403**) and piperazines (**405**), albeit more modest yields were obtained. As preliminary results, arylated products **407** and **408** provide proof of concept that both electron-rich and electron-poor arylboron reagents can access the desired transmetalation step to forge the expected ring-strained quaternary centre.



Scheme 65: Methine C–H activation in tertiary alkylamines. Reaction conducted at 0.3 mmol. ^a Conducted by Samuel McKee. ^b Conducted by Edward Shellard.

Based on the computational studies about β -H elimination of section 2.4., and in line with previous findings of the group,¹²² the isolation of arylated pyrrolidine **406** in 18% yield is a strong indicator that methine C–H activation is slightly more facile than methyl C–H activation, where a 14% ¹H-NMR yield was obtained using the same Pd(PhCN)₂Cl₂ precatalyst. To further corroborate this, Samuel McKee prepared amine **409** to study the direct intramolecular competition between γ -methyl and γ -methine C–H activation (Scheme 66). As expected, a subtle preference for methine C–H activation was obtained in a 1.5:1 product ratio.



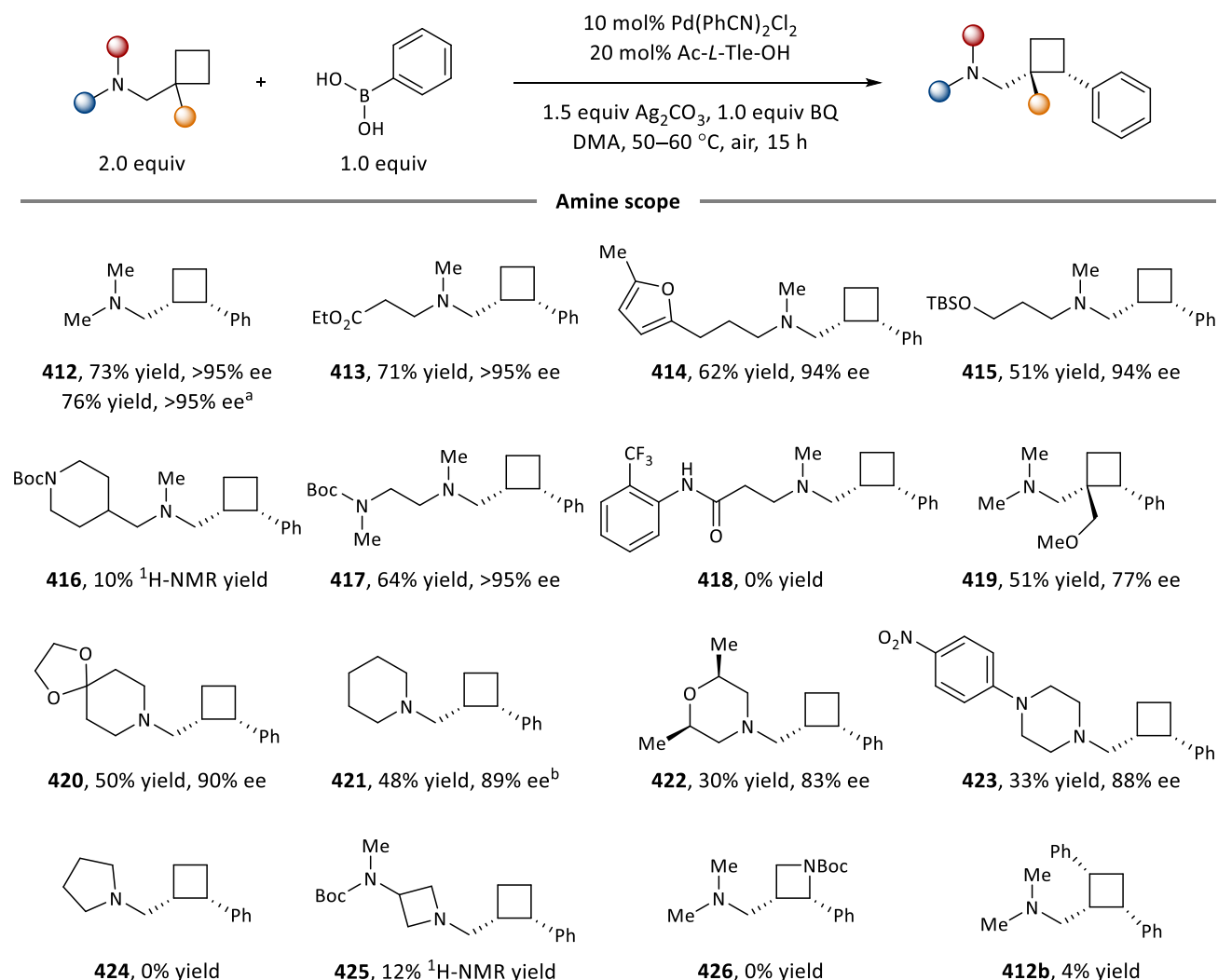
Scheme 66: Competition experiment between methyl and methine γ -C-H activation. Reaction conducted at 0.3 mmol.

^a Conducted by Samuel McKee.

After exploring all the possibilities which cyclopropanes could offer, the *a priori* more demanding C-H arylation of cyclobutanes was targeted as another appealing transformation. The scarce sp^2 character of these methylene C-H bonds makes their cleavage more challenging than in cyclopropane rings. As a result, very few literature examples can perform this in an enantioselective manner,^{140,214,220,233} with no precedents in amine substrates. The ubiquitous acetyl *tert*-leucine ligand performed well in DMA as solvent to deliver arylated dimethylamine **412** in 73% isolated yield and with a greater than 95% ee, along with 4% yield of diarylated product **412b** displaying an all-*cis* configuration (Scheme 67). This by-product only arose when using the simplest dimethylamine substrate, and was detected in less than 2% ¹H-NMR yield when analysing the crude reaction mixtures of all other depicted substrates. It is worth mentioning that a later analysis of this transformation revealed that it could be performed in the absence of Ag₂CO₃ and oxygen to deliver the same yield and enantioselectivity by using 1,4-benzoquinone as the terminal oxidant of the reaction at 60°C (see Section 2.3.). Common functional groups like esters (**413**), heteroaromatic rings (**414**), protected alcohols (**415**) and amines (**417**), all delivered good yields and enantioselectivity of their corresponding arylated cyclobutane amines. Amine **416** afforded a very poor reactivity, thus evidencing the arising steric interactions among the amine backbone during C-H cleavage. As previously observed for similar substrates, the bidentate mode of amine **418** impedes the generation of the required vacant site for C-H activation. Analogously to cyclopropanes, the presence of β -alkyl substituents could still deliver the expected reactivity, although a slightly lower asymmetric induction was observed (**419**).

A range of heterocyclic tertiary amines were tested to determine if it was also possible to direct C-H activation with these more delicate substrates. Piperidine (**420**, **421**), morpholines (**422**), and piperazines (**423**), all accessed their corresponding arylated product, albeit in more moderate yields. Noteworthy is the ability of these substrates to maintain good levels of enantioselectivity, the lowest being an 83% ee of morpholine derivative **422**. Pyrrolidine substrates (**424**) did not deliver any product formation, hence evidencing the facile β -H elimination of these heterocycles over the now more challenging C-H activation of methylene units. This competition between β -H elimination and C-H activation, previously explained in section 2.4., can also be responsible for the diminished yields of heterocycles **420–423**, substrates which performed well in the analogous C-H activation of cyclopropanes (Scheme 63). The use of an azetidine

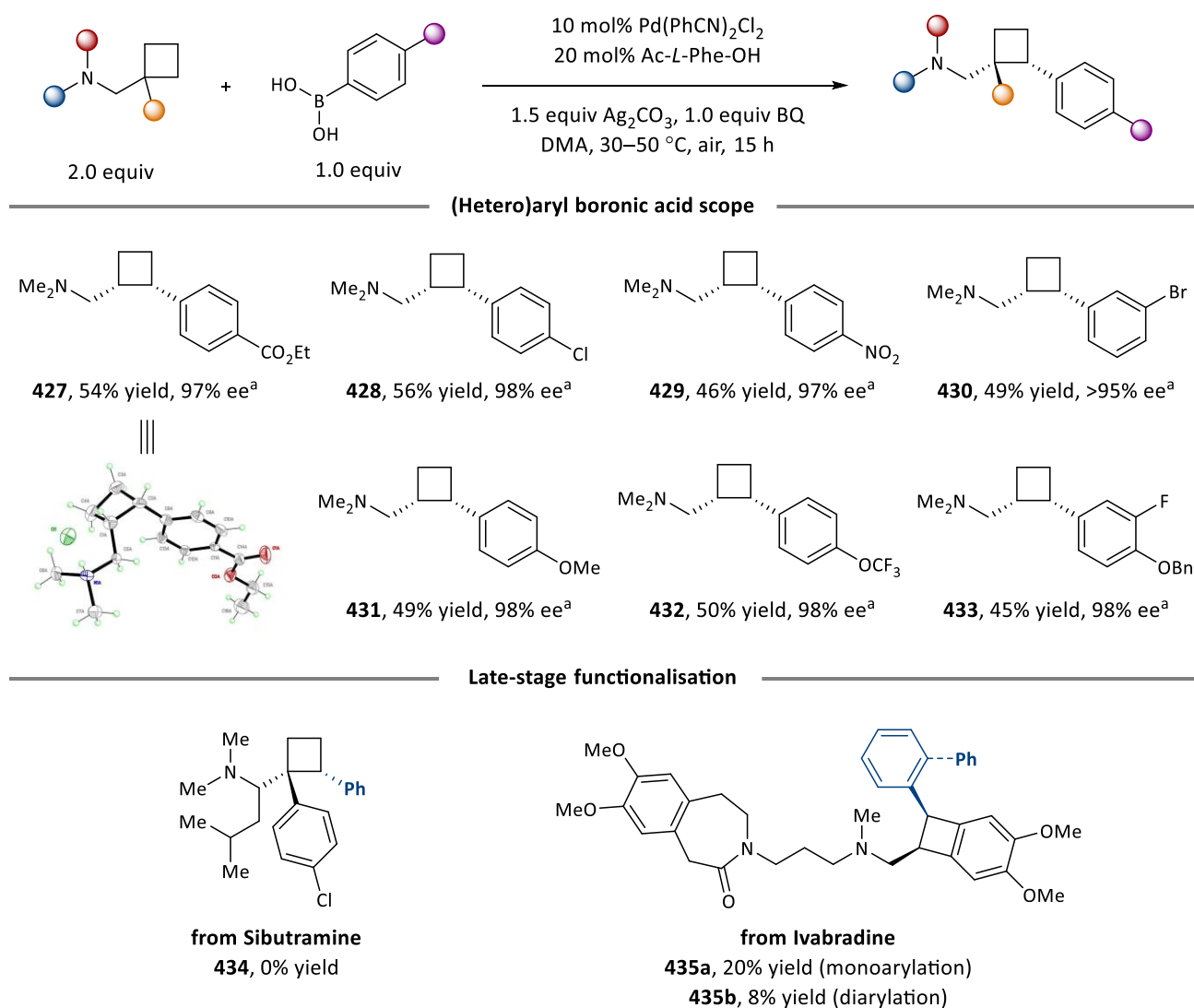
directing group afforded a very poor reactivity (**425**), and targeting C–H activation in the azetidine heterocycle did not deliver any product formation either (**426**).



Scheme 67: Scope of the amine component in the palladium-catalysed C–H arylation of cyclobutanes in tertiary alkylamines. Reactions conducted at 0.3 mmol. ^a 10 mol% Pd(OAc)₂, 20 mol% Ac-L-Tle-OH, 2.0 equiv BQ, no Ag₂CO₃, under N₂, 60 °C. ^b NMP.

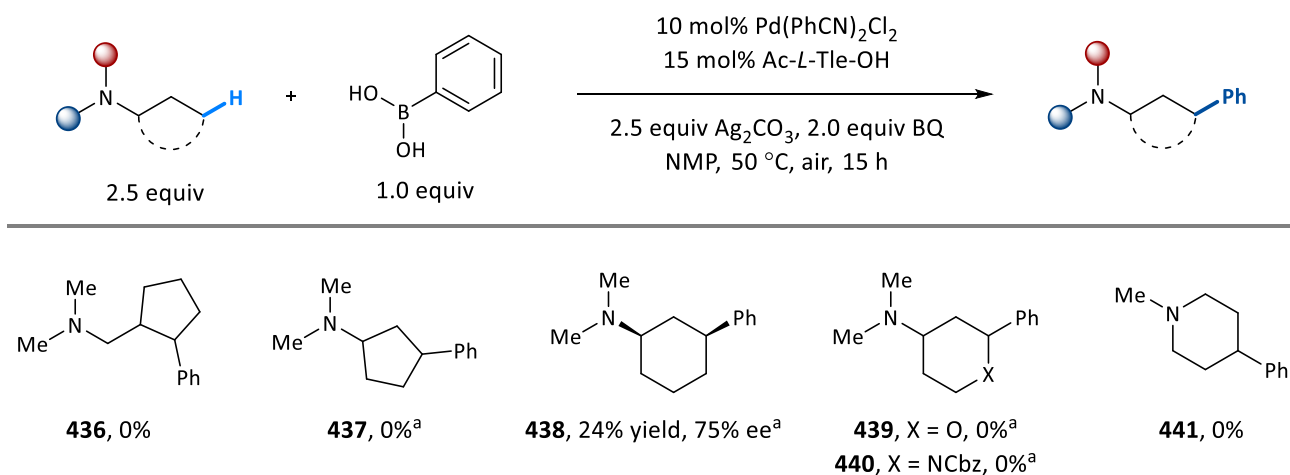
With regards to the boronic acid coupling partner, Luke Reeve found a better reactivity using acetylphenylalanine as the ligand of choice for this palladium-catalysed C–H arylation reaction. Both electron-donating and electron-withdrawing groups were compatible with this transformation to deliver moderate isolated yields ranged between 45% and 56% (**427–433**, Scheme 68). Despite the use of two equivalents of amine starting material, significant amounts of diarylated product were usually observed, accounting for the loss in yield for the reported monoarylated product. Nevertheless, this more challenging C–H activation reaction could also tolerate promiscuous halide functionalities (**430**). Unfortunately, heteroaromatic boron reagents were incompatible with this transformation and did not afford the expected C–C bond formation. Of note is the crystallisation conducted by the present author of product **427** in its hydrochloride salt, which confirmed the absolute configuration of the arylated cyclobutane products.

Lastly, two commercial drugs containing tertiary amines with appendant cyclobutane rings were tested under the reaction conditions to test a potential late-stage functionalisation strategy. Sibutramine, a formerly prescribed appetite suppressant, did not deliver any arylated product (**434**). Based on the similarities between this drug and arylated cyclopropane **379**, some product formation was expected, even if occurring at the δ -C-H bonds of the aromatic ring. However, the α -isobutyl substituent appears to disfavour the required amine conformation during C-H cleavage. On the other hand, Ivabradine, a medication used for the symptomatic management of stable heart chest pain and heart failure, did afford reactivity at its benzocyclobutene ring (**435a**). Despite the isolation of diarylated by-products (**435b**), this provides proof-of-concept that fused cyclobutenes are also compatible with this palladium-mediated C-H activation reaction. It is worth highlighting that no reactivity was observed with the other chiral ligand, opening the possibility to perform kinetic resolution reactions in this drug of interest.



Scheme 68: Scope of the boronic acid component in the palladium-catalysed C-H activation of cyclobutenes in tertiary alkylamines. Application of this reaction as a late-stage functionalisation tool in commercial drugs displaying 4-membered ring alkanes. ^a Conducted by Luke Reeve.

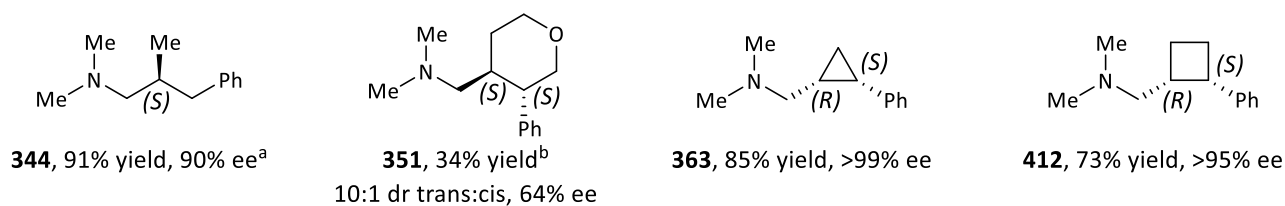
After exploring the reactivity and synthetic applicability of cyclopropane and cyclobutane rings, arylation at the methylene C–H bonds of larger rings was attempted (Scheme 69). Unfortunately, no arylation was achieved in cyclopentane rings (**436–437**). Imitating the methylene arylation discovered by Dr. Azuma (see Section 3.1.), arylated product **438** could be isolated in 24% yield and 75% ee through an unusual axial C–H cleavage. However, this C–H activation mode was incompatible with the presence of heteroatoms (**439–440**). Lastly, arylation at the γ -C–H bonds of the piperidine ring could not be achieved due to the restricted boat conformation required during C–H activation, making a β -H elimination process more favourable.



Scheme 69: Non-ring-strained tertiary alkylamines in C–H activation reactions. ^a Conducted by Samuel McKee.

3.4. Computational findings

The previous section explored asymmetric C–H activation reactions in tertiary alkylamine substrates with appendant ring-strained cycloalkanes while using mono-protected amino acids as chiral ligands. The crystal structures of arylated cyclopropane **374** (Scheme 63) and arylated cyclobutane **427** (Scheme 68) elucidated the absolute configuration of the functionalised amine products. Unexpectedly, the β -carbon of both amine backbones displayed a (*R*) stereodescriptor (**363** & **412**, Scheme 70), while the previously discovered arylations of *gem*-dimethyl amines (**344**) and tetrahydropyran derivatives (**351**) forged a (*S*) stereodescriptor at the same β -carbon and with the same *L*-amino acid ligand.



Scheme 70: Asymmetric C–H activation reactions of tertiary alkylamines. ^a Conducted by Dr. Nappi. ^b Conducted by Dr. Azuma.

Throughout this dissertation it has been proposed that a single ligand in a bidentate coordination mode is responsible of imparting reactivity and selectivity in order to deliver the functionalised tertiary amine products. To corroborate this hypothesis experimentally, non-linear experiments were conducted in the asymmetric reactions leading to arylated amines **344** and **363** using the optimised set of reaction conditions for each one of them, which included the use of Ag₂CO₃ and the same acetyl-*tert*-leucine ligand, but differed in solvent and reaction temperature (Figure 3). Little deviation from linearity was observed for both sets of reactions, thus supporting the premise that a single amino acid ligand per metal centre is involved throughout the catalytic cycle.

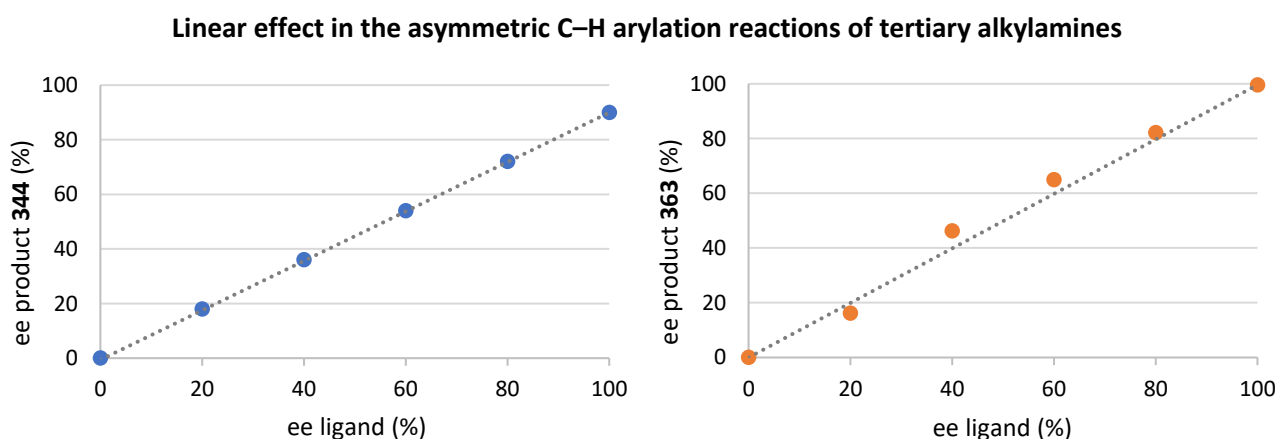
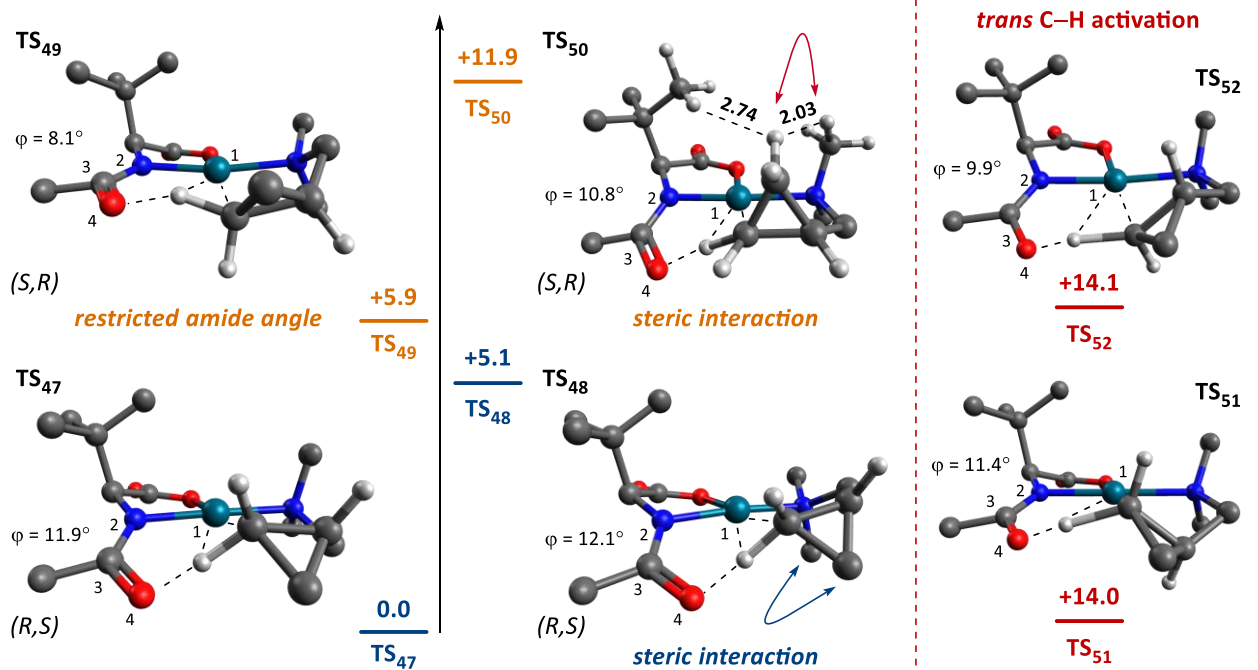
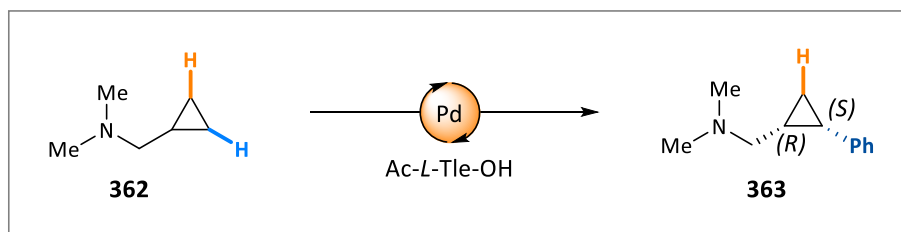


Figure 3: Non-linear experiments for the C–H arylation of amines **344** and **363**. Data determined by HPLC analysis using a CHIRALPAK[®] AD-H column. Each data point represents an average value for two independent reactions.

Taking into account the existing computational knowledge within the research group around tertiary alkylamines in C–H activation, the *in silico* rationalisation of this sharp contrast in asymmetric induction between C–H bonds in strained or non-strained alkyl backbones was attempted. All calculations were made using the Gaussian 16 (Revision A.03) program.²⁰⁵ All geometries were optimised at the B3LYP-D3BJ/[6-31G(d,p)/Lanl2dz(Pd)] level of theory at 323.15 K and accounting for solvation effects using the self-consistent reaction field polarizable continuum model (IEF-PCM) in DMF. Single-point energies of the optimised structures were calculated at the B3LYP-D3BJ/[6-311+G(2d,p)/SDD(Pd)] level of theory, accounting for solvation as above. These functionals and basis sets have been employed in Pd-catalysed C–H activation previously.^{155,157,206} Dispersion was accounted for using Grimme's DFT-D3 scheme²⁰⁷ with Becke-Johnson damping.²⁰⁸ To confirm that the obtained transition states reside along a relevant reaction coordinate, IRC-calculations were undertaken for selected transition states.²⁰⁹ Basis-set superposition error (BSSE) was assumed to be negligible for the large basis sets employed as indicated by previous studies.²¹⁰

It is important to restate the conclusions obtained from the computational analysis in Section 2.4. The flexible tertiary amine backbone grants access to a set of different transition states by which C–H activation can be achieved through a concerted-metalation deprotonation (CMD) transition state in the presence of acetates or the acetamide of the ligand. When activating a methyl C–H bond of a saturated alkane chain, the lowest energetic pathway adopted a chair-like conformation consisting of palladium, the nitrogen of the bound tertiary amine, its 3-carbon amine backbone, and the abstracted *H*-atom. This 6-membered ring transition state finds an optimal orbital overlap with the intramolecular base at a dihedral angle of 10° with palladium. When using amino acid ligands, its α -side chain restricts the mobility of the acetamide base and it positions it out of the plane of geometry of the palladium complex. This has a positive impact in γ -C–H activation, which already occurs through a dihedral angle of 10° and it benefits from the use of a stronger intramolecular base, while disfavoring β -H elimination processes.

The starting hypothesis was that the inherent geometrical restrictions imposed by the cyclopropyl unit, where all atoms display an *eclipsed* conformation, impedes the access to the most favorable chair-like transition state. Indeed, amine **362** generated two diastereomeric pairs of transition states displaying the more typically unstable boat or half-chair conformations (Scheme 71). **TS₄₇** possesses the lowest energetic barrier and leads to the enantiomer observed experimentally. This transition state displays the archetypal desired conformation for C–H cleavage, with an amidate-palladium dihedral angle of 11.9°, capable of minimizing both the steric repulsion of the *tert*-butyl substituent of the ligand and the steric interaction along the amine backbone. All other transition states (**TS₄₈**–**TS₅₀**) do not fulfil one of the above requirements, which results in a higher energetic barrier.



Scheme 71: Transition states leading to an asymmetric C(sp³)-H activation of cyclopropane rings in amine **362** and using acetyl-*tert*-leucine as ligand. Energy values in kcal·mol⁻¹.

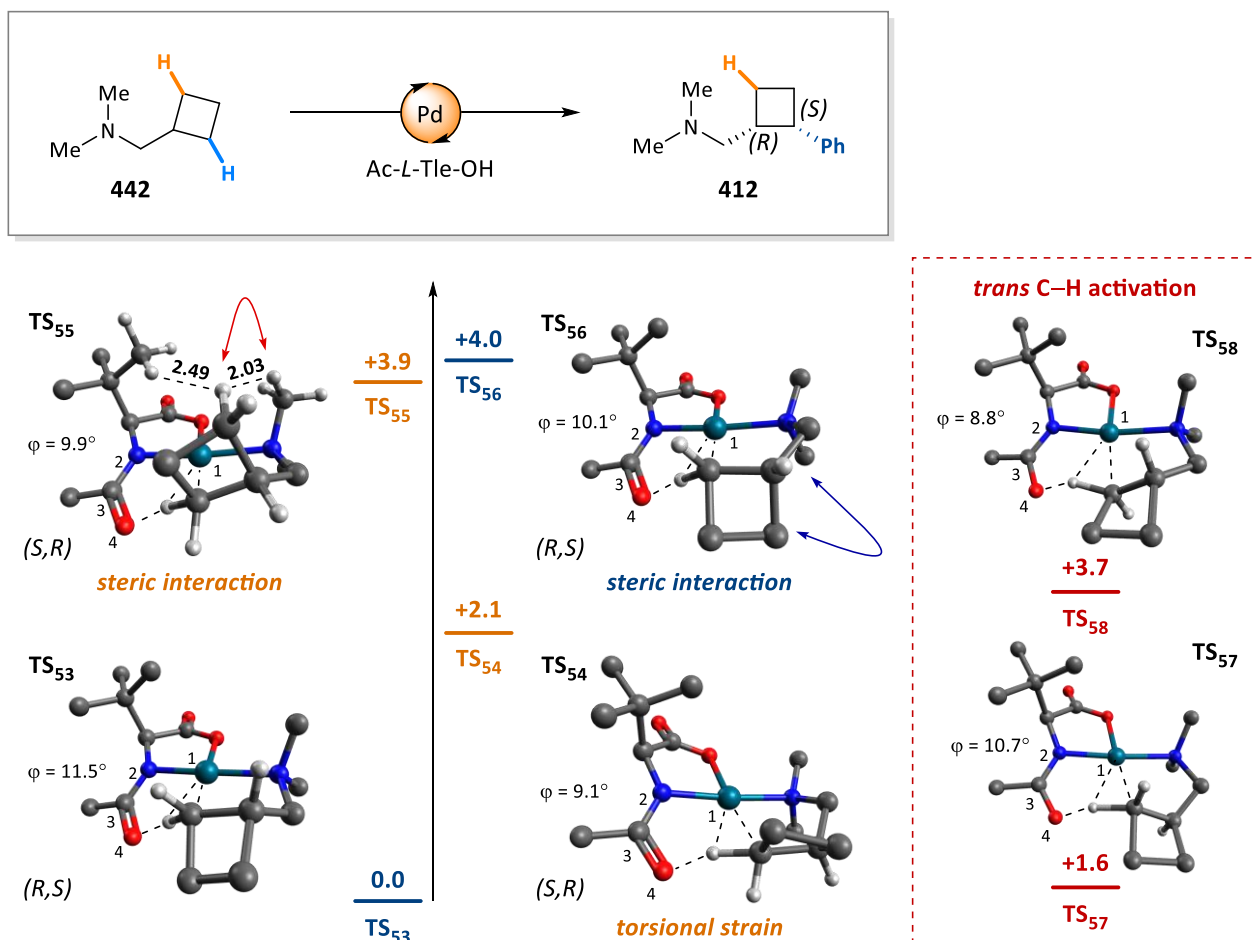
With very similar amine conformations, direct comparison of **TS₄₇** and **TS₅₀** provides a rapid comprehension of the observed enantioselectivity. Both transition states position the amide base in an optimal dihedral angle of 11° or more, meaning that the amine backbone plays again a crucial role in the resultant energy minima obtained. **TS₅₀** exhibits a strong steric interaction above the palladium complex between a methylene unit of the cyclopropyl ring and a *N*-methyl amine substituent, where a H-H distance of 2.03 Å is observed, significantly less than the sum of their Van der Waals radius. To minimise this detrimental clash, the amine backbone suffers from torsional strain with observed *gauche* angles of as little as 26°, which results in a profound increase of the energy barrier. It is worth highlighting that no direct interaction is observed between the ligand *tert*-butyl substituent and the amine backbone, where the closest H-H distance is 2.74 Å. Rather than exploiting more classical ligand-substrate steric interactions, this analysis indicates that these type of ligands induce enantioselectivity by restricting the mobility of the amidate internal base, and it is the amine backbone which is forced to adopt the most stable conformation to bring the reacting C-H bond in close proximity to palladium and its internal base.

The large gap in energy between **TS**₄₇ and **TS**₄₉ yields a predicted enantiomeric excess greater than 99.9% based on Boltzmann populations at the given temperature. Most importantly, the difference in energy between these transition states doesn't rely on steric interactions along the amine backbone, which made this mode of asymmetry amenable for many different types of aliphatic amine heterocycles. Subtle erosion in enantioselectivity for certain substrates may be attributed to an operative background reaction where the carbonate ions, released by silver carbonate upon its reduction with Pd⁰, behave as the intramolecular base needed for C–H cleavage. Lastly, the geometrical constraints of a *trans* C–H cleavage made **TS**₅₁ and **TS**₅₂ energetically inaccessible.

Next, attention was focused on cyclobutane substrates. When compared with the C–H cleavage of cyclopropanes, the non-planar structure of these 4-membered rings grants them access to a few more diastereomeric transition states. For clarity, only the two most relevant pairs will be discussed here, and other transition states with larger energy barriers can be found in Appendix III. Analogously to cyclopropane C–H activation, the lowest transition state was expected to display the minimal torsion strain and/or steric hindrance among the amine backbone, while still accessing the optimum dihedral angle for C–H activation between the acetamide base and palladium. **TS**₅₃ fulfilled all these requirements by adopting a twist-boat conformation (observed between palladium, nitrogen, the 3-carbon backbone, and the cleaved hydrogen) which minimises the eclipsed hydrogen-interactions among the amine backbone thanks to the inherent puckered conformation of a cyclobutane ring (Scheme 72). The lack of steric interactions contrasts with its diastereomeric complex (**TS**₅₅), where a scarce H–H distance of 2.03 Å is observed between the strained ring and the *N*-methyl substituent, resulting in an energy difference of 3.9 kcal·mol⁻¹.

Interestingly, two other transition states (**TS**₅₄ and **TS**₅₆) were found to proceed through a chair-like conformation, resembling the ones predicted when C–H activation is attempted on strained-free systems. When the system loses its strained character, the chair-like transition states recover their predominant stability among other conformations. **TS**₅₆ exhibits a steric interaction between the strained ring and the *N*-methyl substituent through the bottom of the palladium complex, which makes it significantly higher in energy. Nevertheless, **TS**₅₄ presents no detrimental steric interactions and an acceptable acetamide-palladium dihedral angle of 9.1°. Its 2.1 kcal·mol⁻¹ energy difference with **TS**₅₃ lies in the torsional strain of the amine backbone where a *gauche* angle of 40.6° is observed between the hydrogens of the α and β carbons of the amine substrate. In comparison, the most stable transition state **TS**₅₃ displays enviable values of 11.5° (for acetamide-palladium dihedral angle) and 52.9° (for *gauche* conformation in the amine backbone). Taking into account the energy barriers of all transition states found, the predicted enantiomeric excess is 90% ee, which is in line with the range between 83% ee and 95% ee obtained throughout the amine scope of this class of ring-strained systems.

Unexpectedly, a low energy barrier was found for a *trans* C-H cleavage (**TS₅₇**), which should have led to the formation of a minor diastereoisomer not observed experimentally. One potential explanation for this is that transmetalation or reductive elimination from activated *trans* C-H bonds is more challenging, which leads to product decomposition and catalyst deactivation, hence the lower yields observed throughout the amine scope of this ring-strained alkane. Furthermore, this reasoning can also explain the lack of reactivity in cyclopentane rings (Scheme 69, Section 3.3.), and the moderate reactivity of 6-membered ring alkanes discovered by Dr. Azuma (Scheme 61, Section 3.1.).



Scheme 72: Transition states leading to an asymmetric C(sp³)-H activation of cyclobutane rings in amine **442** and using acetyl-*tert*-leucine as ligand. Energy values in kcal·mol⁻¹.

To finish with this section, it is critical to emphasise that the most stable transition state for each diastereomeric complex (**TS₄₇** & **TS₄₉** for cyclopropanes and **TS₅₃** & **TS₅₄** for cyclobutanes) proceeds without evident steric interactions among the amine backbone or with the ligand. Alternatively, asymmetry relies on the restricted geometry of the amidate base, which is clearly exemplified in **TS₄₇** vs **TS₄₉**. The desymmetrisation of cyclobutanes takes this concept to the limit, where a subtle torsional strain of the amine backbone imparts great levels of enantioselectivity (**TS₅₃** vs **TS₅₄**).

3.5. Summary

Mono-protected amino acid ligands and their derivatives are increasingly used as an effective tool for asymmetric palladium-catalysed C–H activation reactions. However, these typically display bespoke bulky functionalities and are used in combination with substrates bearing exogenous directing groups. Focusing solely on amine substrates, only one recently reported method can use unprotected primary amines to achieve functionalisation at the γ -C–H bonds of a cyclopropane, and with the aid of a chiral thioether-amine ligand.¹¹³

In comparison, this chapter has demonstrated that simple and commercial amino acid ligands can also perform asymmetric C–H activation reactions with excellent selectivity and in a wide range of ubiquitous amine substrates. By using aryl boronic acids as coupling partners, tertiary alkylamines displaying both appendant cyclopropane and cyclobutane rings delivered the expected *cis* γ -arylated products with excellent diastereo- and enantioselectivity. *N*-Substituted piperidine, pyrrolidine, morpholine, piperazine and azetidine heterocycles, as well as acyclic amines, were all capable of directing the palladium metal centre to forge the desired C–C bond. Interestingly, the presence of β -substituents within the amine backbone created a Thorpe-Ingold effect which resulted in an unusual product formation in the absence of ligand.

Taking advantage of the exceptional enantioselectivity observed throughout the amine scope, this C–H activation method was applied to *trans* substituted cyclopropyl fragments in a kinetic resolution process. Depending on the reaction conditions, the starting material could be recovered in 93% ee, or it yielded the expected 1,2,3-functionalised cyclopropane ring in 96% ee. Unexpectedly, a minor stereoisomer resulting of the arylation at the benzylic methine γ -C–H bond was also isolated. The hindered nature of this bond makes C–H cleavage and its subsequent functionalisation a great challenge only achieved so far in ring-strained systems or bridgehead positions to typically deliver intramolecular cyclisations. Gratifyingly, this rare intermolecular reactivity could also be accessed in non-biased substrates to forge cyclopropane rings with quaternary centres, and it remains as a research area worth of further investigations.

The isolation of crystal structures of a functionalised cyclopropane and cyclobutane ring elucidated an absolute configuration with opposite chirality to the one obtained when desymmetrising non-ring-strained systems. The *eclipsed* conformation of ring-strained alkanes made inaccessible the favourable chair-like transition states during C–H cleavage. The restricted amidate geometry of the ligand, previously responsible of preventing substrate decomposition through β -H elimination, played a crucial role in delivering asymmetry. Rather than exploiting more classical ligand-substrate steric interactions, computational calculations indicate that these type of ligand induce enantioselectivity by restricting the mobility of the amidate internal base, and it is the amine backbone which is forced to adopt the most stable conformation to bring the reacting C–H bond in close proximity to palladium and its internal base. The most stable transition state for each diastereomeric

complex proceeded without apparent steric interactions along the amine backbone, which made this mode of asymmetry amenable for many different types of aliphatic amine heterocycles. Non-linear experiments corroborate that a single amino acid ligand is involved throughout the catalytic cycle.

Overall, the research presented in this chapter disclosed the asymmetric reactivity of γ -C-H bonds at ring-strained methylene and methine units in tertiary alkylamine substrates, classified the reactivity between them, and provided a computational insight about how asymmetry is induced when using non-bulky amino acid ligands.

Chapter 4

Conclusion and outlook

C–H activation has emerged as a new reaction paradigm capable of expediting organic synthesis. The ubiquity of C–H bonds in any organic framework avoids the use of prefunctionalised reagents and their functionalisation generates in optimal conditions a proton as the only chemical waste. Unfortunately, this overarching goal is far from being fulfilled. The first palladium-catalysed reactions utilised bespoke directing groups instead of common organic functional groups in order to direct the catalytic palladium metal centre towards productive product formation. However, this played against the problems C–H activation was trying to solve. The incorporation and subsequent removal of these engineered directing functionalities made C–H activation strategies lengthier, more expensive, and non-atom economical. The recent use of transient directing groups has masked this problem by the *in situ* incorporation and removal of the enhanced directing functionality needed to access efficient C(sp³)–H cleavage, while very few literature examples can directly take a native molecule functionality to direct C–H activation.

Over the last decade, the Gaunt group made a distinctive progress towards the use of free amines as substrates in palladium-catalysed C–H activation reactions. While others targeted the functionalisation of primary amines through transient directing groups or through their protection as amides or sulfonates, the Gaunt group aimed to exploit direct binding of secondary amines to palladium to direct C–H activation. The seminal use of hindered secondary amines with no α -H was soon followed by a unique carbonylation platform capable of targeting β -H bonds in a wide range of non-hindered secondary amines through the formation of a carbamoyl complex. Nevertheless, none of the aforementioned strategies were applicable to tertiary amines. There is no simple way to attach and remove a directing auxiliary within a tertiary alkylamine motif and its direct coordination to palladium leads to amine decomposition, which have precluded the use of this prevalent functionality of medicinal chemistry in C–H activation reactions.

The research disclosed in this dissertation explored the reactivity of tertiary alkylamines in palladium-catalysed C–H activation reactions. With the aid of mono-protected amino acid ligands, a wide range of tertiary alkylamines, including piperidine, piperazine, pyrrolidine, morpholine, diazepanes and azetidine heterocycles, as well as acyclic amines, were all found to be viable directing groups at promoting γ -C–H cleavage by exploiting its coordination to catalytic amounts of palladium. The resultant palladacycles were subsequently functionalised by using arylboron reagents as coupling partners with the aid of 1,4-benzoquinone as a key additive. This transformation could be performed in the absence of Ag₂CO₃ and O₂ by using the multifaceted 1,4-benzoquinone as the terminal oxidant at slightly higher reaction temperatures in acyclic amine substrates. If compatible with the aforementioned heterocycles, this greener and more atom-economical reaction can facilitate the scalability and applicability of this transformation in industrial settings.

Computational calculations revealed the constant competition between C–H activation and β -H elimination among the multiple amine heterocycles employed, and how the restricted amidate base of the ligand enhances C–H activation over a deleterious β -H elimination pathway. Acyclic amines proved to be

robust directing functionalities which afforded an excellent reactivity. Piperidine substrates benefited from the unfavourable boat conformation needed during the β -H elimination process to also access product formation. However, the less rigid conformations of pyrrolidine and azepane rings made β -H elimination a favourable pathway, resulting in little to no product formation. This was proved experimentally by exploiting KIE of a α -deuterated pyrrolidine substrate. Nevertheless, subtle changes in the heterocycle fragment can reverse this selectivity, as demonstrated for a diazepane fragment.

The intimate role of amino acid ligands in C-H cleavage prompted the study of an asymmetric C-H activation reaction. Taking the preliminary results of other group members as a starting point, methylene C-H activation could be accessed in cyclopropane and cyclobutane rings with excellent reactivity, diastereo- and enantioselectivity. Most importantly, enantioselectivity could be maintained throughout the different amine heterocycles tested. The exquisite asymmetry observed enabled the use of this transformation in a kinetic resolution event by using racemic *trans* cyclopropanes as starting materials. Interestingly, the presence of β -substituents within the amine backbone invoked a Thorpe-Ingold effect which resulted in an unusual product formation in the absence of ligand, a phenomenon not previously observed throughout this research.

Computational analysis of the different diastereomeric transition states disclosed the unique mode of asymmetric induction employed by the ubiquitous acetyl-*tert*-leucine ligand. Rather than exploiting direct ligand-substrate steric interactions, the restricted geometry of the amidate base acts as a chiral relay, forcing the amine backbone to adopt the most stable conformations in order to bring the reacting C-H bond in close proximity to palladium and its internal base. Therefore, the excellent enantioselectivity observed arose from less favourable acetamide dihedral angles and/or the increased torsional strain along the amine backbone during C-H cleavage. Crucially, the absence of direct steric interactions among the amine backbone justified that this asymmetric transformation was compatible with a wide range of substrates bearing different directing nitrogen heterocycles.

Lastly, more distal cyclopropane rings enabled a rare methine C-H arylation reaction which forged a quaternary centre within the 3-membered ring alkane upon reductive elimination, thus becoming a rare example of an intermolecular C-H methine functionalisation through palladium catalysis.

Overall, the research reported in this dissertation become the cornerstone of tertiary alkylamines as native substrates for palladium-catalysed C(sp³)-H activation reactions and discloses a new chemical space full of exciting opportunities. The decomposition of pyrrolidine and azepane heterocycles through a ligand-assisted CMD pathway provides a compelling groundwork for the rational and systematic optimisation of these substrates. The synthesis of non-natural amino acid ligands with bulkier α -side chains, or the use of ligands with highly restricted amide angles, for instance pyroglutamic acid, will certainly influence the subtle energy difference between both C-H cleaving processes. Another key point worth of further investigation are the less well-explored steps of transmetalation and reductive elimination. The sharp contrast in reactivity between 3-

and 4-membered ring alkanes with their 5- and 6- analogues may not be related to C–H cleavage, being the functionalisation of these more hindered methylene C–H bonds rate limiting in the aforementioned elemental steps. Lastly, benzoquinone was proved to be an ubiquitous additive which can be systematically modified to further improve reaction turnovers and efficiency.

This dissertation was largely focused on the reactivity of different tertiary amine heterocycles, achieving the catalytic functionalisation of methyl, methylene and methine C–H bonds with arylboron reagents. Nevertheless, multiple alternative transformations can be attempted. The successful replacement of ArB(OH)_2 by B_2Pin_2 will lead to the formation of a highly versatile C–B bond intermediate, which can be transformed into a vast range of C–O or C–C bonds, through oxidation or cross-coupling, among others. Alternatively, functionalisation with alkyl boron reagents, in particular MeBF_3K or its fluorinated or deuterated analogues, may find applications as a late-stage functionalisation tool in medicinal chemistry. On the other hand, high-valent palladium manifolds could not be accessed. An inherent limitation of this strategy is the incompatibility of the strong oxidant needed to access Pd^{IV} with the delicate tertiary amine substrates. However, polar amino acid residues, for instance aspartic acid or cysteic acid, may offer a third coordination point to stabilise the putative octahedral Pd^{IV} intermediates, being this strategy applicable to the functionalisation through $\text{S}_{\text{N}}2$ mechanisms rather than control of the reductive elimination step.

It is deeply hoped that the knowledge described in these pages will inspire future breakthroughs in the context of substrate compatibility, novel functionalisations, or more environmentally friendly reaction conditions; all imperative features which will unarguably streamline the synthesis of future drug candidates in medicinal chemistry.

Chapter 5

Experimental procedures

5.1. General information

Solvents and reagents: Et₂O and THF were obtained as anhydrous solvents from distillation over LiAlH₄. MeCN, DCM, hexane and toluene were obtained as anhydrous solvents from distillation over from CaH₂. NMP (99.5%), DMA (99.5%) and DMF (99.8%) were purchased from Acros Organics (extra dry, AcroSeal®) and used without further purification. Other solvents used were purchased anhydrous and used without further purification unless otherwise stated. Pd(OAc)₂ (Pd 45.9–48.4% needles), Ag₂CO₃ (99%) and phenyl boronic acid (98+%) were purchased from Alfa Aesar and used without further purification. Pd(PhCN)₂Cl₂ (95%) was purchased from Sigma Aldrich and used without further purification. 1,4-Benzoquinone was purchased from Sigma Aldrich and purified by recrystallisation from petroleum ether (40–60) before use.

Chromatography: Reactions were monitored by thin layer chromatography (TLC) using pre-coated Merck glass-backed silica gel plates (Kieselgel 60 F254 0.2 mm). Visualisation was performed using ultraviolet light ($\lambda_{\text{max}} = 254 \text{ nm}$) and/or chemical staining with basic potassium permanganate solution as appropriate. Alternatively, reactions were also monitored by gas chromatography (GC) using a Shimadzu QP2010-SE GC fitted with a BPX5 column (10 m, 0.1 mm, 0.1 μm film) for FID analysis, or a SHIM-5MS column (30 m, 0.25 mm, 0.25 μm film) for MS analysis. Chiral analysis was performed on a Shimadzu XR high-performance liquid chromatography (HPLC) instrument fitted with a CHIRALPAK® AD-H column, or a Shimadzu QP2010-SE gas chromatography (GC) fitted with a Astec Chiraldex™ B-DM (20 m, 0.25 mm, 0.12 μm film) for FID analysis. Flash column chromatography was performed on Merck Geduran Si 60 [40-63 μm] under a positive pressure of air or by using a Teledyne CombiFlash NextGen 300+.

Characterisation: Nuclear magnetic resonance (NMR) spectra were recorded at room temperature on a 400 MHz Bruker Avance III HD spectrometer, a 500 MHz Bruker Avance III HD Smart Probe spectrometer, or a 700 MHz Bruker Avance II+ spectrometer. Chemical shifts (δ) were reported in ppm and quoted to the nearest 0.01 ppm relative to the residual protons in CDCl₃ (7.26 ppm for ¹H-NMR, 77.16 ppm for ¹³C-NMR) or DMSO-d₆ (2.05 ppm for ¹H-NMR, 39.52 ppm for ¹³C-NMR). Coupling constants (*J*) were quoted to the nearest 0.1 Hz and multiplicity reported according to the following convention: s = singlet, d = doublet, t = triplet, q = quartet, p = quintet, hex = sextet, hept = septet, oct = octet, m = multiplet, br = broad and associated combinations, e.g. dd = doublet of doublets. Where coincident coupling constants have been observed, the apparent (app) multiplicity of the proton resonance has been reported. Data were reported as follows: chemical shift (multiplicity, coupling constants, number of protons and molecular assignment). DEPT135 and 2-dimensional experiments (COSY, HMBC, HSQC and NOESY) were used to support assignments when appropriate, but were not included herein.

Infrared spectra (FT-IR) were recorded on a PerkinElmer FT-IR spectrometer fitted with an ATR sampling accessory or a Thermo Fisher Nicolet Summit PRO FT-IR spectrometer and samples were analysed as neat oils or solids. Absorptions were reported in wavenumbers (cm^{-1}) and only the most relevant peaks were reported.

High-resolution mass spectra (HRMS) were measured on a Thermo Scientific LTQ Orbitrap XL at the EPSRC Mass Spectrometry Service from University of Swansea, or on a Micromass Q-TOF spectrometer or Waters XEVO GII-S Q-TOF spectrometer at the Department of Chemistry from University of Cambridge.

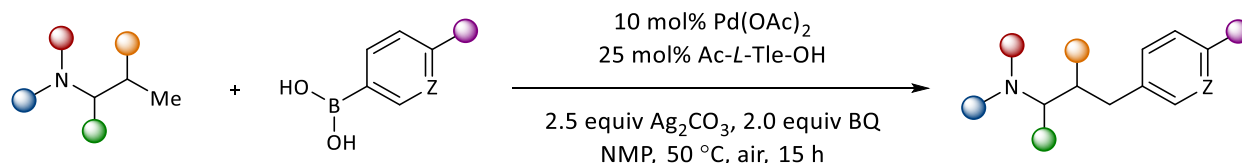
Melting points (mp) were recorded using a Gallenkamp melting point apparatus and are uncorrected.

Optical rotations were measured on a Perkin Elmer Model 343 polarimeter using a Na lamp (λ 589 nm, D-line).

X-Ray crystallography was performed on a Nonius Kappa CCD or a Bruker D8-Quest Photon-100 at the University of Cambridge Chemistry X-ray laboratory by Dr. Andrew Bond.

5.2. Methyl C(sp³)-H activation of tertiary alkylamines

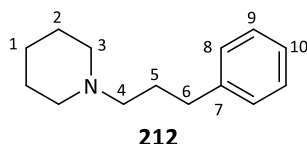
General procedure A: Methyl C-H arylation



The desired tertiary amine (0.750 mmol) was added to a 10–20 mL microwave vial containing Pd(OAc)₂ (6.7 mg, 0.030 mmol), Ac-L-Tle-OH (13.0 mg, 0.0750 mmol), Ag₂CO₃ (207 mg, 0.750 mmol) and 1,4-benzoquinone (BQ) (65.0 mg, 0.600 mmol) in anhydrous NMP (6.50 mL). The reaction was sealed and stirred at 50 °C for 5 minutes. The desired (hetero)aryl boronic acid (0.300 mmol) in NMP (1 mL) was added dropwise and the reaction mixture was stirred at 1000 rpm, at 50 °C for 15 h.

The reaction was cooled to rt and Et₂O (25 mL) added, forcing the formation of a precipitate. The dark mixture was filtered through a pad of Celite and washed with Et₂O (25 mL). The resulting organic layer was washed with aq NaOH (0.25 M, 3 x 50 mL), dried over MgSO₄, filtered and concentrated *in vacuo*. Purification of the crude oil by column chromatography afforded the pure arylated product (*Note: The first aqueous wash is usually dark and can be accompanied with further precipitation, making phase separation difficult to distinguish*).

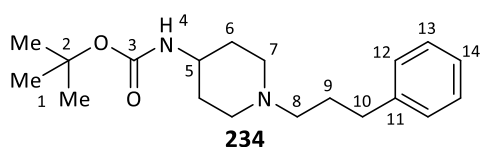
1-(3-Phenylpropyl)piperidine



General procedure A was applied to 1-propylpiperidine (95.4 mg, 0.750 mmol) and phenyl boronic acid (36.6 mg, 0.300 mmol) to provide by column chromatography (DCM to 2% NH₃(MeOH; 2M)) the title compound as a brown oil (49.6 mg, 0.244 mmol, 81% yield).

IR ν_{max} /cm⁻¹ (thin film) 3027, 2932, 2763, 1452, 1155, 1115, 1042, 745, 697; ¹H NMR (400 MHz, CDCl₃) δ (ppm) 7.33 – 7.28 (m, 2H, H₉), 7.26 – 7.16 (m, 3H, H_{8,10}), 2.67 (t, *J* = 7.7 Hz, 2H, H₆), 2.41 (br s, 4H, H₃), 2.37 (t, *J* = 7.7 Hz, 2H, H₄), 1.87 (app qnt, *J* = 7.7 Hz, 2H, H₅), 1.63 (app qnt, *J* = 5.6 Hz, 4H, H₂), 1.51 – 1.42 (m, 2H, H₁); ¹³C NMR (101 MHz, CDCl₃) δ (ppm) 142.3 (C₇), 128.4 (C₈), 128.3 (C₉), 125.7 (C₁₀), 58.9 (C₄), 54.7 (C₃), 34.0 (C₆), 28.8 (C₅), 26.1 (C₂), 24.6 (C₁). HMRS-ESI (*m/z*): found [M+H]⁺ 204.1750, C₁₄H₂₂N requires 204.1747.

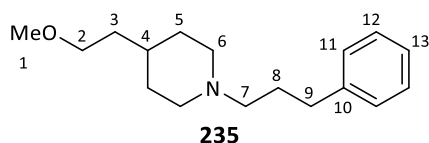
tert-Butyl (1-(3-phenylpropyl)piperidin-4-yl)carbamate



General procedure A was applied to *tert*-butyl (1-propylpiperidin-4-yl)carbamate (182 mg, 0.750 mmol) and phenyl boronic acid (36.6 mg, 0.300 mmol) to provide by column chromatography (DCM to 2% NH₃(MeOH; 2M)) the title compound as a brown oil (67.5 mg, 0.212 mmol, 71% yield).

IR $\nu_{\max}/\text{cm}^{-1}$ (thin film) 3362, 2973, 2938, 2767, 1678, 1514, 1307, 1236, 1163, 1050, 859, 781, 750, 699; **^1H NMR** (400 MHz, CDCl_3) δ (ppm) 7.32 – 7.26 (m, 2H, H_{13}), 7.24 – 7.10 (m, 3H, $\text{H}_{12,14}$), 4.45 (br s, 1H, H_4), 3.47 (br s, 1H, H_5), 2.90 – 2.78 (m, 2H, H_{7a}), 2.64 (t, $J = 7.7$ Hz, 2H, H_{10}), 2.42 – 2.30 (m, 2H, H_8), 2.05 (app t, $J = 11.3$ Hz, 2H, H_{7b}), 1.98 – 1.88 (m, 2H, H_{6a}), 1.82 (app qnt, $J = 7.7$ Hz, 2H, H_9), 1.46 (s, 9H, H_1), 1.50 – 1.38 (m, 2H, H_{6b}); **^{13}C NMR** (101 MHz, CDCl_3) δ (ppm) 155.2 (C_3), 142.1 (C_{11}), 128.4 (C_{12}), 128.3 (C_{13}), 125.7 (C_{14}), 79.2 (C_2), 58.0 (C_8), 52.4 (C_7), 47.8 (C_5), 33.8 (C_{10}), 32.7 (C_6), 28.9 (C_9), 28.4 (C_1); **HMRS-ESI** (m/z): found $[\text{M}+\text{H}]^+$ 319.2380, $\text{C}_{19}\text{H}_{31}\text{N}_2\text{O}_2$ requires 319.2380.

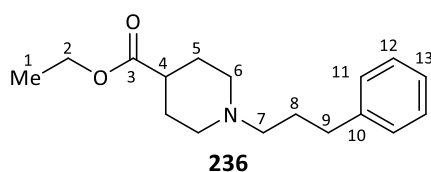
4-(2-Methoxyethyl)-1-(3-phenylpropyl)piperidine



General procedure A was applied to 4-(2-methoxyethyl)-1-propylpiperidine (139 mg, 0.750 mmol) and phenyl boronic acid (36.6 mg, 0.300 mmol) to provide by column chromatography (DCM to 2% $\text{NH}_3(\text{MeOH}; 2\text{M})$) the title compound as a brown oil (60.9 mg, 0.233 mmol, 78% yield).

IR $\nu_{\max}/\text{cm}^{-1}$ (thin film) 3026, 2923, 2860, 2806, 2764, 1602, 1453, 1116, 746, 698; **^1H NMR** (400 MHz, CDCl_3) δ (ppm) 7.33 – 7.25 (m, 2H, H_{12}), 7.24 – 7.16 (m, 3H, $\text{H}_{11,13}$), 3.43 (t, $J = 6.5$ Hz, 2H, H_2), 3.34 (s, 3H, H_1), 3.00 – 2.89 (m, 2H, H_{6a}), 2.64 (t, $J = 7.8$ Hz, 2H, H_9), 2.43 – 2.32 (m, 2H, H_7), 1.94 (app t, $J = 11.1$ Hz, 2H, H_{6b}), 1.85 (app qnt, $J = 7.6$ Hz, 2H, H_8), 1.75 – 1.66 (m, 2H, H_{5a}), 1.54 (app q, $J = 6.5$ Hz, 2H, H_3), 1.49 – 1.37 (m, 1H, H_4), 1.35 – 1.25 (m, 2H, H_{5b}); **^{13}C NMR** (101 MHz, CDCl_3) δ (ppm) 142.2 (C_{10}), 128.4 (C_{11}), 128.3 (C_{12}), 125.7 (C_{13}), 70.4 (C_2), 58.6 (C_1), 58.5 (C_7), 53.9 (C_6), 36.2 (C_3), 33.9 (C_9), 32.7 (C_4), 32.3 (C_5), 28.7 (C_8); **HMRS-ESI** (m/z): found $[\text{M}+\text{H}]^+$ 262.2163, $\text{C}_{17}\text{H}_{28}\text{NO}$ requires 262.2165.

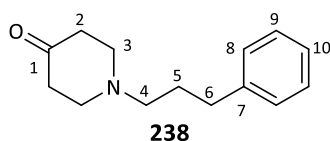
Ethyl 1-(3-phenylpropyl)piperidine-4-carboxylate



General procedure A was applied to ethyl 1-propylpiperidine-4-carboxylate (150 mg, 0.750 mmol) and phenyl boronic acid (36.6 mg, 0.300 mmol) to provide by column chromatography (DCM to 2% $\text{NH}_3(\text{MeOH}; 2\text{M})$) the title compound as a brown oil (52.0 mg, 0.189 mmol,

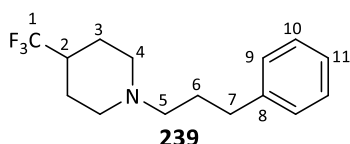
63% yield).

IR $\nu_{\max}/\text{cm}^{-1}$ (thin film) 3027, 2945, 2805, 2767, 1730, 1450, 1377, 1259, 1177, 1047, 1027, 745, 699; **^1H NMR** (400 MHz, CDCl_3) δ (ppm) 7.33 – 7.26 (m, 2H, H_{12}), 7.24 – 7.17 (m, 3H, $\text{H}_{11,13}$), 4.15 (q, $J = 7.1$ Hz, 2H, H_2), 2.95 – 2.85 (m, 2H, H_{6a}), 2.65 (t, $J = 7.7$ Hz, 2H, H_9), 2.41 – 2.34 (m, 2H, H_7), 2.29 (tt, $J = 11.1, 4.0$ Hz, 1H, H_4), 2.00 (app t, $J = 11.1$ Hz, 2H, H_{6b}), 1.95 – 1.75 (m, 6H, $\text{H}_{5,8}$), 1.27 (t, $J = 7.1$ Hz, 3H, H_1); **^{13}C NMR** (101 MHz, CDCl_3) δ (ppm) 175.2 (C_3), 142.2 (C_{10}), 128.4 (C_{11}), 128.3 (C_{12}), 125.7 (C_{13}), 60.3 (C_2), 58.2 (C_7), 53.0 (C_6), 41.3 (C_4), 33.7 (C_9), 28.7 (C_8), 28.3 (C_5), 14.2 (C_1); **HMRS-ESI** (m/z): found $[\text{M}+\text{H}]^+$ 276.1956, $\text{C}_{17}\text{H}_{26}\text{NO}_2$ requires 276.1958.

1-(3-Phenylpropyl)piperidin-4-one

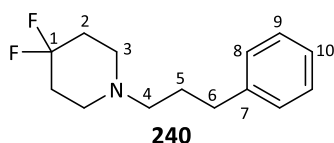
General procedure A was applied to 1-propylpiperidin-4-one (106 mg, 0.750 mmol) and phenyl boronic acid (36.6 mg, 0.300 mmol) to provide by column chromatography (DCM to 3% $\text{NH}_3(\text{MeOH}; 2\text{M})$) the title compound as a yellow oil (31.2 mg, 0.144 mmol, 48% yield).

IR $\nu_{\text{max}}/\text{cm}^{-1}$ (thin film) 3026, 2945, 2806, 1717, 1595, 1453, 1352, 1224, 1130, 747, 699; **$^1\text{H NMR}$** (400 MHz, CDCl_3) δ (ppm) 7.34 – 7.29 (m, 2H, H_9), 7.25 – 7.18 (m, 3H, $\text{H}_{8,10}$), 2.76 (t, $J = 6.1$ Hz, 4H, H_3), 2.71 (t, $J = 7.6$ Hz, 2H, H_6), 2.54 – 2.48 (m, 2H, H_4), 2.48 (t, $J = 6.1$ Hz, 4H, H_2), 1.88 (app qnt, $J = 7.5$ Hz, 2H, H_5); **$^{13}\text{C NMR}$** (101 MHz, CDCl_3) δ (ppm) 209.3 (C_1), 142.0 (C_7), 128.4 (C_8), 128.3 (C_9), 125.9 (C_{10}), 56.7 (C_4), 53.1 (C_3), 41.3 (C_2), 33.6 (C_6), 29.1 (C_5); **HMRS-ESI** (m/z): found $[\text{M}+\text{H}]^+$ 218.1550, $\text{C}_{14}\text{H}_{20}\text{NO}$ requires 218.1545.

1-(3-Phenylpropyl)-4-(trifluoromethyl)piperidine

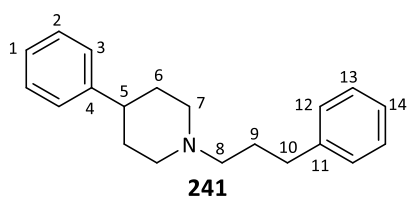
General procedure A was applied to 1-propyl-4-(trifluoromethyl)piperidine (146 mg, 0.750 mmol) and phenyl boronic acid (36.6 mg, 0.300 mmol) to provide by column chromatography (DCM to 2% $\text{NH}_3(\text{MeOH}; 2\text{M})$) the title compound as a brown oil (43.2 mg, 0.159 mmol, 53% yield).

IR $\nu_{\text{max}}/\text{cm}^{-1}$ (thin film) 3027, 2950, 2809, 2773, 1454, 1338, 1252, 1123, 1080, 905, 745, 697; **$^1\text{H NMR}$** (400 MHz, CDCl_3) δ (ppm) 7.34 – 7.27 (m, 2H, H_{10}), 7.25 – 7.17 (m, 3H, $\text{H}_{9,11}$), 3.06 – 2.98 (m, 2H, H_{4a}), 2.66 (t, 2H, $J = 7.7$ Hz, H_7), 2.38 (t, 2H, $J = 7.6$ Hz, H_5), 2.09 – 1.95 (m, 1H, H_2), 1.95 – 1.79 (m, 6H, $\text{H}_{3a,4b,6}$), 1.66 (app qd, $J = 12.5, 3.8$ Hz, 2H, H_{3b}); **$^{13}\text{C NMR}$** (101 MHz, CDCl_3) δ (ppm) 142.1 (C_8), 128.4 (C_9), 128.3 (C_{10}), 127.5 (q, $J = 278.3$ Hz, C_1), 125.8 (C_{11}), 57.9 (C_5), 52.5 (C_4), 40.5 (q, $J = 27.3$ Hz, C_2), 33.7 (C_7), 28.7 (C_6), 24.7 (C_3); **$^{19}\text{F NMR}$** (376 MHz, CDCl_3) δ (ppm) 73.8 (s); **HMRS-ESI** (m/z): found $[\text{M}+\text{H}]^+$ 272.1617, $\text{C}_{15}\text{H}_{21}\text{F}_3\text{N}$ requires 272.1621.

4,4-Difluoro-1-(3-phenylpropyl)piperidine

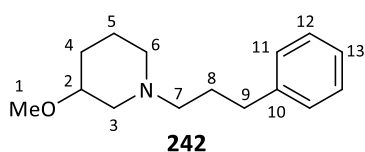
General procedure A was applied to 4,4-difluoro-1-propylpiperidine (122 mg, 0.750 mmol) and phenyl boronic acid (36.6 mg, 0.300 mmol) to provide by column chromatography (DCM to 2% $\text{NH}_3(\text{MeOH}; 2\text{M})$) the title compound as a yellow oil (33.0 mg, 0.138 mmol, 46% yield).

IR $\nu_{\text{max}}/\text{cm}^{-1}$ (thin film) 3027, 2939, 2817, 1601, 1454, 1362, 1094, 950, 747, 699; **$^1\text{H NMR}$** (400 MHz, CDCl_3) δ (ppm) 7.34 – 7.28 (m, 2H, H_9), 7.25 – 7.18 (m, 3H, $\text{H}_{8,10}$), 2.67 (t, $J = 7.7$ Hz, 2H, H_6), 2.56 (br s, 4H, H_3), 2.49 – 2.39 (m, 2H, H_4), 2.09 – 1.93 (m, 4H, H_2), 1.84 (app qnt, $J = 7.7$ Hz, 2H, H_5); **$^{13}\text{C NMR}$** (101 MHz, CDCl_3) δ (ppm) 142.0 (C_7), 128.4 (C_8/C_9), 128.3 (C_8/C_9), 125.8 (C_{10}), 122.2 (t, $J = 241.3$ Hz, C_1), 57.0 (C_4), 50.0 (t, $J = 5.3$ Hz, C_3), 34.0 (t, $J = 22.9$ Hz, C_2), 33.6 (C_6), 28.9 (C_5); **$^{19}\text{F NMR}$** (376 MHz, CDCl_3) δ (ppm) –98.1 (s); **HMRS-ESI** (m/z): found $[\text{M}+\text{H}]^+$ 240.1559, $\text{C}_{14}\text{H}_{20}\text{NF}_2$ requires 240.1558.

4-Phenyl-1-(3-phenylpropyl)piperidine

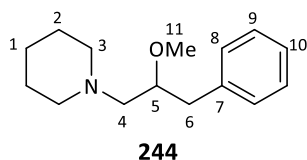
General procedure A was applied to 4-phenyl-1-propylpiperidine (153 mg, 0.750 mmol) and phenyl boronic acid (36.6 mg, 0.300 mmol) to provide by column chromatography (DCM to 2% $\text{NH}_3(\text{MeOH}; 2\text{M})$) the title compound as a brown oil (58.3 mg, 0.209 mmol, 70% yield).

IR $\nu_{\text{max}}/\text{cm}^{-1}$ (thin film) 3026, 2937, 2802, 2764, 1603, 1495, 1452, 1376, 1127, 745, 695; **$^1\text{H NMR}$** (500 MHz, CDCl_3) δ (ppm) 7.35 – 7.29 (m, 4H, $\text{H}_{2,13}$), 7.28 – 7.19 (m, 6H, $\text{H}_{1,3,12,14}$), 3.09 (m, 2H, H_{7a}), 2.68 (t, 2H, $J = 7.7$ Hz, H_{10}), 2.52 (m, 1H, H_5), 2.44 (t, 2H, $J = 7.7$ Hz, H_8), 2.07 (td, $J = 11.2, 3.6$ Hz, 2H, H_{7b}), 1.95 – 1.80 (m, 6H, $\text{H}_{6,9}$); **$^{13}\text{C NMR}$** (126 MHz, CDCl_3) δ (ppm) 146.5 (C_4), 142.2 (C_{11}), 128.4 (C_2 & C_{13}), 128.3 (C_{12}), 126.9 (C_3), 126.1 (C_1), 125.7 (C_{14}), 58.5 (C_8), 54.4 (C_7), 42.8 (C_5), 33.9 (C_{10}), 33.5 (C_6), 28.8 (C_9); **HMRS-ESI** (m/z): found $[\text{M}+\text{H}]^+$ 280.2057, $\text{C}_{20}\text{H}_{26}\text{N}$ requires 280.2060.

3-Methoxy-1-(3-phenylpropyl)piperidine

General procedure A was applied to 3-methoxy-1-propylpiperidine (118 mg, 0.750 mmol) and phenyl boronic acid (36.6 mg, 0.300 mmol) to provide by column chromatography (DCM to 2% $\text{NH}_3(\text{MeOH}; 2\text{M})$) the title compound as a brown oil (42.8 mg, 0.183 mmol, 61% yield).

IR $\nu_{\text{max}}/\text{cm}^{-1}$ (thin film) 3027, 2939, 2773, 1603, 1496, 1454, 1100, 868, 747, 697; **$^1\text{H NMR}$** (400 MHz, CDCl_3) δ (ppm) 7.34 – 7.26 (m, 2H, H_{12}), 7.25 – 7.15 (m, 3H, $\text{H}_{11,13}$), 3.39 (s, 3H, H_1), 3.37 – 3.28 (m, 1H, H_2), 2.98 – 2.87 (m, 1H, H_{3a}), 2.69 – 2.60 (m, 3H, $\text{H}_{6a,9}$), 2.45 – 2.36 (m, 2H, H_7), 2.10 – 1.92 (m, 3H, $\text{H}_{3b,4a,6b}$), 1.86 (app qnt, $J = 7.7$ Hz, 2H, H_8), 1.81 – 1.72 (m, 1H, H_{5a}), 1.59 – 1.47 (m, 1H, H_{5b}), 1.34 – 1.21 (m, 1H, H_{4b}); **$^{13}\text{C NMR}$** (101 MHz, CDCl_3) δ (ppm) 142.2 (C_{10}), 128.4 (C_{11}), 128.3 (C_{12}), 125.7 (C_{13}), 76.3 (C_2), 58.3 (C_7), 57.9 (C_3), 56.1 (C_1), 53.6 (C_6), 33.8 (C_9), 29.9 (C_4), 28.6 (C_8), 23.1 (C_5); **HMRS-ESI** (m/z): found $[\text{M}+\text{H}]^+$ 234.1858, $\text{C}_{15}\text{H}_{24}\text{NO}$ requires 234.1858.

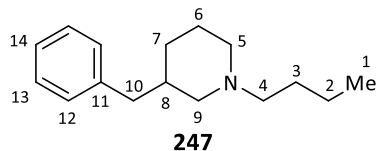
1-(2-Methoxy-3-phenylpropyl)piperidine

General procedure A was applied to 1-(2-methoxypropyl)piperidine (118 mg, 0.750 mmol) and phenyl boronic acid (36.6 mg, 0.300 mmol) to provide by column chromatography (DCM to 2% $\text{NH}_3(\text{MeOH}; 2\text{M})$) the title compound as a brown oil (42.8 mg, 0.183 mmol, 61% yield).

IR $\nu_{\text{max}}/\text{cm}^{-1}$ (thin film) 3027, 2930, 1602, 1495, 1453, 1157, 1101, 742, 697; **$^1\text{H NMR}$** (400 MHz, CDCl_3) δ (ppm) 7.33 – 7.28 (m, 2H, H_9), 7.27 – 7.19 (m, 3H, $\text{H}_{8,10}$), 3.58 (app qnt, $J = 5.9$ Hz, 1H, H_5), 3.38 (s, 3H, H_{11}), 2.88 (dd, $J = 13.9, 5.7$ Hz, 1H, H_{6a}), 2.82 (dd, $J = 13.9, 6.2$ Hz, 1H, H_{6b}), 2.41 (dd, $J = 13.1, 6.6$ Hz, 1H, H_{4a}), 2.39 (br s, 4H, H_3), 2.31 (dd, $J = 13.1, 4.9$ Hz, 1H, H_{4b}), 1.59 (app qnt, $J = 5.6$ Hz, 4H, H_2), 1.47 – 1.38 (m, 2H, H_1); **$^{13}\text{C NMR}$** (101

MHz, CDCl₃) δ (ppm) 139.1 (C₇), 129.5 (C₈), 128.1 (C₉), 125.9 (C₁₀), 80.2 (C₅), 62.1 (C₄), 57.3 (C₁₁), 55.2 (C₃), 38.9 (C₆), 26.1 (C₂), 24.4 (C₁); **HMRS-ESI** (m/z): found [M+H]⁺ 234.1862, C₁₅H₂₄NO requires 234.1858.

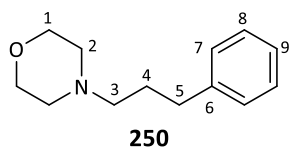
3-Benzyl-1-butylpiperidine



General procedure A was applied to 1-butyl-3-methylpiperidine (116 mg, 0.750 mmol) and phenyl boronic acid (36.6 mg, 0.300 mmol) to provide by column chromatography (DCM to 2% NH₃(MeOH; 2M)) the title compound as a brown oil (21.3 mg, 0.092 mmol, 31% yield).

IR ν_{\max} /cm⁻¹ (thin film) 3026, 2929, 2759, 1603, 1495, 1453, 1096, 745, 697; **¹H NMR** (400 MHz, CDCl₃) δ (ppm) 7.33 – 7.25 (m, 2H, H₁₃), 7.23 – 7.14 (m, 3H, H_{12,14}), 2.87 (app br t, *J* = 13.6 Hz, 2H, H_{5a,9a}), 2.56 (dd, *J* = 13.5, 7.0 Hz, 1H, H_{10a}), 2.49 (dd, *J* = 13.5, 7.5 Hz, 1H, H_{10b}), 2.39 – 2.22 (m, 2H, H₄), 1.97 – 1.81 (m, 2H, H_{5b,8}), 1.77 – 1.42 (m, 6H, H_{3,6,7a,9b}), 1.31 (app hex, *J* = 7.3 Hz, 2H, H₂), 1.01 – 0.80 (m, 4H, H_{1,7b}); **¹³C NMR** (101 MHz, CDCl₃) δ (ppm) 140.4 (C₁₁), 129.1 (C₁₂), 128.2 (C₁₃), 125.8 (C₁₄), 60.4 (C₉), 59.1 (C₄), 54.2 (C₅), 41.2 (C₁₀), 37.9 (C₈), 30.8 (C₇), 29.0 (C₃), 25.3 (C₆), 20.9 (C₂), 14.1 (C₁); **HMRS-ESI** (m/z): found [M+H]⁺ 232.2054, C₁₆H₂₆N requires 232.2060.

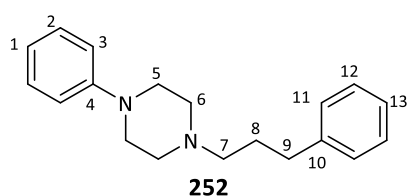
4-(3-Phenylpropyl)morpholine



General procedure A was applied to 4-propylmorpholine (96.9 mg, 0.750 mmol) and phenyl boronic acid (36.6 mg, 0.300 mmol) at 60 °C to provide by column chromatography (DCM to 2% NH₃(MeOH; 2M)) the title compound as a yellow oil (21.5 mg, 0.105 mmol, 35% yield).

IR ν_{\max} /cm⁻¹ (thin film) 3026, 2941, 2853, 2805, 1602, 1495, 1453, 1274, 1115, 1008, 870, 746, 697; **¹H NMR** (400 MHz, CDCl₃) δ (ppm) 7.34 – 7.28 (m, 2H, H₈), 7.27 – 7.15 (m, 3H, H_{7,9}), 3.81 – 3.69 (m, 4H, H₁), 2.71 – 2.63 (m, 2H, H₅), 2.46 (br s, 4H, H₂), 2.42 – 2.35 (m, 2H, H₃), 1.85 (app p, 2H, *J* = 7.4 Hz, H₄); **¹³C NMR** (101 MHz, CDCl₃) δ (ppm) 142.1 (C₆), 128.4 (C₇), 128.3 (C₈), 125.8 (C₉), 67.0 (C₁), 58.4 (C₃), 53.7 (C₂), 33.6 (C₅), 28.3 (C₄); **HMRS-ESI** (m/z): found [M+H]⁺ 206.1539, C₁₃H₂₀NO requires 206.1539.

1-Phenyl-4-(3-phenylpropyl)piperazine

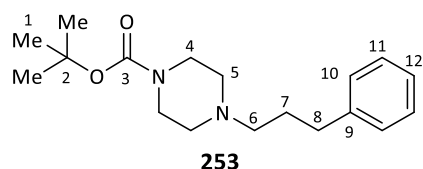


General procedure A was applied to 1-phenyl-4-propylpiperazine (153 mg, 0.75 mmol) and phenyl boronic acid (36.6 mg, 0.300 mmol) at 60 °C to provide by column chromatography (DCM to 20% EtOAc) the title compound as a brown oil (42.1 mg, 0.150 mmol, 50% yield).

IR ν_{\max} /cm⁻¹ (thin film) 3025, 2942, 2815, 1600, 1495, 1452, 1230, 1136, 924, 750, 690; **¹H NMR** (400 MHz, CDCl₃) δ (ppm) 7.34 – 7.26 (m, 4H, H_{2,12}), 7.26 – 7.18 (m, 3H, H_{11,13}), 6.96 (d, *J* = 8.0 Hz, 2H, H₃), 6.88 (t, *J* = 7.3 Hz, 1H, H₁), 3.28 – 3.21 (m, 4H, H₅), 2.73 – 2.67 (m, 2H, H₉), 2.66 – 2.59 (m, 4H, H₆), 2.52 – 2.40 (m, 2H, H₇),

1.90 (app qnt, $J = 7.4$ Hz, 2H, H₈); ¹³C NMR (101 MHz, CDCl₃) δ (ppm) 151.4 (C₄), 142.1 (C₁₀), 129.1 (C₂), 128.4 (C₁₁), 128.3 (C₁₂), 125.8 (C₁₃), 119.6 (C₁), 116.0 (C₃), 58.0 (C₇), 53.3 (C₆), 49.2 (C₅), 33.7 (C₉), 28.6 (C₈); HMRS-ESI (m/z): found [M+H]⁺ 281.2015, C₁₉H₂₅N₂ requires 281.2018.

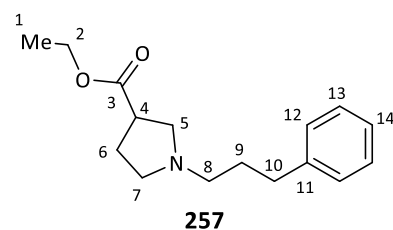
tert-Butyl 4-(3-phenylpropyl)piperazine-1-carboxylate



General procedure A was applied to *tert*-butyl 4-propylpiperazine-1-carboxylate (171 mg, 0.750 mmol) and phenyl boronic acid (36.6 mg, 0.300 mmol) to provide by column chromatography (DCM to 50% EtOAc) the title compound as a yellow oil (41.8 mg, 0.137 mmol, 46% yield).

IR ν_{\max} /cm⁻¹ (thin film) 3026, 2931, 2855, 1693, 1418, 1244, 1168, 1004, 747, 698; ¹H NMR (400 MHz, CDCl₃) δ (ppm) 7.34 – 7.26 (m, 2H, H₁₁), 7.26 – 7.15 (m, 3H, H_{10,12}), 3.53 – 3.38 (m, 4H, H₄), 2.72 – 2.61 (m, 2H, H₈), 2.48 – 2.29 (m, 6H, H_{5,6}), 1.85 (app qnt, $J = 7.5$ Hz, 2H, H₇), 1.48 (s, 9H, H₁); ¹³C NMR (126 MHz, CDCl₃) δ (ppm) 154.8 (C₃), 142.0 (C₉), 128.4 (C₁₀), 128.3 (C₁₁), 125.8 (C₁₂), 79.6 (C₂), 57.9 (C₆), 53.0 (C₅), 44.1 (br s, C_{4a}), 43.1 (br s, C_{4b}), 33.6 (C₈), 28.5 (C₇), 28.4 (C₁); HMRS-ESI (m/z): found [M+H]⁺ 305.2226, C₁₈H₂₉N₂O₂ requires 305.2229.

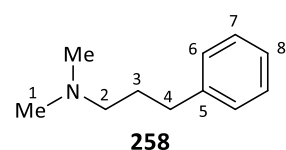
Ethyl 1-(3-phenylpropyl)pyrrolidine-3-carboxylate



General procedure A was applied to ethyl 1-propylpyrrolidine-3-carboxylate (139 mg, 0.750 mmol) and phenyl boronic acid (36.6 mg, 0.300 mmol) to provide by column chromatography (DCM to 80:18:2 DCM:EtOAc:NH₃(MeOH; 2M)) the title compound as a brown oil (17.1 mg, 0.065 mmol, 22% yield).

IR ν_{\max} /cm⁻¹ (thin film) 2933, 2791, 1730, 1453, 1371, 1174, 1030, 746, 698; ¹H NMR (400 MHz, CDCl₃) δ (ppm) 7.33 – 7.27 (m, 2H, H₁₃), 7.23 – 7.17 (m, 3H, H_{12,14}), 4.17 (q, $J = 7.1$ Hz, 2H, H₂), 3.04 (app p, $J = 7.8$ Hz, 1H, H₄), 2.94 (app t, $J = 8.8$ Hz, 1H, H_{5a}), 2.76 – 2.61 (m, 4H, H_{5b,7a,10}), 2.57 – 2.42 (m, 3H, H_{7b,8}), 2.15 – 2.07 (m, $J = 7.8$ Hz, 2H, H₆), 1.91 – 1.81 (app p, $J = 7.7$ Hz, 2H, H₉), 1.28 (t, $J = 7.1$ Hz, 3H, H₁); ¹³C NMR (101 MHz, CDCl₃) δ (ppm) 175.0 (C₃), 142.1 (C₁₁), 128.4 (C₁₂), 128.3 (C₁₃), 125.7 (C₁₄), 60.6 (C₂), 56.8 (C₅), 55.5 (C₈), 53.9 (C₇), 42.1 (C₄), 33.8 (C₁₀), 30.5 (C₉), 27.6 (C₆), 14.2 (C₁); HMRS-ESI (m/z): found [M+H]⁺ 262.1803, C₁₆H₂₄NO₂ requires 262.1802.

***N,N*-Dimethyl-3-phenylpropan-1-amine**

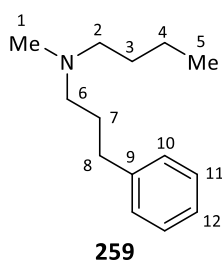


General procedure A was applied to *N,N*-dimethylpropan-1-amine (65.4 mg, 0.750 mmol) and phenyl boronic acid (36.6 mg, 0.300 mmol) to provide by column chromatography (DCM to 2% NH₃(MeOH; 2M)) the title compound as a brown oil (42.5

mg, 0.260 mmol, 87% yield).

IR $\nu_{\max}/\text{cm}^{-1}$ (thin film) 3026, 2942, 1603, 1498, 1262, 1030, 745, 698; **$^1\text{H NMR}$** (400 MHz, CDCl_3) δ (ppm) 7.35 – 7.27 (m, 2H, H_7), 7.26 – 7.15 (m, 3H, $\text{H}_{6,8}$), 2.71 – 2.62 (m, 2H, H_4), 2.36 – 2.29 (m, 2H, H_2), 2.25 (s, 6H, H_1), 1.82 (app qnt, $J = 7.5$ Hz, 2H, H_3); **$^{13}\text{C NMR}$** (101 MHz, CDCl_3) δ (ppm) 142.3 (C_5), 128.4 (C_6), 128.3 (C_7), 125.7 (C_8), 59.3 (C_2), 45.5 (C_1), 33.7 (C_4), 29.5 (C_3); **HMRS-ESI** (m/z): found $[\text{M}+\text{H}]^+$ 164.1431, $\text{C}_{11}\text{H}_{18}\text{N}$ requires 164.1434.

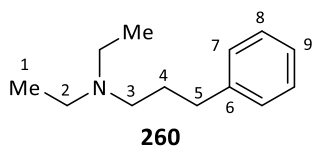
N-Methyl-*N*-(3-phenylpropyl)butan-1-amine



General procedure A was applied to *N*-methyl-*N*-propylbutan-1-amine (97.0 mg, 0.750 mmol) and phenyl boronic acid (36.6 mg, 0.300 mmol) to provide by column chromatography (DCM to 2% $\text{NH}_3(\text{MeOH}; 2\text{M})$) the title compound as a yellow oil (55.9 mg, 0.272 mmol, 91% yield).

IR $\nu_{\max}/\text{cm}^{-1}$ (thin film) 3027, 2954, 2931, 2785, 1603, 1495, 1454, 1377, 1076, 1031, 744, 697; **$^1\text{H NMR}$** (400 MHz, CDCl_3) δ (ppm) 7.33 – 7.27 (m, 2H, H_{11}), 7.25 – 7.18 (m, 3H, $\text{H}_{10,12}$), 2.65 (t, 2H, $J = 7.7$ Hz, H_8), 2.42 – 2.36 (m, 2H, H_6), 2.36 – 2.31 (m, 2H, H_2), 2.24 (s, 3H, H_1), 1.82 (app qnt, $J = 7.7$ Hz, 2H, H_7), 1.51 – 1.41 (m, 2H, H_3), 1.39 – 1.29 (m, 2H, H_4), 0.94 (t, $J = 7.3$ Hz, 3H, H_5); **$^{13}\text{C NMR}$** (101 MHz, CDCl_3) δ (ppm) 142.4 (C_9), 128.4 (C_{10}), 128.3 (C_{11}), 125.7 (C_{12}), 57.6 (C_2), 57.4 (C_6), 42.3 (C_1), 33.8 (C_8), 29.5 (C_3), 29.1 (C_7), 20.8 (C_4), 14.1 (C_5); **HMRS-ESI** (m/z): found $[\text{M}+\text{H}]^+$ 206.1913, $\text{C}_{14}\text{H}_{24}\text{N}$ requires 206.1909.

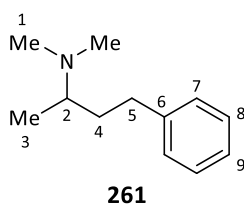
N,N-Diethyl-3-phenylpropan-1-amine



General procedure A was applied to *N,N*-diethylpropan-1-amine (86.4 mg, 0.750 mmol) and phenyl boronic acid (36.6 mg, 0.300 mmol) to provide by column chromatography (DCM to 2% $\text{NH}_3(\text{MeOH}; 2\text{M})$) the title compound as a brown oil (29.7 mg, 0.155 mmol, 52% yield).

IR $\nu_{\max}/\text{cm}^{-1}$ (thin film) 3028, 2928, 2853, 2807, 1600, 1489, 1237, 745, 697; **$^1\text{H NMR}$** (400 MHz, CDCl_3) δ (ppm) 7.34 – 7.26 (m, 2H, H_8), 7.26 – 7.16 (m, 3H, $\text{H}_{7,9}$), 2.64 (t, $J = 7.6$ Hz, 2H, H_5), 2.55 (q, $J = 7.1$ Hz, 4H, H_2), 2.52 – 2.46 (m, 2H, H_3), 1.81 (app qnt, $J = 7.6$ Hz, 2H, H_4), 1.03 (t, $J = 7.1$ Hz, 6H, H_1); **$^{13}\text{C NMR}$** (101 MHz, CDCl_3) δ (ppm) 142.4 (C_6), 128.4 (C_7), 128.3 (C_8), 125.7 (C_9), 52.5 (C_3), 46.9 (C_2), 33.9 (C_5), 28.8 (C_4), 11.7 (C_1); **HMRS-ESI** (m/z): found $[\text{M}+\text{H}]^+$ 192.1745, $\text{C}_{13}\text{H}_{22}\text{N}$ requires 192.1747.

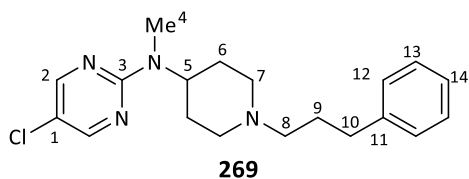
N,N-Dimethyl-4-phenylbutan-2-amine



General procedure A was applied to *N,N*-dimethylbutan-2-amine (75.9 mg, 0.750 mmol) and phenyl boronic acid (36.6 mg, 0.300 mmol) to provide by column chromatography (DCM to 2% $\text{NH}_3(\text{MeOH}; 2\text{M})$) the title compound as a brown oil (48.8 mg, 0.275 mmol, 92% yield).

IR $\nu_{\max}/\text{cm}^{-1}$ (thin film) 3025, 2942, 2810, 2770, 1599, 1495, 1078, 746, 699; **$^1\text{H NMR}$** (400 MHz, CDCl_3) δ (ppm) 7.34 – 7.27 (m, 2H, H_8), 7.26 – 7.17 (m, 3H, $\text{H}_{7,9}$), 2.74 – 2.61 (m, 2H, H_5), 2.57 (app hex, $J = 6.5$ Hz, 1H, H_2), 2.26 (s, 6H, H_1), 1.85 (ddt, $J = 12.7, 9.8, 6.2$ Hz, 1H, H_{4a}), 1.64 – 1.53 (m, 1H, H_{4b}), 1.02 (d, $J = 6.5$ Hz, 3H, H_3); **$^{13}\text{C NMR}$** (101 MHz, CDCl_3) δ (ppm) 142.8 (C_6), 128.4 (C_7), 128.3 (C_8), 125.6 (C_9), 58.5 (C_2), 40.5 (C_1), 35.5 (C_4), 33.0 (C_5), 13.3 (C_3); **HMRS-ESI** (m/z): found $[\text{M}+\text{H}]^+$ 178.1597, $\text{C}_{12}\text{H}_{20}\text{N}$ requires 178.1596.

5-Chloro-*N*-methyl-*N*-(1-(3-phenylpropyl)piperidin-4-yl)pyrimidin-2-amine

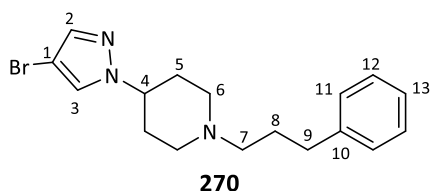


General procedure A was applied to 5-chloro-*N*-methyl-*N*-(1-propylpiperidin-4-yl)pyrimidin-2-amine (202 mg, 0.750 mmol) and phenyl boronic acid (36.6 mg, 0.300 mmol) to provide by column chromatography (EtOAc) the title compound as a brown oil (61.9

mg, 0.180 mmol, 60% yield).

IR $\nu_{\max}/\text{cm}^{-1}$ (thin film) 3025, 2942, 2802, 2767, 1583, 1496, 1367, 1030, 745, 697; **$^1\text{H NMR}$** (400 MHz, CDCl_3) δ (ppm) 8.23 (s, 2H, H_2), 7.33 – 7.28 (m, 2H, H_{13}), 7.24 – 7.17 (m, 3H, $\text{H}_{12,14}$), 4.57 (tt, $J = 12.0, 4.1$ Hz, 1H, H_5), 3.08 – 2.99 (m, 5H, $\text{H}_{4,7a}$), 2.67 (t, $J = 7.6$ Hz, 2H, H_{10}), 2.48 – 2.36 (m, 2H, H_8), 2.12 (app td, $J = 11.9, 2.0$ Hz, 2H, H_{7b}), 1.93 – 1.81 (m, 4H, $\text{H}_{6a,9}$), 1.73 – 1.65 (m, 2H, H_{6b}); **$^{13}\text{C NMR}$** (101 MHz, CDCl_3) δ (ppm) 159.9 (C_3), 155.7 (C_2), 142.1 (C_{11}), 128.4 (C_{12}), 128.3 (C_{13}), 125.8 (C_{14}), 117.4 (C_1), 58.0 (C_8), 53.2 (C_7), 52.9 (C_5), 33.8 (C_{10}), 29.1 (C_4), 29.0 (C_6), 28.9 (C_9); **HMRS-ESI** (m/z): found $[\text{M}+\text{H}]^+$ 345.1844, $\text{C}_{19}\text{H}_{26}\text{N}_4\text{Cl}$ requires 345.1846.

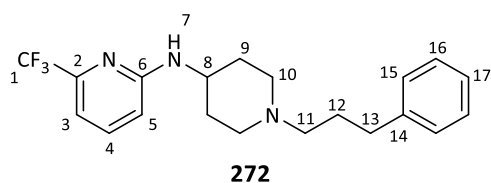
4-(4-Bromo-1*H*-pyrazol-1-yl)-1-(3-phenylpropyl)piperidine



General procedure A was applied to 4-(4-bromo-1*H*-pyrazol-1-yl)-1-propylpiperidine (163.3 mg, 0.600 mmol) and phenyl boronic acid (36.6 mg, 0.300 mmol) to provide by column chromatography (DCM to 80:19:1 DCM:EtOAc: $\text{NH}_3(\text{MeOH}; 2\text{M})$) the title compound as a brown oil

(35.1 mg, 0.101 mmol, 34% yield).

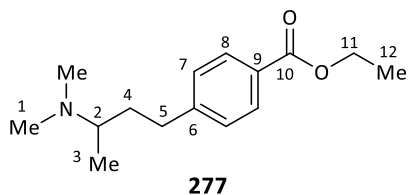
IR $\nu_{\max}/\text{cm}^{-1}$ (thin film) 2945, 2807, 2769, 1452, 1372, 1304, 1110, 976, 952, 838, 731, 698; **$^1\text{H NMR}$** (400 MHz, CDCl_3) δ (ppm) 7.47 (s, 1H, H_2), 7.45 (s, 1H, H_3), 7.34 – 7.29 (m, 2H, H_{12}), 7.24 – 7.17 (m, 3H, $\text{H}_{11,13}$), 4.12 (tt, $J = 11.5, 4.1$ Hz, 1H, H_4), 3.09 – 3.00 (m, 2H, H_{6a}), 2.67 (t, $J = 7.7$ Hz, 2H, H_9), 2.46 – 2.38 (m, 2H, H_7), 2.18 – 2.07 (m, 4H, $\text{H}_{5a,6b}$), 2.06 – 1.94 (m, 2H, H_{5b}), 1.86 (app p, $J = 7.7$ Hz, 2H, H_8); **$^{13}\text{C NMR}$** (101 MHz, CDCl_3) δ (ppm) 142.1 (C_{10}), 139.2 (C_2), 128.4 (C_{11}), 128.3 (C_{12}), 126.7 (C_3), 125.8 (C_{13}), 92.7 (C_1), 60.3 (C_4), 57.6 (C_7), 52.4 (C_6), 33.6 (C_9), 32.5 (C_5), 28.9 (C_8); **HMRS-ESI** (m/z): found $[\text{M}+\text{H}]^+$ 348.1070, $\text{C}_{17}\text{H}_{23}\text{N}_3\text{Br}$ requires 348.1074.

***N*-(1-(3-Phenylpropyl)piperidin-4-yl)-6-(trifluoromethyl)pyridin-2-amine****272**

General procedure A was applied to *N*-(1-Propylpiperidin-4-yl)-6-(trifluoromethyl)pyridin-2-amine (216 mg, 0.750 mmol) and phenyl boronic acid (36.6 mg, 0.300 mmol) to provide by column chromatography (EtOAc) the title compound as a brown oil (67.2

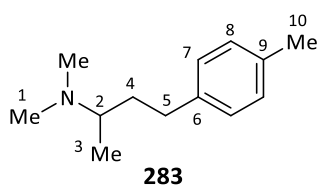
mg, 0.185 mmol, 62% yield).

IR $\nu_{\max}/\text{cm}^{-1}$ (thin film) 2942, 2804, 1512, 1470, 1367, 1294, 1182, 978, 736, 698; **$^1\text{H NMR}$** (400 MHz, CDCl_3) δ (ppm) 7.52 (app t, $J = 7.8$ Hz, 1H, H_4), 7.34 – 7.28 (m, 2H, H_{16}), 7.25 – 7.18 (m, 3H, $\text{H}_{15,17}$), 6.92 (d, $J = 7.3$ Hz, 1H, H_3), 6.52 (d, $J = 8.5$ Hz, 1H, H_5), 4.69 (d, $J = 7.5$ Hz, 1H, H_7), 3.70 – 3.59 (m, 1H, H_8), 2.90 (br d, $J = 11.5$ Hz, 2H, H_{10a}), 2.66 (t, $J = 7.5$ Hz, 2H, H_{13}), 2.47 – 2.37 (m, 2H, H_{11}), 2.18 (app t, $J = 11.3$ Hz, 2H, H_{10b}), 2.12 – 2.04 (m, 2H, H_{9a}), 1.86 (app qnt, $J = 7.5$ Hz, 2H, H_{12}), 1.62 – 1.51 (m, 2H, H_{9b}); **$^{13}\text{C NMR}$** (101 MHz, CDCl_3) δ (ppm) 157.7 (C_6), 146.7 (q, $J = 33.7$ Hz, C_2), 142.1 (C_{14}), 138.1 (C_4), 128.4 (C_{15}), 128.3 (C_{16}), 125.8 (C_{17}), 121.6 (q, $J = 274.0$ Hz, C_1), 109.8 (C_5), 108.7 (q, $J = 3.1$ Hz, C_3), 58.0 (C_{11}), 52.2 (C_{10}), 48.5 (C_8), 33.8 (C_{13}), 32.1 (C_9), 28.8 (C_{12}); **$^{19}\text{F NMR}$** (376 MHz, CDCl_3) δ (ppm) 68.9 (s); **HMRS-ESI** (m/z): found $[\text{M}+\text{H}]^+$ 364.2002, $\text{C}_{20}\text{H}_{25}\text{N}_3\text{F}_3$ requires 364.2001.

Ethyl 4-(3-(dimethylamino)butyl)benzoate**277**

General procedure A was applied to *N,N*-dimethylbutan-2-amine (75.9 mg, 0.750 mmol) and (4-(ethoxycarbonyl)phenyl)boronic acid (58.2 mg, 0.300 mmol) to provide by column chromatography (DCM to 3% $\text{NH}_3(\text{MeOH}; 2\text{M})$) the title compound as a yellow oil (65.9 mg, 0.264 mmol, 88% yield).

IR $\nu_{\max}/\text{cm}^{-1}$ (thin film) 2963, 2932, 2775, 1714, 1610, 1453, 1270, 1176, 1100, 1021, 763; **$^1\text{H NMR}$** (400 MHz, CDCl_3) δ (ppm) 7.98 (d, $J = 8.2$ Hz, 2H, H_8), 7.28 (d, $J = 8.2$ Hz, 2H, H_7), 4.38 (q, $J = 7.1$ Hz, 2H, H_{11}), 2.79 – 2.65 (m, 2H, H_5), 2.61 – 2.50 (app hex, $J = 6.5$ Hz, 1H, H_2), 2.25 (s, 6H, H_1), 1.89 – 1.79 (m, 1H, H_{4a}), 1.64 – 1.53 (m, 1H, H_{4b}), 1.41 (t, $J = 7.1$ Hz, 3H, H_{12}), 1.00 (d, $J = 6.5$ Hz, 3H, H_3); **$^{13}\text{C NMR}$** (101 MHz, CDCl_3) δ (ppm) 166.7 (C_{10}), 148.2 (C_6), 129.6 (C_8), 128.4 (C_7), 128.0 (C_9), 60.7 (C_{11}), 58.2 (C_2), 40.4 (C_1), 35.3 (C_4), 33.0 (C_5), 14.4 (C_{12}), 13.0 (C_3); **HMRS-ESI** (m/z): found $[\text{M}+\text{H}]^+$ 250.1802, $\text{C}_{15}\text{H}_{24}\text{NO}_2$ requires 250.1802.

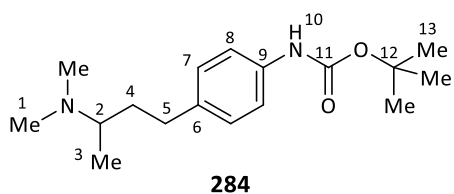
***N,N*-Dimethyl-4-(*p*-tolyl)butan-2-amine****283**

General procedure A was applied to *N,N*-dimethylbutan-2-amine (75.9 mg, 0.750 mmol) and *p*-tolylboronic acid (40.8 mg, 0.300 mmol) to provide by column chromatography (DCM to 2% $\text{NH}_3(\text{MeOH}; 2\text{M})$) the title compound as a yellow oil (42.4 mg, 0.222 mmol, 74% yield).

IR $\nu_{\max}/\text{cm}^{-1}$ (thin film) 2962, 2927, 2817, 2773, 1514, 1451, 1375, 1267, 1158, 1128, 1045, 806; **$^1\text{H NMR}$** (400 MHz, CDCl_3) δ (ppm) 7.12 (app s, 4H, $\text{H}_{7,8}$), 2.70 – 2.52 (m, 3H, $\text{H}_{2,5}$), 2.34 (s, 3H, H_{10}), 2.26 (s, 6H, H_1), 1.90 –

1.77 (m, 1H, H_{4a}), 1.62 – 1.51 (m, 1H, H_{4b}), 1.01 (d, $J = 6.5$ Hz, 3H, H₃); ¹³C NMR (101 MHz, CDCl₃) δ (ppm) 139.6 (C₆), 135.1 (C₉), 129.0 (C₈), 128.2 (C₇), 58.5 (C₂), 40.5 (C₁), 35.6 (C₄), 32.5 (C₅), 21.0 (C₁₀), 13.3 (C₃); HMRS-ESI (m/z): found [M+H]⁺ 192.1747, C₁₃H₂₂N requires 192.1746.

tert-Butyl (4-(3-(dimethylamino)butyl)phenyl)carbamate



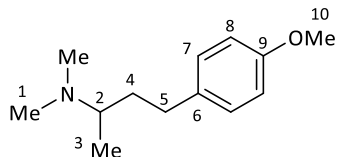
284

General procedure A was applied to *N,N*-dimethylbutan-2-amine (75.9 mg, 0.750 mmol) and 4-((*tert*-butoxycarbonyl)amino)phenylboronic acid (71.1 mg, 0.300 mmol) to provide by column chromatography (DCM to 3% NH₃(MeOH; 2M)) the title compound as a

brown oil (56.1 mg, 0.192 mmol, 64% yield).

IR ν_{\max} /cm⁻¹ (thin film) 2971, 2773, 1722, 1520, 1411, 1365, 1049, 830; ¹H NMR (400 MHz, CDCl₃) δ (ppm) 7.32 – 7.24 (m, 2H, H₈), 7.13 (d, $J = 8.4$ Hz, 2H, H₇), 6.41 (s, 1H, H₁₀), 2.68 – 2.51 (m, 3H, H_{2,5}), 2.25 (s, 6H, H₁), 1.81 (ddt, $J = 12.2, 9.9, 6.0$ Hz, 1H, H_{4a}), 1.58 – 1.49 (m, 10H, H_{4b,13}), 0.99 (d, $J = 6.5$ Hz, 3H, H₃); ¹³C NMR (101 MHz, CDCl₃) δ (ppm) 152.9 (C₁₁), 137.5 (C₆), 136.0 (C₉), 128.8 (C₇), 118.7 (C₈), 80.3 (C₁₂), 58.3 (C₂), 40.4 (C₁), 35.5 (C₄), 32.3 (C₅), 28.4 (C₁₃), 13.2 (C₃); HMRS-ESI (m/z): found [M+H]⁺ 293.2224, C₁₇H₂₉N₂O₂ requires 293.2224.

4-(4-Methoxyphenyl)-*N,N*-dimethylbutan-2-amine

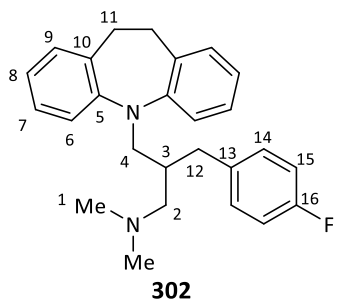


286

General procedure A was applied to *N,N*-dimethylbutan-2-amine (75.9 mg, 0.750 mmol) and 4-methoxyphenylboronic acid (45.6 mg, 0.300 mmol) to provide by column chromatography (DCM to 2% NH₃(MeOH; 2M)) the title compound as a brown oil (30.8 mg, 0.149 mmol, 50% yield).

IR ν_{\max} /cm⁻¹ (thin film) 2961, 2932, 2818, 2774, 1612, 1510, 1454, 1242, 1175, 1037, 820; ¹H NMR (400 MHz, CDCl₃) δ (ppm) 7.14 (d, $J = 8.5$ Hz, 2H, H₇), 6.85 (d, $J = 8.6$ Hz, 2H, H₈), 3.81 (s, 3H, H₁₀), 2.67 – 2.53 (m, 3H, H_{2,5}), 2.26 (s, 6H, H₁), 1.88 – 1.77 (m, 1H, H_{4a}), 1.55 (dddd, $J = 13.6, 9.8, 7.6, 6.3$ Hz, 1H, H_{4b}), 1.01 (d, $J = 6.5$ Hz, 3H, H₃); ¹³C NMR (101 MHz, CDCl₃) δ (ppm) 157.7 (C₉), 134.7 (C₆), 129.2 (C₇), 113.7 (C₈), 58.4 (C₂), 55.3 (C₁₀), 40.4 (C₁), 35.6 (C₄), 32.0 (C₅), 13.3 (C₃); HMRS-ESI (m/z): found [M+H]⁺ 208.1696, C₁₃H₂₂NO requires 208.1696.

3-(10,11-dihydro-5H-dibenzo[*b,f*]azepin-5-yl)-2-(4-fluorobenzyl)-*N,N*-dimethylpropan-1-amine

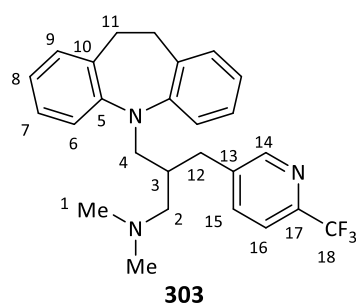


302

General procedure A was applied to 3-(10,11-dihydro-5H-dibenzo[*b,f*]azepin-5-yl)-*N,N*-dimethylpropan-1-amine (221 mg, 0.750 mmol) and 4-fluorophenylboronic acid (42.0 mg, 0.300 mmol) to provide by column chromatography (DCM to 3% NH₃(MeOH; 2M)) the title compound as a pale yellow oil (74.3 mg, 0.191 mmol, 64% yield).

IR $\nu_{\max}/\text{cm}^{-1}$ (thin film) 2940, 2857, 2820, 2768, 1598, 1508, 1486, 1220, 906, 728; **$^1\text{H NMR}$** (400 MHz, CDCl_3) δ (ppm) 7.20 – 7.06 (m, 4H, $\text{H}_{7,9}$), 7.02 – 6.80 (m, 8H, $\text{H}_{6,8,14,15}$), 3.84 (dd, $J = 12.9, 5.3$ Hz, 1H, H_{4a}), 3.46 (dd, $J = 12.9, 7.0$ Hz, 1H, H_{4b}), 3.25 (s, 4H, H_{11}), 2.73 (dd, $J = 13.8, 5.6$ Hz, 1H, H_{12a}), 2.65 (dd, $J = 13.8, 5.6$ Hz, 1H, H_{12b}), 2.31 – 2.17 (m, 1H, H_{2a}), 2.17 – 2.01 (m, 8H, $\text{H}_{1,2b,3}$); **$^{13}\text{C NMR}$** (101 MHz, CDCl_3) δ (ppm) 161.3 (d, $J = 243.4$ Hz, C_{16}), 148.3 (C_5), 135.9 (d, $J = 3.3$ Hz, C_{13}), 134.1 (C_{10}), 130.7 (d, $J = 7.7$ Hz, C_{14}), 129.9 (C_9), 126.4 (C_7), 122.5 (C_8), 120.1 (C_6), 114.8 (d, $J = 21.0$ Hz, C_{15}), 62.5 (C_2), 52.7 (C_4), 46.1 (C_1), 36.5 (C_{12}), 36.2 (C_3), 32.4 (C_{11}); **$^{19}\text{F NMR}$** (376 MHz, CDCl_3) δ (ppm) –117.7 (s); **HMRS-ESI** (m/z): found $[\text{M}+\text{H}]^+$ 389.2382, $\text{C}_{26}\text{H}_{30}\text{N}_2\text{F}$ requires 389.2388.

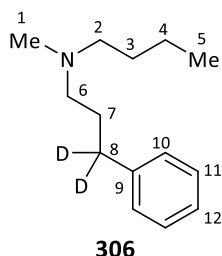
3-(10,11-dihydro-5H-dibenzo[b,f]azepin-5-yl)-*N,N*-dimethyl-2-((6-(trifluoromethyl)pyridin-3-yl)methyl)propan-1-amine



General procedure A was applied to 3-(10,11-dihydro-5H-dibenzo[b,f]azepin-5-yl)-*N,N*-dimethylpropan-1-amine (221 mg, 0.750 mmol) and (6-(trifluoromethyl)pyridin-3-yl)boronic acid (57.3 mg, 0.300 mmol) to provide by column chromatography (DCM to 3% $\text{NH}_3(\text{MeOH}; 2\text{M})$) the title compound as a pale yellow oil (107.9 mg, 0.246 mmol, 82% yield).

IR $\nu_{\max}/\text{cm}^{-1}$ (thin film) 2943, 2822, 2770, 1487, 1335, 1130, 1086, 907, 727; **$^1\text{H NMR}$** (400 MHz, CDCl_3) δ (ppm) 8.42 (d, $J = 1.4$ Hz, 1H, H_{14}), 7.53 (d, $J = 8.0$ Hz, 1H, H_{16}), 7.44 (dd, $J = 8.0, 1.4$ Hz, 1H, H_{15}), 7.19 – 7.10 (m, 4H, $\text{H}_{7,9}$), 7.04 (d, $J = 7.8$ Hz, 2H, H_6), 6.98 (td, $J = 7.4, 1.0$ Hz, 2H, H_8), 3.98 (dd, $J = 13.0, 4.6$ Hz, 1H, H_{4a}), 3.37 (dd, $J = 13.0, 8.2$ Hz, 1H, H_{4b}), 3.24 (s, $J = 11.4$ Hz, 4H, H_{11}), 2.92 (dd, $J = 13.7, 4.5$ Hz, 1H, H_{12a}), 2.69 (dd, $J = 13.7, 6.2$ Hz, 1H, H_{12b}), 2.29 – 2.17 (m, 2H, $\text{H}_{2a,3}$), 2.16 – 2.03 (m, 7H, $\text{H}_{1,2b}$); **$^{13}\text{C NMR}$** (101 MHz, CDCl_3) δ (ppm) 150.9 (C_{14}), 148.0 (C_5), 145.9 (q, $J = 34.6$ Hz, C_{17}), 139.3 (C_{13}), 137.9 (C_{15}), 134.0 (C_{10}), 130.0 (C_9), 126.5 (C_7), 122.8 (C_8), 121.8 (q, $J = 273.7$ Hz, C_{18}), 120.0 – 119.8 (m, $\text{C}_{6,16}$), 61.9 (C_2), 52.6 (C_4), 46.0 (C_1), 36.0 (C_3), 34.0 (C_{12}), 32.3 (C_{11}); **$^{19}\text{F NMR}$** (376 MHz, CDCl_3) δ (ppm) –67.6 (s); **HMRS-ESI** (m/z): found $[\text{M}+\text{H}]^+$ 440.2299, $\text{C}_{26}\text{H}_{29}\text{N}_3\text{F}_3$ requires 440.2308.

N-Methyl-*N*-(3-phenylpropyl-3,3- d_2)butan-1-amine

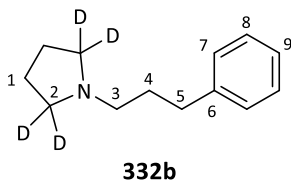


General procedure A was applied to *N*-methyl-*N*-(propyl-3,3- d_3)butan-1-amine (99.1 mg, 0.750 mmol) and phenyl boronic acid (36.6 mg, 0.300 mmol) to provide by column chromatography (DCM to 2% $\text{NH}_3(\text{MeOH}; 2\text{M})$) the title compound as a brown oil (16.3 mg, 0.079 mmol, 26% yield).

IR $\nu_{\max}/\text{cm}^{-1}$ (thin film) 2930, 2786, 1447, 1073, 734, 697; **$^1\text{H NMR}$** (700 MHz, CDCl_3) δ (ppm) 7.32 – 7.28 (m, 2H, H_{11}), 7.23 – 7.19 (m, 3H, $\text{H}_{10,12}$), 2.42 – 2.36 (m, 2H, H_6), 2.36 – 2.32 (m, 2H, H_2), 2.24 (s, 3H, H_1), 1.84 – 1.78 (t, $J = 7.4$ Hz, 2H, H_7), 1.50 – 1.43 (m, 2H, H_3), 1.34 (hex, $J = 7.4$ Hz, 2H, H_4), 0.94 (t, $J = 7.4$ Hz, 3H, H_5); **$^{13}\text{C NMR}$** (176 MHz, CDCl_3) δ (ppm) 142.4 (C_9), 128.4 (C_{10}), 128.3 (C_{11}), 125.7 (C_{12}), 57.6 (C_2),

57.3 (C₆), 42.3 (C₁), 33.1 (p, $J = 19.7$ Hz, C₈), 29.5 (C₃), 29.0 (C₇), 20.8 (C₄), 14.1 (C₅); **HMRS-ESI** (m/z): found [M+H]⁺ 208.2065, C₁₄H₂₂ND₂ requires 208.2029.

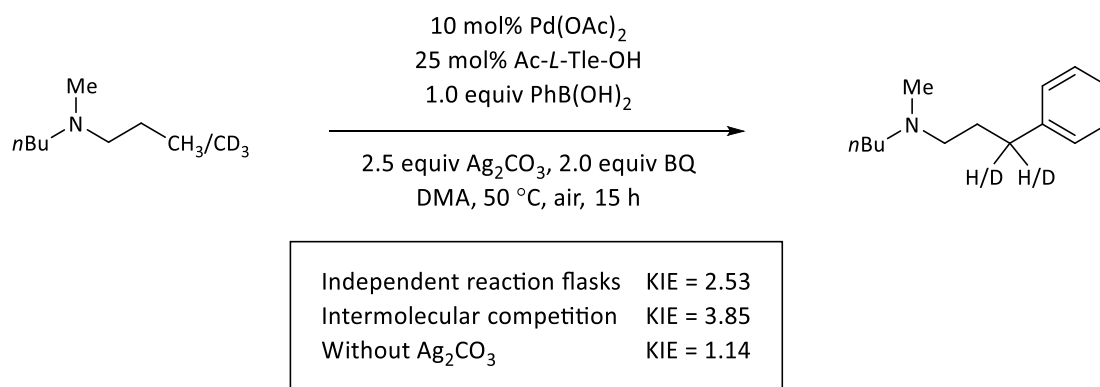
1-(3-Phenylpropyl)pyrrolidine-2,2,5,5-d₄



General procedure A was applied at 0.1 mmol scale to 1-propylpyrrolidine-2,2,5,5-d₄ (29.3 mg, 0.250 mmol) and phenyl boronic acid (12.2 mg, 0.100 mmol) with Pd(PhCN)₂Cl₂ (4.3 mg, 0.010 mmol) to provide by column chromatography (DCM to 3% NH₃(MeOH; 2M)) the title compound as a brown oil (9.6 mg, 0.050 mmol, 50% yield).

IR $\nu_{\max}/\text{cm}^{-1}$ (thin film) 2941, 2785, 1496, 1453, 1219, 1124, 743, 696; **¹H NMR** (400 MHz, CDCl₃) δ (ppm) 7.34 – 7.26 (m, 2H, H₈), 7.26 – 7.17 (m, 3H, H_{7,9}), 2.73 – 2.64 (m, 2H, H₅), 2.53 – 2.45 (m, 2H, H₃), 1.88 (app p, $J = 7.8$ Hz, 2H, H₄), 1.78 (s, 4H, H₁); **¹³C NMR** (101 MHz, CDCl₃) δ (ppm) 142.3 (C₆), 128.4 (C₇), 128.3 (C₈), 125.7 (C₉), 56.1 (C₃), 53.5 (p, $J = 20.6$ Hz, C₂), 34.0 (C₅), 30.8 (C₄), 23.2 (C₁); **HMRS-ESI** (m/z): found [M+H]⁺ 194.1833, C₁₃H₁₆D₄N requires 194.1841.

Kinetic isotope effect (KIE) experiments



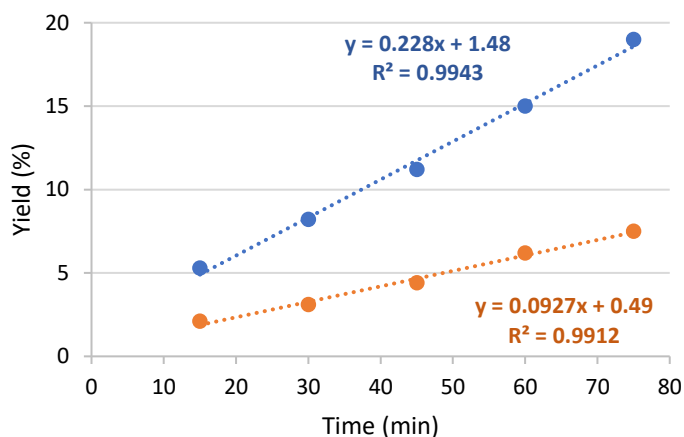
The desired tertiary amine (0.750 mmol) was added to a 10–20 mL microwave vial containing Pd(OAc)₂ (6.7 mg, 0.030 mmol), Ac-L-Tle-OH (13.0 mg, 0.0750 mmol), Ag₂CO₃ (207 mg, 0.750 mmol), 1,4-benzoquinone (BQ) (65.0 mg, 0.600 mmol) and 1,4-dimethoxybenzene (20.7 mg, 0.150 mmol) as internal standard in anhydrous DMA (6.50 mL). The reaction was sealed and pre-stirred at 1000 rpm and at 50 °C for 5 minutes. Phenyl boronic acid (36.6 mg, 0.300 mmol) was added as a solution in 1 mL of DMA, initiating the reaction (*Note: for an intermolecular experiment, 1.25 equiv of each amine were added to the same reaction flask*).

Aliquots of 0.5 mL were taken over time, diluted in 10 mL of Et₂O, and filtered through a Pasteur pipette with pad of Celite. The resulting organic layer was washed with 10 mL of aq NaOH (0.25 M), dried by filtration over MgSO₄ with the aid of a second Pasteur pipette, and concentrated *in vacuo*. The resultant crude was analysed by ¹H-NMR in CDCl₃ integrating the benzylic protons of product **259** and the overlapped *ortho*- and *para*-aromatic protons of both products obtained. The represented values are an average of two reaction replicates. Graphs illustrate data in its linear region.

i) Independent KIE experiments

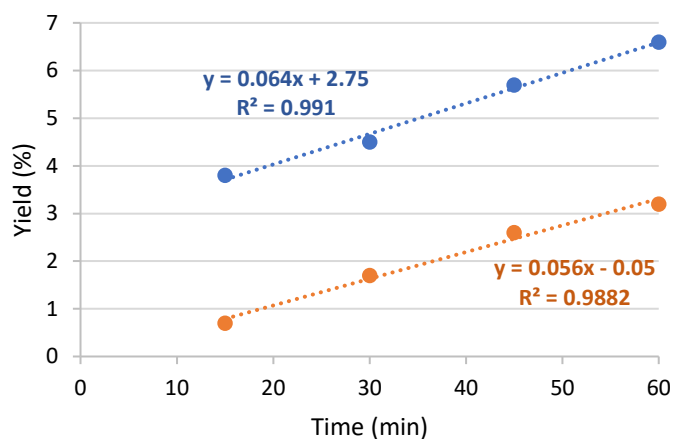
Time (min)	Yield 259 (%)	Yield 306 (%)
15	5.3	2.1
30	8.2	3.1
45	11.2	4.4
60	15.0	6.2
75	19.0	7.5
90	22.7	8.3
120	27.5	11.1
900	88.0	34.9

$$KIE = \frac{0.2280}{0.0927} = 2.53$$

ii) Independent KIE experiments without Ag_2CO_3

Time (min)	Yield 259 (%)	Yield 306 (%)
15	3.8	0.7
30	4.5	1.7
45	5.7	2.6
60	6.6	3.2
75	7.5	3.5
90	8.3	3.7
120	10.0	4.4

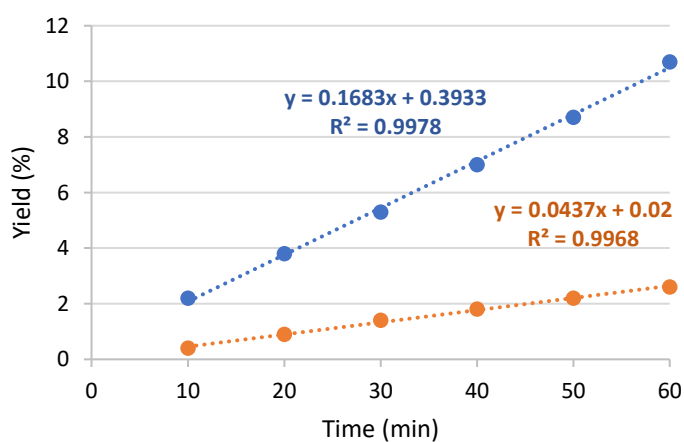
$$KIE = \frac{0.0640}{0.0560} = 1.14$$



iii) Intermolecular KIE experiments

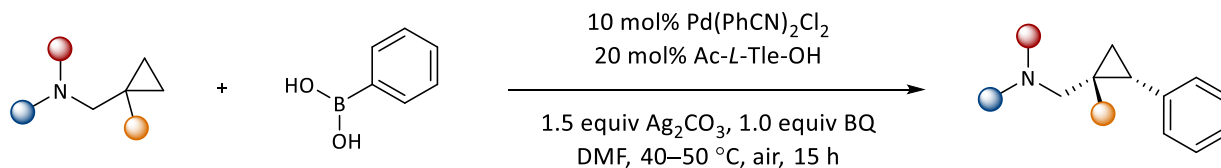
Time (min)	Yield 259 (%)	Yield 306 (%)
10	2.2	0.4
20	3.8	0.9
30	5.3	1.4
40	7.0	1.8
50	8.7	2.2
60	10.7	2.6

$$KIE = \frac{0.1683}{0.0437} = 3.85$$



5.3. Enantioselective methylene C(sp³)-H activation of tertiary alkylamines

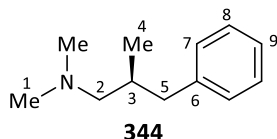
General procedure B: Methylene cyclopropane C-H arylation



The desired tertiary amine (0.600 mmol) was added to a 2–5 mL microwave vial containing Pd(PhCN)₂Cl₂ (11.5 mg, 0.030 mmol), Ac-L-Tle-OH (10.4 mg, 0.060 mmol), Ag₂CO₃ (124 mg, 0.450 mmol) and 1,4-benzoquinone (BQ) (32.5 mg, 0.300 mmol) in anhydrous DMF (0.75 mL). The reaction was sealed and stirred at 50 °C for 5 minutes. Phenyl boronic acid (36.6 mg, 0.300 mmol) in DMF (0.75 mL) was added dropwise and the reaction mixture was stirred at 1000 rpm, at 50 °C for 15 h.

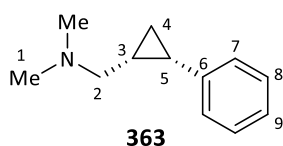
The reaction was cooled to rt and Et₂O (5 mL) added, forcing the formation of a precipitate. The dark mixture was filtered through a pad of Celite and washed with Et₂O (25 mL). The resulting organic layer was washed with aq NaOH (0.25 M, 3 x 50 mL), dried over MgSO₄, filtered and concentrated *in vacuo*. Purification of the crude oil by column chromatography afforded the pure arylated product. Asymmetry was determined by HPLC analysis using a CHIRALPAK® AD-H column, GC-FID analysis using a Astec ChiralDex™ B-DM column, or ¹H-NMR analysis of the methylated tertiary amine product following a literature procedure reported by Lacour.²²⁴

N,N,2-Trimethyl-3-phenylpropan-1-amine



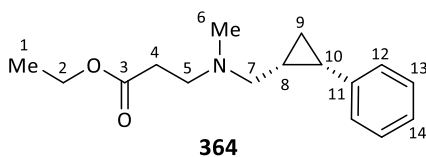
General procedure A was applied at 3.0 mmol scale to *N,N*,2-trimethylpropan-1-amine (911 mg, 9.00 mmol) in DMF (15.0 mL) at 40 °C to provide by column chromatography (DCM to 5% NH₃(MeOH; 2M)) the title compound as a brown oil (483 mg, 2.72 mmol, 91% yield, 90% ee). Enantiomeric excess was determined by GC-FID analysis.

IR ν_{\max} /cm⁻¹ (thin film) 3027, 2937, 2816, 2763, 1494, 1380, 1263, 1036, 739, 699; **¹H NMR** (400 MHz, CDCl₃) δ (ppm) 7.34 – 7.26 (m, 2H, H₈), 7.25 – 7.14 (m, 3H, H_{7,9}), 2.84 (dd, J = 13.4, 4.8 Hz, 1H, H_{5a}), 2.32 (dd, J = 13.4, 8.8 Hz, 1H, H_{5b}), 2.24 (s, 6H, H₁), 2.18 (dd, J = 11.8, 7.2 Hz, 1H, H_{2a}), 2.10 (dd, J = 11.8, 7.4 Hz, 1H, H_{2b}), 1.99 – 1.86 (m, 1H, H₃), 0.88 (d, J = 6.6 Hz, 3H, H₄); **¹³C NMR** (101 MHz, CDCl₃) δ (ppm) 141.1 (C₆), 129.3 (C₇), 128.1 (C₈), 125.6 (C₉), 66.6 (C₂), 45.9 (C₁), 41.4 (C₅), 33.2 (C₃), 17.9 (C₄); **HMRS-ESI** (m/z): found [M+H]⁺ 178.1596, C₁₂H₂₀N requires 178.1596; **ee analysis**: GC-FID ChiralDex β -DM (60 °C to 150 °C; 2 °C/min; linear velocity 40 cm·s⁻¹; split ratio 10.0) t_R = 12.6 min (minor), t_R = 12.8 min (major); $[\alpha]_D^{25.0}$ = -3.8° (c = 1.0, CHCl₃).

***N,N*-Dimethyl-1-(((1*R*,2*S*)-2-phenylcyclopropyl)methanamine**

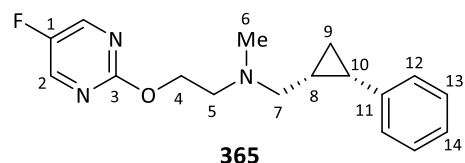
General procedure B was applied to 1-cyclopropyl-*N,N*-dimethylmethanamine (59.6 mg, 0.600 mmol) at 40 °C to provide by column chromatography (DCM to 4% NH₃(MeOH; 2M)) the title compound as a brown oil (44.6 mg, 0.254 mmol, 85% yield, >99% ee). Enantiomeric excess was determined by ¹H-NMR analysing H₄ from the corresponding methylated ammonium derivative.

IR ν_{\max} /cm⁻¹ (thin film) 2941, 2814, 1497, 1457, 1262, 1029, 844; **¹H NMR** (600 MHz, CDCl₃) δ (ppm) 7.31 – 7.26 (m, 2H, H₈), 7.24 – 7.17 (m, 3H, H_{7,9}), 2.30 (dd, $J = 12.7, 5.0$ Hz, 1H, H_{2a}), 2.23 – 2.15 (m, 7H, H_{1,5}), 1.67 (dd, $J = 12.7, 8.4$ Hz, 1H, H_{2b}), 1.31 – 1.24 (m, 1H, H₃), 1.17 – 1.07 (m, 1H, H_{4a}), 0.82 (q, $J = 5.8$ Hz, 1H, H_{4b}); **¹³C NMR** (151 MHz, CDCl₃) δ (ppm) 138.8 (C₆), 129.0 (C₇), 127.9 (C₈), 125.8 (C₉), 59.0 (C₂), 45.4 (C₁), 20.3 (C₅), 17.0 (C₃), 9.6 (C₄); **HMRS-ESI** (m/z): found [M+H]⁺ 176.1428, C₁₂H₁₈N requires 176.1434; **ee analysis**: ¹H-NMR (H₄) from the corresponding methylated ammonium derivative; HPLC Chiralpak AD-H (hexane(0.1% DEA):2-propanol 98:2, 1.0 mL·min⁻¹, 30 °C) $t_R = 5.1$ min (major), $t_R = 5.5$ min (minor); $[\alpha]_D^{25.0} = -77^\circ$ (c = 1.0, CHCl₃).

Ethyl 3-(methyl(((1*R*,2*S*)-2-phenylcyclopropyl)methyl)amino)propanoate

General procedure B was applied to ethyl 3-((cyclopropylmethyl)-(methyl)amino)propanoate (111 mg, 0.600 mmol) at 60 °C to provide by column chromatography (DCM to 5% NH₃(MeOH; 2M)) the title compound as a brown oil (50.8 mg, 0.194 mmol, 65% yield, 92% ee). Enantiomeric excess was determined by HPLC analysis.

IR ν_{\max} /cm⁻¹ (thin film) 2980, 2772, 1731, 1459, 1179, 1028; **¹H NMR** (600 MHz, CDCl₃) δ (ppm) 7.31 – 7.26 (m, 2H, H₁₃), 7.23 – 7.17 (m, 3H, H_{12,14}), 4.12 (q, $J = 7.1$ Hz, 2H, H₂), 2.64 (t, $J = 7.4$ Hz, 2H, H₅), 2.41 – 2.30 (m, 3H, H_{4,7a}), 2.24 – 2.16 (m, 4H, H_{6,10}), 1.83 (dd, $J = 12.9, 7.9$ Hz, 1H, H_{7b}), 1.31 – 1.23 (m, 4H, H_{1,8}), 1.12 (td, $J = 8.4, 5.3$ Hz, 1H, H_{9a}), 0.82 (q, $J = 5.8$ Hz, 1H, H_{9b}); **¹³C NMR** (151 MHz, CDCl₃) δ (ppm) 172.7 (C₃), 138.8 (C₁₁), 129.0 (C₁₂), 128.0 (C₁₃), 125.8 (C₁₄), 60.4 (C₂), 56.7 (C₇), 52.5 (C₅), 42.1 (C₆), 32.4 (C₄), 20.4 (C₁₀), 16.9 (C₈), 14.2 (C₁), 9.6 (C₉); **HMRS-ESI** (m/z): found [M+H]⁺ 262.1794, C₁₆H₂₄NO₂ requires 262.1807; **ee analysis**: HPLC Chiralpak AD-H (hexane:2-propanol 99.5:0.5, 1.0 mL·min⁻¹, 30 °C) $t_R = 13.1$ min (major), $t_R = 17.2$ min (minor); $[\alpha]_D^{25.0} = -36^\circ$ (c = 1.0, CHCl₃).

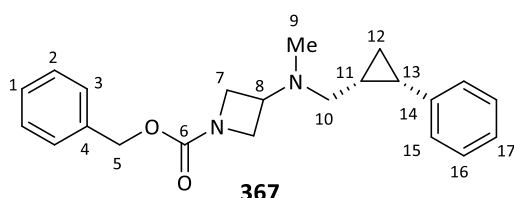
2-((5-Fluoropyrimidin-2-yl)oxy)-*N*-methyl-*N*-(((1*R*,2*S*)-2-phenylcyclopropyl)methyl)ethan-1-amine

General procedure B was applied to *N*-(cyclopropylmethyl)-2-((5-fluoropyrimidin-2-yl)oxy)-*N*-methylethan-1-amine (135.2 mg, 0.600 mmol) in NMP at 50 °C to provide by column chromatography (DCM

to 6% NH₃(MeOH; 2M)) the title compound as a brown oil (43.3 mg, 0.144 mmol, 48% yield, 78% ee). Enantiomeric excess was determined by HPLC analysis.

IR $\nu_{\max}/\text{cm}^{-1}$ (thin film) 3077, 2774, 1570, 1426, 1325, 1242, 1029; **$^1\text{H NMR}$** (400 MHz, CDCl_3) δ (ppm) 8.36 (s, 2H, H_2), 7.28 – 7.23 (m, 2H, H_{13}), 7.23 – 7.13 (m, 3H, $\text{H}_{12,14}$), 4.34 (t, $J = 6.2$ Hz, 2H, H_4), 2.76 (t, $J = 6.2$ Hz, 2H, H_5), 2.44 (dd, $J = 12.9, 5.5$ Hz, 1H, H_{7a}), 2.30 (s, 3H, H_6), 2.21 (td, $J = 8.7, 6.3$ Hz, 1H, H_{10}), 1.97 (dd, $J = 13.0, 7.6$ Hz, 1H, H_{7b}), 1.36 – 1.26 (m, 1H, H_8), 1.12 (td, $J = 8.4, 5.2$ Hz, 1H, H_{9a}), 0.84 (q, $J = 5.7$ Hz, 1H, H_{9b}); **$^{13}\text{C NMR}$** (151 MHz, CDCl_3) δ (ppm) 161.4 (d, $J = 0.8$ Hz, C_3), 154.2 (d, $J = 253.4$ Hz, C_1), 146.5 (d, $J = 22.6$ Hz, C_2), 138.8 (C_{11}), 129.0 (C_{12}), 127.9 (C_{13}), 125.8 (C_{14}), 66.3 (C_4), 57.3 (C_7), 55.5 (C_5), 42.8 (C_6), 20.4 (C_{10}), 16.9 (C_8), 9.6 (C_9); **$^{19}\text{F NMR}$** (377 MHz, CDCl_3) δ (ppm) –150.5 (s); **HMRS-ESI** (m/z): found $[\text{M}+\text{H}]^+$ 302.1660, $\text{C}_{17}\text{H}_{21}\text{N}_3\text{OF}$ requires 302.1669; **ee analysis**: HPLC Chiralpak AD-H (hexane:2-propanol 98:2, 1.0 $\text{mL}\cdot\text{min}^{-1}$, 30 °C) $t_{\text{R}} = 13.0$ min (major), $t_{\text{R}} = 14.4$ min (minor); $[\alpha]_{\text{D}}^{25.0} = -29^\circ$ ($c = 1.0$, CHCl_3).

Benzyl 3-(methyl(((1*R*,2*S*)-2-phenylcyclopropyl)methyl)amino)azetidine-1-carboxylate

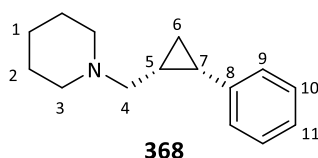


General procedure B was applied to benzyl 3-((cyclopropylmethyl)(methyl)amino)azetidine-1-carboxylate (164.6 mg, 0.600 mmol) at 50 °C to provide by column chromatography (DCM to 5% $\text{NH}_3(\text{MeOH}; 2\text{M})$) the title compound as a brown oil (48.1

mg, 0.138 mmol, 46% yield, 84% ee). Enantiomeric excess was determined by HPLC analysis.

IR $\nu_{\max}/\text{cm}^{-1}$ (thin film) 3029, 2955, 1704, 1415, 1351, 1127; **$^1\text{H NMR}$** (600 MHz, CDCl_3) δ (ppm) 7.40 – 7.31 (m, 5H, $\text{H}_{1,2,3}$), 7.29 – 7.24 (m, 2H, H_{16}), 7.18 (app br d, $J = 7.7$ Hz, 3H, $\text{H}_{15,17}$), 5.09 (s, 2H, H_5), 3.87 (t, $J = 7.9$ Hz, 1H, H_{7a}), 3.81 (t, $J = 7.9$ Hz, 1H, H_{7b}), 3.76 – 3.72 (m, 1H, H_{7c}), 3.67 (br s, 1H, H_{7d}), 3.08 (br s, 1H, H_8), 2.26 – 2.15 (m, 2H, $\text{H}_{10a,13}$), 2.13 (s, 3H, H_9), 1.78 (dd, $J = 13.0, 7.5$ Hz, 1H, H_{10b}), 1.29 – 1.21 (m, 1H, H_{11}), 1.11 (td, $J = 8.4, 5.5$ Hz, 1H, H_{12a}), 0.80 (q, $J = 5.7$ Hz, 1H, H_{12b}); **$^{13}\text{C NMR}$** (151 MHz, CDCl_3) δ (ppm) 156.4 (C_6), 138.3 (C_{14}), 136.7 (C_4), 128.9 (C_{15}), 128.4 (C_3), 128.0 (C_{16}), 128.0 (C_1), 127.9 (C_2), 126.0 (C_{17}), 66.5 (C_5), 54.1 (C_8), 53.8 (C_{10}), 38.1 (C_9), 20.6 (C_{13}), 16.4 (C_{11}), 9.3 (C_{12}); **HMRS-ESI** (m/z): found $[\text{M}+\text{H}]^+$ 351.2060, $\text{C}_{22}\text{H}_{27}\text{N}_2\text{O}_2$ requires 351.2073; **ee analysis**: HPLC Chiralpak AD-H (hexane:2-propanol 97:3, 1.0 $\text{mL}\cdot\text{min}^{-1}$, 30 °C) $t_{\text{R}} = 20.3$ min (major), $t_{\text{R}} = 23.1$ min (minor); $[\alpha]_{\text{D}}^{25.0} = -39^\circ$ ($c = 0.7$, CHCl_3).

1-(((1*R*,2*S*)-2-Phenylcyclopropyl)methyl)piperidine

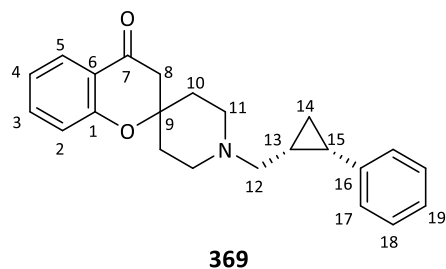


General procedure B was applied to 1-(cyclopropylmethyl)piperidine (83.5 mg, 0.600 mmol) at 50 °C to provide by column chromatography (DCM to 4% $\text{NH}_3(\text{MeOH}; 2\text{M})$) the title compound as a brown oil (49.2 mg, 0.229 mmol, 76% yield, >95% ee). Enantiomeric excess was determined by $^1\text{H-NMR}$ analysing H_7 from the corresponding methylated ammonium derivative.

IR $\nu_{\max}/\text{cm}^{-1}$ (thin film) 2931, 1497, 1453, 1299, 1115, 1028, 763, 696; **$^1\text{H NMR}$** (600 MHz, CDCl_3) δ (ppm) 7.30 – 7.25 (m, 2H, H_{10}), 7.22 – 7.16 (m, 3H, $\text{H}_{9,11}$), 2.36 (dd, $J = 12.9, 5.0$ Hz, 1H, H_{4a}), 2.34 (br s, 4H, H_3), 2.21 – 2.15

(m, 1H, H₇), 1.79 (dd, $J = 12.9, 8.0$ Hz, 1H, H_{4b}), 1.58 (app p, $J = 5.6$ Hz, 4H, H₂), 1.39 (br s, 2H, H₁), 1.36 – 1.28 (m, 1H, H₅), 1.12 (td, $J = 8.4, 5.2$ Hz, 1H, H_{6a}), 0.82 (q, $J = 5.7$ Hz, 1H, H_{6b}); ¹³C NMR (151 MHz, CDCl₃) δ (ppm) 138.8 (C₈), 129.0 (C₉), 127.9 (C₁₀), 125.8 (C₁₁), 58.7 (C₄), 54.4 (C₃), 25.8 (C₂), 24.3 (C₁), 20.2 (C₇), 16.4 (C₅), 10.0 (C₆); **HMRS-ESI** (m/z): found [M+H]⁺ 216.1739, C₁₅H₂₂N requires 216.1747; **ee analysis**: ¹H-NMR (H₇) from the corresponding methylated ammonium derivative; $[\alpha]_D^{25.0} = -51^\circ$ ($c = 0.8, \text{CHCl}_3$).

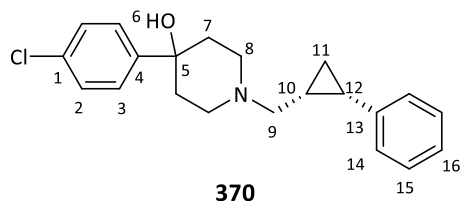
1'-(((1R,2S)-2-Phenylcyclopropyl)methyl)spiro[chromane-2,4'-piperidin]-4-one



General procedure B was applied to 1'-(cyclopropylmethyl)-spiro[chromane-2,4'-piperidin]-4-one (163 mg, 0.600 mmol) at 40 °C to provide by column chromatography (DCM to 5% NH₃(MeOH; 2M)) the title compound as a yellow oil (74.8 mg, 0.215 mmol, 72% yield, >99% ee). Enantiomeric excess was determined by HPLC analysis.

IR $\nu_{\text{max}}/\text{cm}^{-1}$ (thin film) 3076, 2919, 2786, 1687, 1605, 1461, 1298, 1228, 1114; **¹H NMR** (600 MHz, CDCl₃) δ (ppm) 7.85 (dd, $J = 8.0, 1.7$ Hz, 1H, H₅), 7.47 (td, $J = 7.7, 1.7$ Hz, 1H, H₃), 7.32 – 7.26 (m, 2H, H₁₈), 7.25 – 7.17 (m, 3H, H_{17,19}), 6.99 (td, $J = 7.6, 0.8$ Hz, 1H, H₄), 6.94 (d, $J = 8.3$ Hz, 1H, H₂), 2.81 – 2.65 (m, 3H, H_{8,11a}), 2.57 (br d, $J = 11.0$ Hz, 1H, H_{11b}), 2.45 (dd, $J = 12.9, 4.7$ Hz, 1H, H_{12a}), 2.31 (br q, $J = 10.2$ Hz, 2H, H_{11c}), 2.20 (app q, $J = 8.3$ Hz, 1H, H₁₅), 2.06 – 1.97 (m, 2H, H_{10a}), 1.79 (dd, $J = 12.9, 8.3$ Hz, 1H, H_{12b}), 1.76 – 1.70 (m, 2H, H_{10b}), 1.32 – 1.24 (m, 1H, H₁₃), 1.13 (td, $J = 8.3, 5.2$ Hz, 1H, H_{14a}), 0.83 (q, $J = 5.7$ Hz, 1H, H_{14b}); ¹³C NMR (101 MHz, CDCl₃) δ (ppm) 192.1 (C₇), 159.2 (C₁), 138.8 (C₁₆), 136.1 (C₃), 129.0 (C₁₇), 127.9 (C₁₈), 126.5 (C₅), 125.9 (C₁₉), 120.9 (C₄), 120.8 (C₆), 118.4 (C₂), 77.9 (C₉), 58.1 (C₁₂), 48.9 (C_{11a}), 48.5 (C_{11b}), 48.0 (C₈), 34.3 (C_{10a}), 34.3 (C_{10b}), 20.1 (C₁₅), 16.5 (C₁₃), 10.0 (C₁₄); **HMRS-ESI** (m/z): found [M+H]⁺ 348.1963, C₂₃H₂₆NO₂ requires 348.1964; **ee analysis**: HPLC Chiralpak AD-H (hexane:2-propanol 97:3, 1.0 mL·min⁻¹, 30 °C) $t_R = 14.5$ min (major), $t_R = 16.4$ min (minor); $[\alpha]_D^{25.0} = -37^\circ$ ($c = 1.0, \text{CHCl}_3$).

4-(4-Chlorophenyl)-1-(((1R,2S)-2-phenylcyclopropyl)methyl)piperidin-4-ol

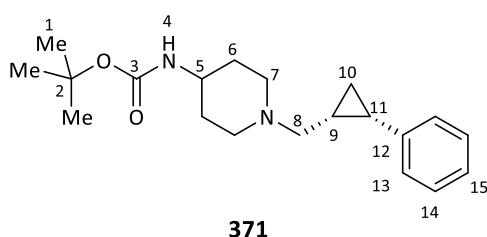


General procedure B was applied to 4-(4-chlorophenyl)-1-(cyclopropylmethyl)piperidin-4-ol (159.5 mg, 0.600 mmol) at 50 °C to provide by column chromatography (DCM to 7% NH₃(MeOH; 2M)) the title compound as a colourless oil (52.1 mg, 0.152 mmol, 51% yield, 98% ee). Enantiomeric excess was determined by HPLC analysis.

IR $\nu_{\text{max}}/\text{cm}^{-1}$ (thin film) 3063, 2924, 2833, 1495, 1082, 1047; **¹H NMR** (400 MHz, CDCl₃) δ (ppm) 7.45 – 7.41 (m, 2H, H₂), 7.33 – 7.27 (m, 4H, H_{3,15}), 7.23 – 7.18 (m, 3H, H_{14,16}), 2.94 (app br d, $J = 11.1$ Hz, 1H, H_{8a}), 2.79 (app br d, $J = 11.4$ Hz, 1H, H_{8b}), 2.48 (dd, $J = 12.9, 5.0$ Hz, 1H, H_{9a}), 2.39 (br t, $J = 11.8$ Hz, 1H, H_{8c}), 2.31 (br t, $J = 11.5$ Hz, 1H, H_{8d}), 2.23 (app q, $J = 8.1$ Hz, 1H, H₁₂), 2.15 (br t, $J = 11.3$ Hz, 2H, H_{7a}), 1.93 (dd, $J = 12.1, 8.3$ Hz, 1H, H_{9b}),

1.90 – 1.75 (br s, 1H, H₆), 1.74 – 1.64 (m, 2H, H_{7b}), 1.39 – 1.30 (m, 1H, H₁₀), 1.15 (td, $J = 8.4, 5.3$ Hz, 1H, H_{11a}), 0.89 (q, $J = 5.7$ Hz, 1H, H_{11b}); ¹³C NMR (101 MHz, CDCl₃) δ (ppm) 146.8 (C₄), 138.5 (C₁₃), 132.8 (C₁), 128.9 (C₁₄), 128.4 (C₃), 128.0 (C₁₅), 126.1 (C₂), 125.9 (C₁₆), 70.9 (C₅), 58.0 (C₉), 49.1 (C₈), 38.1 (C₇), 20.3 (C₁₂), 16.1 (C₁₀), 10.0 (C₁₁); **HMRS-ESI** (m/z): found [M+H]⁺ 342.1617, C₂₁H₂₅NOCl requires 342.1625; **ee analysis**: HPLC Chiralpak AD-H (hexane:2-propanol 95:5, 1.0 mL·min⁻¹, 30 °C) t_R = 24.2 min (minor), t_R = 26.1 min (major); [α]_D^{25.0} = -32° (c = 1.0, CHCl₃).

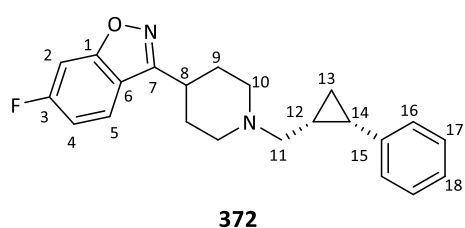
tert-Butyl (1-(((1*R*,2*S*)-2-phenylcyclopropyl)methyl)piperidin-4-yl)carbamate



General procedure B was applied to *tert*-butyl (1-(cyclopropylmethyl)piperidin-4-yl)carbamate (153 mg, 0.600 mmol) at 40 °C to provide by column chromatography (DCM to 6% NH₃(MeOH; 2M)) the title compound as a yellow oil (75.0 mg, 0.227 mmol, 76% yield, >99% ee). Enantiomeric excess was determined by HPLC analysis.

IR ν_{\max} /cm⁻¹ (thin film) 3321, 2930, 2781, 1686, 1497, 1168, 765; ¹H NMR (600 MHz, CDCl₃) δ (ppm) 7.29 – 7.23 (m, 2H, H₁₄), 7.21 – 7.15 (m, 3H, H_{13,15}), 4.43 (br s, 1H, H₄), 3.39 (app br s, 1H, H₅), 2.89 (br s, 1H, H_{7a}), 2.77 (br s, 1H, H_{7b}), 2.35 (dd, $J = 12.9, 5.2$ Hz, 1H, H_{8a}), 2.18 (app q, $J = 7.8$ Hz, 1H, H₁₁), 1.97 (br t, $J = 11.2$ Hz, 1H, H_{7c}), 1.88 (br s, 3H, H_{6a,7d}), 1.83 (dd, $J = 12.9, 7.9$ Hz, 1H, H_{8b}), 1.50 – 1.37 (m, 11H, H_{1,6b}), 1.31 – 1.24 (m, 1H, H₉), 1.11 (td, $J = 8.4, 5.2$ Hz, 1H, H_{10a}), 0.81 (q, $J = 5.7$ Hz, 1H, H_{10b}); ¹³C NMR (151 MHz, CDCl₃) δ (ppm) 155.2 (C₃), 138.6 (C₁₂), 128.9 (C₁₃), 127.9 (C₁₄), 125.9 (C₁₅), 79.2 (C₂), 57.9 (C₈), 52.3 (C₇), 47.6 (C₅), 32.5 (C₆), 28.4 (C₁), 20.3 (C₁₁), 16.4 (C₉), 9.8 (C₁₀); **HMRS-ESI** (m/z): found [M+H]⁺ 331.2380, C₂₀H₃₁N₂O₂ requires 331.2386; **ee analysis**: HPLC Chiralpak AD-H (hexane(0.1% DEA):2-propanol 98:2, 1.0 mL·min⁻¹, 45 °C) t_R = 17.9 min (minor), t_R = 18.7 min (major); [α]_D^{25.0} = -39° (c = 1.0, CHCl₃).

6-Fluoro-3-(1-(((1*R*,2*S*)-2-phenylcyclopropyl)methyl)piperidin-4-yl)benzo[*d*]isoxazole

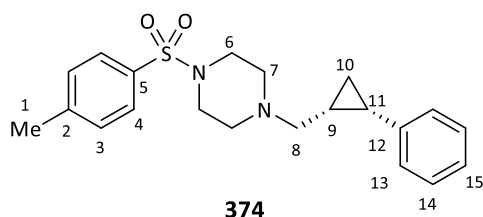


General procedure B was applied to 3-(1-(cyclopropylmethyl)piperidin-4-yl)-6-fluorobenzo[*d*]isoxazole (164 mg, 0.600 mmol) at 50 °C to provide by column chromatography (DCM to 3% NH₃(MeOH; 2M)) the title compound as a brown oil (39.9 mg, 0.114 mmol, 38% yield, 99% ee). Enantiomeric excess was determined by HPLC analysis.

IR ν_{\max} /cm⁻¹ (thin film) 2943, 1614, 1495, 1122, 955, 698; ¹H NMR (700 MHz, CDCl₃) δ (ppm) 7.71 (dd, $J = 8.6, 5.1$ Hz, 1H, H₅), 7.30 (t, $J = 7.5$ Hz, 2H, H₁₇), 7.26 – 7.20 (m, 4H, H_{2,16,18}), 7.06 (td, $J = 8.8, 1.8$ Hz, 1H, H₄), 3.20 – 3.12 (m, 1H, H₈), 3.06 – 2.97 (m, 2H, H_{10a}), 2.44 (dd, $J = 12.8, 5.1$ Hz, 1H, H_{11a}), 2.23 (app q, $J = 8.0$ Hz, 1H, H₁₄), 2.11 – 1.96 (m, 6H, H_{9,10b}), 1.92 (dd, $J = 12.8, 7.8$ Hz, 1H, H_{11b}), 1.38 – 1.32 (m, 1H, H₁₂), 1.18 – 1.13 (m, 1H, H_{13a}), 0.86 (app q, $J = 5.6$ Hz, 1H, H_{13b}); ¹³C NMR (176 MHz, CDCl₃) δ (ppm) 164.1 (d, $J = 250.5$ Hz, C₃), 163.9 (d, $J =$

13.6 Hz, C₁), 161.2 (C₇), 138.8 (C₁₅), 129.0 (C₁₆), 127.9 (C₁₇), 125.9 (C₁₈), 122.6 (d, *J* = 11.1 Hz, C₅), 117.3 (C₆), 112.2 (d, *J* = 25.3 Hz, C₄), 97.4 (d, *J* = 26.6 Hz, C₂), 58.2 (C₁₁), 53.6 (C₁₀), 34.6 (C₈), 30.5 (C₉), 20.3 (C₁₄), 16.5 (C₁₂), 9.9 (C₁₃); ¹⁹F NMR (377 MHz, CDCl₃) δ (ppm) -109.8 (s); **HMRS-ESI** (*m/z*): found [M+H]⁺ 351.1877, C₂₂H₂₄N₂O requires 351.1873; **ee analysis**: HPLC Chiralpak AD-H (hexane(0.1% DEA):2-propanol 90:10, 1.0 mL·min⁻¹, 30 °C) *t_R* = 6.2 min (major), *t_R* = 8.2 min (minor); [α]_D^{25.0} = -30° (*c* = 1.0, CHCl₃).

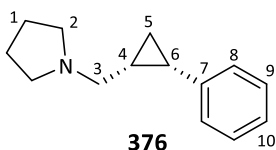
1-(((1*R*,2*S*)-2-Phenylcyclopropyl)methyl)-4-tosylpiperazine



General procedure B was applied to 1-(cyclopropylmethyl)-4-tosylpiperazine (176.6 mg, 0.600 mmol) at 40 °C to provide by column chromatography (DCM to 3% NH₃(MeOH; 2M)) the title compound as a white solid (55.3 mg, 0.149 mmol, 50% yield, 97% ee). Enantiomeric excess was determined by HPLC analysis.

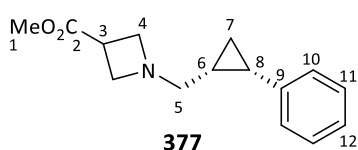
mp 72 – 74 °C; **IR** ν_{\max} /cm⁻¹ (thin film) 2856, 2801, 1595, 1452, 1347, 1301, 1163; **¹H NMR** (600 MHz, CDCl₃) δ (ppm) 7.63 (d, *J* = 8.0 Hz, 2H, H₄), 7.32 (d, *J* = 8.0 Hz, 2H, H₃), 7.28 – 7.25 (m, 2H, H₁₄), 7.22 – 7.17 (m, 1H, H₁₅), 7.15 (d, *J* = 7.2 Hz, 2H, H₁₃), 2.98 (br s, 4H, H₆), 2.44 (app br s, 7H, H_{1,7}), 2.32 (dd, *J* = 13.0, 5.5 Hz, 1H, H_{8a}), 2.18 (td, *J* = 8.7, 6.1 Hz, 1H, H₁₁), 1.87 (dd, *J* = 13.0, 7.7 Hz, 1H, H_{8b}), 1.19 (qt, *J* = 8.4, 5.7 Hz, 1H, H₉), 1.08 (td, *J* = 8.4, 5.3 Hz, 1H, H_{10a}), 0.77 (q, *J* = 5.8 Hz, 1H, H_{10b}); **¹³C NMR** (151 MHz, CDCl₃) δ (ppm) 143.6 (C₅), 138.4 (C₁₂), 132.2 (C₂), 129.6 (C₃), 128.9 (C₁₃), 128.0 (C₁₄), 127.9 (C₄), 126.0 (C₁₅), 57.4 (C₈), 52.0 (C₇), 46.0 (C₆), 21.5 (C₁), 20.3 (C₁₁), 16.2 (C₉), 9.4 (C₁₀); **HMRS-ESI** (*m/z*): found [M+H]⁺ 371.1785, C₂₁H₂₇N₂O₂S requires 371.1793; **ee analysis**: HPLC Chiralpak AD-H (hexane:2-propanol 90:10, 1.0 mL·min⁻¹, 30 °C) *t_R* = 16.3 min (major), *t_R* = 19.2 min (minor); [α]_D^{25.0} = -23° (*c* = 1.0, CHCl₃).

1-(((1*R*,2*S*)-2-Phenylcyclopropyl)methyl)pyrrolidine



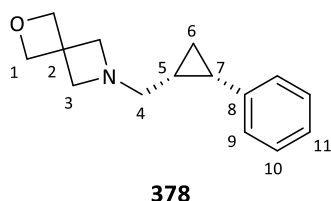
General procedure B was applied to 1-(cyclopropylmethyl)pyrrolidine (94.0 mg, 0.750 mmol) at 50 °C to provide by column chromatography (DCM to 3% NH₃(MeOH; 2M)) the title compound as a brown oil (19.2 mg, 0.095 mmol, 32% yield, >95% ee). Enantiomeric excess was determined by ¹H-NMR analysing H₅ from the corresponding methylated ammonium derivative.

IR ν_{\max} /cm⁻¹ (thin film) 2969, 2901, 2777, 1394, 1230, 1056; **¹H NMR** (600 MHz, CDCl₃) δ (ppm) 7.30 – 7.26 (m, 2H, H₉), 7.24 – 7.17 (m, 3H, H_{8,10}), 2.50 (dd, *J* = 12.5, 4.7 Hz, 1H, H_{3a}), 2.48 – 2.38 (m, 4H, H₂), 2.20 (dt, *J* = 8.7, 6.4 Hz, 1H, H₆), 1.81 (dd, *J* = 12.5, 8.8 Hz, 1H, H_{3b}), 1.78 – 1.70 (m, 4H, H₁), 1.37 – 1.30 (m, 1H, H₄), 1.10 (tdd, *J* = 8.3, 5.2, 0.7 Hz, 1H, H_{5a}), 0.85 (q, *J* = 5.7 Hz, 1H, H_{5b}); **¹³C NMR** (151 MHz, CDCl₃) δ (ppm) 139.0 (C₇), 129.1 (C₈), 127.9 (C₉), 125.7 (C₁₀), 55.9 (C₃), 54.3 (C₂), 23.4 (C₁), 20.3 (C₆), 17.9 (C₄), 9.7 (C₅); **HMRS-ESI** (*m/z*): found [M+H]⁺ 202.1588, C₁₄H₂₀N requires 202.1596; **ee analysis**: ¹H-NMR (H₅) from the corresponding methylated ammonium derivative; [α]_D^{25.0} = -42° (*c* = 1.0, CHCl₃).

Methyl 1-(((1*R*,2*S*)-2-phenylcyclopropyl)methyl)azetidine-3-carboxylate

General procedure B was applied to methyl 1-(cyclopropylmethyl)-azetidine-3-carboxylate (101.4 mg, 0.600 mmol) at 50 °C to provide by column chromatography (DCM to 5% NH₃(MeOH; 2M)) the title compound as a brown oil (21.9 mg, 0.089 mmol, 30% yield, 98% ee). Enantiomeric excess was determined by HPLC analysis.

IR ν_{\max} /cm⁻¹ (thin film) 3060, 2834, 1732, 1436, 1197, 1172; **¹H NMR** (600 MHz, CDCl₃) δ (ppm) 7.30 – 7.26 (m, 2H, H₁₁), 7.23 – 7.16 (m, 3H, H_{10,12}), 3.68 (s, 3H, H₁), 3.49 – 3.42 (m, 2H, H_{4a}), 3.28 (p, J = 7.6 Hz, 1H, H₃), 3.19 (t, J = 7.5 Hz, 1H, H_{4b}), 3.10 (t, J = 7.5 Hz, 1H, H_{4c}), 2.46 (dd, J = 12.3, 5.0 Hz, 1H, H_{5a}), 2.16 (td, J = 8.7, 6.2 Hz, 1H, H₈), 1.79 (dd, J = 12.3, 8.8 Hz, 1H, H_{5a}), 1.21 – 1.12 (m, 1H, H₆), 1.04 (tdd, J = 8.3, 5.2, 0.8 Hz, 1H, H_{7a}), 0.81 (q, J = 5.6 Hz, 1H, H_{7b}); **¹³C NMR** (151 MHz, CDCl₃) δ (ppm) 173.5 (C₂), 138.8 (C₉), 129.0 (C₁₀), 128.0 (C₁₁), 125.9 (C₁₂), 58.7 (C₅), 57.0 (C_{4a}), 56.9 (C_{4b}), 51.8 (C₁), 34.2 (C₃), 19.5 (C₈), 16.6 (C₆), 8.9 (C₇); **HMRS-ESI** (m/z): found [M+H]⁺ 246.1482, C₁₅H₂₀NO₂ requires 246.1494; **ee analysis**: HPLC Chiralpak AD-H (hexane:2-propanol 97:3, 1.0 mL·min⁻¹, 30 °C) t_R = 7.8 min (major), t_R = 8.8 min (minor); $[\alpha]_D^{25.0}$ = -47° (c = 0.8, CHCl₃).

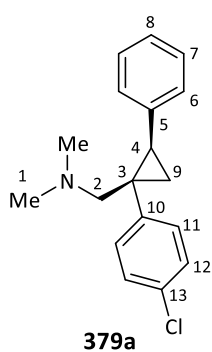
6-(((1*R*,2*S*)-2-phenylcyclopropyl)methyl)-2-oxa-6-azaspiro[3.3]heptane

General procedure B was applied to 6-(cyclopropylmethyl)-2-oxa-6-azaspiro[3.3]heptane (91.9 mg, 0.600 mmol) and phenyl boronic acid pinacol ester (61.2 mg, 0.300 mmol) at 50 °C to provide by column chromatography (DCM to 8% NH₃(MeOH; 2M)) the title compound as a yellow oil (21.8 mg, 0.095

mmol, 32% yield, >99% ee). Enantiomeric excess was determined by HPLC analysis.

IR ν_{\max} /cm⁻¹ (thin film) 2927, 2860, 2814, 1458, 1247, 970, 728, 698; **¹H NMR** (600 MHz, CDCl₃) δ (ppm) 7.30 – 7.26 (m, 2H, H₁₀), 7.24 – 7.16 (m, 3H, H_{9,11}), 4.72 – 4.65 (m, 4H, H₁), 3.27 (d, J = 7.3 Hz, 2H, H_{3a}), 3.21 (d, J = 7.3 Hz, 2H, H_{3b}), 2.37 (dd, J = 12.3, 5.1 Hz, 1H, H_{4a}), 2.16 (app q, J = 8.0 Hz, 1H, H₇), 1.77 (dd, J = 12.3, 8.6 Hz, 1H, H_{4b}), 1.14 (qt, J = 8.8, 5.5 Hz, 1H, H₅), 1.05 (td, J = 8.3, 5.3 Hz, 1H, H_{6a}), 0.80 (q, J = 5.7 Hz, 1H, H_{6b}); **¹³C NMR** (151 MHz, CDCl₃) δ (ppm) 138.8 (C₈), 129.0 (C₉), 128.0 (C₁₀), 125.9 (C₁₁), 81.3 (C₁), 63.8 (C₃), 58.8 (C₄), 39.2 (C₂), 19.6 (C₇), 16.8 (C₅), 8.9 (C₆); **HMRS-ESI** (m/z): found [M+H]⁺ 230.1543, C₁₅H₂₀NO requires 230.1545; **ee analysis**: HPLC Chiralpak AD-H (hexane(0.1% DEA):2-propanol 97:3, 1.0 mL·min⁻¹, 30 °C) t_R = 9.4 min (major), t_R = 11.0 min (minor); $[\alpha]_D^{25.0}$ = -54° (c = 0.7, CHCl₃).

1-((1*R*,2*R*)-1-(4-Chlorophenyl)-2-phenylcyclopropyl)-*N,N*-dimethylmethanamine

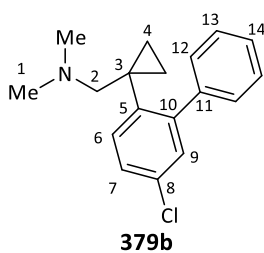


General procedure B was applied to 1-(1-(4-chlorophenyl)cyclopropyl)-*N,N*-dimethylmethanamine (126.0 mg, 0.600 mmol) at 50 °C to provide by column chromatography (DCM to 3% NH₃(MeOH; 2M)) the title compound as a brown oil (18.2 mg, 0.064 mmol, 22% yield, 92% ee). Enantiomeric excess was determined by HPLC analysis.

IR ν_{max} /cm⁻¹ (thin film) 2968, 2815, 2764, 1493, 1456, 1093; **¹H NMR** (600 MHz, CDCl₃) δ (ppm) 7.39 – 7.36 (m, 2H, H₁₁), 7.36 – 7.33 (m, 2H, H₇), 7.33 – 7.31 (m, 2H, H₁₂), 7.31 – 7.28 (m, 2H, H₆), 7.27 – 7.24 (m, 1H, H₈), 2.78 (dd, J = 13.0, 1.5 Hz, 1H, H_{2a}), 2.22 (dd, J = 8.8, 6.7

Hz, 1H, H₄), 2.07 (s, 6H, H₁), 1.68 (ddd, J = 8.8, 5.5, 1.5 Hz, 1H, H_{9a}), 1.65 (d, J = 13.1 Hz, 1H, H_{2b}), 1.44 (dd, J = 6.7, 5.5 Hz, 1H, H_{9b}); **¹³C NMR** (151 MHz, CDCl₃) δ (ppm) 144.1 (C₁₀), 137.8 (C₅), 131.7 (C₁₃), 129.4 (C₁₁), 129.0 (C₆), 128.5 (C₁₂), 128.2 (C₇), 126.3 (C₈), 64.0 (C₂), 45.8 (C₁), 30.3 (C₄), 30.0 (C₃), 16.5 (C₉); **HMRS-ESI** (m/z): found [M+H]⁺ 286.1354, C₁₈H₂₁NCl requires 286.1363; **ee analysis**: HPLC Chiralpak AD-H (hexane:2-propanol 99:1, 1.0 mL·min⁻¹, 30 °C) t_R = 8.5 min (major), t_R = 12.4 min (minor); $[\alpha]_D^{25.0}$ = +84° (c = 1.0, CHCl₃).

1-(1-(5-Chloro-[1,1'-biphenyl]-2-yl)cyclopropyl)-*N,N*-dimethylmethanamine

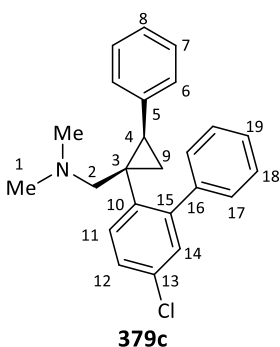


General procedure B was applied to 1-(1-(4-chlorophenyl)cyclopropyl)-*N,N*-dimethylmethanamine (126.0 mg, 0.600 mmol) at 50 °C to provide by column chromatography (DCM to 3% NH₃(MeOH; 2M)) the title compound as a pale oil (42.9 mg, 0.150 mmol, 50%).

IR ν_{max} /cm⁻¹ (thin film) 2941, 2811, 2763, 1461, 1267, 1113, 1034; **¹H NMR** (600 MHz, CDCl₃) δ (ppm) 7.45 – 7.41 (m, 2H, H₁₃), 7.41 – 7.36 (m, 3H, H_{12,14}), 7.31 (d, J = 8.3 Hz, 1H, H₆), 7.26 (dd, J = 8.3, 2.3 Hz, 1H, H₇), 7.17 (d, J = 2.3 Hz, 1H, H₉), 2.08 (s, 6H, H₁), 1.91 (s, 2H, H₂), 0.87 (app

q, J = 4.5 Hz, 2H, H_{4a}), 0.55 (app q, J = 4.5 Hz, 2H, H_{4b}); **¹³C NMR** (151 MHz, CDCl₃) δ (ppm) 145.1 (C₁₀), 141.6 (C₁₁), 139.9 (C₅), 131.8 (C₆), 131.7 (C₈), 130.6 (C₉), 129.3 (C₁₂), 127.8 (C₁₃), 127.1 (C₁₄), 127.1 (C₇), 67.6 (C₂), 46.0 (C₁), 23.1 (C₃), 13.3 (C₄); **HMRS-ESI** (m/z): found [M+H]⁺ 286.1353, C₁₈H₂₁NCl requires 286.1363.

1-((1*R*,2*R*)-1-(5-Chloro-[1,1'-biphenyl]-2-yl)-2-phenylcyclopropyl)-*N,N*-dimethylmethanamine



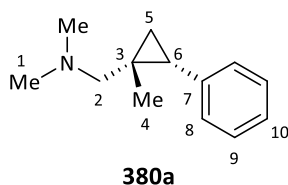
General procedure B was applied to 1-(1-(4-chlorophenyl)cyclopropyl)-*N,N*-dimethylmethanamine (126 mg, 0.600 mmol) at 50 °C to provide by column chromatography (DCM to 3% NH₃(MeOH; 2M)) the title compound (13.3 mg, 0.036 mmol, 12% yield).

IR ν_{max} /cm⁻¹ (thin film) 3061, 2941, 2813, 2761, 1587, 1461, 1038; **¹H NMR** (600 MHz, CDCl₃) δ (ppm) 7.50 (d, J = 8.4 Hz, 1H, H₁₁), 7.46 – 7.41 (m, 3H, H_{18,19}), 7.41 – 7.36 (m, 2H, H₁₇), 7.32 (dd, J = 8.4, 2.4 Hz, 1H, H₁₂), 7.17 (d, J = 2.3 Hz, 1H, H₁₄), 7.16 – 7.10 (m, 3H, H_{7,8}), 6.61 (d, J = 6.4 Hz, 2H, H₆), 2.38 (d, J = 13.2 Hz, 1H, H_{2a}), 2.19 (dd, J = 8.5, 7.1

Hz, 1H, H₄), 2.03 (s, 6H, H₁), 1.65 (d, J = 13.2 Hz, 1H, H_{2b}), 1.43 (dd, J = 8.9, 5.0 Hz, 1H, H_{9a}), 1.31 – 1.27 (m, 1H,

H_{9b}); **¹³C NMR** (151 MHz, CDCl₃) δ (ppm) 145.0 (C₁₅), 141.7 (C₁₀), 141.6 (C₁₆), 137.8 (C₅), 132.6 (C₁₁), 131.7 (C₁₃), 130.8 (C₁₄), 129.4 (C₁₇), 129.1 (C₆), 128.2 (C₁₈), 127.6 (C₇), 127.3 (C₁₉), 127.2 (C₁₂), 125.8 (C₈), 63.8 (C₂), 46.0 (C₁), 30.6 (C₃), 29.5 (C₄), 18.4 (C₉); **HMRS-ESI** (m/z): found [M+H]⁺ 362.1669, C₂₄H₂₅NCl requires 362.1676.

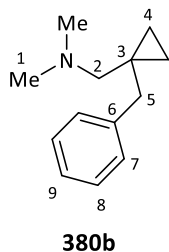
N,N-Dimethyl-1-((1*R*,2*R*)-1-methyl-2-phenylcyclopropyl)methanamine



General procedure B was applied to *N,N*-dimethyl-1-(1-methylcyclopropyl)methanamine (102 mg, 0.900 mmol) at 50 °C to provide by column chromatography (DCM to 2% NH₃(MeOH; 2M)) the title compound as a yellow oil (22.6 mg, 0.119 mmol, 40% yield, 78% ee). Enantiomeric excess was determined by GC-FID analysis.

IR ν_{max}/cm⁻¹ (thin film) 2942, 2812, 2761, 1455, 1265, 1026, 857, 696; **¹H NMR** (700 MHz, CDCl₃) δ (ppm) 7.30 – 7.25 (m, 2H, H₉), 7.22 – 7.16 (m, 3H, H_{8,10}), 2.30 (d, *J* = 12.5 Hz, 1H, H_{2a}), 2.11 (s, 6H, H₁), 1.96 – 1.91 (m, 1H, H₆), 1.52 (d, *J* = 12.5 Hz, 1H, H_{2b}), 1.30 (s, 3H, H₄), 1.02 (app t, *J* = 5.6 Hz, 1H, H_{5a}), 0.92 (dd, *J* = 8.4, 5.0 Hz, 1H, H_{5b}); **¹³C NMR** (176 MHz, CDCl₃) δ (ppm) 139.2 (C₇), 128.9 (C₈), 127.8 (C₉), 125.6 (C₁₀), 63.5 (C₂), 45.6 (C₁), 28.6 (C₆), 24.0 (C₄), 21.4 (C₃), 17.8 (C₅); **HMRS-ESI** (m/z): found [M+H]⁺ 190.1591, C₁₃H₂₀N requires 190.1596; **ee analysis**: GC-FID ChiralDex β-DM (50 °C to 150 °C; 5 °C/min; linear velocity 40 cm·s⁻¹; split ratio 10.0) t_R = 9.0 min (minor), t_R = 9.2 min (major); [α]_D^{25.0} = +7.4° (c = 0.4, CHCl₃).

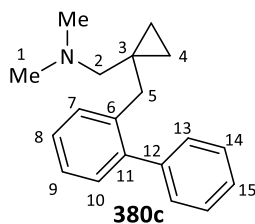
1-(1-Benzylcyclopropyl)-*N,N*-dimethylmethanamine



General procedure B was applied to *N,N*-dimethyl-1-(1-methylcyclopropyl)methanamine (102 mg, 0.900 mmol) at 50 °C to provide by column chromatography (DCM to 2% NH₃(MeOH; 2M)) the title compound as an inseparable mixture with 1-(1-([1,1'-biphenyl]-2-ylmethyl)-cyclopropyl)-*N,N*-dimethylmethanamine (9.0 mg, 4:1 ratio (major), 0.035 mmol, 12% yield).

¹H NMR (700 MHz, CDCl₃) δ (ppm) 7.32 – 7.17 (m, 5H, H_{7,8,9}), 4.96 (s, 1H, H_{4a}), 4.91 (s, 1H, H_{4b}), 2.86 (s, 2H, H₂), 2.83 – 2.79 (app t, *J* = 8.0 Hz, 2H, H₅), 2.44 – 2.39 (app t, *J* = 8.0 Hz, 2H, H_{4c}), 2.21 (s, 6H, H₁); **¹³C NMR** (176 MHz, CDCl₃) δ (ppm) 146.6 (C₃), 142.2 (C₆), 128.4 (C_{7/8}), 128.2 (C_{7/8}), 125.7 (C₉), 112.4 (C_{4a}), 65.8 (C₂), 45.5 (C₁), 35.6 (C_{4b}), 34.1 (C₅); **HMRS-ESI** (m/z): found [M+H]⁺ 176.1435, C₁₂H₁₈N requires 176.1434.

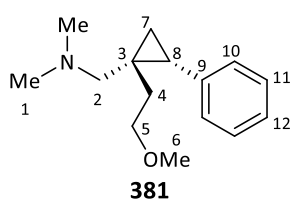
1-(1-([1,1'-Biphenyl]-2-ylmethyl)cyclopropyl)-*N,N*-dimethylmethanamine



General procedure B was applied to *N,N*-dimethyl-1-(1-methylcyclopropyl)methanamine (102 mg, 0.900 mmol) at 50 °C to provide by column chromatography (DCM to 2% NH₃(MeOH; 2M)) the title compound as an inseparable mixture with 1-(1-benzylcyclopropyl)-*N,N*-dimethylmethanamine (9.0 mg, 4:1 ratio (minor), 0.009 mmol, 3% yield).

¹H NMR (700 MHz, CDCl₃) δ (ppm) 7.32 – 7.17 (m, 9H), 2.70 (s, 2H, H_{2/5}), 2.27 (s, 6H, H₁), 2.01 (s, 2H, H_{2/5}), 0.49 – 0.45 (m, 2H, H_{4a}), 0.31 – 0.27 (m, 2H, H_{4b}); **HMRS-ESI** (m/z): found [M+H]⁺ 252.1738, C₁₈H₂₂N requires 252.1747.

1-((1*S*,2*R*)-1-(2-Methoxyethyl)-2-phenylcyclopropyl)-*N,N*-dimethylmethanamine

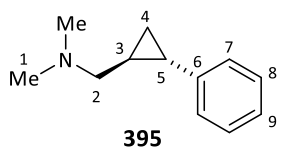


381

General procedure B was applied to 1-(1-(2-methoxyethyl)cyclopropyl)-*N,N*-dimethylmethanamine (94.4 mg, 0.600 mmol) at 50 °C to provide by column chromatography (DCM to 3% NH₃(MeOH; 2M)) the title compound as a yellow oil (30.7 mg, 0.132 mmol, 44% yield, 75% ee). Enantiomeric excess was determined by ¹H-NMR analysing H₆ from the corresponding methylated ammonium derivative.

IR $\nu_{\max}/\text{cm}^{-1}$ (thin film) 2936, 2813, 1456, 1263, 1115, 1030, 728, 697; **¹H NMR** (700 MHz, CDCl₃) δ (ppm) 7.28 (t, $J = 7.2$ Hz, 2H, H₁₁), 7.23 – 7.17 (m, 3H, H_{10,12}), 3.67 – 3.58 (m, 2H, H₅), 3.42 (s, 3H, H₆), 2.40 (d, $J = 12.8$ Hz, 1H, H_{2a}), 2.22 – 2.16 (m, 1H, H_{4a}), 2.11 (s, 6H, H₁), 2.04 (t, $J = 7.3$ Hz, 1H, H₈), 1.34 (dt, $J = 13.9, 7.1$ Hz, 1H, H_{4b}), 1.26 (d, $J = 12.8$ Hz, 1H, H_{2b}), 1.01 (t, $J = 5.4$ Hz, 1H, H_{7a}), 0.96 – 0.92 (m, 1H, H_{7b}); **¹³C NMR** (176 MHz, CDCl₃) δ (ppm) 139.0 (C₉), 129.0 (C₁₀), 127.8 (C₁₁), 125.7 (C₁₂), 71.1 (C₅), 61.1 (C₂), 58.7 (C₆), 45.7 (C₁), 36.3 (C₄), 26.8 (C₈), 22.6 (C₃), 17.2 (C₇); **HMRS-ESI** (m/z): found [M+H]⁺ 234.1853, C₁₅H₂₄NO requires 234.1858; **ee analysis**: ¹H-NMR (H₆) from the corresponding methylated ammonium derivative; $[\alpha]_D^{25.0} = +13^\circ$ ($c = 0.5$, CHCl₃).

trans-*N,N*-Dimethyl-1-(2-phenylcyclopropyl)methanamine

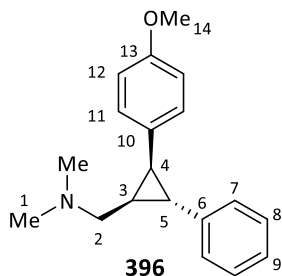


395

Subjecting the title compound (105 mg, 0.600 mmol) to general procedure B with (4-methoxyphenyl)boronic acid (45.6 mg, 0.300 mmol) in DMA at 50 °C provided by column chromatography (DCM to 2% NH₃(MeOH; 2M)) the unreacted starting material as a yellow oil (43.0 mg, 0.245 mmol, 82% yield, 51% ee). Enantiomeric excess was determined by HPLC analysis.

IR $\nu_{\max}/\text{cm}^{-1}$ (thin film) 2940, 2761, 1604, 1497, 1455, 1033, 753, 695; **¹H NMR** (700 MHz, CDCl₃) δ (ppm) 7.27 (app t, $J = 7.7$ Hz, 2H, H₈), 7.16 (t, $J = 7.0$ Hz, 1H, H₉), 7.09 (d, $J = 7.7$ Hz, 2H, H₇), 2.43 (dd, $J = 12.5, 6.3$ Hz, 1H, H_{2a}), 2.34 – 2.29 (m, 7H, H_{1,2b}), 1.74 – 1.68 (m, 1H, H₅), 1.28 – 1.22 (m, 1H, H₃), 0.99 (dt, $J = 8.7, 5.1$ Hz, 1H, H_{4a}), 0.86 (dt, $J = 8.9, 5.3$ Hz, 1H, H_{4b}); **¹³C NMR** (176 MHz, CDCl₃) δ (ppm) 143.0 (C₆), 128.3 (C₈), 125.7 (C₇), 125.4 (C₉), 64.1 (C₂), 45.5 (C₁), 22.6 (C₅), 21.6 (C₃), 15.0 (C₄); **HMRS-ESI** (m/z): found [M+H]⁺ 176.1438, C₁₂H₁₈N requires 176.1439; **ee analysis**: HPLC Chiralpak AD-H (hexane(0.1% DEA):2-propanol 98:2, 1.0 mL·min⁻¹, 30 °C) $t_R = 5.4$ min (major), $t_R = 5.8$ min (minor); $[\alpha]_D^{25.0} = -49^\circ$ ($c = 0.4$, CHCl₃).

1-((1*R*,2*S*,3*S*)-2-(4-Methoxyphenyl)-3-phenylcyclopropyl)-*N,N*-dimethylmethanamine

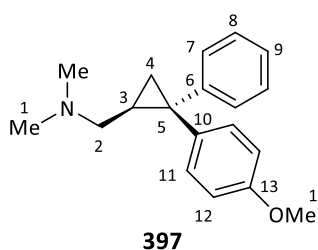


396

General procedure B was applied to *trans*-*N,N*-dimethyl-1-(2-phenylcyclopropyl)-methanamine (105 mg, 0.600 mmol) and (4-methoxyphenyl)boronic acid (45.6 mg, 0.300 mmol) in DMA at 50 °C to provide by column chromatography (DCM to 2% NH₃(MeOH; 2M)) the title compound as a yellow oil (51.4 mg, 0.183 mmol, 61% yield, 96% ee). Enantiomeric excess was determined by HPLC analysis.

IR $\nu_{\max}/\text{cm}^{-1}$ (thin film) 2937, 2764, 1609, 1512, 1454, 1243, 1031, 830, 755, 695; **$^1\text{H NMR}$** (700 MHz, CDCl_3) δ (ppm) 7.32 (t, $J = 7.5$ Hz, 2H, H_8), 7.26 – 7.18 (m, 5H, $\text{H}_{7,9,11}$), 6.88 (d, $J = 8.4$ Hz, 2H, H_{12}), 3.83 (s, 3H, H_{14}), 2.54 (dd, $J = 12.6, 4.6$ Hz, 1H, H_{2a}), 2.49 (dd, $J = 8.6, 6.2$ Hz, 1H, H_4), 2.25 (t, $J = 5.2$ Hz, 1H, H_5), 2.22 (s, 6H, H_1), 1.88 (dd, $J = 12.6, 8.4$ Hz, 1H, H_{2b}), 1.66 – 1.60 (m, 1H, H_3); **$^{13}\text{C NMR}$** (176 MHz, CDCl_3) δ (ppm) 158.1 (C_{13}), 142.3 (C_6), 130.1 (C_{10}), 129.9 (C_{11}), 128.4 (C_8), 126.1 (C_7), 125.7 (C_9), 113.6 (C_{12}), 58.9 (C_2), 55.3 (C_{14}), 45.5 (C_1), 30.6 (C_4), 28.6 (C_5), 27.7 (C_3); **HMRS-ESI** (m/z): found $[\text{M}+\text{H}]^+$ 282.1852, $\text{C}_{19}\text{H}_{24}\text{NO}$ requires 282.1858; **ee analysis**: HPLC Chiralpak AD-H (hexane(0.1% DEA):2-propanol 98:2, $1.0 \text{ mL}\cdot\text{min}^{-1}$, 30°C) $t_{\text{R}} = 11.6$ min (minor), $t_{\text{R}} = 14.0$ min (major); $[\alpha]_{\text{D}}^{25.0} = -130^\circ$ ($c = 1.0$, CHCl_3).

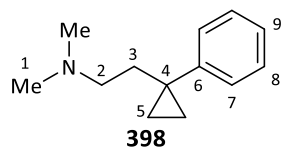
1-((1S,2R)-2-(4-Methoxyphenyl)-2-phenylcyclopropyl)-N,N-dimethylmethanamine



General procedure B was applied to *trans*-N,N-dimethyl-1-(2-phenylcyclopropyl)methanamine (105 mg, 0.600 mmol) and (4-methoxyphenyl)boronic acid (45.6 mg, 0.300 mmol) in DMA at 50°C to provide by column chromatography (DCM to 2% $\text{NH}_3(\text{MeOH}; 2\text{M})$) the title compound as a yellow oil (5.2 mg, 0.019 mmol, 6% yield, 99% ee). Enantiomeric excess was determined by HPLC analysis.

$^1\text{H NMR}$ (700 MHz, CDCl_3) δ (ppm) 7.30 – 7.26 (m, 2H, H_{11}), 7.24 (t, $J = 7.4$ Hz, 2H, H_8), 7.20 (d, $J = 7.6$ Hz, 2H, H_7), 7.14 (t, $J = 7.0$ Hz, 1H, H_9), 6.86 (d, $J = 8.5$ Hz, 2H, H_{12}), 3.82 (s, 3H, H_{14}), 2.60 (dd, $J = 12.4, 3.4$ Hz, 1H, H_{2a}), 2.26 (s, 6H, H_1), 1.82 – 1.76 (m, 1H, H_3), 1.55 (dd, $J = 12.4, 9.2$ Hz, 1H, H_{2b}), 1.37 (dd, $J = 8.0, 4.7$ Hz, 1H, H_{4a}), 1.33 – 1.29 (m, 1H, H_{4b}); **$^{13}\text{C NMR}$** (176 MHz, CDCl_3) δ (ppm) 158.1 (C_{13}), 147.3 (C_6), 133.5 (C_{10}), 131.4 (C_{11}), 128.2 ($\text{C}_{7/8}$), 127.5 ($\text{C}_{7/8}$), 125.6 (C_9), 113.6 (C_{12}), 61.3 (C_2), 55.2 (C_{14}), 45.7 (C_1), 33.4 (C_5), 24.3 (C_3), 21.3 (C_4); **HMRS-ESI** (m/z): found $[\text{M}+\text{H}]^+$ 282.1854, $\text{C}_{19}\text{H}_{24}\text{NO}$ requires 282.1858; **ee analysis**: HPLC Chiralpak AD-H (hexane(0.1% DEA):2-propanol 98:2, $1.0 \text{ mL}\cdot\text{min}^{-1}$, 30°C) $t_{\text{R}} = 8.3$ min (minor), $t_{\text{R}} = 12.2$ min (major).

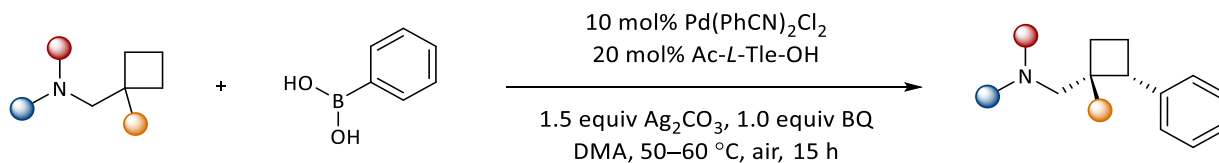
N,N-Dimethyl-2-(1-phenylcyclopropyl)ethan-1-amine



General procedure B was applied to 2-cyclopropyl-N,N-dimethylethan-1-amine (84.9 mg, 0.750 mmol) to provide by column chromatography (DCM to 2% $\text{NH}_3(\text{MeOH}; 2\text{M})$) the title compound as a brown oil (45.5 mg, 0.240 mmol, 80% yield).

IR $\nu_{\max}/\text{cm}^{-1}$ (thin film) 3660, 2972, 2762, 1460, 1260, 1066; **$^1\text{H NMR}$** (400 MHz, CDCl_3) δ (ppm) 7.32 – 7.16 (m, 5H, $\text{H}_{7,8,9}$), 2.30 – 2.23 (m, 2H, H_2), 2.18 (s, 6H, H_1), 1.81 – 1.72 (m, 2H, H_3), 0.84 (dd, $J = 5.9, 4.3$ Hz, 2H, H_{5a}), 0.73 (dd, $J = 5.9, 4.3$ Hz, 2H, H_{5b}); **$^{13}\text{C NMR}$** (101 MHz, CDCl_3) δ (ppm) 144.9 (C_6), 128.7 ($\text{C}_{7/8}$), 128.1 ($\text{C}_{7/8}$), 125.9 (C_9), 57.6 (C_2), 45.6 (C_1), 38.3 (C_3), 24.0 (C_4), 13.2 (C_5); **HMRS-ESI** (m/z): found $[\text{M}+\text{H}]^+$ 190.1583, $\text{C}_{13}\text{H}_{20}\text{N}$ requires 190.1596.

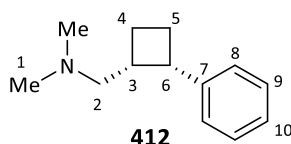
General procedure C: Methylene cyclobutane C–H arylation



The desired tertiary amine (0.600 mmol) was added to a 2–5 mL microwave vial containing Pd(PhCN)₂Cl₂ (11.5 mg, 0.030 mmol), Ac-*L*-Tle-OH (10.4 mg, 0.060 mmol), Ag₂CO₃ (124 mg, 0.450 mmol) and 1,4-benzoquinone (BQ) (32.5 mg, 0.300 mmol) in anhydrous DMA (0.75 mL). The reaction was sealed and stirred at 50 °C for 5 minutes. Phenyl boronic acid (36.6 mg, 0.300 mmol) in DMA (0.75 mL) was added dropwise and the reaction mixture was stirred at 1000 rpm, at 50 °C for 15 h.

The reaction was cooled to rt and Et₂O (5 mL) added, forcing the formation of a precipitate. The dark mixture was filtered through a pad of Celite and washed with Et₂O (25 mL). The resulting organic layer was washed with aq NaOH (0.25 M, 3 x 50 mL), dried over MgSO₄, filtered and concentrated *in vacuo*. Purification of the crude oil by column chromatography afforded the pure arylated product. Asymmetry was determined by HPLC analysis using a CHIRALPAK® AD-H column, GC-FID analysis using a Astec Chiraldex™ B-DM column, or ¹H-NMR analysis of the methylated tertiary amine product following a literature procedure reported by Lacour.²²⁴

N,N-Dimethyl-1-((1*R*,2*S*)-2-phenylcyclobutyl)methanamine

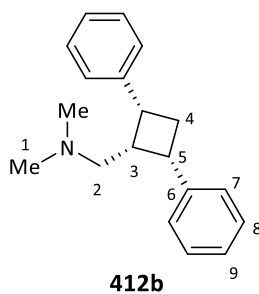


General procedure C was applied to 1-cyclobutyl-*N,N*-dimethylmethanamine (67.9 mg, 0.600 mmol) at 60 °C to provide by column chromatography (DCM to 4% NH₃(MeOH; 2M)) the title compound as a brown oil (41.3 mg, 0.218 mmol, 73% yield,

>95% ee). Enantiomeric excess was determined by ¹H-NMR analysing H₆ from the corresponding methylated ammonium derivative.

IR ν_{\max} /cm⁻¹ (thin film) 2941, 2763, 1494, 1455, 1031, 764, 737, 697; **¹H NMR** (600 MHz, CDCl₃) δ (ppm) 7.34 – 7.30 (m, 2H, H₉), 7.23 – 7.19 (m, 3H, H_{8,10}), 3.77 (q, *J* = 8.3 Hz, 1H, H₆), 2.90 – 2.81 (m, 1H, H₃), 2.41 – 2.29 (m, 2H, H₅), 2.24 (tt, *J* = 7.9, 4.9 Hz, 1H, H_{4a}), 2.13 – 2.06 (m, 7H, H_{1,2a}), 1.92 – 1.84 (m, 2H, H_{2b,4b}); **¹³C NMR** (151 MHz, CDCl₃) δ (ppm) 141.6 (C₇), 128.0 (C₈), 127.8 (C₉), 125.8 (C₁₀), 61.2 (C₂), 45.9 (C₁), 41.8 (C₆), 37.5 (C₃), 24.2 (C₄), 23.5 (C₅); **HMRS-ESI** (*m/z*): found [M+H]⁺ 190.1584, C₁₃H₂₀N requires 190.1590; **ee analysis**: ¹H-NMR (H₆) from the corresponding methylated ammonium derivative; $[\alpha]_D^{25.0} = -69^\circ$ (*c* = 1.0, CHCl₃).

1-((1*S*,2*R*,4*S*)-2,4-Diphenylcyclobutyl)-*N,N*-dimethylmethanamine

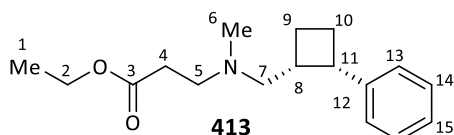


General procedure C was applied to 1-cyclobutyl-*N,N*-dimethylmethanamine (67.9 mg, 0.600 mmol) at 60 °C to provide by column chromatography (DCM to 4% NH₃(MeOH; 2M)) the title compound as a brown oil (3.2 mg, 0.012 mmol, 4% yield).

¹H NMR (600 MHz, CDCl₃) δ (ppm) 7.34 (t, *J* = 7.6 Hz, 4H, H₈), 7.30 – 7.25 (m, 4H, H₇), 7.22 (t, *J* = 7.2 Hz, 2H, H₉), 3.86 (dt, *J* = 11.0, 8.1 Hz, 2H, H₅), 3.16 (br s, 1H, H₃), 2.75 (q, *J* = 11.1 Hz, 1H, H_{4a}), 2.46 (dtd, *J* = 11.1, 7.5, 3.7 Hz, 1H, H_{4b}), 2.01 (br s, 2H, H₂), 1.75

(s, 6H, H₁); ¹³C NMR (151 MHz, CDCl₃) δ (ppm) 140.9 (C₆), 128.1 (C₇), 127.9 (C₈), 125.9 (C₉), 55.0 (C₂), 45.1 (C₁), 43.8 (C₃), 39.1 (C₄), 27.8 (C₅); **HMRS-ESI** (*m/z*): found [M+H]⁺ 266.1893, C₁₉H₂₄N requires 266.1903.

Ethyl 3-(methyl(((1*R*,2*S*)-2-phenylcyclobutyl)methyl)amino)propanoate

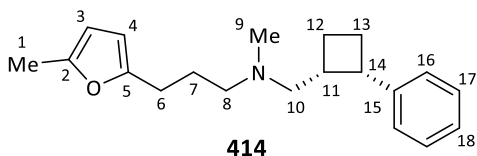


General procedure C was applied to ethyl 3-((cyclobutylmethyl)(methyl)amino)propanoate (120 mg, 0.600 mmol) at 50 °C to provide by column chromatography (DCM to 3% NH₃(MeOH; 2M)) the title compound as a brown oil (58.5 mg, 0.212 mmol, 71% yield, 95% ee). Enantiomeric excess was determined by

¹H-NMR analysing H₆ from the corresponding methylated ammonium derivative.

IR ν_{max}/cm⁻¹ (thin film) 2973, 1731, 1458, 1177, 1030, 698; ¹H NMR (700 MHz, CDCl₃) δ (ppm) 7.32 (t, *J* = 7.5 Hz, 2H, H₁₄), 7.24 – 7.18 (m, 3H, H_{13,15}), 4.12 (q, *J* = 7.1 Hz, 2H, H₂), 3.77 (q, *J* = 8.3 Hz, 1H, H₁₁), 2.91 – 2.83 (m, 1H, H₈), 2.63 – 2.57 (m, 1H, H_{5a}), 2.55 – 2.50 (m, 1H, H_{5b}), 2.40 – 2.29 (m, 4H, H_{4,10}), 2.24 – 2.17 (m, 1H, H_{9a}), 2.14 (app t, *J* = 11.4 Hz, 1H, H_{7a}), 2.10 (s, 3H, H₆), 1.99 (dd, *J* = 12.6, 4.7 Hz, 1H, H_{7b}), 1.86 (tt, *J* = 11.3, 5.7 Hz, 1H, H_{9b}), 1.26 (t, *J* = 7.1 Hz, 3H, H₁); ¹³C NMR (176 MHz, CDCl₃) δ (ppm) 172.7 (C₃), 141.6 (C₁₂), 128.0 (C₁₃), 127.8 (C₁₄), 125.8 (C₁₅), 60.3 (C₂), 58.7 (C₇), 53.1 (C₅), 42.3 (C₆), 41.8 (C₁₁), 37.2 (C₈), 32.5 (C₄), 24.0 (C₉), 23.5 (C₁₀), 14.2 (C₁); **HMRS-ESI** (*m/z*): found [M+H]⁺ 276.1964, C₁₇H₂₆NO₂ requires 276.1964; **ee analysis**: ¹H-NMR (H₆) from the corresponding methylated ammonium derivative; [α]_D^{25.0} = -71° (c = 0.6, CHCl₃).

N-Methyl-3-(5-methylfuran-2-yl)-*N*-(((1*R*,2*S*)-2-phenylcyclobutyl)methyl)propan-1-amine



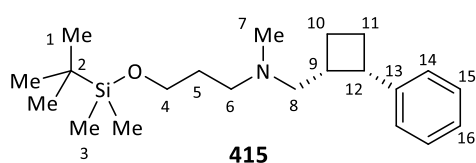
General procedure C was applied to *N*-(cyclobutylmethyl)-*N*-methyl-3-(5-methylfuran-2-yl)propan-1-amine (133 mg, 0.600 mmol) at 50 °C to provide by column chromatography (DCM to 4%

NH₃(MeOH; 2M)) the title compound as a yellow oil (55.0 mg, 0.185 mmol, 62% yield, 94% ee). Enantiomeric excess was determined by HPLC analysis.

IR ν_{max}/cm⁻¹ (thin film) 2942, 2788, 1453, 1218, 1018, 776, 697; ¹H NMR (700 MHz, CDCl₃) δ (ppm) 7.31 (t, *J* = 7.4 Hz, 2H, H₁₇), 7.24 – 7.18 (m, 3H, H_{16,18}), 5.85 (s, 1H, H₃), 5.83 (s, 1H, H₄), 3.76 (q, *J* = 8.3 Hz, 1H, H₁₄), 2.92 – 2.83 (m, 1H, H₁₁), 2.58 – 2.48 (m, 2H, H₆), 2.40 – 2.29 (m, 2H, H₁₃), 2.27 (s, 3H, H₉), 2.26 – 2.16 (m, 3H, H_{8,12a}),

2.13 (app t, $J = 11.3$ Hz, 1H, H_{10a}), 2.09 (s, 3H, H₁), 1.98 (dd, $J = 12.6, 4.6$ Hz, 1H, H_{10b}), 1.92 – 1.86 (m, 1H, H_{12b}), 1.69 – 1.64 (m, 2H, H₇); ¹³C NMR (176 MHz, CDCl₃) δ (ppm) 154.4 (C₅), 150.1 (C₂), 141.8 (C₁₅), 127.9 (C₁₆), 127.8 (C₁₇), 125.7 (C₁₈), 105.7 (C₃), 105.2 (C₄), 59.1 (C₁₀), 57.4 (C₈), 42.6 (C₉), 41.9 (C₁₄), 37.4 (C₁₁), 25.9 (C₆), 25.8 (C₇), 24.3 (C₁₂), 23.6 (C₁₃), 13.5 (C₁); **HMRS-ESI** (m/z): found [M+H]⁺ 298.2168, C₂₀H₂₈NO requires 298.2171; **ee analysis**: HPLC Chiralpak AD-H (hexane(0.1% DEA):2-propanol 99.6:0.4, 1.0 mL·min⁻¹, 15 °C) $t_R = 4.8$ min (major), $t_R = 5.1$ min (minor); $[\alpha]_D^{25.0} = -64^\circ$ ($c = 1.0$, CHCl₃).

3-((*tert*-Butyldimethylsilyloxy)-*N*-methyl-*N*-(((1*R*,2*S*)-2-phenylcyclobutyl)methyl)propan-1-amine

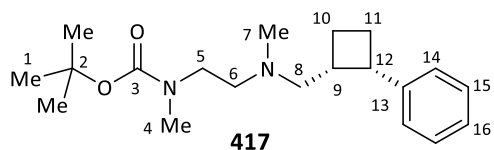


General procedure C was applied to 3-((*tert*-butyldimethylsilyloxy)-*N*-(cyclobutylmethyl)-*N*-methylpropan-1-amine (163 mg, 0.600 mmol) at 50 °C to provide by column chromatography (DCM to 3% NH₃(MeOH; 2M)) the title compound as a yellow oil (53.0 mg, 0.152

mmol, 51% yield, 94% ee). Enantiomeric excess was determined by ¹H-NMR analysing H₁₂ from the corresponding methylated ammonium derivative.

IR $\nu_{\max}/\text{cm}^{-1}$ (thin film) 2950, 2855, 1461, 1253, 1094, 832, 772, 697; **¹H NMR** (700 MHz, CDCl₃) δ (ppm) 7.32 (app t, $J = 7.6$ Hz, 2H, H₁₅), 7.24 – 7.18 (m, 3H, H_{14,16}), 3.77 (q, $J = 8.3$ Hz, 1H, H₁₂), 3.62 – 3.56 (m, 2H, H₄), 2.92 – 2.85 (m, 1H, H₉), 2.40 – 2.28 (m, 3H, H_{6a,11}), 2.26 – 2.20 (m, 2H, H_{6b,10a}), 2.13 (dd, $J = 12.4, 10.4$ Hz, 1H, H_{8a}), 2.09 (s, 3H, H₇), 1.98 (dd, $J = 12.4, 4.7$ Hz, 1H, H_{8b}), 1.89 (tt, $J = 11.2, 5.7$ Hz, 1H, H_{10b}), 1.57 (app p, $J = 6.8$ Hz, 2H, H₅), 0.91 (s, 9H, H₁), 0.06 (s, 6H, H₃); ¹³C NMR (176 MHz, CDCl₃) δ (ppm) 141.7 (C₁₃), 128.0 (C₁₄), 127.8 (C₁₅), 125.7 (C₁₆), 61.5 (C₄), 59.1 (C₈), 54.7 (C₆), 42.7 (C₇), 41.9 (C₁₂), 37.4 (C₉), 30.5 (C₅), 26.0 (C₁), 24.3 (C₁₀), 23.6 (C₁₁), 18.3 (C₂), -5.3 (C₃); **HMRS-ESI** (m/z): found [M+H]⁺ 348.2718, C₂₁H₃₈NOSi requires 348.2723; **ee analysis**: ¹H-NMR (H₁₂) from the corresponding methylated ammonium derivative; $[\alpha]_D^{25.0} = -62^\circ$ ($c = 1.0$, CHCl₃).

tert-Butyl methyl(2-(methyl(((1*R*,2*S*)-2-phenylcyclobutyl)methyl)amino)ethyl)carbamate



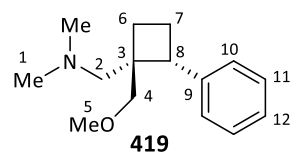
General procedure C was applied to *tert*-butyl (2-((cyclobutylmethyl)(methyl)amino)ethyl)(methyl)carbamate (155 mg, 0.600

mmol) at 50 °C to provide by column chromatography (DCM to 3% NH₃(MeOH; 2M)) the title compound as a brown oil (63.3 mg, 0.190 mmol, 64% yield, >95% ee). Enantiomeric excess was determined by ¹H-NMR from the corresponding methylated ammonium derivative.

IR $\nu_{\max}/\text{cm}^{-1}$ (thin film) 2971, 1691, 1390, 1153, 1044, 765, 698; **¹H NMR** (700 MHz, CDCl₃) δ (ppm) 7.31 (t, $J = 7.6$ Hz, 2H, H₁₅), 7.24 – 7.18 (m, 3H, H_{14,16}), 3.77 (q, $J = 8.2$ Hz, 1H, H₁₂), 3.28 – 3.04 (m, 2H, H₅), 2.89 – 2.77 (m, 4H, H_{4,9}), 2.40 – 2.26 (m, 4H, H_{6,11}), 2.23 – 2.17 (m, 1H, H_{10a}), 2.17 – 2.09 (m, 4H, H_{7,8a}), 2.07 – 2.00 (m, 1H, H_{8b}), 1.87 (tt, $J = 11.2, 5.8$ Hz, 1H, H_{10b}), 1.45 (s, 9H, H₁); ¹³C NMR (176 MHz, CDCl₃) δ (ppm) 155.7 (C₃), 141.6 (C₁₃), 127.9 (C₁₄), 127.8 (C₁₅), 125.8 (C₁₆), 79.1 (C₂), 59.4 (C₈), 55.6 (C₆), 47.0 (C₅), 42.8 (C₇), 41.8 (C₁₂), 37.3 (C₉), 34.6

(C₄), 28.5 (C₁), 24.0 (C₁₀), 23.5 (C₁₁); **HMRS-ESI** (m/z): found [M+H]⁺ 333.2535, C₂₀H₃₃N₂O₂ requires 333.2542; **ee analysis**: ¹H-NMR from the corresponding methylated ammonium derivative; [α]_D^{25.0} = -63° (c = 1.0, CHCl₃).

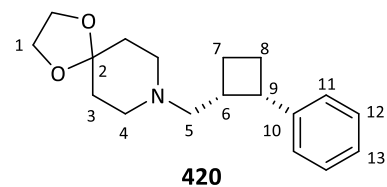
1-((1*S*,2*R*)-1-(Methoxymethyl)-2-phenylcyclobutyl)-*N,N*-dimethylmethanamine



General procedure C was applied to 1-(1-(methoxymethyl)cyclobutyl)-*N,N*-dimethylmethanamine (94.3 mg, 0.600 mmol) at 50 °C to provide by column chromatography (DCM to 2% NH₃(MeOH; 2M)) the title compound as a yellow oil (33.8 mg, 0.151 mmol, 51% yield, 77% ee). Enantiomeric excess was determined by GC-FID analysis.

IR ν_{max}/cm⁻¹ (thin film) 2973, 2939, 2815, 2763, 1452, 1103, 1032, 697; **¹H NMR** (700 MHz, CDCl₃) δ (ppm) 7.31 (t, *J* = 7.6 Hz, 2H, H₁₁), 7.24 (d, *J* = 7.5 Hz, 2H, H₁₀), 7.20 (t, *J* = 7.3 Hz, 1H, H₁₂), 3.71 (t, *J* = 9.0 Hz, 1H, H₈), 3.55 – 3.45 (m, 5H, H_{4,5}), 2.32 (app p, *J* = 9.3 Hz, 1H, H_{7a}), 2.21 – 2.16 (m, 1H, H_{7b}), 2.13 (s, 6H, H₁), 2.10 – 2.03 (m, 2H, H₂), 2.03 – 1.97 (m, 1H, H_{6a}), 1.91 (td, *J* = 10.7, 3.9 Hz, 1H, H_{6b}); **¹³C NMR** (176 MHz, CDCl₃) δ (ppm) 140.9 (C₉), 128.1 (C₁₀), 127.8 (C₁₁), 125.7 (C₁₂), 77.8 (C₄), 61.1 (C₂), 59.2 (C₅), 47.8 (C₁), 47.1 (C₃), 44.7 (C₈), 24.9 (C₆), 20.2 (C₇); **HMRS-ESI** (m/z): found [M+H]⁺ 234.1857, C₁₅H₂₄NO requires 234.1858; **ee analysis**: GC-FID ChiralDex β-DM (50 °C to 72 °C; 0.15 °C/min; linear velocity 40 cm·s⁻¹; split ratio 10.0) t_R = 131.3 min (minor), t_R = 134.3 min (major); [α]_D^{25.0} = -20° (c = 1.0, CHCl₃).

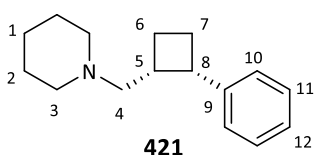
8-(((1*R*,2*S*)-2-Phenylcyclobutyl)methyl)-1,4-dioxo-8-azaspiro[4.5]decane



General procedure C was applied to 8-(cyclobutylmethyl)-1,4-dioxo-8-azaspiro[4.5]decane (127 mg, 0.600 mmol) at 50 °C to provide by column chromatography (DCM to 4% NH₃(MeOH; 2M)) the title compound as a yellow oil (42.6 mg, 0.148 mmol, 50% yield, 90% ee). Enantiomeric excess was

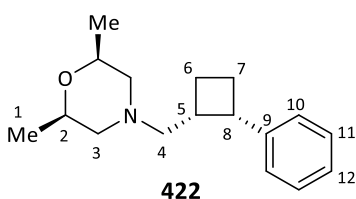
determined by HPLC analysis.

IR ν_{max}/cm⁻¹ (thin film) 2948, 2808, 1308, 1142, 1090, 1038, 913, 765, 698; **¹H NMR** (700 MHz, CDCl₃) δ (ppm) 7.33 – 7.27 (m, 2H, H₁₂), 7.22 (d, *J* = 7.5 Hz, 2H, H₁₁), 7.20 (t, *J* = 7.3 Hz, 1H, H₁₃), 3.93 (s, 4H, H₁), 3.77 (q, *J* = 8.2 Hz, 1H, H₉), 2.90 (app hex, *J* = 7.2 Hz, 1H, H₆), 2.44 – 2.26 (m, 6H, H_{4,8}), 2.23 (app p, *J* = 8.1 Hz, 1H, H_{7a}), 2.11 (d, *J* = 7.2 Hz, 2H, H₅), 1.92 – 1.86 (m, 1H, H_{7b}), 1.66 (br s, 4H, H₃); **¹³C NMR** (176 MHz, CDCl₃) δ (ppm) 141.7 (C₁₀), 128.0 (C₁₁), 127.9 (C₁₂), 125.7 (C₁₃), 107.3 (C₂), 64.1 (C₁), 59.4 (C₅), 51.5 (C₄), 42.2 (C₉), 37.4 (C₆), 34.8 (C₃), 24.8 (C₇), 23.6 (C₈); **HMRS-ESI** (m/z): found [M+H]⁺ 288.1962, C₁₈H₂₈NO₂ requires 288.1964; **ee analysis**: HPLC Chiralpak AD-H (hexane(0.1% DEA):2-propanol 97:3, 1.0 mL·min⁻¹, 30 °C) t_R = 5.7 min (major), t_R = 6.0 min (minor); [α]_D^{25.0} = -52° (c = 1.0, CHCl₃).

1-(((1*R*,2*S*)-2-Phenylcyclobutyl)methyl)piperidine**421**

General procedure C was applied to 1-(cyclobutylmethyl)piperidine (67.9 mg, 0.600 mmol) and phenyl boronic acid (36.6 mg, 0.300 mmol) in NMP at 50 °C to provide by column chromatography (DCM to 4% NH₃(MeOH; 2M)) the title compound as a brown oil (33.1 mg, 0.144 mmol, 48% yield, 89% ee). Enantiomeric excess was determined by ¹H-NMR analysing H₈ from the corresponding methylated ammonium derivative.

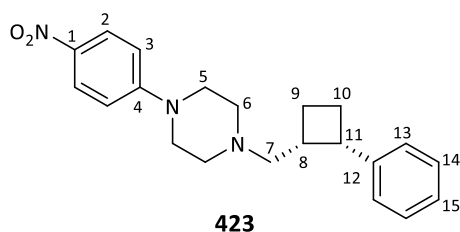
IR ν_{\max} /cm⁻¹ (thin film) 2932, 2850, 2765, 1602, 1494, 1441, 1302, 1153, 1121, 1038, 995, 736, 696; **¹H NMR** (600 MHz, CDCl₃) δ (ppm) 7.31 (app t, $J = 7.6$ Hz, 2H, H₁₁), 7.24 – 7.17 (m, 3H, H_{10,12}), 3.75 (q, $J = 8.2$ Hz, 1H, H₈), 2.95 – 2.86 (m, 1H, H₅), 2.37 – 2.28 (m, 2H, H₇), 2.28 – 2.08 (m, 5H, H_{3,6a}), 2.07 – 2.00 (m, 2H, H₄), 1.94 – 1.88 (m, 1H, H_{6b}), 1.54 – 1.46 (m, 4H, H₂), 1.42 – 1.29 (m, 2H, H₁); **¹³C NMR** (151 MHz, CDCl₃) δ (ppm) 141.8 (C₉), 128.0 (C₁₀), 127.9 (C₁₁), 125.7 (C₁₂), 60.8 (C₄), 54.8 (C₃), 42.3 (C₈), 37.4 (C₅), 26.0 (C₂), 25.3 (C₆), 24.4 (C₁), 23.7 (C₇); **HMRS-ESI** (m/z): found [M+H]⁺ 230.1896, C₁₆H₂₄N requires 230.1903; **ee analysis**: ¹H-NMR (H₈) from the corresponding methylated ammonium derivative following Lacour's procedure; $[\alpha]_D^{25.0} = -55^\circ$ (c = 1.0, CHCl₃).

(2*S*,6*R*)-2,6-Dimethyl-4-(((1*R*,2*S*)-2-phenylcyclobutyl)methyl)morpholine**422**

General procedure C was applied to (2*S*,6*R*)-4-(cyclobutylmethyl)-2,6-dimethylmorpholine (110 mg, 0.600 mmol) and phenyl boronic acid (36.6 mg, 0.300 mmol) in DMA at 50 °C to provide by column chromatography (DCM to 3% NH₃(MeOH; 2M)) the title compound as a yellow oil (23.1 mg, 0.089 mmol, 30% yield, 83% ee). Enantiomeric excess was determined by GC-FID analysis.

IR ν_{\max} /cm⁻¹ (thin film) 2969, 2933, 2864, 1454, 1322, 1142, 1080, 766, 697; **¹H NMR** (700 MHz, CDCl₃) δ (ppm) 7.31 (t, $J = 7.4$ Hz, 2H, H₁₁), 7.25 – 7.18 (m, 3H, H_{10,12}), 3.78 (q, $J = 8.2$ Hz, 1H, H₈), 3.65 – 3.59 (m, 1H, H_{2a}), 3.58 – 3.52 (m, 1H, H_{2b}), 2.95 – 2.87 (m, 1H, H₅), 2.58 (d, $J = 11.1$ Hz, 1H, H_{3a}), 2.43 (d, $J = 11.1$ Hz, 1H, H_{3b}), 2.41 – 2.29 (m, 2H, H₇), 2.22 (app p, $J = 8.8$ Hz, 1H, H_{6a}), 2.08 (app t, $J = 10.9$ Hz, 1H, H_{4a}), 2.03 (dd, $J = 12.5, 5.0$ Hz, 1H, H_{4b}), 1.92 – 1.86 (m, 1H, H_{6b}), 1.63 (app t, $J = 10.7$ Hz, 1H, H_{3c}), 1.51 (app t, $J = 10.7$ Hz, 1H, H_{3d}), 1.12 (d, $J = 6.2$ Hz, 3H, H_{1a}), 1.09 (d, $J = 6.2$ Hz, 3H, H_{1b}); **¹³C NMR** (176 MHz, CDCl₃) δ (ppm) 141.5 (C₉), 128.0 (C₁₀), 127.9 (C₁₁), 125.8 (C₁₂), 71.6 (C_{2a}), 71.6 (C_{2b}), 60.2 (C_{3a}), 59.8 (C₄), 59.4 (C_{3b}), 42.0 (C₈), 36.8 (C₅), 24.5 (C₆), 23.5 (C₇), 19.2 (C_{1a}), 19.1 (C_{1b}); **HMRS-ESI** (m/z): found [M+H]⁺ 260.2012, C₁₇H₂₆NO requires 260.2014; **ee analysis**: GC-FID ChiralDex β -DM (110 °C; isocratic; linear velocity 40 cm·s⁻¹; split ratio 10.0) $t_R = 25.6$ min (major), $t_R = 26.5$ min (minor); $[\alpha]_D^{25.0} = -60^\circ$ (c = 0.8, CHCl₃).

1-(4-Nitrophenyl)-4-(((1*R*,2*S*)-2-phenylcyclobutyl)methyl)piperazine

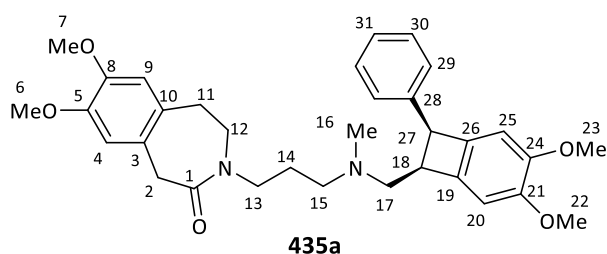


General procedure C was applied to 1-(cyclobutylmethyl)-4-(4-nitrophenyl)piperazine (165 mg, 0.600 mmol) and phenyl boronic acid (36.6 mg, 0.300 mmol) in DMA at 50 °C to provide by column chromatography (DCM to 3% NH₃(MeOH; 2M)) the title compound as a yellow oil (34.6 mg, 0.098 mmol, 33% yield, 88% ee). Enantiomeric

excess was determined by HPLC analysis.

IR ν_{max} /cm⁻¹ (thin film) 2970, 1956, 1492, 1320, 1239, 1112, 1001, 732, 699; **¹H NMR** (700 MHz, CDCl₃) δ (ppm) 8.17 – 8.08 (m, 2H, H₂), 7.36 – 7.29 (m, 2H, H₁₄), 7.27 – 7.19 (m, 3H, H_{13,15}), 6.81 – 6.76 (m, 2H, H₃), 3.81 (q, J = 8.3 Hz, 1H, H₁₁), 3.39 – 3.29 (m, 4H, H₅), 2.99 – 2.88 (m, 1H, H₈), 2.45 – 2.31 (m, 6H, H_{6,10}), 2.30 – 2.20 (m, 1H, H_{9a}), 2.19 – 2.10 (m, 2H, H₇), 1.94 – 1.85 (m, 1H, H_{9b}); **¹³C NMR** (176 MHz, CDCl₃) δ (ppm) 154.9 (C₄), 141.4 (C₁₂), 138.2 (C₁), 128.0 (C_{13,14}), 126.0 (C₁₅), 125.9 (C₂), 112.5 (C₃), 59.6 (C₇), 52.7 (C₆), 47.0 (C₅), 42.0 (C₁₁), 36.8 (C₈), 24.2 (C₉), 23.5 (C₁₀); **HMRS-ESI** (m/z): found [M+H]⁺ 352.2031, C₂₁H₂₆N₃O₂ requires 352.2025; **ee analysis**: HPLC Chiralpak AD-H (hexane(0.1% DEA):2-propanol 98:2, 1.0 mL·min⁻¹, 30 °C) t_R = 23.3 min (major), t_R = 26.5 min (minor); $[\alpha]_D^{25.0}$ = -5.9° (c = 0.8, CHCl₃).

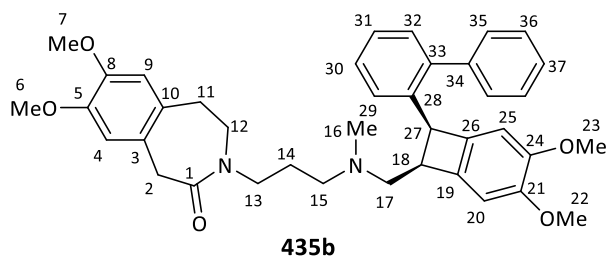
3-(3-(((7*S*,8*S*)-3,4-Dimethoxy-8-phenylbicyclo[4.2.0]octa-1(6),2,4-trien-7-yl)methyl)(methyl)amino)-propyl)-7,8-dimethoxy-1,3,4,5-tetrahydro-2H-benzo[d]azepin-2-one



General procedure C was applied to Ivabradine (70.3 mg, 0.150 mmol) with *D*-Ac-Tle-OH (3.5 mg, 0.020 mmol) at 50 °C to provide by column chromatography (DCM to 3% NH₃(MeOH; 2M)) the title compound as a yellow oil (10.8 mg, 0.020 mmol, 20% yield).

¹H NMR (700 MHz, CDCl₃) δ (ppm) 7.30 (t, J = 7.5 Hz, 2H, H₃₀), 7.24 (t, J = 7.2 Hz, 1H, H₃₁), 7.17 (d, J = 7.5 Hz, 2H, H₂₉), 6.84 (s, 1H, H₂₀), 6.79 (s, 1H, H₂₅), 6.60 (s, 1H, H₄), 6.55 (s, 1H, H₉), 4.79 (d, J = 5.3 Hz, 1H, H₂₇), 3.92 (s, 3H, H₂₂), 3.89 (s, 3H, H₂₃), 3.88 – 3.86 (m, 1H, H₁₈), 3.85 (s, 3H, H₇), 3.84 (s, 3H, H₆), 3.83 – 3.77 (m, 2H, H₂), 3.70 – 3.62 (m, 2H, H₁₂), 3.50 – 3.41 (m, 1H, H_{13a}), 3.37 – 3.28 (m, 1H, H_{13b}), 3.06 – 2.97 (m, 2H, H₁₁), 2.21 (t, J = 7.1 Hz, 2H, H₁₅), 2.17 (s, 3H, H₁₆), 2.12 (d, J = 7.4 Hz, 2H, H₁₇), 1.64 – 1.54 (m, 2H, H₁₄); **¹³C NMR** (176 MHz, CDCl₃) δ (ppm) 172.0 (C₁), 150.1 (C_{21/24}), 150.0 (C_{21/24}), 147.8 (C₈), 147.1 (C₅), 140.0 (C₂₈), 138.9 (C₁₉), 136.3 (C₂₆), 128.8 (C₂₉), 128.0 (C₃₀), 127.4 (C₁₀), 126.6 (C₃₁), 123.5 (C₃), 114.0 (C₄), 113.1 (C₉), 107.5 (C₂₀), 107.1 (C₂₅), 58.8 (C₁₇), 56.4 (C₂₂), 56.3 (C₂₃), 55.9 (C_{6/7}), 55.9 (C_{6/7}), 55.1 (C₁₅), 50.3 (C₂₇), 46.5 (C₁₂), 45.9 (C₁₈), 44.9 (C₁₃), 42.7 (C₁₆), 42.3 (C₂), 32.4 (C₁₁), 26.2 (C₁₄); **HMRS-ESI** (m/z): found [M+H]⁺ 545.3014, C₃₃H₄₁N₂O₅ requires 545.3015; $[\alpha]_D^{25.0}$ = -93° (c = 0.5, CHCl₃).

3-(3-(((7S,8R)-8-([1,1'-biphenyl]-2-yl)-3,4-dimethoxybicyclo[4.2.0]octa-1(6),2,4-trien-7-yl)methyl)-(methyl)amino)propyl)-7,8-dimethoxy-1,3,4,5-tetrahydro-2H-benzo[d]azepin-2-one



General procedure C was applied to Ivabradine (70.3 mg, 0.150 mmol) with *D*-Ac-Tle-OH (3.5 mg, 0.020 mmol) at 50 °C to provide by column chromatography (DCM to 3% NH₃(MeOH; 2M)) the title compound as a brown oil (5.1 mg, 0.008 mmol, 8% yield).

¹H NMR (700 MHz, CDCl₃) δ (ppm) 7.54 (d, *J* = 7.4 Hz, 2H, H₃₅), 7.46 (t, *J* = 7.6 Hz, 2H, H₃₆), 7.38 (t, *J* = 7.4 Hz, 1H, H₃₇), 7.33 – 7.25 (m, 3H, H_{29/30/31/32}), 7.12 (d, *J* = 7.5 Hz, 1H, H_{29/32}), 6.80 (s, 1H, H₂₀), 6.67 (s, 1H, H₂₅), 6.59 (s, 1H, H₄), 6.50 (s, 1H, H₉), 4.78 (d, *J* = 5.1 Hz, 1H, H₂₇), 3.90 (s, 3H, H_{6/7/22/23}), 3.85 (s, 2H, H_{6/7/22/23}), 3.84 (s, 3H, H_{6/7/22/23}), 3.81 (s, 3H, H_{6/7/22/23}), 3.80 – 3.76 (m, 2H, H₂), 3.74 (app q, *J* = 6.8 Hz, 1H, H₁₈), 3.63 – 3.55 (m, 2H, H₁₂), 3.44 – 3.34 (m, 1H, H_{13a}), 3.22 – 3.13 (m, 1H, H_{13b}), 2.95 – 2.87 (m, 2H, H₁₁), 2.41 (dd, *J* = 12.9, 7.0 Hz, 1H, H_{17a}), 2.31 (dd, *J* = 12.8, 7.9 Hz, 1H, H_{17b}), 2.27 – 2.20 (m, 4H, H_{15a,16}), 2.20 – 2.12 (m, 1H, H_{15b}), 1.55 – 1.43 (m, 2H, H₁₄); **HMRS-ESI** (m/z): found [M+H]⁺ 621.3328, C₃₉H₄₅N₂O₅ requires 621.3328.

Chapter 6

References

1. Bollinger, J. M. J.; Broderick, J. B. *Curr. Opin. Chem. Biol.* **2009**, *13*, 51–57.
2. Arnold, F. H. *Angew. Chem. Int. Ed.* **2019**, *58*, 14420–14426.
3. Ryabov, A. D. *Chem. Rev.* **1990**, *90*, 403–424.
4. Dick, A. R.; Sanford, M. S. *Tetrahedron* **2006**, *62*, 2439–2463.
5. Rouquet, G.; Chatani, N. *Angew. Chem. Int. Ed.* **2013**, *52*, 11726–11743.
6. Gensch, T.; Hopkinson, M. N.; Glorius, F.; Wencel-Delord, J. *Chem. Soc. Rev.* **2016**, *110*, 2900–2936.
7. Davies, H. M. L.; Morton, D. *Chem. Soc. Rev.* **2011**, *40*, 1857–1869.
8. Zhang, R. K.; Chen, K.; Huang, X.; Wohlschlagel, L.; Renata, H.; Arnold, F. H. *Nature* **2019**, *565*, 67–72.
9. Yang, Y.; Cho, I.; Qi, X.; Liu, P.; Arnold, F. H. *Nat. Chem.* **2019**, *11*, 987–993.
10. Lyons, T.; Sanford, M. *Chem. Rev.* **2010**, No. 110, 1147–1169.
11. He, J.; Wasa, M.; Chan, K. S. L.; Shao, Q.; Yu, J. Q. *Chem. Rev.* **2017**, *117*, 8754–8786.
12. Xu, Y.; Dong, G. *Chem. Sci.* **2018**, *9*, 1424–1432.
13. Sambiagio, C.; Schönbauer, D.; Blicke, R.; Dao-Huy, T.; Pototschnig, G.; Schaaf, P.; Wiesinger, T.; Zia, M. F.; Wencel-Delord, J.; Besset, T.; et al. *Chem. Soc. Rev.* **2018**, *47*, 6603–6743.
14. He, C.; Whitehurst, W. G.; Gaunt, M. J. *Chem* **2019**, *5*, 1–28.
15. Chen, G.; Gong, W.; Zhuang, Z.; Chen, Y.-Q.; Hong, X.; Yang, Y.-F.; Liu, T.; Houk, K. N.; Yu, J.-Q. *Science* **2016**, *353*, 1023–1027.
16. Wu, Q. F.; Shen, P. X.; He, J.; Wang, X. B.; Zhang, F.; Shao, Q.; Zhu, R. Y.; Mapelli, C.; Qiao, J. X.; Yu, J. Q. *Science* **2017**, *355*, 499–503.
17. Zhu, R.-Y.; Li, Z.-Q.; Park, H. S.; Senanayake, C. H.; Yu, J.-Q. *J. Am. Chem. Soc.* **2018**, *140*, 3564–3568.
18. Shao, Q.; Wu, K.; Zhuang, Z.; Qian, S.; Yu, J.-Q. *Acc. Chem. Res.* **2020**, *53*, 833–851.
19. Lawrence, J. D.; Takahashi, M.; Bae, C.; Hartwig, J. F. *J. Am. Chem. Soc.* **2004**, *126*, 15334–15335.
20. Murphy, J. M.; Lawrence, J. D.; Kawamura, K.; Incarvito, C.; Hartwig, J. F. *J. Am. Chem. Soc.* **2006**, *128*, 13684–13685.
21. Shang, R.; Ilies, L.; Matsumoto, A.; Nakamura, E. *J. Am. Chem. Soc.* **2013**, *135*, 6030–6032.
22. Aihara, Y.; Chatani, N. *J. Am. Chem. Soc.* **2014**, *136*, 898–901.

23. Li, Q.; Liskey, C. W.; Hartwig, J. F. *J. Am. Chem. Soc.* **2014**, *136*, 8755–8765.
24. Li, M.; Yang, Y.; Zhou, D.; Wan, D.; You, J. *Org. Lett.* **2015**, *17*, 2546–2549.
25. Yoshino, T.; Matsunaga, S. *Asian J. Org. Chem.* **2018**, *7*, 1193–1205.
26. Wang, H.; Park, Y.; Bai, Z.; Chang, S.; He, G.; Chen, G. *J. Am. Chem. Soc.* **2019**, *141*, 7194–7201.
27. Cope, A.; Siekman, R. *J. Am. Chem. Soc.* **1965**, *87*, 3272–3273.
28. Cope, A.; Friedrichlb, E. *J. Am. Chem. Soc.* **1968**, *90*, 909–913.
29. Constable, A. G.; McDonald, W. S.; Sawkins, L. C.; Shaw, B. L. *J. Chem. Soc., Chem. Commun.* **1978**, *23*, 1061–1062.
30. Fuchita, Y.; Hiraki, K.; Uchiyama, T. *J. Chem. Soc., Dalt. Trans.* **1983**, *5*, 897–899.
31. Dupont, J.; Consorti, C. S.; Spencer, J. *Chem. Rev.* **2005**, *105*, 2527–2571.
32. Ryabov, A. D.; Sakodinskaya, I.; Yatsimirsky, A. *J. Chem. Soc. Dalt. Trans* **1985**, No. 12, 2629–2638.
33. Davies, D. L.; Donald, S. M. A.; Macgregor, S. A. *J. Am. Chem. Soc.* **2005**, *127*, 13754–13755.
34. Lafrance, M.; Rowley, C. N.; Woo, T. K.; Fagnou, K. *J. Am. Chem. Soc.* **2006**, *128*, 8754–8756.
35. Gorelsky, S. I.; Lapointe, D.; Fagnou, K. *J. Am. Chem. Soc.* **2008**, *130*, 10848–10849.
36. Lafrance, M.; Gorelsky, S. I.; Fagnou, K. *J. Am. Chem. Soc.* **2007**, *129*, 14570–14571.
37. Ren, Z.; Mo, F.; Dong, G. *J. Am. Chem. Soc.* **2012**, *134*, 16991–16994.
38. Ren, Z.; Dong, G. *Organometallics* **2016**, *35*, 1057–1059.
39. Gulia, N.; Daugulis, O. *Angew. Chem. Int. Ed.* **2017**, *56*, 3630–3634.
40. Hogg, K. F.; Trowbridge, A.; Álvarez-Pérez, A.; Gaunt, M. J. *Chem. Sci.* **2017**, *8*, 8198–8203.
41. Chen, Y.-Q.; Wang, Z.; Wu, Y.; Wisniewski, S. R.; Qiao, J. X.; Ewing, W. R.; Eastgate, M. D.; Yu, J.-Q. *J. Am. Chem. Soc.* **2018**, *140*, 17884–17894.
42. Xia, G.; Weng, J.; Liu, L.; Verma, P.; Li, Z.; Yu, J.-Q. *Nat. Chem.* **2019**, *11*, 571–577.
43. Grennberg, H.; Gogoll, A.; Bäckvall, J. *Organometallics* **1993**, *12*, 1790–1793.
44. Plata, J. J.; García-Mota, M.; Braga, A. A. C.; Ria López, N.; Maseras, F. *J. Phys. Chem* **2009**, *113*, 11758–11762.
45. Nahra, F.; Liron, F.; Prestat, G.; Mealli, C.; Messaoudi, A.; Poli, G. *Chem. Eur. J.* **2009**, *15*, 11078–

- 11082.
46. Yamamoto, Y. *Adv. Synth. Catal.* **2010**, *352*, 478–492.
47. Sköld, C.; Kleimark, J.; Trejos, A.; Odell, L. R.; Nilsson Lill, S. O.; Norrby, P. O.; Larhed, M. *Chem. Eur. J.* **2012**, *18*, 4714–4722.
48. Campbell, A. N.; Stahl, S. S. *Acc. Chem. Res.* **2012**, *45*, 851–863.
49. Pérez-Temprano, M. H.; Racowski, J. M.; Kampf, J. W.; Sanford, M. S. *J. Am. Chem. Soc.* **2014**, *136*, 4097–4100.
50. Park, H.; Verma, P.; Hong, K.; Yu, J.-Q. *Nat. Chem.* **2018**, *10*, 755–762.
51. Samanta, R.; Antonchick, A. P. *Angew. Chem. Int. Ed.* **2011**, *50*, 5217–5220.
52. Wong, N. W. Y.; Forgione, P. *Org. Lett.* **2012**, *14*, 2738–2741.
53. Powers, D.; Ritter, T. *Acc. Chem. Res.* **2012**, *45*, 840–850.
54. He, G.; Lu, G.; Guo, Z.; Liu, P.; Chen, G. *Nat. Chem.* **2016**, *8*, 1131–1136.
55. Plata, R. E.; Hill, D. E.; Haines, B. E.; Musaev, D. G.; Chu, L.; Hickey, D. P.; Sigman, M. S.; Yu, J.-Q.; Blackmond, D. G. *J. Am. Chem. Soc.* **2017**, *139*, 9238–9245.
56. Yang, Y.-F.; Cheng, G.-J.; Liu, P.; Leow, D.; Sun, T.-Y.; Chen, P.; Zhang, X.; Yu, J.-Q.; Wu, Y.-D.; Houk, K. *N. J. Am. Chem. Soc.* **2014**, *136*, 344–355.
57. Anand, M.; Sunoj, R. B.; Schaefer, H. F. *J. Am. Chem. Soc.* **2014**, *136*, 5535–5538.
58. Feng, W.; Wang, T.; Liu, D.; Wang, X.; Dang, Y. *ACS Catal.* **2019**, *9*, 6672–6680.
59. Whitaker, D.; Burés, J.; Larrosa, I. *J. Am. Chem. Soc.* **2016**, *138*, 8384–8387.
60. Lee, S. Y.; Hartwig, J. F. *J. Am. Chem. Soc.* **2016**, *138*, 15278–15284.
61. Lotz, M. D.; Camasso, N. M.; Canty, A. J.; Sanford, M. S. *Organometallics* **2017**, *36*, 165–171.
62. Colletto, C.; Panigrahi, A.; Fernández-Casado, J.; Larrosa, I. *J. Am. Chem. Soc.* **2018**, *140*, 9638–9643.
63. Panigrahi, A.; Whitaker, D.; Vitorica-Yrezabal, I. J.; Larrosa, I. *ACS Catal.* **2020**, *10*, 2100–2107.
64. Miyaura, N.; Suzuki, A. *Chem. Rev.* **1995**, *95*, 2457–2483.
65. Pérez-Rodríguez, M.; Braga, A. A. C.; Garcia-Melchor, M.; Pérez-Temprano, M. H.; Casares, J. A.; Ujaque, G.; de Lera, A. R.; Álvarez, R.; Maseras, F.; Espinet, P. *J. Am. Chem. Soc.* **2009**, *131*, 3650–3657.

66. Desai, L.; Hull, K.; Sanford, M. S. *J. Am. Chem. Soc.* **2004**, *126*, 9542–9543.
67. Zaitsev, V. G.; Shabashov, D.; Daugulis, O. *J. Am. Chem. Soc.* **2005**, *127*, 13154–13155.
68. Kalia, J.; Raines, R. T. *Angew. Chem. Int. Ed.* **2008**, *47*, 7523–7526.
69. Neufeldt, S. R.; Sanford, M. S. *Org. Lett.* **2010**, *12*, 532–535.
70. Ano, Y.; Tobisu, M.; Chatani, N. *J. Am. Chem. Soc.* **2011**, *133*, 12984–12986.
71. Roman, D. S.; Charette, A. B. *Org. Lett.* **2013**, *15*, 4394–4397.
72. Zhang, S.; He, G.; Nack, W. A.; Zhao, Y.; Li, Q.; Chen, G. *J. Am. Chem. Soc.* **2013**, *135*, 2124–2127.
73. Wang, P. L.; Li, Y.; Wu, Y.; Li, C.; Lan, Q.; Wang, X. S. *Org. Lett.* **2015**, *17*, 3698–3701.
74. Wang, H.; Tong, H. R.; He, G.; Chen, G. *Angew. Chem. Int. Ed.* **2016**, *55*, 15387–15391.
75. Nadres, E. T.; Daugulis, O. *J. Am. Chem. Soc.* **2012**, *134*, 7–10.
76. He, G.; Zhao, Y.; Zhang, S.; Lu, C.; Chen, G. *J. Am. Chem. Soc.* **2012**, *134*, 3–6.
77. Zhang, S.; He, G.; Zhao, Y.; Wright, K.; Nack, W. A.; Chen, G. *J. Am. Chem. Soc.* **2012**, *134*, 7313–7316.
78. Zhang, L. S.; Chen, G.; Wang, X.; Guo, Q. Y.; Zhang, X. S.; Pan, F.; Chen, K.; Shi, Z. *J. Angew. Chem. Int. Ed.* **2014**, *53*, 3899–3903.
79. He, G.; Chen, G. *Angew. Chem. Int. Ed.* **2011**, *50*, 5192–5196.
80. Li, K.; Wu, Q.; Lan, J.; You, J. *Nat. Commun.* **2015**, *6*, 8404.
81. Landge, V. G.; Midya, S. P.; Rana, J.; Shinde, D. R.; Balaraman, E. *Org. Lett.* **2016**, *18*, 5252–5255.
82. Donovan, D. H. O.; De Fusco, C.; Spring, D. R. *Tetrahedron Lett.* **2016**, *57*, 2962–2964.
83. Biswas, S.; Bheemireddy, N. R.; Bal, M.; Steijvoort, B. F. Van; Maes, B. U. W. *J. Org. Chem.* **2019**, *84*, 13112–13123.
84. Rodríguez, N.; Romero-Revilla, J. A.; Fernández-Ibáñez, M. Á.; Carretero, J. C. *Chem. Sci.* **2013**, *4*, 175–179.
85. Fan, M.; Ma, D. *Angew. Chem. Int. Ed.* **2013**, *52*, 12152–12155.
86. Chan, K. S. L.; Wasa, M.; Chu, L.; Laforteza, B. N.; Miura, M.; Yu, J. Q. *Nat. Chem.* **2014**, *6*, 146–150.
87. Chan, K. S. L.; Fu, H. Y.; Yu, J. Q. *J. Am. Chem. Soc.* **2015**, *137*, 2042–2046.
88. Spangler, J. E.; Kobayashi, Y.; Verma, P.; Wang, D. H.; Yu, J. Q. *J. Am. Chem. Soc.* **2015**, *137*, 11876–

- 11879.
89. Topczewski, J. J.; Cabrera, P. J.; Saper, N. I.; Sanford, M. S. *Nature* **2016**, *531*, 220–224.
90. Cabrera, P. J.; Lee, M.; Sanford, M. S. *J. Am. Chem. Soc.* **2018**, *140*, 5599–5606.
91. Huang, Z.; Wang, C.; Dong, G. *Angew. Chem. Int. Ed.* **2016**, *55*, 5299–5303.
92. Zhang, F.-L.; Hong, K.; Li, T.-J.; Park, H.; Yu, J.-Q. *Science* **2016**, *351*, 252–256.
93. Yang, K.; Li, Q.; Liu, Y.; Li, G.; Ge, H. *J. Am. Chem. Soc.* **2016**, *138*, 12775–12778.
94. John-Campbell, S. S.; White, A. J. P.; Bull, J. A. *Chem. Sci.* **2017**, *8*, 4840–4847.
95. Hong, K.; Park, H.; Yu, J.-Q. *ACS Catal.* **2017**, *7*, 6938–6941.
96. Pan, L.; Yang, K.; Li, G.; Ge, H. *Chem. Commun.* **2018**, *54*, 2759–2762.
97. Liu, Y.; Ge, H. *Nat. Chem.* **2017**, *9*, 26–32.
98. Xu, Y.; Young, M. C.; Wang, C.; Magness, D. M.; Dong, G. *Angew. Chem. Int. Ed.* **2016**, *55*, 9084–9087.
99. John-Campbell, S. S.; Ou, A. K.; Bull, J. A. *Chem. Eur. J.* **2018**, *24*, 17838–17843.
100. Wu, Y.; Chen, Y. Q.; Liu, T.; Eastgate, M. D.; Yu, J. Q. *J. Am. Chem. Soc.* **2016**, *138*, 14554–14557.
101. Wang, P.; Farmer, M. E.; Huo, X.; Jain, P.; Shen, P.-X.; Ishoey, M.; Bradner, J. E.; Wisniewski, S. R.; Eastgate, M. D.; Yu, J.-Q. *J. Am. Chem. Soc.* **2016**, *138*, 9269–9276.
102. Wang, P.; Verma, P.; Xia, G.; Shi, J.; Qiao, J. X.; Tao, S.; Peter, T. W. C.; Poss, M. A.; Farmer, M. E.; Yeung, K.-S.; et al. *Nature* **2017**, *551*, 489–493.
103. Chen, Y.-Q.; Wu, Y.; Wang, Z.; Qiao, J. X.; Yu, J.-Q. *ACS Catal.* **2020**, *10*, 5657–5662.
104. Chen, Y.-Q.; Singh, S.; Wu, Y.; Wang, Z.; Hao, W.; Verma, P.; Qiao, J. X.; Sunoj, R. B.; Yu, J.-Q. *J. Am. Chem. Soc.* **2020**, No. 142, 9966.
105. Su, B.; Bunescu, A.; Qiu, Y.; Zuend, S. J.; Ernst, M.; Hartwig, J. F. *J. Am. Chem. Soc.* **2020**, *142*, 7912–7919.
106. Kapoor, M.; Liu, D.; Young, M. C. *J. Am. Chem. Soc.* **2018**, *140*, 6818–6822.
107. Fuchita, Y.; Hiraki, K.; Matsumoto, Y. *J. Organomet. Chem.* **1985**, *280*, C51–C53.
108. Schultz, M. J.; Adler, R. S.; Zierkiewicz, W.; Privalov, T.; Sigman, M. S. *J. Am. Chem. Soc.* **2005**, *127*, 8499–8507.

109. Chen, K.; Wang, D.; Li, Z.-W.; Liu, Z.; Pan, F.; Zhang, Y.-F.; Shi, Z.-J. *Org. Chem. Front.* **2017**, *4*, 2097–2101.
110. Pramanick, P. K.; Zhou, Z.; Hou, Z.-L.; Yao, B. *J. Org. Chem.* **2019**, *84*, 5684–5694.
111. Yuan, F.; Hou, Z.-L.; Pramanick, P. K.; Yao, B. *Org. Lett.* **2019**, *21*, 9381–9385.
112. Lin, H.; Pan, X.; Barsamian, A. L.; Kamenecka, T. M.; Bannister, T. D. *ACS Catal.* **2019**, *9*, 4887–4891.
113. Zhuang, Z.; Yu, J.-Q. *J. Am. Chem. Soc.* **2020**, No. 142, 12015–12019.
114. McNally, A.; Haffemayer, B.; Collins, B. S. L.; Gaunt, M. J. *Nature* **2014**, *510*, 129–133.
115. Buettner, C. S.; Willcox, D.; Chappell, B. G. N.; Gaunt, M. J. *Chem. Sci.* **2019**, *10*, 83–89.
116. Smalley, A. P.; Gaunt, M. J. *J. Am. Chem. Soc.* **2015**, *137*, 10632–10641.
117. Nappi, M.; He, C.; Whitehurst, W. G.; Chappell, B. G. N.; Gaunt, M. J. *Angew. Chem. Int. Ed.* **2018**, *57*, 3178–3182.
118. Smalley, A. P.; Cuthbertson, J. D.; Gaunt, M. J. *J. Am. Chem. Soc.* **2017**, *139*, 1412–1415.
119. He, C.; Gaunt, M. J. *Angew. Chem. Int. Ed.* **2015**, *54*, 15840–15844.
120. He, C.; Gaunt, M. J. *Chem. Sci.* **2017**, *8*, 3586–3592.
121. Calleja, J.; Pla, D.; Gorman, T. W.; Domingo, V.; Haffemayer, B.; Gaunt, M. J. *Nat. Chem.* **2015**, *7*, 1009–1016.
122. Ho, D. K. H.; Calleja, J.; Gaunt, M. J. *Synlett* **2019**, *30*, 454–458.
123. Willcox, D.; Chappell, B. G. N.; Hogg, K. F.; Calleja, J.; Smalley, A. P.; Gaunt, M. J. *Science* **2016**, *354*, 851–857.
124. Stromnova, T. A.; Vargaftik, M. N.; Moiseev, I. I. *J. Organomet. Chem.* **1983**, *252*, 113–120.
125. Cabrera-Pardo, J. R.; Trowbridge, A.; Nappi, M.; Ozaki, K.; Gaunt, M. J. *Angew. Chem. Int. Ed.* **2017**, *56*, 11958–11962.
126. Png, Z. M.; Cabrera-Pardo, J. R.; Peiró Cadahía, J.; Gaunt, M. J. *Chem. Sci.* **2018**, *9*, 7628–7633.
127. Whitehurst, W. G.; Blackwell, J. H.; Hermann, G. N.; Gaunt, M. J. *Angew. Chem. Int. Ed.* **2019**, *58*, 9054–9059.
128. Heck, R. F.; Nolley, J. P. J. *J. Org. Chem.* **1972**, *37*, 2320–2322.
129. Yap, J. S. L.; Ding, Y.; Yang, X. Y.; Wong, J.; Li, Y.; Pullarkat, S. A.; Leung, P. H. *Eur. J. Inorg. Chem.* **2014**,

- 2014, 5046–5052.
130. Liu, Y.; Yao, B.; Deng, C.-L.; Tang, R.-Y.; Zhang, X.-G.; Li, J.-H. *Org. Lett.* **2011**, *13*, 2184–2187.
131. Li, S.; Wu, J. *Org. Lett.* **2011**, *13*, 712–715.
132. Fang, T.; Gao, X.-H.; Tang, R.-Y.; Zhang, X.-G.; Deng, C.-L. *Chem. Commun.* **2014**, *50*, 14775–14777.
133. Cai, G.; Fu, Y.; Li, Y.; Wan, X.; Shi, Z. *J. Am. Chem. Soc.* **2007**, *129*, 7666–7673.
134. Lei, A.; Liu, W.; Liu, C.; Chen, M.; Shi, Z.-J. *Dalt. Trans.* **2010**, *39*, 10442–10446.
135. Feng, R.; Yao, J.; Liang, Z.; Liu, Z.; Zhang, Y. *J. Org. Chem.* **2013**, *78*, 3688–3696.
136. Zhang, J. C.; Shi, J. L.; Wang, B. Q.; Hu, P.; Zhao, K. Q.; Shi, Z. *J. Chem. Asian J.* **2015**, *10*, 840–843.
137. Tan, P. W.; Haughey, M.; Dixon, D. J. *Chem. Commun.* **2015**, *51*, 4406–4409.
138. Dong, Z.; Wang, J.; Dong, G. *J. Am. Chem. Soc.* **2015**, *137*, 5887–5890.
139. Wasa, M.; Chan, K. S. L.; Zhang, X.-G.; He, J.; Miura, M.; Yu, J.-Q. *J. Am. Chem. Soc.* **2012**, *134*, 18570–18572.
140. Xiao, K.; Lin, D. W.; Miura, M.; Zhu, R.; Gong, W.; Wasa, M.; Yu, J. Q. *J. Am. Chem. Soc.* **2014**, *136*, 8138–8142.
141. Shen, P.-X.; Hu, L.; Shao, Q.; Hong, K.; Yu, J.-Q. *J. Am. Chem. Soc.* **2018**, *140*, 6545–6549.
142. Zhuang, Z.; Yu, C.; Chen, G.; Wu, Q.; Hsiao, Y.; Joe, C. L.; Qiao, J. X.; Poss, M. A.; Yu, J.-Q. *J. Am. Chem. Soc.* **2018**, *140*, 10363–10367.
143. Shao, Q.; Wu, K.; Zhuang, Z.; Qian, S.; Yu, J.-Q. *Acc. Chem. Res.* **2020**, *53*, 833–851.
144. Sokolov, V. I.; Troitskaya, L. L. *Chimia* **1978**, *32*, 122–123.
145. Sokolov, V. I.; Troitskaya, L. L.; Reutov, O. A. *J. Organomet. Chem.* **1979**, *182*, 537–546.
146. Gaunt, J. C.; Shaw, B. L. *J. Organomet. Chem.* **1975**, *102*, 511–516.
147. Shi, B. F.; Maugel, N.; Zhang, Y. H.; Yu, J. Q. *Angew. Chem. Int. Ed.* **2008**, *47*, 4882–4886.
148. Shi, B.-F.; Zhang, Y.-H.; Lam, J. K.; Wang, D.-H.; Yu, J.-Q. *J. Am. Chem. Soc.* **2010**, *132*, 460–461.
149. Cheng, X.-F.; Li, Y.; Su, Y.-M.; Yin, F.; Wang, J.-Y.; Sheng, J.; Vora, H. U.; Wang, X.-S.; Yu, J.-Q. *J. Am. Chem. Soc.* **2013**, *135*, 1236–1239.
150. Laforteza, B. N.; Chan, K. S. L.; Yu, J.-Q. *Angew. Chem. Int. Ed.* **2015**, *54*, 11143–11146.

151. Chu, L.; Wang, X.-C.; Moore, C. E.; Rheingold, A. L.; Yu, J.-Q. *J. Am. Chem. Soc.* **2013**, *135*, 16344–16347.
152. Chu, L.; Xiao, K.-J.; Yu, J.-Q. *Science* **2014**, *346*, 451–455.
153. Xiao, K.-J.; Chu, L.; Chen, G.; Yu, J.-Q. *J. Am. Chem. Soc.* **2016**, *138*, 7796–7800.
154. Musaev, D. G.; Kaledin, A.; Shi, B.; Yu, J. Q. *J. Am. Chem. Soc.* **2012**, *134*, 1690–1698.
155. Haines, B. E.; Musaev, D. G. *ACS Catal.* **2015**, *5*, 830–840.
156. Günay, M. E.; Richards, C. J. *Organometallics* **2009**, *28*, 5833–5836.
157. Cheng, G. J.; Yang, Y. F.; Liu, P.; Chen, P.; Sun, T. Y.; Li, G.; Zhang, X.; Houk, K. N.; Yu, J. Q.; Wu, Y. D. *J. Am. Chem. Soc.* **2014**, *136*, 894–897.
158. Musaev, D. G.; Figg, T. M.; Kaledin, A. L. *Chem. Soc. Rev.* **2014**, *43*, 5009–5031.
159. Gair, J. J.; Haines, B. E.; Filatov, A. S.; Musaev, D. G.; Lewis, J. C. *Chem. Sci.* **2017**, *8*, 5746–5756.
160. Shao, Q.; Wu, Q. F.; He, J.; Yu, J.-Q. *J. Am. Chem. Soc.* **2018**, *140*, 5322–5325.
161. Asensio, G.; González-Núñez, M. E.; Bernardini, C. B.; Mello, R.; Adam, W. *J. Am. Chem. Soc.* **1993**, *115*, 7250–7253.
162. Lee, M.; Sanford, M. S. *J. Am. Chem. Soc.* **2015**, *137*, 12796–12799.
163. Howell, J. M.; Feng, K.; Clark, J. R.; Trzepakowski, L. J.; White, M. C. *J. Am. Chem. Soc.* **2015**, *137*, 14590–14593.
164. Schultz, D. M.; Lévesque, F.; DiRocco, D. A.; Reibarkh, M.; Ji, Y.; Joyce, L. A.; Dropinski, J. F.; Sheng, H.; Sherry, B. D.; Davies, I. W. *Angew. Chem. Int. Ed.* **2017**, *56*, 15274–15278.
165. Mack, J. B. C.; Gipson, J. D.; Du Bois, J.; Sigman, M. S. *J. Am. Chem. Soc.* **2017**, *139*, 9503–9506.
166. Lee, M.; Sanford, M. S. *Org. Lett.* **2017**, *19*, 572–575.
167. Bertrand, S.; Hoffmann, N.; Pete, J. *Eur. J. Org. Chem.* **2000**, *1*, 2227–2238.
168. Pan, Y.; Wang, S.; Kee, C. W.; Dubuisson, E.; Yang, Y.; Loh, K. P.; Tan, C. H. *Green Chem.* **2011**, *13*, 3341–3344.
169. McNally, A.; Prier, C. K.; MacMillan, D. W. C. *Science* **2011**, *334*, 1114–1117.
170. Miyake, Y.; Nakajima, K.; Nishibayashi, Y. *J. Am. Chem. Soc.* **2012**, *134*, 3338–3341.
171. Singh, A.; Arora, A.; Weaver, J. D. *Org. Lett.* **2013**, *15*, 5390–5393.

172. Xie, J.; Shi, S.; Zhang, T.; Mehrkens, N.; Rudolph, M.; Hashmi, A. S. K. *Angew. Chem. Int. Ed.* **2015**, *54*, 6046–6050.
173. Beatty, J. W.; Stephenson, C. R. J. *Acc. Chem. Res.* **2015**, *48*, 1474–1484.
174. Thullen, S. M.; Rovis, T. *J. Am. Chem. Soc.* **2017**, *139*, 15504–15508.
175. Yilmaz, O.; Oderinde, M. S.; Emmert, M. H. *J. Org. Chem.* **2018**, *83*, 11089–11100.
176. Aycock, R. A.; Pratt, C. J.; Jui, N. T. *ACS Catal.* **2018**, *8*, 9115–9119.
177. Zhuang, Z.; Yu, C.; Chen, G.; Wu, Q.; Hsiao, Y.; Joe, C. L.; Qiao, J. X.; Poss, M. A.; Yu, J.-Q. *J. Am. Chem. Soc.* **2018**, *140*, 10363–10367.
178. Zhuang, Z.; Yu, J.-Q. *Nature* **2020**, *577*, 656–659.
179. Park, H.; Chekshin, N.; Shen, P.; Yu, J.-Q. *ACS Catal.* **2018**, *8*, 9292–9297.
180. Park, H.; Li, Y.; Yu, J.-Q. *Angew. Chem. Int. Ed.* **2019**, *58*, 11424–11428.
181. Vitaku, E.; Smith, D. T.; Njardarson, J. T. *J. Med. Chem.* **2014**, *57*, 10257–10274.
182. Takahashi, O.; Kohno, Y.; Nishio, M. *Chem. Rev.* **2010**, No. 110, 6049–6076.
183. Kittakoop, P.; Mahidol, C.; Ruchirawat, S. *Curr. Top. Med. Chem.* **2014**, *14*, 239–252.
184. Roughley, S. D.; Jordan, A. M. *J. Med. Chem.* **2011**, *54*, 3451–3479.
185. Mcgrath, N. A.; Brichacek, M.; Njardarson, J. T. *J. Chem. Educ.* **2010**, *87*, 1348–1349.
186. Rodrigalvarez, J. **2017**, (Master's thesis), University of Cambridge, UK.
187. Carrow, B. P.; Hartwig, J. F. *J. Am. Chem. Soc.* **2011**, *133*, 2116–2119.
188. Lennox, A. J. J.; Lloyd-Jones, G. C. *Angew. Chem. Int. Ed.* **2013**, *52*, 7362–7370.
189. Thomas, A. A.; Denmark, S. E. *Science* **2016**, *352*, 329–332.
190. Carole, W. A.; Colacot, T. J. *Chem. Eur. J.* **2016**, *22*, 7686–7695.
191. Li, W.; Ivanov, S.; Shanaiah, N.; Karim, A. M. *Organometallics* **2019**, *38*, 451–460.
192. Astruc, D. *Inorg. Chem.* **2007**, *46*, 1884–1894.
193. Zawartka, W.; Gniewek, A.; Trzeciak, A. M.; Ziólkowski, J. J.; Pernak, J. *J. Mol. Catal. A Chem.* **2009**, *304*, 8–15.
194. Albéniz, A. C.; Espinet, P.; Martín-Ruiz, B. *Chem. Eur. J.* **2001**, *7*, 2481–2489.

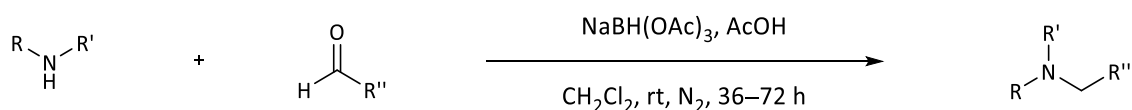
195. Chu, J.; Chen, C.; Wu, M. *Organometallics* **2008**, *27*, 5173–5176.
196. Hull, K. L.; Sanford, M. S. *J. Am. Chem. Soc.* **2009**, *131*, 9651–9653.
197. Chu, J.-H.; Tsai, S.; Wu, M.-J. *Synthesis* **2009**, *22*, 3757–3764.
198. Wang, D.-H.; Engle, K. M.; Shi, B.-F.; Yu, J. Q. *Science* **2010**, *327*, 315–320.
199. Salazar, C. A.; Flesch, K. N.; Haines, B. E.; Zhou, P. S.; Musaev, D. G.; Stahl, S. S. *Science* **2020**, *370*, 1454–1460.
200. Hu, J.; Wang, J.; Nguyen, T. H.; Zheng, N. *Beilstein J. Org. Chem.* **2013**, *9*, 1977–2001.
201. Tomberg, A.; Muratore, M. É.; Johansson, M. J.; Terstiege, I.; Sköld, C.; Noorby, P.-O. *iScience* **2019**, *20*, 373–391.
202. Rodrigalvarez, J.; Nappi, M.; Azuma, H.; Flodén, N. J.; Burns, M. E.; Gaunt, M. J. *Nat. Chem.* **2020**, *12*, 76–81.
203. Simmons, E. M.; Hartwig, J. F. *Angew. Chem. Int. Ed.* **2012**, *51*, 3066–3072.
204. Bruns, D. L.; Musaev, D. G.; Stahl, S. S. *J. Am. Chem. Soc.* **2020**, *142*, 19678–19688.
205. Frisch, M. J.; Trucks, G. W.; Schlegel, H. B.; Scuseria, G. E.; Robb, M. A.; Cheeseman, J. R.; Scalmani, G.; Barone, V.; Petersson, G. A.; Nakatsuji, H.; et al. *Gaussian 16 Revis. A.03* Wallingford CT, 2016.
206. Haines, B. E.; Yu, J. Q.; Musaev, D. G. *ACS Catal.* **2017**, *7*, 4344–4354.
207. Grimme, S.; Antony, J.; Ehrlich, S.; Krieg, H. *J. Chem. Phys.* **2010**, *132*, 154104.
208. Grimme, S.; Ehrlich, S.; Goerigk, L. *J. Comput. Chem.* **2011**, *32*, 1456–1465.
209. Hratchian, H. P.; Schlegel, H. B. *J. Chem. Theory Comput.* **2005**, *1*, 61–69.
210. Armstrong, A.; Boto, R. A.; Dingwall, P.; Contreras-garc, J.; Harvey, M. J.; Mason, N. J.; Rzepa, H. S. *Chem. Sci.* **2014**, *5*, 2057–2071.
211. Murahashi, S. I.; Yano, T. *J. Chem. Soc., Chem. Commun.* **1979**, No. 6, 270–271.
212. Nielsen, R. J.; Goddard III, W. A. *J. Am. Chem. Soc.* **2006**, *128*, 9651–9660.
213. Xiao, K.; Lin, D. W.; Miura, M.; Zhu, R.; Gong, W.; Wasa, M.; Yu, J. *J. Am. Chem. Soc.* **2014**, *136*, 8138–8142.
214. Hu, L.; Shen, P.-X.; Shao, Q.; Hong, K.; Qiao, J. X.; Yu, J.-Q. *Angew. Chem. Int. Ed.* **2019**, *58*, 2134–2138.
215. Saget, T.; Cramer, N. *Angew. Chem. Int. Ed.* **2012**, *51*, 12842–12845.

216. Pedroni, J.; Saget, T.; Donets, P. A.; Cramer, N. *Chem. Sci.* **2015**, *6*, 5164–5171.
217. Pedroni, J.; Cramer, N. *Angew. Chem. Int. Ed.* **2015**, *54*, 11826–11829.
218. Mayer, C.; Ladd, C. L.; Charette, A. B. *Org. Lett.* **2019**, *21*, 2639–2644.
219. Wasa, M.; Engle, K. M.; Lin, D. W.; Yoo, E. J.; Yu, J.-Q. *J. Am. Chem. Soc.* **2011**, *133*, 19598–19601.
220. Wu, Q.-F.; Wang, X.-B.; Shen, P.-X.; Yu, J.-Q. *ACS Catal.* **2018**, *8*, 2577–2581.
221. Jerhaoui, S.; Djukic, J.-P.; Wencel-Delord, J.; Colobert, F. *ACS Catal.* **2019**, *9*, 2532–2542.
222. Xiao, L.-J.; Hong, K.; Luo, F.; Hu, L.; Ewing, W. R.; Yeung, K.-S.; Yu, J.-Q. *Angew. Chem. Int. Ed.* **2020**, *59*, 2–9.
223. Shi, Y.; Gao, Q.; Xu, S. *J. Am. Chem. Soc.* **2019**, *141*, 10599–10604.
224. Lacour, J.; Vial, L.; Herse, C. *Org. Lett.* **2002**, *4*, 1351–1354.
225. Rousseaux, S.; Liégault, B.; Fagnou, K. *Chem. Sci.* **2012**, *3*, 244–248.
226. Ren, Z.; Mo, F.; Dong, G. *J. Am. Chem. Soc.* **2012**, *134*, 16991–16994.
227. Saget, T.; Perez, D.; Cramer, N. *Org. Lett.* **2013**, *15*, 1354–1357.
228. Ladd, C. L.; Roman, D. S.; Charette, A. B. *Org. Lett.* **2013**, *15*, 1350–1353.
229. Hoshiya, N.; Kobayashi, T.; Arisawa, M.; Shuto, S. *Org. Lett.* **2013**, *15*, 6202–6205.
230. Tsukano, C.; Okuno, M.; Takemoto, Y. *Chem. Lett.* **2013**, *42*, 753–755.
231. Parella, R.; Babu, S. A. *Synlett* **2014**, *25*, 1395–1402.
232. Hoshiya, N.; Takenaka, K.; Shuto, S.; Uenishi, J. *Org. Lett.* **2016**, *18*, 48–51.
233. He, J.; Shao, Q.; Wu, Q.; Yu, J. Q. *J. Am. Chem. Soc.* **2017**, *139*, 3344–3347.

Appendix

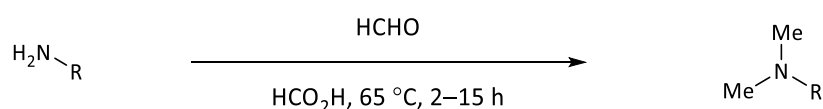
Appendix I – Synthesis and characterisation of starting materials

General procedure D: Reductive amination



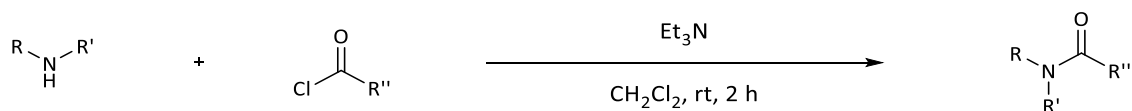
To a solution of amine (1 equiv) in DCM [0.2 – 0.4 M] at 0 °C under N₂, was added the desired aldehyde (1 – 2 equiv) and AcOH (1 equiv). NaBH(OAc)₃ (1.2 – 2 equiv) was added portionwise over 15 min while stirring. The resultant mixture was purged briefly with N₂, warmed to rt and stirred for 36–72 h. The reaction was quenched with aq NaOH (2.5 M) and the solution was left stirring until no further effervescence was observed. The phases were separated and the aqueous layer was extracted twice with DCM. The combined organic layers were dried over MgSO₄, filtered and concentrated *in vacuo*. The crude product was purified by distillation or column chromatography.

General procedure E: Eschweiler-Clarke methylation

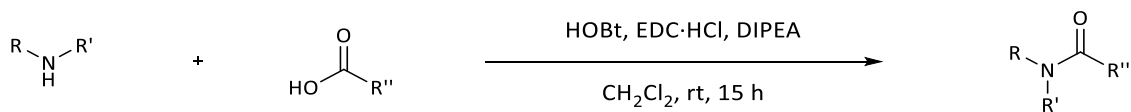


To a solution of formaldehyde (37% in H₂O, 6 equiv) and amine (1 equiv), formic acid was added dropwise while stirring to reach a 1 M solution. The flask was fitted with a condenser and the reaction mixture was heated to 65 °C for 2–15 h. After cooling to 0 °C, the reaction mixture was basified with aq NaOH (2.5 M). The resultant tertiary amine was separated from the aqueous layer as a supernatant, dried over MgSO₄ and filtered. The crude product was purified by distillation or column chromatography.

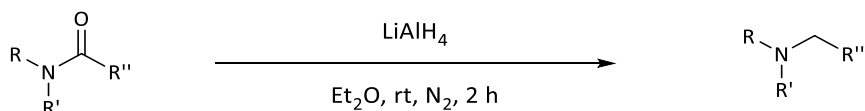
General procedure F: Amine acylation



To a solution of amine (1 equiv), Et₃N (1.2 equiv) in DCM [0.5 M] at 0 °C, was added the desired acyl chloride (1.2 equiv). The resultant mixture was warmed to rt and stirred for 2 h. The reaction was quenched with aq NH₄Cl (sat). The organic layer was washed twice with aq HCl (0.5 M), twice with aq NaOH (0.5 M), dried over MgSO₄, filtered and concentrated *in vacuo*. The crude product was typically used without further purification.

General procedure G: Amide coupling

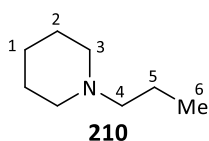
To a solution of amine (1 – 1.2 equiv), carboxylic acid (1 – 1.2 equiv) and DIPEA (1.5 equiv) in DCM [0.3 – 0.5 M] was added HOBT·hydrate (1.5 equiv) and EDC·HCl (1.2 equiv). The resultant mixture was warmed to rt and stirred for 15 h. The reaction was quenched with aq NaOH (2.5 M) and the resultant layers were separated. The organic layer was washed once with aq NaOH (0.5 M), twice with aq HCl (0.5 M), dried over MgSO₄, filtered and concentrated *in vacuo*. The crude product was typically used without further purification.

General procedure H: Amide reduction

To a solution of LiAlH₄ (2 equiv) in Et₂O [1 M] under N₂ at 0 °C, was added dropwise the desired amide (1 equiv) in Et₂O [1 M]. The resultant mixture was warmed to rt and stirred for 2 h. After this time, the reaction was cooled to 0 °C and further Et₂O was added. The reaction was quenched with a dropwise addition of H₂O (2 equiv), NaOH (10%) (2 equiv), and H₂O (6 equiv). The resultant solution was dried over MgSO₄, filtered and concentrated *in vacuo*. The crude product was purified by distillation or column chromatography.

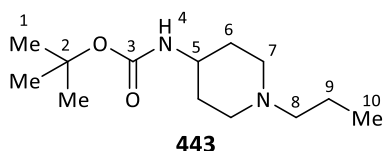
General procedure I: Amine alkylation

To a solution of amine (1 – 2.5 equiv) and K₂CO₃ (1.5 equiv) or DIPEA (1.5 equiv) in MeCN [0.5 M] was added the desired alkyl bromide (1.0 – 1.5 equiv). The resultant mixture was heated to reflux for 15 h. After this time, volatiles were evaporated *in vacuo*. DCM was added to the reaction crude and the organic layer was washed twice with aq NaOH (2.5 M), dried over MgSO₄, filtered and concentrated *in vacuo*. The crude product was typically purified by column chromatography.

1-Propylpiperidine

General procedure D was applied to piperidine (9.90 mL, 100 mmol) with propionaldehyde (18.1 mL, 250 mmol), AcOH (5.70 mL, 100 mmol) and NaBH(OAc)₃ (25.4 g, 120 mmol) in DCM (200 mL) to provide by distillation at 90 °C under 100 mbar the title compound as a colourless oil (9.38 g, 73.7 mmol, 74% yield).

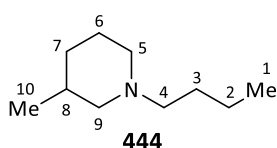
IR ν_{\max} /cm⁻¹ (thin film) 2927, 2765, 1443, 1376, 1302, 1158, 1133, 1098; **¹H NMR** (400 MHz, CDCl₃) δ (ppm) 2.38 (br s, 4H, H₃), 2.29 – 2.22 (m, 2H, H₄), 1.60 (dt, J = 11.2, 5.7 Hz, 4H, H₂), 1.52 (m, 2H, H₅), 1.45 (m, 2H, H₁), 0.90 (t, J = 7.4 Hz, 3H, H₆); **¹³C NMR** (101 MHz, CDCl₃) δ (ppm) 61.7 (C₄), 54.7 (C₃), 26.0 (C₂), 24.5 (C₁), 20.1 (C₅), 12.1 (C₆); **HMRS-ESI** (m/z): found [M+H]⁺ 128.1437, C₈H₁₈N requires 128.1439.

tert-Butyl (1-propylpiperidin-4-yl)carbamate

General procedure D was applied to *tert*-butyl piperidin-4-ylcarbamate (10.0 g, 50.0 mmol) with propionaldehyde (7.30 mL, 100 mmol), AcOH (2.90 mL, 50.0 mmol) and NaBH(OAc)₃ (12.7 g, 60.0 mmol) in DCM (150 mL) to

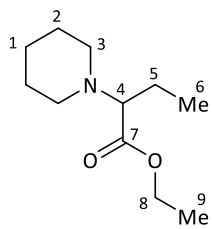
provide by column chromatography (DCM to EtOAc) the title compound as a colourless oil (10.2 g, 42.1 mmol, 84% yield).

IR ν_{\max} /cm⁻¹ (thin film) 3361, 2973, 2938, 2768, 1680, 1307, 1236, 1161, 1052, 863; **¹H NMR** (400 MHz, CDCl₃) δ (ppm) 4.43 (br s, 1H, H₄), 3.47 (br s, 1H, H₅), 2.91 – 2.78 (m, 2H, H_{7a}), 2.32 – 2.19 (m, 2H, H₈), 2.05 (app t, J = 11.5 Hz, 2H, H_{7b}), 2.00 – 1.90 (m, 2H, H_{6a}), 1.56 – 1.30 (m, 4H, H_{6b,9}), 1.47 (s, 9H, H₁), 0.91 (t, J = 7.4 Hz, 3H, H₁₀); **¹³C NMR** (101 MHz, CDCl₃) δ (ppm) 155.2 (C₃), 79.1 (C₂), 60.7 (C₈), 52.4 (C₇), 47.9 (C₅), 32.7 (C₆), 28.4 (C₁), 20.3 (C₉), 12.0 (C₁₀); **HMRS-ESI** (m/z): found [M+H]⁺ 243.2070, C₁₃H₂₇N₂O₂ requires 243.2067.

1-Butyl-3-methylpiperidine

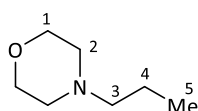
General procedure D was applied to 3-methylpiperidine (11.7 mL, 100 mmol) with butyraldehyde (13.5 mL, 150 mmol), AcOH (5.70 mL, 100 mmol) and NaBH(OAc)₃ (31.8 g, 150 mmol) in DCM (200 mL) to provide by distillation at 100 °C under 30 mbar the title compound as a colourless oil (10.7 g, 69.0 mmol, 69% yield).

IR ν_{\max} /cm⁻¹ (thin film) 2952, 2928, 2871, 2759, 1457, 1375, 1136; **¹H NMR** (400 MHz, CDCl₃) δ (ppm) 2.86 (app br t, J = 14.2 Hz, 2H, H_{5a,9a}), 2.35 – 2.21 (m, 2H, H₄), 1.79 (td, J = 11.3, 3.2 Hz, 1H, H_{5b}), 1.75 – 1.55 (m, 4H, H_{6,7a,8}), 1.54 – 1.45 (m, 3H, H_{3,9b}), 1.32 (app hex, J = 7.3 Hz, 2H, H₂), 0.93 (t, J = 7.3 Hz, 3H, H₁), 0.90 – 0.80 (m, 4H, H_{7b,10}); **¹³C NMR** (101 MHz, CDCl₃) δ (ppm) 62.3 (C₉), 59.2 (C₄), 54.2 (C₅), 33.2 (C₇), 31.2 (C₈), 29.2 (C₃), 25.7 (C₆), 21.0 (C₂), 19.9 (C₁₀), 14.1 (C₁); **HMRS-ESI** (m/z): found [M+H]⁺ 156.1748, C₁₀H₂₂N requires 156.1747.

Ethyl 2-(piperidin-1-yl)butanoate**445**

General procedure I was applied to piperidine (4.90 mL, 50.0 mmol), with ethyl 2-bromobutyrate (7.40 mL, 50.0 mmol), and K_2CO_3 (10.4 g, 75.0 mmol) in MeCN (100 mL) to provide by distillation at 120 °C under 15 mbar the title compound as a pale yellow oil (6.20 g, 31.0 mmol, 62% yield).

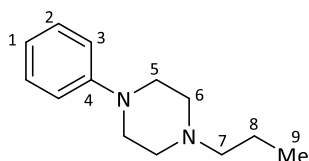
IR ν_{max}/cm^{-1} (thin film) 2968, 2854, 1728, 1443, 1376, 1222, 1176, 1132, 1026, 860; **1H NMR** (400 MHz, $CDCl_3$) δ (ppm) 4.18 (q, $J = 7.1$ Hz, 2H, H_8), 3.03 (dd, $J = 8.8, 6.1$ Hz, 1H, H_4), 2.58 (ddd, $J = 10.8, 7.0, 3.6$ Hz, 2H, H_{3a}), 2.50 (ddd, $J = 10.8, 7.0, 3.6$ Hz, 2H, H_{3b}), 1.84 – 1.61 (m, 2H, H_5), 1.61 – 1.48 (m, 4H, H_2), 1.47 – 1.39 (m, 2H, H_1), 1.29 (t, $J = 7.1$ Hz, 3H, H_9), 0.91 (t, $J = 7.4$ Hz, 3H, H_6); **^{13}C NMR** (100 MHz, $CDCl_3$) δ (ppm) 172.5 (C_7), 70.1 (C_4), 59.8 (C_8), 50.8 (C_3), 26.5 (C_2), 24.7 (C_1), 22.8 (C_5), 14.5 (C_9), 10.8 (C_6); **HMRS-ESI** (m/z): found $[M+H]^+$ 200.1643, $C_{11}H_{22}NO_2$ requires 200.1645.

4-Propylmorpholine**446**

General procedure F was applied to morpholine (4.40 mL, 50.0 mmol) and propionyl chloride (1.75 mL, 20.0 mmol) in CH_2Cl_2 (60.0 mL) without triethylamine addition. The resultant crude amide was used without further purification in General procedure H with

$LiAlH_4$ (1.62 g, 42.0 mmol) in Et_2O (60.0 mL). Purification by distillation at 85 °C under 100 mbar provided the title compound as a colourless oil (1.98 g, 15.3 mmol, 76% yield).

IR ν_{max}/cm^{-1} (thin film) 2960, 2808, 1457, 1278, 1116, 1071, 861; **1H NMR** (400 MHz, $CDCl_3$) δ (ppm) 3.82 – 3.67 (m, 4H, H_1), 2.45 (br s, 4H, H_2), 2.36 – 2.26 (m, 2H, H_3), 1.52 (app hex, $J = 7.4$ Hz, 2H, H_4), 0.92 (t, $J = 7.4$ Hz, 3H, H_5); **^{13}C NMR** (101 MHz, $CDCl_3$) δ (ppm) 67.0 (C_1), 61.1 (C_3), 53.8 (C_2), 19.7 (C_4), 11.9 (C_5); **HMRS-ESI** (m/z): found $[M+H]^+$ 130.1223, $C_7H_{16}NO$ requires 130.1226.

1-Phenyl-4-propylpiperazine**447**

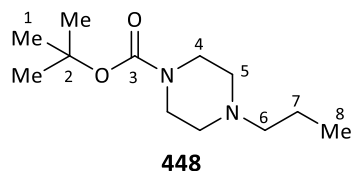
General procedure F was applied to 1-phenylpiperazine (2.30 mL, 15.0 mmol) with Et_3N (2.50 mL, 18.0 mmol) and propionyl chloride (1.60 mL, 18.0 mmol) in DCM (45.0 mL). The resultant crude amide was used without further purification.

General procedure H was applied to the crude amide (3.27 g, 15.0 mmol) and $LiAlH_4$ (1.14 g, 30.0 mmol) in Et_2O (20.0 mL) to provide without further purification the title compound as a colourless oil (2.93 g, 14.3 mmol, 95% yield).

IR ν_{max}/cm^{-1} (thin film) 2959, 2816, 1600, 1501, 1229, 1154, 754, 689; **1H NMR** (400 MHz, $CDCl_3$) δ (ppm) 7.29 (m, 2H, H_2), 6.96 (d, $J = 8.2$ Hz, 2H, H_3), 6.88 (t, $J = 7.3$ Hz, 1H, H_1), 3.30 – 3.18 (m, 4H, H_5), 2.68 – 2.58 (m, 4H, H_6), 2.42 – 2.33 (m, 2H, H_7), 1.58 (app hex, $J = 7.5$ Hz, 2H, H_8), 0.96 (t, $J = 7.5$ Hz, 3H, H_9); **^{13}C NMR** (101 MHz,

CDCl_3) δ (ppm) 151.4 (C_4), 129.1 (C_2), 119.6 (C_1), 116.0 (C_3), 60.8 (C_7), 53.3 (C_6), 49.2 (C_5), 20.1 (C_8), 12.0 (C_9);
HMRS-ESI (m/z): found $[\text{M}+\text{H}]^+$ 205.1698, $\text{C}_{13}\text{H}_{21}\text{N}_2$ requires 205.1699.

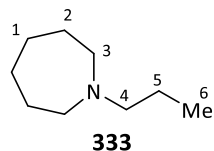
tert-Butyl 4-propylpiperazine-1-carboxylate



Boc_2O (1.70 g, 7.80 mmol) in DCM (10.0 mL) was added dropwise to a solution of 1-propylpiperazine (1.00 g, 7.80 mmol) and Et_3N (1.30 mL, 9.40 mmol) in DCM (10.0 mL) at 0 °C. The resultant mixture was warmed to rt and stirred for 15 h. The reaction was quenched with aq NaOH (2.5 M, 50 mL) and the layers separated. The aqueous layer was extracted with DCM (2 x 25 mL). The combined organic layers were dried over MgSO_4 , filtered and concentrated *in vacuo*. Purification by column chromatography (DCM to EtOAc) provided the title compound as a colourless oil (1.04 g, 4.55 mmol, 58% yield).

IR $\nu_{\text{max}}/\text{cm}^{-1}$ (thin film) 2967, 2810, 1694, 1418, 1241, 1166, 1133, 1003, 866, 770; **$^1\text{H NMR}$** (400 MHz, CDCl_3) δ (ppm) 3.55 – 3.38 (m, 4H, H_4), 2.46 – 2.34 (m, 4H, H_5), 2.34 – 2.26 (m, 2H, H_6), 1.53 (app hex, $J = 7.4$ Hz, 2H, H_7), 1.48 (s, 9H, H_1), 0.92 (t, $J = 7.4$ Hz, 3H, H_8); **$^{13}\text{C NMR}$** (101 MHz, CDCl_3) δ (ppm) 154.7 (C_3), 79.5 (C_2), 60.7 (C_6), 53.0 (C_5), 44.0 (br s, C_{4a}), 43.2 (br s, C_{4b}), 28.4 (C_1), 19.9 (C_7), 11.9 (C_8); **HMRS-ESI** (m/z): found $[\text{M}+\text{H}]^+$ 229.1912, $\text{C}_{12}\text{H}_{25}\text{N}_2\text{O}_2$ requires 229.1911.

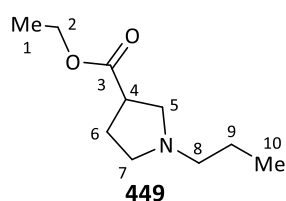
1-Propylazepane



General procedure D was applied to azepane (11.3 mL, 100 mmol) with propionaldehyde (14.4 mL, 200 mmol), AcOH (5.70 mL, 100 mmol) and $\text{NaBH}(\text{OAc})_3$ (31.8 g, 150 mmol) in DCM (250 mL) to provide by distillation at 100 °C under 70 mbar the title compound as a colourless oil (7.50 g, 53.0 mmol, 53% yield).

IR $\nu_{\text{max}}/\text{cm}^{-1}$ (thin film) 2925, 2805, 1456, 1358, 1184, 1137, 1081; **$^1\text{H NMR}$** (400 MHz, CDCl_3) δ (ppm) 2.69 – 2.60 (m, 4H, H_3), 2.47 – 2.40 (m, 2H, H_4), 1.69 – 1.57 (m, 8H, $\text{H}_{1,2}$), 1.49 (app hex, $J = 7.4$ Hz, 2H, H_5), 0.88 (t, $J = 7.4$ Hz, 3H, H_6); **$^{13}\text{C NMR}$** (101 MHz, CDCl_3) δ (ppm) 60.3 (C_4), 55.5 (C_3), 27.9 (C_2), 27.1 (C_1), 20.6 (C_5), 12.0 (C_6); **HMRS-ESI** (m/z): found $[\text{M}+\text{H}]^+$ 142.1591, $\text{C}_9\text{H}_{20}\text{N}$ requires 142.1590.

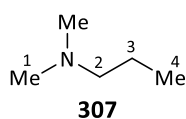
Ethyl 1-propylpyrrolidine-3-carboxylate



Ethyl pyrrolidine-3-carboxylate hydrochloride (1.00 g, 5.50 mmol) was stirred with Et_3N (762 μL , 5.50 mmol) for 10 min in DCM (20.0 mL). Then, General procedure D was applied by adding propionaldehyde (1.98 mL, 27.5 mmol), AcOH (315 μL , 5.50 mmol), and $\text{NaBH}(\text{OAc})_3$ (2.33 g, 11.0 mmol) to provide by column chromatography (EtOAc to 20% MeOH), followed by a short path distillation, the title compound as a colourless oil (651 mg, 3.51 mmol, 63% yield).

IR $\nu_{\max}/\text{cm}^{-1}$ (thin film) 2960, 2933, 2791, 1732, 1449, 1372, 1161, 1095, 1033; **$^1\text{H NMR}$** (400 MHz, CDCl_3) δ (ppm) 4.16 (q, $J = 7.1$ Hz, 2H, H_2), 3.04 (app p, $J = 7.8$ Hz, 1H, H_4), 2.94 (app t, $J = 8.8$ Hz, 1H, H_{5a}), 2.78 – 2.68 (m, 1H, H_{7a}), 2.61 (dd, $J = 9.2, 7.1$ Hz, 1H, H_{5b}), 2.53 – 2.32 (m, 3H, $\text{H}_{7b,8}$), 2.10 (app q, $J = 7.8$ Hz, 2H, H_6), 1.54 (app hex, $J = 7.4$ Hz, 2H, H_9), 1.28 (t, $J = 7.1$ Hz, 3H, H_1), 0.93 (t, $J = 7.4$ Hz, 3H, H_{10}); **$^{13}\text{C NMR}$** (101 MHz, CDCl_3) δ (ppm) 175.1 (C_3), 60.6 (C_2), 58.1 (C_8), 56.9 (C_5), 54.0 (C_7), 42.1 (C_4), 27.6 (C_6), 22.1 (C_9), 14.2 (C_1), 12.0 (C_{10}); **HMRS-ESI** (m/z): found $[\text{M}+\text{H}]^+$ 186.1488, $\text{C}_{10}\text{H}_{20}\text{NO}_2$ requires 186.1489.

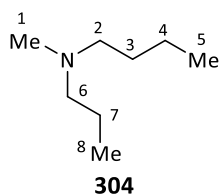
N,N-Dimethylpropan-1-amine



General procedure E was applied to propylamine (8.20 mL, 100 mmol) with formaldehyde (37%, 45.0 mL, 600 mmol) in formic acid (50.0 mL). Purification by distillation at 70 °C under 1 bar provided the title compound as a colourless oil (4.60 g, 52.8 mmol, 53% yield).

IR $\nu_{\max}/\text{cm}^{-1}$ (thin film) 2961, 2779, 1460, 1259, 1040, 835; **$^1\text{H NMR}$** (400 MHz, CDCl_3) δ (ppm) 2.27 – 2.19 (m, 8H, $\text{H}_{1,2}$), 1.50 (app hex, $J = 7.4$ Hz, 2H, H_3), 0.92 (t, $J = 7.4$ Hz, 3H, H_4); **$^{13}\text{C NMR}$** (101 MHz, CDCl_3) δ (ppm) 61.9 (C_2), 45.5 (C_1), 20.9 (C_3), 11.9 (C_4); **HMRS-ESI** (m/z): found $[\text{M}+\text{H}]^+$ 88.1120, $\text{C}_5\text{H}_{14}\text{N}$ requires 88.1121.

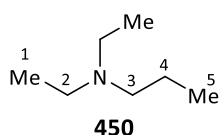
N-Methyl-*N*-propylbutan-1-amine



General procedure D was applied to *N*-butylmethylamine (7.10 mL, 60.0 mmol) with propionaldehyde (6.50 mL, 90.0 mmol), AcOH (3.50 mL, 60.0 mmol) and $\text{NaBH}(\text{OAc})_3$ (15.2 g, 72.0 mmol) in DCM (150 mL) to provide by distillation at 80 °C under 110 mbar the title compound as a colourless oil (2.72 g, 21.0 mmol, 35% yield).

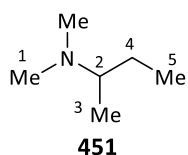
IR $\nu_{\max}/\text{cm}^{-1}$ (thin film) 2959, 2934, 2788, 1459, 1379, 1067; **$^1\text{H NMR}$** (400 MHz, CDCl_3) δ (ppm) 2.36 – 2.26 (m, 4H, $\text{H}_{2,6}$), 2.22 (s, 3H, H_1), 1.56 – 1.41 (m, 4H, $\text{H}_{3,7}$), 1.38 – 1.27 (m, 2H, H_4), 0.93 (t, $J = 7.3$ Hz, 3H, H_5), 0.90 (t, $J = 7.4$ Hz, 3H, H_8); **$^{13}\text{C NMR}$** (101 MHz, CDCl_3) δ (ppm) 59.9 (C_6), 57.6 (C_2), 42.4 (C_1), 29.5 (C_3), 20.8 (C_4), 20.5 (C_7), 14.1 (C_5), 12.0 (C_8); **HMRS-ESI** (m/z): found $[\text{M}+\text{H}]^+$ 130.1592, $\text{C}_8\text{H}_{20}\text{N}$ requires 130.1590.

N,N-Diethylpropan-1-amine



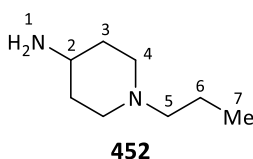
General procedure H was applied to *N,N*-diethylpropionamide (5.70 mL, 40.0 mmol) and LiAlH_4 (3.10 g, 80.0 mmol) in Et_2O (40.0 mL) to provide by distillation at 120 °C under 1 bar the title compound as a colourless oil (2.67 g, 23.2 mmol, 58% yield).

IR $\nu_{\max}/\text{cm}^{-1}$ (thin film) 2952, 2931, 2862, 1452, 1378, 1075; **$^1\text{H NMR}$** (400 MHz, CDCl_3) δ (ppm) 2.54 (q, $J = 7.2$ Hz, 4H, H_2), 2.42 – 2.36 (m, 2H, H_3), 1.54 – 1.42 (m, 2H, H_4), 1.04 (t, $J = 7.2$ Hz, 6H, H_1), 0.90 (t, $J = 7.4$ Hz, 3H, H_5); **$^{13}\text{C NMR}$** (101 MHz, CDCl_3) δ (ppm) 55.1 (C_3), 46.9 (C_2), 20.2 (C_4), 12.1 (C_5), 11.7 (C_1); **HMRS-ESI** (m/z): found $[\text{M}+\text{H}]^+$ 116.1435, $\text{C}_7\text{H}_{18}\text{N}$ requires 116.1434.

***N,N*-Dimethylbutan-2-amine**

General procedure E was applied to butan-2-amine (12.2 mL, 120 mmol) with formaldehyde (37%, 45.0 mL, 600 mmol) in formic acid (50.0 mL) to provide by distillation at 95 °C under 1 bar the title compound as a colourless oil (8.50 g, 84.0 mmol, 70% yield).

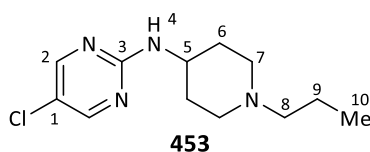
IR $\nu_{\max}/\text{cm}^{-1}$ (thin film) 2967, 2930, 1455, 1379, 1268, 1081, 1057; **$^1\text{H NMR}$** (400 MHz, CDCl_3) δ (ppm) 2.44 – 2.34 (m, 1H, H_2), 2.24 (s, 6H, H_1), 1.62 – 1.49 (m, 1H, H_{4a}), 1.35 – 1.22 (m, 1H, H_{4b}), 0.96 (d, $J = 6.5$ Hz, 3H, H_3), 0.91 (t, $J = 7.4$ Hz, 3H, H_5); **$^{13}\text{C NMR}$** (101 MHz, CDCl_3) δ (ppm) 60.8 (C_2), 40.8 (C_1), 26.2 (C_4), 13.3 (C_3), 11.2 (C_5); **HMRS-ESI** (m/z): found $[\text{M}]$ 101.1202, $\text{C}_6\text{H}_{15}\text{N}$ requires 101.1205.

1-Propylpiperidin-4-amine

TFA (40.0 mL) was added dropwise to a solution of *tert*-butyl (1-propylpiperidin-4-yl)carbamate (12.1 g, 50.0 mmol) in DCM (40.0 mL) at 0 °C. The mixture was warmed to rt and stirred for 2 h. The organic layer was extracted with aq HCl (1M, 2 x 30 mL).

The aqueous layers were combined and basified with NaOH (s) before extraction with DCM (2 x 50 mL). The resultant organic layers were combined, dried over MgSO_4 , filtered and concentrated *in vacuo*. Purification by distillation at 110 °C under 30 mbar provided the title compound as a colourless oil (3.42 g, 24.0 mmol, 48% yield).

IR $\nu_{\max}/\text{cm}^{-1}$ (thin film) 2931, 2766, 1466, 1373, 1142, 1089, 815; **$^1\text{H NMR}$** (400 MHz, CDCl_3) δ (ppm) 2.87 (br d, $J = 11.9$ Hz, 2H, H_{4a}), 2.70 – 2.60 (m, 1H, H_2), 2.33 – 2.24 (m, 2H, H_5), 1.98 (app t, $J = 12.3$ Hz, 2H, H_{4b}), 1.88 – 1.77 (m, 2H, H_{3a}), 1.51 (app hex, $J = 7.4$ Hz, 2H, H_6), 1.40 (ddd, $J = 15.2, 12.9, 3.7$ Hz, 2H, H_{3b}), 1.14 (br s, 2H, H_1), 0.90 (t, $J = 7.4$ Hz, 3H, H_7); **$^{13}\text{C NMR}$** (101 MHz, CDCl_3) δ (ppm) 60.8 (C_5), 52.6 (C_4), 48.9 (C_2), 36.2 (C_3), 20.4 (C_6), 12.0 (C_7); **HMRS-ESI** (m/z): found $[\text{M}+\text{H}]^+$ 143.1539, $\text{C}_8\text{H}_{19}\text{N}_2$ requires 143.1543.

5-Chloro-*N*-(1-propylpiperidin-4-yl)pyrimidin-2-amine

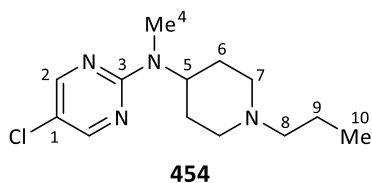
1-propylpiperidin-4-amine (356 mg, 2.50 mmol) was added to a solution of 2,5-dichloropyrimidine (373 mg, 2.50 mmol) and Cs_2CO_3 (1.63 g, 5.00 mmol) in DMF (2.50 mL). The mixture was heated to 70 °C for 15 h. After cooling to

rt, Et_2O (40 mL) was added and washed with aq NaOH (0.25 M, 3 x 50 mL). The organic layer was dried over MgSO_4 , filtered and concentrated *in vacuo*. Purification by column chromatography (DCM to 3% $\text{NH}_3(\text{MeOH}; 2\text{M})$) provided the title compound as a pale brown solid (495 mg, 1.95 mmol, 78% yield).

mp (°C) 95–97; **IR** $\nu_{\max}/\text{cm}^{-1}$ (thin film) 3265, 2955, 2927, 2764, 1600, 1514, 1439, 1367, 1113, 1094, 787, 715; **$^1\text{H NMR}$** (400 MHz, CDCl_3) δ (ppm) 8.21 (s, 2H, H_2), 5.10 (d, $J = 7.4$ Hz, 1H, H_4), 3.81 (td, $J = 14.5, 7.4$ Hz, 1H, H_5), 2.88 (br d, $J = 11.5$ Hz, 2H, H_{7a}), 2.37 – 2.28 (m, 2H, H_8), 2.15 (app t, $J = 11.2$ Hz, 2H, H_{7b}), 2.10 – 2.01 (m, 2H, H_{6a}), 1.61 – 1.48 (m, 4H, $\text{H}_{6b,9}$), 0.92 (t, $J = 7.4$ Hz, 3H, H_{10}); **$^{13}\text{C NMR}$** (101 MHz, CDCl_3) δ (ppm) 160.0 (C_3), 156.2

(C₂), 118.7 (C₁), 60.8 (C₈), 52.3 (C₇), 48.4 (C₅), 32.2 (C₆), 20.3 (C₉), 12.0 (C₁₀); **HMRS-ESI** (m/z): found [M+H]⁺ 255.1373, C₁₂H₂₀N₄Cl requires 255.1371.

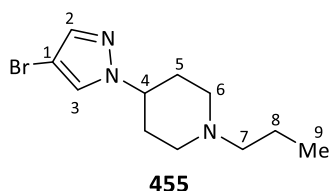
5-Chloro-N-methyl-N-(1-propylpiperidin-4-yl)pyrimidin-2-amine



Et₃N (8.32 mL, 60.0 mmol) was added to a solution of 1-propylpiperidin-4-one (4.24 g, 30.0 mmol) and dimethylamine hydrochloride (4.05 g, 60.0 mmol) in DCM (150 mL) under N₂. The resultant solution was stirred at rt for 30 min. AcOH (3.45 mL, 60.0 mmol) was subsequently added and stirred for 2 h. The solution was cooled to 0 °C and NaBH(OAc)₃ (12.7 g, 60 mmol) was added portionwise. The resultant mixture was stirred at rt for 72 h. The reaction was quenched with aq NaOH (2.5 M, 150 mL) and stirred for 1 h. Phases were separated and the organic layer was washed with aq NaOH (2.5 M, 100 mL). The organic layer was dried over MgSO₄, filtered and concentrated *in vacuo* to provide the crude secondary amine. 2.50 mmol of this was added to a solution of 2,5-dichloropyrimidine (373 mg, 2.50 mmol) and Cs₂CO₃ (1.63 g, 5.00 mmol) in DMF (2.50 mL). The mixture was heated to 70 °C for 15 h. After cooling to rt, Et₂O (40 mL) was added and washed with aq NaOH (0.25 M, 3 x 50 mL). The organic layer was dried over MgSO₄, filtered and concentrated *in vacuo*. Purification by column chromatography (EtOAc) provided the title compound as a pale brown solid (406 mg, 1.51 mmol, 60% yield).

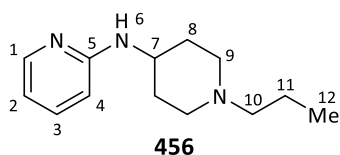
mp (°C) 52–54; **IR** ν_{\max} /cm⁻¹ (thin film) 2935, 2764, 1586, 1505, 1469, 1112, 1030, 1004, 783; **¹H NMR** (400 MHz, CDCl₃) δ (ppm) 8.23 (s, 2H, H₂), 4.56 (tt, *J* = 12.1, 4.1 Hz, 1H, H₅), 3.08 – 2.99 (m, 5H, H_{4,7a}), 2.38 – 2.30 (m, 2H, H₈), 2.11 (td, *J* = 11.9, 2.1 Hz, 2H, H_{7b}), 1.87 (app qd, *J* = 12.1, 3.7 Hz, 2H, H_{6a}), 1.73 – 1.64 (m, 2H, H_{6b}), 1.54 (app hex, *J* = 7.4 Hz, 2H, H₉), 0.93 (t, *J* = 7.4 Hz, 3H, H₁₀); **¹³C NMR** (101 MHz, CDCl₃) δ (ppm) 159.9 (C₃), 155.7 (C₂), 117.4 (C₁), 60.8 (C₈), 53.3 (C₇), 53.0 (C₅), 29.1 (C₄), 29.0 (C₆), 20.4 (C₉), 12.1 (C₁₀); **HMRS-ESI** (m/z): found [M+H]⁺ 269.1533, C₁₃H₂₂N₄Cl requires 269.1533.

4-(4-Bromo-1H-pyrazol-1-yl)-1-propylpiperidine



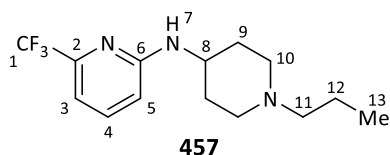
General procedure D was applied to 4-(4-bromo-1H-pyrazol-1-yl)piperidine (1.67 g, 7.30 mmol) with propionaldehyde (1.05 mL, 14.6 mmol), AcOH (420 μ L, 7.30 mmol), and NaBH(OAc)₃ (1.87 g, 8.80 mmol) in DCM (25.0 mL) to provide by column chromatography (DCM to 5% NH₃(MeOH; 2M)) the title compound as a pale yellow oil (1.37 g, 5.03 mmol, 69% yield).

IR ν_{\max} /cm⁻¹ (thin film) 3099, 2953, 2808, 1452, 1378, 1130, 1091, 949, 870; **¹H NMR** (400 MHz, CDCl₃) δ (ppm) 7.46 (s, 1H, H₂), 7.45 (s, 1H, H₃), 4.12 (tt, *J* = 11.4, 4.0 Hz, 1H, H₄), 3.09 – 3.00 (m, 2H, H_{6a}), 2.38 – 2.31 (m, 2H, H₇), 2.18 – 2.06 (m, 4H, H_{5a,6b}), 1.99 (ddd, *J* = 16.3, 12.0, 3.2 Hz, 2H, H_{5b}), 1.48 (app hex, *J* = 7.4 Hz, 2H, H₈), 0.93 (t, *J* = 7.4 Hz, 3H, H₉); **¹³C NMR** (101 MHz, CDCl₃) δ (ppm) 139.1 (C₂), 126.6 (C₃), 92.6 (C₁), 60.4 (C₇), 60.3 (C₄), 52.5 (C₆), 32.5 (C₅), 20.3 (C₈), 12.0 (C₉); **HMRS-ESI** (m/z): found [M+H]⁺ 272.0751, C₁₁H₁₉N₃Br requires 272.0757.

***N*-(1-Propylpiperidin-4-yl)pyridin-2-amine**

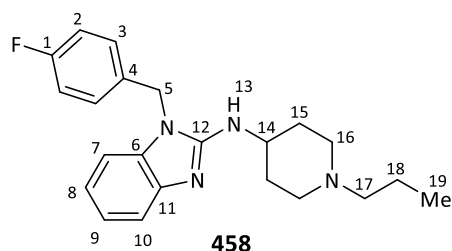
A solution of 1-propylpiperidin-4-amine (356 mg, 2.50 mmol), 2-bromopyridine (240 μ L, 2.50 mmol), Pd₂(dba)₃ (90.0 mg, 0.100 mmol), BINAP (124 mg, 0.200 mmol) and NaOtBu (360 mg, 3.75 mmol) in PhMe (5.0 mL) was stirred at 70 °C for 24 h. After this time, Et₂O (15 mL) was added and the resultant mixture filtered through a pad of Celite and washed with Et₂O (25 mL). Volatiles were gently removed *in vacuo* and the title compound was obtained by column chromatography (DCM to 4% NH₃(MeOH; 2M)) as a pale orange solid (275 mg, 1.25 mmol, 50% yield).

mp (°C) 101–103; **IR** ν_{max} /cm⁻¹ (thin film) 3270, 2935, 2770, 1607, 1519, 1485, 1417, 1287, 1091, 977, 859, 769; **¹H NMR** (400 MHz, CDCl₃) δ (ppm) 8.09 (dd, *J* = 5.0, 1.0 Hz, 1H, H₁), 7.46 – 7.36 (m, 1H, H₃), 6.60 – 6.51 (m, 1H, H₂), 6.38 (d, *J* = 8.4 Hz, 1H, H₄), 4.39 (d, *J* = 7.5 Hz, 1H, H₆), 3.71 – 3.58 (m, 1H, H₇), 2.89 (br d, *J* = 11.6 Hz, 2H, H_{9a}), 2.38 – 2.29 (m, 2H, H₁₀), 2.16 (app t, *J* = 11.5 Hz, 2H, H_{9b}), 2.12 – 2.04 (m, 2H, H_{8a}), 1.60 – 1.49 (m, 4H, H_{8b,11}), 0.93 (t, *J* = 7.4 Hz, 3H, H₁₂); **¹³C NMR** (101 MHz, CDCl₃) δ (ppm) 158.0 (C₅), 148.3 (C₁), 137.3 (C₃), 112.6 (C₂), 107.1 (C₄), 60.9 (C₁₀), 52.4 (C₉), 48.4 (C₇), 32.5 (C₈), 20.3 (C₁₁), 12.0 (C₁₂); **HMRS-ESI** (*m/z*): found [M+H]⁺ 220.1809, C₁₃H₂₂N₃ requires 220.1808.

***N*-(1-Propylpiperidin-4-yl)-6-(trifluoromethyl)pyridin-2-amine**

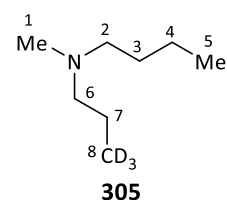
A solution of 1-propylpiperidin-4-amine (940 mg, 6.60 mmol), 2-chloro-6-(trifluoromethyl)pyridine (1.09 g, 6.00 mmol), Pd(OAc)₂ (40.4 mg, 0.180 mmol), DavePhos (70.8 mg, 0.180 mmol) and NaOtBu (692 mg, 7.20 mmol) in PhMe (18.0 mL) was fitted with a condenser and heated to reflux under N₂ for 15 h. After this time, DCM (50 mL) and aq NaOH (2.5 M, 100 mL) were added and phases separated. The organic layer was dried over MgSO₄, filtered and concentrated *in vacuo*. The title compound was obtained by column chromatography (DCM to 4% NH₃(MeOH; 2M)) as a pale orange solid (1.29 g, 4.49 mmol, 75% yield).

mp (°C) 62–63; **IR** ν_{max} /cm⁻¹ (thin film) 3269, 2955, 2926, 1606, 1514, 1360, 1134, 1093, 976, 788; **¹H NMR** (400 MHz, CDCl₃) δ (ppm) 7.52 (app t, *J* = 7.9 Hz, 1H, H₄), 6.91 (d, *J* = 7.3 Hz, 1H, H₃), 6.52 (d, *J* = 8.5 Hz, 1H, H₅), 4.70 (d, *J* = 7.4 Hz, 1H, H₇), 3.71 – 3.56 (m, 1H, H₈), 2.89 (br d, *J* = 11.7 Hz, 2H, H_{10a}), 2.38 – 2.28 (m, 2H, H₁₁), 2.15 (app t, *J* = 11.4 Hz, 2H, H_{10b}), 2.12 – 2.04 (m, 2H, H_{9a}), 1.62 – 1.48 (m, 4H, H_{9b,12}), 0.93 (t, *J* = 7.4 Hz, 3H, H₁₃); **¹³C NMR** (101 MHz, CDCl₃) δ (ppm) 157.7 (C₆), 146.7 (q, *J* = 33.8 Hz, C₂), 138.1 (C₄), 121.6 (q, *J* = 274.0 Hz, C₁), 109.7 (C₅), 108.7 (q, *J* = 3.2 Hz, C₃), 60.8 (C₁₁), 52.3 (C₁₀), 48.6 (C₈), 32.2 (C₉), 20.3 (C₁₂), 12.0 (C₁₃); **¹⁹F NMR** (376 MHz, CDCl₃) δ (ppm) 68.9 (s); **HMRS-ESI** (*m/z*): found [M+H]⁺ 288.1682, C₁₄H₂₁N₃F₃ requires 288.1682.

1-(4-Fluorobenzyl)-N-(1-propylpiperidin-4-yl)-1H-benzo[d]imidazol-2-amine

A solution of 1-propylpiperidin-4-amine (427 mg, 3.00 mmol), 2-chloro-1-(4-fluorobenzyl)-1H-benzo[d]imidazole (652 mg, 2.50 mmol), Pd₂(dba)₃ (286 mg, 0.0313 mmol), BINAP (58.4 mg, 0.0938 mmol) and NaOtBu (721 mg, 7.50 mmol) in PhMe (8.0 mL) under N₂ was stirred at 85 °C for 15 h. After this time, DCM (40 mL) and aq NaOH (2.5 M, 50 mL) were added and phases separated. The organic layer was dried over MgSO₄, filtered and concentrated *in vacuo*. The title compound was obtained by column chromatography (EtOAc to 5% NH₃(MeOH; 2M)) to afford the title compound as a pale yellow solid (841 mg, 2.30 mmol, 92% yield).

mp (°C) 158–160 (decomp); **IR** ν_{max} /cm⁻¹ (thin film) 3236, 3034, 2942, 2806, 2771, 1600, 1566, 1523, 1508, 1462, 1354, 1224, 1090, 818, 735; **¹H NMR** (400 MHz, CDCl₃) δ (ppm) 7.54 (d, *J* = 7.8 Hz, 1H, H₁₀), 7.19 – 7.11 (m, 3H, H_{3,9}), 7.11 – 7.00 (m, 4H, H_{2,7,8}), 5.07 (s, 2H, H₅), 4.04 – 3.89 (m, 1H, H₁₄), 3.75 (d, *J* = 8.0 Hz, 1H, H₁₃), 2.74 (br d, *J* = 8.6 Hz, 2H, H_{16a}), 2.34 – 2.22 (m, 2H, H₁₇), 2.21 – 2.06 (m, 4H, H_{15a,16b}), 1.55 – 1.35 (m, 4H, H_{15b,18}), 0.91 (t, *J* = 7.4 Hz, 3H, H₁₉); **¹³C NMR** (101 MHz, CDCl₃) δ (ppm) 162.5 (d, *J* = 247.6 Hz, C₁), 153.3 (C₁₂), 142.4 (C₁₁), 134.5 (C₆), 131.1 (d, *J* = 3.2 Hz, C₄), 128.3 (d, *J* = 8.2 Hz, C₃), 121.5 (C₉), 119.7 (C₈), 116.6 (C₁₀), 116.2 (d, *J* = 21.8 Hz, C₂), 107.0 (C₇), 60.7 (C₁₇), 52.1 (C₁₆), 49.7 (C₁₄), 45.0 (C₅), 32.7 (C₁₅), 20.3 (C₁₈), 12.0 (C₁₉); **¹⁹F NMR** (376 MHz, CDCl₃) δ (ppm) –113.5 (s); **HMRS-ESI** (*m/z*): found [M+H]⁺ 367.2293, C₂₂H₂₈N₄F requires 367.2284.

N-Methyl-N-(propyl-3,3,3-d₃)butan-1-amine

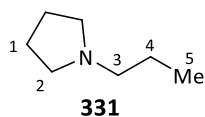
General procedure F was applied to *N*-methylbutan-1-amine (4.70 mL, 40.0 mmol) with Et₃N (6.10 mL, 44.0 mmol) and ethyl malonyl chloride (5.60 mL, 44.0 mmol) in DCM (100 mL). The crude amide was used without further purification and was added to a solution of KOtBu (4.94 g, 44.0 mmol) in THF (100 mL) at 0 °C. After 10 minutes, iodomethane-d₃

(2.74 mL, 44.0 mmol) was added dropwise and the reaction was stirred for 15 h at rt. After this time, volatiles were evaporated and the mixture was dissolved in DCM (100 mL), dried over MgSO₄, filtered and concentrated *in vacuo*. The resultant methylated amide was stirred in aq NaOH (1.0 M, 100 mL) with EtOH (10 mL) at rt for 15 h. After this time, the solution was acidified with aq HCl (3.0 M, 100 mL) to reach pH = 1 and concentrated *in vacuo*. The crude mixture was dissolved in DCM (100 mL), dried over MgSO₄, filtered and concentrated *in vacuo*, and then subjected to 140 °C for 1 h. General procedure H was applied to the resultant decarboxylated amide with LiAlH₄ (2.66 g, 70.0 mmol) in Et₂O (150.0 mL) stirring at rt for 2 h. The title compound was obtained by distillation at 80 °C under 110 mbar as a colourless oil (2.14 g, 16.2 mmol, 41% yield).

IR ν_{max} /cm⁻¹ (thin film) 2932, 2872, 2785, 2217, 1458, 1376, 1054, 733; **¹H NMR** (700 MHz, CDCl₃) δ (ppm) 2.33 – 2.30 (m, 2H, H₂), 2.30 – 2.26 (m, 2H, H₆), 2.21 (s, 3H, H₁), 1.50 – 1.41 (m, 4H, H_{3,7}), 1.35 – 1.29 (m, 2H, H₄), 0.92 (t, *J* = 7.4 Hz, 3H, H₅); **¹³C NMR** (176 MHz, CDCl₃) δ (ppm) 59.9 (C₆), 57.6 (C₂), 42.4 (C₁), 29.5 (C₃), 20.8 (C₄),

20.2 (C₇), 14.1 (C₅), 11.1 (hept, $J = 19.2$ Hz, C₈); **HMRS-ESI** (m/z): found [M+H]⁺ 133.1776, C₈H₁₇ND₃ requires 133.1779.

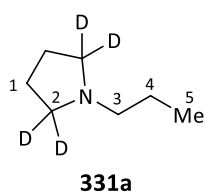
1-Propylpyrrolidine



General procedure I was applied to propylamine (16.5 mL, 200 mmol), with 1,4-dibromobutane (12.0 mL, 100 mmol), and K₂CO₃ (13.8 g, 100 mmol) in MeCN (100 mL) to provide by distillation at 70 °C under 100 mbar the title compound as a colourless oil (6.41 g, 57.0 mmol, 57% yield).

IR $\nu_{\max}/\text{cm}^{-1}$ (thin film) 2962, 2776, 1460, 1349, 1178, 932; **¹H NMR** (400 MHz, CDCl₃) δ (ppm) 2.54 – 2.46 (m, 4H, H₂), 2.44 – 2.36 (m, 2H, H₃), 1.85 – 1.73 (m, 4H, H₁), 1.61 – 1.49 (m, 2H, H₄), 0.93 (t, $J = 7.4$ Hz, 3H, H₅); **¹³C NMR** (100 MHz, CDCl₃) δ (ppm) 58.7 (C₃), 54.3 (C₂), 23.4 (C₁), 22.3 (C₄), 12.2 (C₅); **HMRS-ESI** (m/z): found [M+H]⁺ 114.1275, C₇H₁₆N requires 114.1277.

1-Propylpyrrolidine-2,2,5,5-d₄

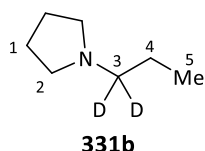


To a solution of pyrrolidine-2,5-dione (3.96 g, 40.0 mmol) and K₂CO₃ (6.08 g, 44.0 mmol) in acetone (100 mL) was added iodopropane (5.86 mL, 60.0 mmol). The resultant mixture was heated to reflux for 15 h. After this time, the reaction was diluted with DCM (50 mL), filtered and concentrated in vacuo. The resultant crude was dissolved in DCM (50 mL),

washed with aq NaOH (1.0 M, 2 x 50 mL), dried over MgSO₄, filtered and concentrated *in vacuo*. The crude product was used without further purification in General procedure H (1.70 g, 12.0 mmol) with LiAlD₄ (1.00 g, 24.0 mmol) in Et₂O (25 mL) heating to reflux for 4 h. Purification by distillation at 75 °C under 90 mbar provided the title compound as a colourless oil (0.71 g, 6.06 mmol, 50% yield).

IR $\nu_{\max}/\text{cm}^{-1}$ (thin film) 2958, 2932, 2876, 2784, 2037, 1467, 1382, 1220, 1127, 954; **¹H NMR** (400 MHz, CDCl₃) δ (ppm) 2.45 – 2.36 (m, 2H, H₃), 1.78 (s, 4H, H₁), 1.55 (app hex, $J = 7.5$ Hz, 2H, H₄), 0.94 (t, $J = 7.4$ Hz, 3H, H₅); **¹³C NMR** (101 MHz, CDCl₃) δ (ppm) 58.7 (C₃), 53.5 (p, $J = 20.8$ Hz, C₂), 23.2 (C₁), 22.3 (C₄), 12.2 (C₅); **HMRS-ESI** (m/z): found [M+H]⁺ 118.1526, C₇H₁₂D₄N requires 118.1528.

1-(Propyl-1,1-d₂)pyrrolidine

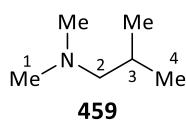


General procedure F was applied to pyrrolidine (4.20 mL, 50.0 mmol) with propionyl chloride (2.62 mL, 30.0 mmol) in the absence of Et₃N. The resultant crude amide was used without further purification in General procedure H with LiAlD₄ (1.00 g, 24.0 mmol) in Et₂O

(40 mL) heating to reflux for 4 h. The resultant crude showed large amounts of unreacted amide. The title compound was purified by distillation at 80 °C under 100 mbar and isolated with the starting amide as a minor impurity (250 mg, 2.20 mmol, 9% yield).

IR ν_{\max} /cm⁻¹ (thin film) 2958, 2775, 2024, 1652, 1459, 1181, 910; **¹H NMR** (600 MHz, CDCl₃) δ (ppm) 2.53 – 2.45 (m, 4H, H₂), 1.80 – 1.75 (m, 4H, H₁), 1.52 (q, J = 7.4 Hz, 2H, H₄), 0.92 (t, J = 7.4 Hz, 3H, H₅); **¹³C NMR** (151 MHz, CDCl₃) δ (ppm) 57.8 (p, J = 20.0 Hz, C₃), 54.2 (C₂), 23.4 (C₁), 22.1 (C₄), 12.1 (C₅); **HMRS-ESI** (m/z): found [M+H]⁺ 116.1403, C₇H₁₄D₂N requires 116.1408.

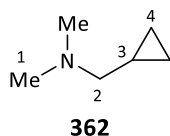
***N,N*,2-Trimethylpropan-1-amine**



General procedure E was applied to 2-methylpropan-1-amine (10.0 mL, 100 mmol) with formaldehyde (37%, 45.0 mL, 600 mmol) in formic acid (50.0 mL) to provide by distillation at 95 °C under 1 bar provided the title compound as a colourless oil (5.40 g, 53.4 mmol, 53% yield).

IR ν_{\max} /cm⁻¹ (thin film) 2951, 2764, 1459, 1264, 1110, 1039, 842; **¹H NMR** (400 MHz, CDCl₃) δ (ppm) 2.21 (s, 6H, H₁), 2.03 (d, J = 7.4 Hz, 2H, H₂), 1.75 (app non, J = 6.6 Hz, 1H, H₃), 0.92 (d, J = 6.6 Hz, 6H, H₄); **¹³C NMR** (101 MHz, CDCl₃) δ (ppm) 68.5 (C₂), 45.9 (C₁), 26.1 (C₃), 20.9 (C₄); **HMRS-ESI** (m/z): found [M+H]⁺ 102.1277, C₆H₁₆N requires 102.1277.

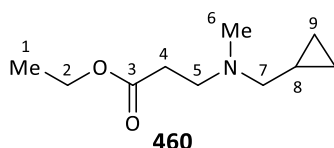
1-Cyclopropyl-*N,N*-dimethylmethanamine



General procedure E was applied to cyclopropylmethanamine (8.70 mL, 10.0 mmol) with formaldehyde (37%, 45.0 mL, 600 mmol) in formic acid (50.0 mL) to provide by distillation at 100 °C under 1 bar the title compound as a colourless oil (6.54 g, 66.0 mmol, 66% yield).

IR ν_{\max} /cm⁻¹ (thin film) 3079, 2944, 2814, 2763, 1464, 1263, 1183, 1029; **¹H NMR** (400 MHz, CDCl₃) δ (ppm) 2.28 (s, 6H, H₁), 2.16 (app d, J = 6.7 Hz, 2H, H₂), 0.94 – 0.79 (m, 1H, H₃), 0.58 – 0.45 (m, 2H, H_{4a}), 0.11 (app q, J = 4.7 Hz, 2H, H_{4b}); **¹³C NMR** (101 MHz, CDCl₃) δ (ppm) 64.7 (C₂), 45.5 (C₁), 9.2 (C₃), 3.8 (C₄); **HMRS-ESI** (m/z): found [M+H]⁺ 100.1124, C₆H₁₄N requires 100.1121.

Ethyl 3-((cyclopropylmethyl)(methyl)amino)propanoate



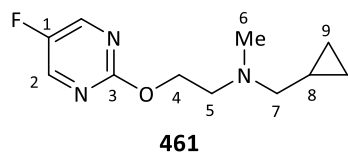
To a solution of cyclopropylmethanamine (5.20 mL, 60.0 mmol) in EtOH (40 mL) at 0 °C was added ethyl acrylate (3.26 mL, 30.0 mmol) in EtOH (10 mL). The resultant mixture was warmed to rt and stirred for 15 h. After this time, the

reaction was concentrated *in vacuo* and the crude product was used without further purification in General procedure E with formaldehyde (37%, 6.75 mL, 90.0 mmol) in formic acid (7.0 mL). The title compound was obtained without further purification (4.35 g, 23.5 mmol, 78% yield).

IR ν_{\max} /cm⁻¹ (thin film) 2981, 2769, 1733, 1464, 1369, 1180, 1031; **¹H NMR** (400 MHz, CDCl₃) δ (ppm) 4.15 (q, J = 7.1 Hz, 2H, H₂), 2.78 (t, J = 7.4 Hz, 2H, H₅), 2.49 (t, J = 7.4 Hz, 2H, H₄), 2.32 (s, 3H, H₆), 2.28 (d, J = 6.6 Hz, 2H, H₇), 1.27 (t, J = 7.1 Hz, 3H, H₁), 0.95 – 0.78 (m, 1H, H₈), 0.57 – 0.47 (m, 2H, H_{9a}), 0.12 (q, J = 4.7 Hz, 2H, H_{9b}); **¹³C NMR**

NMR (101 MHz, CDCl₃) δ (ppm) 172.7 (C₃), 62.5 (C₇), 60.3 (C₂), 52.7 (C₅), 42.1 (C₆), 32.6 (C₄), 14.2 (C₁), 8.8 (C₈), 3.9 (C₉); **HMRS-ESI** (m/z): found [M+H]⁺ 186.1482, C₁₀H₁₉NO₂ requires 186.1494.

***N*-(Cyclopropylmethyl)-2-((5-fluoropyrimidin-2-yl)oxy)-*N*-methylethan-1-amine**

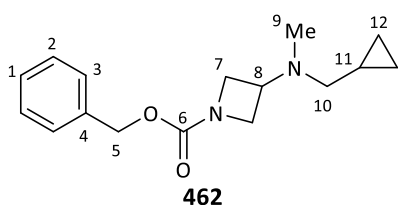


To a solution of NaH (60% in mineral oil, 0.80 g, 20.0 mmol) in THF (30 mL) at 0 °C under N₂ was added 2-(methylamino)ethan-1-ol (1.60 mL, 20.0 mmol) dropwise in THF (10 mL). The resultant mixture was stirred at rt for 30 min

before adding 2-chloro-5-fluoropyrimidine (1.84 mL, 20.0 mmol) dropwise at 0 °C. The reaction mixture was stirred at rt for 15 h. After this time, the reaction was concentrated *in vacuo*. The crude mixture was dissolved in DCM (50 mL), washed with aq NaOH (0.5 M, 2 x 50 mL), dried over MgSO₄, filtered and concentrated *in vacuo*. The crude amine was used without further purification in General procedure D with cyclopropanecarboxaldehyde (2.24 mL, 30.0 mmol), AcOH (1.15 mL, 20.0 mmol) and NaBH(OAc)₃ (6.36 g, 30.0 mmol) in DCM (60 mL). Purification by column chromatography (DCM to 10% NH₃(MeOH; 2M)) provided the title compound as a colourless oil (1.11 g, 4.93 mmol, 25% yield).

IR ν_{\max} /cm⁻¹ (thin film) 3077, 2948, 2775, 1570, 1426, 1325, 1242, 1032; **¹H NMR** (600 MHz, CDCl₃) δ (ppm) 8.38 (s, 2H, H₂), 4.46 (t, *J* = 6.1 Hz, 2H, H₄), 2.91 (t, *J* = 6.1 Hz, 2H, H₅), 2.43 (s, 3H, H₆), 2.37 (d, *J* = 6.6 Hz, 2H, H₇), 0.94 – 0.86 (m, 1H, H₈), 0.57 – 0.49 (m, 2H, H_{9a}), 0.15 – 0.10 (m, 2H, H_{9b}); **¹³C NMR** (151 MHz, CDCl₃) δ (ppm) 161.4 (d, *J* = 1.2 Hz, C₃), 154.2 (d, *J* = 253.4 Hz, C₁), 146.6 (d, *J* = 22.5 Hz, C₂), 66.4 (C₄), 63.2 (C₇), 55.6 (C₅), 42.9 (C₆), 8.9 (C₈), 3.9 (C₉); **¹⁹F NMR** (377 MHz, CDCl₃) δ (ppm) –150.5 (s); **HMRS-ESI** (m/z): found [M+H]⁺ 226.1355, C₁₁H₁₆N₃OF requires 226.1356.

Benzyl 3-((cyclopropylmethyl)(methyl)amino)azetidone-1-carboxylate



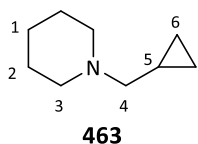
General procedure D was applied to benzyl 3-oxoazetidone-1-carboxylate (2.57 g, 15.0 mmol) with cyclopropylmethanamine (1.73 mL, 20.0 mmol), AcOH (1.15 mL, 20.0 mmol) and NaBH(OAc)₃ (4.24 g, 20.0 mmol) in DCM (60.0 mL). The crude product was used without further purification in

General procedure B with formaldehyde (37%, 6.75 mL, 90.0 mmol) in formic acid (7.0 mL). Purification by column chromatography (DCM to 5% NH₃(MeOH; 2M)) provided the title compound as a yellow oil (1.76 g, 6.43 mmol, 43% yield).

IR ν_{\max} /cm⁻¹ (thin film) 2952, 2882, 2799, 1703, 1414, 1350, 1127; **¹H NMR** (600 MHz, CDCl₃) δ (ppm) 7.40 – 7.35 (m, 4H, H_{2,3}), 7.35 – 7.29 (m, 1H, H₁), 5.11 (s, 2H, H₅), 4.02 (t, *J* = 8.0 Hz, 2H, H_{7a}), 3.92 (dd, *J* = 8.5, 5.8 Hz, 2H, H_{7b}), 3.28 (p, *J* = 6.3 Hz, 1H, H₈), 2.27 (s, 3H, H₉), 2.18 (d, *J* = 6.4 Hz, 2H, H₁₀), 0.90 – 0.81 (m, 1H, H₁₁), 0.55 (app q, *J* = 5.1 Hz, 2H, H_{12a}), 0.11 (app q, *J* = 5.1 Hz, 2H, H_{12b}); **¹³C NMR** (151 MHz, CDCl₃) δ (ppm) 156.4 (C₆),

136.7 (C₄), 128.4 (C₃), 128.0 (C₁), 127.9 (C₂), 66.6 (C₅), 59.8 (C₁₀), 54.1 (C₈), 54.0 (br s, C_{7a}), 53.5 (br s, C_{7b}), 38.4 (C₉), 8.4 (C₁₁), 4.0 (C₁₂); **HMRS-ESI** (m/z): found [M+H]⁺ 275.1750, C₁₆H₂₃N₂O₂ requires 275.1760.

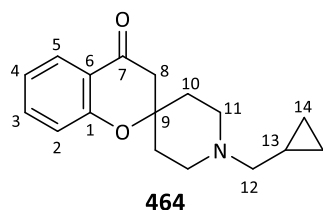
1-(Cyclopropylmethyl)piperidine



General procedure G was applied to piperidine (1.98 mL, 20.0 mmol) with cyclopropanecarboxylic acid (1.67 mL, 21.0 mmol), DIPEA (5.24 mL, 30.0 mmol), HOBt hydrate (4.00 g, 30.0 mmol) and EDC·HCl (4.22 g, 22.0 mmol) in DCM (40 mL). The resultant crude amide was used without further purification in General procedure H with LiAlH₄ (1.52 g, 40.0 mmol) in Et₂O (60 mL). Purification by distillation at 100 °C under 60 mbar provided the title compound as a colourless oil (1.73 g, 12.4 mmol, 62% yield).

IR ν_{max} /cm⁻¹ (thin film) 2931, 2769, 1442, 1377, 1332, 1299, 1149, 1018; **¹H NMR** (600 MHz, CDCl₃) δ (ppm) 2.46 (br s, 4H, H₃), 2.22 (d, *J* = 6.5 Hz, 2H, H₄), 1.61 (app p, *J* = 5.7 Hz, 4H, H₂), 1.44 (br s, 2H, H₁), 0.93 – 0.83 (m, 1H, H₅), 0.53 – 0.47 (m, 2H, H_{6a}), 0.12 – 0.06 (m, 2H, H_{6b}); **¹³C NMR** (151 MHz, CDCl₃) δ (ppm) 64.6 (C₄), 54.6 (C₃), 26.0 (C₂), 24.5 (C₁), 8.4 (C₅), 4.0 (C₆); **HMRS-ESI** (m/z): found [M+H]⁺ 140.1432, C₉H₁₈N requires 140.1434.

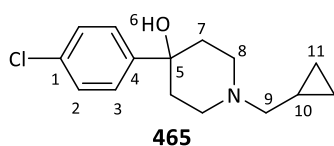
1'-(Cyclopropylmethyl)spiro[chromane-2,4'-piperidin]-4-one



General procedure I was applied to spiro[chromane-2,4'-piperidin]-4-one (1.01 g, 4.00 mmol) with (bromomethyl)cyclopropane (430 μ L, 4.40 mmol) and K₂CO₃ (880 mg, 6.0 mmol) in MeCN (20 mL) to provide by column chromatography (DCM to 5% NH₃(MeOH; 2M)) the title compound as a yellow oil (750 mg, 2.76 mmol, 69% yield).

IR ν_{max} /cm⁻¹ (thin film) 3076, 2919, 2817, 2780, 1688, 1606, 1461, 1298, 1228, 1114; **¹H NMR** (400 MHz, CDCl₃) δ (ppm) 7.87 (d, *J* = 8.0 Hz, 1H, H₅), 7.49 (t, *J* = 7.7 Hz, 1H, H₃), 7.13 – 6.91 (m, 2H, H_{2,4}), 2.85 – 2.75 (m, 2H, H_{11a}), 2.73 (s, 2H, H₈), 2.46 (br t, *J* = 10.7 Hz, 2H, H_{11b}), 2.31 (d, *J* = 6.5 Hz, 2H, H₁₂), 2.08 (br d, *J* = 12.6 Hz, 2H, H_{10a}), 1.85 – 1.74 (m, 2H, H_{10b}), 0.94 – 0.82 (m, 1H, H₁₃), 0.53 (q, *J* = 5.1 Hz, 2H, H_{14a}), 0.13 (q, *J* = 5.1 Hz, 2H, H_{14b}); **¹³C NMR** (101 MHz, CDCl₃) δ (ppm) 192.1 (C₇), 159.2 (C₁), 136.2 (C₃), 126.5 (C₅), 120.9 (C₄), 120.8 (C₆), 118.4 (C₂), 77.9 (C₉), 63.7 (C₁₂), 48.8 (C₁₁), 48.0 (C₈), 34.3 (C₁₀), 8.6 (C₁₃), 4.0 (C₁₄); **HMRS-ESI** (m/z): found [M+H]⁺ 272.1640, C₁₇H₂₂NO₂ requires 272.1651.

4-(4-Chlorophenyl)-1-(cyclopropylmethyl)piperidin-4-ol

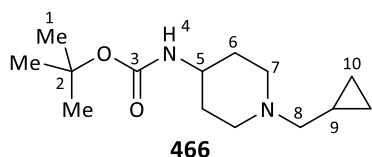


General procedure D was applied to 4-(4-chlorophenyl)piperidin-4-ol (2.12 g, 10.0 mmol) with cyclopropanecarboxaldehyde (1.12 mL, 15.0 mmol), AcOH (572 μ L, 10.0 mmol) and NaBH(OAc)₃ (4.24 g, 20.0 mmol) in DCM (50 mL) to provide

by trituration in a mixture of PE:DCM (9:1) the title compound as a white solid (2.03 g, 7.64 mmol, 76% yield).

mp (°C) 94–96; **IR** $\nu_{\max}/\text{cm}^{-1}$ (thin film) 3072, 2918, 2835, 1482, 1378, 1097, 996; **$^1\text{H NMR}$** (600 MHz, CDCl_3) δ (ppm) 7.51 – 7.41 (m, 2H, H_2), 7.36 – 7.29 (m, 2H, H_3), 2.98 (app br d, $J = 11.4$ Hz, 2H, H_{8a}), 2.46 (td, $J = 12.2$, 2.3 Hz, 2H, H_{8b}), 2.34 (d, $J = 6.5$ Hz, 2H, H_9), 2.16 (td + br s, $J = 13.3$, 4.5 Hz, 3H, H_{7a+6}), 1.74 (dd, $J = 14.1$, 2.3 Hz, 2H, H_{7b}), 0.96 – 0.85 (m, 1H, H_{10}), 0.59 – 0.51 (m, 2H, H_{11a}), 0.14 (q, $J = 4.7$ Hz, 2H, H_{11b}); **$^{13}\text{C NMR}$** (151 MHz, CDCl_3) δ (ppm) 147.0 (C_4), 132.7 (C_1), 128.4 (C_3), 126.1 (C_2), 71.0 (C_5), 63.9 (C_9), 49.4 (C_8), 38.4 (C_7), 8.4 (C_{10}), 4.0 (C_{11}); **HMRS-ESI** (m/z): found $[\text{M}+\text{H}]^+$ 266.1301, $\text{C}_{15}\text{H}_{21}\text{NOCl}$ requires 266.1312.

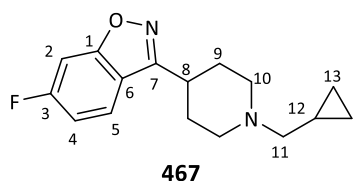
***tert*-Butyl (1-(cyclopropylmethyl)piperidin-4-yl)carbamate**



General procedure D was applied to *tert*-butyl piperidin-4-ylcarbamate (3.00 g, 15.0 mmol) with cyclopropanecarboxaldehyde (1.50 mL, 20.0 mmol), AcOH (860 μL , 15.0 mmol) and $\text{NaBH}(\text{OAc})_3$ (4.24 g, 20.0 mmol) in DCM (50 mL) to provide by column chromatography (DCM to 5% $\text{NH}_3(\text{MeOH}; 2\text{M})$) the title compound as a colourless oil (1.31 g, 7.80 mmol, 78% yield).

mp (°C) 88–90; **IR** $\nu_{\max}/\text{cm}^{-1}$ (thin film) 3170, 2943, 2783, 1702, 1535, 1274, 1242, 1170; **$^1\text{H NMR}$** (600 MHz, CDCl_3) δ (ppm) 4.44 (br s, 1H, H_4), 3.47 (app br s, 1H, H_5), 2.98 (app br d, $J = 8.3$ Hz, 2H, H_{7a}), 2.24 (d, $J = 6.5$ Hz, 2H, H_8), 2.08 (app br t, $J = 10.9$ Hz, 2H, H_{7b}), 1.95 (app br d, $J = 12.1$ Hz, 2H, H_{6a}), 1.51 – 1.41 (m, 11H, $\text{H}_{1,6b}$), 0.90 – 0.81 (m, 1H, H_9), 0.54 – 0.49 (m, 2H, H_{10a}), 0.10 (app q, $J = 4.7$ Hz, 2H, H_{10b}); **$^{13}\text{C NMR}$** (151 MHz, CDCl_3) δ (ppm) 155.2 (C_3), 79.1 (C_2), 63.8 (C_8), 52.4 (C_7), 47.8 (C_5), 32.6 (C_6), 28.4 (C_1), 8.5 (C_9), 3.9 (C_{10}); **HMRS-ESI** (m/z): found $[\text{M}+\text{H}]^+$ 255.2062, $\text{C}_{14}\text{H}_{27}\text{N}_2\text{O}_2$ requires 255.2073.

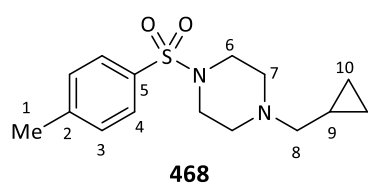
3-(1-(Cyclopropylmethyl)piperidin-4-yl)-6-fluorobenzo[*d*]isoxazole



General procedure I was applied to 6-fluoro-3-(piperidin-4-yl)benzo[*d*]isoxazole hydrochloride (1.28 g, 5.00 mmol) with (bromomethyl)cyclopropane (534 μL , 5.50 mmol) and DIPEA (2.10 mL, 12.0 mmol) in MeCN (10 mL) to provide by column chromatography (DCM to 4% $\text{NH}_3(\text{MeOH}; 2\text{M})$) the title compound as a

white solid (846 mg, 3.08 mmol, 62% yield).

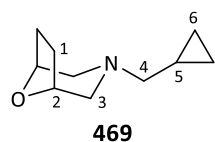
mp (°C) 82–84; **IR** $\nu_{\max}/\text{cm}^{-1}$ (thin film) 2962, 1609, 1414, 1270, 1232, 1120, 954, 829; **$^1\text{H NMR}$** (700 MHz, CDCl_3) δ (ppm) 7.74 (dd, $J = 8.7$, 5.1 Hz, 1H, H_5), 7.25 (dd, $J = 8.5$, 1.8 Hz, 1H, H_2), 7.06 (td, $J = 8.8$, 2.0 Hz, 1H, H_4), 3.23 (app br d, $J = 11.3$ Hz, 2H, H_{10a}), 3.09 (tt, $J = 11.2$, 4.0 Hz, 1H, H_8), 2.34 (d, $J = 6.5$ Hz, 2H, H_{11}), 2.23 – 2.18 (m, 2H, H_{10b}), 2.14 (ddd, $J = 14.7$, 12.1, 3.1 Hz, 2H, H_{9a}), 2.09 (app br d, $J = 10.7$ Hz, 2H, H_{9b}), 0.97 – 0.90 (m, 1H, H_{12}), 0.59 – 0.53 (m, 2H, H_{13a}), 0.17 – 0.12 (m, 2H, H_{13b}); **$^{13}\text{C NMR}$** (176 MHz, CDCl_3) δ (ppm) 164.1 (d, $J = 250.5$ Hz, C_3), 163.9 (d, $J = 13.6$ Hz, C_1), 161.2 (C_7), 122.7 (d, $J = 11.1$ Hz, C_5), 117.3 (d, $J = 1.3$ Hz, C_6), 112.3 (d, $J = 25.3$ Hz, C_4), 97.4 (d, $J = 26.7$ Hz, C_2), 64.1 (C_{11}), 53.5 (C_{10}), 34.7 (C_8), 30.5 (C_9), 8.4 (C_{12}), 4.0 (C_{13}); **$^{19}\text{F NMR}$** (377 MHz, CDCl_3) δ (ppm) –109.8 (s); **HMRS-ESI** (m/z): found $[\text{M}+\text{H}]^+$ 275.1563, $\text{C}_{16}\text{H}_{20}\text{N}_2\text{OF}$ requires 275.1560.

1-(Cyclopropylmethyl)-4-tosylpiperazine

General procedure D was applied to 4-tosylpiperazine (3.61 g, 15.0 mmol) with cyclopropanecarboxaldehyde (1.49 mL, 20.0 mmol), AcOH (860 μ L, 15.0 mmol) and NaBH(OAc)₃ (4.24 g, 20.0 mmol) in DCM (50 mL) to provide by trituration in a mixture of PE:Et₂O (1:1) the title compound as a white solid

(3.26 g, 11.1 mmol, 74% yield).

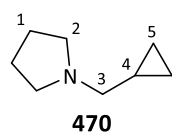
mp ($^{\circ}$ C) 106–108; **IR** ν_{\max} /cm⁻¹ (thin film) 3074, 2776, 1456, 1344, 1325, 1161, 952; **¹H NMR** (600 MHz, CDCl₃) δ (ppm) 7.64 (d, J = 8.0 Hz, 2H, H₄), 7.33 (d, J = 8.0 Hz, 2H, H₃), 3.04 (br s, 4H, H₆), 2.61 (br s, 4H, H₇), 2.43 (s, 3H, H₁), 2.24 (d, J = 6.6 Hz, 2H, H₈), 0.82 – 0.73 (m, 1H, H₉), 0.54 – 0.46 (m, 2H, H_{10a}), 0.09 (q, J = 4.7 Hz, 2H, H_{10b}); **¹³C NMR** (151 MHz, CDCl₃) δ (ppm) 143.7 (C₅), 131.8 (C₂), 129.6 (C₃), 128.0 (C₄), 63.3 (C₈), 52.2 (C₇), 46.0 (C₆), 21.6 (C₁), 8.3 (C₉), 3.9 (C₁₀); **HMRS-ESI** (m/z): found [M+H]⁺ 295.1466, C₁₅H₂₃N₂O₂S requires 295.1480.

(1R,5S)-3-(cyclopropylmethyl)-8-oxa-3-azabicyclo[3.2.1]octane

To a solution of (1R,5S)-8-oxa-3-azabicyclo[3.2.1]octane hydrochloride (1.50 g, 10.0 mmol) and cyclopropanecarboxaldehyde (1.12 mL, 15.0 mmol) in DCM (40 mL) at 0 $^{\circ}$ C under N₂ was added NaBH(OAc)₃ (3.18 g, 15.0 mmol) portionwise. The resultant mixture

was stirred at rt for 48 h. After this time, the reaction was quenched with aq NaOH (2.5 M, 10 mL) and concentrated *in vacuo*. Et₂O (50 mL) was added and the organic layer was washed with aq NaOH (3 x 50 mL, 0.25 M), dried over MgSO₄, filtered and concentrated *in vacuo*. Purification by distillation at 110 $^{\circ}$ C under 15 mbar provided the title compound as a colourless oil (775 mg, 4.63 mmol, 46% yield).

IR ν_{\max} /cm⁻¹ (thin film) 2949, 2804, 1457, 1280, 1163, 1142, 1005; **¹H NMR** (600 MHz, CDCl₃) δ (ppm) 4.34 – 4.24 (m, 2H, H₂), 2.71 (d, J = 11.2 Hz, 2H, H_{3a}), 2.31 (d, J = 11.2 Hz, 2H, H_{3b}), 2.19 (d, J = 6.5 Hz, 2H, H₄), 2.01 – 1.92 (m, 2H, H_{1a}), 1.90 – 1.81 (m, 2H, H_{1b}), 0.85 – 0.75 (m, 1H, H₅), 0.47 (q, J = 5.1 Hz, 2H, H_{6a}), 0.07 (q, J = 5.1 Hz, 2H, H_{6b}); **¹³C NMR** (151 MHz, CDCl₃) δ (ppm) 74.8 (C₂), 63.1 (C₄), 58.8 (C₃), 28.6 (C₁), 8.3 (C₅), 3.7 (C₆); **HMRS-ESI** (m/z): found [M+H]⁺ 168.1380, C₁₀H₁₈NO requires 168.1388.

1-(Cyclopropylmethyl)pyrrolidine

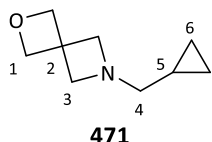
General procedure F was applied to pyrrolidine (4.05 mL, 48.0 mmol) with cyclopropanecarbonyl chloride (3.63 mL, 40.0 mmol) and Et₃N (6.75 mL, 48.0 mmol) in DCM (100 mL). The crude product was used without further purification in General procedure E with LiAlH₄ (3.03 g, 80.0 mmol) in Et₂O (80 mL). Purification by distillation at 90 $^{\circ}$ C under 80 mbar provided the title compound

as a colourless oil (2.84 g, 22.7 mmol, 57% yield).

IR ν_{\max} /cm⁻¹ (thin film) 3076, 2964, 2773, 1346, 1147, 1018; **¹H NMR** (600 MHz, CDCl₃) δ (ppm) 2.61 – 2.52 (m, 4H, H₂), 2.33 (d, J = 6.7 Hz, 2H, H₃), 1.88 – 1.74 (m, 4H, H₁), 1.01 – 0.85 (m, 1H, H₄), 0.57 – 0.44 (m, 2H, H_{5a}),

0.14 (app q, $J = 5.0$ Hz, 2H, H_{5b}); ¹³C NMR (151 MHz, CDCl₃) δ (ppm) 61.4 (C₃), 54.4 (C₂), 23.4 (C₁), 10.2 (C₄), 3.8 (C₅); **HMRS-ESI** (m/z): found [M+H]⁺ 126.1273, C₈H₁₆N requires 126.1283.

6-(Cyclopropylmethyl)-2-oxa-6-azaspiro[3.3]heptane

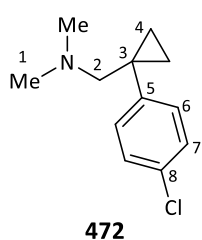


To a solution of 2-oxa-6-azaspiro[3.3]heptane oxalate (2:1) (2.16 g, 15.0 mmol) in DCM (50 mL) at 0 °C under N₂ was added cyclopropanecarboxaldehyde (1.10 mL, 15.0 mmol). NaBH(OAc)₃ (4.25 g, 20.0 mmol) was added portionwise over 15 min while stirring. The

resultant mixture was purged briefly with N₂, warmed to rt and stirred for 36 h. The reaction was quenched with aq NaOH (2.5 M, 50 mL) and the solution was left stirring until no further effervescence was observed. The phases were separated and the aqueous layer was extracted with further DCM (50 mL). The combined organic layers were extracted twice with 1M HCl (2 x 30 mL), the combined aqueous solution were basified with NaOH (s) until a basic pH > 12 was reached, and it was extracted twice with DCM (2 x 30 mL). The resultant new organic layer was dried over MgSO₄, filtered and concentrated *in vacuo* to provide the title compound without further purification (1.24 g, 8.10 mmol, 54% yield).

IR ν_{\max} /cm⁻¹ (thin film) 2924, 2861, 2806, 1248, 971, 830; **¹H NMR** (600 MHz, CDCl₃) δ (ppm) 4.74 (s, 4H, H₁), 3.37 (s, 4H, H₃), 2.23 (d, $J = 6.8$ Hz, 2H, H₄), 0.78 – 0.70 (m, 1H, H₅), 0.47 – 0.42 (m, 2H, H_{6a}), 0.08 (app q, $J = 4.6$ Hz, 2H, H_{6b}); ¹³C NMR (151 MHz, CDCl₃) δ (ppm) 81.4 (C₁), 64.2 (C₄), 64.0 (C₃), 39.5 (C₂), 9.0 (C₅), 2.8 (C₆); **HMRS-ESI** (m/z): found [M+H]⁺ 154.1226, C₉H₁₆NO requires 154.1232.

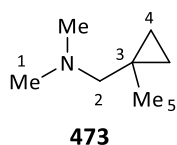
1-(1-(4-Chlorophenyl)cyclopropyl)-N,N-dimethylmethanamine



General procedure G was applied to dimethylamine (2.0 M in MeOH, 12.5 mL, 25.0 mmol) with 1-(4-chlorophenyl)cyclopropane-1-carboxylic acid (3.93 g, 20.0 mmol), DIPEA (5.24 mL, 30.0 mmol), HOBT hydrate (4.00 g, 30.0 mmol) and EDC·HCl (4.80 g, 25.0 mmol) in DCM (50 mL). The resultant crude amide was used without further purification in General procedure H with LiAlH₄ (1.52 g, 40.0 mmol) in Et₂O (50 mL) heating to reflux for 4 h. The

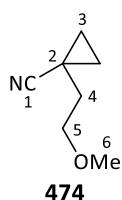
title compound was obtained as a colourless oil without further purification (2.37 g, 11.3 mmol, 57% yield).

IR ν_{\max} /cm⁻¹ (thin film) 3078, 2941, 2813, 2764, 1494, 1456, 1102, 1035, 1013; **¹H NMR** (600 MHz, CDCl₃) δ (ppm) 7.32 – 7.23 (m, 4H, H_{6,7}), 2.47 (s, 2H, H₂), 2.22 (s, 6H, H₁), 0.87 (dd, $J = 6.2, 4.4$ Hz, 2H, H_{4a}), 0.74 (dd, $J = 6.2, 4.3$ Hz, 2H, H_{4b}); ¹³C NMR (151 MHz, CDCl₃) δ (ppm) 143.0 (C₅), 131.5 (C₈), 129.7 (C₆), 128.3 (C₇), 68.8 (C₂), 46.0 (C₁), 23.2 (C₃), 12.7 (C₄); **HMRS-ESI** (m/z): found [M+H]⁺ 210.1043, C₁₂H₁₇NCl requires 210.1050.

***N,N*-Dimethyl-1-(1-methylcyclopropyl)methanamine**

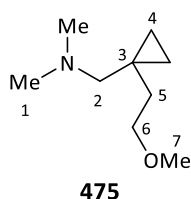
General procedure G was applied to dimethylamine (2.0 M in THF, 30.0 mL, 60.0 mmol) with 1-methylcyclopropane-1-carboxylic acid (5.00 g, 50.0 mmol), DIPEA (13.1 mL, 75.0 mmol), HOBT hydrate (10.0 g, 75.0 mmol) and EDC-HCl (11.5 g, 60.0 mmol) in DCM (100 mL). The resultant crude amide was used without further purification in General procedure H with LiAlH₄ (3.80 g, 100.0 mmol) in Et₂O (100 mL) heating to reflux for 16 h. Purification by distillation at 70 °C under 200 mbar provided the title compound as a colourless oil (1.17 g, 10.3 mmol, 21% yield).

IR $\nu_{\max}/\text{cm}^{-1}$ (thin film) 2947, 2812, 2761, 1455, 1252, 1035; **¹H NMR** (600 MHz, CDCl₃) δ (ppm) 2.24 (s, 6H, H₁), 2.09 (s, 2H, H₂), 1.10 (s, 3H, H₅), 0.33 – 0.28 (m, 2H, H_{4a}), 0.28 – 0.24 (m, 2H, H_{4b}); **¹³C NMR** (151 MHz, CDCl₃) δ (ppm) 68.7 (C₂), 45.8 (C₁), 21.6 (C₅), 13.8 (C₃), 12.0 (C₄); **HMRS-ESI** (m/z): found [M+H]⁺ 114.1270, C₇H₁₆N requires 114.1283.

1-(2-Methoxyethyl)cyclopropane-1-carbonitrile

To a solution of cyclopropanecarbonitrile (3.70 mL, 50.0 mmol) in THF (75 mL) at -78 °C was added LDA (30.0 mL, 60.0 mmol, 2 M in THF) dropwise while stirring. The solution was stirred for 30 min at this temperature before the dropwise addition of 1-bromo-2-methoxyethane (5.15 mL, 55.0 mmol). The resultant mixture was left to warm up overnight while stirring. The reaction was quenched with aq NaOH and volatiles were evaporated *in vacuo*. The resultant crude was dissolved in DCM (50 mL) and aq NaOH (2.5 M, 150 mL). The layers were separated and the aqueous solution was extracted with further DCM (2 x 50 mL). The organic layers were combined, dried over MgSO₄, filtered and concentrated *in vacuo*. Purification by column chromatography (PE to DCM) provided the title compound as a colourless oil (2.73 g, 21.8 mmol, 44% yield).

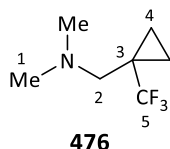
IR $\nu_{\max}/\text{cm}^{-1}$ (thin film) 3071, 3025, 2890, 2246, 1422, 1148; **¹H NMR** (700 MHz, CDCl₃) δ (ppm) 3.61 (t, *J* = 6.4 Hz, 2H, H₅), 3.39 (s, 3H, H₆), 1.75 (t, *J* = 6.4 Hz, 2H, H₄), 1.27 – 1.23 (m, 2H, H_{3a}), 0.90 – 0.86 (m, 2H, H_{3b}); **¹³C NMR** (176 MHz, CDCl₃) δ (ppm) 123.3 (C₁), 70.4 (C₅), 58.9 (C₆), 35.1 (C₄), 13.8 (C₃), 7.3 (C₂); **HMRS-ESI** (m/z): found [M+Na]⁺ 148.0729, C₇H₁₁NO requires 148.0733.

1-(1-(2-Methoxyethyl)cyclopropyl)-*N,N*-dimethylmethanamine

General procedure H was applied to 1-(2-methoxyethyl)cyclopropane-1-carbonitrile (2.73 g, 21.8 mmol) with LiAlH₄ (1.67 g, 44.0 mmol) in Et₂O (100 mL). The resultant primary amine was used without further purification in General procedure E with formaldehyde (37%, 10.0 mL, 130 mmol) in formic acid (11.0 mL). Purification by column chromatography (DCM to 5% NH₃(MeOH; 2M)) provided the title compound as a colourless oil (524 mg, 3.33 mmol, 15% yield).

IR $\nu_{\max}/\text{cm}^{-1}$ (thin film) 2938, 2812, 2762, 1455, 1188, 1117, 1035; **$^1\text{H NMR}$** (700 MHz, CDCl_3) δ (ppm) 3.50 (t, $J = 6.8$ Hz, 2H, H_5), 3.34 (s, 3H, H_7), 2.23 (s, 6H, H_1), 2.07 (s, 2H, H_2), 1.63 (t, $J = 6.8$ Hz, 2H, H_5), 0.38 (br s, 2H, H_{4a}), 0.26 (br s, 2H, H_{4b}); **$^{13}\text{C NMR}$** (176 MHz, CDCl_3) δ (ppm) 71.2 (C_6), 66.1 (C_2), 58.6 (C_7), 45.9 (C_1), 34.3 (C_5), 15.8 (C_3), 10.8 (C_4); **HMRS-ESI** (m/z): found $[\text{M}+\text{H}]^+$ 158.1543, $\text{C}_9\text{H}_{20}\text{NO}$ requires 158.1545.

***N,N*-Dimethyl-1-(1-(trifluoromethyl)cyclopropyl)methanamine**



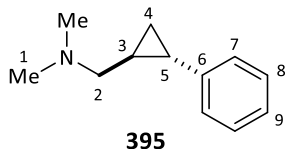
476

General procedure G was applied to dimethylamine (2.0 M in THF, 16.5 mL, 33.0 mmol) with 1-(trifluoromethyl)cyclopropane-1-carboxylic acid (4.62 g, 30.0 mmol), DIPEA (7.90 mL, 45.0 mmol), HOBt hydrate (6.00 g, 45.0 mmol) and EDC·HCl (6.90 g, 36.0 mmol) in DCM (100 mL).

The resultant crude amide was used without further purification in General procedure H with LiAlH_4 (2.28 g, 60.0 mmol) in Et_2O (100 mL) heating to reflux for 4 h. The title compound was obtained as a colourless oil without further purification (1.03 g, 6.16 mmol, 21% yield).

IR $\nu_{\max}/\text{cm}^{-1}$ (thin film) 2947, 2821, 2770, 1458, 1394, 1263, 1126, 1037; **$^1\text{H NMR}$** (700 MHz, CDCl_3) δ (ppm) 2.46 (s, 2H, H_2), 2.28 (s, 6H, H_1), 1.03 (app s, 2H, H_{4a}), 0.65 (app s, 2H, H_{4b}); **$^{13}\text{C NMR}$** (176 MHz, CDCl_3) δ (ppm) 127.0 (q, $J = 273.8$ Hz, C_5), 61.4 (C_2), 46.1 (C_1), 21.1 (q, $J = 31.4$ Hz, C_3), 8.4 (q, $J = 2.4$ Hz, C_4); **HMRS-ESI** (m/z): found $[\text{M}+\text{H}]^+$ 167.0920, $\text{C}_7\text{H}_{13}\text{NF}_3$ requires 167.0922.

***trans-N,N*-Dimethyl-1-(2-phenylcyclopropyl)methanamine**

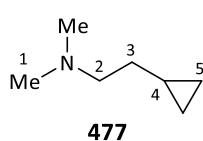


395

General procedure G was applied to dimethylamine (2.0 M in THF, 15.0 mL, 30.0 mmol) with *trans* 2-phenylcyclopropane-1-carboxylic acid (3.24 g, 20.0 mmol), DIPEA (5.3 mL, 30.0 mmol), HOBt hydrate (3.33 g, 25.0 mmol) and EDC·HCl (4.78 g,

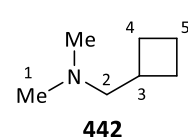
25.0 mmol) in DCM (100 mL). The resultant crude amide was used without further purification in THF (20.0 mL) in General procedure H with LiAlH_4 (1.52 g, 40.0 mmol) in Et_2O (80.0 mL). The title compound was obtained without further purification as a colourless oil (3.00 g, 17.1 mmol, 86% yield).

IR $\nu_{\max}/\text{cm}^{-1}$ (thin film) 2940, 2761, 1604, 1497, 1455, 1033, 753, 695; **$^1\text{H NMR}$** (700 MHz, CDCl_3) δ (ppm) 7.27 (app t, $J = 7.7$ Hz, 2H, H_8), 7.16 (t, $J = 7.0$ Hz, 1H, H_9), 7.09 (d, $J = 7.7$ Hz, 2H, H_7), 2.43 (dd, $J = 12.5, 6.3$ Hz, 1H, H_{2a}), 2.34 – 2.29 (m, 7H, $\text{H}_{1,2b}$), 1.74 – 1.68 (m, 1H, H_5), 1.28 – 1.22 (m, 1H, H_3), 0.99 (dt, $J = 8.7, 5.1$ Hz, 1H, H_{4a}), 0.86 (dt, $J = 8.9, 5.3$ Hz, 1H, H_{4b}); **$^{13}\text{C NMR}$** (176 MHz, CDCl_3) δ (ppm) 143.0 (C_6), 128.3 (C_8), 125.7 (C_7), 125.4 (C_9), 64.1 (C_2), 45.5 (C_1), 22.6 (C_5), 21.6 (C_3), 15.0 (C_4); **HMRS-ESI** (m/z): found $[\text{M}+\text{H}]^+$ 176.1438, $\text{C}_{12}\text{H}_{18}\text{N}$ requires 176.1439.

2-Cyclopropyl-*N,N*-dimethylethan-1-amine

General procedure G was applied to dimethylamine (2.0 M in THF, 12.5 mL, 25.0 mmol) with 2-cyclopropylacetic acid (2.43 mL, 25.0 mmol), DIPEA (7.00 mL, 40.0 mmol), HOBt hydrate (5.33 g, 40.0 mmol) and EDC·HCl (5.75 g, 30.0 mmol) in DCM (75 mL). The resultant crude was used without further purification in General procedure H with LiAlH₄ (1.90 g, 50.0 mmol) in Et₂O (50 mL). Purification by distillation at 70 °C under 150 mbar provided the title compound as a colourless oil (0.60 g, 5.30 mmol, 21% yield).

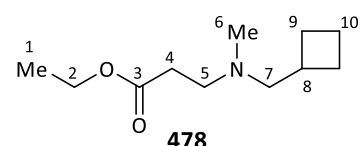
IR $\nu_{\max}/\text{cm}^{-1}$ (thin film) 2971, 2938, 2762, 1461, 1065, 1042; **¹H NMR** (400 MHz, CDCl₃) δ (ppm) 2.40 – 2.34 (m, 2H, H₂), 2.24 (s, 6H, H₁), 1.42 – 1.32 (m, 2H, H₃), 0.75 – 0.61 (m, 1H, H₄), 0.51 – 0.38 (m, 2H, H_{5a}), 0.11 – 0.00 (m, 2H, H_{5b}); **¹³C NMR** (101 MHz, CDCl₃) δ (ppm) 59.8 (C₂), 45.6 (C₁), 33.1 (C₃), 9.0 (C₄), 4.3 (C₅); **HMRS-ESI** (m/z): found [M+H]⁺ 114.1274, C₇H₁₆N requires 114.1277.

1-Cyclobutyl-*N,N*-dimethylmethanamine

To an aq solution of dimethylamine (40%, 32.0 mL, 250 mmol) at 0 °C was added (bromomethyl)cyclobutane (5.62 mL, 50.0 mmol). The resultant mixture was stirred at rt for 15 h.

After this time, aq NaOH (50 mL, 2.5 M) and sat NaCl (150 mL) were added and an organic layer was collected as a supernatant. The crude product was dissolved in Et₂O (50 mL) and the organic solution was extracted with HCl (0.5 M, 2 x 50 mL). The aqueous layers were combined and basified with NaOH while stirring at 0 °C. The resultant aqueous solution was extracted with Et₂O (2 x 50 mL), dried over MgSO₄, filtered and concentrated *in vacuo* to provide the title compound as a colourless oil (1.28 g, 11.3 mmol, 23% yield).

IR $\nu_{\max}/\text{cm}^{-1}$ (thin film) 2969, 2940, 2763, 1456, 1265, 1041, 1023, 842; **¹H NMR** (400 MHz, CDCl₃) δ (ppm) 2.51 (app hept, $J = 7.7$ Hz, 1H, H₃), 2.31 (d, $J = 7.1$ Hz, 2H, H₂), 2.21 (s, 6H, H₁), 2.14 – 2.03 (m, 2H, H_{4a}), 1.96 – 1.86 (m, 1H, H_{5a}), 1.85 – 1.78 (m, 1H, H_{5b}), 1.72 – 1.64 (m, 2H, H_{4b}); **¹³C NMR** (101 MHz, CDCl₃) δ (ppm) 66.5 (C₂), 45.8 (C₁), 34.3 (C₃), 27.5 (C₄), 18.7 (C₅); **HMRS-ESI** (m/z): found [M+H]⁺ 114.1276, C₇H₁₆N requires 114.1277.

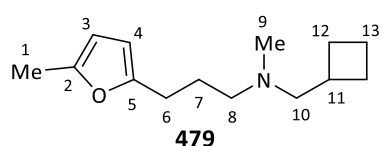
Ethyl 3-((cyclobutylmethyl)(methyl)amino)propanoate

To a solution of methylamine (33% in EtOH, 6.17 mL, 50.0 mmol) in EtOH (40 mL) at 0 °C was added ethyl acrylate (2.72 mL, 25.0 mmol) in EtOH (10 mL).

The resultant mixture was warmed to rt and stirred for 15 h. After this time, the reaction was concentrated *in vacuo* and the crude product was dissolved in DCM (50 mL) and washed with aq NaOH (2.5 M, 2 x 50 mL), dried over MgSO₄, filtered and concentrated *in vacuo*. The crude mixture was used without further purification in General procedure I with (bromomethyl)cyclobutane (2.80 mL, 25.0 mmol) and DIPEA (5.24 mL, 30.0 mmol) in MeCN (50 mL). Purification by column chromatography (DCM to 3% NH₃(MeOH; 2M)) provided the title compound as a colourless oil (690 mg, 3.46 mmol, 14% yield).

IR $\nu_{\text{max}}/\text{cm}^{-1}$ (thin film) 2972, 2772, 1733, 1178, 1027; **$^1\text{H NMR}$** (700 MHz, CDCl_3) δ (ppm) 4.15 (q, $J = 7.1$ Hz, 2H, H_2), 2.69 (t, $J = 7.3$ Hz, 2H, H_5), 2.52 (hept, $J = 7.8$ Hz, 1H, H_8), 2.47 (t, $J = 7.3$ Hz, 2H, H_4), 2.40 (d, $J = 7.0$ Hz, 2H, H_7), 2.21 (s, 3H, H_6), 2.12 – 2.03 (m, 2H, H_{9a}), 1.95 – 1.87 (app hex, $J = 9.2$ Hz, 1H, H_{10a}), 1.87 – 1.75 (m, 1H, H_{10b}), 1.67 (app p, $J = 9.1$ Hz, 2H, H_{9b}), 1.28 (t, $J = 7.1$ Hz, 3H, H_1); **$^{13}\text{C NMR}$** (176 MHz, CDCl_3) δ (ppm) 172.8 (C_3), 63.9 (C_7), 60.4 (C_2), 53.0 (C_5), 42.3 (C_6), 34.0 (C_8), 32.5 (C_4), 27.5 (C_9), 18.8 (C_{10}), 14.2 (C_1); **HMRS-ESI** (m/z): found $[\text{M}+\text{H}]^+$ 200.1646, $\text{C}_{11}\text{H}_{22}\text{NO}_2$ requires 200.1651.

***N*-(Cyclobutylmethyl)-*N*-methyl-3-(5-methylfuran-2-yl)propan-1-amine**

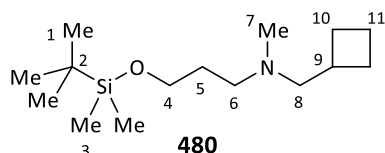


To a solution of methylamine hydrochloride (10.1 g, 150 mmol) in MeOH (100 mL), KOH (8.40 g, 150 mmol) was added portionwise while stirring at 0 °C. (Bromomethyl)cyclobutane (5.60 mL, 50.0 mmol) was added to the resultant

mixture and the reaction was heated to 50 °C for 15 h. The reaction was quenched with aq HCl (3 M, 30 mL) and volatiles were evaporated *in vacuo*. The resultant aqueous layer was basified with aq NaOH until a basic pH > 12 was reached, and extracted with Et₂O (3 x 30 mL). The organic layers were combined, dried over MgSO₄, filtered and concentrated *in vacuo*. 7.5 mmol of the resultant crude amine were used without further purification in General procedure D with 3-(5-methylfuran-2-yl)propanal (1.33 mL, 10.0 mmol), AcOH (430 μL , 7.5 mmol) and NaBH(OAc)₃ (2.54 g, 12.0 mmol) in DCM (30 mL). Purification by column chromatography (DCM to 4% NH₃(MeOH; 2M)) provided the title compound as a yellow oil (862 mg, 3.90 mmol, 52% yield).

IR $\nu_{\text{max}}/\text{cm}^{-1}$ (thin film) 2945, 2783, 1569, 1453, 1219, 1018, 775; **$^1\text{H NMR}$** (700 MHz, CDCl_3) δ (ppm) 5.86 (m, 2H, $\text{H}_{3,4}$), 2.59 (t, $J = 7.5$ Hz, 2H, H_6), 2.56 – 2.48 (app hept, $J = 7.2$ Hz, 1H, H_{11}), 2.39 (d, $J = 7.0$ Hz, 2H, H_{10}), 2.36 (t, $J = 7.4$ Hz, 2H, H_8), 2.27 (s, 3H, H_1), 2.21 (s, 3H, H_9), 2.11 – 2.03 (m, 2H, H_{12a}), 1.95 – 1.88 (m, 1H, H_{13a}), 1.85 – 1.76 (m, 3H, $\text{H}_{7,13b}$), 1.68 (p, $J = 9.0$ Hz, 2H, H_{12b}); **$^{13}\text{C NMR}$** (176 MHz, CDCl_3) δ (ppm) 154.3 (C_5), 150.1 (C_2), 105.7 (C_3), 105.3 (C_4), 64.2 (C_{10}), 57.3 (C_8), 42.7 (C_9), 34.2 (C_{11}), 27.6 (C_{12}), 26.0 (C_6), 25.8 (C_7), 18.8 (C_{13}), 13.5 (C_1); **HMRS-ESI** (m/z): found $[\text{M}+\text{H}]^+$ 222.1858, $\text{C}_{14}\text{H}_{24}\text{NO}$ requires 222.1858.

3-((*tert*-Butyldimethylsilyloxy)-*N*-(cyclobutylmethyl)-*N*-methylpropan-1-amine



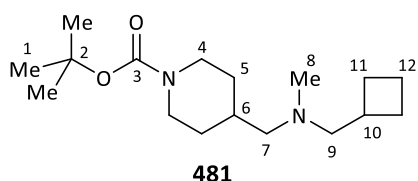
To a solution of methylamine hydrochloride (10.1 g, 150 mmol) in MeOH (100 mL), KOH (8.40 g, 150 mmol) was added portionwise while stirring at 0 °C. (Bromomethyl)cyclobutane (5.60 mL, 50.0 mmol) was added to the

resultant mixture and the reaction was heated to 50 °C for 15 h. The reaction was quenched with aq HCl (3 M, 30 mL) and volatiles were evaporated *in vacuo*. The resultant aqueous layer was basified with aq NaOH until a basic pH > 12 was reached, and extracted with Et₂O (3 x 30 mL). The organic layers were combined, dried over MgSO₄, filtered and concentrated *in vacuo*. 12.0 mmol of the resultant crude amine were used without further purification in General procedure I with (3-bromopropoxy)(*tert*-butyl)dimethylsilane (2.32 mL, 10.0

mmol) and DIPEA (2.62 mL, 15.0 mmol) in MeCN (20 mL). Purification by column chromatography (DCM to 4% $\text{NH}_3(\text{MeOH}; 2\text{M})$) provided the title compound as a colourless oil (1.62 g, 5.97 mmol, 60% yield).

IR $\nu_{\text{max}}/\text{cm}^{-1}$ (thin film) 2952, 2856, 1462, 1251, 1096, 832, 772; **$^1\text{H NMR}$** (700 MHz, CDCl_3) δ (ppm) 3.66 (t, $J = 6.4$ Hz, 2H, H_4), 2.56 – 2.48 (m, 1H, H_9), 2.42 – 2.36 (m, 4H, $\text{H}_{6,8}$), 2.19 (s, 3H, H_7), 2.11 – 2.04 (m, 2H, H_{10a}), 1.95 – 1.87 (m, 1H, H_{11a}), 1.85 – 1.79 (m, 1H, H_{11b}), 1.72 – 1.64 (m, 4H, $\text{H}_{5,10b}$), 0.91 (s, 9H, H_1), 0.07 (s, 6H, H_3); **$^{13}\text{C NMR}$** (176 MHz, CDCl_3) δ (ppm) 64.3 (C_8), 61.6 (C_4), 54.6 (C_6), 42.7 (C_7), 34.2 (C_9), 30.5 (C_5), 27.7 (C_{10}), 26.0 (C_1), 18.8 (C_{11}), 18.3 (C_2), -5.3 (C_3); **HMRS-ESI** (m/z): found $[\text{M}+\text{H}]^+$ 272.2409, $\text{C}_{15}\text{H}_{34}\text{NOSi}$ requires 272.2410.

***tert*-Butyl 4-(((cyclobutylmethyl)(methyl)amino)methyl)piperidine-1-carboxylate**

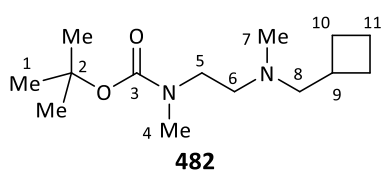


General procedure I was applied to *tert*-butyl 4-((methylamino)methyl)piperidine-1-carboxylate (1.00 g, 4.4 mmol) with (bromomethyl)cyclobutane (740 μL , 6.6 mmol) and K_2CO_3 (912 mg, 6.6 mmol) in MeCN (10 mL) to provide by column chromatography (DCM to 5% $\text{NH}_3(\text{MeOH}; 2\text{M})$) the

title compound as a colourless oil (904 mg, 3.05 mmol, 70% yield).

IR $\nu_{\text{max}}/\text{cm}^{-1}$ (thin film) 2927, 2846, 2781, 1690, 1419, 1238, 1158; **$^1\text{H NMR}$** (700 MHz, CDCl_3) δ (ppm) 4.08 (br s, 2H, H_{4a}), 2.71 (br s, 2H, H_{4b}), 2.49 (hept, $J = 7.6$ Hz, 1H, H_{10}), 2.34 (d, $J = 7.1$ Hz, 2H, H_9), 2.17 (s, 3H, H_8), 2.12 (d, $J = 7.1$ Hz, 2H, H_7), 2.09 – 2.02 (m, 2H, H_{11a}), 1.94 – 1.86 (m, 1H, H_{12a}), 1.86 – 1.78 (m, 1H, H_{12b}), 1.73 (br d, $J = 13.0$ Hz, 2H, H_{5a}), 1.70 – 1.63 (m, 2H, H_{11b}), 1.63 – 1.55 (m, 1H, H_6), 1.47 (s, 9H, H_1), 1.10 – 1.00 (m, 2H, H_{5b}); **$^{13}\text{C NMR}$** (176 MHz, CDCl_3) δ (ppm) 154.9 (C_3), 79.2 (C_2), 64.8 (C_9), 64.2 (C_7), 43.4 (C_8), 34.4 (C_6), 34.2 (C_{10}), 30.8 (C_5), 28.5 (C_1), 27.5 (C_{11}), 18.8 (C_{12}), C_4 not observed; **HMRS-ESI** (m/z): found $[\text{M}+\text{H}]^+$ 297.2538, $\text{C}_{17}\text{H}_{33}\text{N}_2\text{O}_2$ requires 297.2542.

***tert*-Butyl (2-((cyclobutylmethyl)(methyl)amino)ethyl)(methyl)carbamate**



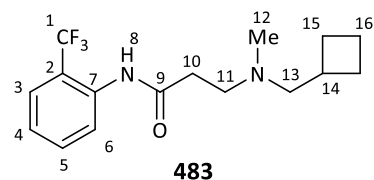
N^1, N^2 -dimethylethane-1,2-diamine (8.00 mL, 75.0 mmol) was added to a solution of Boc_2O (5.46 g, 25.0 mmol) and Et_3N (3.48 mL, 25.0 mmol) in DCM (100 mL) at 0 °C. The resultant mixture was warmed to rt and stirred for 15 h. After this time, the organic layer was washed with aq NaOH (2.5 M, 2 x

50 mL), dried over MgSO_4 , filtered and concentrated *in vacuo*. The crude mixture was used without further purification in General procedure I with (bromomethyl)cyclobutane (2.80 mL, 25.0 mmol) and DIPEA (5.24 mL, 30.0 mmol) in MeCN (50 mL). Purification by column chromatography (DCM to 3% $\text{NH}_3(\text{MeOH}; 2\text{M})$) provided the title compound as a colourless oil (600 mg, 2.34 mmol, 9% yield).

IR $\nu_{\text{max}}/\text{cm}^{-1}$ (thin film) 2971, 2931, 2781, 1692, 1389, 1159; **$^1\text{H NMR}$** (700 MHz, CDCl_3) δ (ppm) 3.30 (m, 2H, H_5), 2.88 (s, 3H, H_4), 2.56 – 2.45 (m, 3H, $\text{H}_{6,9}$), 2.42 (d, $J = 7.0$ Hz, 2H, H_8), 2.24 (s, 3H, H_7), 2.12 – 2.02 (m, 2H, H_{10a}), 1.95 – 1.87 (m, 1H, H_{11a}), 1.86 – 1.80 (m, 1H, H_{11b}), 1.71 – 1.64 (m, 2H, H_{10b}), 1.48 (s, 9H, H_1); **$^{13}\text{C NMR}$**

(126 MHz, CDCl₃) δ (ppm) 155.7 (C₃), 79.2 (C₂), 64.5 (C₈), 55.4 (C₆), 47.0 (C₅), 42.9 (C₇), 34.6 (C₄), 34.2 (C₉), 28.5 (C₁), 27.5 (C₁₀), 18.8 (C₁₁); **HMRS-ESI** (m/z): found [M+H]⁺ 257.2220, C₁₄H₂₉N₂O₂ requires 257.2229.

3-((Cyclobutylmethyl)(methyl)amino)-N-(2-(trifluoromethyl)phenyl)propenamide

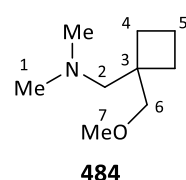


General procedure I was applied to methylamine (12.0 mL, 24.0 mmol, 2 M in THF) with 3-chloro-N-(2-(trifluoromethyl)phenyl)propenamide (2.51 g, 10.0 mmol) in MeCN (50 mL). The resultant crude amine was used without further purification in General procedure I with (bromomethyl)cyclobutane

(1.35 mL, 12.0 mmol) and DIPEA (2.10 mL, 12.0 mmol) in MeCN (20 mL). Purification by column chromatography (DCM to 5% NH₃(MeOH; 2M)) provided the title compound as a colourless oil (1.49 g, 4.74 mmol, 47% yield).

IR ν_{\max} /cm⁻¹ (thin film) 2958, 2855, 2800, 1689, 1587, 1532, 1454, 1318, 1278, 1165, 1108, 759; **¹H NMR** (700 MHz, CDCl₃) δ (ppm) 11.17 (br s, 1H, H₈), 8.06 (d, *J* = 8.2 Hz, 1H, H₃), 7.62 (d, *J* = 7.9 Hz, 1H, H₆), 7.55 (t, *J* = 7.8 Hz, 1H, H₅), 7.22 (t, *J* = 7.6 Hz, 1H, H₄), 2.73 – 2.68 (m, 2H, H₁₁), 2.62 – 2.55 (m, 3H, H_{10,14}), 2.53 (d, *J* = 6.9 Hz, 2H, H₁₃), 2.32 (s, 3H, H₁₂), 2.05 – 1.99 (m, 2H, H_{15a}), 1.88 (app hex, *J* = 9.1 Hz, 1H, H_{16a}), 1.81 – 1.75 (m, 1H, H_{16b}), 1.70 – 1.62 (m, 2H, H_{15b}); **¹³C NMR** (176 MHz, CDCl₃) δ (ppm) 171.5 (C₉), 135.7 (C₇), 132.4 (C₅), 126.2 (C₆), 125.9 (q, *J* = 5.4 Hz, C₃), 124.2 (C₄), 123.9 (q, *J* = 273.0 Hz, C₁), 121.6 (q, *J* = 29.5 Hz, C₂), 63.1 (C₁₃), 52.7 (C₁₁), 41.5 (C₁₂), 33.2 (C₁₀), 33.0 (C₁₄), 27.8 (C₁₅), 18.7 (C₁₆); **¹⁹F NMR** (376 MHz, CDCl₃) δ (ppm) –61.4 (s); **HMRS-ESI** (m/z): found [M+H]⁺ 315.1682, C₁₆H₂₂F₃N₂O requires 315.1684.

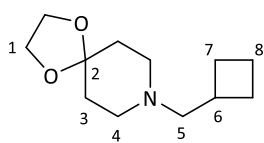
1-(1-(Methoxymethyl)cyclobutyl)-N,N-dimethylmethanamine



To a solution of 1-(methoxymethyl)cyclobutylmethanamine (1.00 g, 6.00 mmol) and aq formaldehyde (37%, 2.23 mL, 30.0 mmol) in MeOH (12 mL) under N₂ at 0 °C was added NaBH₃CN (1.51 g, 24.0 mmol). The resultant mixture was stirred at rt for 15 h. The reaction was quenched with aq HCl (3 M, 15 mL) and concentrated *in vacuo*. DCM was added (50 mL)

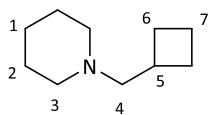
and the organic layer was washed with NaOH (2.5 M, 2 x 50 mL), dried over MgSO₄, filtered and concentrated *in vacuo*. Purification by column chromatography (DCM to 5% NH₃(MeOH; 2M)) provided the title compound as a colourless oil (577 mg, 3.67 mmol, 61% yield).

IR ν_{\max} /cm⁻¹ (thin film) 2973, 2938, 2871, 2814, 2763, 1456, 1108, 1032; **¹H NMR** (700 MHz, CDCl₃) δ (ppm) 3.46 (s, 2H, H₆), 3.41 (s, 3H, H₇), 2.37 (s, 2H, H₂), 2.22 (s, 6H, H₁), 1.97 – 1.77 (m, 6H, H_{4,5}); **¹³C NMR** (176 MHz, CDCl₃) δ (ppm) 76.7 (C₆), 66.3 (C₂), 59.3 (C₇), 47.2 (C₁), 42.5 (C₃), 28.7 (C₄), 16.0 (C₅); **HMRS-ESI** (m/z): found [M+H]⁺ 158.1546, C₉H₂₀NO requires 158.1545.

8-(Cyclobutylmethyl)-1,4-dioxo-8-azaspiro[4.5]decane**485**

General procedure I was applied to 1,4-dioxo-8-azaspiro[4.5]decane (1.28 mL, 10.0 mmol) with (bromomethyl)cyclobutane (1.23 mL, 11.0 mmol) and DIPEA (2.62 mL, 15.0 mmol) in MeCN (25 mL) to provide by column chromatography (DCM to 5% $\text{NH}_3(\text{MeOH}; 2\text{M})$) the title compound as a yellow oil (1.16 g, 5.50 mmol, 55% yield).

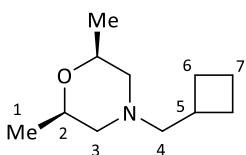
IR $\nu_{\text{max}}/\text{cm}^{-1}$ (thin film) 2953, 2873, 2807, 1307, 1089, 1039, 915; **$^1\text{H NMR}$** (700 MHz, CDCl_3) δ (ppm) 3.96 (s, 4H, H_1), 2.60 – 2.45 (m, 5H, $\text{H}_{4,6}$), 2.44 (d, $J = 6.7$ Hz, 2H, H_5), 2.12 – 2.03 (m, 2H, H_{7a}), 1.94 – 1.85 (m, 1H, H_{8a}), 1.85 – 1.77 (m, 1H, H_{8b}), 1.76 – 1.72 (m, 4H, H_3), 1.72 – 1.65 (m, 2H, H_{7b}); **$^{13}\text{C NMR}$** (176 MHz, CDCl_3) δ (ppm) 107.3 (C_2), 65.0 (C_5), 64.2 (C_1), 51.4 (C_4), 34.8 (C_3), 34.3 (C_6), 28.1 (C_7), 18.8 (C_8); **HMRS-ESI** (m/z): found $[\text{M}+\text{H}]^+$ 212.1652, $\text{C}_{11}\text{H}_{22}\text{NO}_2$ requires 212.1651.

1-(Cyclobutylmethyl)piperidine**486**

General procedure G was applied to piperidine (1.98 mL, 20.0 mmol) with cyclobutanecarboxylic acid (2.00 mL, 21.0 mmol), DIPEA (5.24 mL, 30.0 mmol), HOBt hydrate (4.00 g, 30.0 mmol) and EDC·HCl (4.22 g, 22.0 mmol) in DCM (40 mL). The resultant crude amide

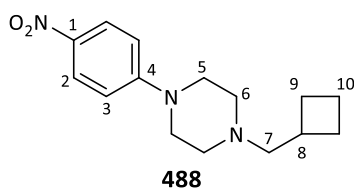
was used without further purification in General procedure H with LiAlH_4 (1.52 g, 40.0 mmol) in Et_2O (60 mL). Purification by distillation at 100 °C under 30 mbar provided the title compound as a colourless oil (2.33 g, 15.2 mmol, 76% yield).

IR $\nu_{\text{max}}/\text{cm}^{-1}$ (thin film) 2931, 2854, 2756, 1442, 1154, 1125, 1038, 995; **$^1\text{H NMR}$** (600 MHz, CDCl_3) δ (ppm) 2.56 (app hept, $J = 7.6$ Hz, 1H, H_5), 2.38 (d, $J = 6.7$ Hz, 2H, H_4), 2.34 (br s, 4H, H_3), 2.11 – 2.02 (m, 2H, H_{6a}), 1.89 (app hept, $J = 8.8$ Hz, 1H, H_{7a}), 1.82 – 1.75 (m, 1H, H_{7b}), 1.68 (pd, $J = 8.9, 2.1$ Hz, 2H, H_{6b}), 1.57 (app p, $J = 5.6$ Hz, 4H, H_2), 1.47 – 1.35 (m, 2H, H_1); **$^{13}\text{C NMR}$** (151 MHz, CDCl_3) δ (ppm) 66.2 (C_4), 54.6 (C_3), 34.2 (C_5), 28.3 (C_6), 25.9 (C_2), 24.3 (C_1), 18.8 (C_7); **HMRS-ESI** (m/z): found $[\text{M}+\text{H}]^+$ 154.1588, $\text{C}_{10}\text{H}_{20}\text{N}$ requires 154.1590.

(2S,6R)-4-(Cyclobutylmethyl)-2,6-dimethylmorpholine**487**

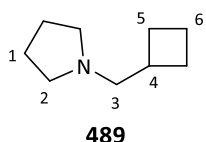
General procedure I was applied to (2R,6S)-2,6-dimethylmorpholine (1.23 mL, 10.0 mmol) with (bromomethyl)cyclobutane (1.23 mL, 11.0 mmol) and DIPEA (2.62 mL, 15.0 mmol) in MeCN (25 mL) to provide by column chromatography (DCM to 5% $\text{NH}_3(\text{MeOH}; 2\text{M})$) the title compound as a yellow oil (1.01 g, 5.51 mmol, 55% yield).

IR $\nu_{\text{max}}/\text{cm}^{-1}$ (thin film) 2969, 2931, 2865, 1455, 1373, 1322, 1143, 1083; **$^1\text{H NMR}$** (700 MHz, CDCl_3) δ (ppm) 3.71 – 3.62 (m, 2H, H_2), 2.67 (d, $J = 11.2$ Hz, 2H, H_{3a}), 2.55 (hept, $J = 7.0$ Hz, 1H, H_5), 2.38 (d, $J = 6.8$ Hz, 2H, H_4), 2.12 – 2.02 (m, 2H, H_{6a}), 1.95 – 1.86 (m, 1H, H_{7a}), 1.86 – 1.78 (m, 1H, H_{7b}), 1.74 – 1.65 (m, 4H, $\text{H}_{3b,6b}$), 1.15 (d, $J = 6.2$ Hz, 6H, H_1); **$^{13}\text{C NMR}$** (176 MHz, CDCl_3) δ (ppm) 71.6 (C_2), 65.3 (C_4), 59.7 (C_3), 33.7 (C_5), 27.9 (C_6), 19.2 (C_1), 18.9 (C_7); **HMRS-ESI** (m/z): found $[\text{M}+\text{H}]^+$ 184.1698, $\text{C}_{11}\text{H}_{22}\text{NO}$ requires 184.1701.

1-(Cyclobutylmethyl)-4-(4-nitrophenyl)piperazine

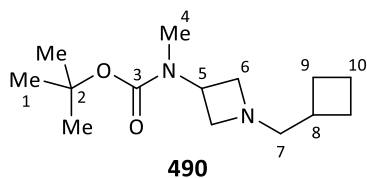
General procedure I was applied to 1-(4-nitrophenyl)piperazine (2.07 g, 10.0 mmol) with (bromomethyl)cyclobutane (1.12 mL, 10.0 mmol) and DIPEA (2.10 mL, 12.0 mmol) in MeCN (20.0 mL) to provide by column chromatography (DCM to 3% $\text{NH}_3(\text{MeOH}; 2\text{M})$) the title compound as a yellow solid (1.46 g, 5.30 mmol, 53% yield).

mp ($^{\circ}\text{C}$) 88–90; **IR** $\nu_{\text{max}}/\text{cm}^{-1}$ (thin film) 2922, 1588, 1492, 1324, 1239, 1114, 1002, 923, 823; **$^1\text{H NMR}$** (700 MHz, CDCl_3) δ (ppm) 8.13 (d, $J = 9.1$ Hz, 2H, H_2), 6.82 (d, $J = 9.1$ Hz, 2H, H_3), 3.42 (br s, $J = 4.1$ Hz, 4H, H_5), 2.62–2.52 (m, 5H, $\text{H}_{6,8}$), 2.47 (d, $J = 6.9$ Hz, 2H, H_7), 2.15–2.06 (m, 2H, H_{9a}), 1.98–1.89 (app hex, $J = 9.3$ Hz, 1H, H_{10a}), 1.88–1.80 (m, 1H, H_{10b}), 1.73 (app p, $J = 9.2$ Hz, 2H, H_{9b}); **$^{13}\text{C NMR}$** (176 MHz, CDCl_3) δ (ppm) 154.9 (C_4), 138.3 (C_1), 125.9 (C_2), 112.5 (C_3), 65.0 (C_7), 52.8 (C_6), 47.0 (C_5), 33.7 (C_8), 27.8 (C_9), 18.9 (C_{10}); **HMRS-ESI** (m/z): found $[\text{M}+\text{H}]^+$ 276.1711, $\text{C}_{15}\text{H}_{22}\text{N}_3\text{O}_2$ requires 276.1712.

1-(Cyclobutylmethyl)pyrrolidine

General procedure G was applied to pyrrolidine (3.51 mL, 42.0 mmol) with cyclobutanecarboxylic acid (3.81 mL, 40.0 mmol), DIPEA (10.5 mL, 60.0 mmol), HOBt hydrate (8.00 g, 60.0 mmol) and EDC·HCl (8.43 g, 44.0 mmol) in DCM (100 mL). The resultant crude amide was used without further purification in General procedure H with LiAlH_4 (3.03 g, 80.0 mmol) in Et_2O (80 mL). Purification by distillation at 100 $^{\circ}\text{C}$ under 50 mbar provided the title compound as a colourless oil (4.32 g, 31.0 mmol, 78% yield).

IR $\nu_{\text{max}}/\text{cm}^{-1}$ (thin film) 2964, 2777, 1459, 1315, 1150; **$^1\text{H NMR}$** (600 MHz, CDCl_3) δ (ppm) 2.59–2.50 (m, 1H, H_4), 2.49–2.43 (m, 6H, $\text{H}_{2,3}$), 2.12–2.03 (m, 2H, H_{5a}), 1.94–1.85 (m, 1H, H_{6a}), 1.84–1.66 (m, 7H, $\text{H}_{1,5b,6b}$); **$^{13}\text{C NMR}$** (101 MHz, CDCl_3) δ (ppm) 63.2 (C_3), 54.5 (C_2), 35.6 (C_4), 27.7 (C_5), 23.4 (C_1), 18.7 (C_6); **HMRS-ESI** (m/z): found $[\text{M}+\text{H}]^+$ 140.1428, $\text{C}_9\text{H}_{18}\text{N}$ requires 140.1439.

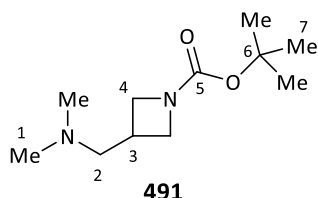
***tert*-Butyl (1-(cyclobutylmethyl)azetidin-3-yl)(methyl)carbamate**

General procedure I was applied to *tert*-butyl azetidin-3-yl(methyl)carbamate hydrochloride (2.23 g, 10.0 mmol) with (bromomethyl)cyclobutane (1.18 mL, 10.5 mmol) and DIPEA (4.36 mL, 25.0 mmol) in MeCN (30 mL) to provide by column chromatography (DCM to 4% $\text{NH}_3(\text{MeOH}; 2)$) the title compound as a colourless oil (792 mg, 3.11 mmol, 31% yield).

IR $\nu_{\text{max}}/\text{cm}^{-1}$ (thin film) 2970, 2931, 1693, 1364, 1331, 1148; **$^1\text{H NMR}$** (700 MHz, CDCl_3) δ (ppm) 3.57 (t, $J = 6.9$ Hz, 2H, H_{6a}), 2.92 (br s, 2H, H_{6b}), 2.82 (s, 3H, H_4), 2.47 (d, $J = 7.1$ Hz, 2H, H_7), 2.35 (app hept, $J = 7.2$ Hz, 1H, H_8), 2.07–2.00 (m, 2H, H_{9a}), 1.94–1.85 (m, 2H, $\text{H}_{5,10a}$), 1.85–1.77 (m, 1H, H_{10b}), 1.68 (p, $J = 9.0$ Hz, 2H, H_{9b}), 1.45

(s, 9H, H₁); ¹³C NMR (176 MHz, CDCl₃) δ (ppm) 155.5 (C₃), 79.7 (C₂), 66.1 (C₇), 60.1 (C₆), 34.4 (C₈), 30.4 (C₄), 28.4 (C₁), 28.3 (C₅), 27.0 (C₉), 18.9 (C₁₀); HMRS-ESI (m/z): found [M+Na]⁺ 277.1878, C₁₄H₂₇N₂O₂ requires 277.1886.

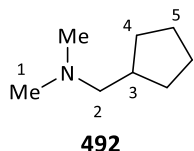
tert-Butyl 3-((dimethylamino)methyl)azetidine-1-carboxylate



To a solution of *tert*-butyl 3-(aminomethyl)azetidine-1-carboxylate (1.86 g, 10.0 mmol) and aq formaldehyde (37%, 3.00 mL, 40.0 mmol) in EtOH (50 mL) under N₂ at 0 °C was added NaBH₃CN (2.51 g, 40.0 mmol). The resultant mixture was stirred at rt for 48 h. The reaction was quenched with aq NaOH (2.5 M, 10 mL) and concentrated *in vacuo*. DCM was added (50 mL) and the organic layer was washed with NaOH (0.5 M, 2 x 50 mL), dried over MgSO₄, filtered and concentrated *in vacuo*. The crude product was crystallised as white needles in a 9:1 mixture of EtOAc:PE (0.89 g, 4.2 mmol, 42% yield).

mp (°C) 114–116; **IR** ν_{max}/cm⁻¹ (thin film) 2652, 2338, 2182, 1695, 1382, 1125; ¹H NMR (600 MHz, CDCl₃) δ (ppm) 4.20 (t, *J* = 8.8 Hz, 2H, H_{4a}), 3.77 (dd, *J* = 8.8, 5.6 Hz, 2H, H_{4b}), 3.37 (d, *J* = 7.2 Hz, 2H, H₂), 3.14 – 3.02 (m, 1H, H₃), 2.87 (s, 6H, H₁), 1.46 (s, 9H, H₇); ¹³C NMR (101 MHz, DMSO-*d*₆) δ (ppm) 155.8 (C₅), 79.2 (C₆), 59.6 (C₂), 53.4 (br s, C_{4a}), 52.4 (br s, C_{4b}), 42.7 (C₁), 28.5 (C₇), 24.4 (C₃); HMRS-ESI (m/z): found [M+H]⁺ 237.1574, C₁₁H₂₂N₂O₂Na requires 237.1573.

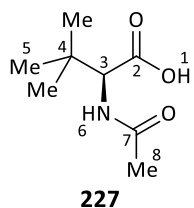
1-Cyclopentyl-*N,N*-dimethylmethanamine



General procedure G was applied to dimethylamine (2.0 M in THF, 10.0 mL, 20.0 mmol) with cyclopentanecarboxylic acid (2.28 mL, 21.0 mmol), DIPEA (5.24 mL, 30.0 mmol), HOBT hydrate (4.00 g, 30.0 mmol) and EDC·HCl (4.22 g, 22.0 mmol) in DCM (50 mL). The resultant crude amide was used without further purification in General procedure H with LiAlH₄ (1.52 g, 40.0 mmol) in Et₂O (60 mL). The title compound was obtained without further purification as a colourless oil (1.67 g, 13.1 mmol, 66% yield).

IR ν_{max}/cm⁻¹ (thin film) 2980, 2942, 1459, 1263, 1100, 1035; ¹H NMR (600 MHz, CDCl₃) δ (ppm) 2.23 (s, 6H, H₁), 2.18 (d, *J* = 7.5 Hz, 2H, H₂), 2.03 (app hept, *J* = 7.7 Hz, 1H, H₃), 1.81 – 1.74 (m, 2H, H_{4a}), 1.65 – 1.58 (m, 1H, H_{5a}), 1.57 – 1.50 (m, 1H, H_{5b}), 1.22 – 1.14 (m, 2H, H_{4b}); ¹³C NMR (101 MHz, CDCl₃) δ (ppm) 66.1 (C₂), 45.9 (C₁), 37.9 (C₃), 31.3 (C₄), 25.3 (C₅); HMRS-ESI (m/z): found [M+H]⁺ 128.1436, C₈H₁₈N requires 128.1439.

(*S*)-2-Acetamido-3,3-dimethylbutanoic acid

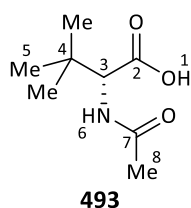


Ac₂O (11.3 mL, 120 mmol) was added to a solution of (*S*)-2-amino-3,3-dimethylbutanoic acid (13.2 g, 100 mmol) in AcOH (100 mL) and stirred for 15 h. After this time, volatiles were removed *in vacuo* and the resultant white solid was washed with Et₂O (150 mL). The solid was dissolved in a hot mixture of MeCN:MeOH (3:1) and allowed to cool down to rt, and

then to $-20\text{ }^{\circ}\text{C}$ for 15 h. The crystalline product was filtered, washed with Et_2O (100 mL) and dried *in vacuo* to provide the title compound as a white solid (13.3 g, 76.9 mmol, 77% yield).

mp ($^{\circ}\text{C}$) 232–233; **IR** $\nu_{\text{max}}/\text{cm}^{-1}$ (thin film) 3352, 2969, 2901, 1700, 1613, 1542, 1254, 1221, 1060, 723; **$^1\text{H NMR}$** (400 MHz, DMSO-d_6) δ (ppm) 12.49 (s, 1H, H_1), 7.93 (d, $J = 8.9\text{ Hz}$, 1H, H_6), 4.10 (d, $J = 8.9\text{ Hz}$, 1H, H_3), 1.89 (s, 3H, H_8), 0.94 (s, 9H, H_5); **$^{13}\text{C NMR}$** (101 MHz, DMSO-d_6) δ (ppm) 173.0 (C_2), 169.8 (C_7), 60.7 (C_3), 33.7 (C_4), 27.1 (C_5), 22.8 (C_8); **HMRS-ESI** (m/z): found $[\text{M-H}]^-$ 172.0982, $\text{C}_8\text{H}_{14}\text{NO}_3$ requires 172.0979; $[\alpha]_{\text{D}}^{25} -3.2$ ($c = 1.0$, EtOH).

(*R*)-2-Acetamido-3,3-dimethylbutanoic acid



Ac_2O (3.40 mL, 36.0 mmol) was added to a solution of (*R*)-2-amino-3,3-dimethylbutanoic acid (3.80 g, 30.0 mmol) in AcOH (30.0 mL) and stirred for 15 h. After this time, the volatiles were removed *in vacuo* and the resultant white solid was washed with Et_2O (50 mL). The solid was dissolved in hot $\text{MeCN}:\text{MeOH}$ (3:1) and cooled down to $-20\text{ }^{\circ}\text{C}$ for 15 h. The

crystalline product was filtered, washed with Et_2O (50 mL) and dried *in vacuo* to provide the title compound as a white solid (4.02 g, 23.2 mmol, 77% yield).

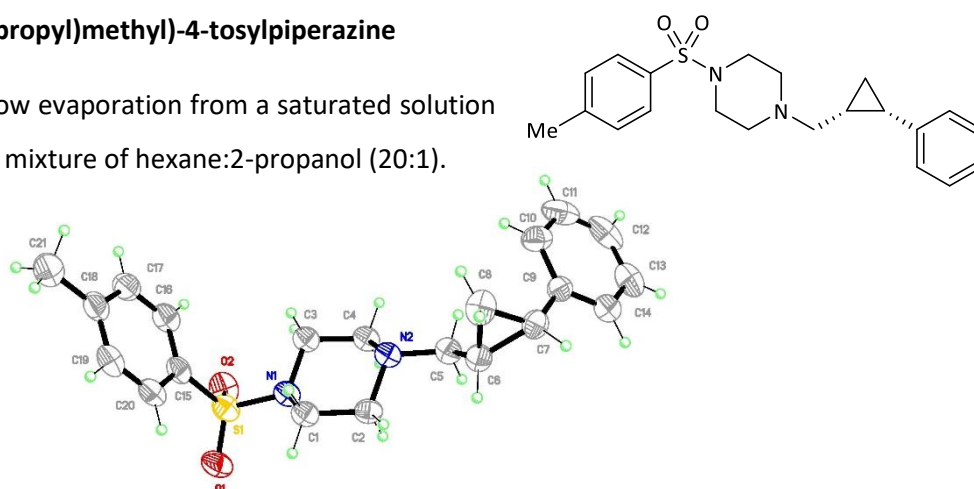
mp ($^{\circ}\text{C}$) 231–232; **IR** $\nu_{\text{max}}/\text{cm}^{-1}$ (thin film) 3352, 2974, 2902, 1700, 1614, 1544, 1404, 1254, 1060, 723; **$^1\text{H NMR}$** (400 MHz, DMSO-d_6) δ (ppm) 12.49 (s, 1H, H_1), 7.93 (d, $J = 8.9\text{ Hz}$, 1H, H_6), 4.10 (d, $J = 8.9\text{ Hz}$, 1H, H_3), 1.89 (s, 3H, H_8), 0.94 (s, 9H, H_5); **$^{13}\text{C NMR}$** (101 MHz, DMSO-d_6) δ (ppm) 173.0 (C_2), 169.8 (C_7), 60.7 (C_3), 33.7 (C_4), 27.1 (C_5), 22.8 (C_8); $[\alpha]_{\text{D}}^{25} +3.0$ ($c = 1.0$, EtOH).

Appendix II – Supplementary Data

II.I. X-Ray Crystallography

1-(((1*R*,2*S*)-2-Phenylcyclopropyl)methyl)-4-tosylpiperazine

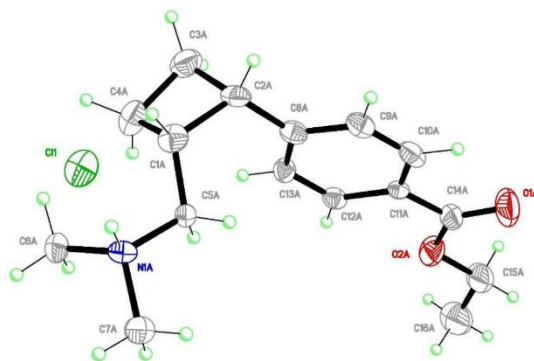
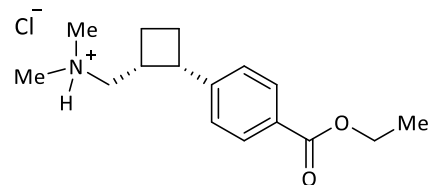
Crystals were grown by slow evaporation from a saturated solution of the title compound in a mixture of hexane:2-propanol (20:1).



Identification code	mg_k1_0010	
Empirical formula	C ₂₁ H ₂₆ N ₂ O ₂ S	
Formula weight	370.50	
Temperature	180(2) K	
Wavelength	0.71073 Å	
Crystal system	Monoclinic	
Space group	P 21	
Unit cell dimensions	a = 9.2198(2) Å	a = 90°.
	b = 6.02920(10) Å	b = 98.1862(9)°.
	c = 17.5266(4) Å	g = 90°.
Volume	964.34(3) Å ³	
Z	2	
Density (calculated)	1.276 Mg/m ³	
Absorption coefficient	0.185 mm ⁻¹	
F(000)	396	
Crystal size	0.500 x 0.250 x 0.150 mm ³	
Theta range for data collection	3.523 to 27.490°.	
Index ranges	-11<=h<=11, -7<=k<=7, -22<=l<=22	
Reflections collected	14403	
Independent reflections	4365 [R(int) = 0.0502]	
Completeness to theta = 25.242°	99.5 %	
Absorption correction	Semi-empirical from equivalents	
Max. and min. transmission	0.959 and 0.765	
Refinement method	Full-matrix least-squares on F ²	
Data / restraints / parameters	4365 / 1 / 236	
Goodness-of-fit on F ²	0.980	
Final R indices [I>2sigma(I)]	R1 = 0.0324, wR2 = 0.0768	
R indices (all data)	R1 = 0.0414, wR2 = 0.0790	
Absolute structure parameter	-0.02(2)	
Extinction coefficient	n/a	
Largest diff. peak and hole	0.145 and -0.270 e.Å ⁻³	

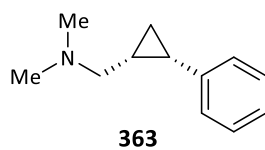
Ethyl 4-((1*S*,2*R*)-2-((dimethylamino)methyl)cyclobutyl)benzoate hydrochloride

Crystals were grown by slow evaporation from a saturated solution of the title compound in a mixture of MeCN:Et₂O (1:2).

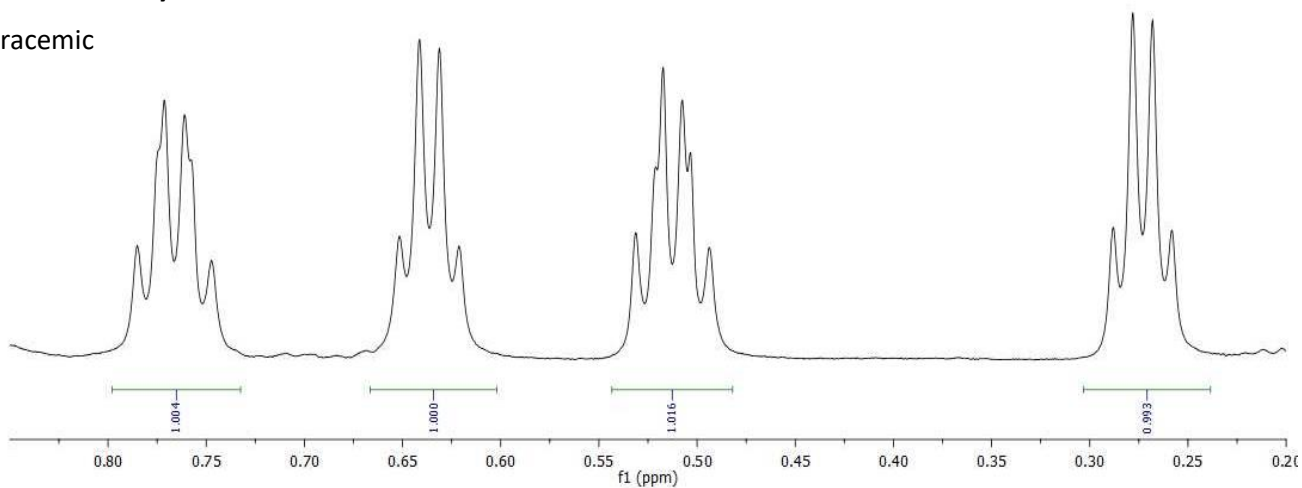
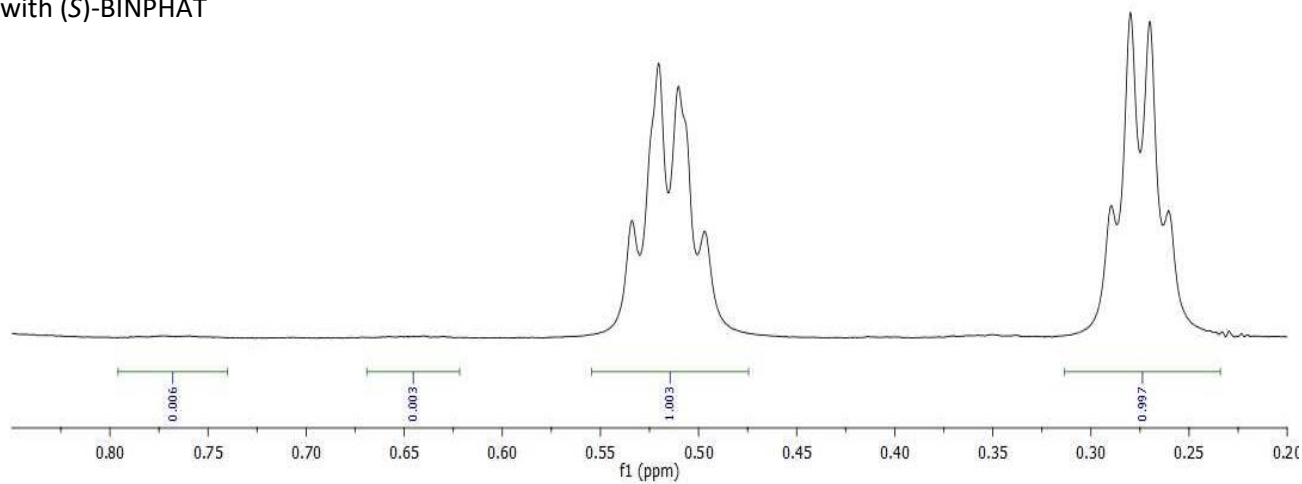
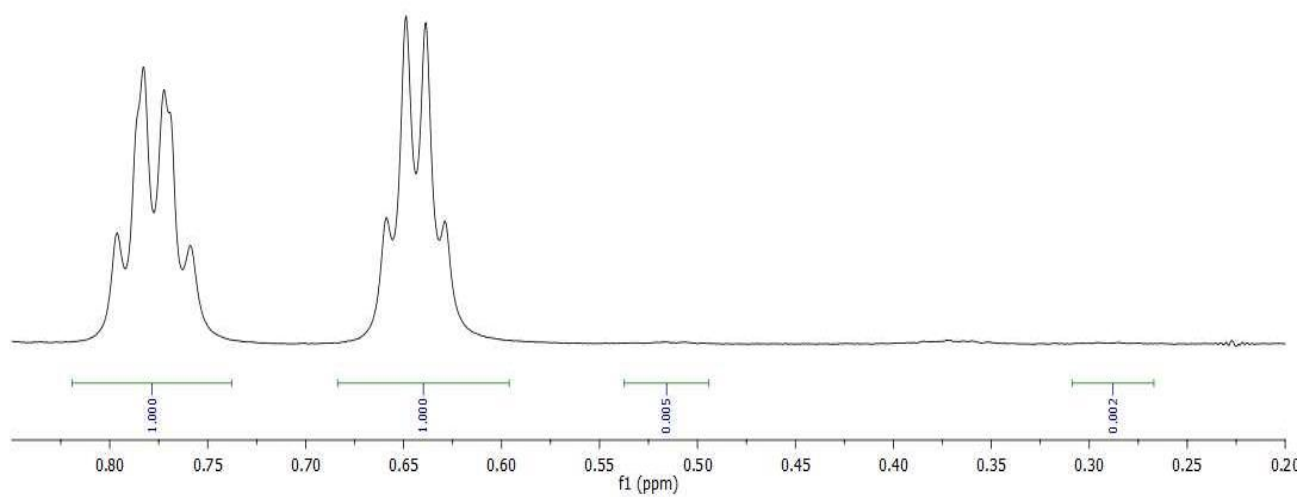


Identification code	mg_k3_0060	
Empirical formula	C ₁₆ H ₂₄ Cl N O ₂	
Formula weight	297.81	
Temperature	180(2) K	
Wavelength	0.71073 Å	
Crystal system	Triclinic	
Space group	P 1	
Unit cell dimensions	a = 11.2519(5) Å	a = 85.667(2)°.
	b = 11.9268(6) Å	b = 77.085(2)°.
	c = 12.4492(7) Å	g = 89.656(3)°.
Volume	1623.65(14) Å ³	
Z	4	
Density (calculated)	1.218 Mg/m ³	
Absorption coefficient	0.237 mm ⁻¹	
F(000)	640	
Crystal size	0.520 x 0.220 x 0.020 mm ³	
Theta range for data collection	3.661 to 25.324°.	
Index ranges	-13<=h<=12, -13<=k<=13, -14<=l<=14	
Reflections collected	15080	
Independent reflections	9384 [R(int) = 0.0773]	
Completeness to theta = 25.242°	96.7 %	
Absorption correction	Semi-empirical from equivalents	
Max. and min. transmission	0.994 and 0.665	
Refinement method	Full-matrix least-squares on F ²	
Data / restraints / parameters	9384 / 273 / 733	
Goodness-of-fit on F ²	1.079	
Final R indices [I>2sigma(I)]	R1 = 0.0786, wR2 = 0.1797	
R indices (all data)	R1 = 0.1114, wR2 = 0.2031	
Absolute structure parameter	0.06(10)	
Extinction coefficient	n/a	
Largest diff. peak and hole	0.787 and -0.280 e.Å ⁻³	

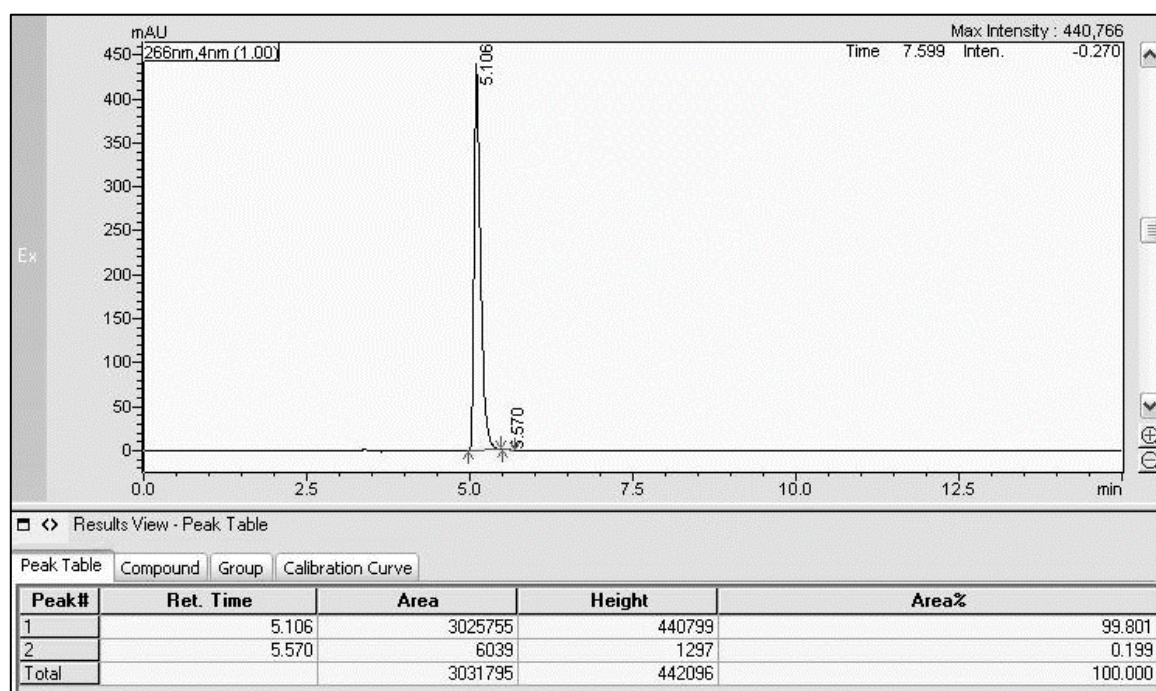
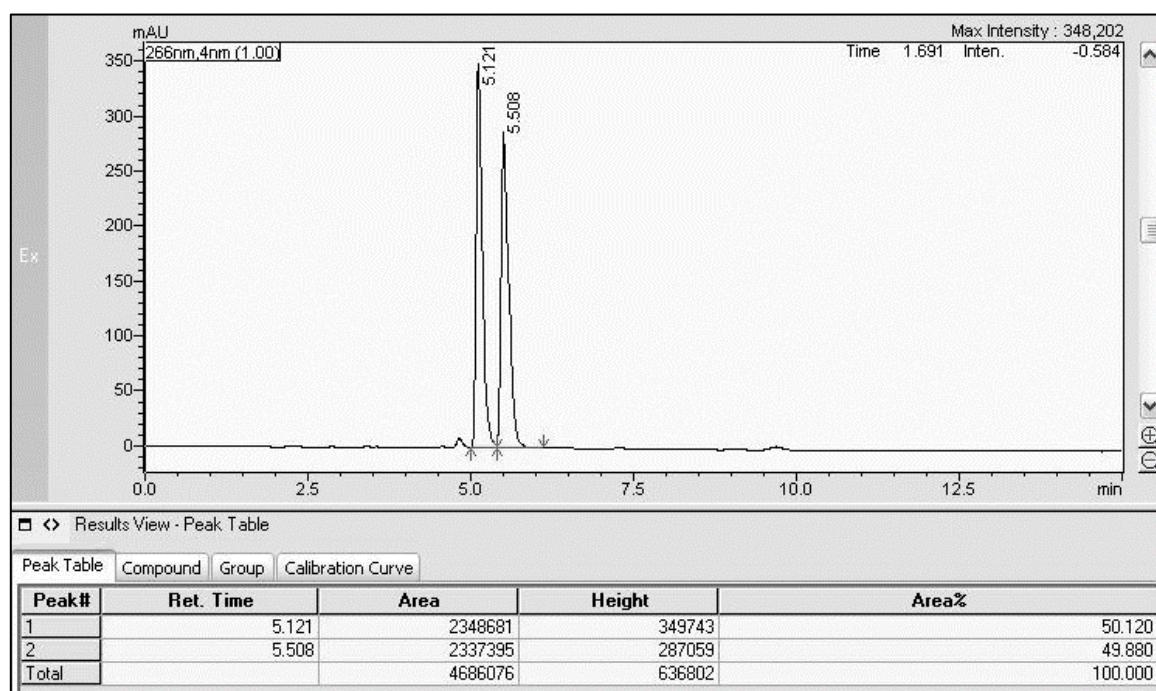
II.II. Asymmetric Analysis

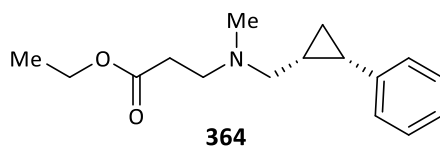
***N,N*-Dimethyl-1-((1*R*,2*S*)-2-phenylcyclopropyl)methanamine****¹H-NMR analysis:**

racemic

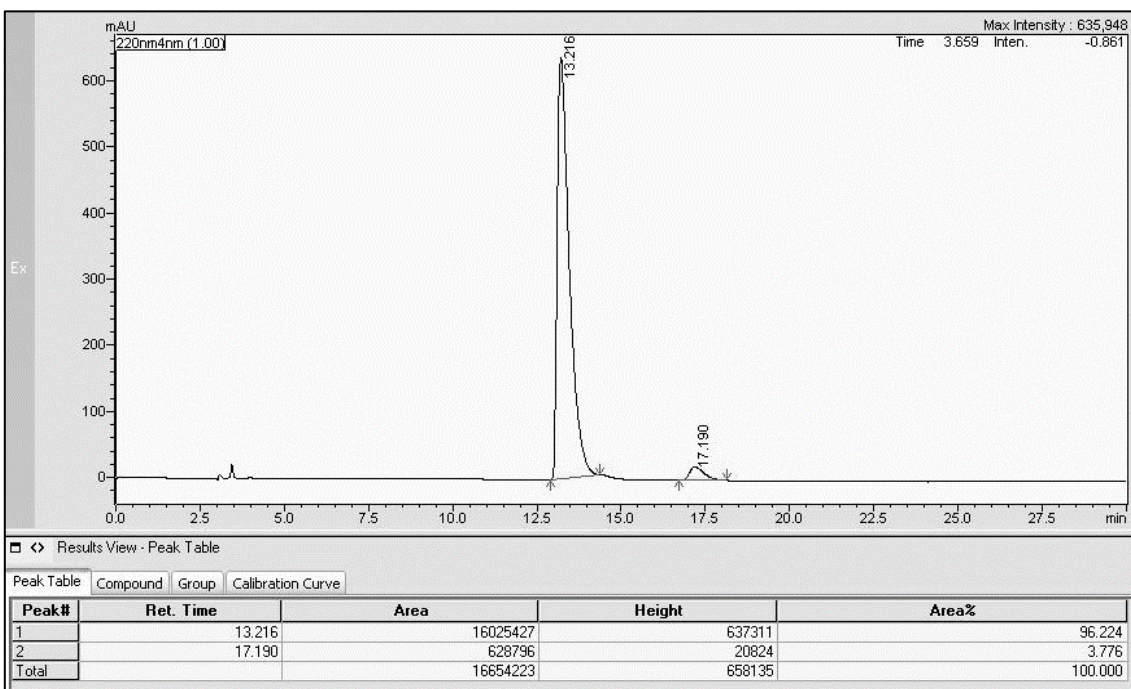
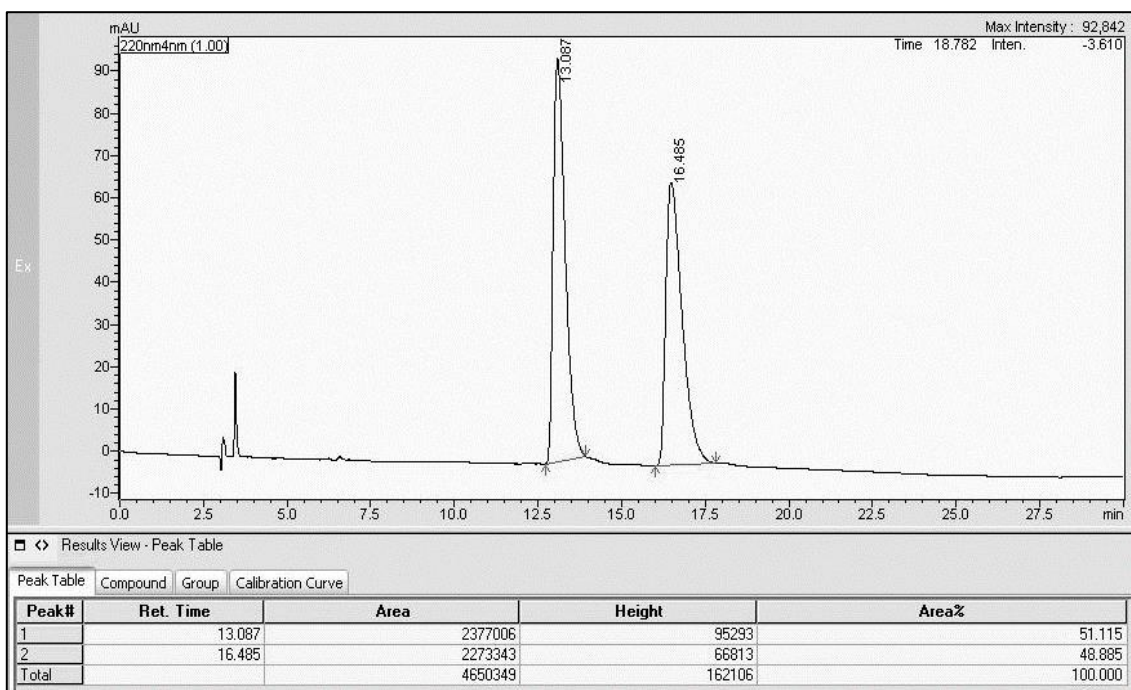
with (*S*)-BINPHATwith (*R*)-BINPHAT

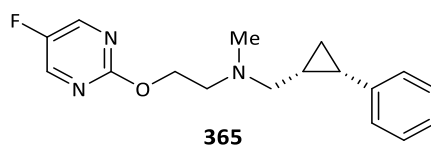
HPLC analysis: Chiralpak AD-H (hexane(0.1% DEA):2-propanol 98:2, 1.0 mL·min⁻¹, 30 °C) t_R = 5.1 min (major, 99.8%), t_R = 5.5 min (minor, 0.2%)



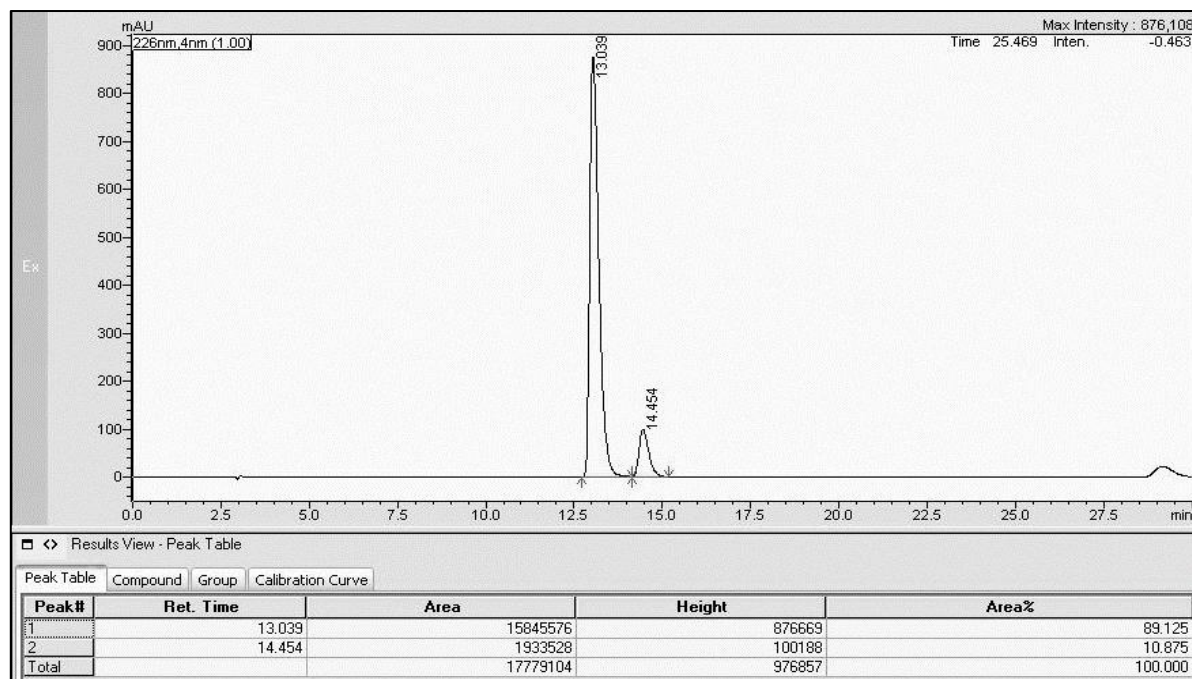
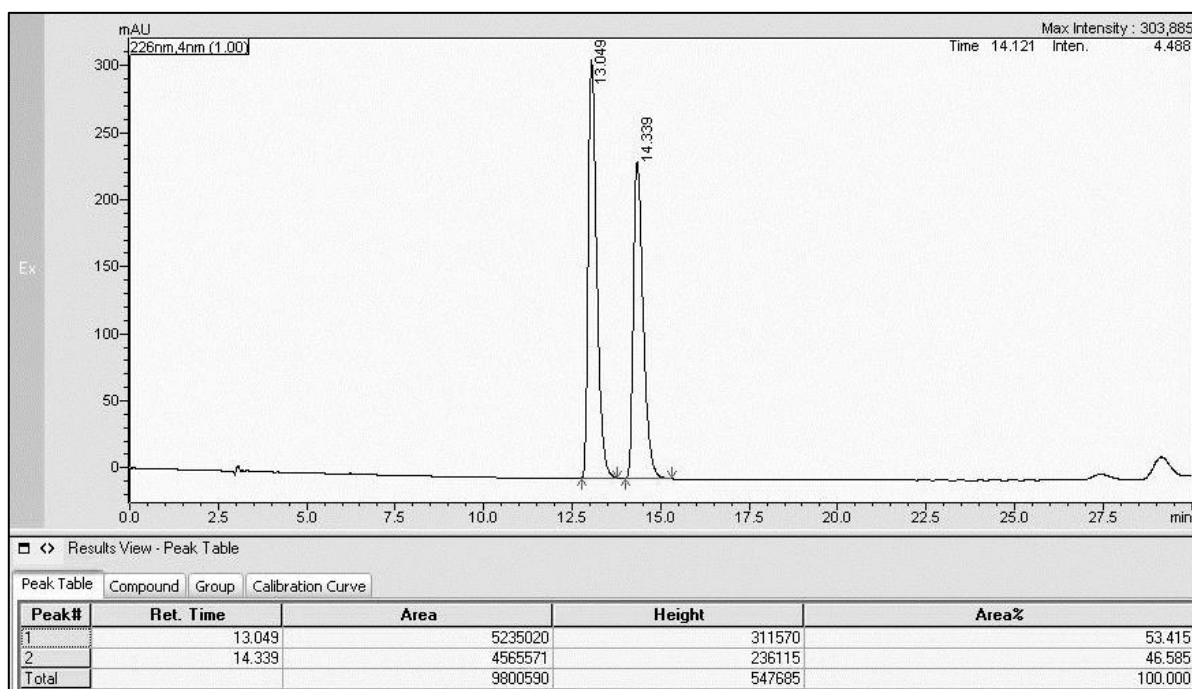
Ethyl 3-(methyl((1*R*,2*S*)-2-phenylcyclopropyl)methyl)amino)propanoate

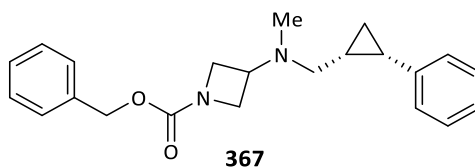
HPLC analysis: Chiralpak AD-H (hexane:2-propanol 99.5:0.5, 1.0 mL·min⁻¹, 30 °C) t_R = 13.1 min (major, 96.2%), t_R = 17.2 min (minor, 3.8%)



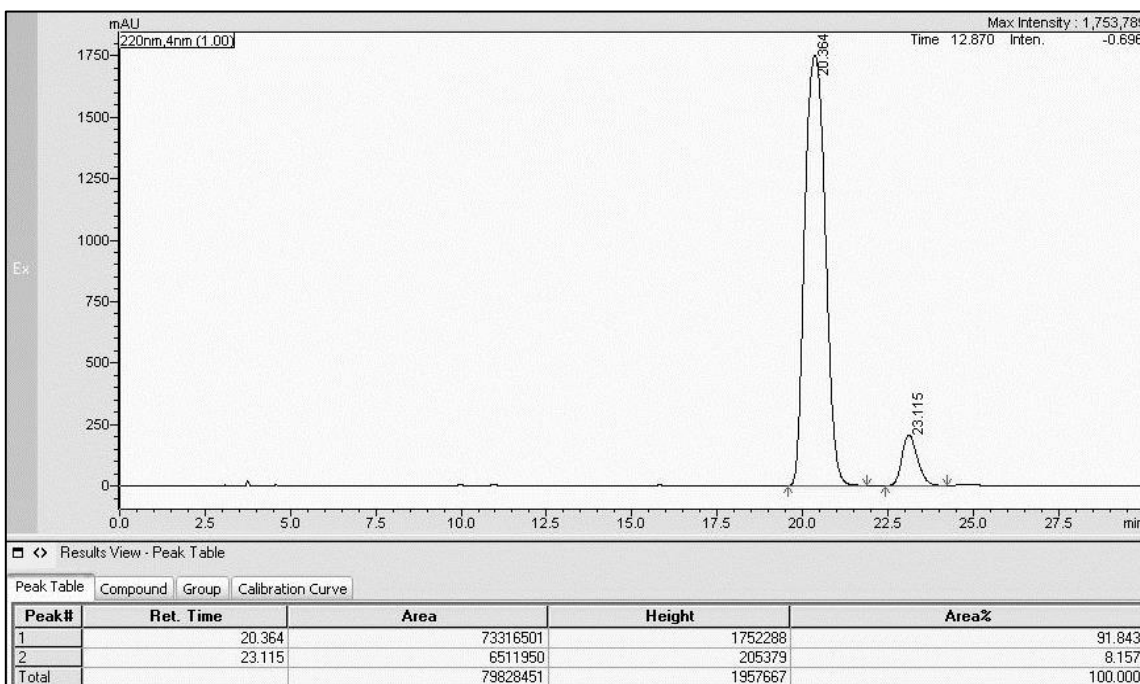
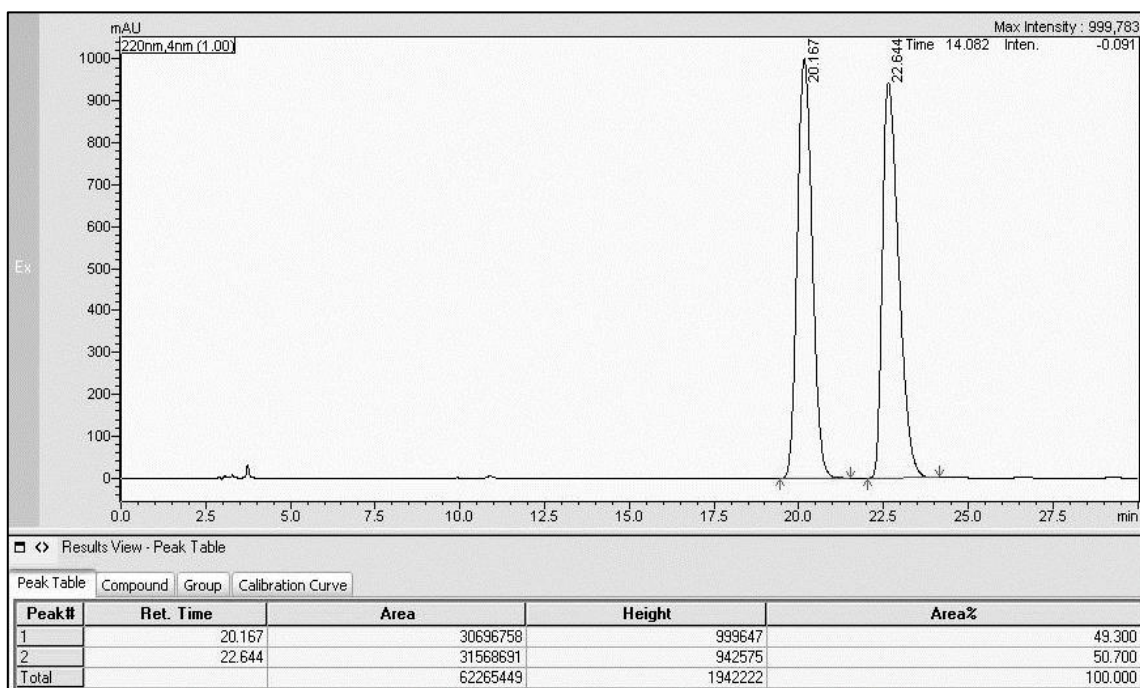
2-((5-Fluoropyrimidin-2-yl)oxy)-*N*-methyl-*N*-(((1*R*,2*S*)-2-phenylcyclopropyl)methyl)ethan-1-amine

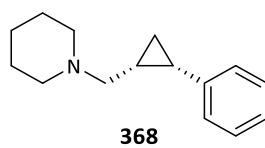
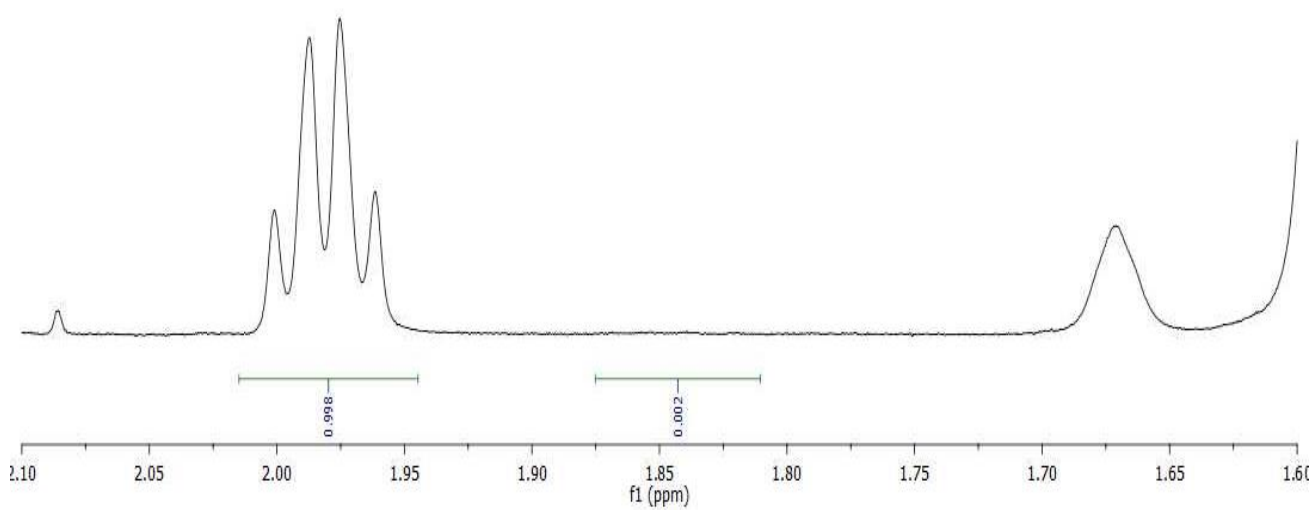
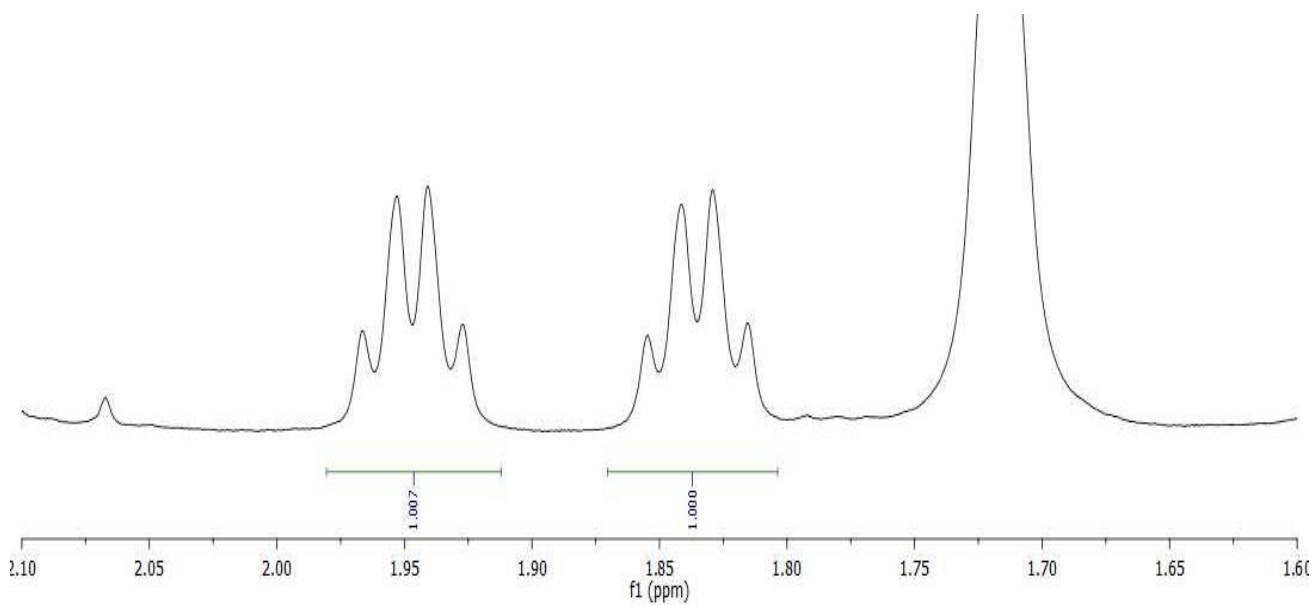
HPLC analysis: Chiralpak AD-H (hexane:2-propanol 98:2, 1.0 mL·min⁻¹, 30 °C) t_R = 13.0 min (major, 89.1%), t_R = 14.4 min (minor, 10.9%)

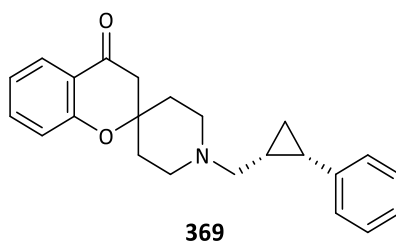


Benzyl 3-(methyl(((1*R*,2*S*)-2-phenylcyclopropyl)methyl)amino)azetidine-1-carboxylate


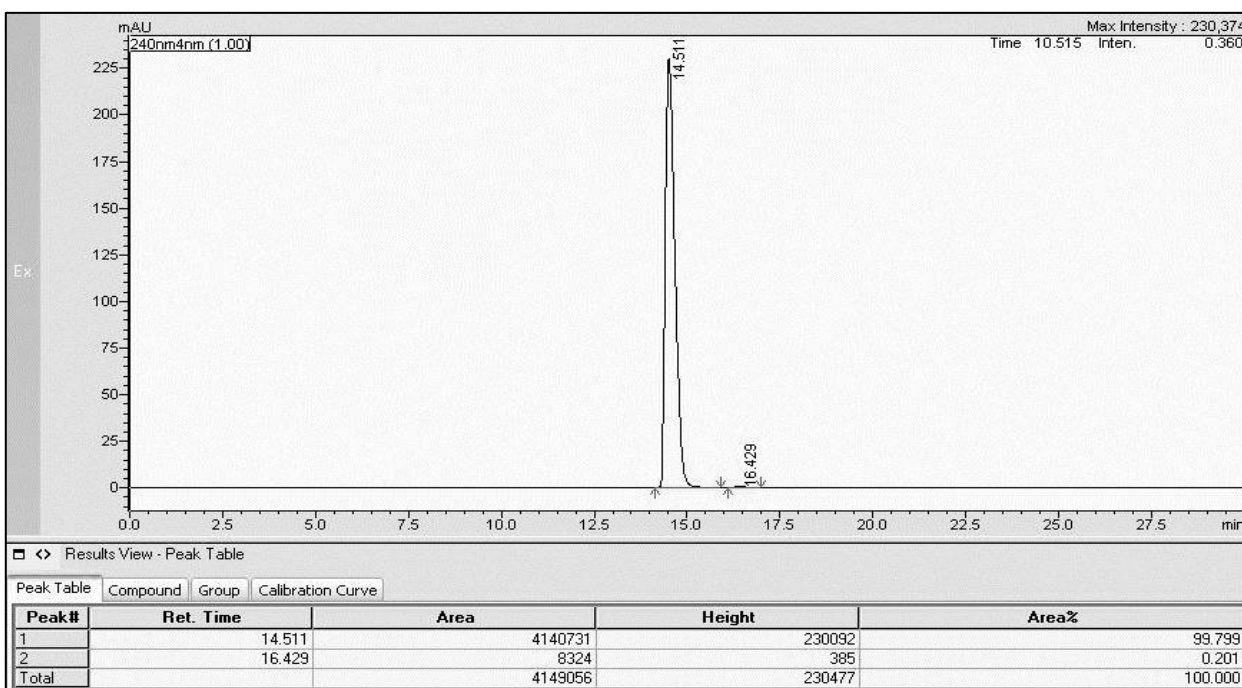
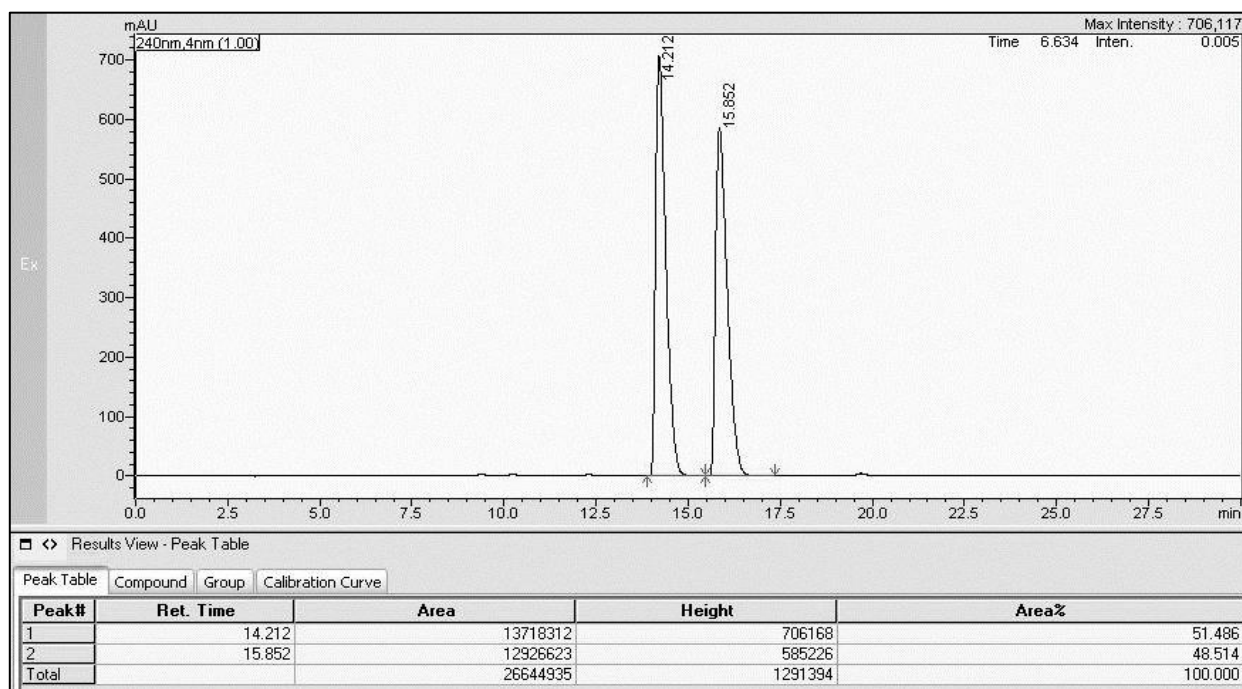
HPLC analysis: Chiralpak AD-H (hexane:2-propanol 97:3, 1.0 mL·min⁻¹, 30 °C) t_R = 20.3 min (major, 91.8%), t_R = 23.1 min (minor, 8.2%)

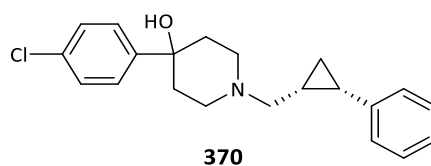


1-(((1*R*,2*S*)-2-Phenylcyclopropyl)methyl)piperidine¹H-NMR analysis:

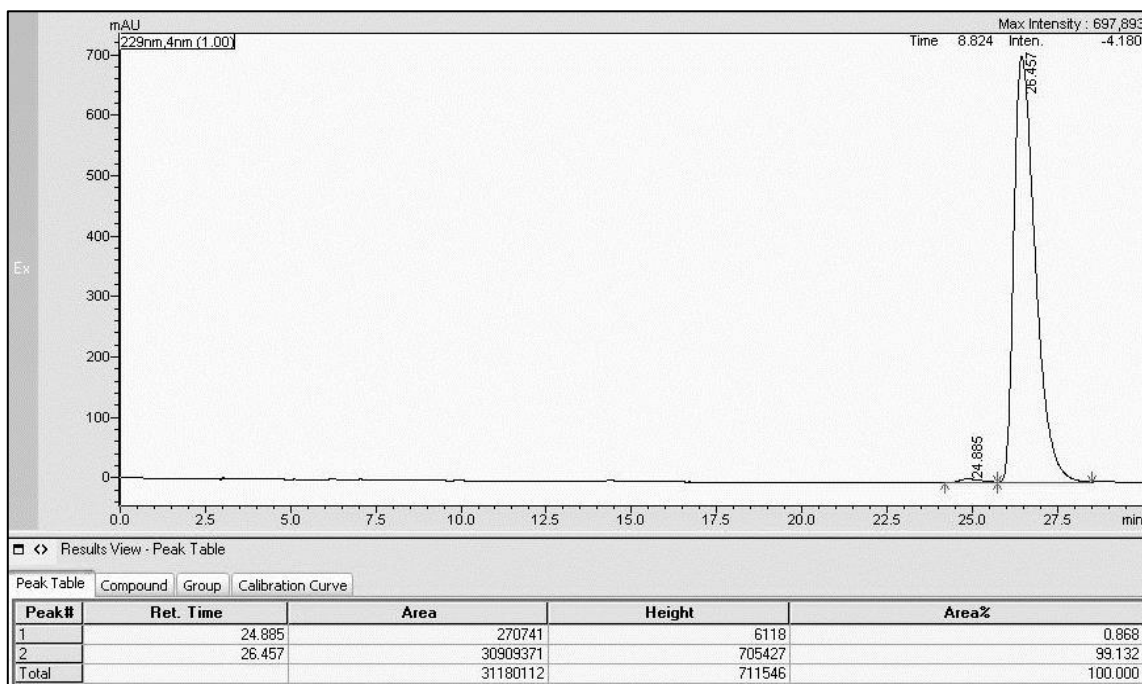
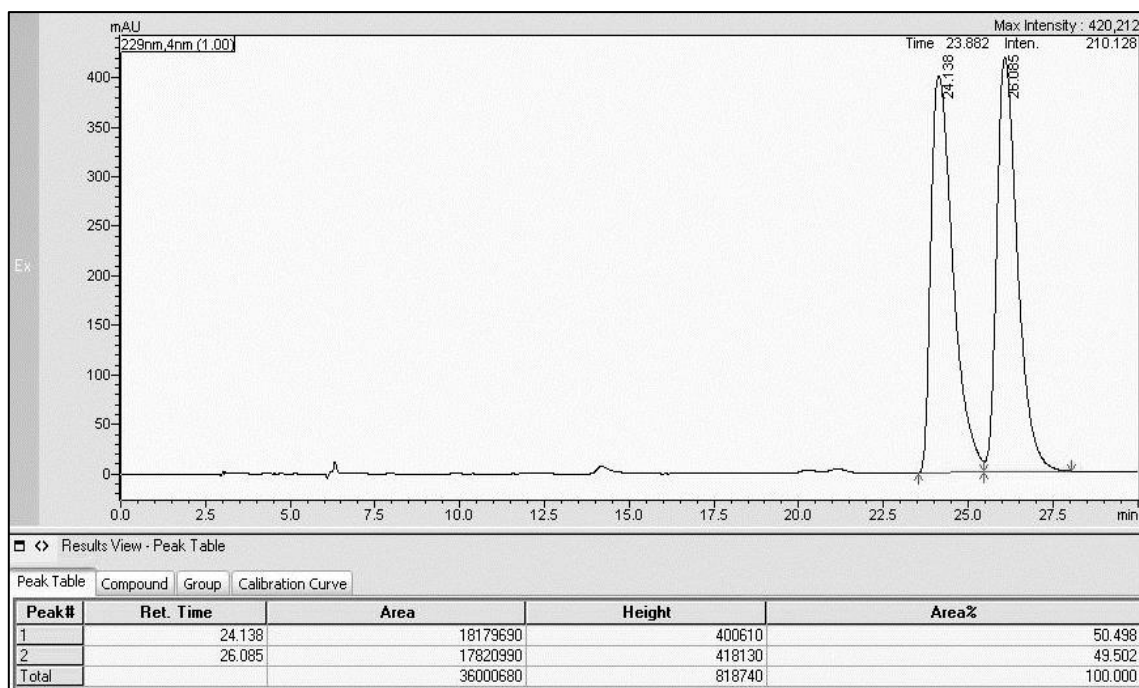
1'-(((1*R*,2*S*)-2-Phenylcyclopropyl)methyl)spiro[chromane-2,4'-piperidin]-4-one

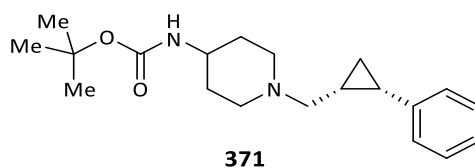
HPLC analysis: Chiralpak AD-H (hexane:2-propanol 97:3, 1.0 mL·min⁻¹, 30 °C) t_R = 14.5 min (major, 99.8%), t_R = 16.4 min (minor, 0.2%)



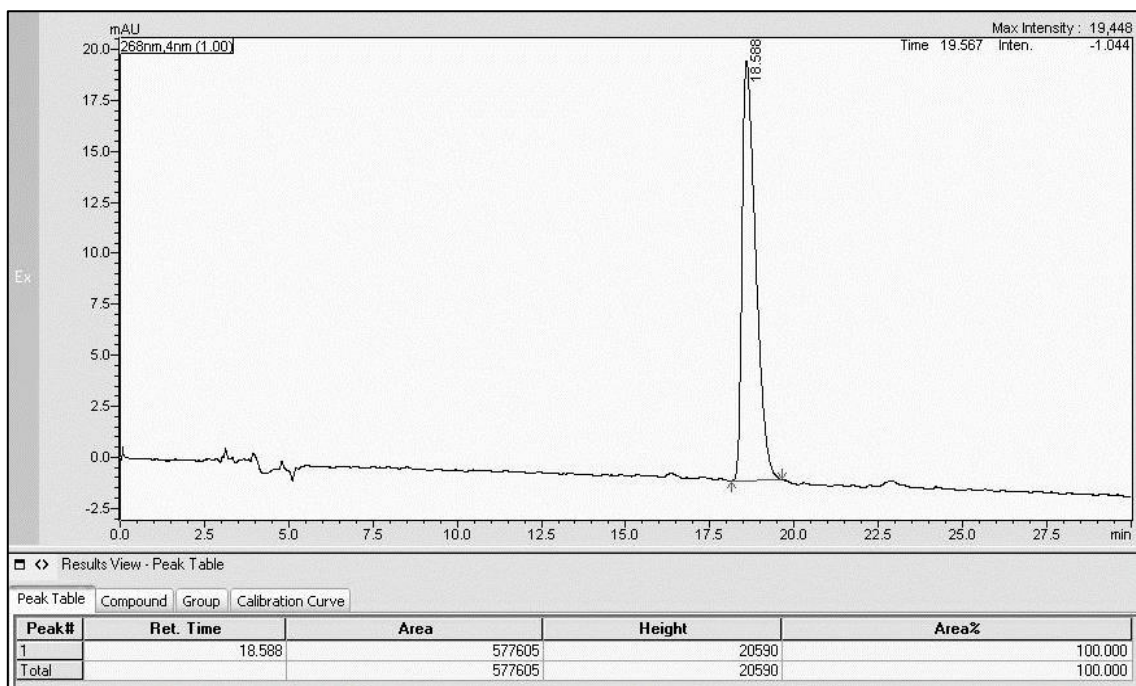
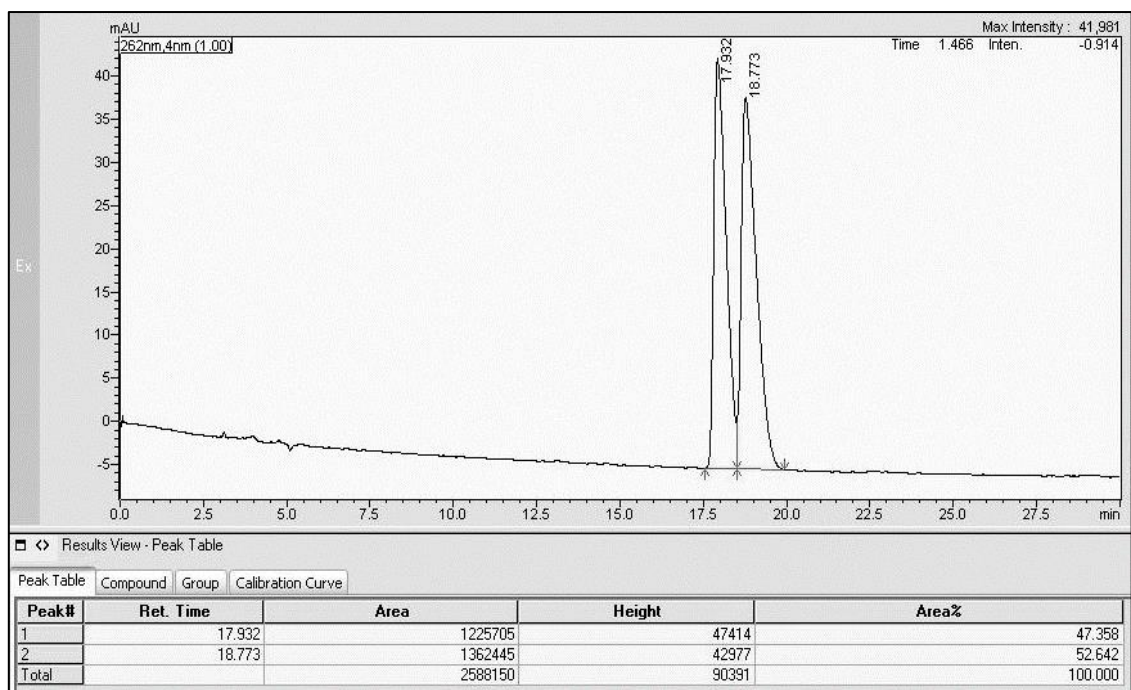
4-(4-Chlorophenyl)-1-(((1*R*,2*S*)-2-phenylcyclopropyl)methyl)piperidin-4-ol

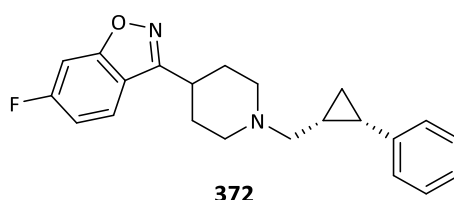
HPLC analysis: Chiralpak AD-H (hexane:2-propanol 95:5, 1.0 mL·min⁻¹, 30 °C) $t_R = 24.2$ min (minor, 0.9%), $t_R = 26.1$ min (major, 99.1%)



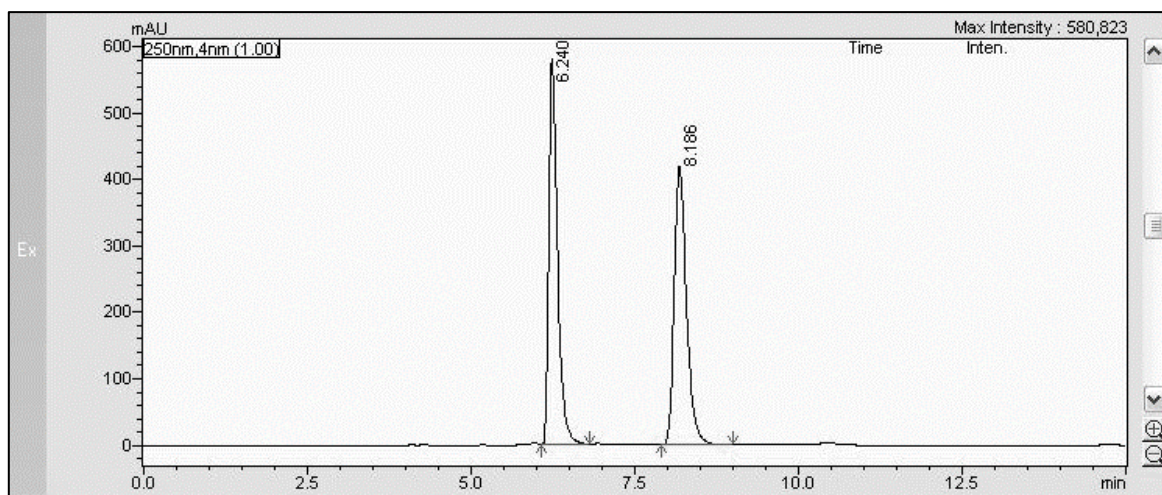
***tert*-Butyl (1-(((1*R*,2*S*)-2-phenylcyclopropyl)methyl)piperidin-4-yl)carbamate**

HPLC analysis: Chiralpak AD-H (hexane(0.1% DEA):2-propanol 98:2, 1.0 mL·min⁻¹, 45 °C) t_R = 17.9 min (minor, <0.1%), t_R = 18.7 min (major, >99.9%)



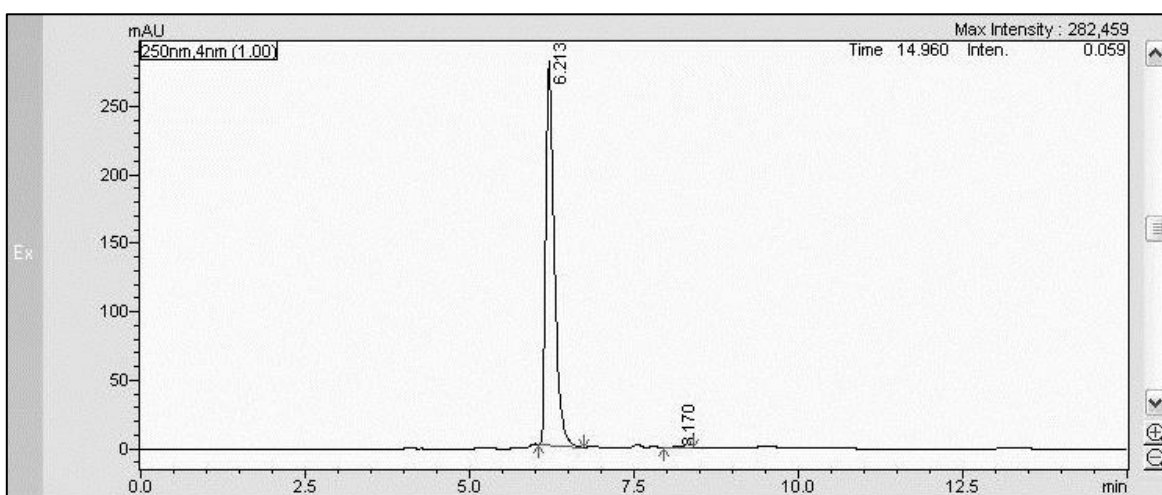
6-Fluoro-3-(1-(((1*R*,2*S*)-2-phenylcyclopropyl)methyl)piperidin-4-yl)benzo[*d*]isoxazole

HPLC analysis: Chiralpak AD-H (hexane(0.1% DEA):2-propanol 90:10, 1.0 mL·min⁻¹, 30 °C) t_R = 6.2 min (major, 99.3%), t_R = 8.2 min (minor, 0.7%)



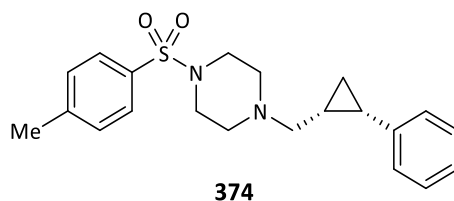
Results View - Peak Table

Peak#	Ret. Time	Area	Height	Area%
1	6.240	5337513	579249	49.233
2	8.186	5503841	419122	50.767
Total		10841354	998370	100.000

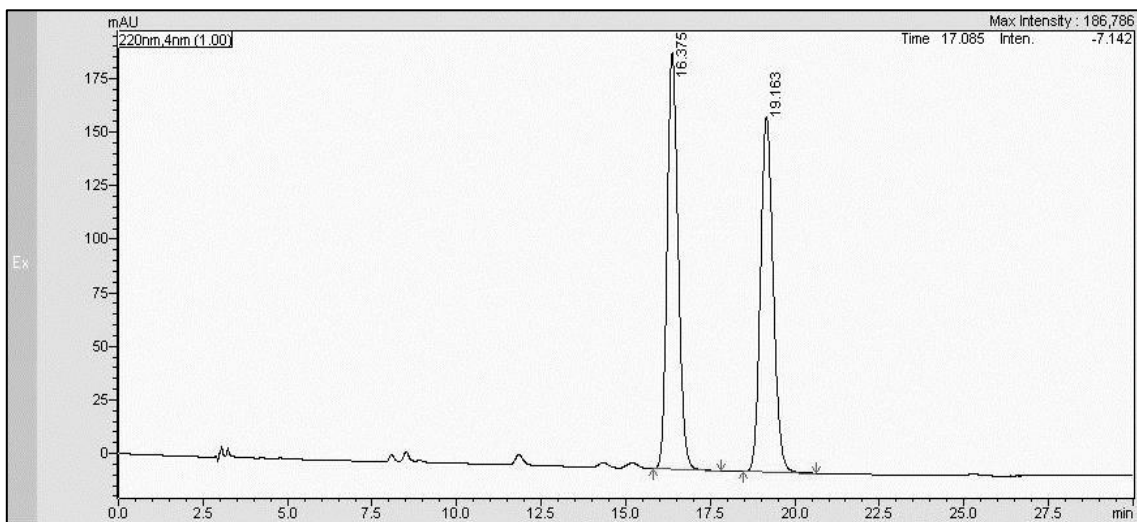


Results View - Peak Table

Peak#	Ret. Time	Area	Height	Area%
1	6.213	2532025	280129	99.256
2	8.170	18981	1756	0.744
Total		2551005	281885	100.000

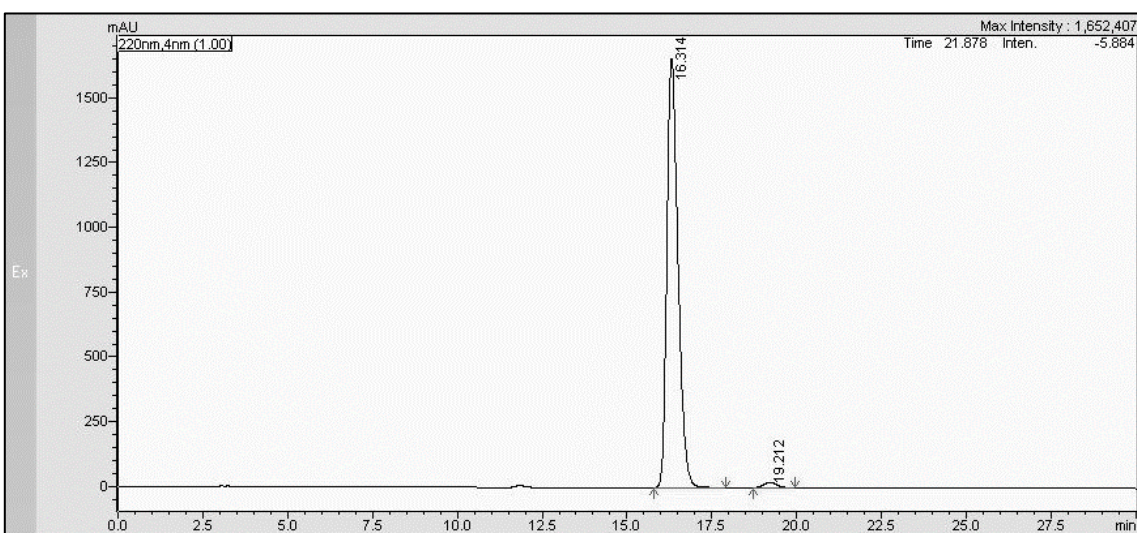
1-(((1*R*,2*S*)-2-Phenylcyclopropyl)methyl)-4-tosylpiperazine

HPLC analysis: Chiralpak AD-H (hexane:2-propanol 90:10, 1.0 mL·min⁻¹, 30 °C) t_R = 16.3 min (major, 98.6%), t_R = 19.2 min (minor, 1.4%)



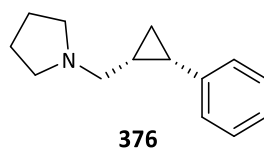
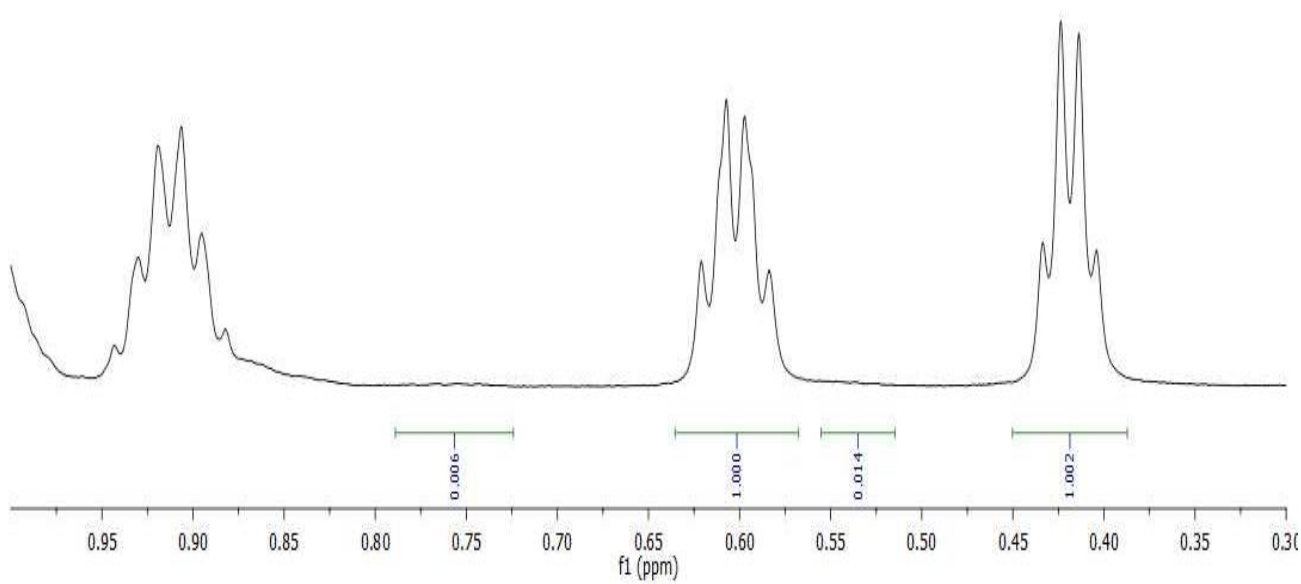
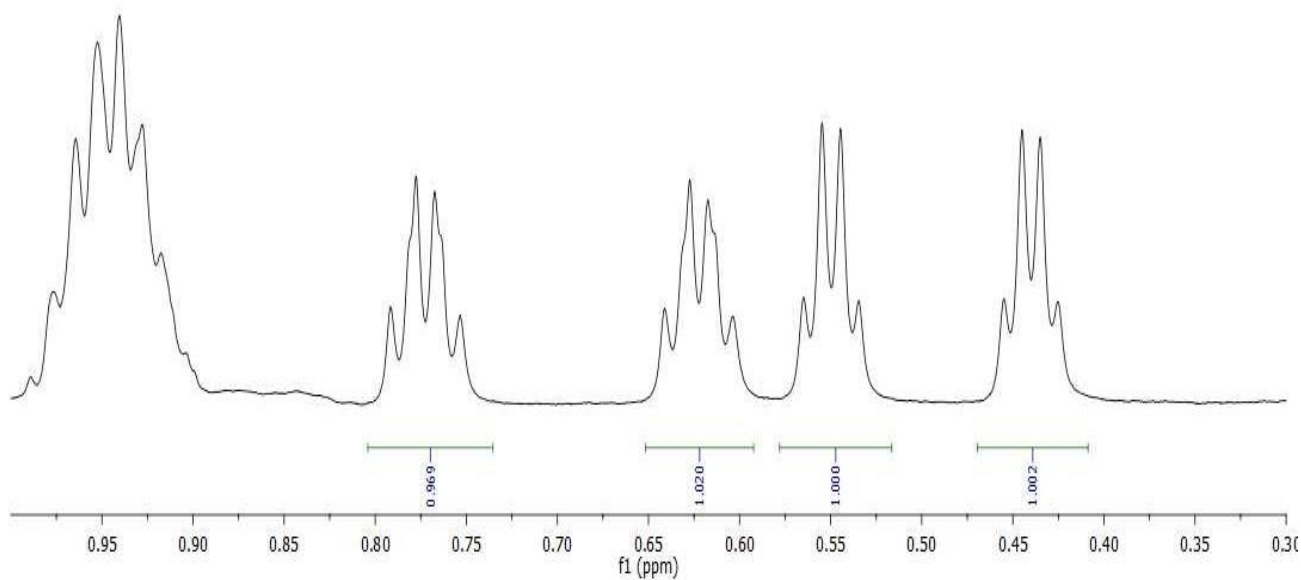
Results View - Peak Table

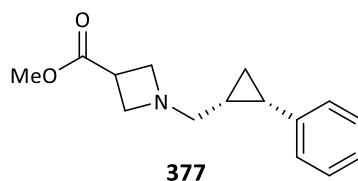
Peak#	Ret. Time	Area	Height	Area%
1	16.375	4399813	194308	50.291
2	19.163	4348926	165790	49.709
Total		8748740	360098	100.000



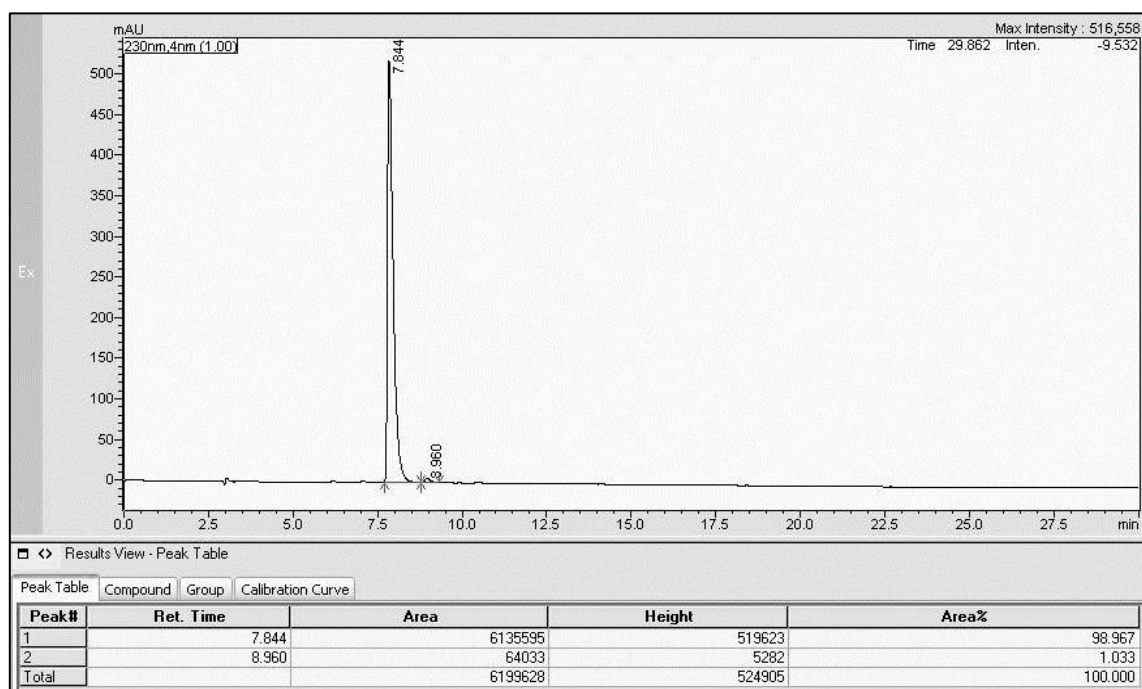
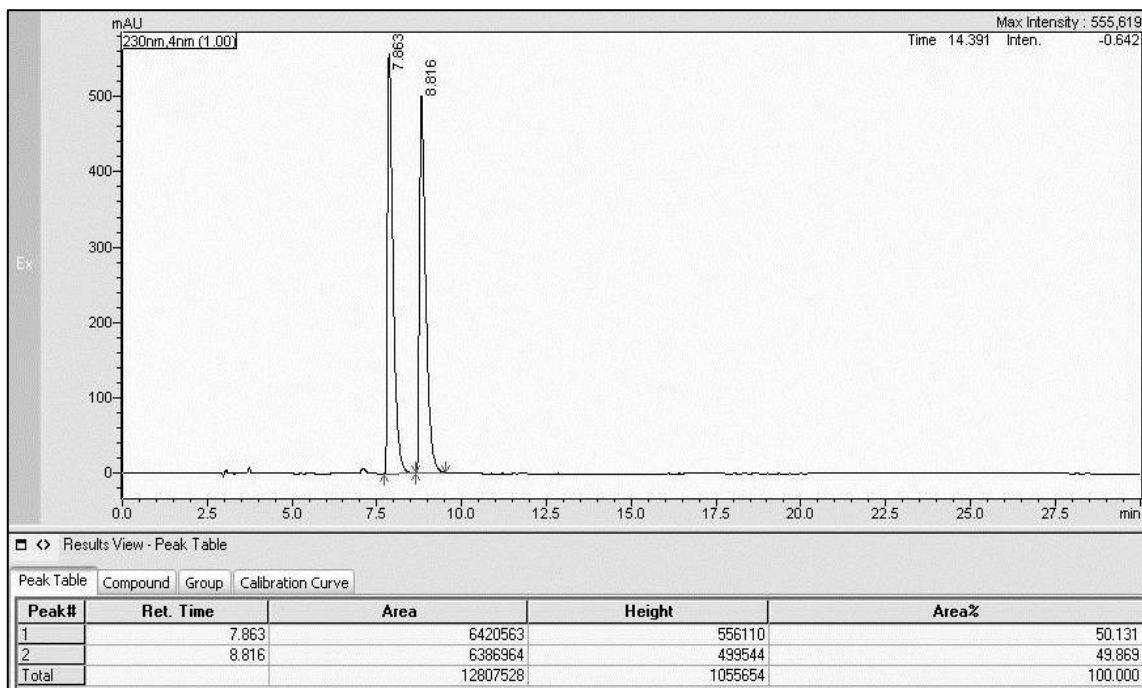
Results View - Peak Table

Peak#	Ret. Time	Area	Height	Area%
1	16.314	37612537	1656764	98.595
2	19.212	535881	20880	1.405
Total		38148417	1677644	100.000

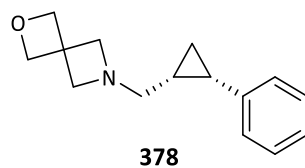
1-(((1*R*,2*S*)-2-Phenylcyclopropyl)methyl)pyrrolidine**¹H-NMR analysis:**

Methyl 1-(((1*R*,2*S*)-2-phenylcyclopropyl)methyl)azetidine-3-carboxylate

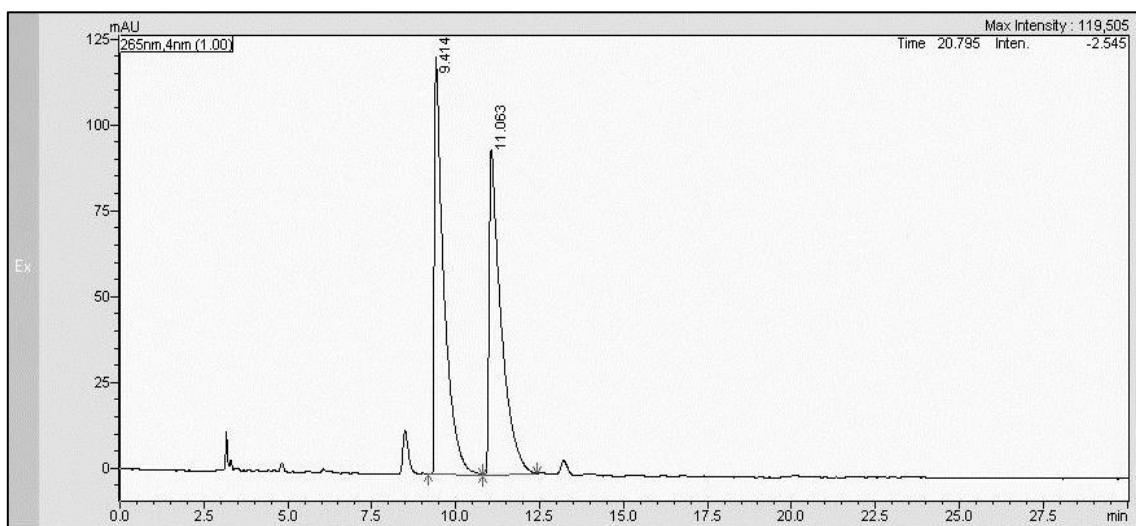
HPLC analysis: Chiralpak AD-H (hexane:2-propanol 97:3, 1.0 mL·min⁻¹, 30 °C) t_R = 7.8 min (major, 99.0%), t_R = 8.8 min (minor, 1.0%)



6-(((1R,2S)-2-phenylcyclopropyl)methyl)-2-oxa-6-azaspiro[3.3]heptane



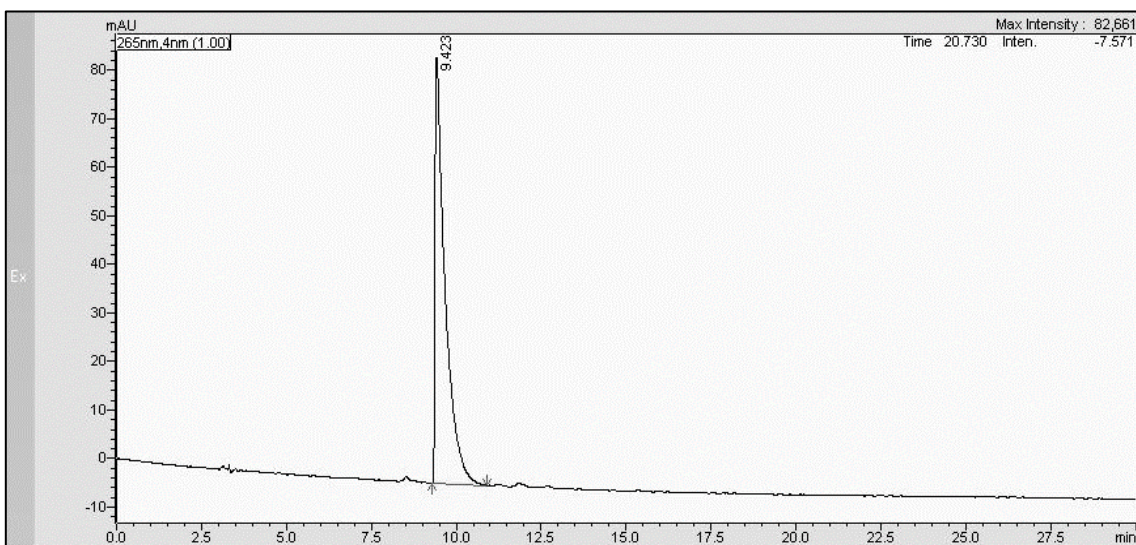
HPLC analysis: Chiralpak AD-H (hexane(0.1% DEA):2-propanol 97:3, 1.0 mL·min⁻¹, 30 °C) t_R = 9.4 min (major, >99.9%), t_R = 11.0 min (minor, <0.1%)



Results View - Peak Table

Peak Table Compound Group Calibration Curve

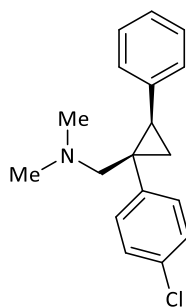
Peak#	Ret. Time	Area	Height	Area%
1	9.414	2378319	121321	50.534
2	11.063	2328026	94463	49.466
Total		4706345	215784	100.000



Results View - Peak Table

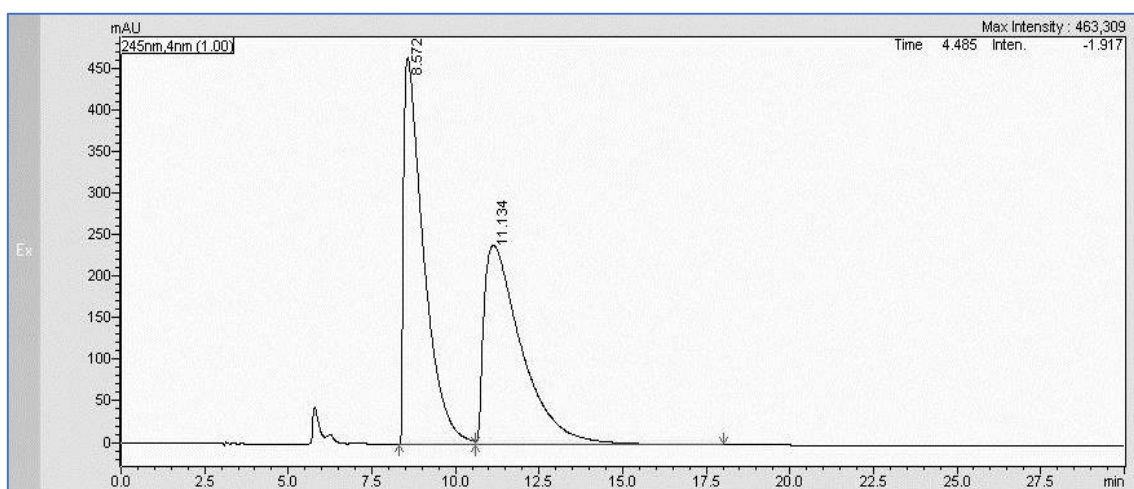
Peak Table Compound Group Calibration Curve

Peak#	Ret. Time	Area	Height	Area%
1	9.423	1829787	87818	100.000
Total		1829787	87818	100.000

1-((1*R*,2*R*)-1-(4-Chlorophenyl)-2-phenylcyclopropyl)-*N,N*-dimethylmethanamine

379a

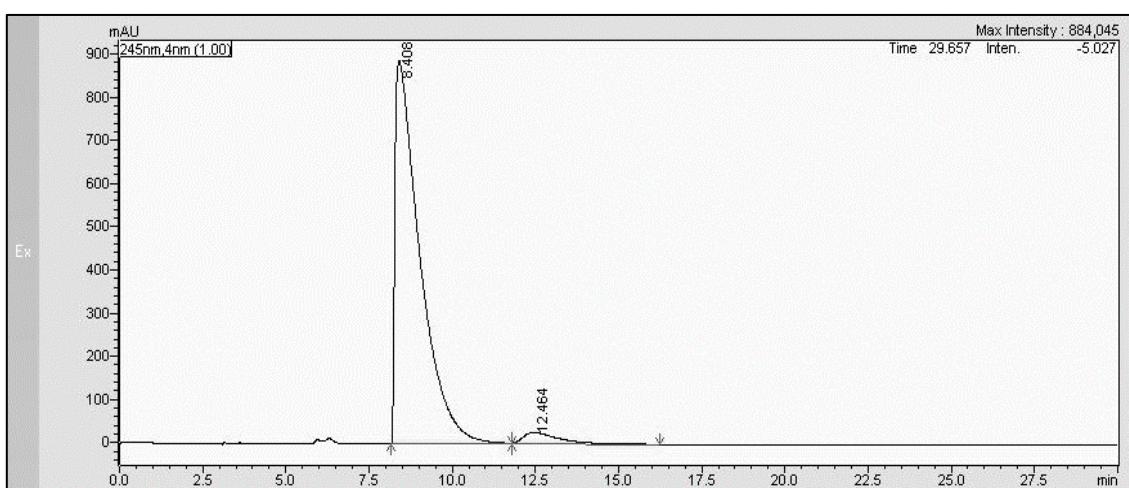
HPLC analysis: Chiralpak AD-H (hexane:2-propanol 99:1, 1.0 mL·min⁻¹, 30 °C) t_R = 8.5 min (major, 95.7%), t_R = 12.4 min (minor, 4.3%)



Results View - Peak Table

Peak Table Compound Group Calibration Curve

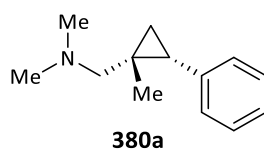
Peak#	Ret. Time	Area	Height	Area%
1	8.572	19441293	465865	50.710
2	11.134	18896622	240167	49.290
Total		38337915	706032	100.000



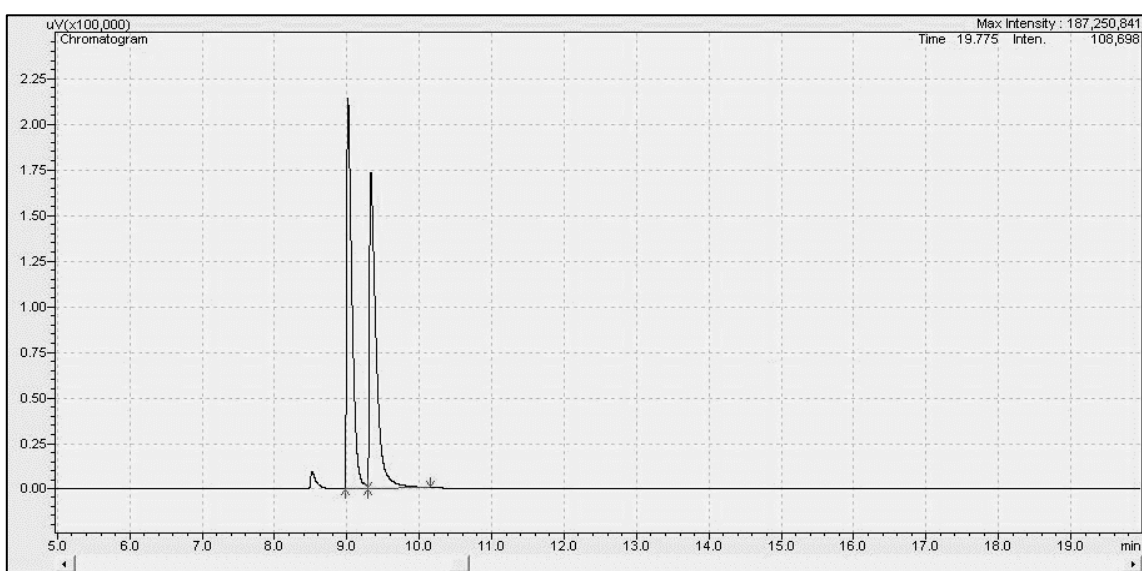
Results View - Peak Table

Peak Table Compound Group Calibration Curve

Peak#	Ret. Time	Area	Height	Area%
1	8.408	46349307	886827	95.675
2	12.464	2095110	26925	4.325
Total		48444417	913752	100.000

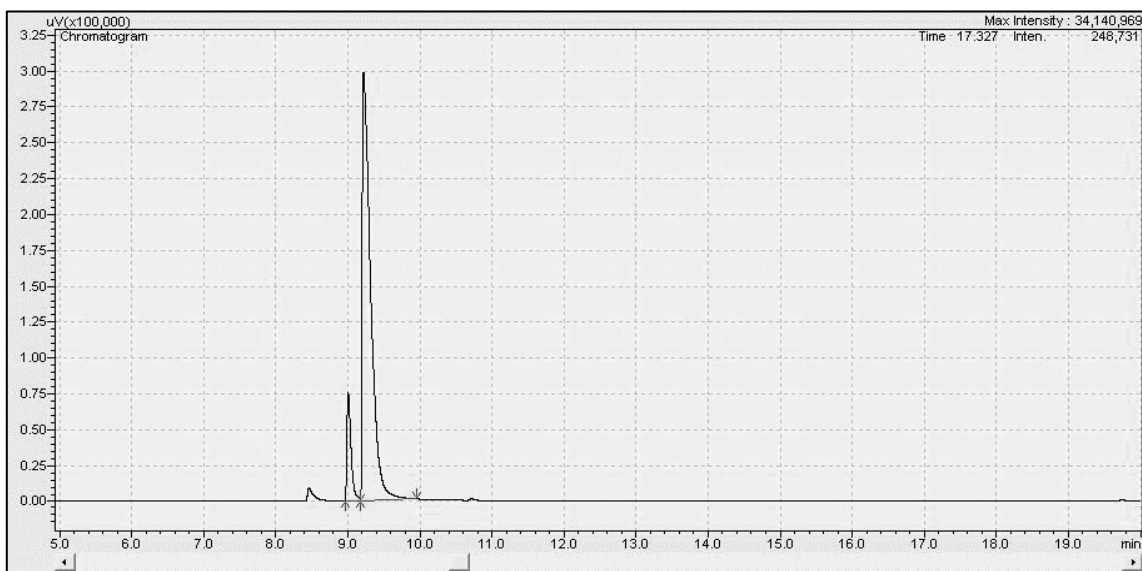
***N,N*-Dimethyl-1-((1*R*,2*R*)-1-methyl-2-phenylcyclopropyl)methanamine**

GC-FID analysis: ChiralDex β -DM (50 °C to 150 °C; 5 °C/min; linear velocity 40 cm·s⁻¹; split ratio 10.0) t_R = 9.0 min (minor, 11.1%), t_R = 9.2 min (major, 88.9%)



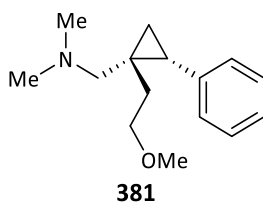
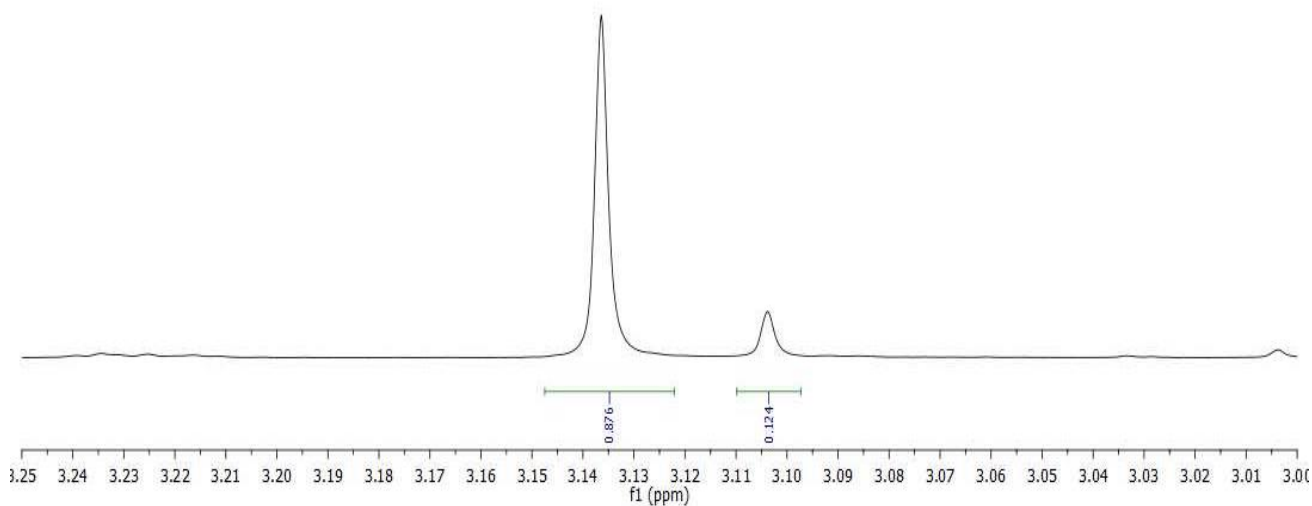
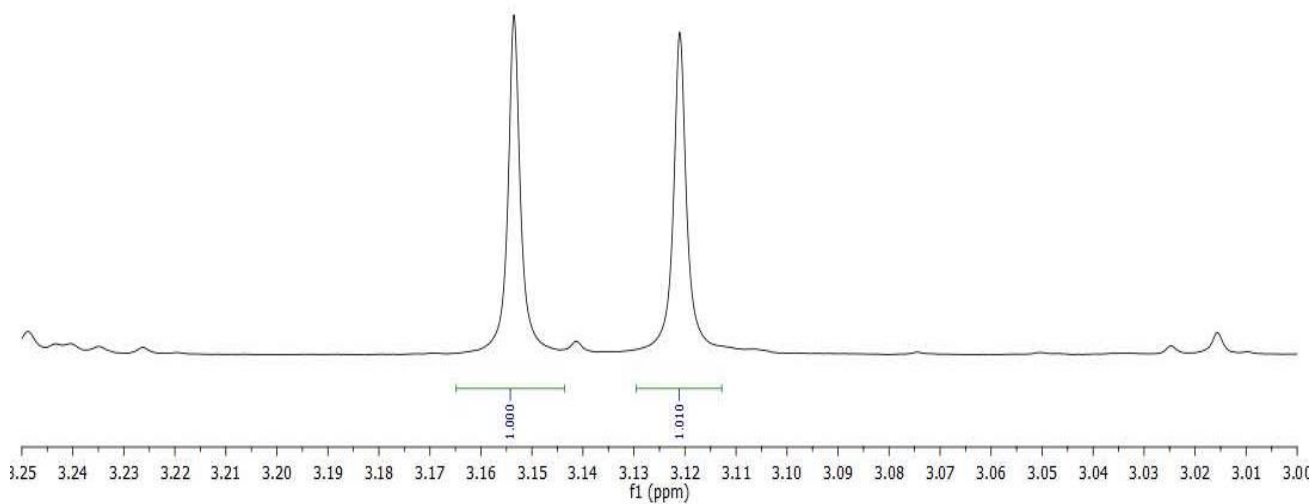
Results - Peak Table

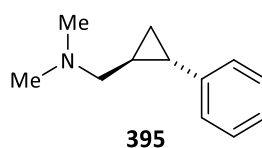
Peak#	Ret. Time	Area	Height	Conc.	Units	Mark	Compound ID#	Compound Name
1	9.016	1103626.0	214260.9	49.62123				
2	9.331	1120474.5	173196.3	50.37877		V		



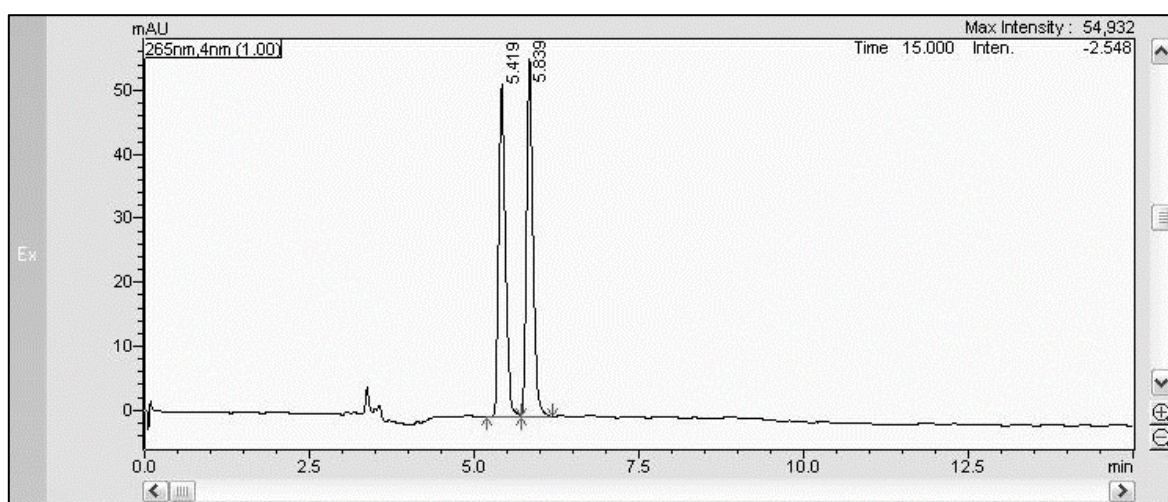
Results - Peak Table

Peak#	Ret. Time	Area	Height	Conc.	Units	Mark	Compound ID#	Compound Name
1	9.007	304270.9	75062.1	11.05783				
2	9.219	2447362.9	298048.2	88.94217		V		

1-((1*S*,2*R*)-1-(2-Methoxyethyl)-2-phenylcyclopropyl)-*N,N*-dimethylmethanamine**¹H-NMR analysis:**

***N,N*-Dimethyl-1-((1*S*,2*S*)-2-phenylcyclopropyl)methanamine**

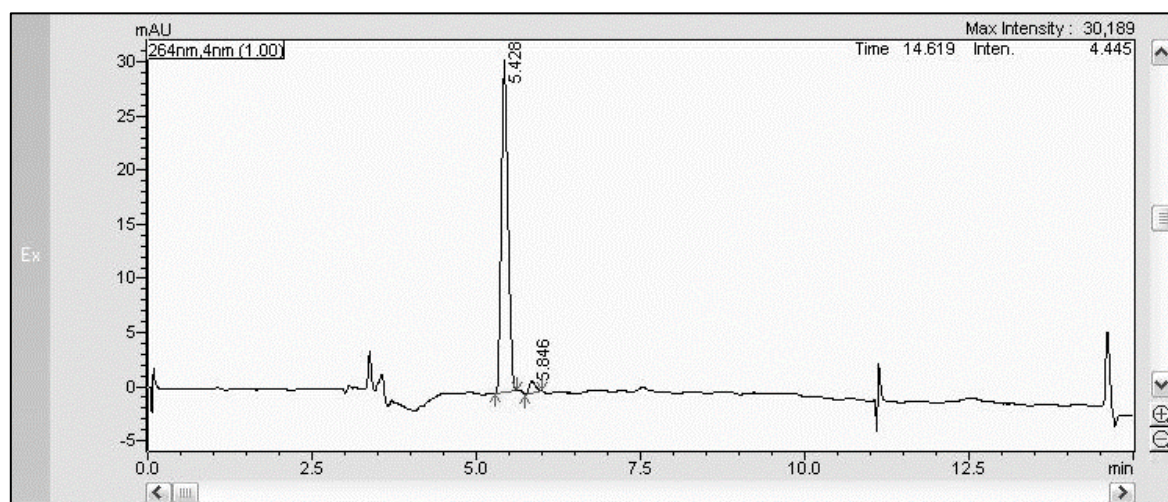
HPLC analysis: Chiralpak AD-H (hexane(0.1% DEA):2-propanol 98:2, 1.0 mL·min⁻¹, 30 °C) *t_R* = 5.4 min (major, 96.4%), *t_R* = 5.8 min (minor, 3.6%)



Results View - Peak Table

Peak Table Compound Group Calibration Curve

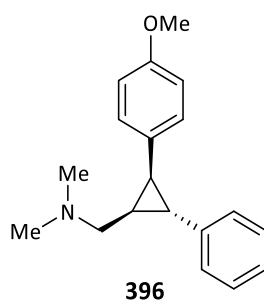
Peak#	Ret. Time	Area	Height	Area%
1	5.419	369906	51884	49.402
2	5.839	378859	55946	50.598
Total		748765	107830	100.000



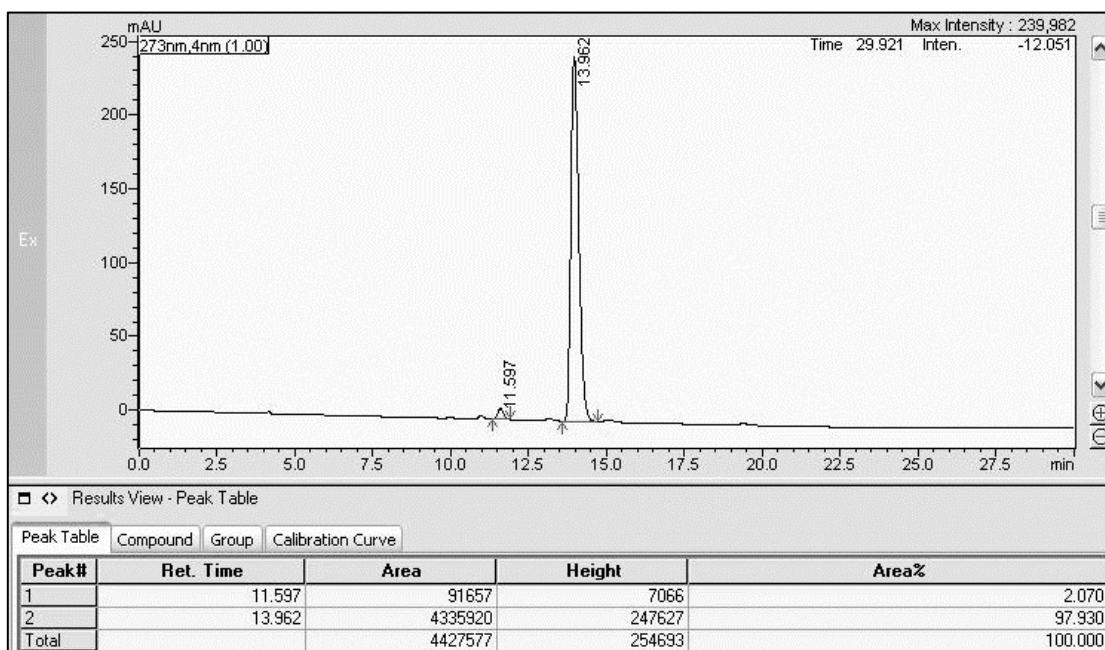
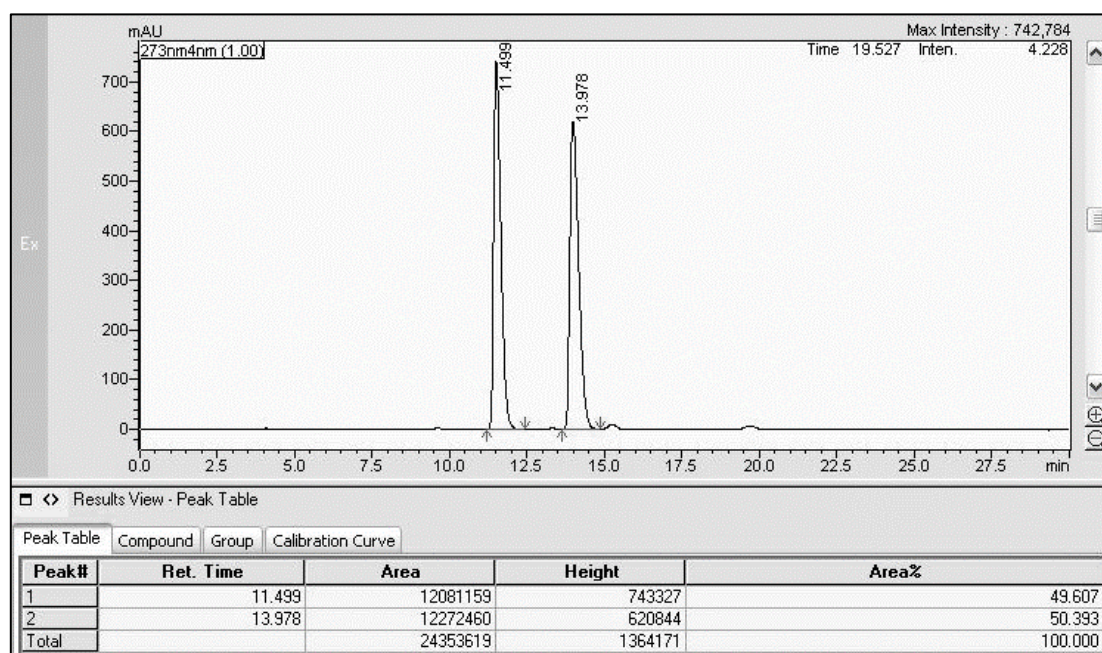
Results View - Peak Table

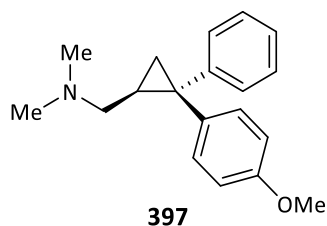
Peak Table Compound Group Calibration Curve

Peak#	Ret. Time	Area	Height	Area%
1	5.428	214369	30739	96.376
2	5.846	8062	1194	3.624
Total		222431	31933	100.000

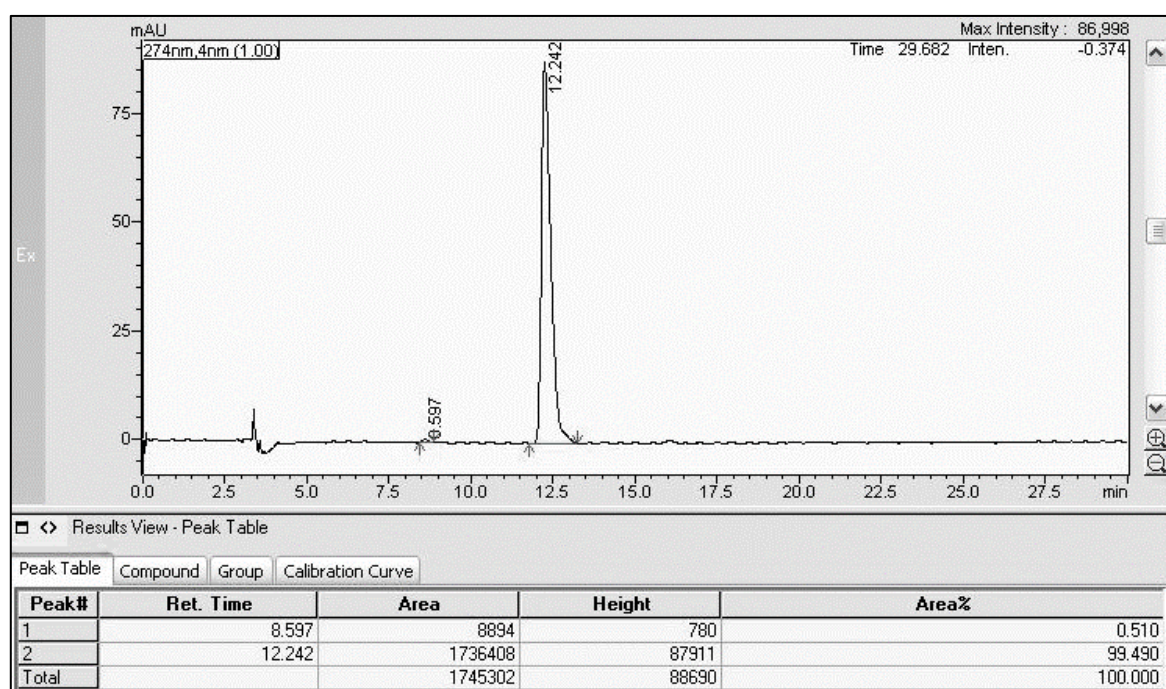
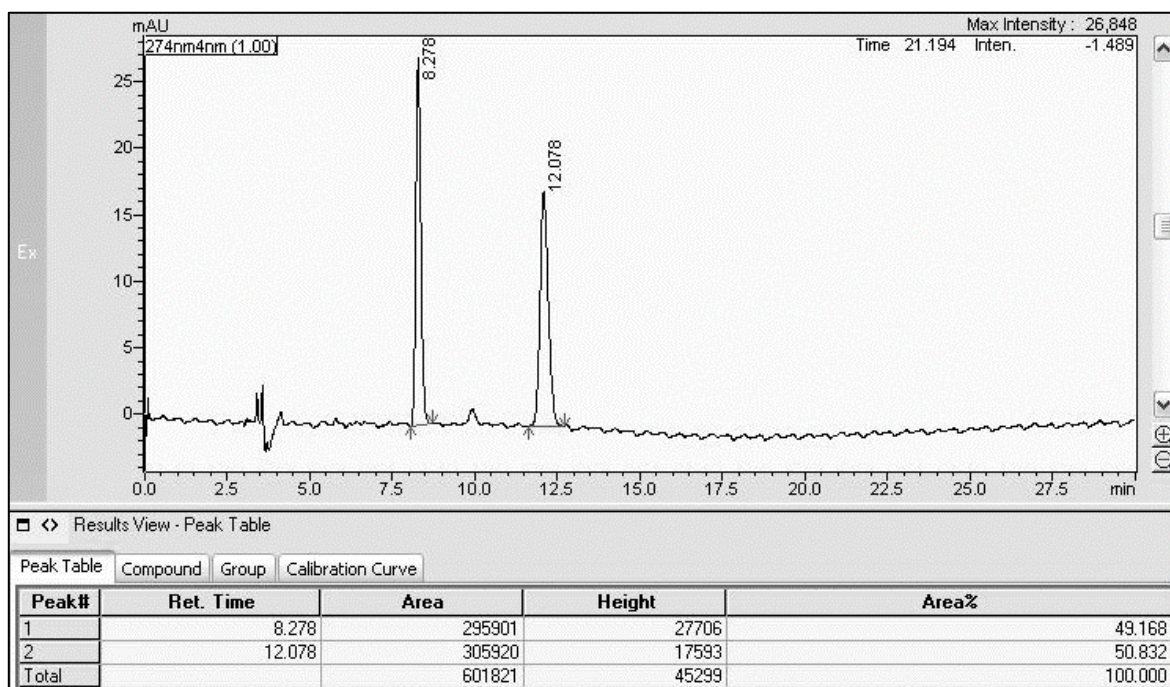
1-((1*R*,2*S*,3*S*)-2-(4-Methoxyphenyl)-3-phenylcyclopropyl)-*N,N*-dimethylmethanamine

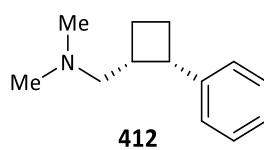
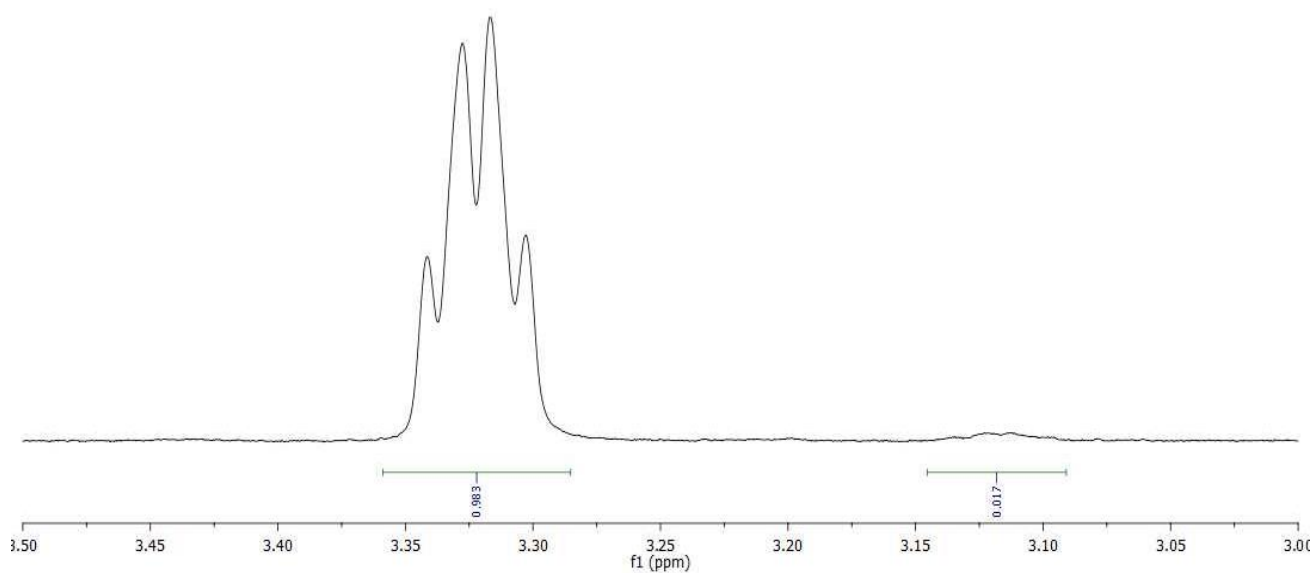
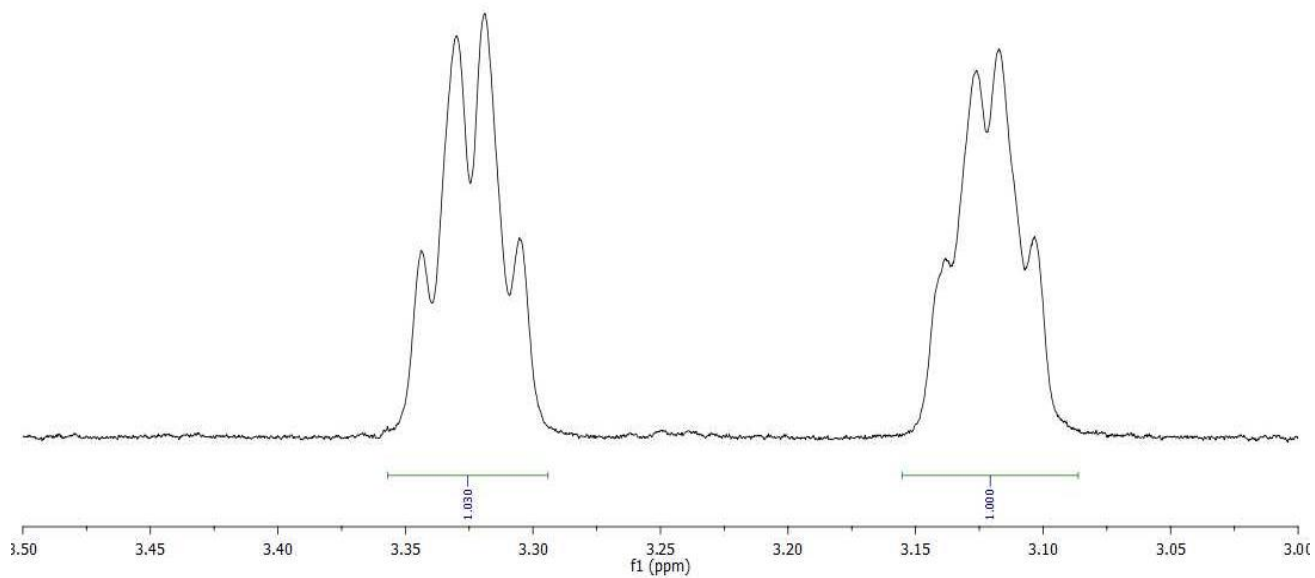
HPLC analysis: Chiralpak AD-H (hexane(0.1% DEA):2-propanol 98:2, 1.0 mL·min⁻¹, 30 °C) t_R = 11.6 min (minor, 2.1%), t_R = 14.0 min (major, 97.9%)

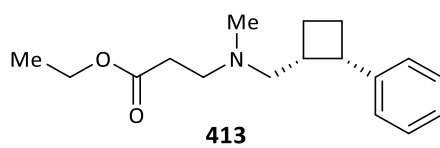
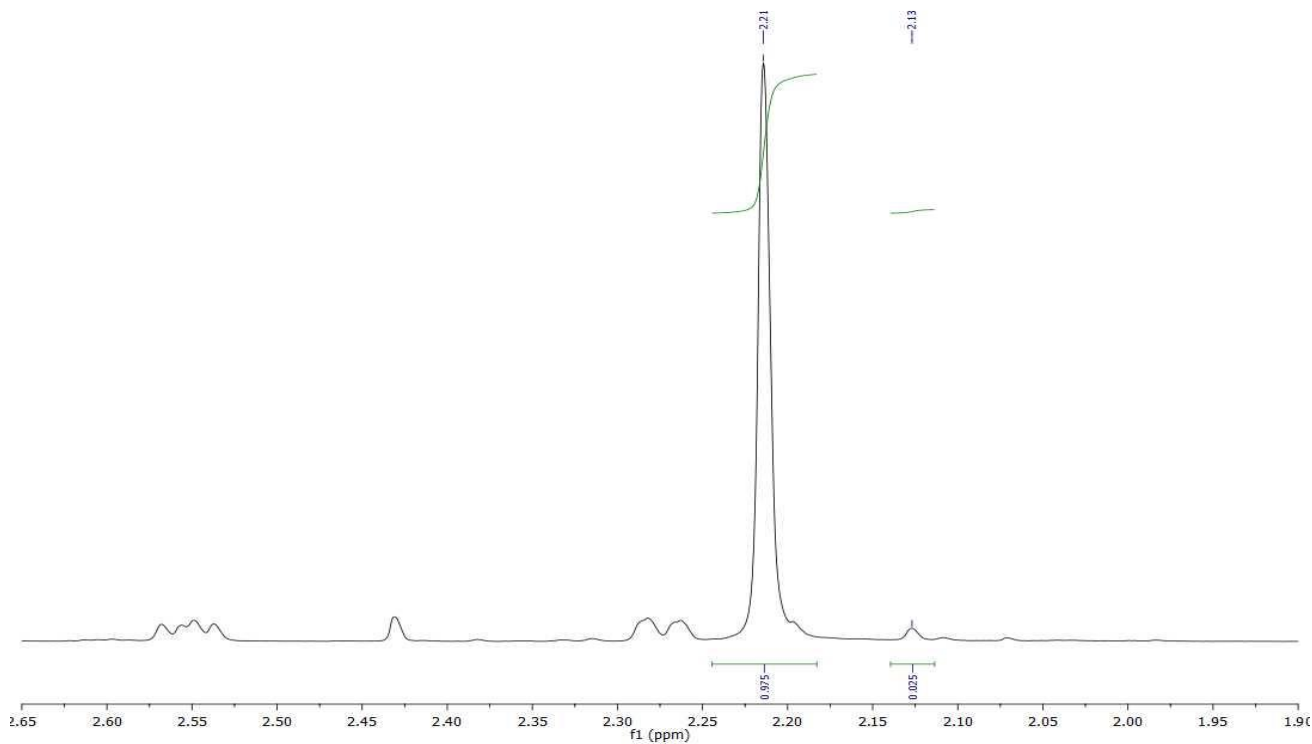
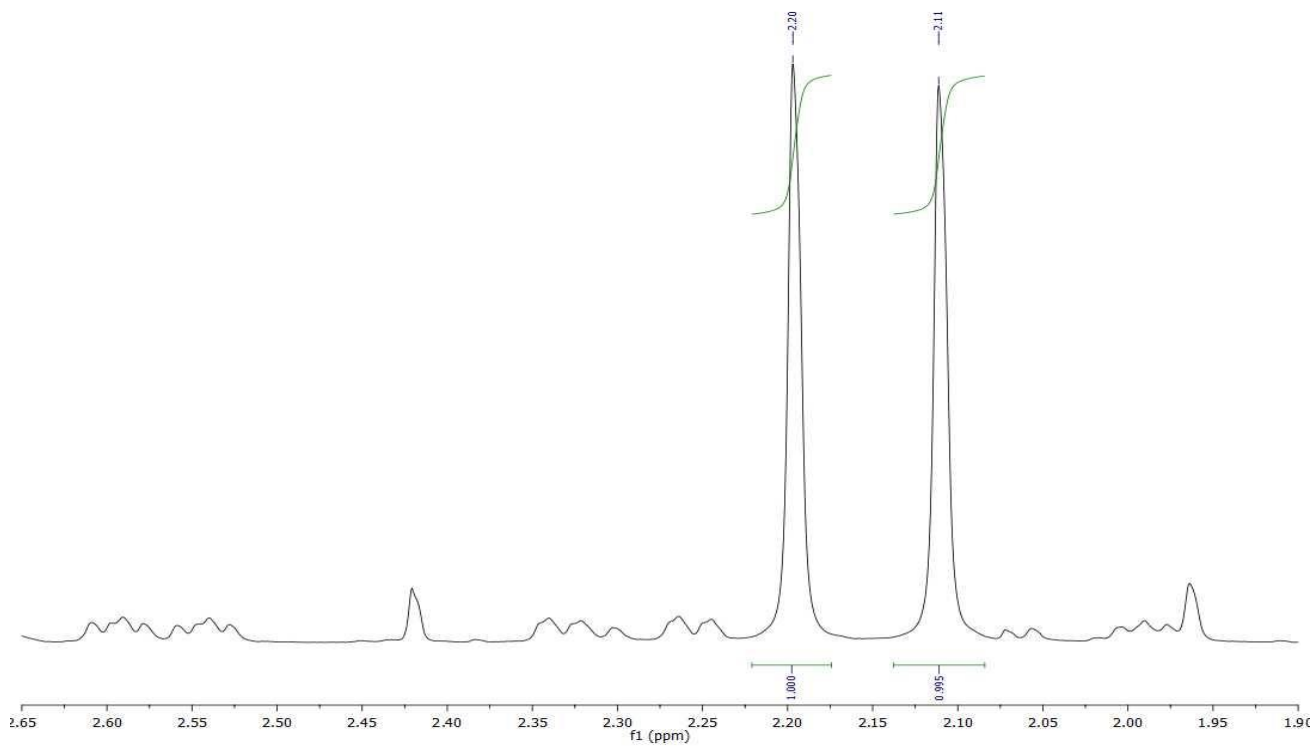


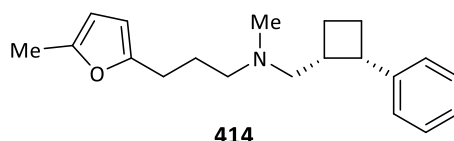
1-((1*S*,2*R*)-2-(4-Methoxyphenyl)-2-phenylcyclopropyl)-*N,N*-dimethylmethanamine

HPLC analysis: Chiralpak AD-H (hexane(0.1% DEA):2-propanol 98:2, 1.0 mL·min⁻¹, 30 °C) t_R = 8.3 min (minor, 0.5%), t_R = 12.2 min (major, 99.5%)

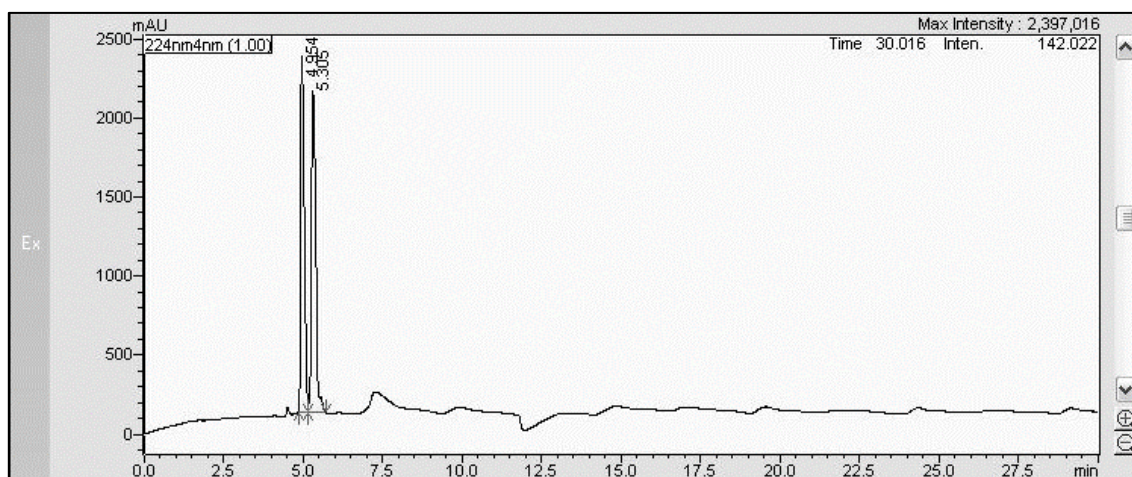


***N,N*-Dimethyl-1-((1*R*,2*S*)-2-phenylcyclobutyl)methanamine****¹H-NMR analysis:**

Ethyl 3-(methyl(((1*R*,2*S*)-2-phenylcyclobutyl)methyl)amino)propanoate**¹H-NMR analysis:**

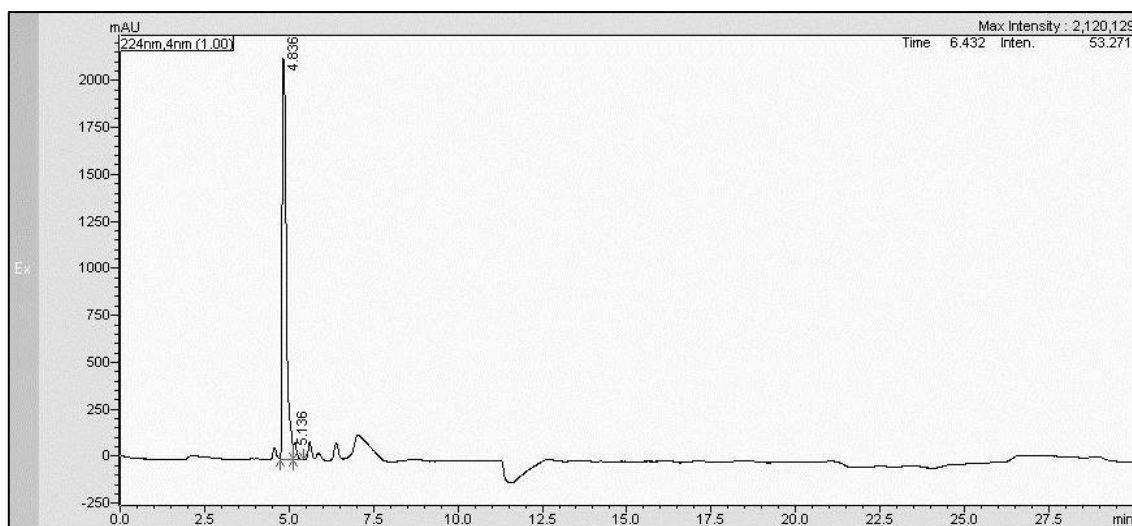
***N*-Methyl-3-(5-methylfuran-2-yl)-*N*-(((1*R*,2*S*)-2-phenylcyclobutyl)methyl)propan-1-amine**

HPLC analysis: Chiralpak AD-H (hexane(0.1% DEA):2-propanol 99.6:0.4, 1.0 mL·min⁻¹, 15 °C) t_R = 4.8 min (major, 97.0%), t_R = 5.1 min (minor, 3.0%)



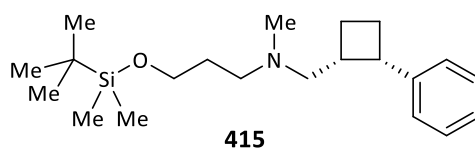
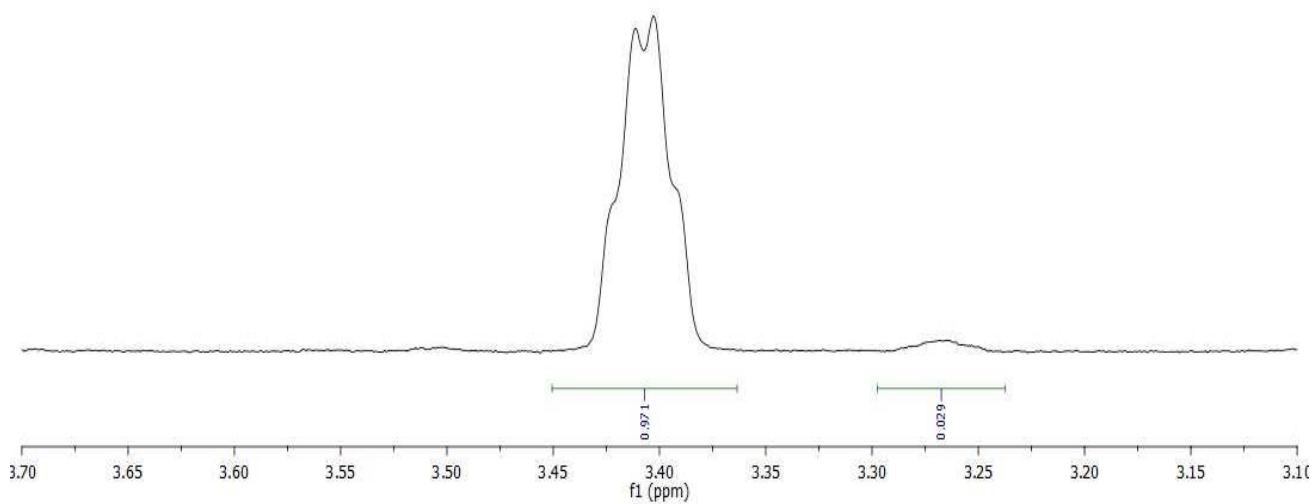
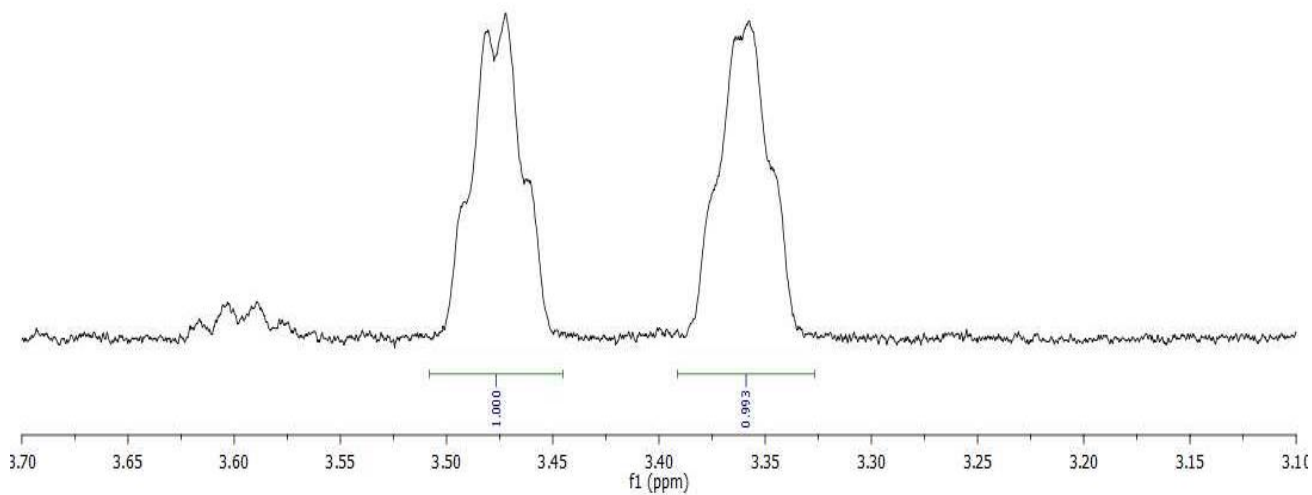
Results View - Peak Table

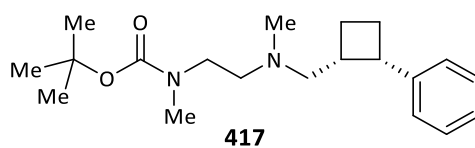
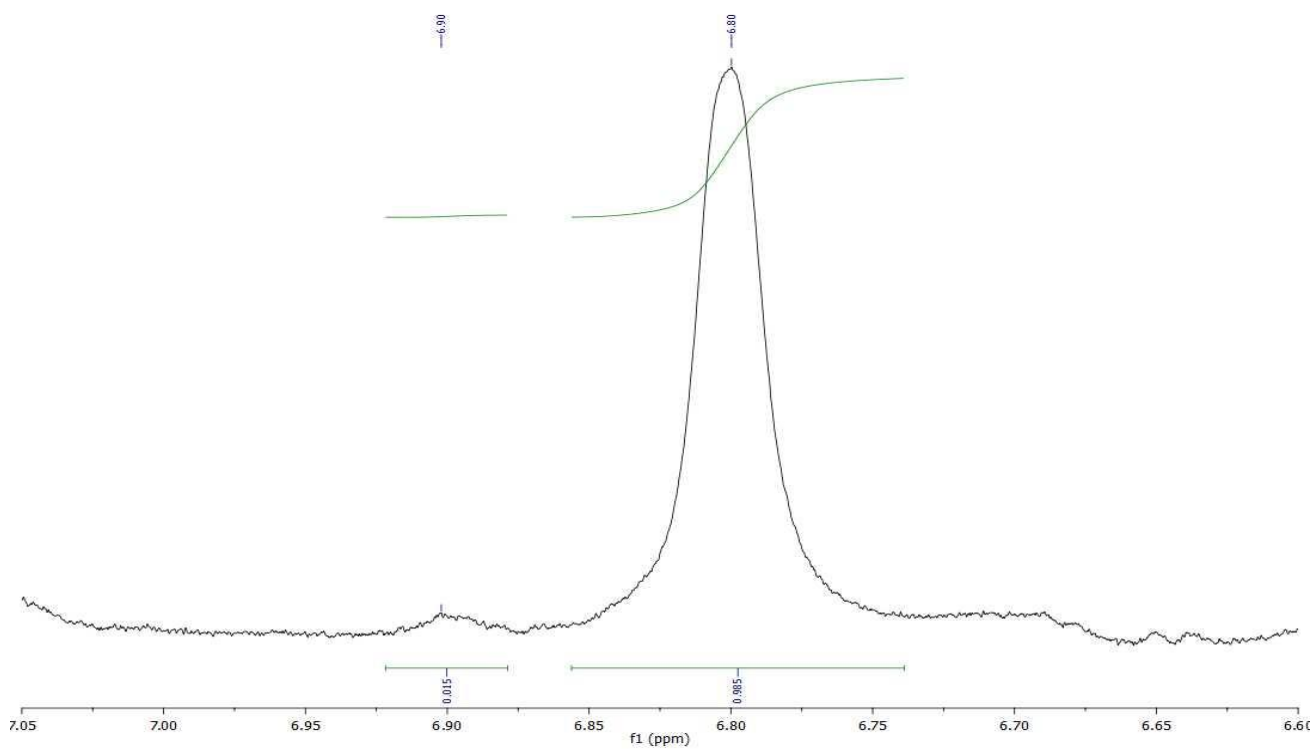
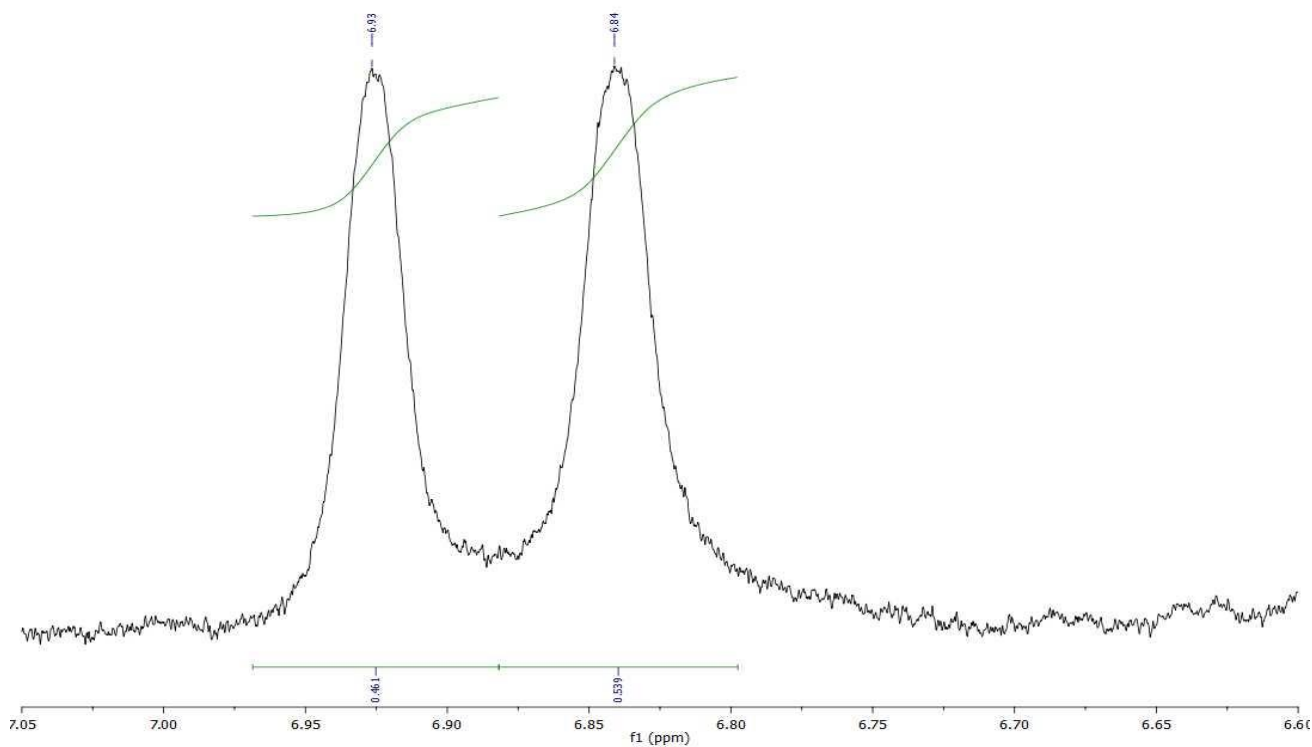
Peak#	Ret. Time	Area	Height	Area%
1	4.954	18434716	2261315	49.074
2	5.305	19130780	2033664	50.926
Total		37565496	4294979	100.000

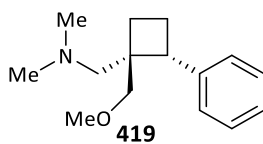


Results View - Peak Table

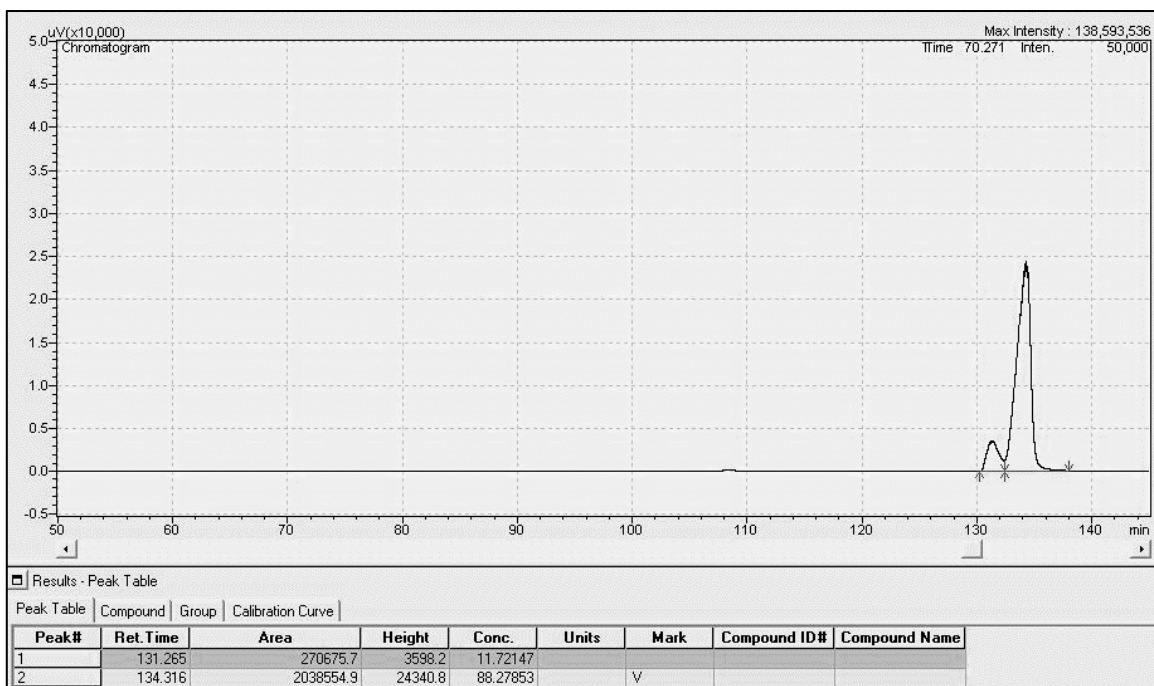
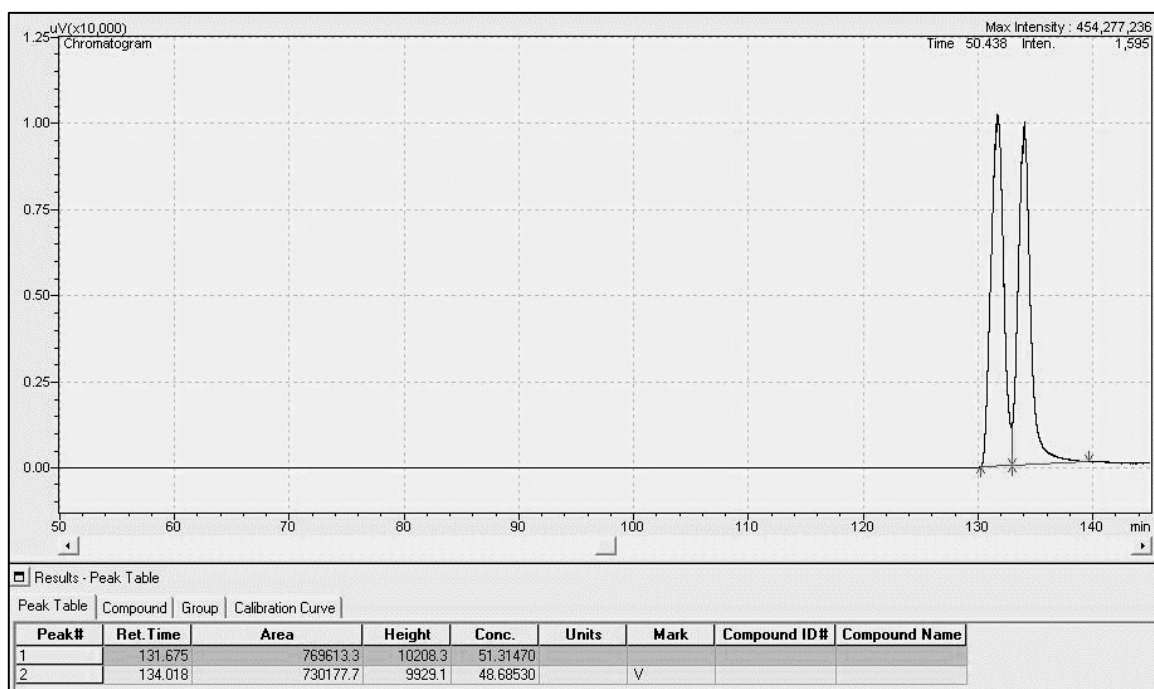
Peak#	Ret. Time	Area	Height	Area%
1	4.836	18618715	2135269	96.954
2	5.136	584913	73976	3.046
Total		19203628	2209246	100.000

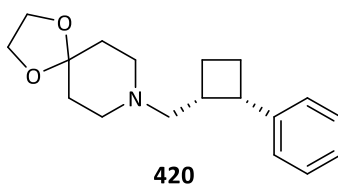
3-((*tert*-Butyldimethylsilyl)oxy)-*N*-methyl-*N*-(((1*R*,2*S*)-2-phenylcyclobutyl)methyl)propan-1-amine**¹H-NMR analysis:**

***tert*-Butyl methyl(2-(methyl((1*R*,2*S*)-2-phenylcyclobutyl)methyl)amino)ethyl)carbamate****¹H-NMR analysis:**

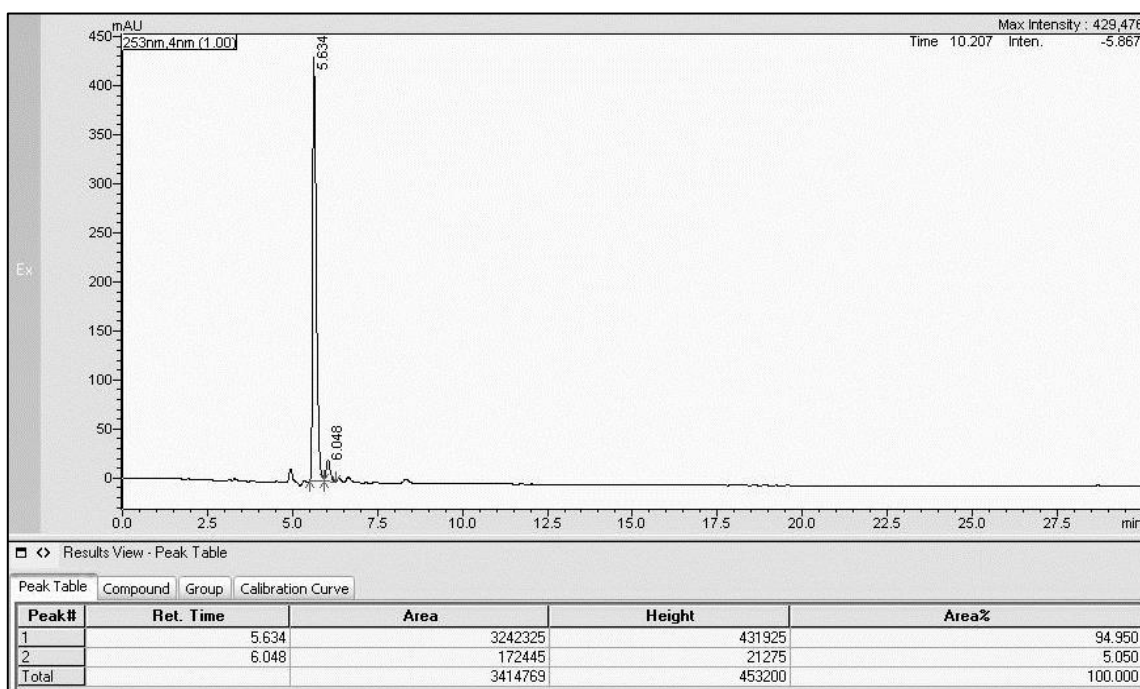
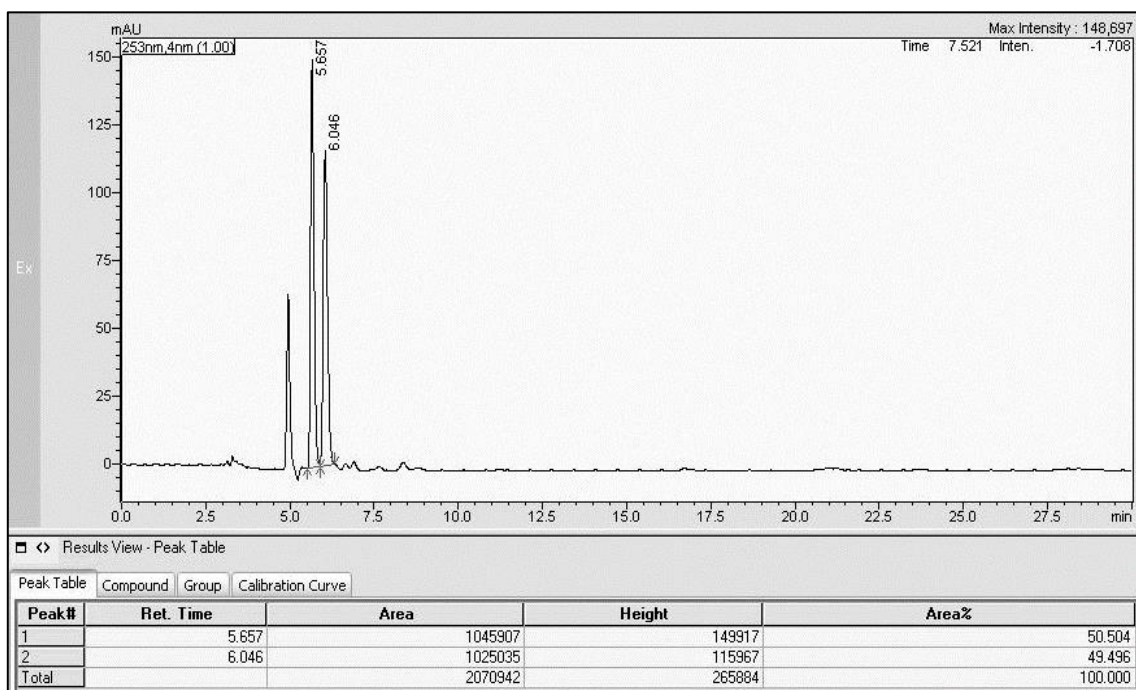
1-((1*S*,2*R*)-1-(Methoxymethyl)-2-phenylcyclobutyl)-*N,N*-dimethylmethanamine

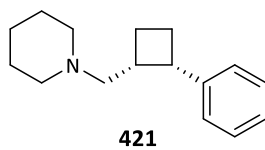
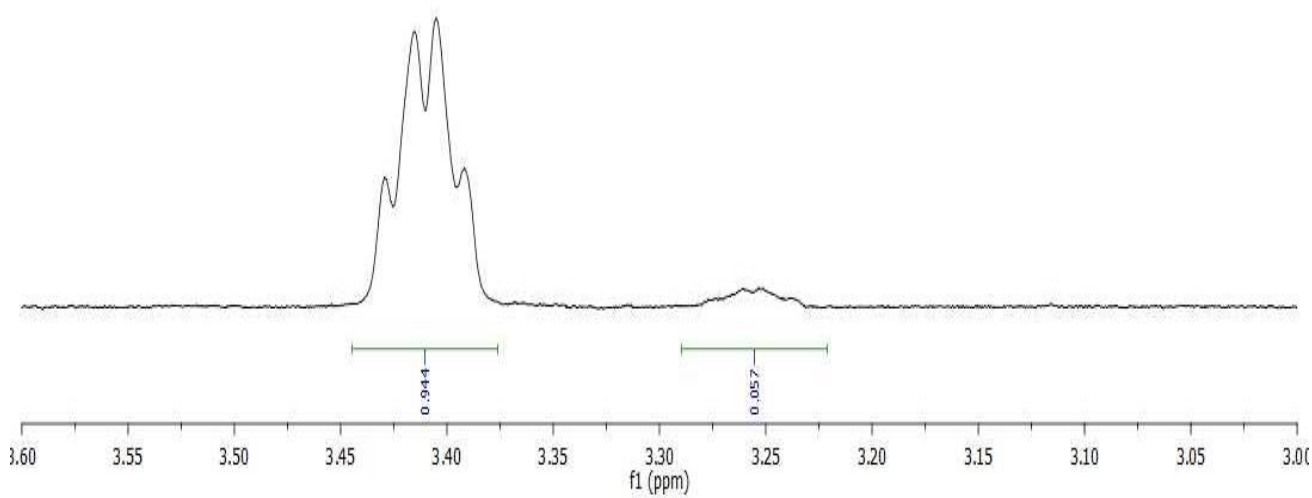
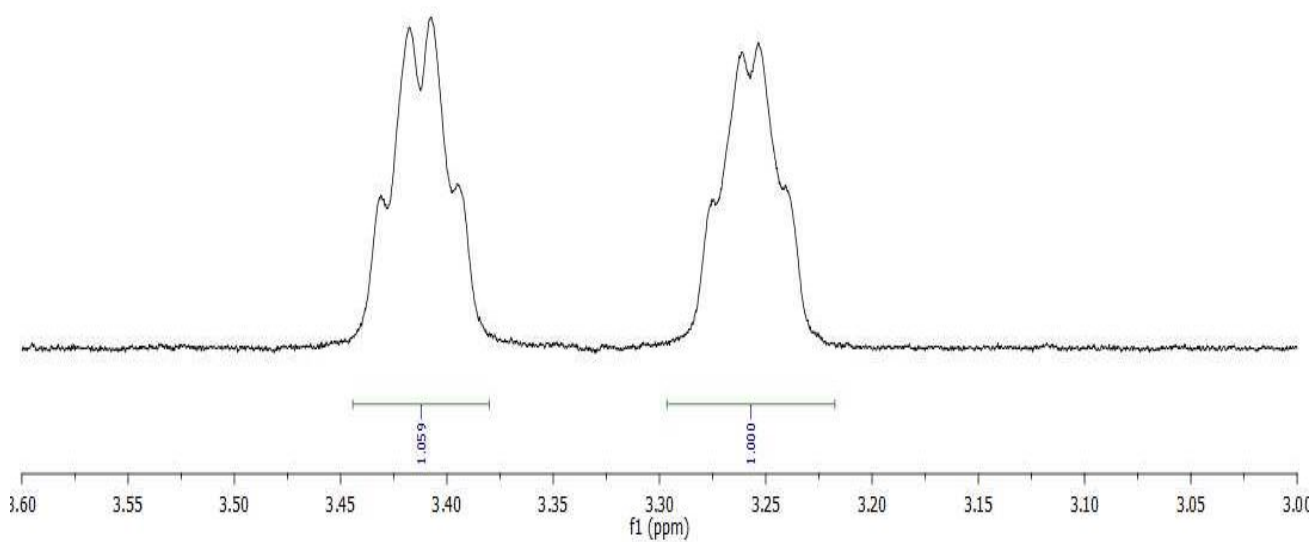
GC-FID analysis: ChiralDex β -DM (50 °C to 72 °C; 0.15 °C/min; linear velocity 40 cm·s⁻¹; split ratio 10.0) t_R = 131.3 min (minor, 11.7%), t_R = 134.3 min (major, 88.3%)

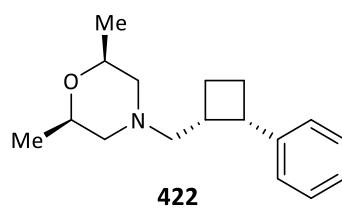


8-(((1*R*,2*S*)-2-Phenylcyclobutyl)methyl)-1,4-dioxaspiro[4.5]decane

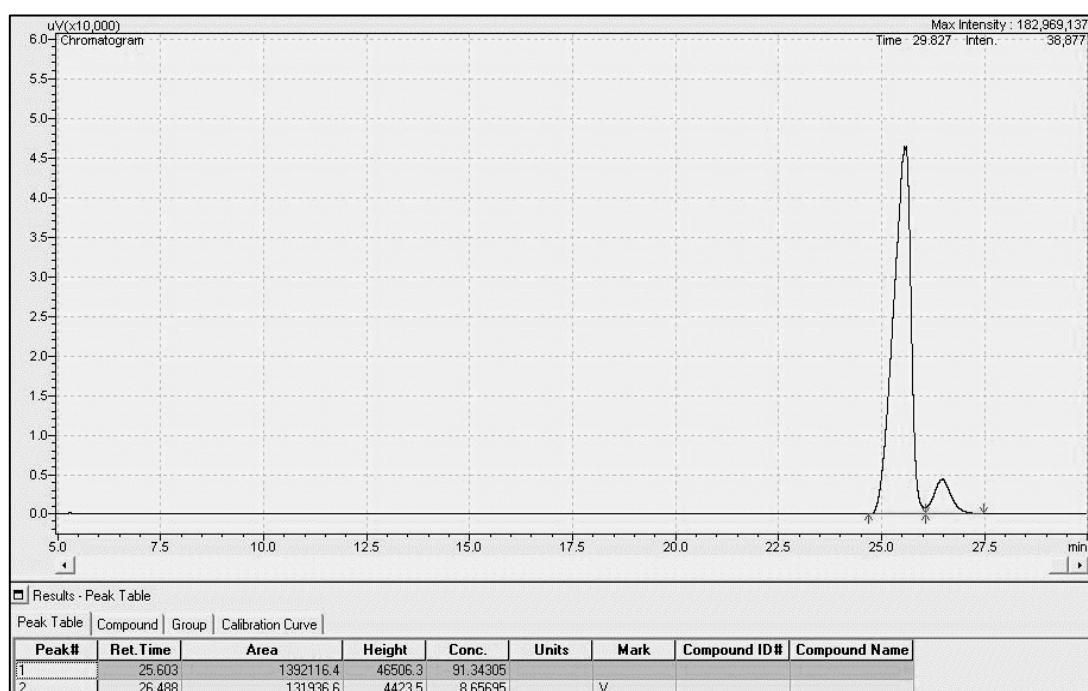
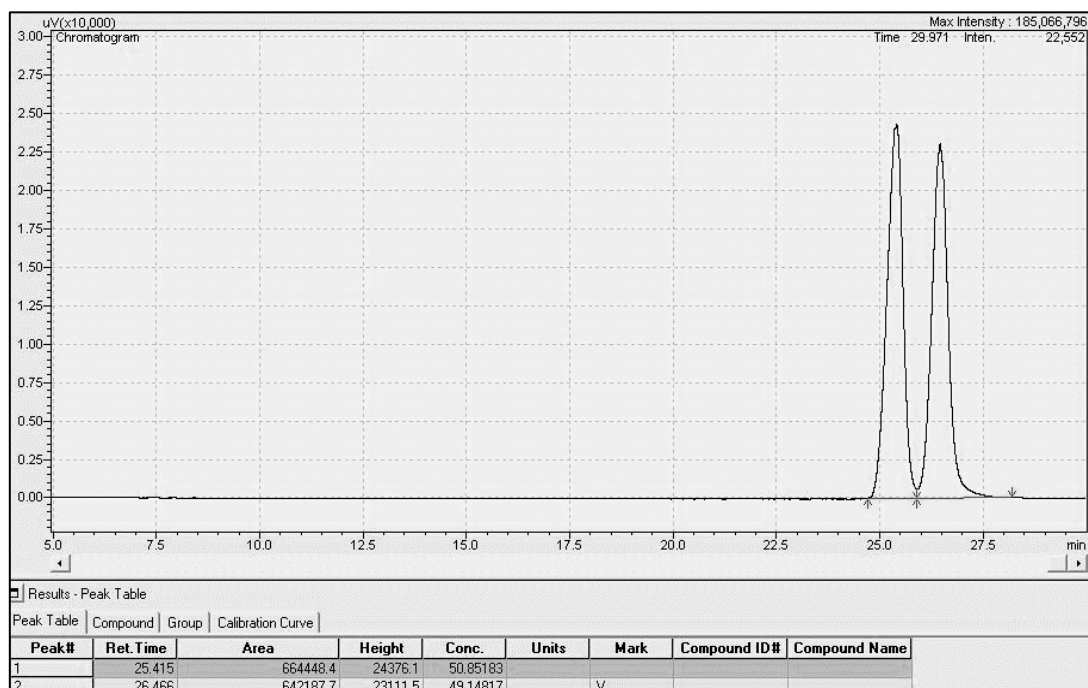
HPLC analysis: Chiralpak AD-H (hexane(0.1% DEA):2-propanol 97:3, 1.0 mL·min⁻¹, 30 °C) t_R = 5.7 min (major, 95.0%), t_R = 6.0 min (minor, 5.0%)



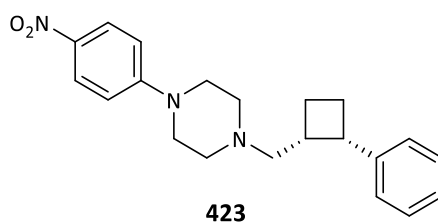
1-(((1*R*,2*S*)-2-Phenylcyclobutyl)methyl)piperidine¹H-NMR analysis:

(2S,6R)-2,6-Dimethyl-4-(((1R,2S)-2-phenylcyclobutyl)methyl)morpholine

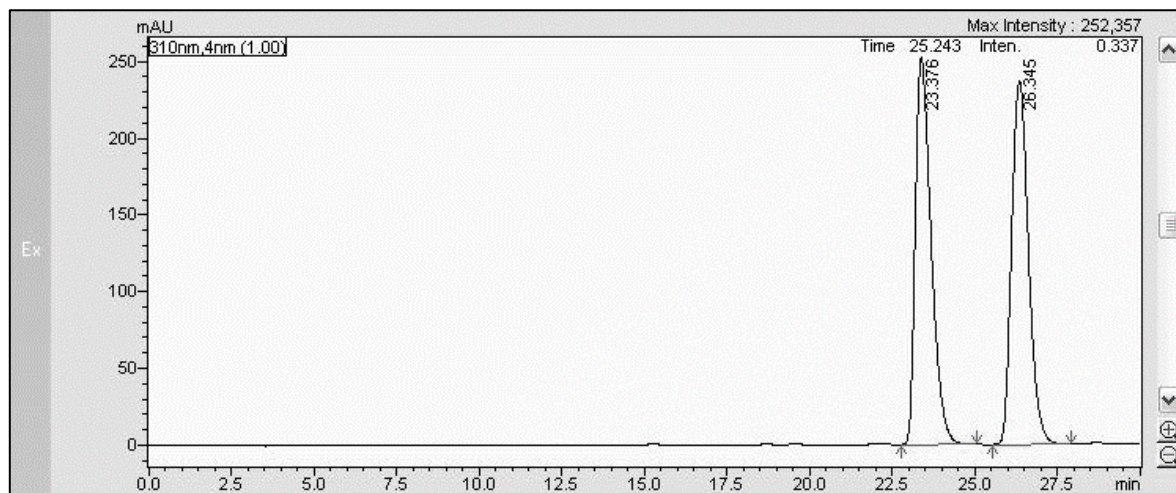
GC-FID analysis: ChiralDex β -DM (110 °C; isocratic; linear velocity 40 cm·s⁻¹; split ratio 10.0) t_R = 25.6 min (major, 91.3%), t_R = 26.5 min (minor, 8.7%)



1-(4-Nitrophenyl)-4-(((1R,2S)-2-phenylcyclobutyl)methyl)piperazine



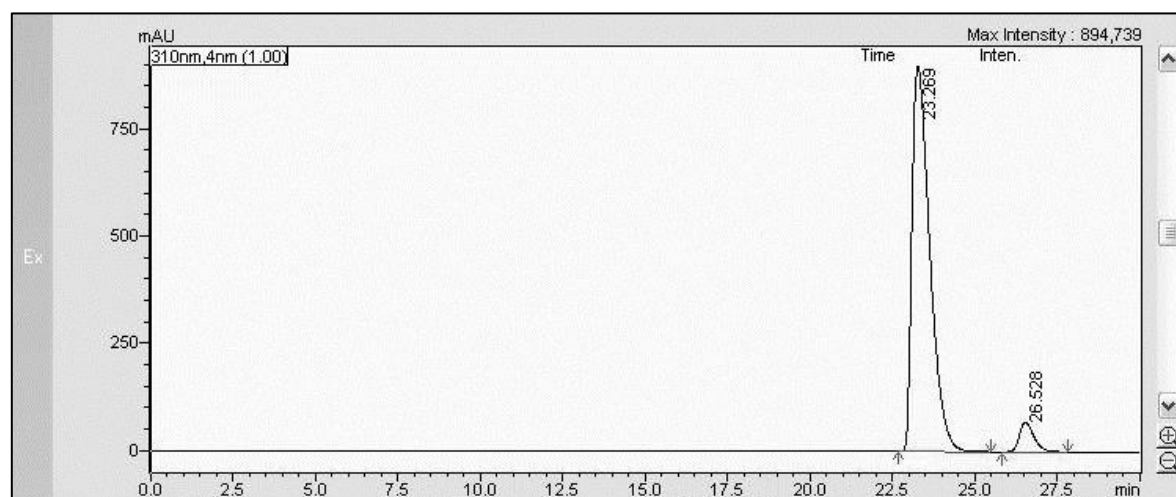
HPLC analysis: Chiralpak AD-H (hexane(0.1% DEA):2-propanol 98:2, 1.0 mL·min⁻¹, 30 °C) t_R = 23.3 min (major, 94.1%), t_R = 26.5 min (minor, 5.9%)



Results View - Peak Table

Peak Table Compound Group Calibration Curve

Peak#	Ret. Time	Area	Height	Area%
1	23.376	8405251	252063	50.042
2	26.345	8391033	237142	49.958
Total		16796285	489206	100.000

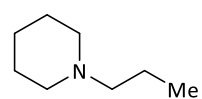


Results View - Peak Table

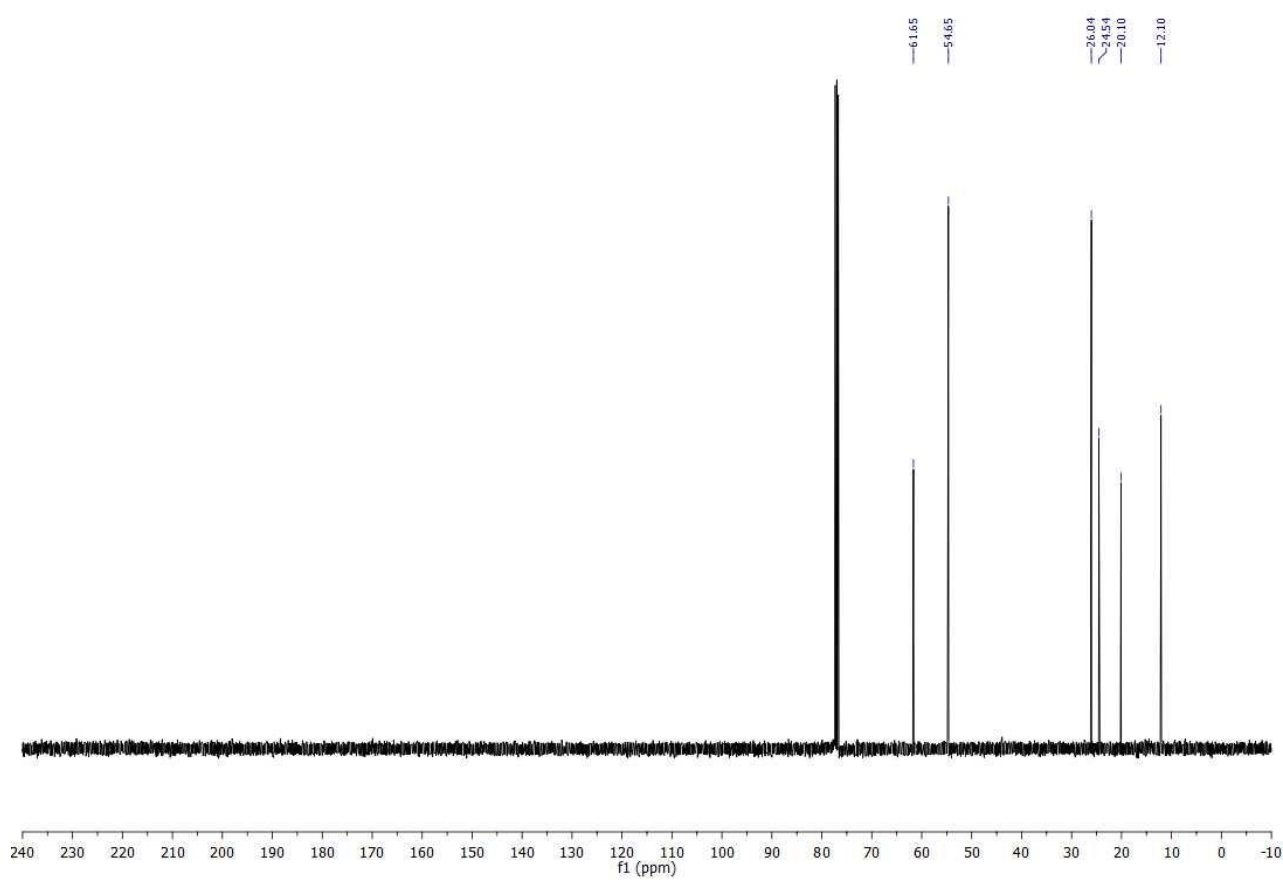
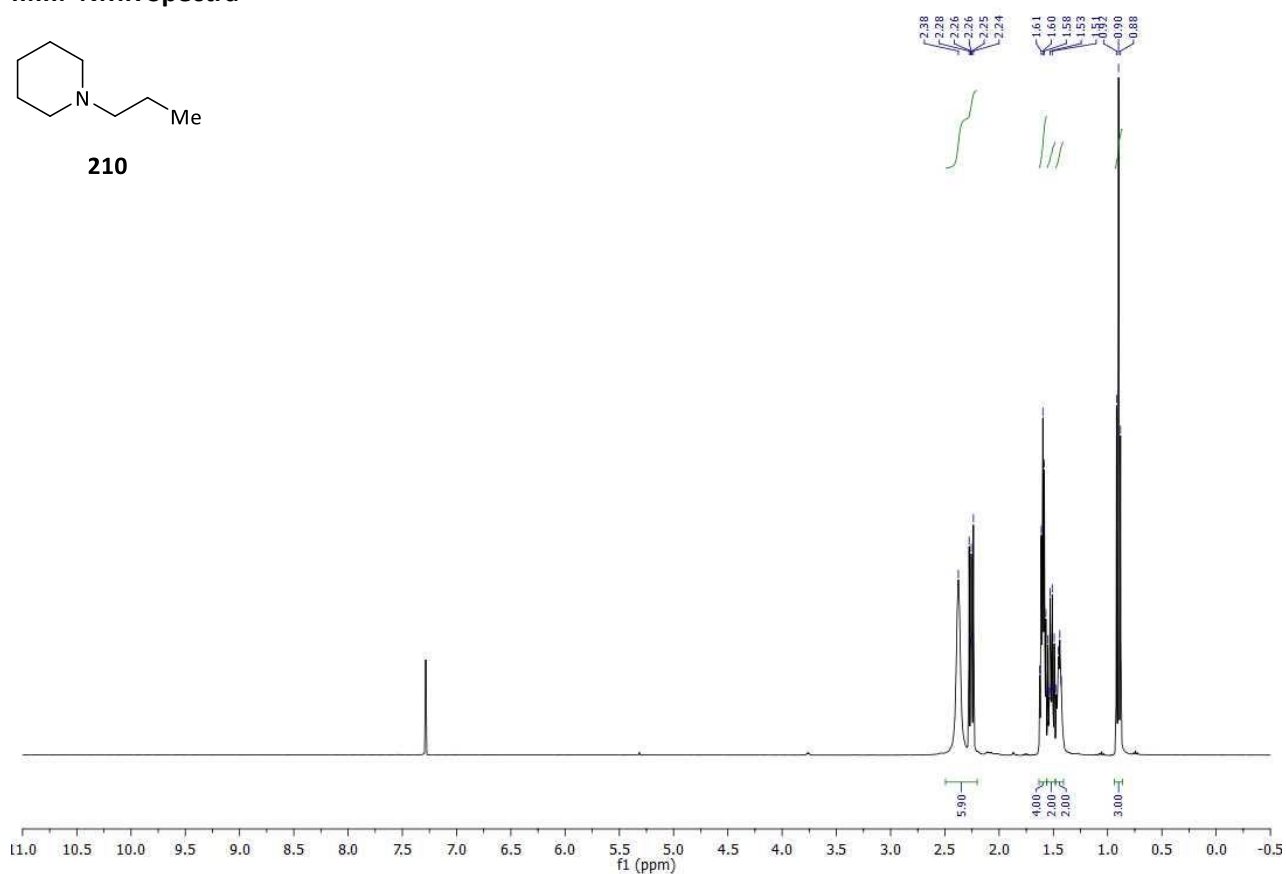
Peak Table Compound Group Calibration Curve

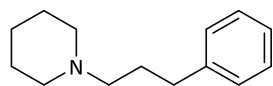
Peak#	Ret. Time	Area	Height	Area%
1	23.269	33898114	897172	94.062
2	26.528	2139766	69422	5.938
Total		36037880	966594	100.000

II.III. NMR Spectra

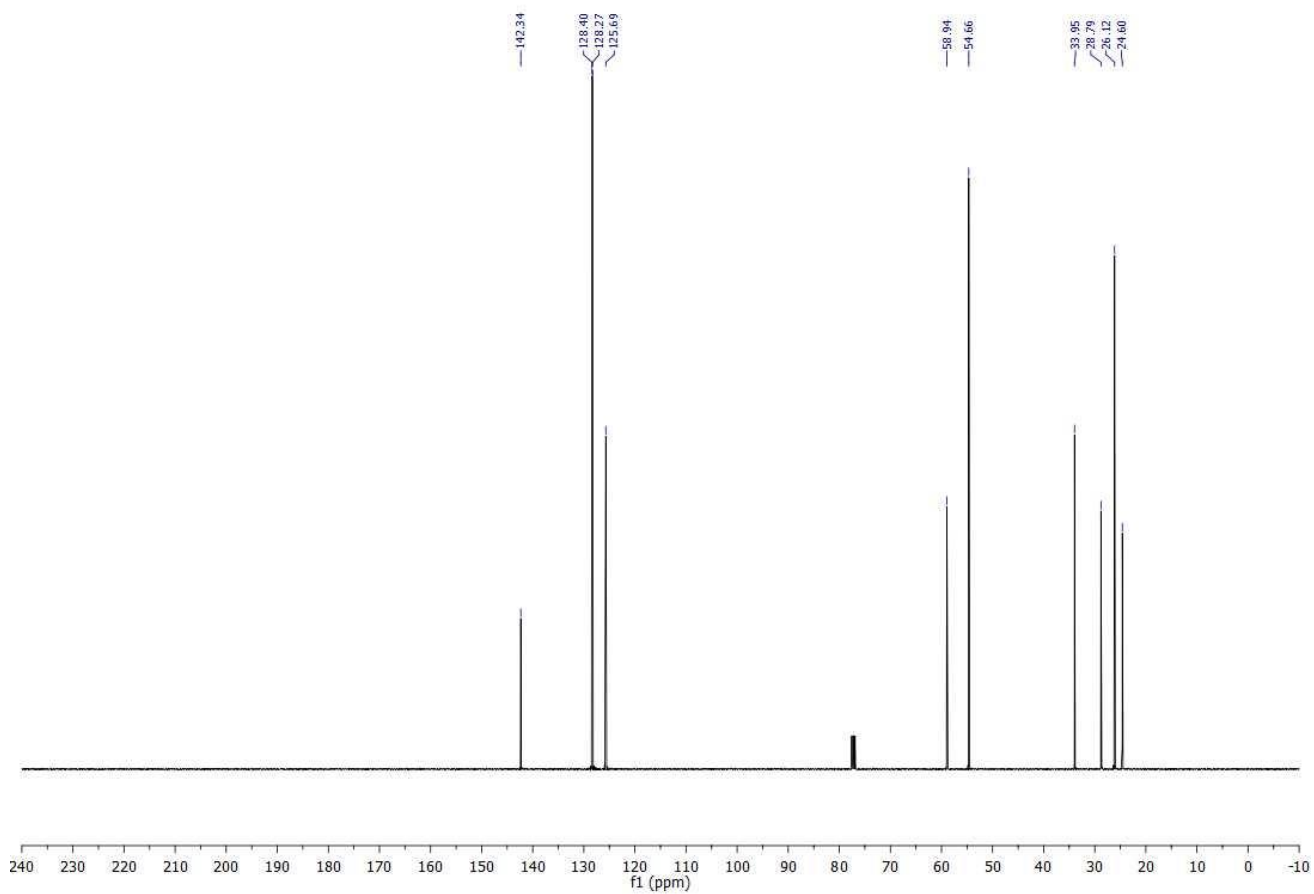
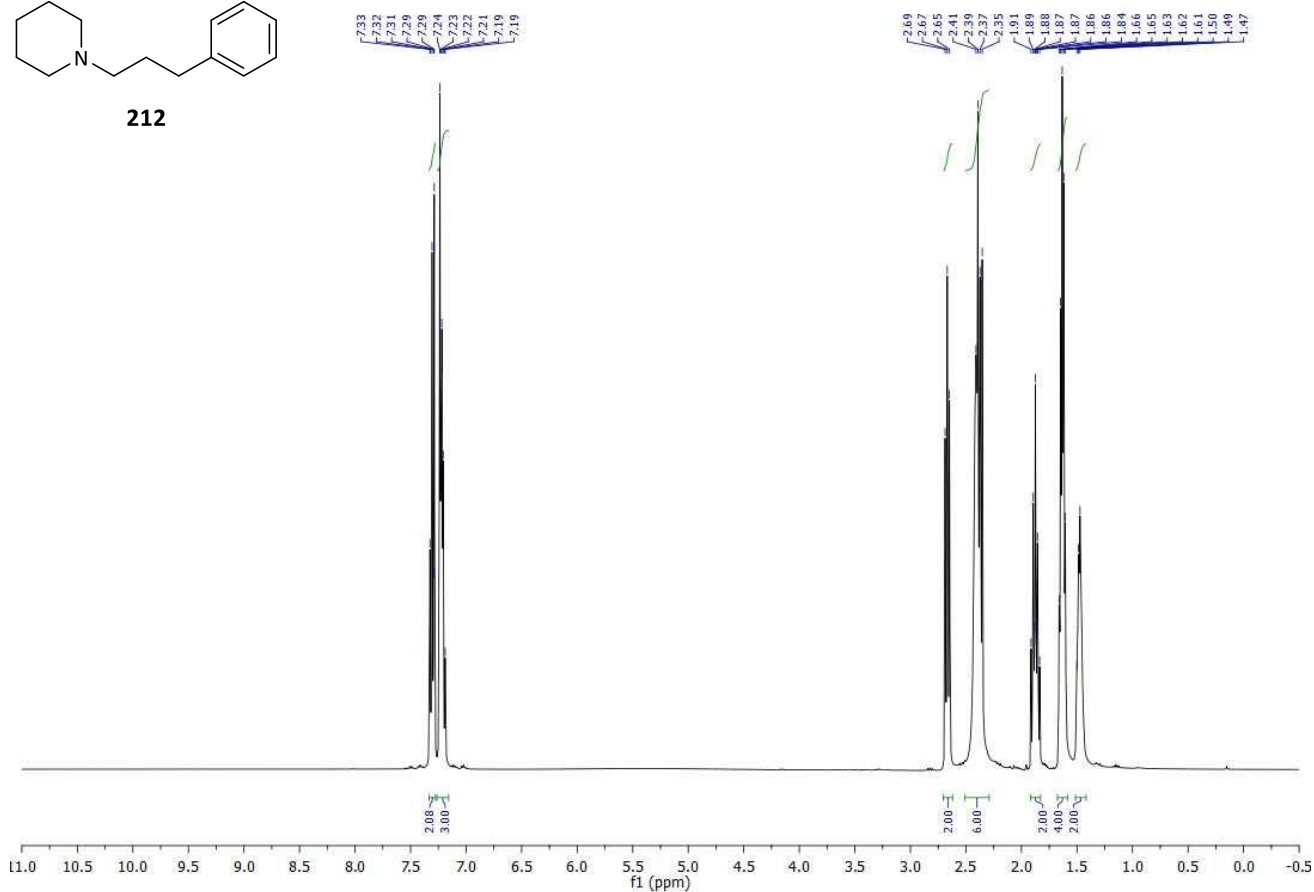


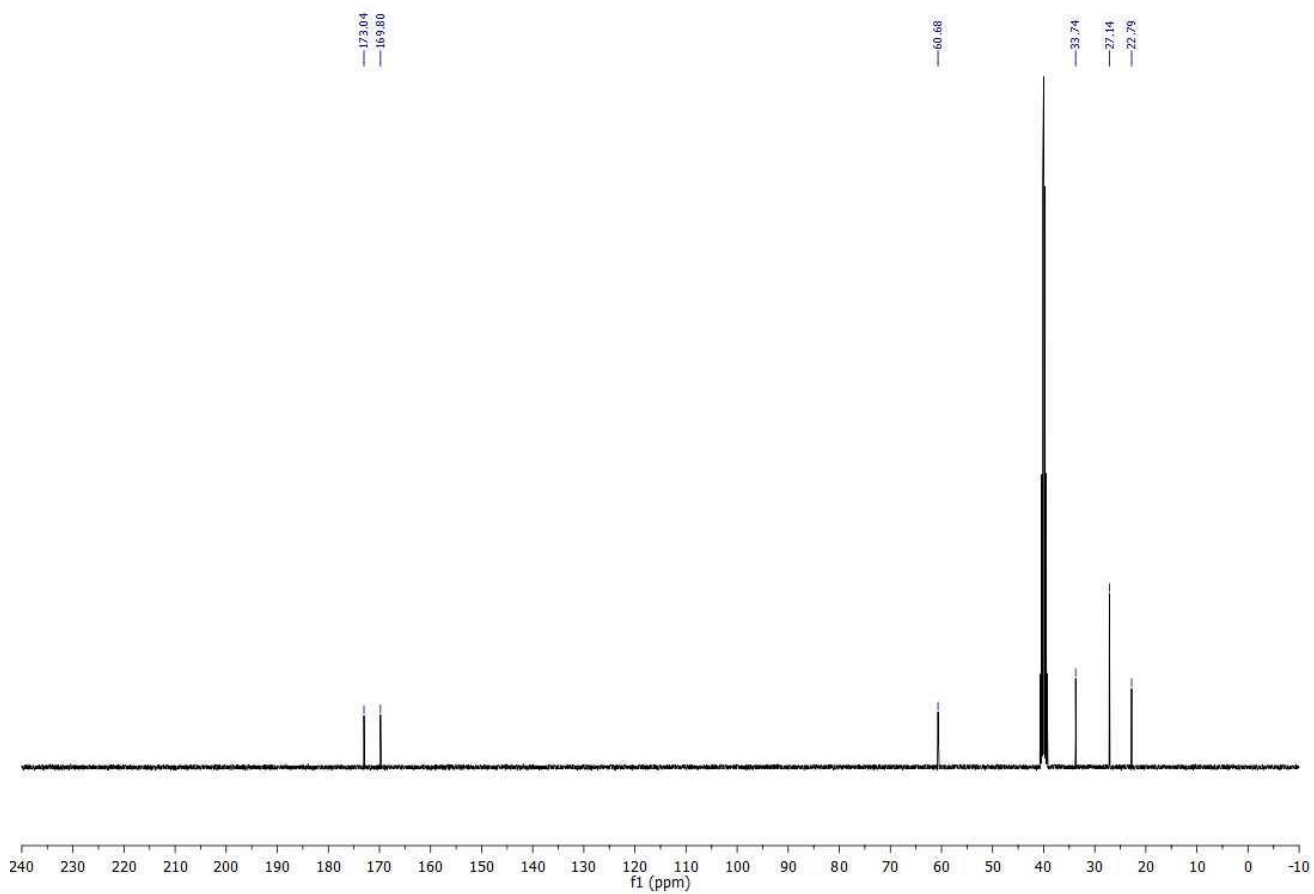
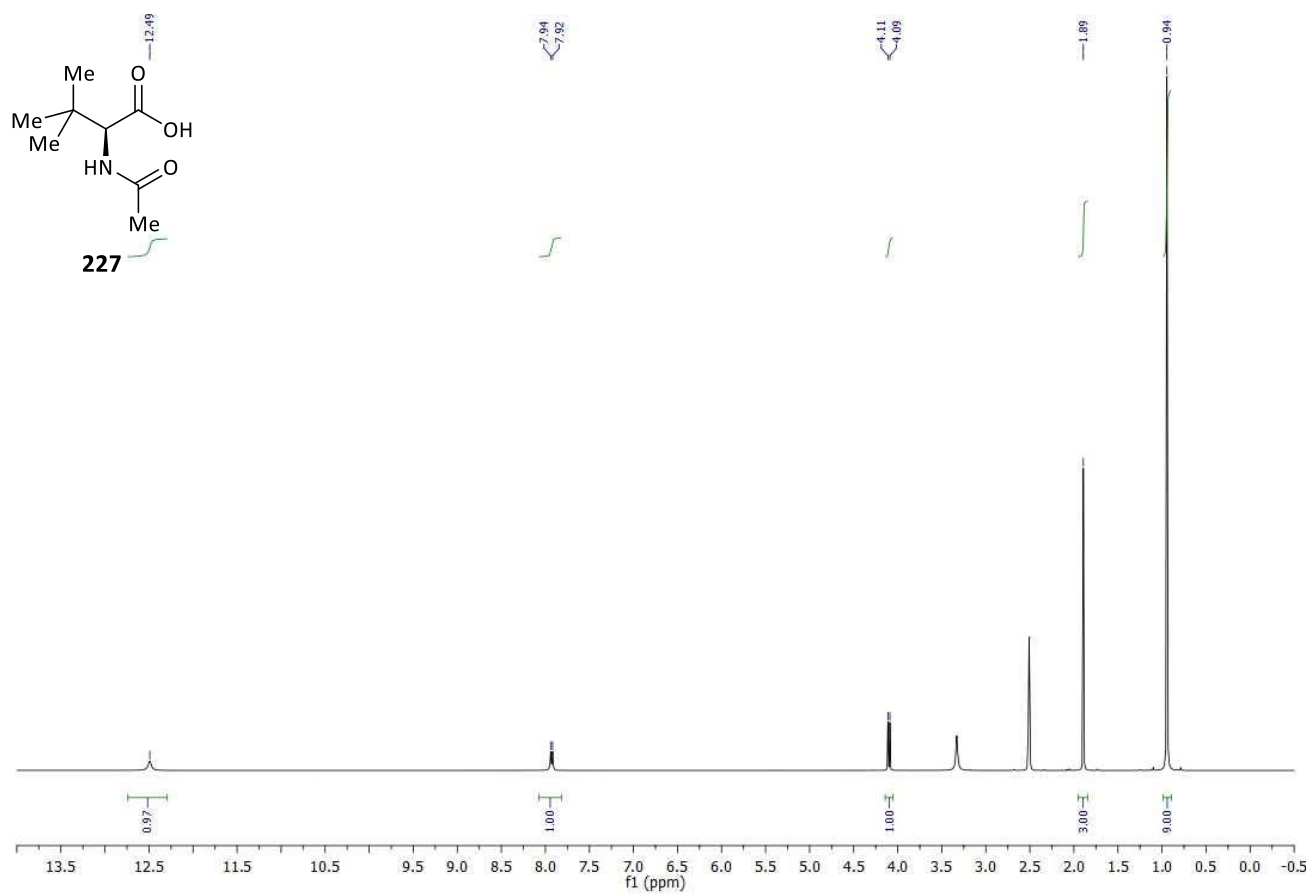
210

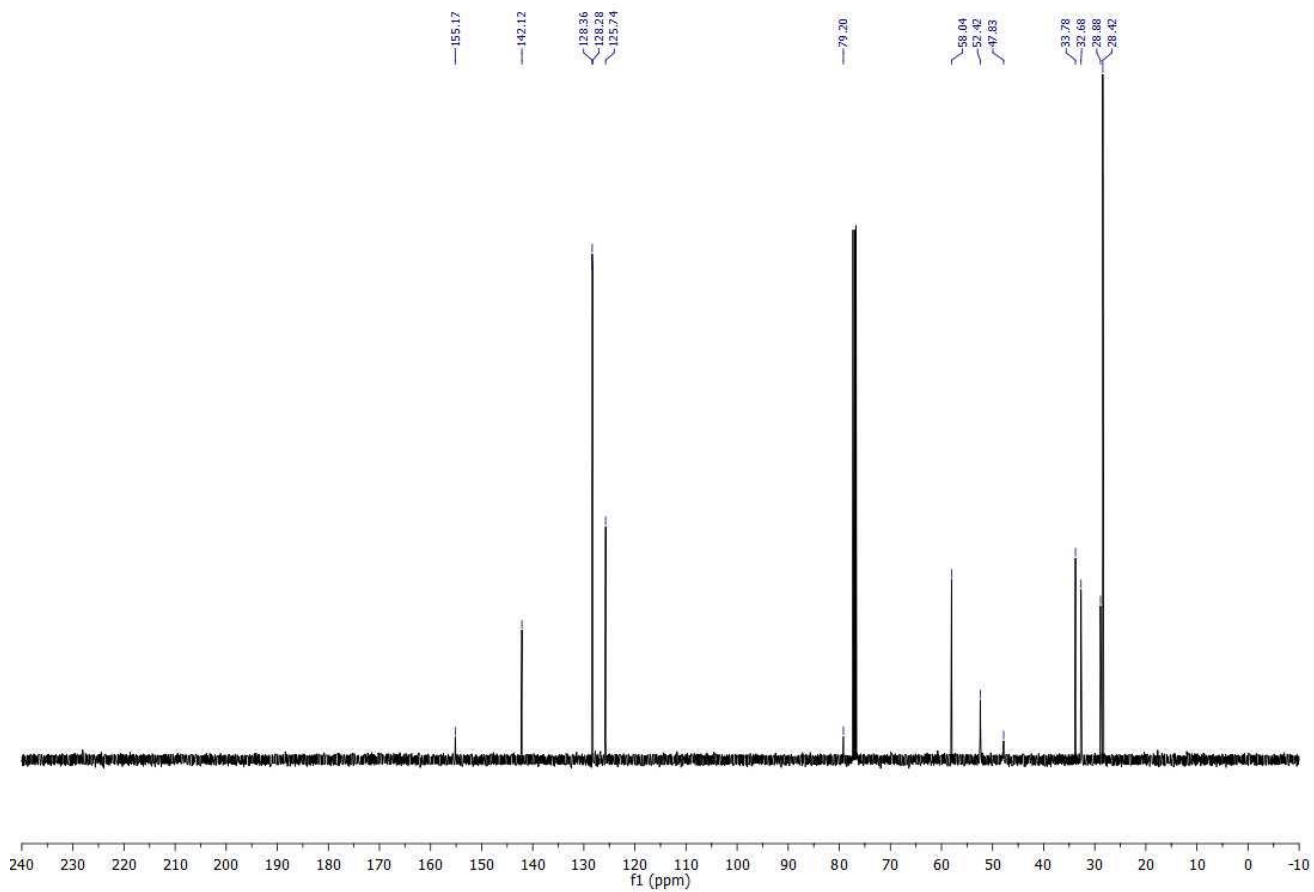
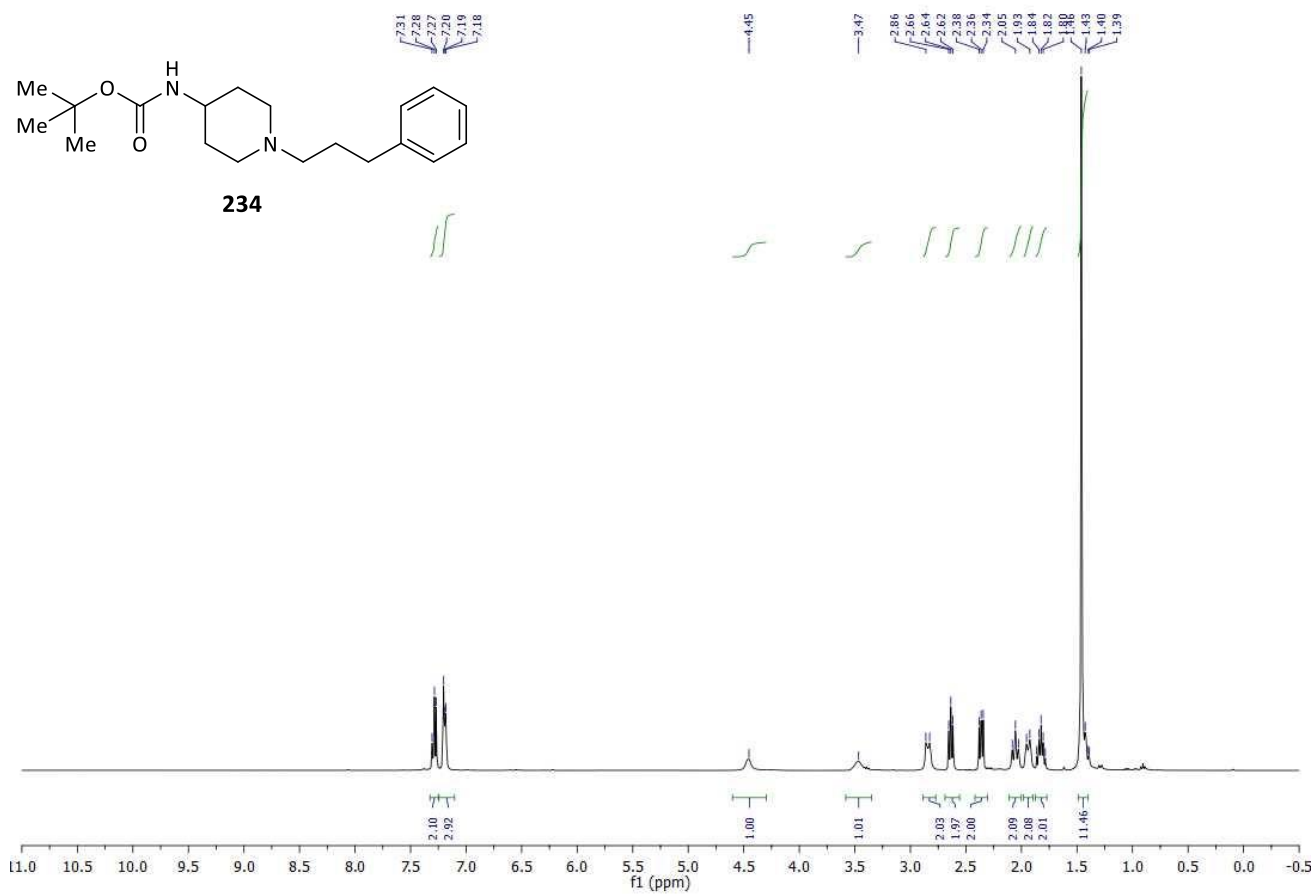


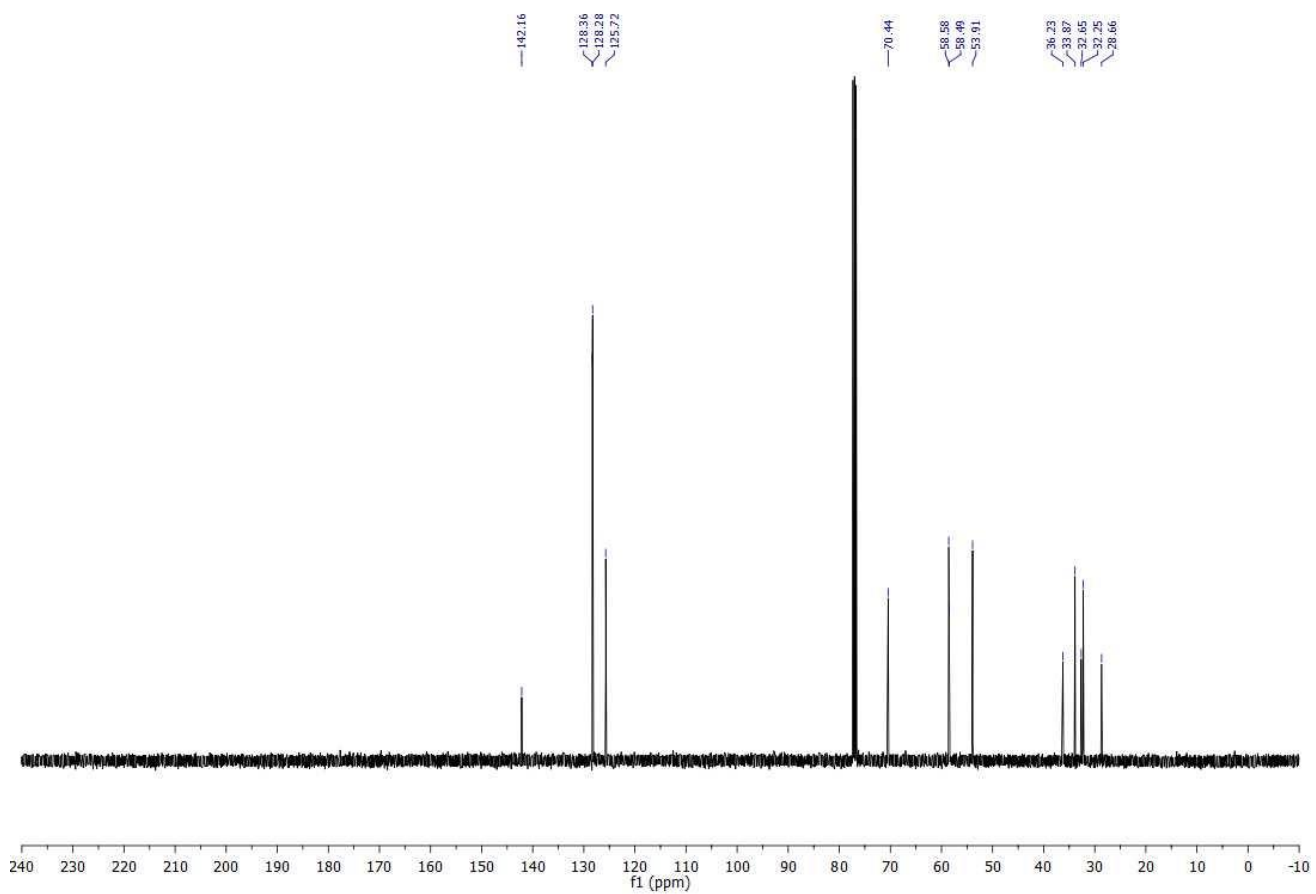
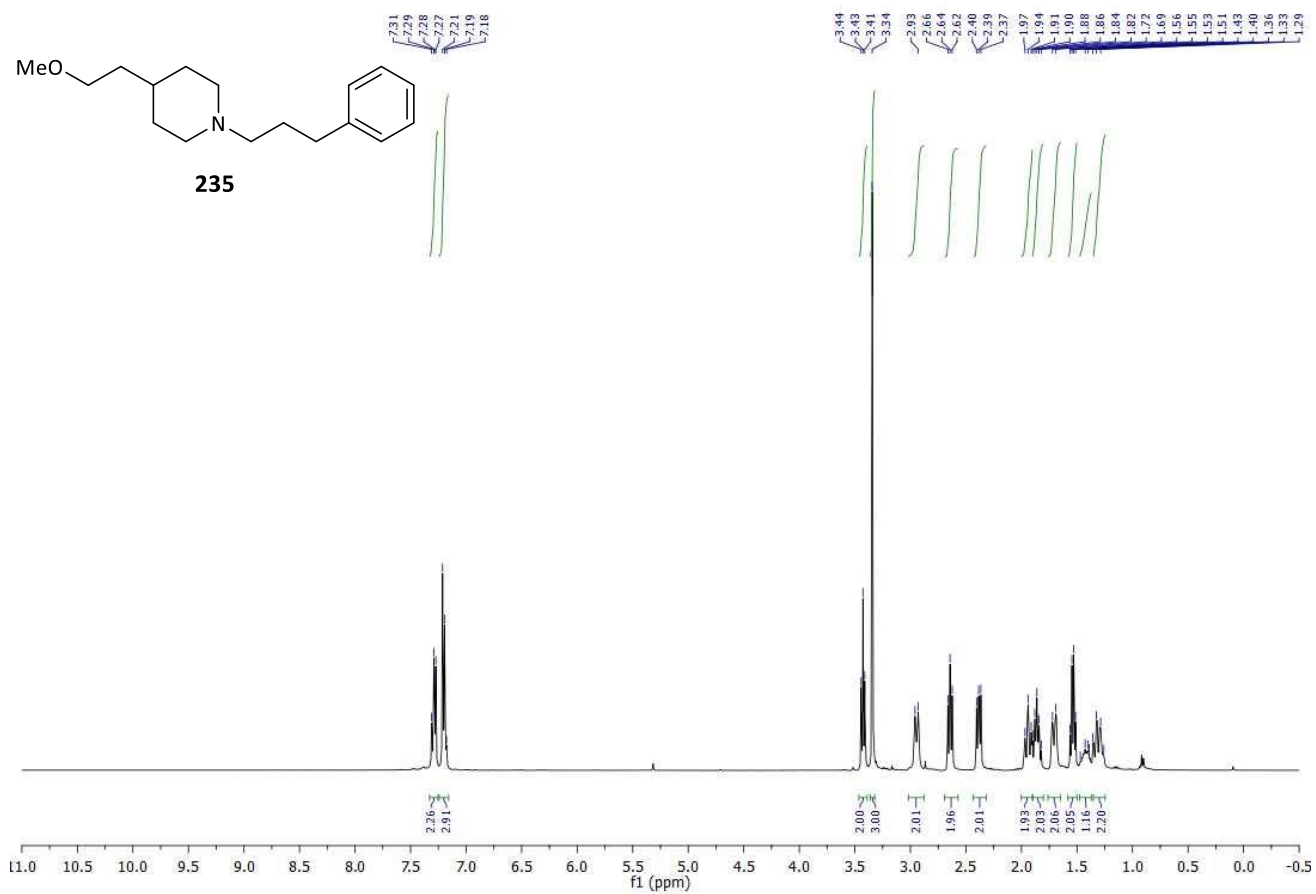


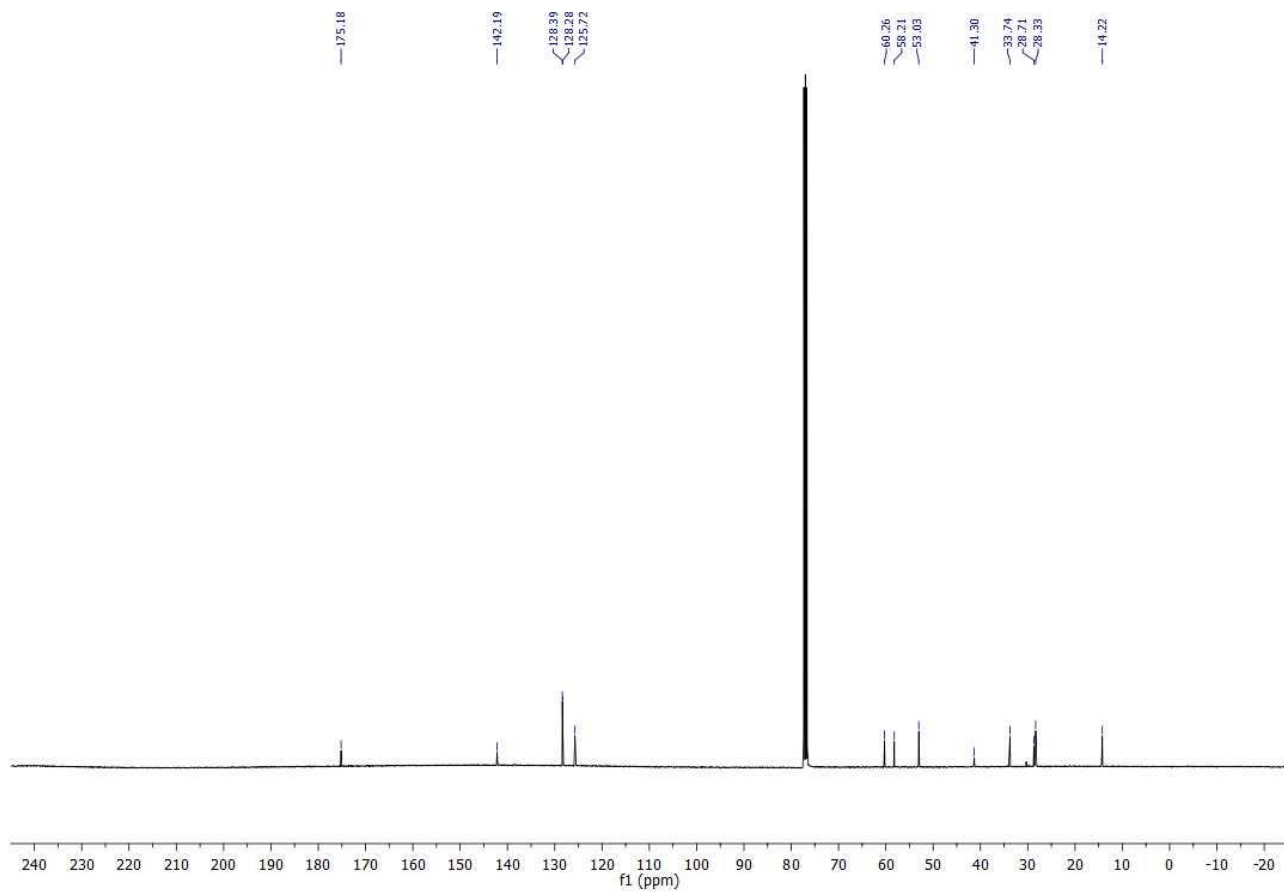
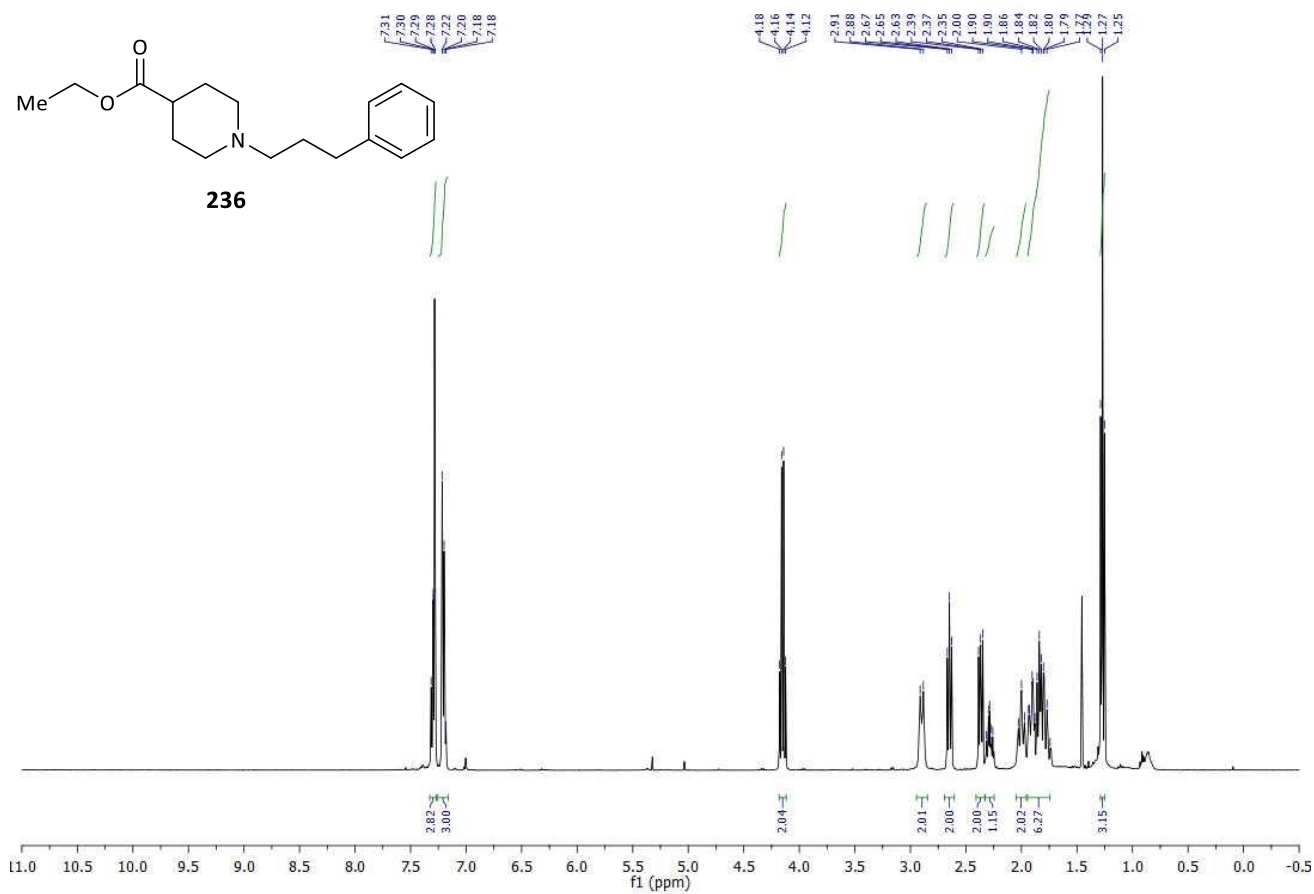
212

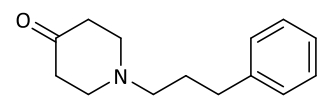




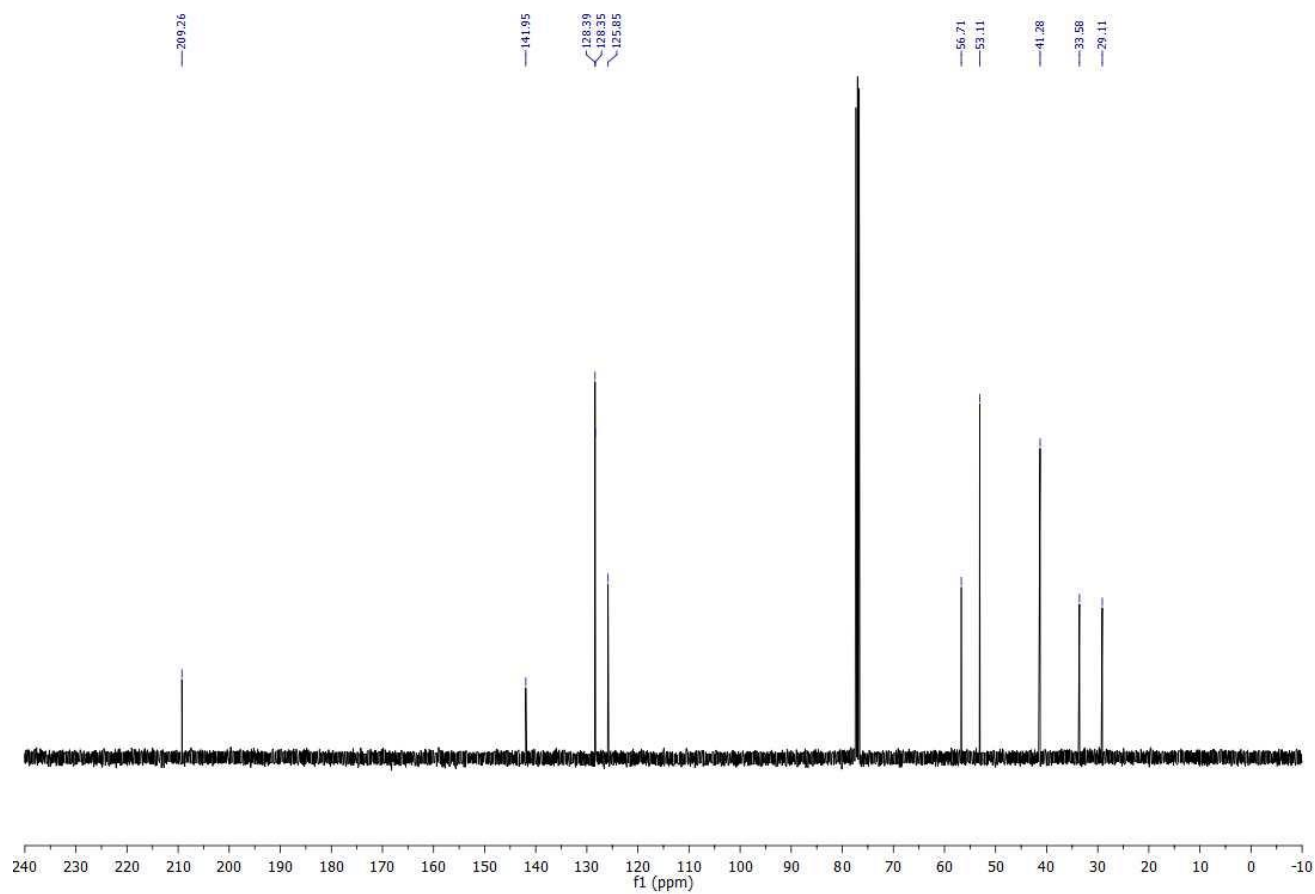
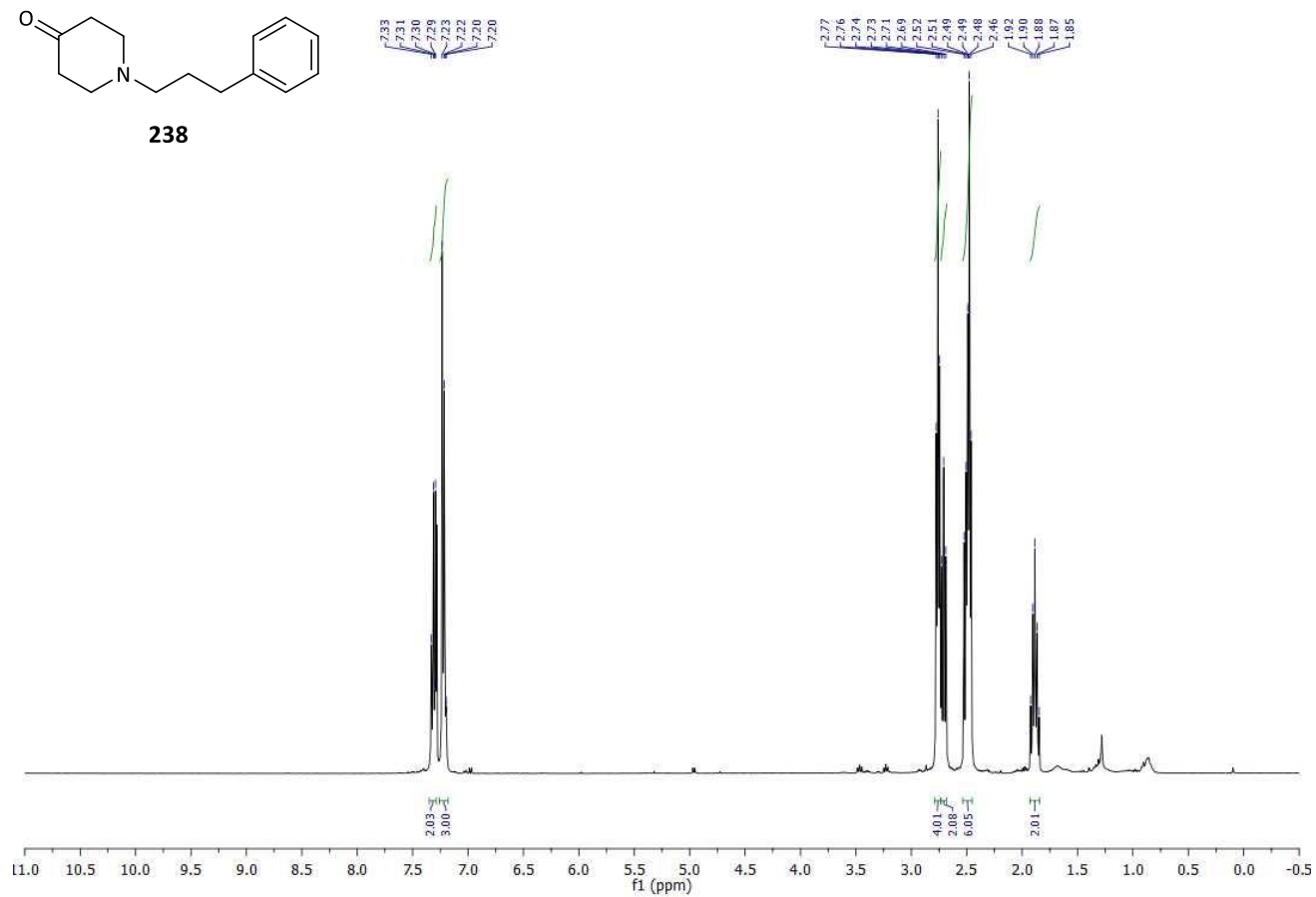


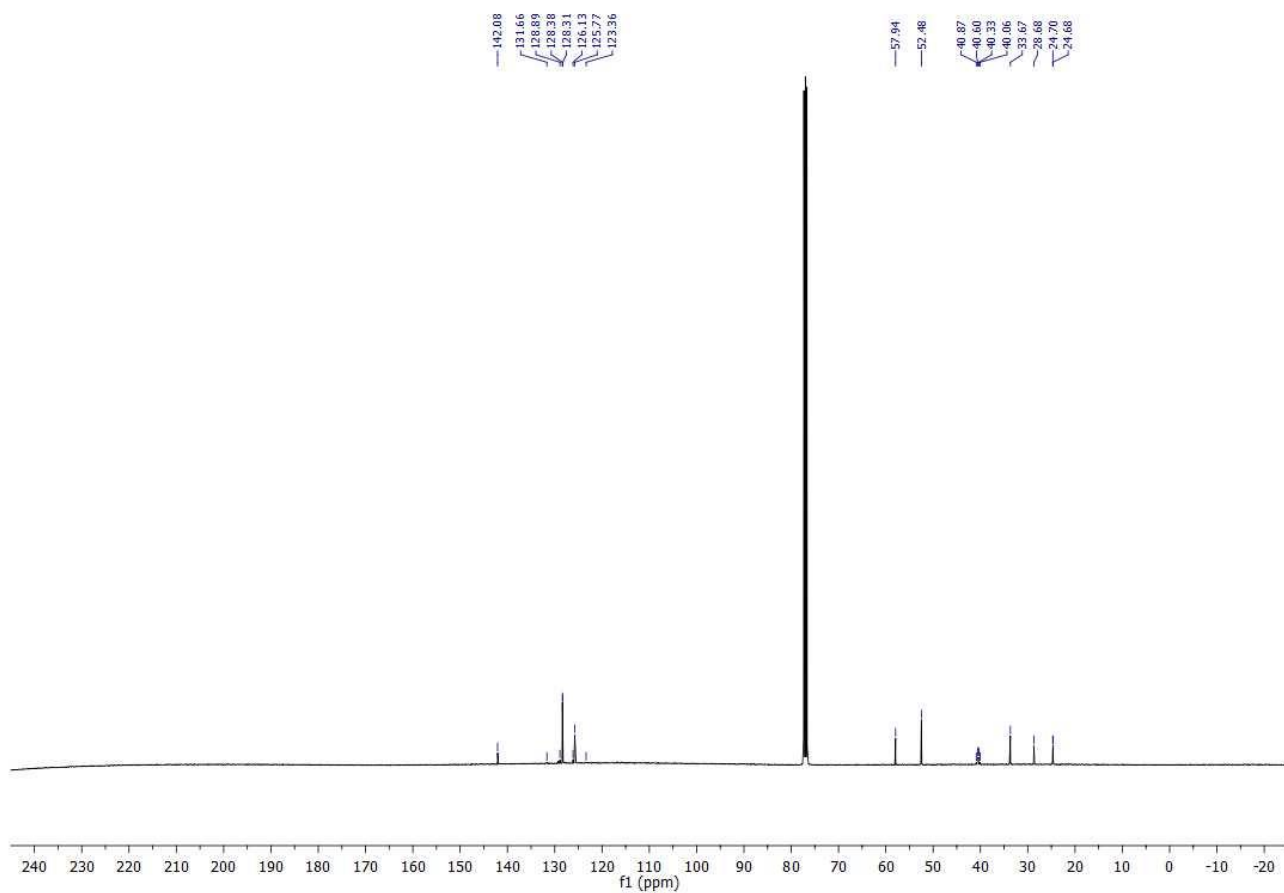
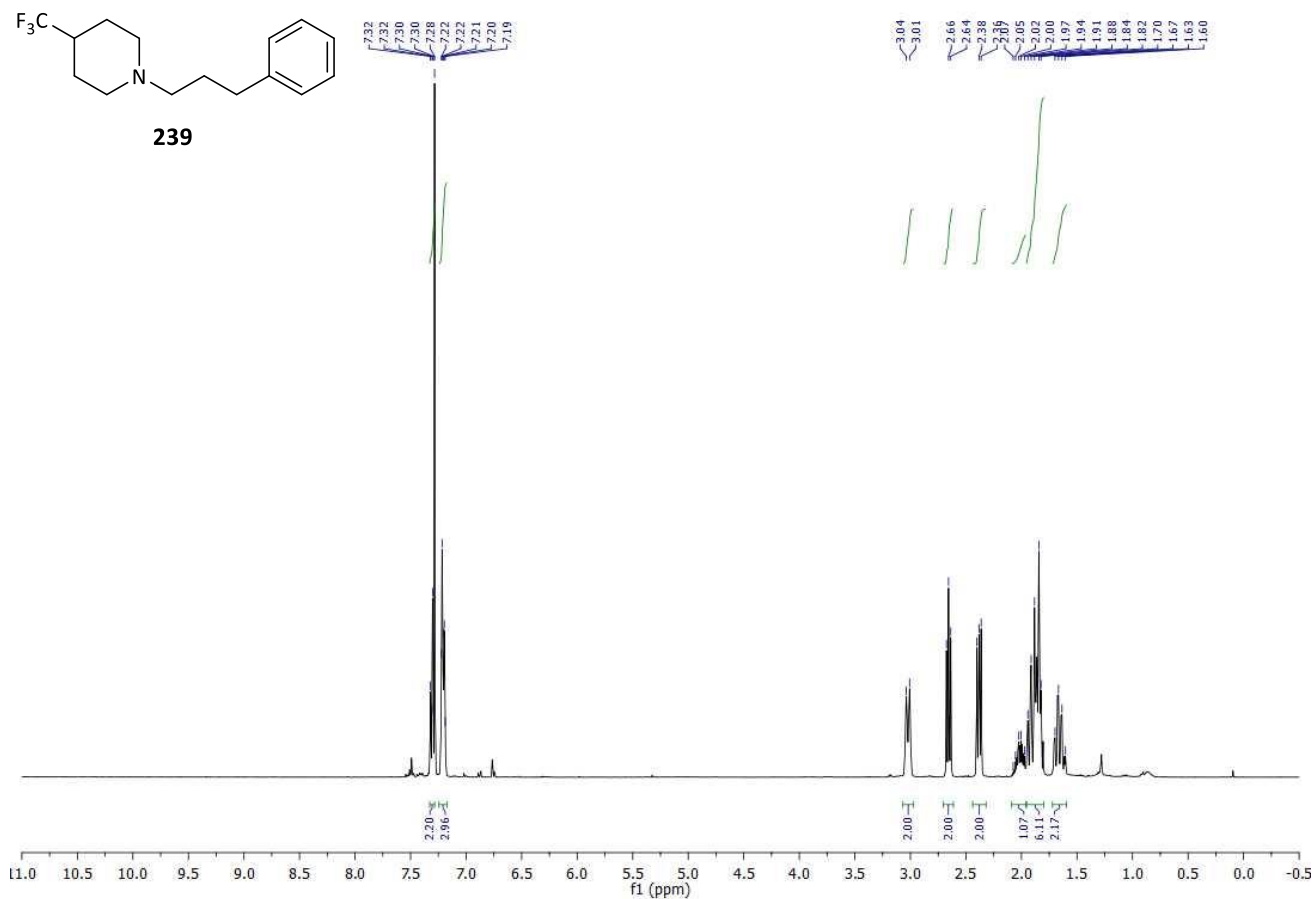


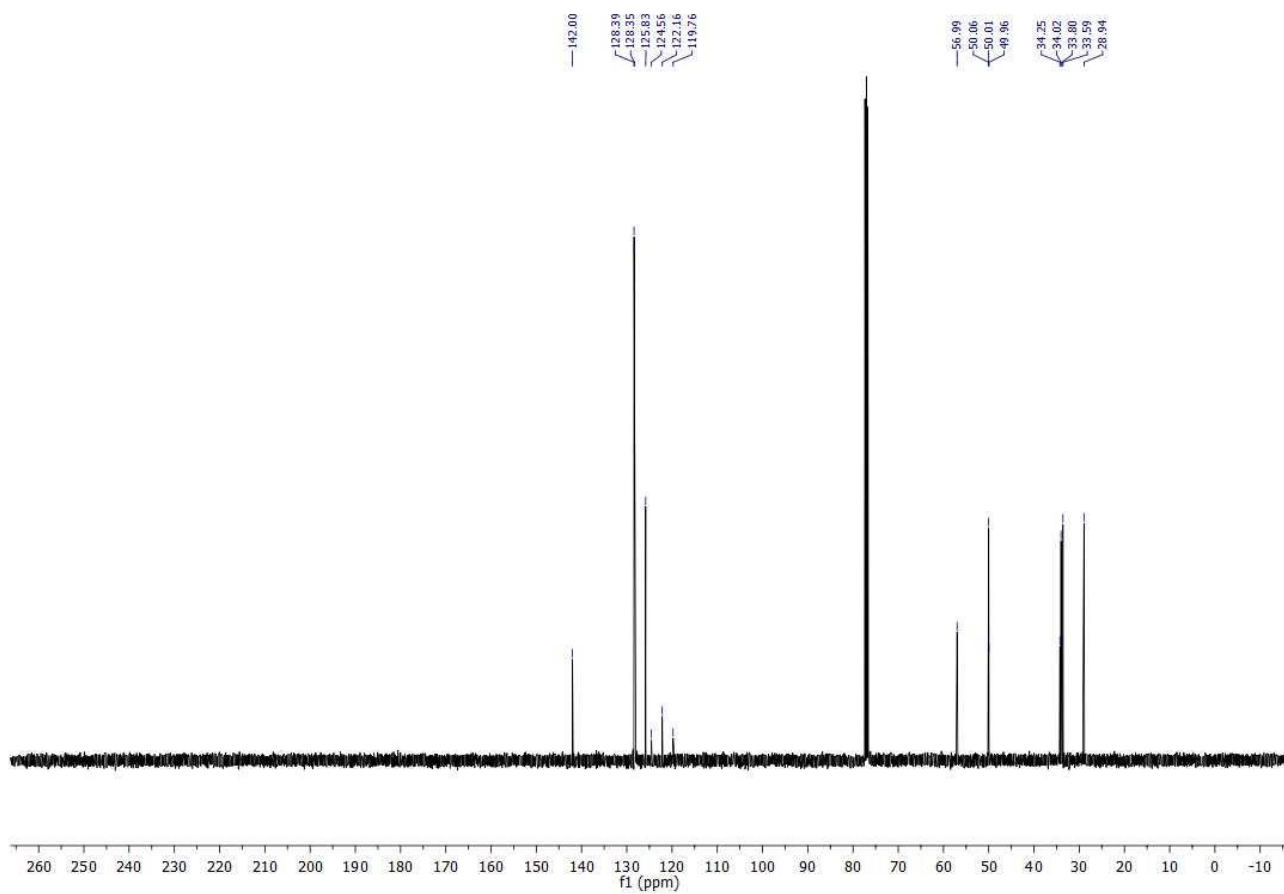
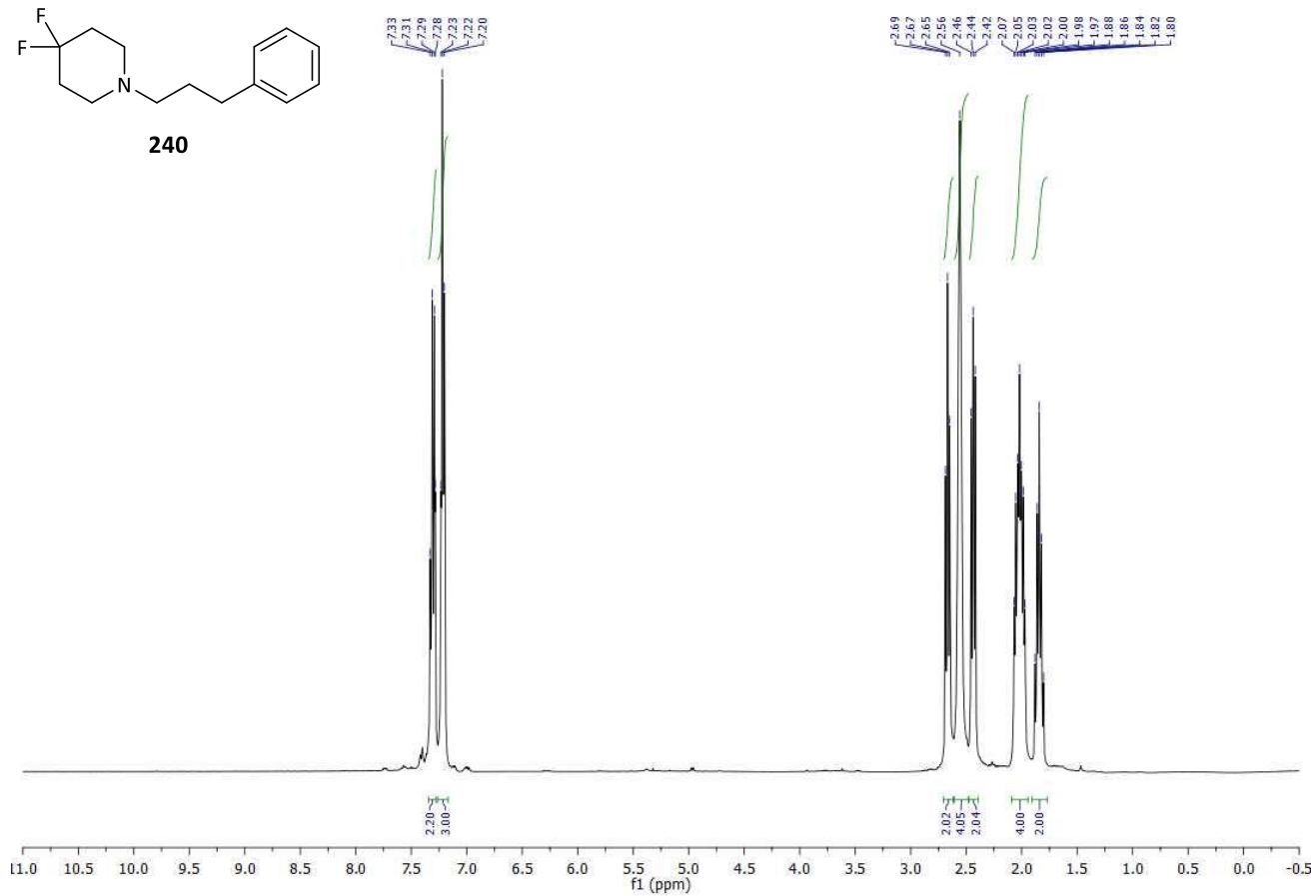
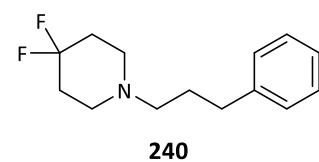


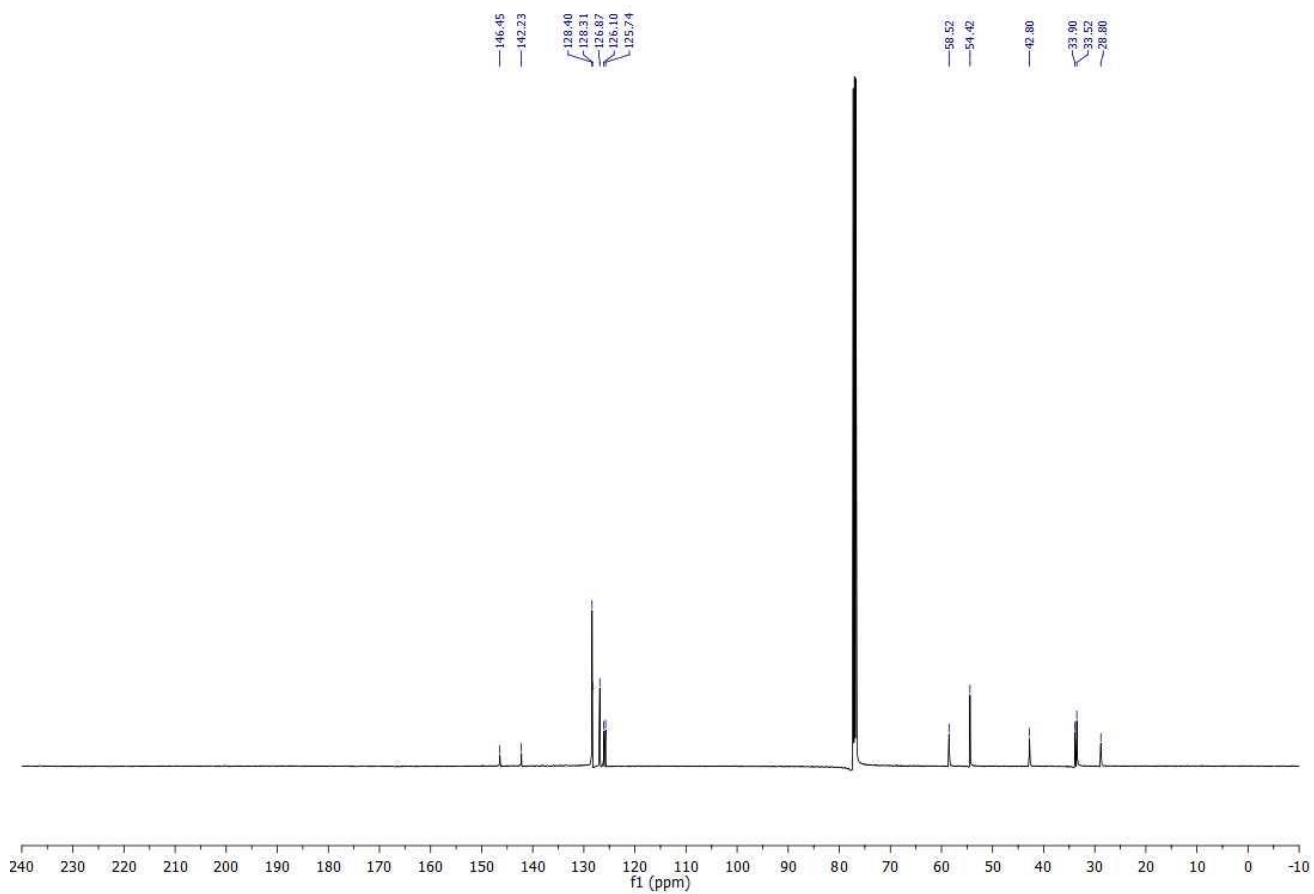
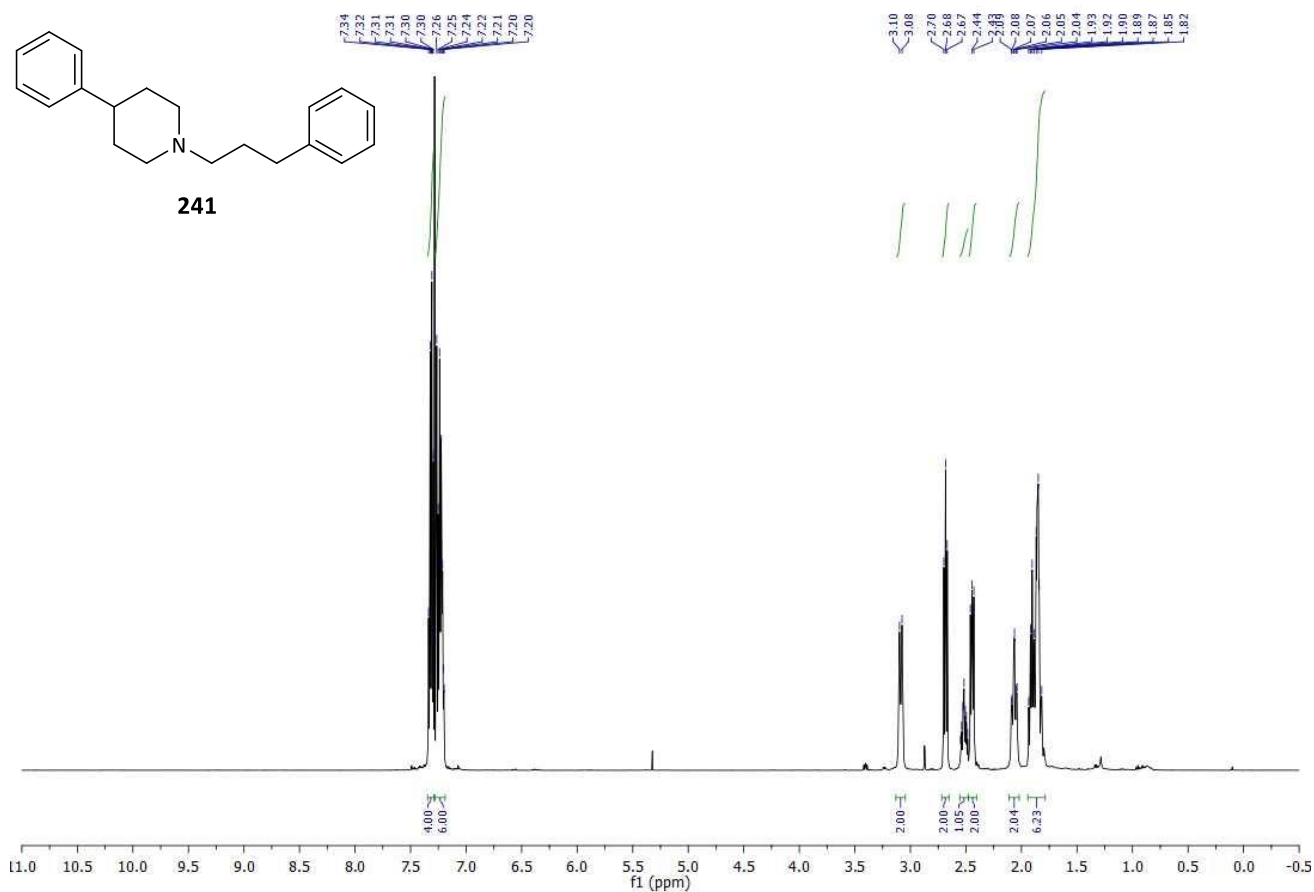


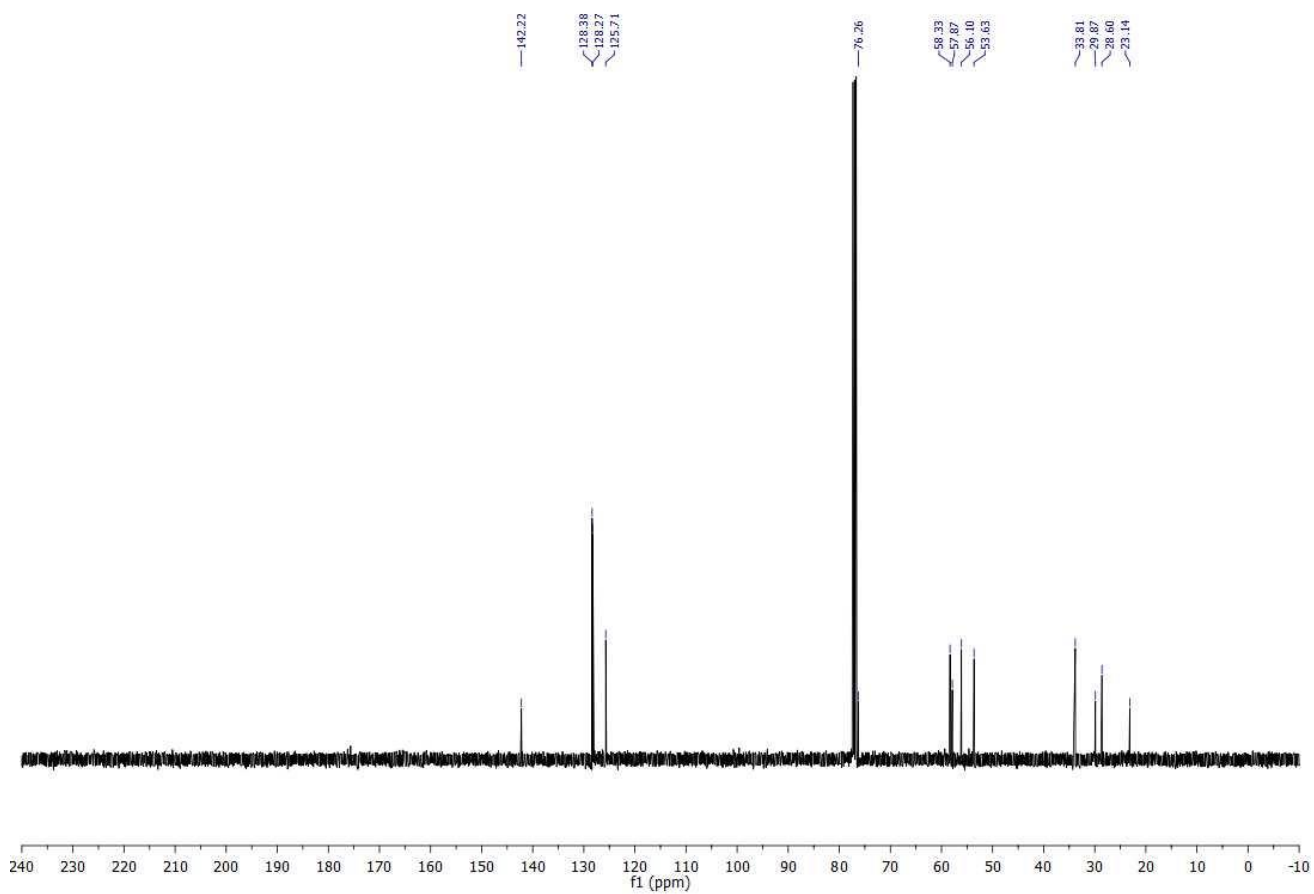
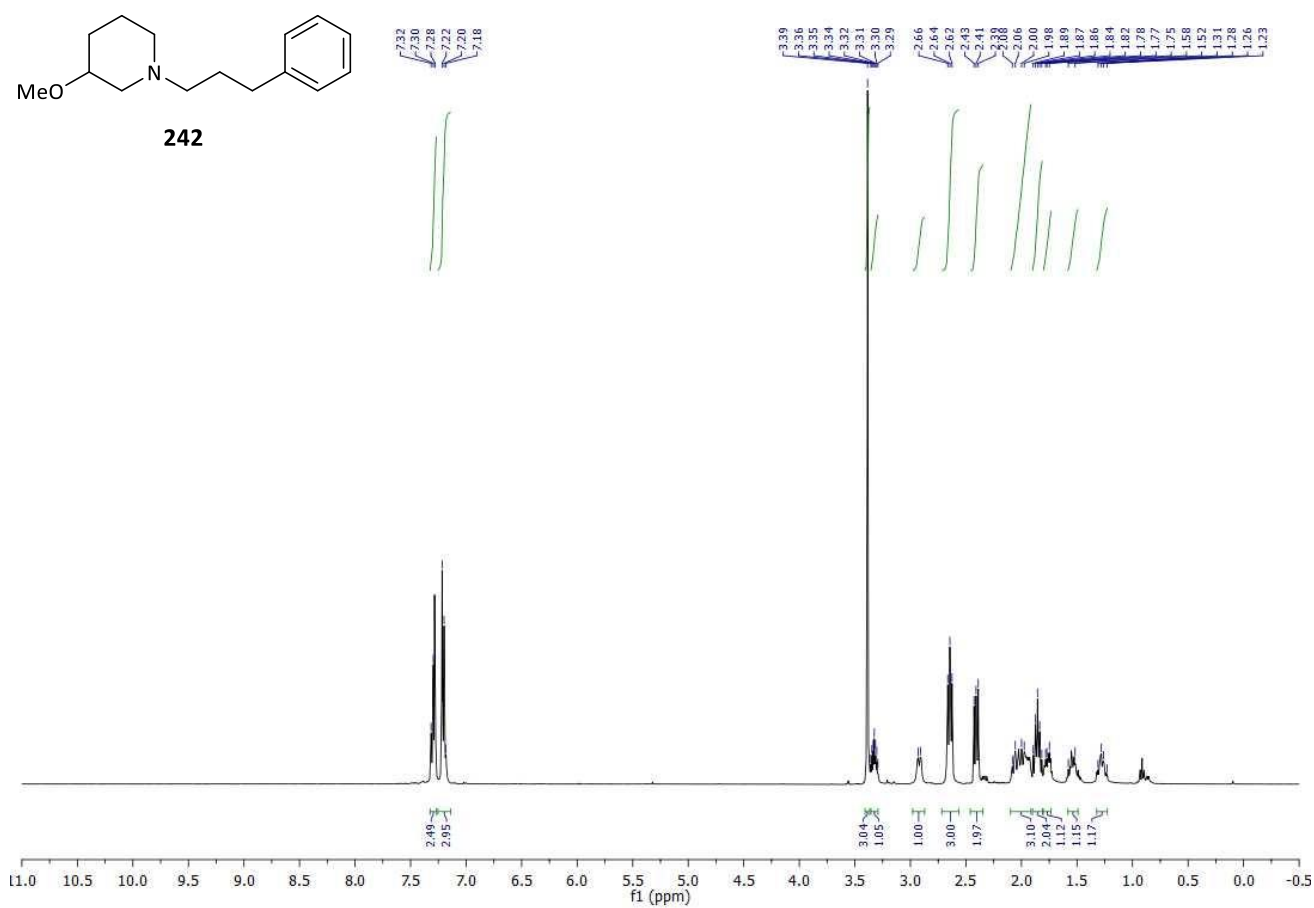
238

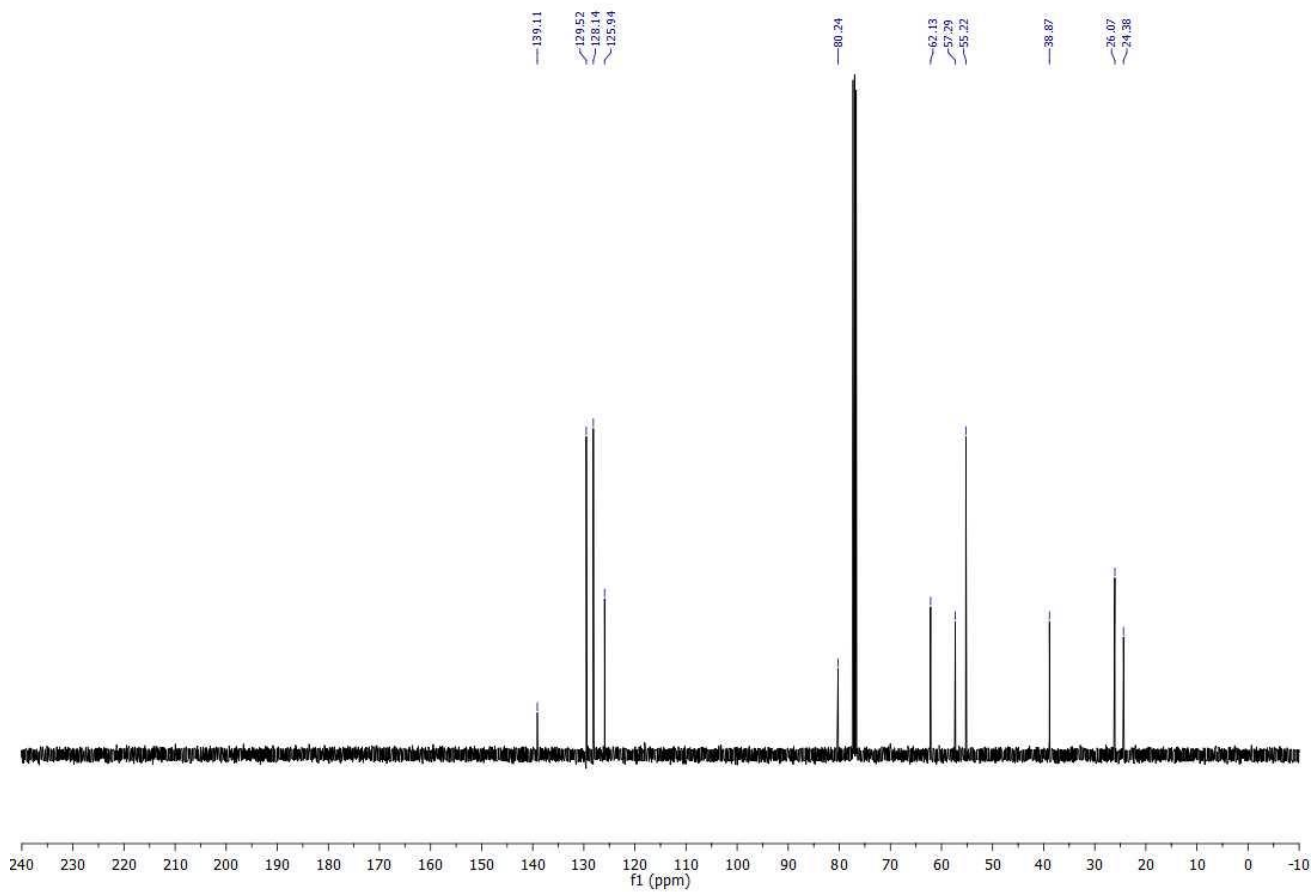
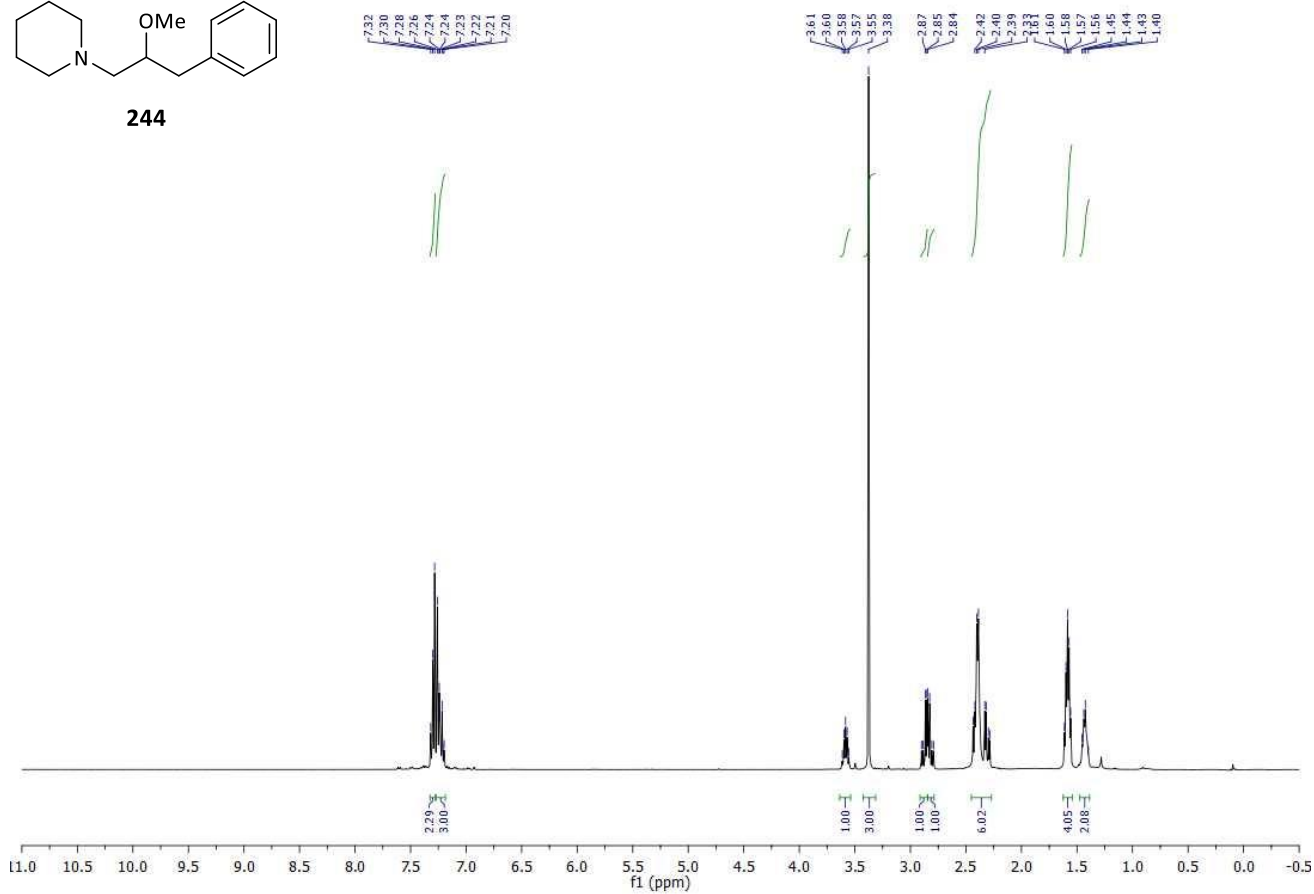
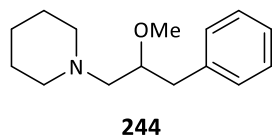


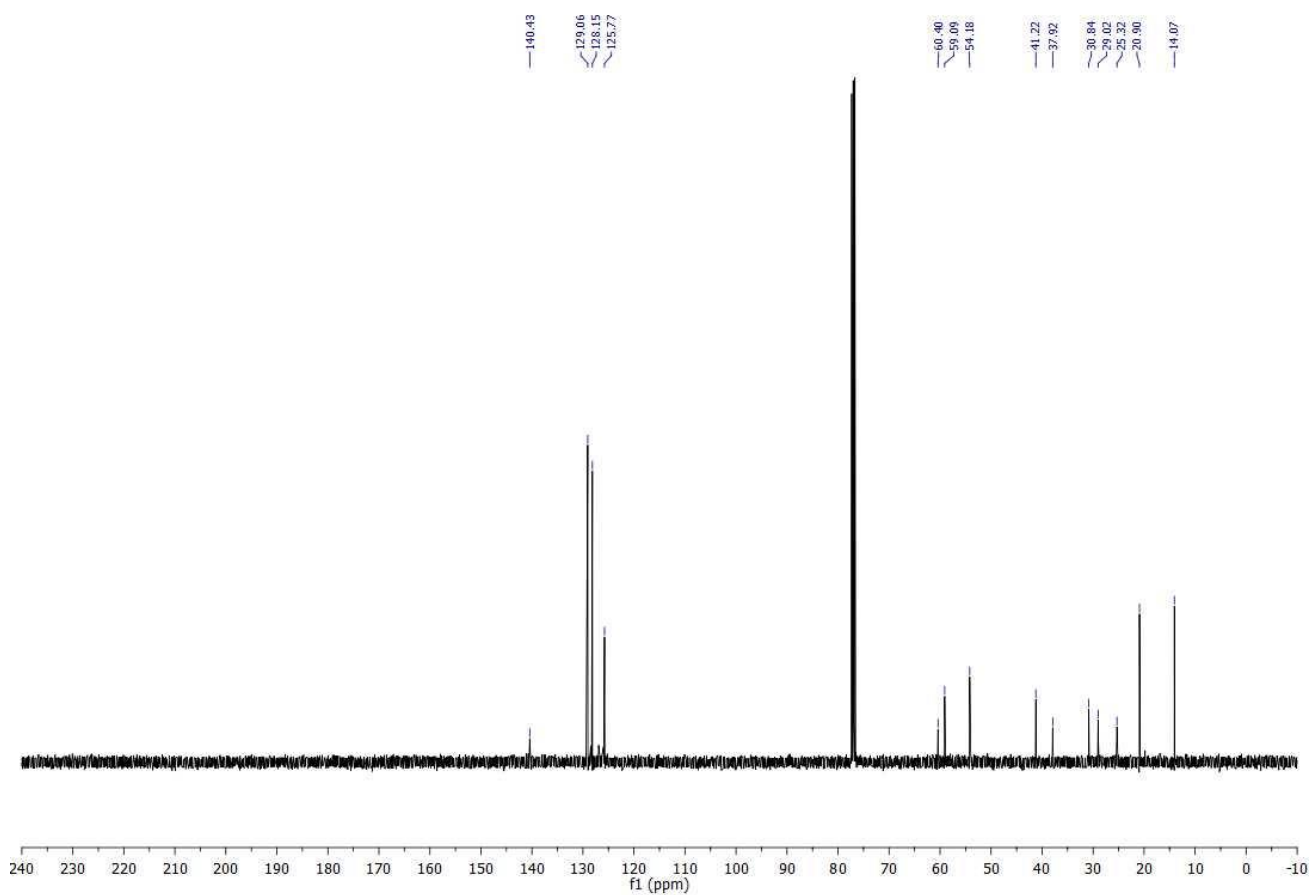
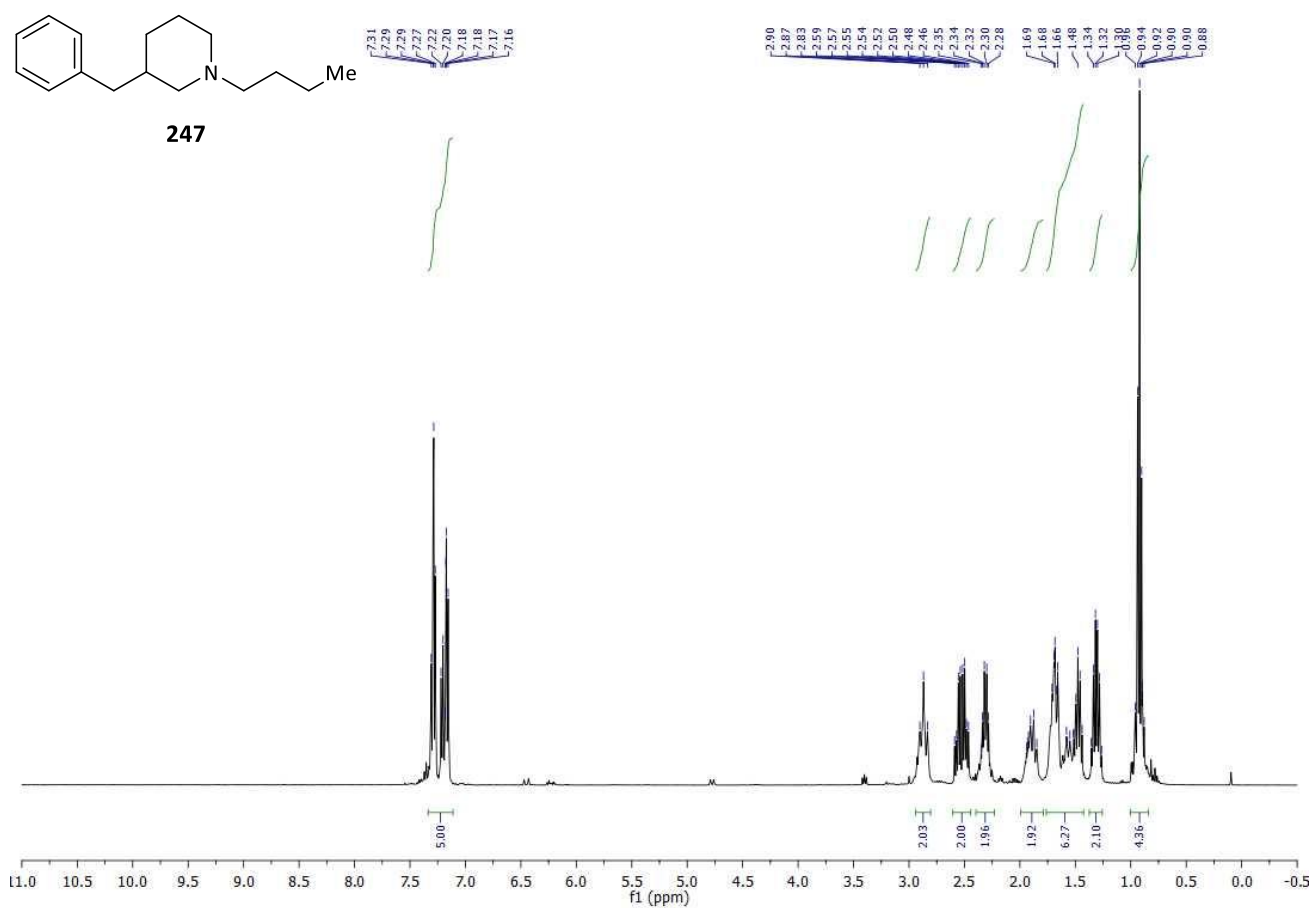


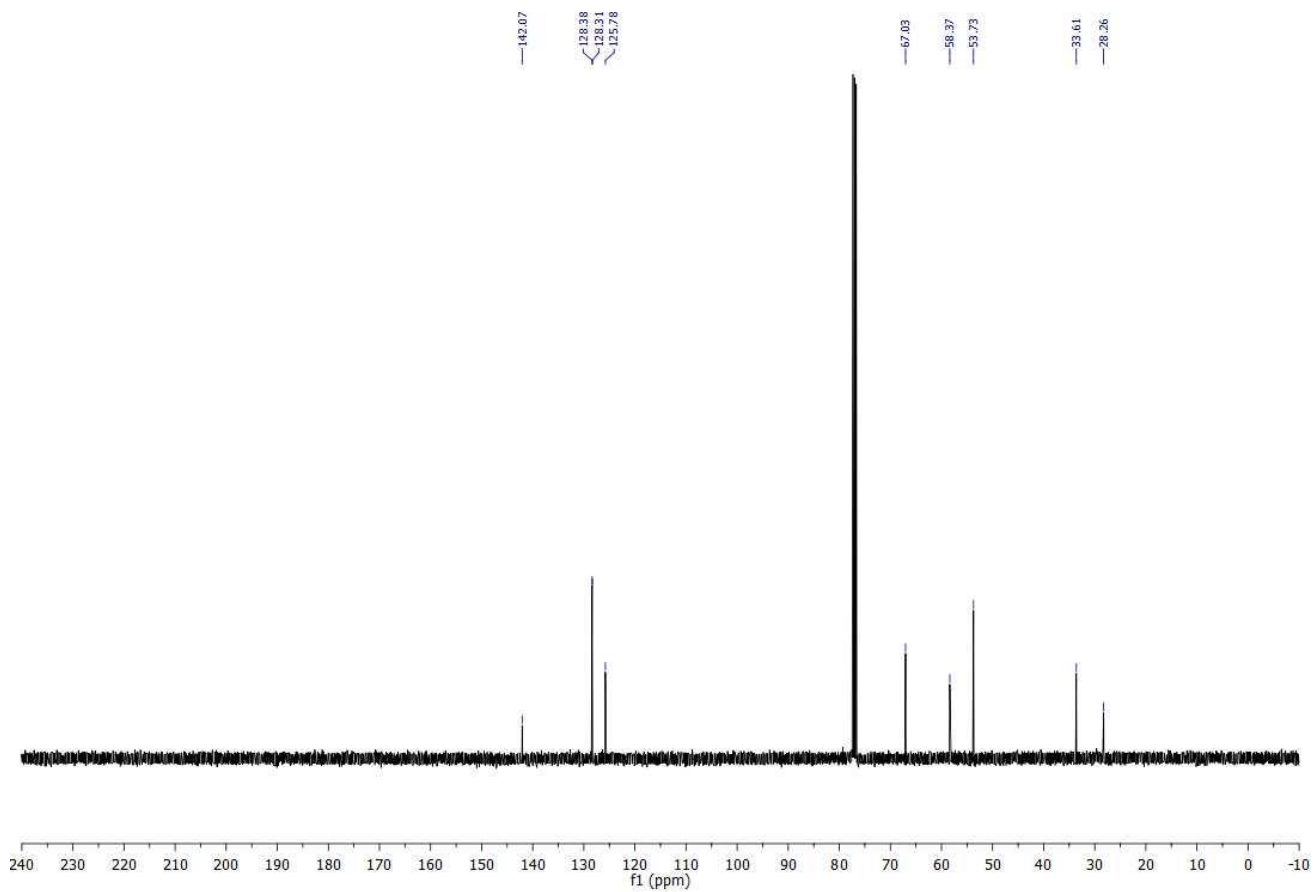
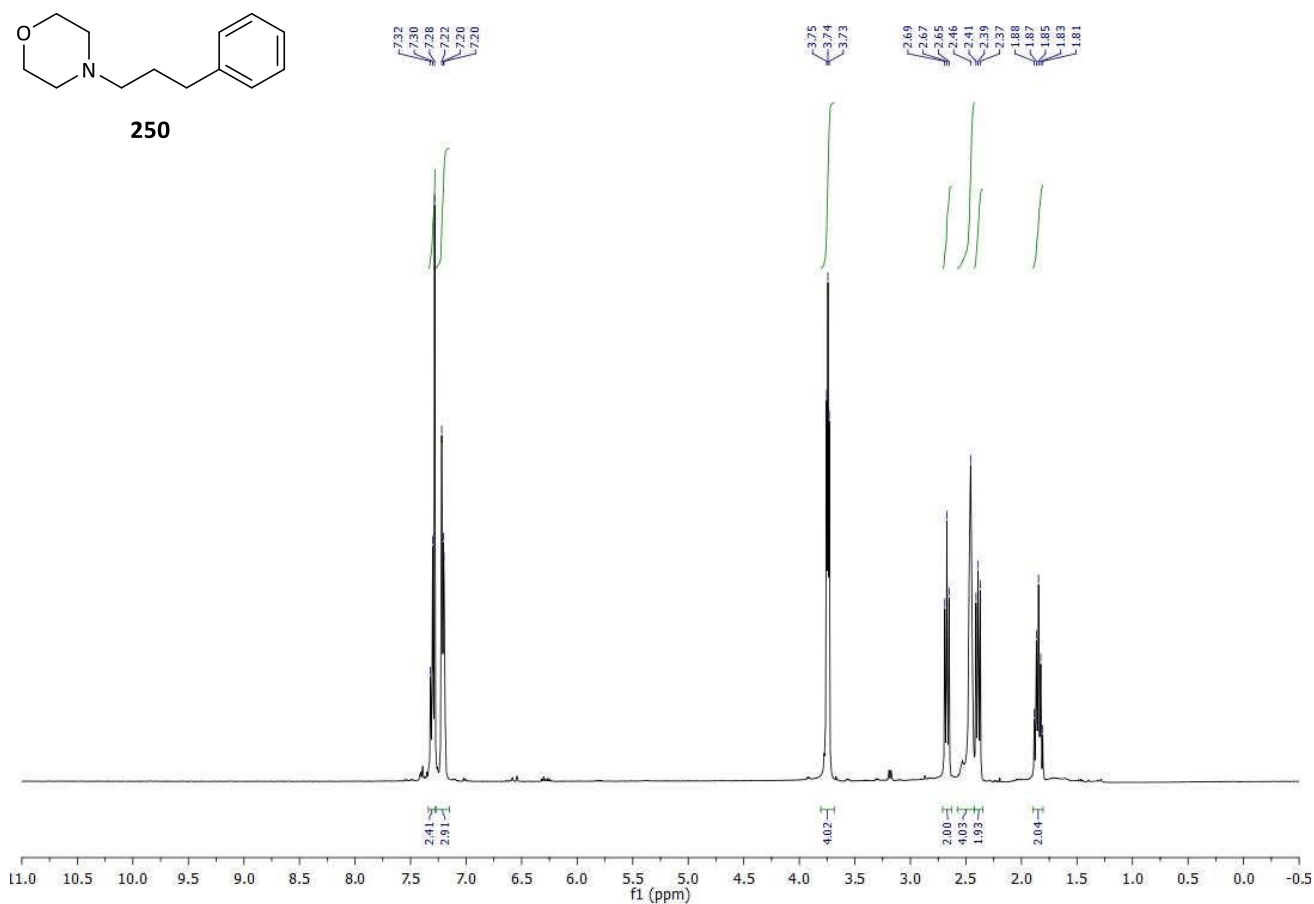


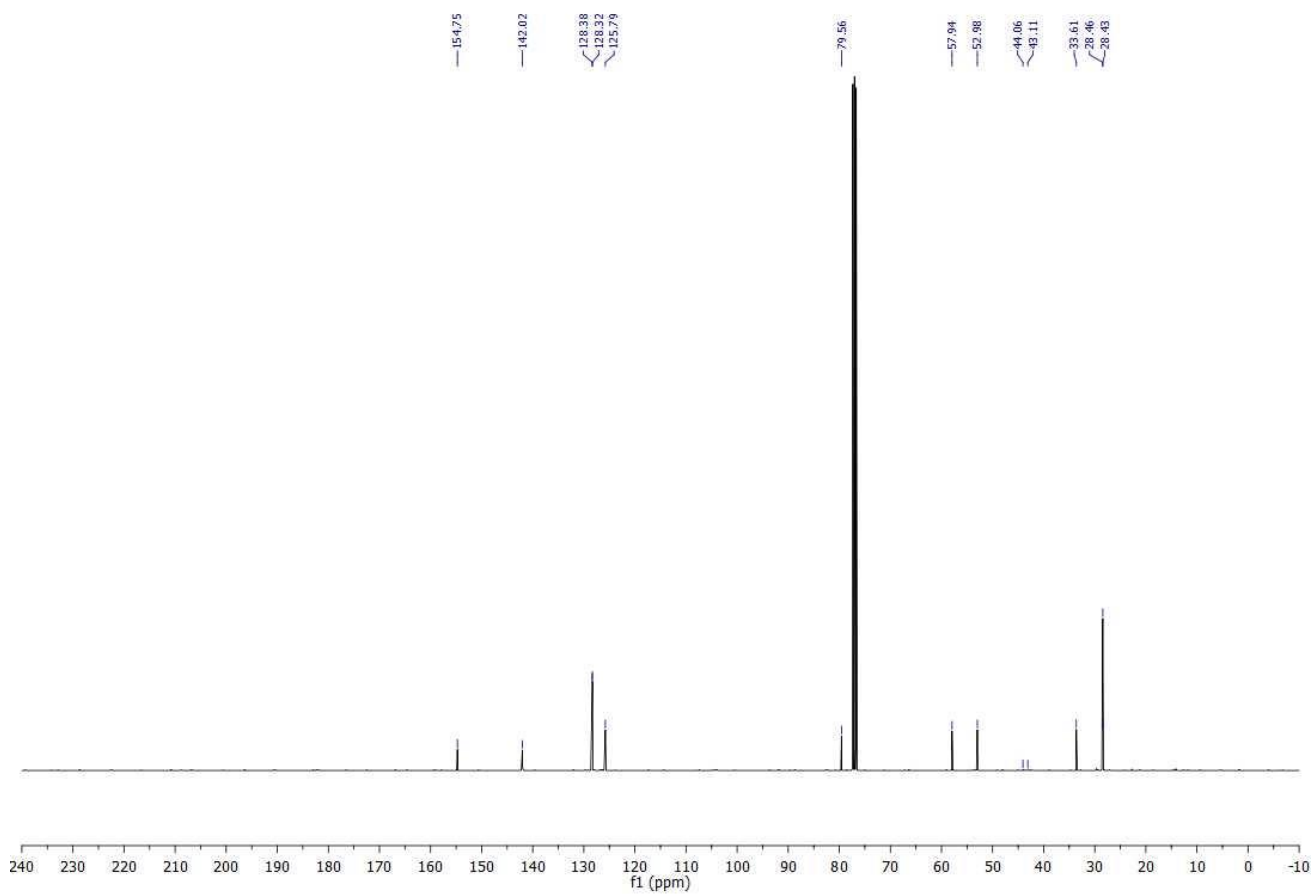
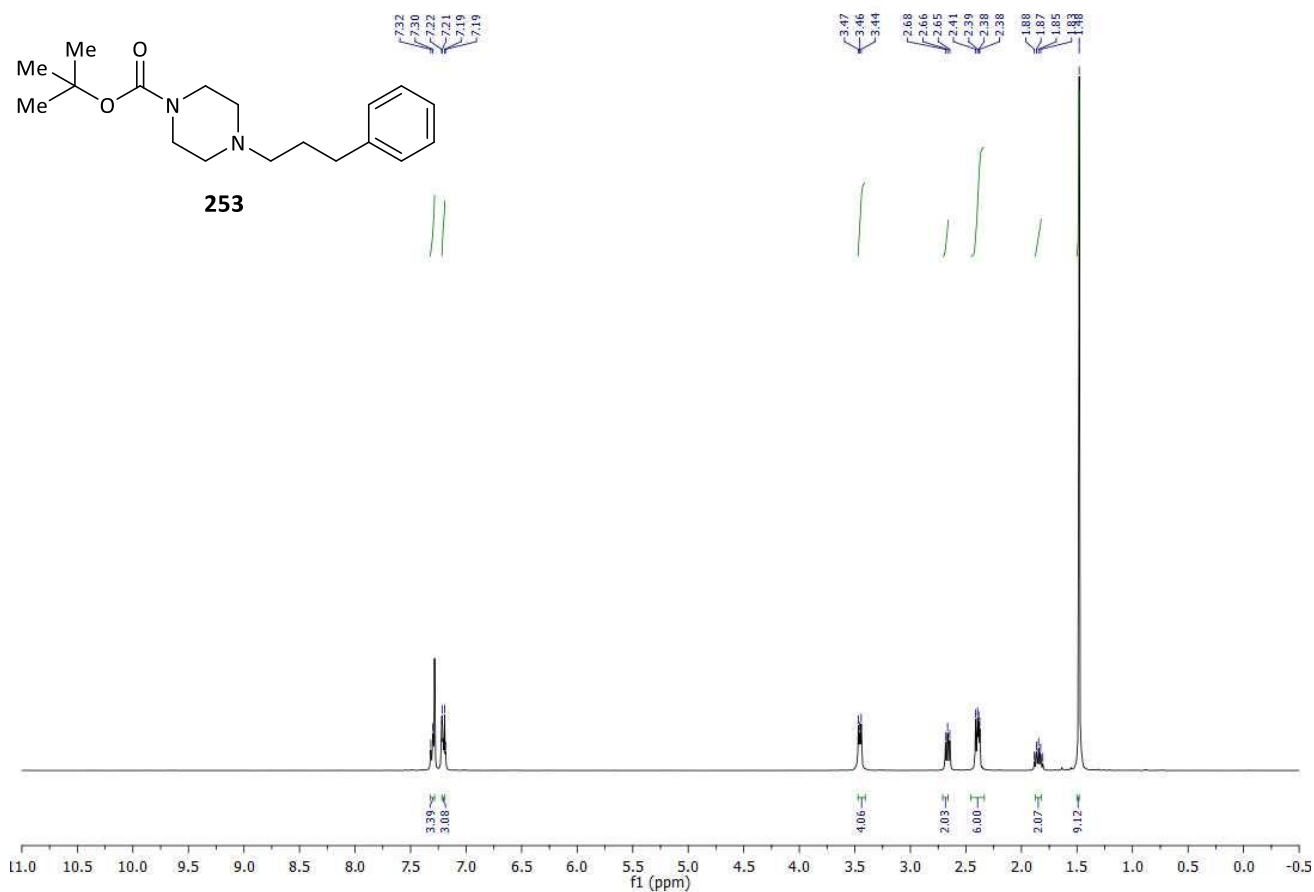


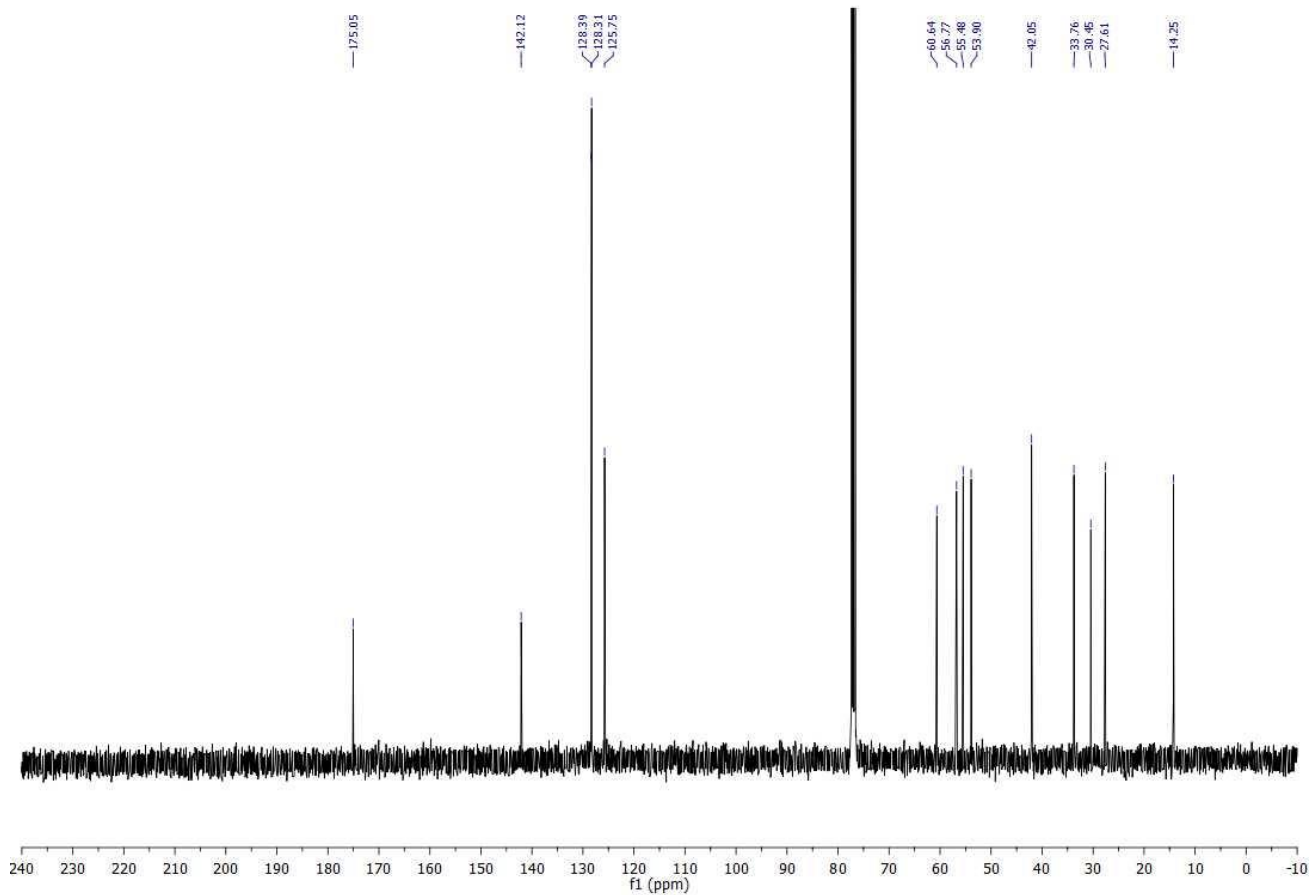
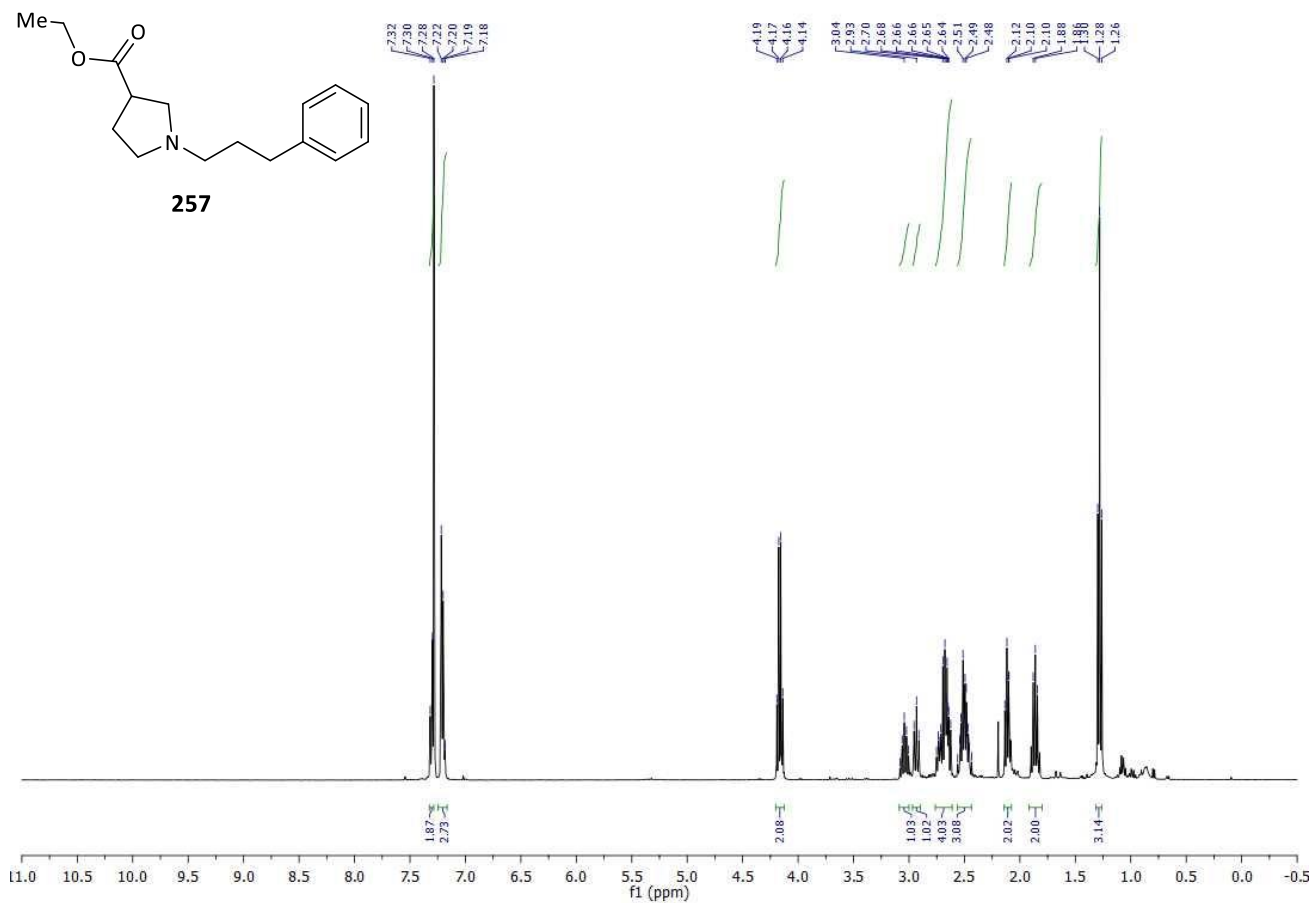


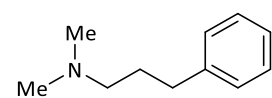




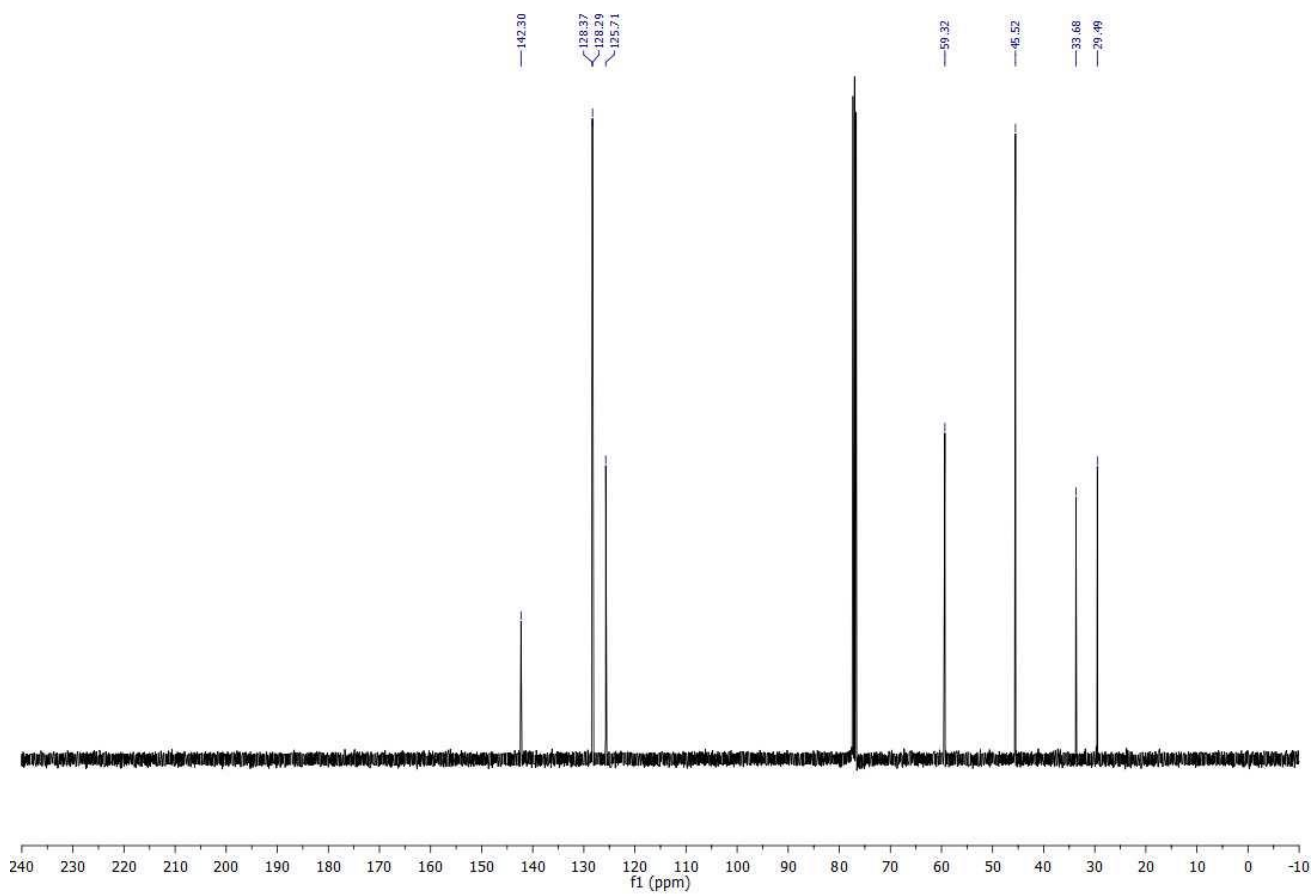
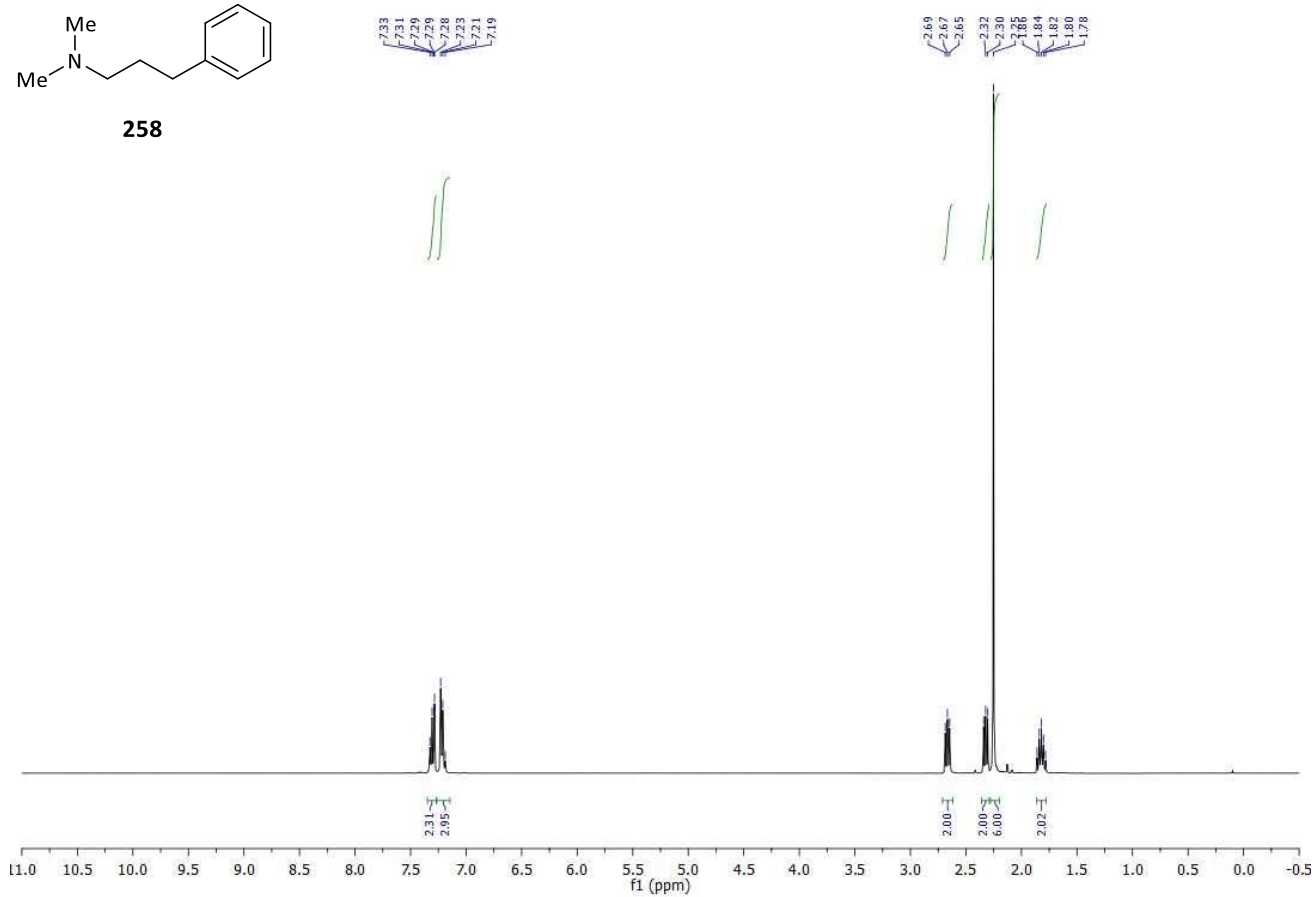


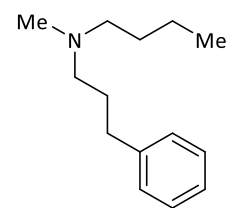




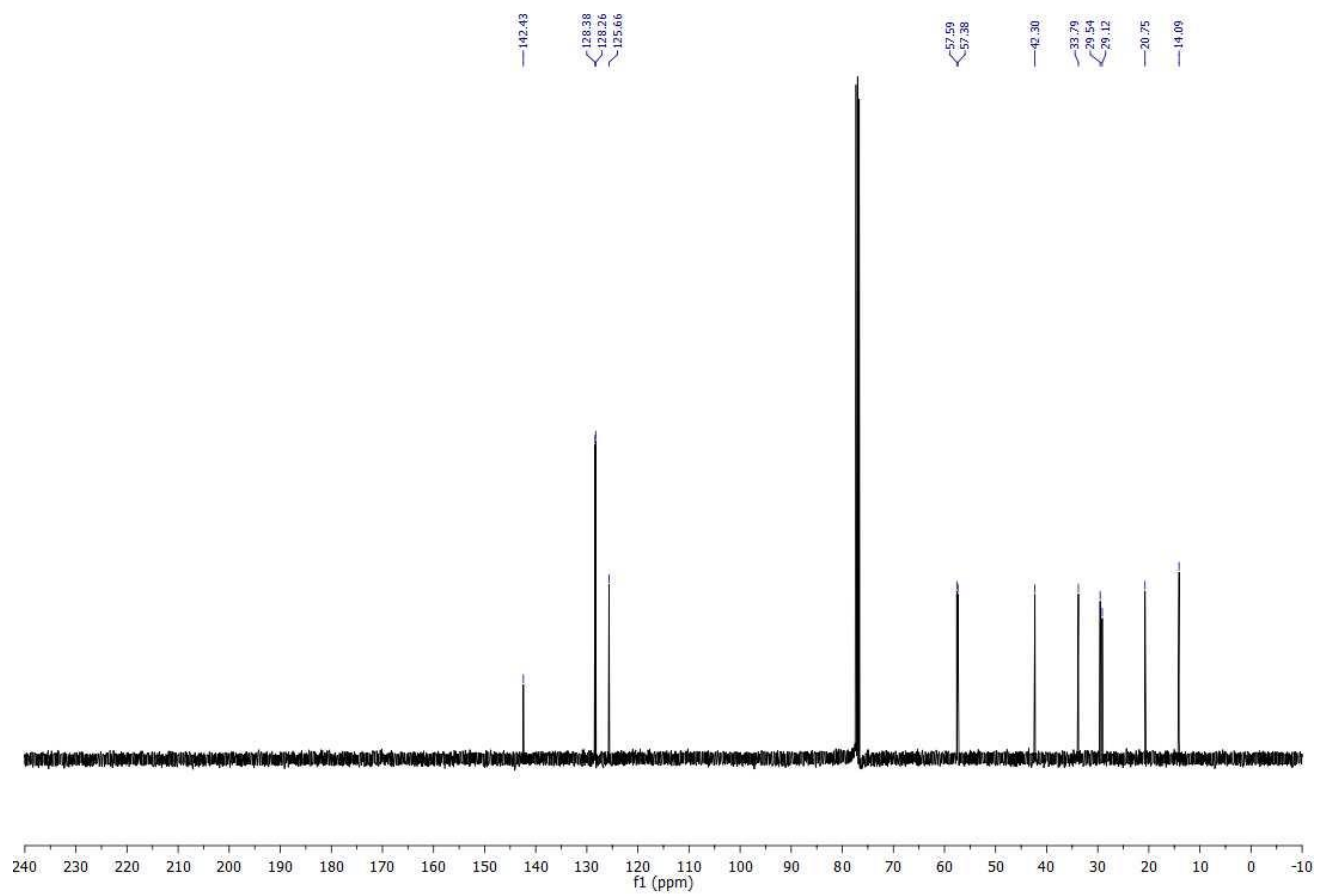
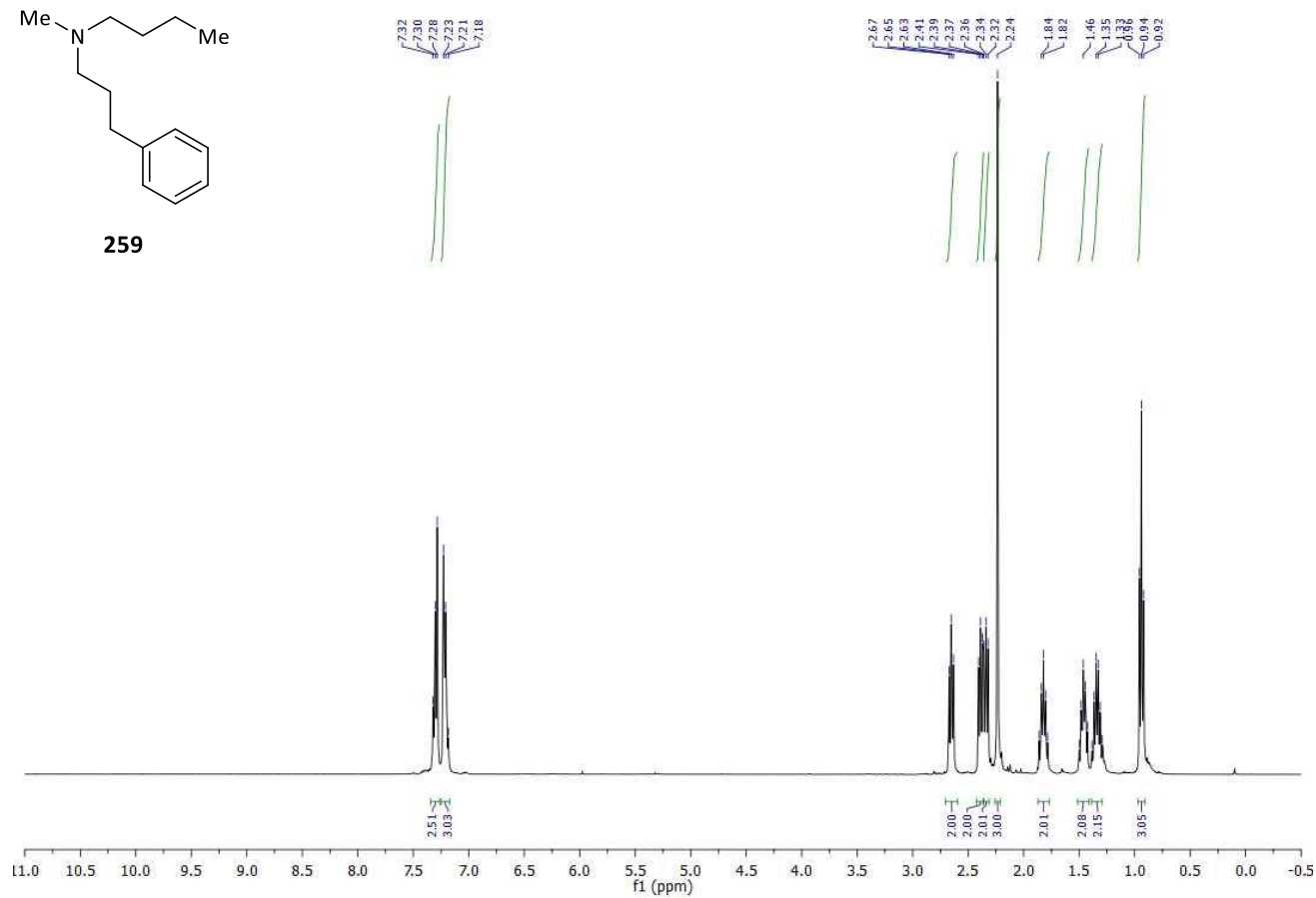


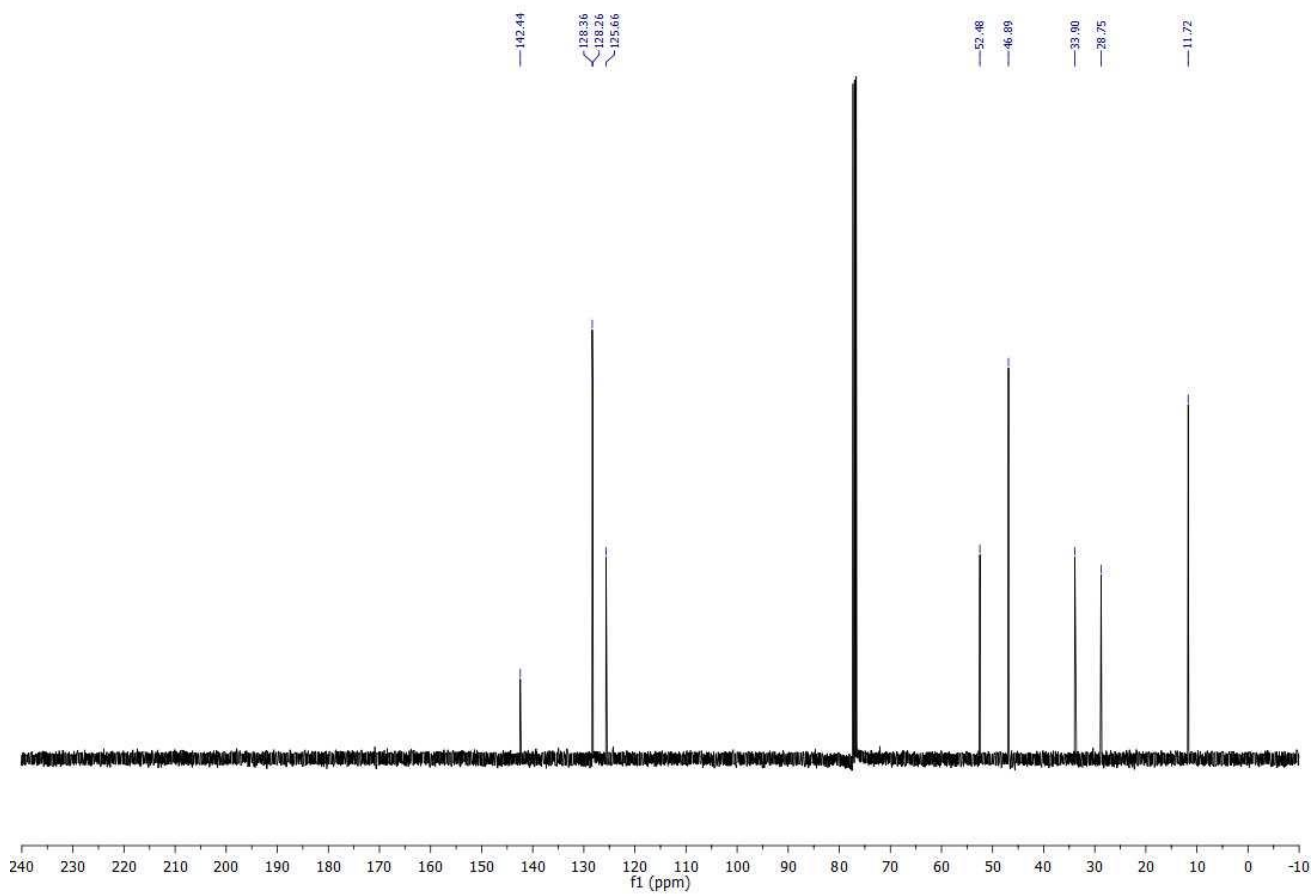
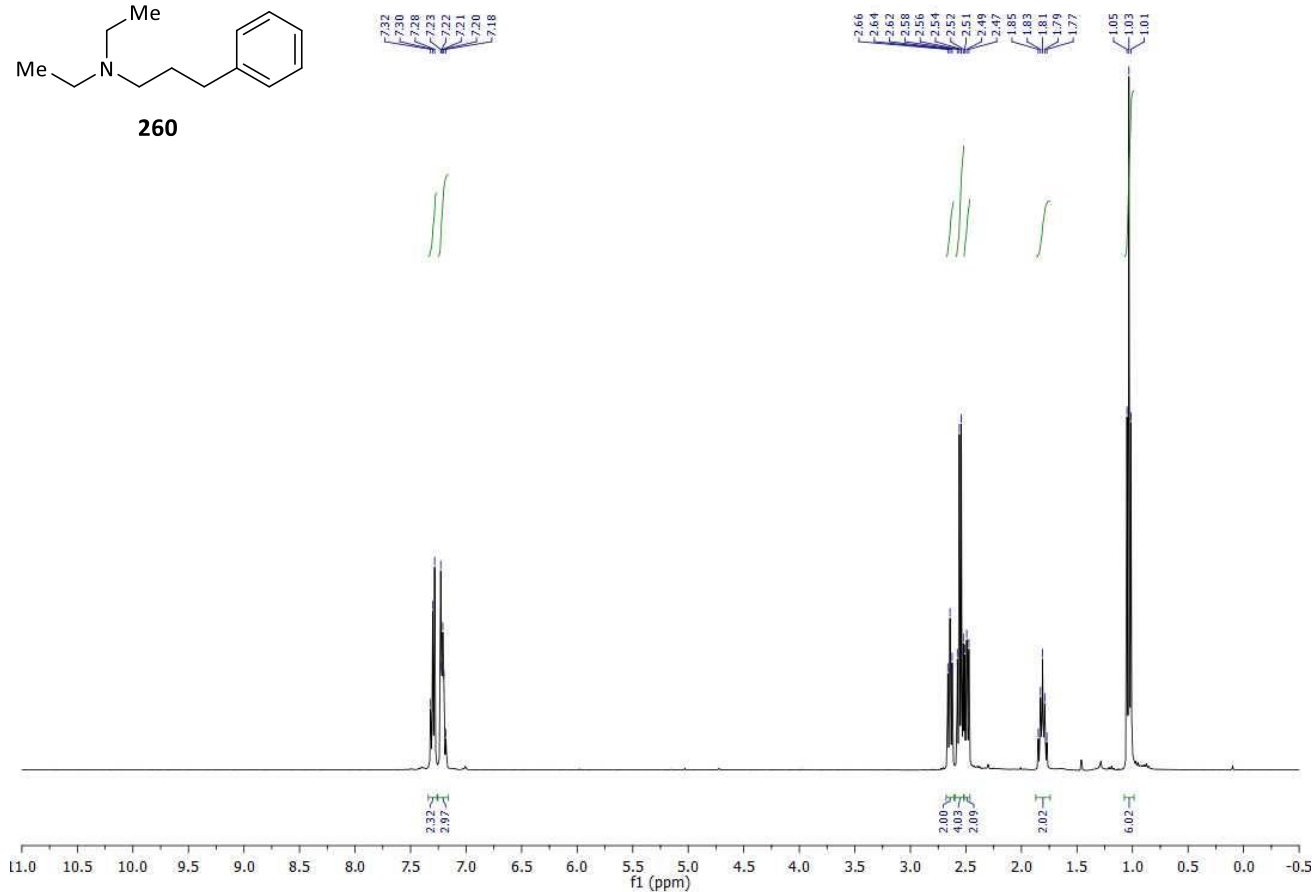
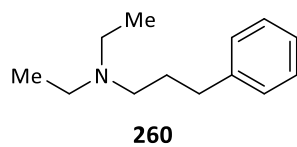
258

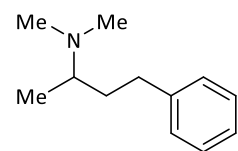




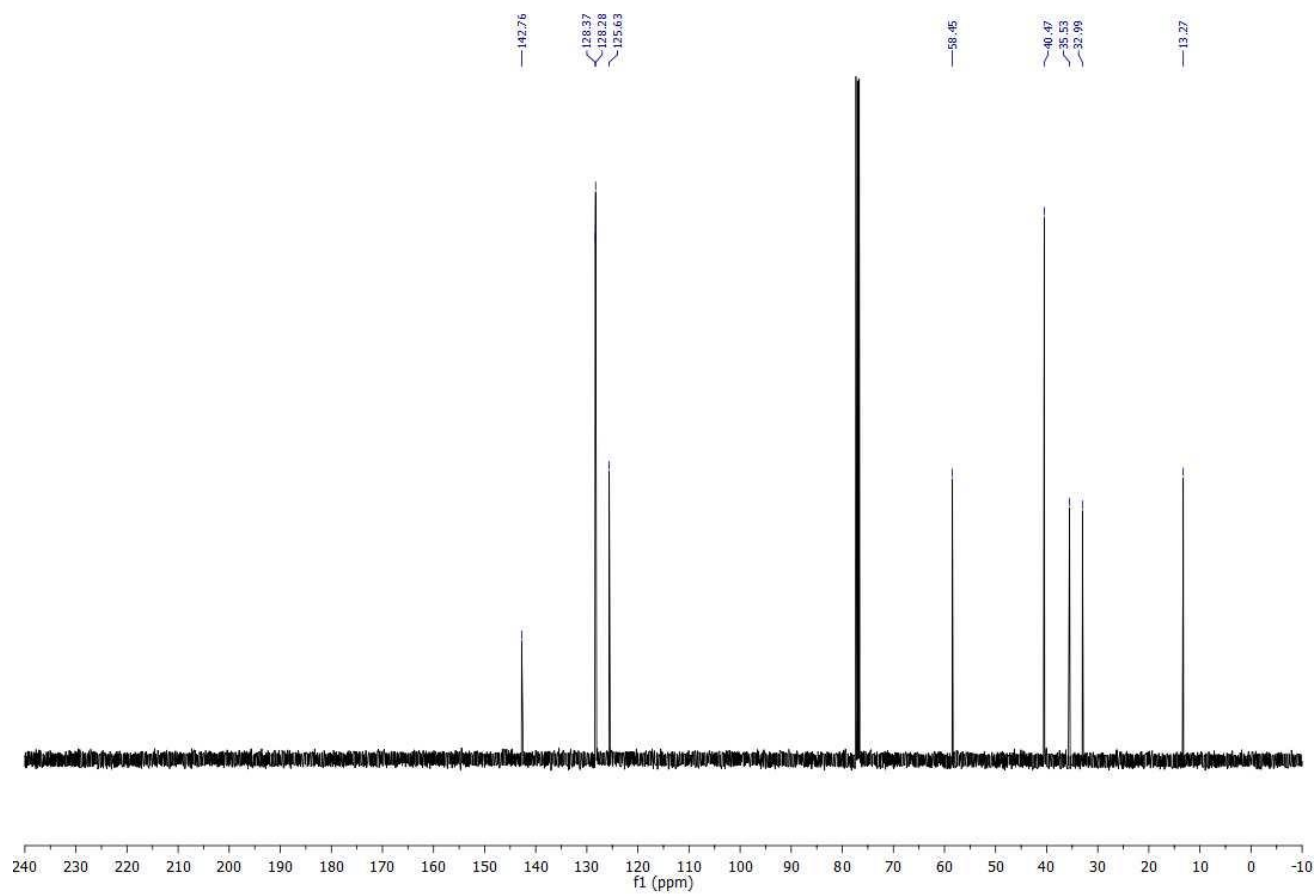
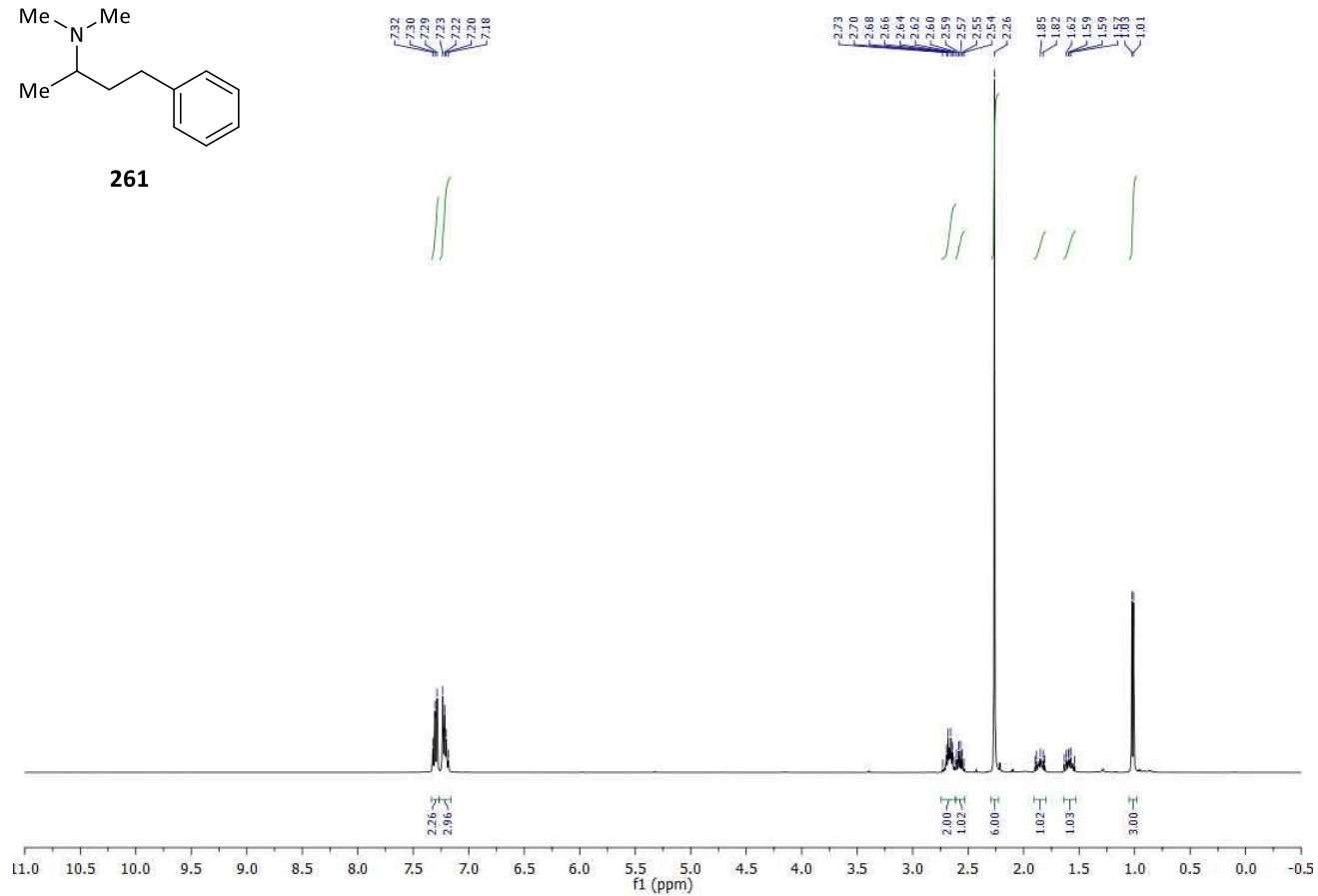
259

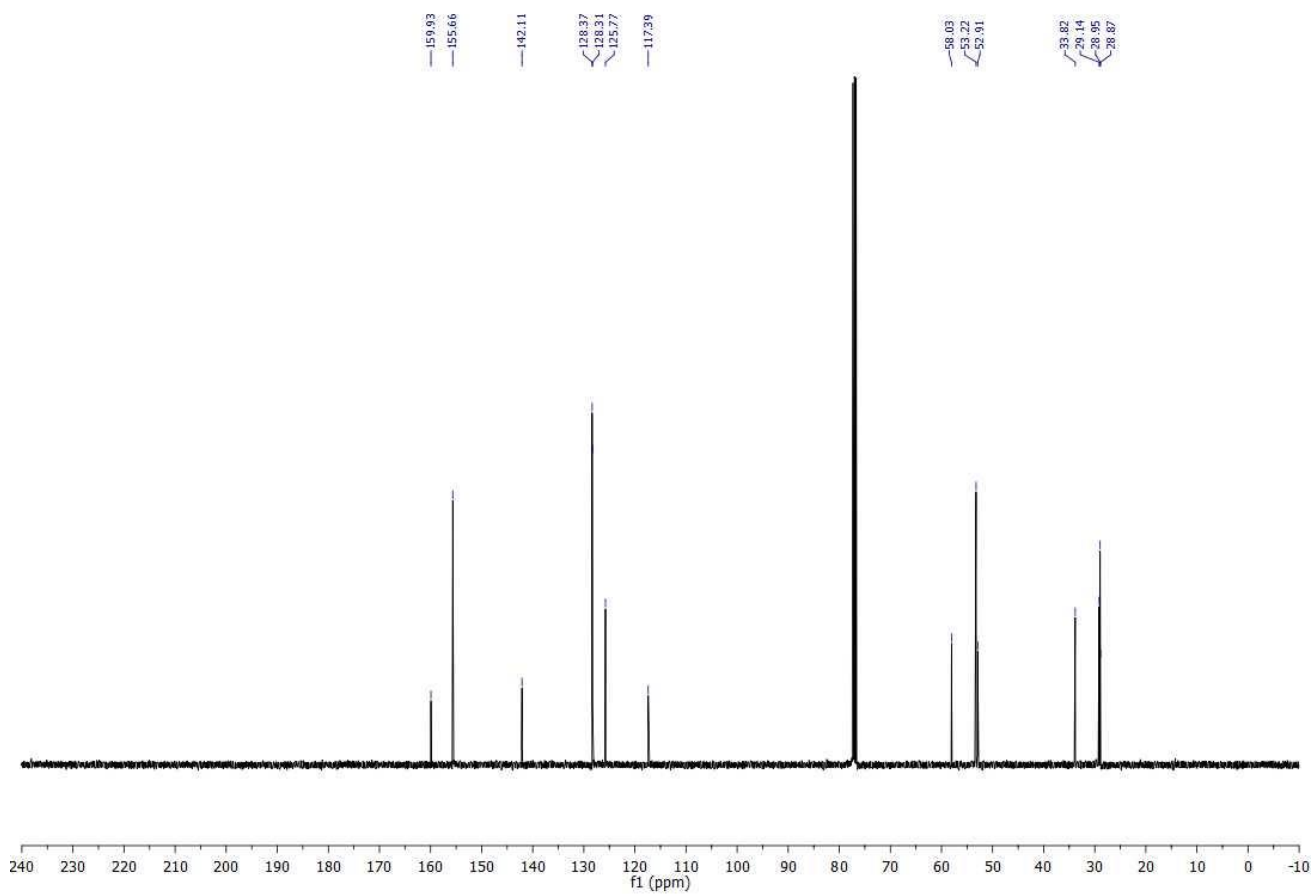
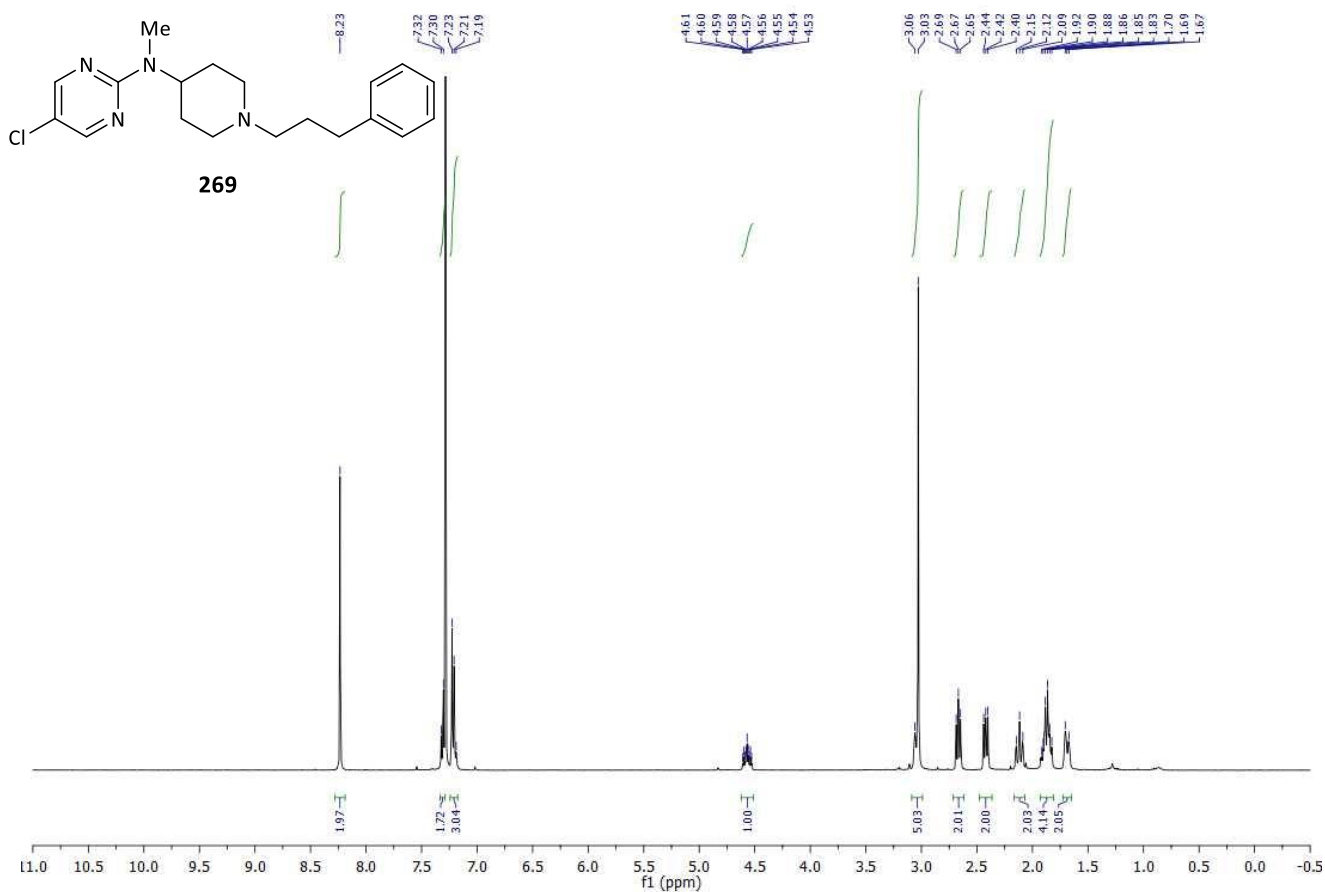


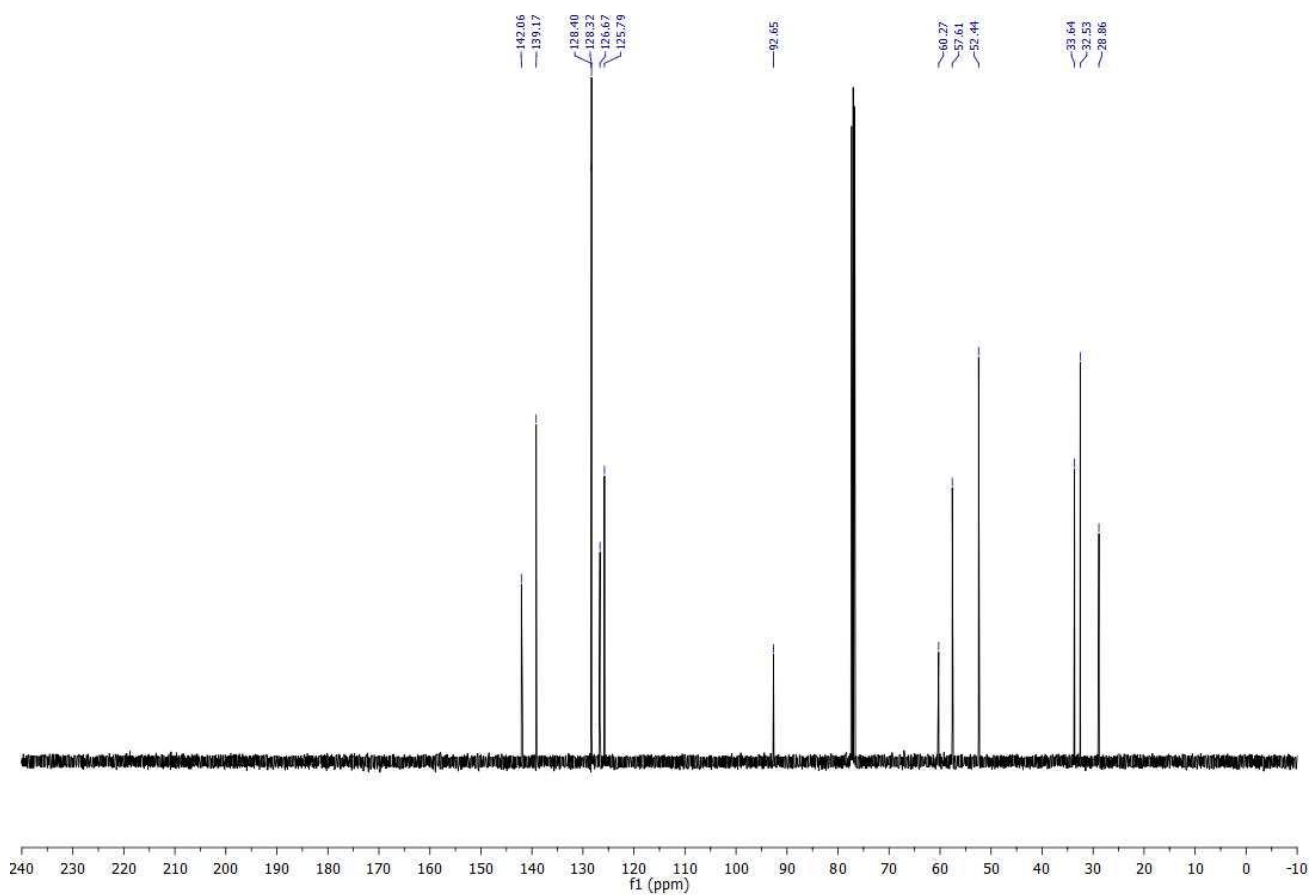
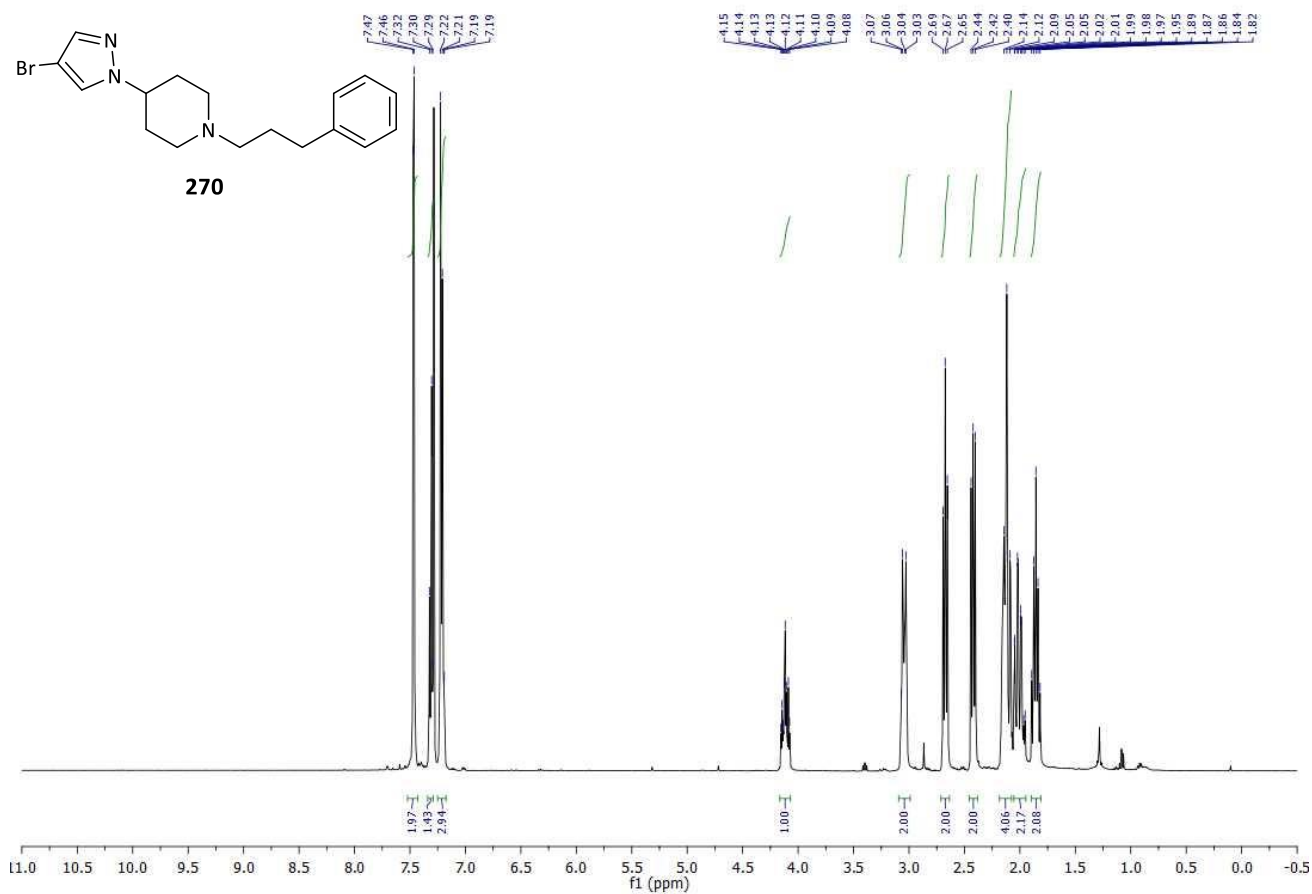


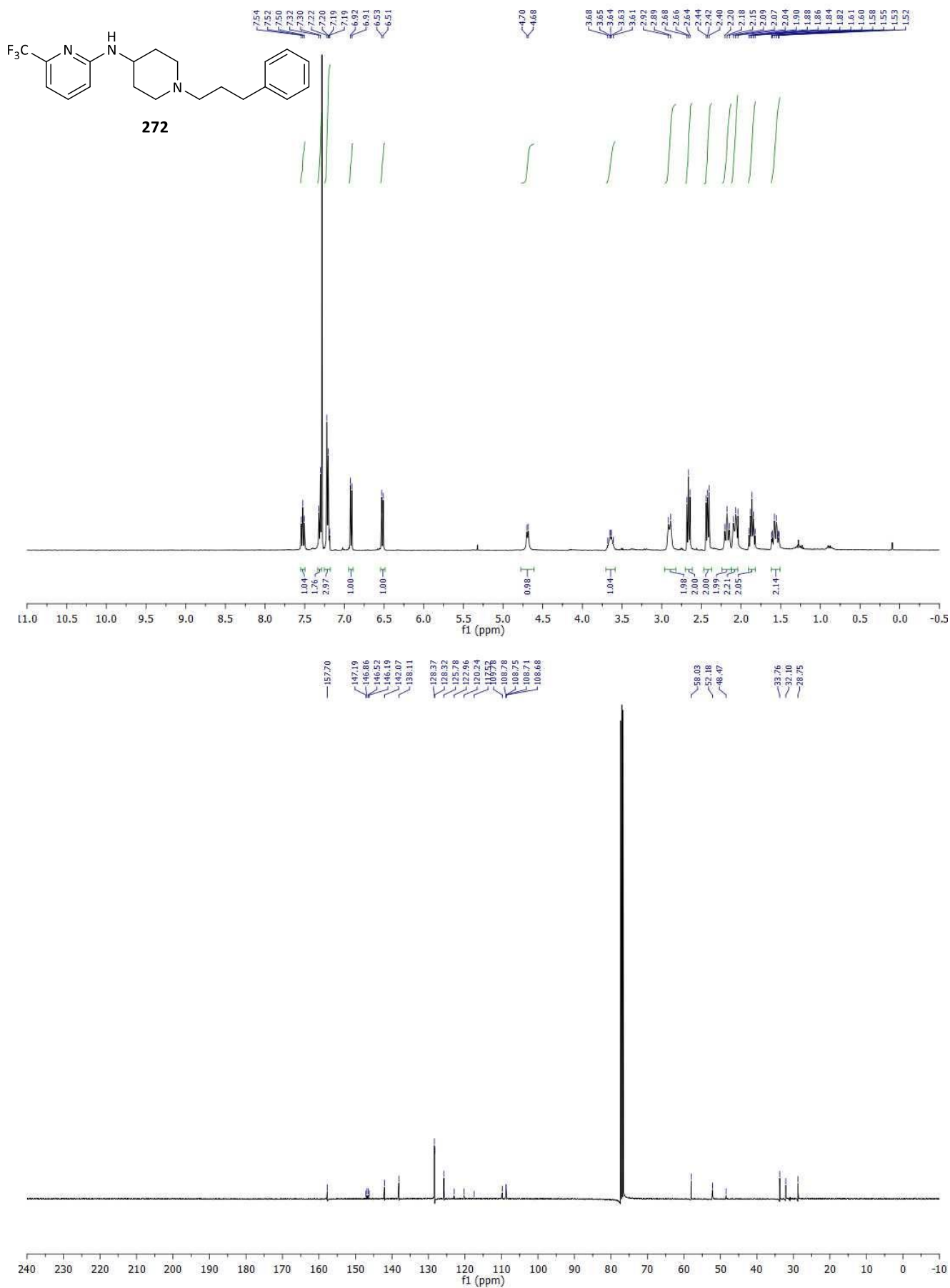


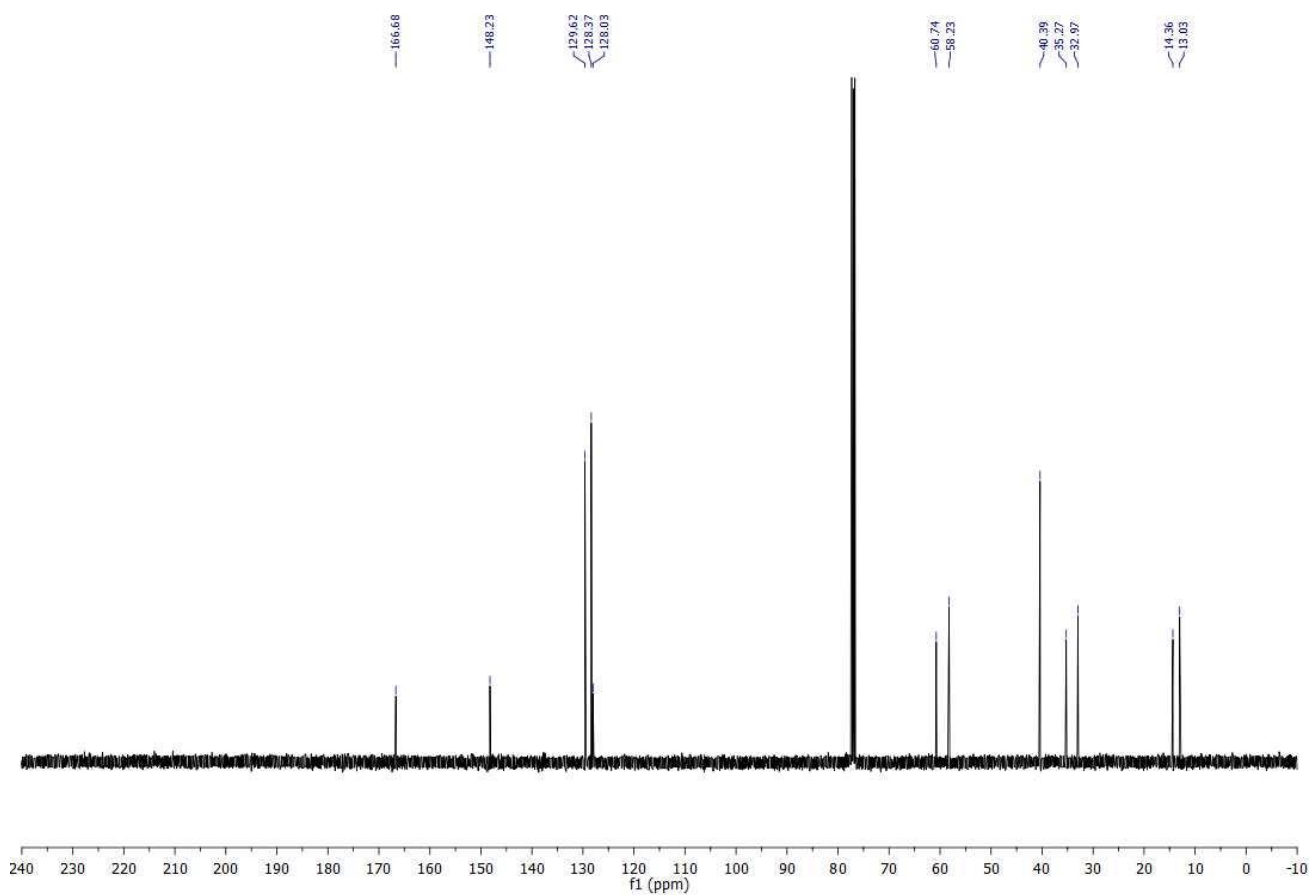
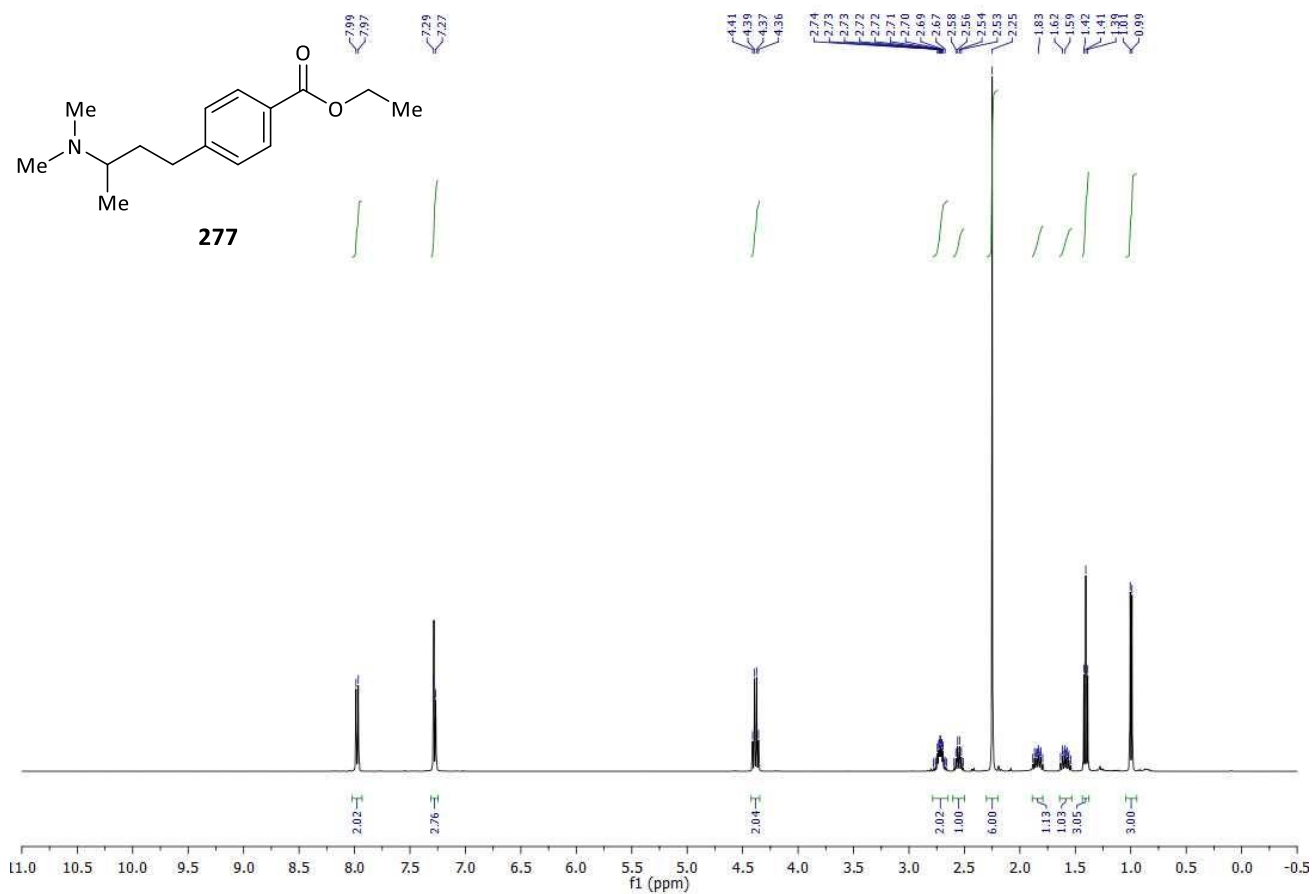
261

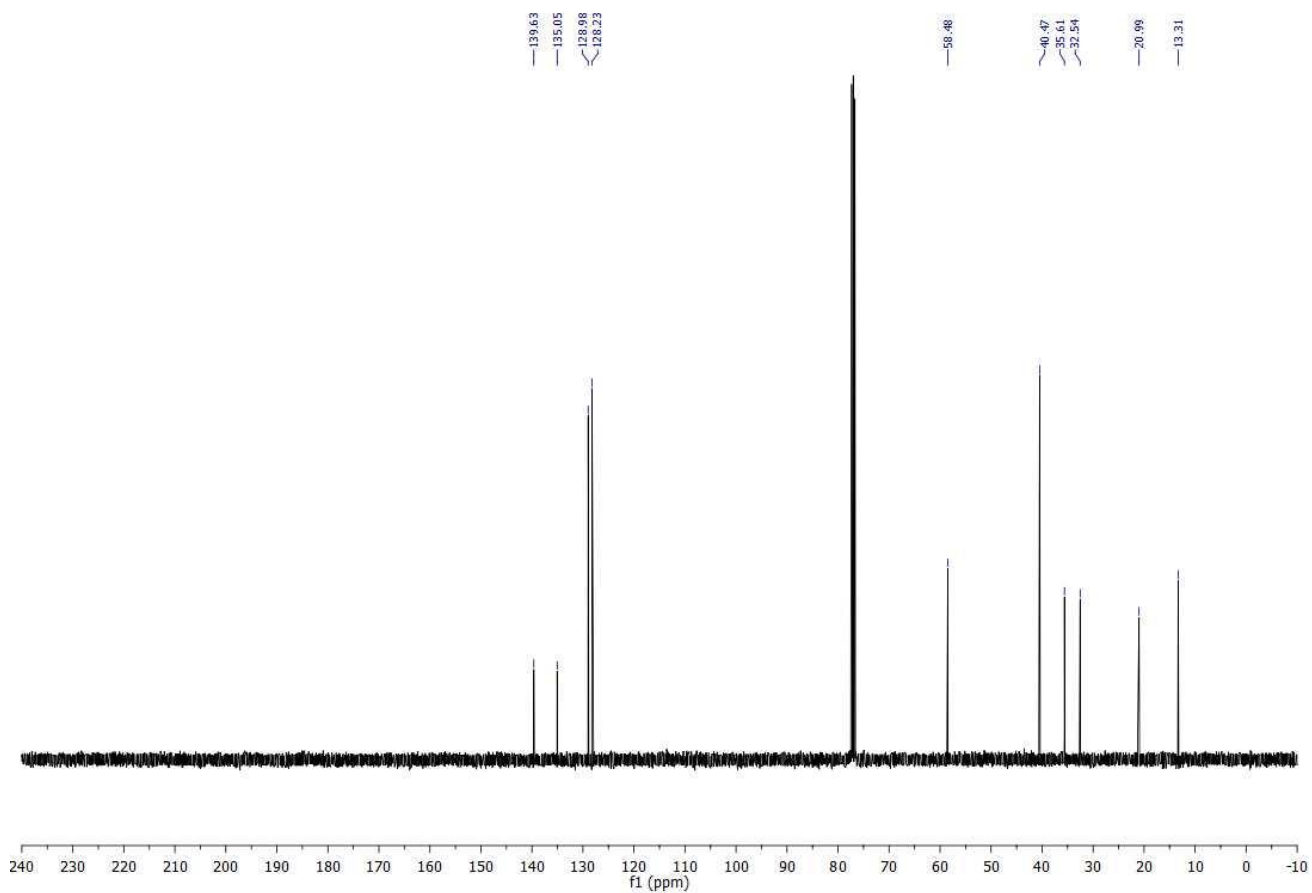
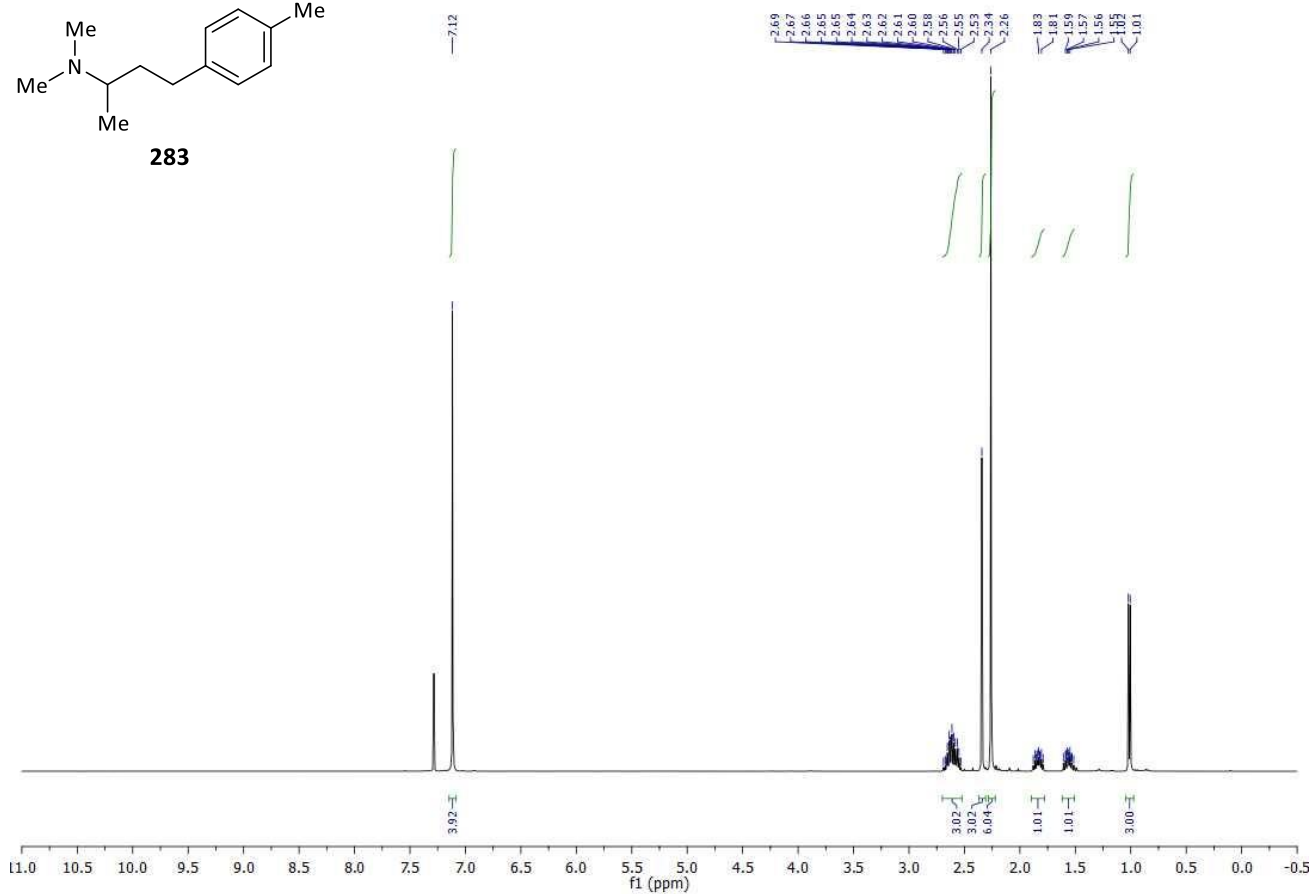
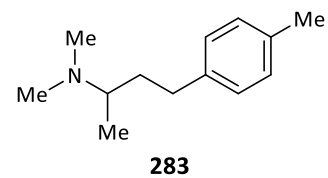


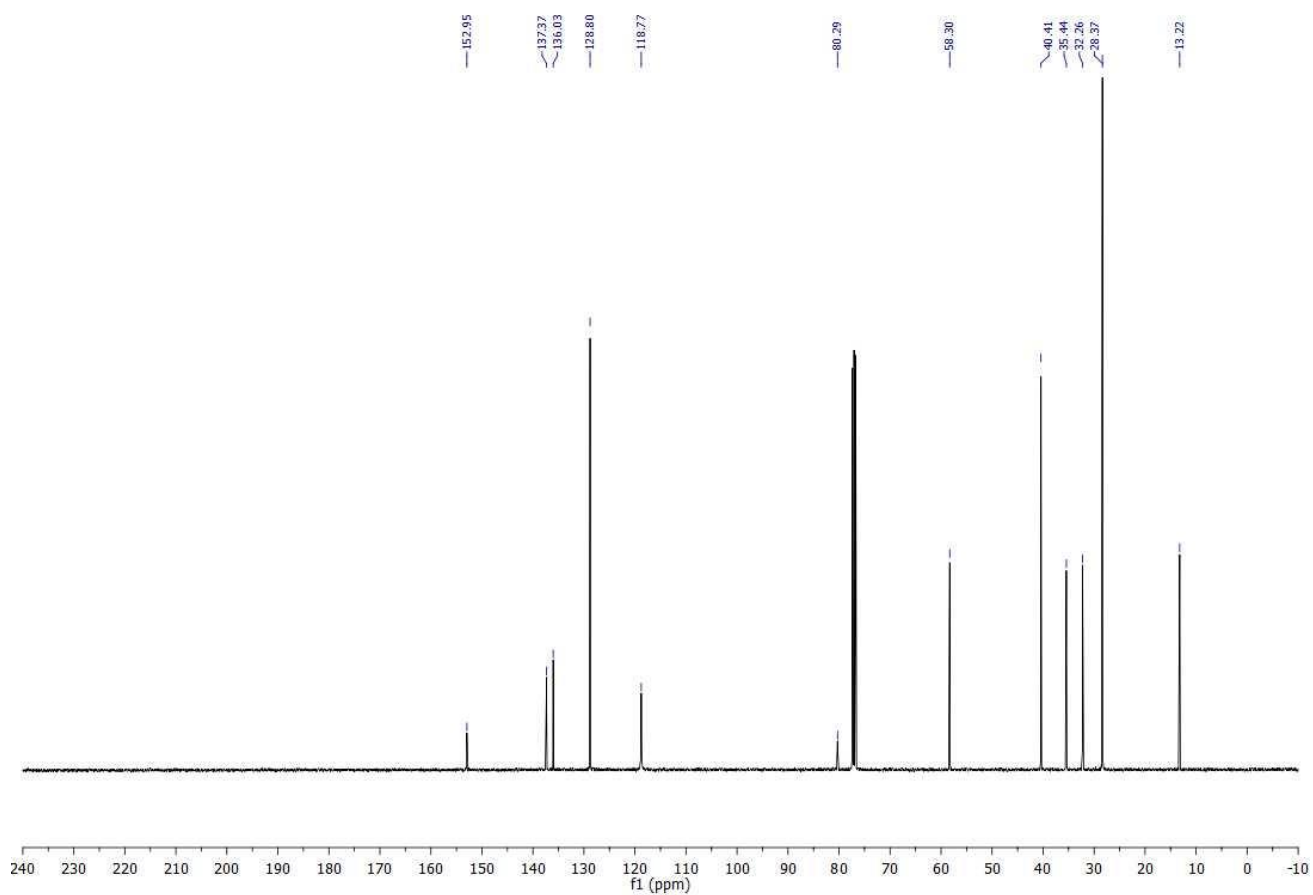
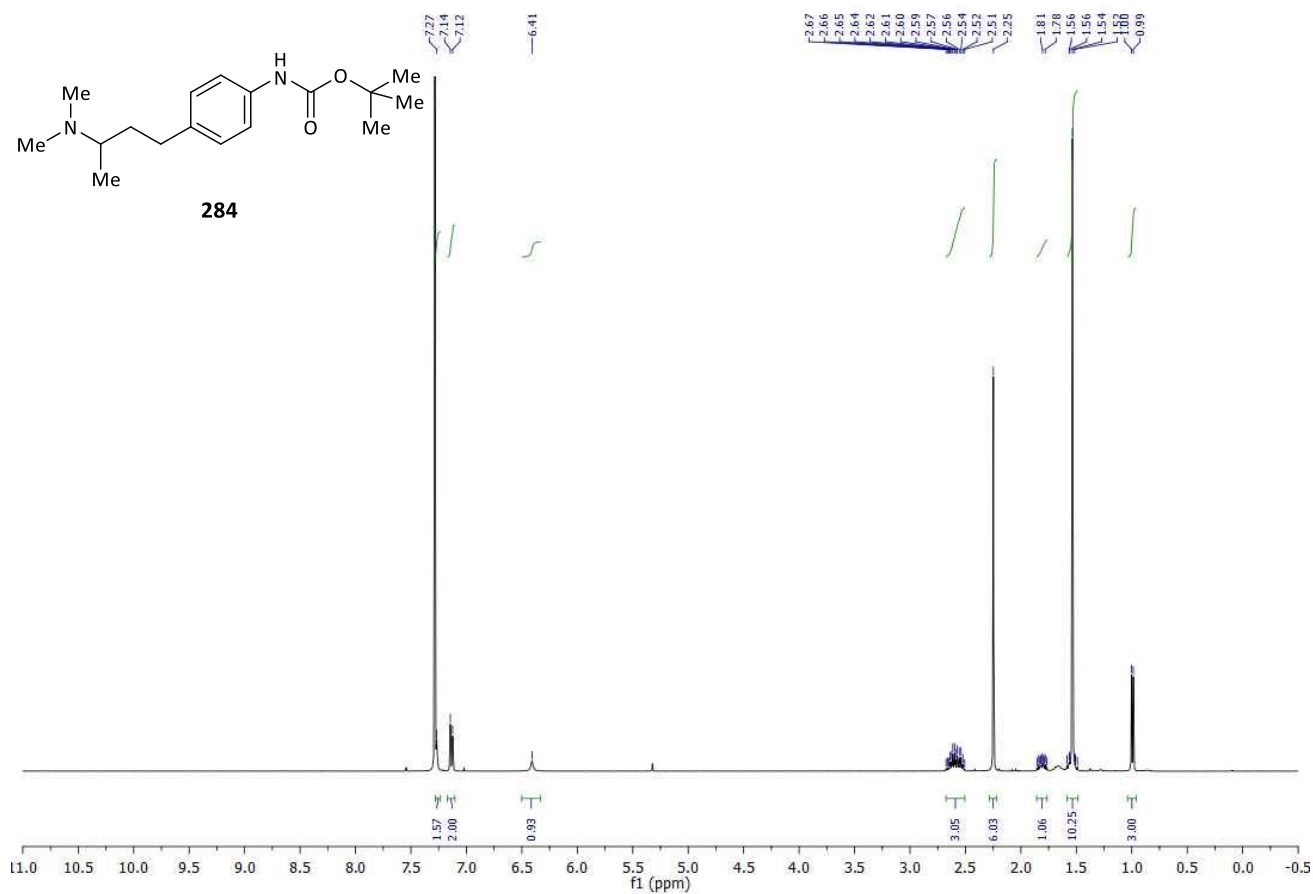


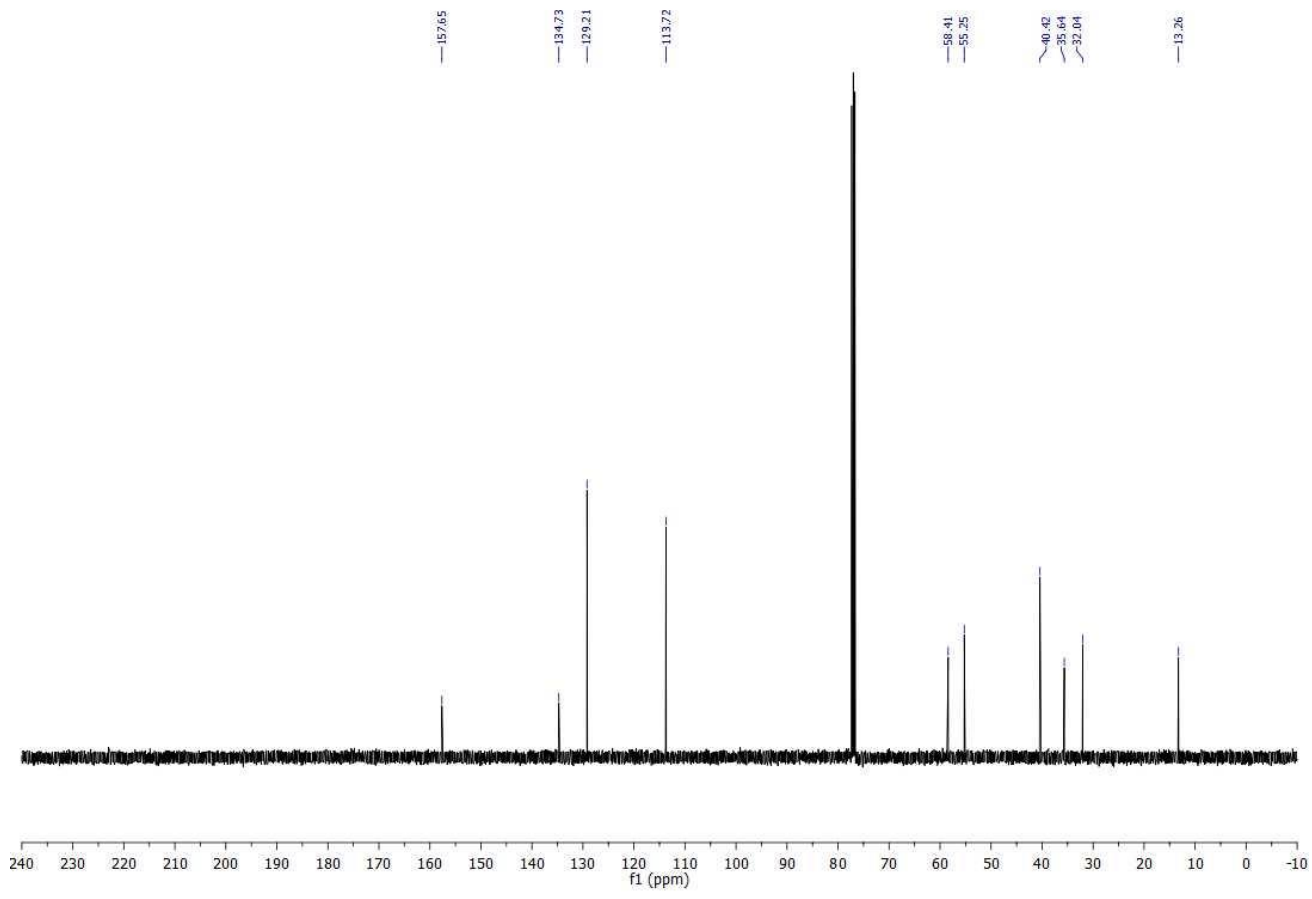
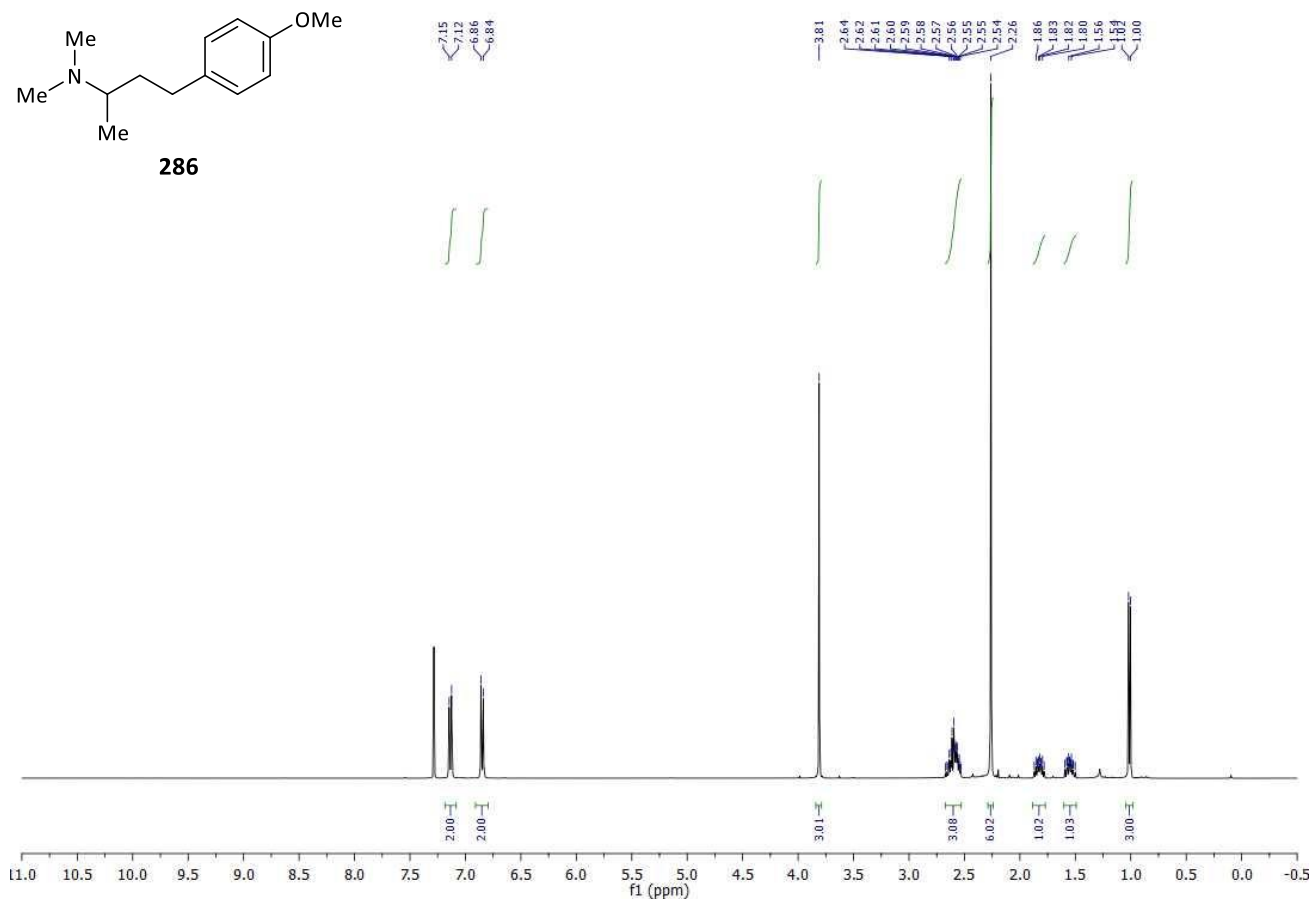


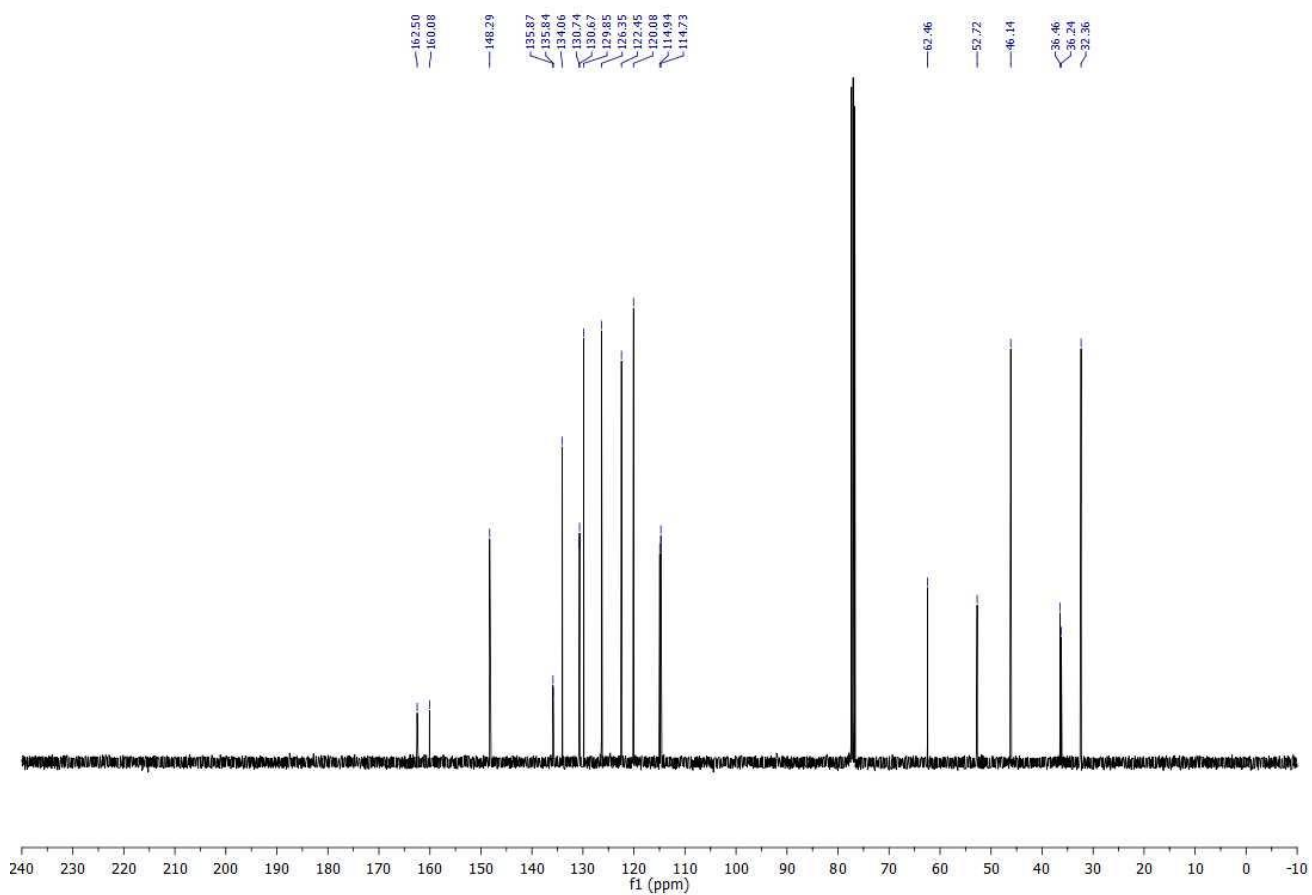
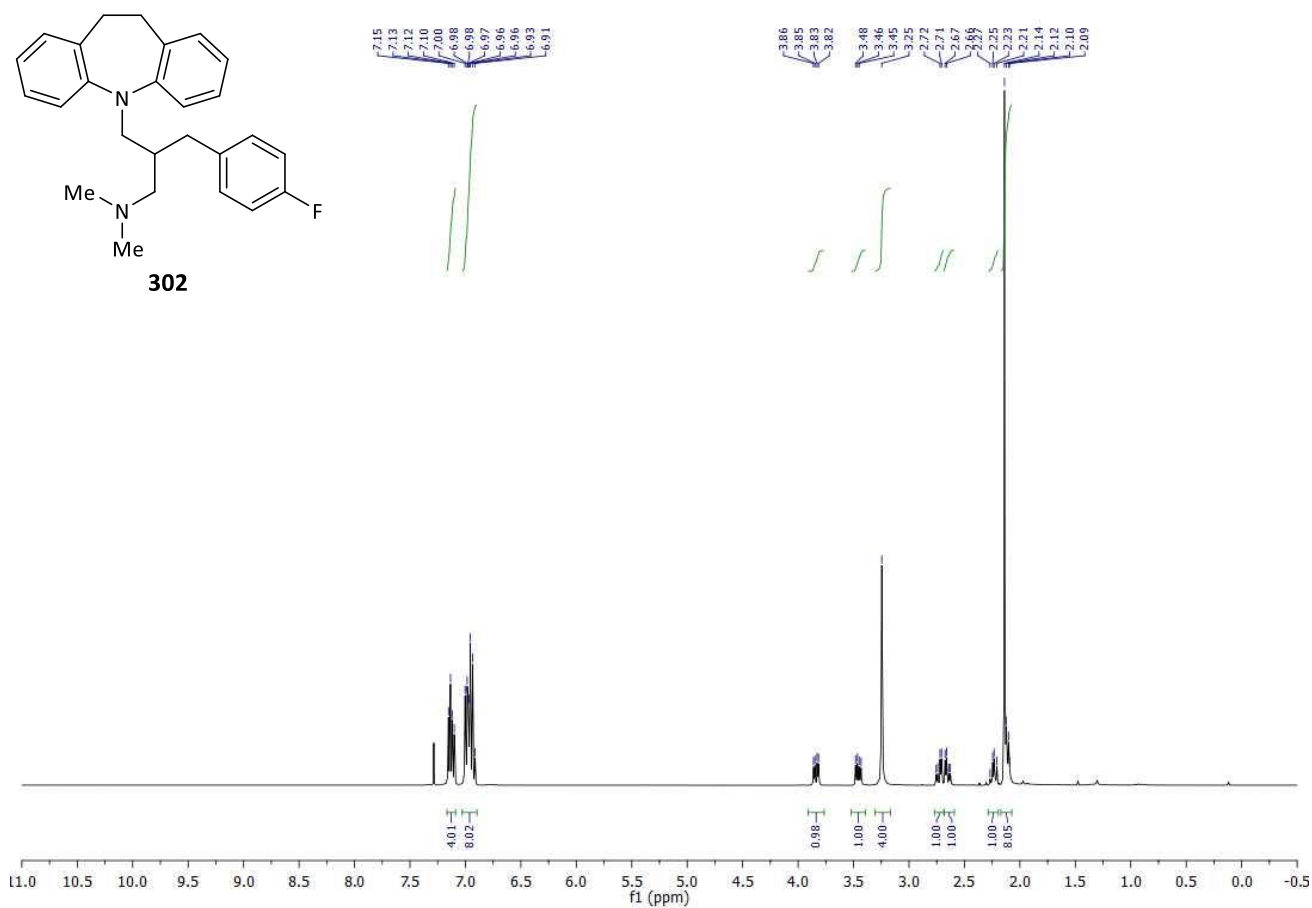


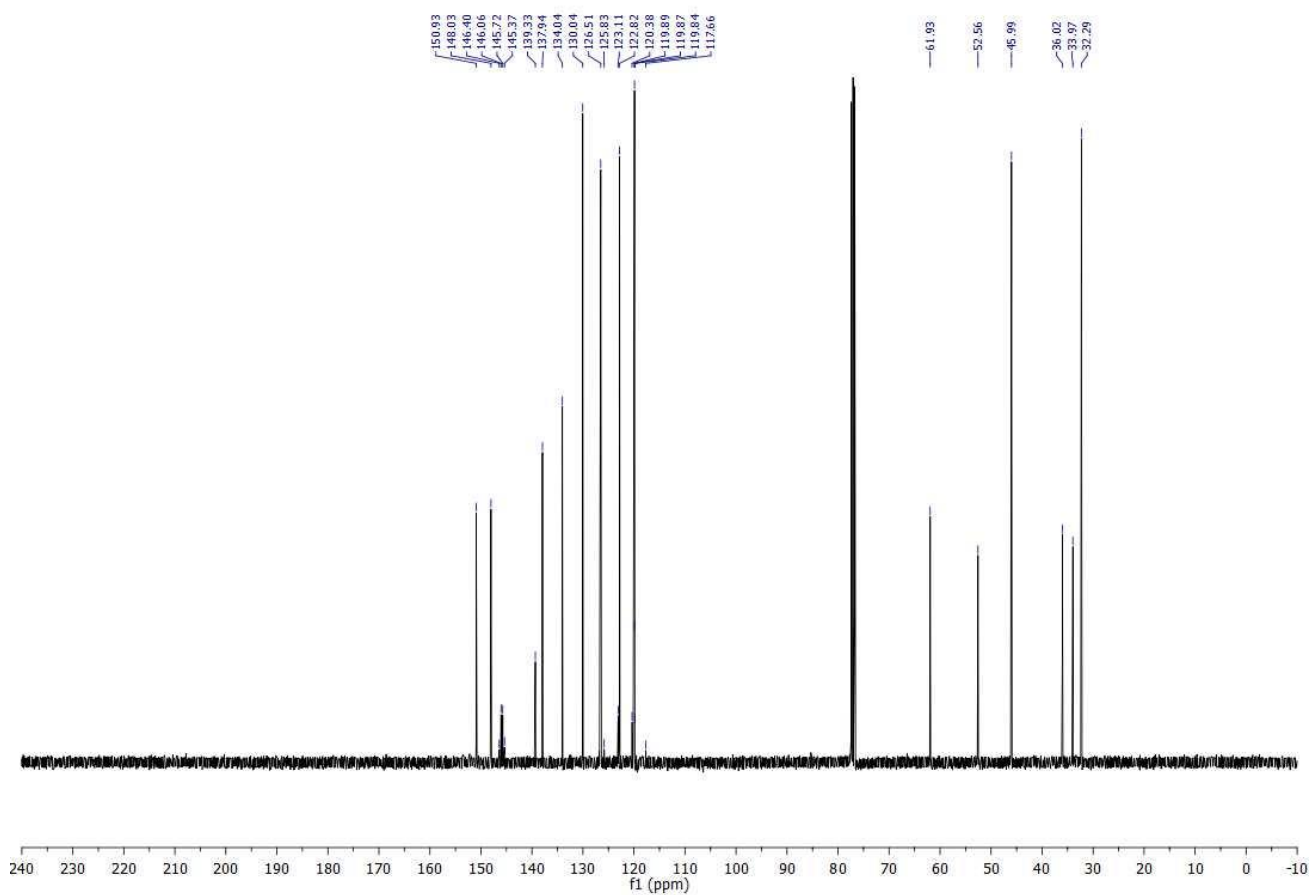
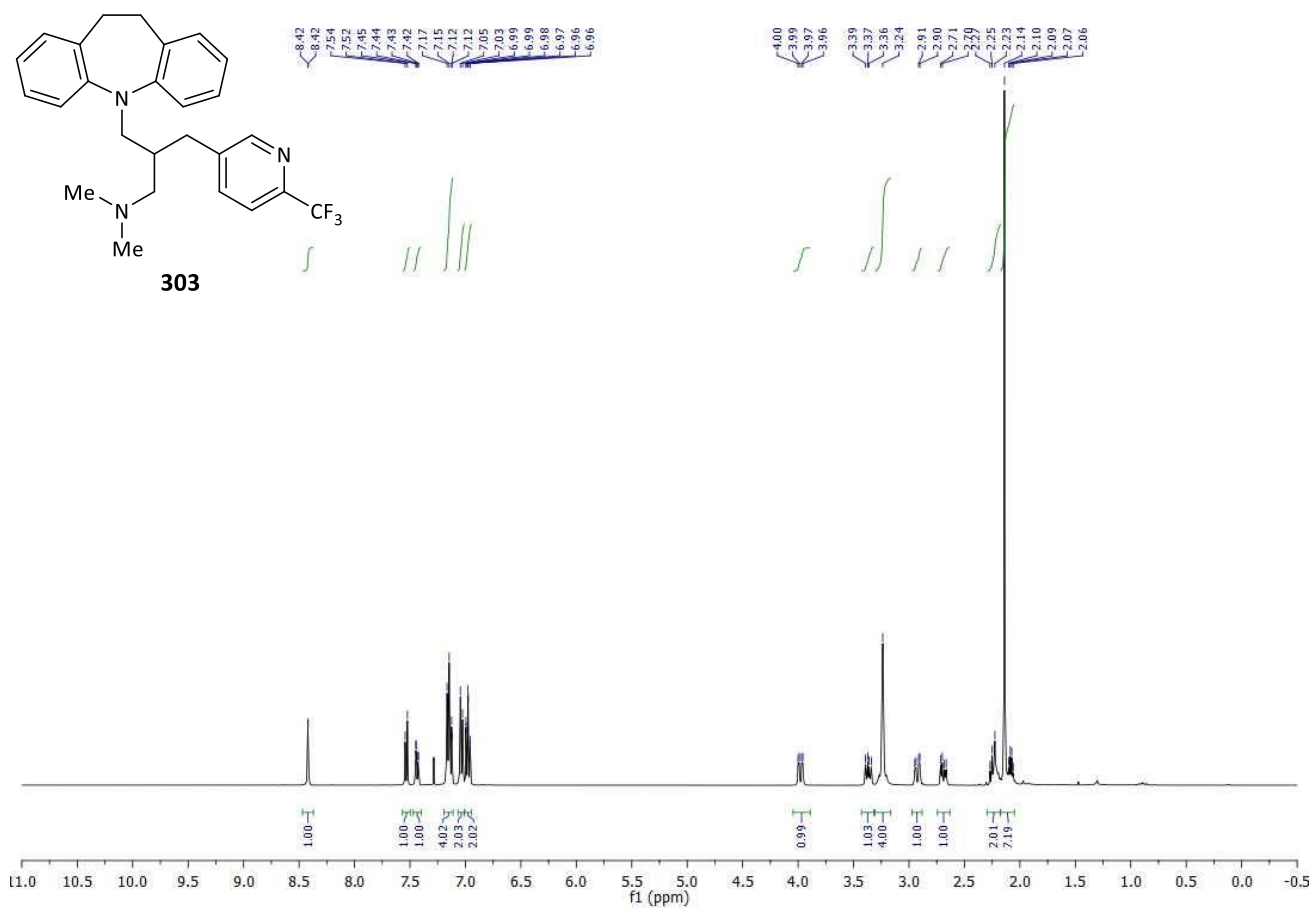


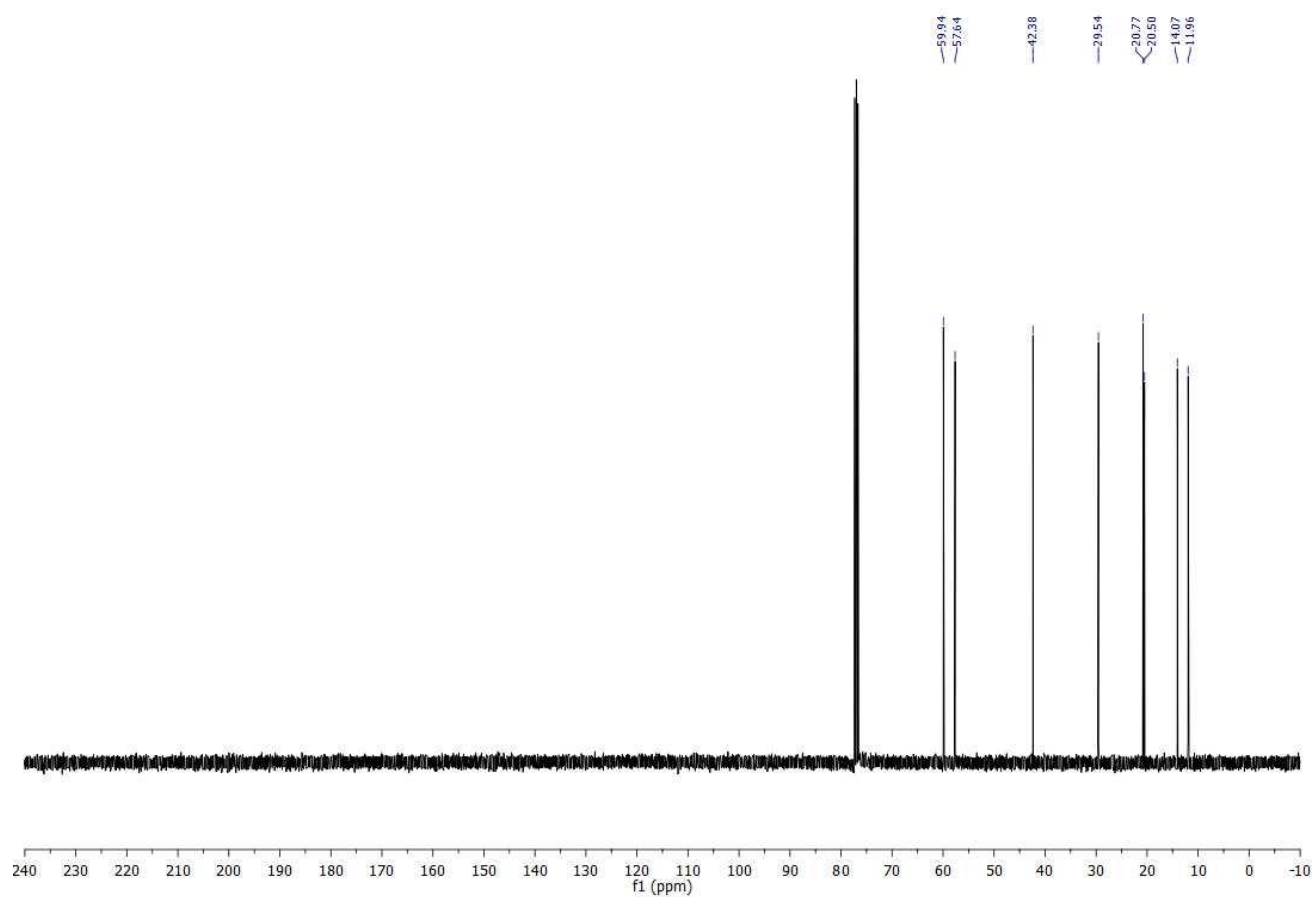
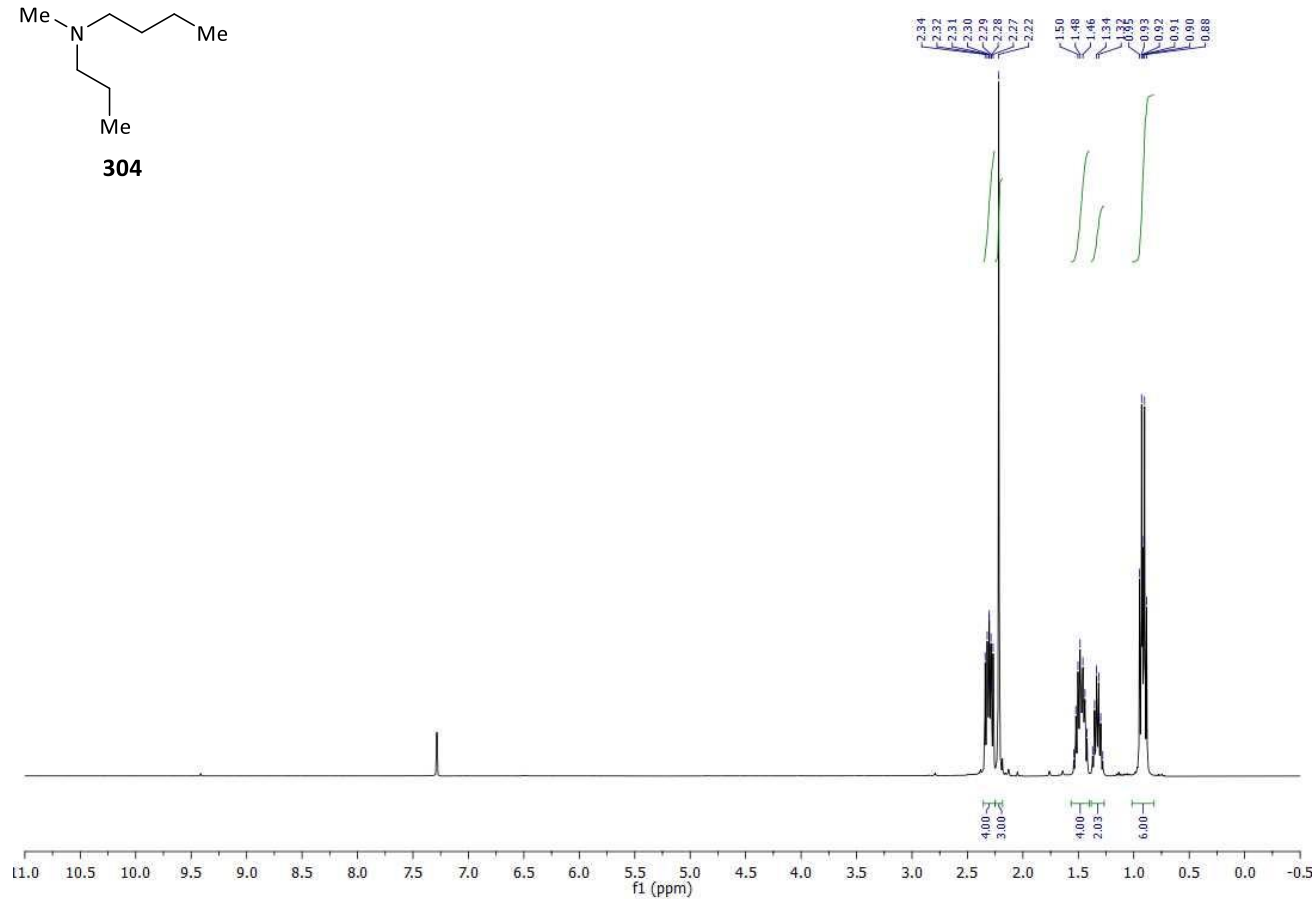
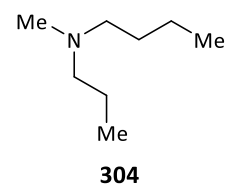


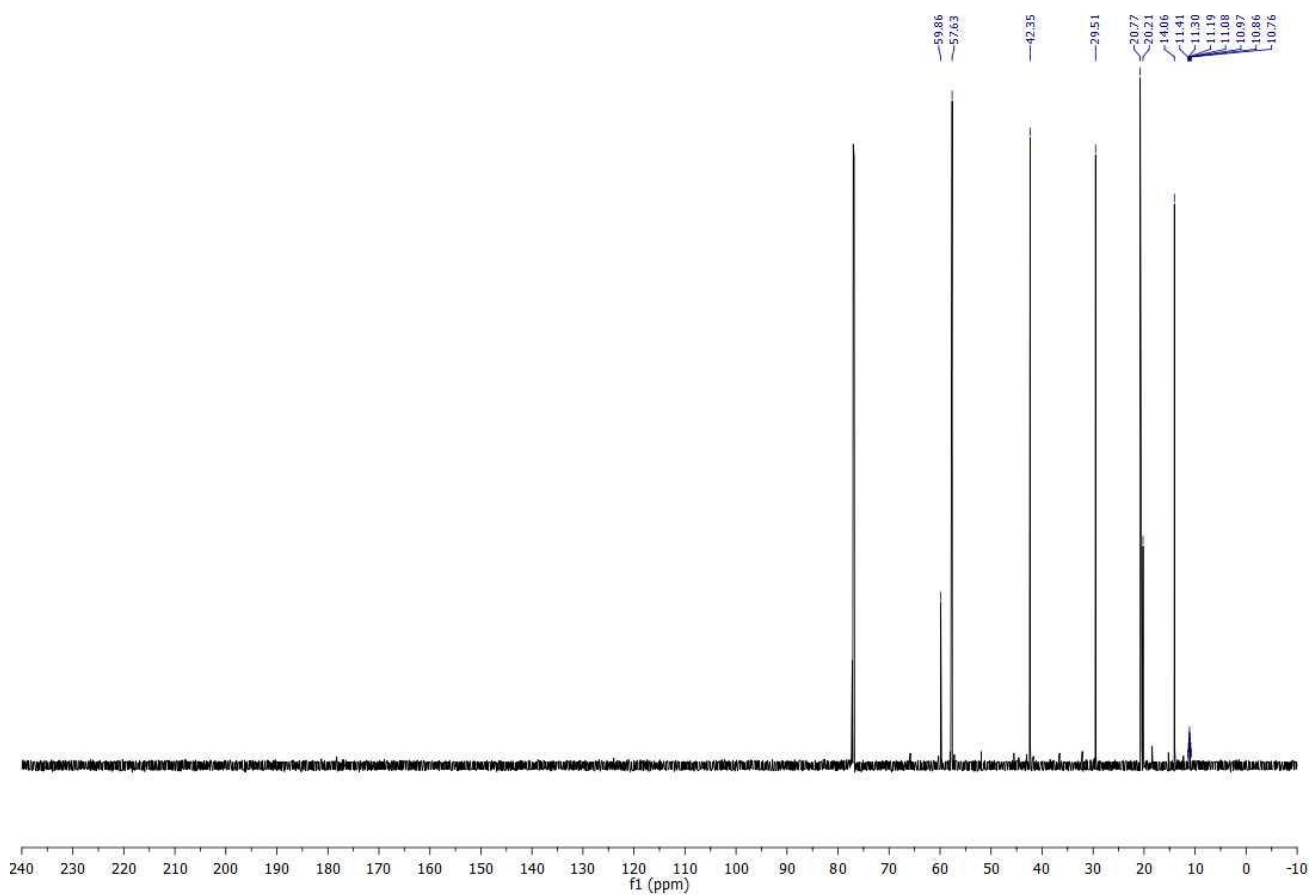
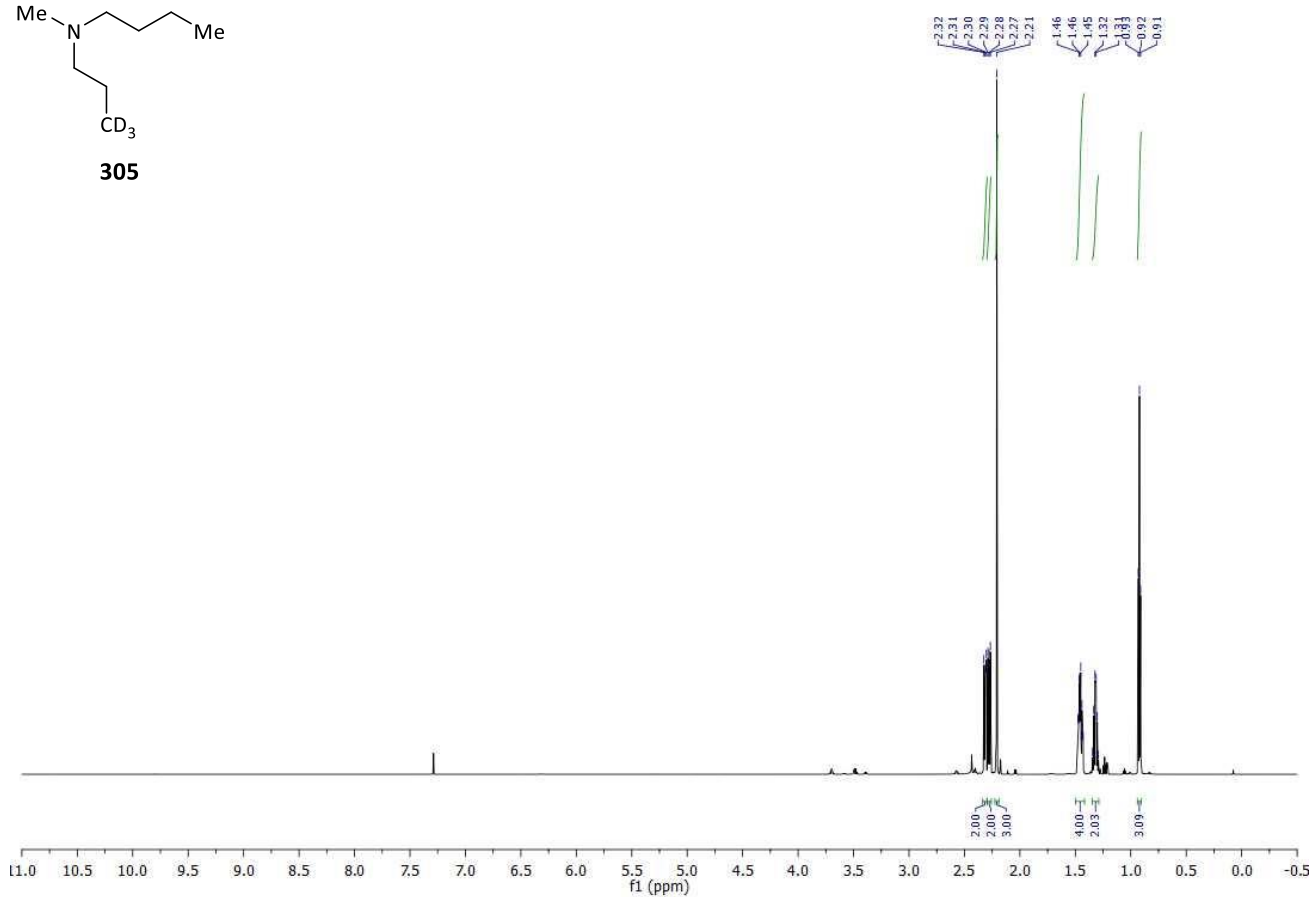
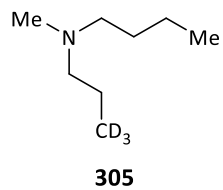


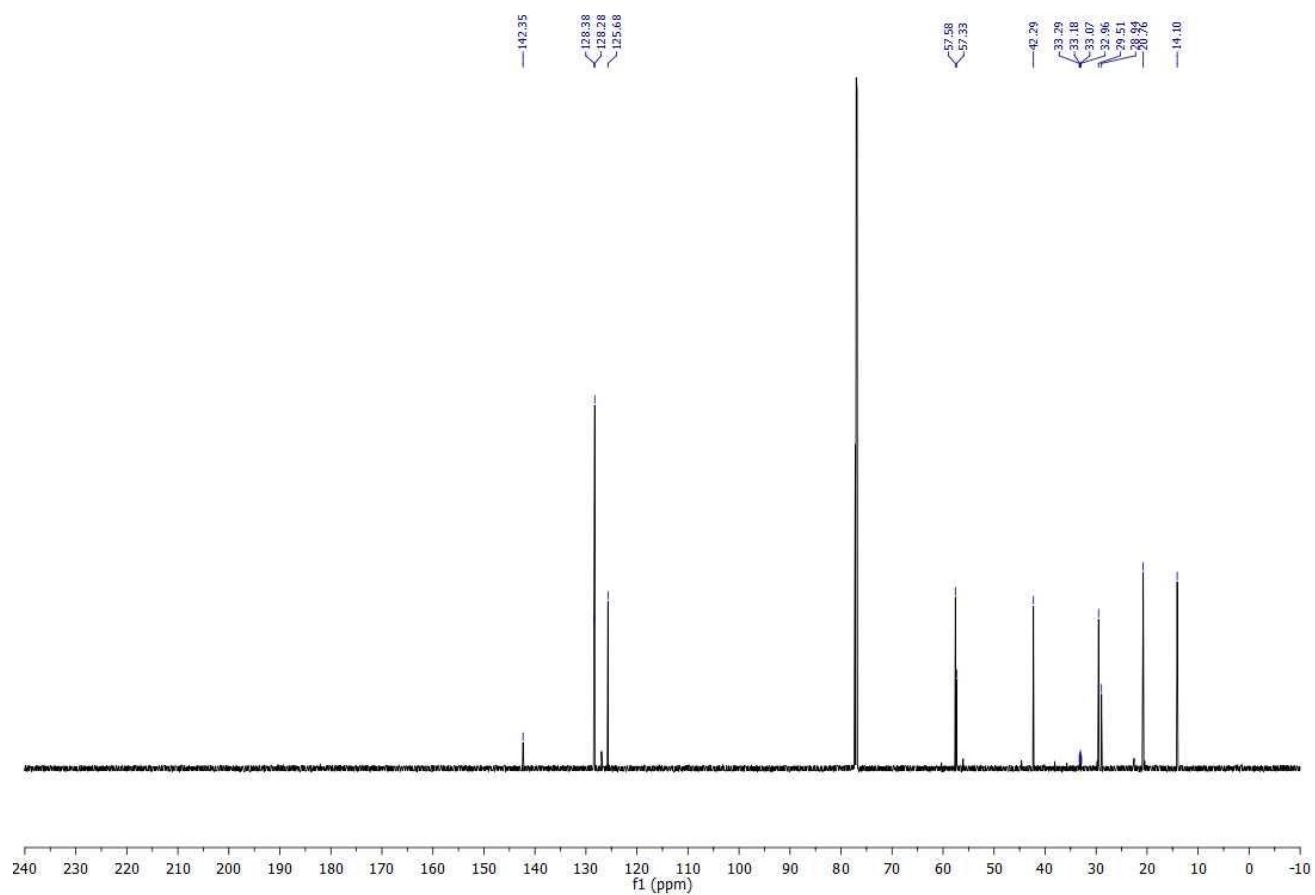
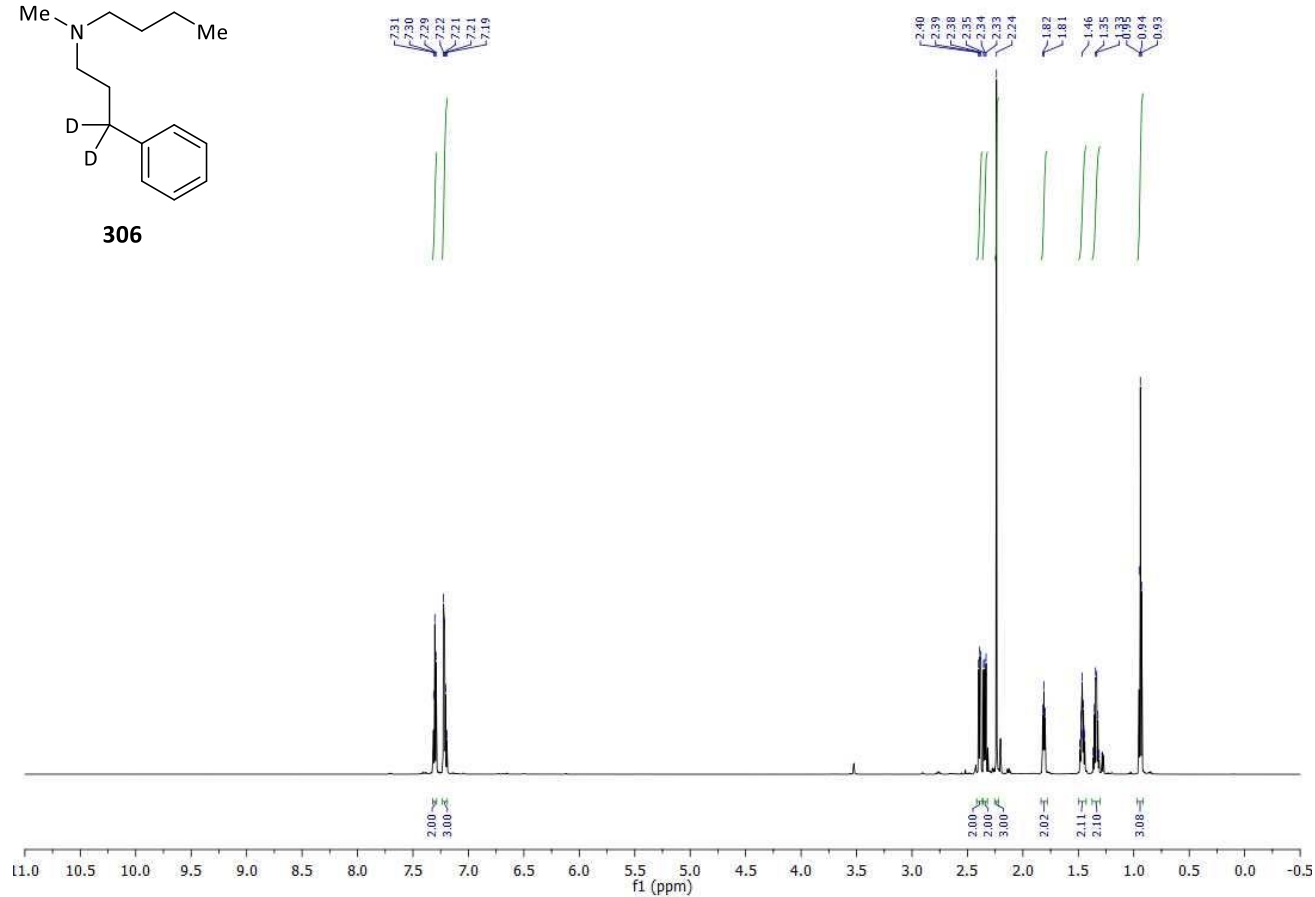
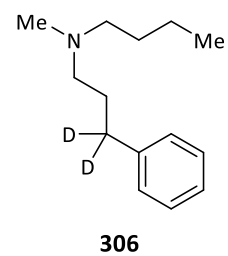


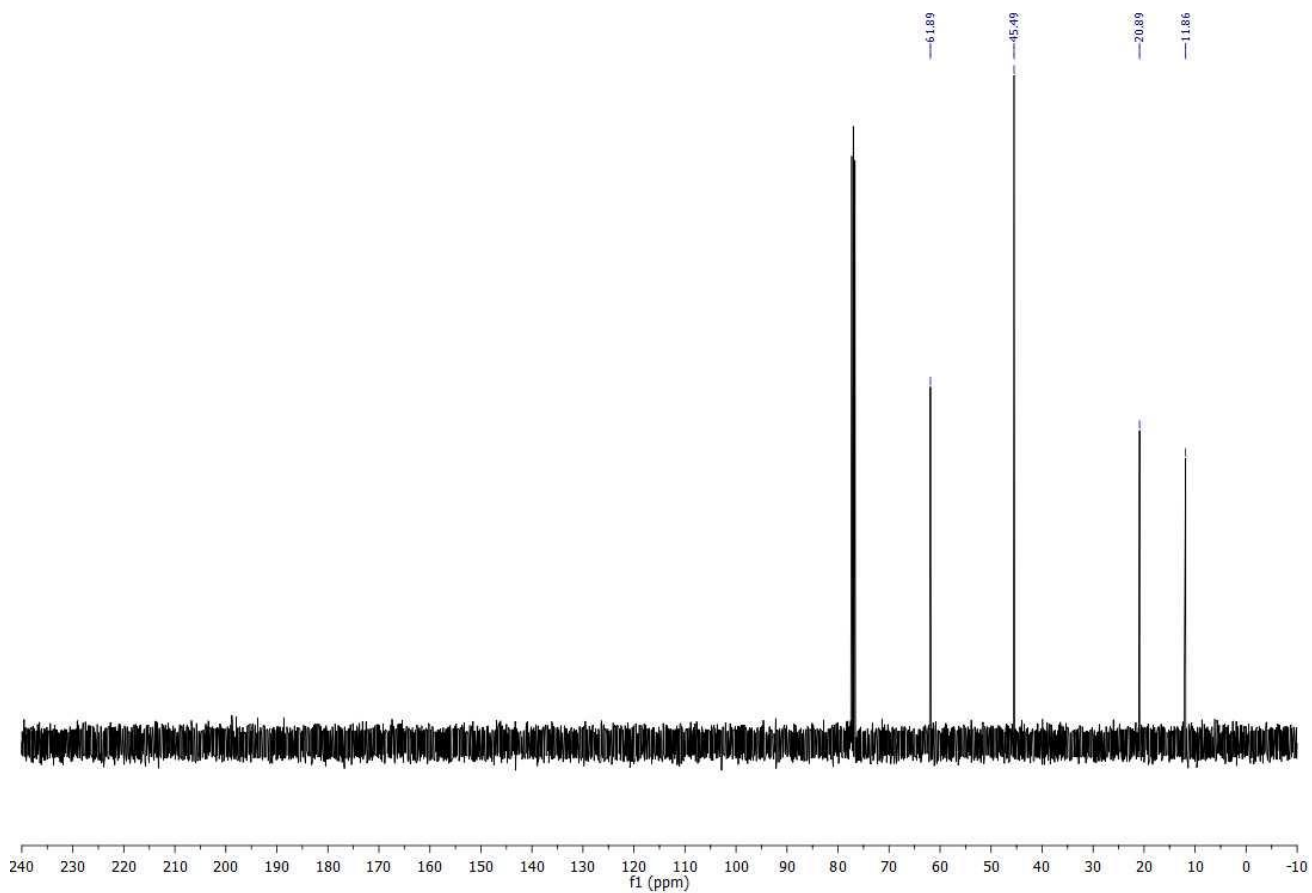
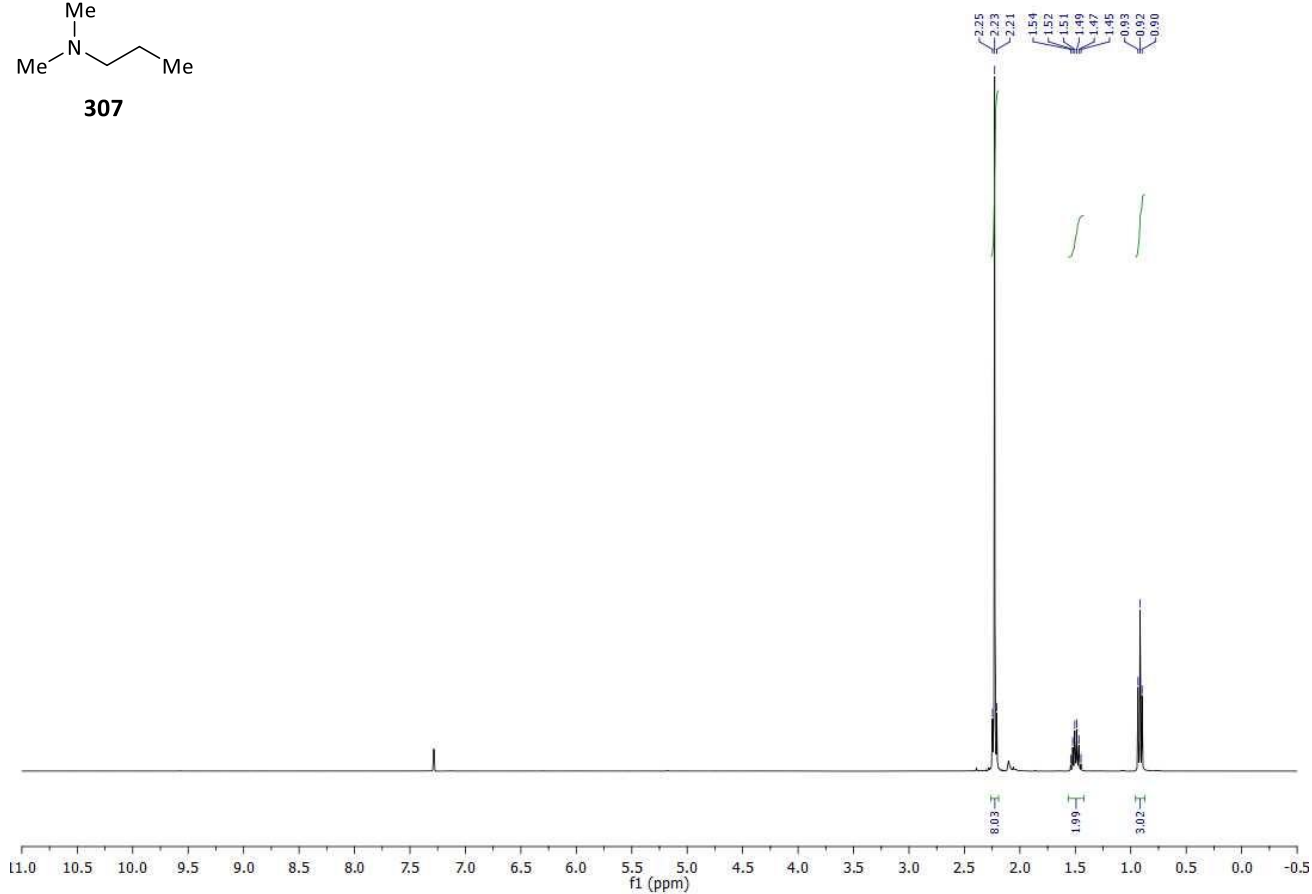
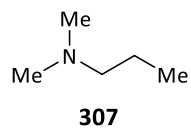


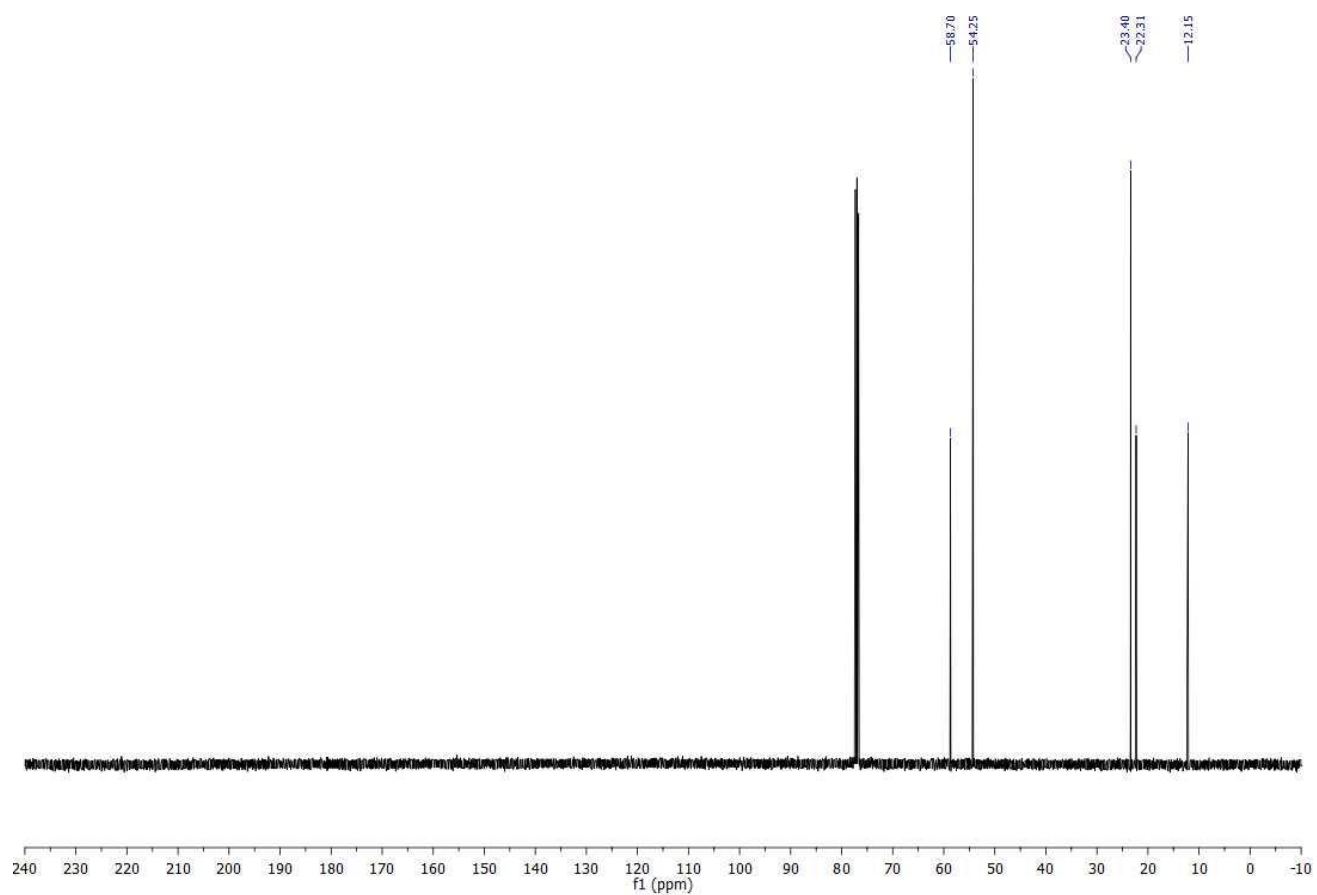
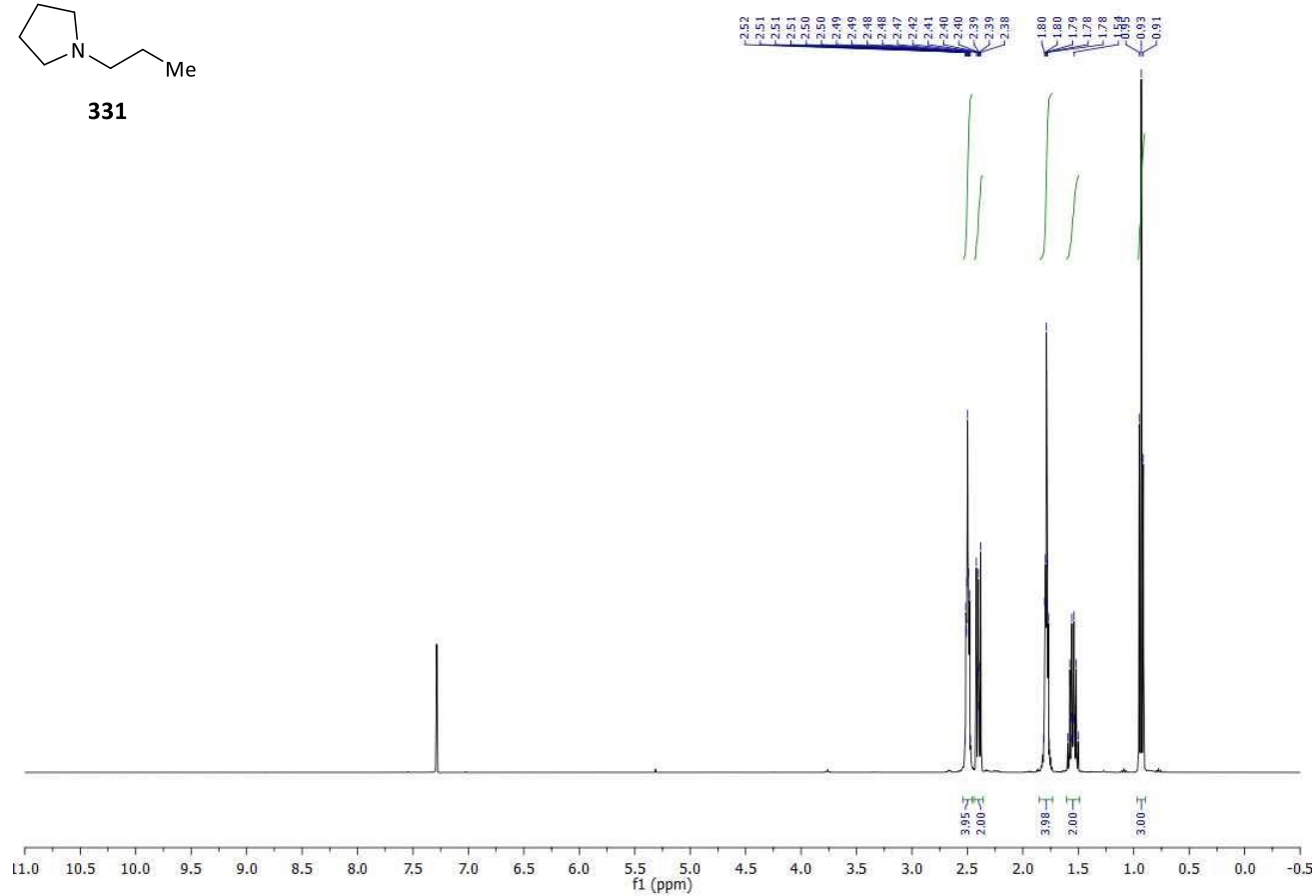
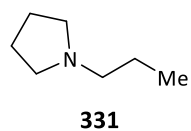


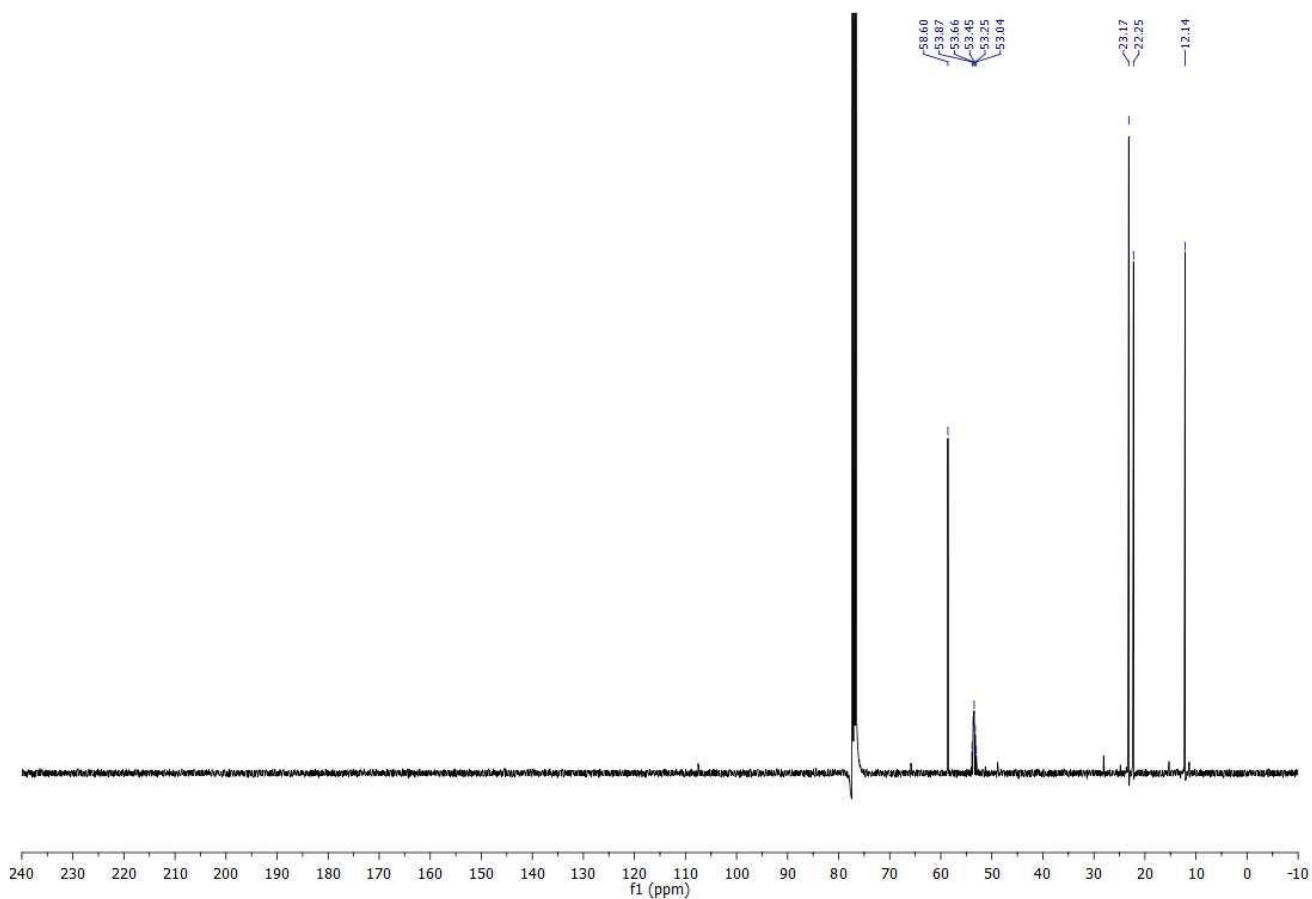
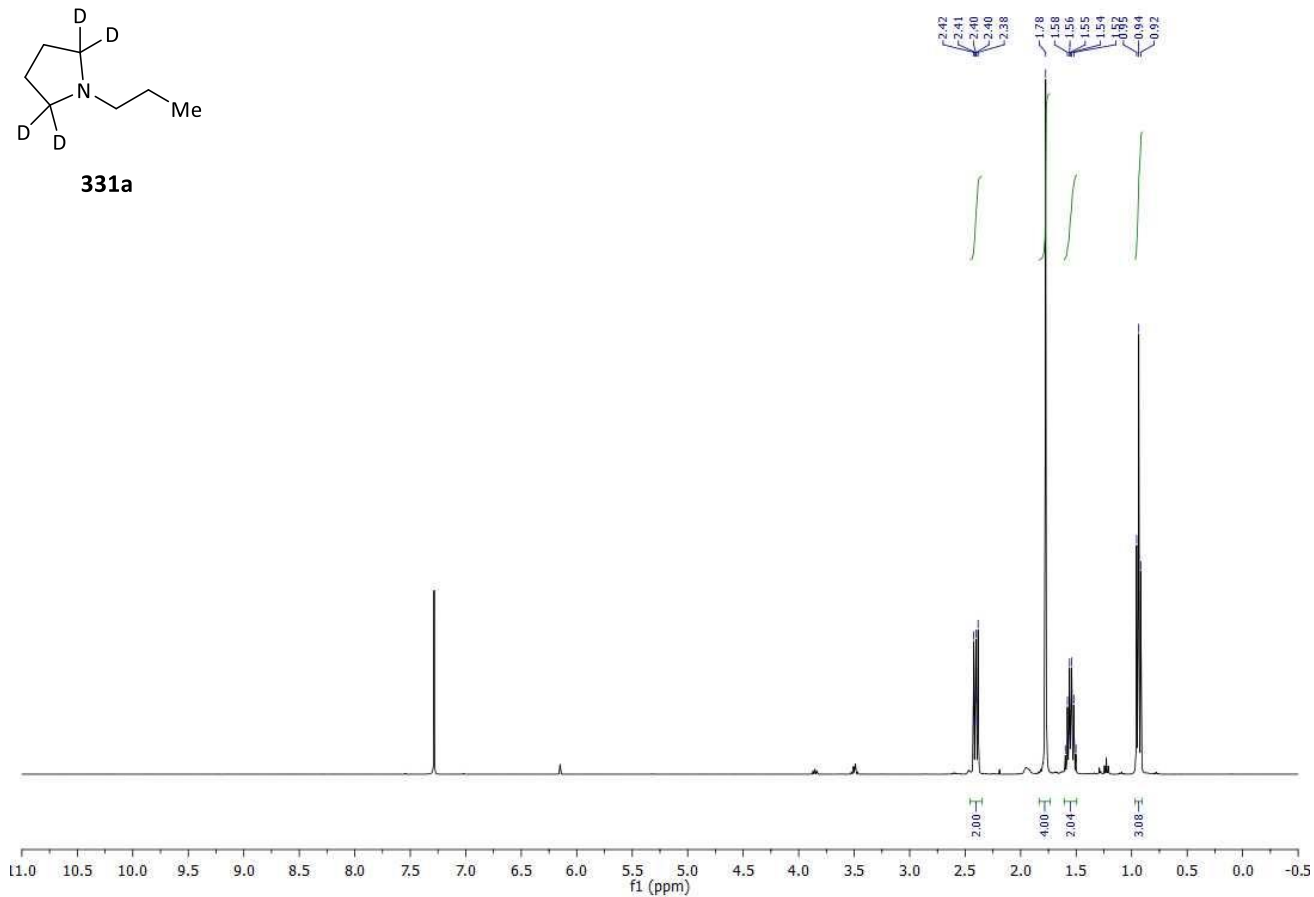
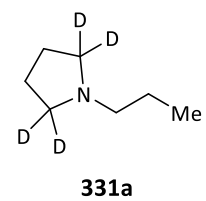


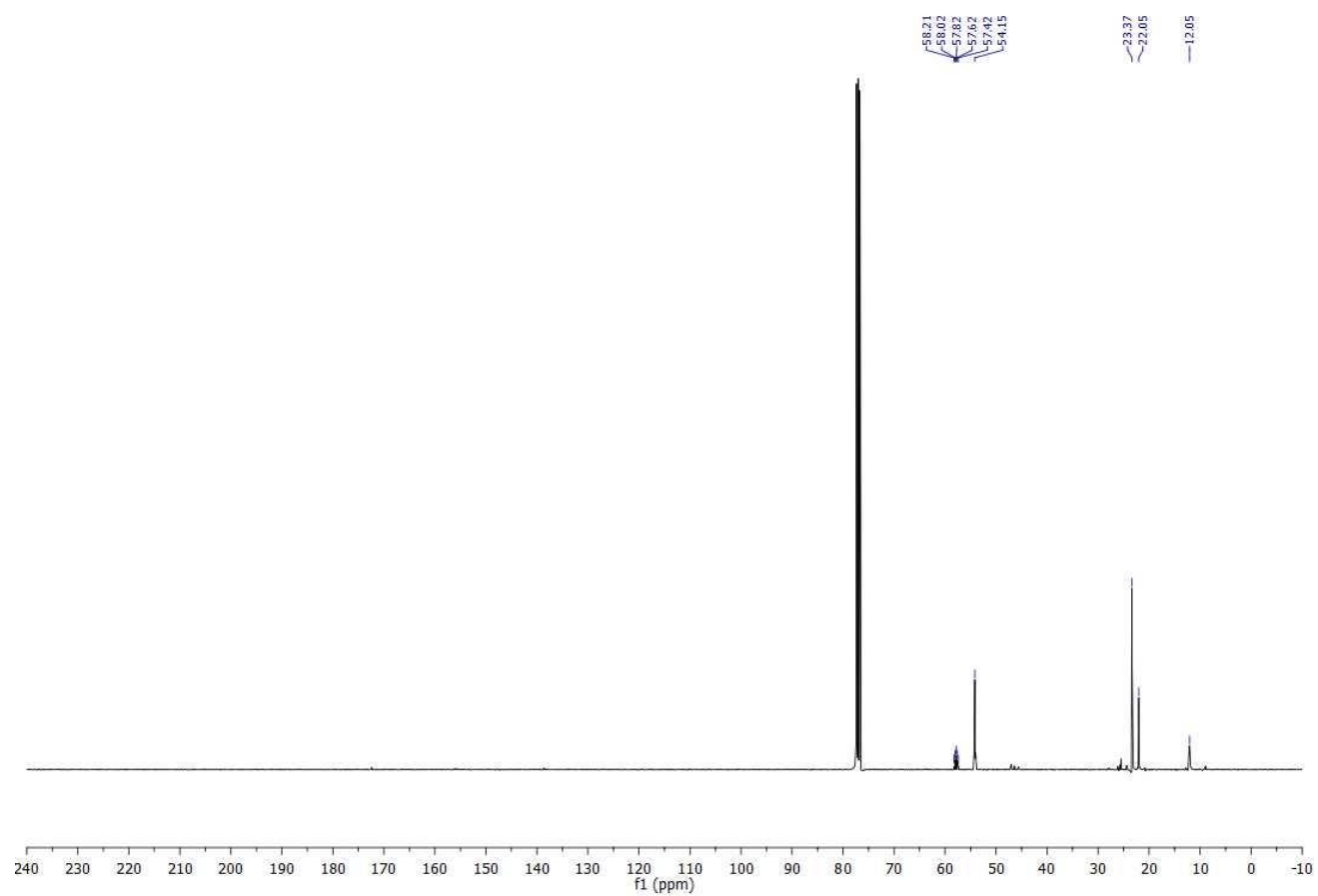
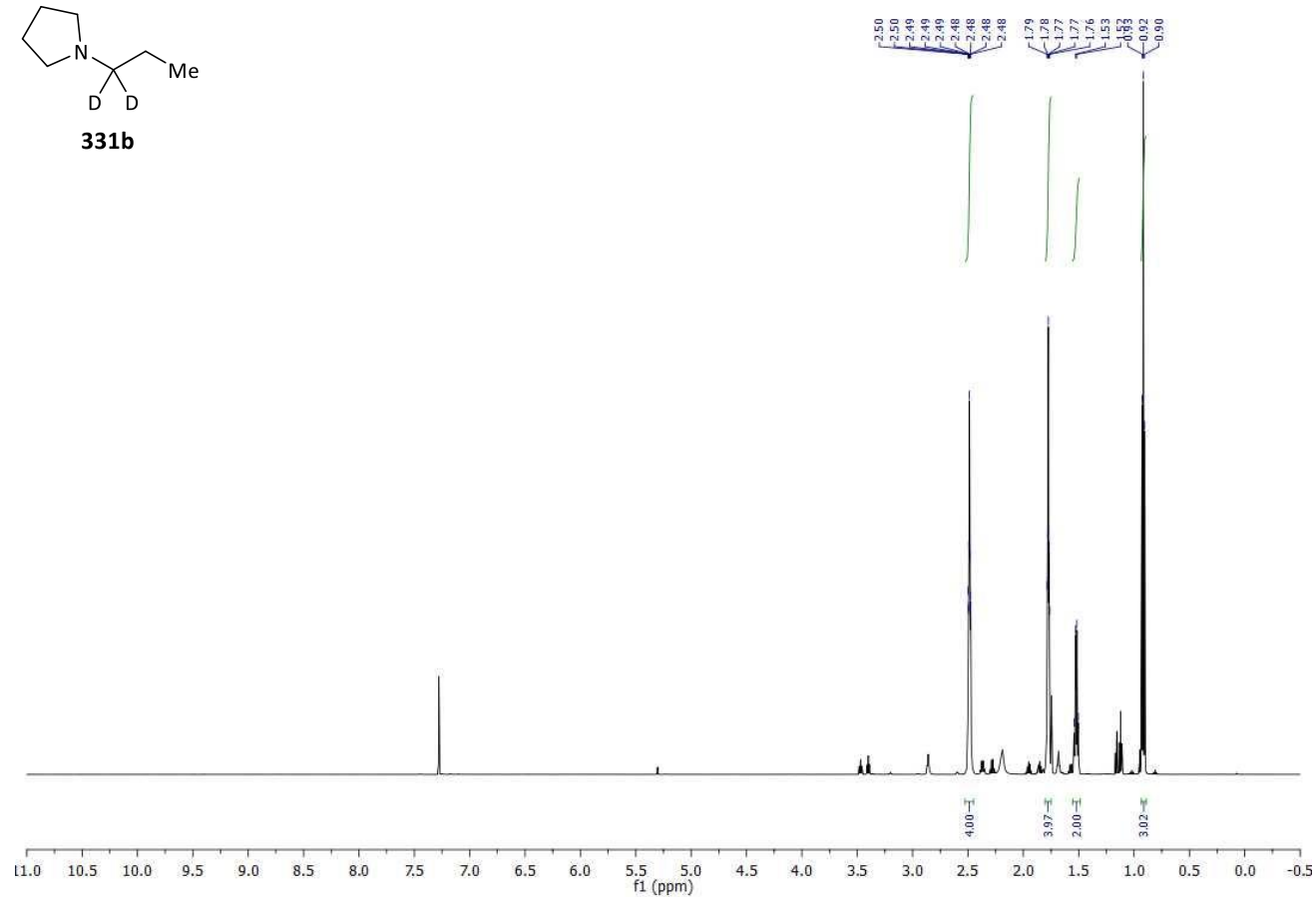
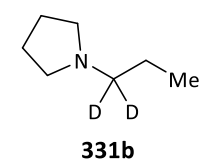


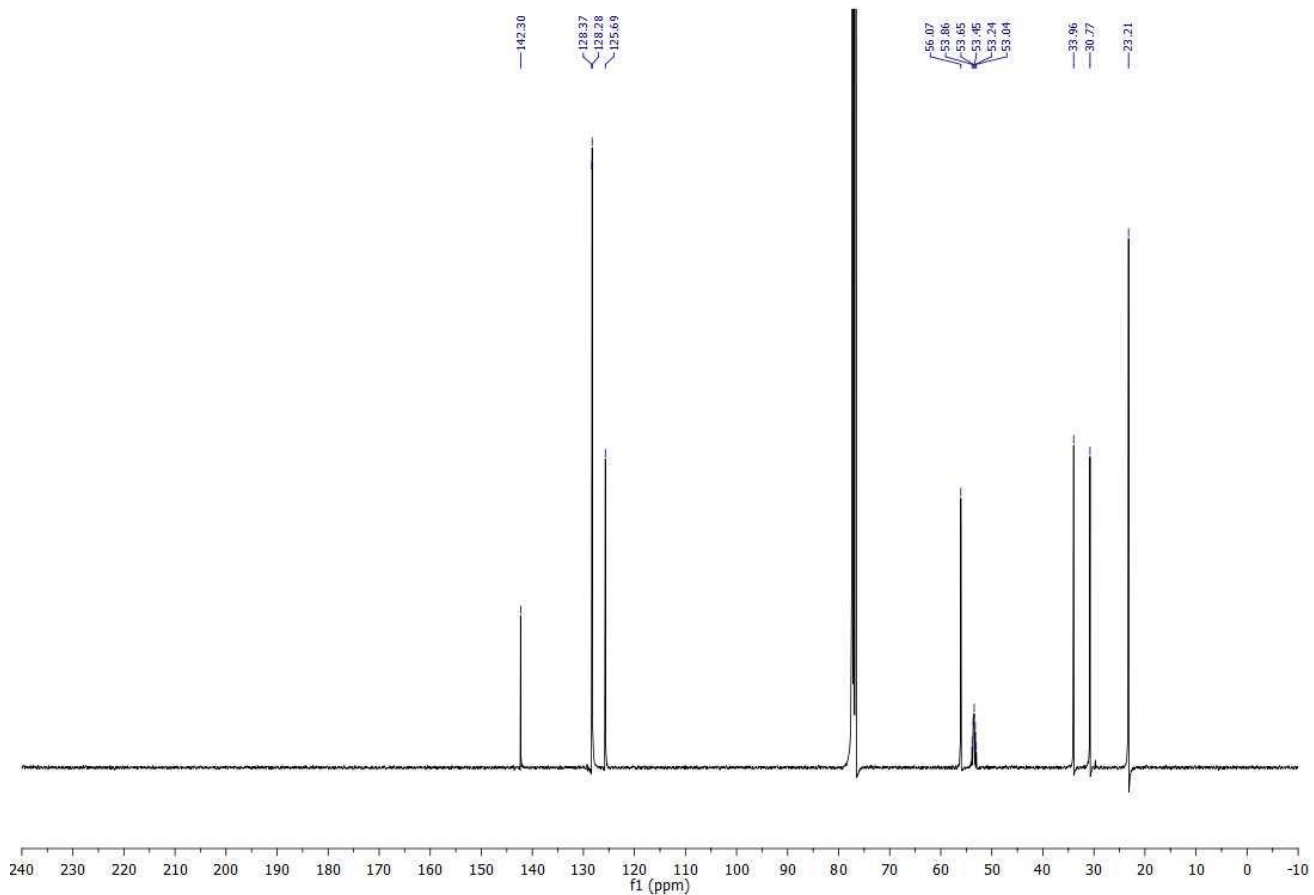
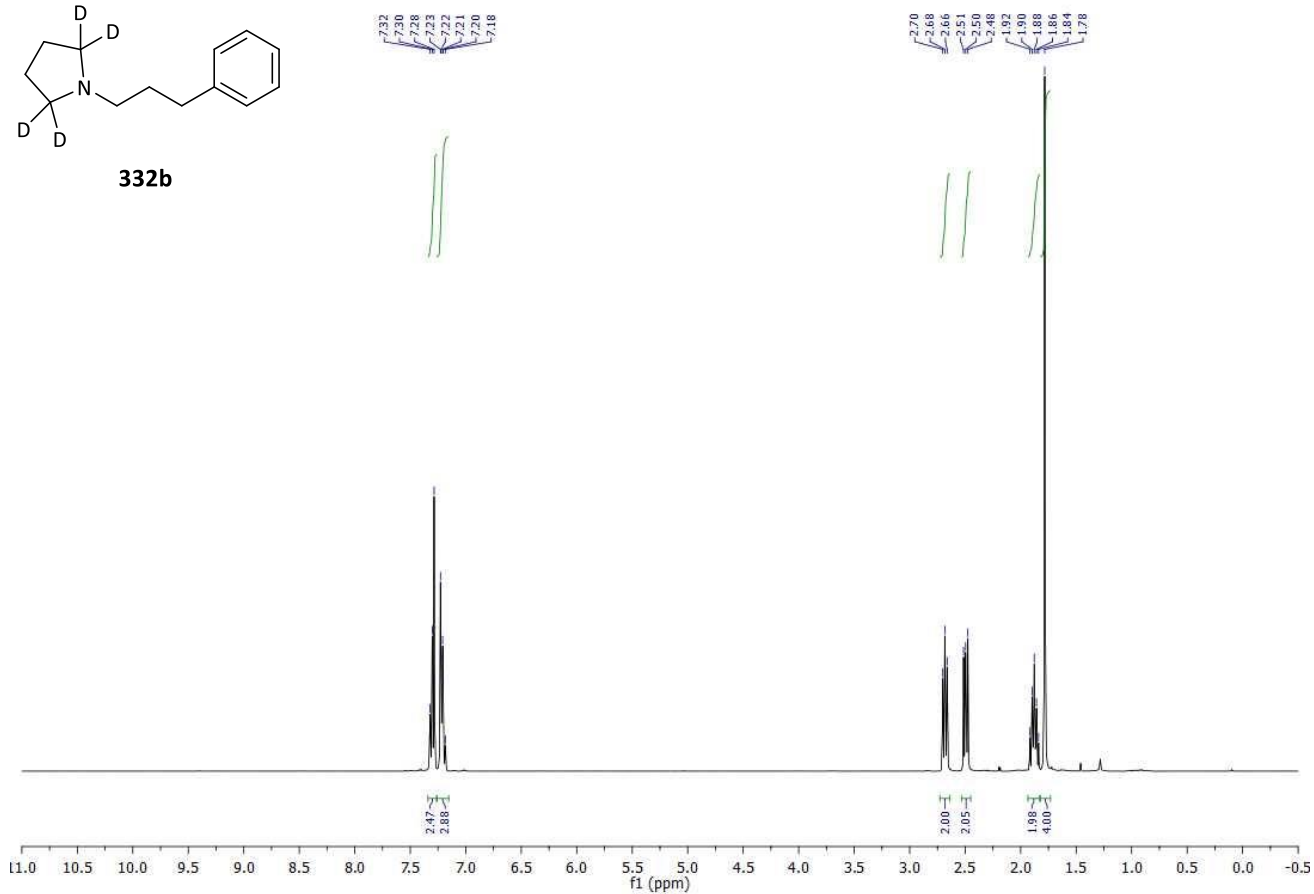
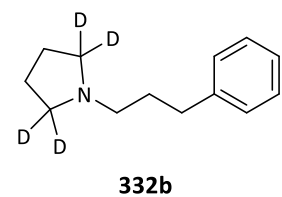


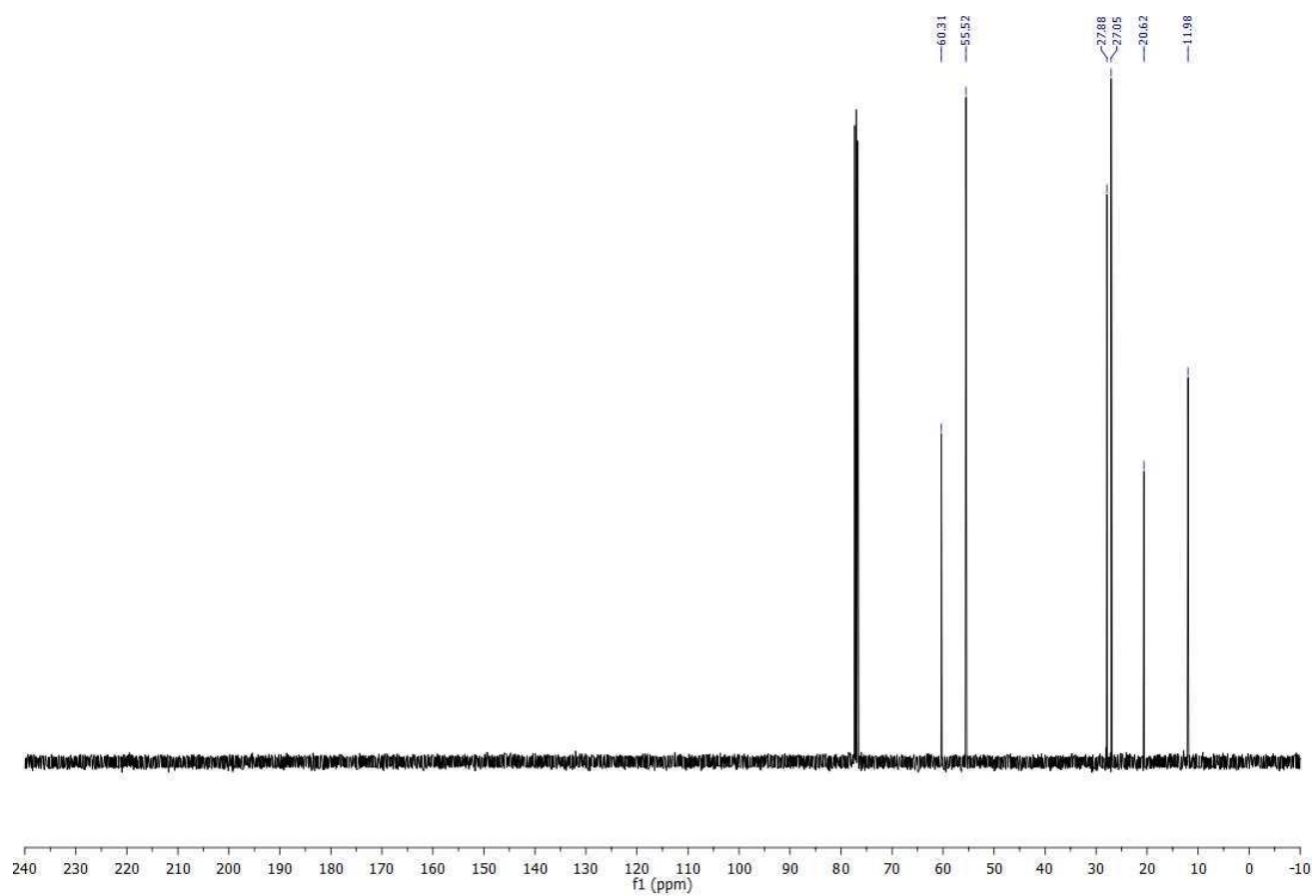
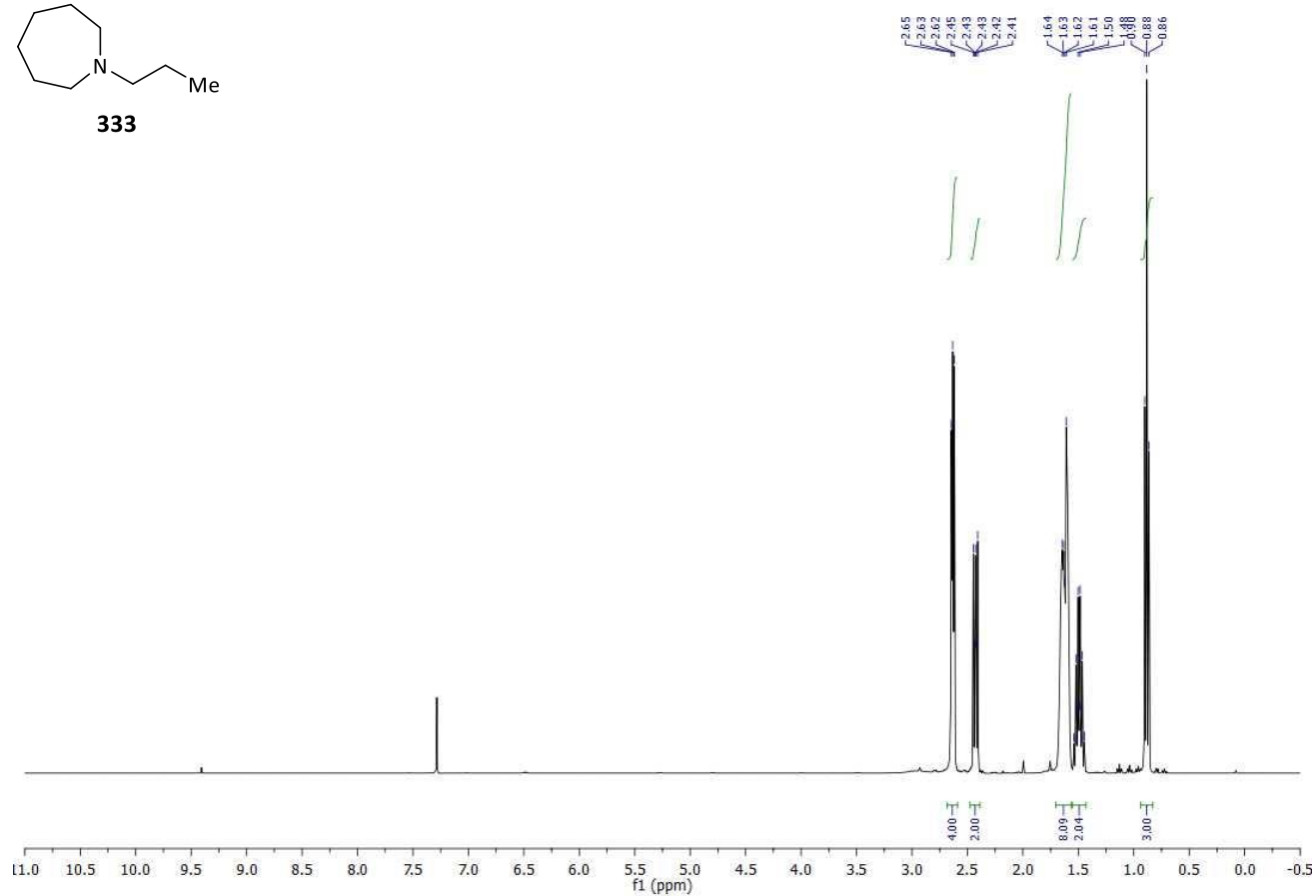
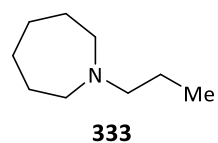


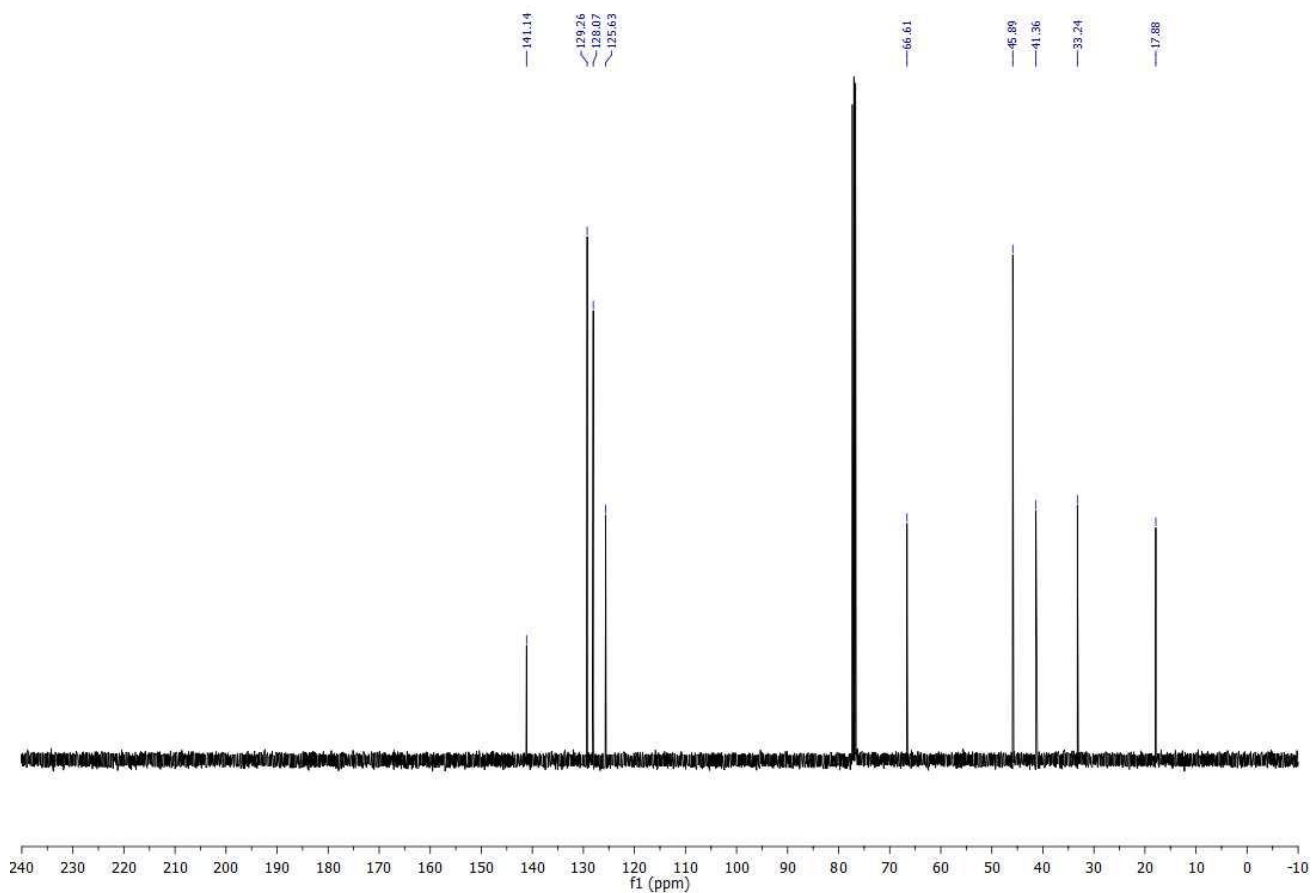
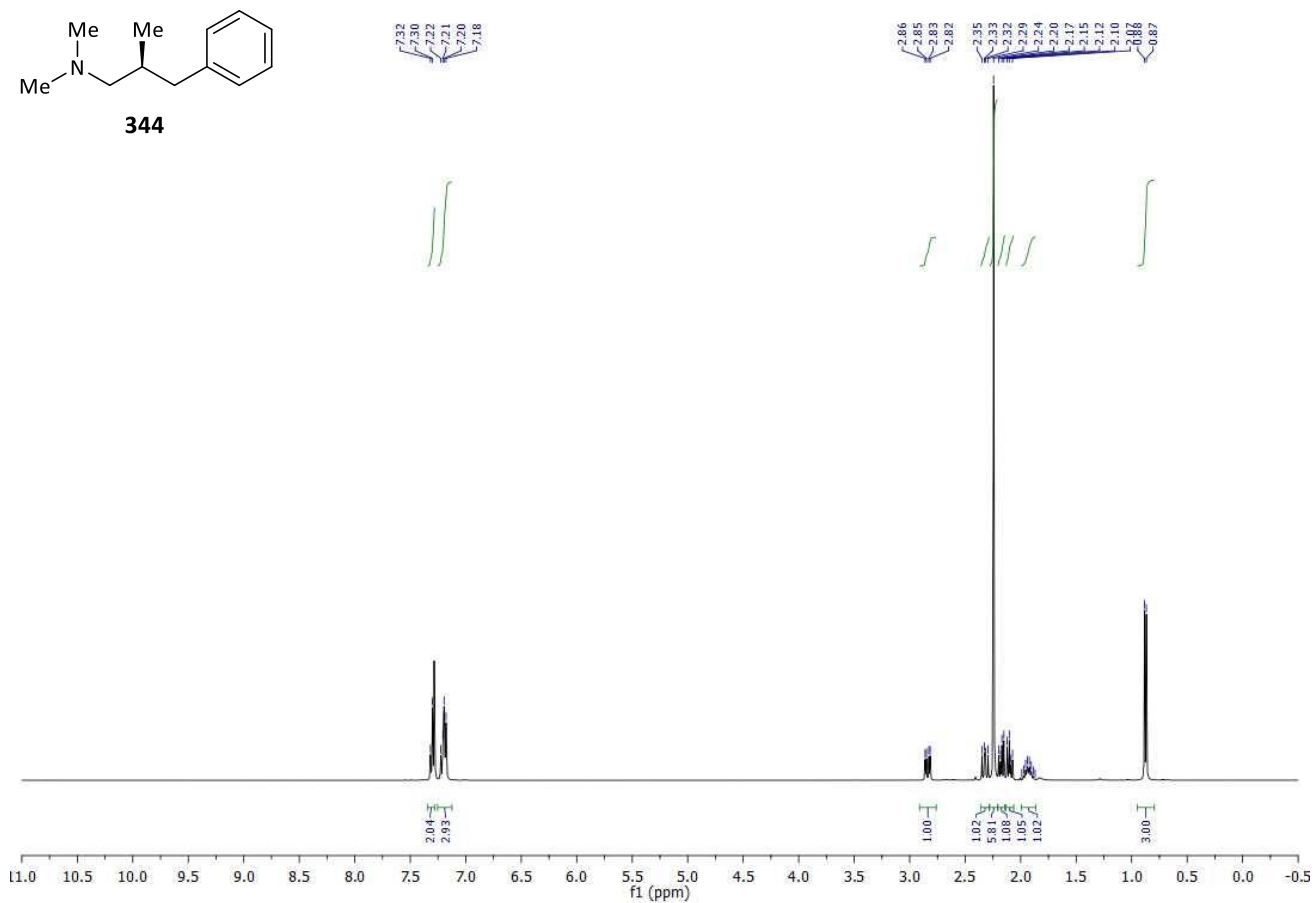


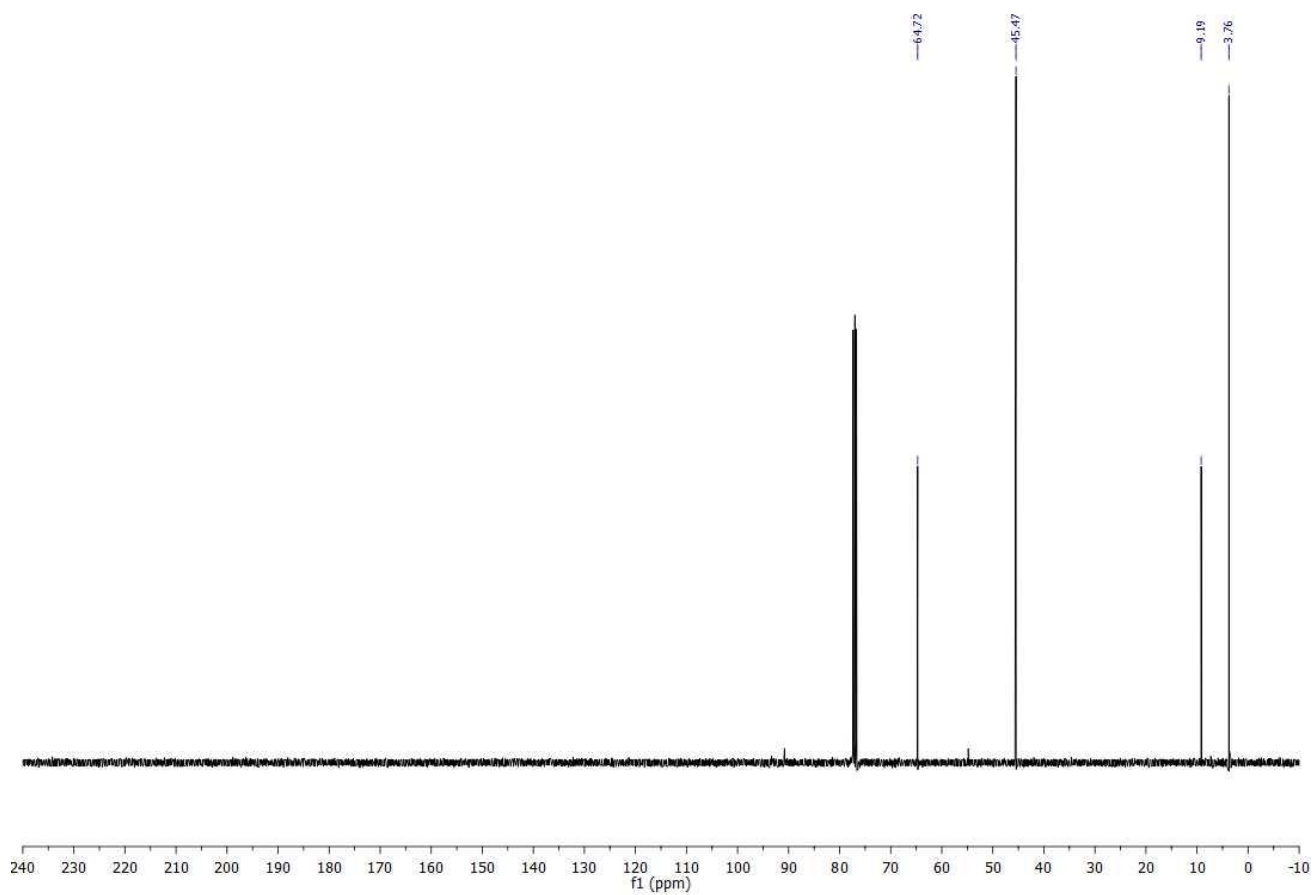
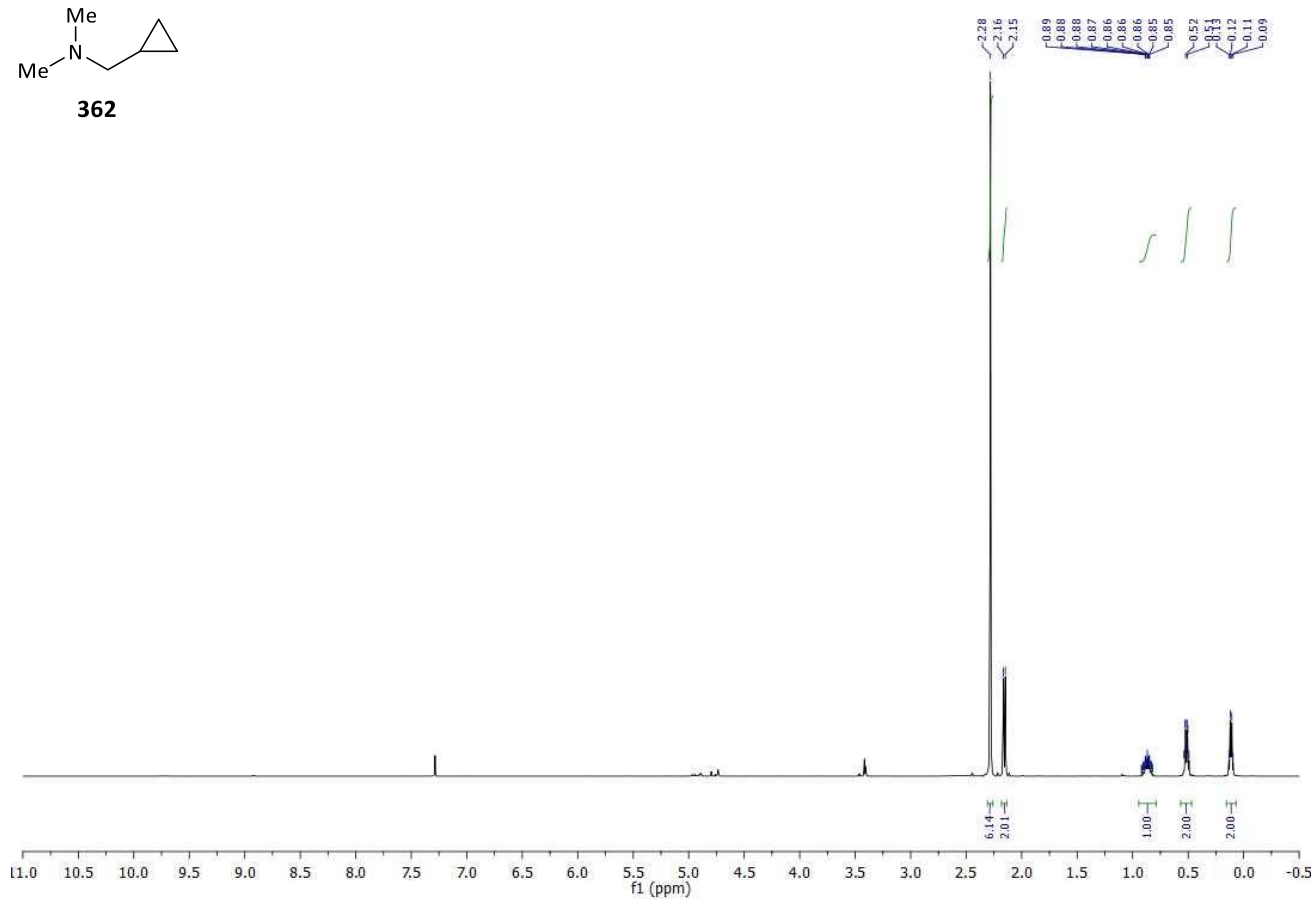
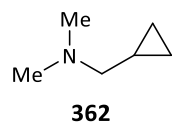


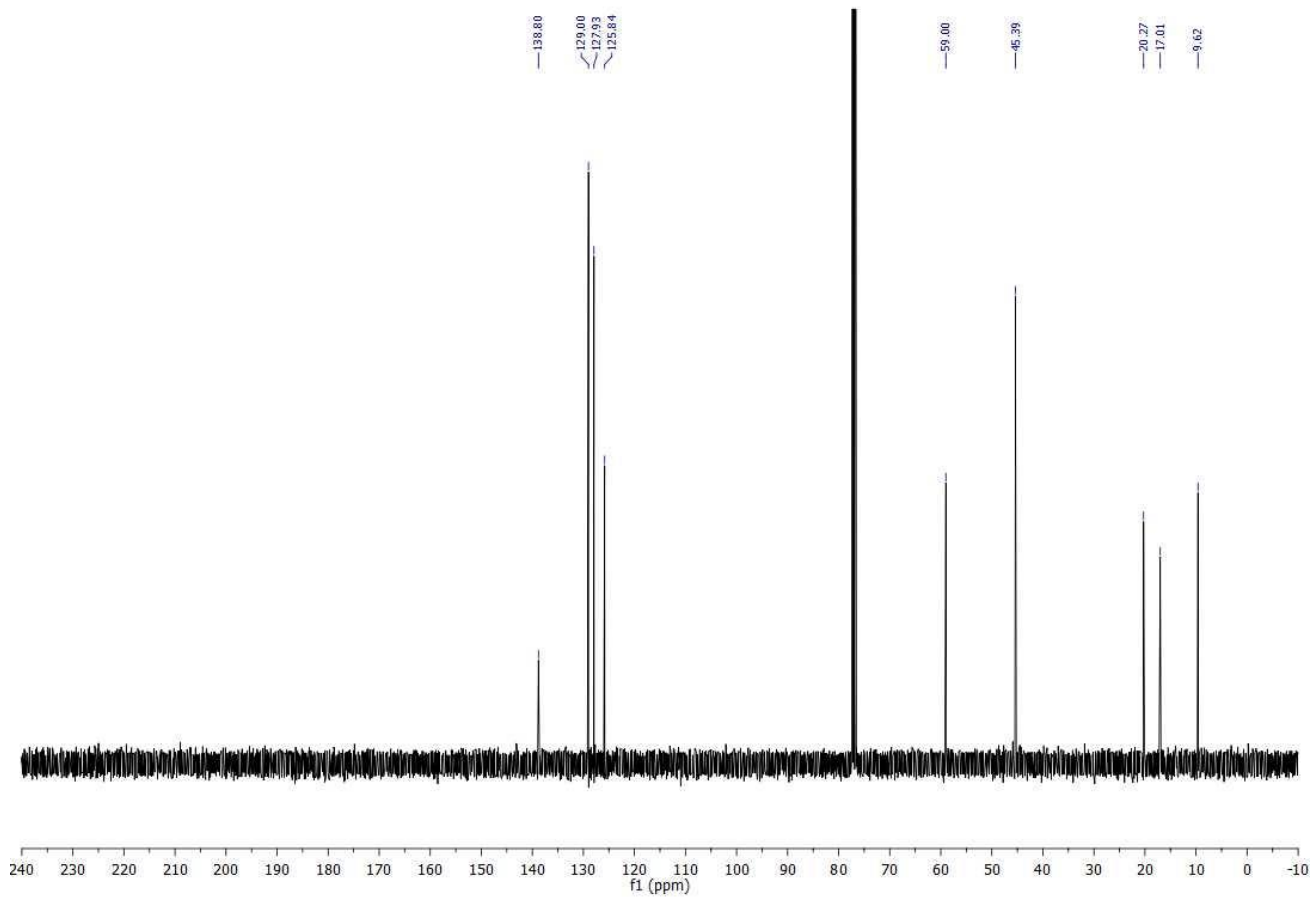
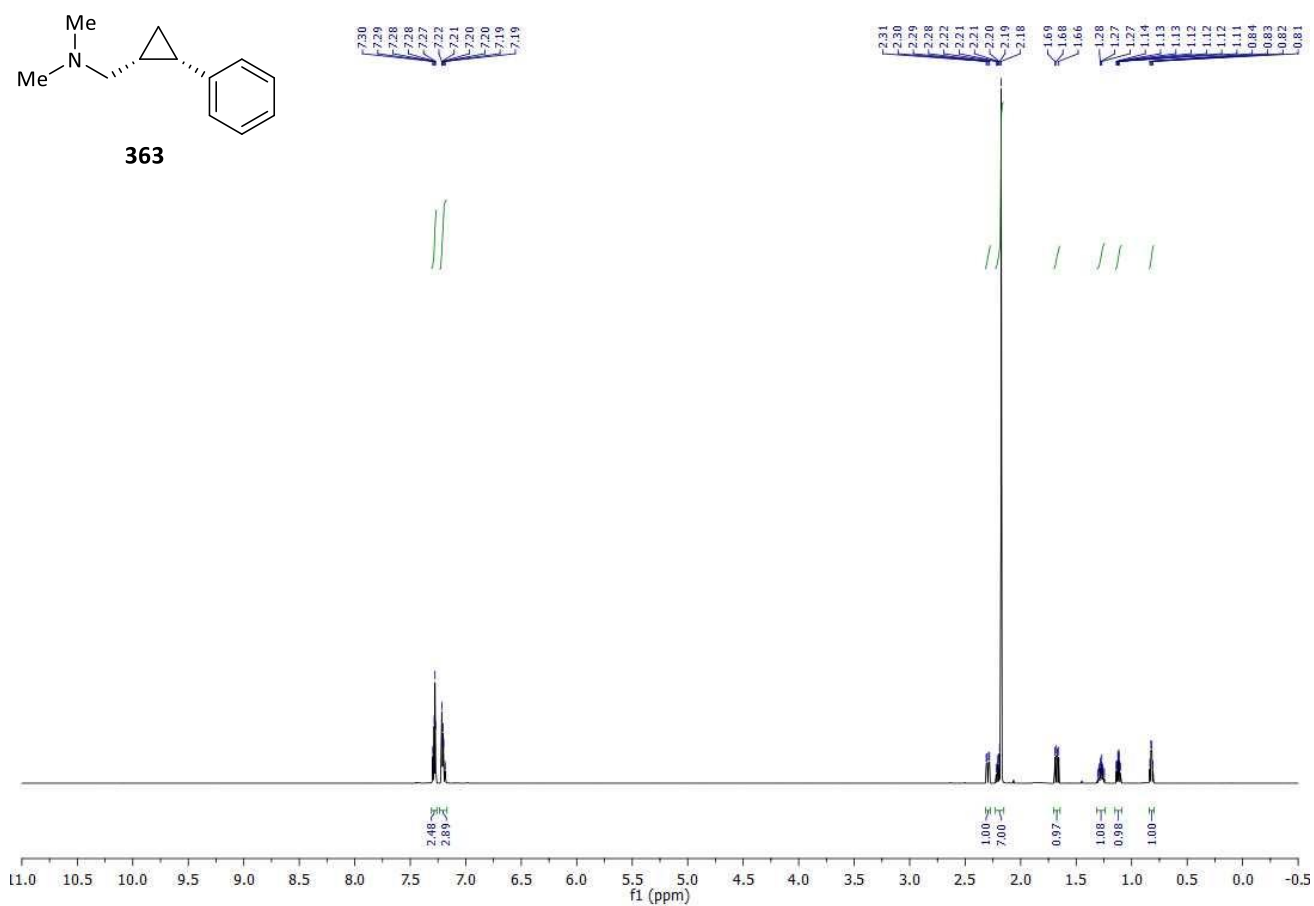


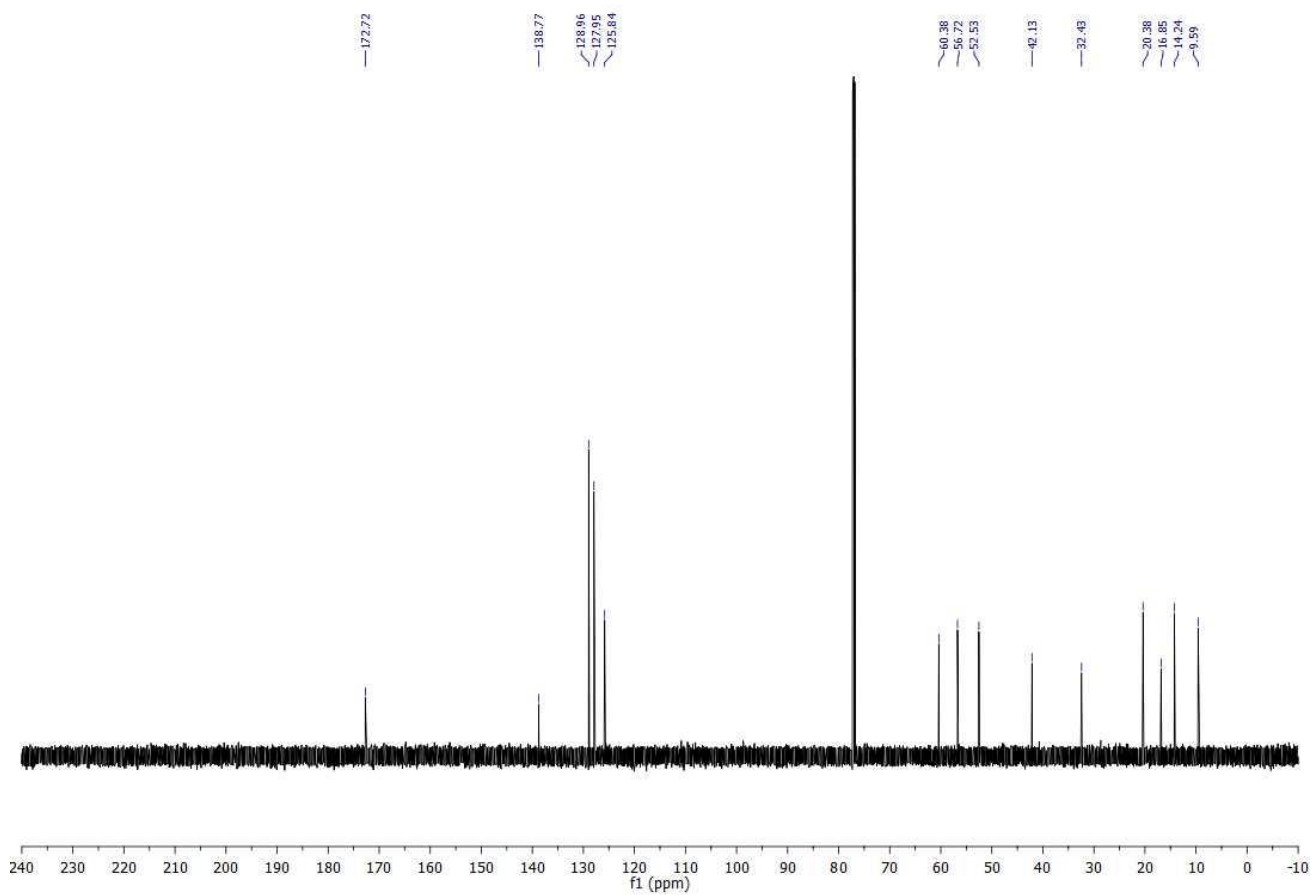
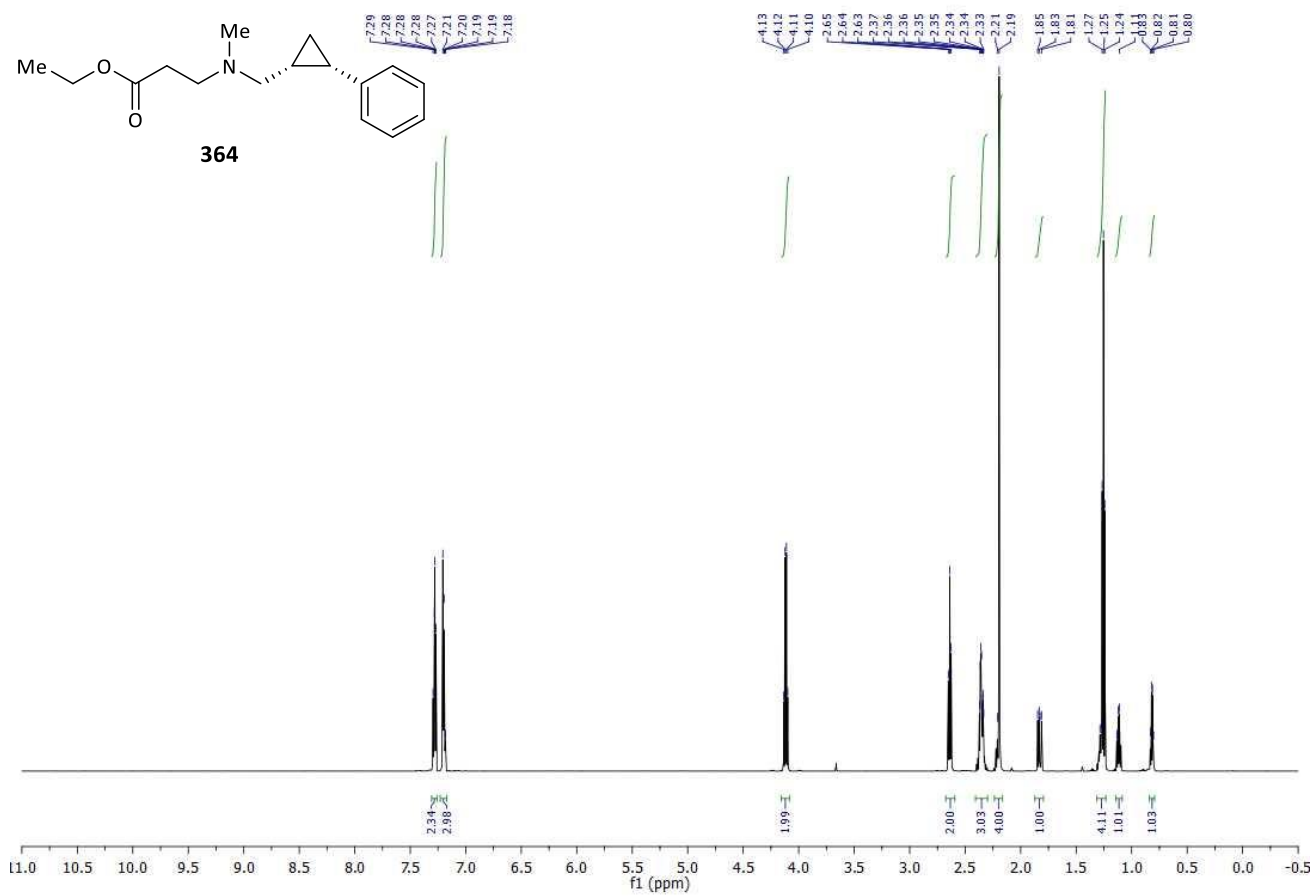


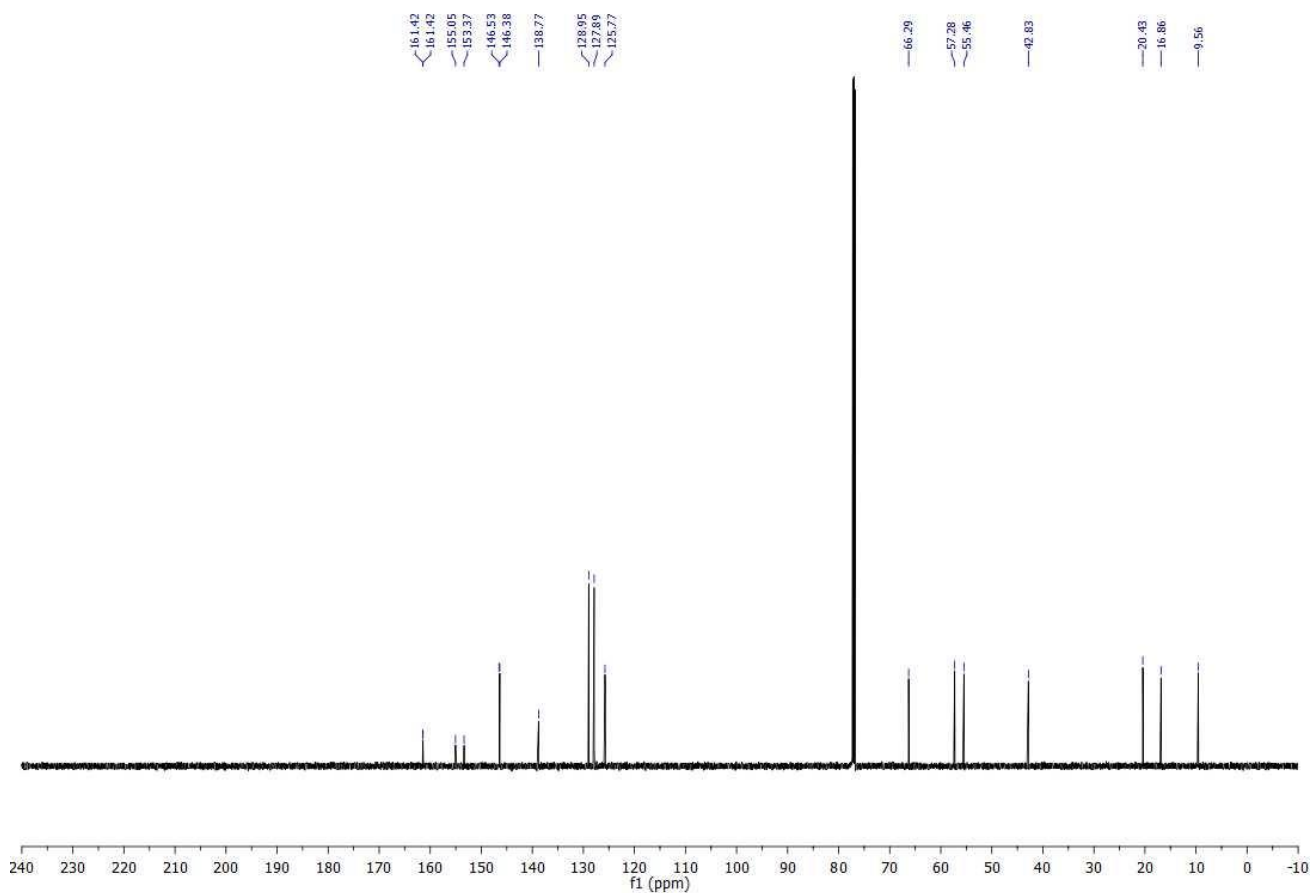
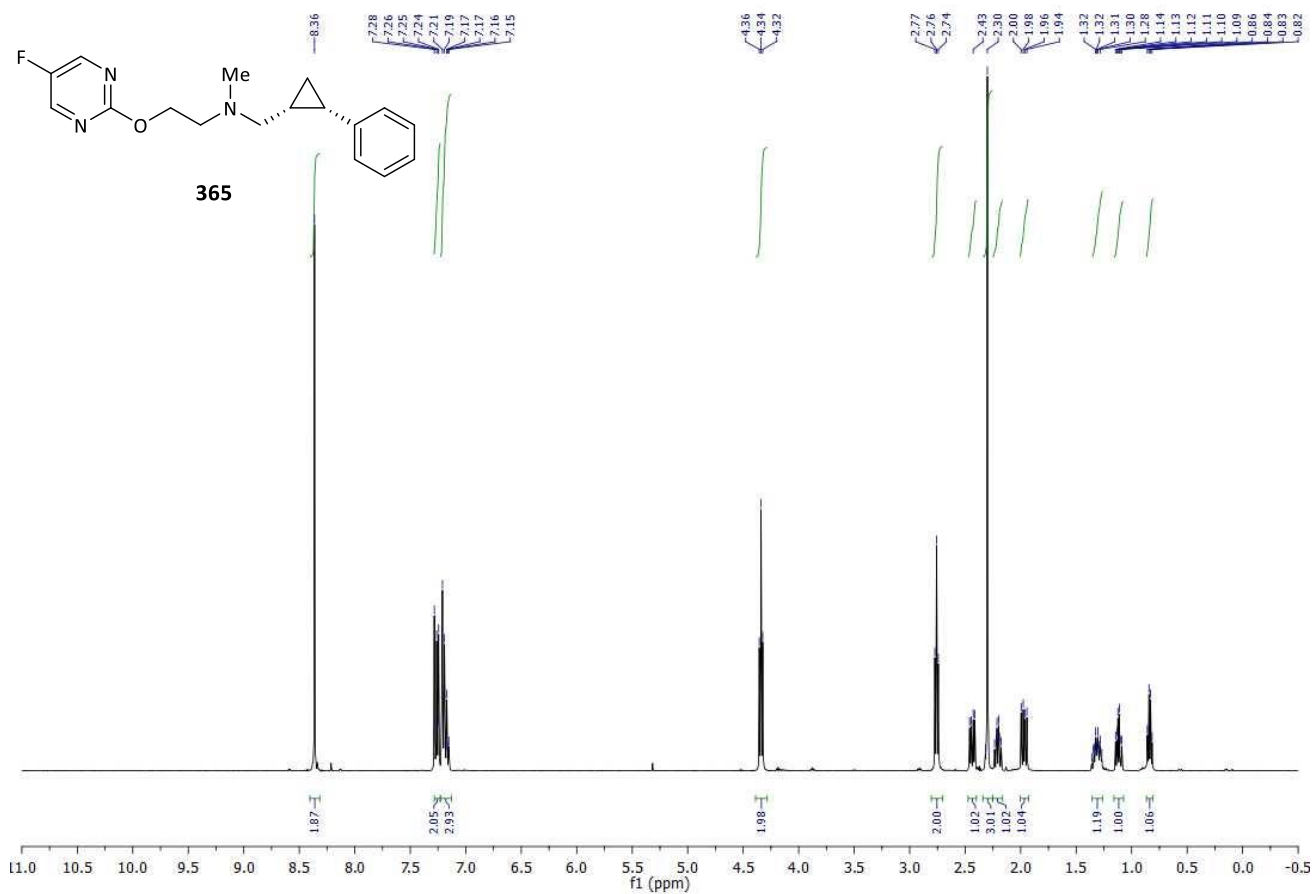


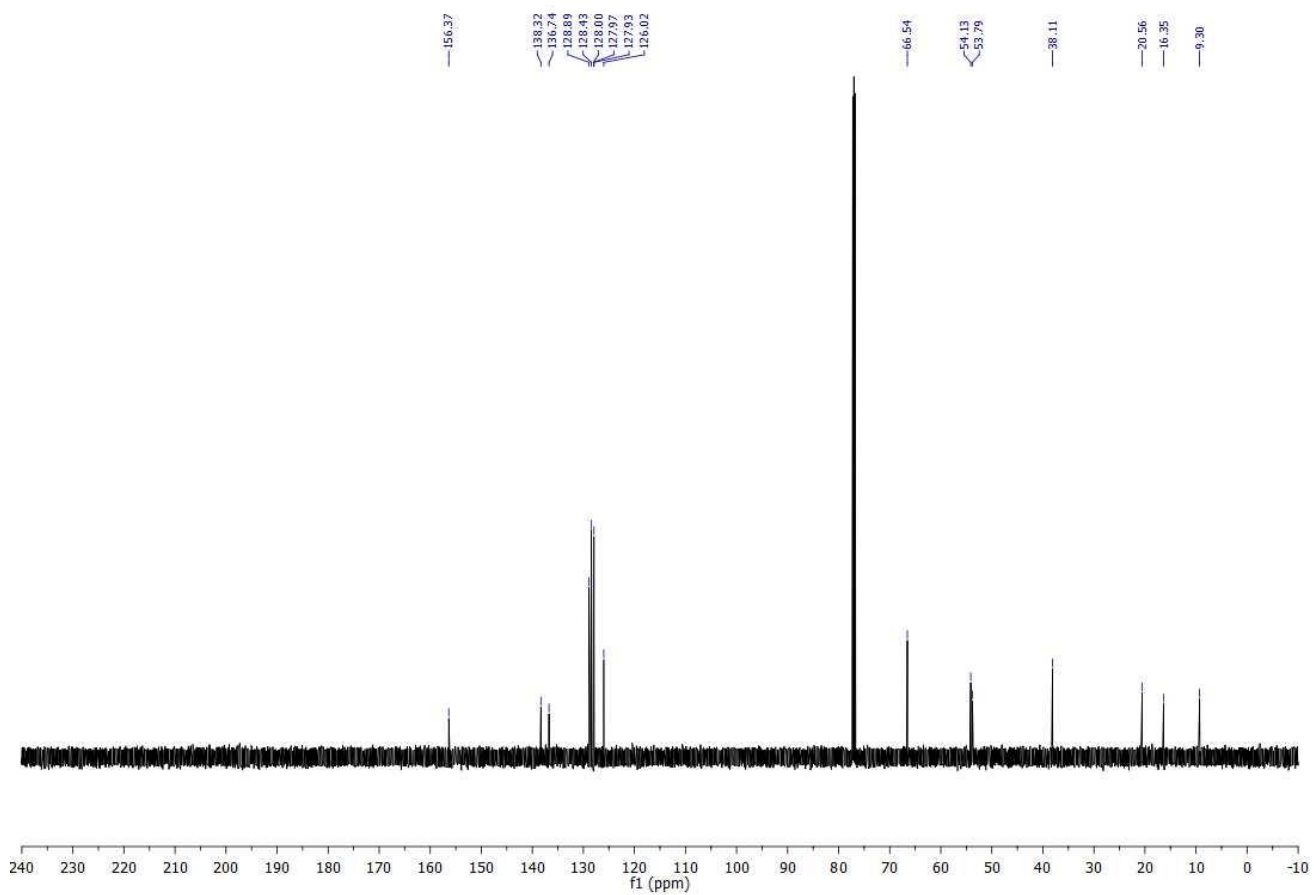
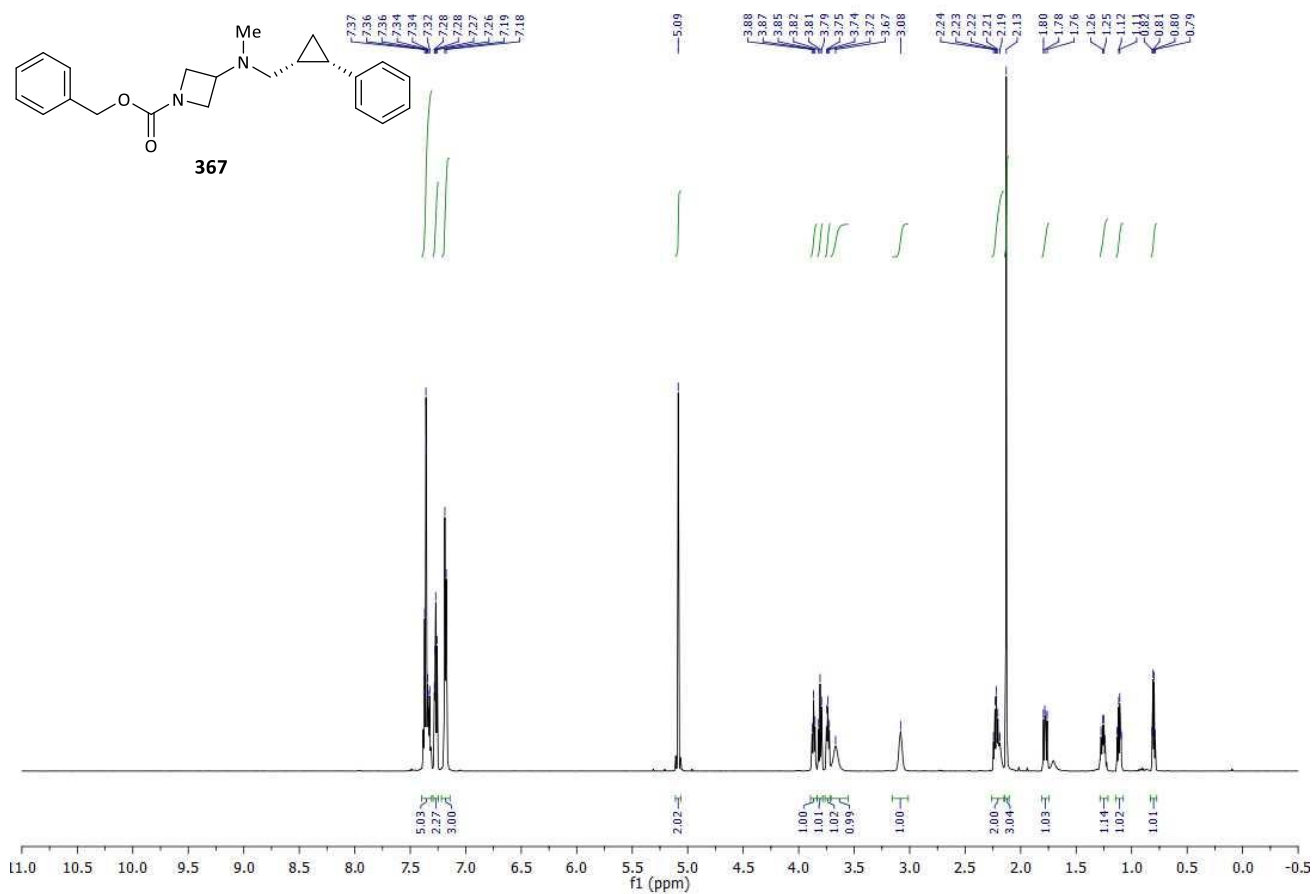


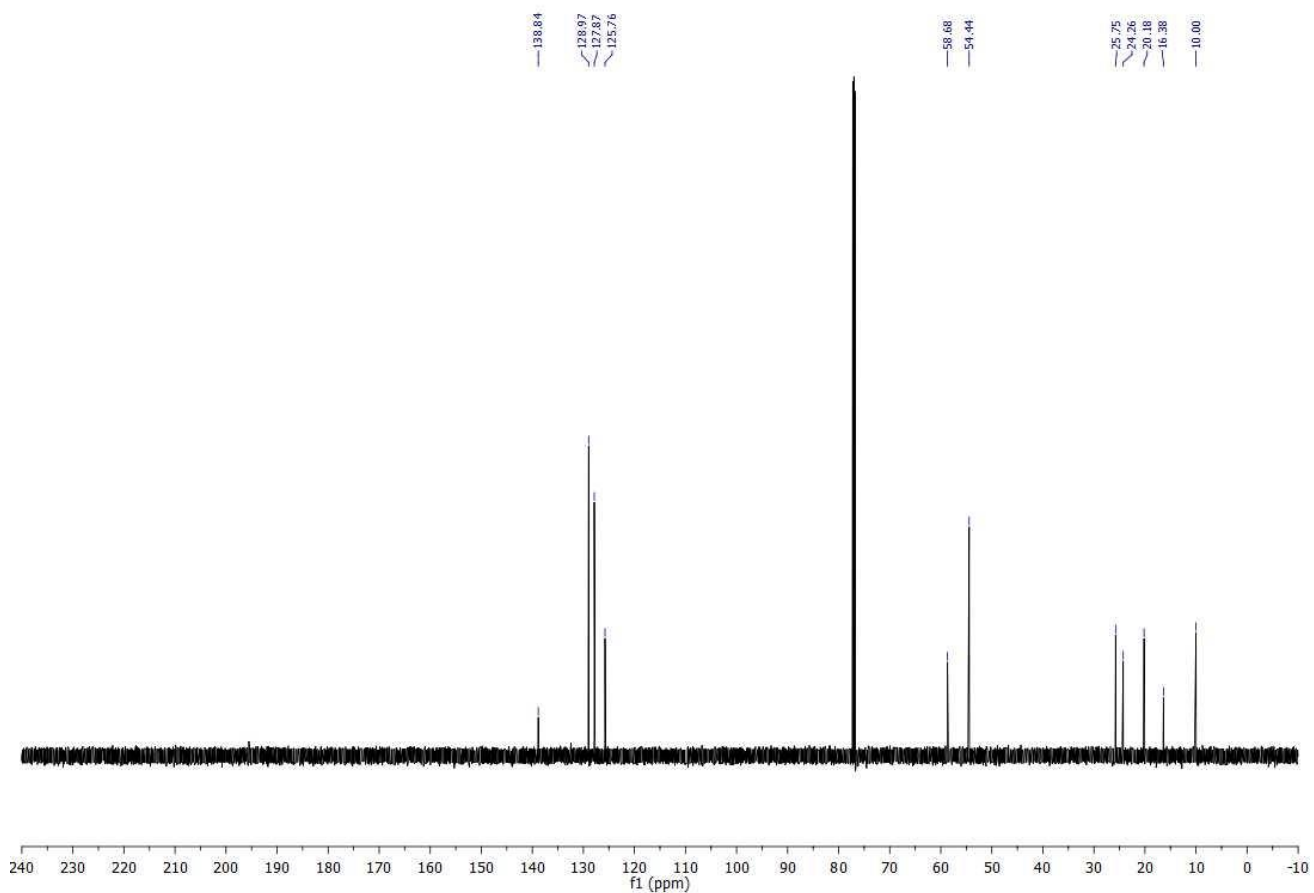
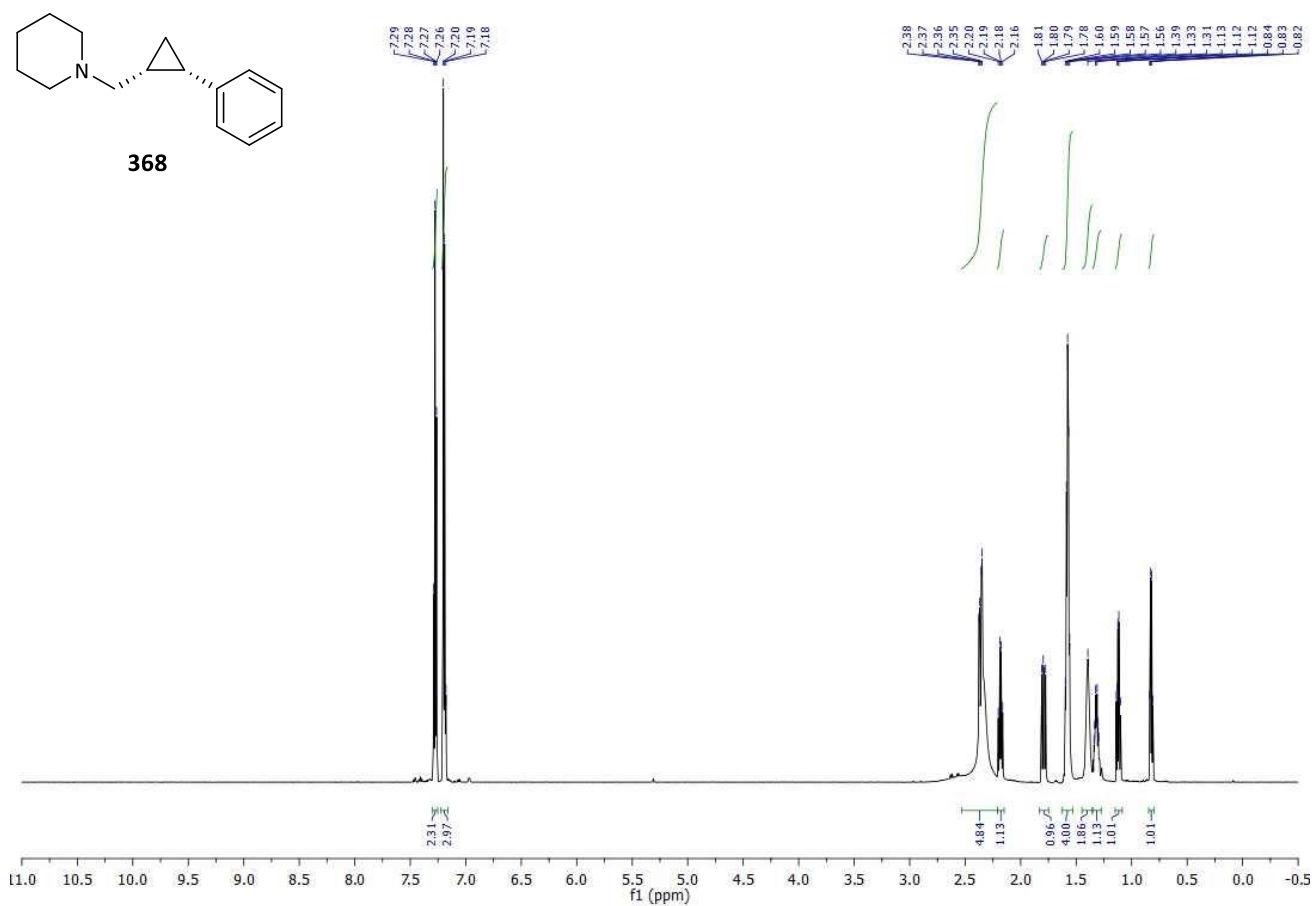


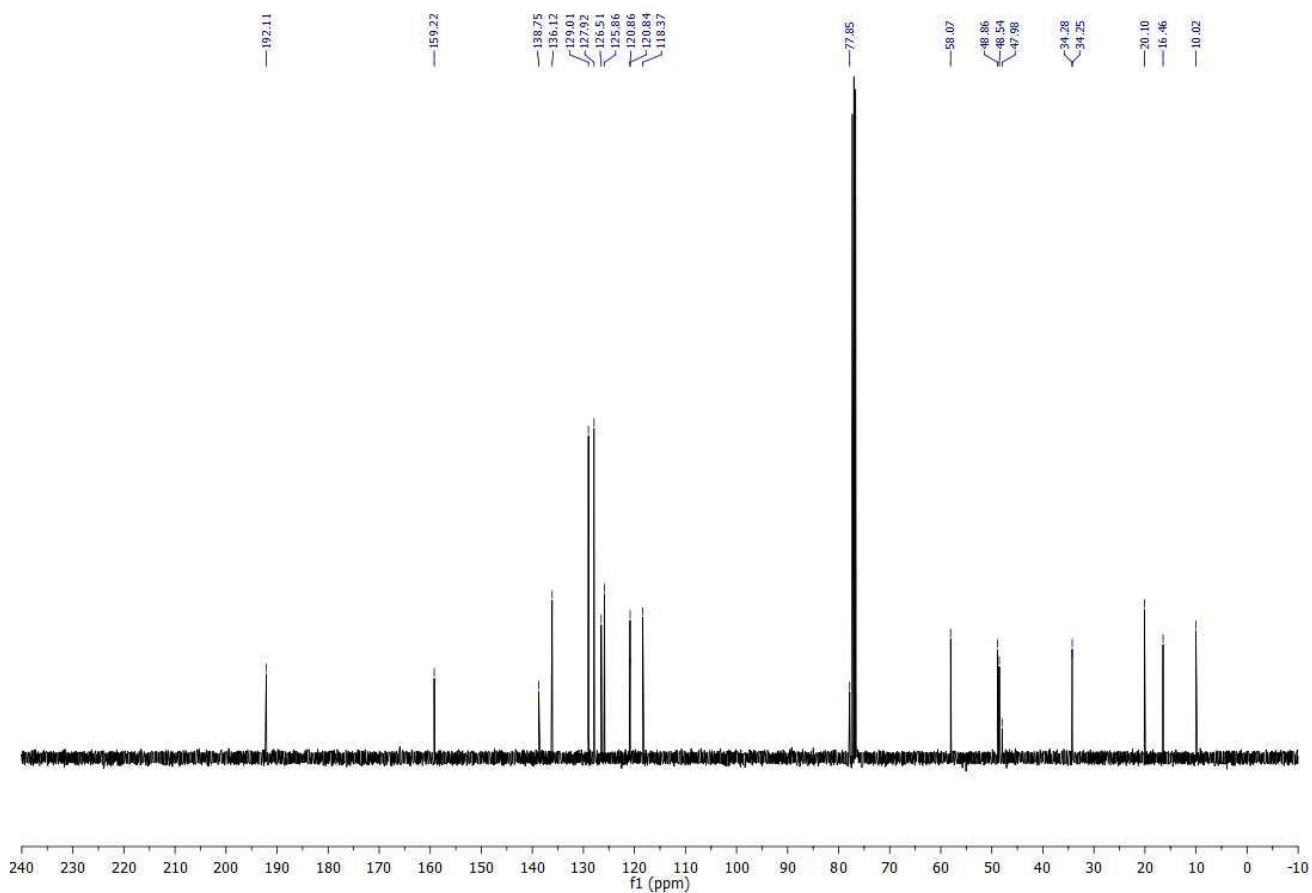
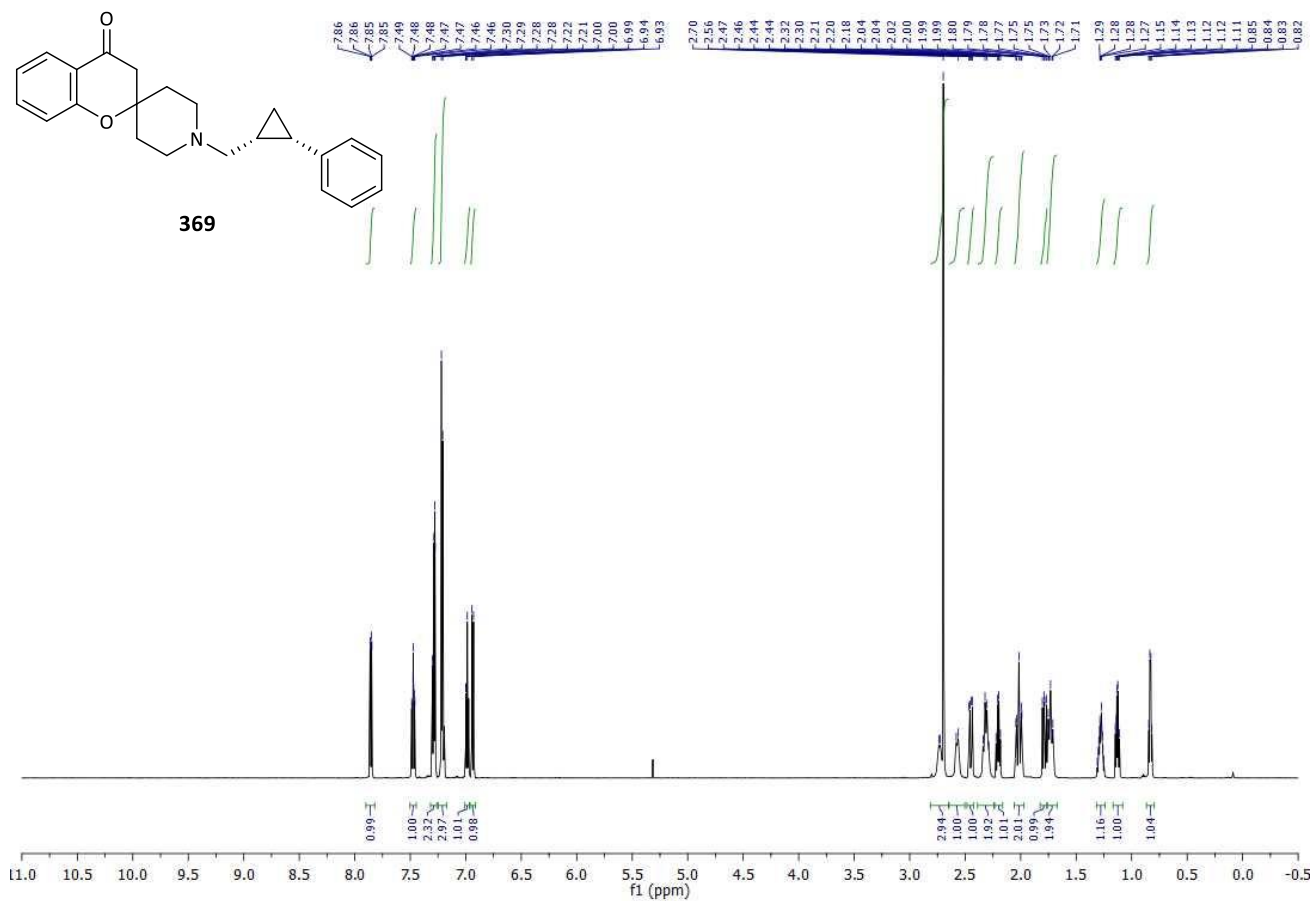


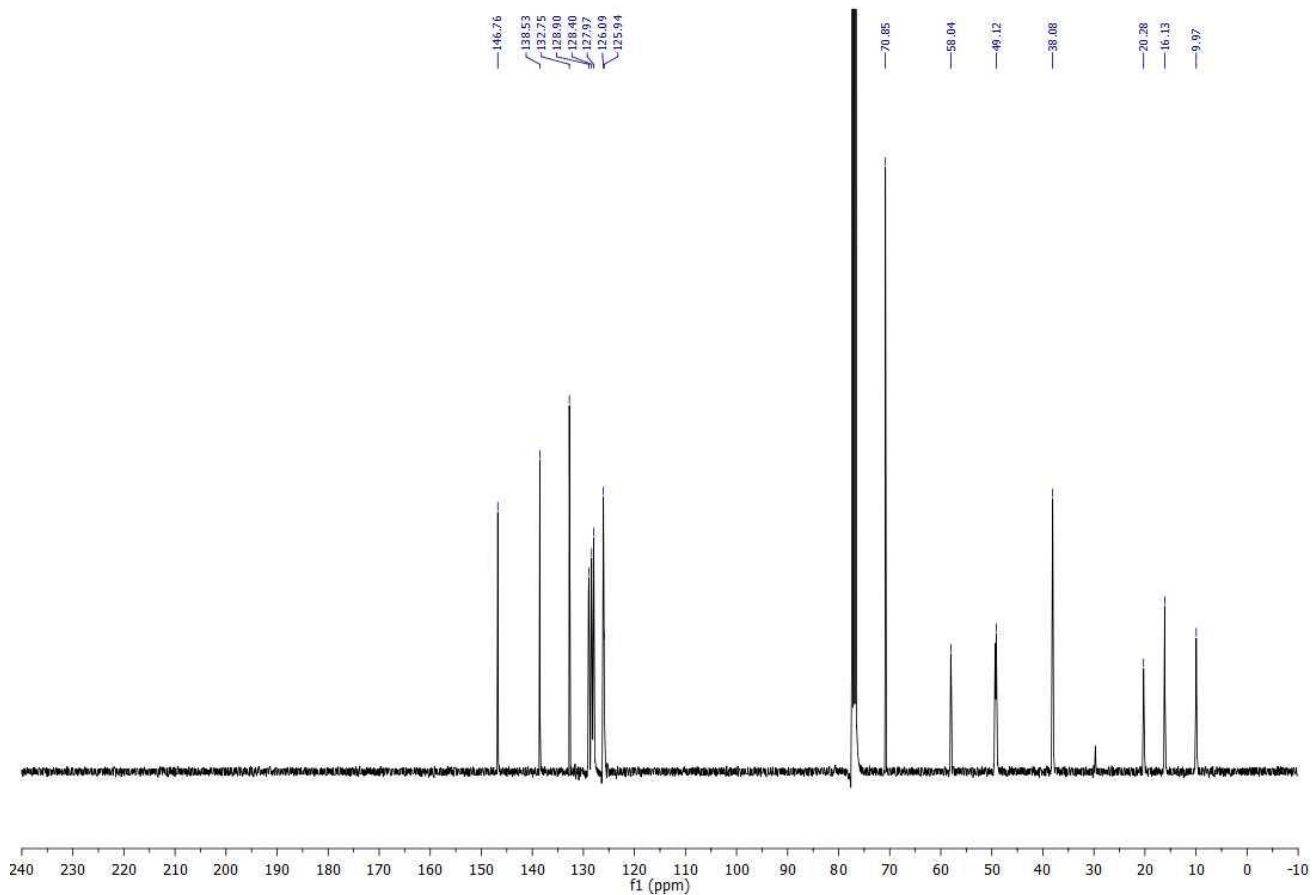
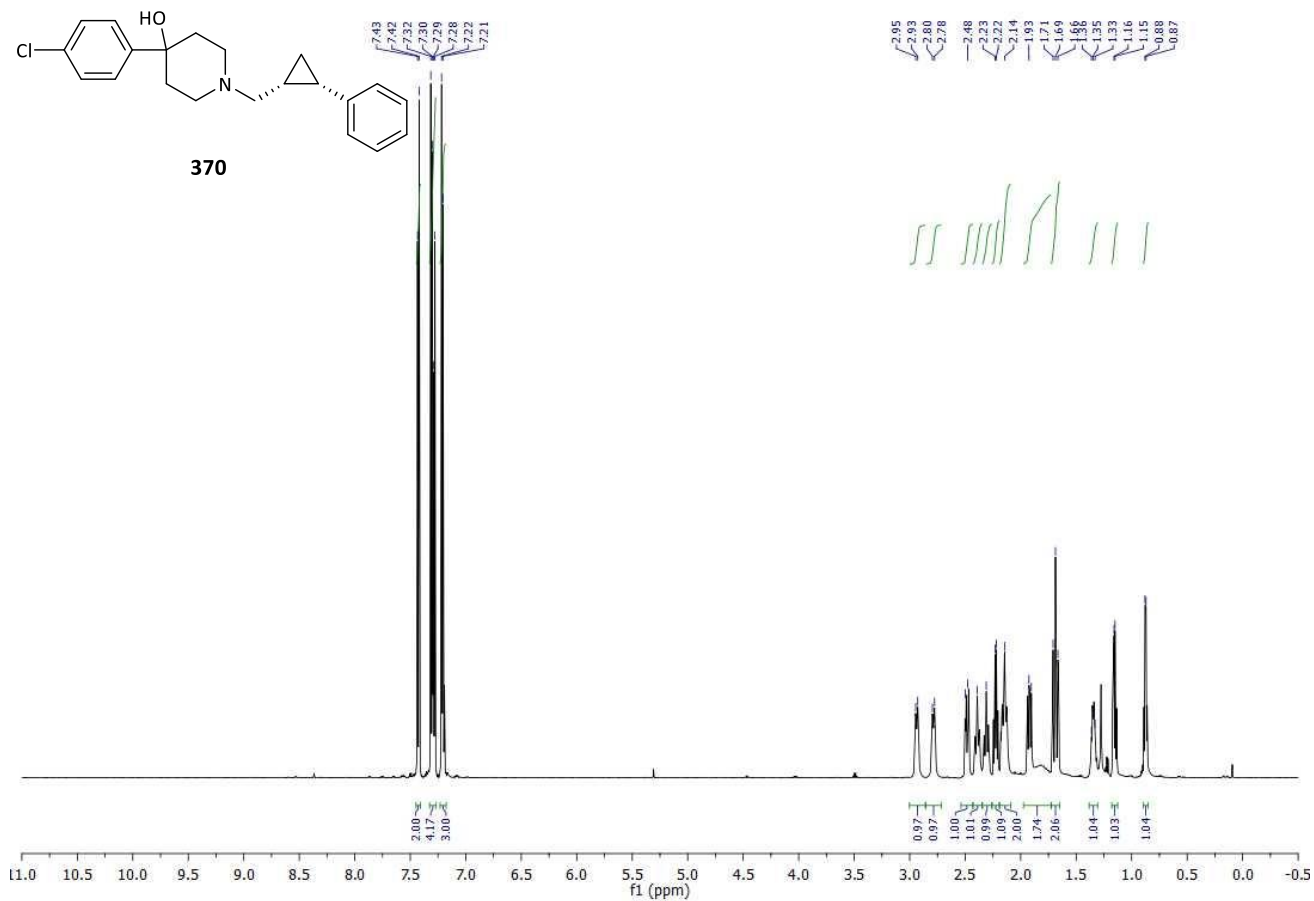


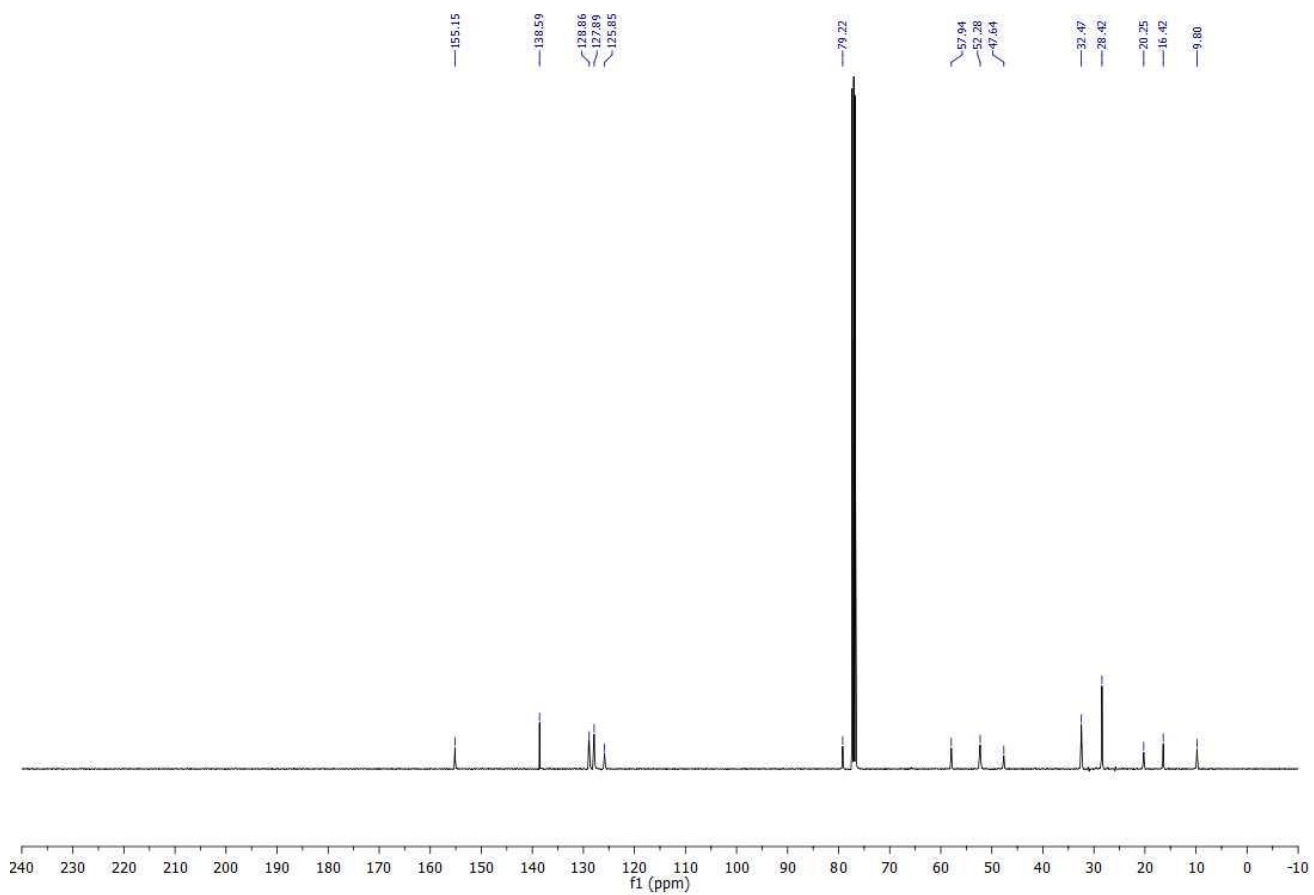
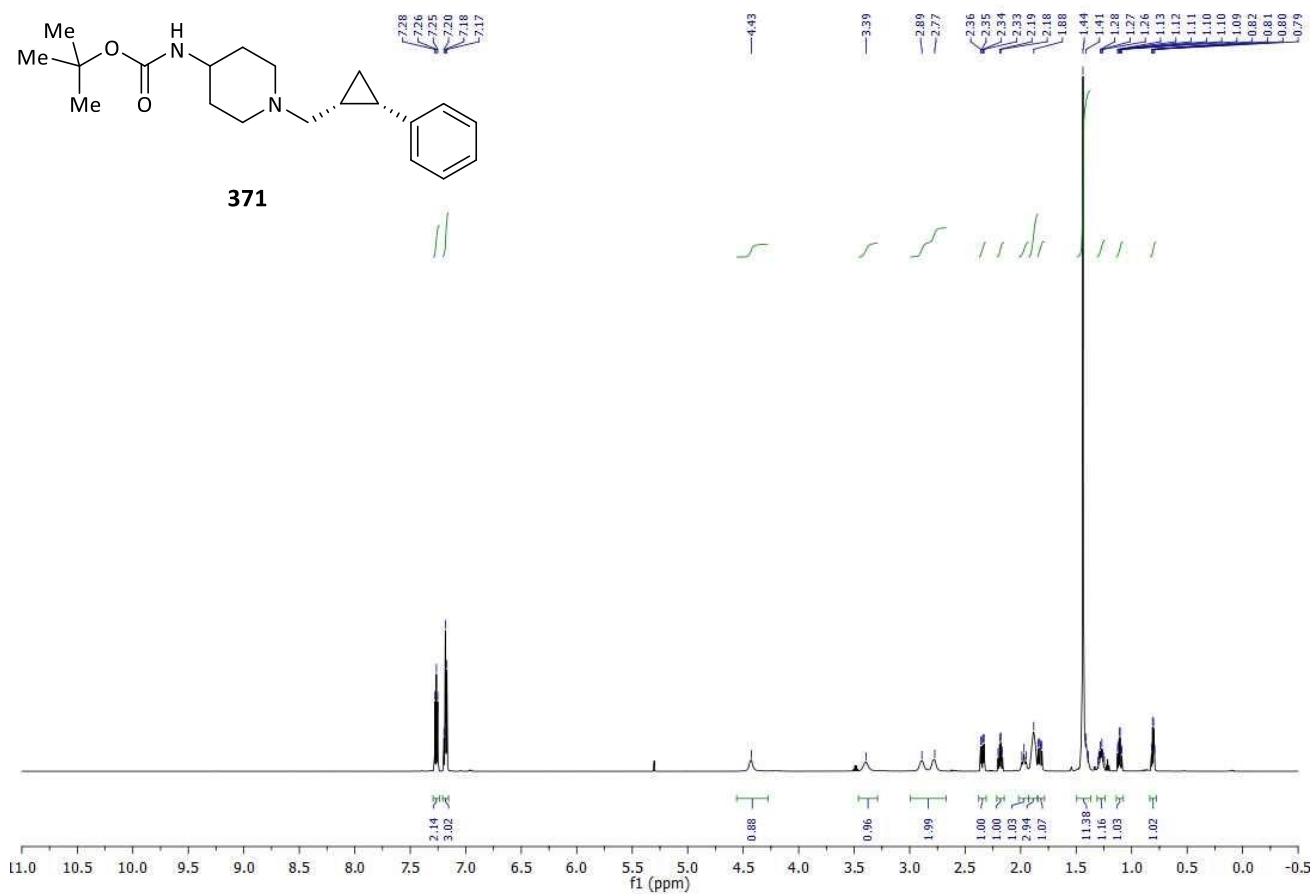


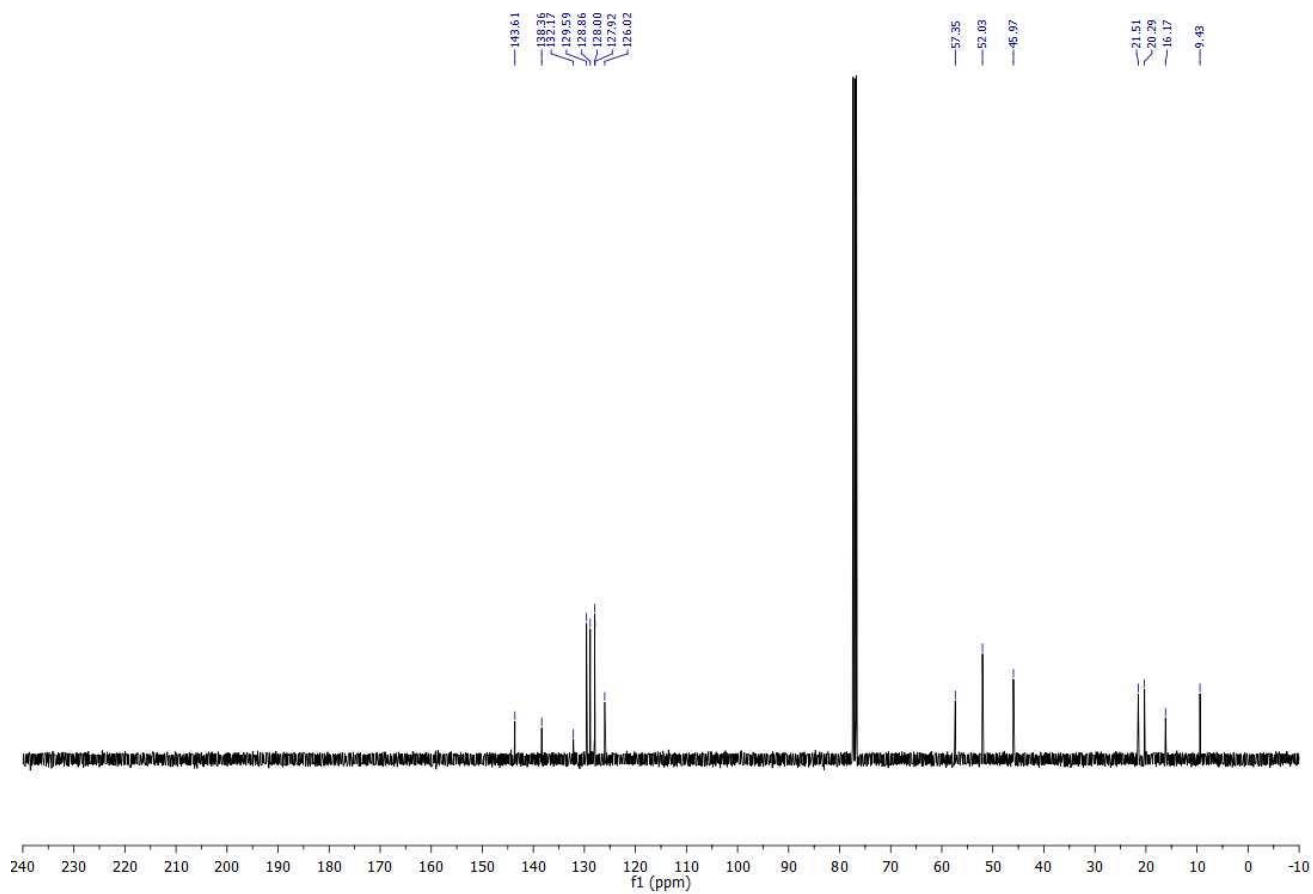
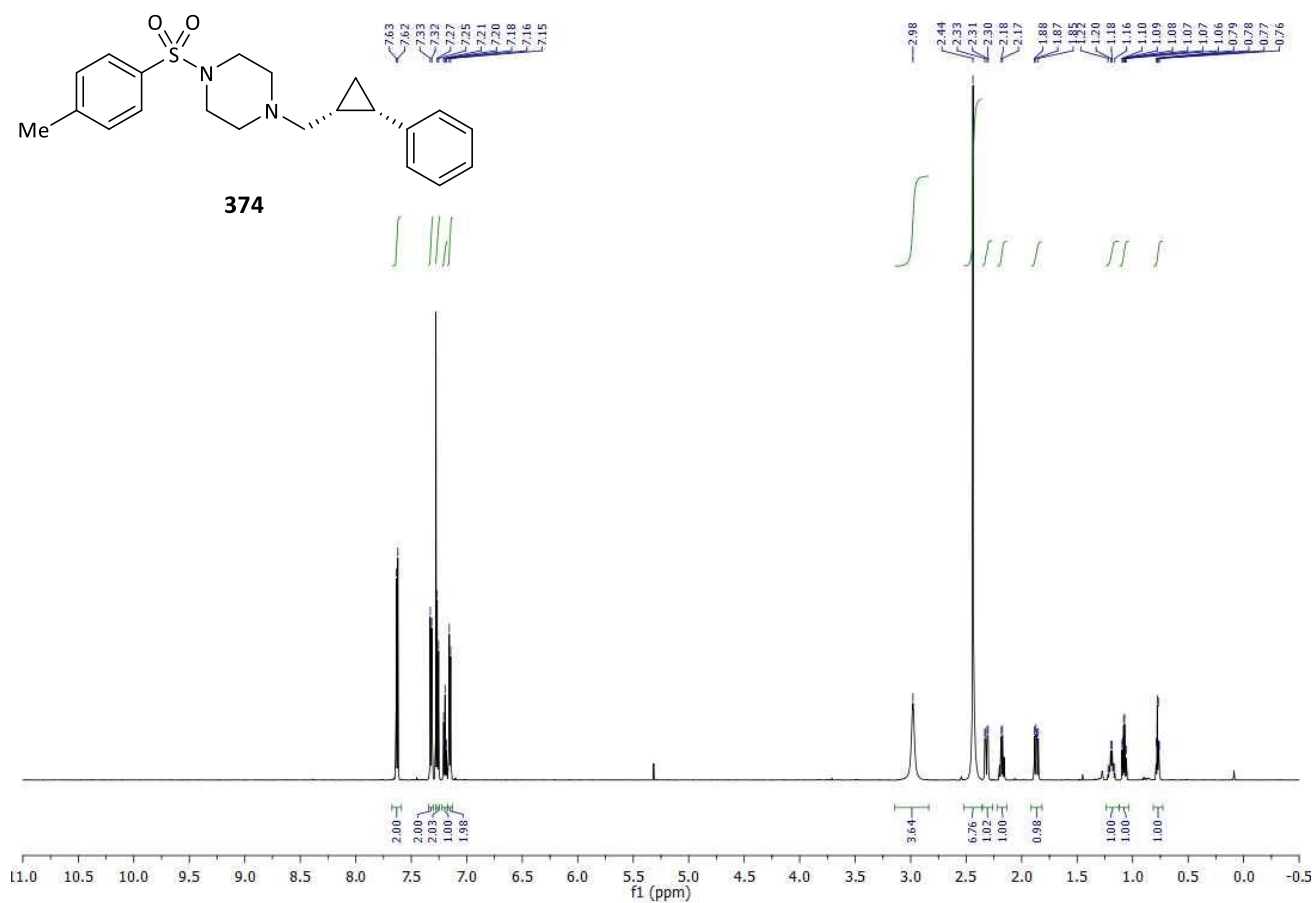


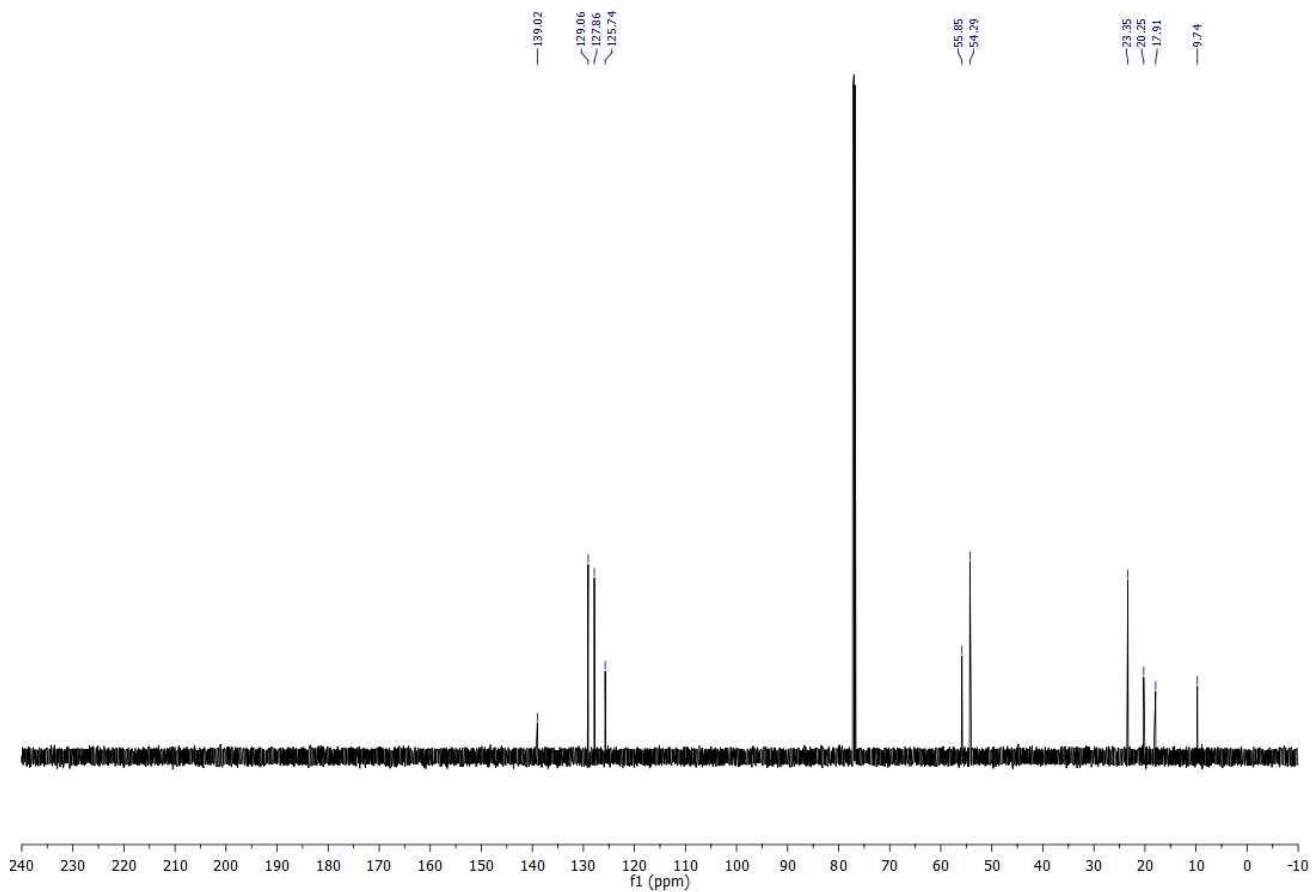
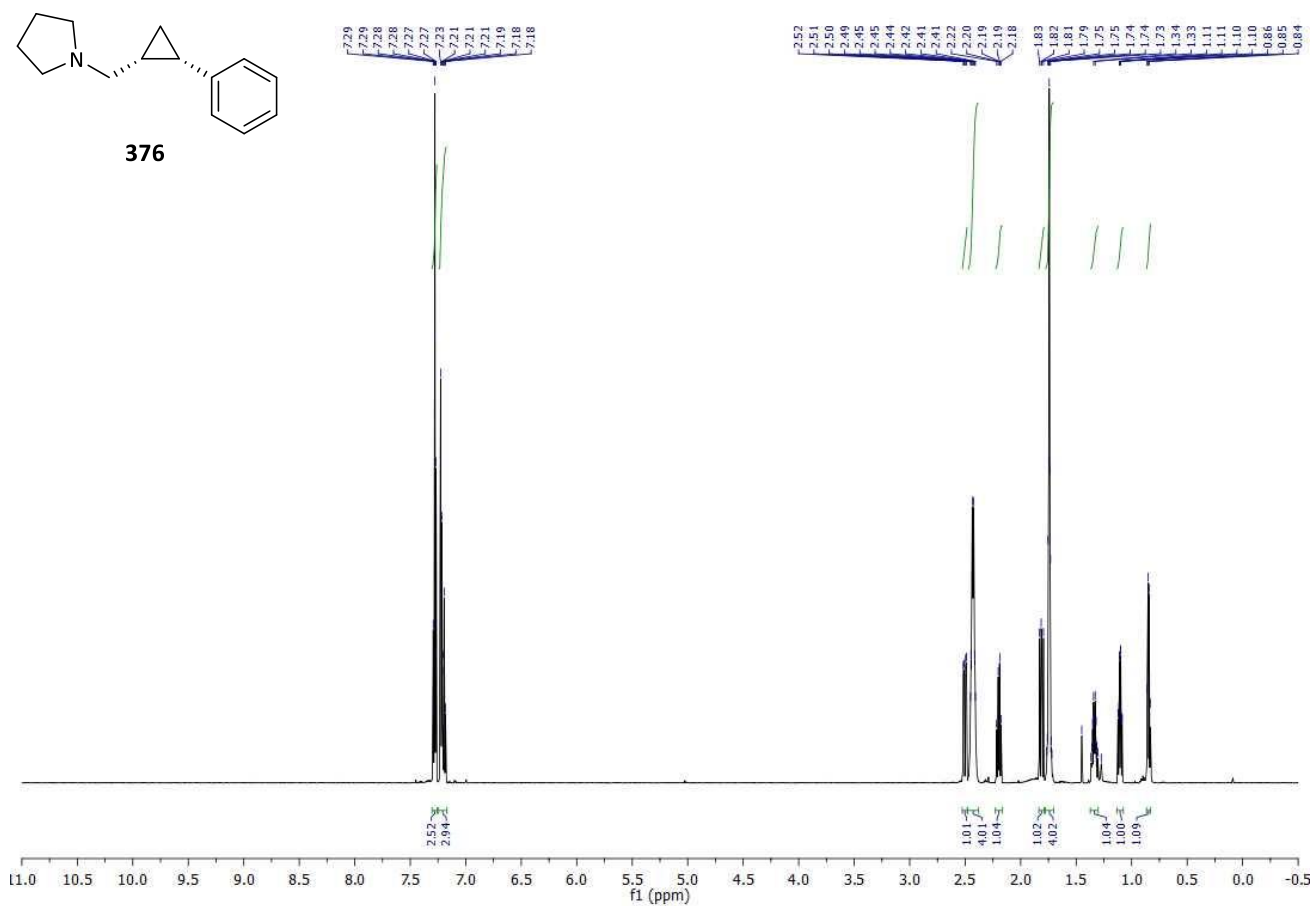


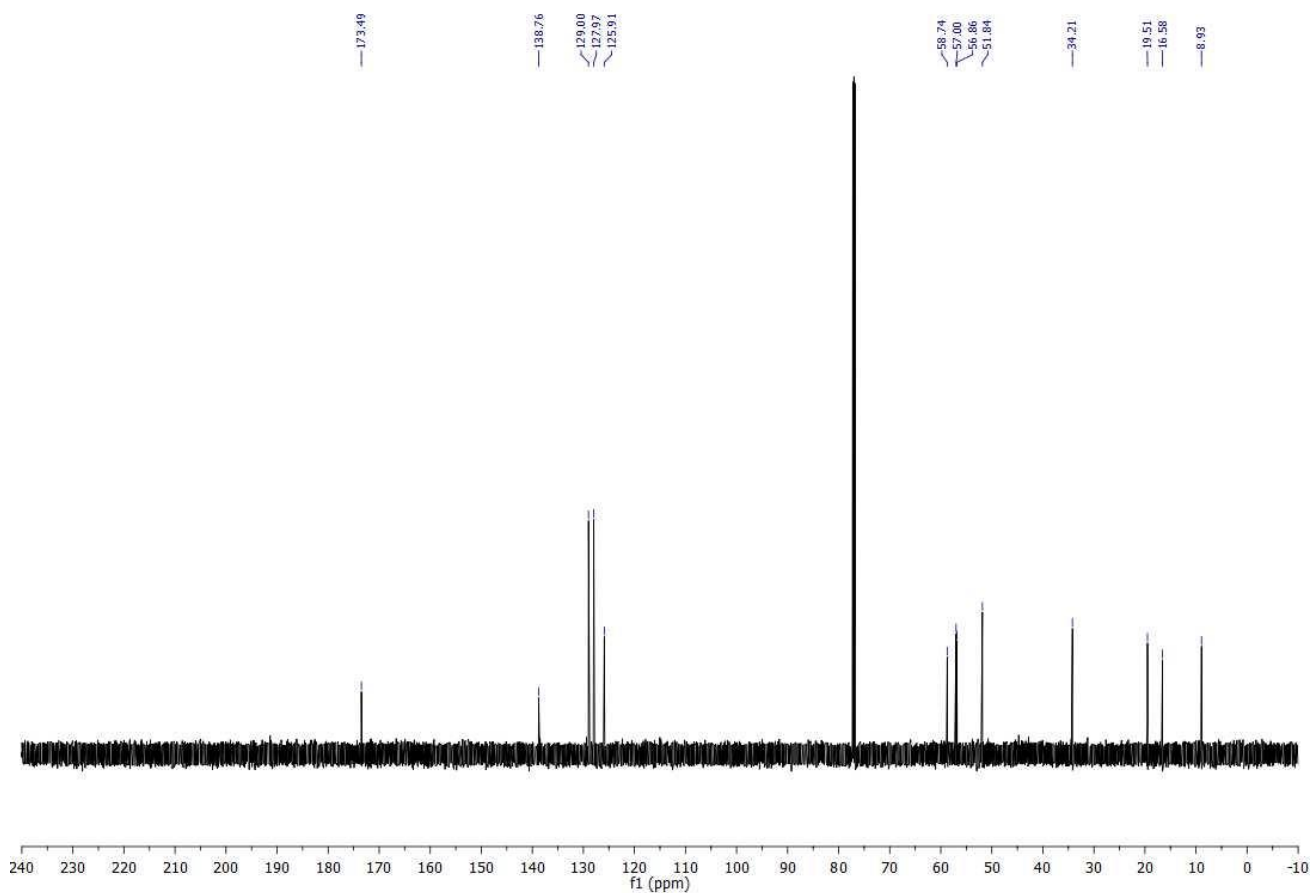
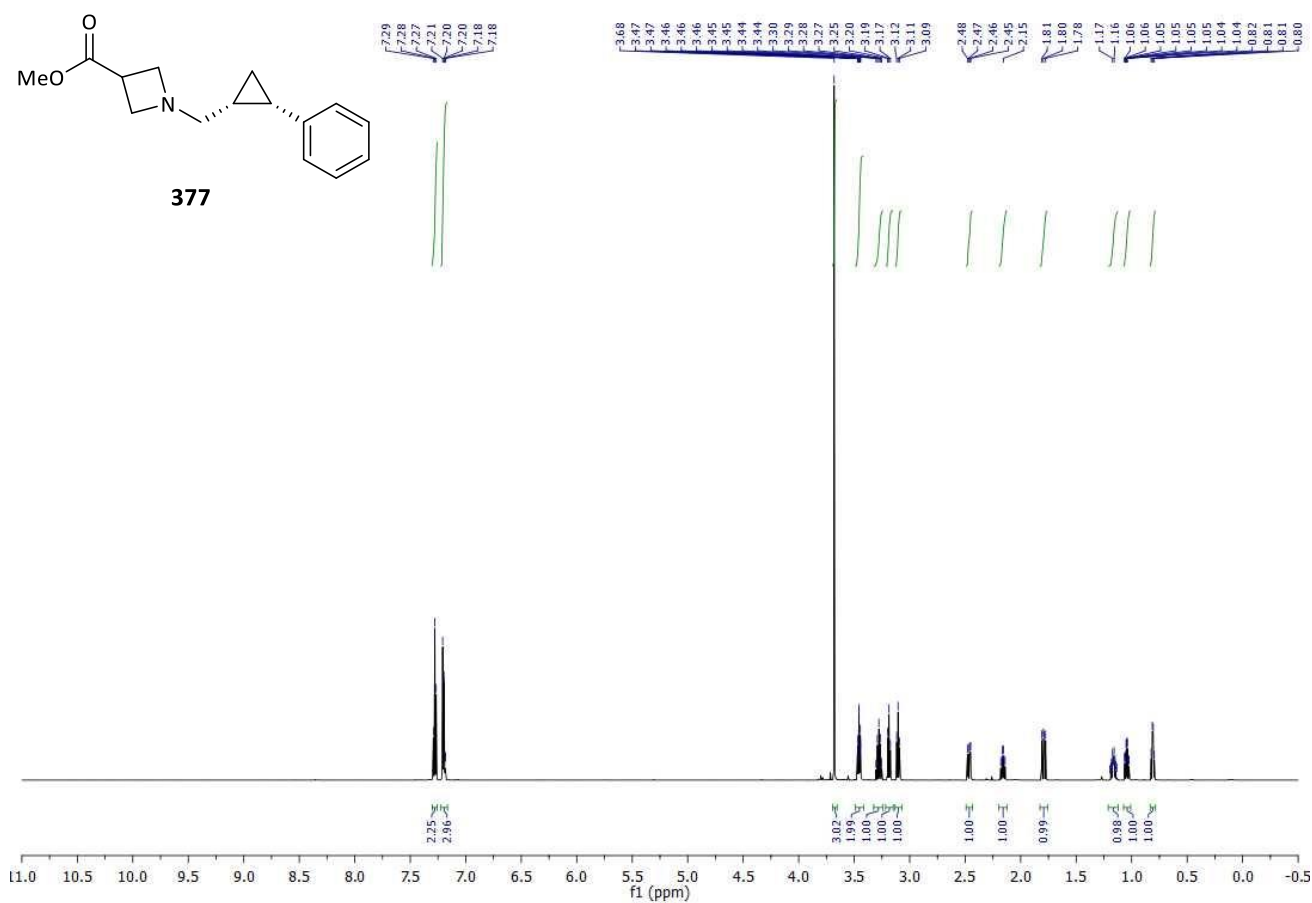


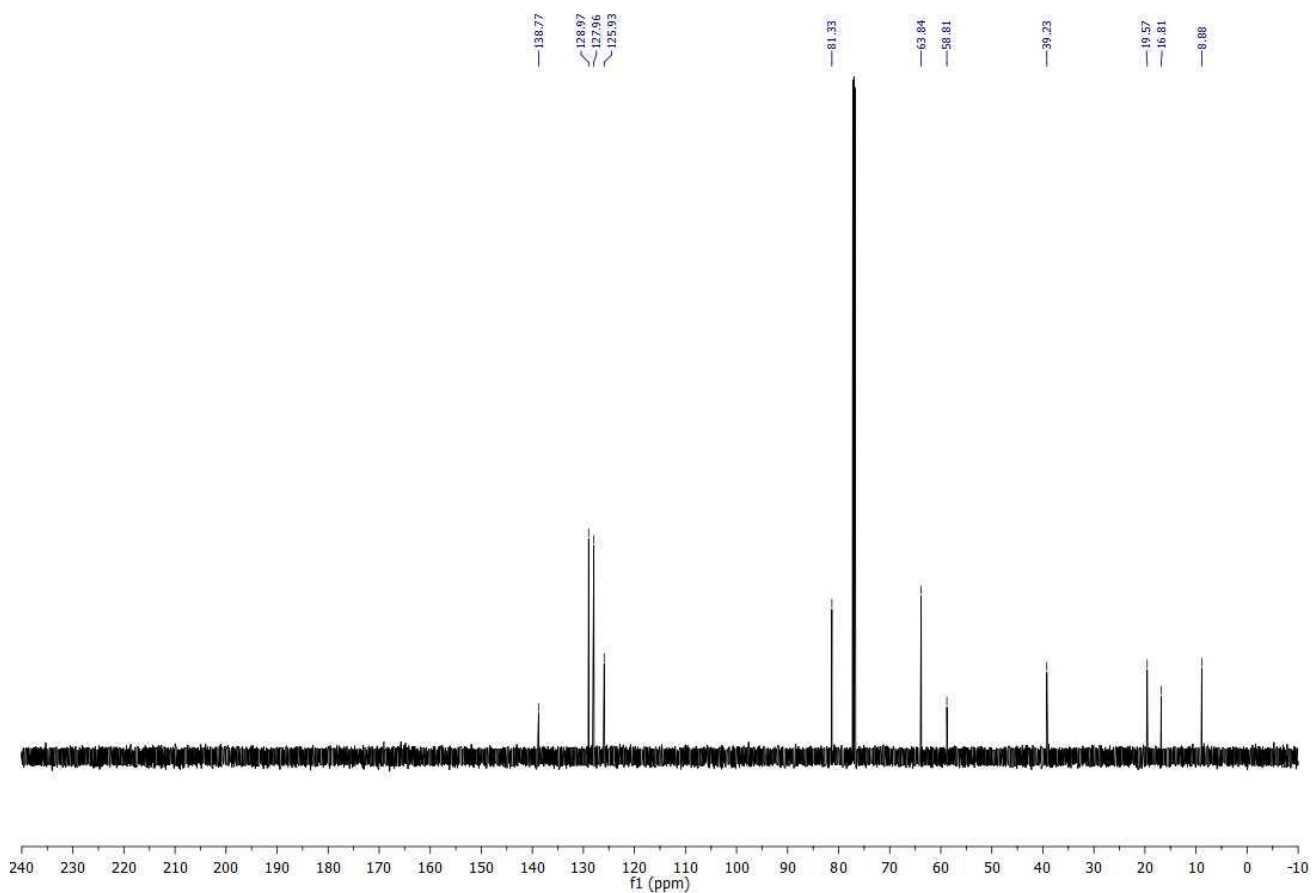
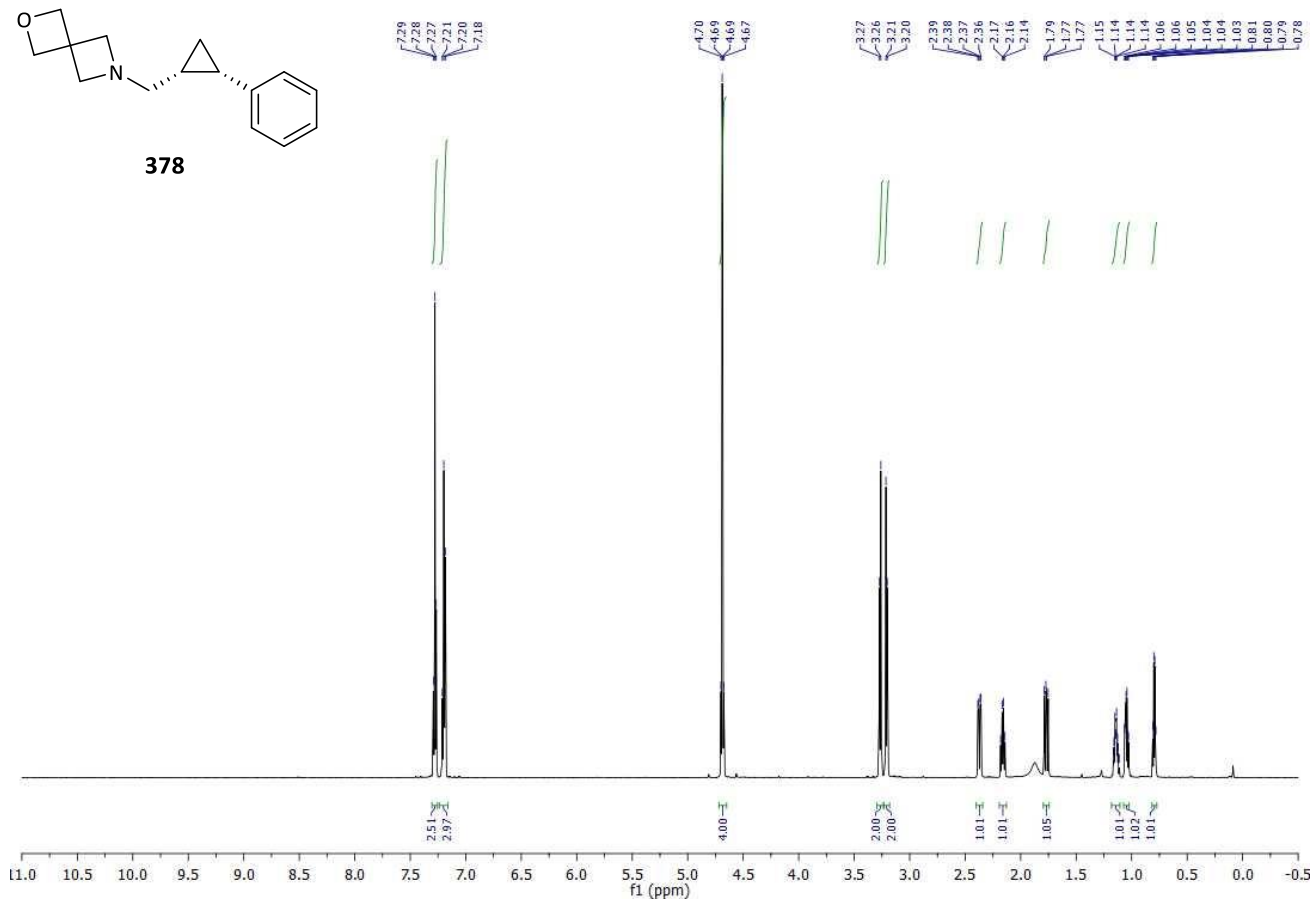


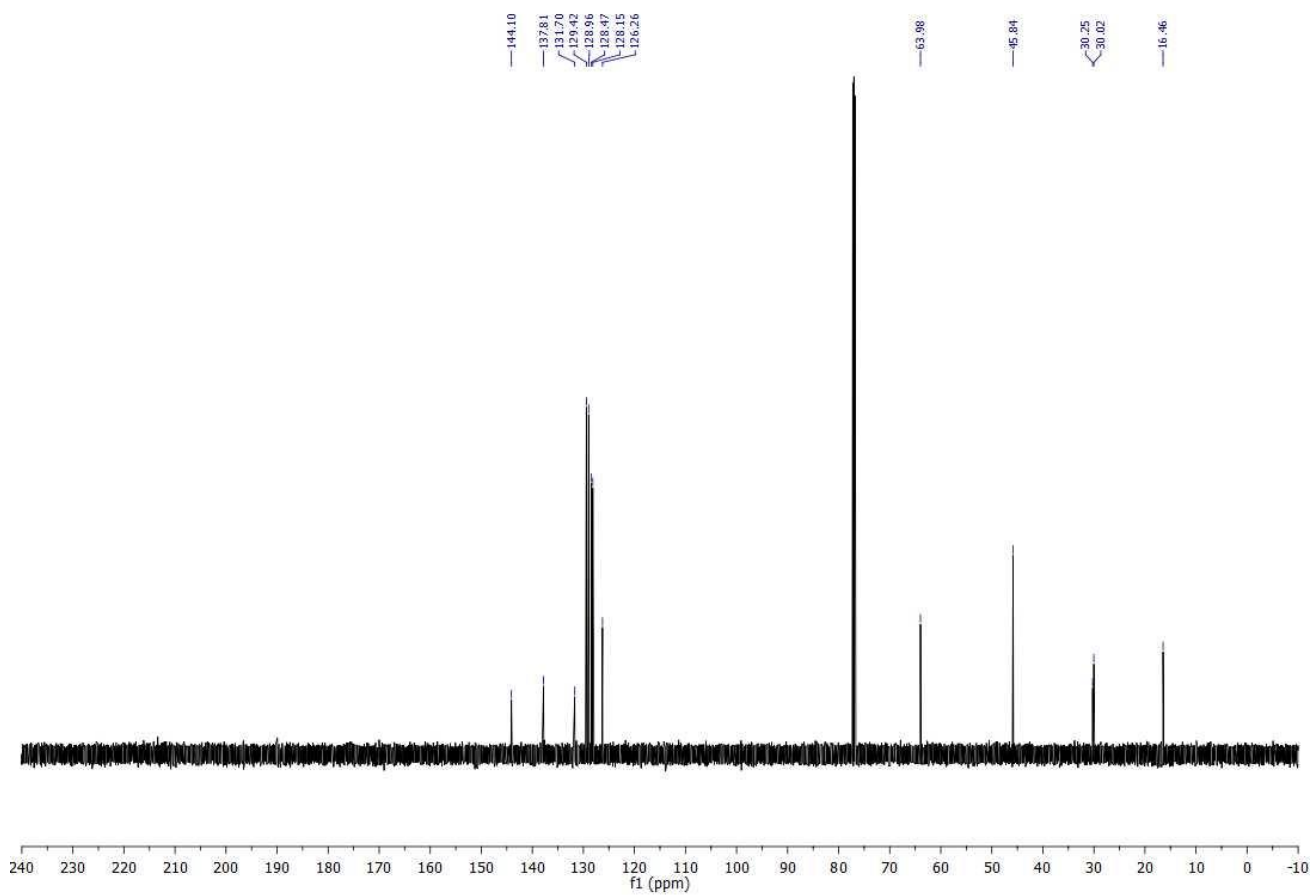
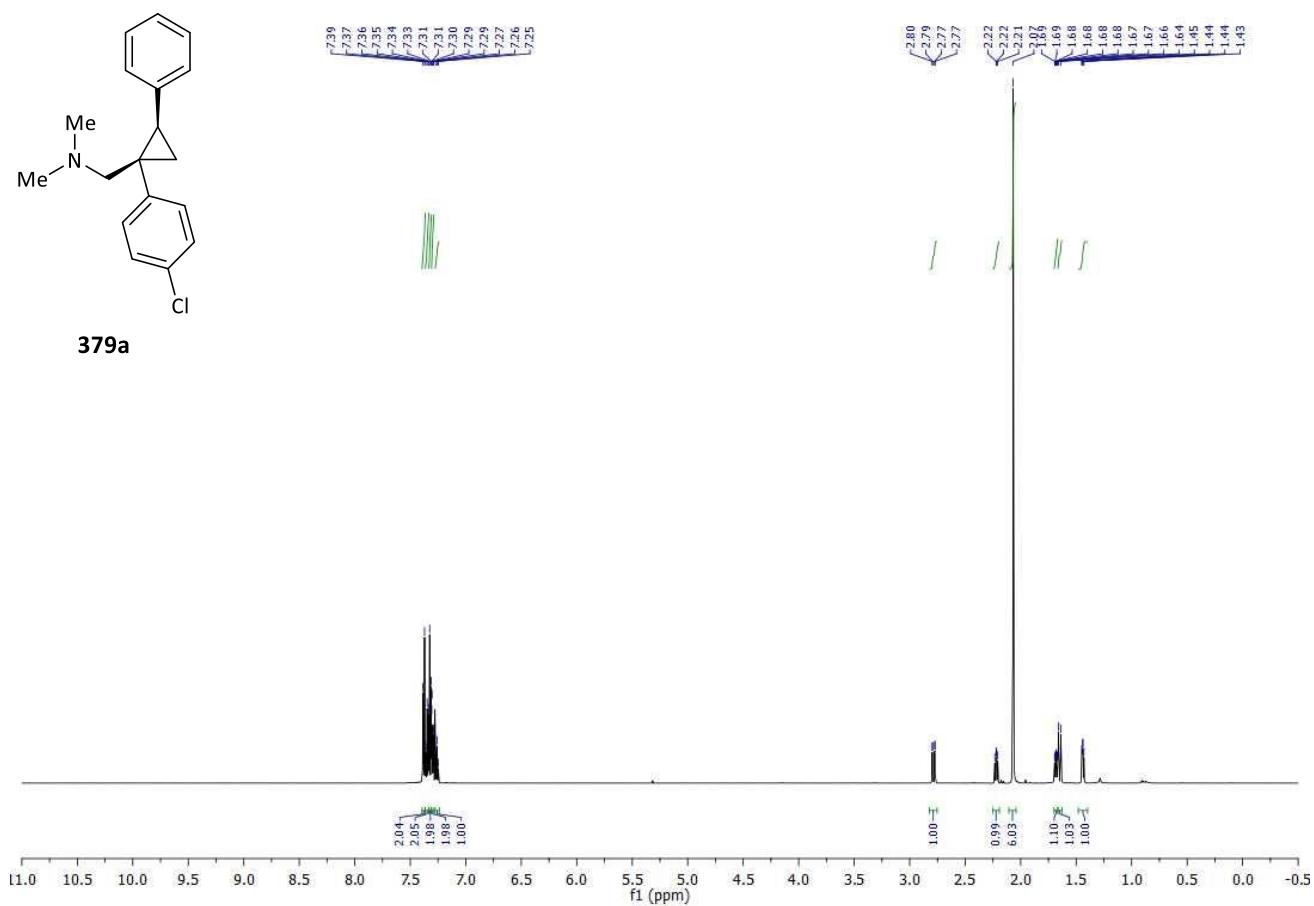


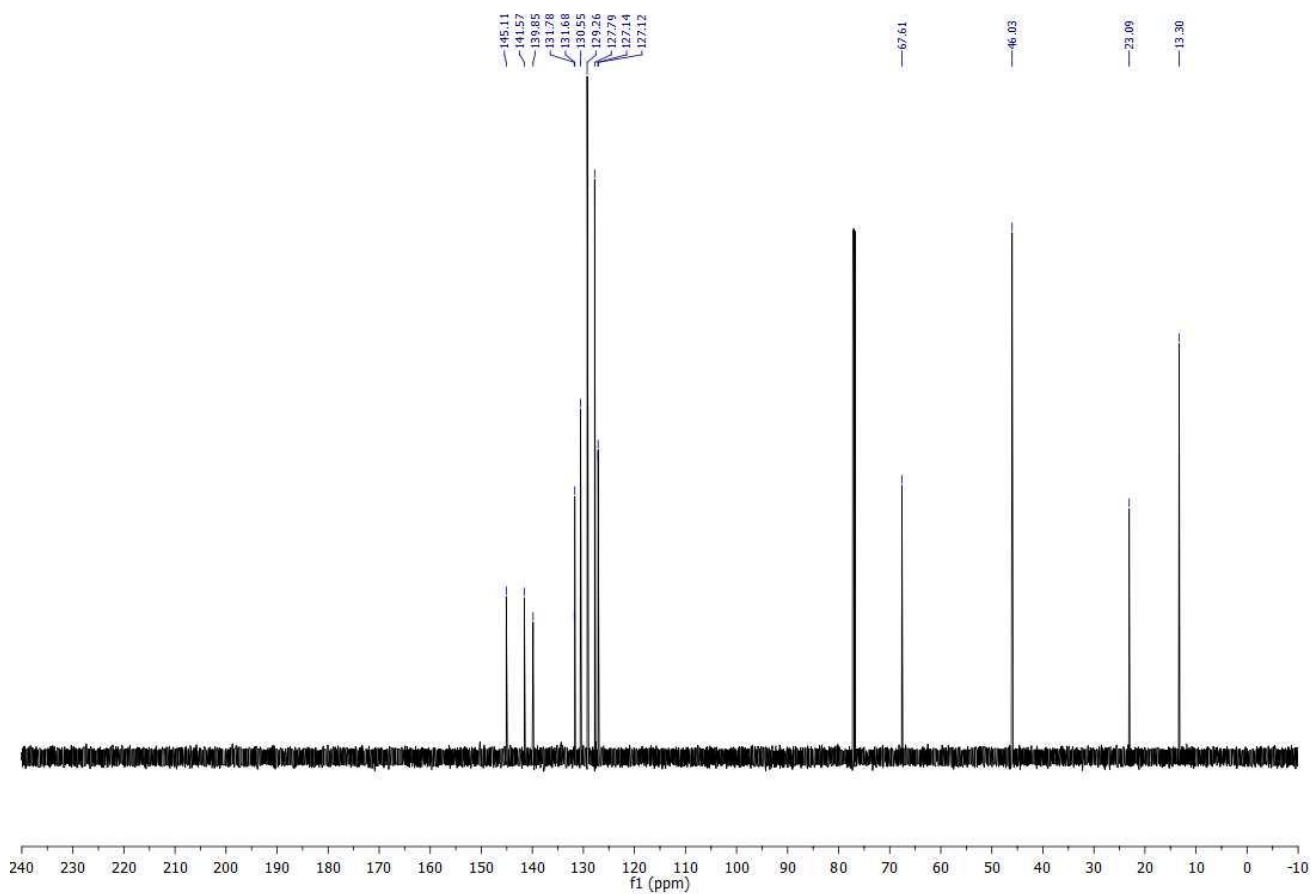
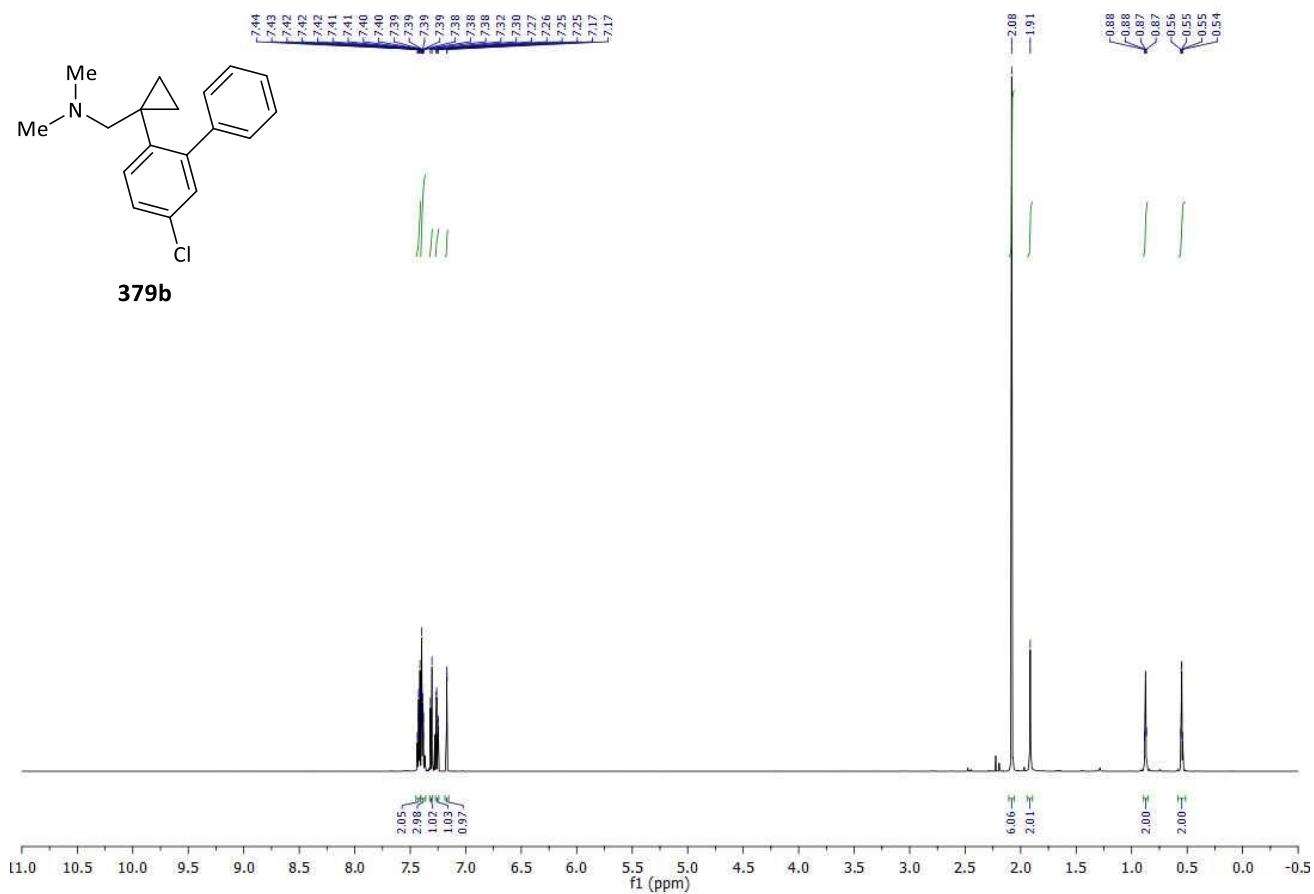


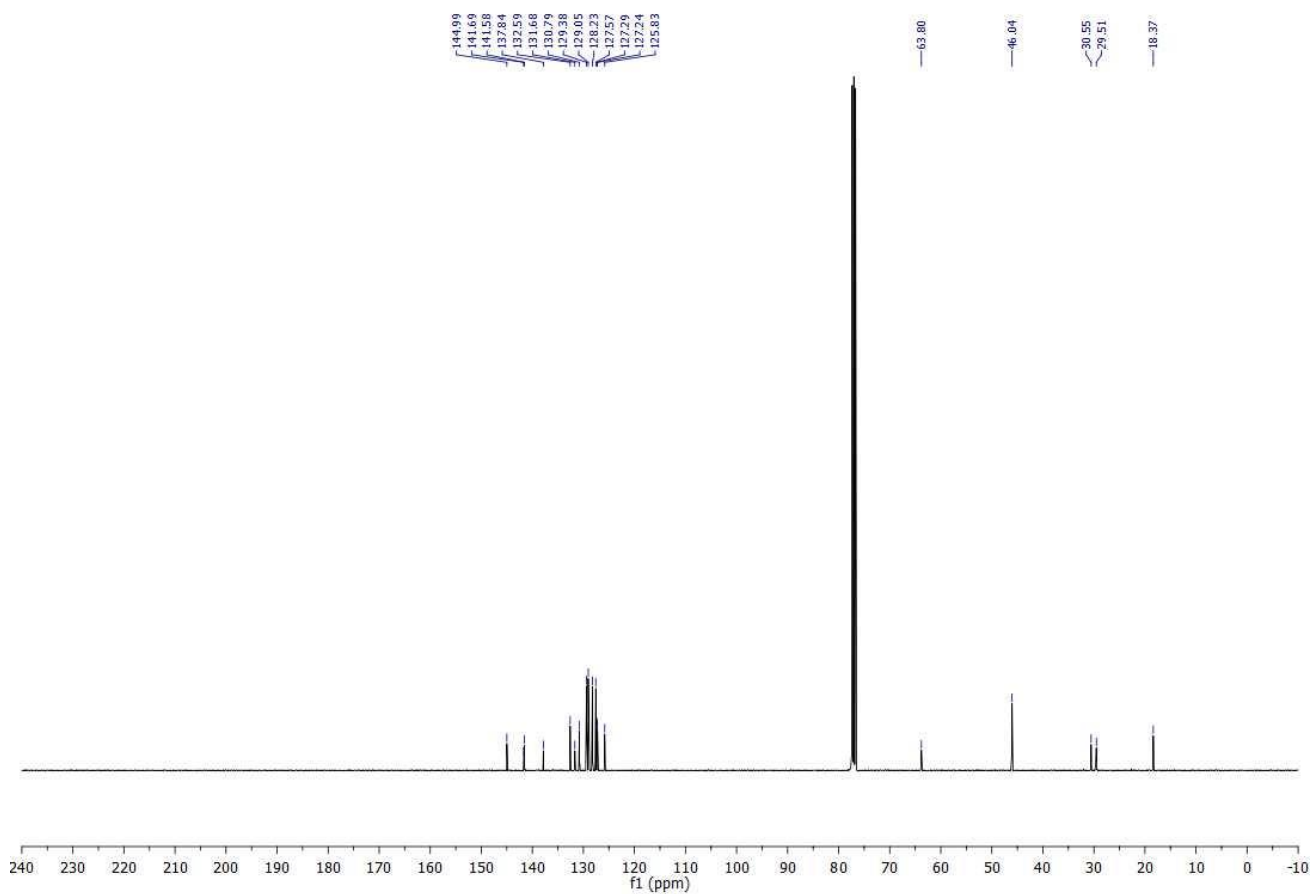
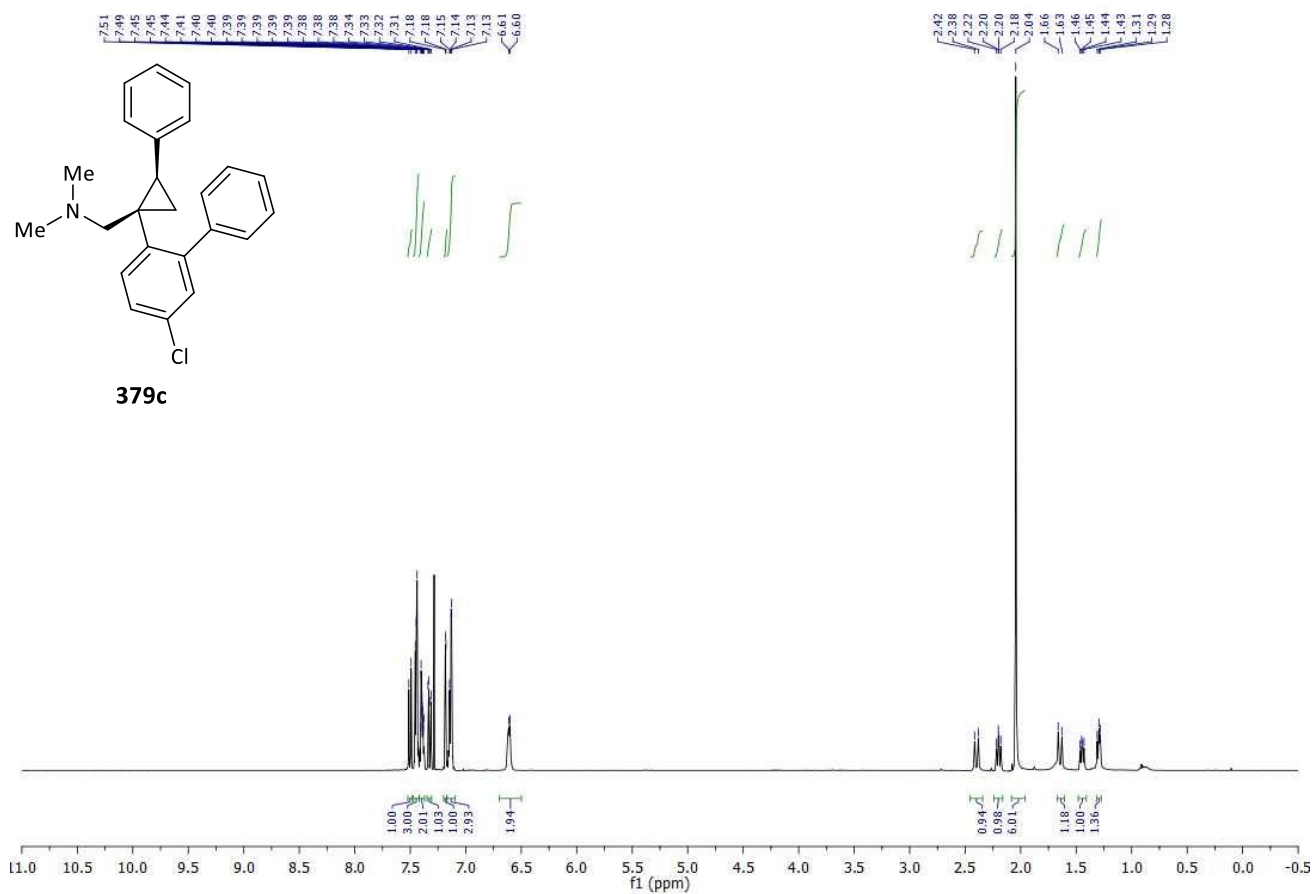


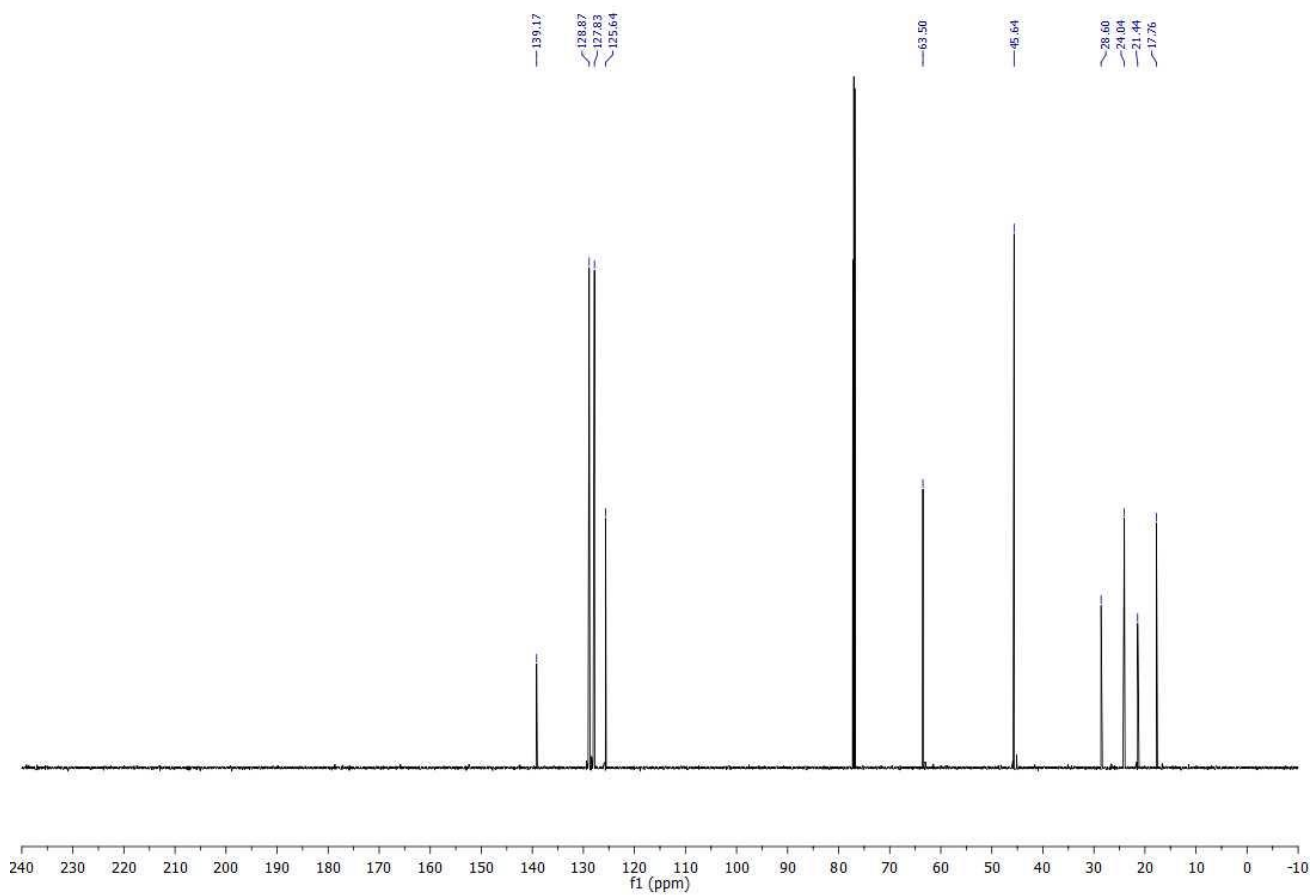
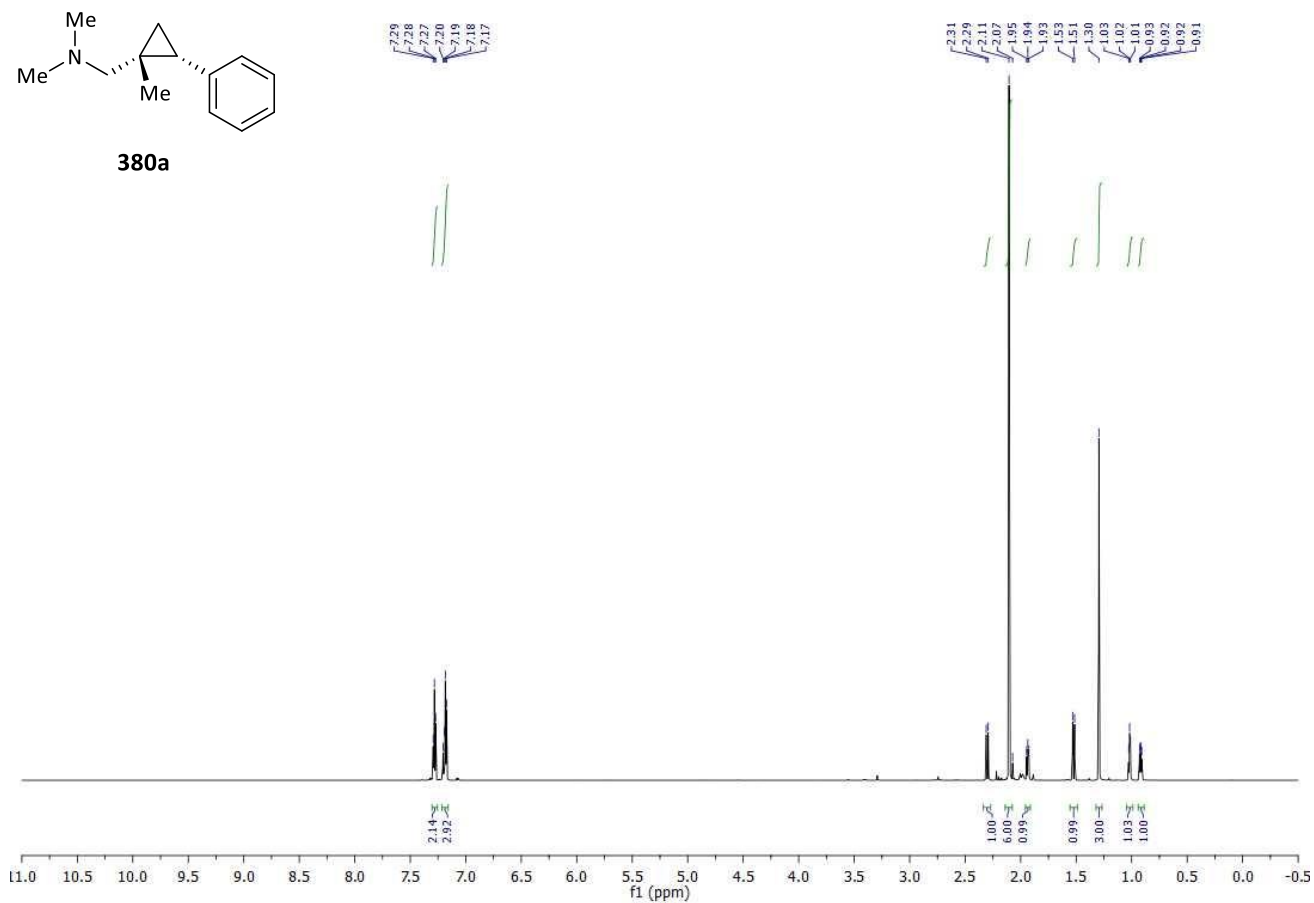


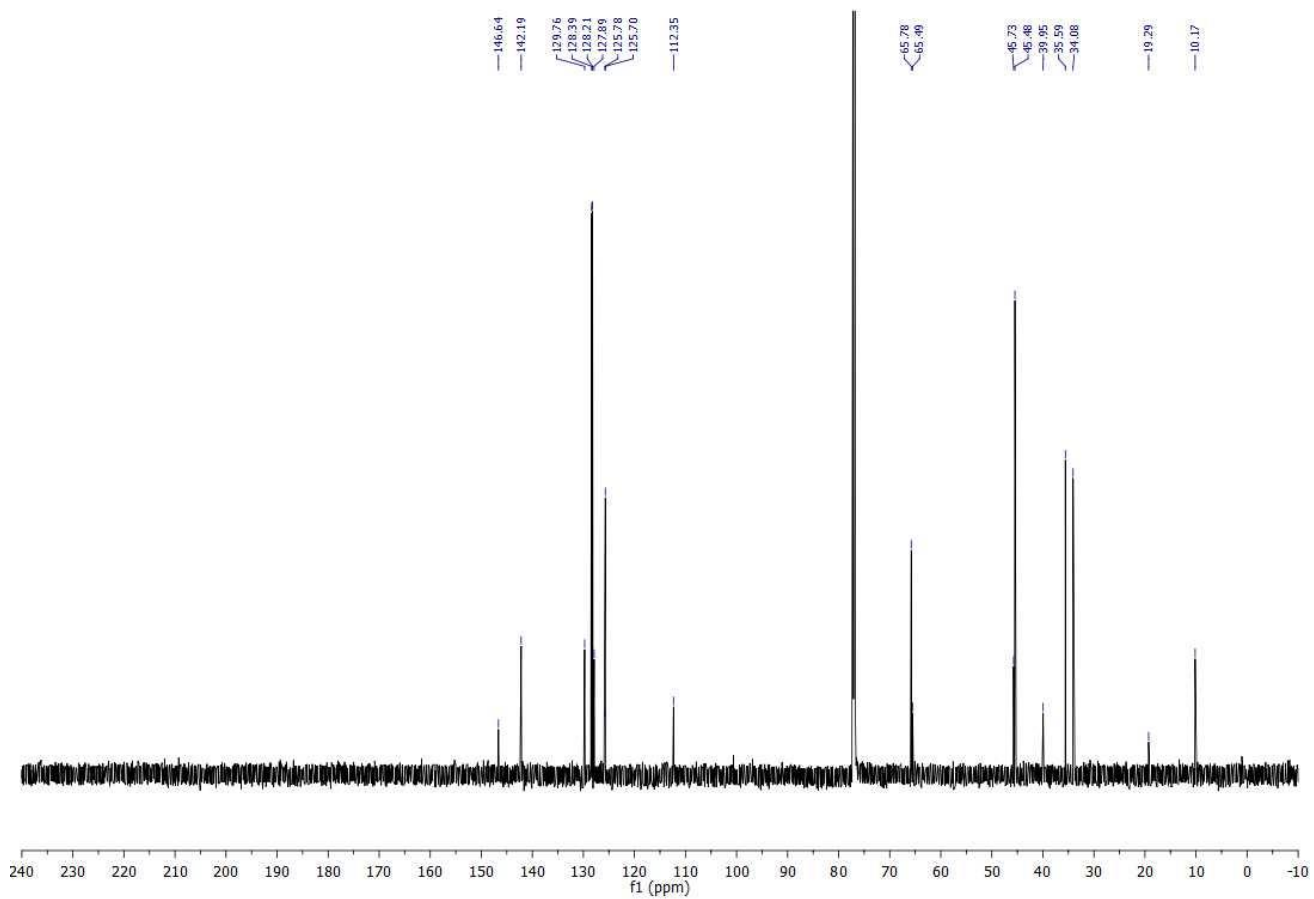
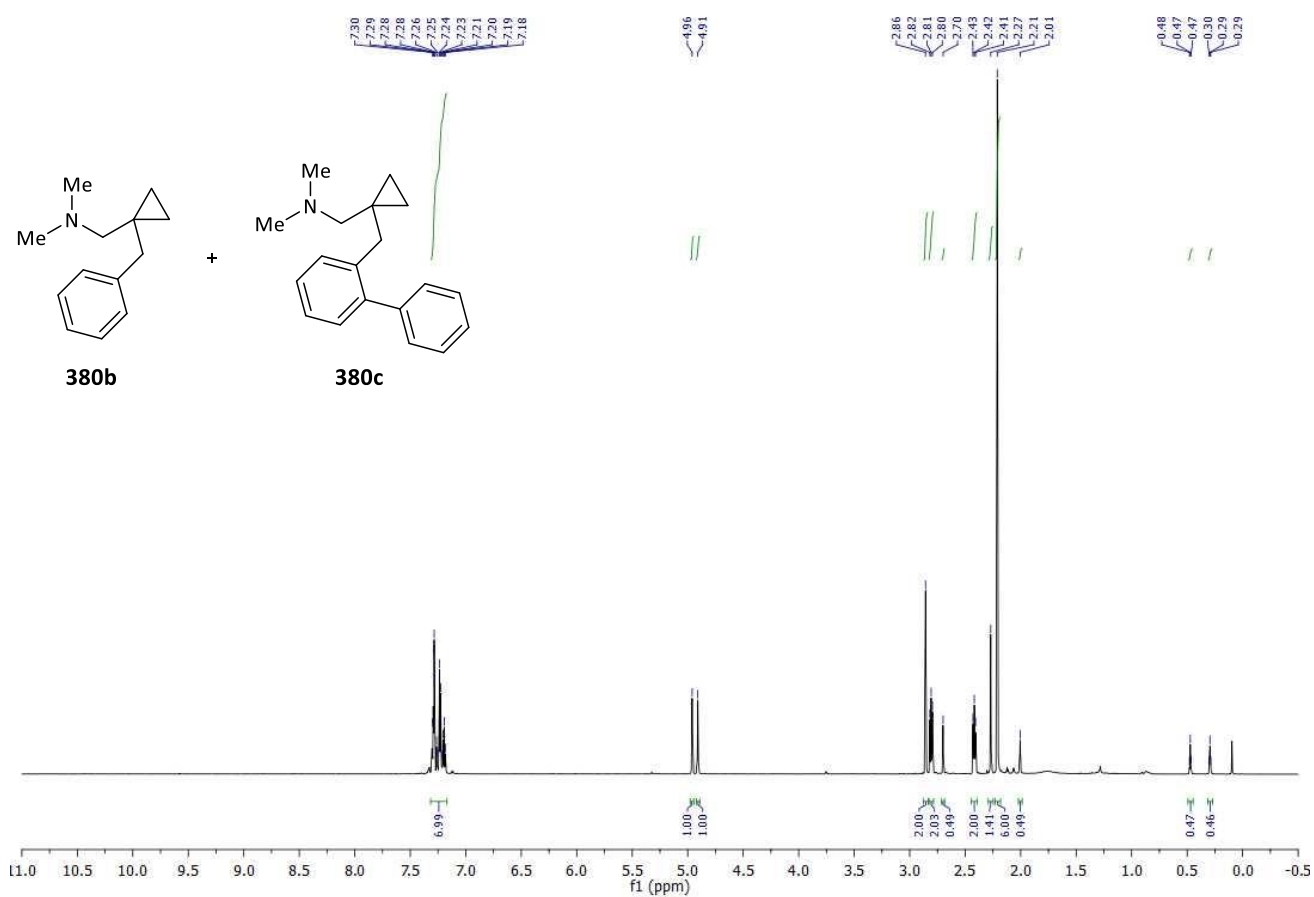


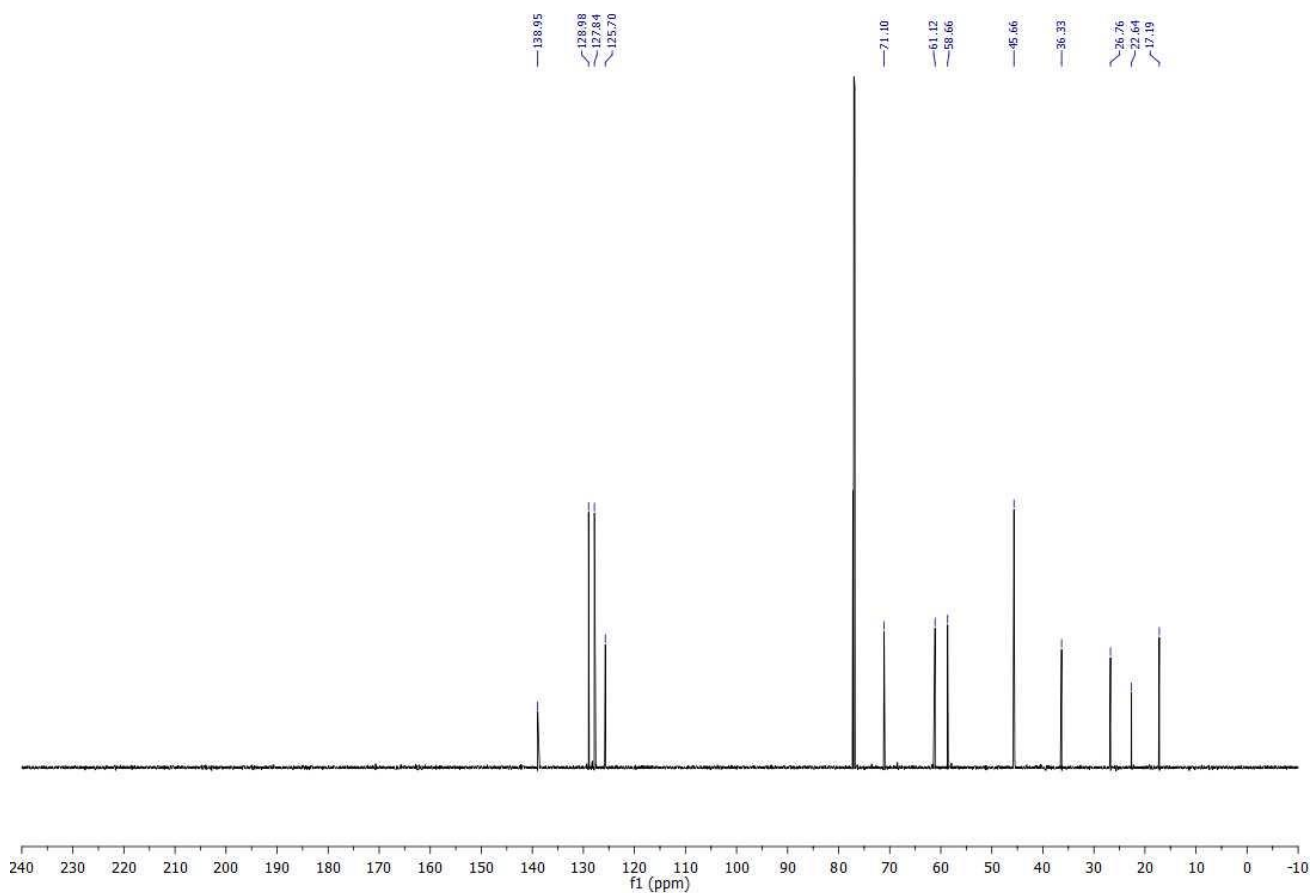
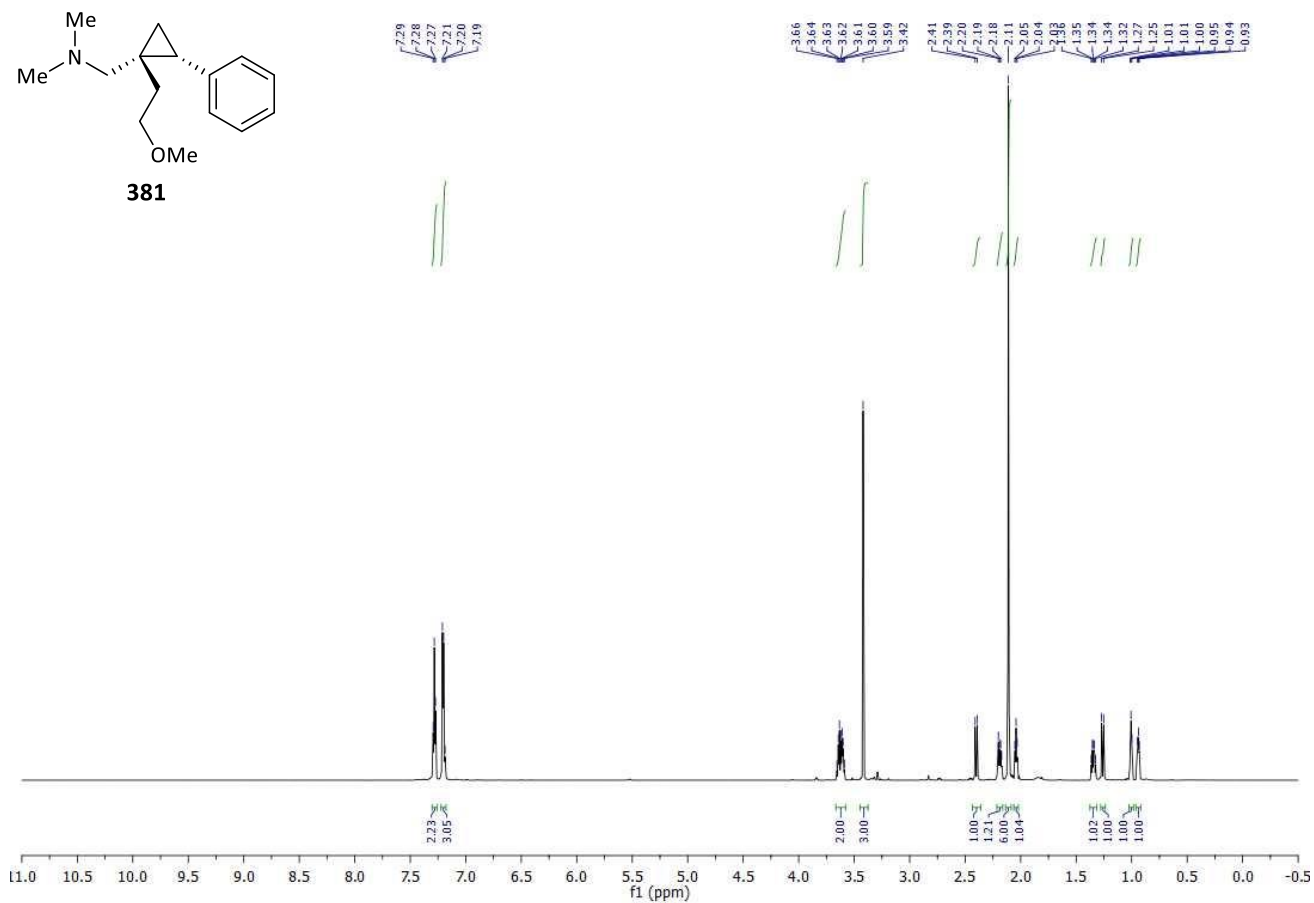


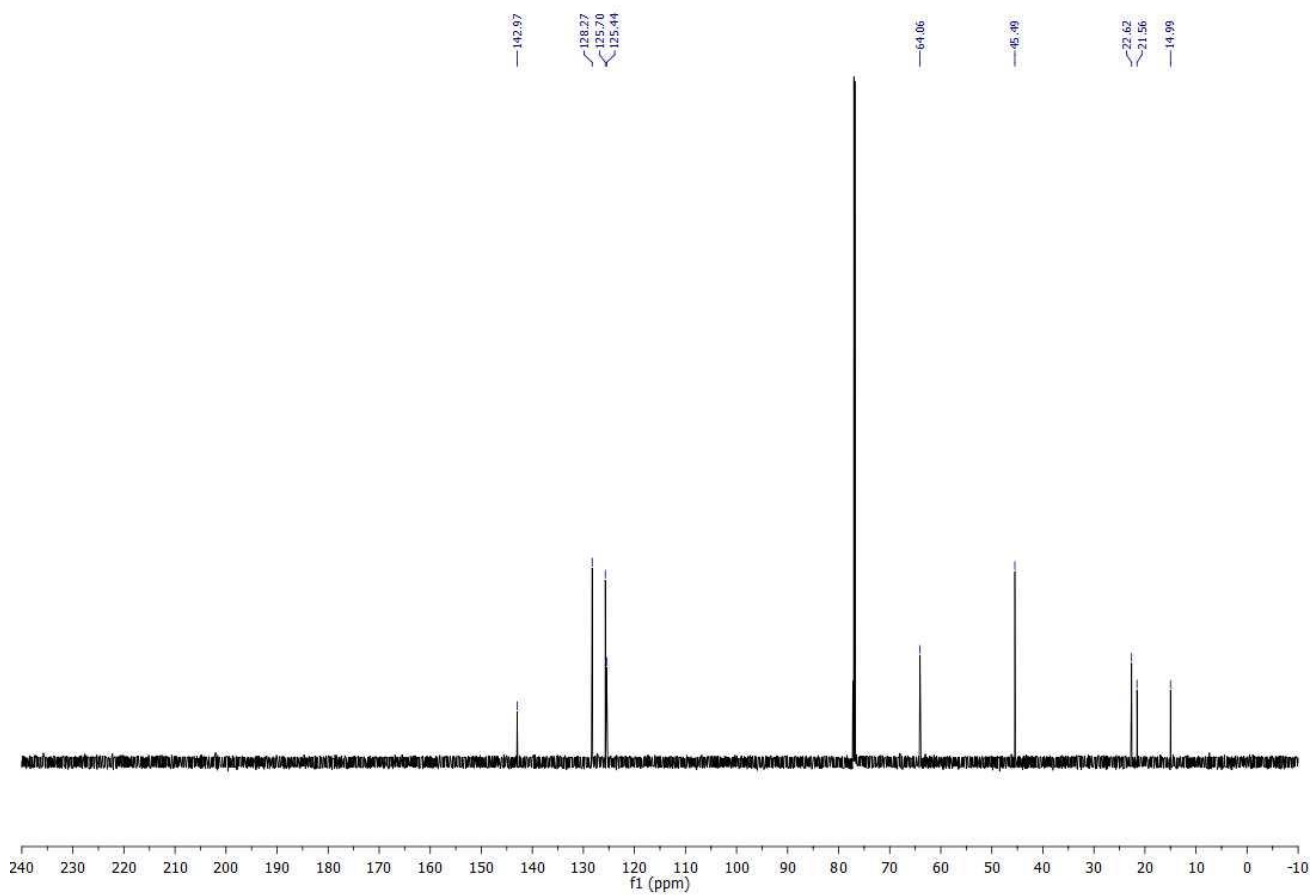
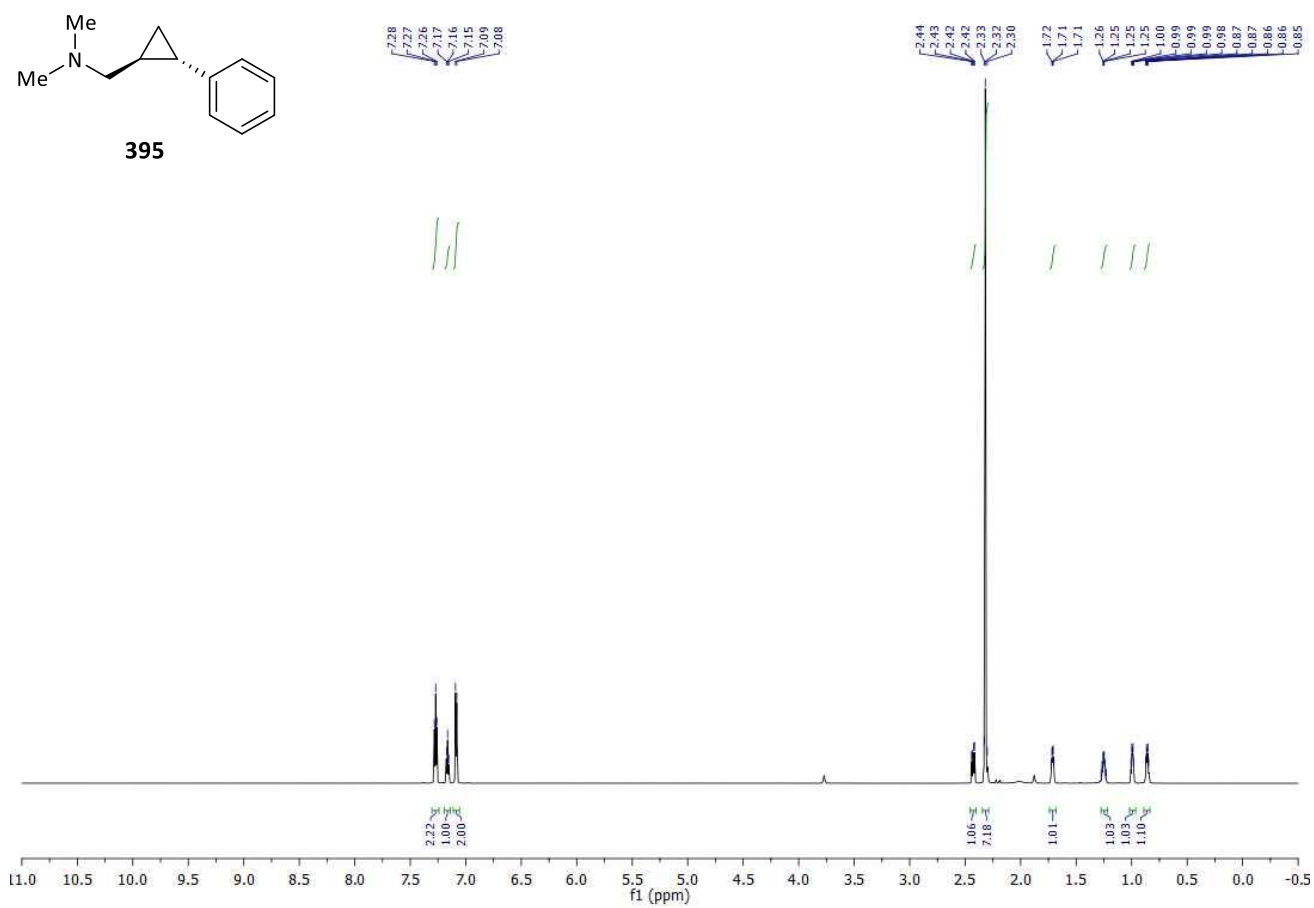


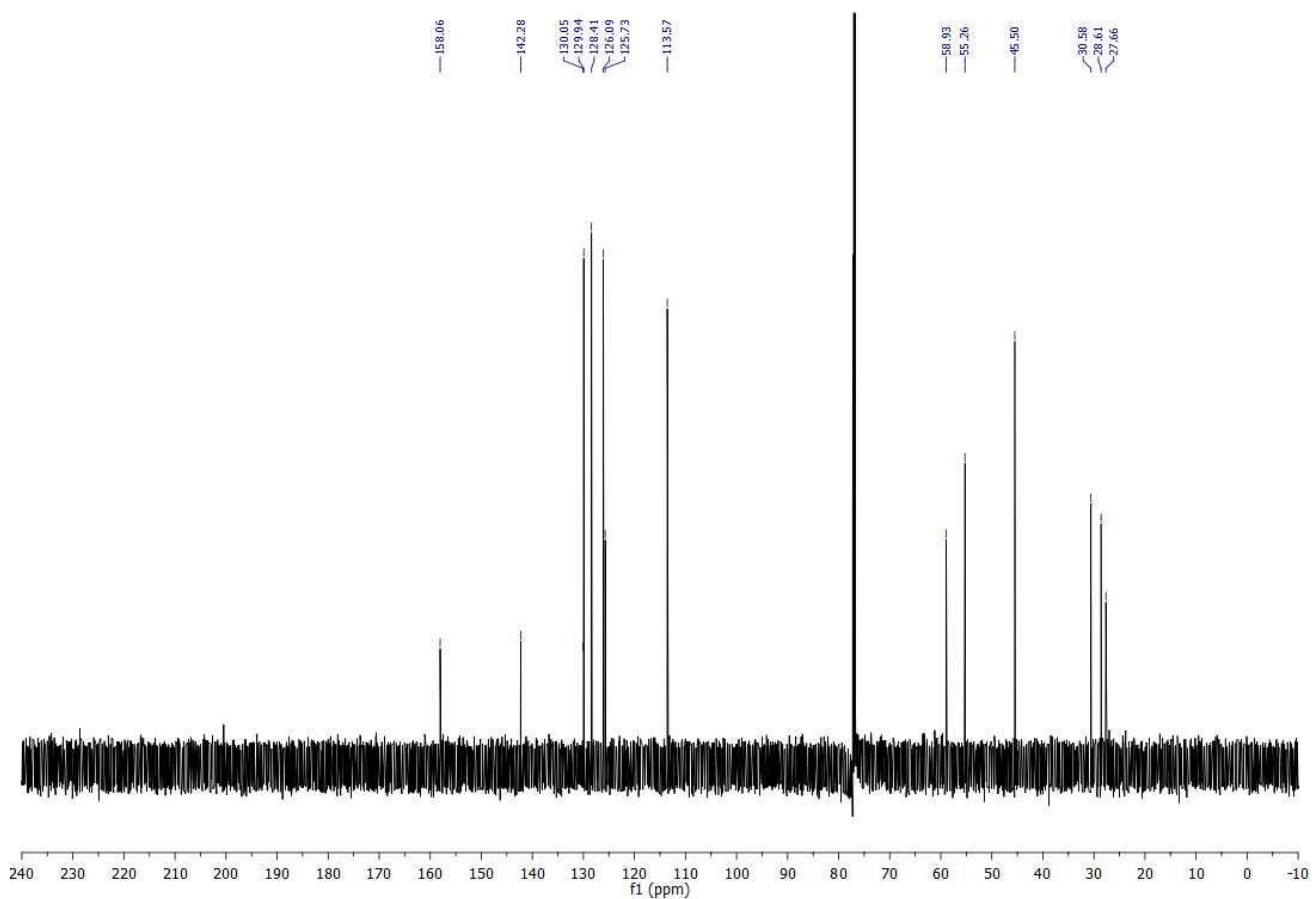
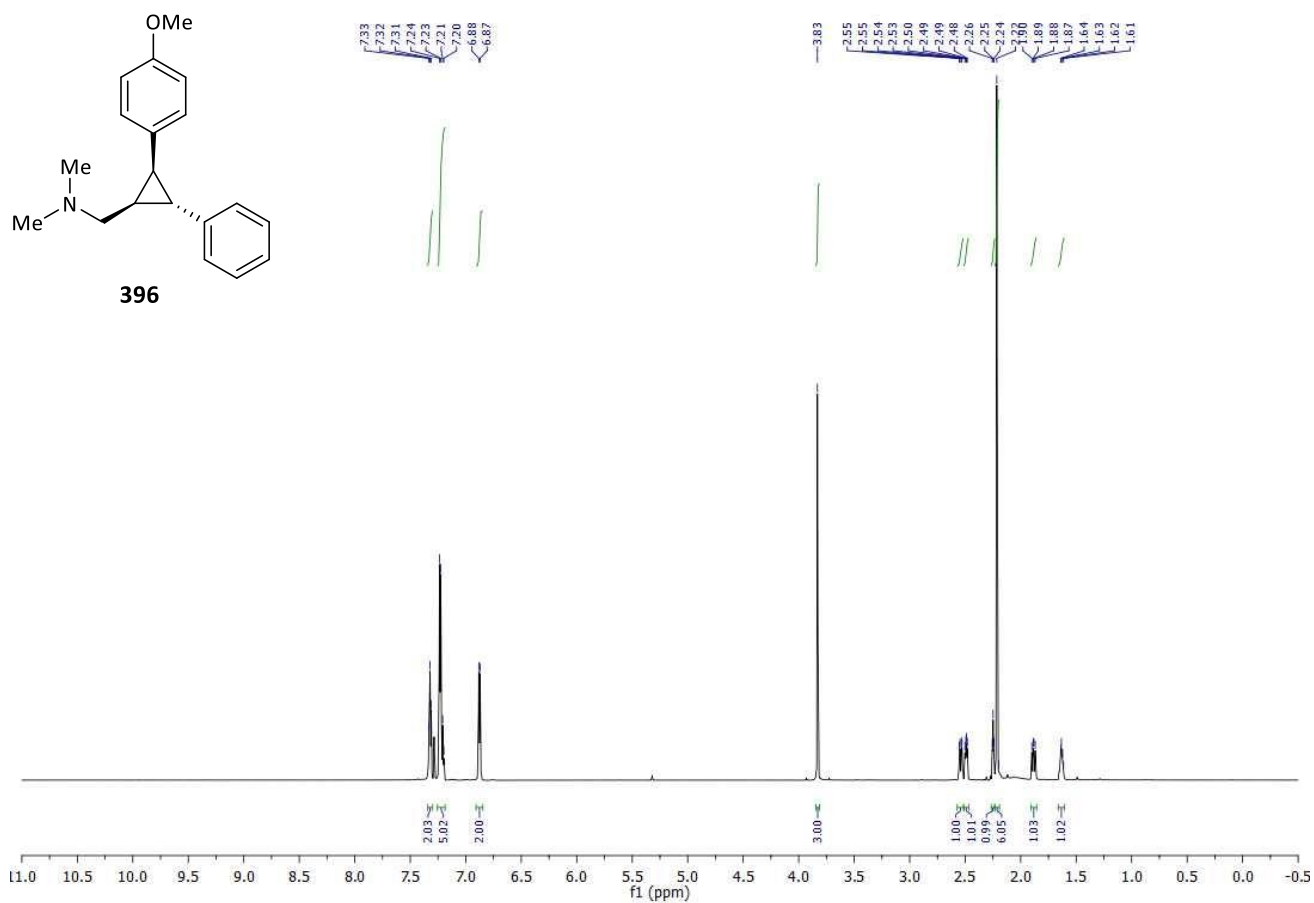


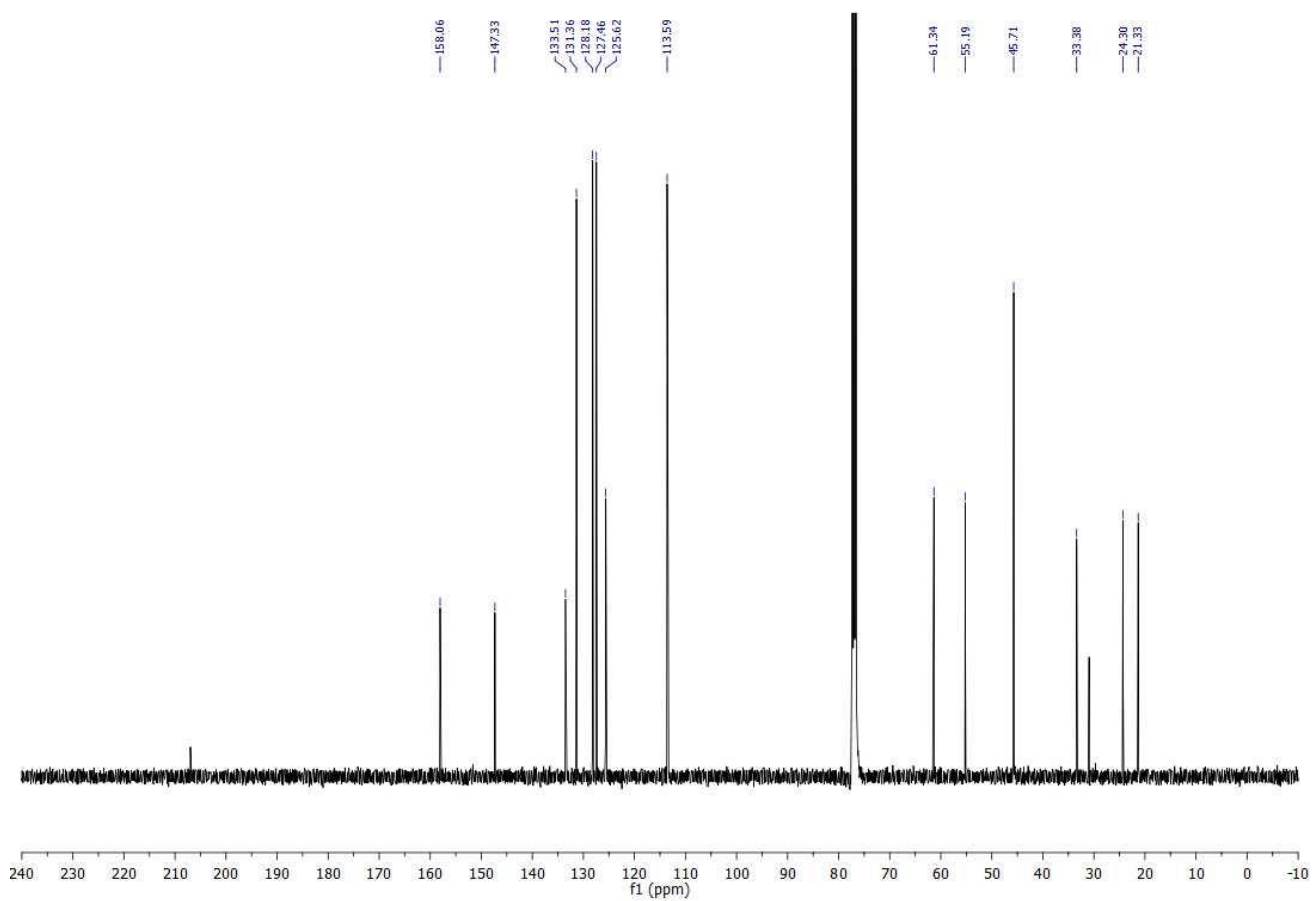
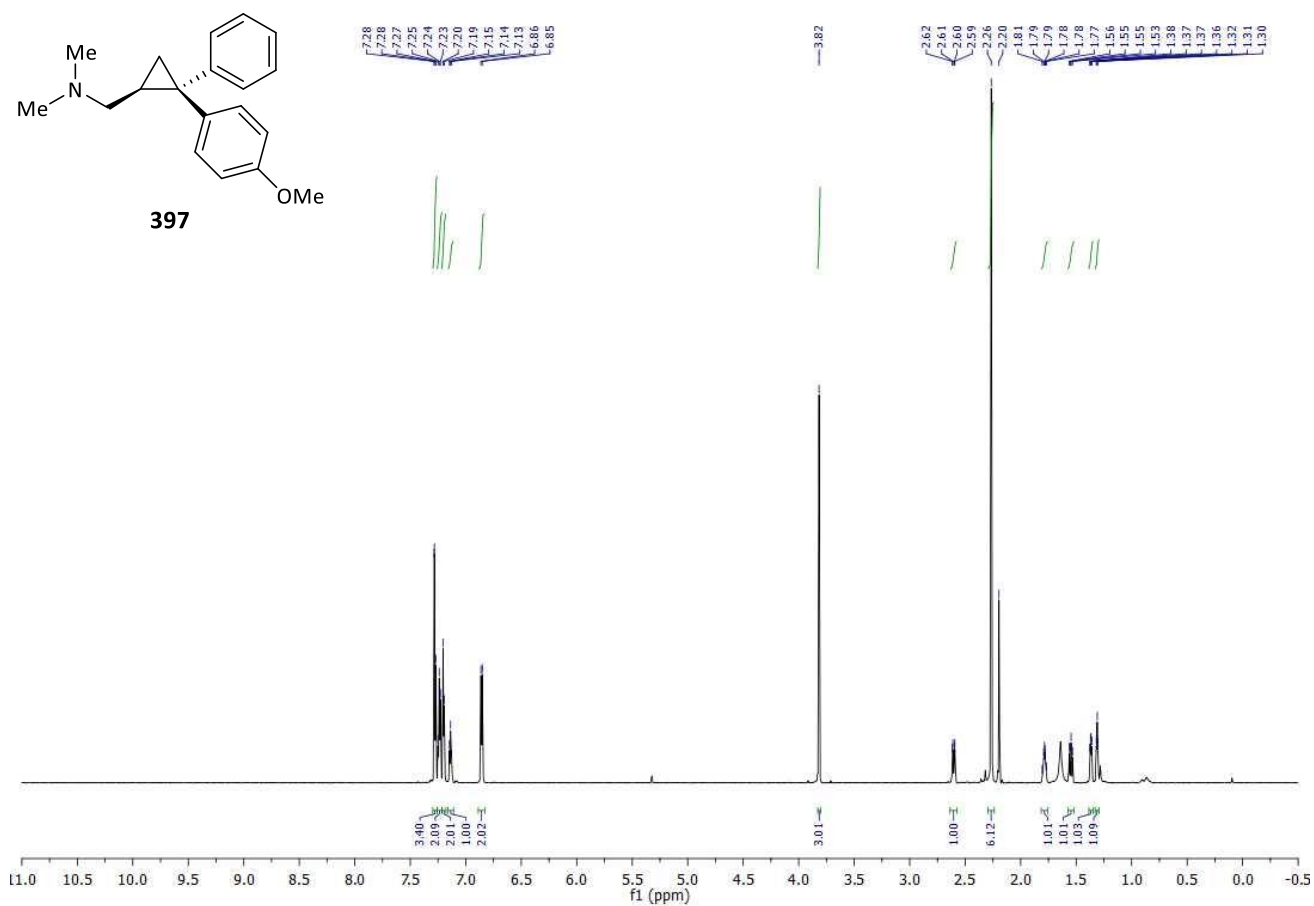


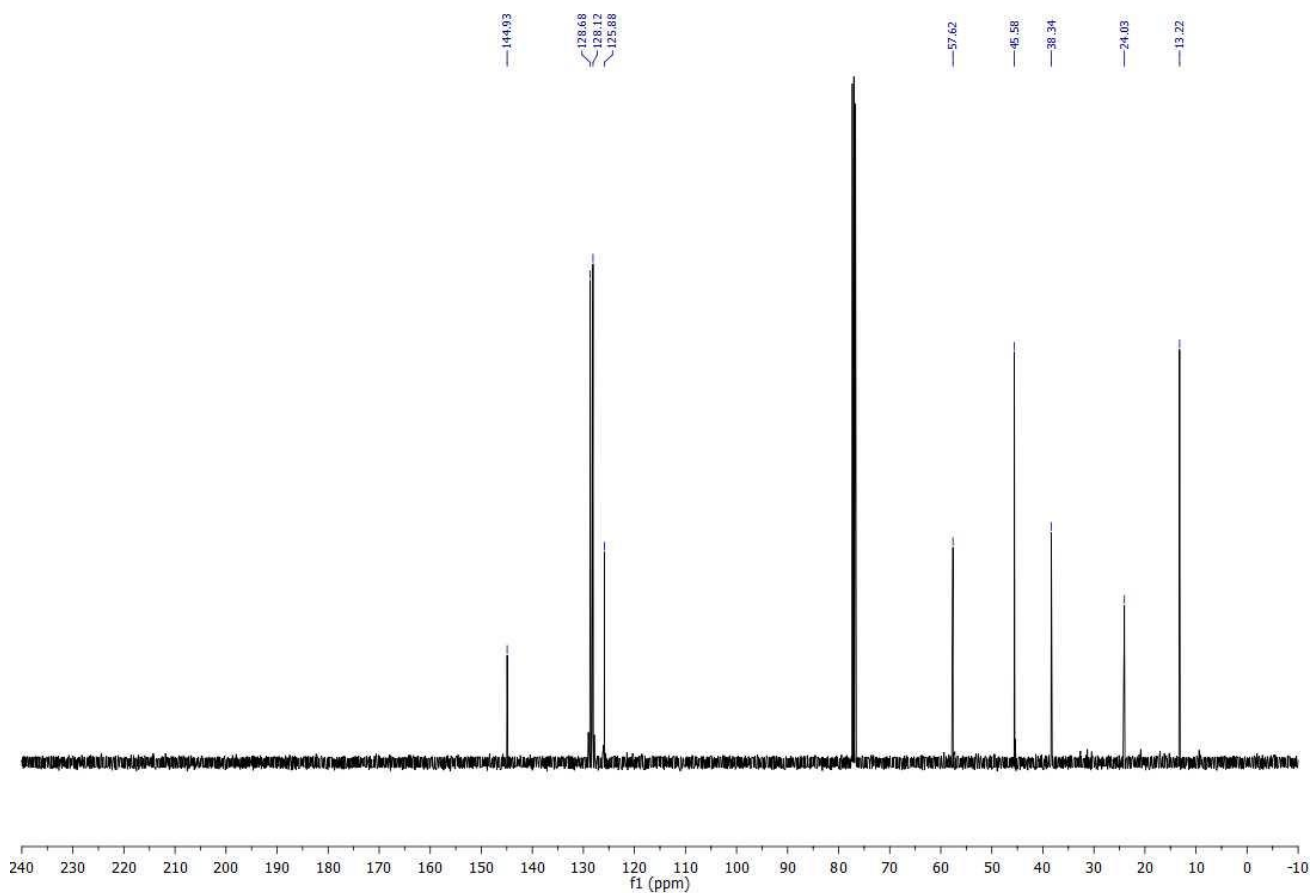
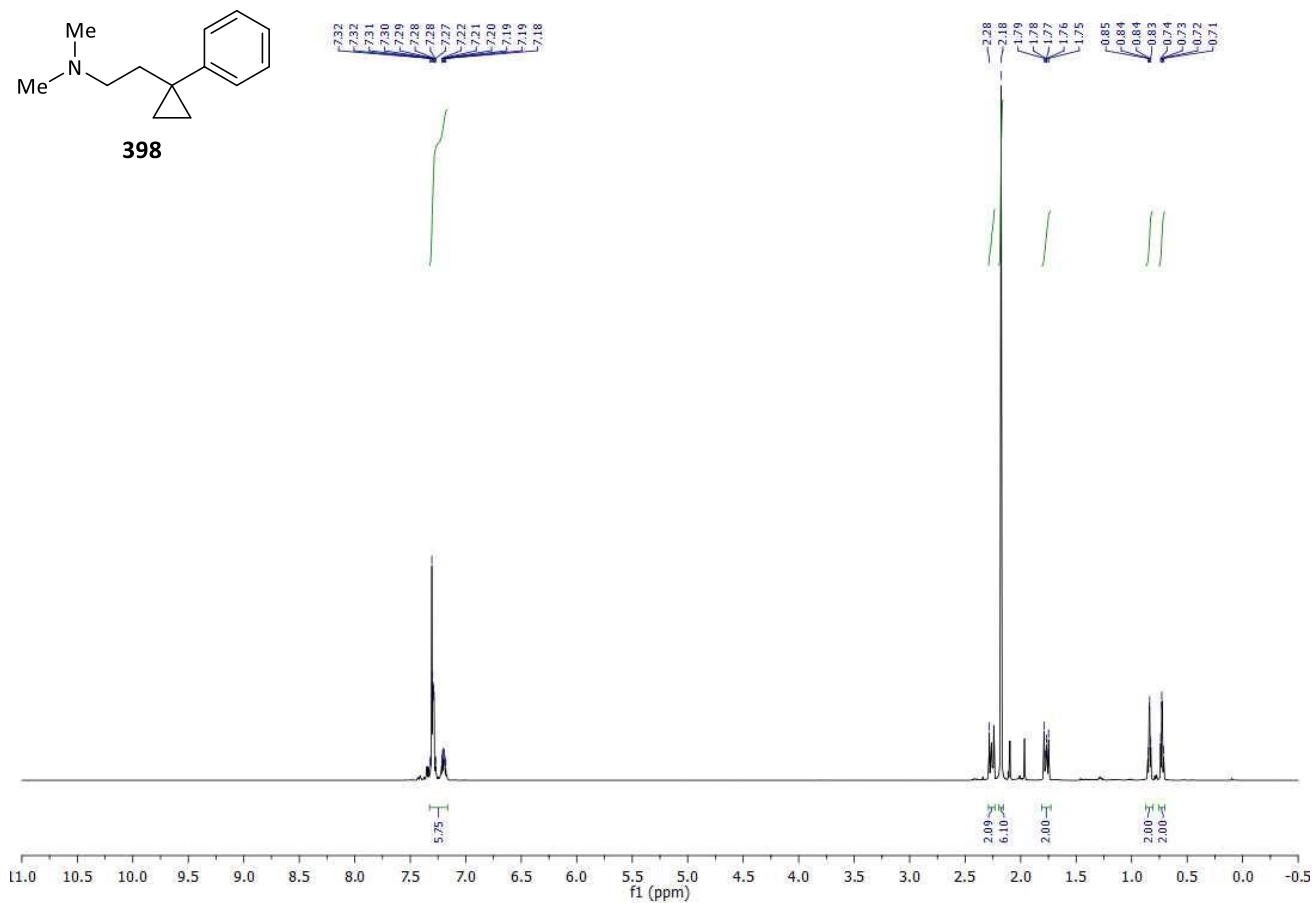


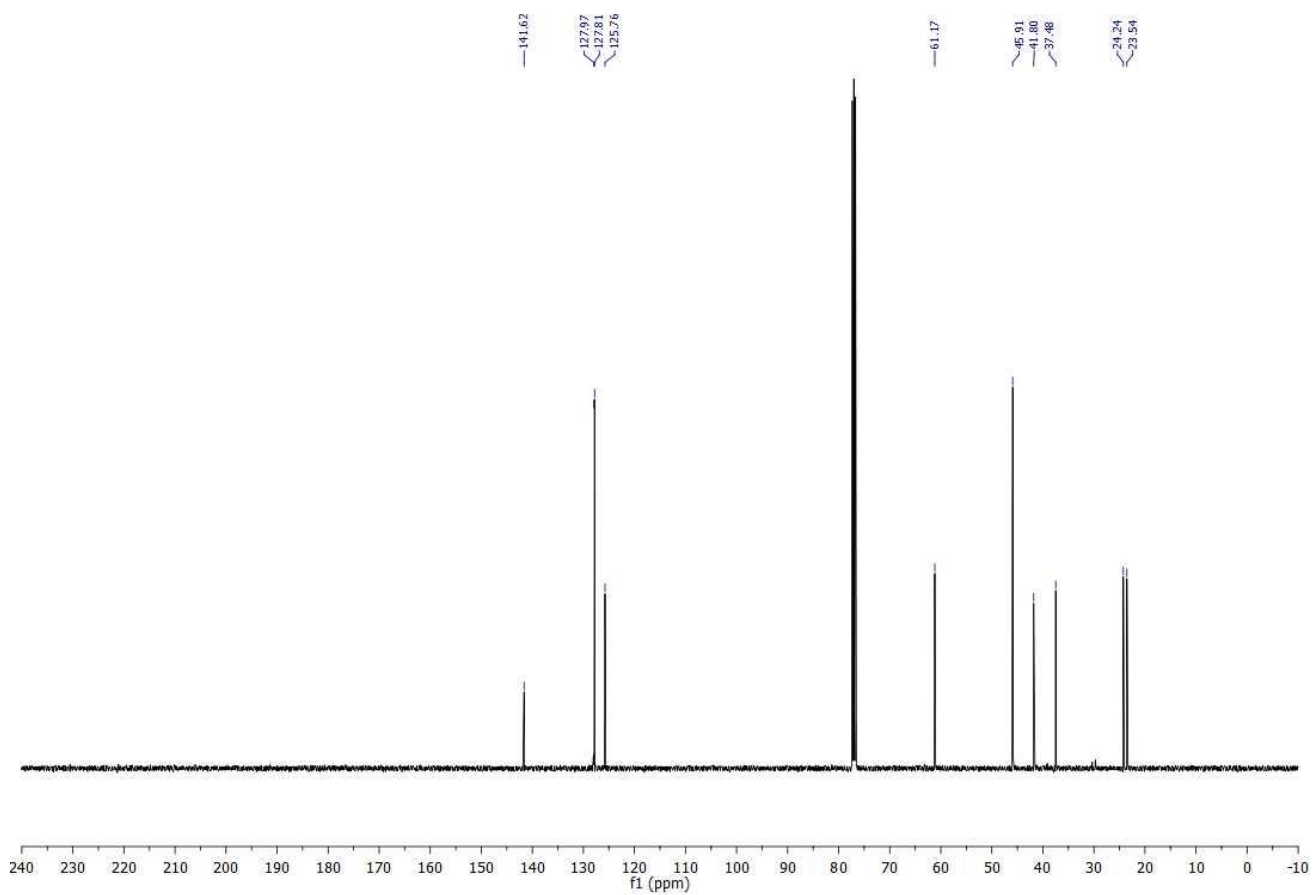
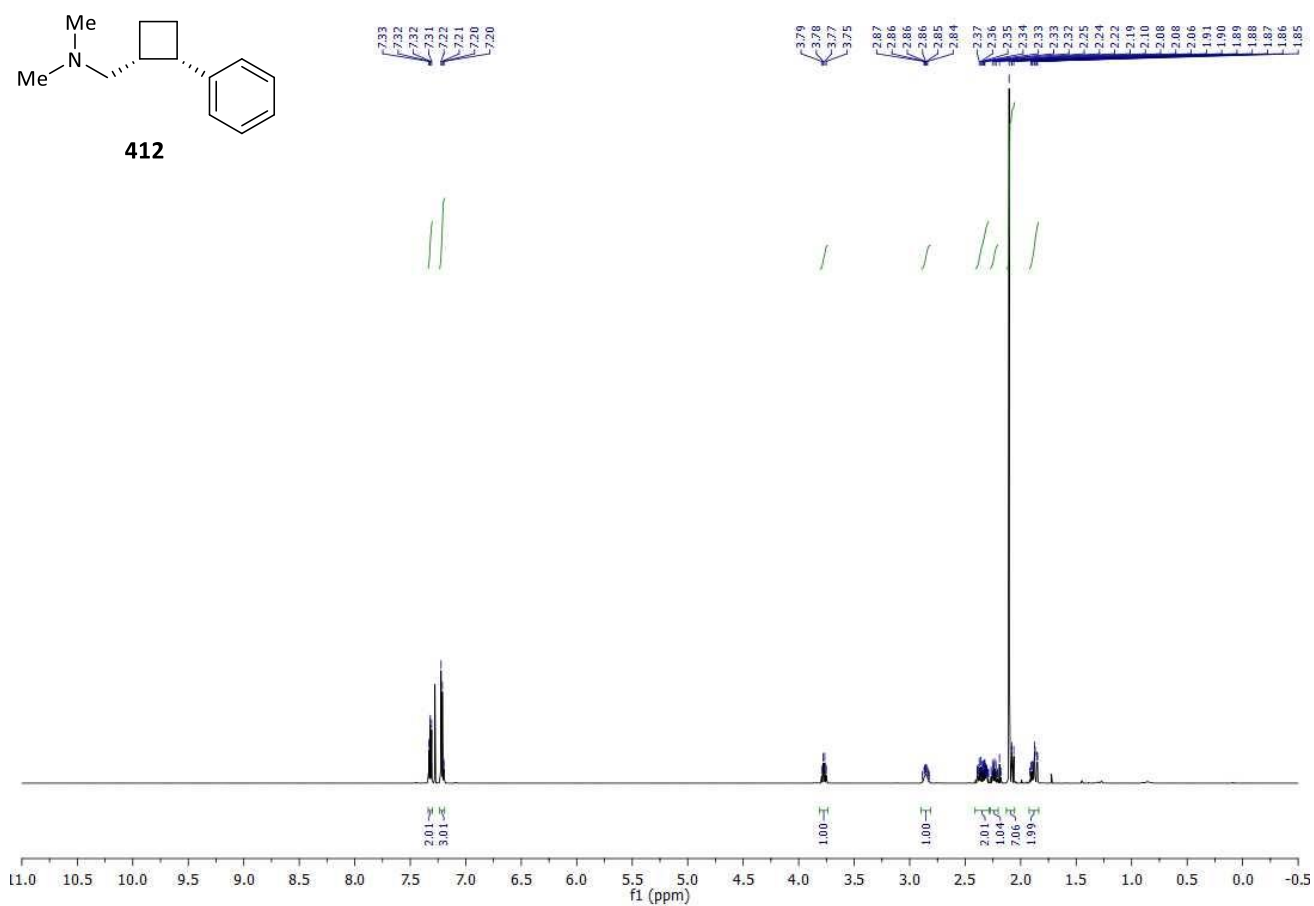


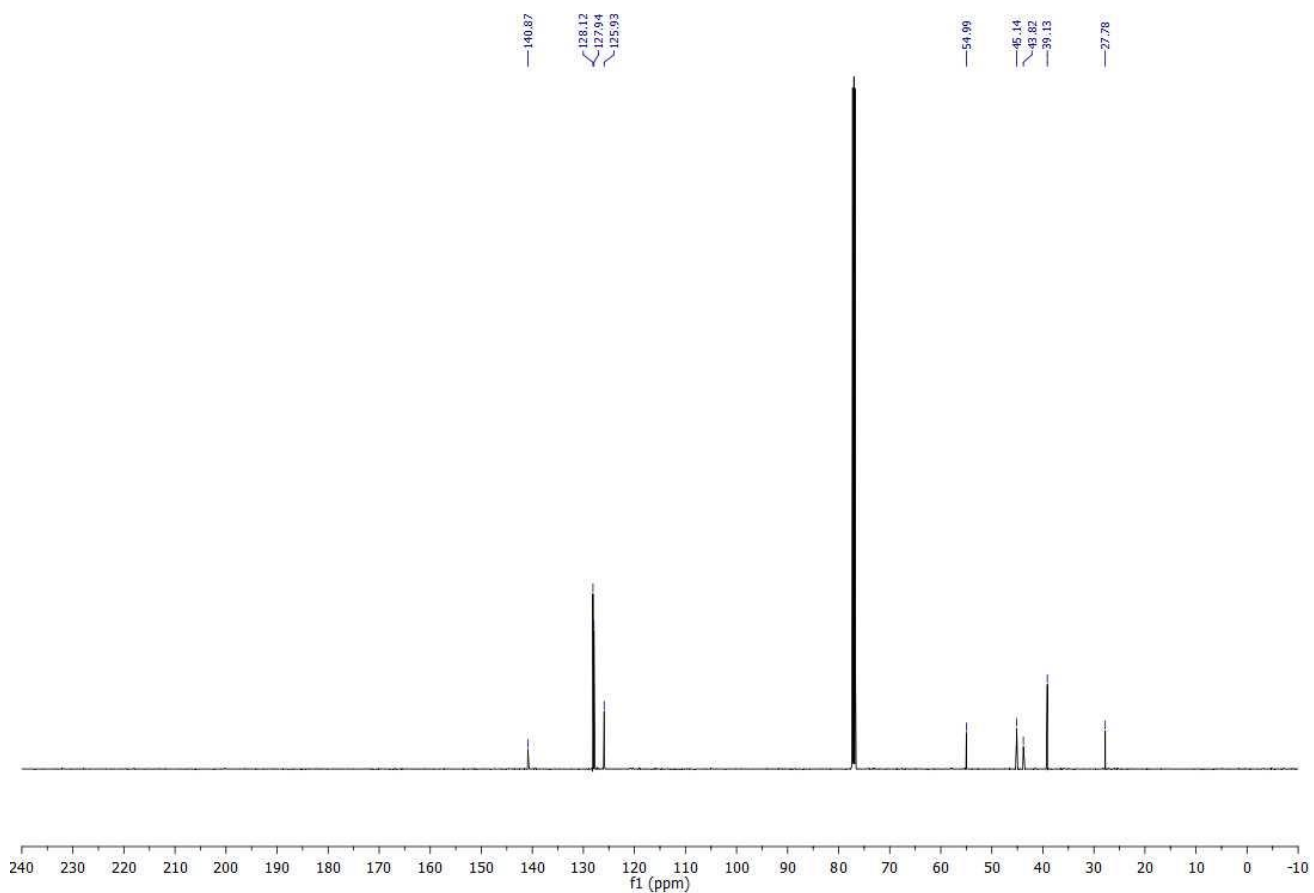
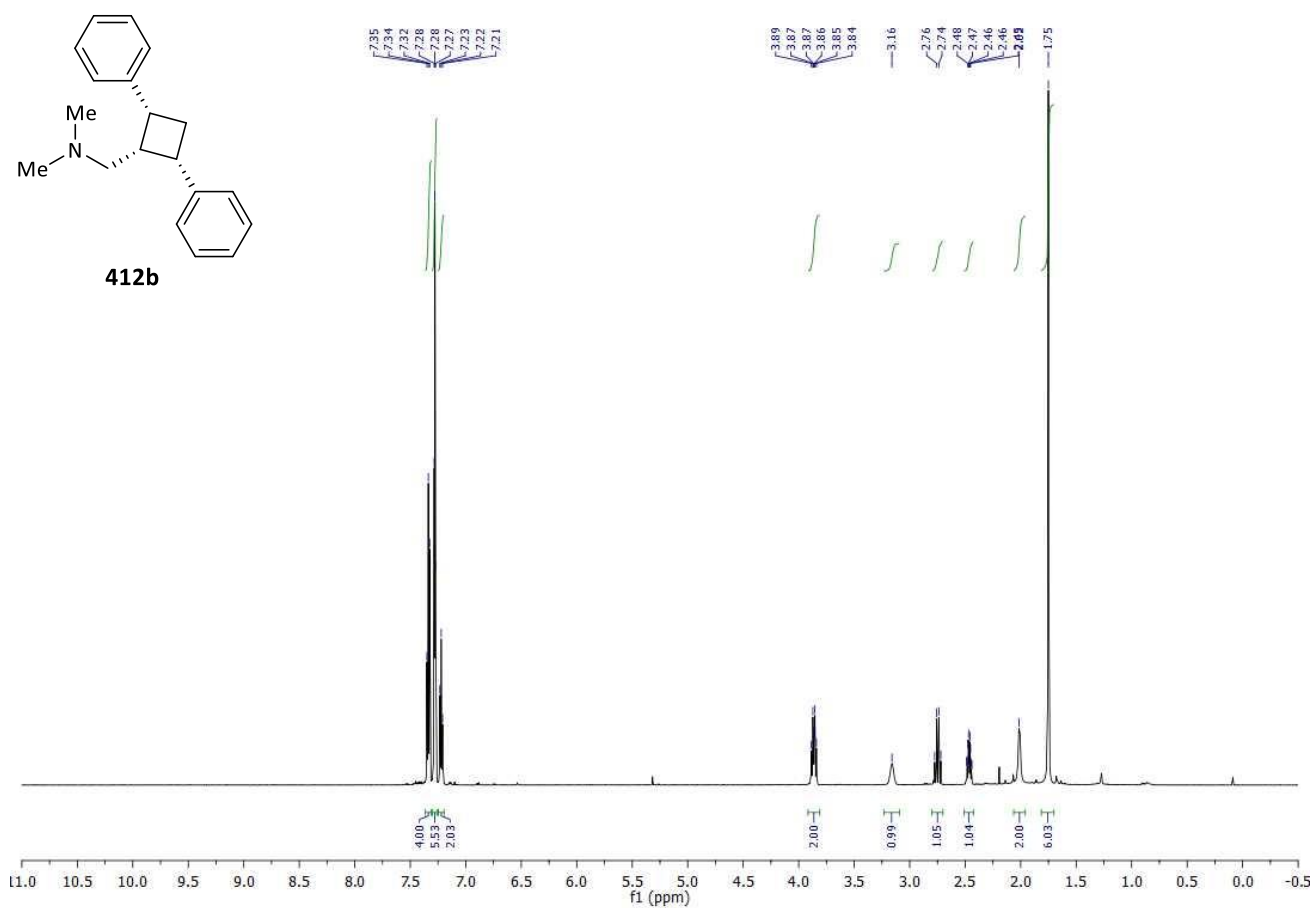


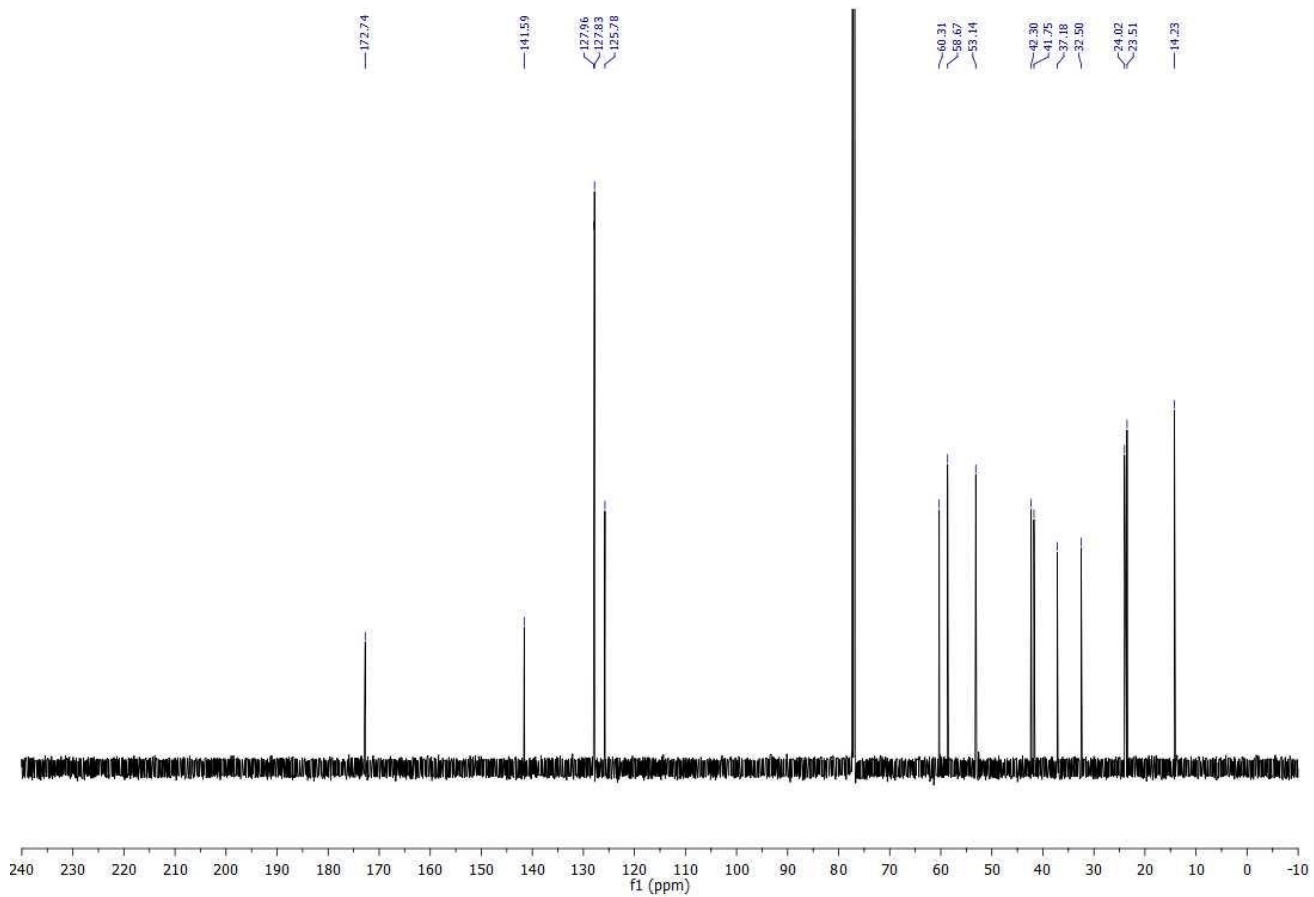
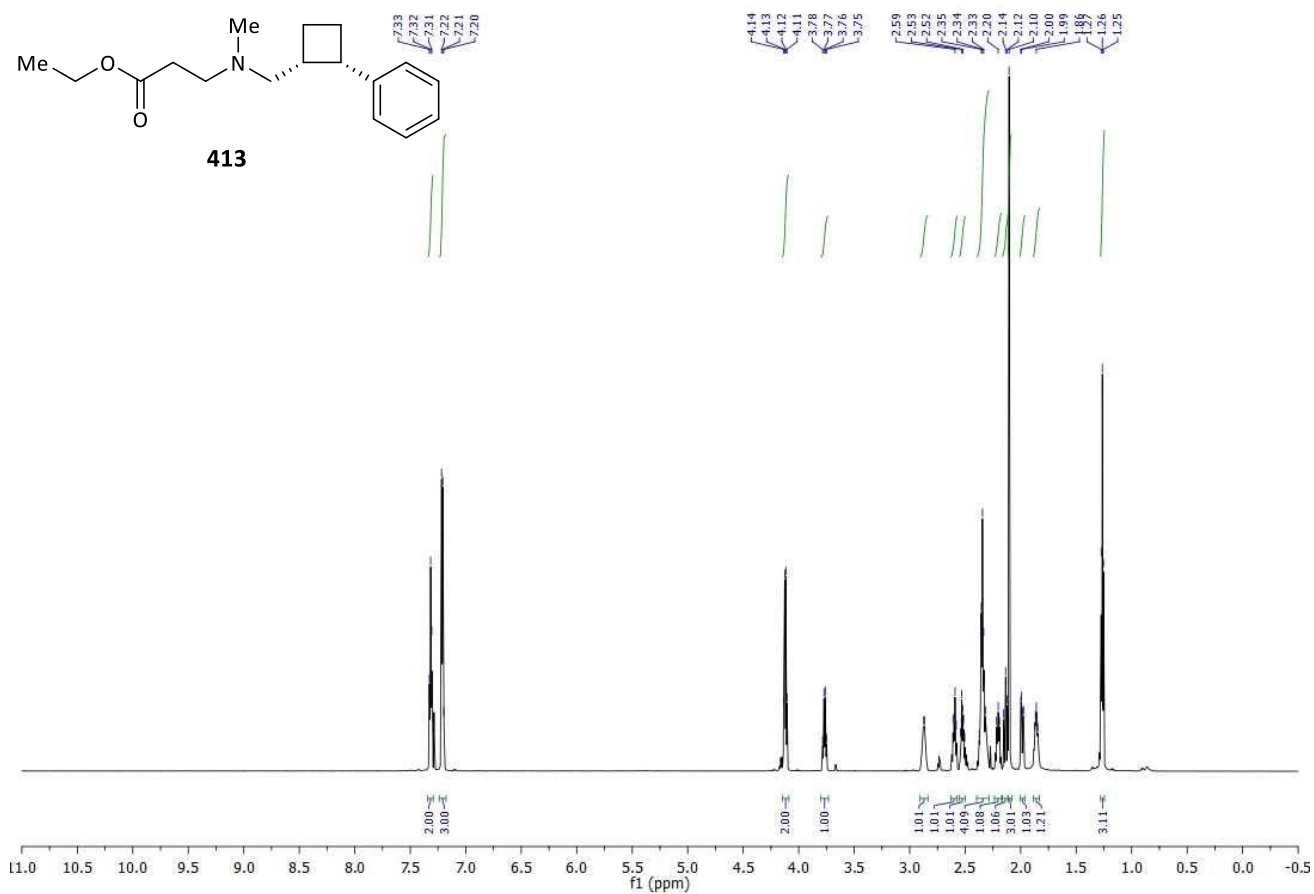


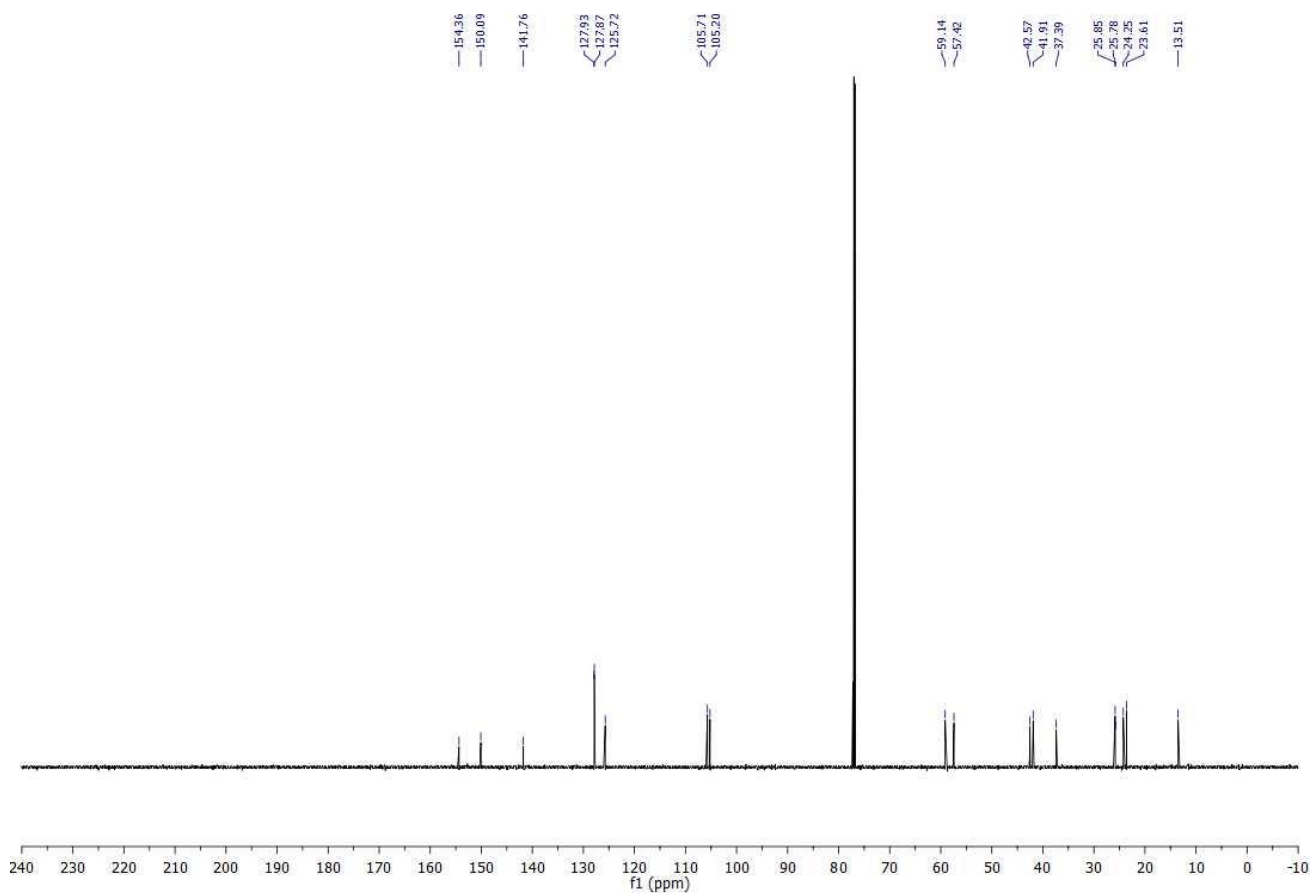
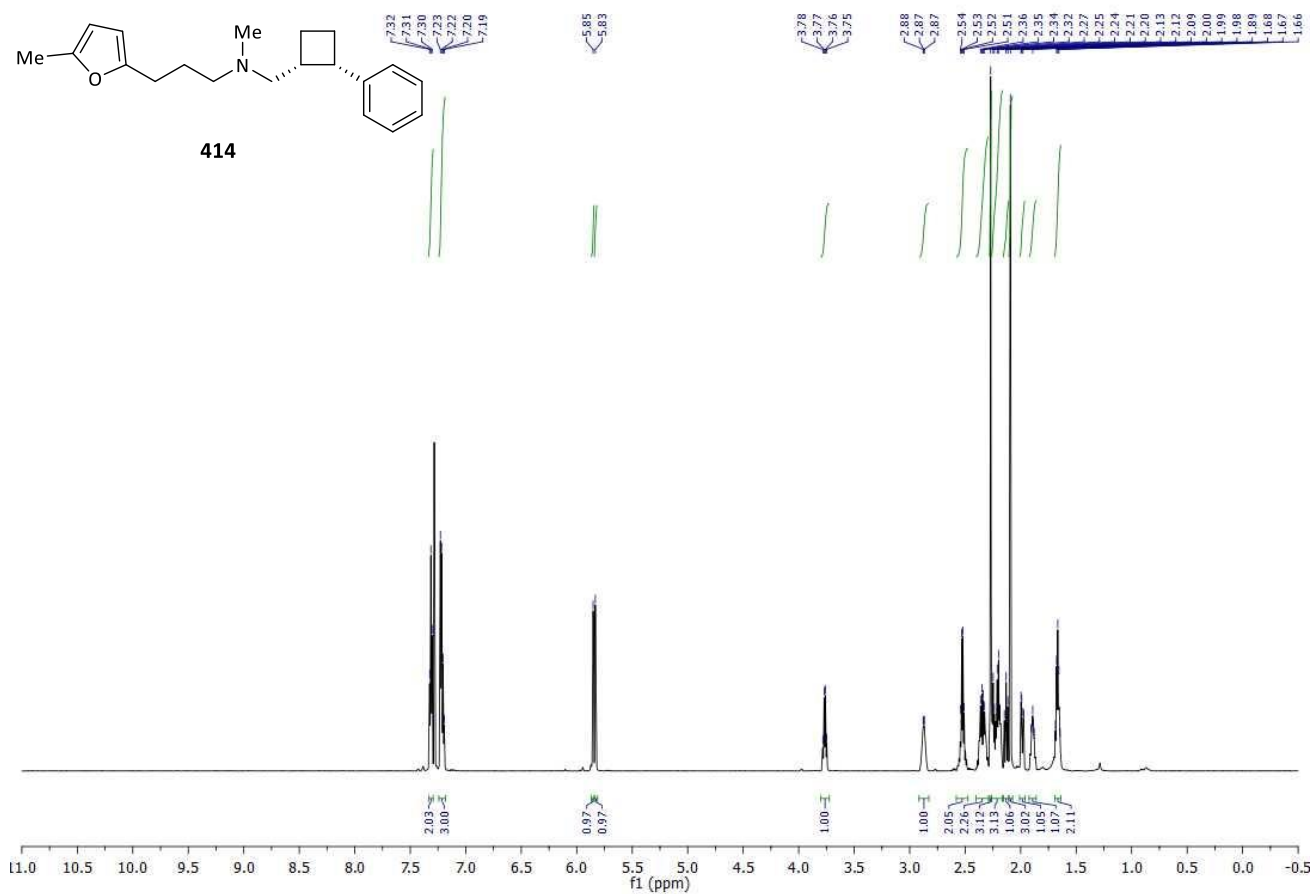


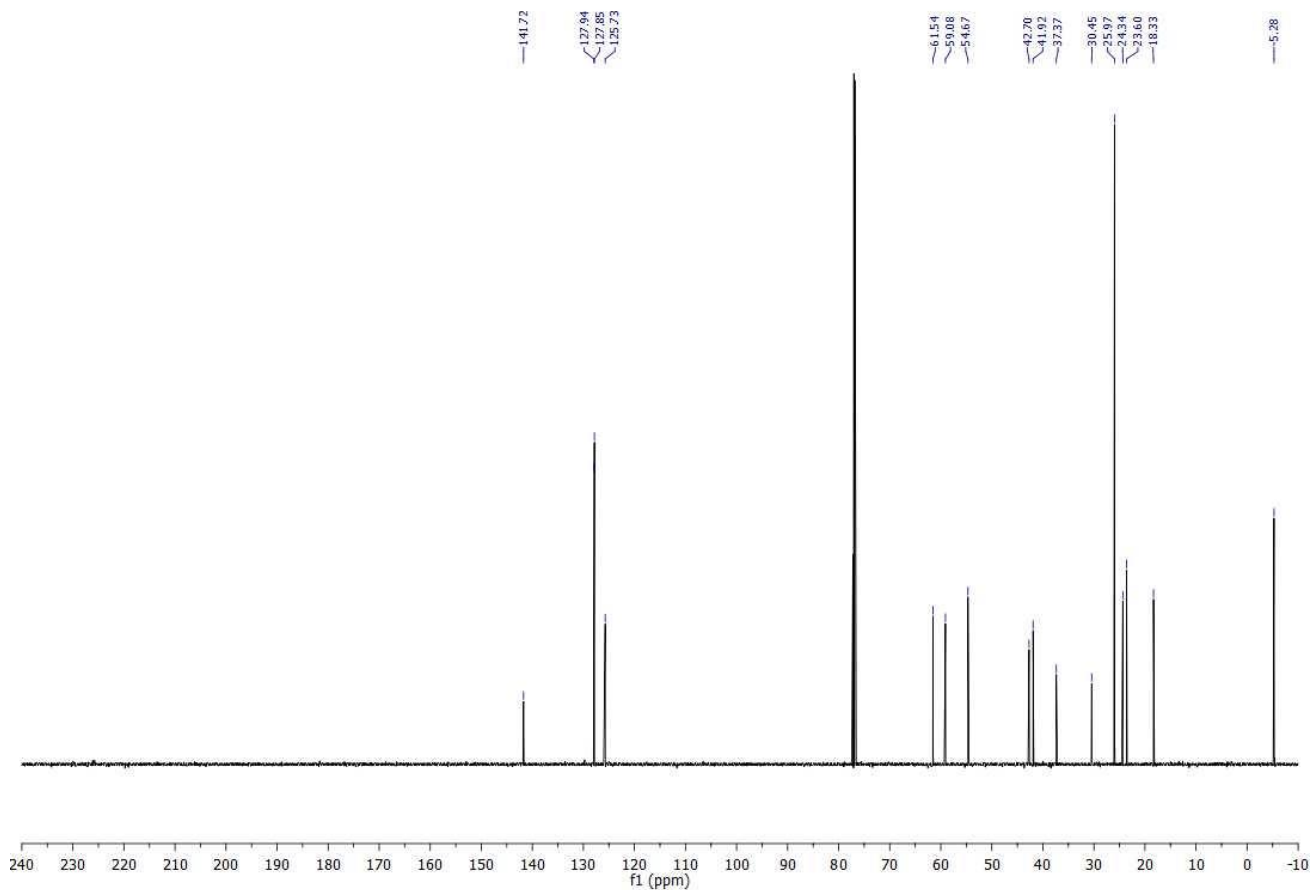
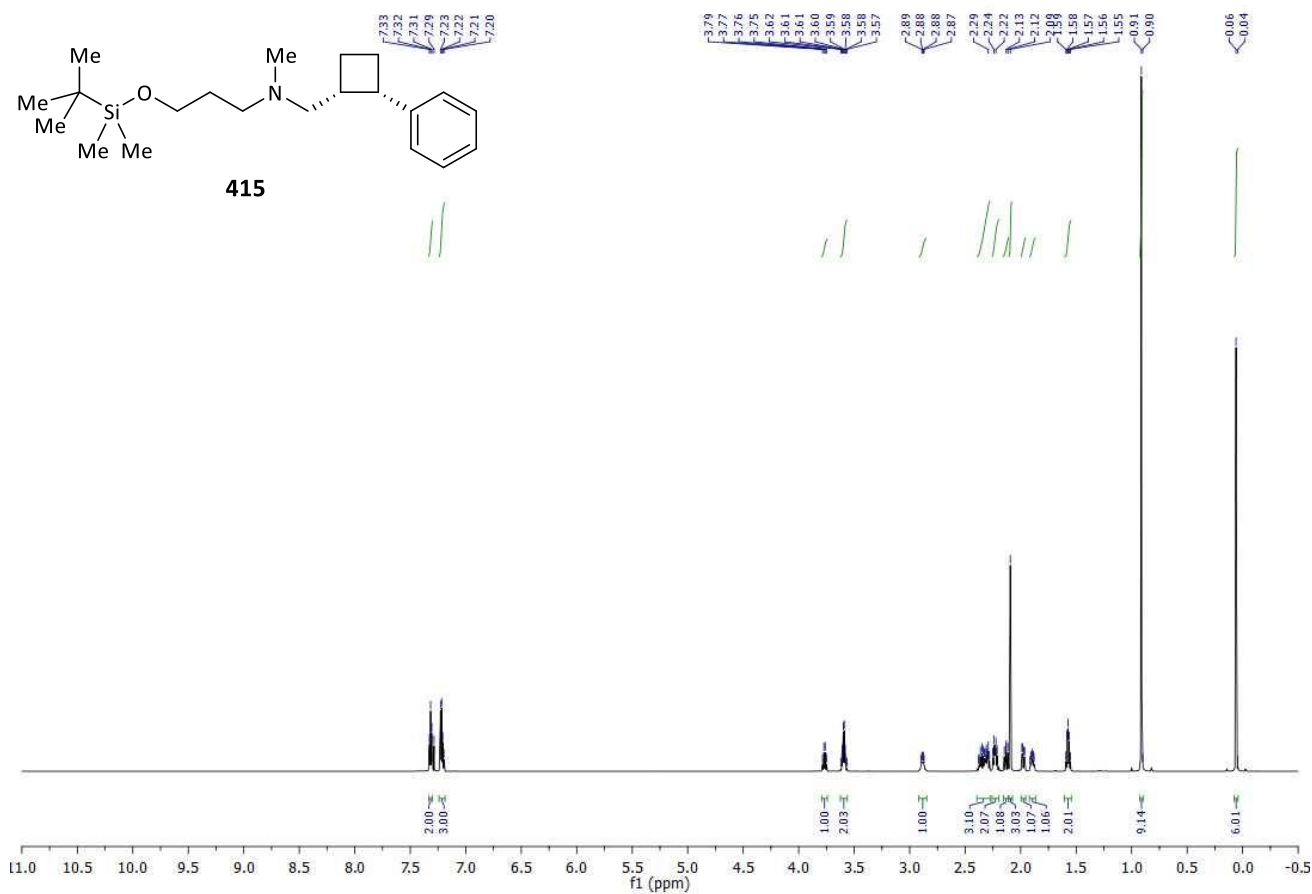


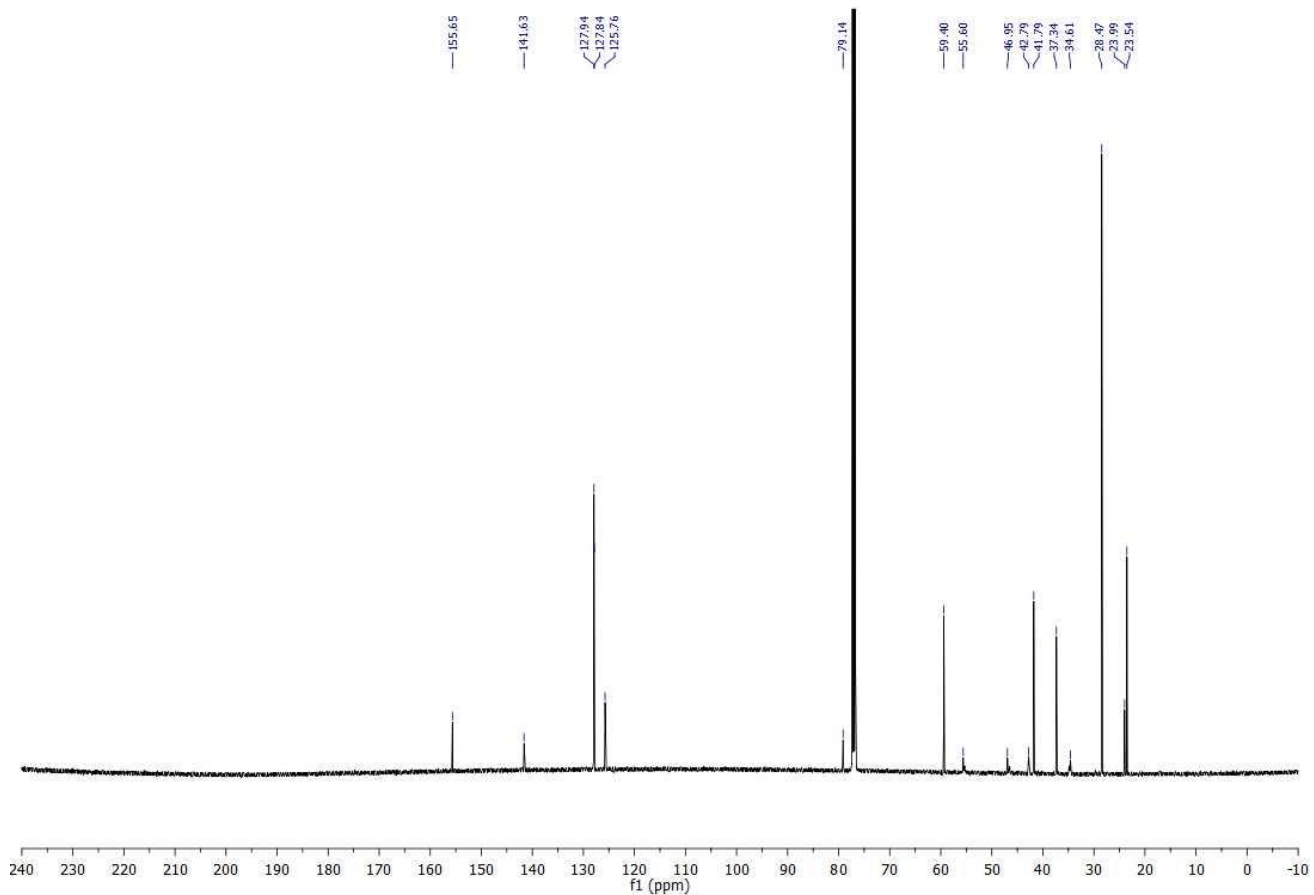
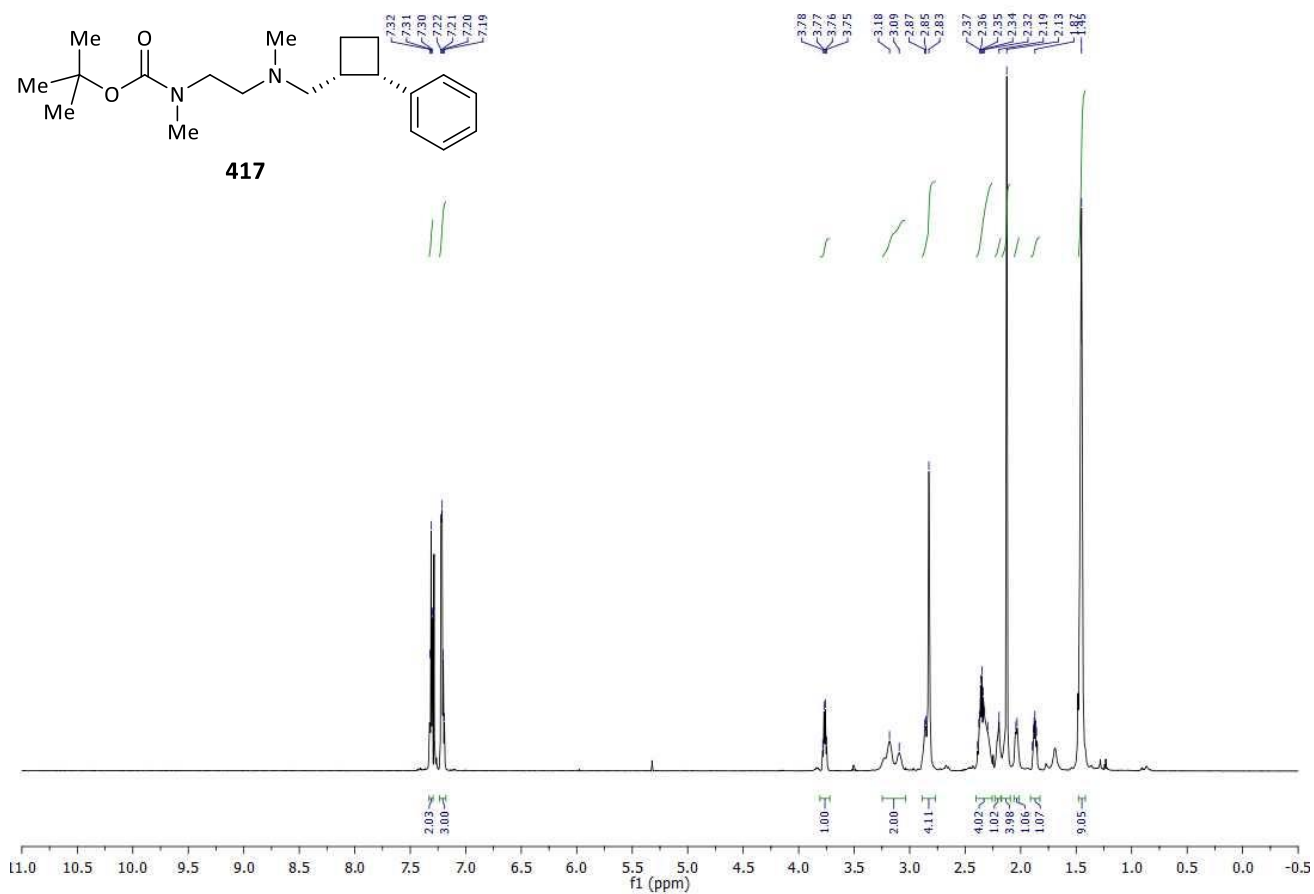


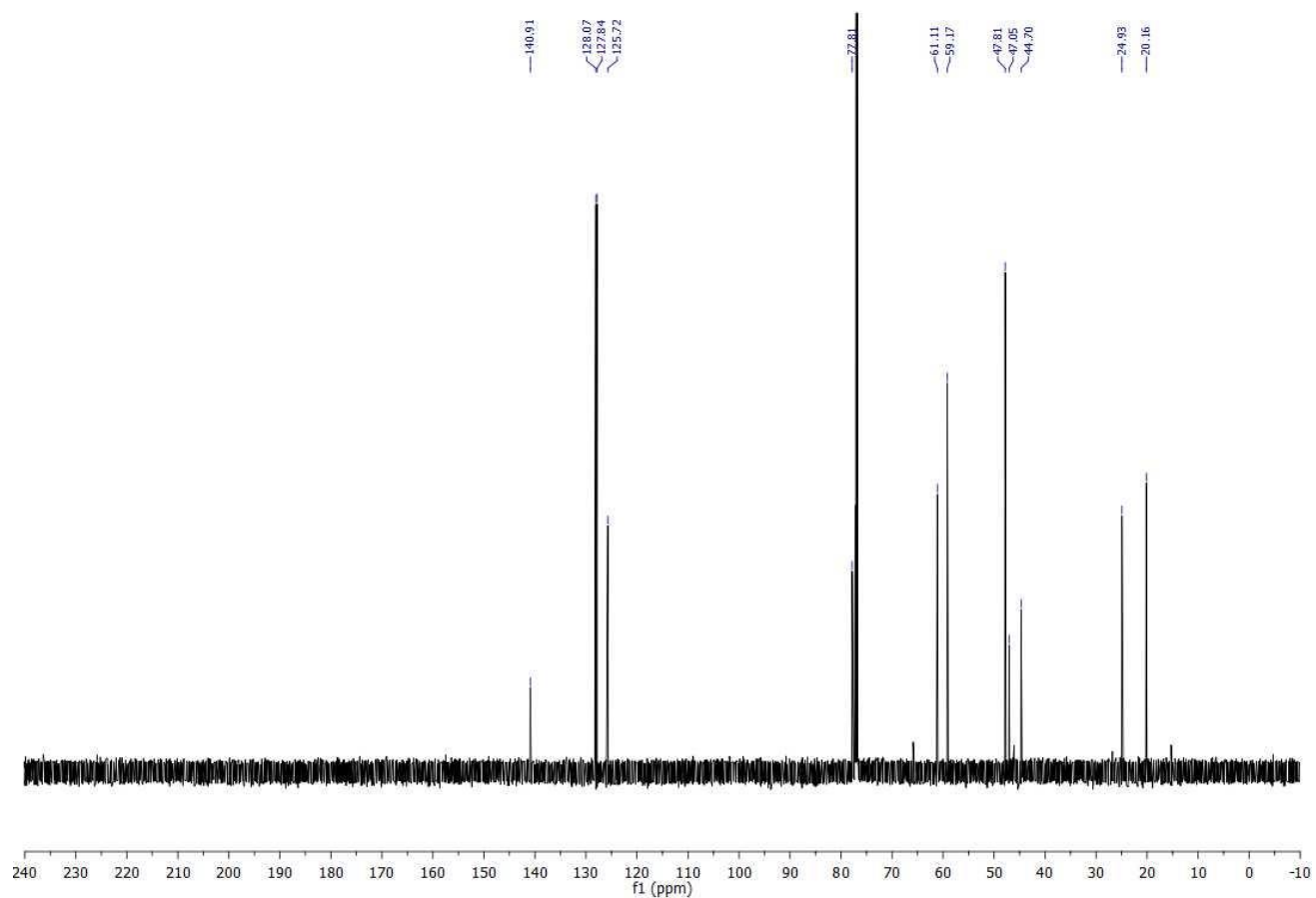
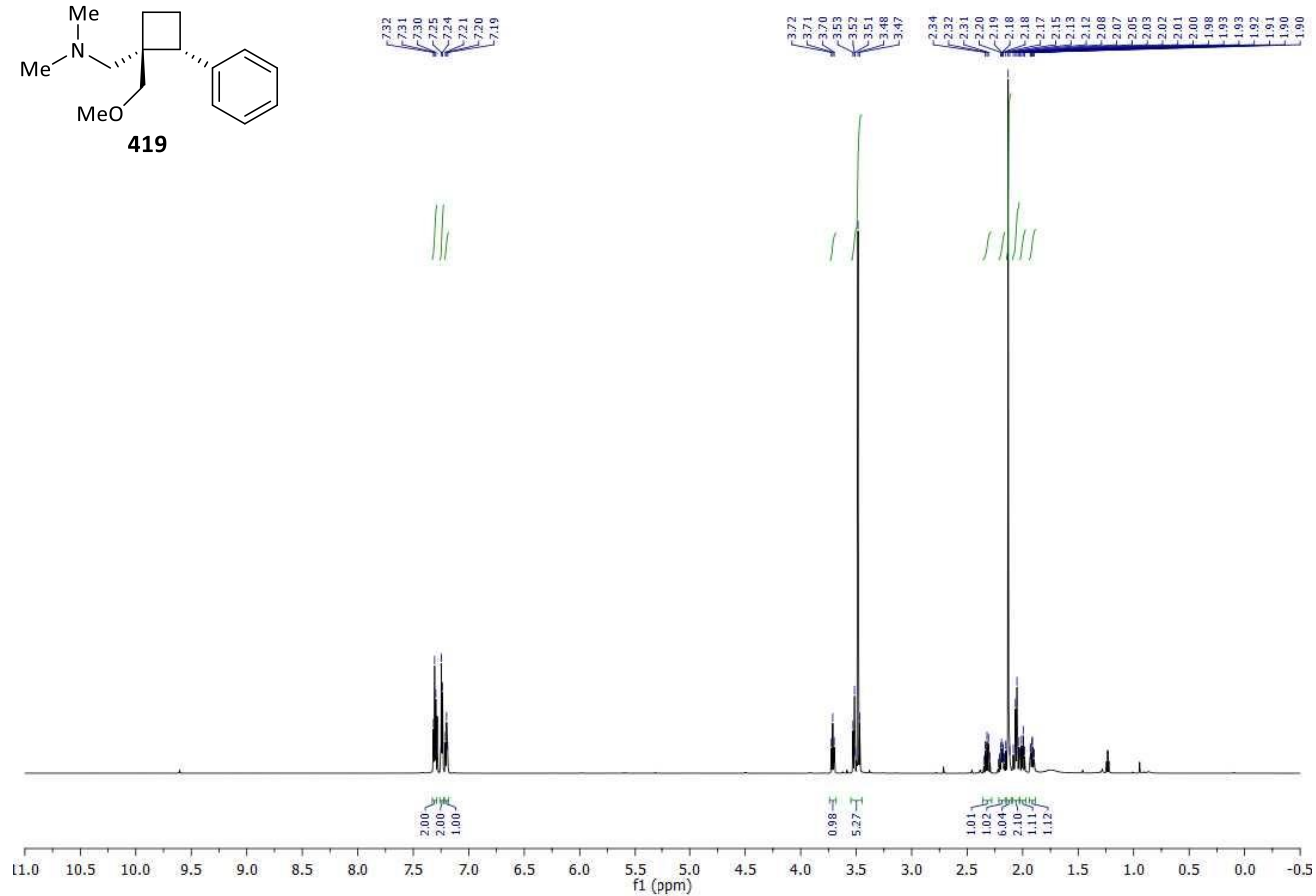
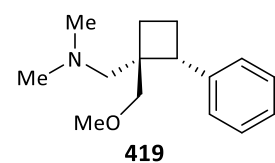


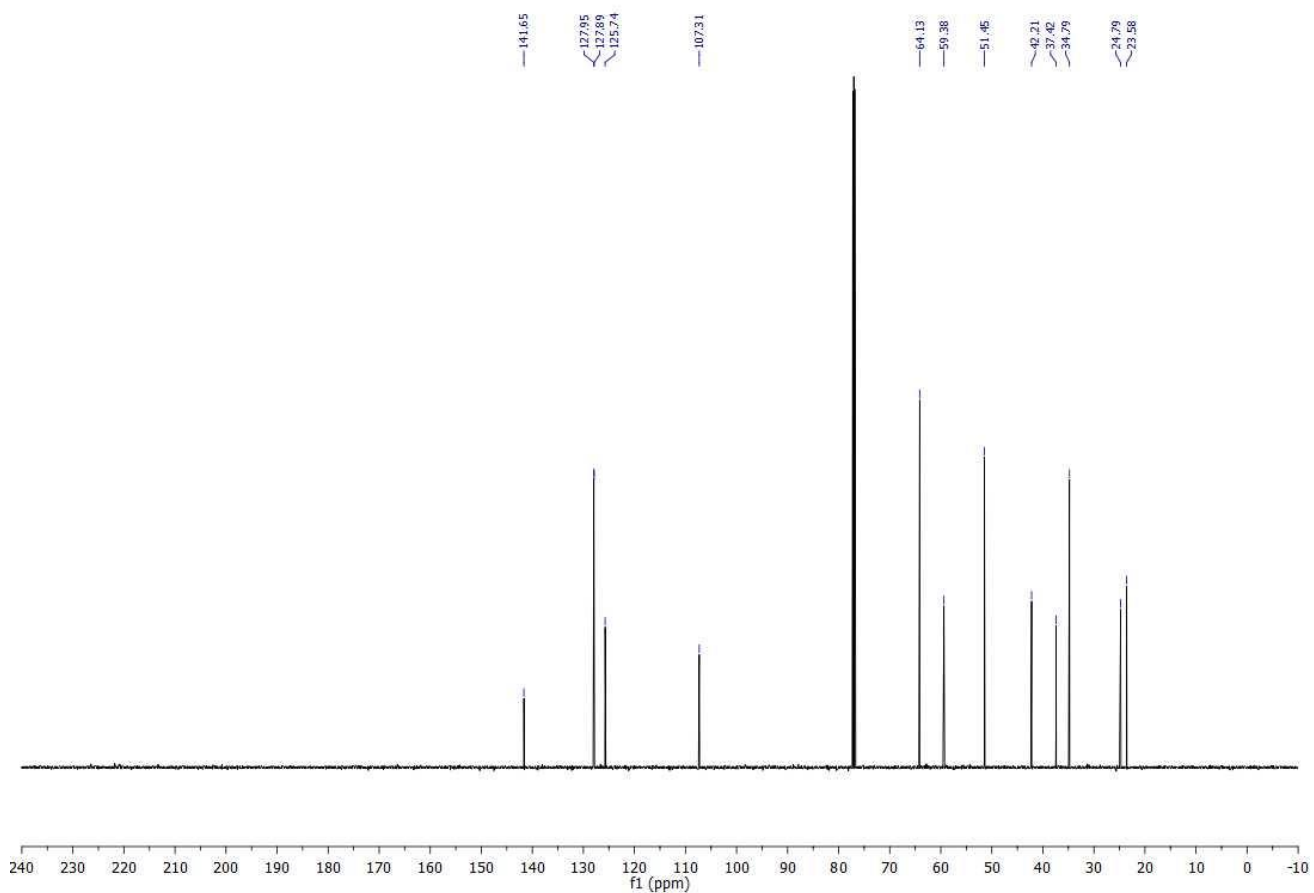
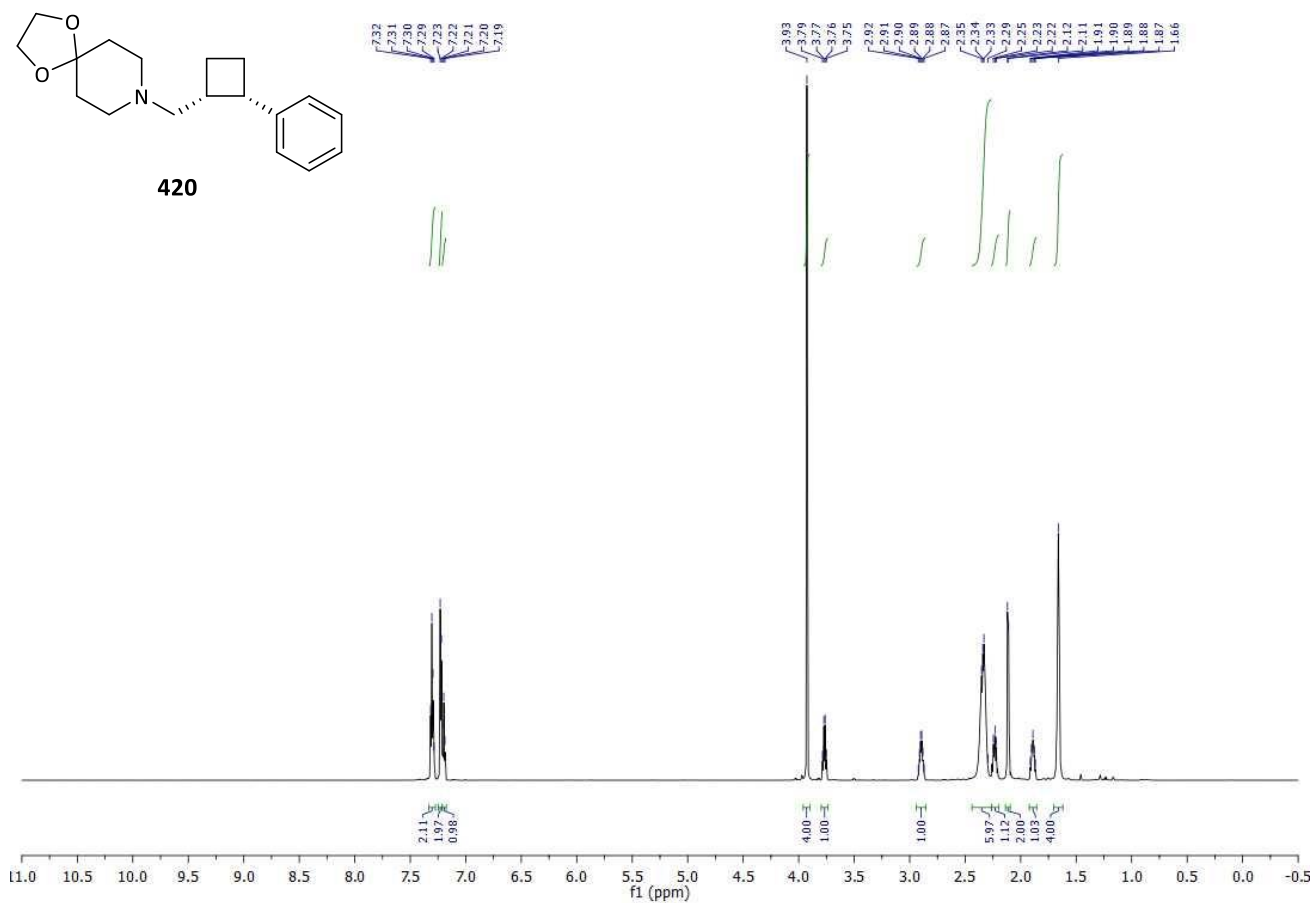


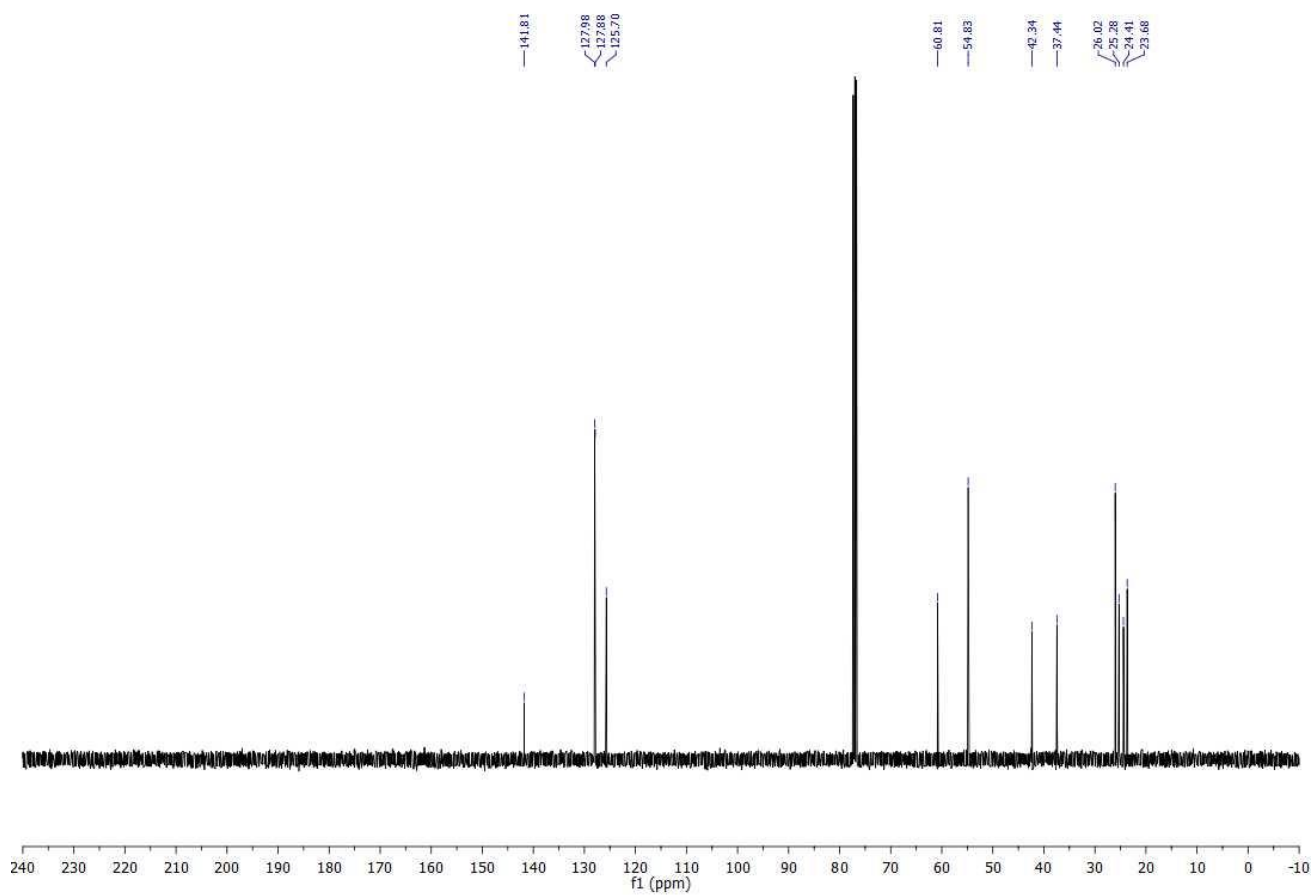
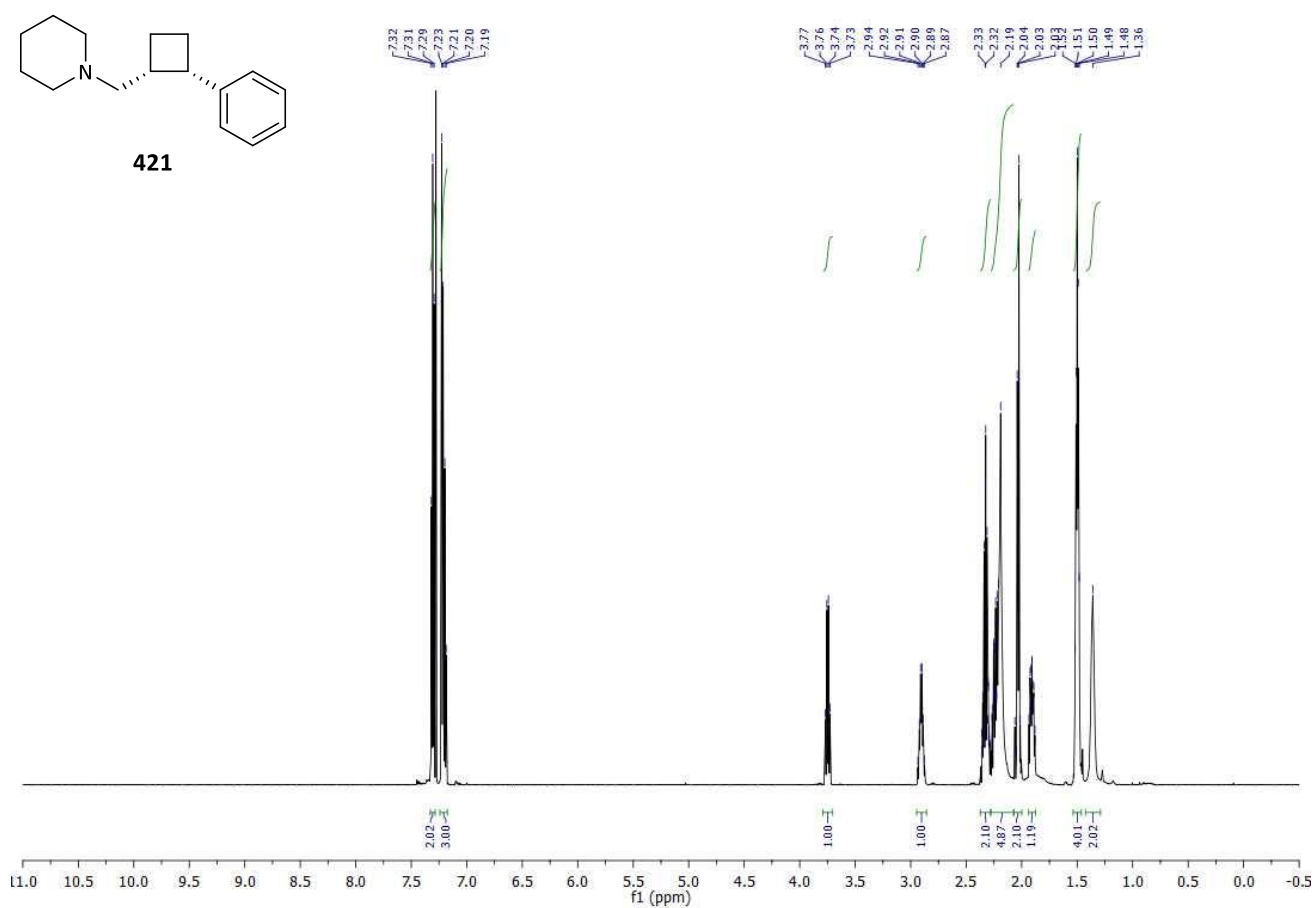


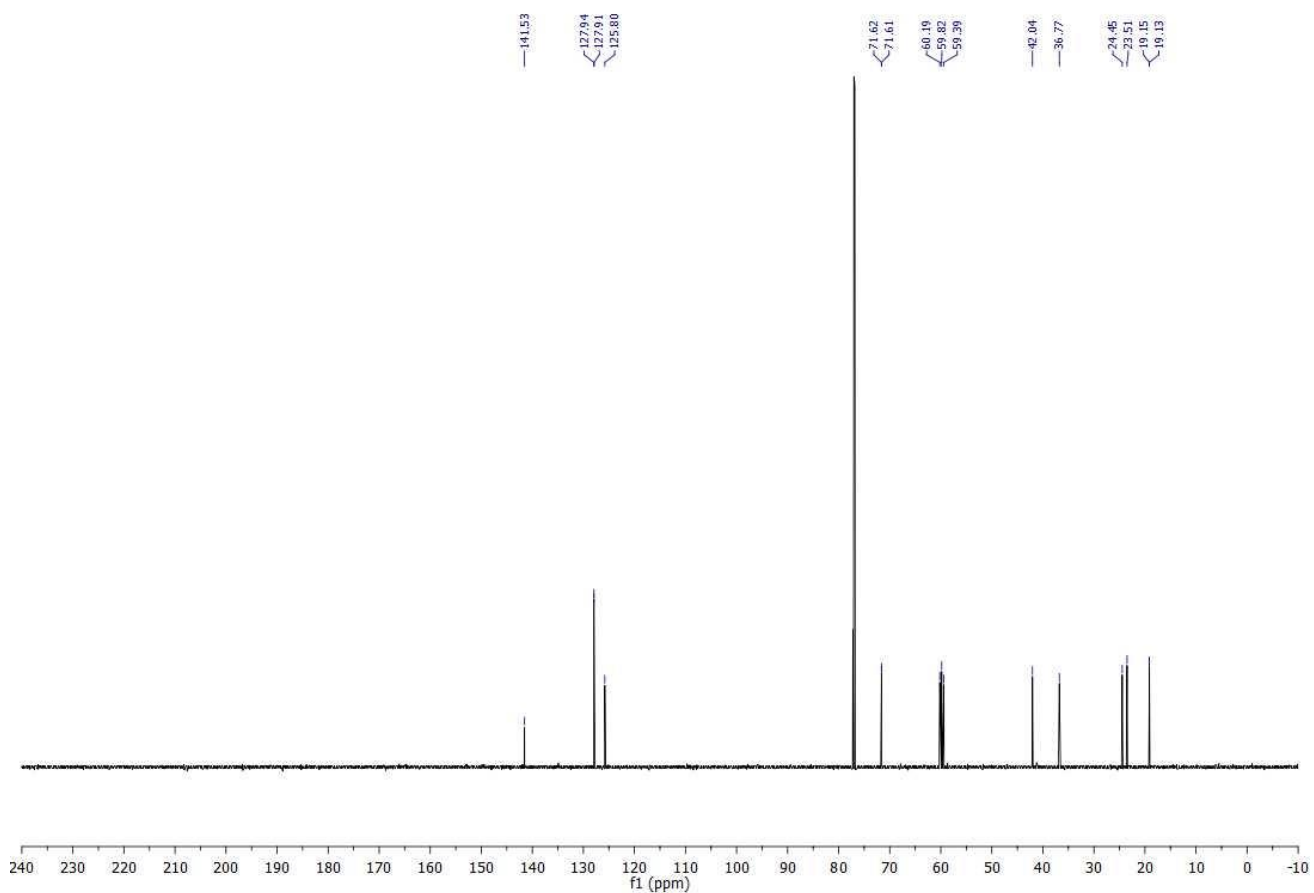
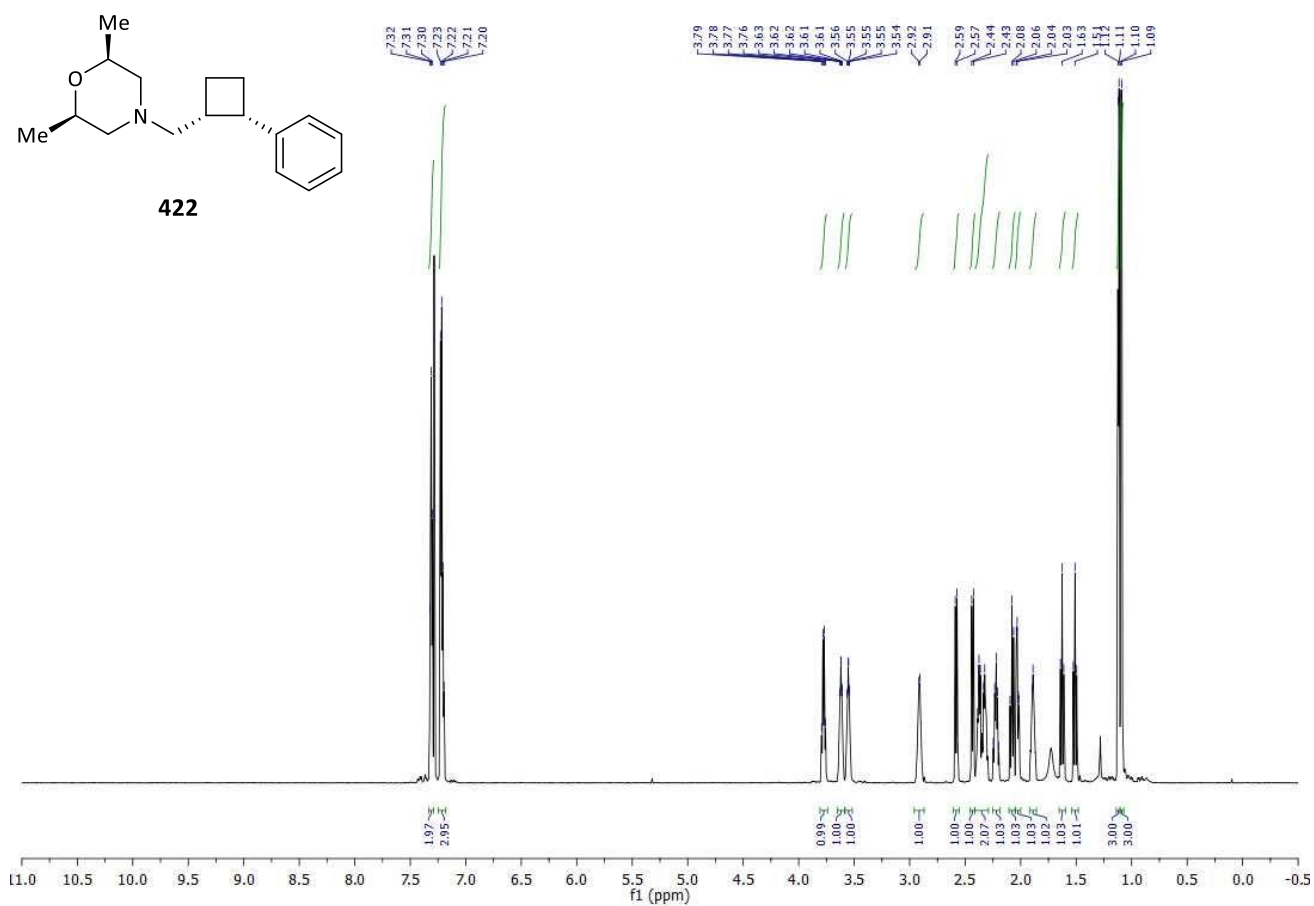


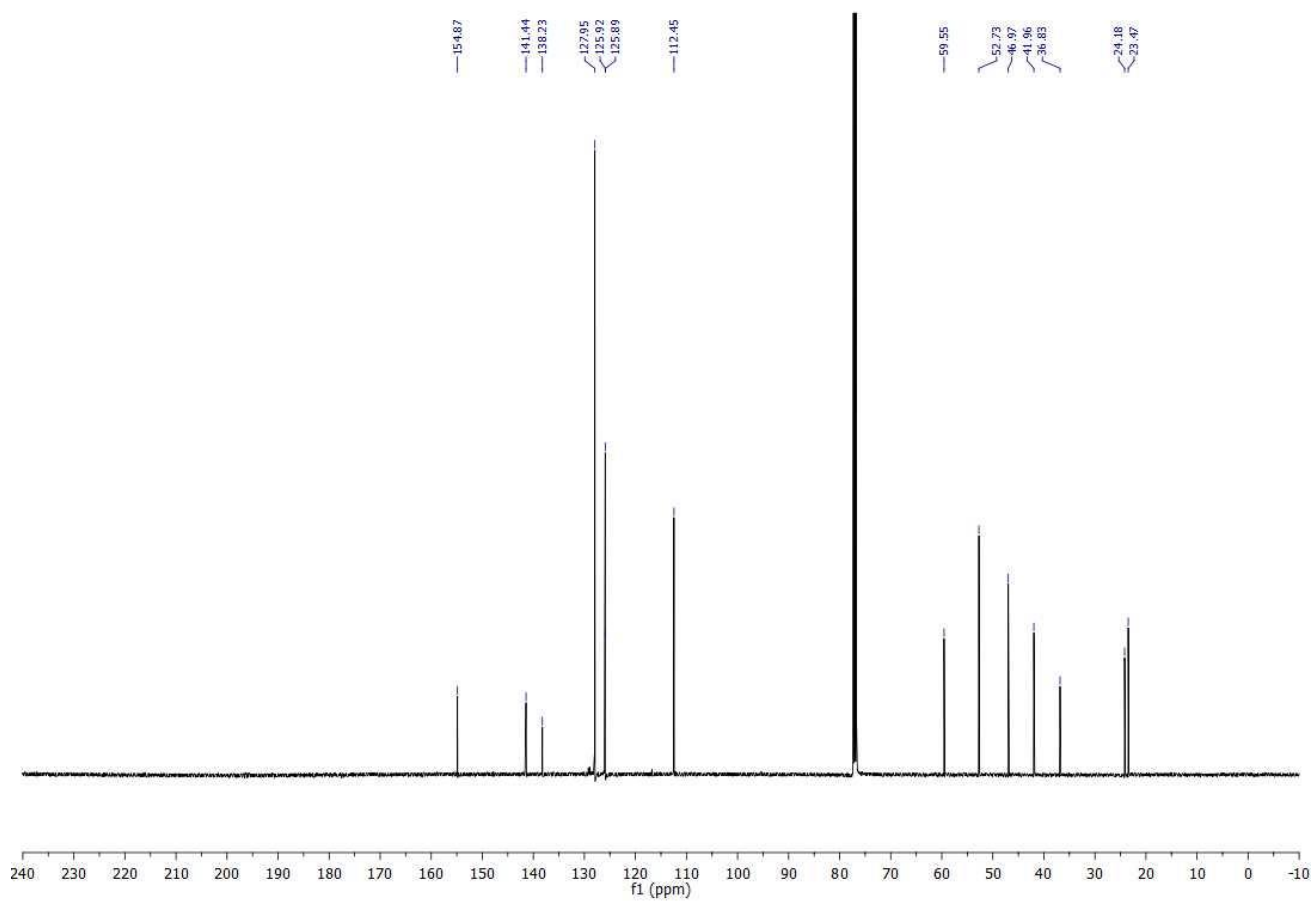
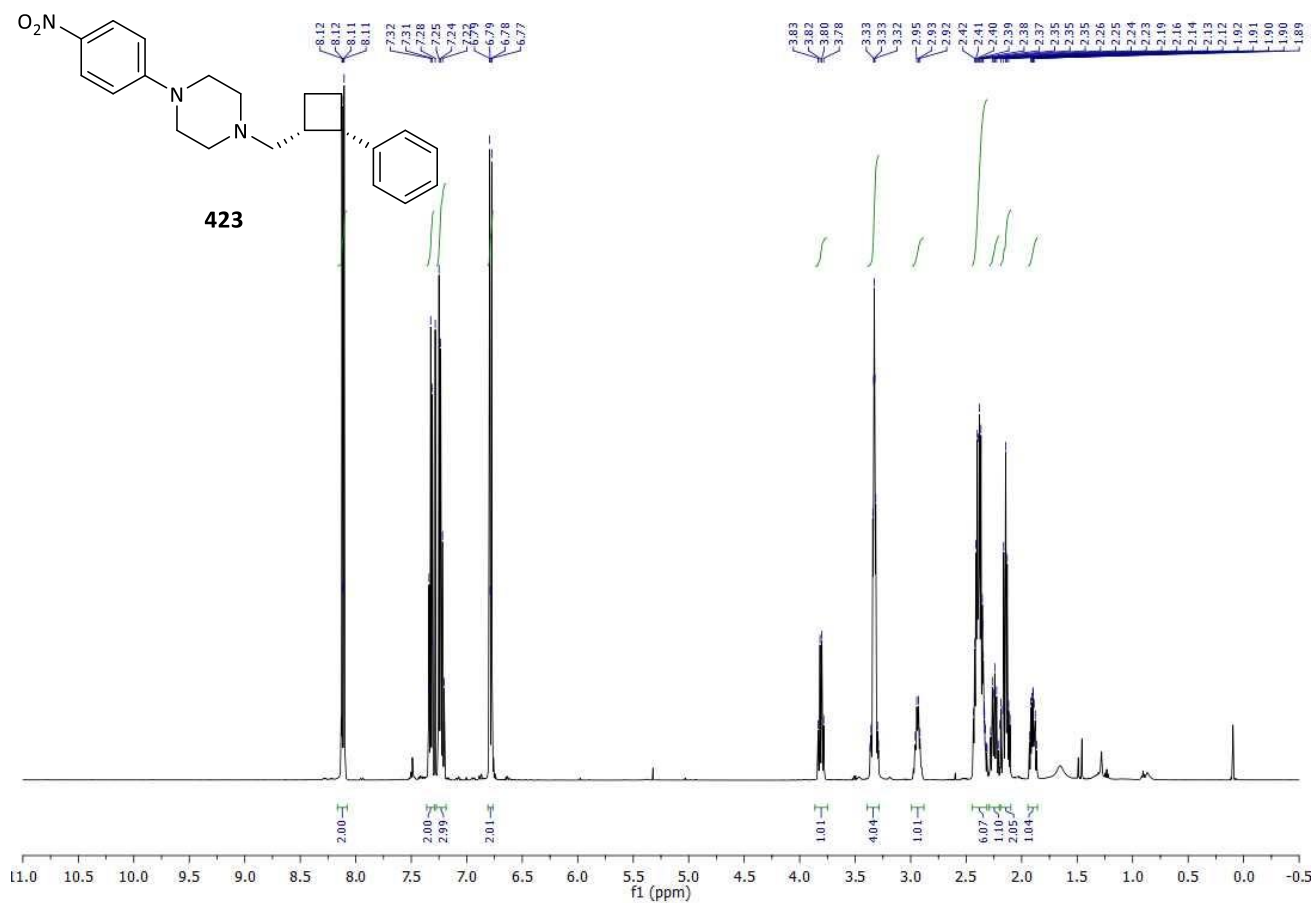


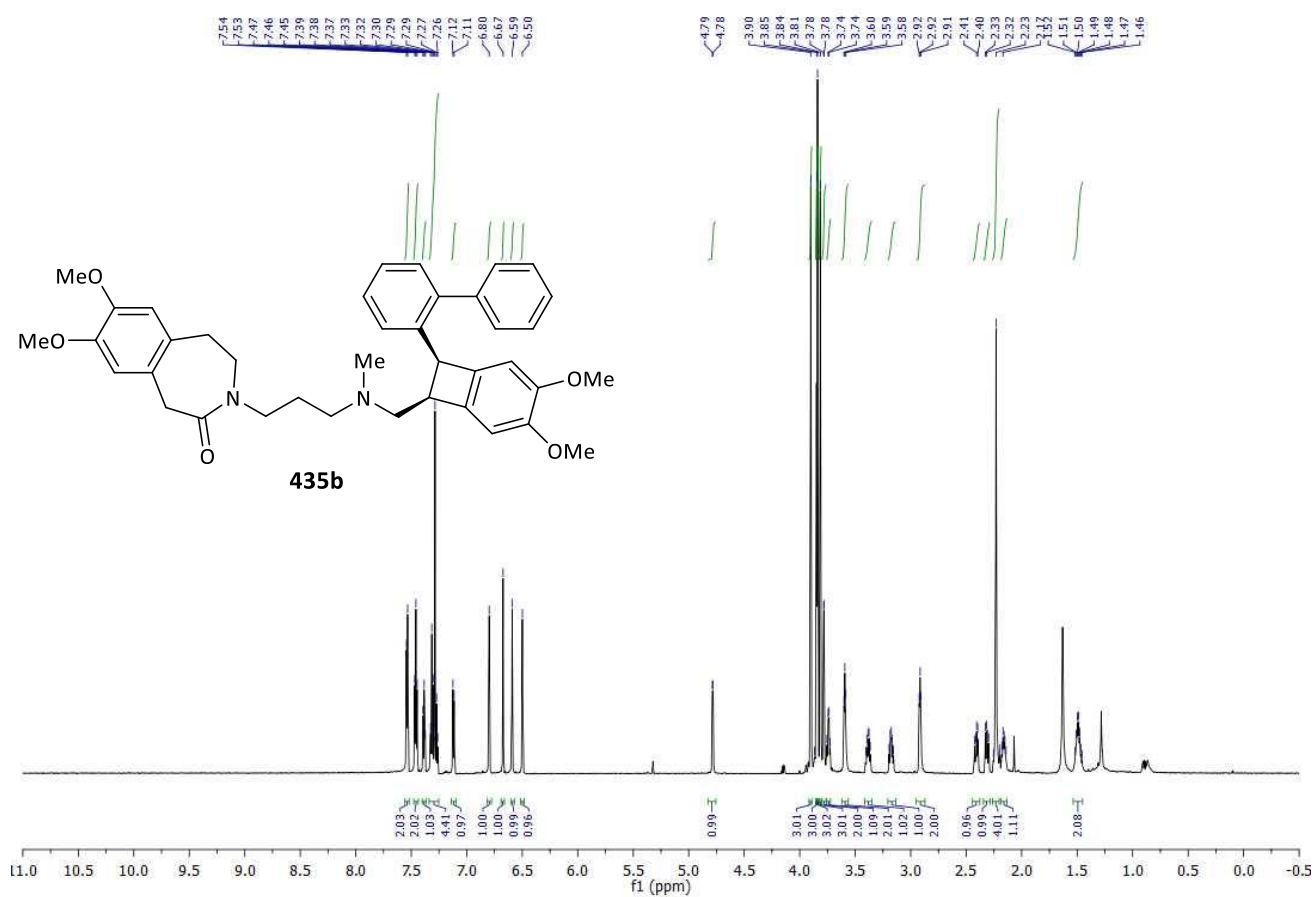


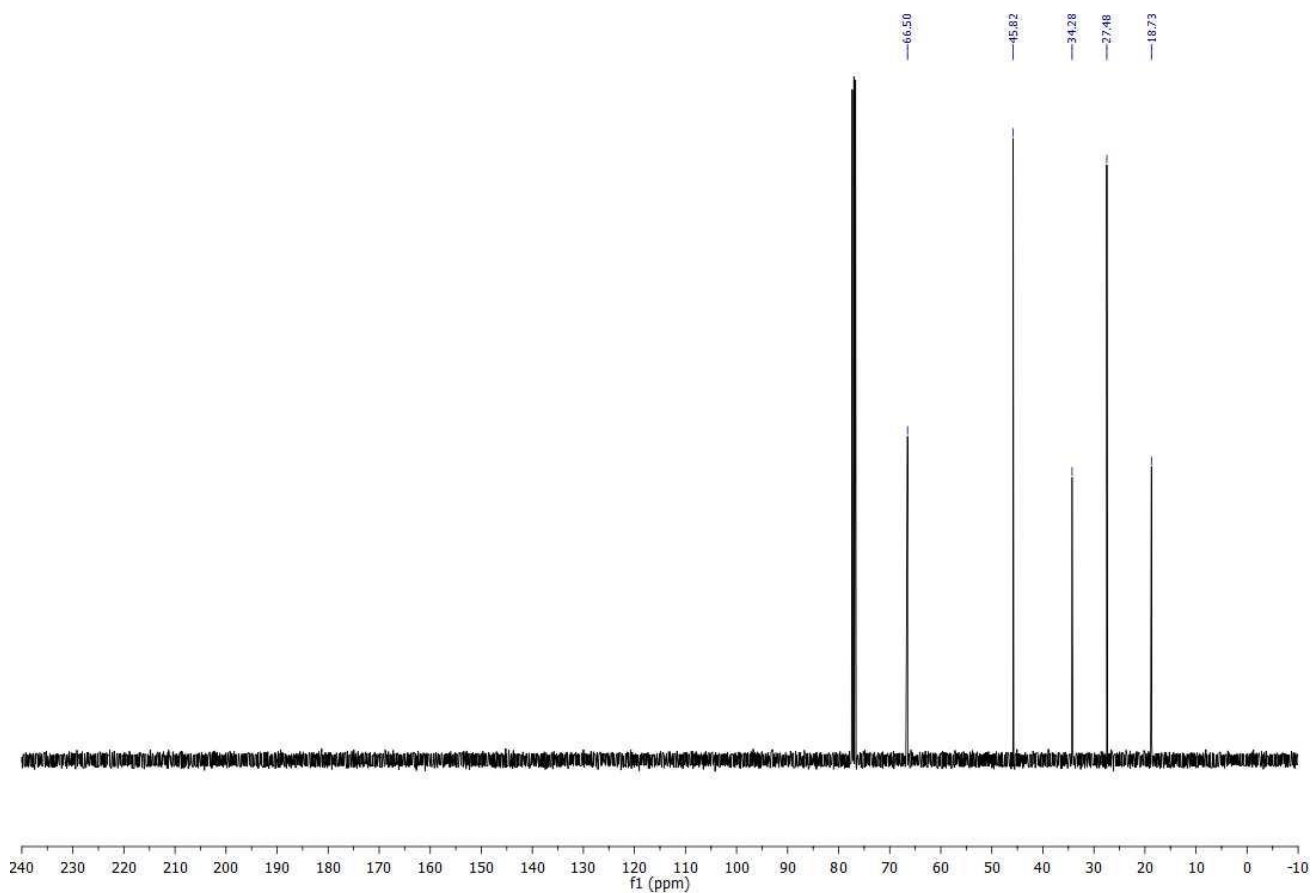
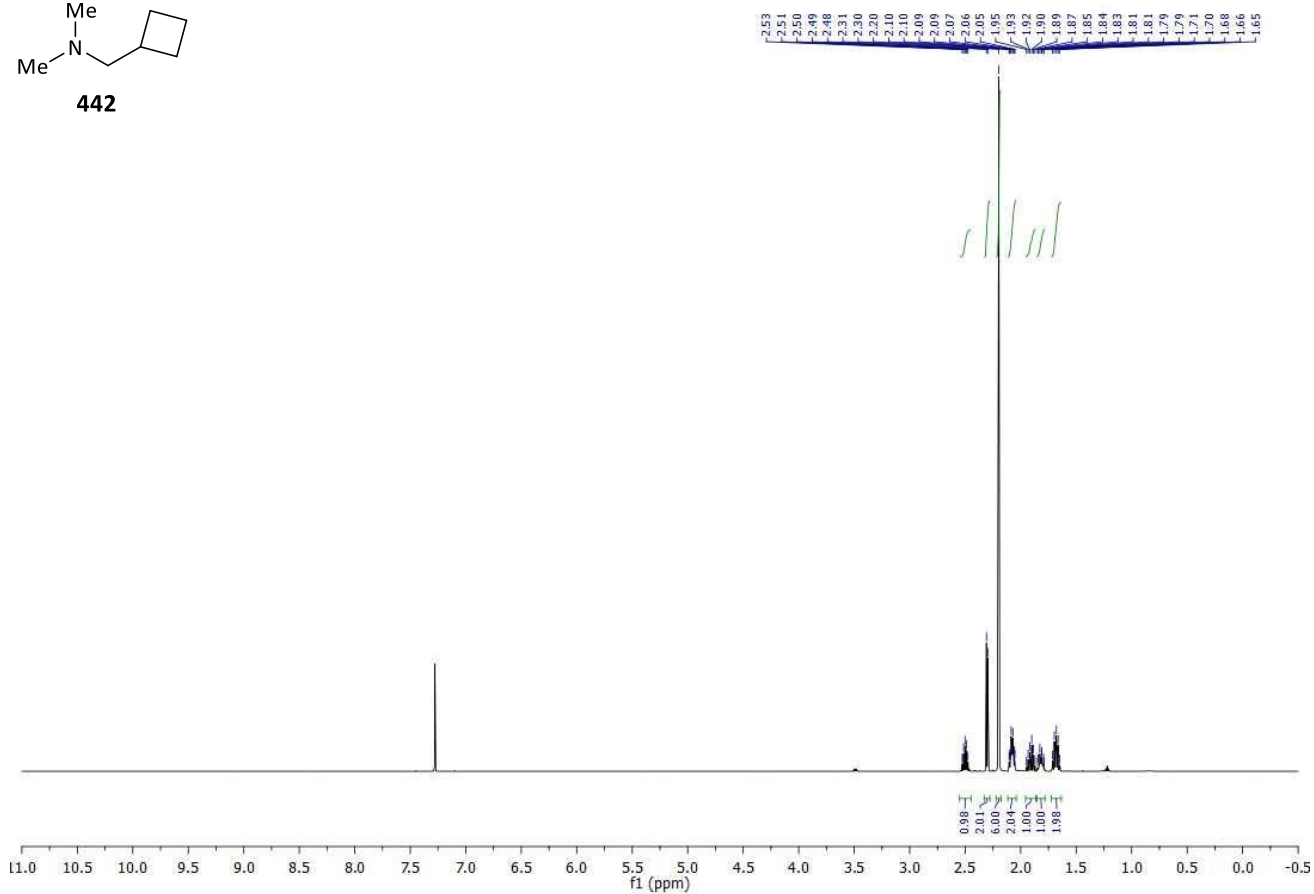
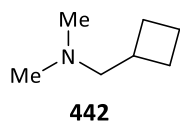


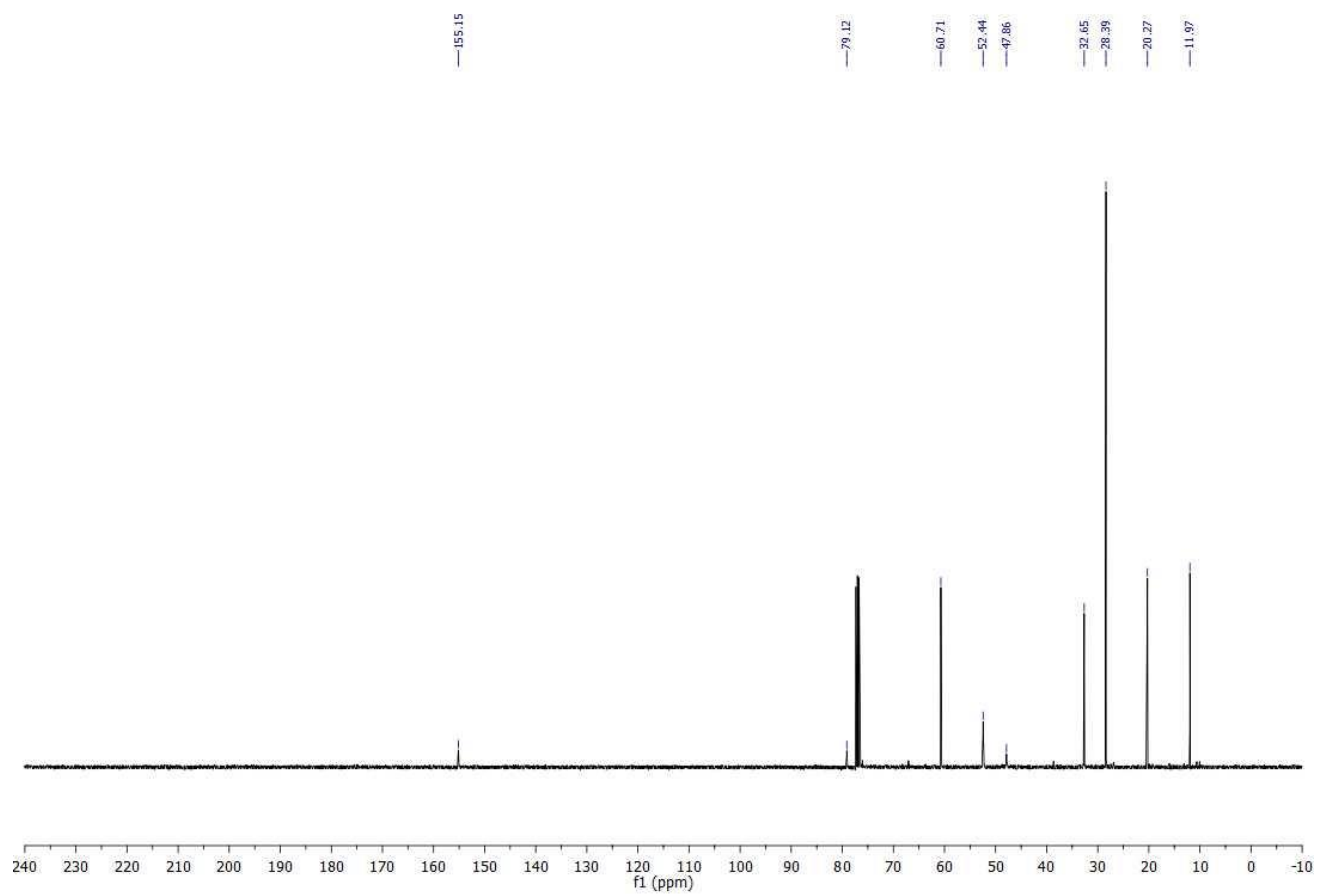
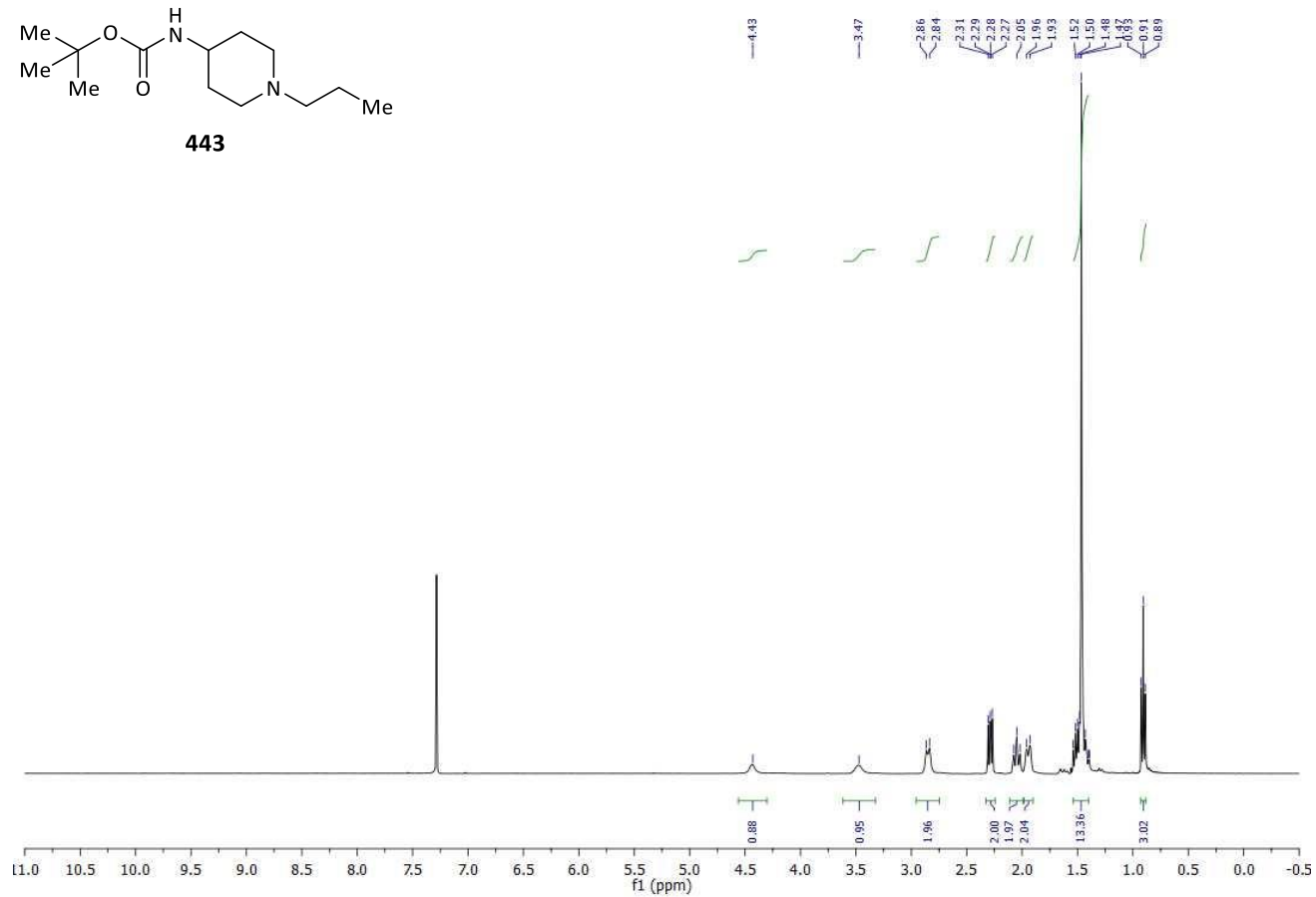
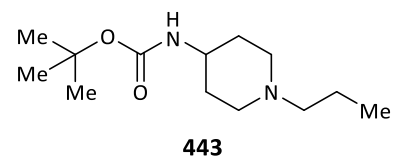


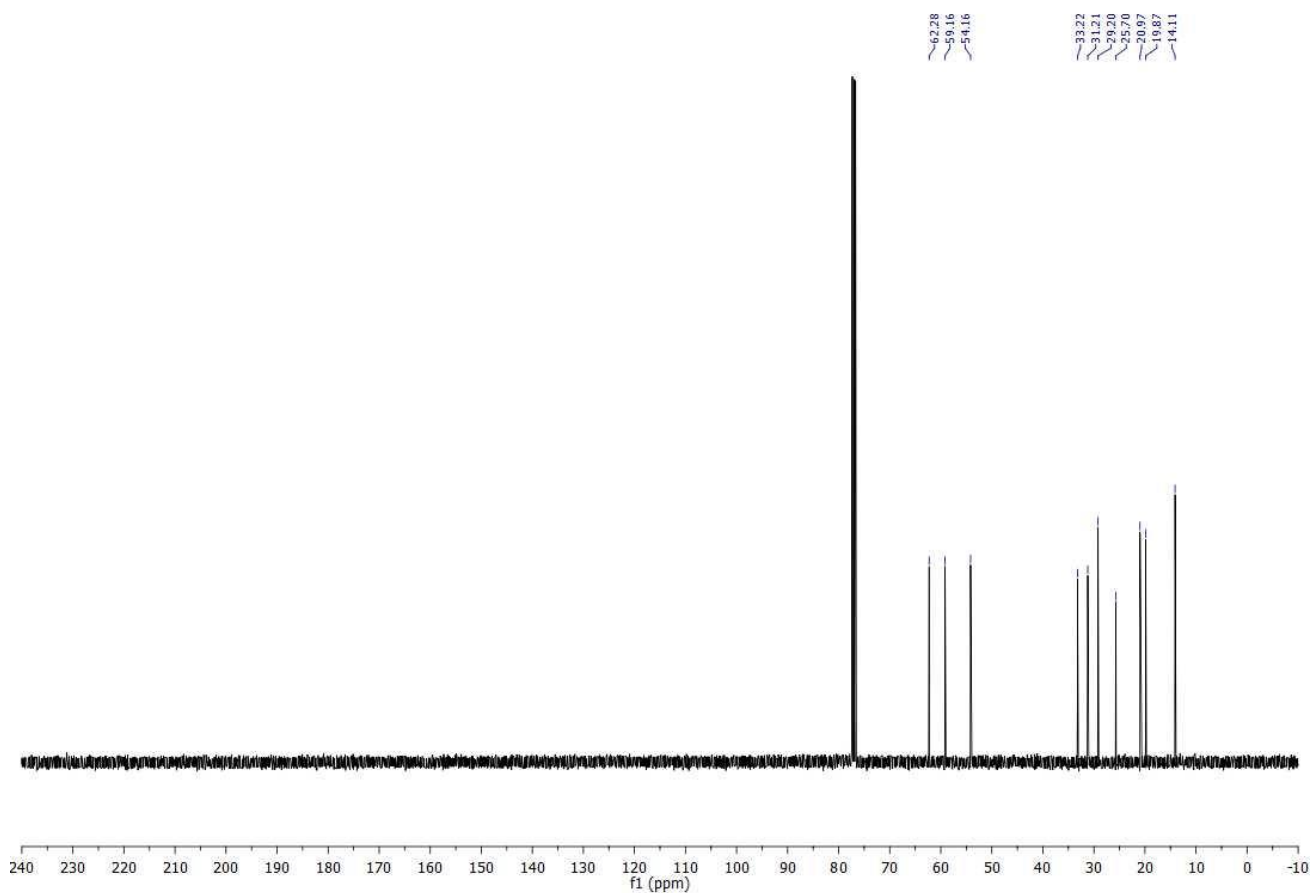
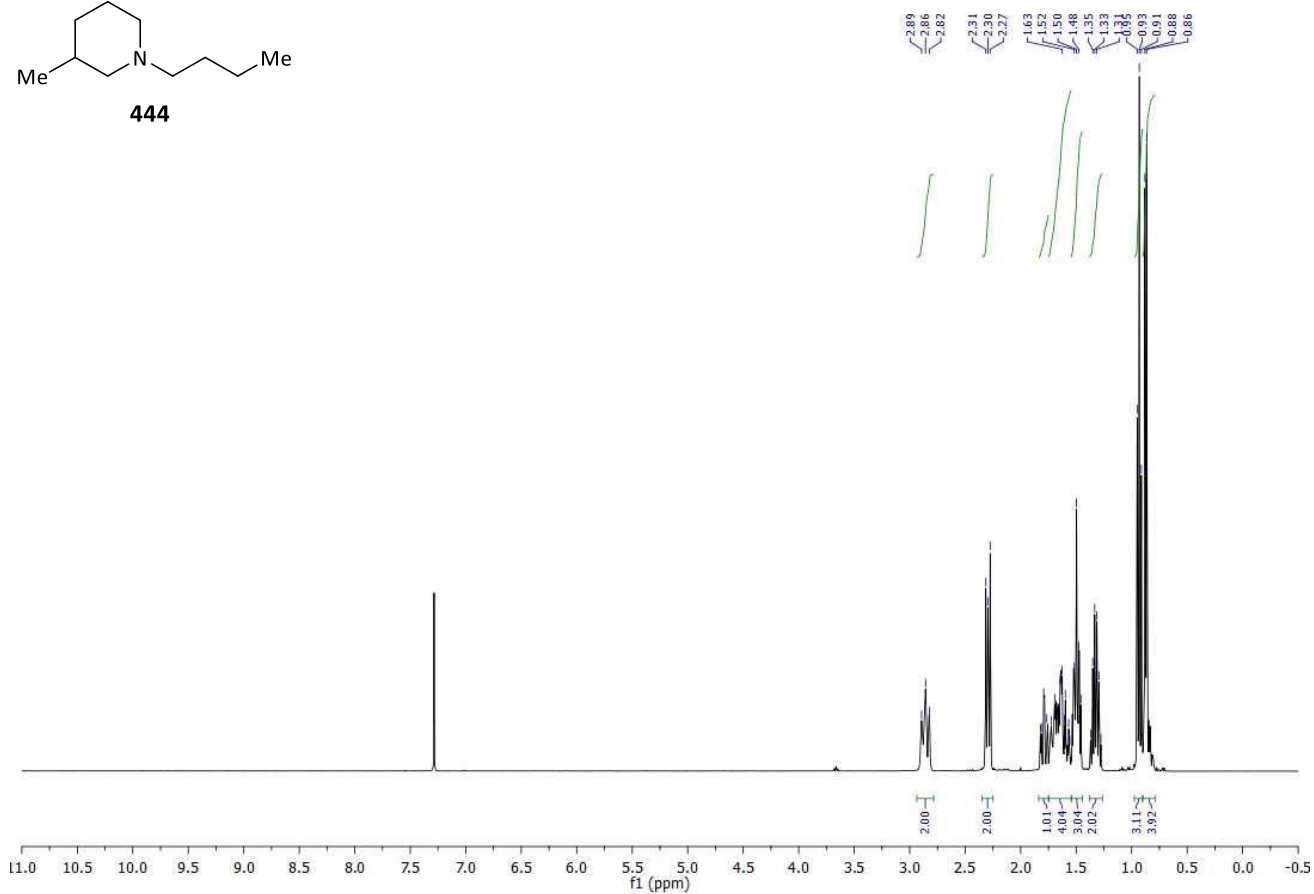
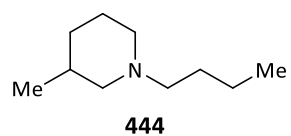


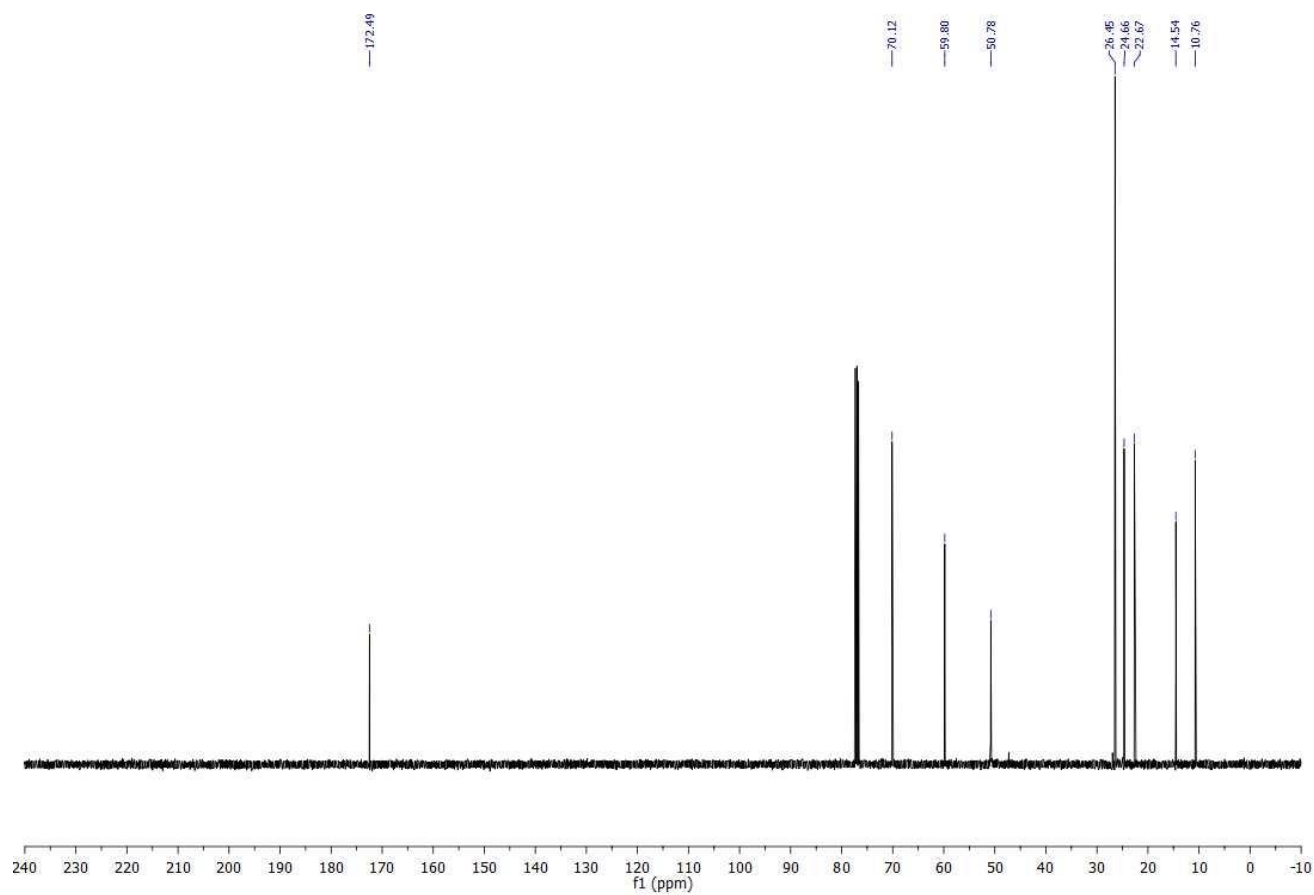
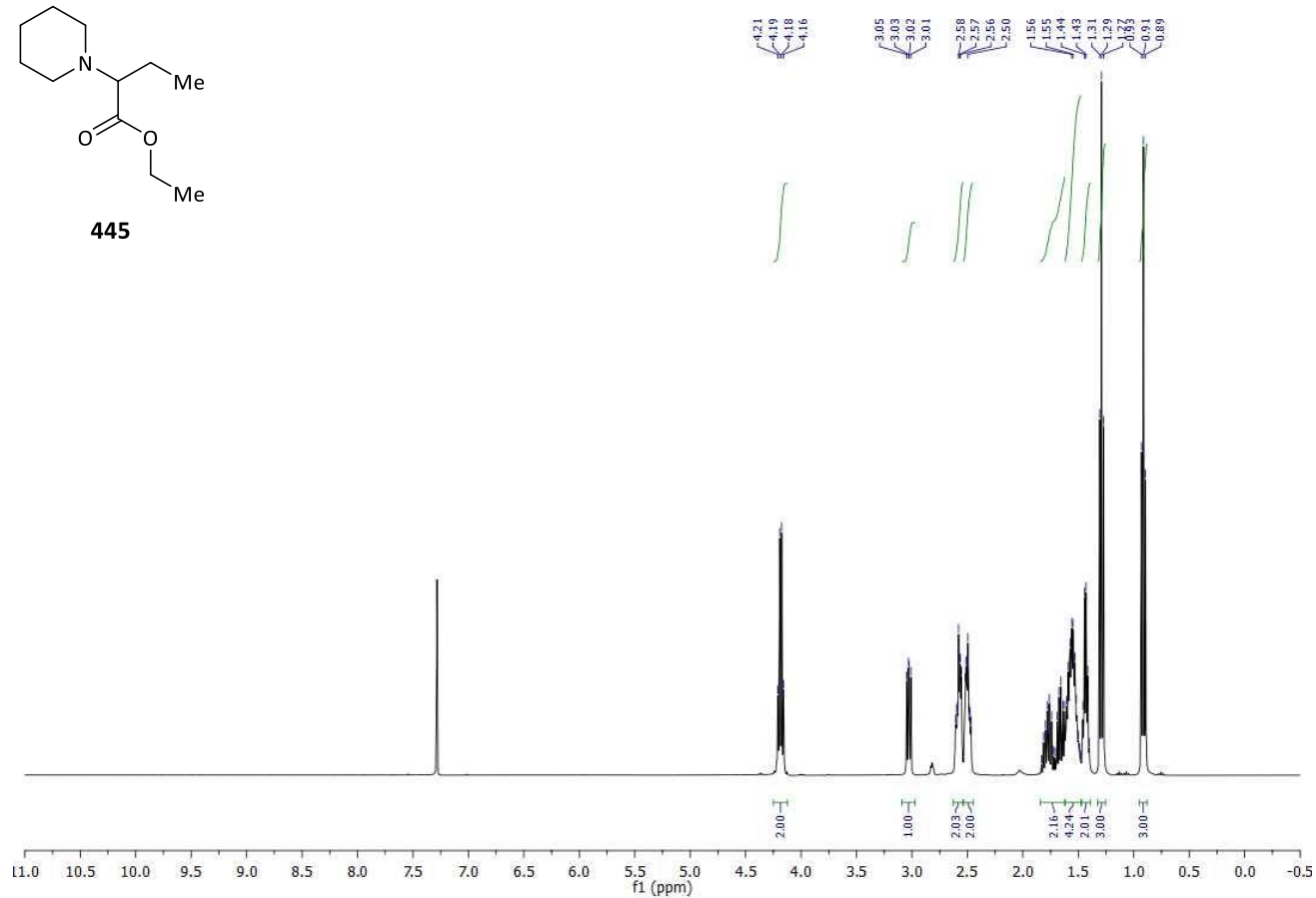
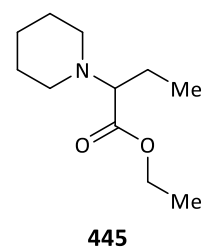


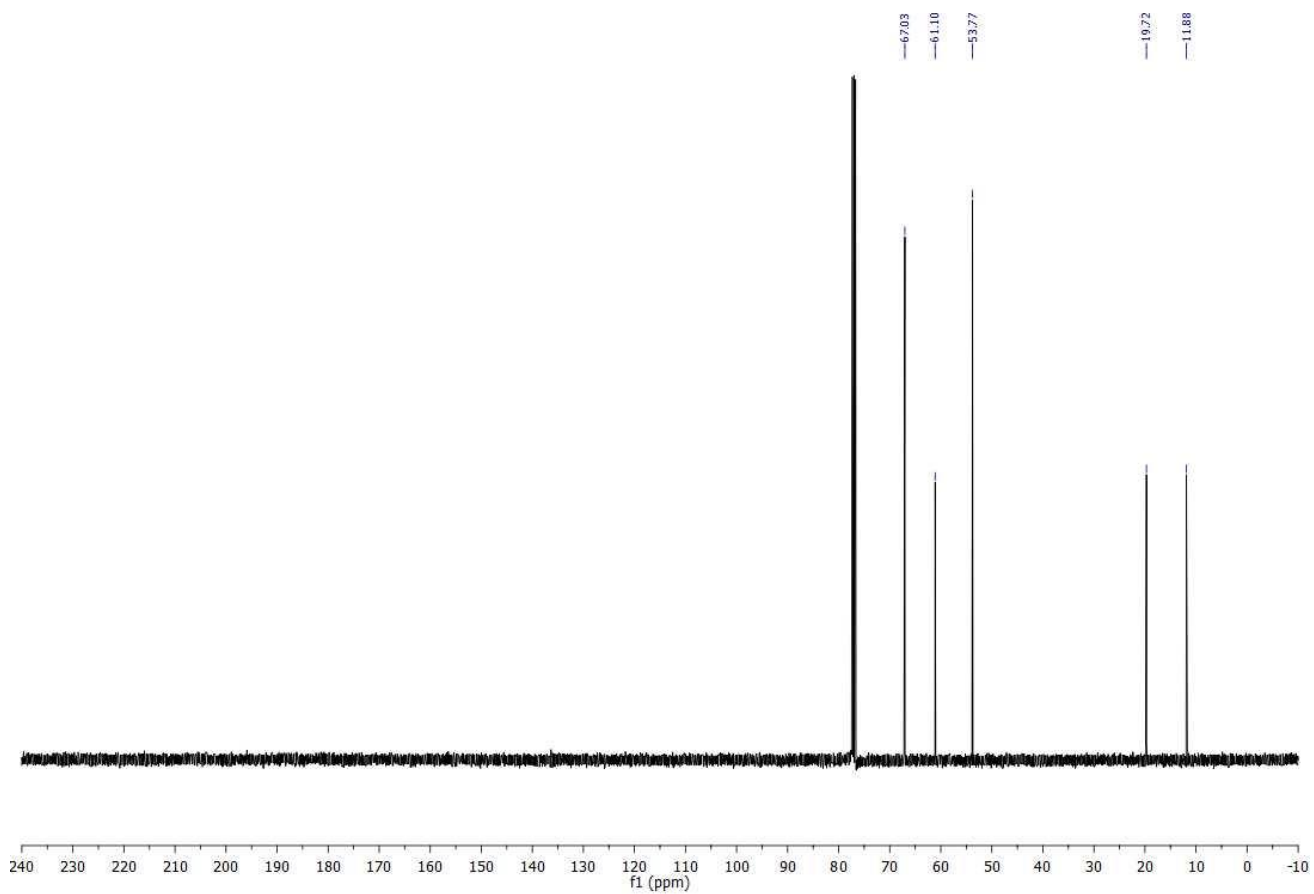
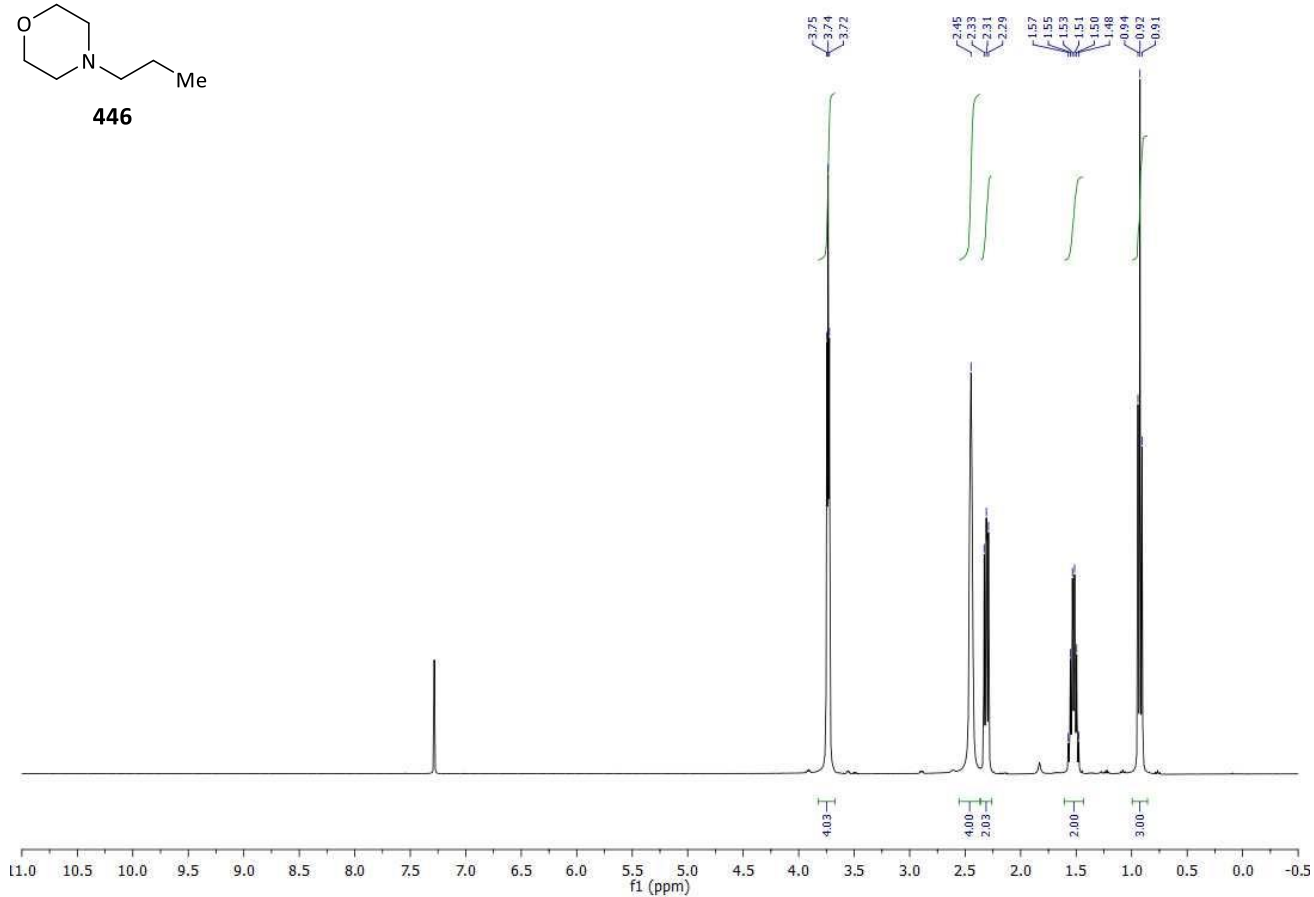
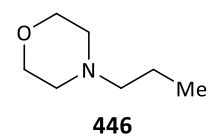


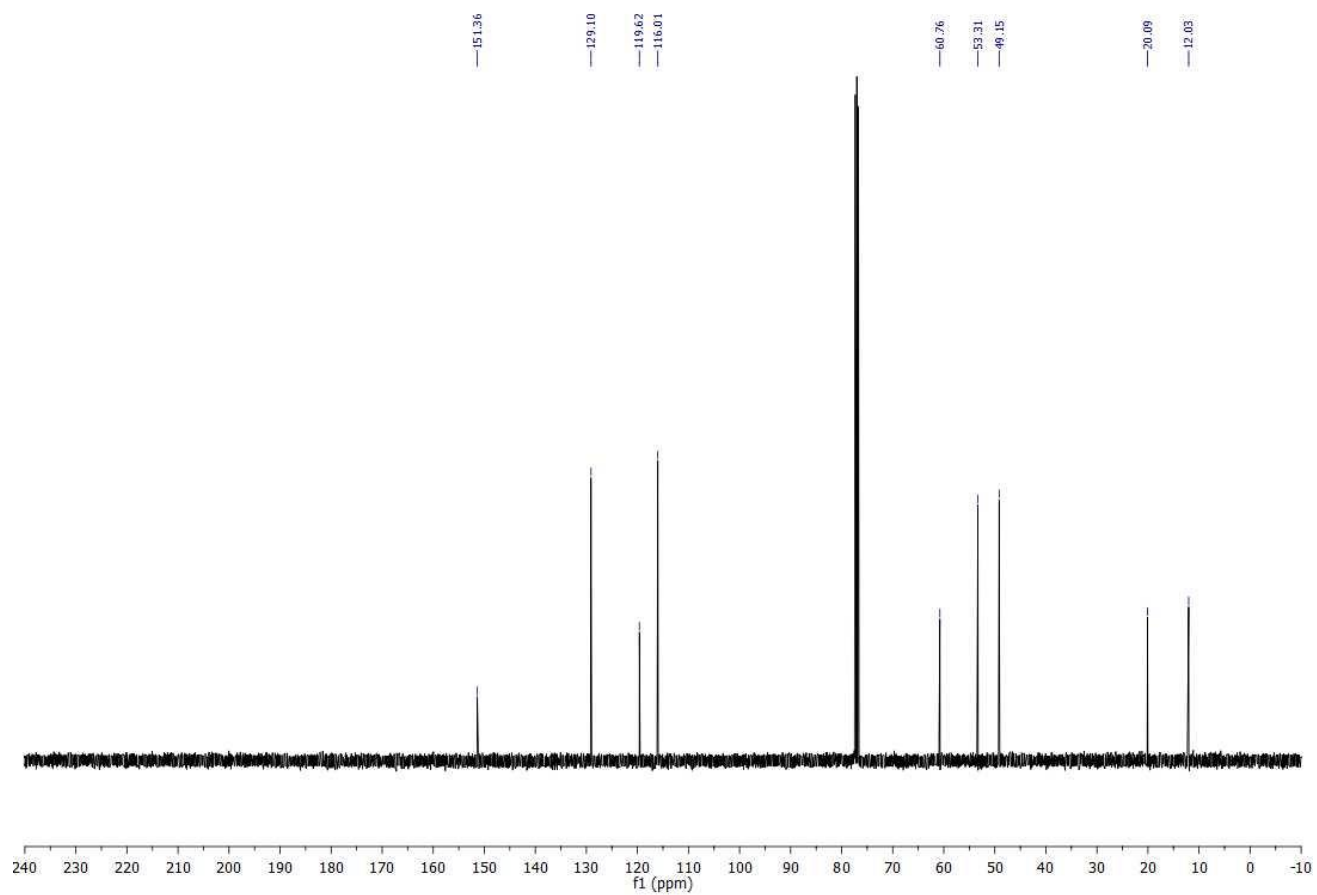
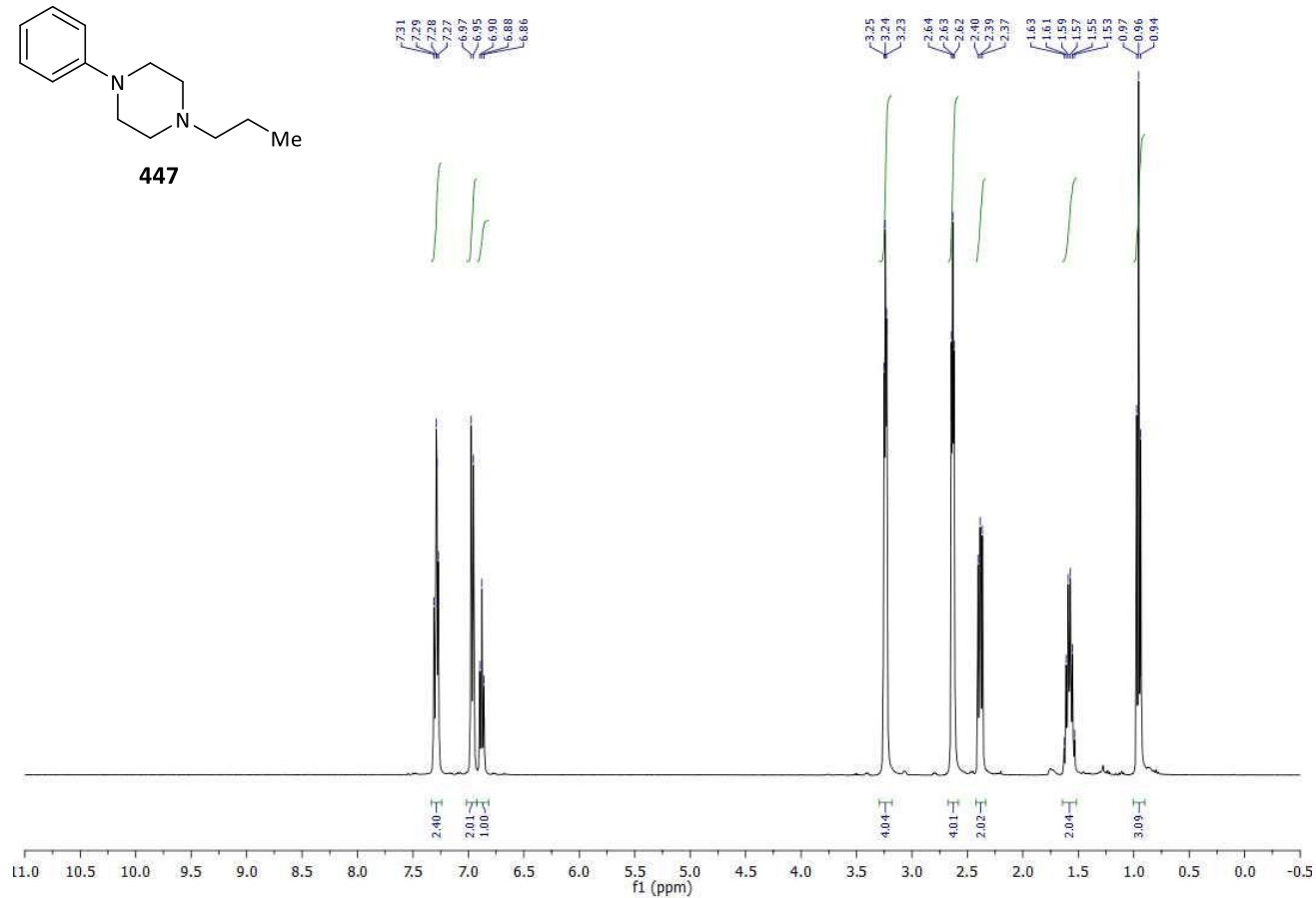
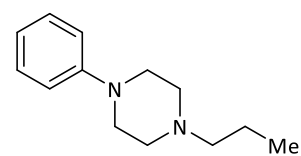


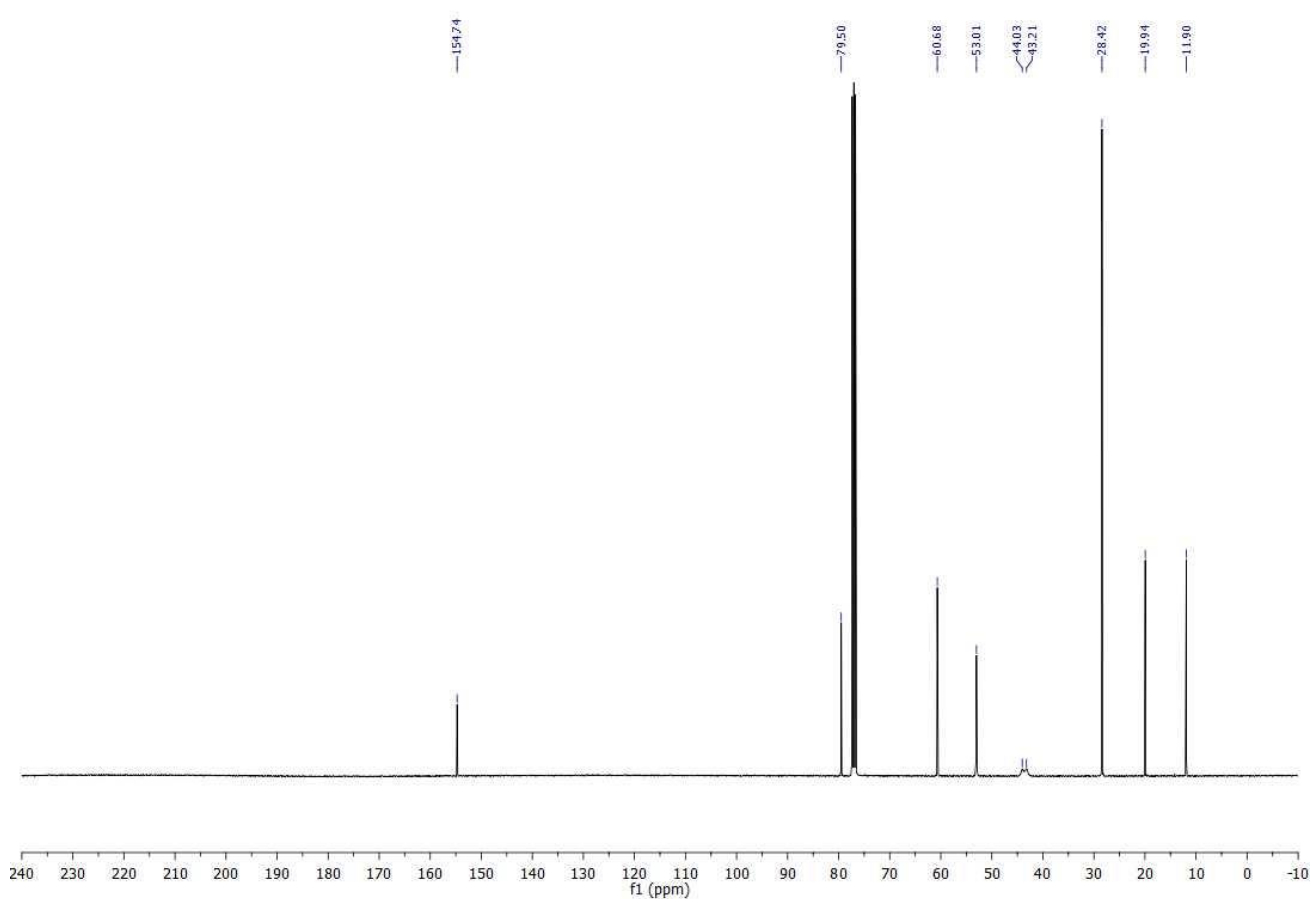
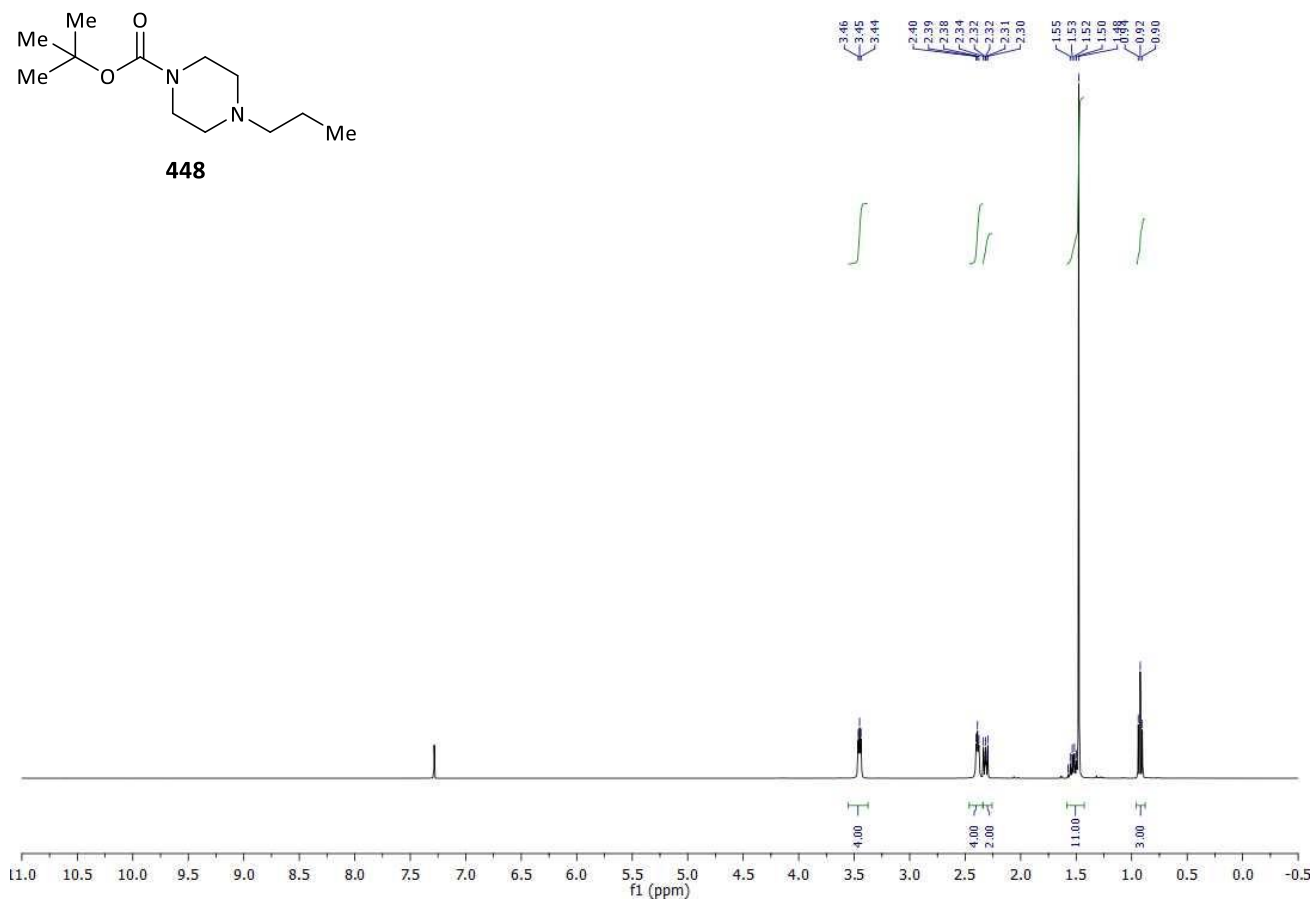
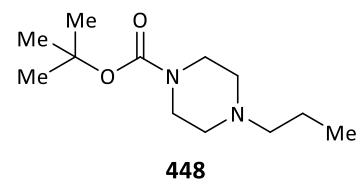


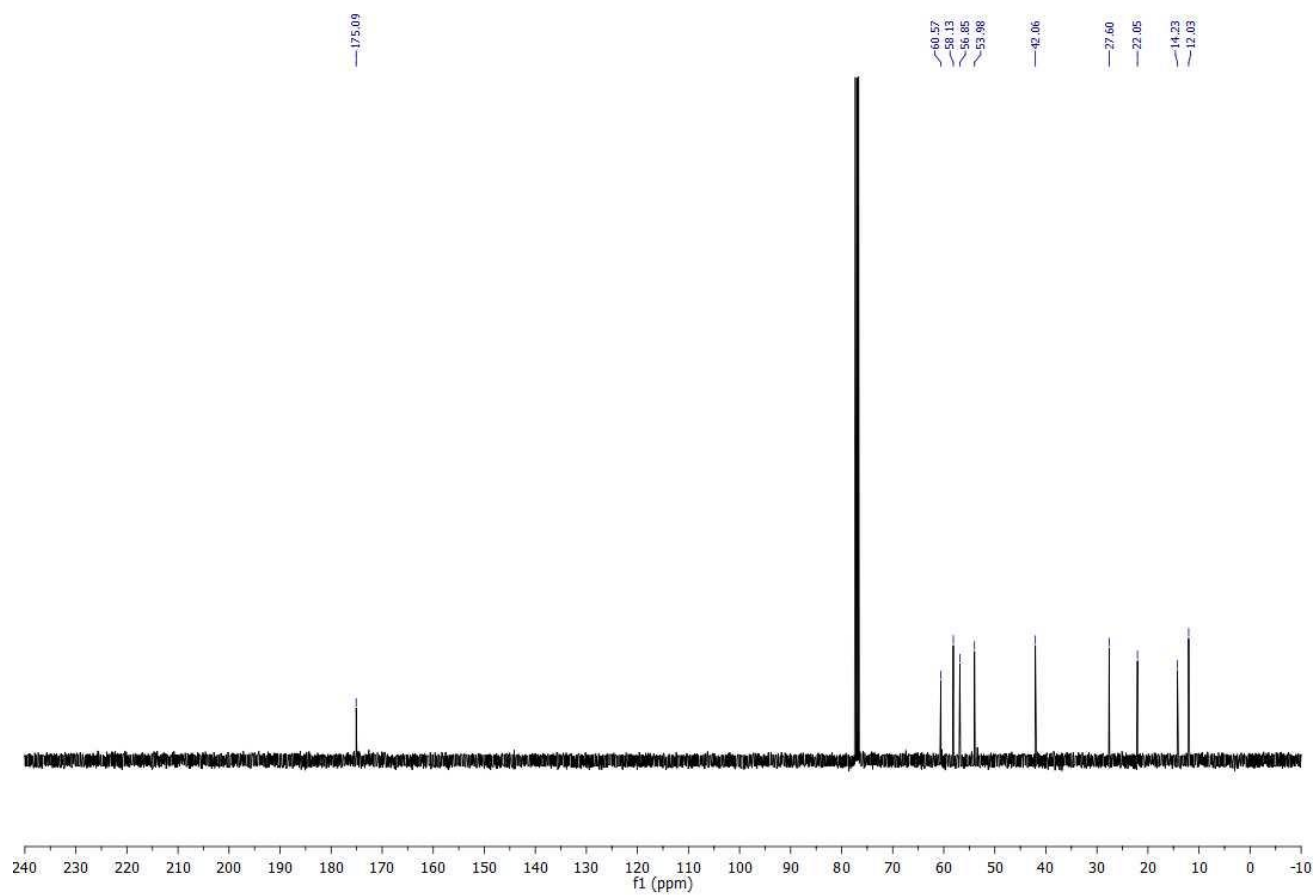
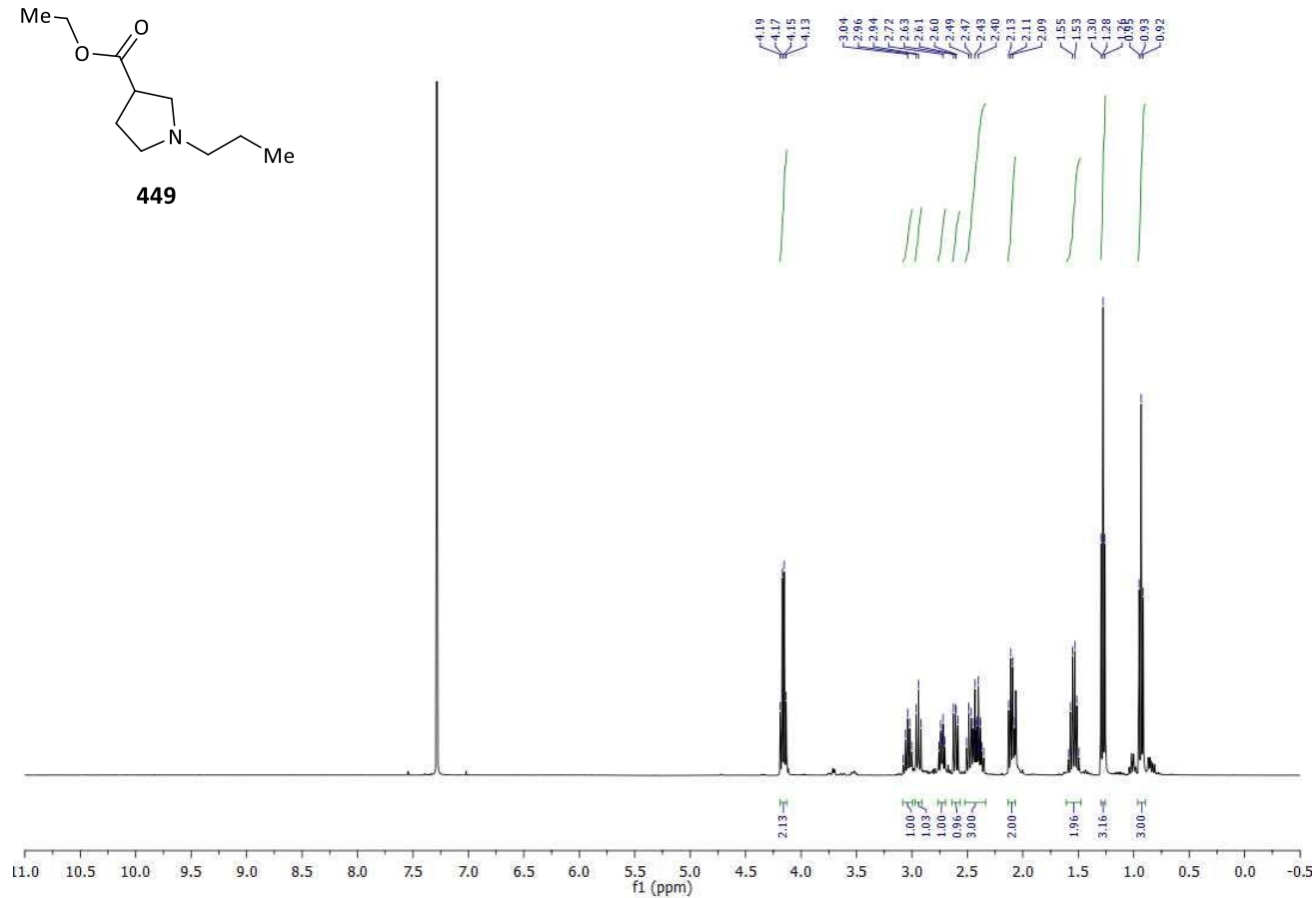
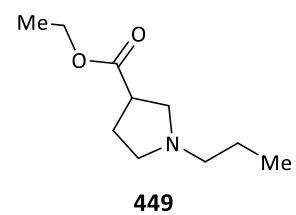


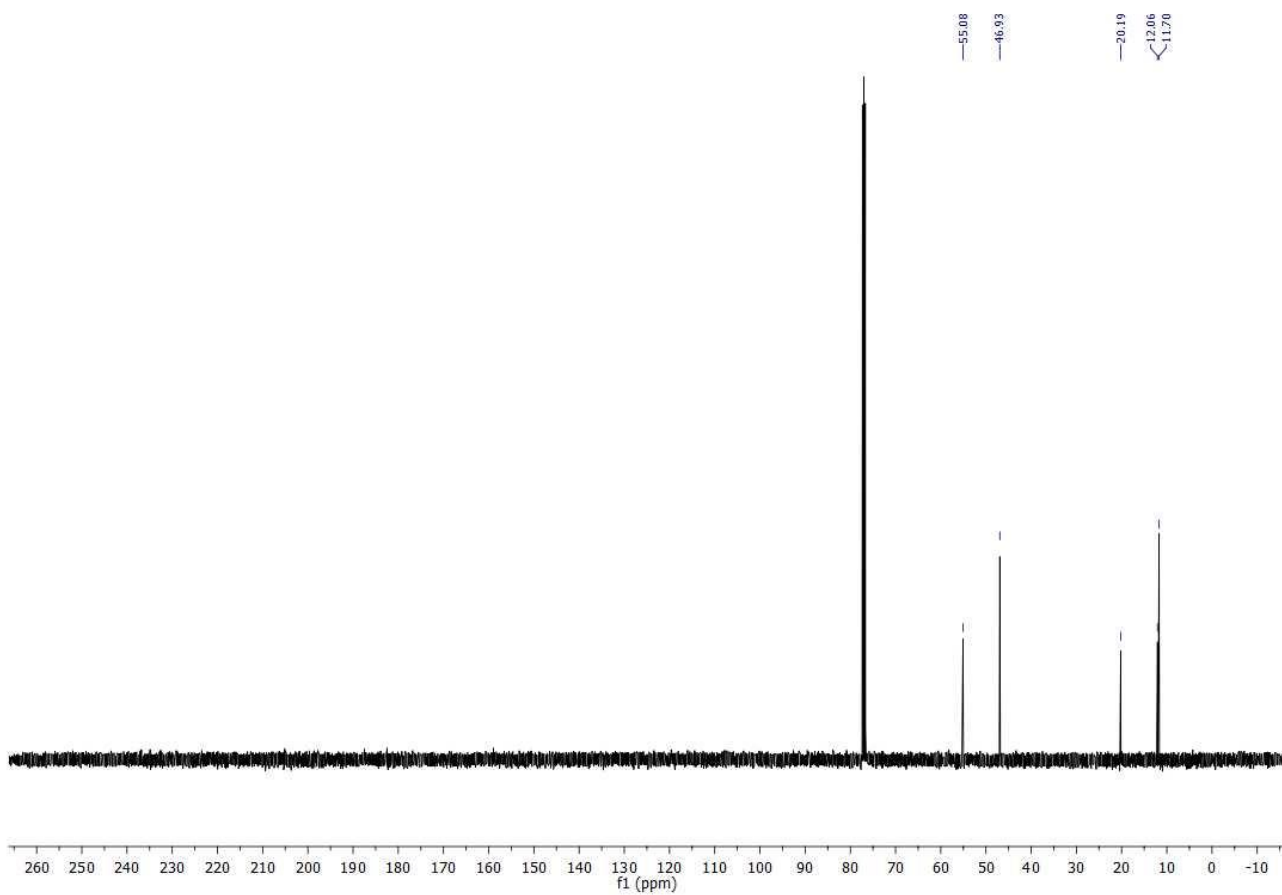
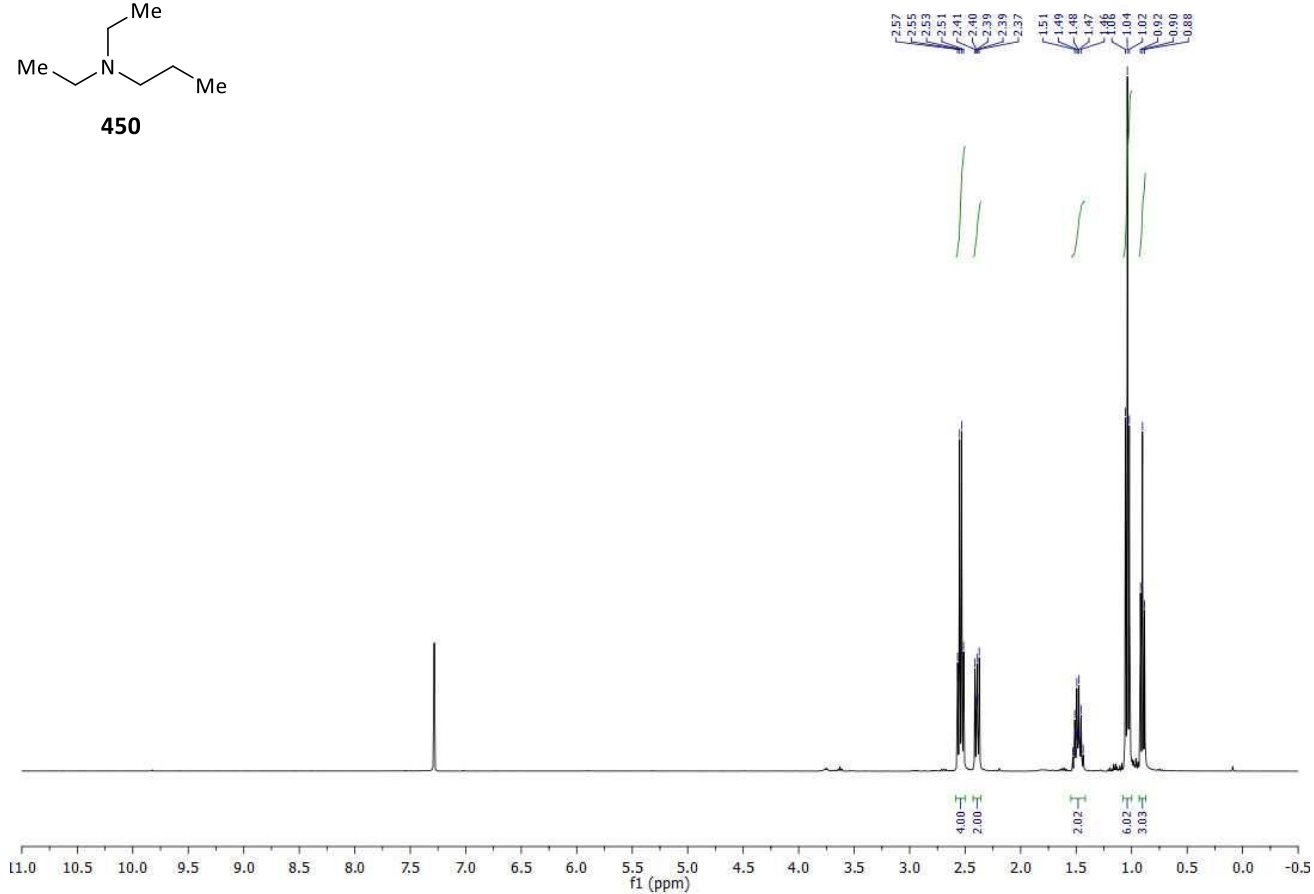
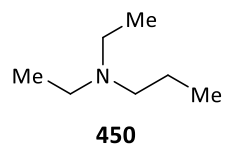


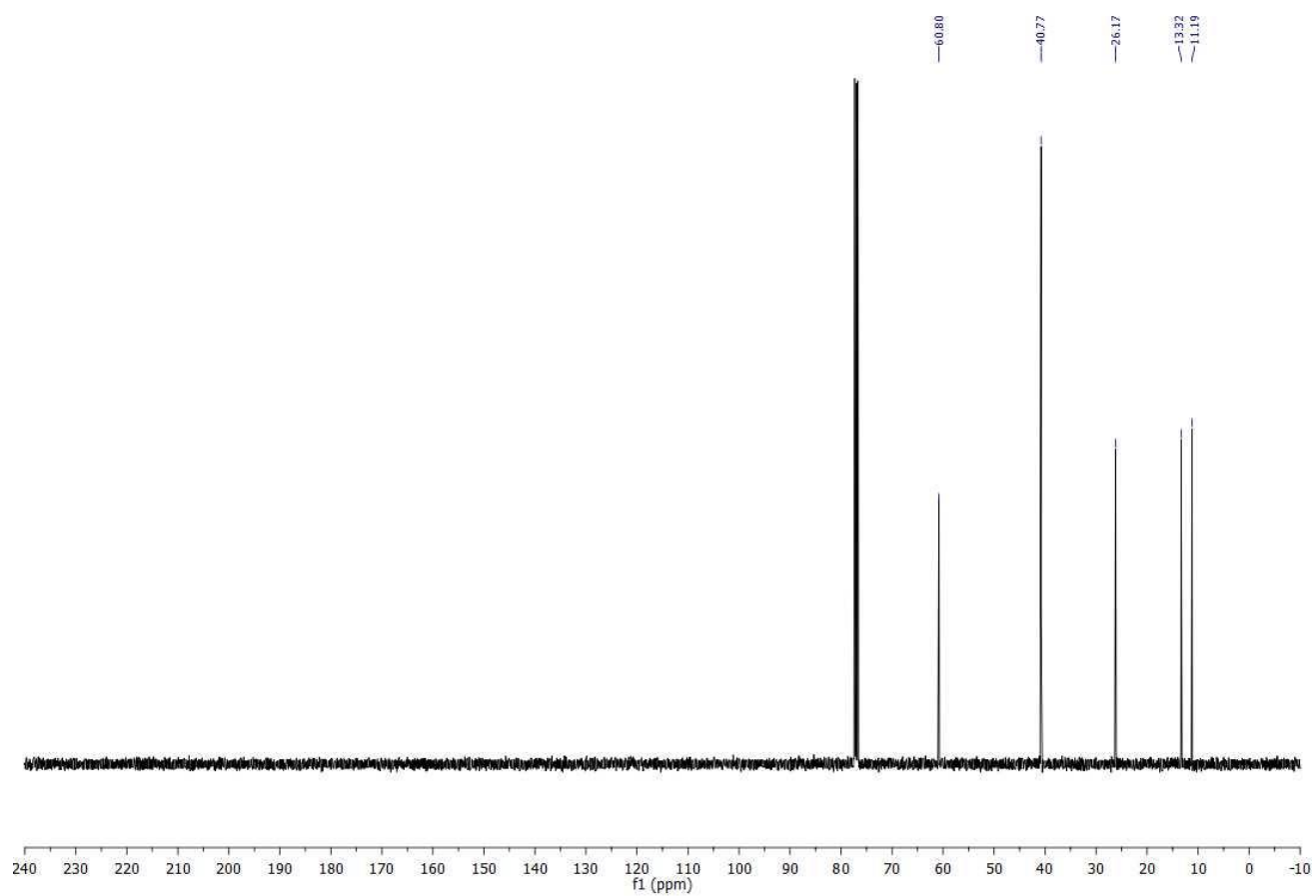
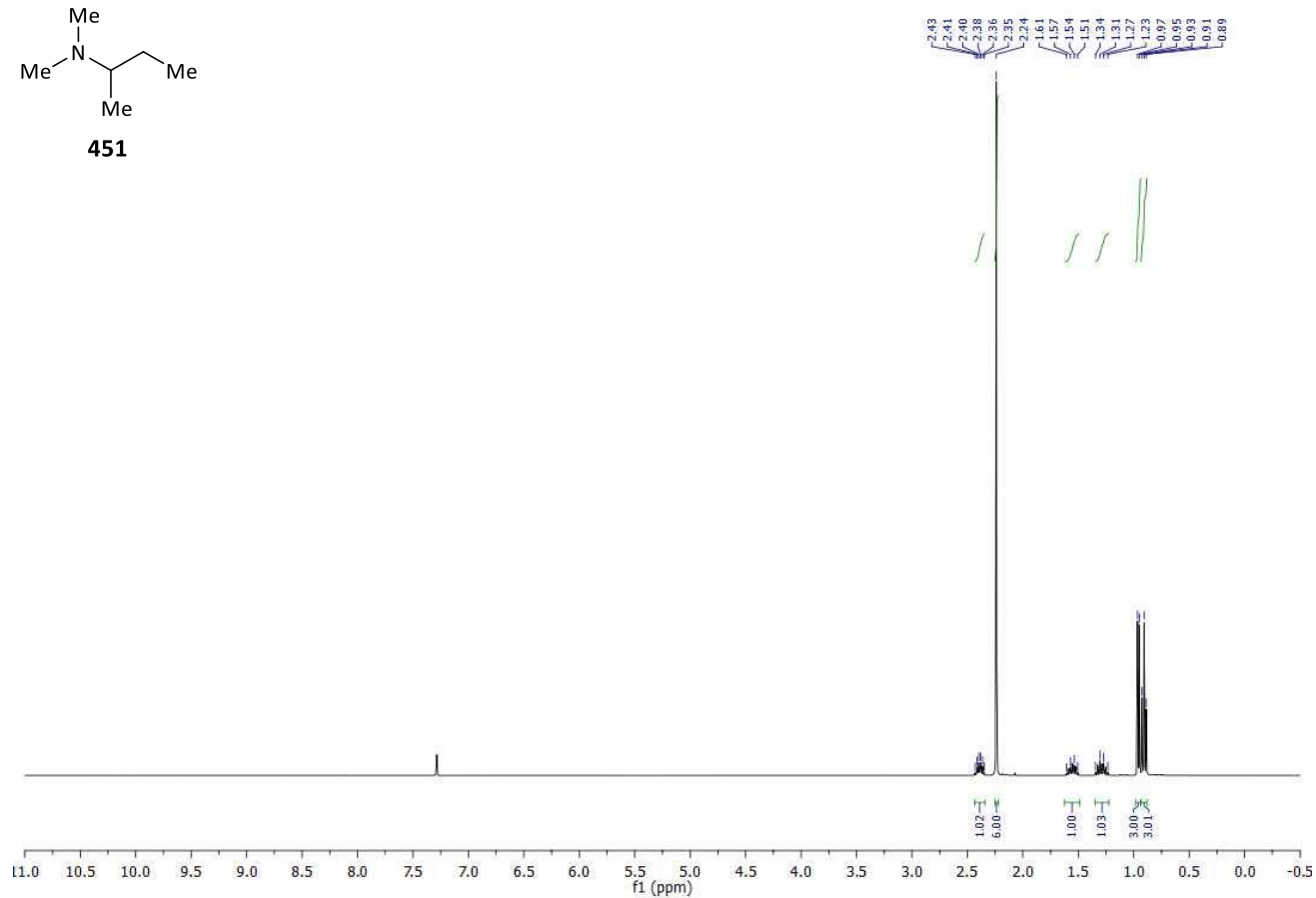
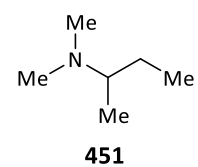


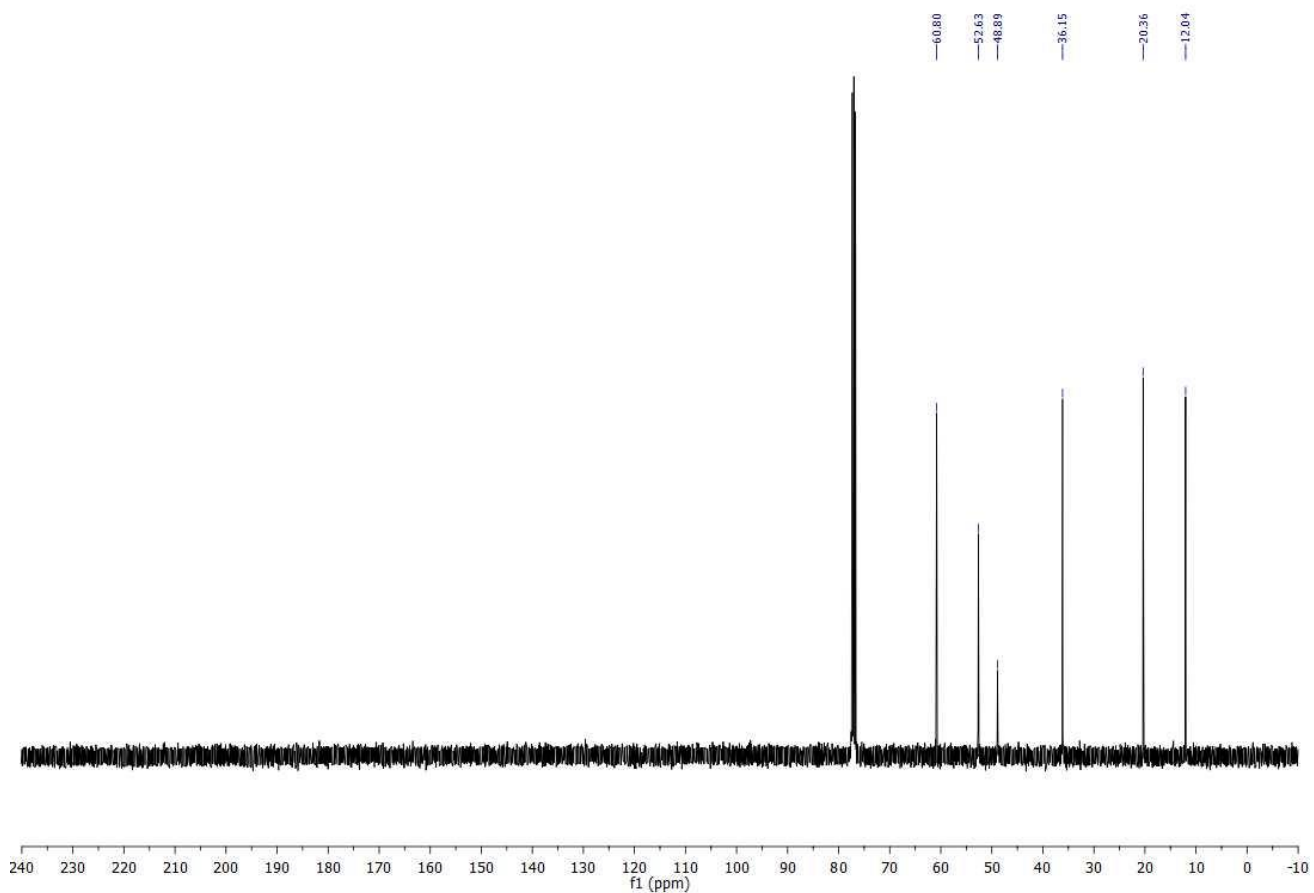
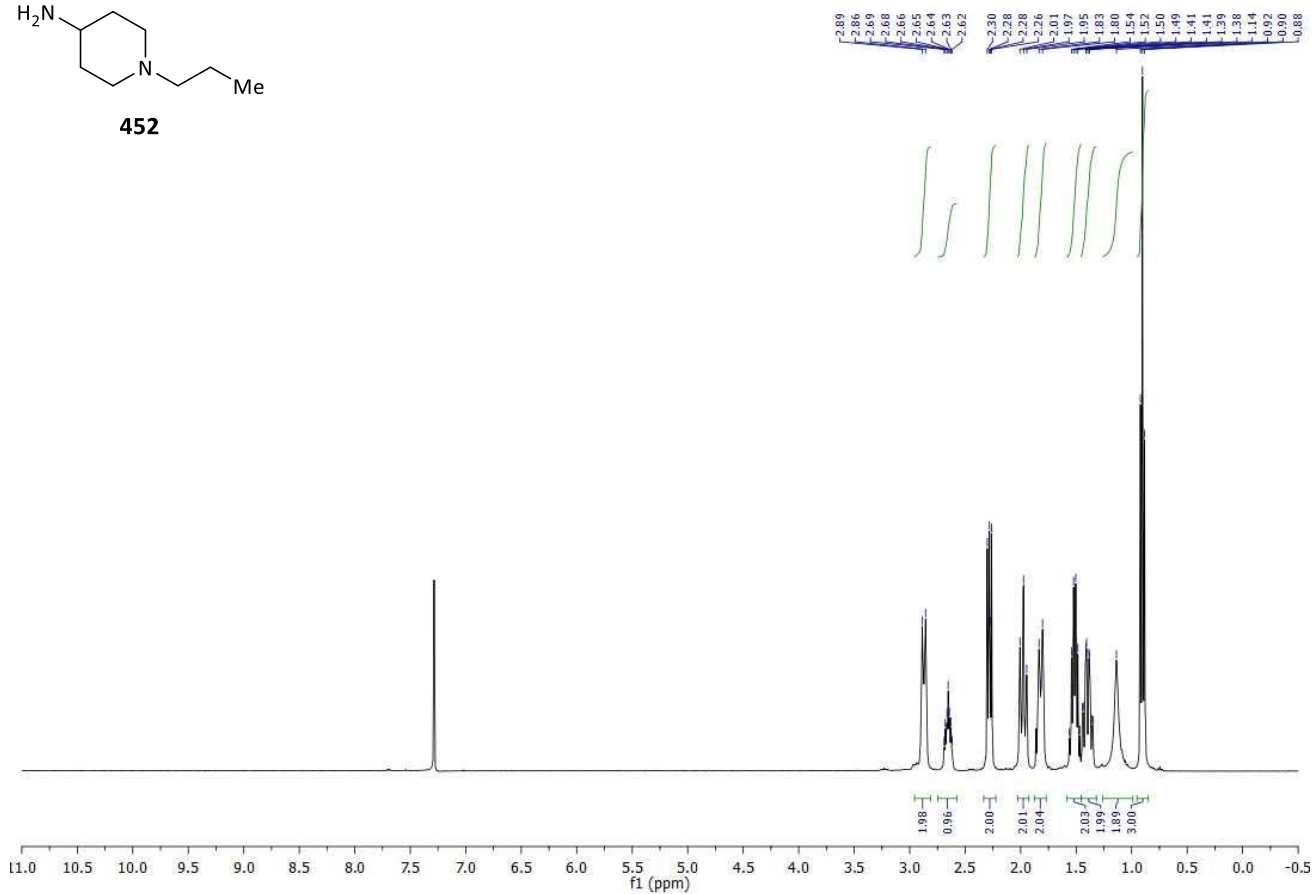
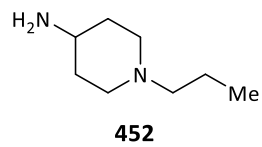


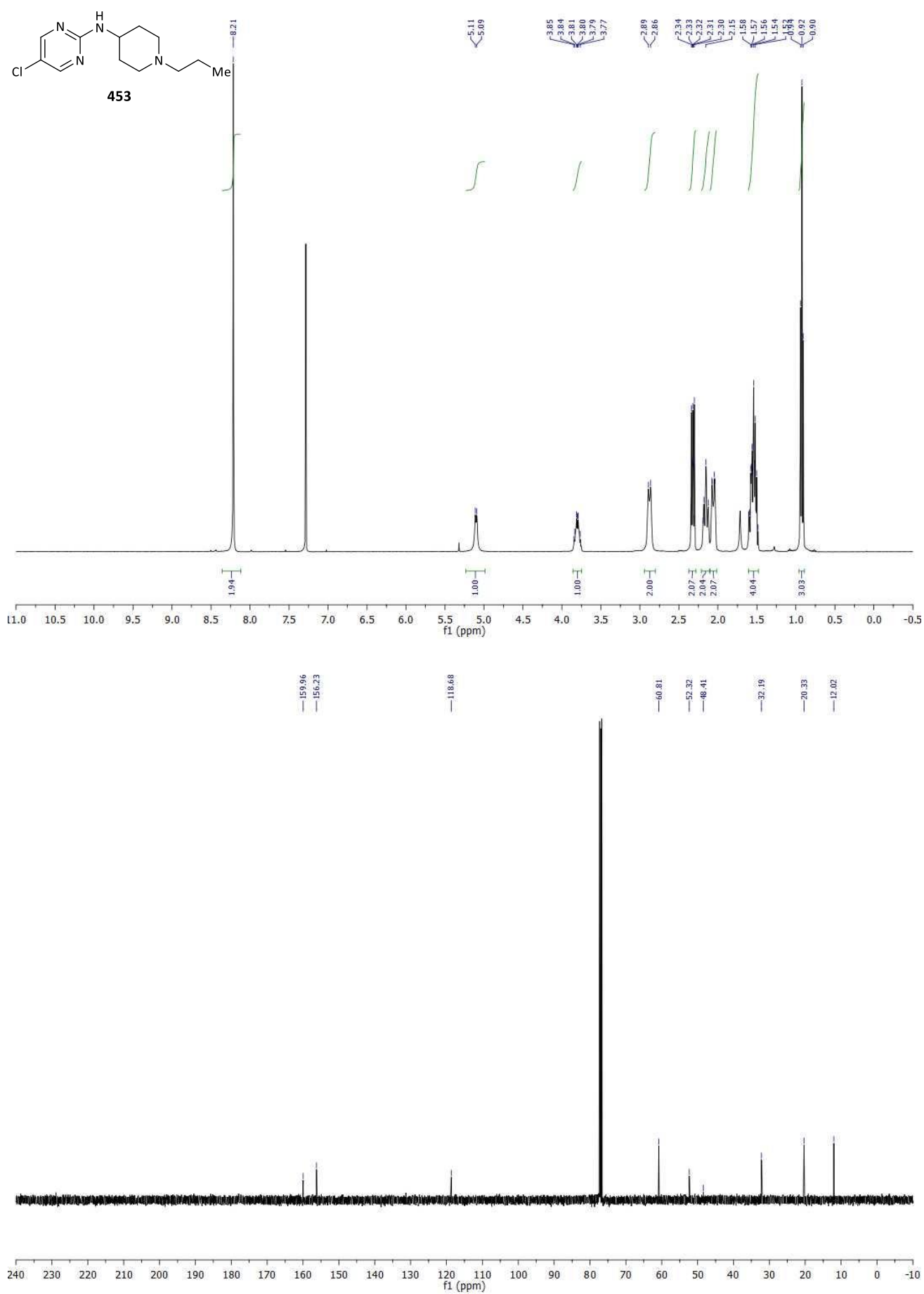


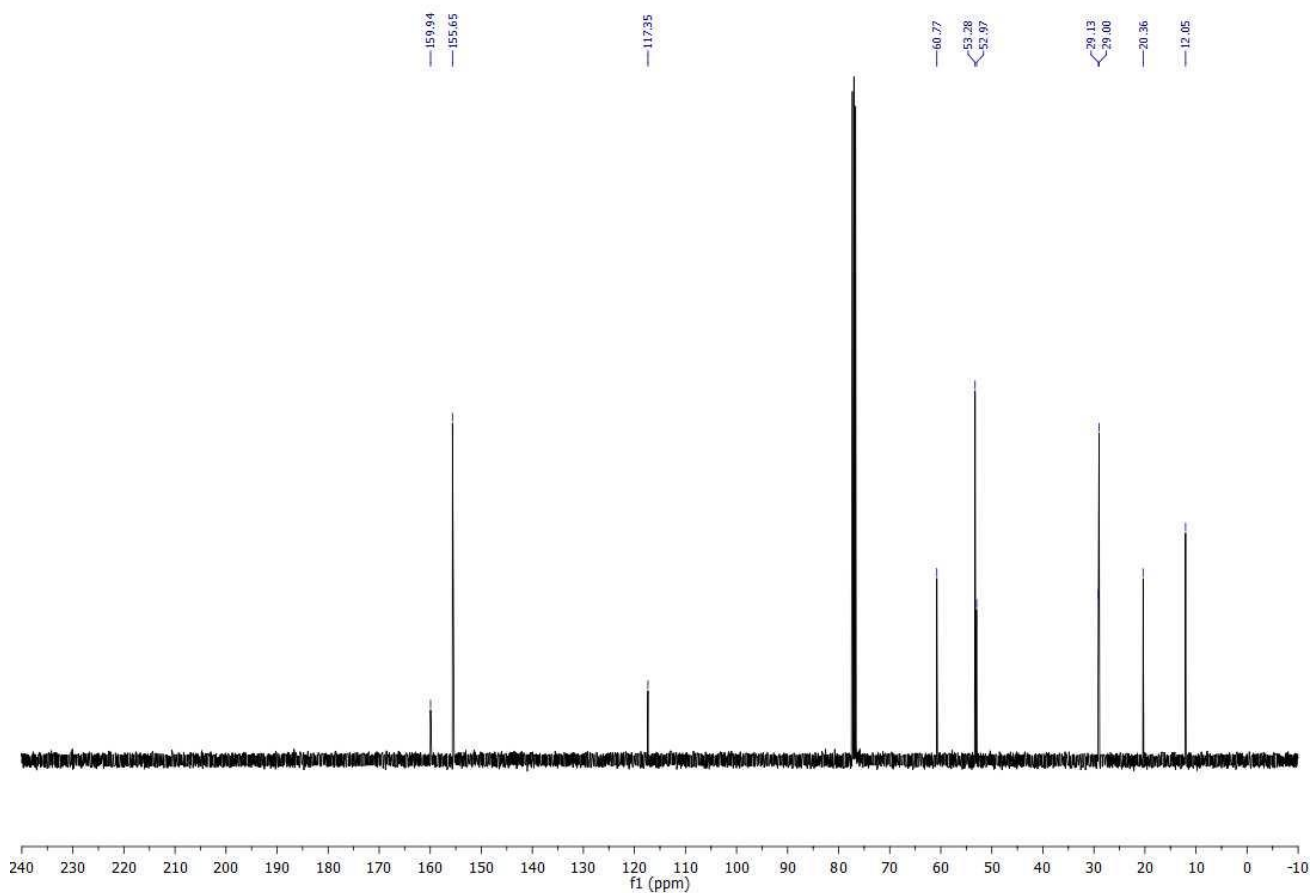
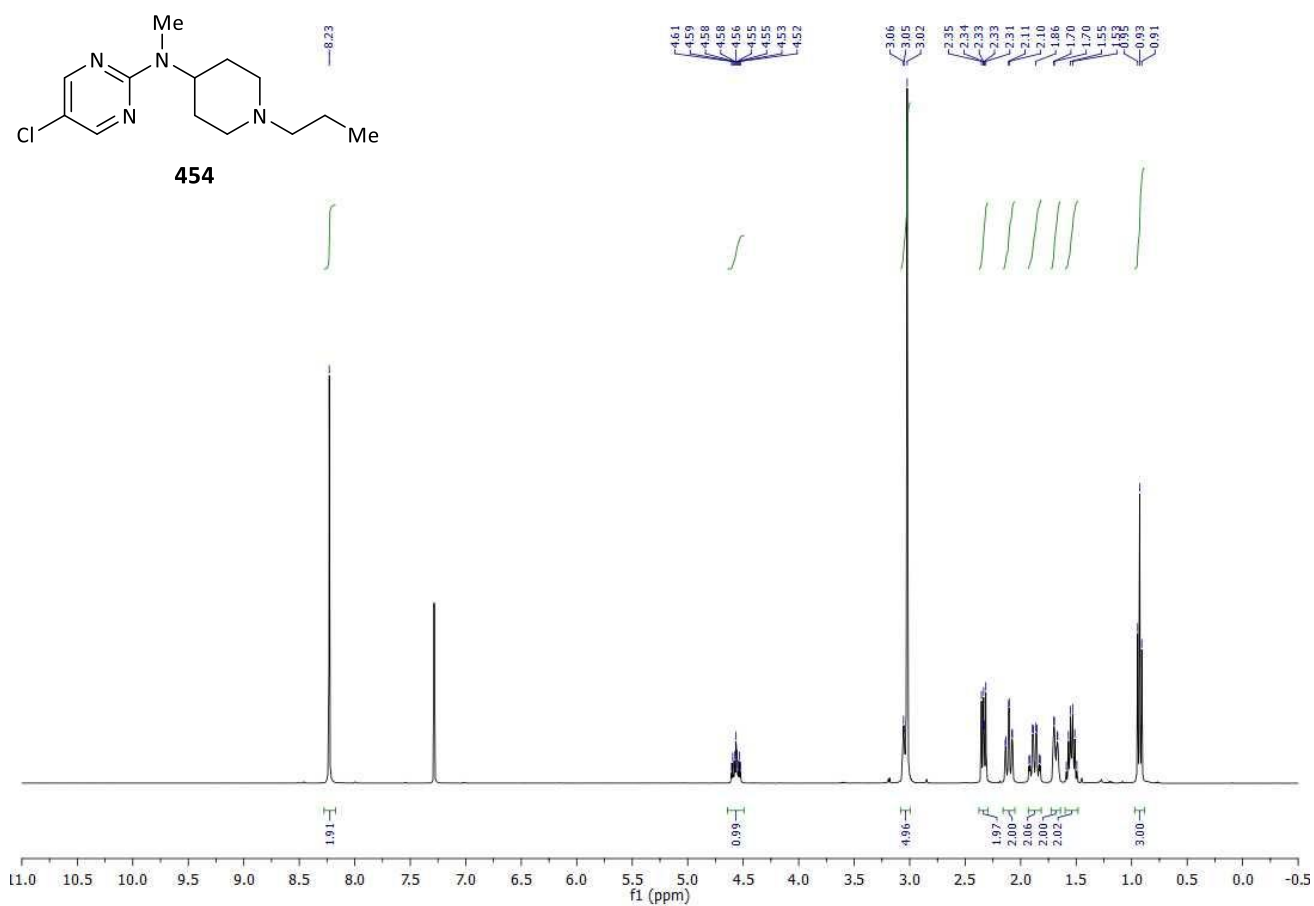


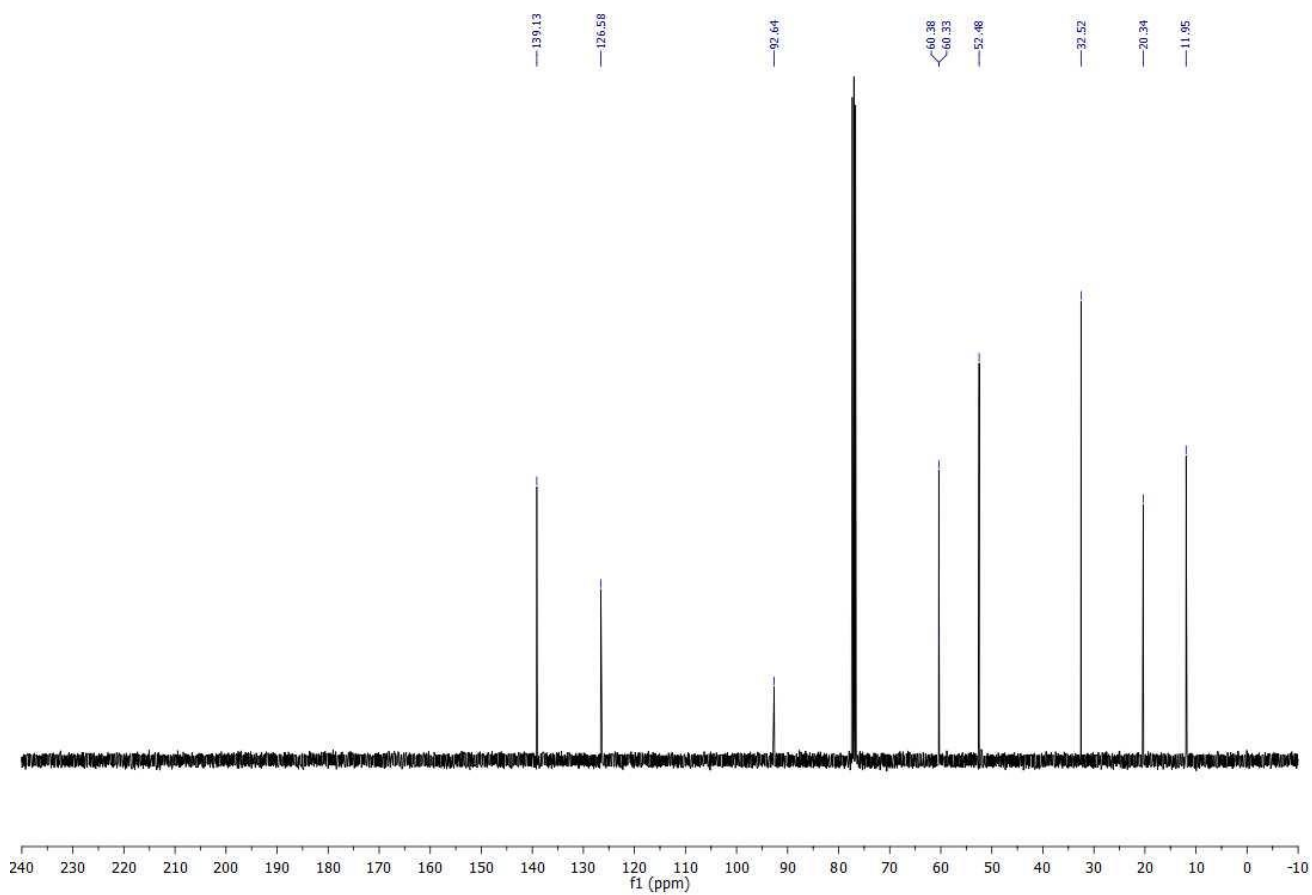
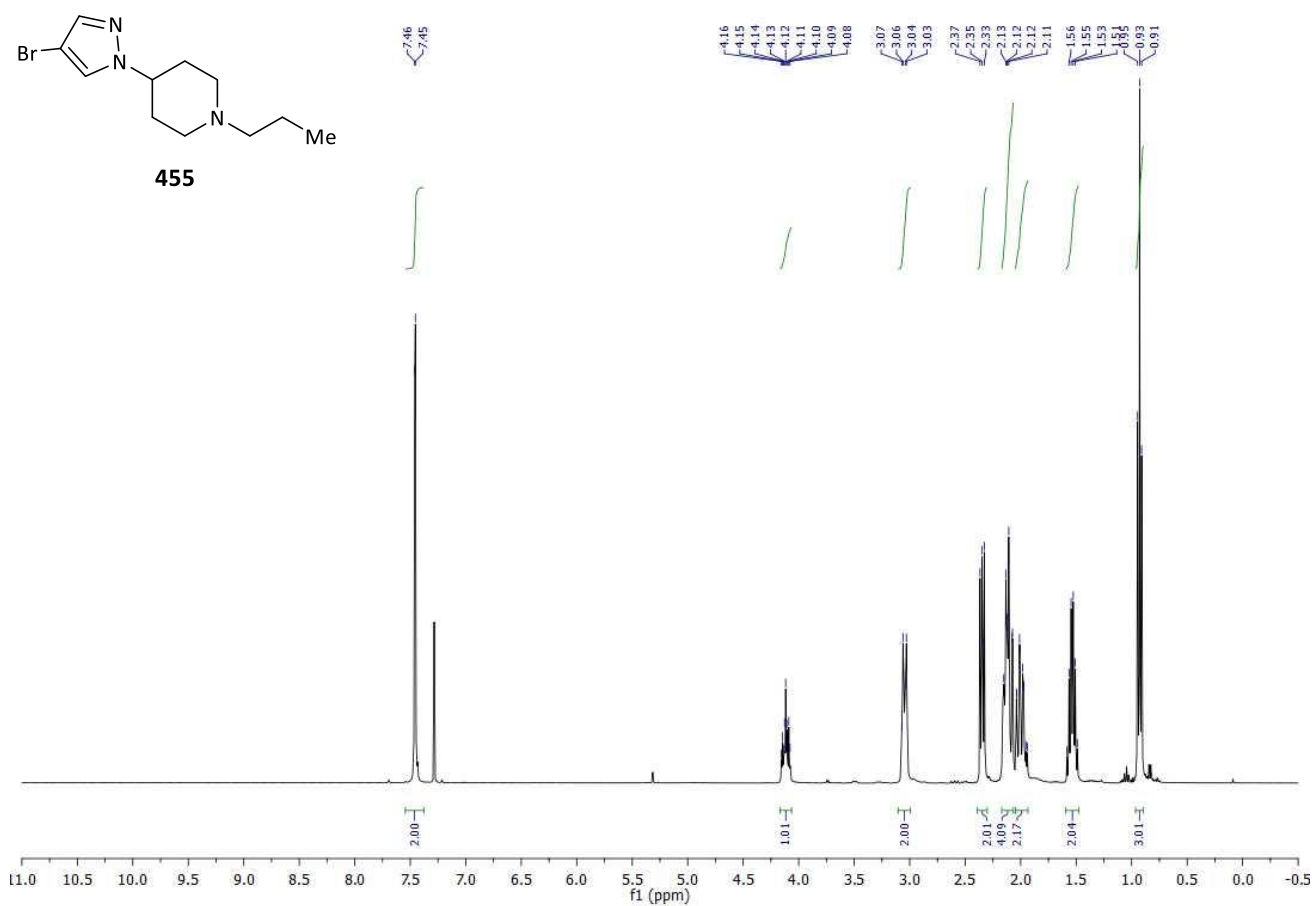


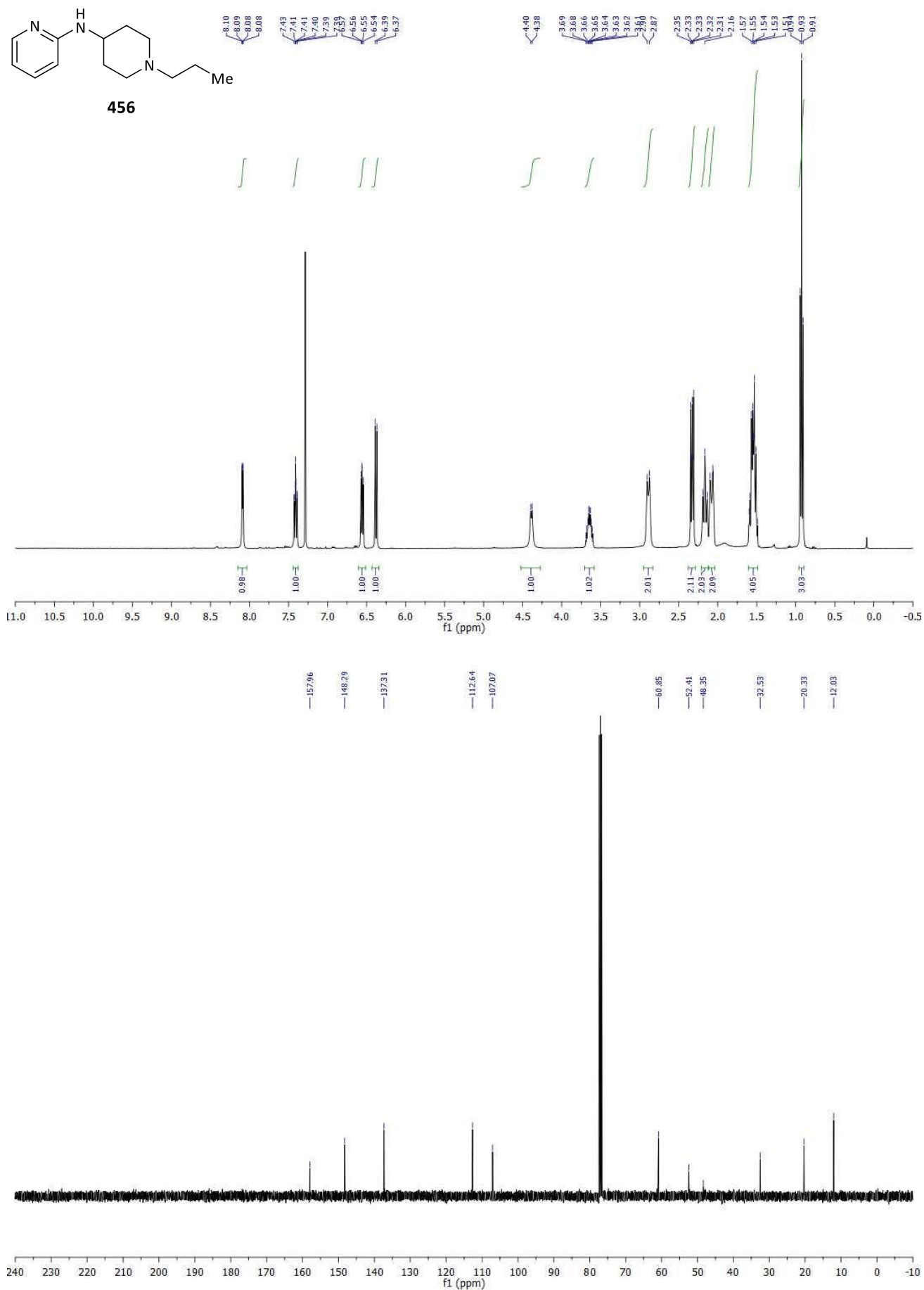


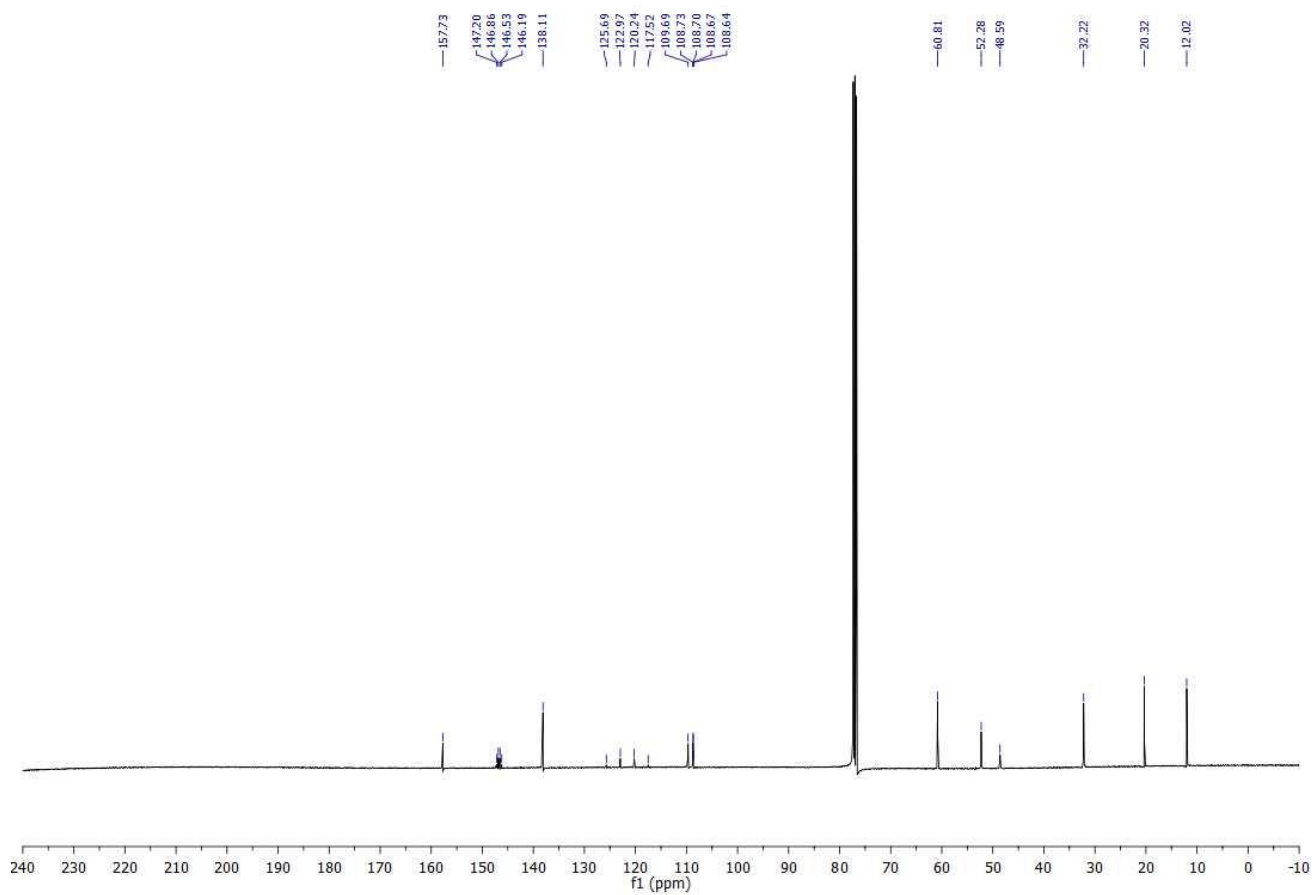
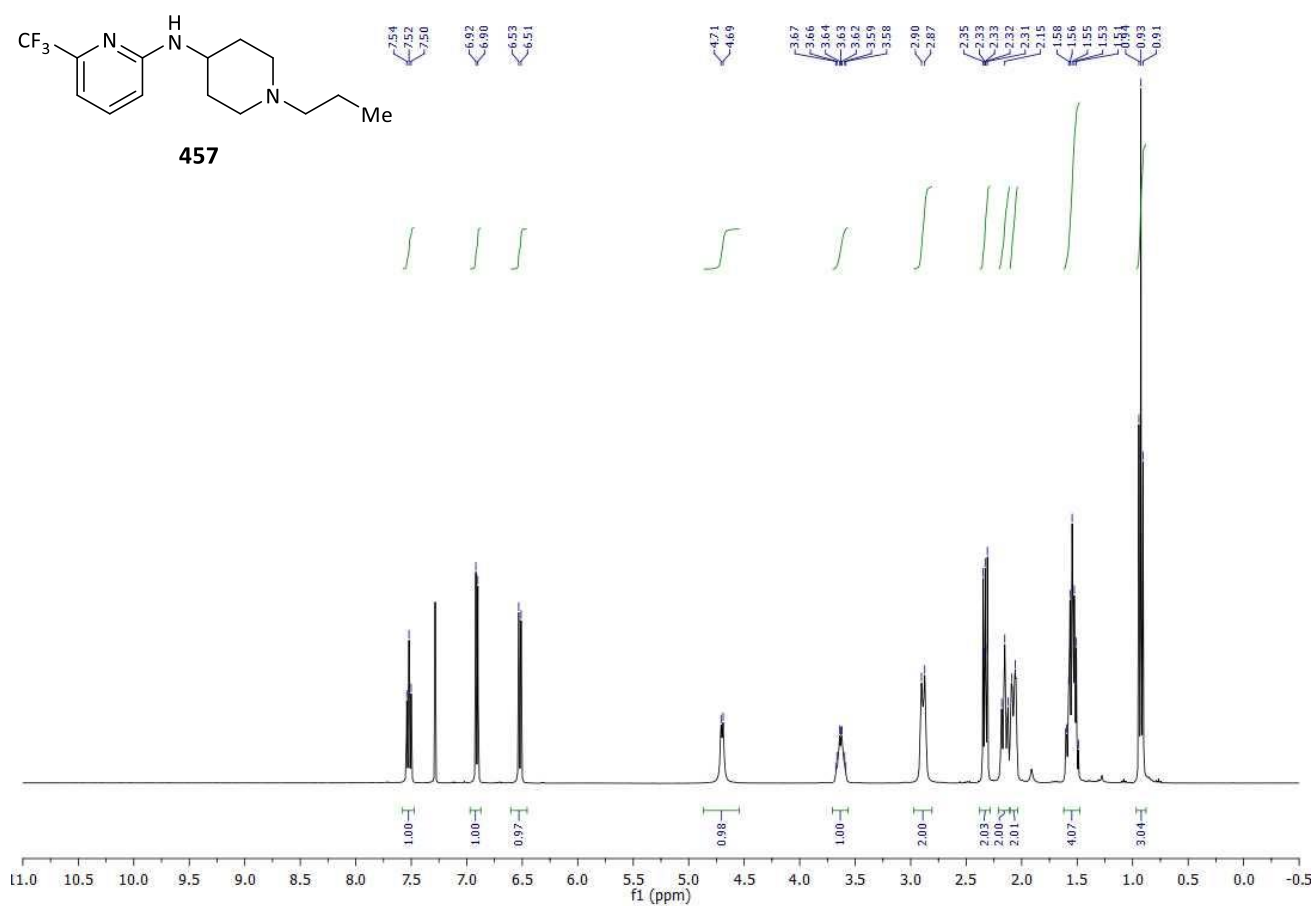


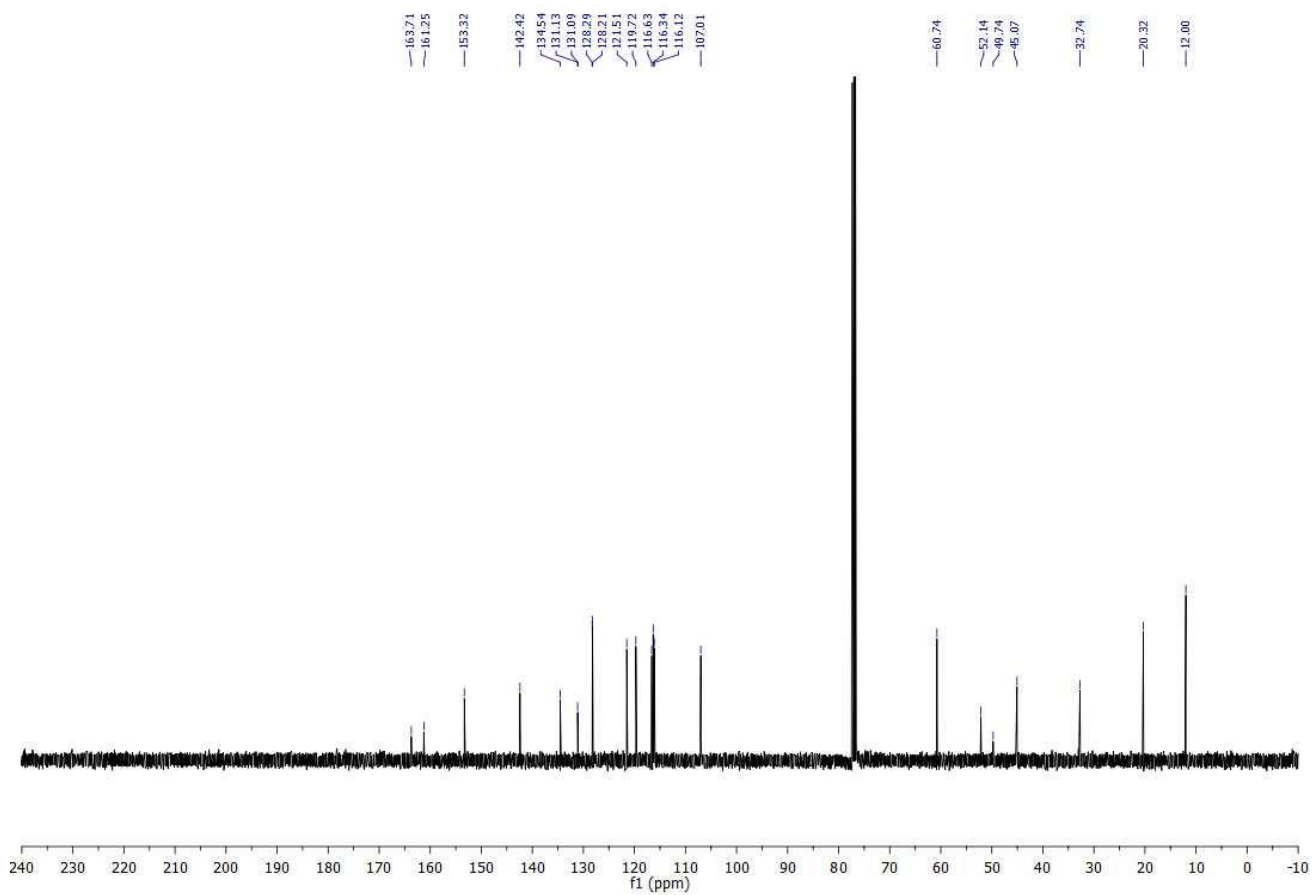
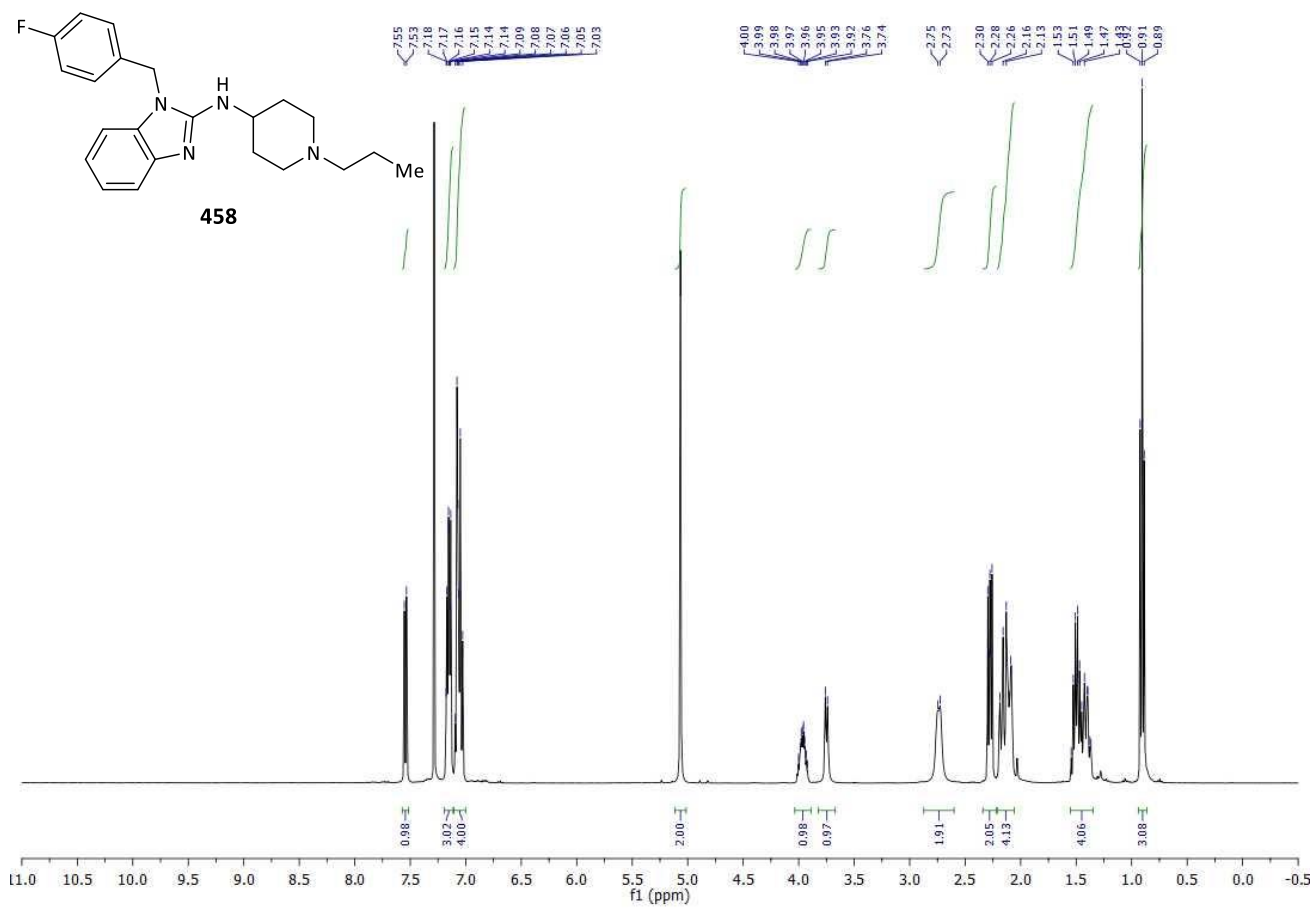


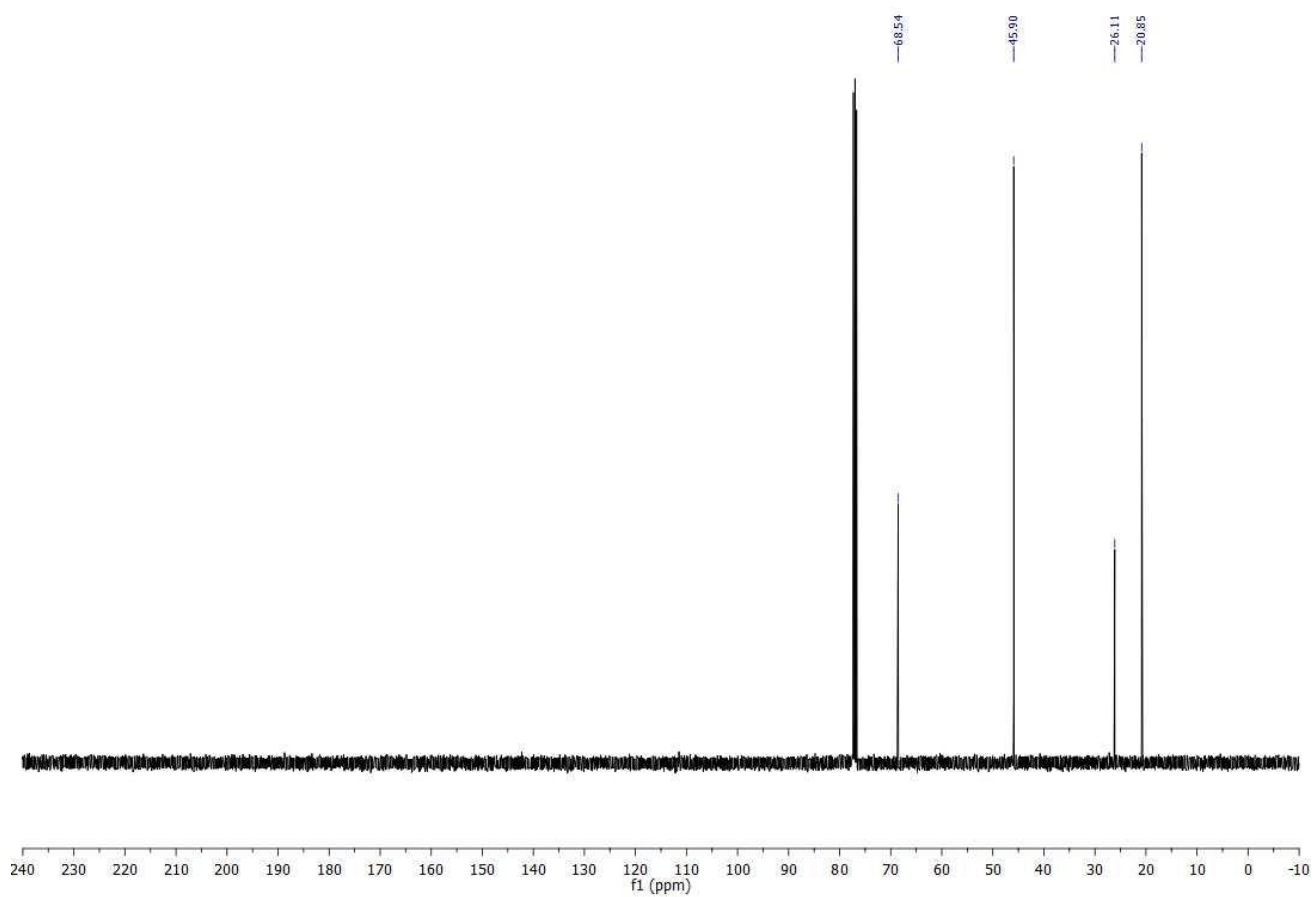
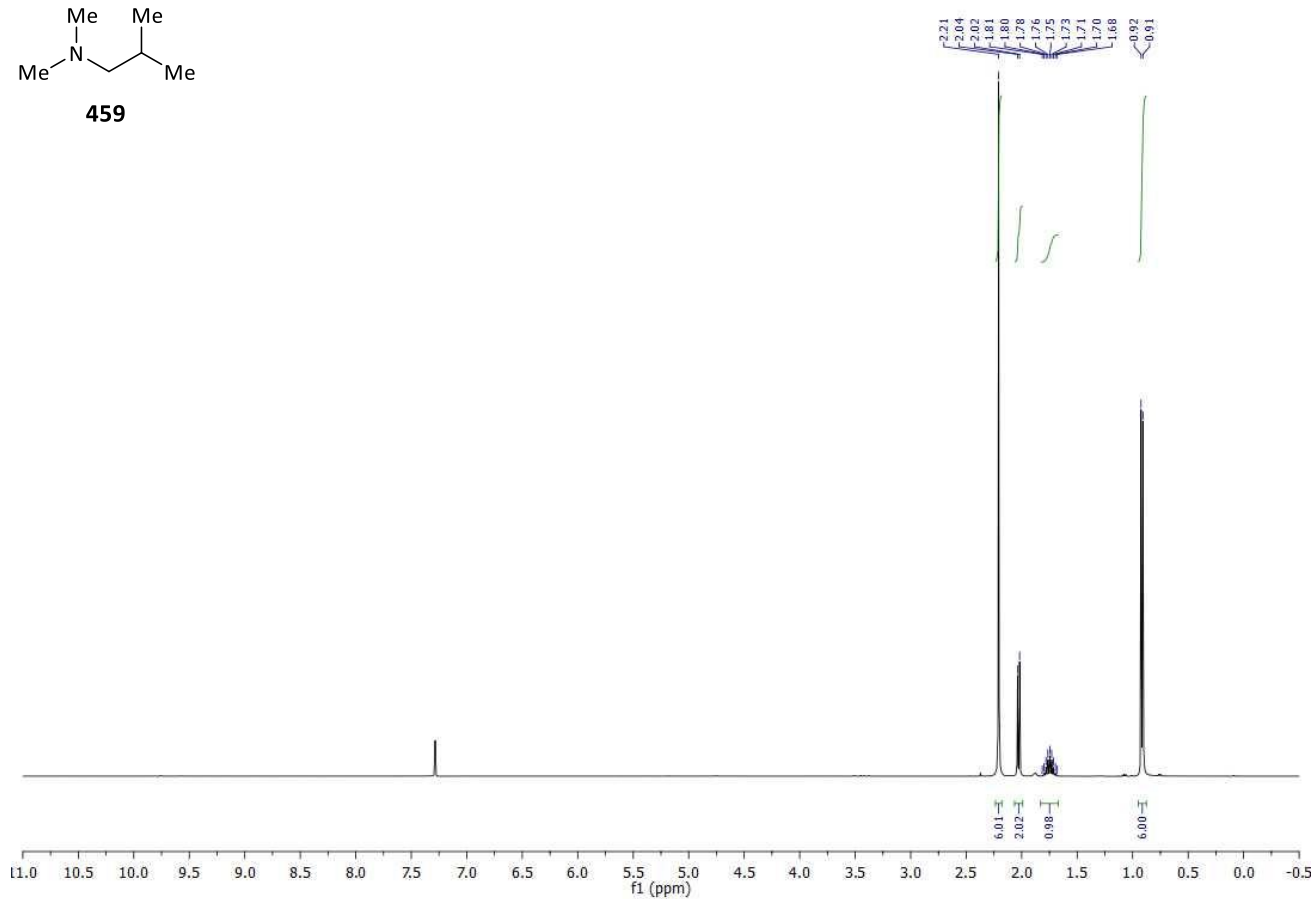
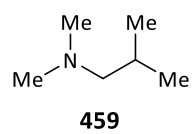


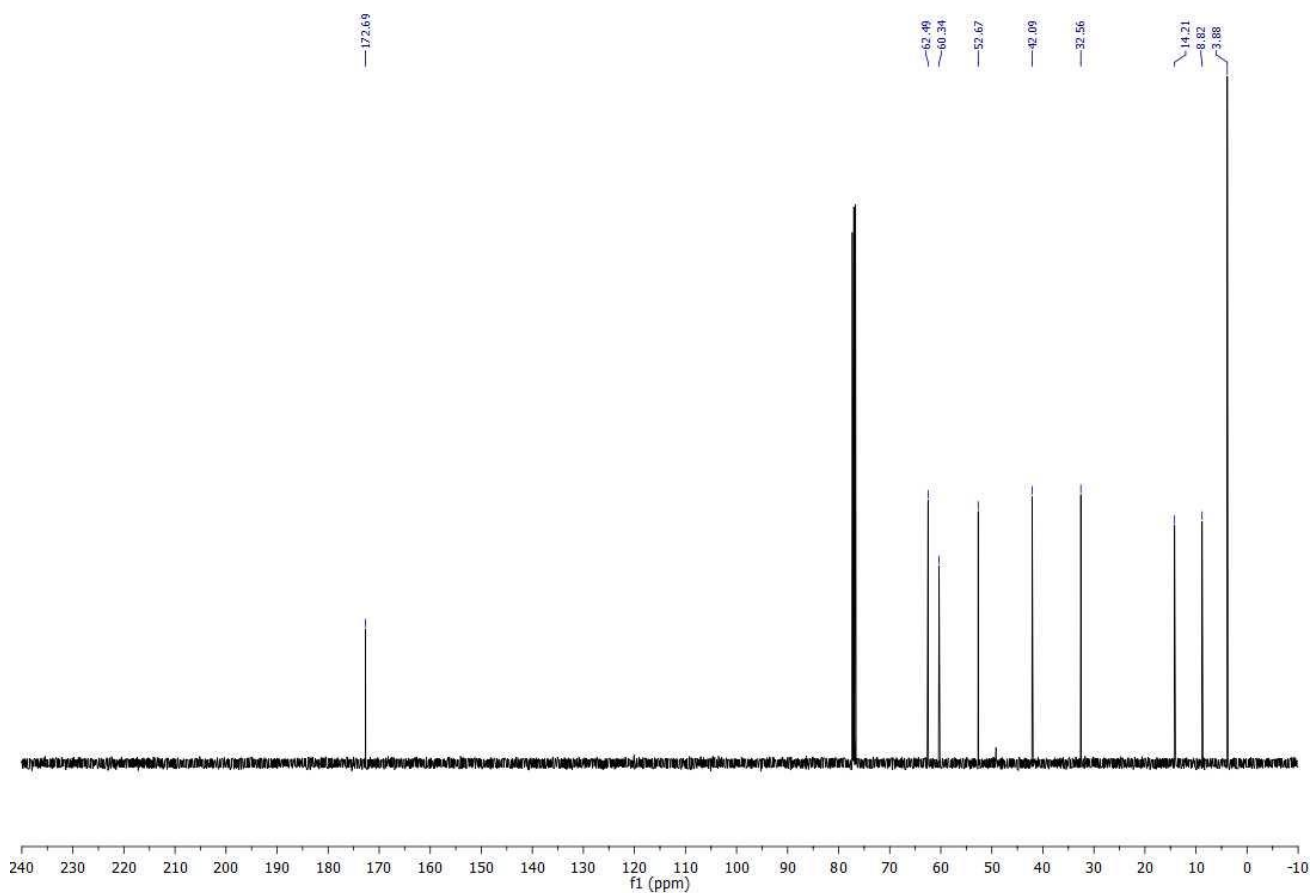
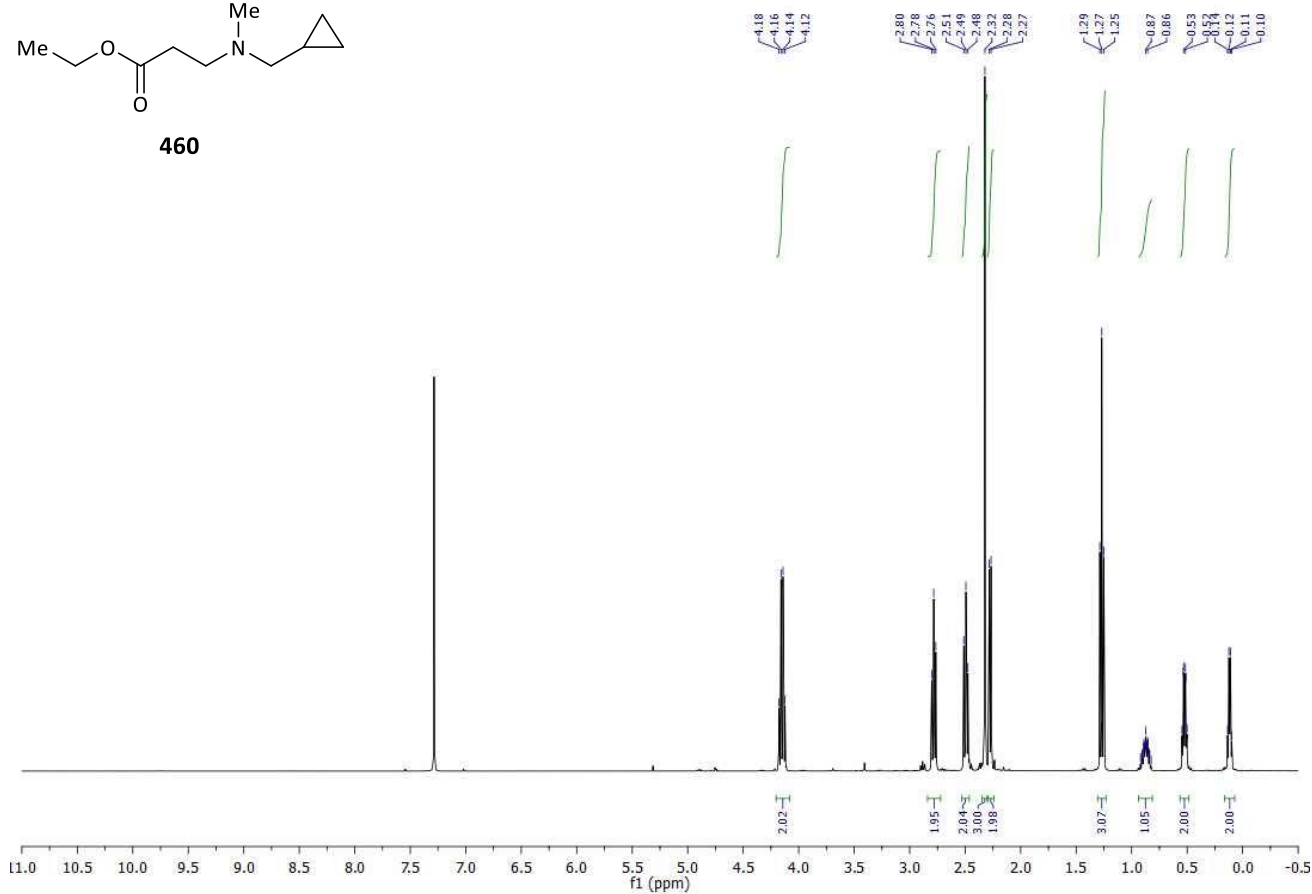
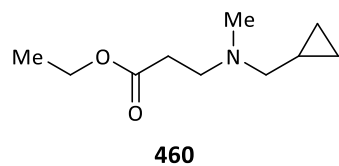


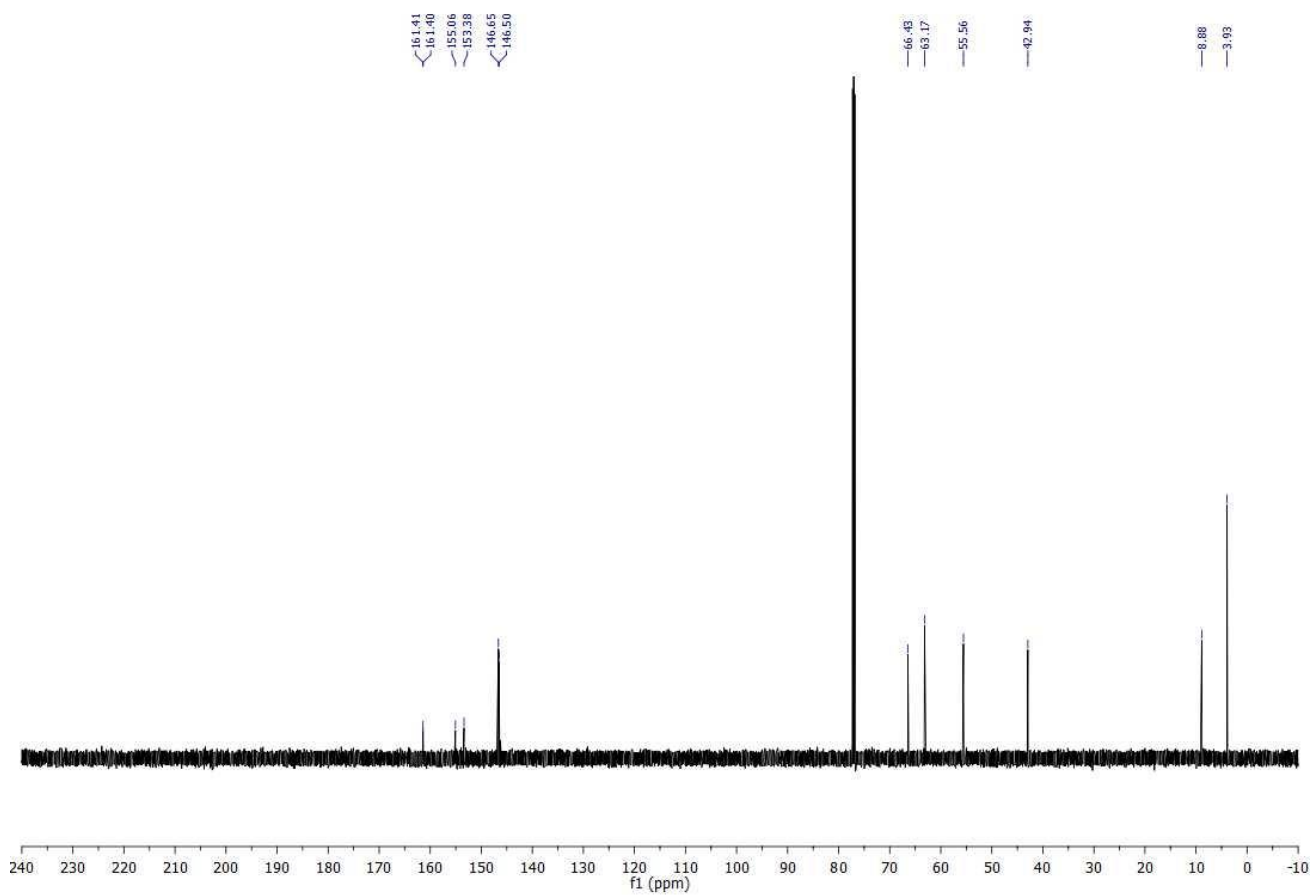
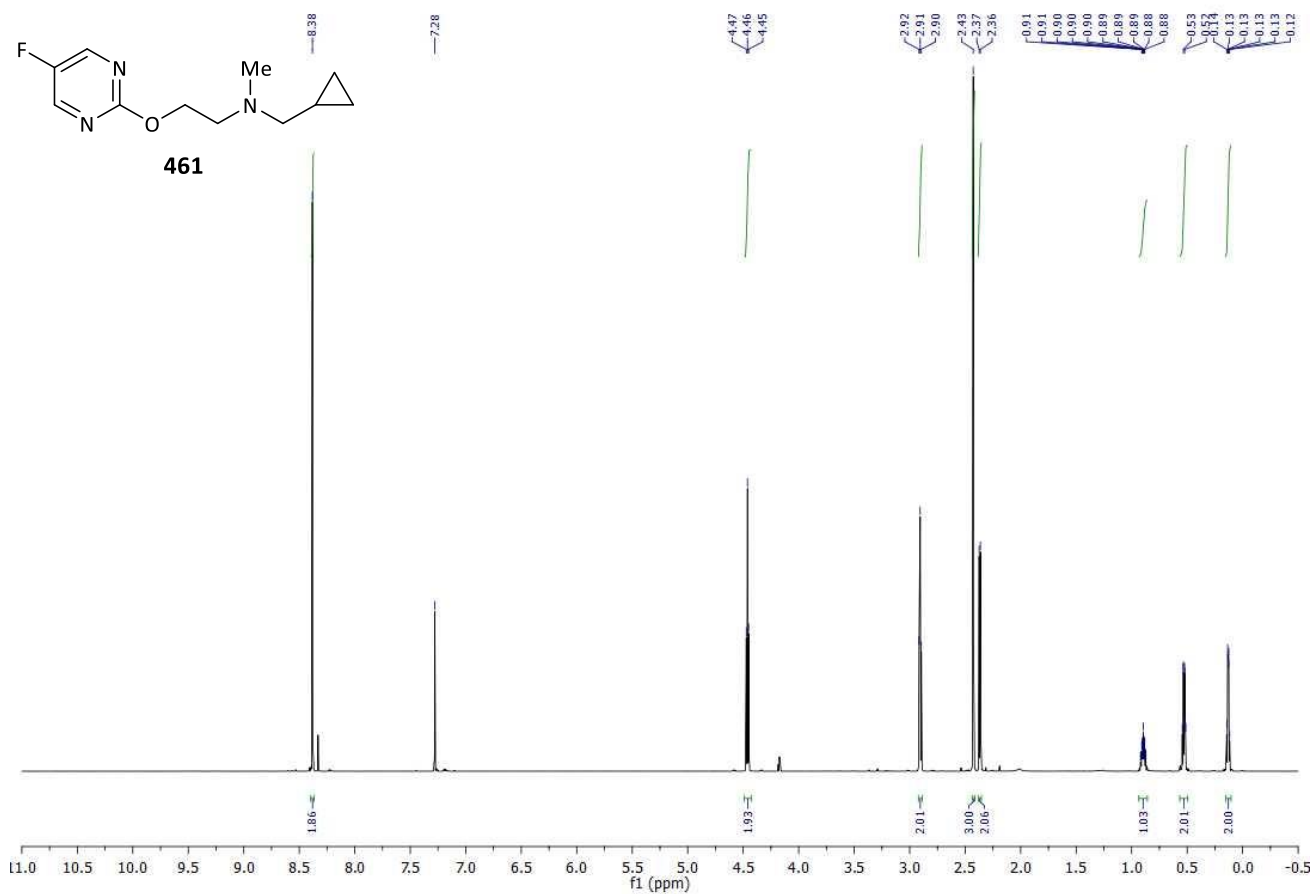


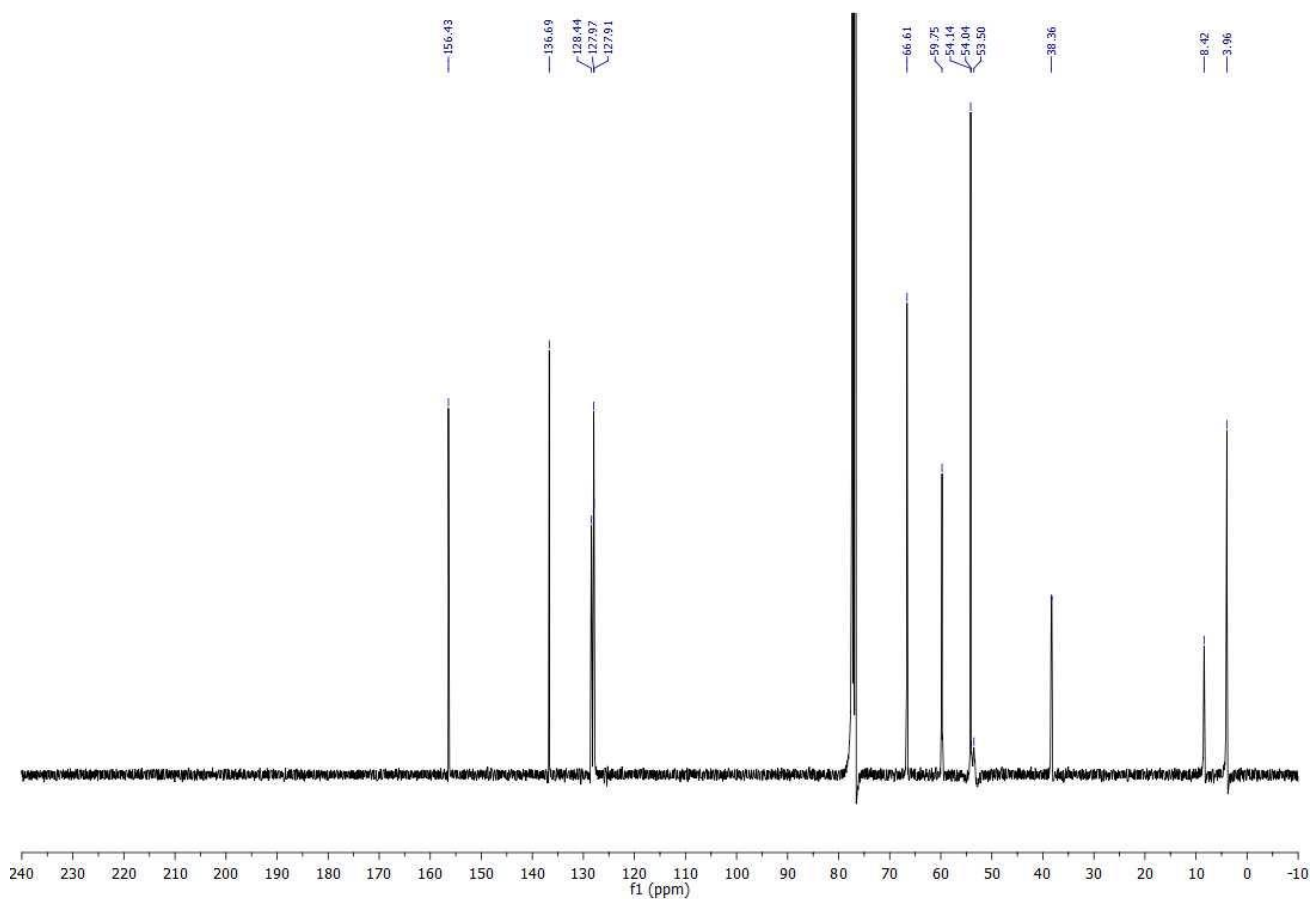
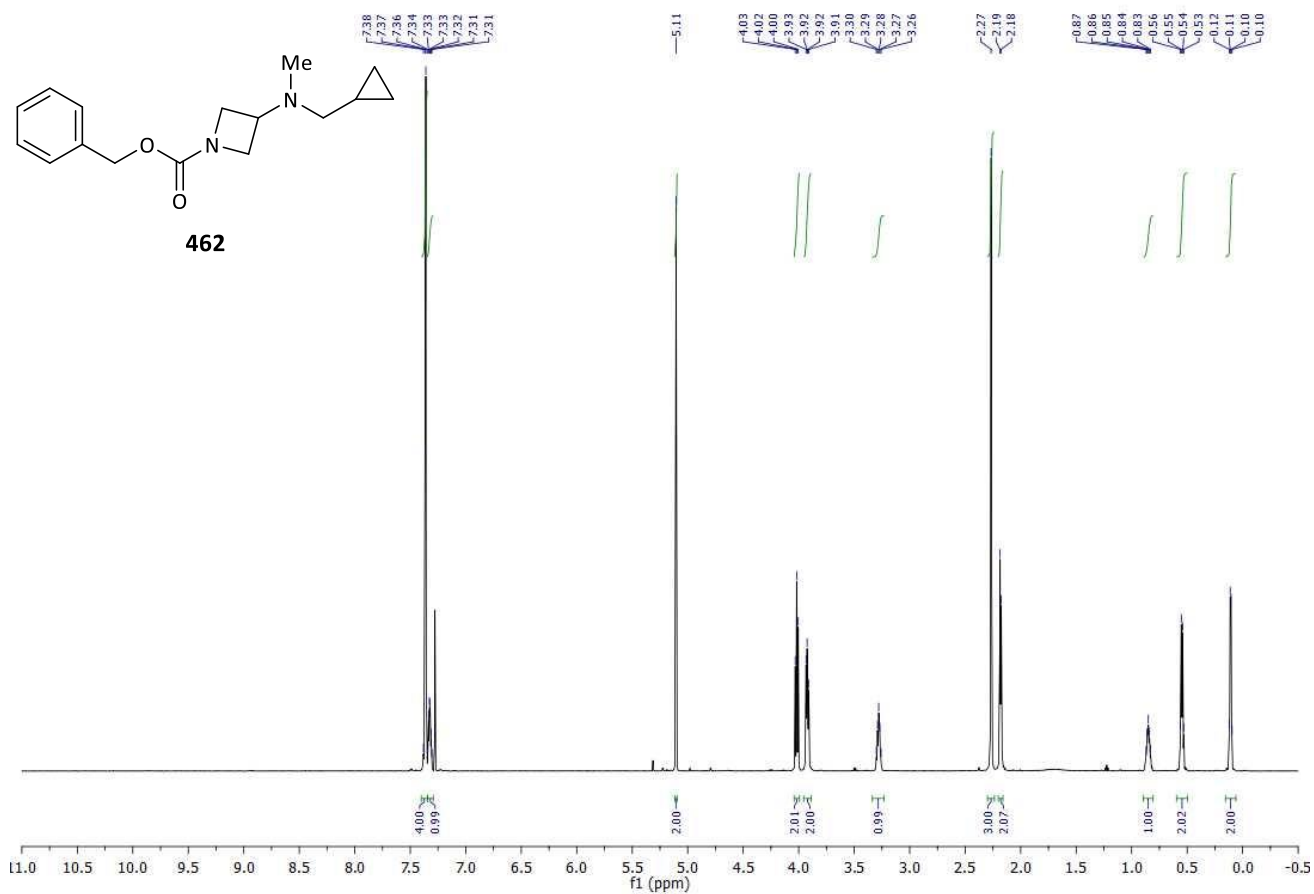


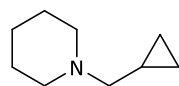




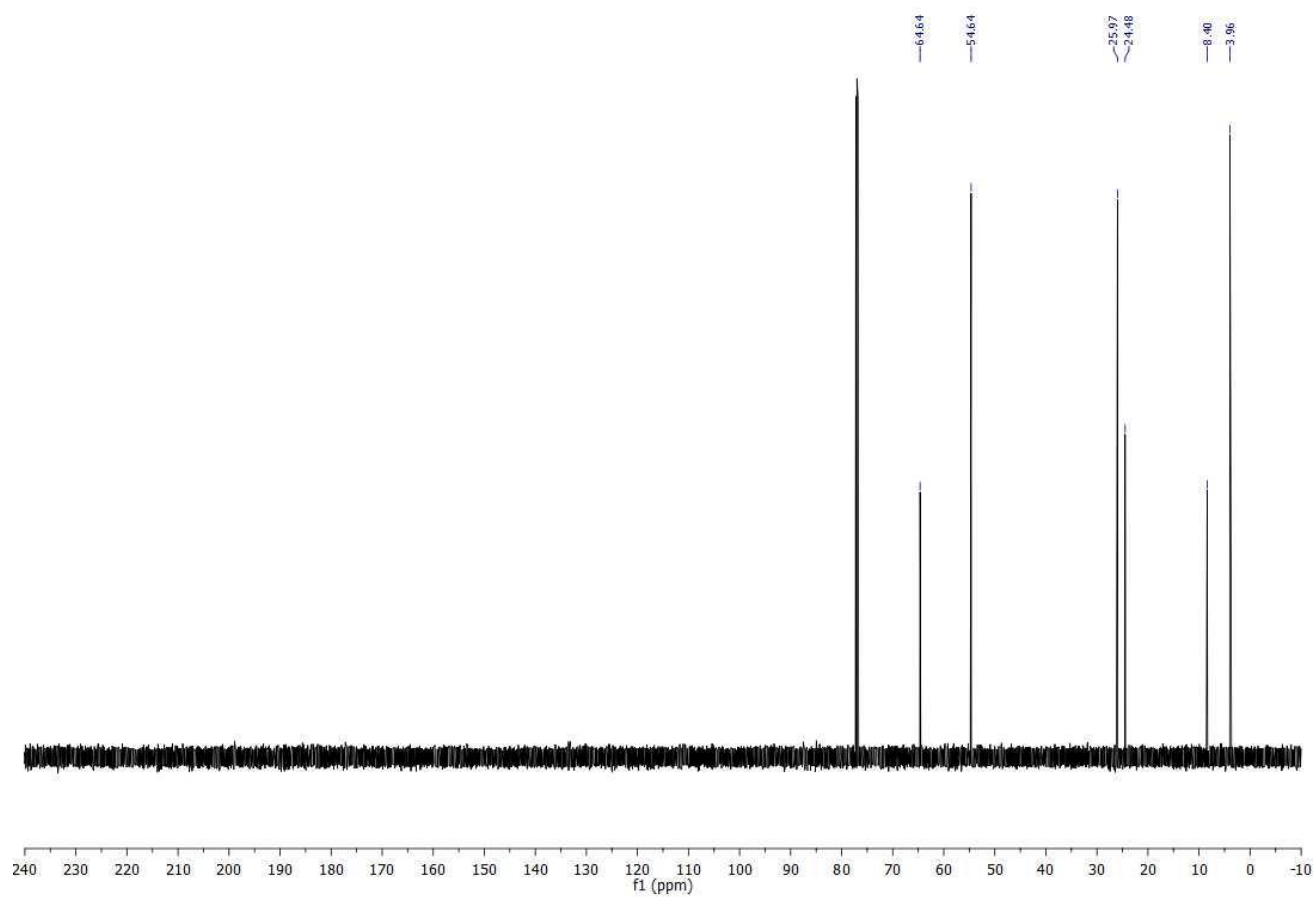
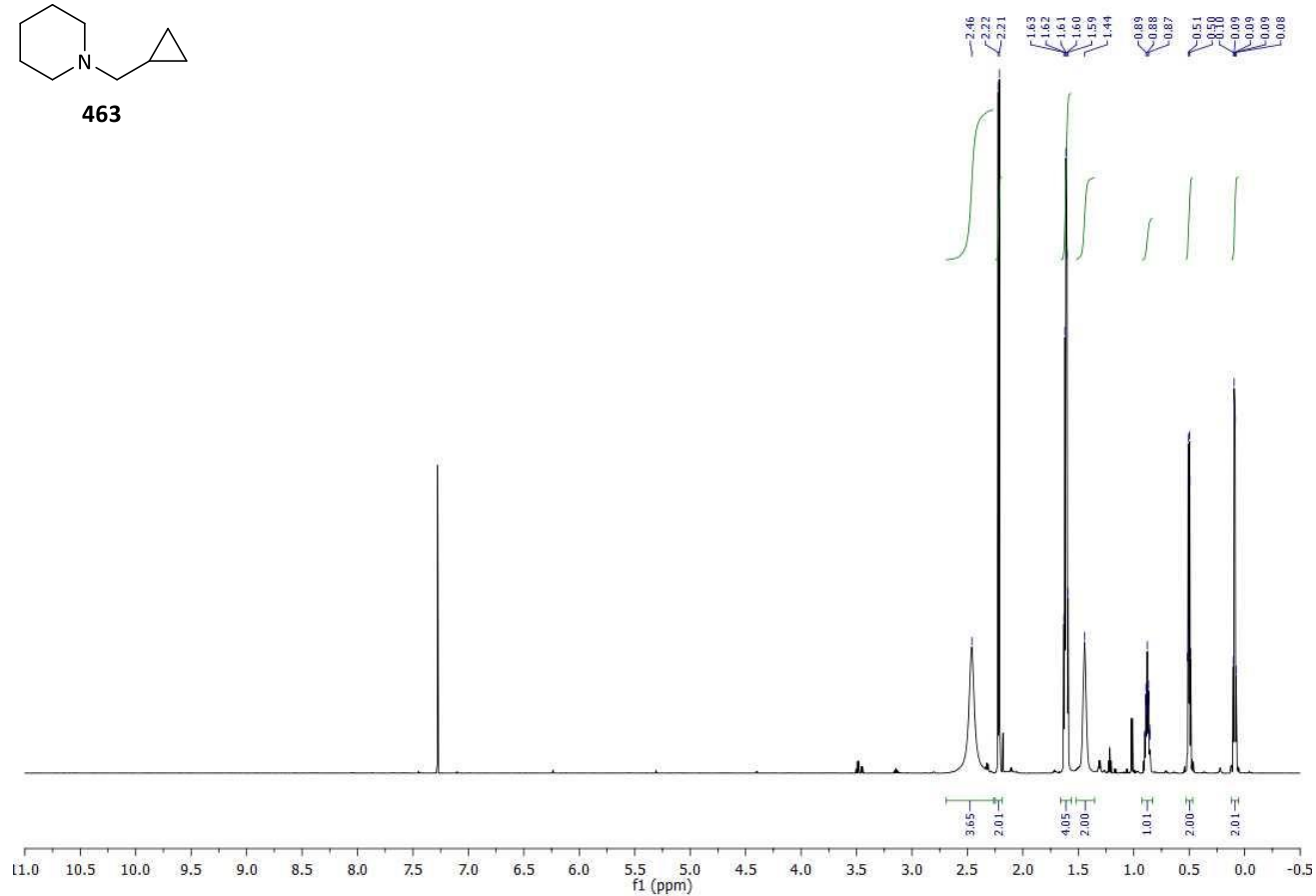


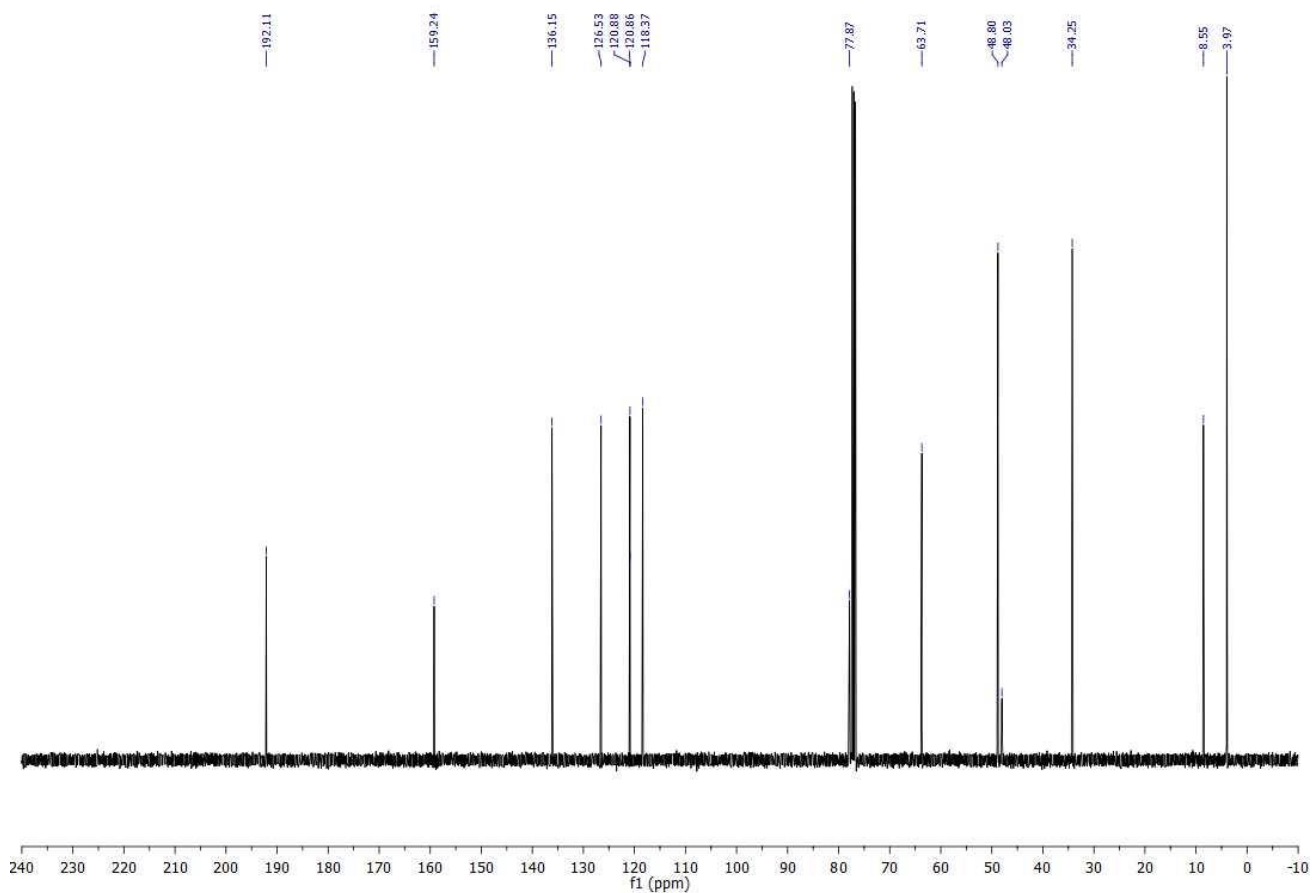
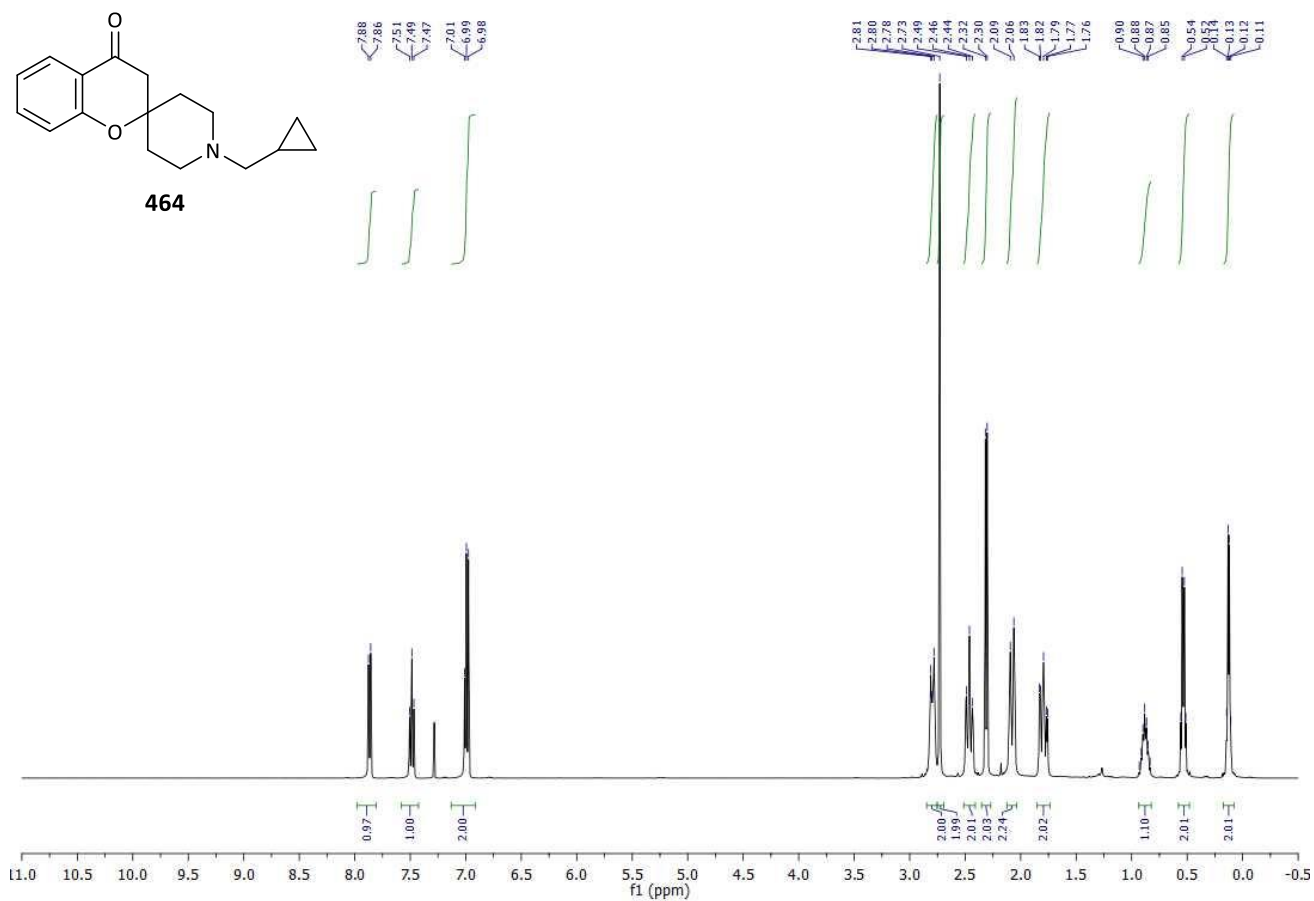


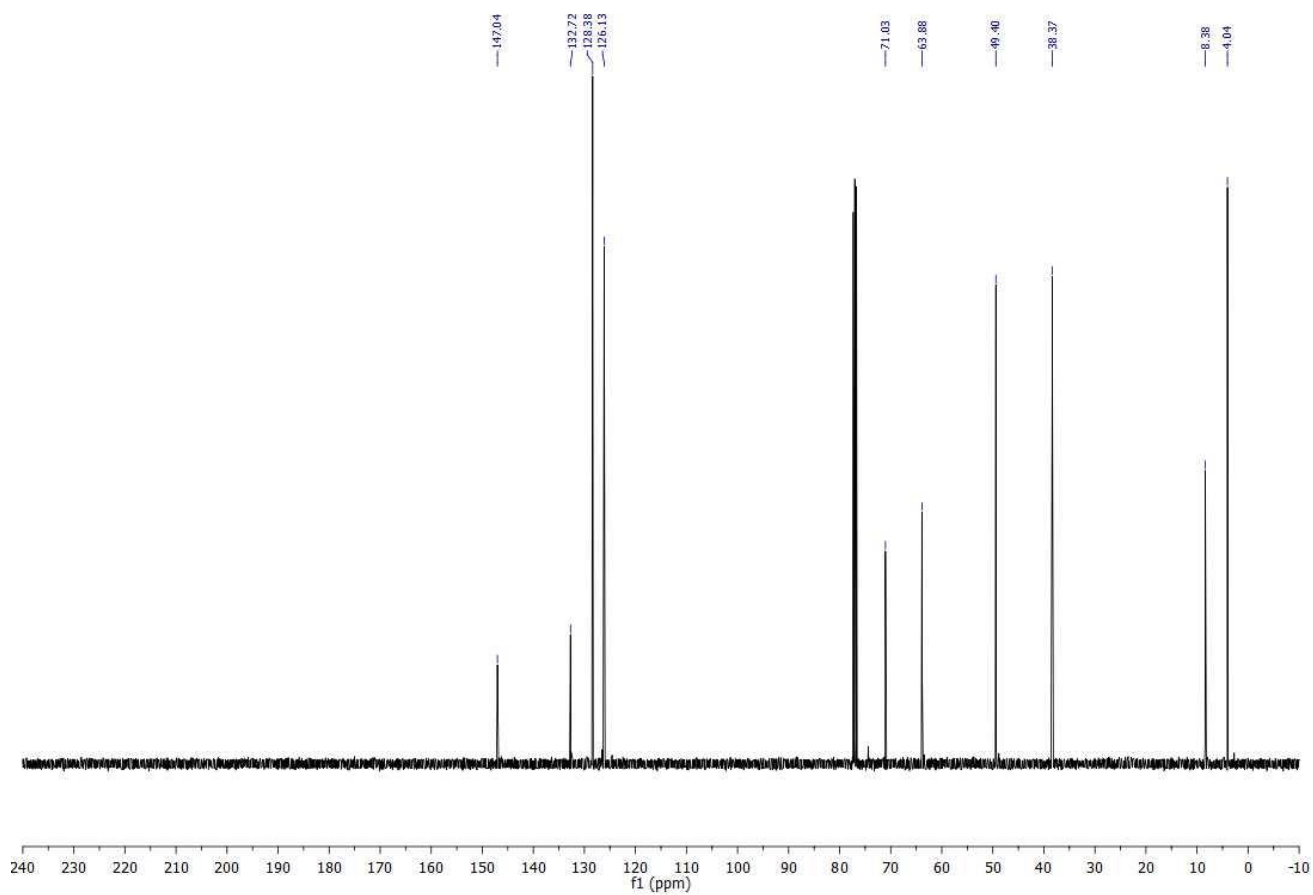
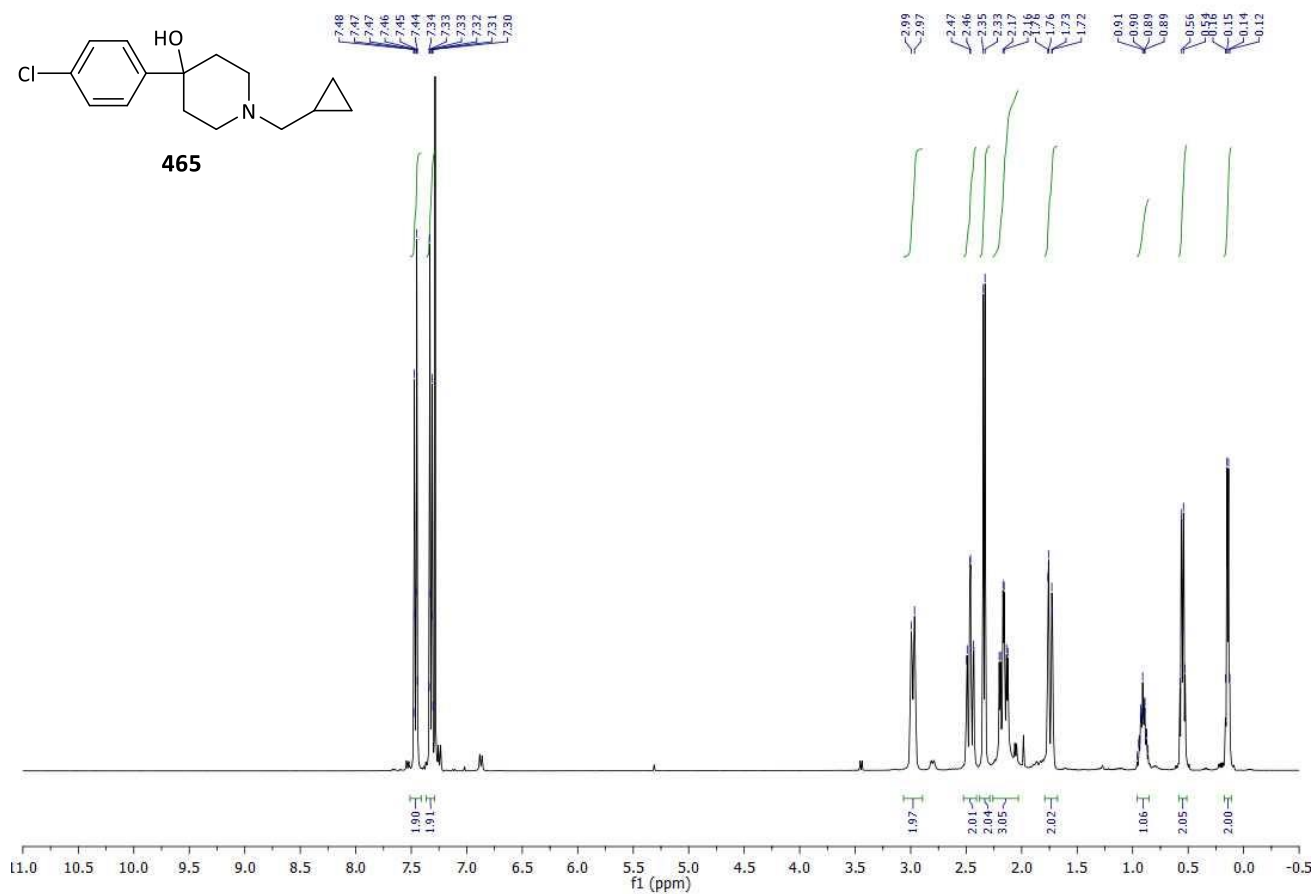


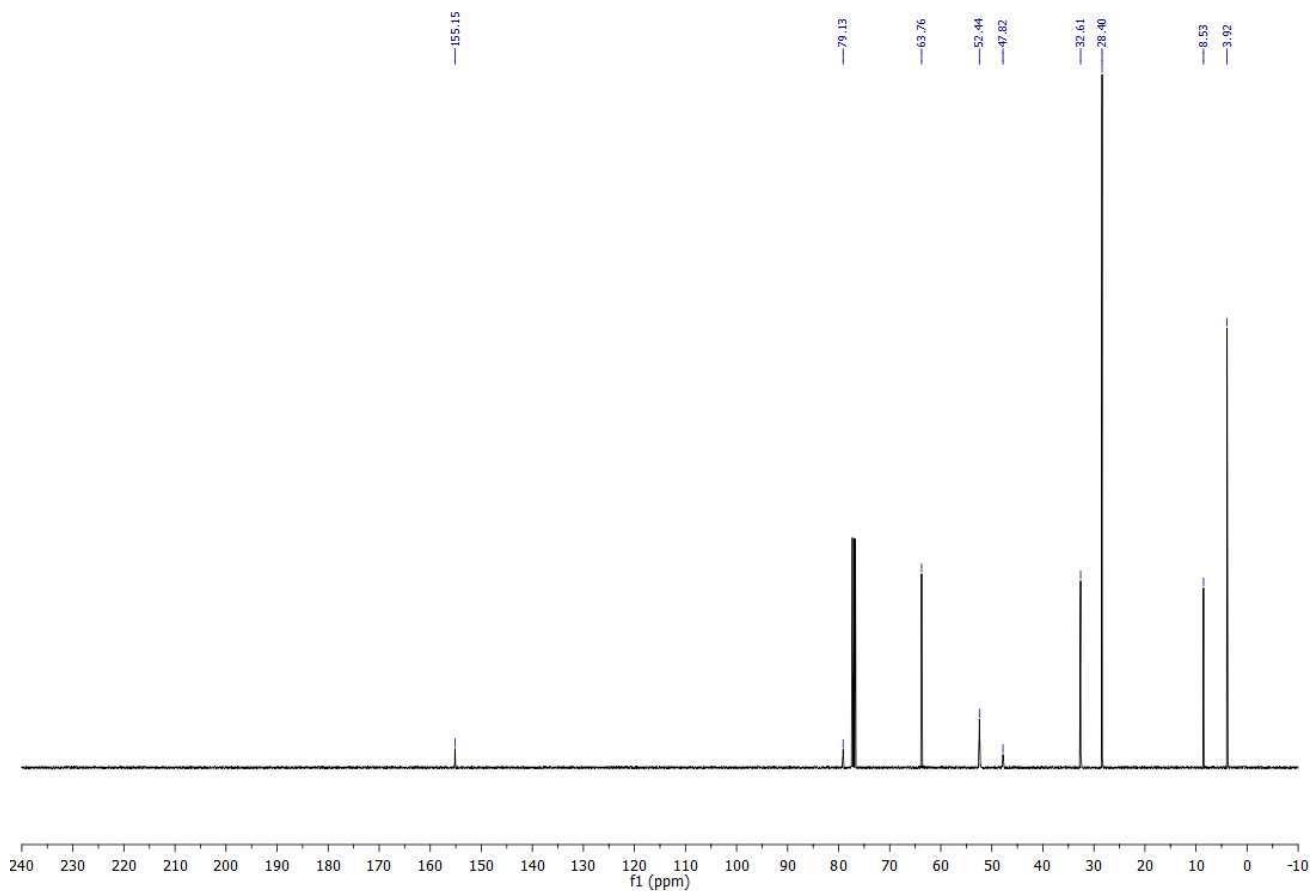
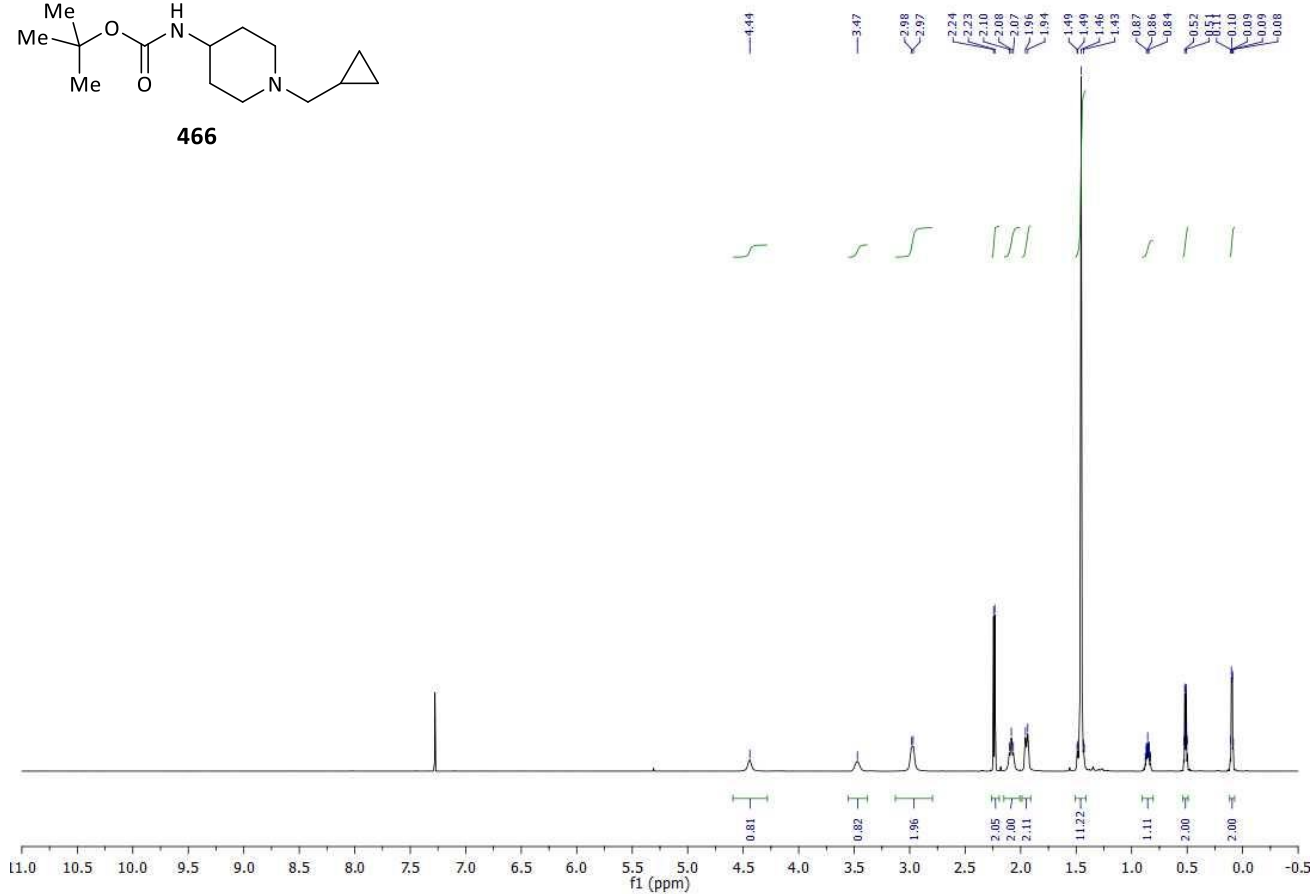
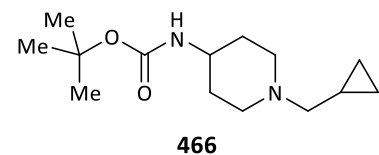


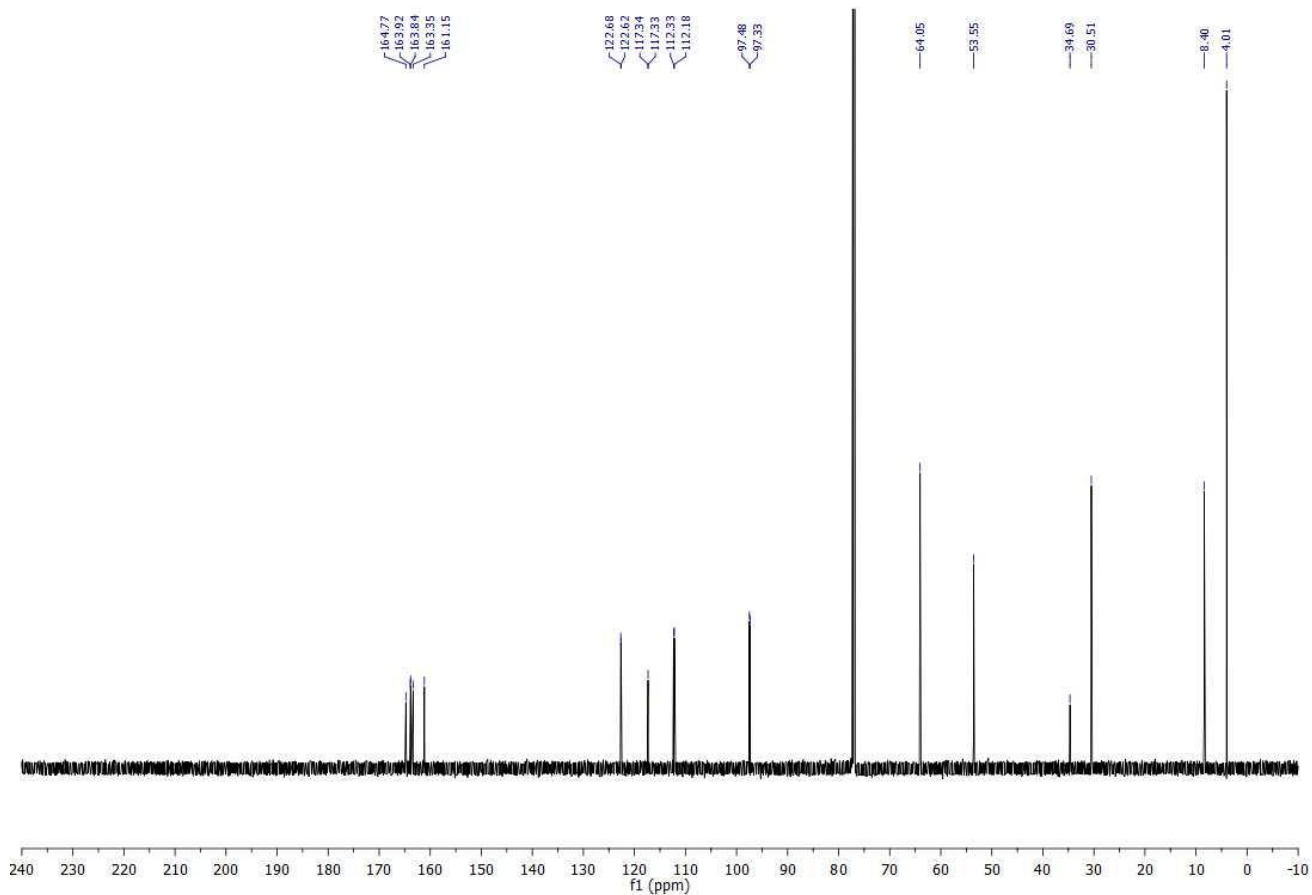
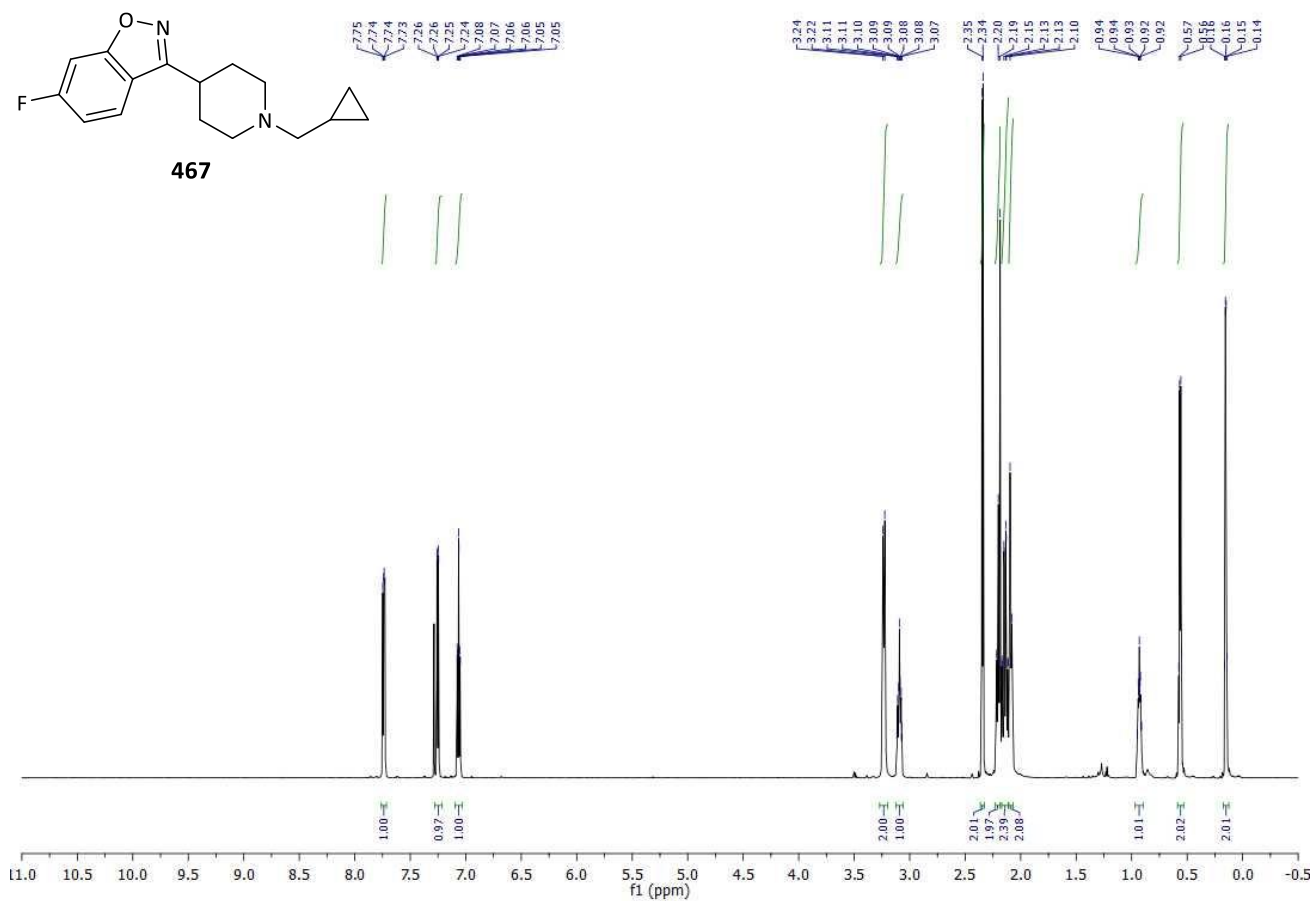
463

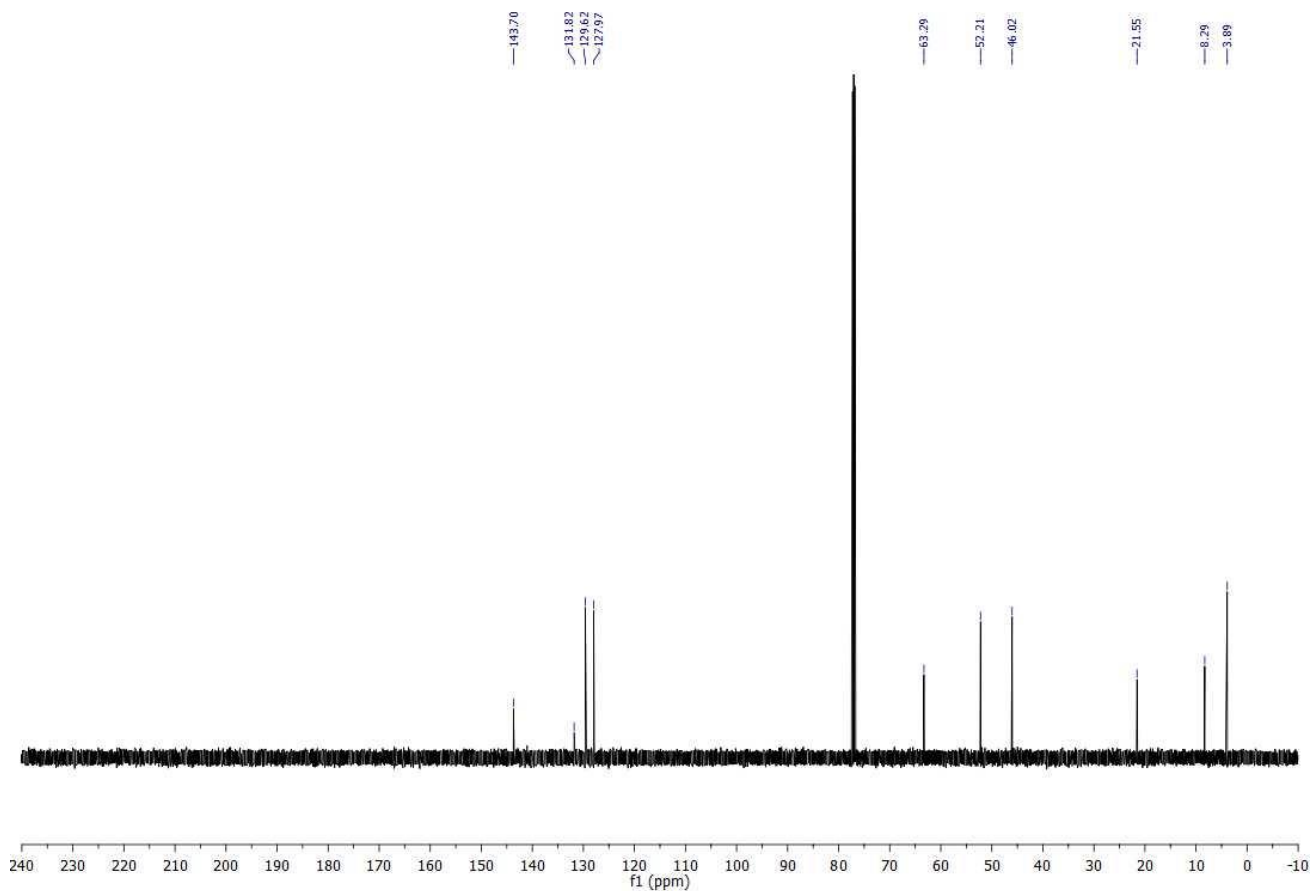
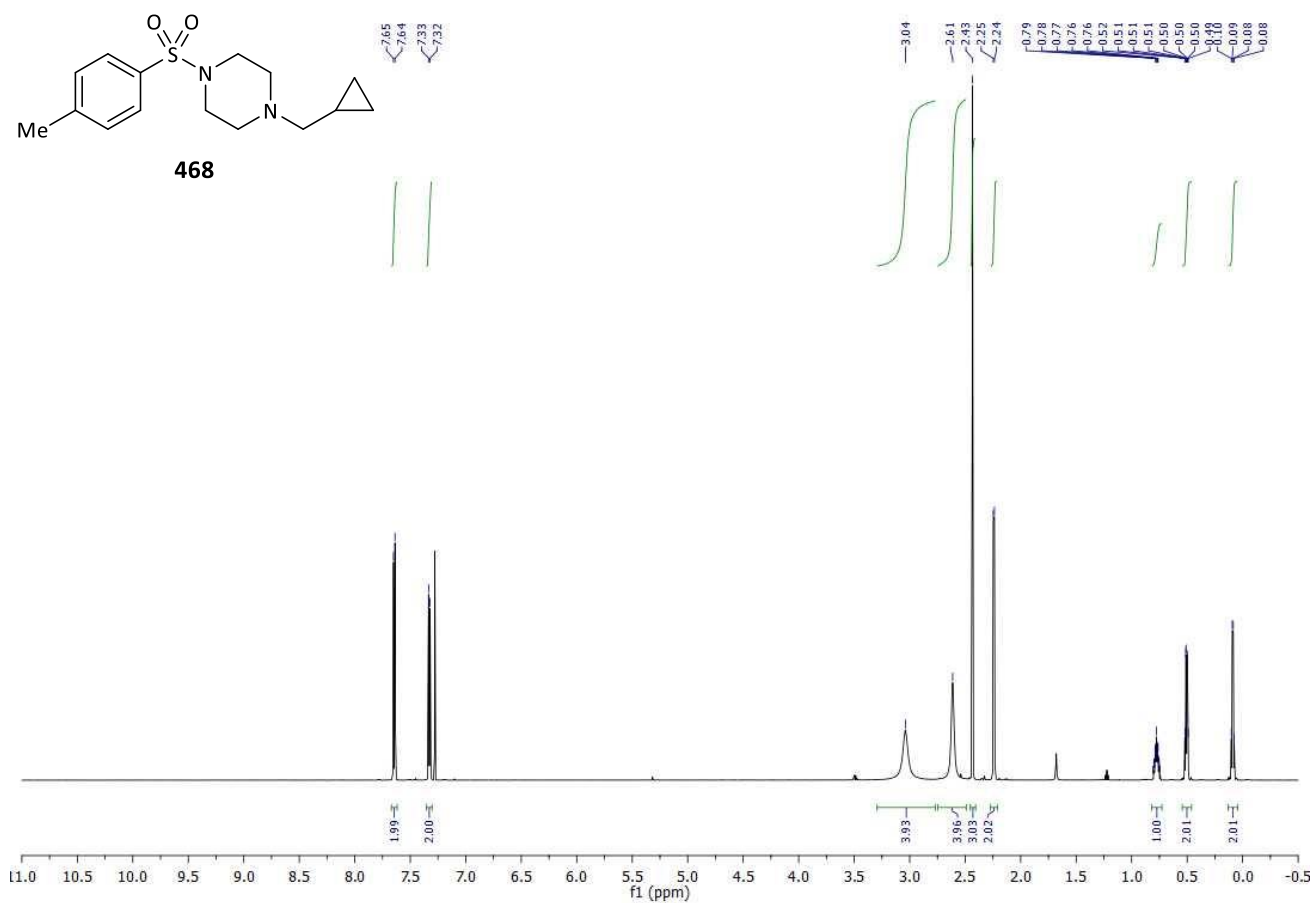


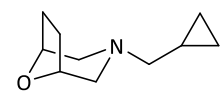




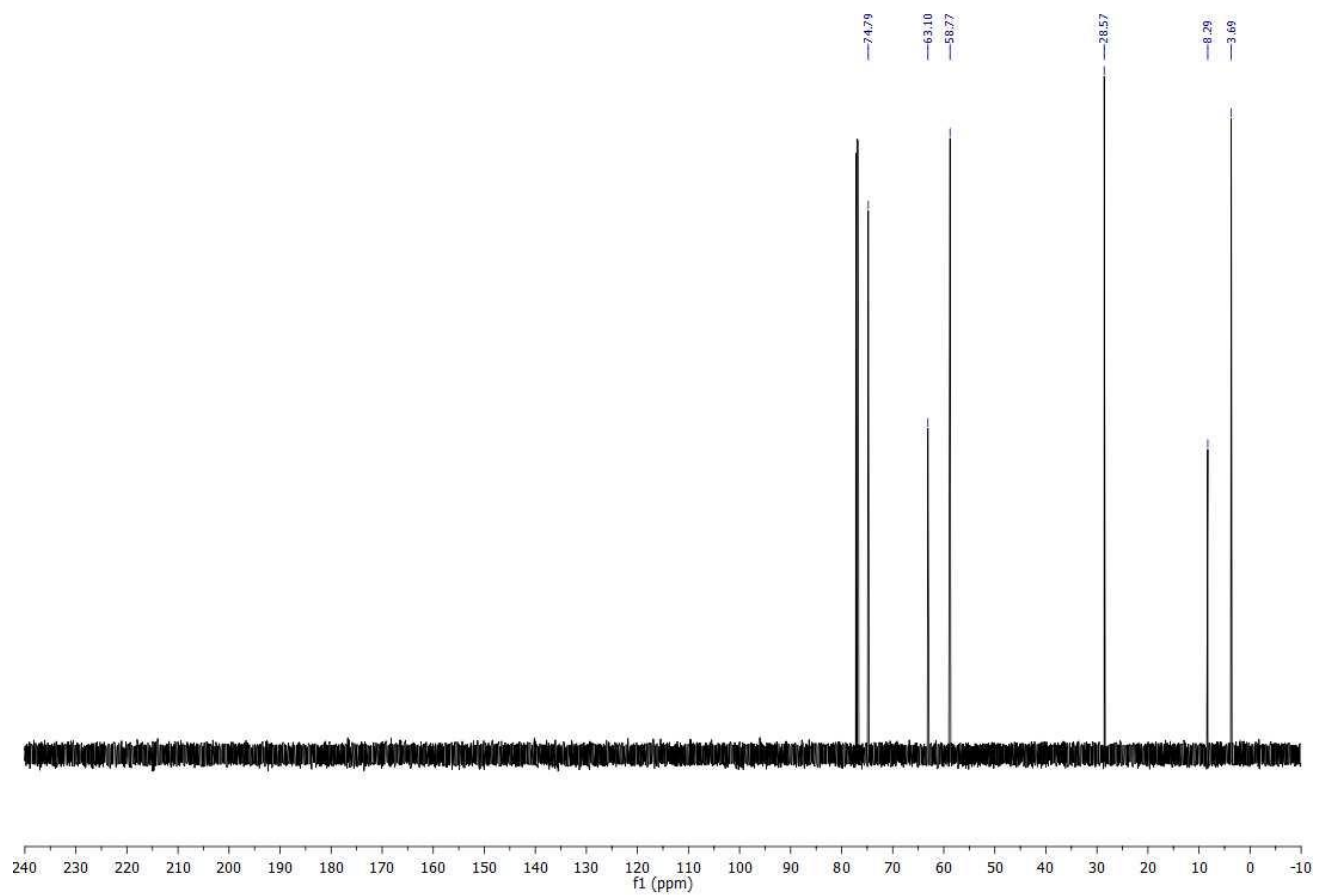
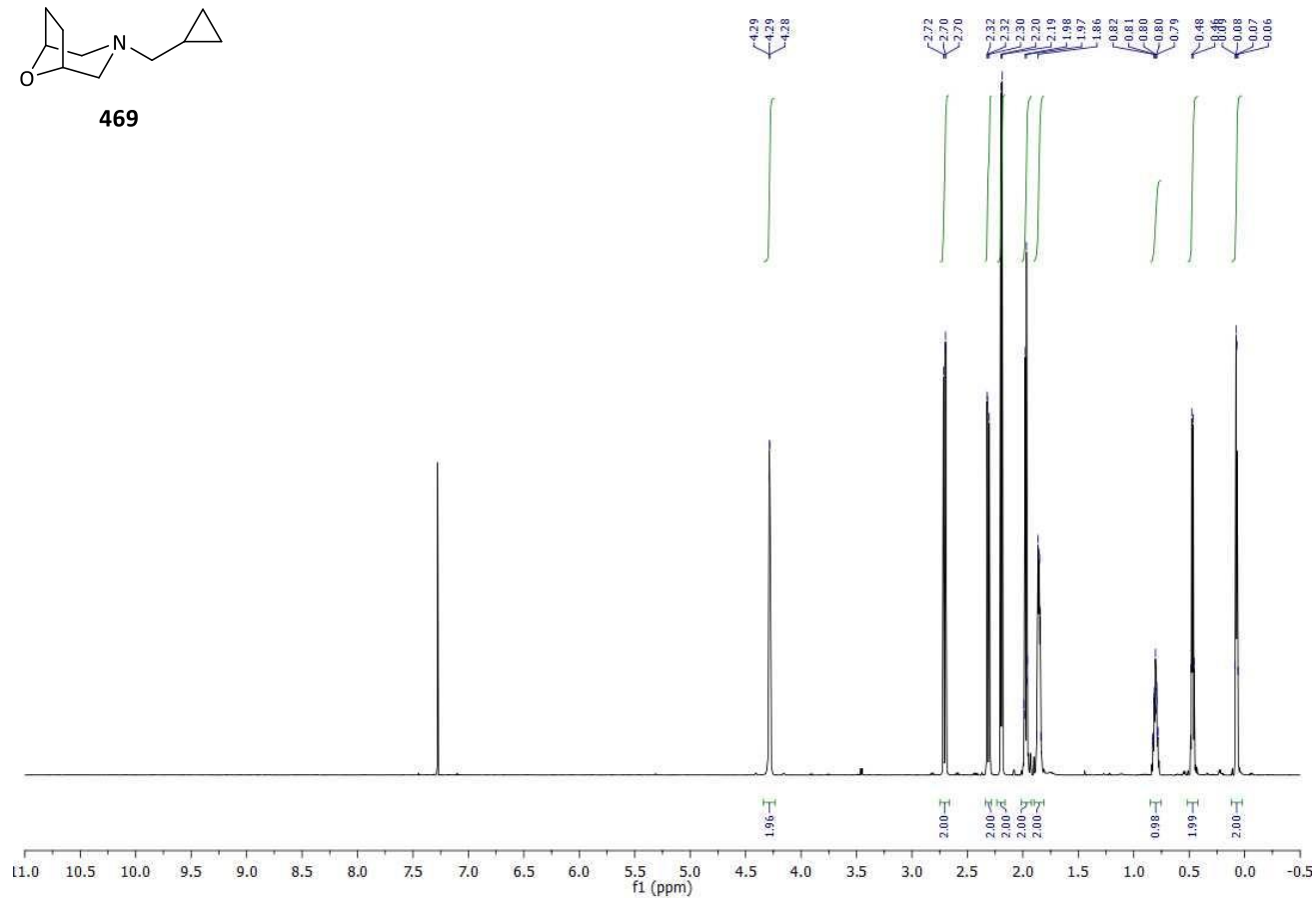


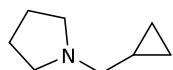




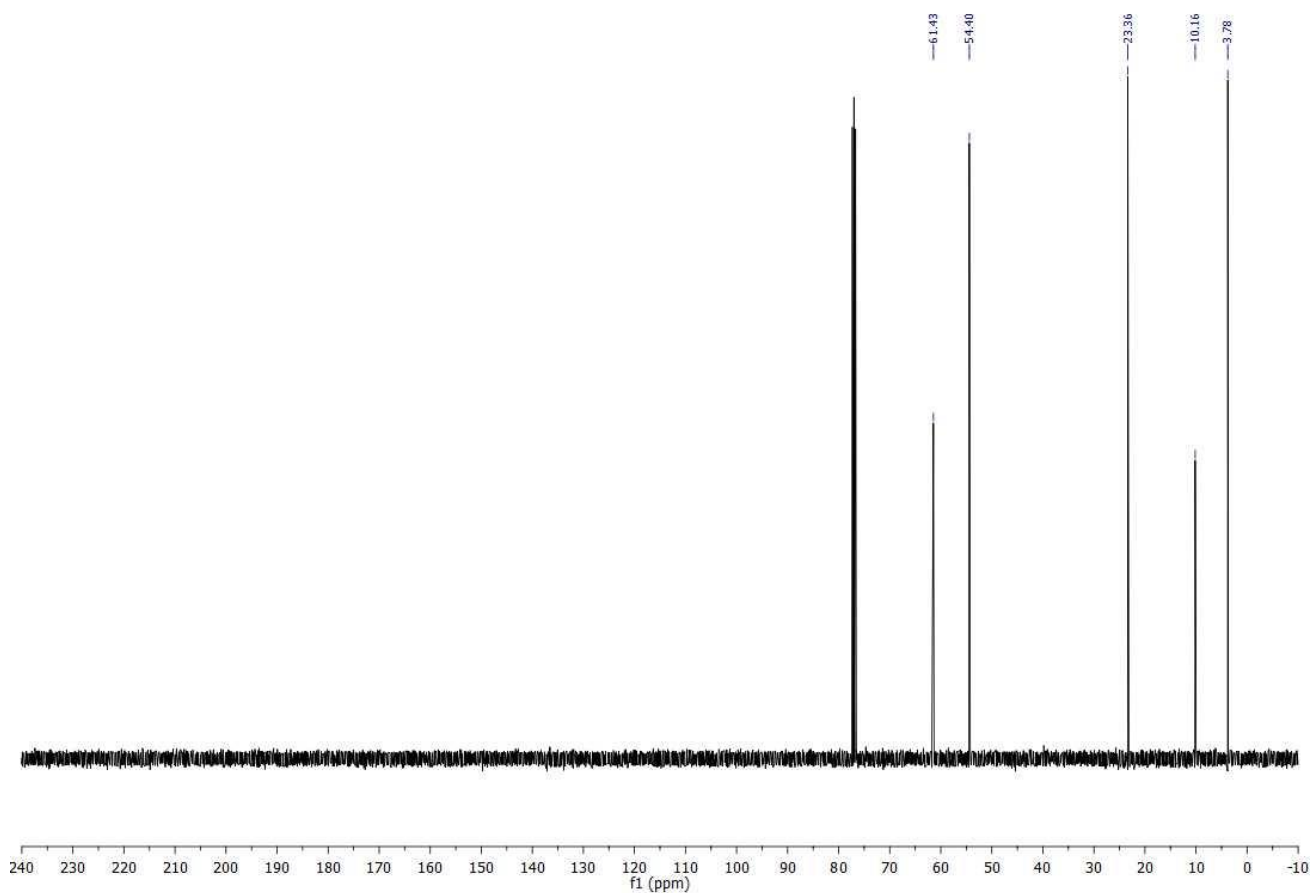
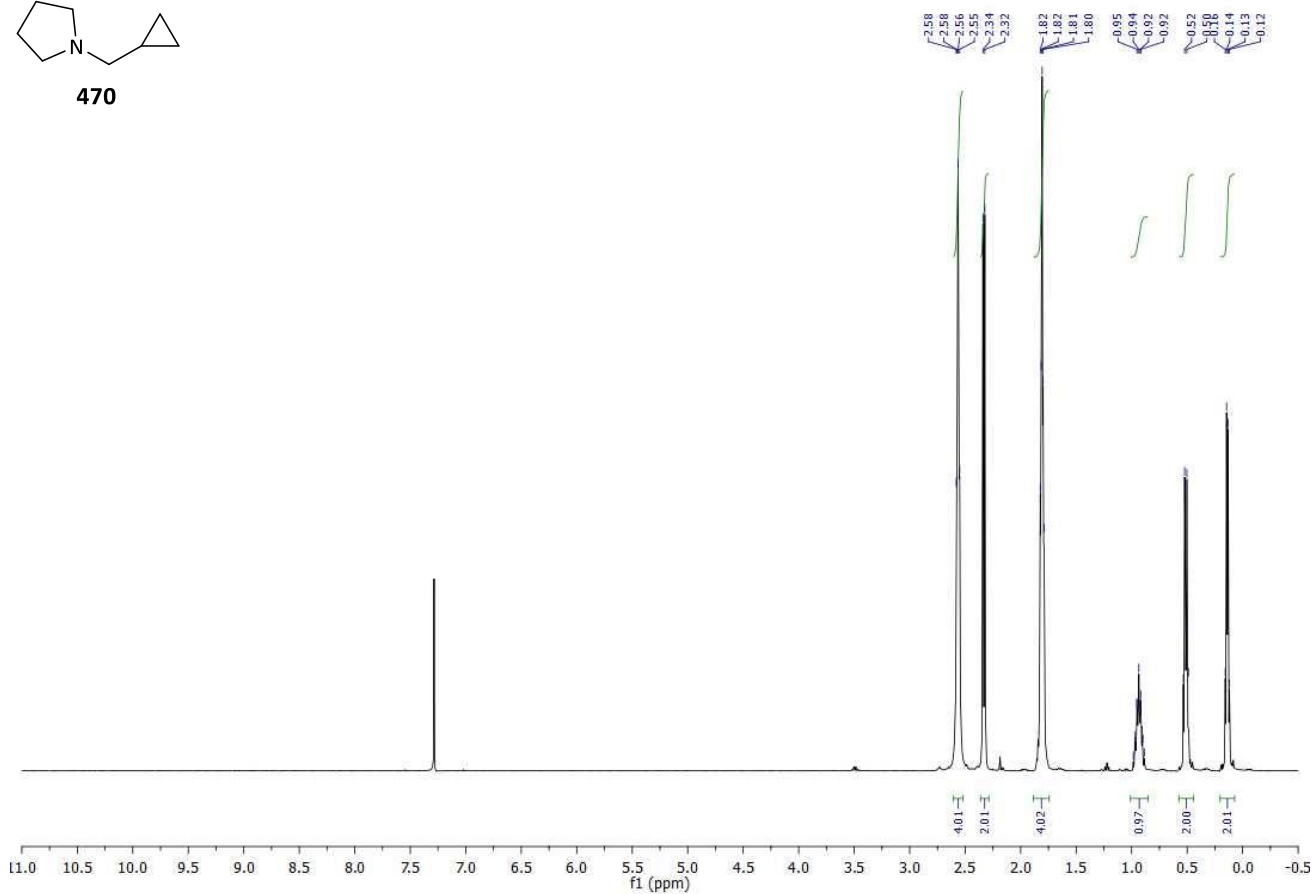


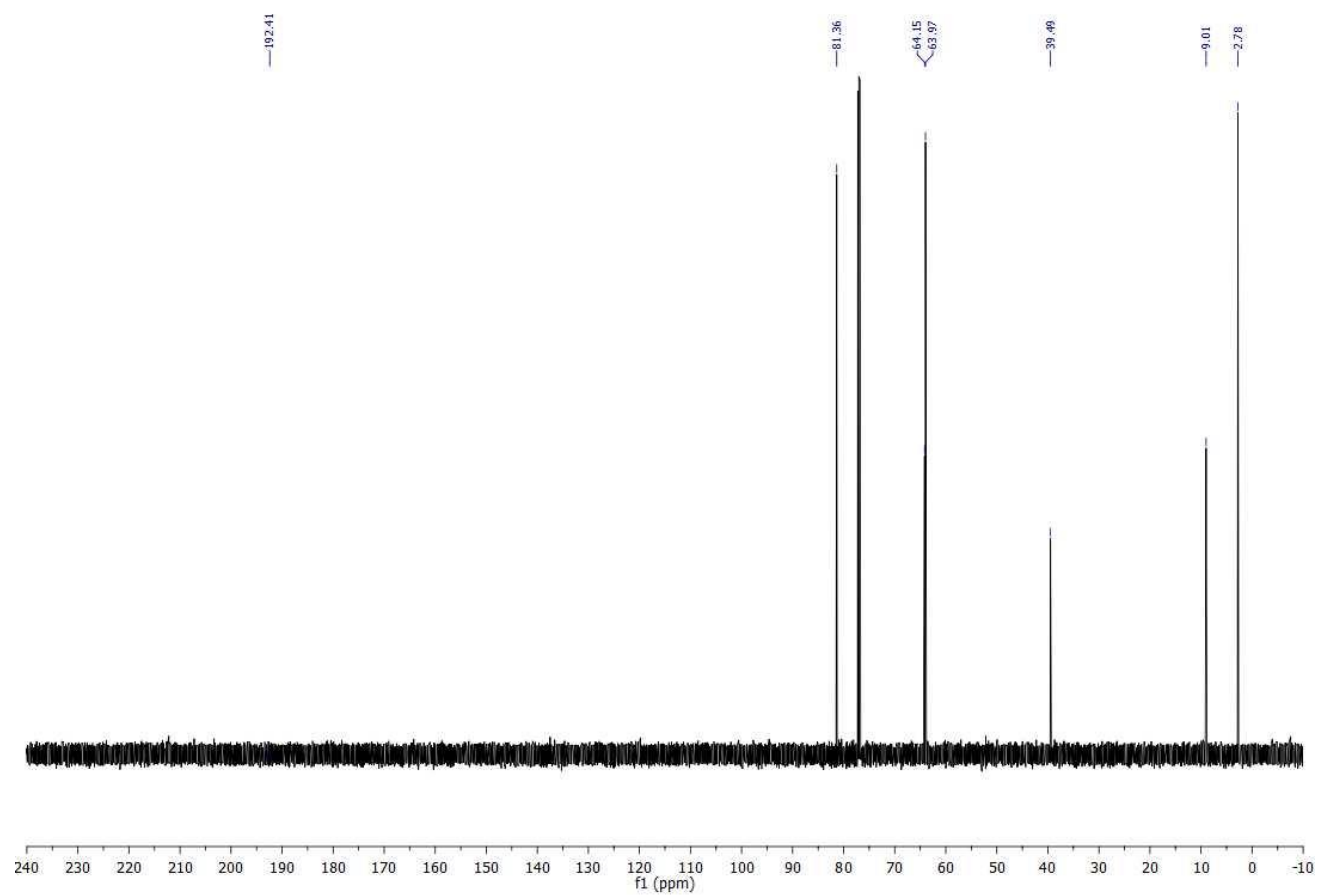
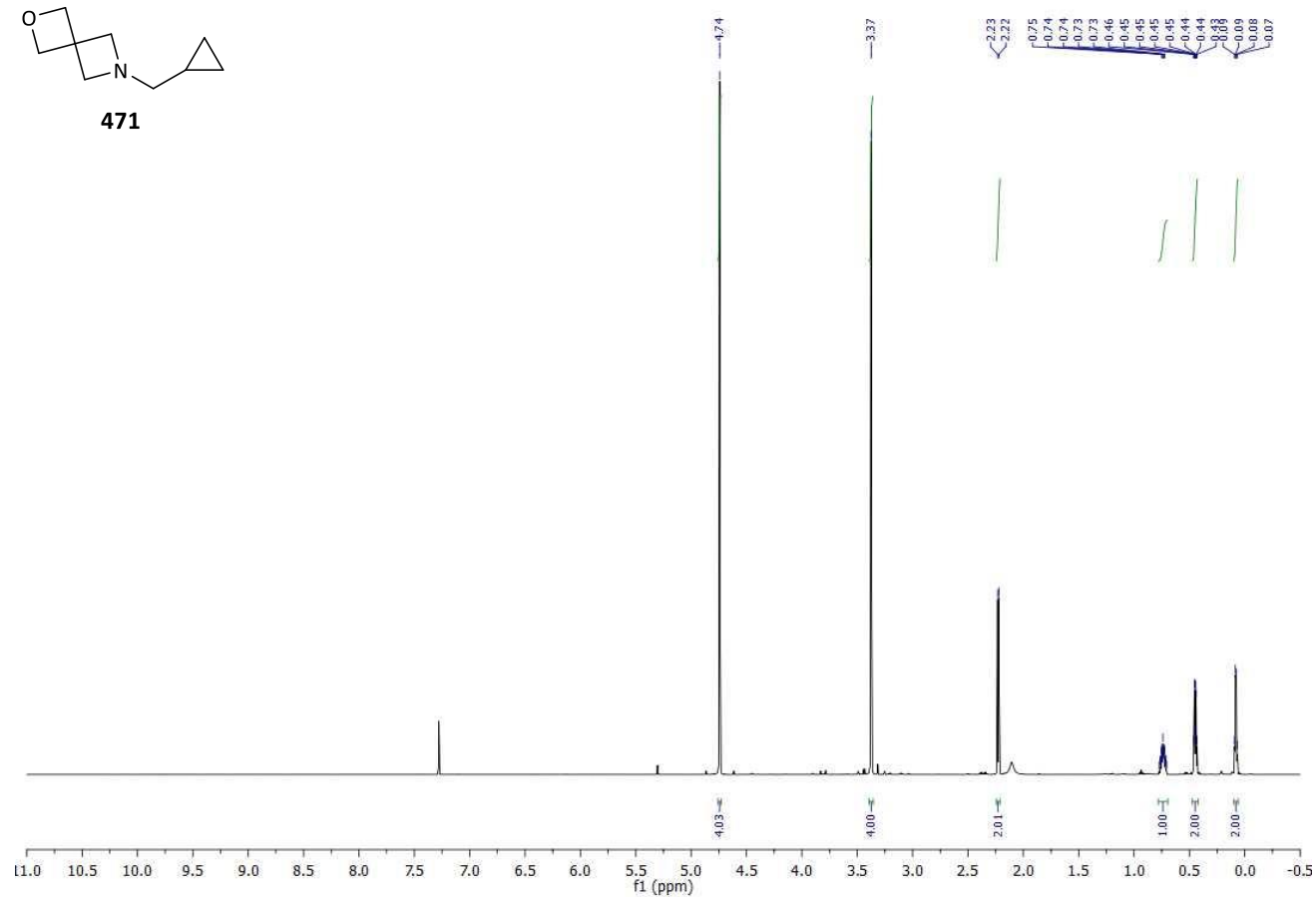
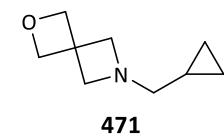
469

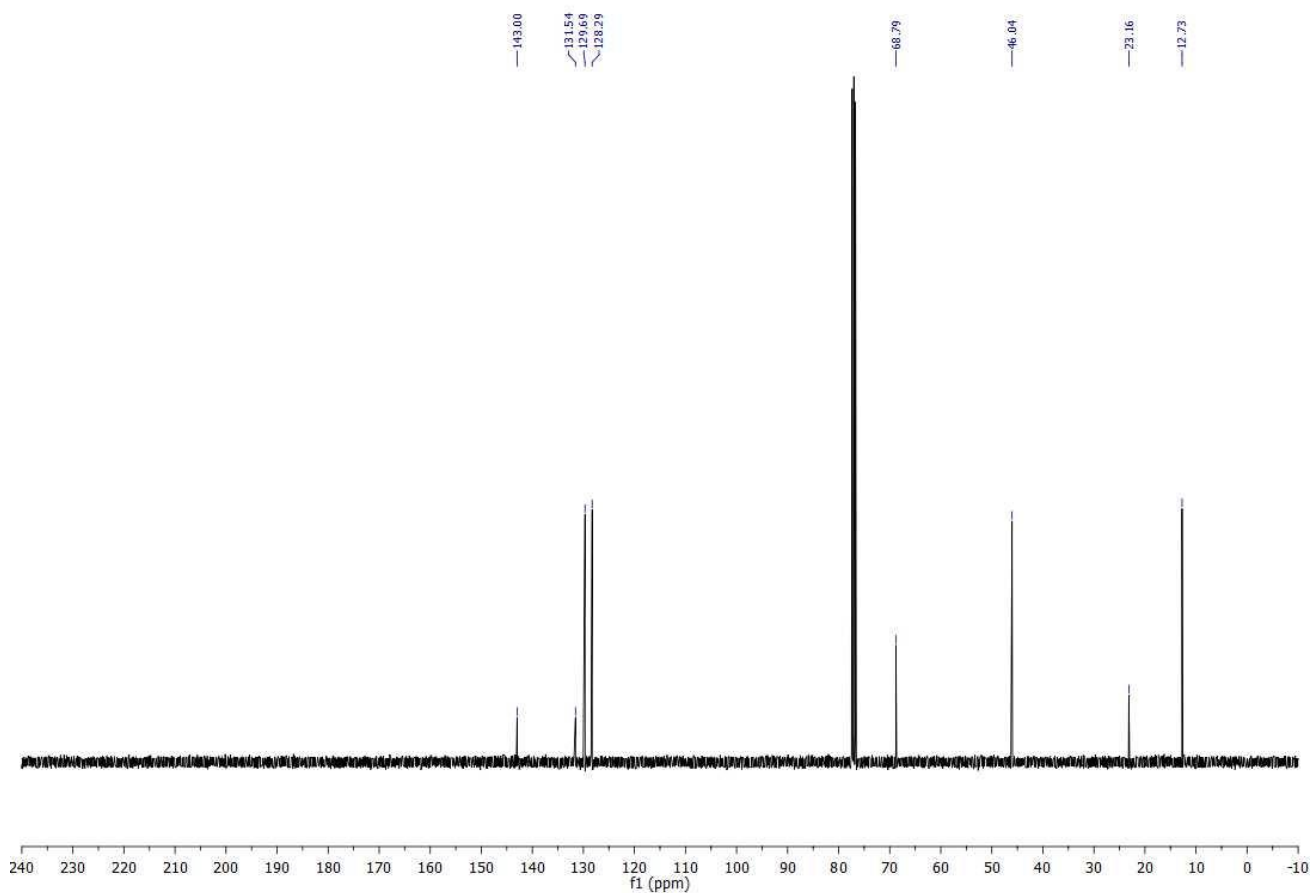
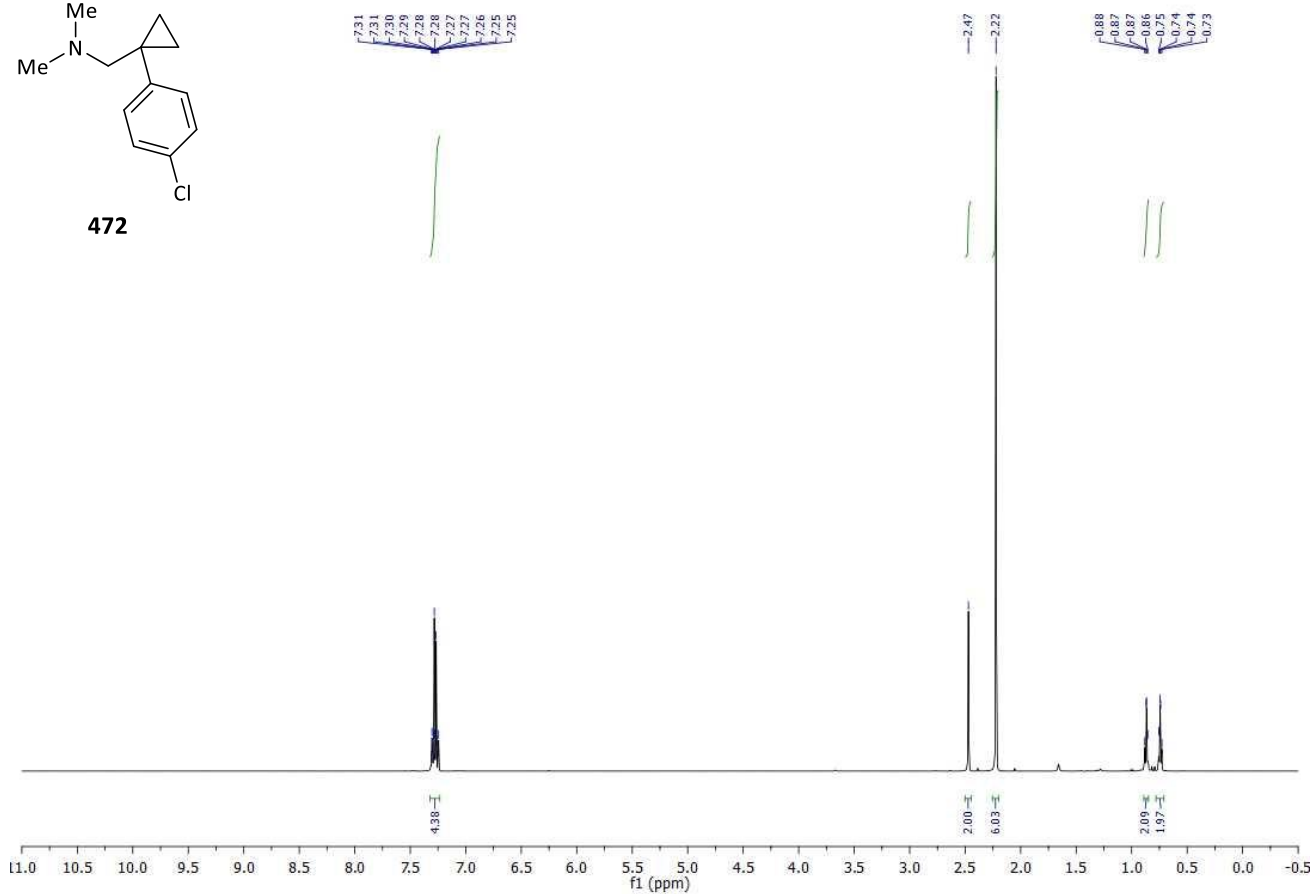
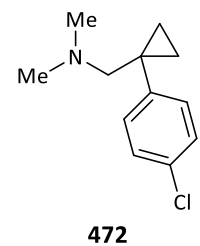


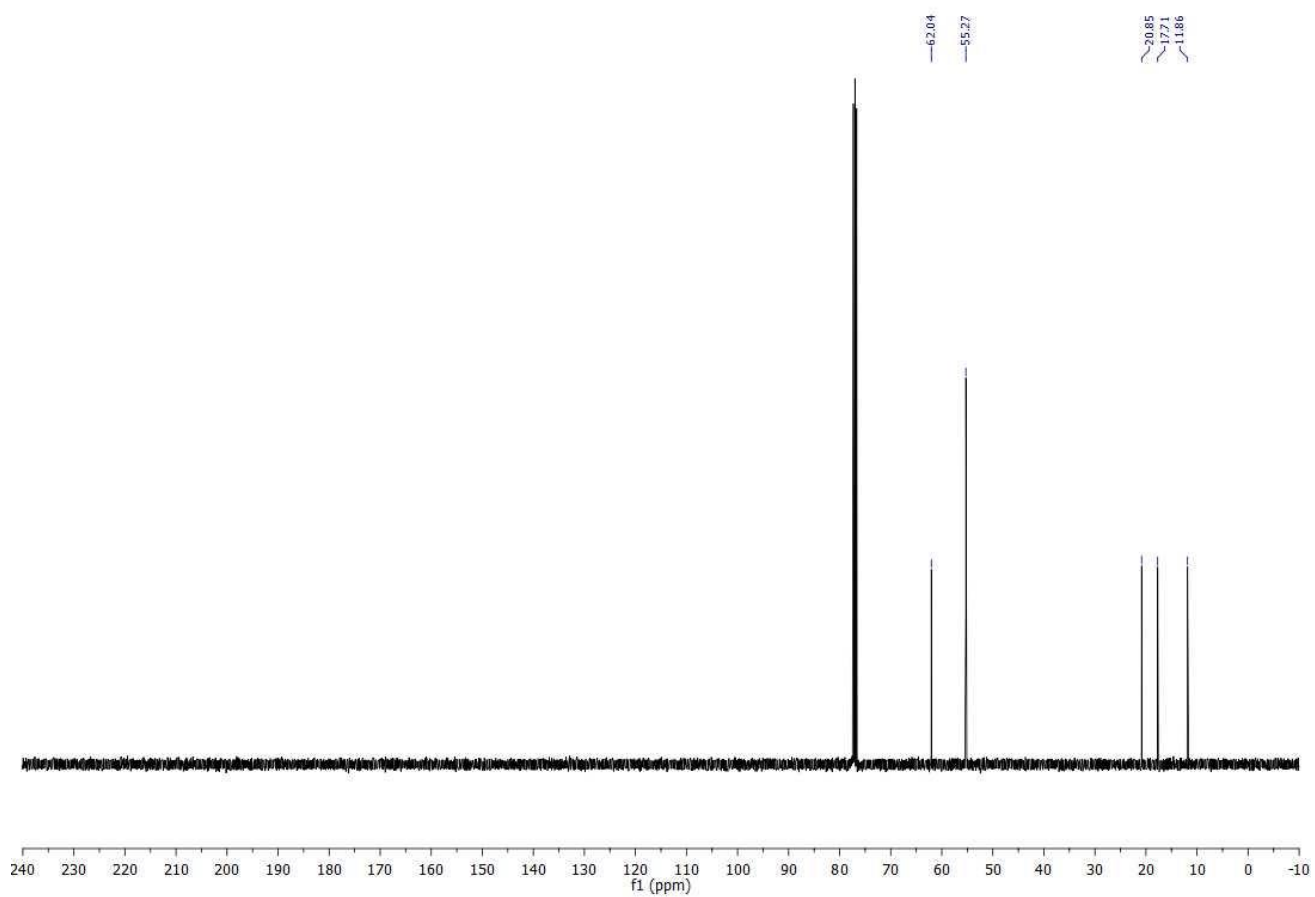
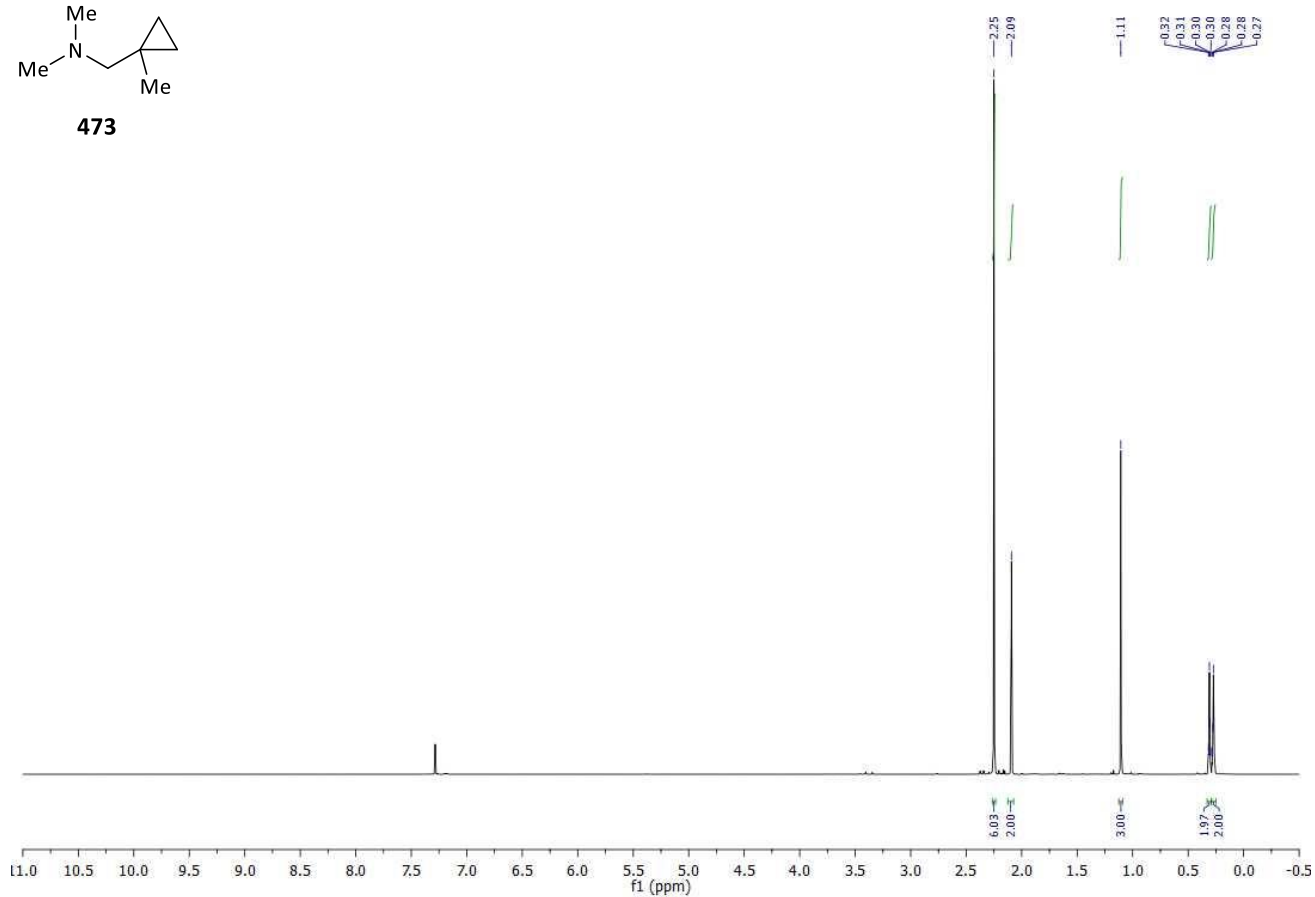
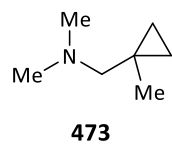


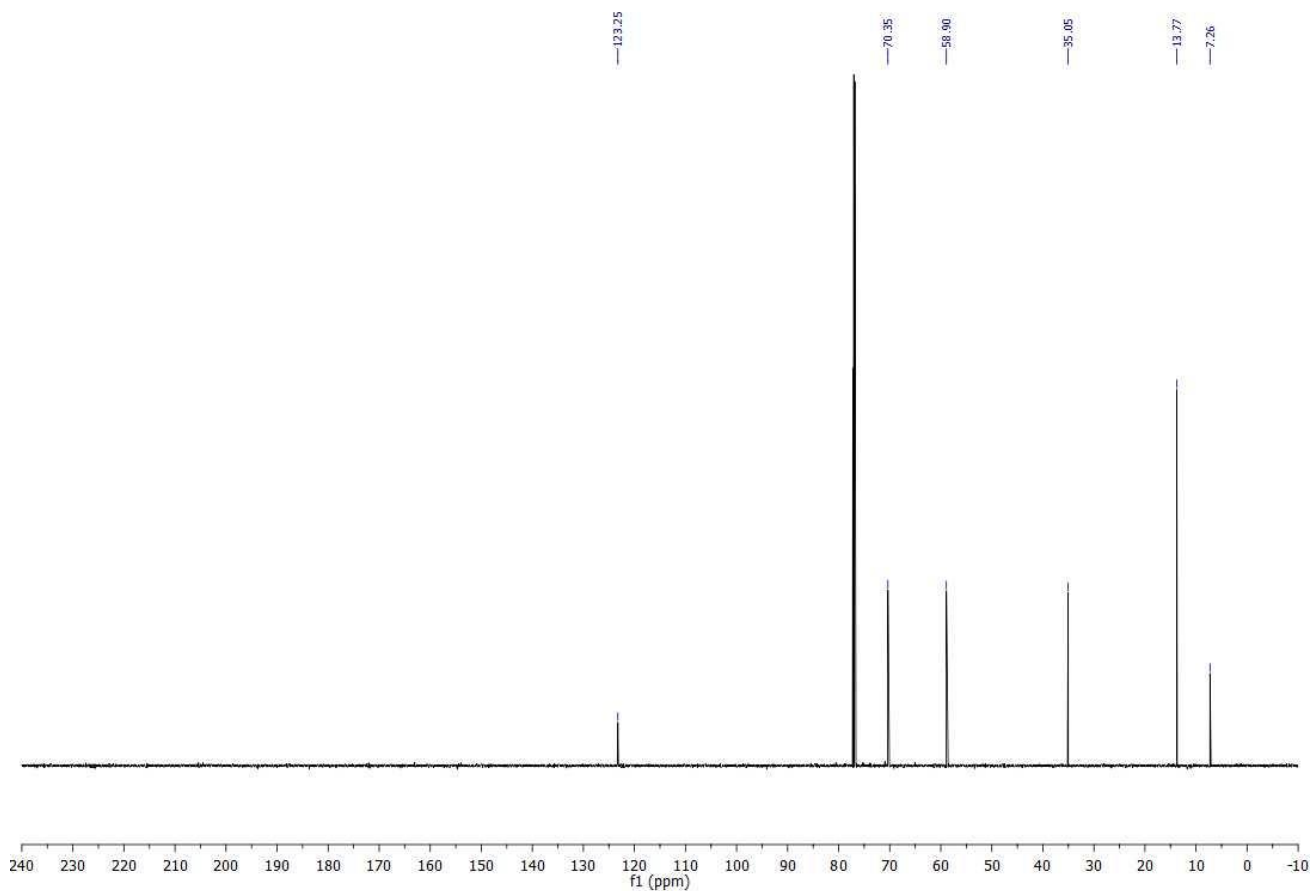
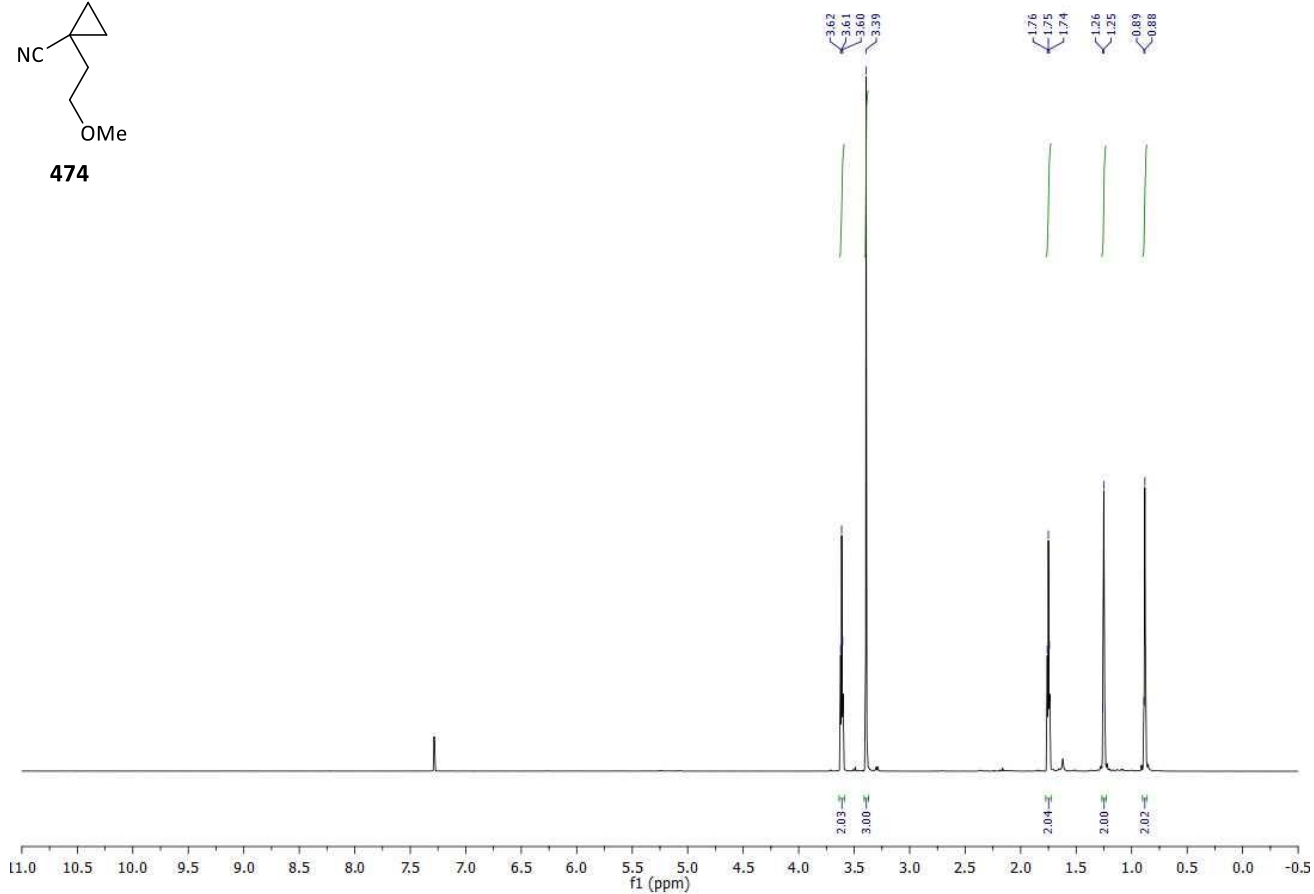
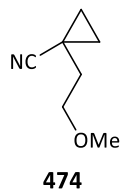
470

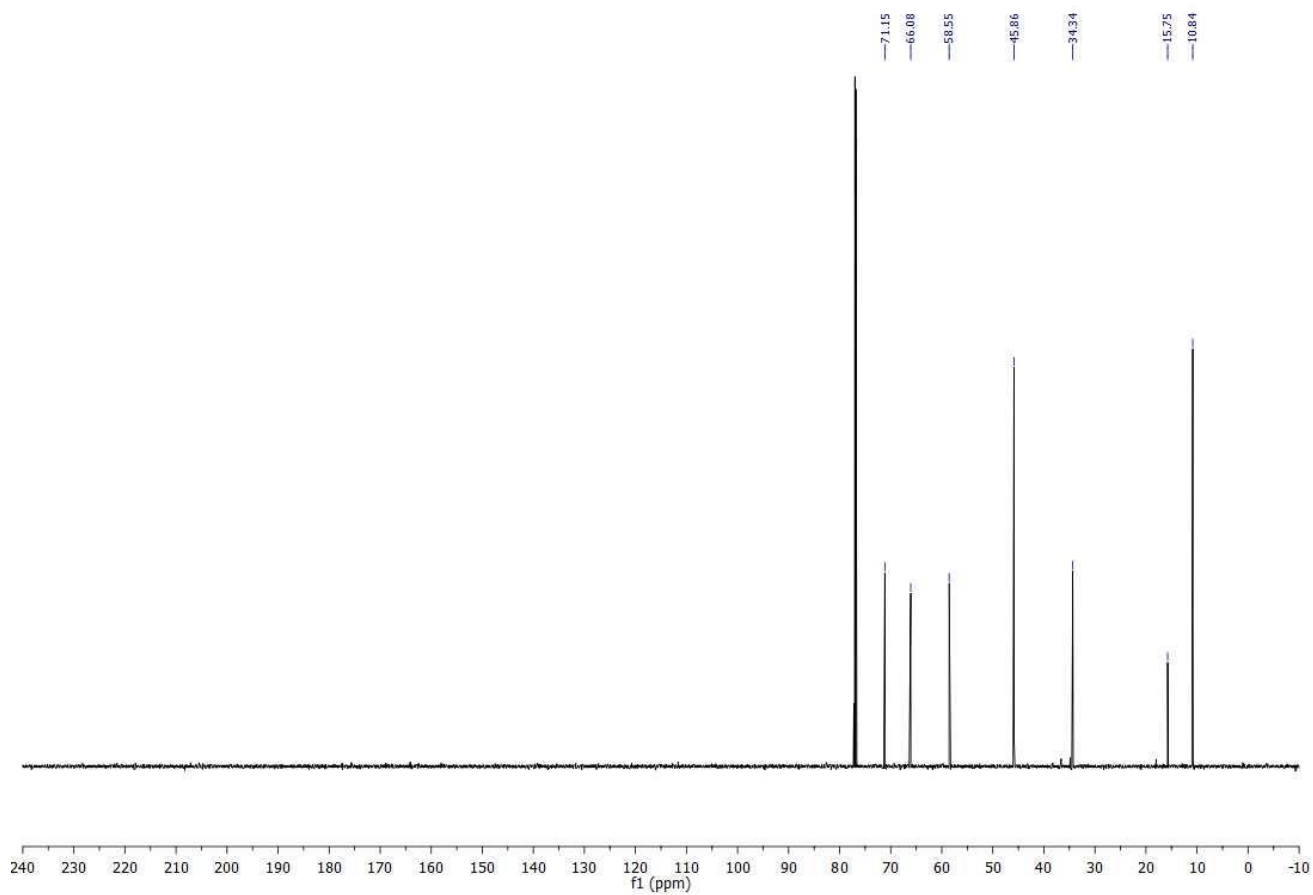
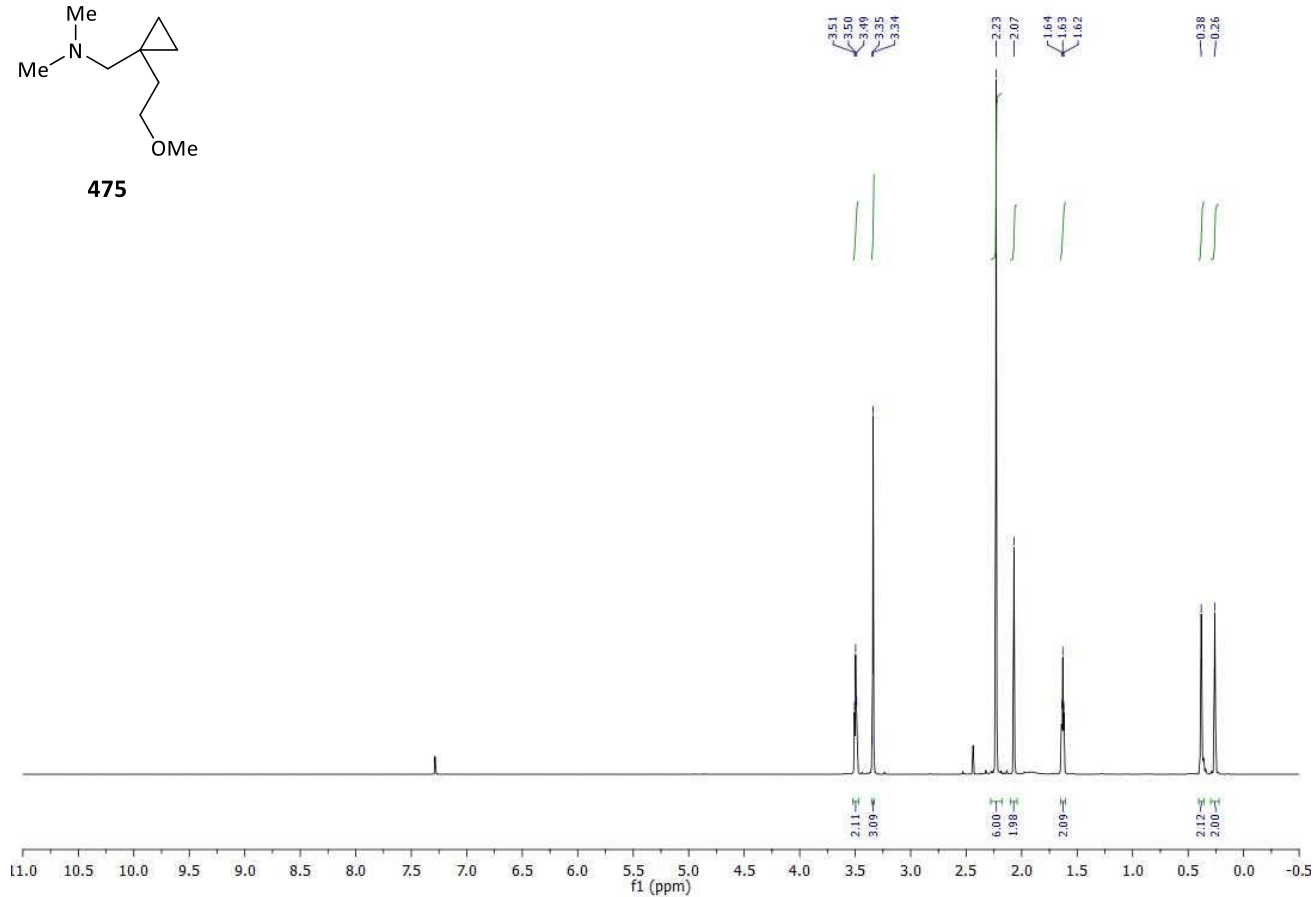
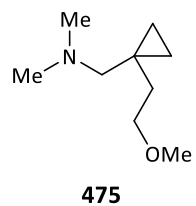


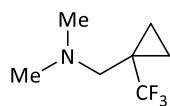




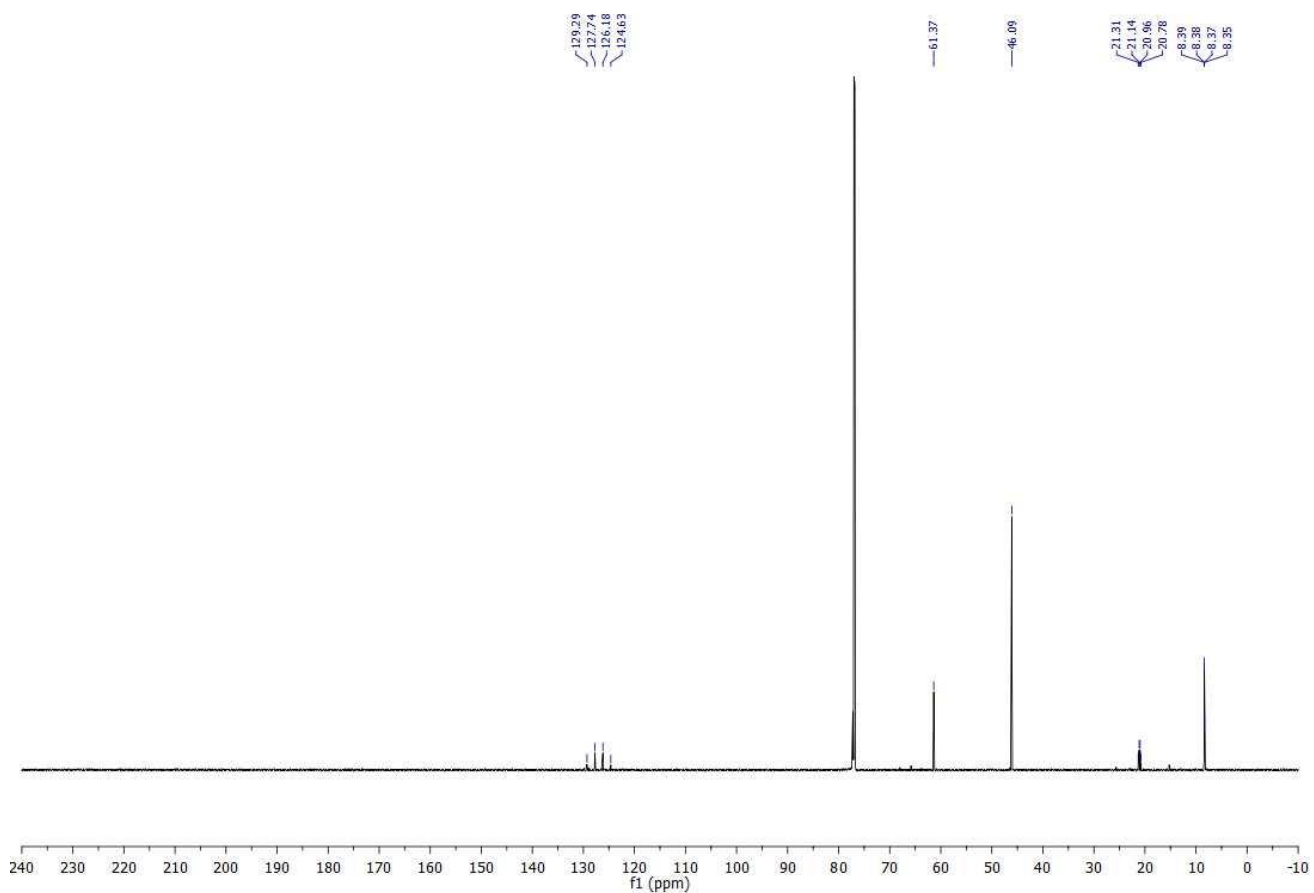
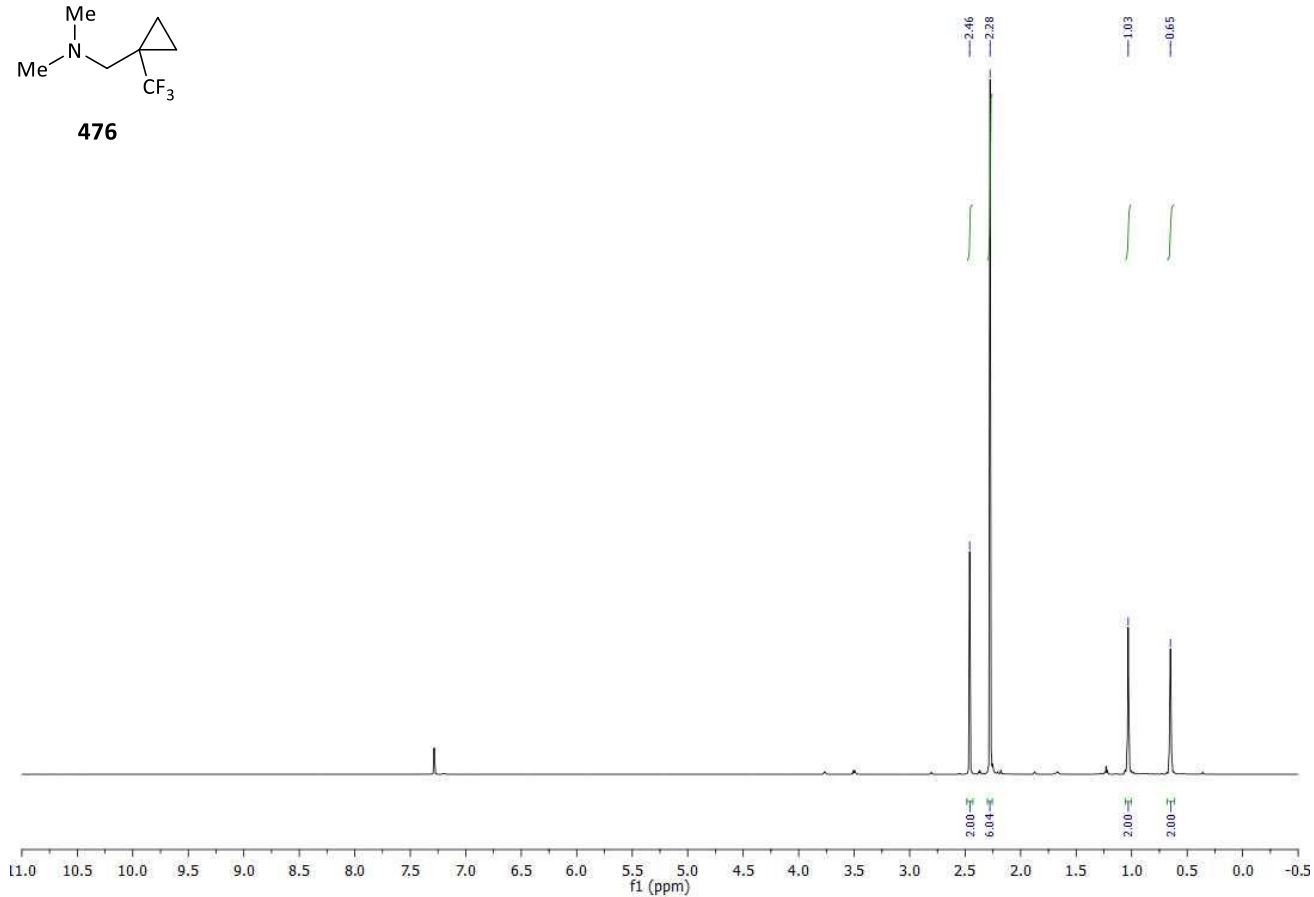


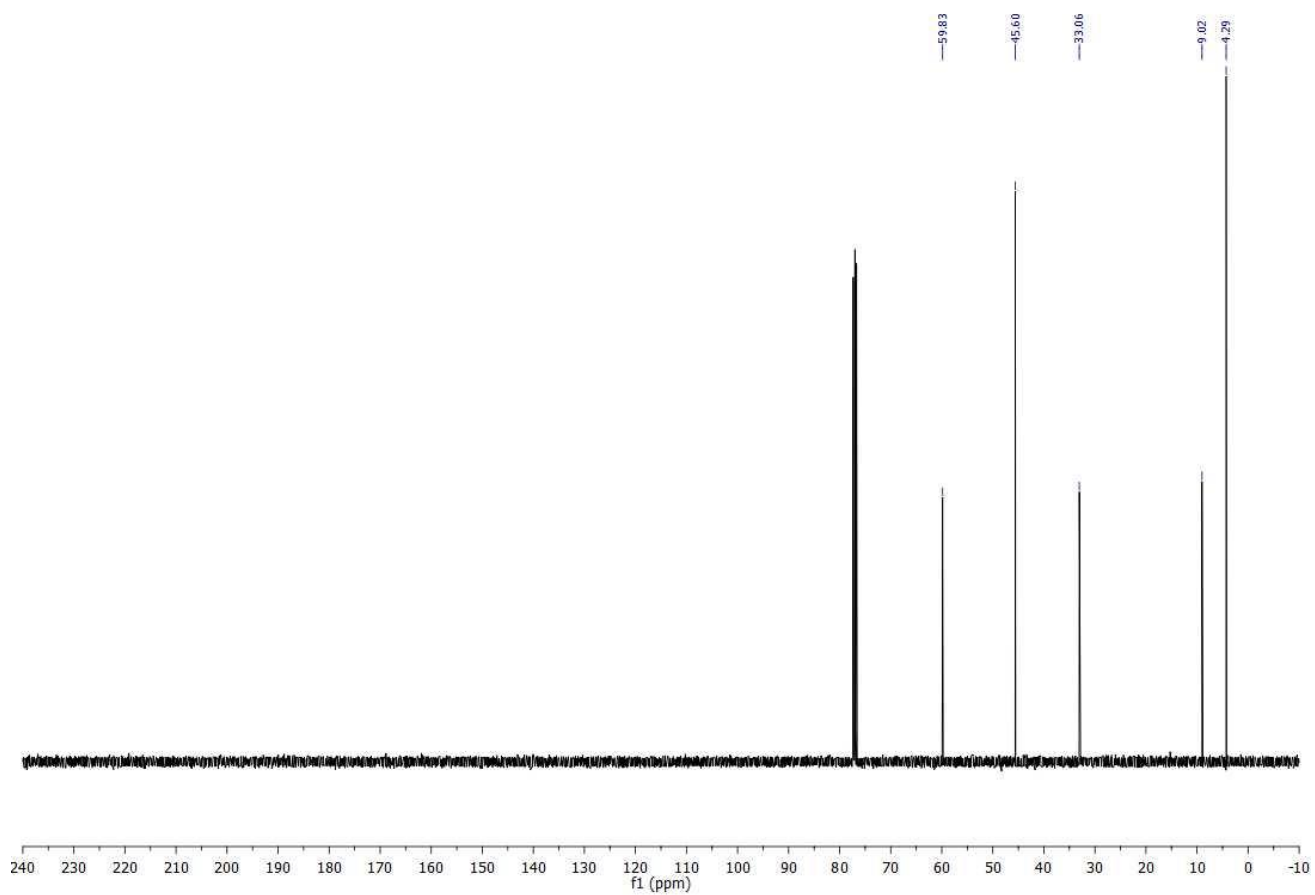
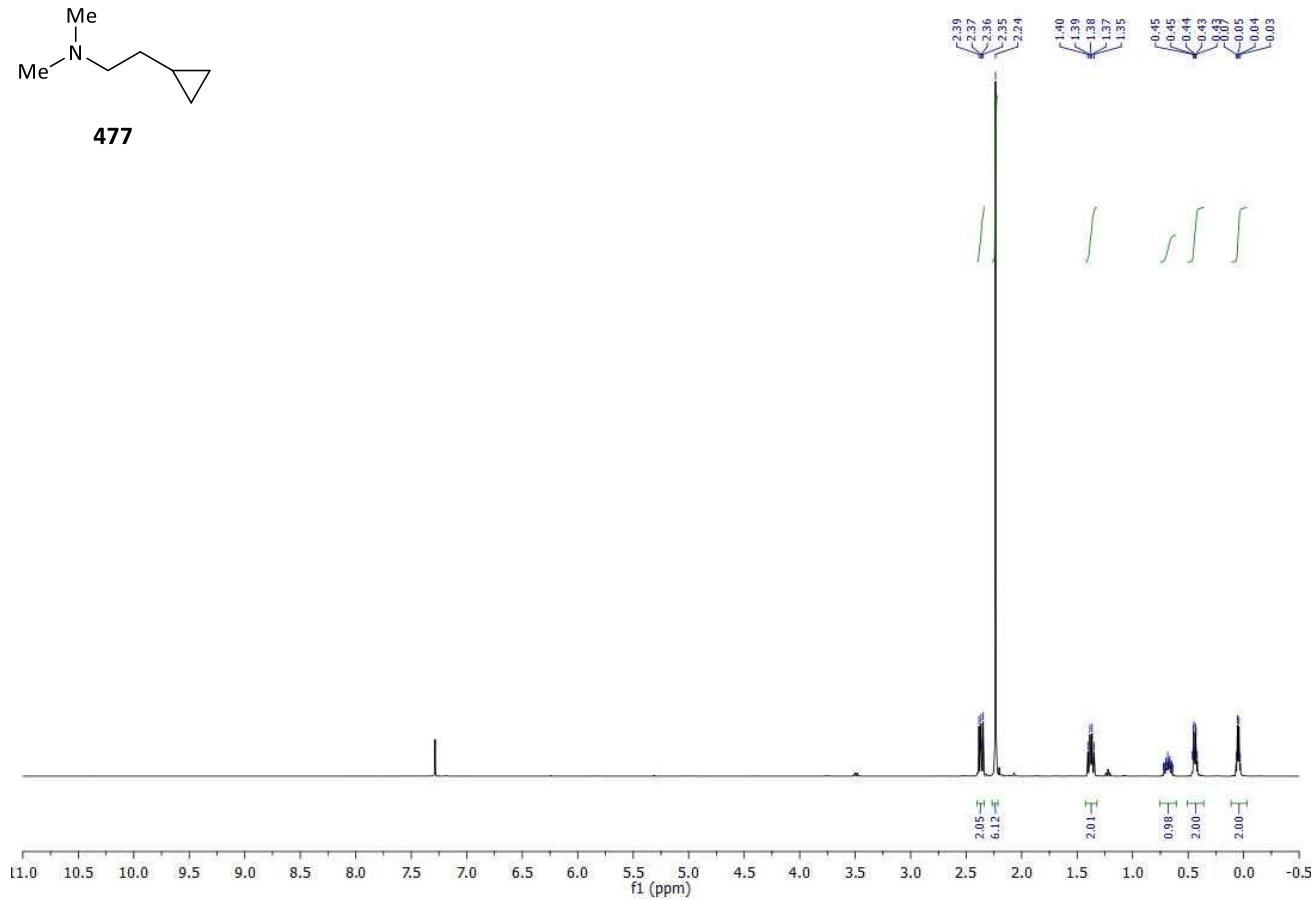
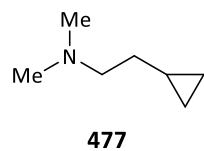


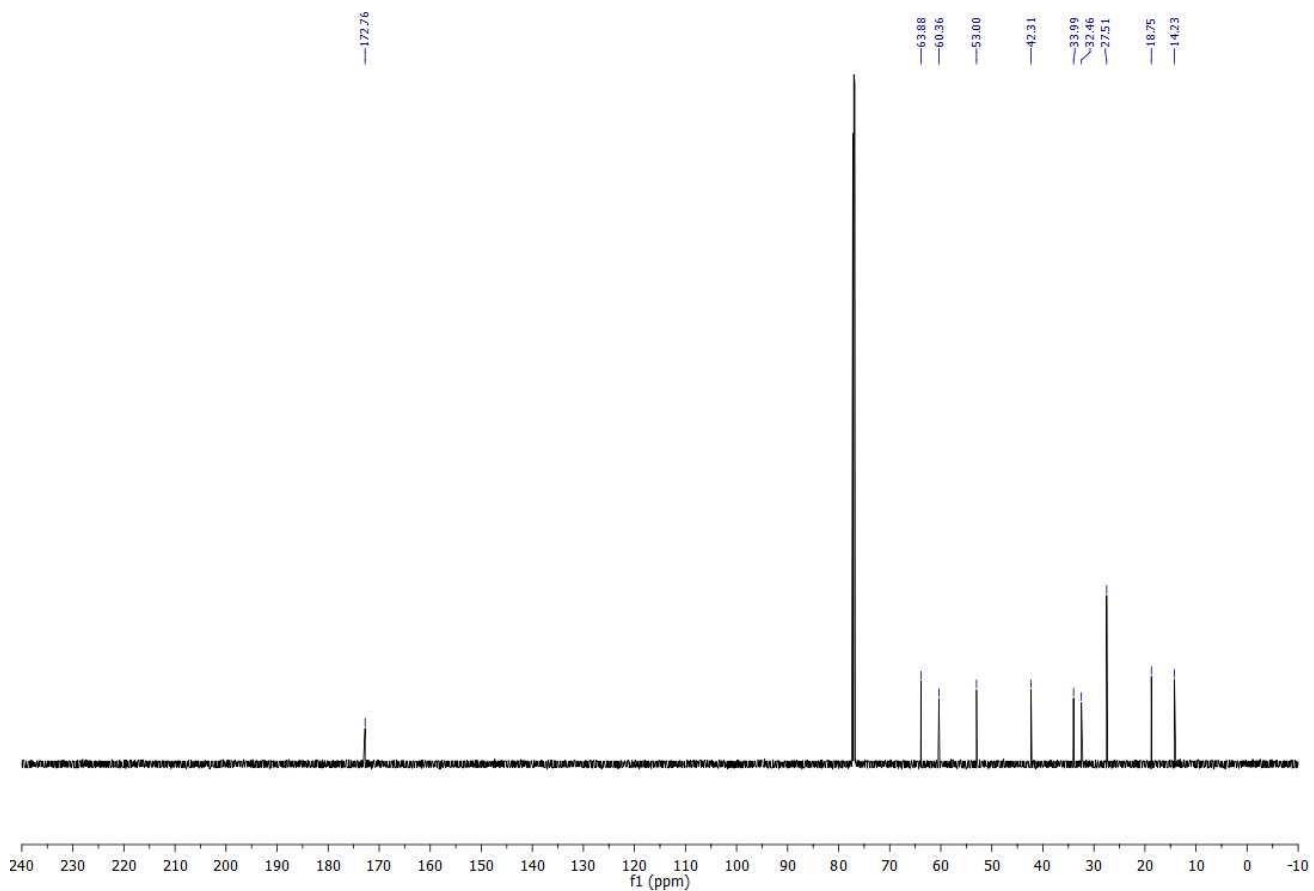
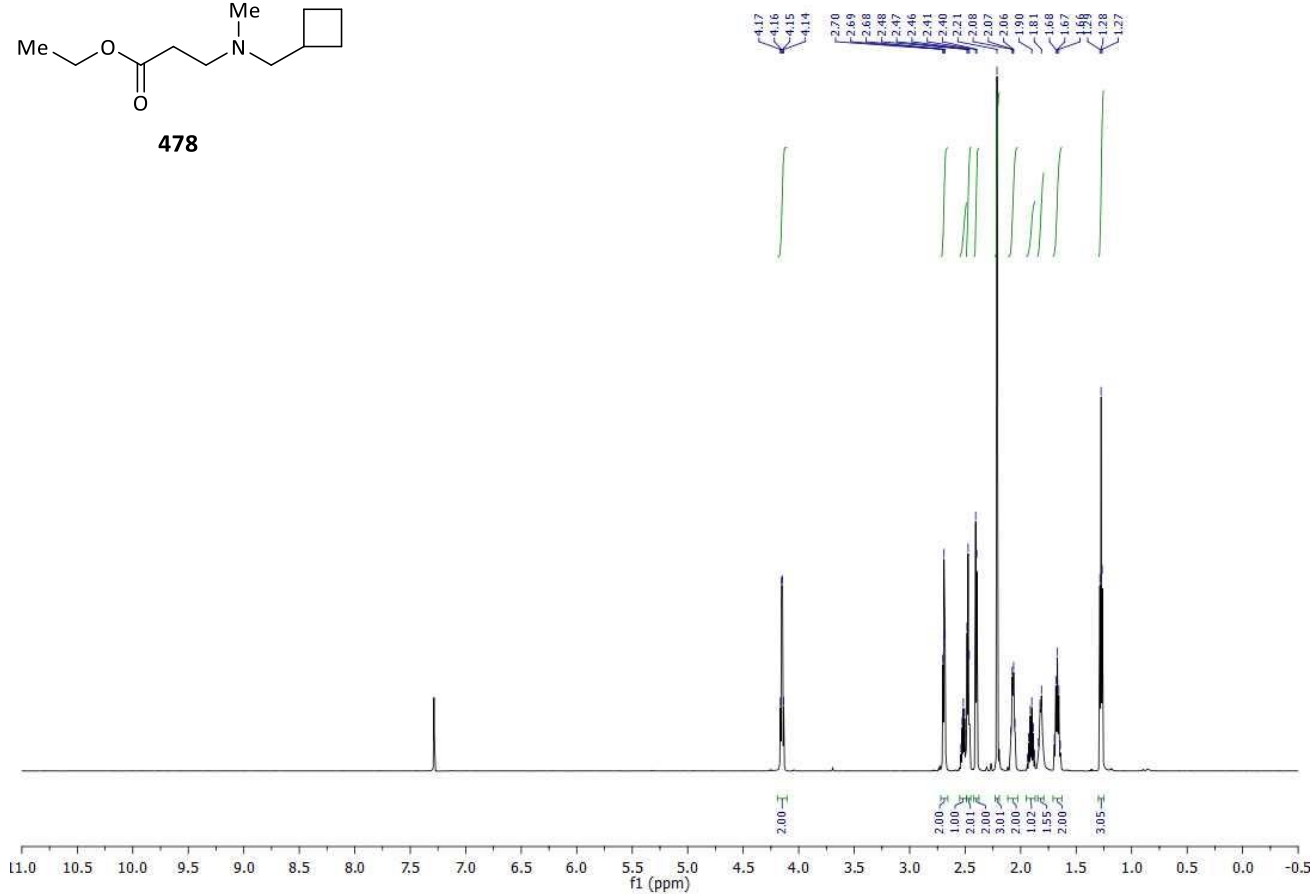
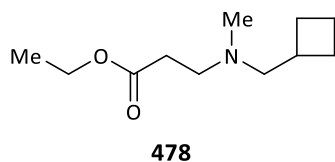


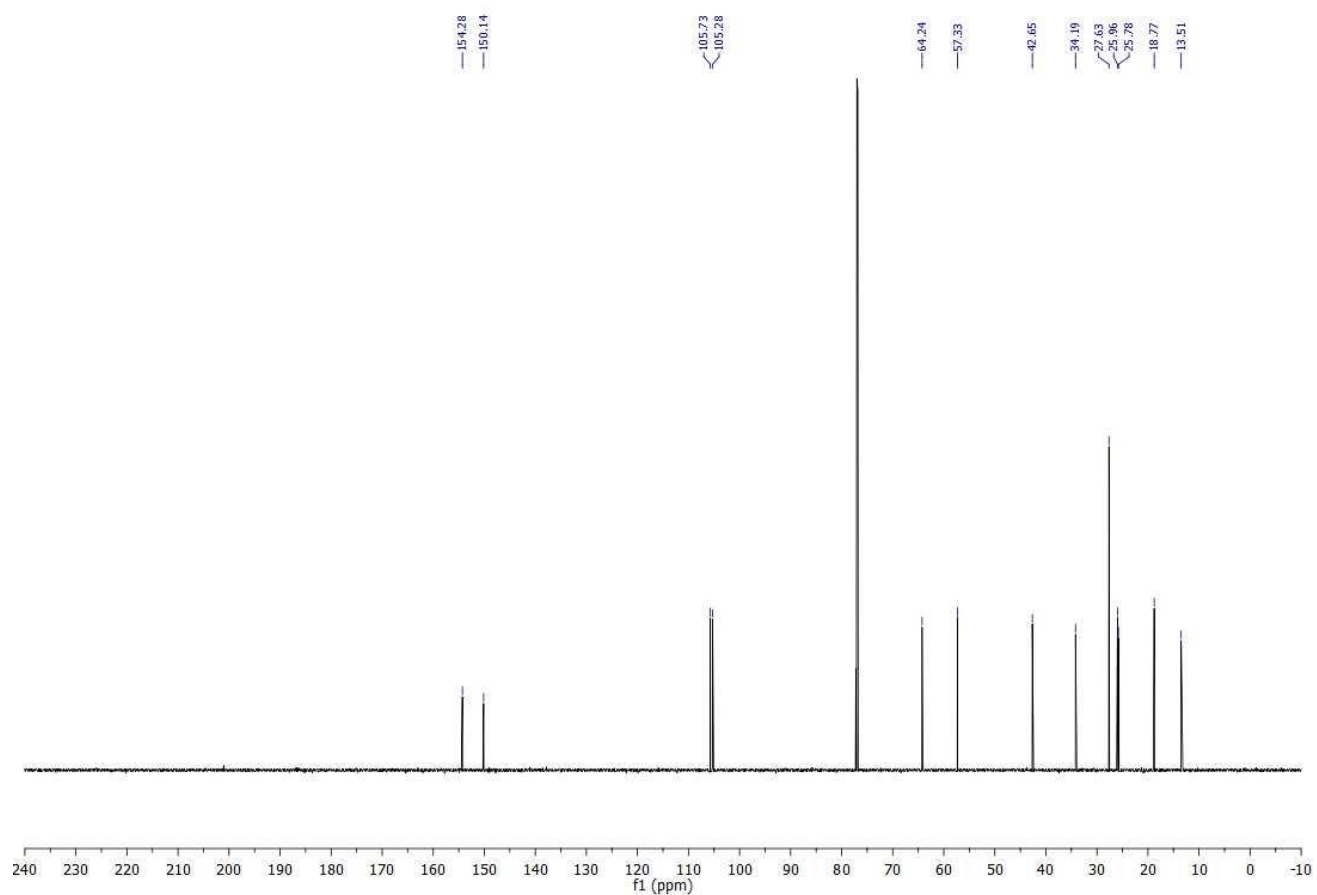
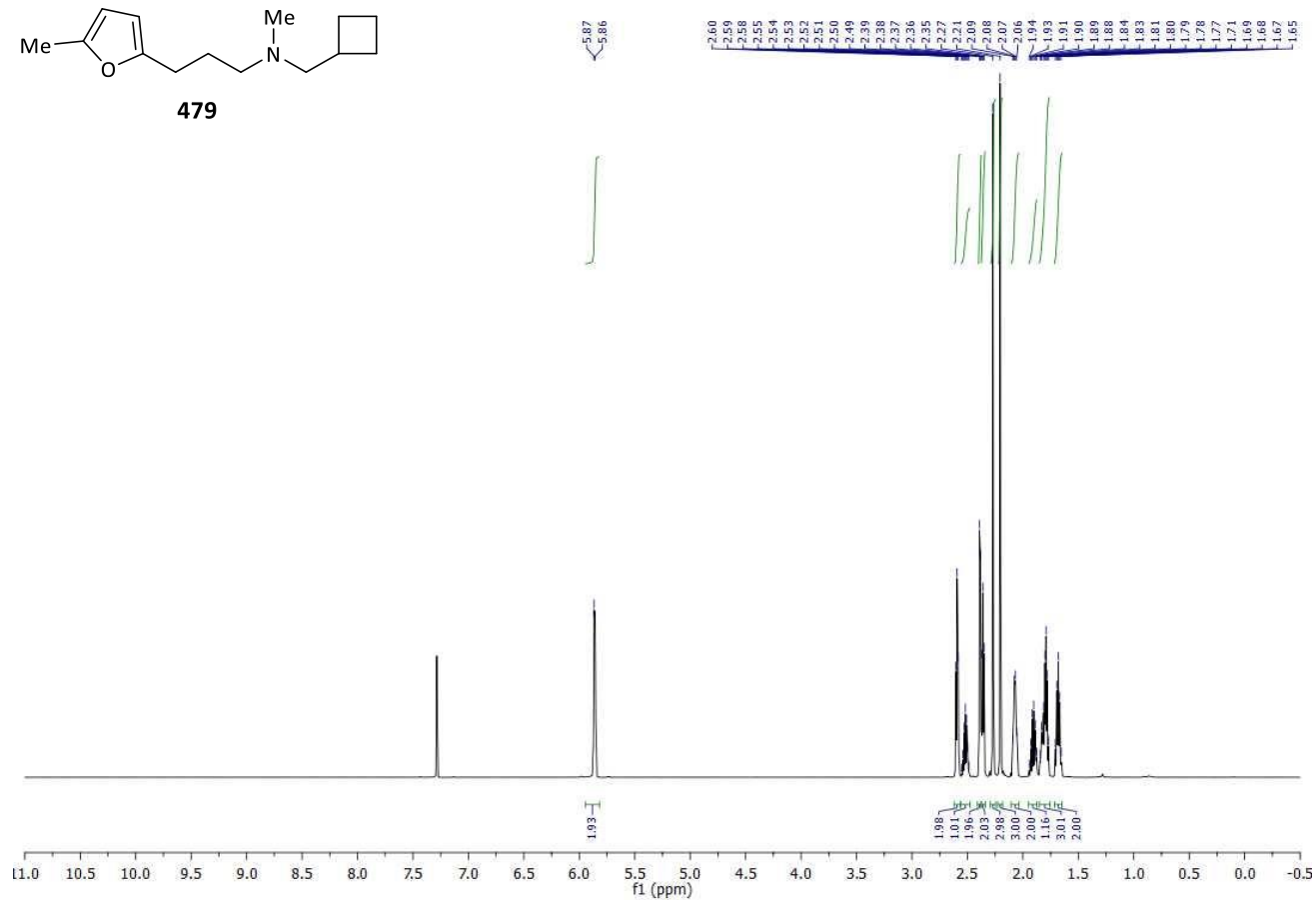
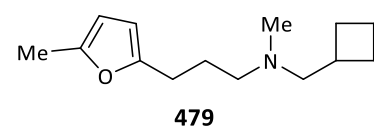


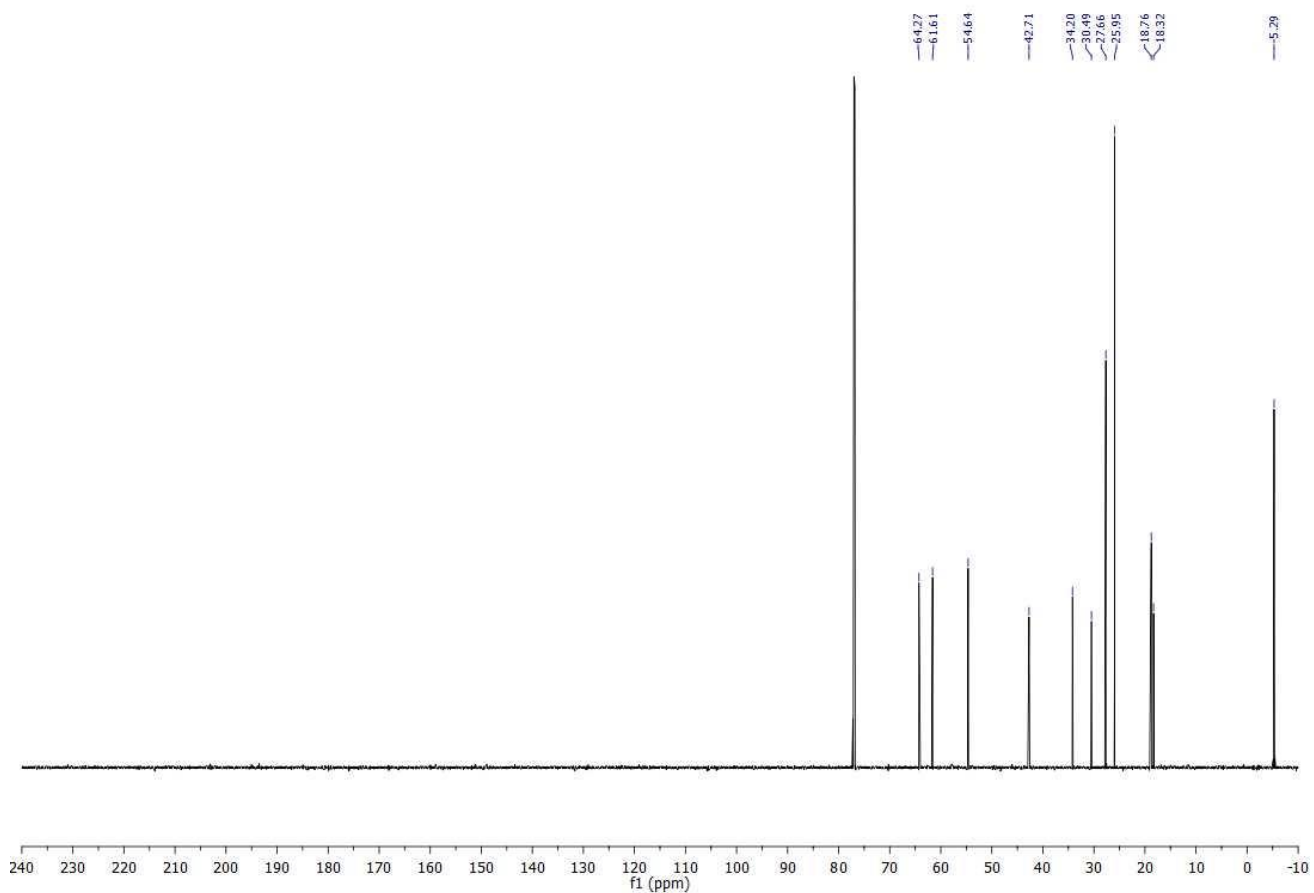
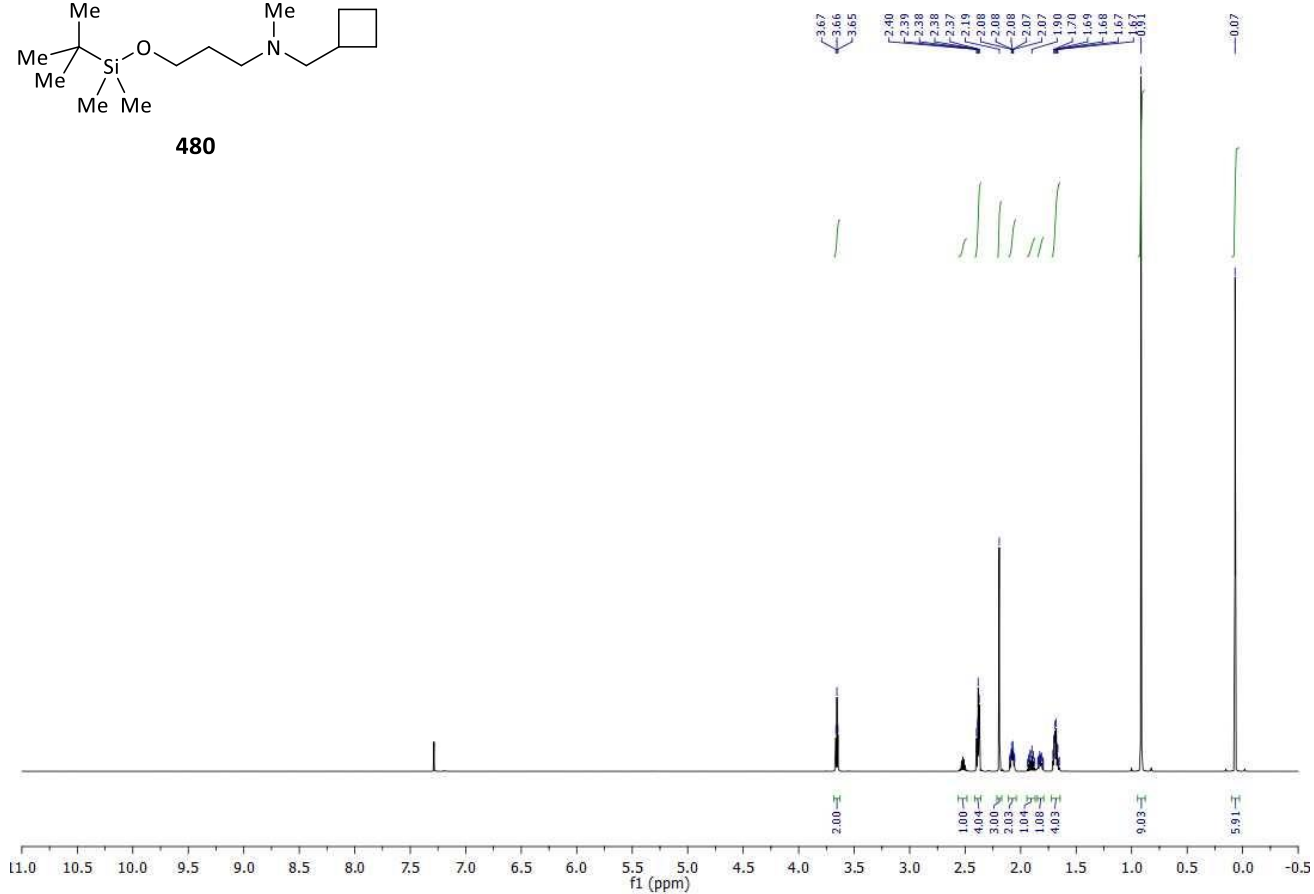
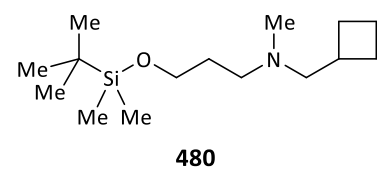
476

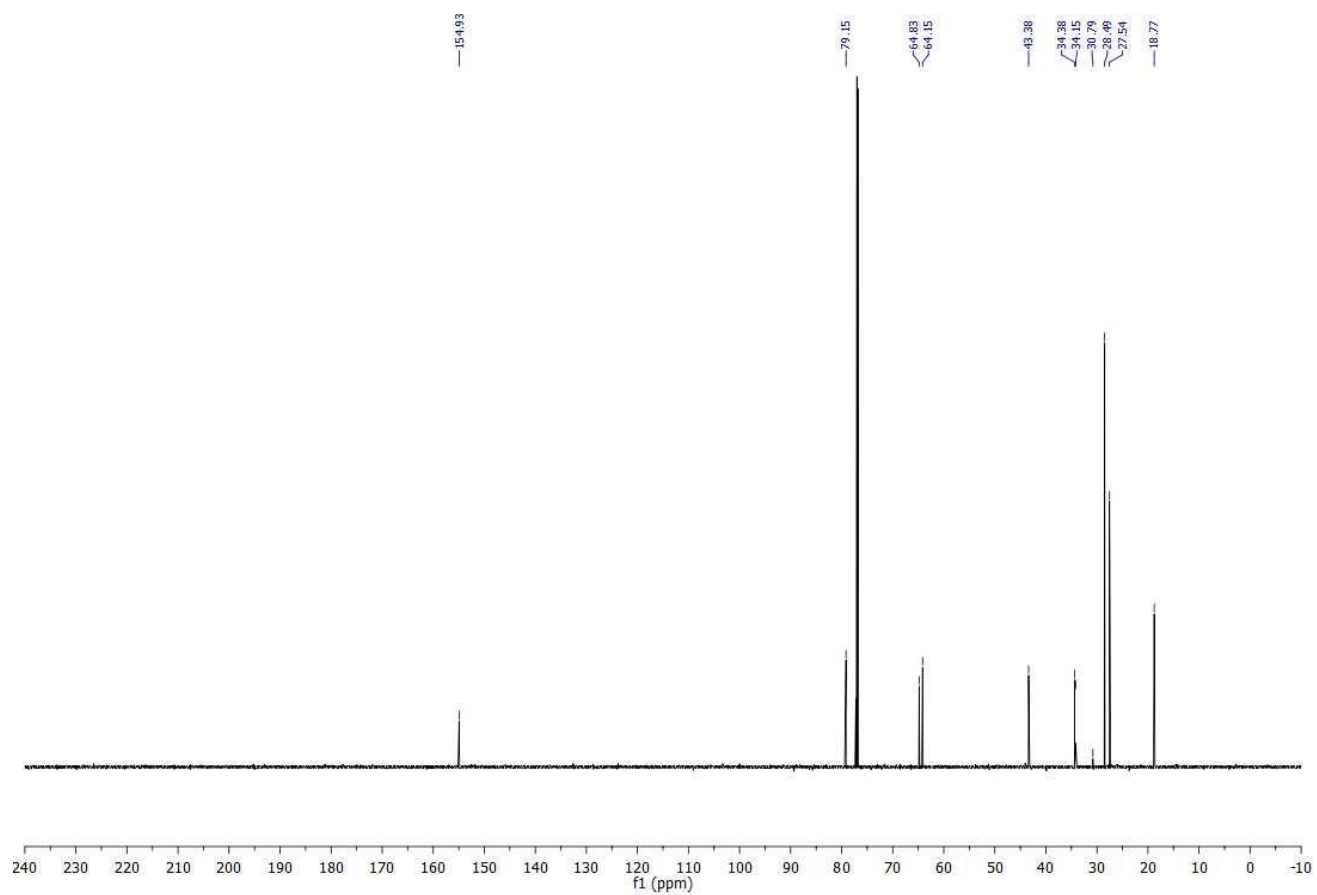
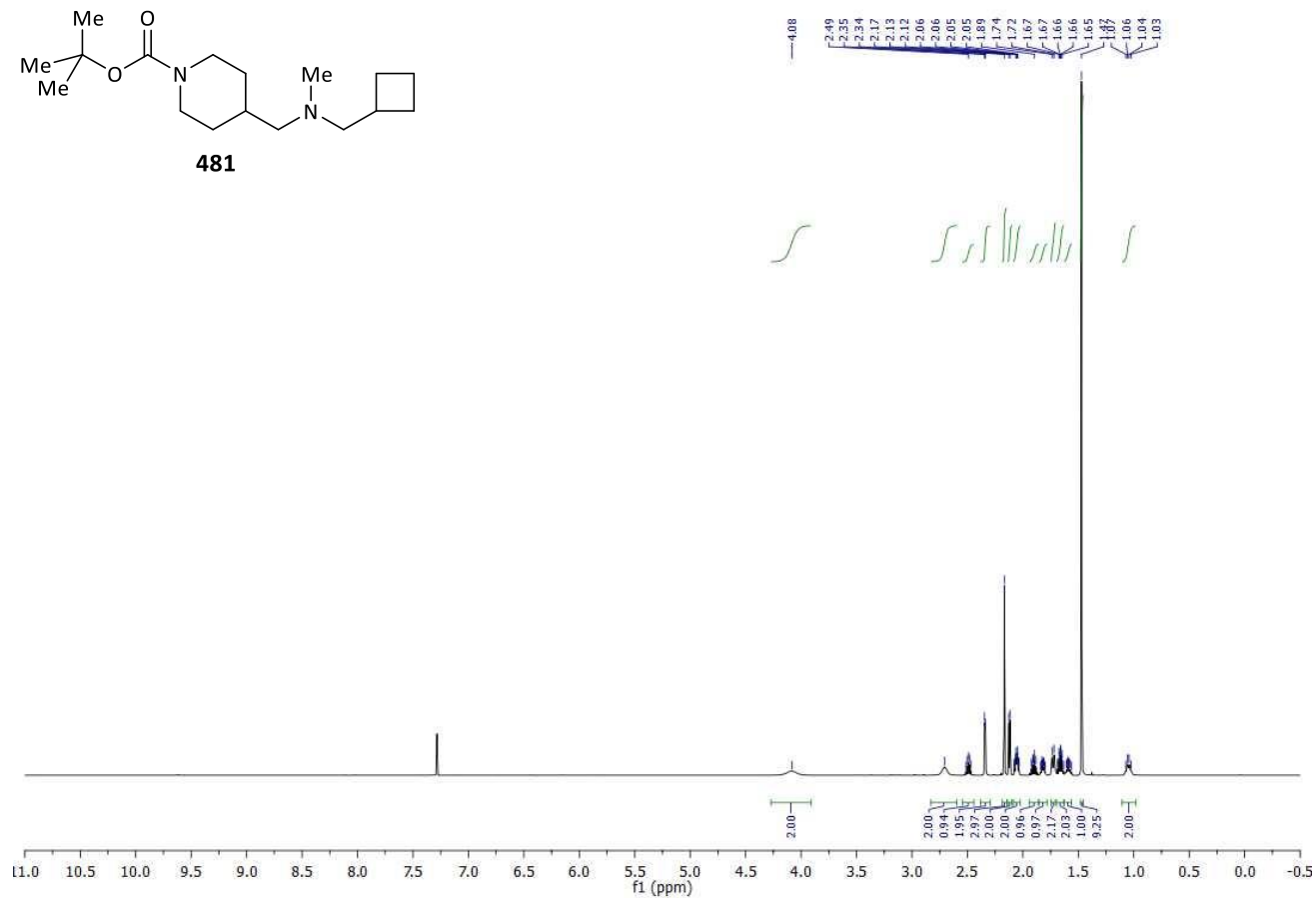
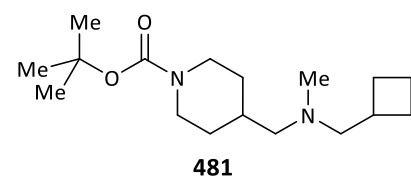


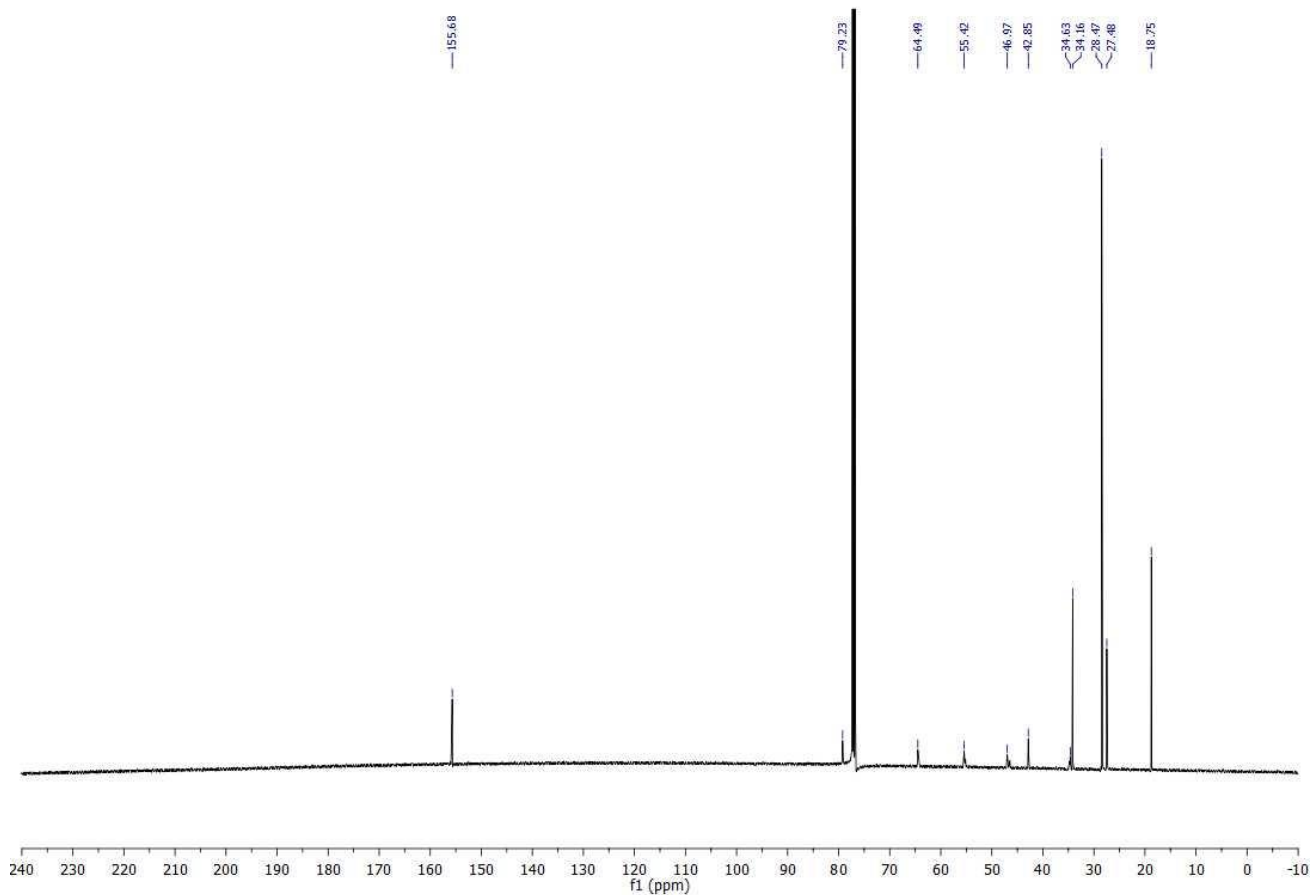
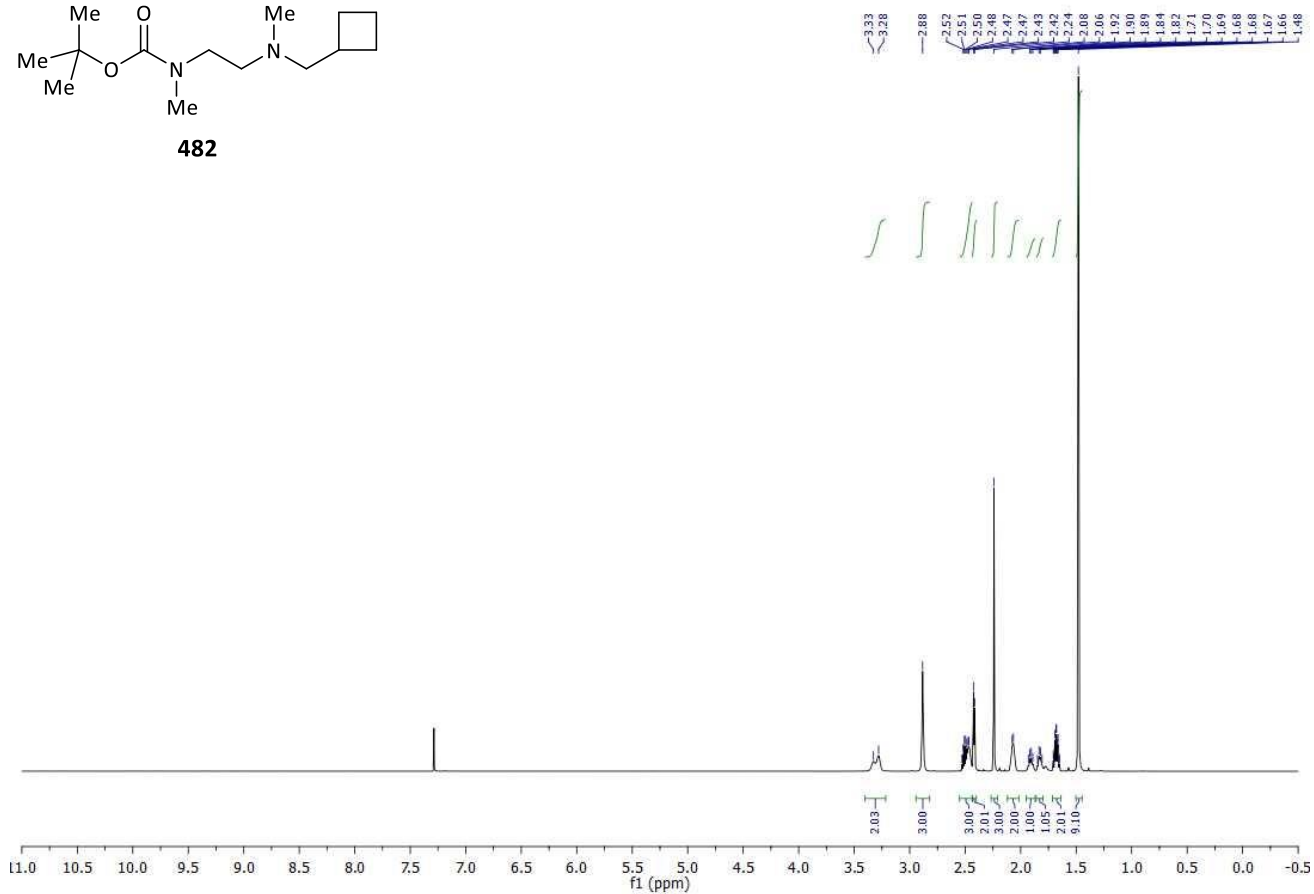
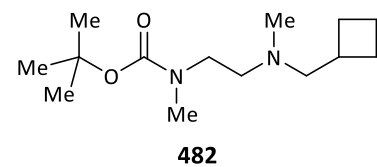


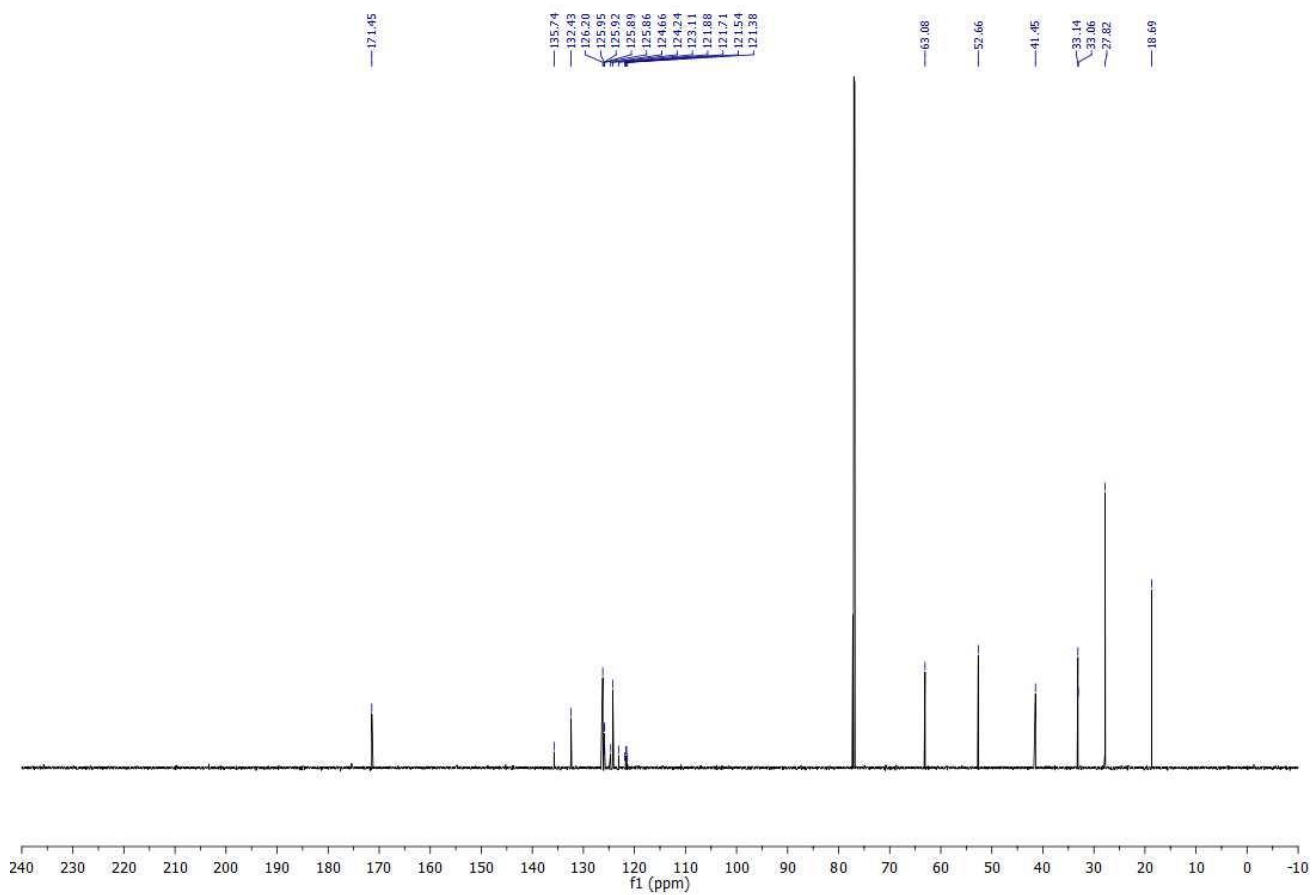
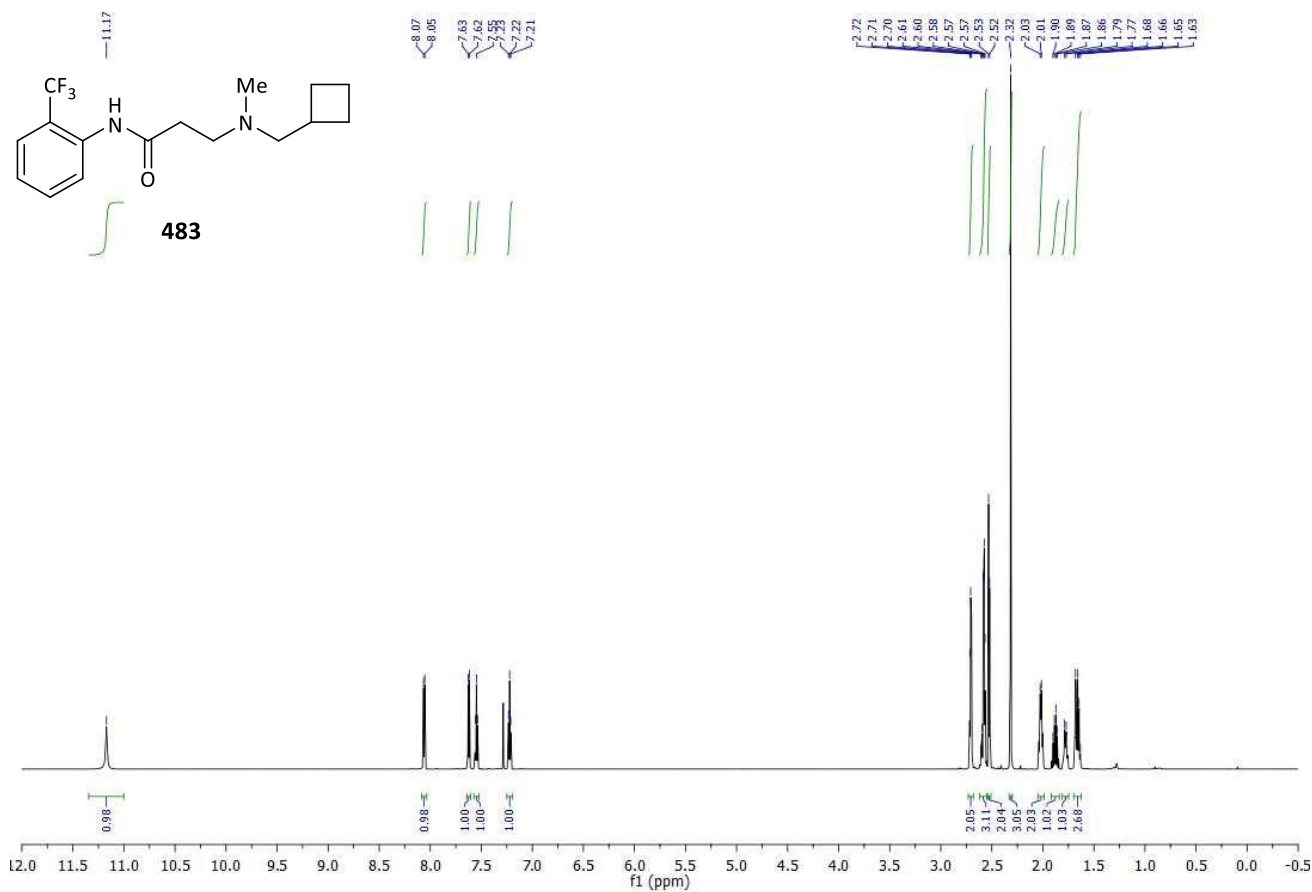


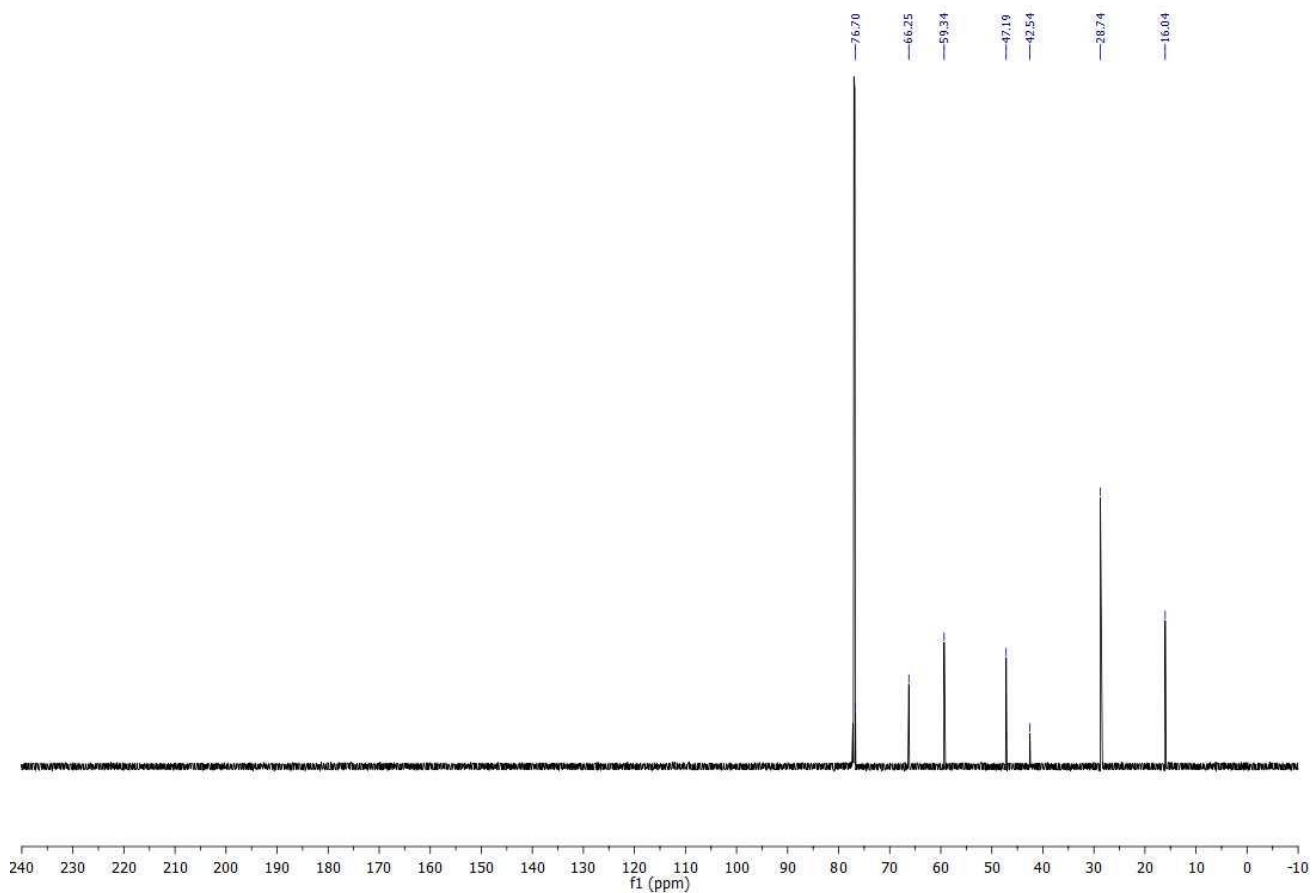
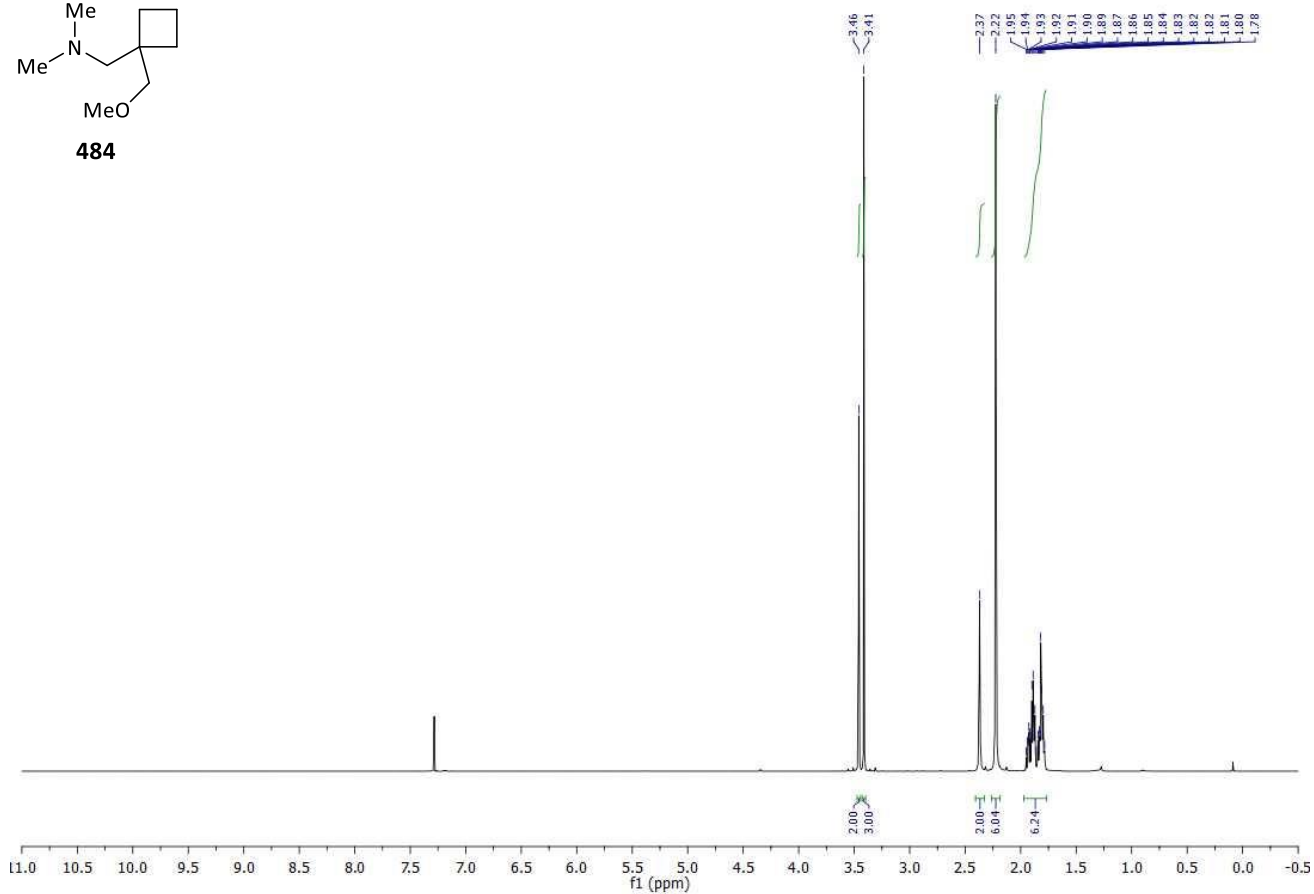
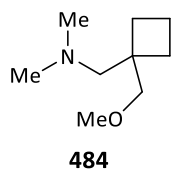


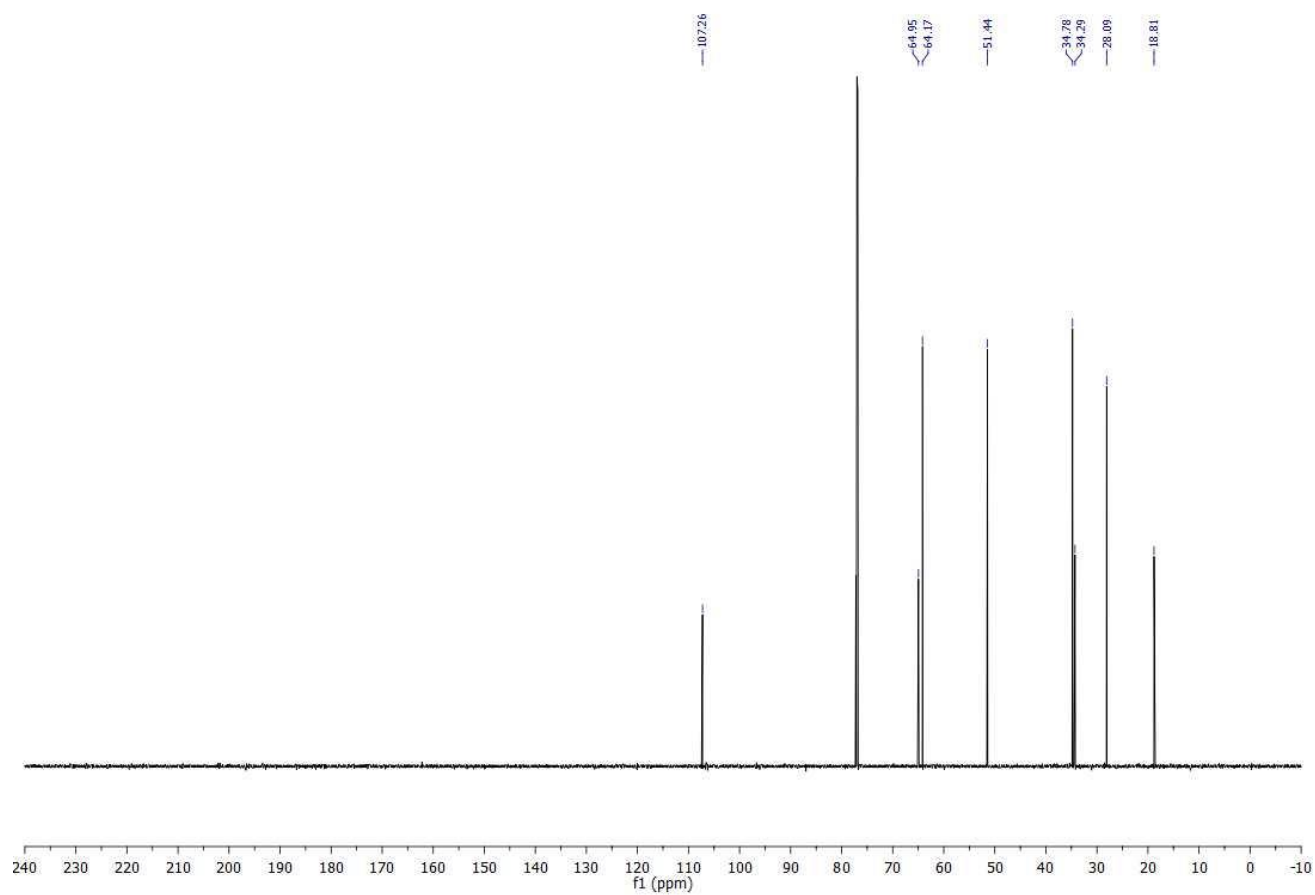
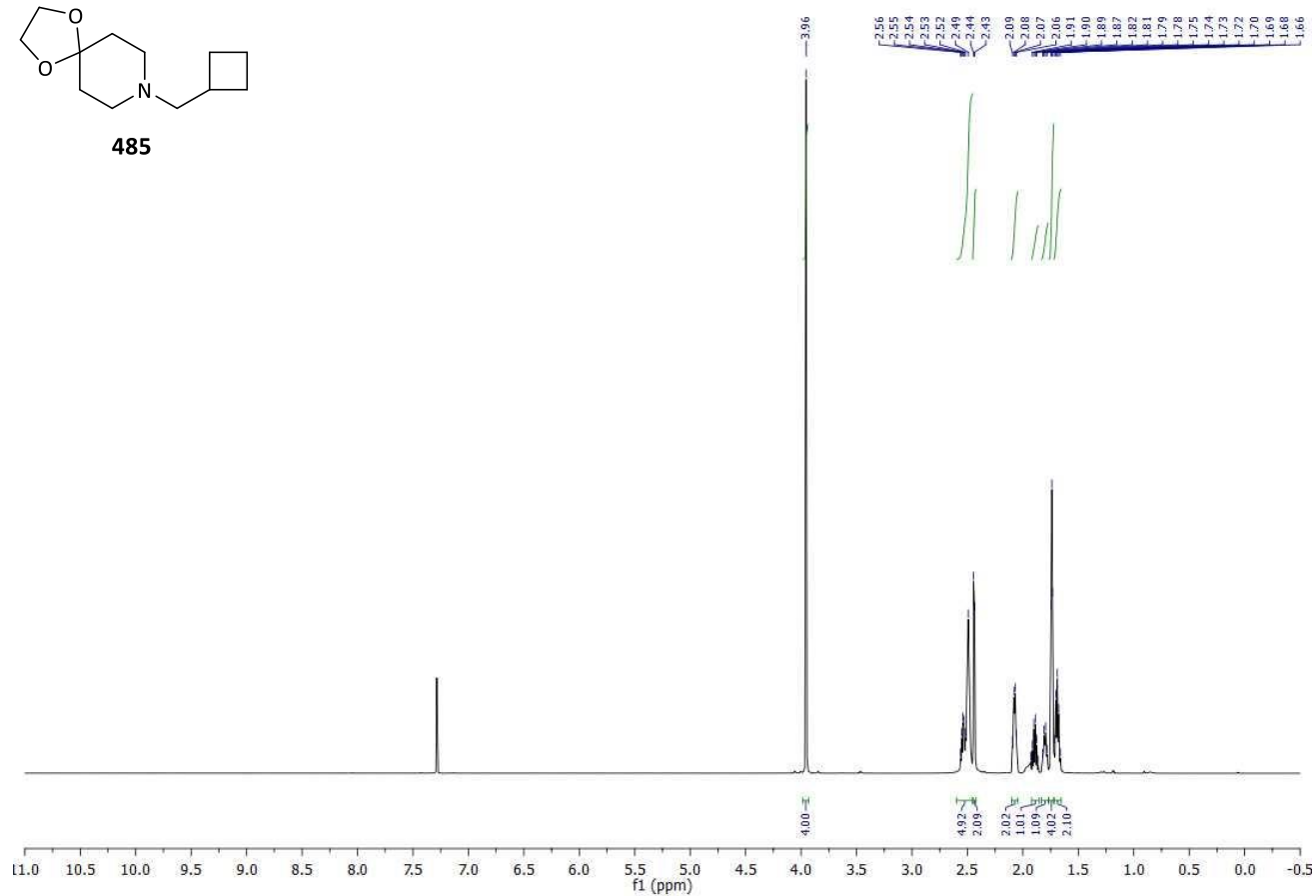
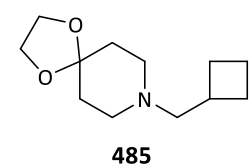


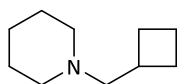




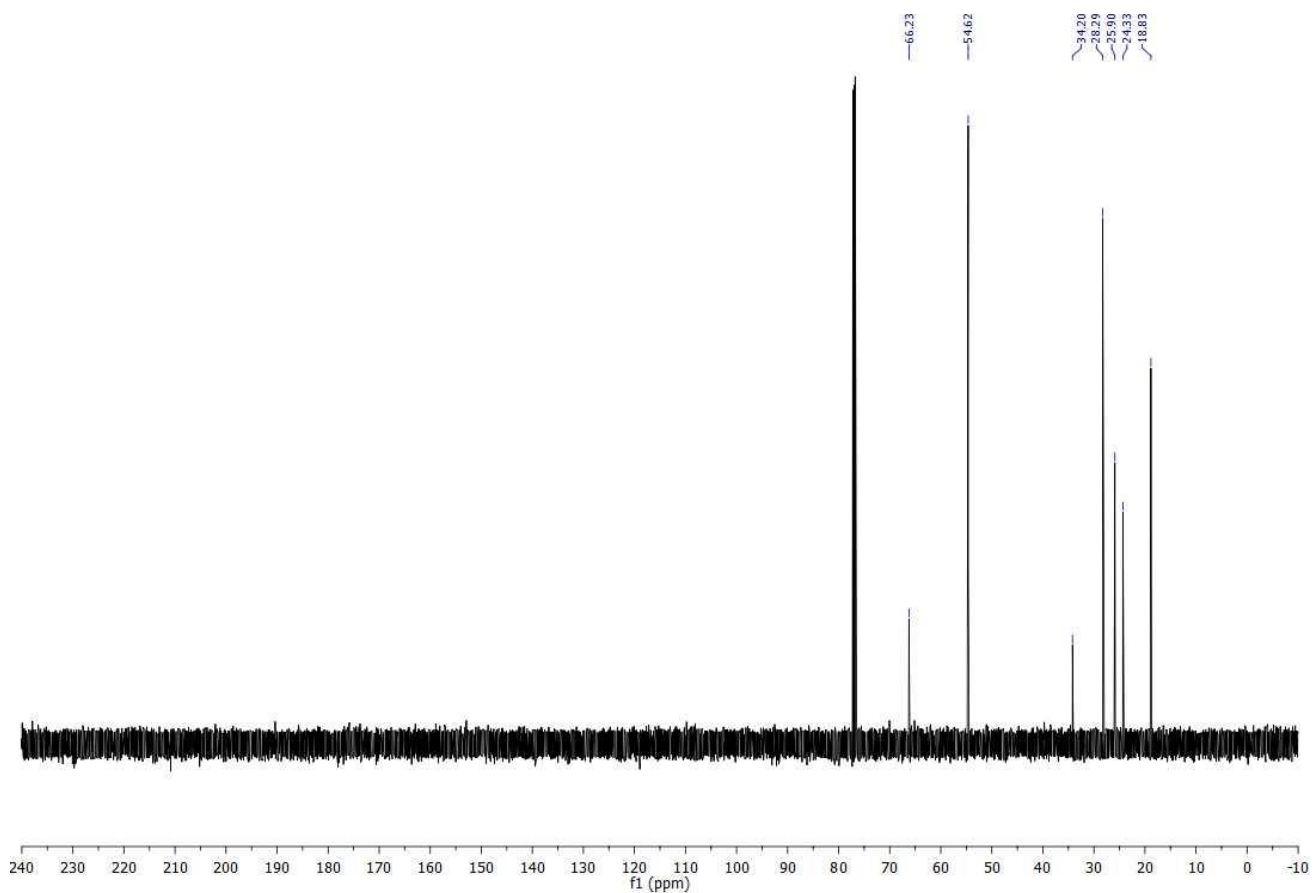
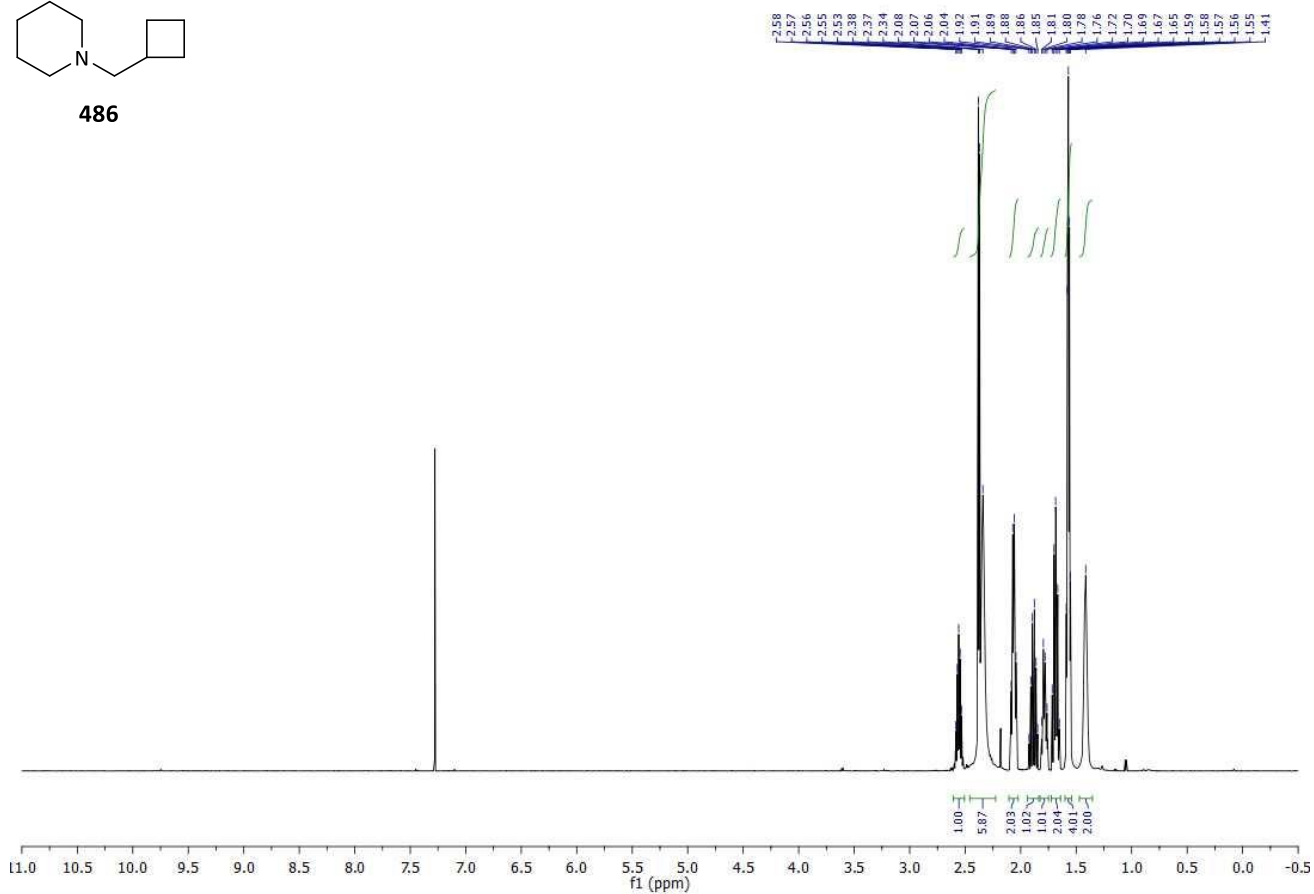


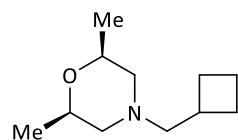




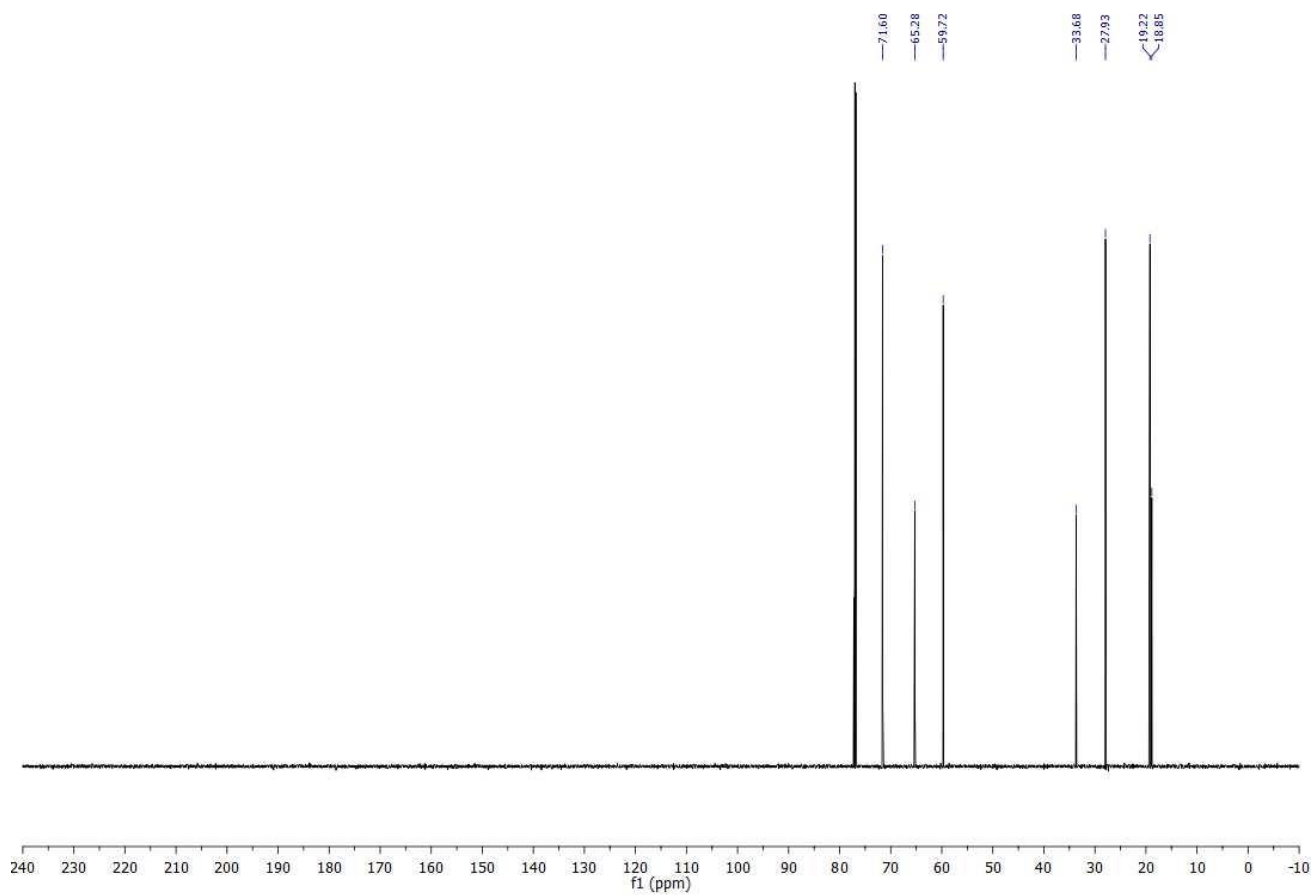
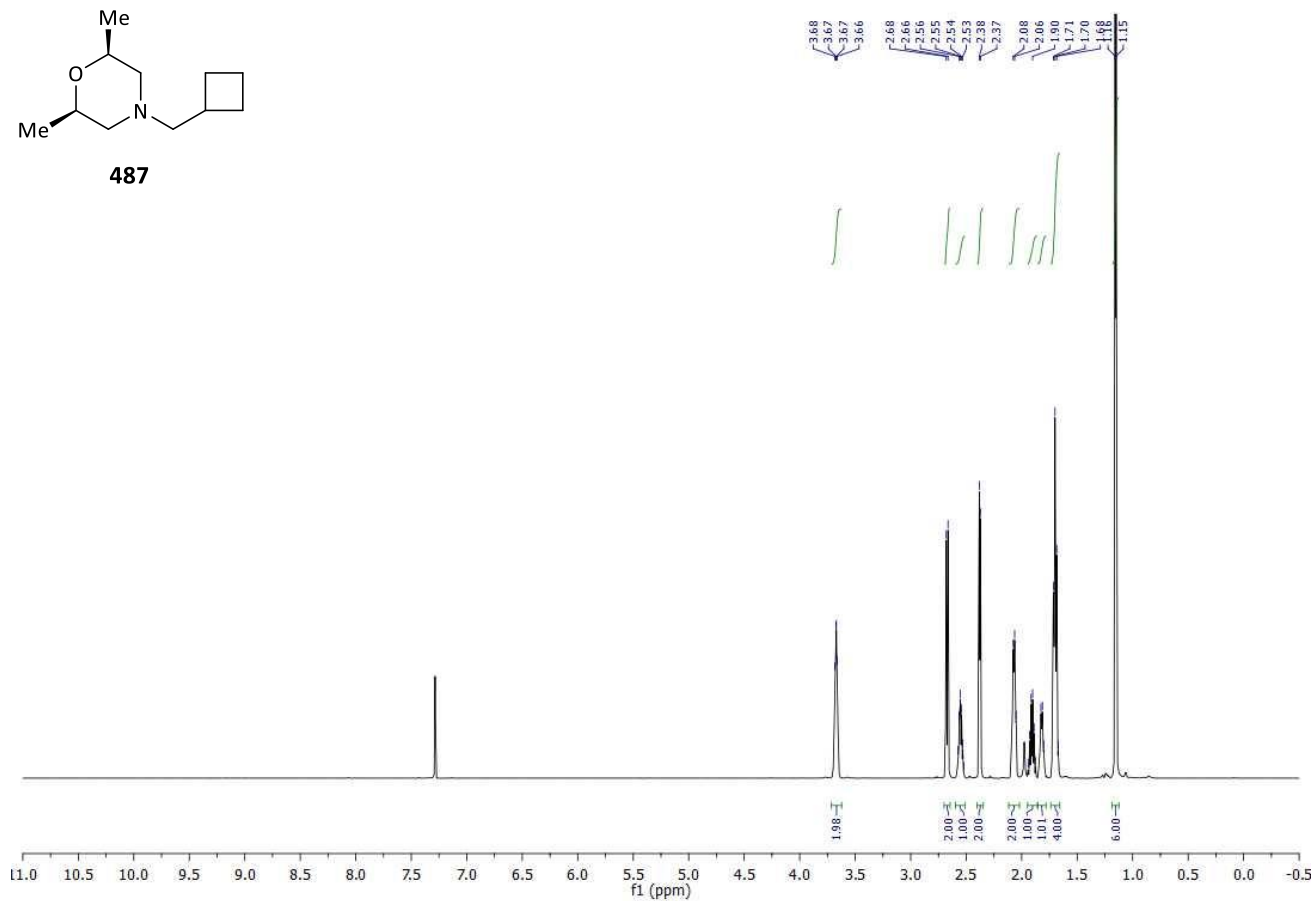


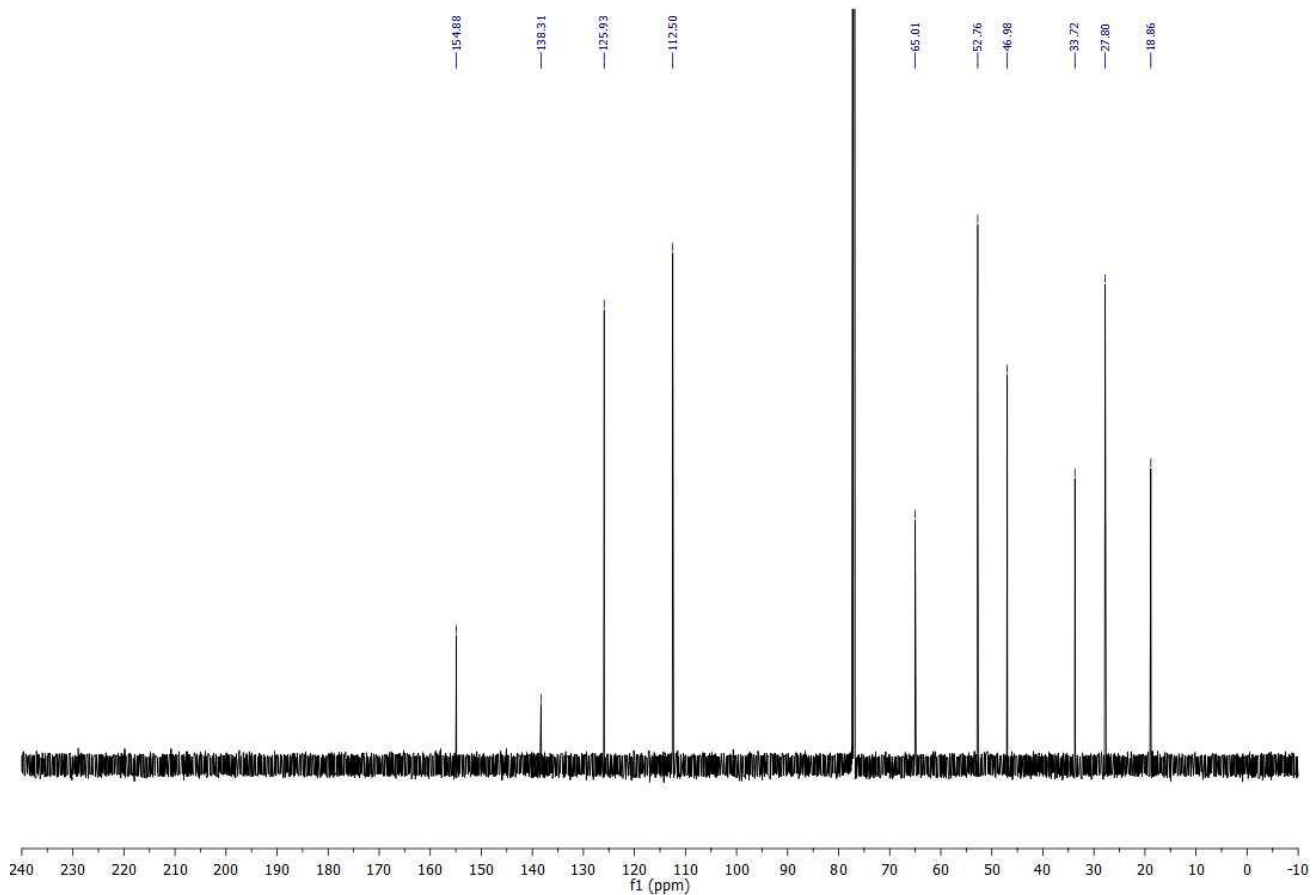
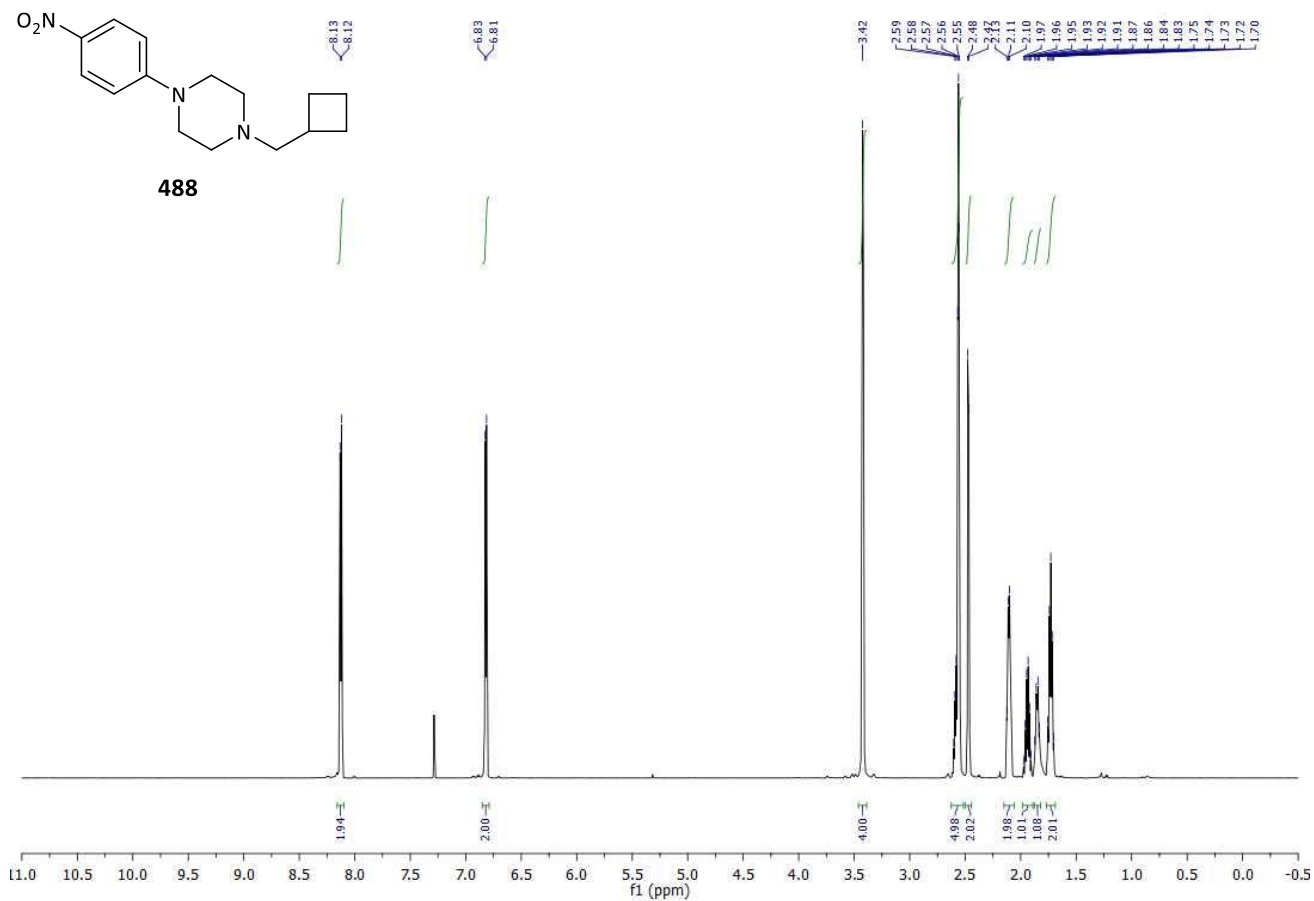
486

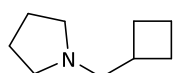




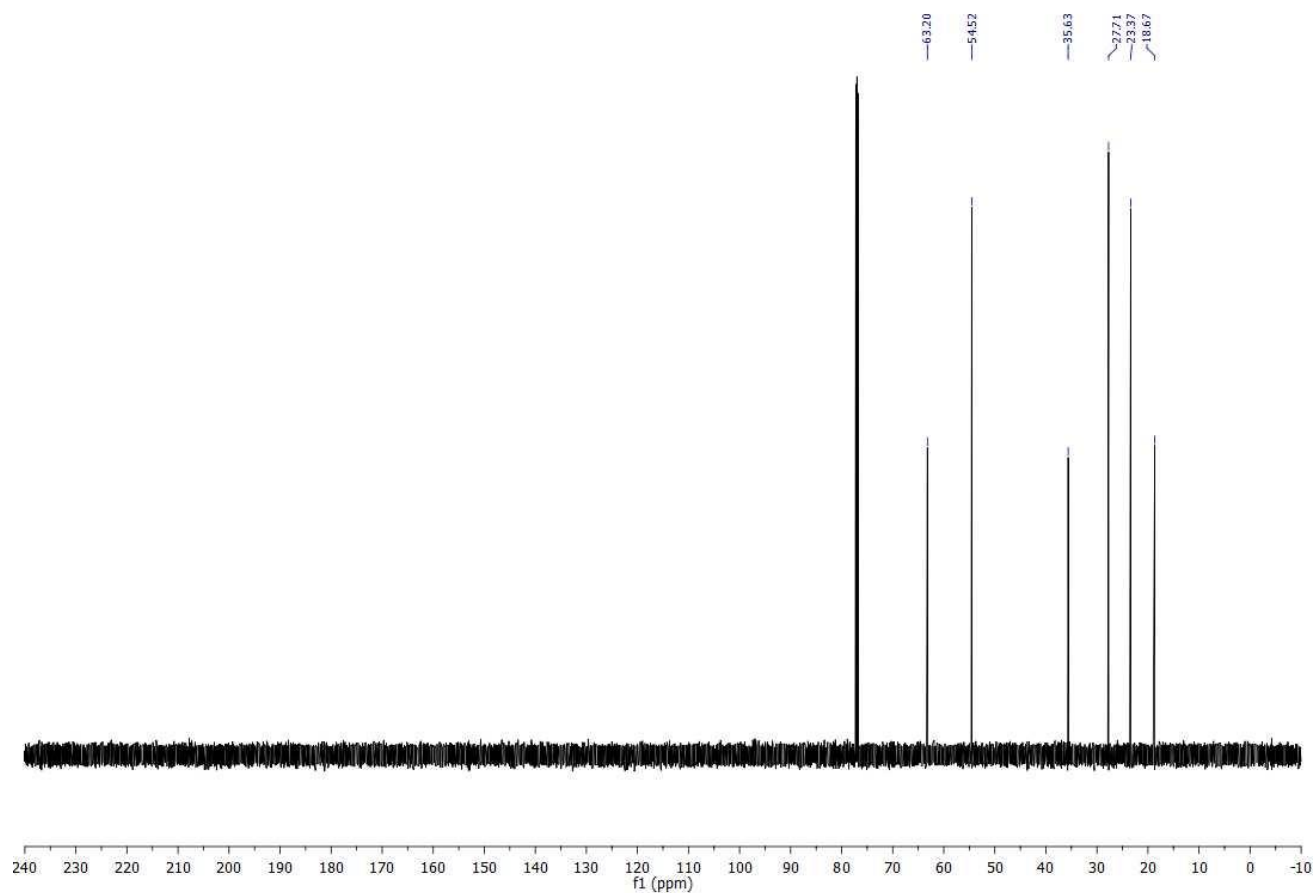
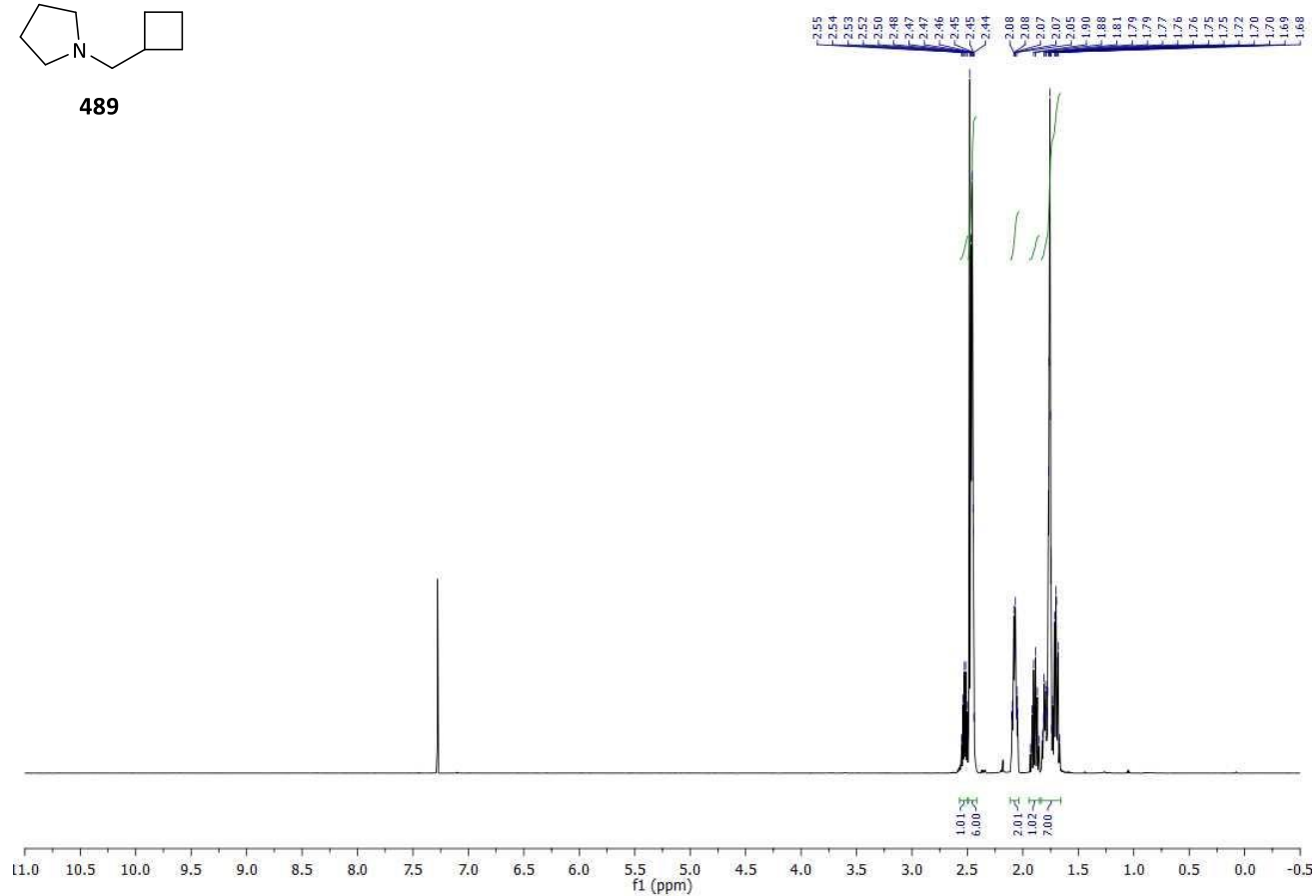
487

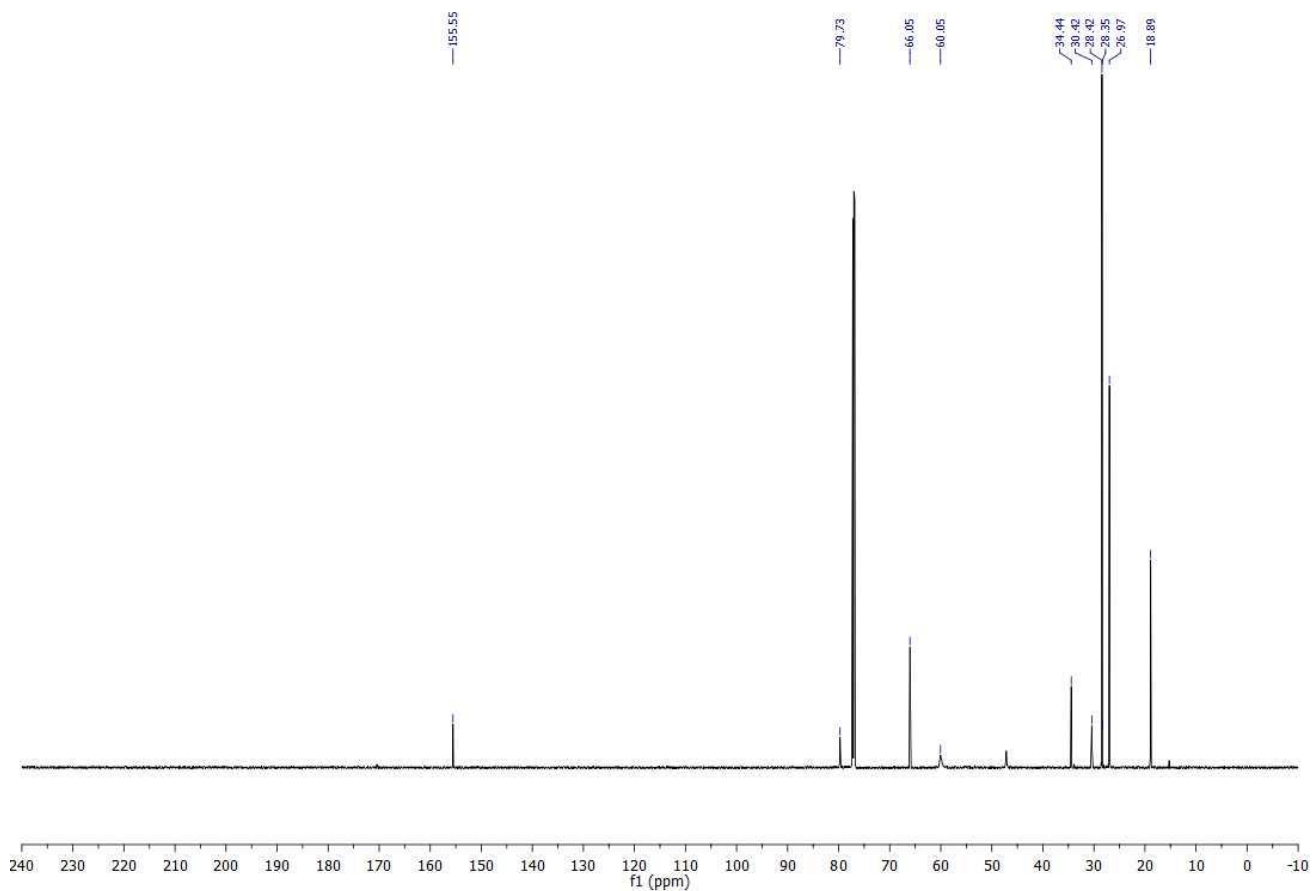
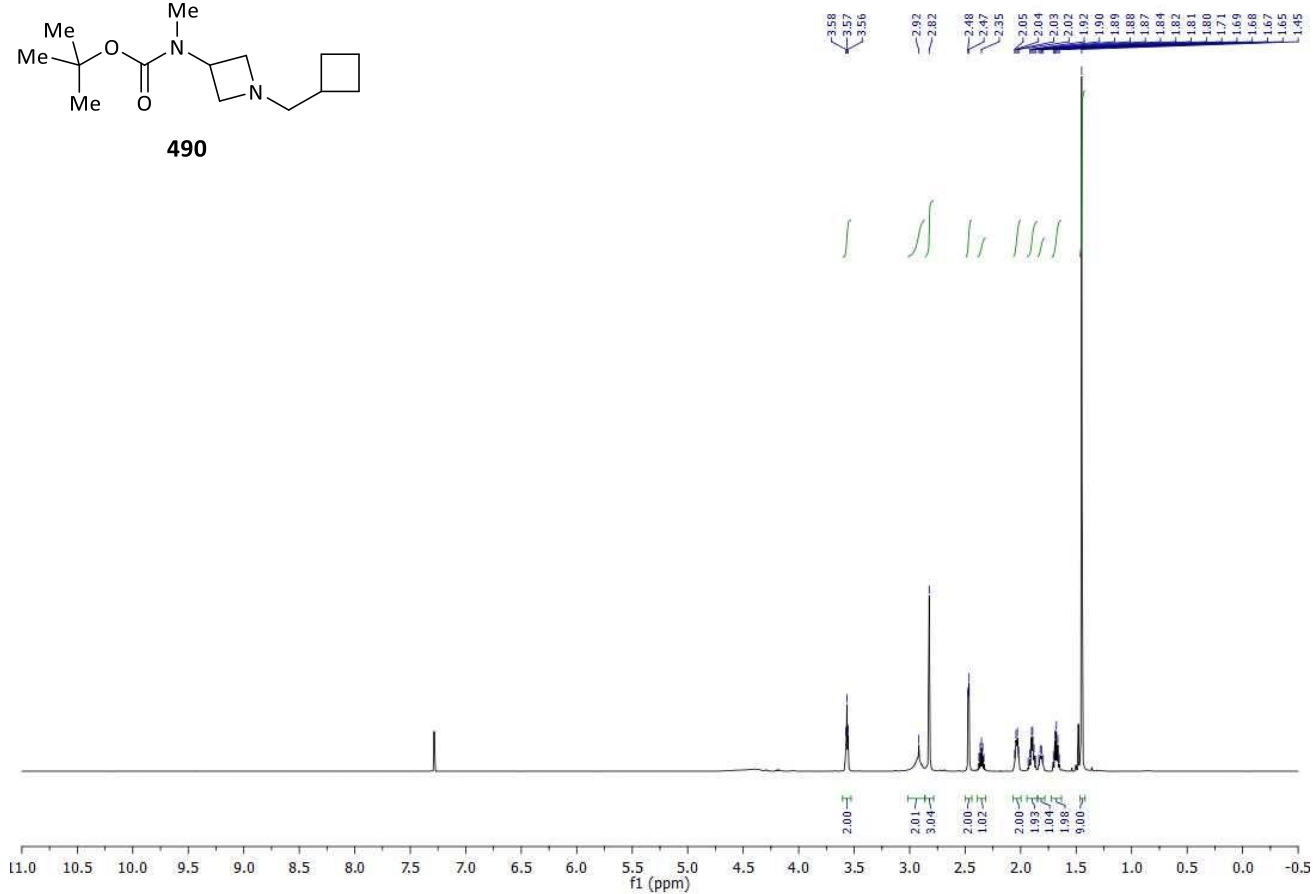
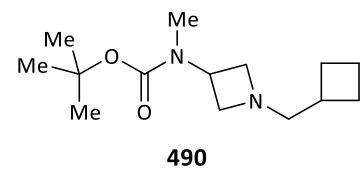


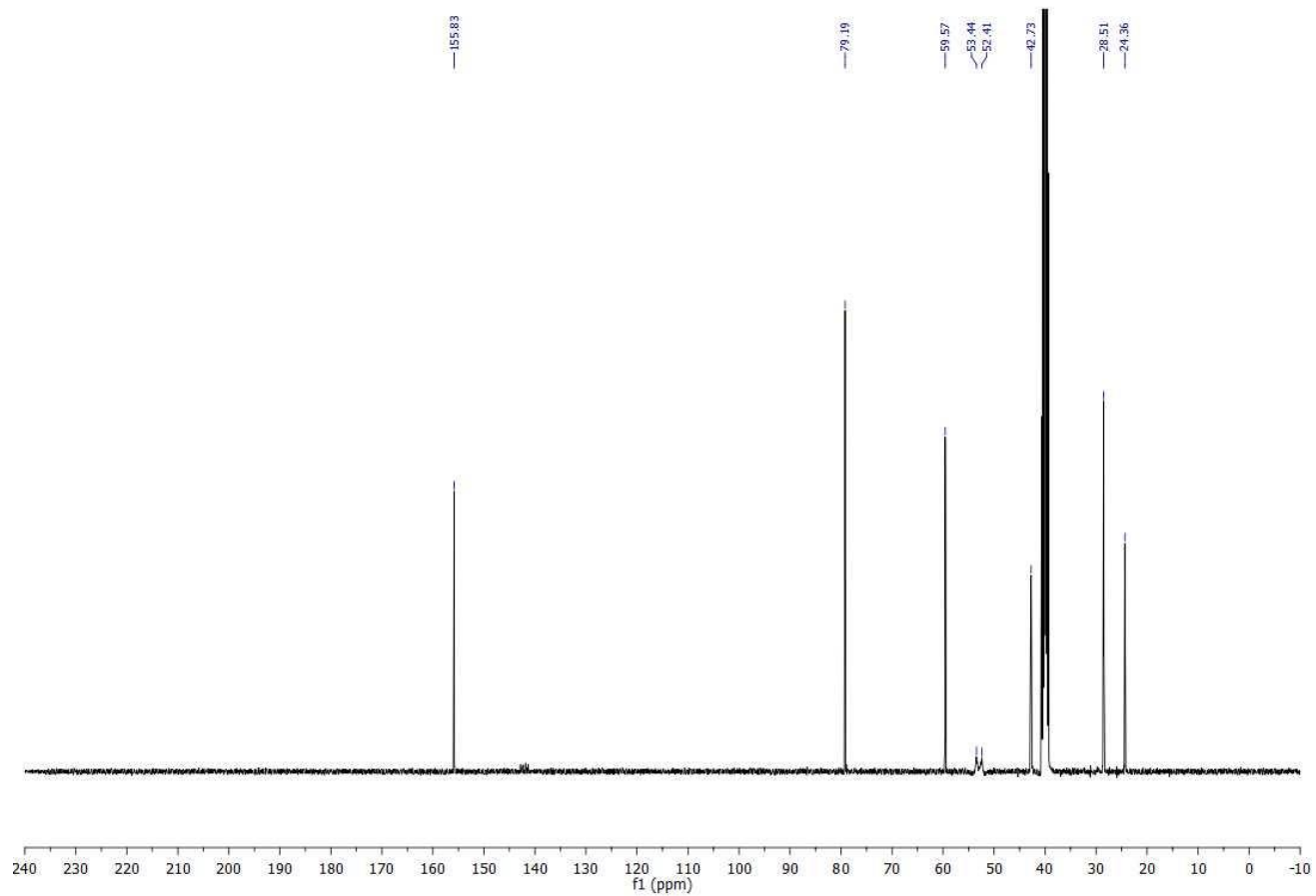
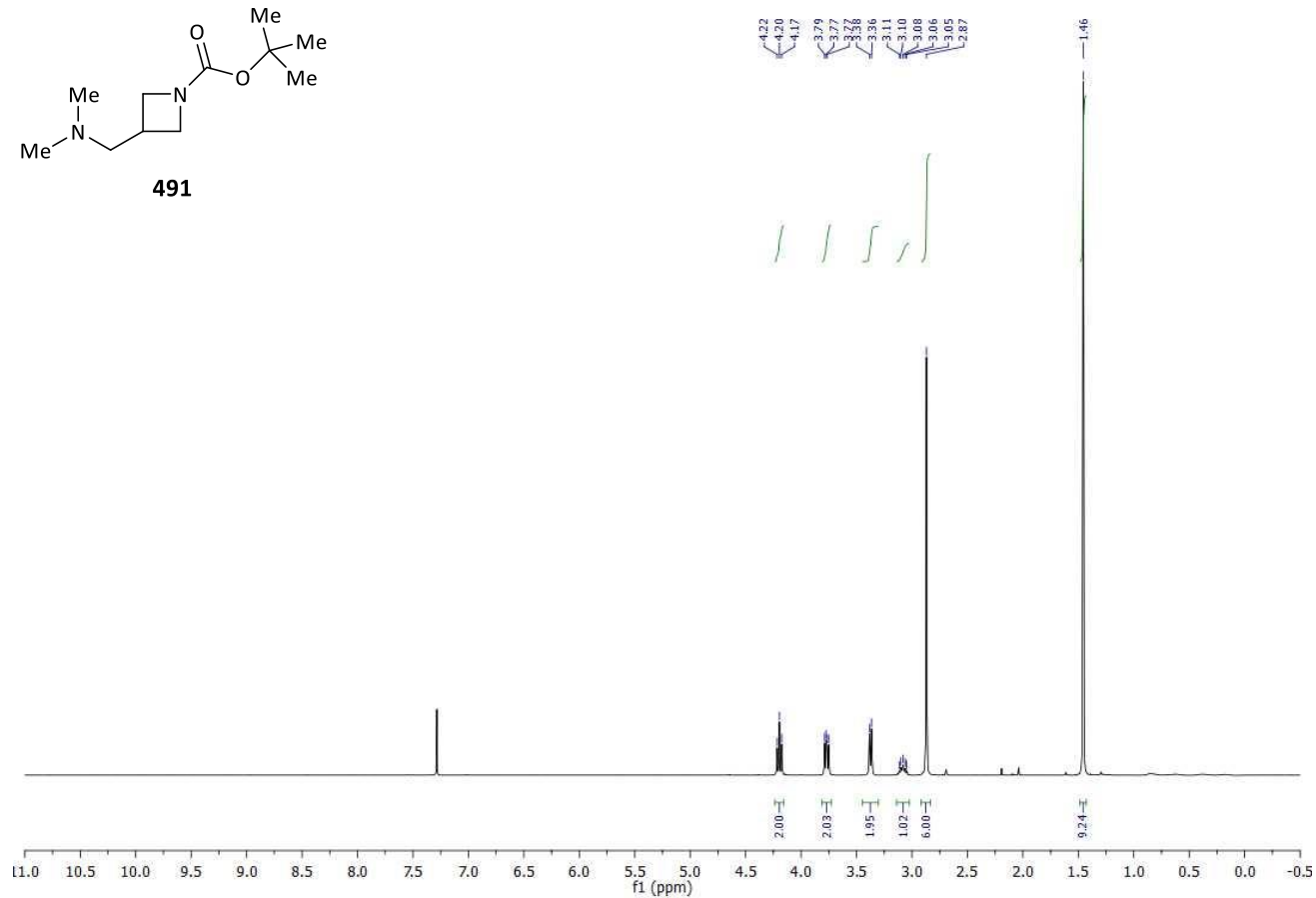
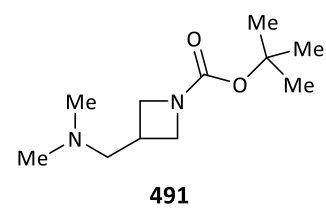


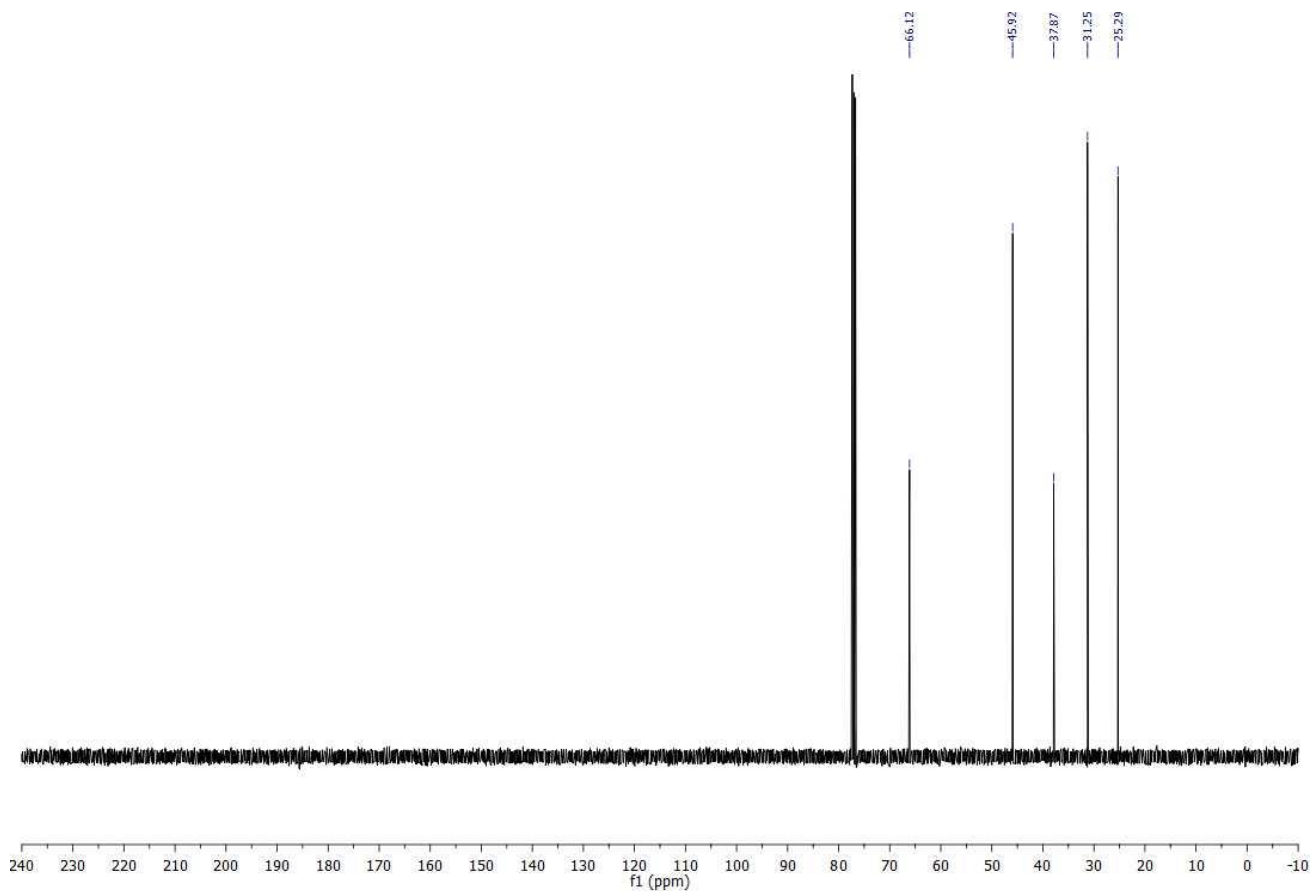
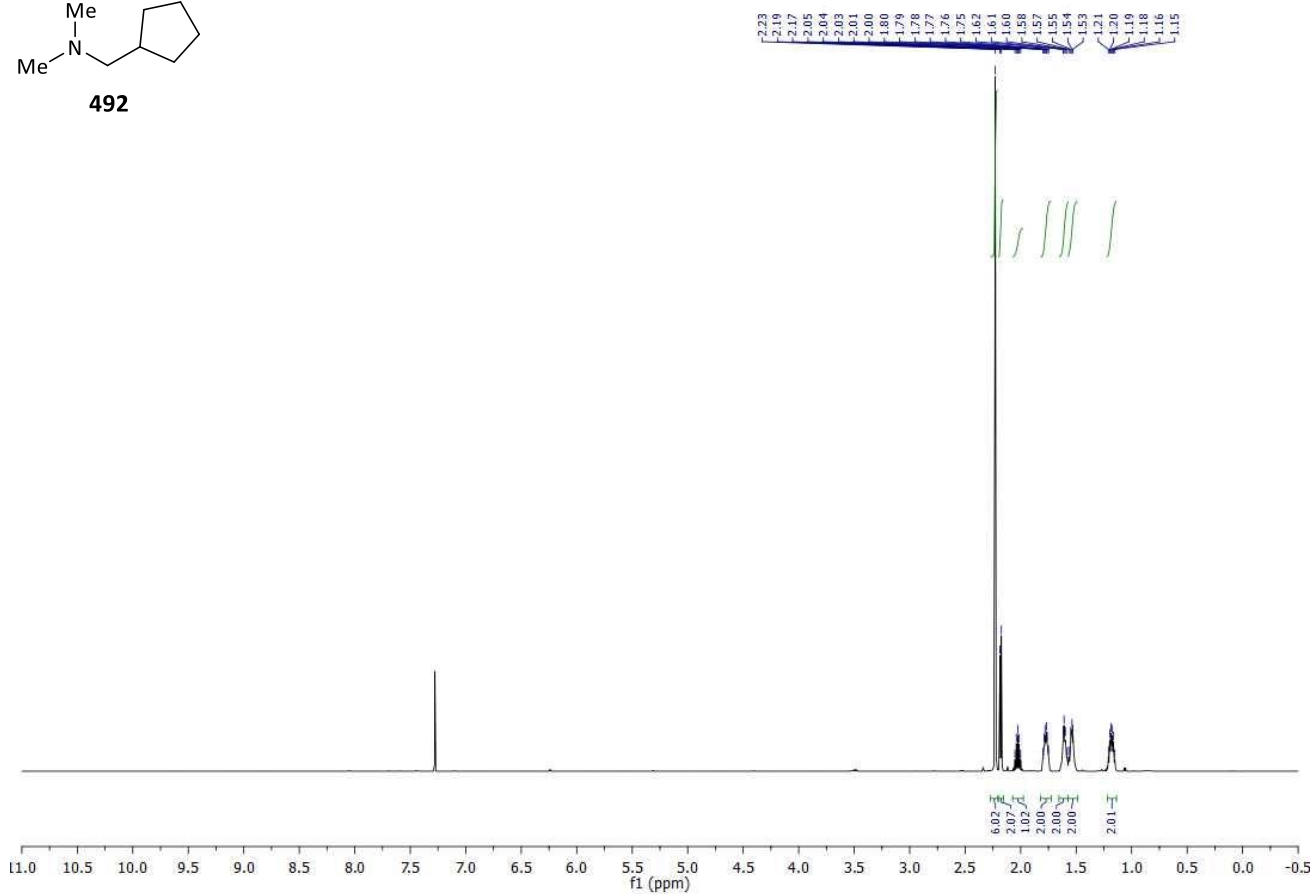
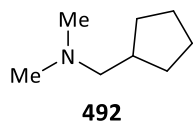


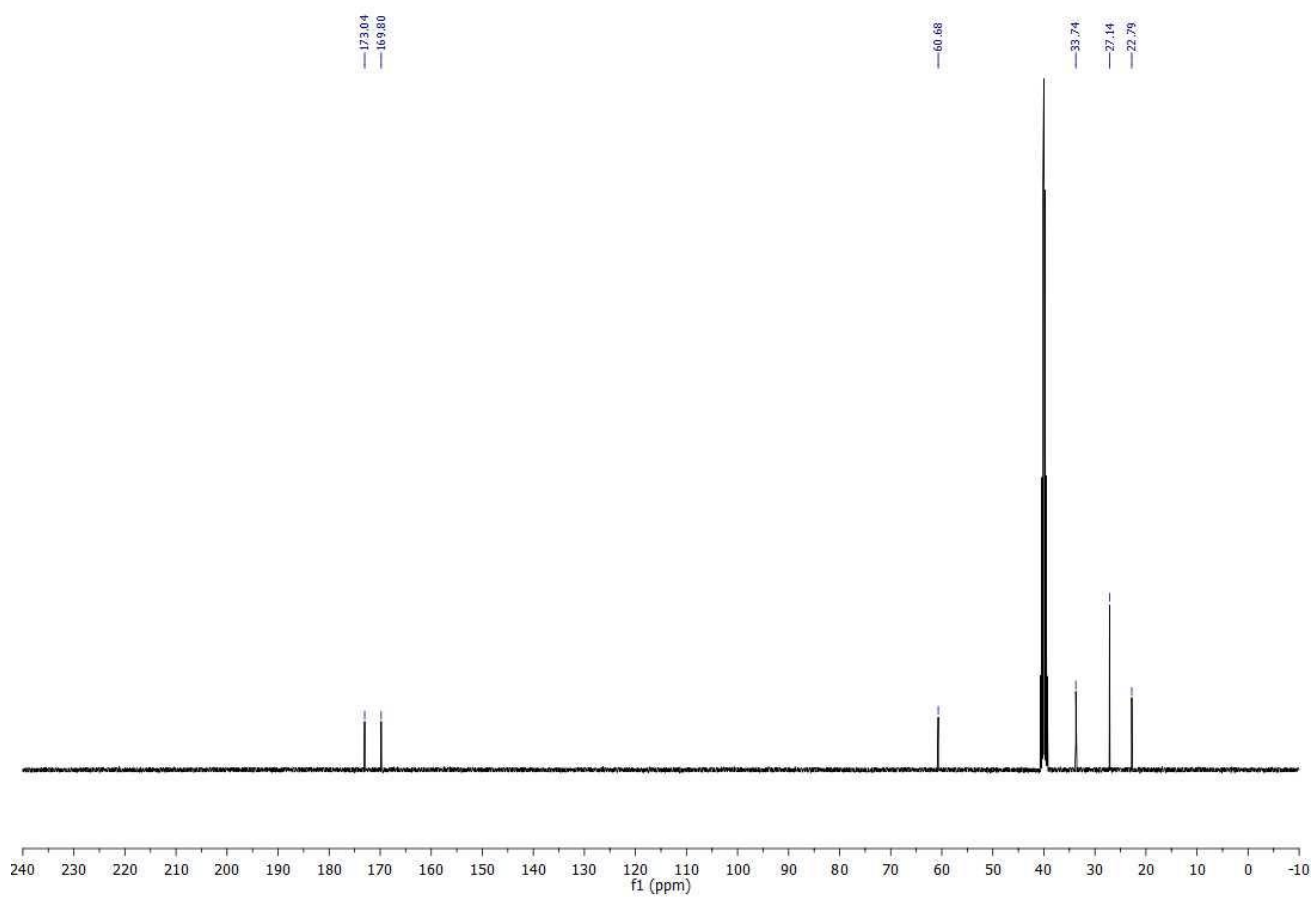
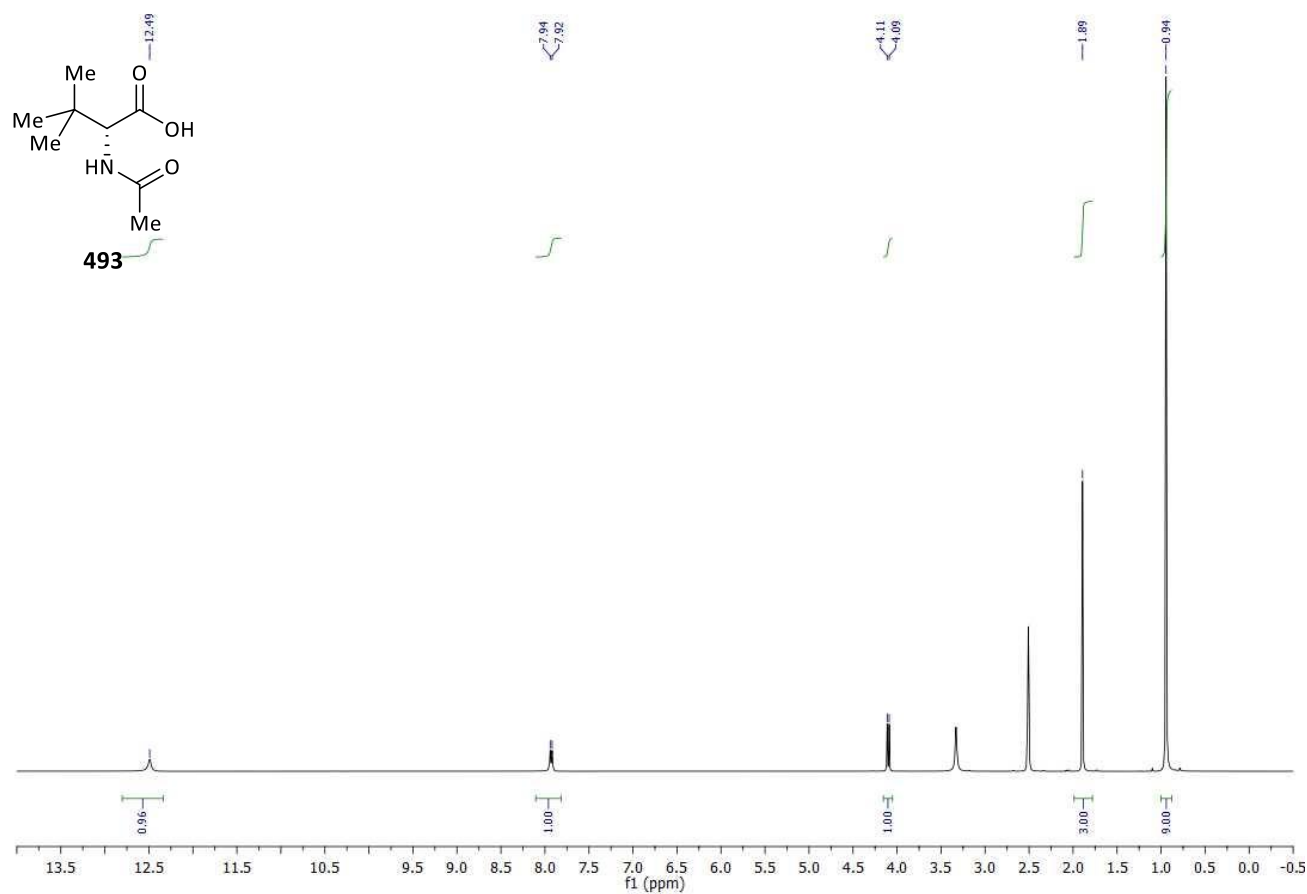
489











Appendix III – Computational complexes

Pd(OAc)₂

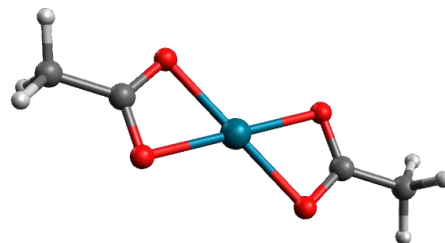
Geometry optimisation:

B3LYP-D3BJ/631G(d,p)/LANL2DZ-IEFPCM(DMF) Energy = -583.771757264

Thermal correction to Gibbs Free Energy = 0.058944

Single-point energy calculation:

B3LYP-D3BJ/6311+G(2d,p)/SDD-IEFPCM(DMF) Energy = -585.112621003



O	-1.78198	1.08817	0.01863	O	1.78197	1.08817	-0.01855
O	-1.78198	-1.08816	0.01866	O	1.78199	-1.08816	-0.01858
C	-2.45819	0.00000	0.01787	C	2.45819	0.00001	-0.01794
C	-3.94916	-0.00000	-0.01478	C	3.94917	0.00001	0.01428
H	-4.27949	-0.00016	-1.05899	H	4.27984	-0.00078	1.05838
H	-4.33544	0.89783	0.47017	H	4.33527	0.89813	-0.47027
H	-4.33541	-0.89769	0.47046	H	4.33530	-0.89740	-0.47160
Pd	0.00000	-0.00000	0.00009				

Acetic acid

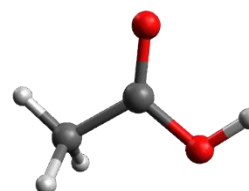
Geometry optimisation:

B3LYP-D3BJ/631G(d,p)/LANL2DZ-IEFPCM(DMF) Energy = -229.104946426

Thermal correction to Gibbs Free Energy = 0.031838

Single-point energy calculation:

B3LYP-D3BJ/6311+G(2d,p)-IEFPCM(DMF) Energy = -229.184280273



C	1.39486	-0.11172	-0.00000	H	1.91733	0.84351	-0.00006
C	-0.09155	0.12155	-0.00000	H	1.67914	-0.69301	-0.88158
O	-0.64226	1.20444	-0.00000	H	1.67915	-0.69290	0.88165
O	-0.77906	-1.04221	-0.00000	H	-1.72493	-0.81435	0.00001

Acetyl-tert-leucine (Ac-Tle-OH; 227)

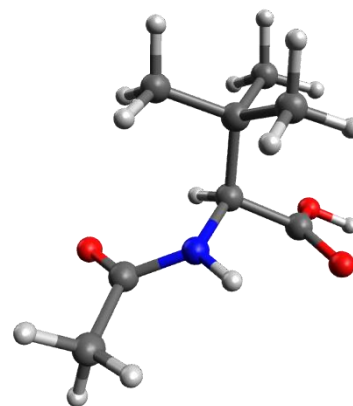
Geometry optimisation:

B3LYP-D3BJ/631G(d,p)/LANL2DZ-IEFPCM(DMF) Energy = -594.431973806

Thermal correction to Gibbs Free Energy = 0.184621

Single-point energy calculation:

B3LYP-D3BJ/6311+G(2d,p)-IEFPCM(DMF) Energy = -594.606787127



C	0.22365	-0.19449	-0.31215	H	-4.06360	0.55615	0.66923
C	0.99689	-1.48096	-0.06465	C	2.33679	1.18062	-0.65945
H	0.01510	-0.10258	-1.37997	C	1.33455	1.01749	1.64357
C	1.02720	1.07711	0.13913	C	0.16029	2.31165	-0.15857
N	-1.05246	-0.32320	0.36666	H	1.96309	0.15912	1.89720
O	1.80695	-1.80313	-1.08558	H	0.41484	0.95319	2.23296
O	0.90637	-2.14464	0.95044	H	1.86350	1.92501	1.95005
H	2.29276	-2.60869	-0.83314	H	3.02180	0.35893	-0.43670
C	-2.23856	-0.06402	-0.24806	H	2.84427	2.11754	-0.41032
H	-1.04446	-0.80467	1.25459	H	2.14485	1.17701	-1.73743
O	-2.31092	0.39331	-1.39008	H	-0.09350	2.37055	-1.22078
C	-3.47526	-0.36050	0.57710	H	0.70562	3.21971	0.11702
H	-4.08742	-1.09231	0.04321	H	-0.77102	2.28961	0.41241
H	-3.25115	-0.74186	1.57531				

Acetyl-alanine (Ac-Ala-OH; 224)

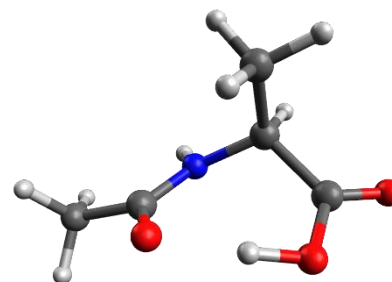
Geometry optimisation:

B3LYP-D3BJ/631G(d,p)/LANL2DZ-IEFPCM(DMF) Energy = -476.467823025

Thermal correction to Gibbs Free Energy = 0.107374

Single-point energy calculation:

B3LYP-D3BJ/6311+G(2d,p)-IEFPCM(DMF) Energy = -476.618223940



C	0.70789	0.85410	-0.30528	H	-1.00694	1.07519	-1.53043
C	1.61469	-0.39052	-0.26250	O	-1.25749	-0.82661	0.97665
H	1.12838	1.48177	-1.09014	C	-3.00418	-0.11511	-0.50440
C	0.76760	1.60733	1.03297	H	-3.13222	0.42695	-1.44242
N	-0.67602	0.57169	-0.72035	H	-3.36255	-1.14011	-0.62207
O	1.18371	-1.42884	0.44890	H	-3.61421	0.36287	0.26753
O	2.70454	-0.39211	-0.80273	H	1.80721	1.83662	1.28058
H	0.25250	-1.24971	0.79183	H	0.33665	1.01065	1.83823
C	-1.57513	-0.15079	-0.02491	H	0.21190	2.54432	0.95158

Bisligand complex

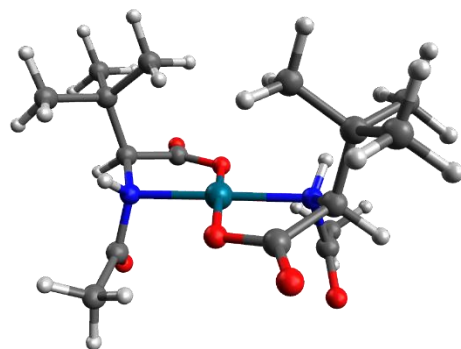
Geometry optimisation:

B3LYP-D3BJ/631G(d,p)/LANL2DZ-IEFPCM(DMF) Energy = -1314.43793443

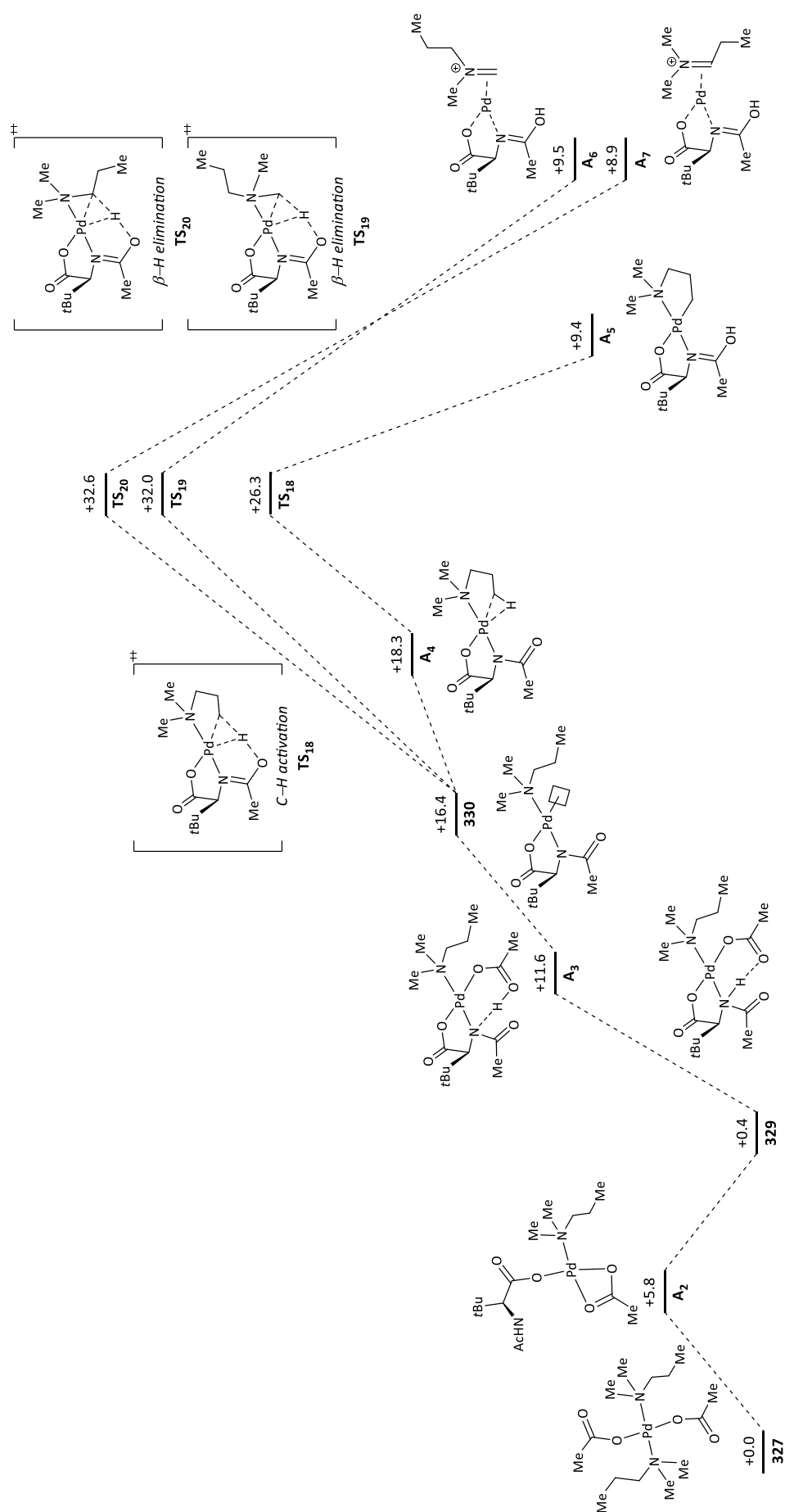
Thermal correction to Gibbs Free Energy = 0.376572

Single-point energy calculation:

B3LYP-D3BJ/6311+G(2d,p)/SDD-IEFPCM(DMF) Energy = -1315.98202403



Pd	-0.00001	0.37033	-0.00000	H	5.25922	-1.37467	-0.62032
O	1.11976	0.38678	-1.67223	C	-1.99127	-2.49567	0.22944
N	-1.89189	0.38233	-0.92721	H	-1.15004	-2.30302	-0.44258
O	-1.11978	0.38679	1.67223	H	-2.26292	-3.54982	0.12097
N	1.89188	0.38232	0.92721	H	-1.64603	-2.33863	1.25532
C	2.89609	-0.09334	-0.08059	C	-4.37261	-1.97808	0.84022
C	2.06504	1.75454	1.37379	H	-4.11004	-1.82232	1.88725
C	2.41578	0.26307	-1.49836	H	-4.63434	-3.03064	0.69764
C	3.20762	-1.61306	0.09829	H	-5.25922	-1.37473	0.62025
H	3.81957	0.46329	0.09136	C	-3.66179	-1.87260	-1.54893
C	-2.89609	-0.09335	0.08058	H	-2.85101	-1.77525	-2.28030
C	-2.41580	0.26306	1.49836	H	-4.47122	-1.19607	-1.84084
H	-3.81958	0.46326	-0.09137	H	-4.02931	-2.89888	-1.63589
C	-3.20759	-1.61308	-0.09831	C	1.47748	2.04231	2.72592
O	-3.21926	0.38502	2.41385	H	0.45804	1.65216	2.79417
O	3.21924	0.38505	-2.41386	H	1.48953	3.11744	2.90014
C	1.99130	-2.49567	-0.22943	H	2.08285	1.54606	3.49310
C	3.66184	-1.87258	1.54890	O	2.64732	2.54314	0.66338
H	1.15008	-2.30304	0.44260	C	-2.06505	1.75456	-1.37375
H	2.26297	-3.54982	-0.12098	C	-1.47749	2.04237	-2.72587
H	1.64603	-2.33862	-1.25530	H	-2.08286	1.54615	-3.49307
H	2.85108	-1.77523	2.28029	H	-0.45805	1.65222	-2.79413
H	4.47128	-1.19605	1.84079	H	-1.48952	3.11750	-2.90006
H	4.02937	-2.89885	1.63585	O	-2.64734	2.54314	-0.66333
C	4.37262	-1.97805	-0.84026	H	1.81589	-0.24668	1.72486
H	4.11002	-1.82230	-1.88729	H	-1.81590	-0.24665	-1.72487
H	4.63437	-3.03059	-0.69769				

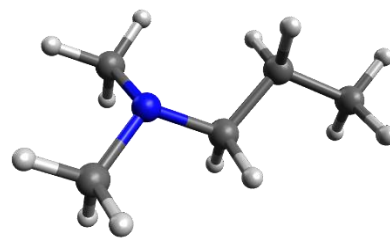
III.I. Nuclear coordinates for complexes containing *N,N*-dimethylpropan-1-amineScheme 73: Full computational pathway for C-H activation or β-H elimination in acyclic amines using acetyl-*tert*-leucine as ligand. Energy values in kcal·mol⁻¹.

307 – *N,N*-dimethylpropan-1-amine

Geometry optimisation:

B3LYP-D3BJ/631G(d,p)/LANL2DZ-IEFPCM(DMF) Energy = -253.145309959

Thermal correction to Gibbs Free Energy = 0.142261



Single-point energy calculation:

B3LYP-D3BJ/6311+G(2d,p)-IEFPCM(DMF) Energy = -253.208069296

N	1.03364	-0.01353	-0.33842	C	-1.44593	0.37497	-0.31934
C	-0.26176	-0.44901	0.18860	H	-1.39743	0.41682	-1.41410
C	2.06862	-0.99246	-0.02493	H	-1.37234	1.40804	0.03845
C	1.41802	1.30227	0.16185	C	-2.78459	-0.21630	0.12909
H	2.22608	-1.12320	1.06298	H	-2.91468	-1.23538	-0.25182
H	3.02036	-0.67963	-0.46549	H	-3.62451	0.38532	-0.23101
H	1.79965	-1.96624	-0.44559	H	-2.85055	-0.26030	1.22194
H	1.49719	1.33392	1.26583	H	-0.26376	-0.45045	1.29819
H	0.69370	2.05925	-0.14679	H	-0.40635	-1.49118	-0.12155
H	2.39102	1.58089	-0.25369				

327 – Bisamine complex

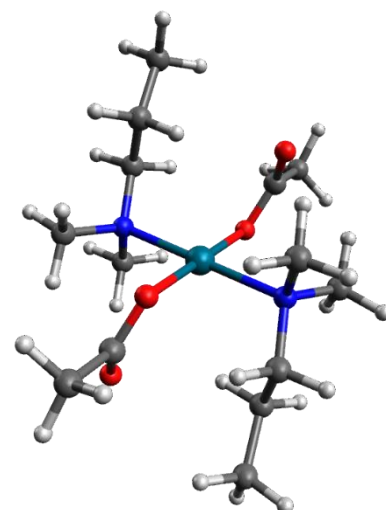
Geometry optimisation:

B3LYP-D3BJ/631G(d,p)/LANL2DZ-IEFPCM(DMF) Energy = -1090.15399653

Thermal correction to Gibbs Free Energy = 0.396856

Single-point energy calculation:

B3LYP-D3BJ/6311+G(2d,p)/SDD-IEFPCM(DMF) Energy = -1091.61657466



Pd	0.00000	-0.00000	0.00000	H	3.60012	-1.98952	-2.00781
O	1.31088	-1.20380	-1.02448	O	2.33926	-1.83094	0.88498
N	1.12794	1.66509	-0.77026	C	-2.90104	-1.41824	-1.02664
O	-1.31088	1.20380	1.02448	H	-2.90581	-0.59079	0.96521
N	-1.12795	-1.66509	0.77026	H	-3.11493	-2.34451	0.92066
C	0.93207	1.61936	-2.24181	C	-4.36937	-1.04420	-1.24323
H	-0.13140	1.73606	-2.45083	H	-2.68588	-2.37377	-1.51642
H	1.27990	0.65472	-2.61028	H	-2.26257	-0.65524	-1.48258
H	1.49710	2.42769	-2.72386	H	-5.04292	-1.76152	-0.76104
C	2.57924	1.50035	-0.46237	H	-4.61300	-1.02192	-2.30948
C	0.65520	2.97685	-0.26354	H	-4.57539	-0.05154	-0.83088
C	-0.65521	-2.97686	0.26354	H	0.13139	-1.73607	2.45084
H	0.34691	-3.15829	0.64316	H	-1.49710	-2.42770	2.72386
H	-0.63212	-2.97241	-0.82363	H	-1.27991	-0.65472	2.61028
H	-1.32986	-3.76640	0.61731	C	2.90104	1.41823	1.02664
C	-2.57924	-1.50035	0.46236	H	-0.34691	3.15829	-0.64316
C	-0.93207	-1.61936	2.24181	H	1.32986	3.76640	-0.61731
C	-2.22673	1.83461	0.34743	H	0.63212	2.97241	0.82363
O	-2.33927	1.83094	-0.88497	C	4.36936	1.04419	1.24322
C	-3.17812	2.63066	1.22870	H	2.26257	0.65524	1.48258
H	-3.98014	3.06430	0.63042	H	2.68589	2.37377	1.51641
H	-2.62575	3.43172	1.73036	H	4.57538	0.05153	0.83088
H	-3.59995	1.98964	2.00796	H	4.61300	1.02191	2.30947
C	2.22673	-1.83461	-0.34742	H	5.04292	1.76151	0.76103
C	3.17815	-2.63063	-1.22870	H	2.90581	0.59079	-0.96521
H	2.62577	-3.43156	-1.73054	H	3.11492	2.34451	-0.92067
H	3.98007	-3.06440	-0.63039				

328 – Monoamine complex

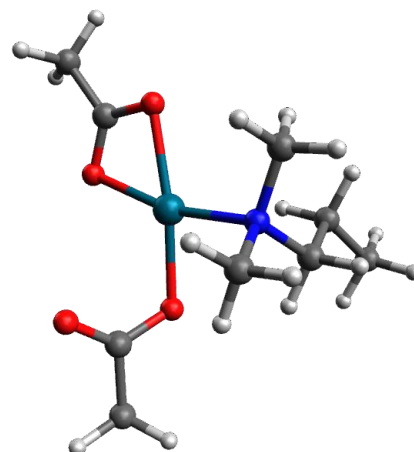
Geometry optimisation:

B3LYP-D3BJ/631G(d,p)/LANL2DZ-IEFPCM(DMF) Energy = -836.962267957

Thermal correction to Gibbs Free Energy = 0.225513

Single-point energy calculation:

B3LYP-D3BJ/6311+G(2d,p)/SDD-IEFPCM(DMF) Energy = -838.366051363



Pd	0.45475	0.00385	0.02417	H	-1.10342	4.74953	-0.19530
O	1.99975	-1.40531	0.33140	H	-2.40201	3.54792	-0.45218
O	2.35801	0.38997	-0.87264	H	-2.58245	-0.01025	-0.25571
C	2.80689	-0.69100	-0.36245	H	-3.17595	-1.37562	0.71247
C	4.23743	-1.09747	-0.53639	C	-2.03983	-1.94261	-1.04375
H	4.33994	-2.17898	-0.43605	H	-1.91842	1.07757	1.66889
H	4.83871	-0.61704	0.24294	H	-0.73835	0.34220	2.78148
H	4.60848	-0.76521	-1.50753	H	-2.40854	-0.28586	2.71332
N	-1.18007	-0.79996	1.05925	H	-0.33893	-2.73972	0.91115
C	-2.32796	-1.00195	0.12220	H	-1.58947	-2.55750	2.17441
C	-1.58912	0.14776	2.12825	H	0.04141	-1.86585	2.40382
O	-0.77340	1.50860	-0.56071	C	-3.20858	-1.94994	-2.03329
C	-0.44914	2.69647	-0.11438	H	-1.86193	-2.96036	-0.68214
C	-1.35538	3.79263	-0.65359	H	-1.12360	-1.61759	-1.55112
O	0.48042	2.93267	0.65943	H	-4.13614	-2.27381	-1.54905
C	-0.74056	-2.07680	1.67460	H	-3.00911	-2.63200	-2.86438
H	-1.24054	3.86641	-1.73930	H	-3.37842	-0.95127	-2.44935

A₁ – Agostic complex without ligand

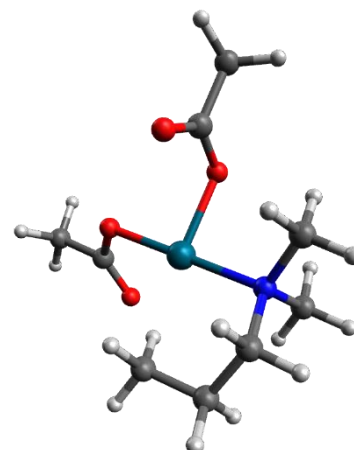
Geometry optimisation:

B3LYP-D3BJ/631G(d,p)/LANL2DZ-IEFPCM(DMF) Energy = -836.945290296

Thermal correction to Gibbs Free Energy = 0.226179

Single-point energy calculation:

B3LYP-D3BJ/6311+G(2d,p)/SDD-IEFPCM(DMF) Energy = -838.350094446



O	2.07145	0.16992	-0.38965	H	-2.60450	1.12720	-0.87973
Pd	0.09383	-0.13627	-0.02131	H	-2.46000	1.51391	0.84701
O	-0.03433	1.77836	0.64882	H	-3.83219	0.52244	0.27617
N	-1.95762	-0.46744	0.34204	H	4.60303	0.53946	0.52281
C	-2.43832	-1.52973	-0.60088	H	4.54796	-0.30164	-1.02630
C	-1.59045	-2.79627	-0.60520	H	4.91597	-1.21386	0.46795
C	-0.13454	-2.54033	-0.99118	H	-0.04699	-1.98414	-1.92911
C	-2.08275	-0.89662	1.75846	H	0.43133	-3.46902	-1.11362
C	-2.77180	0.75682	0.13082	H	0.45838	-2.06850	-0.16086
C	2.84447	-0.66256	0.25083	H	-2.04197	-3.47655	-1.33466
C	4.32630	-0.40281	0.03928	H	-1.64294	-3.30678	0.36106
O	2.43726	-1.58005	0.97585	C	-0.16821	2.65986	-0.30976
H	-2.43317	-1.07983	-1.59734	O	-0.28170	2.39827	-1.50848
H	-3.47862	-1.76431	-0.34232	C	-0.22764	4.08746	0.21315
H	-1.73367	-0.08646	2.39893	H	-1.22301	4.27126	0.63137
H	-1.47430	-1.78163	1.94095	H	-0.05365	4.78965	-0.60302
H	-3.13038	-1.12213	1.99116	H	0.50201	4.24469	1.01003

TS₁₅ – Acetate-assisted C–H activation

Geometry optimisation:

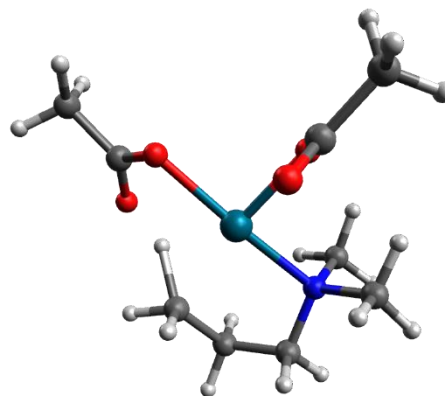
B3LYP-D3BJ/631G(d,p)/LANL2DZ-IEFPCM(DMF) Energy = -836.924082284

Thermal correction to Gibbs Free Energy = 0.223602

Imaginary frequency = -1344.9802

Single-point energy calculation:

B3LYP-D3BJ/6311+G(2d,p)/SDD-IEFPCM(DMF) Energy = -838.328365284



O	-1.17349	2.21266	-1.47075	H	-2.17569	-3.27496	-0.04510
C	-1.30107	2.38721	-0.25330	H	0.04510	-3.96989	-0.98695
O	1.84044	1.07599	-0.22025	H	0.24354	-3.33422	0.63596
Pd	0.11002	-0.08729	-0.05982	H	1.92312	-2.41242	-1.08757
O	-0.89301	1.56521	0.67120	H	0.62444	-1.62401	-1.91200
N	-1.60727	-1.25695	0.27742	H	-1.72272	-0.50370	2.23803
C	-1.45687	-2.55393	-0.45305	H	-0.77036	-1.99752	2.08033
C	-0.02449	-3.05317	-0.38821	H	-2.55101	-2.07036	1.99954
C	0.92744	-1.98256	-0.92114	H	-2.98472	0.32526	0.42942
C	-1.66576	-1.47445	1.74586	H	-3.70667	-1.24706	-0.01721
C	-2.85083	-0.57744	-0.16228	H	-2.76229	-0.31117	-1.21494
C	2.87755	0.46094	0.17887	H	4.94457	0.75373	-0.26455
C	4.16237	1.23327	0.32955	H	4.47723	1.20022	1.37652
O	2.87936	-0.78245	0.45637	H	4.03530	2.26877	0.01672
H	1.74642	-1.24419	-0.03959	H	-2.99009	3.31515	0.69956
C	-2.01446	3.61369	0.30111	H	-2.16462	4.35440	-0.48550
H	-1.72541	-2.35914	-1.49489	H	-1.44579	4.05233	1.12487

TS₁₆ – Acetate-assisted β -H elimination on the methyl substituent

Geometry optimisation:

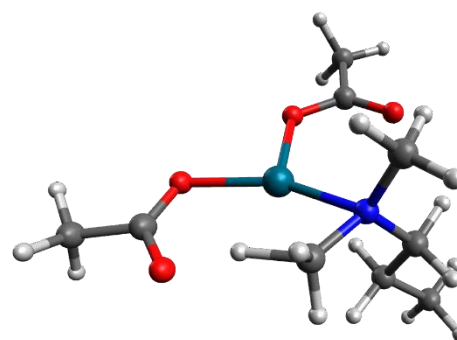
B3LYP-D3BJ/631G(d,p)/LANL2DZ-IEFPCM(DMF) Energy = -836.918528993

Thermal correction to Gibbs Free Energy = 0.220532

Imaginary frequency = -1107.9989

Single-point energy calculation:

B3LYP-D3BJ/6311+G(2d,p)/SDD-IEFPCM(DMF) Energy = -838.326257635



O	-2.27206	0.91218	-0.44842	H	2.80124	-1.04471	0.24912
Pd	-0.41087	0.17925	0.20386	C	1.60920	-1.79520	-1.36876
O	0.41556	2.00610	-0.22707	H	2.25149	-2.72243	0.49015
N	0.88340	-1.21275	0.99121	H	-0.78417	-2.11411	1.93501
C	1.39065	-0.87325	2.34022	C	1.69525	2.18692	-0.07794
C	-0.39654	-1.88029	0.94457	O	2.51052	1.33973	0.30548
C	1.96780	-1.73225	0.11074	C	2.13710	3.60464	-0.42464
C	-3.16272	0.00182	-0.33847	H	1.65437	4.31744	0.25109
C	-4.56135	0.34741	-0.79678	H	1.82421	3.85830	-1.44154
O	-2.94294	-1.16640	0.10039	H	3.22024	3.69855	-0.33795
H	-1.53263	-1.27575	0.45587	C	2.79104	-2.32215	-2.18826
H	-5.29859	-0.14859	-0.16346	H	1.33889	-0.78844	-1.70552
H	-4.69304	-0.02046	-1.81981	H	0.73577	-2.43508	-1.53506
H	-4.71687	1.42634	-0.79234	H	3.67047	-1.68110	-2.06692
H	0.56247	-0.53195	2.96099	H	2.54035	-2.35152	-3.25208
H	2.11851	-0.07251	2.22172	H	3.06811	-3.33572	-1.87981
H	1.85428	-1.75568	2.79368	H	-0.41008	-2.73745	0.27385

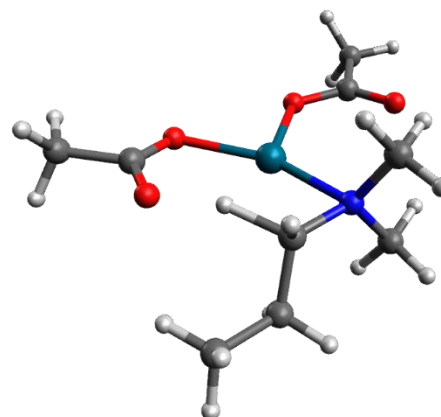
TS₁₇ – Acetate-assisted β -H elimination on the propyl substituent

Geometry optimisation:

B3LYP-D3BJ/631G(d,p)/LANL2DZ-IEFPCM(DMF) Energy = -836.918609707

Thermal correction to Gibbs Free Energy = 0.221642

Imaginary frequency = -1156.1505



Single-point energy calculation:

B3LYP-D3BJ/6311+G(2d,p)/SDD-IEFPCM(DMF) Energy = -838.325066532

O	-0.87532	2.10171	-0.16631	H	0.74064	-3.20974	1.80137
Pd	0.13930	0.25911	0.02390	H	-1.67896	-3.19193	-0.90553
O	1.91295	1.26087	-0.30791	H	-1.61838	-1.67123	-1.79194
N	0.32058	-1.76154	0.31838	C	-3.42962	-1.96041	-0.64663
C	0.89796	-2.13951	1.62877	H	-3.75435	-2.42237	0.29169
C	-1.11141	-1.52885	0.30521	H	-3.96581	-2.44879	-1.46463
C	0.94763	-2.51330	-0.78953	H	-3.71539	-0.90723	-0.62222
C	-2.09416	1.95247	0.17831	H	2.01455	-2.30320	-0.74289
C	-2.99524	3.16419	0.12433	H	0.55365	-2.17359	-1.74470
O	-2.59940	0.84793	0.54789	H	0.75688	-3.58497	-0.66699
C	-1.91999	-2.12360	-0.84298	H	-1.53350	-1.76426	1.28524
H	-1.58949	-0.19277	0.38716	C	3.05492	0.66094	-0.15777
H	-3.55976	3.24488	1.05612	O	3.22313	-0.51295	0.19871
H	-3.71692	3.02964	-0.68737	C	4.24660	1.56086	-0.46968
H	-2.42223	4.07446	-0.04895	H	4.23271	2.43770	0.18469
H	0.41166	-1.56289	2.41570	H	4.18031	1.92391	-1.49974
H	1.95917	-1.90052	1.59845	H	5.18238	1.01752	-0.33281

A₂ – Monodentate ligand-amine complex

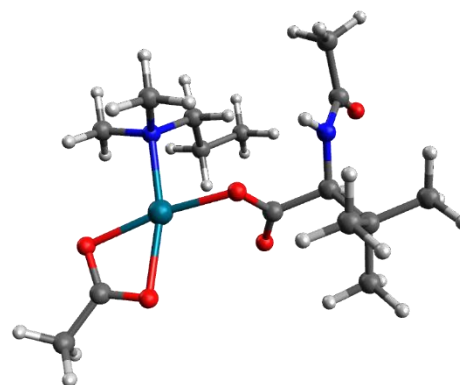
Geometry optimisation:

B3LYP-D3BJ/631G(d,p)/LANL2DZ-IEFPCM(DMF) Energy = -1202.29143457

Thermal correction to Gibbs Free Energy = 0.381018

Single-point energy calculation:

B3LYP-D3BJ/6311+G(2d,p)/SDD-IEFPCM(DMF) Energy = -1203.79543617



Pd	1.74466	-0.15665	-0.24868	H	-2.72809	-1.81721	-2.29319
N	1.38823	1.86272	-0.69018	H	-2.81148	-3.52256	-1.84774
C	1.00699	1.92568	-2.12540	H	-1.33416	-2.59631	-1.52601
C	2.65763	2.60124	-0.47659	H	-4.94325	-1.85414	0.76290
C	0.27864	2.44192	0.12976	H	-4.93482	-3.06461	-0.53203
O	3.83295	-0.24609	0.00364	H	-4.84423	-1.34014	-0.92980
O	-0.25157	-0.44022	-0.51334	H	-2.94345	-3.01541	1.87182
H	-0.63102	1.93240	-0.18666	H	-3.01452	-4.22605	0.57985
H	0.18745	3.50060	-0.14930	H	-1.49591	-3.38187	0.92527
C	0.44715	2.30101	1.63876	H	4.89857	-3.32627	0.18586
C	-0.92539	-0.78417	0.54892	H	5.13775	-2.30922	1.61848
C	3.77296	-1.51161	0.20538	H	5.88216	-1.82927	0.08184
C	5.00458	-2.29664	0.53136	H	3.42838	2.17672	-1.11892
O	-0.44748	-1.06652	1.64832	H	2.97069	2.50574	0.56131
C	-2.44801	-0.79811	0.32918	H	2.51342	3.65941	-0.72267
H	-2.90147	-0.57071	1.29493	O	2.62506	-2.06713	0.14738
C	-2.98518	-2.18348	-0.14867	H	-2.37644	0.32227	-1.46113
N	-2.83223	0.28568	-0.56144	H	0.61350	1.24773	1.88552
C	-3.53297	1.37211	-0.13871	C	-0.80497	2.80663	2.36355
O	-4.00282	1.46630	0.99874	H	1.32188	2.86247	1.98256
C	-3.67910	2.48362	-1.15989	H	-1.69466	2.24199	2.06604
H	-4.70176	2.86464	-1.12863	H	-0.99165	3.86347	2.14280
H	-3.43946	2.16675	-2.17739	H	-0.68937	2.70792	3.44663
H	-3.00960	3.30436	-0.88242	H	1.82400	1.53431	-2.73221
C	-4.51956	-2.10222	-0.21607	H	0.80522	2.96432	-2.41224
C	-2.58093	-3.26329	0.86872	H	0.11425	1.32026	-2.27742
C	-2.42643	-2.54693	-1.53454				

329 – Bidentate ligand-amine complex

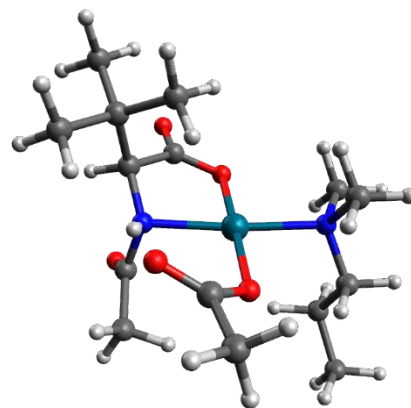
Geometry optimisation:

B3LYP-D3BJ/631G(d,p)/LANL2DZ-IEFPCM(DMF) Energy = -1202.30685337

Thermal correction to Gibbs Free Energy = 0.386185

Single-point energy calculation:

B3LYP-D3BJ/6311+G(2d,p)/SDD-IEFPCM(DMF) Energy = -1203.80917498



Pd	0.43563	-0.21868	-0.09507	O	-0.50142	2.77942	-0.57452
O	-0.55929	-1.95054	0.22330	C	1.60133	3.81349	-1.11588
N	-1.28354	0.57028	0.85464	H	2.01480	3.59571	-2.10580
O	1.40339	1.56883	-0.42209	H	2.44282	3.93697	-0.42954
N	2.05692	-1.13170	-1.10339	H	1.01582	4.73179	-1.16177
C	-1.82540	-1.81839	0.53915	C	1.91154	-2.60718	-1.11997
O	-2.54892	-2.77990	0.77991	C	3.33479	-0.71937	-0.44629
C	-2.39223	-0.38632	0.57515	C	2.03948	-0.62203	-2.49924
C	-3.18652	0.00765	-0.70777	H	1.10051	-0.91061	-2.97310
C	-2.31512	-0.05556	-1.97462	H	2.87771	-1.04833	-3.06325
C	-3.74339	1.43496	-0.53325	H	2.12069	0.46369	-2.47922
C	-4.37569	-0.95841	-0.85933	H	-0.55157	2.84318	2.10466
H	-4.04453	-1.98713	-1.00862	H	0.88931	1.83287	2.15494
H	-4.97882	-0.65648	-1.72100	H	-0.06710	2.05979	3.64304
H	-5.01711	-0.93683	0.02781	H	4.16200	-1.17095	-1.01138
H	-1.49490	0.66690	-1.93820	C	3.43427	-1.09195	1.03023
H	-2.92651	0.18073	-2.85145	H	3.39624	0.36419	-0.55556
H	-1.89014	-1.05336	-2.11949	H	1.84261	-2.98707	-0.10372
H	-2.95769	2.19470	-0.52698	H	2.77492	-3.05222	-1.62838
H	-4.31972	1.52119	0.39399	H	0.99537	-2.86771	-1.64706
H	-4.41146	1.66958	-1.36767	C	4.68195	-0.46967	1.66314
C	-0.94287	0.72890	2.23561	H	3.46462	-2.17926	1.15333
H	-3.08388	-0.34817	1.41969	H	2.53672	-0.73564	1.55033
C	-0.11965	1.94907	2.56071	H	5.59392	-0.80967	1.16063
O	-1.30299	-0.09507	3.05421	H	4.75997	-0.74295	2.71906
H	-1.29283	1.47094	0.33786	H	4.65114	0.62330	1.59841
C	0.73388	2.65118	-0.67157				

A₃ – Deprotonated ligand complex

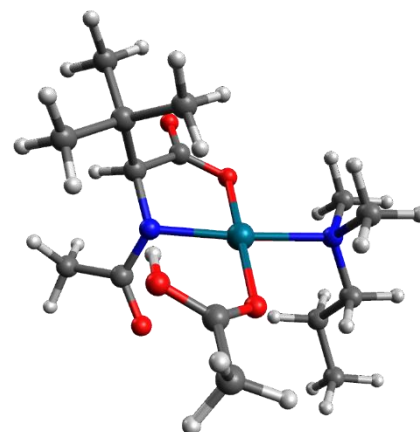
Geometry optimisation:

B3LYP-D3BJ/631G(d,p)/LANL2DZ-IEFPCM(DMF) Energy = -1202.28951164

Thermal correction to Gibbs Free Energy = 0.385896

Single-point energy calculation:

B3LYP-D3BJ/6311+G(2d,p)/SDD-IEFPCM(DMF) Energy = -1203.79102065



Pd	0.49324	-0.24681	-0.05523	C	1.32849	3.82783	-1.45569
O	-0.41903	-1.96575	0.43446	H	2.36395	3.63273	-1.72958
N	-1.24840	0.55058	0.70242	H	1.29384	4.59342	-0.67407
O	1.37406	1.57586	-0.66116	H	0.76712	4.20378	-2.31394
N	2.22144	-1.22081	-0.86535	C	2.16131	-2.68487	-0.64516
C	-1.70507	-1.85951	0.68847	C	3.45490	-0.63655	-0.25945
O	-2.38083	-2.82942	1.02199	C	2.22330	-0.95106	-2.32531
C	-2.32031	-0.45395	0.54875	H	1.31759	-1.36855	-2.76718
C	-3.14379	-0.27657	-0.76939	H	3.10143	-1.41199	-2.79487
C	-2.26920	-0.43865	-2.02375	H	2.24505	0.12566	-2.49152
C	-3.78732	1.12165	-0.75753	H	4.32397	-1.13128	-0.71658
C	-4.27405	-1.32130	-0.80909	C	3.52796	-0.74414	1.26164
H	-3.88402	-2.33909	-0.85826	H	3.47562	0.41496	-0.55161
H	-4.90337	-1.14587	-1.68765	H	2.08364	-2.89971	0.41807
H	-4.90885	-1.24924	0.08053	H	3.06152	-3.15781	-1.05641
H	-1.49941	0.33434	-2.08871	H	1.27519	-3.08133	-1.13800
H	-2.89102	-0.36121	-2.92180	C	4.75175	0.00281	1.79945
H	-1.77196	-1.41355	-2.04158	H	3.57576	-1.79327	1.57054
H	-3.04548	1.92250	-0.74452	H	2.61468	-0.32321	1.69901
H	-4.43635	1.24558	0.11626	H	5.67949	-0.40246	1.38118
H	-4.40355	1.25602	-1.65243	H	4.81098	-0.08028	2.88821
C	-1.09063	1.22888	1.89547	H	4.70613	1.06715	1.54464
H	-3.04263	-0.36398	1.36167	H	-3.18402	1.54732	2.41580
O	-0.05323	1.85740	2.13144	H	-1.99167	1.99659	3.66181
C	-2.24003	1.26750	2.89099	H	-2.38124	0.28992	3.36337
C	0.68468	2.58030	-0.93439	H	-0.95583	1.79347	-0.29933
O	-0.60955	2.63319	-0.79195				

330 – Amine-ligand complex with vacant site

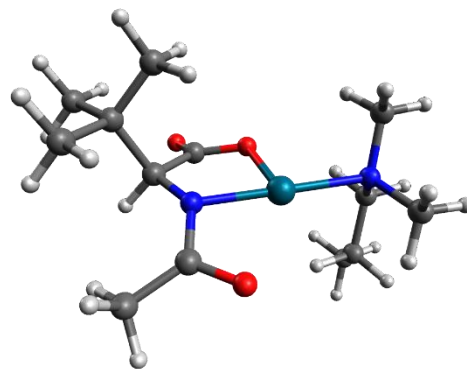
Geometry optimisation:

B3LYP-D3BJ/631G(d,p)/LANL2DZ-IEFPCM(DMF) Energy = -973.143454999

Thermal correction to Gibbs Free Energy = 0.326354

Single-point energy calculation:

B3LYP-D3BJ/6311+G(2d,p)/SDD-IEFPCM(DMF) Energy = -974.571293387



O	-1.42552	-2.56239	1.35221	H	-4.43989	1.02875	0.49420
C	-1.08991	-1.55632	0.73667	H	-3.55356	-1.17986	-2.38668
C	-2.02528	-0.32119	0.64781	H	-2.16856	-1.98998	-1.64060
H	-2.42957	-0.14378	1.65222	H	-2.04417	-0.28825	-2.11745
C	-3.23233	-0.60628	-0.31619	C	3.39792	-0.06588	1.41833
C	-4.13418	-1.69867	0.28058	H	-2.72638	2.03882	2.06255
C	-4.05791	0.68118	-0.47133	H	-2.84676	3.31473	0.84224
C	-2.71488	-1.04335	-1.69654	H	-1.63606	3.45105	2.12628
N	-1.22815	0.80304	0.19337	H	3.35696	1.79284	-0.53345
Pd	0.59795	0.39692	-0.40126	H	2.84915	1.56153	-2.21708
O	0.05860	-1.49880	0.08691	H	4.37378	0.83431	-1.64245
N	2.58778	-0.12553	-0.98760	H	1.96199	-0.49676	-2.96911
C	3.34275	1.08963	-1.36566	H	1.87972	-1.89861	-1.87679
C	3.24883	-0.86567	0.12641	H	3.46041	-1.34640	-2.50191
C	2.46820	-1.02525	-2.15973	H	4.10793	0.75613	1.28035
C	-1.13100	2.06433	0.59535	C	3.87484	-0.96541	2.56203
C	-2.14891	2.74818	1.46668	H	2.43248	0.38504	1.67853
O	-0.10193	2.69102	0.17519	H	4.83697	-1.43210	2.32438
H	-4.99392	-1.86550	-0.37681	H	3.15368	-1.76592	2.75848
H	-4.51610	-1.39714	1.26250	H	4.00042	-0.39070	3.48389
H	-3.59848	-2.64071	0.40344	H	4.23438	-1.20889	-0.22115
H	-4.91797	0.49288	-1.12190	H	2.62936	-1.74665	0.31233
H	-3.46679	1.48386	-0.91952				

A₄ – Agostic complex with ligand

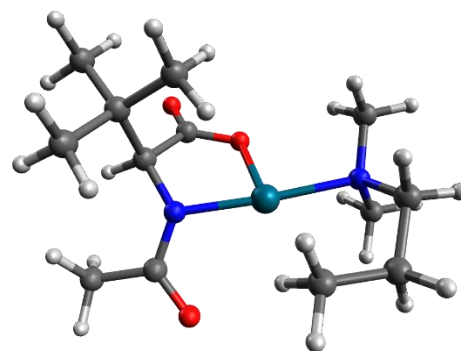
Geometry optimisation:

B3LYP-D3BJ/631G(d,p)/LANL2DZ-IEFPCM(DMF) Energy = -973.144763814

Thermal correction to Gibbs Free Energy = 0.332255

Single-point energy calculation:

B3LYP-D3BJ/6311+G(2d,p)/SDD-IEFPCM(DMF) Energy = -974.574235357



O	2.18579	-2.16067	-1.73158	H	3.60349	0.35216	2.74565
C	1.50911	-1.32963	-1.13586	H	2.44672	1.38779	1.88908
C	2.12583	-0.14404	-0.37444	H	4.06363	1.10068	1.21266
H	2.97121	0.21140	-0.97045	H	2.04290	-1.57609	2.83761
C	2.70118	-0.59781	1.01580	H	1.21155	-2.16305	1.38936
C	3.86293	-1.58079	0.79277	H	0.78811	-0.58627	2.07537
C	3.23237	0.63938	1.75637	H	-2.98728	-0.71868	1.95931
C	1.61852	-1.27092	1.87551	H	-4.46152	-0.74681	0.97872
N	1.10002	0.88970	-0.25582	H	-2.71078	-1.06805	-2.18958
Pd	-0.73767	0.10121	-0.15509	H	-3.43090	0.42872	-1.56714
O	0.19205	-1.42497	-1.09128	H	-4.31050	-1.11377	-1.39746
N	-2.64367	-0.87892	-0.09443	H	-1.94165	-2.50645	1.04798
C	-3.44560	-0.33493	1.04346	H	-1.82309	-2.71822	-0.70911
C	-3.48669	1.18845	1.10257	H	-3.41619	-2.85119	0.10017
C	-2.10772	1.82233	1.28929	H	2.88515	2.17898	-2.10655
C	-3.32009	-0.64123	-1.39223	H	3.34511	2.47073	-0.42677
C	-2.44777	-2.33623	0.09692	H	2.48871	3.73274	-1.34563
C	1.20459	2.14255	-0.74104	H	-1.55192	1.36499	2.11269
C	2.57151	2.65951	-1.17335	H	-2.17708	2.89351	1.50304
O	0.20916	2.89132	-0.83171	H	-1.48894	1.86635	0.35095
H	4.30705	-1.85438	1.75558	H	-4.11988	1.45525	1.95535
H	4.64792	-1.12748	0.17725	H	-3.97847	1.60264	0.21696
H	3.52983	-2.49211	0.29285				

TS₁₈ – Ligand-assisted C–H activation

Geometry optimisation:

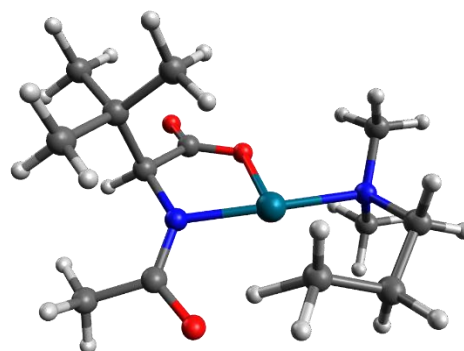
B3LYP-D3BJ/631G(d,p)/LANL2DZ-IEFPCM(DMF) Energy = -973.128193134

Thermal correction to Gibbs Free Energy = 0.328440

Imaginary frequency = -1330.6650

Single-point energy calculation:

B3LYP-D3BJ/6311+G(2d,p)/SDD-IEFPCM(DMF) Energy = -974.557695057



O	2.07875	-2.32945	-1.65787	H	3.89367	0.58463	2.38098
C	1.41166	-1.47435	-1.07711	H	2.55489	1.49680	1.67073
C	2.08545	-0.20982	-0.49619	H	4.06270	1.27253	0.76118
H	2.85191	0.10291	-1.21170	H	2.37096	-1.34878	2.81791
C	2.81264	-0.52089	0.86143	H	1.45576	-2.11481	1.51003
C	3.99088	-1.47352	0.59817	H	0.99876	-0.50339	2.08155
C	3.35935	0.79074	1.44796	H	-3.40669	-0.29089	1.91072
C	1.84855	-1.16079	1.87422	H	-4.63977	-0.28035	0.63858
N	1.05587	0.81271	-0.35967	H	-2.45843	-1.52393	-1.95564
Pd	-0.78105	0.05592	-0.05833	H	-3.27470	0.04508	-1.78372
O	0.12077	-1.59075	-0.88766	H	-4.15459	-1.45765	-1.39508
N	-2.69008	-0.87277	0.03333	H	-2.19294	-2.17193	1.61665
C	-3.59648	-0.02858	0.86626	H	-1.86615	-2.80550	-0.01114
C	-3.29809	1.44945	0.66324	H	-3.54844	-2.73602	0.59912
C	-1.83134	1.75321	0.98792	H	3.15260	2.05855	-1.49206
C	-3.17850	-0.95690	-1.36507	H	2.78465	3.37565	-0.36717
C	-2.57107	-2.23754	0.59561	H	2.12432	3.41883	-2.00506
C	1.12047	2.08489	-0.68997	H	-1.53288	1.33266	1.95525
C	2.38045	2.75803	-1.17469	H	-1.70377	2.83510	1.11786
O	0.07514	2.82122	-0.58371	H	-0.88070	2.05295	0.04471
H	4.52551	-1.66800	1.53380	H	-3.96453	2.02260	1.31975
H	4.70123	-1.03180	-0.10959	H	-3.53837	1.75552	-0.36088
H	3.65183	-2.42428	0.18390				

As – Cyclopalladated amine

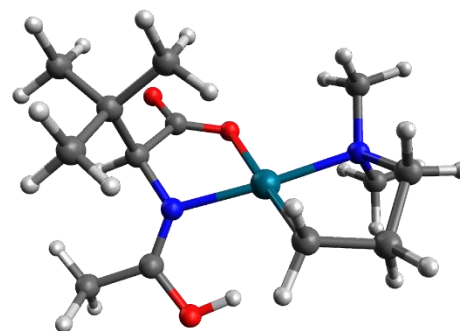
Geometry optimisation:

B3LYP-D3BJ/631G(d,p)/LANL2DZ-IEFPCM(DMF) Energy = -973.158971609

Thermal correction to Gibbs Free Energy = 0.331680

Single-point energy calculation:

B3LYP-D3BJ/6311+G(2d,p)/SDD-IEFPCM(DMF) Energy = -974.587943691



O	2.18749	-2.20560	-1.78552	H	3.62712	1.06647	1.46657
C	1.43426	-1.37303	-1.26378	H	1.74748	-1.93111	2.68139
C	2.07385	-0.24895	-0.39913	H	1.14901	-2.47918	1.10781
H	2.98426	0.05910	-0.91787	H	0.48886	-1.00958	1.84099
C	2.50496	-0.76170	1.02061	C	-3.13701	1.35984	1.11213
C	3.76172	-1.63334	0.85070	H	3.58573	1.92286	-0.85241
C	2.84776	0.44133	1.91502	H	2.97405	3.48284	-0.26803
C	1.40300	-1.59391	1.69818	H	2.78336	3.05242	-1.96896
N	1.12737	0.87190	-0.33576	H	-2.08334	-2.37856	1.12637
Pd	-0.79653	0.14739	-0.13872	H	-1.93018	-2.62407	-0.62486
O	0.14795	-1.37151	-1.36671	H	-3.54458	-2.70225	0.15036
N	-2.70983	-0.75489	-0.06221	H	-2.74559	-0.95086	-2.16065
C	-2.56289	-2.21157	0.16112	H	-3.48209	0.54405	-1.54598
C	-3.49132	-0.11661	1.04442	H	-4.35491	-1.00398	-1.38786
C	-3.36675	-0.52538	-1.37186	H	-3.51361	1.88105	0.22456
C	1.43449	2.08222	-0.64535	C	-1.61502	1.48129	1.20544
C	2.78512	2.65061	-0.95186	H	-3.64111	1.81551	1.97611
O	0.47330	3.01091	-0.71895	H	-3.18364	-0.60572	1.97292
H	4.07973	-2.02394	1.82293	H	-4.56213	-0.30723	0.89721
H	4.58988	-1.04810	0.43522	H	-1.25152	1.10261	2.17006
H	3.56822	-2.46990	0.17729	H	-1.28381	2.52157	1.12802
H	3.22211	0.08826	2.88130	H	-0.37908	2.55640	-0.55062
H	1.97061	1.06720	2.10064				

TS₁₉ – Ligand-assisted β -H elimination on the methyl substituent

Geometry optimisation:

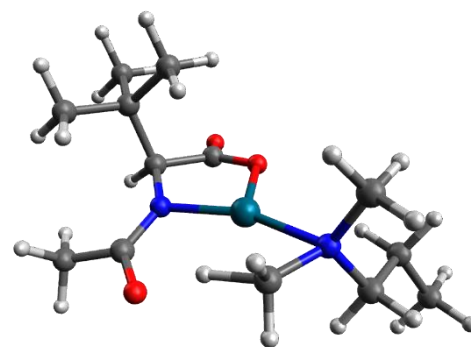
B3LYP-D3BJ/631G(d,p)/LANL2DZ-IEFPCM(DMF) Energy = -973.112087402

Thermal correction to Gibbs Free Energy = 0.325599

Imaginary frequency = -1152.4688

Single-point energy calculation:

B3LYP-D3BJ/6311+G(2d,p)/SDD-IEFPCM(DMF) Energy = -974.545843759



O	1.70586	-2.77269	-1.28876	H	4.47246	0.92269	-0.04011
C	1.25192	-1.75527	-0.76621	H	2.94658	-0.97557	2.76985
C	2.13123	-0.48814	-0.61687	H	1.73700	-1.87290	1.83809
H	2.76289	-0.41573	-1.50897	H	1.53803	-0.13434	2.09848
C	3.08047	-0.62832	0.63260	H	-0.70770	2.03652	-0.00092
C	4.08386	-1.76658	0.38065	H	2.24267	2.95377	-2.54180
C	3.86484	0.67746	0.83620	H	3.22916	1.57361	-2.00077
C	2.27313	-0.92248	1.90820	H	3.14714	3.05414	-1.02902
N	1.22504	0.64402	-0.51904	H	-2.03507	0.49080	2.83770
Pd	-0.60722	0.21554	0.14722	H	-3.04705	-0.84833	2.27035
O	0.04157	-1.69426	-0.26744	H	-3.77711	0.75810	2.53598
N	-2.56458	0.58191	0.80397	H	-2.44458	2.49708	-0.11621
C	-2.87919	0.22567	2.20169	H	-1.77214	2.40819	1.55902
C	-1.92897	1.87999	0.62036	H	-3.38213	0.73128	-1.10748
C	-3.64412	0.25097	-0.16156	H	-4.58196	0.69605	0.19770
C	1.35225	1.89382	-0.93217	C	-3.80250	-1.25124	-0.38122
C	2.57501	2.38102	-1.67326	C	-4.83555	-1.54103	-1.47348
O	0.41654	2.74313	-0.73108	H	-4.10867	-1.74090	0.54920
H	4.77022	-1.84908	1.22989	H	-2.82817	-1.66946	-0.65970
H	4.68141	-1.57055	-0.51667	H	-5.81788	-1.13506	-1.20948
H	3.57900	-2.72412	0.24444	H	-4.94785	-2.61815	-1.62438
H	4.54168	0.56912	1.68985	H	-4.53446	-1.09719	-2.42852
H	3.19950	1.51917	1.04540				

A₆ – Imine complex I

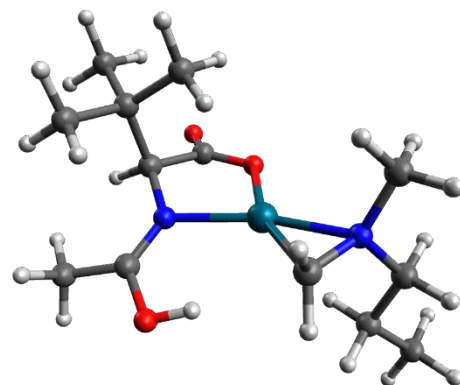
Geometry optimisation:

B3LYP-D3BJ/631G(d,p)/LANL2DZ-IEFPCM(DMF) Energy = -973.153013549

Thermal correction to Gibbs Free Energy = 0.328162

Single-point energy calculation:

B3LYP-D3BJ/6311+G(2d,p)/SDD-IEFPCM(DMF) Energy = -974.584174216



Pd	0.66902	-0.10855	-0.17982	C	-3.53892	0.31950	-1.44496
N	2.54177	-0.65950	-0.96538	H	-2.72457	0.81338	-1.98235
O	-0.28076	-1.24910	1.43525	H	-4.15611	1.08781	-0.96822
N	-1.15070	0.91631	0.11190	H	-4.16247	-0.19365	-2.18411
C	-1.50817	-0.93849	1.66965	C	3.74315	-0.53837	-0.09850
O	-2.19291	-1.39316	2.59792	C	3.70983	0.61688	0.89618
C	-2.18472	0.05511	0.68788	C	2.54098	-1.91775	-1.73886
C	-1.26676	2.18822	-0.03454	C	2.01400	0.49195	-1.60026
O	-0.24934	2.88289	-0.56359	C	4.93342	0.57563	1.81634
C	-2.43034	3.06799	0.30382	H	2.78781	0.55238	1.48613
H	-3.18098	2.55718	0.90212	H	3.68389	1.57649	0.36982
H	-2.89642	3.41763	-0.62223	H	4.96616	-0.35747	2.38859
H	-2.06662	3.94454	0.84494	H	4.90937	1.40581	2.52743
C	-3.01135	-0.69604	-0.41760	H	5.86376	0.65142	1.24345
H	-2.89405	0.64464	1.27478	H	3.81886	-1.48425	0.44519
C	-2.16117	-1.75025	-1.14626	H	4.62165	-0.45955	-0.75246
H	-1.28305	-1.29654	-1.61708	H	3.43831	-1.97354	-2.36512
H	-2.75821	-2.23169	-1.92792	H	1.65173	-1.95535	-2.36687
H	-1.80937	-2.52531	-0.46000	H	2.52806	-2.76088	-1.04661
C	-4.21211	-1.38552	0.25312	H	2.56875	1.41177	-1.43383
H	-3.88620	-2.10128	1.00926	H	1.69215	0.34264	-2.62805
H	-4.80649	-1.91135	-0.50142	H	0.46085	2.23430	-0.76456
H	-4.86202	-0.65163	0.74267				

TS₂₀ – Ligand-assisted β -H elimination on the propyl substituent

Geometry optimisation:

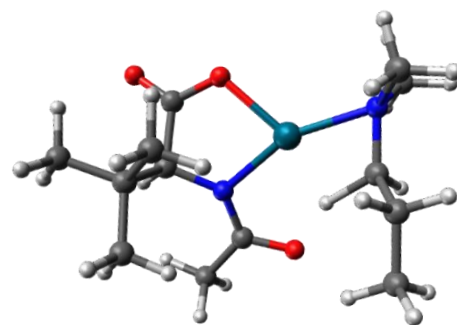
B3LYP-D3BJ/631G(d,p)/LANL2DZ-IEFPCM(DMF) Energy = -973.112699884

Thermal correction to Gibbs Free Energy = 0.325991

Imaginary frequency = -1185.6646

Single-point energy calculation:

B3LYP-D3BJ/6311+G(2d,p)/SDD-IEFPCM(DMF) Energy = -974.545300918



O	2.84071	-2.38247	-0.98593	H	3.63498	2.11946	0.39451
C	1.92797	-1.62695	-0.65008	H	2.40653	-0.17873	3.05350
C	2.19868	-0.11339	-0.45662	H	1.85559	-1.49528	2.00437
H	2.92462	0.19206	-1.21789	H	0.95760	0.02844	2.05293
C	2.84215	0.15666	0.95449	H	-1.42384	1.07413	-0.57144
C	4.23409	-0.49504	1.01016	H	1.36812	3.02885	-2.70128
C	3.00041	1.67083	1.16502	H	2.67607	2.16902	-1.85159
C	1.96047	-0.40945	2.08054	H	1.83017	3.51531	-1.06823
N	0.92811	0.56703	-0.63621	H	-2.51695	-1.17485	2.16106
Pd	-0.69664	-0.53324	-0.24468	H	-2.95478	-2.63824	1.26395
O	0.71429	-2.04484	-0.39642	H	-4.18518	-1.38190	1.55670
N	-2.73166	-0.94376	0.06902	H	-3.22928	-2.60950	-1.10957
C	-3.12471	-1.56430	1.34772	H	-3.10650	-1.07704	-2.00018
C	-2.59026	0.51279	0.00750	H	-4.52965	-1.39381	-0.96534
C	-3.44911	-1.54170	-1.07555	C	-2.82976	1.30556	1.28643
C	0.64591	1.73977	-1.17395	C	-2.69873	2.81500	1.06535
C	1.70832	2.65556	-1.73305	H	-2.90351	3.34919	1.99688
O	-0.56834	2.14123	-1.24638	H	-3.41211	3.16501	0.31173
H	4.70354	-0.28398	1.97671	H	-1.69562	3.07760	0.72282
H	4.88578	-0.09484	0.22540	H	-2.12987	0.98813	2.06441
H	4.17612	-1.57658	0.87798	H	-3.84011	1.07657	1.64787
H	3.47121	1.86020	2.13514	H	-3.17219	0.90262	-0.83247
H	2.03344	2.18079	1.15950				

A₇ – Imine complex II

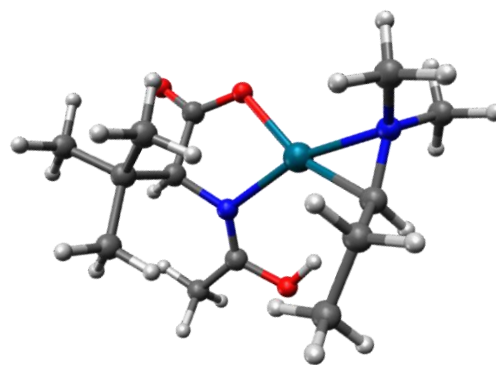
Geometry optimisation:

B3LYP-D3BJ/631G(d,p)/LANL2DZ-IEFPCM(DMF) Energy = -973.157025370

Thermal correction to Gibbs Free Energy = 0.330053

Single-point energy calculation:

B3LYP-D3BJ/6311+G(2d,p)/SDD-IEFPCM(DMF) Energy = -974.586995895



Pd	-0.83523	-0.38531	-0.39154	C	2.67274	1.28462	1.60247
N	-2.86326	-0.72768	0.04624	H	1.72889	1.83099	1.52202
O	0.57242	-2.02373	-0.87011	H	3.42491	1.80212	0.99827
N	1.00391	0.61096	-0.67492	H	2.99703	1.33206	2.64704
C	1.81459	-1.69536	-0.80995	C	-3.71902	-1.08606	-1.10215
O	2.76713	-2.44761	-1.06758	H	-3.54625	-2.13110	-1.36349
C	2.14389	-0.24719	-0.35154	H	-3.46374	-0.45657	-1.95391
C	1.10322	1.76073	-1.23968	H	-4.77406	-0.94556	-0.84042
O	-0.01337	2.44536	-1.53377	C	-3.16165	-1.54391	1.23754
C	2.33813	2.51133	-1.63137	H	-2.43917	-1.34263	2.02479
H	3.23704	1.90341	-1.56332	H	-3.09403	-2.59593	0.95801
H	2.44981	3.37919	-0.97432	H	-4.17367	-1.32868	1.59923
H	2.22292	2.88034	-2.65316	C	-2.50665	0.64446	0.18347
C	2.51842	-0.18395	1.17269	H	-0.76822	1.88428	-1.25114
H	3.03004	0.06331	-0.91144	C	-2.49631	1.32181	1.53635
C	1.45028	-0.85264	2.05382	H	-1.98274	0.70674	2.28014
H	0.47601	-0.36765	1.93537	H	-3.53249	1.44352	1.88589
H	1.74057	-0.77980	3.10726	C	-1.81640	2.69182	1.46112
H	1.33086	-1.91102	1.80625	H	-0.76226	2.58750	1.18863
C	3.86452	-0.90130	1.37402	H	-1.87070	3.20321	2.42581
H	3.80766	-1.94286	1.05435	H	-2.29526	3.33309	0.71326
H	4.14920	-0.86734	2.43087	H	-2.95786	1.25724	-0.59907
H	4.65775	-0.41481	0.79537				

329a – Bidentate ligand-amine complex with Ac-Ala-OH

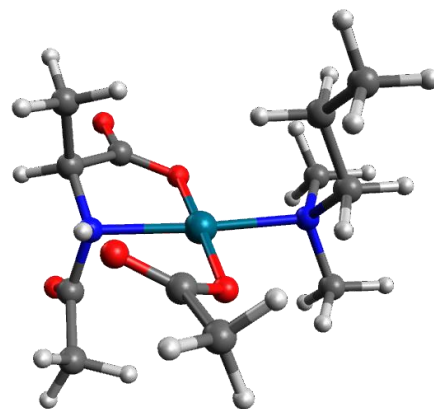
Geometry optimisation:

B3LYP-D3BJ/631G(d,p)/LANL2DZ-IEFPCM(DMF) Energy = -1084.33978871

Thermal correction to Gibbs Free Energy = 0.306336

Single-point energy calculation:

B3LYP-D3BJ/6311+G(2d,p)/SDD-IEFPCM(DMF) Energy = -1085.81744372



Pd	0.01613	-0.18591	-0.37552	C	-1.54255	-2.63127	-1.10264
O	1.12457	-1.88111	-0.24895	H	2.00455	3.19393	-0.49755
N	1.79827	0.66149	0.39331	H	1.15888	2.34273	-1.78473
O	-1.06536	1.55669	-0.48739	H	2.87101	2.78681	-2.01340
N	-1.72888	-1.16065	-1.07174	H	-3.02274	0.29321	-0.33280
C	2.17268	-1.78733	0.53218	C	-2.70382	-1.09964	1.27493
O	2.91339	-2.73223	0.78332	H	-3.77853	-1.29018	-0.59935
C	2.41583	-0.42316	1.20038	C	-3.84929	-0.50811	2.10105
C	1.83463	-0.41445	2.61548	H	-2.65340	-2.18135	1.43552
C	2.56438	1.12641	-0.71976	H	-1.74967	-0.68015	1.61486
H	3.49493	-0.26096	1.23704	H	-4.81819	-0.90519	1.77972
C	2.12833	2.45191	-1.29032	H	-3.88289	0.58197	1.99851
O	3.48714	0.46024	-1.14835	H	-3.72598	-0.74296	3.16189
H	1.33418	1.42677	0.92638	H	2.03936	0.53795	3.11191
C	-0.89745	2.49944	0.38890	H	2.29770	-1.21575	3.19496
O	0.01053	2.54855	1.23942	H	0.75299	-0.57671	2.60003
C	-1.94547	3.59337	0.30935	H	-1.13162	-0.94445	-3.08592
H	-2.89819	3.20109	0.68019	H	-2.06583	0.42152	-2.42186
H	-2.09762	3.89717	-0.72906	H	-2.89318	-1.10521	-2.85091
H	-1.64966	4.45040	0.91468	H	-0.72231	-2.87224	-1.77656
C	-1.97252	-0.66346	-2.45079	H	-2.46552	-3.10800	-1.45303
C	-2.88775	-0.78139	-0.20581	H	-1.29018	-2.99553	-0.10972

330a – Amine-ligand complex with vacant site and Ac-Ala-OH

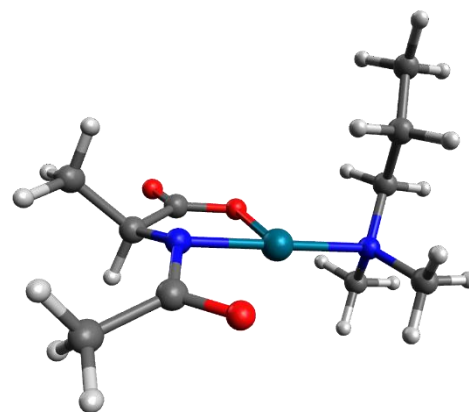
Geometry optimisation:

B3LYP-D3BJ/631G(d,p)/LANL2DZ-IEFPCM(DMF) Energy = -855.177860678

Thermal correction to Gibbs Free Energy = 0.248373

Single-point energy calculation:

B3LYP-D3BJ/6311+G(2d,p)/SDD-IEFPCM(DMF) Energy = -856.579692254



O	-1.79063	3.02521	-0.98519	C	2.93127	0.36108	1.50278
C	-1.44753	1.89626	-0.65230	H	2.47441	1.49367	-0.27280
C	-2.49875	0.87879	-0.13982	H	3.95721	0.52999	-0.39856
H	-3.08115	0.58490	-1.02724	H	-4.09170	-1.67798	1.42741
C	-3.43528	1.53898	0.87364	H	-3.68535	-3.04117	0.35948
N	-1.79035	-0.26595	0.41194	H	-4.16493	-1.46325	-0.32430
Pd	0.09775	-0.41257	-0.11494	H	2.12587	-2.57209	-1.13451
O	-0.19325	1.49818	-0.73627	H	2.58480	-2.13698	0.52254
N	2.14577	-0.50355	-0.75065	H	3.74884	-1.90609	-0.80979
C	2.68923	-1.86198	-0.52679	H	1.89924	0.23927	1.85427
C	2.17216	-0.18776	-2.19910	C	3.57339	1.57062	2.18759
C	2.92644	0.53231	-0.01431	H	3.47427	-0.54731	1.78331
C	-2.17146	-1.54219	0.48752	H	3.01715	2.48813	1.96785
C	-3.61693	-1.95980	0.48246	H	4.60543	1.71540	1.85018
O	-1.22926	-2.38936	0.58176	H	3.59164	1.43925	3.27311
H	1.72393	0.79395	-2.35424	H	-4.24870	0.86499	1.15255
H	1.59178	-0.93672	-2.74022	H	-3.85909	2.44461	0.43368
H	3.20353	-0.18777	-2.57459	H	-2.88193	1.80995	1.77767

TS_{18a} – Ligand-assisted C–H activation with Ac-Ala-OH

Geometry optimisation:

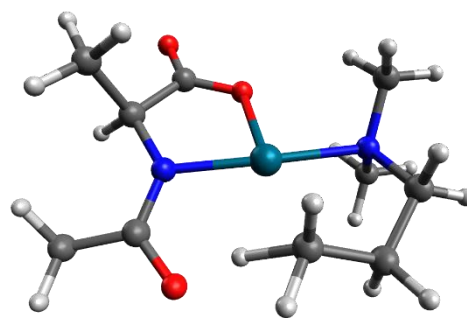
B3LYP-D3BJ/631G(d,p)/LANL2DZ-IEFPCM(DMF) Energy = -855.161047727

Thermal correction to Gibbs Free Energy = 0.247925

Imaginary frequency = -1336.3442

Single-point energy calculation:

B3LYP-D3BJ/6311+G(2d,p)/SDD-IEFPCM(DMF) Energy = -856.564871645



O	2.32577	-2.96155	-0.48002	H	-4.29252	0.25438	0.04877
C	1.71368	-1.91194	-0.29302	H	3.57680	1.77974	-1.67001
C	2.49432	-0.63038	0.07146	H	4.03691	1.68198	0.03442
H	3.28437	-0.51841	-0.67963	H	3.40967	3.20979	-0.63460
C	3.13505	-0.80908	1.45537	H	-1.27650	1.62281	1.77545
N	1.58549	0.51005	0.03368	H	-1.08082	3.02344	0.78309
Pd	-0.36132	0.02567	0.08258	H	-0.17688	2.03674	-0.01084
O	0.40942	-1.82308	-0.35156	H	-3.42354	2.52734	0.60098
N	-2.37251	-0.64645	-0.08955	H	-2.74179	1.98969	-0.92324
C	-3.28305	0.40488	0.45119	H	3.77098	-1.69732	1.45651
C	-2.73981	1.79451	0.15469	H	2.35738	-0.92918	2.21625
C	-1.32904	1.95593	0.73212	H	3.74155	0.06148	1.71896
C	-2.60697	-0.85656	-1.53937	H	-2.36577	-1.77366	1.69148
C	-2.55661	-1.92853	0.62871	H	-1.84265	-2.65337	0.23836
C	1.89928	1.73187	-0.34058	H	-3.58005	-2.29956	0.49179
C	3.32211	2.12396	-0.66166	H	-3.62439	-1.23223	-1.70705
O	0.98389	2.61934	-0.46087	H	-1.88336	-1.58224	-1.91154
H	-3.32771	0.26275	1.53446	H	-2.47820	0.08421	-2.07497

TS_{19a} – Ligand-assisted β -H elimination on the methyl substituent with Ac-Ala-OH

Geometry optimisation:

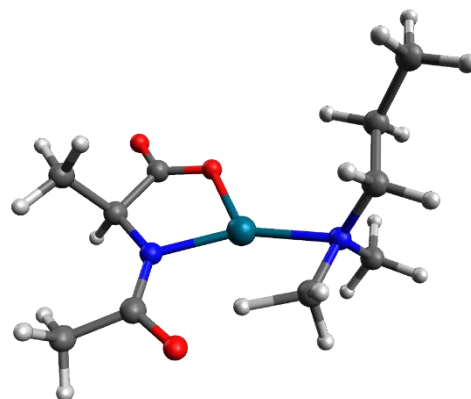
B3LYP-D3BJ/631G(d,p)/LANL2DZ-IEFPCM(DMF) Energy = -855.147365032

Thermal correction to Gibbs Free Energy = 0.244748

Imaginary frequency = -1118.8913

Single-point energy calculation:

B3LYP-D3BJ/6311+G(2d,p)/SDD-IEFPCM(DMF) Energy = -856.555901610



O	-2.04451	3.14665	-0.91344	H	-3.98866	-1.78860	1.57450
C	-1.59545	2.04009	-0.61913	C	3.48070	1.06328	0.39924
C	-2.55506	0.96294	-0.05667	H	1.29950	-2.85848	-0.60908
H	-3.37417	0.86177	-0.78102	H	1.52121	-2.34441	1.10965
C	-3.12119	1.46071	1.28147	C	4.34264	1.60642	1.54238
N	-1.82170	-0.28640	0.06841	H	3.95235	-1.03772	0.68877
Pd	0.14648	-0.20242	-0.23449	H	2.57175	-0.45010	1.63316
O	-0.32774	1.73344	-0.72365	H	2.57662	1.67220	0.28562
N	2.11976	-0.91255	-0.34752	H	4.03713	1.13491	-0.54097
C	3.07073	-0.38275	0.66345	H	3.79621	1.58845	2.49141
C	1.29019	-2.02591	0.09418	H	4.64014	2.63998	1.34539
C	2.70203	-1.06318	-1.69621	H	5.25458	1.01321	1.66864
C	-2.28110	-1.50110	0.31828	H	-3.86487	0.76730	1.68024
C	-3.75842	-1.75857	0.50480	H	-3.59109	2.43620	1.13757
O	-1.48440	-2.49485	0.41549	H	-2.31457	1.56140	2.01460
H	-0.07977	-1.96833	0.19957	H	3.57218	-1.72908	-1.66178
H	-4.00355	-2.73391	0.08149	H	3.00593	-0.08625	-2.06944
H	-4.38067	-0.99215	0.04022	H	1.94811	-1.47573	-2.36619

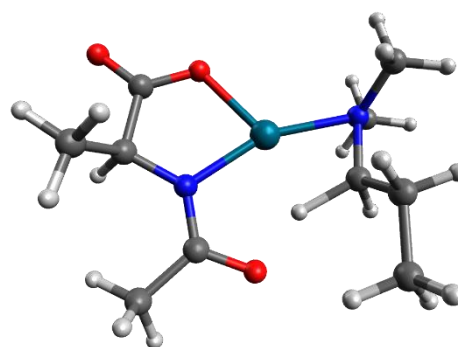
TS_{20a} – Ligand-assisted β -H elimination on the propyl substituent with Ac-Ala-OH

Geometry optimisation:

B3LYP-D3BJ/631G(d,p)/LANL2DZ-IEFPCM(DMF) Energy = -855.147240531

Thermal correction to Gibbs Free Energy = 0.245436

Imaginary frequency = -1202.6684



Single-point energy calculation:

B3LYP-D3BJ/6311+G(2d,p)/SDD-IEFPCM(DMF) Energy = -856.554328796

O	3.47984	-2.21975	0.14009	H	2.29926	3.55220	0.15907
C	2.48873	-1.49394	0.06299	C	-2.75931	1.14566	1.02107
C	2.68761	0.04212	0.03880	C	-2.79549	2.66414	0.82797
H	3.37786	0.25408	-0.78832	H	-3.25080	3.14020	1.70054
C	3.33325	0.48260	1.36035	H	-3.39132	2.93244	-0.05098
N	1.39816	0.67084	-0.19360	H	-1.79097	3.06866	0.69062
Pd	-0.21003	-0.51358	-0.11996	H	-2.18351	0.90139	1.91830
O	1.26563	-1.95201	0.03040	H	-3.78015	0.77872	1.18434
N	-2.23027	-1.04932	-0.17596	H	-2.59906	0.78589	-1.12902
C	-2.79568	-1.73335	1.00211	H	4.25891	-0.07533	1.51833
C	-2.18483	0.41453	-0.18822	H	2.65281	0.28248	2.19423
C	-2.68408	-1.66499	-1.44037	H	3.56171	1.55099	1.35095
C	1.13337	1.91178	-0.55712	H	-2.21346	-1.15514	-2.28104
C	2.22884	2.93459	-0.74207	H	-3.77435	-1.59284	-1.52683
O	-0.07447	2.28788	-0.75064	H	-2.38667	-2.71433	-1.44700
H	-0.95734	1.09659	-0.43043	H	-3.88766	-1.64032	1.01730
H	1.96915	3.58821	-1.57638	H	-2.37798	-1.31973	1.91718
H	3.20379	2.48002	-0.92407	H	-2.52654	-2.78809	0.93651

III.II. Nuclear coordinates for complexes containing 1-propylpiperidine

210 – 1-propylpiperidine

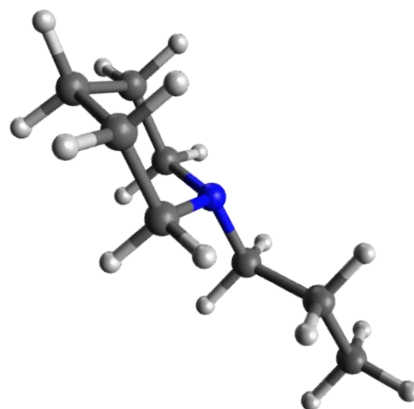
Geometry optimisation:

B3LYP-D3BJ/631G(d,p)/LANL2DZ-IEFPCM(DMF) Energy = -369.908534444

Thermal correction to Gibbs Free Energy = 0.205055

Single-point energy calculation:

B3LYP-D3BJ/6311+G(2d,p)-IEFPCM(DMF) Energy = -369.995744353



N	0.03783	-0.21075	-0.17504	H	4.02567	0.02036	1.09171
C	-0.45958	1.06008	0.36210	H	4.62966	0.63623	-0.45199
C	-1.85154	1.38680	-0.18197	H	4.08934	-1.04341	-0.31922
H	0.23708	1.85720	0.09054	C	-2.27126	-1.07899	-0.36542
H	-0.49648	1.02826	1.47094	H	-0.92275	-1.42657	1.29072
C	1.40555	-0.49561	0.26216	H	-0.44915	-2.23946	-0.20977
C	-0.86474	-1.30763	0.18899	C	-2.83829	0.25659	0.12613
C	2.46232	0.40726	-0.37747	H	-1.78056	1.52727	-1.26778
H	1.62760	-1.53352	-0.01438	H	-2.19584	2.33438	0.24729
H	1.49513	-0.44301	1.36629	H	-3.81442	0.45664	-0.32957
C	3.88173	-0.01787	0.00613	H	-2.99785	0.20301	1.21191
H	2.30727	1.44970	-0.07767	H	-2.91940	-1.91164	-0.06989
H	2.33661	0.37228	-1.46621	H	-2.22181	-1.07624	-1.46148

335 – Bisamine complex

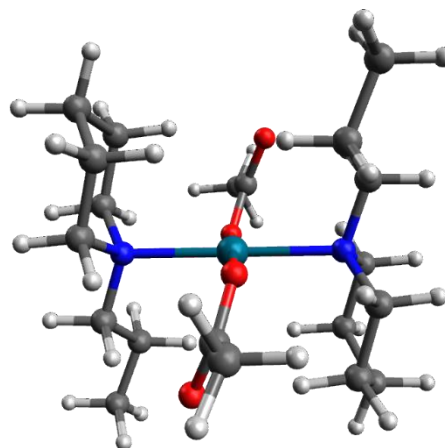
Geometry optimisation:

B3LYP-D3BJ/631G(d,p)/LANL2DZ-IEFPCM(DMF) Energy = -1323.67811778

Thermal correction to Gibbs Free Energy = 0.523247

Single-point energy calculation:

B3LYP-D3BJ/6311+G(2d,p)/SDD-IEFPCM(DMF) Energy = -1325.19342190



Pd	0.00000	0.00000	0.00000	H	-0.99205	1.02060	-2.36238
O	-0.40696	-1.34129	-1.51545	H	-3.57492	2.45312	-3.24099
N	2.16203	-0.39077	-0.12172	H	-2.17668	2.12303	-4.27344
O	0.40695	1.34130	1.51545	H	-2.02905	3.25065	-2.91775
N	-2.16204	0.39077	0.12172	C	-2.29442	-0.06338	2.59095
C	2.55584	-0.92620	-1.46289	H	-3.63069	1.15678	1.41514
C	2.29442	0.06338	-2.59095	H	-2.02469	1.86136	1.61738
H	2.02468	-1.86137	-1.61736	C	2.07687	-1.15264	2.32748
H	3.63069	-1.15679	-1.41513	C	2.71866	1.91032	-0.95138
C	2.50256	-1.43969	0.89118	H	4.01264	0.56449	0.14997
C	2.95125	0.85394	0.12690	H	2.67731	1.23556	1.10643
C	-2.95125	-0.85394	-0.12690	C	2.48858	-2.31024	3.24175
C	-2.71866	-1.91033	0.95137	H	0.99208	-1.02053	2.36241
H	-2.67731	-1.23555	-1.10643	H	2.51634	-0.21909	2.69040
H	-4.01264	-0.56449	-0.14997	H	2.02900	-3.25062	2.91777
C	-2.50257	1.43969	-0.89117	H	2.17671	-2.12302	4.27346
C	-2.55585	0.92619	1.46289	H	3.57491	-2.45317	3.24098
C	0.28915	2.62567	1.35537	H	2.00891	-2.35151	0.55340
O	-0.11707	3.19987	0.33710	H	3.59145	-1.59377	0.85191
C	0.72455	3.41117	2.58552	C	3.04637	1.37476	-2.34770
H	0.49512	4.47047	2.46436	H	1.67625	2.23896	-0.91034
H	1.80277	3.28966	2.73284	H	3.33859	2.78149	-0.71156
H	0.22818	3.02071	3.47807	H	4.12660	1.19358	-2.42870
C	-0.28915	-2.62567	-1.35538	H	2.78836	2.11537	-3.11215
C	-0.72455	-3.41116	-2.58554	H	1.21742	0.24341	-2.66218
H	-1.80277	-3.28962	-2.73287	H	2.60771	-0.39992	-3.53305
H	-0.49514	-4.47046	-2.46438	C	-3.04636	-1.37478	2.34770
H	-0.22816	-3.02070	-3.47808	H	-1.67623	-2.23896	0.91033
O	0.11707	-3.19988	-0.33712	H	-3.33859	-2.78150	0.71155
C	-2.07685	1.15265	-2.32746	H	-2.78836	-2.11538	3.11214
H	-2.00894	2.35152	-0.55337	H	-4.12660	-1.19360	2.42869
H	-3.59145	1.59375	-0.85192	H	-2.60771	0.39991	3.53305
C	-2.48859	2.31024	-3.24174	H	-1.21742	-0.24342	2.66219
H	-2.51627	0.21908	-2.69039				

336 – Monoamine complex

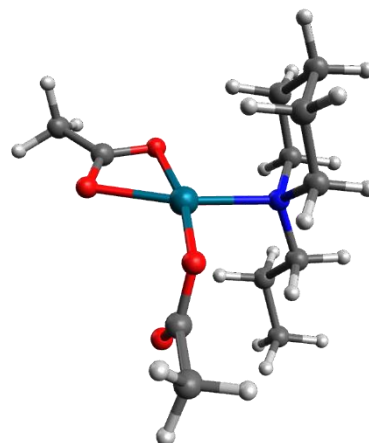
Geometry optimisation:

B3LYP-D3BJ/631G(d,p)/LANL2DZ-IEFPCM(DMF) Energy = -953.728100582

Thermal correction to Gibbs Free Energy = 0.289342

Single-point energy calculation:

B3LYP-D3BJ/6311+G(2d,p)/SDD-IEFPCM(DMF) Energy = -955.156305780



Pd	0.28571	-0.53036	-0.22618	C	-1.46612	0.65441	2.27280
O	2.04792	-0.98969	0.86056	C	-2.88733	0.60897	2.84035
O	1.11225	-2.49492	-0.42849	H	-0.77391	1.03817	3.02906
C	2.05465	-2.17433	0.37143	H	-1.15078	-0.36114	2.01418
C	3.15550	-3.13362	0.70292	H	-3.26195	1.61269	3.06943
H	3.53209	-2.94306	1.70933	H	-2.91936	0.02122	3.76210
H	3.97796	-2.98626	-0.00536	H	-3.56849	0.14548	2.11963
H	2.80219	-4.16201	0.61380	C	2.28596	2.16041	0.27501
N	-0.14336	1.47473	0.24833	H	1.12145	1.38340	1.92689
C	-1.42610	1.52069	1.01778	H	0.66039	3.01964	1.42477
C	-0.32376	2.27395	-1.00624	C	0.95251	2.35716	-1.83462
O	-1.32629	-0.50311	-1.45499	H	-0.64304	3.28209	-0.70801
C	-2.37784	-1.14589	-1.01207	H	-1.13112	1.80185	-1.56490
C	-3.55536	-1.07579	-1.97187	C	2.09672	2.96006	-1.01605
O	-2.44842	-1.72978	0.07162	H	2.66643	1.16090	0.04490
C	0.98278	2.03325	1.06287	H	3.02137	2.63979	0.92973
H	-3.94036	-0.05112	-1.99643	H	3.02438	2.96860	-1.59706
H	-4.34821	-1.74930	-1.64488	H	1.85868	4.00433	-0.77434
H	-3.24038	-1.33176	-2.98653	H	0.74194	2.96003	-2.72403
H	-2.20776	1.20034	0.32738	H	1.22647	1.35323	-2.18255
H	-1.62058	2.57066	1.27539				

337 – Bidentate ligand-amine complex

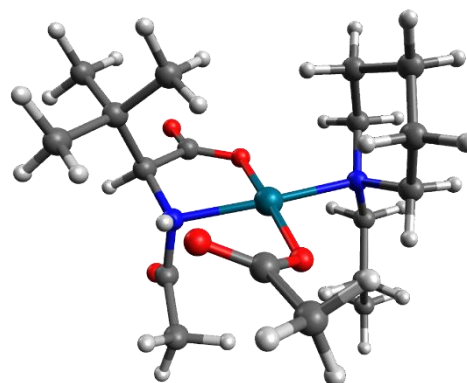
Geometry optimisation:

B3LYP-D3BJ/631G(d,p)/LANL2DZ-IEFPCM(DMF) Energy = -1319.07145791

Thermal correction to Gibbs Free Energy = 0.449159

Single-point energy calculation:

B3LYP-D3BJ/6311+G(2d,p)/SDD-IEFPCM(DMF) Energy = -1320.59932117



Pd	-0.30083	0.11765	-0.15688	H	-1.74874	2.93843	3.21553
O	0.52457	-0.93100	-1.67187	H	-0.45944	2.45486	4.35890
N	1.64573	0.96047	-0.10260	C	-2.00331	-2.25332	-0.82010
O	-1.07582	1.23174	1.38769	C	-2.78060	-0.12097	-1.66280
N	-2.19710	-0.80933	-0.46778	C	-3.11105	-0.69498	0.70993
C	1.83249	-0.87279	-1.75848	C	-2.62526	-1.50137	1.91116
O	2.45862	-1.45307	-2.63965	H	-4.09949	-1.05163	0.38663
C	2.57465	-0.04826	-0.68885	H	-3.18679	0.35648	0.97460
C	3.26355	-0.91056	0.41274	H	1.48607	3.44501	0.93136
C	2.26002	-1.80581	1.15843	H	-0.06679	3.21151	0.13563
C	3.97017	0.02491	1.41458	H	1.14996	4.27192	-0.62328
C	4.33226	-1.79303	-0.25773	C	-3.02802	1.37711	-1.50187
H	3.89142	-2.48196	-0.97934	H	-1.31851	-2.28863	-1.66623
H	4.85499	-2.37333	0.50875	H	-2.97944	-2.64351	-1.14054
H	5.07298	-1.18197	-0.78416	C	-1.47596	-3.07680	0.34826
H	1.49778	-1.21864	1.67903	C	-2.40526	-2.97400	1.55956
H	2.78685	-2.40540	1.90751	H	-0.47434	-2.72626	0.61675
H	1.75775	-2.49354	0.47195	H	-1.37412	-4.11451	0.01361
H	3.26671	0.59168	2.02991	H	-1.98516	-3.51349	2.41456
H	4.62845	0.73091	0.89713	H	-3.36821	-3.44546	1.32285
H	4.58512	-0.57093	2.09593	H	-3.36697	-1.39297	2.70965
C	1.55613	2.19601	-0.82195	H	-1.69255	-1.06298	2.27886
H	3.35864	0.49890	-1.21707	C	-3.47239	1.99274	-2.83171
C	1.00127	3.36133	-0.04431	H	-2.11183	1.86624	-1.15478
O	1.90981	2.25328	-1.98418	H	-3.79375	1.55787	-0.74122
H	1.68142	1.09364	0.92533	H	-2.70118	1.86903	-3.59965
C	-0.34523	1.51334	2.42159	H	-3.66616	3.06299	-2.71832
O	0.88365	1.33074	2.51452	H	-4.39070	1.52290	-3.20023
C	-1.13170	2.11013	3.57312	H	-2.08263	-0.29541	-2.48618
H	-1.80717	1.34966	3.97771	H	-3.72346	-0.62685	-1.91376

TS₂₁ – Acetate-assisted C–H activation with equatorial binding

Geometry optimisation:

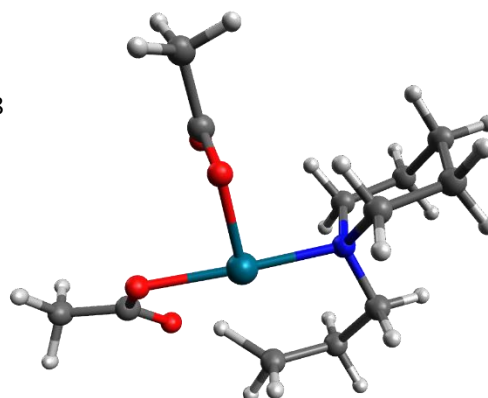
B3LYP-D3BJ/631G(d,p)/LANL2DZ-IEFPCM(DMF) Energy = -953.685235968

Thermal correction to Gibbs Free Energy = 0.287919

Imaginary frequency = -1345.0032

Single-point energy calculation:

B3LYP-D3BJ/6311+G(2d,p)/SDD-IEFPCM(DMF) Energy = -955.114906219



O	0.58753	2.25270	1.32950	H	0.79619	-2.47381	-1.39814
C	0.29889	2.58332	0.17241	C	-3.27471	-0.25409	1.59168
O	2.61594	0.25721	-0.60244	C	-3.79647	0.01576	-0.85333
Pd	0.58528	-0.21889	-0.43388	H	5.02350	0.87006	-0.23318
O	0.16749	1.76959	-0.83429	H	5.39833	-0.82010	0.21147
N	-1.46285	-0.64564	-0.14311	H	4.94264	0.33029	1.46817
C	-1.65482	-2.12343	-0.30155	C	-4.11283	0.51121	0.56192
C	-0.49851	-2.89214	0.31216	H	-1.42216	0.84175	1.33103
C	0.82229	-2.43572	-0.30251	H	-1.19114	-0.78827	1.94326
C	-1.78244	-0.18505	1.25231	H	-1.96285	1.14844	-1.08566
C	-2.29496	0.11083	-1.13359	H	-2.04341	-0.27419	-2.12454
C	3.31937	-0.34871	0.26397	H	-3.40590	0.16732	2.59387
C	4.76450	0.04429	0.42805	H	-3.60953	-1.29605	1.64828
O	2.85695	-1.28304	0.99694	H	-4.14696	-1.01504	-0.98112
H	1.71109	-1.62107	0.43087	H	-4.31736	0.61943	-1.60399
C	0.01283	4.03635	-0.18594	H	-5.18023	0.40309	0.77961
H	-1.69003	-2.31942	-1.37678	H	-3.87773	1.58177	0.62839
H	-2.61449	-2.42784	0.12319	H	-1.05804	4.15433	-0.38311
H	-0.66573	-3.96134	0.13009	H	0.54578	4.32165	-1.09650
H	-0.48346	-2.76591	1.40016	H	0.29808	4.69509	0.63541
H	1.62823	-3.12907	-0.03151				

TS₂₂ – Acetate-assisted C–H activation with axial binding

Geometry optimisation:

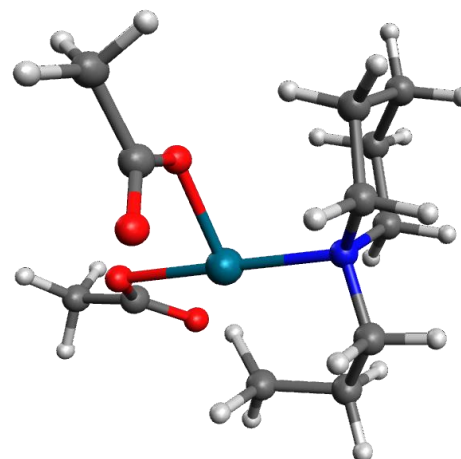
B3LYP-D3BJ/631G(d,p)/LANL2DZ-IEFPCM(DMF) Energy = -953.682186473

Thermal correction to Gibbs Free Energy = 0.288701

Imaginary frequency = -1359.2072

Single-point energy calculation:

B3LYP-D3BJ/6311+G(2d,p)/SDD-IEFPCM(DMF) Energy = -955.111293784



O	2.41321	2.21993	-1.82407	H	4.52030	-1.13999	-2.08688
C	2.32552	2.54819	-0.63265	C	1.08170	-1.11260	2.11764
O	5.34628	0.93447	0.11731	H	2.46371	-2.44101	1.11375
Pd	3.49631	-0.00512	-0.18377	H	0.76270	-2.70594	0.70070
O	2.65071	1.79946	0.37991	C	-0.11148	0.44973	0.59094
N	1.68456	-1.11483	-0.33070	H	-0.32153	-1.05382	-0.94093
C	1.91373	-2.02540	-1.49884	H	0.66210	0.34074	-1.43600
C	3.23817	-2.75814	-1.37887	H	7.51150	1.80859	1.03760
C	4.39387	-1.77778	-1.20460	H	8.30036	0.25332	0.65021
C	1.51939	-1.93635	0.91355	H	7.59352	0.49533	2.24800
C	0.43444	-0.32932	-0.60575	H	0.69957	3.76469	0.05265
C	6.17244	0.15838	0.69231	H	1.79595	4.59638	-1.06883
C	7.47543	0.73037	1.18705	H	2.27521	4.31110	0.63316
O	5.95273	-1.08647	0.85665	C	-0.25580	-0.42733	1.83552
H	4.93426	-1.35066	0.04392	H	-1.07686	0.87168	0.29096
C	1.74950	3.89916	-0.23086	H	0.55919	1.27707	0.81989
H	1.91350	-1.39515	-2.39256	H	1.84886	-0.36490	2.35047
H	1.06853	-2.72168	-1.57298	H	1.01174	-1.78588	2.97827
H	3.38228	-3.35228	-2.28973	H	-1.02933	-1.19104	1.67844
H	3.21112	-3.47466	-0.55286	H	-0.57048	0.17846	2.69134
H	5.33677	-2.33368	-1.13137				

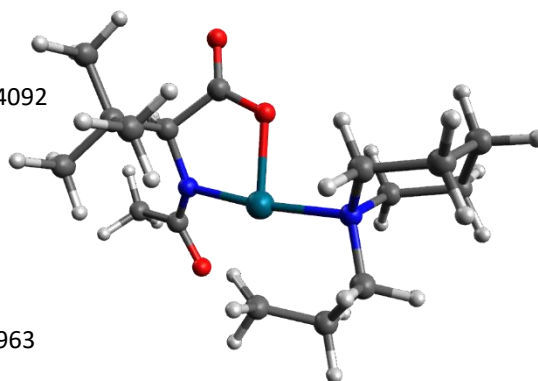
TS₂₃ – Ligand-assisted C–H activation with equatorial binding

Geometry optimisation:

B3LYP-D3BJ/631G(d,p)/LANL2DZ-IEFPCM(DMF) Energy = -1089.88874092

Thermal correction to Gibbs Free Energy = 0.392493

Imaginary frequency = -1325.8891



Single-point energy calculation:

B3LYP-D3BJ/6311+G(2d,p)/SDD-IEFPCM(DMF) Energy = -1091.34427963

O	1.74930	-2.69738	-1.62722	H	2.53421	-1.75995	2.79169
C	1.38581	-1.67471	-1.04762	H	1.37714	-2.25743	1.54744
C	2.42139	-0.64487	-0.54179	H	1.42082	-0.57356	2.09031
H	3.20938	-0.58320	-1.29845	H	-2.76009	0.95356	2.08154
C	3.09488	-1.12320	0.79492	H	-3.98226	1.26994	0.84930
C	3.94351	-2.37444	0.51257	C	-4.31484	-0.44143	-1.22801
C	4.01590	-0.00923	1.31828	C	-3.95126	-1.70787	0.91776
C	2.04000	-1.44742	1.86598	H	3.43059	2.78208	-2.18046
N	1.73617	0.63401	-0.40178	H	4.04504	1.19236	-1.66448
Pd	-0.22522	0.44829	0.00832	H	4.12941	2.58197	-0.57036
O	0.12815	-1.41121	-0.79532	H	-0.50294	1.95679	1.98301
N	-2.30976	0.08272	0.23378	H	-0.27052	3.41328	1.08148
C	-2.90560	1.20116	1.02617	H	0.26041	2.39033	0.02698
C	-2.20351	2.51573	0.72126	H	-2.65978	3.29435	1.34567
C	-0.70224	2.40766	1.00376	H	-2.38106	2.81336	-0.31829
C	-2.85475	0.01892	-1.16143	C	-4.50332	-1.78327	-0.51060
C	-2.49397	-1.24061	0.90618	H	-2.09021	-1.15008	1.91735
C	2.14912	1.82415	-0.78132	H	-1.87205	-1.95250	0.35807
C	3.52474	2.09235	-1.33952	H	-4.56160	-1.02767	1.52392
O	1.36688	2.83426	-0.66140	H	-3.99396	-2.68782	1.40468
H	4.44393	-2.69760	1.43135	H	-5.56051	-2.06756	-0.50178
H	4.71631	-2.16294	-0.23493	H	-3.96513	-2.56578	-1.06194
H	3.33148	-3.19675	0.13869	H	-2.72677	1.00372	-1.61566
H	4.51510	-0.34155	2.23418	H	-2.21795	-0.68535	-1.70342
H	3.45400	0.89895	1.55244	H	-4.59511	-0.51986	-2.28374
H	4.79228	0.24252	0.58868	H	-4.97463	0.31497	-0.78778

TS₂₄ – Ligand-assisted C–H activation with axial binding

Geometry optimisation:

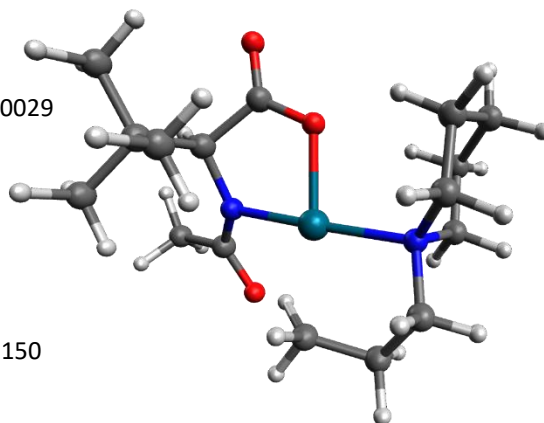
B3LYP-D3BJ/631G(d,p)/LANL2DZ-IEFPCM(DMF) Energy = -1089.88840029

Thermal correction to Gibbs Free Energy = 0.392120

Imaginary frequency = -1319.7876

Single-point energy calculation:

B3LYP-D3BJ/6311+G(2d,p)/SDD-IEFPCM(DMF) Energy = -1091.34317150



O	4.01567	-2.65165	-1.17871	H	4.88366	-0.99891	2.98563
C	3.61143	-1.56229	-0.77304	H	3.72766	-1.74839	1.87384
C	4.59785	-0.41551	-0.47040	H	3.67066	-0.00338	2.16470
H	5.35790	-0.42980	-1.25695	H	-0.28617	1.35718	2.32052
C	5.33947	-0.63055	0.89668	H	-1.69575	1.65685	1.29229
C	6.27096	-1.84836	0.77608	C	-0.71173	-0.82221	-1.67539
C	6.18658	0.61458	1.20502	H	-0.61376	1.32712	-1.37649
C	4.34187	-0.85902	2.04449	H	-2.00975	0.54252	-0.61930
N	3.83698	0.82507	-0.51108	H	0.01735	-0.85550	2.13514
Pd	1.91143	0.62226	0.04292	C	-0.43341	-2.13582	0.44032
O	2.34650	-1.31394	-0.55204	H	-1.64205	-0.71535	1.53033
N	-0.20579	0.39233	0.46583	H	5.30194	2.71653	-2.74362
C	-0.60156	1.57172	1.29514	H	6.02671	1.25878	-2.02264
C	0.07167	2.85116	0.83258	H	6.09446	2.80693	-1.16683
C	1.58894	2.69253	0.88109	H	1.92620	2.30088	1.84774
C	-0.93678	0.43364	-0.83929	H	2.07277	3.67445	0.81229
C	-0.59097	-0.83873	1.22751	H	2.33603	2.56373	-0.25553
C	4.14918	1.94155	-1.13504	H	-0.25370	3.66139	1.49705
C	5.47694	2.17507	-1.81230	H	-0.25949	3.12834	-0.17381
O	3.31148	2.91291	-1.15637	C	-1.16106	-2.06790	-0.90608
H	6.81526	-1.99326	1.71510	H	0.34866	-0.90892	-1.93085
H	7.00840	-1.70024	-0.02073	H	-1.27261	-0.71222	-2.60964
H	5.71108	-2.75734	0.55074	H	-0.83163	-2.94798	1.05861
H	6.73735	0.46671	2.13953	H	0.62657	-2.32803	0.26930
H	5.56265	1.50524	1.31886	H	-0.96211	-2.97236	-1.49029
H	6.91877	0.80449	0.41343	H	-2.24667	-2.02276	-0.74323

TS₂₅ – Acetate-assisted β -H elimination on the heterocycle

Geometry optimisation:

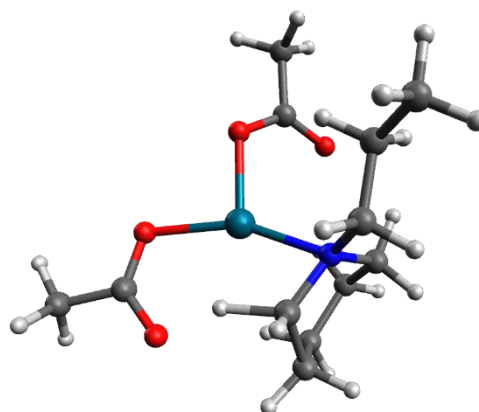
B3LYP-D3BJ/631G(d,p)/LANL2DZ-IEFPCM(DMF) Energy = -953.681966304

Thermal correction to Gibbs Free Energy = 0.283031

Imaginary frequency = -1082.6931

Single-point energy calculation:

B3LYP-D3BJ/6311+G(2d,p)/SDD-IEFPCM(DMF) Energy = -955.114688428



O	-1.95930	0.99008	1.80240	H	-2.08341	-1.39888	1.30705
C	-1.76946	1.95613	1.05276	C	1.27460	-2.21885	1.82565
O	2.06230	1.63759	-0.33665	H	2.39074	-2.85271	0.06712
Pd	0.35888	0.39665	-0.19029	H	0.85247	-3.68438	0.27013
O	-0.83837	2.04769	0.15074	H	1.98429	-1.39355	1.94405
N	-0.67981	-1.38480	-0.23393	H	1.60024	-3.01826	2.49654
C	-1.68505	-1.49526	-1.32869	H	-0.53609	-2.26851	3.06360
C	0.68304	-1.74058	-0.57951	H	-0.14880	-0.67026	2.44292
C	-1.16447	-1.92740	1.06640	C	-3.84314	-0.69368	-2.34213
C	3.09423	0.92910	-0.58961	H	-2.06462	-2.52504	-1.32667
C	4.42120	1.64291	-0.71179	H	-1.15279	-1.33604	-2.26942
O	3.07704	-0.32929	-0.74547	H	-2.41376	0.51808	-1.24908
H	1.68950	-0.76946	-0.59671	H	-3.32802	-0.59314	-0.24370
H	4.31318	2.71228	-0.53433	H	-3.37195	-0.57292	-3.32370
H	4.82898	1.47361	-1.71234	H	-4.65308	0.03730	-2.26803
H	5.12685	1.21599	0.00604	H	-4.28890	-1.69345	-2.30537
C	-2.83010	-0.49305	-1.21212	C	-2.68781	3.17221	1.09942
C	1.35309	-2.71367	0.37841	H	-3.23420	3.20040	2.04346
H	0.76129	-2.02105	-1.63016	H	-3.41078	3.10112	0.27905
C	-0.15156	-1.73284	2.19049	H	-2.12354	4.09752	0.96289
H	-1.38826	-2.98940	0.90370				

TS₂₆ – Acetate-assisted β–H elimination on the propyl substituent

Geometry optimisation:

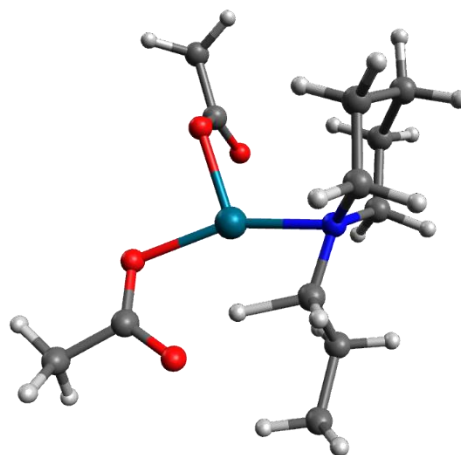
B3LYP-D3BJ/631G(d,p)/LANL2DZ-IEFPCM(DMF) Energy = -953.682590499

Thermal correction to Gibbs Free Energy = 0.284360

Imaginary frequency = -1169.2647

Single-point energy calculation:

B3LYP-D3BJ/6311+G(2d,p)/SDD-IEFPCM(DMF) Energy = -955.115519718



O	-1.41811	1.83933	1.79946	H	1.12172	-1.76417	2.05572
C	-1.63184	2.30672	0.67111	C	2.72240	-2.88360	1.12777
O	1.92785	1.70583	-0.20499	H	2.87836	-3.56936	0.28825
Pd	0.30345	0.36323	-0.18856	H	3.00094	-3.40784	2.04577
O	-1.05472	1.91695	-0.42302	H	3.39075	-2.03066	0.99738
N	-0.63680	-1.46401	-0.19724	C	-2.89262	-1.10376	0.79765
C	-1.25446	-1.79717	-1.51467	H	-1.05408	-1.50051	1.86452
C	0.77782	-1.77541	-0.07943	H	-1.66522	-2.89084	0.94422
C	-1.54128	-1.79983	0.93876	H	1.11494	-2.30338	-0.97506
C	3.01365	1.05817	-0.37542	C	-3.54188	-1.37515	-0.56285
C	4.30332	1.84369	-0.41948	H	-2.74526	-0.03213	0.95054
O	3.07696	-0.20389	-0.49409	H	-3.53295	-1.46025	1.61119
C	1.25913	-2.43971	1.20657	H	-2.98645	-1.30494	-2.66998
H	1.73997	-0.74576	-0.28586	H	-2.35428	0.03515	-1.70023
H	4.11175	2.91551	-0.45674	H	-3.82835	-2.43288	-0.63078
H	4.89254	1.53515	-1.28618	H	-4.45983	-0.78792	-0.66490
H	4.88751	1.61001	0.47599	C	-2.67147	3.40072	0.45894
H	-0.53136	-1.54096	-2.29091	H	-3.54874	2.96935	-0.03507
C	-2.56566	-1.04008	-1.69495	H	-2.28121	4.18526	-0.19409
H	-1.42178	-2.88212	-1.53720	H	-2.97743	3.82797	1.41482
H	0.62879	-3.31839	1.38990				

TS₂₇ – Ligand-assisted β -H elimination on the heterocycle

Geometry optimisation:

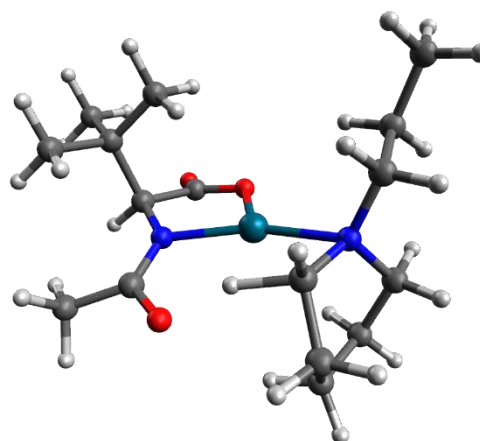
B3LYP-D3BJ/631G(d,p)/LANL2DZ-IEFPCM(DMF) Energy = -1089.87564087

Thermal correction to Gibbs Free Energy = 0.387778

Imaginary frequency = -1138.6981

Single-point energy calculation:

B3LYP-D3BJ/6311+G(2d,p)/SDD-IEFPCM(DMF) Energy = -1091.33454353



O	2.54148	1.19283	2.60819	H	1.46664	1.42897	-1.53000
C	1.85805	0.78428	1.66861	H	-0.73553	-1.47757	-0.91710
C	2.49120	-0.11024	0.57224	H	2.30666	-3.97194	-0.20549
H	3.22258	-0.76559	1.05783	H	3.42501	-2.61191	0.05939
C	3.26477	0.78173	-0.47179	H	2.97404	-3.09733	-1.58571
C	4.47189	1.43704	0.22071	C	-2.55005	2.72361	-0.26156
C	3.78016	-0.09465	-1.62420	C	-2.75262	-2.24119	-0.67827
C	2.34758	1.87086	-1.05409	H	-2.03089	-0.72110	-2.09925
N	1.41011	-0.87561	-0.02418	C	-3.00821	-1.28295	1.67499
Pd	-0.40674	-0.04974	0.12075	H	-4.41028	-0.26631	0.35322
O	0.60159	1.11237	1.50698	H	-3.52432	0.80453	1.44494
N	-2.45558	0.21008	-0.24926	C	-2.66493	-2.53356	0.82318
C	-2.78700	1.42788	-1.03365	H	-2.31885	-3.05848	-1.25819
C	-2.02901	-0.94844	-1.03334	H	-3.79751	-2.13858	-0.99722
C	-3.43550	-0.08804	0.82600	H	-1.64499	-2.86127	1.04581
C	1.39637	-2.08653	-0.55234	H	-3.33089	-3.36536	1.06767
C	2.61038	-2.98463	-0.56078	H	-3.82213	-1.49473	2.37422
O	0.32075	-2.55719	-1.06381	H	-2.14326	-0.98813	2.27689
H	5.03295	2.03747	-0.50308	C	-2.81858	3.94583	-1.14374
H	5.15051	0.67774	0.62535	H	-3.83235	1.35529	-1.36288
H	4.16098	2.08174	1.04426	H	-2.15381	1.41594	-1.92414
H	4.34089	0.52397	-2.33241	H	-1.51399	2.73545	0.09555
H	2.95920	-0.56421	-2.17236	H	-3.19371	2.76404	0.62322
H	4.45272	-0.87899	-1.26412	H	-2.16200	3.95141	-2.02051
H	2.89042	2.44835	-1.80953	H	-2.64364	4.87079	-0.58747
H	2.00063	2.56322	-0.28227	H	-3.85414	3.95944	-1.50003

TS₂₈ – Ligand-assisted β -H elimination on the propyl substituent

Geometry optimisation:

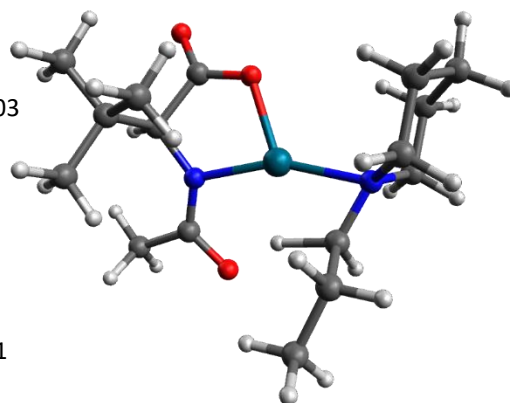
B3LYP-D3BJ/631G(d,p)/LANL2DZ-IEFPCM(DMF) Energy = -1089.87886303

Thermal correction to Gibbs Free Energy = 0.390159

Imaginary frequency = -1195.4260

Single-point energy calculation:

B3LYP-D3BJ/6311+G(2d,p)/SDD-IEFPCM(DMF) Energy = -1091.33765931



O	2.28998	-2.93643	-1.07254	H	1.32109	-0.14043	2.05650
C	1.68732	-1.92553	-0.70870	H	-0.54575	1.74697	-0.53112
C	2.45852	-0.60194	-0.46742	H	2.77065	2.71257	-2.59452
H	3.25179	-0.53942	-1.22036	H	3.70091	1.43373	-1.77526
C	3.14463	-0.61648	0.94979	H	3.35312	2.96157	-0.94662
C	4.23428	-1.70170	0.97363	H	-2.32557	0.02281	2.13967
C	3.80390	0.74611	1.21573	C	-3.15089	-1.77801	1.26567
C	2.11603	-0.89279	2.05968	H	-3.97611	0.21840	1.51731
N	1.49981	0.47827	-0.61933	C	-3.48829	-1.59945	-1.22193
Pd	-0.40699	-0.01416	-0.25853	H	-2.87568	0.33608	-1.99703
O	0.40262	-1.91197	-0.46317	H	-4.30642	0.39532	-0.94434
N	-2.45830	0.25501	0.05424	C	-1.85777	2.41662	1.28673
C	-3.00339	-0.25905	1.33587	C	-1.29536	3.82213	1.05753
C	-1.86098	1.58492	0.00953	H	-1.33219	4.39751	1.98633
C	-3.33153	-0.08700	-1.09992	H	-1.88003	4.36027	0.30384
C	1.63892	1.69578	-1.11019	H	-0.26033	3.78005	0.71156
C	2.95400	2.21550	-1.63952	H	-1.27876	1.91352	2.06599
O	0.63364	2.48896	-1.16190	H	-2.89087	2.49075	1.64891
H	4.74025	-1.69744	1.94481	H	-2.26711	2.14021	-0.84037
H	4.98860	-1.51618	0.20080	C	-4.02490	-2.20284	0.08079
H	3.81537	-2.69442	0.80152	H	-3.57689	-2.12707	2.21156
H	4.30334	0.72943	2.18989	H	-2.15236	-2.22121	1.17106
H	3.06660	1.55308	1.23373	H	-5.05419	-1.85798	0.24500
H	4.55885	0.98156	0.45931	H	-4.06096	-3.29423	0.00799
H	2.60799	-0.86441	3.03749	H	-2.51138	-2.03563	-1.46190
H	1.64929	-1.87482	1.94311	H	-4.15916	-1.81421	-2.05976

III.III. Nuclear coordinates for complexes containing 1-propylpyrrolidine

331 – 1-propylpyrrolidine

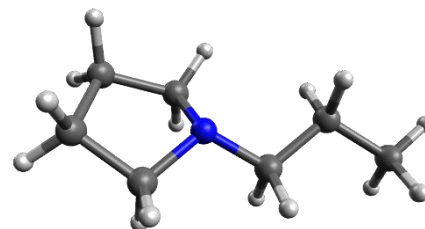
Geometry optimisation:

B3LYP-D3BJ/631G(d,p)/LANL2DZ-IEFPCM(DMF) Energy = -330.578787318

Thermal correction to Gibbs Free Energy = 0.176270

Single-point energy calculation:

B3LYP-D3BJ/6311+G(2d,p)-IEFPCM(DMF) Energy = -330.658289978



N	0.27119	-0.19734	-0.26447	H	1.11419	-2.12926	-0.45109
C	0.79870	1.05321	0.29163	C	-1.07250	-0.53719	0.18427
C	2.30569	0.99803	-0.02416	C	-2.14412	0.42218	-0.33469
H	0.63744	1.09705	1.38707	H	-1.12302	-0.57851	1.29246
H	0.30275	1.92267	-0.14800	H	-1.29829	-1.54934	-0.17483
C	2.61084	-0.51680	-0.19287	C	-3.55424	-0.02269	0.05868
H	2.89305	1.45630	0.77546	H	-2.05679	0.48634	-1.42602
H	2.52920	1.54174	-0.94590	H	-1.95951	1.43051	0.05387
C	1.26992	-1.20197	0.10995	H	-3.78506	-1.01255	-0.35068
H	3.40215	-0.86533	0.47545	H	-4.30975	0.67676	-0.31166
H	2.92626	-0.73185	-1.21751	H	-3.66011	-0.08201	1.14768
H	1.20343	-1.44981	1.18798				

338 – Bisamine complex

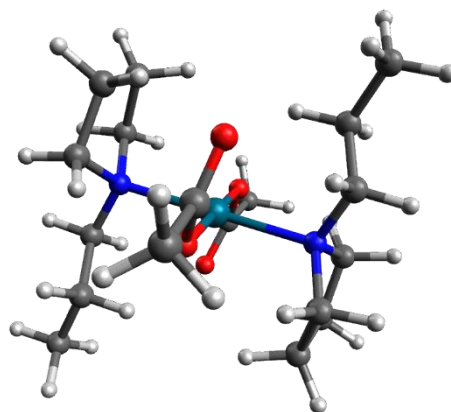
Geometry optimisation:

B3LYP-D3BJ/631G(d,p)/LANL2DZ-IEFPCM(DMF) Energy = -1245.02327889

Thermal correction to Gibbs Free Energy = 0.467986

Single-point energy calculation:

B3LYP-D3BJ/6311+G(2d,p)/SDD-IEFPCM (DMF) Energy = -1246.52087026



Pd	0.00810	0.01561	-0.01415	H	1.89827	0.11198	2.00283
O	-0.05566	-1.53979	1.34840	H	4.93756	0.61968	2.10672
N	-2.00477	0.61970	0.62143	H	3.84924	0.62667	3.50126
O	0.06314	1.59074	-1.35200	H	3.68720	1.86434	2.24628
N	2.01688	-0.60199	-0.64119	C	1.40741	-1.47207	-2.77735
C	-2.11052	0.50923	2.10821	H	3.26963	-0.43801	-2.32773
C	-1.36565	1.73843	2.62497	H	1.85647	0.64904	-2.35861
H	-1.69445	-0.43906	2.43966	C	-2.90119	-0.23516	-1.58126
H	-3.17527	0.55607	2.37569	C	-1.61637	2.82104	1.54234
C	-2.99078	-0.26224	-0.05885	H	-3.38523	2.19127	0.42665
C	-2.29495	2.06828	0.38353	H	-1.94785	2.35957	-0.60328
C	2.22068	-2.08017	-0.55316	C	-3.89997	-1.21344	-2.20322
C	3.01320	0.15541	0.16328	H	-1.88349	-0.50790	-1.87907
C	2.19768	-0.35020	-2.10358	H	-3.08389	0.77767	-1.95647
C	0.69872	2.68664	-1.05026	H	-3.69563	-2.23673	-1.87149
O	1.33632	2.89089	-0.00976	H	-3.83954	-1.19423	-3.29534
C	0.56346	3.76613	-2.11495	H	-4.92956	-0.96724	-1.92052
H	1.32255	4.53654	-1.97263	H	-2.81180	-1.27924	0.28832
H	-0.42634	4.22808	-2.02825	H	-3.99573	0.04743	0.26502
H	0.64075	3.33953	-3.11766	H	-0.29659	1.52105	2.70468
C	-0.67965	-2.65217	1.08462	H	-1.72221	2.03290	3.61458
C	-0.66732	-3.62791	2.25383	H	-2.27011	3.61783	1.90516
H	0.32474	-3.67516	2.70940	H	-0.67685	3.26924	1.22184
H	-0.97754	-4.62025	1.92390	C	1.49310	-2.65691	-1.77753
H	-1.36459	-3.27572	3.02191	H	1.85855	-2.45198	0.40042
O	-1.25762	-2.92722	0.02640	H	3.30219	-2.26372	-0.61665
C	2.92017	-0.08865	1.66688	H	1.82174	-1.71108	-3.75942
H	2.84886	1.21343	-0.04322	H	0.36771	-1.16380	-2.91903
H	4.01500	-0.12351	-0.19721	H	0.49776	-2.99994	-1.49657
C	3.90526	0.80564	2.42352	H	2.04936	-3.50409	-2.18598
H	3.12276	-1.14098	1.89378				

339 – Monoamine complex

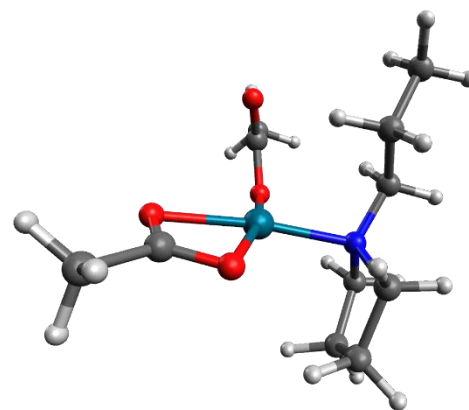
Geometry optimisation:

B3LYP-D3BJ/631G(d,p)/LANL2DZ-IEFPCM(DMF) Energy = -914.400153699

Thermal correction to Gibbs Free Energy = 0.260318

Single-point energy calculation:

B3LYP-D3BJ/6311+G(2d,p)/SDD-IEFPCM(DMF) Energy = -915.820005834



Pd	0.47258	-0.32861	-0.21213	H	-2.45885	0.68726	0.06870
O	2.29137	0.00728	0.80911	H	-2.29817	2.30491	0.76700
O	1.89850	-1.93228	-0.13318	C	-1.65642	0.69779	2.07358
C	2.68575	-1.18204	0.53486	C	-3.02074	0.42055	2.70897
C	4.04157	-1.65433	0.96020	H	-1.06828	1.36194	2.71635
H	4.33267	-1.17267	1.89527	H	-1.10611	-0.24293	1.97254
H	4.77014	-1.37797	0.19044	H	-3.61839	1.33462	2.79537
H	4.04815	-2.73982	1.06952	H	-2.90549	-0.00068	3.71162
N	-0.54435	1.49386	-0.05166	H	-3.58401	-0.29804	2.10450
C	-1.82119	1.31807	0.69038	C	1.35151	2.87968	-0.55325
C	-0.77495	2.04550	-1.42208	H	0.87227	2.04969	1.44094
O	-1.07695	-0.98498	-1.34222	H	-0.22143	3.34374	0.90092
C	-1.87135	-1.84880	-0.76175	C	0.60547	2.53088	-1.87186
C	-3.01496	-2.29135	-1.66148	H	-1.47838	2.88297	-1.33063
O	-1.74667	-2.26207	0.39329	H	-1.21966	1.27197	-2.04677
C	0.38192	2.48813	0.57288	H	0.51769	3.38663	-2.54430
H	-3.67122	-1.43876	-1.86291	H	1.12945	1.73600	-2.40883
H	-3.58869	-3.08384	-1.17996	H	2.27656	2.30693	-0.46914
H	-2.62980	-2.64115	-2.62291	H	1.60340	3.93998	-0.48681

340 – Bidentate ligand-amine complex

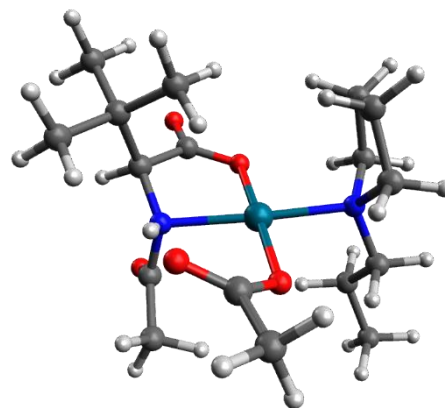
Geometry optimisation:

B3LYP-D3BJ/631G(d,p)/LANL2DZ-IEFPCM(DMF) Energy = -1279.74464415

Thermal correction to Gibbs Free Energy = 0.422035

Single-point energy calculation:

B3LYP-D3BJ/6311+G(2d,p)/SDD-IEFPCM(DMF) Energy = -1281.26383512



Pd	0.40019	0.02017	0.07091	H	1.58081	3.00246	-3.22072
O	-0.38180	-1.59258	1.00655	H	1.90044	3.97228	-1.78259
N	-1.46148	0.85397	0.65054	H	0.41529	4.26166	-2.74050
O	1.15820	1.67919	-0.87799	C	2.15545	-2.40727	-0.18688
N	2.21552	-0.93689	-0.44949	C	3.31625	-0.24772	0.27494
C	-1.66968	-1.53641	1.24872	C	2.40803	-0.86689	-1.93138
O	-2.27259	-2.43820	1.82208	H	3.45215	-1.13198	-2.14315
C	-2.42068	-0.28184	0.76296	H	2.22337	0.14976	-2.27313
C	-3.21883	-0.49597	-0.55921	H	-1.11913	3.50777	0.92930
C	-2.30753	-0.91782	-1.72429	H	0.44466	2.83246	1.37490
C	-3.94917	0.81302	-0.92122	H	-0.63036	3.45457	2.65359
C	-4.27694	-1.58797	-0.31895	H	1.71137	-2.59804	0.78694
H	-3.81915	-2.54628	-0.06981	H	3.18538	-2.78601	-0.19927
H	-4.87999	-1.71194	-1.22362	C	3.18809	-0.30141	1.79484
H	-4.94837	-1.31228	0.50089	C	1.45142	-1.92393	-2.48713
H	-1.56931	-0.14628	-1.96007	C	1.33321	-2.97790	-1.35179
H	-2.91180	-1.08481	-2.62165	H	1.83615	-2.34777	-3.41705
H	-1.77640	-1.84724	-1.49962	H	0.47718	-1.47844	-2.70203
H	-3.26242	1.60845	-1.22204	H	0.29380	-3.10401	-1.04469
H	-4.55219	1.17238	-0.08064	H	1.71872	-3.95496	-1.65049
H	-4.62184	0.63262	-1.76530	C	4.30661	0.49817	2.46755
C	-1.21227	1.56872	1.86495	H	3.31269	0.78917	-0.06897
H	-3.13855	-0.03097	1.54705	H	4.26367	-0.70776	-0.03936
C	-0.59535	2.93388	1.69744	H	3.21706	-1.34123	2.13756
O	-1.48569	1.06609	2.93810	H	2.21247	0.10329	2.08950
H	-1.56245	1.47904	-0.17090	H	5.29286	0.10368	2.20026
C	0.37138	2.47513	-1.53473	H	4.21351	0.45831	3.55636
O	-0.87354	2.43713	-1.52183	H	4.27368	1.55044	2.16477
C	1.10720	3.50474	-2.37081				

TS₂₉ – Acetate-assisted C–H activation with pseudo-equatorial binding

Geometry optimisation:

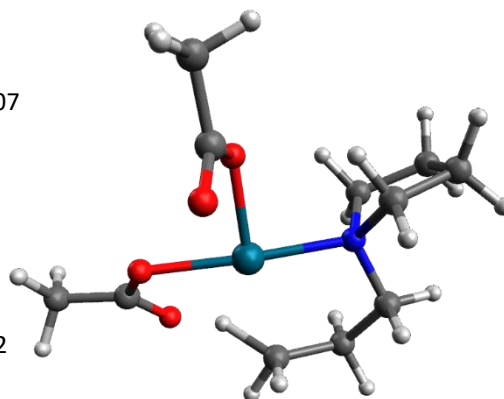
B3LYP-D3BJ/631G(d,p)/LANL2DZ-IEFPCM(DMF) Energy = -914.355926407

Thermal correction to Gibbs Free Energy = 0.258677

Imaginary frequency = -1343.3404

Single-point energy calculation:

B3LYP-D3BJ/6311+G(2d,p)/SDD-IEFPCM(DMF) Energy = -915.778013722



O	0.39598	2.57805	-1.49722	H	-0.66758	-3.16773	0.45279
C	0.11710	2.73754	-0.30403	H	1.40231	-2.91570	-1.07797
O	2.44449	0.36773	-0.05700	H	0.55025	-1.72481	-1.99435
Pd	0.40828	-0.10670	-0.14733	H	4.77719	-0.53732	1.79634
O	-0.01994	1.78195	0.57209	H	4.85741	0.72325	0.53232
N	-1.63117	-0.59150	-0.05416	H	5.21875	-0.98452	0.14846
C	-1.86524	-1.87262	-0.79711	H	-1.19811	4.21614	0.54097
C	-0.70866	-2.83299	-0.58954	H	0.11386	4.89344	-0.45547
C	0.60559	-2.16607	-0.99209	H	0.44020	4.27068	1.18883
C	-2.01731	-0.71592	1.39121	C	-3.92215	0.13762	0.10051
C	-2.56265	0.47821	-0.53319	C	-3.55633	-0.58979	1.42341
C	3.14432	-0.57635	0.42431	H	-1.54735	0.11994	1.91135
C	4.59325	-0.31229	0.74233	H	-1.63098	-1.64851	1.80200
O	2.67667	-1.74115	0.64240	H	-2.55740	0.51155	-1.62293
H	1.52246	-1.76925	-0.00085	H	-2.18065	1.41934	-0.14207
C	-0.14013	4.12344	0.27412	H	-4.50701	-0.51323	-0.55410
H	-1.93503	-1.61090	-1.85624	H	-4.50678	1.04418	0.26937
H	-2.82082	-2.31095	-0.49309	H	-3.86784	-0.02483	2.30428
H	-0.89583	-3.72889	-1.19487	H	-4.03411	-1.57049	1.47970

TS₃₀ – Acetate-assisted C–H activation with pseudo-axial binding

Geometry optimisation:

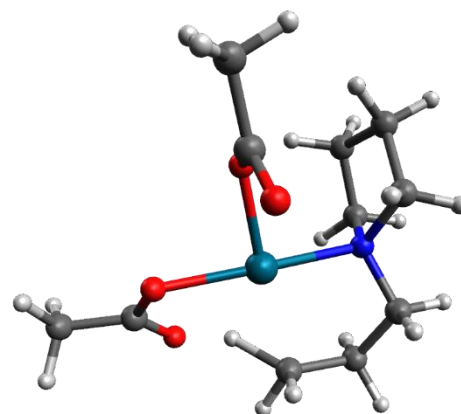
B3LYP-D3BJ/631G(d,p)/LANL2DZ-IEFPCM(DMF) Energy = -914.358413546

Thermal correction to Gibbs Free Energy = 0.261209

Imaginary frequency = -1349.4954

Single-point energy calculation:

B3LYP-D3BJ/6311+G(2d,p)/SDD-IEFPCM(DMF) Energy = -915.779043963



O	-0.98068	2.08791	-1.77293	H	0.33315	-3.42866	0.20638
C	-1.06306	2.38625	-0.57265	H	2.31418	-2.36485	-0.96674
O	2.13247	1.07787	-0.09968	H	1.25287	-1.45556	-1.98766
Pd	0.37298	-0.05627	-0.16133	C	-2.22251	-0.51588	2.02230
O	-0.63115	1.66020	0.41310	C	-3.17163	0.03114	0.93227
N	-1.35766	-1.25952	-0.06945	H	4.25771	2.24964	0.54833
C	-1.13281	-2.40165	-0.99850	H	5.17286	0.76322	0.17182
C	0.25259	-2.98608	-0.79216	H	4.61245	1.04381	1.82056
C	1.31645	-1.90897	-0.99139	H	-2.83984	3.47266	-0.06706
C	-1.54024	-1.70268	1.35122	H	-1.61308	4.44815	-0.88524
C	-2.63522	-0.53700	-0.39804	H	-1.41462	4.00627	0.83929
C	3.08539	0.44613	0.45434	H	-3.33126	-1.27445	-0.81304
C	4.35912	1.18752	0.76713	H	-2.42758	0.21386	-1.15847
O	3.01639	-0.79277	0.74514	H	-4.19679	-0.31097	1.09389
H	1.96209	-1.23754	0.07793	H	-3.17572	1.12070	0.93029
C	-1.76370	3.66708	-0.13728	H	-1.48151	0.24124	2.28461
H	-1.22497	-2.00994	-2.01573	H	-2.74771	-0.82014	2.93024
H	-1.92647	-3.14368	-0.84395	H	-0.58224	-1.97959	1.79082
H	0.39602	-3.80541	-1.50738	H	-2.19568	-2.58432	1.34981

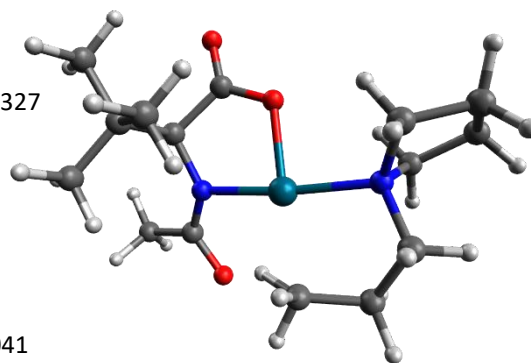
TS₃₁ – Ligand-assisted C–H activation with pseudo-equatorial binding

Geometry optimisation:

B3LYP-D3BJ/631G(d,p)/LANL2DZ-IEFPCM(DMF) Energy = -1050.56049327

Thermal correction to Gibbs Free Energy = 0.364104

Imaginary frequency = -1325.1427



Single-point energy calculation:

B3LYP-D3BJ/6311+G(2d,p)/SDD-IEFPCM(DMF) Energy = -1052.00759041

O	1.80386	-2.64880	-1.57871	H	4.59581	0.55039	0.60602
C	1.35705	-1.64942	-1.01748	H	2.49236	-1.59415	2.82859
C	2.30446	-0.53401	-0.51965	H	1.38011	-2.19300	1.58824
H	3.08864	-0.41855	-1.27415	H	1.29397	-0.50433	2.11121
C	3.00845	-0.94015	0.82549	H	-3.01755	0.66318	2.03609
C	3.95352	-2.12492	0.56352	H	-4.24487	0.87186	0.77883
C	3.83747	0.24954	1.33593	H	3.04983	2.94123	-2.19087
C	1.97835	-1.33104	1.89832	H	3.78830	1.41594	-1.64354
N	1.51823	0.68737	-0.39823	H	3.74731	2.82502	-0.57208
Pd	-0.42689	0.35120	-0.00776	H	-0.83910	1.85108	1.95504
O	0.07956	-1.48206	-0.78021	H	-0.71603	3.31291	1.04045
N	-2.46683	-0.16024	0.19063	H	-0.09872	2.32459	0.00073
C	-3.16851	0.89906	0.97910	H	-3.09065	3.00627	1.30095
C	-2.57181	2.26551	0.67955	H	-2.76459	2.54670	-0.36189
C	-1.06712	2.27579	0.97051	C	-4.08087	-1.94708	0.34465
C	-3.06243	-0.31237	-1.17607	C	-4.32068	-1.18882	-0.98955
C	-2.66682	-1.51994	0.77774	H	-2.31953	-0.82434	-1.79026
C	1.83832	1.90312	-0.78676	H	-3.25633	0.66941	-1.60913
C	3.19251	2.27490	-1.33792	H	-2.51353	-1.48117	1.85708
O	0.97712	2.84864	-0.68329	H	-1.90622	-2.16641	0.33644
H	4.47614	-2.39277	1.48774	H	-4.82035	-1.65570	1.09495
H	4.70875	-1.86524	-0.18674	H	-4.14167	-3.03103	0.22724
H	3.40895	-2.99892	0.20275	H	-4.43635	-1.86823	-1.83658
H	4.35613	-0.02968	2.25872	H	-5.22479	-0.57779	-0.93655
H	3.20547	1.11445	1.55447				

TS₃₂ – Ligand-assisted C–H activation with pseudo-axial binding

Geometry optimisation:

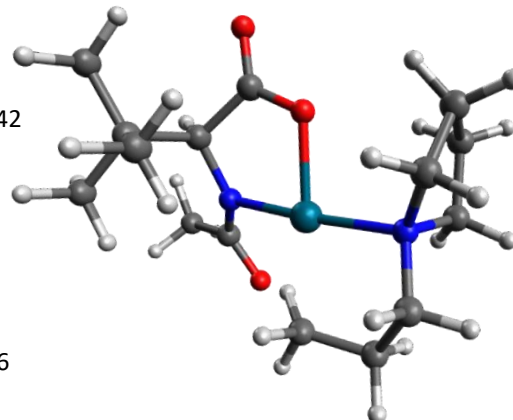
B3LYP-D3BJ/631G(d,p)/LANL2DZ-IEFPCM(DMF) Energy = -1050.56157242

Thermal correction to Gibbs Free Energy = 0.364337

Imaginary frequency = -1346.0304

Single-point energy calculation:

B3LYP-D3BJ/6311+G(2d,p)/SDD-IEFPCM(DMF) Energy = -1052.00803526



O	3.31953	-2.75958	-1.19788	H	5.93023	0.90381	0.44217
C	2.82412	-1.71434	-0.77656	H	4.03197	-1.06996	2.98610
C	3.71376	-0.48925	-0.46752	H	2.95409	-1.91569	1.86478
H	4.47353	-0.43503	-1.25302	H	2.74122	-0.18345	2.15721
C	4.46741	-0.65783	0.90062	H	-1.22334	0.62489	2.31283
C	5.49461	-1.79520	0.77247	H	-2.71239	0.79783	1.36401
C	5.21134	0.64722	1.22694	H	4.18231	2.74938	-2.65539
C	3.48639	-0.97620	2.04142	H	5.02386	1.34958	-1.94559
N	2.85583	0.68699	-0.49628	H	4.94173	2.88397	-1.06577
Pd	0.94785	0.31007	0.01264	H	0.81569	2.00414	1.84439
O	1.54504	-1.58386	-0.53801	H	0.69807	3.36255	0.77902
N	-1.10221	-0.16498	0.38308	H	1.18017	2.27838	-0.23915
C	-1.61726	0.86543	1.32056	H	-1.54684	2.97925	1.61967
C	-1.14358	2.24929	0.90684	H	-1.55551	2.51377	-0.07311
C	0.38506	2.31658	0.88621	C	-1.34682	-2.47836	-0.31134
C	-1.83482	-0.17687	-0.92034	C	-1.48244	-1.53190	-1.53060
C	-1.29805	-1.54968	0.91739	H	-0.52755	-1.46803	-2.05600
C	3.08179	1.84558	-1.07755	H	-2.24661	-1.85703	-2.24000
C	4.39203	2.21015	-1.72977	H	-2.19629	-3.16065	-0.23186
O	2.16325	2.74254	-1.08179	H	-0.43262	-3.06483	-0.38824
H	6.04385	-1.90672	1.71321	H	-2.24932	-1.57010	1.46375
H	6.22196	-1.57821	-0.01787	H	-0.49359	-1.78034	1.61675
H	5.01154	-2.74386	0.53307	H	-1.54087	0.67802	-1.53030
H	5.76753	0.53243	2.16289	H	-2.91158	-0.10629	-0.71153
H	4.51844	1.48431	1.34783				

TS₃₃ – Acetate-assisted β -H elimination on the heterocycle

Geometry optimisation:

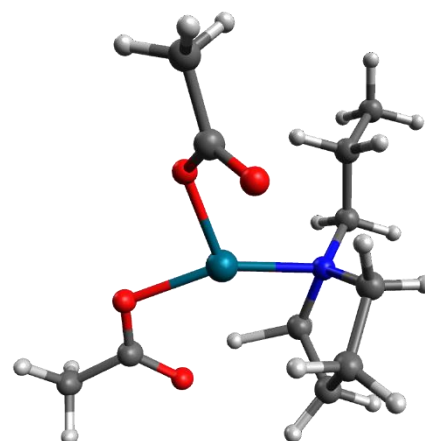
B3LYP-D3BJ/631G(d,p)/LANL2DZ-IEFPCM(DMF) Energy = -914.361915216

Thermal correction to Gibbs Free Energy = 0.254981

Imaginary frequency = -1088.7877

Single-point energy calculation:

B3LYP-D3BJ/6311+G(2d,p)/SDD-IEFPCM(DMF) Energy = -915.786345125



O	1.57597	1.42089	1.83560	C	2.88145	-0.57837	-1.04939
C	1.48263	2.17230	0.85542	C	3.88802	-0.82870	-2.17457
O	-2.24439	1.31228	-0.40349	H	3.38833	-0.62333	-0.07976
Pd	-0.43105	0.26066	-0.16042	H	2.44957	0.42326	-1.13847
O	0.66494	2.01579	-0.14205	H	4.34345	-1.82099	-2.08808
N	0.77066	-1.39728	0.00691	H	4.69142	-0.08744	-2.14657
C	1.26360	-1.69371	1.38867	H	3.40718	-0.76501	-3.15671
C	-0.57223	-1.92745	-0.14887	C	2.39698	3.38275	0.71128
C	1.74874	-1.59966	-1.08848	C	-0.93585	-2.63560	1.15262
C	-3.21135	0.48591	-0.52413	C	-0.01446	-1.96137	2.18198
C	-4.59346	1.06032	-0.73627	H	1.83515	-0.84105	1.74849
O	-3.08206	-0.77503	-0.50196	H	1.89532	-2.58796	1.32824
H	-1.66195	-1.07538	-0.33086	H	0.17269	-2.58622	3.05705
H	-5.32701	0.48987	-0.16337	H	-0.44688	-1.01448	2.51903
H	-4.85115	0.96582	-1.79627	H	-0.69758	-3.70079	1.05538
H	-4.62752	2.11330	-0.45759	H	-1.99667	-2.54250	1.39015
H	-0.70794	-2.47450	-1.08195	H	2.79423	3.67713	1.68404
H	1.20208	-1.52255	-2.03151	H	1.87402	4.22168	0.24724
H	2.14021	-2.62161	-1.00265	H	3.23669	3.11342	0.06063

TS₃₄ – Acetate-assisted β -H elimination on the propyl substituent

Geometry optimisation:

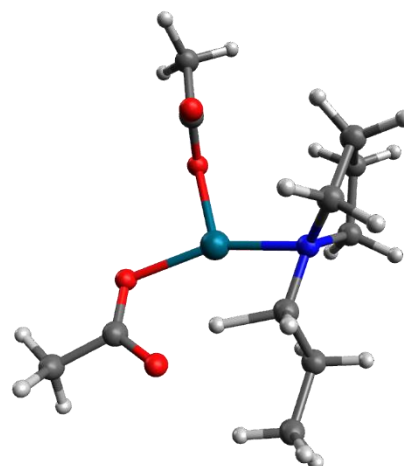
B3LYP-D3BJ/631G(d,p)/LANL2DZ-IEFPCM(DMF) Energy = -914.353336646

Thermal correction to Gibbs Free Energy = 0.254810

Imaginary frequency = -1195.2711

Single-point energy calculation:

B3LYP-D3BJ/6311+G(2d,p)/SDD-IEFPCM(DMF) Energy = -915.777003481



O	-2.15300	-1.54976	1.27529	C	3.20334	2.58286	-0.19833
C	-2.28702	-1.81775	0.07162	H	3.35273	2.93581	0.82751
O	1.53258	-1.93074	-0.35223	H	3.70312	3.28466	-0.87121
Pd	0.14641	-0.34801	-0.18481	H	3.68355	1.60716	-0.29253
O	-1.44362	-1.50606	-0.86429	C	-2.63438	1.81594	-0.72361
N	-0.50069	1.54766	0.21861	H	1.15149	1.80723	1.46871
C	-1.40087	1.69398	1.40292	C	-3.53844	-2.52505	-0.43370
C	0.92783	1.61418	0.41646	H	-4.01881	-3.07490	0.37729
C	-1.18288	2.26218	-0.89399	H	-3.30704	-3.19876	-1.26136
C	2.64211	-1.57610	0.16776	H	-4.24223	-1.77148	-0.80486
C	3.77235	-2.57847	0.17056	C	-2.82150	1.66041	0.81033
O	2.85857	-0.43032	0.67033	H	-1.17548	2.65811	1.87144
C	1.71330	2.50560	-0.53887	H	-1.20214	0.88851	2.10729
H	1.68620	0.39613	0.43832	H	-3.42097	2.47225	1.22690
H	4.56737	-2.21566	-0.48797	H	-3.30547	0.71372	1.04867
H	3.43416	-3.55575	-0.17202	H	-2.77534	0.85401	-1.22134
H	4.19015	-2.65667	1.17720	H	-3.32492	2.53708	-1.16432
H	1.27922	3.51222	-0.48528	H	-1.06872	3.34135	-0.73373
H	1.58248	2.15559	-1.56689	H	-0.73884	1.99272	-1.85071

TS₃₅ – Ligand-assisted β -H elimination on the heterocycle

Geometry optimisation:

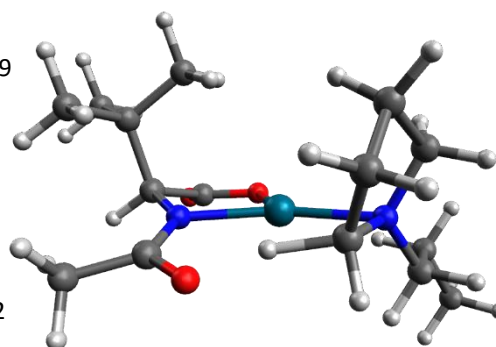
B3LYP-D3BJ/631G(d,p)/LANL2DZ-IEFPCM(DMF) Energy = -1050.55515579

Thermal correction to Gibbs Free Energy = 0.360837

Imaginary frequency = -1121.3581

Single-point energy calculation:

B3LYP-D3BJ/6311+G(2d,p)/SDD-IEFPCM(DMF) Energy = -1052.00582612



O	-2.11646	3.07706	-0.44241	H	-1.76274	1.26294	2.27272
C	-1.55954	1.99187	-0.27414	H	-1.47093	-0.45439	1.96796
C	-2.35123	0.67063	-0.44780	H	0.64082	-1.67929	-0.81326
H	-3.06787	0.81727	-1.26336	H	-2.46885	-2.05361	-3.29689
C	-3.17159	0.35288	0.85968	H	-3.47429	-0.98216	-2.29145
C	-4.24461	1.43700	1.05898	H	-3.21845	-2.67372	-1.82420
C	-3.87289	-1.00683	0.71460	C	1.98584	-1.81446	2.13558
C	-2.25210	0.30213	2.09185	H	2.37614	-1.94942	-1.20326
N	-1.38085	-0.36020	-0.77487	C	1.91725	-2.67875	0.86529
Pd	0.47987	-0.01468	-0.12848	H	3.16946	0.22472	-1.58922
O	-0.31046	1.88343	0.10239	H	4.46095	-0.20776	-0.45160
N	2.49623	-0.41684	0.27423	C	3.60933	1.76974	-0.14626
C	2.86033	-0.63658	1.70366	C	4.57833	2.52356	-1.05988
C	1.91463	-1.64955	-0.26090	H	3.94826	1.84357	0.89310
C	3.49249	0.30218	-0.54785	H	2.61210	2.22297	-0.19129
C	-1.48927	-1.45141	-1.51281	H	5.58275	2.08887	-1.01868
C	-2.74851	-1.79457	-2.27316	H	4.65516	3.57318	-0.76308
O	-0.50039	-2.25547	-1.63108	H	4.24186	2.49274	-2.10185
H	-4.84448	1.20506	1.94526	H	2.81265	-3.30411	0.77784
H	-4.92066	1.48217	0.19784	H	1.04238	-3.33025	0.83029
H	-3.79909	2.42472	1.18709	H	0.98787	-1.46344	2.41607
H	-4.46463	-1.21187	1.61262	H	2.41307	-2.34672	2.98737
H	-3.15317	-1.82151	0.59958	H	3.92600	-0.89471	1.74849
H	-4.55374	-1.01946	-0.14184	H	2.69263	0.27642	2.27491
H	-2.83710	0.04523	2.98102				

TS₃₆ – Ligand-assisted β -H elimination on the propyl substituent

Geometry optimisation:

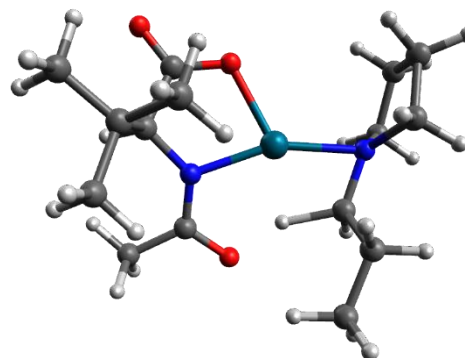
B3LYP-D3BJ/631G(d,p)/LANL2DZ-IEFPCM(DMF) Energy = -1050.54799886

Thermal correction to Gibbs Free Energy = 0.359273

Imaginary frequency = -1204.4477

Single-point energy calculation:

B3LYP-D3BJ/6311+G(2d,p)/SDD-IEFPCM(DMF) Energy = -1051.99818655



O	1.76929	-4.18973	-1.03155	H	1.02851	-3.18108	1.96213
C	1.06069	-3.24384	-0.68409	H	0.50742	-1.49356	2.06439
C	1.68570	-1.84302	-0.45870	H	-1.54843	0.18112	-0.54732
H	2.46679	-1.70402	-1.21418	H	1.64563	1.46338	-2.61762
C	2.37122	-1.76926	0.95699	H	2.70600	0.29947	-1.78536
C	3.57659	-2.72426	0.98532	H	2.19610	1.78981	-0.97229
C	2.87300	-0.33930	1.21255	C	-4.14975	-3.53476	0.85057
C	1.38174	-2.15188	2.07090	C	-4.36151	-3.47775	-0.69086
N	0.61667	-0.87357	-0.62067	C	-2.95407	0.70291	1.25484
Pd	-1.22887	-1.56147	-0.26153	C	-2.44270	2.13566	1.08803
O	-0.21934	-3.36408	-0.44357	H	-2.57159	2.69165	2.02045
N	-3.29523	-1.49170	0.03198	H	-2.99647	2.66105	0.30269
C	-3.84683	-2.08967	1.27292	H	-1.38536	2.14803	0.81472
C	-2.84344	-0.11340	-0.02683	H	-2.40610	0.20549	2.06019
C	-4.15491	-2.00443	-1.06465	H	-4.01068	0.72441	1.55099
C	0.62684	0.34719	-1.12316	H	-3.29374	0.38989	-0.88735
C	1.87982	0.99839	-1.65759	H	-4.76275	-1.55262	1.54910
O	-0.45637	1.02959	-1.18255	H	-3.12937	-2.01004	2.08804
H	4.07778	-2.65991	1.95687	H	-5.10080	-1.44812	-1.05149
H	4.30598	-2.45663	0.21255	H	-3.66346	-1.84740	-2.02522
H	3.27274	-3.75828	0.81526	H	-3.62597	-4.10427	-1.20006
H	3.37170	-0.29295	2.18613	H	-5.35487	-3.81824	-0.98847
H	2.04966	0.37971	1.22592	H	-5.02534	-3.91558	1.37933
H	3.59644	-0.02583	0.45371	H	-3.30386	-4.18121	1.09447
H	1.86872	-2.06158	3.04744				

III.IV. Nuclear coordinates for complexes containing 1-propylazepane

333 – 1-Propylazepane

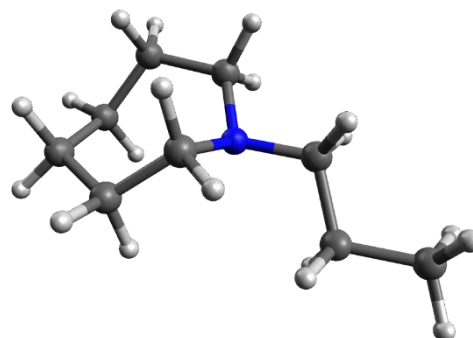
Geometry optimisation:

B3LYP-D3BJ/631G(d,p)/LANL2DZ-IEFPCM(DMF) Energy = -409.220627721

Thermal correction to Gibbs Free Energy = 0.232031

Single-point energy calculation:

B3LYP-D3BJ/6311+G(2d,p)-IEFPCM(DMF) Energy = -409.315591490



C	-2.52702	-1.12431	-0.21119	H	-0.72912	-0.38425	1.84008
C	-2.51633	0.27245	-0.85241	H	0.63488	-1.32839	1.27543
H	-3.03619	-1.82886	-0.88062	H	-0.31202	2.11445	1.15294
C	-1.15275	-1.70142	0.15075	H	-0.21715	2.23884	-0.60523
H	-3.14162	-1.07085	0.69850	C	1.67771	0.61447	0.22763
H	-1.88748	0.27567	-1.75106	C	2.55678	-0.44968	-0.43280
H	-3.53650	0.50153	-1.18269	H	1.97115	0.73412	1.28951
C	-2.05571	1.37055	0.12119	H	1.88505	1.57764	-0.25401
H	-1.29922	-2.62031	0.73370	C	4.04810	-0.13940	-0.28734
C	-0.23039	-0.75595	0.92919	H	2.28153	-0.51439	-1.49222
H	-0.62069	-1.98704	-0.76491	H	2.34619	-1.43433	0.00164
C	-0.53622	1.57715	0.20984	H	4.29758	0.82600	-0.74192
H	-2.49493	2.33379	-0.16254	H	4.66298	-0.90459	-0.77074
H	-2.46030	1.14167	1.11461	H	4.34084	-0.09339	0.76758
N	0.24715	0.34851	0.08611				

341 – Bisamine complex

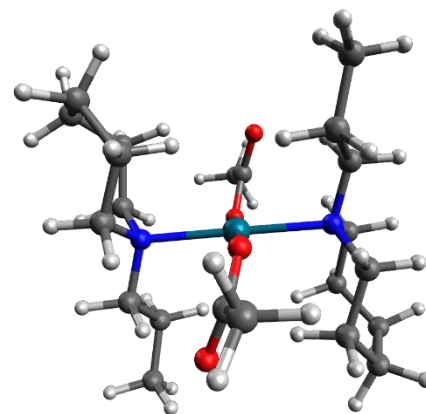
Geometry optimisation:

B3LYP-D3BJ/631G(d,p)/LANL2DZ-IEFPCM(DMF) Energy = -1402.29615318

Thermal correction to Gibbs Free Energy = 0.576630

Single-point energy calculation:

B3LYP-D3BJ/6311+G(2d,p)/SDD-IEFPCM(DMF) Energy = -1403.82966801



Pd	-0.00004	0.59310	-0.01850	C	0.21415	4.83282	-1.77048
O	-0.19514	0.94695	2.00782	H	-0.11703	2.69605	-1.76769
N	1.88178	1.73142	-0.13310	H	1.35531	3.19059	-2.58743
O	0.19227	0.19963	-2.03126	H	-0.47073	5.03717	-0.94048
N	-1.89717	-0.52607	0.09906	H	-0.32293	5.02106	-2.70479
C	2.58134	1.72143	1.19263	H	1.03834	5.55219	-1.70794
C	2.82044	0.32467	1.77423	H	0.87597	3.46944	0.42298
C	1.49595	3.15561	-0.41639	H	2.41833	3.75571	-0.42023
C	2.78601	1.25785	-1.22437	C	4.17364	-0.31357	1.43250
C	-2.85486	0.12320	1.04598	C	-4.31508	1.89940	-0.20405
C	-3.14969	1.59620	0.74596	C	-4.32118	1.11393	-1.53296
C	-1.57267	-1.91737	0.56881	C	4.60865	-0.13282	-0.03298
C	-2.51856	-0.69315	-1.25111	H	-3.39554	-1.34488	-1.12265
C	0.54149	-0.98376	-2.44149	H	-1.79872	-1.24262	-1.85073
O	0.71525	-1.97734	-1.72428	H	-3.02688	0.29802	-3.04187
C	0.74545	-1.05060	-3.94823	H	-2.17720	1.33931	-1.92405
H	0.84061	-2.08682	-4.27489	H	-4.73373	1.75330	-2.32111
H	1.65924	-0.50742	-4.21218	H	-5.00627	0.26046	-1.45460
H	-0.08498	-0.56677	-4.46863	H	-4.28477	2.97471	-0.41616
C	-0.47140	2.09271	2.55301	H	-5.26369	1.72333	0.31714
C	-0.68515	1.98196	4.05807	H	-2.23056	2.06155	0.38105
H	-1.62577	1.45486	4.25088	H	-3.35559	2.08890	1.70209
H	-0.73192	2.97262	4.51212	H	-3.77782	-0.47515	1.04960
H	0.11669	1.39640	4.51510	H	-2.40410	0.04983	2.03125
O	-0.57707	3.17891	1.97131	H	3.52882	2.26576	1.07433
C	-0.89072	-2.05378	1.92759	H	1.95759	2.30500	1.86502
H	-0.92039	-2.33777	-0.19747	H	2.71628	0.38784	2.86223
H	-2.51261	-2.48950	0.57654	H	2.00715	-0.32447	1.44010
C	-0.47873	-3.51130	2.15779	H	4.10885	-1.38288	1.66675
H	-1.55683	-1.73276	2.73485	H	4.95262	0.09474	2.08755
H	-0.01455	-1.40496	1.97235	H	5.30412	-0.93738	-0.29605
H	-1.34273	-4.18402	2.11516	H	5.17829	0.79912	-0.13973
H	-0.00872	-3.63358	3.13808	H	2.70345	-0.87117	-0.81428
H	0.23793	-3.84137	1.39769	H	3.84840	-0.36498	-2.03336
C	-2.95724	0.57540	-1.98376	H	3.57070	2.02069	-1.33986
C	0.72620	3.39050	-1.71422	H	2.19058	1.24739	-2.13268
C	3.45224	-0.10807	-1.04375				

342 – Monoamine complex

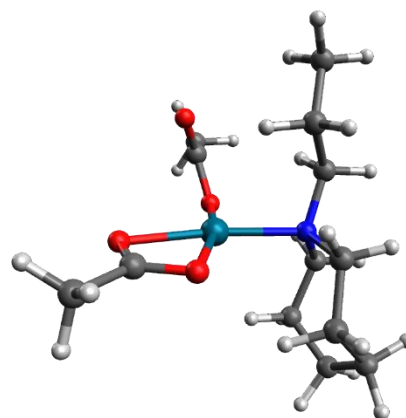
Geometry optimisation:

B3LYP-D3BJ/631G(d,p)/LANL2DZ-IEFPCM(DMF) Energy = -993.037907754

Thermal correction to Gibbs Free Energy = 0.316654

Single-point energy calculation:

B3LYP-D3BJ/6311+G(2d,p)/SDD-IEFPCM(DMF) Energy = -994.475446658



Pd	0.24923	0.63599	-0.22906	H	2.08758	-3.10655	2.98548
O	-0.78079	2.14788	0.84091	H	2.78625	-1.61123	3.62205
O	0.80945	2.67628	-0.57152	H	3.07183	-2.06760	1.93478
C	-0.07632	3.05241	0.26787	C	-2.99363	-0.19749	0.80597
C	-0.31345	4.50320	0.55272	H	-1.29103	-0.17434	2.11804
H	-0.69926	4.63152	1.56533	H	-1.99925	-1.77596	1.88250
H	-1.05993	4.88478	-0.15217	C	-1.97505	-1.20992	-1.76590
H	0.60867	5.07103	0.41865	H	-1.58811	-2.87022	-0.39874
N	-0.63013	-1.16742	0.40927	H	-0.17261	-2.27388	-1.27950
C	0.42063	-1.97410	1.11597	C	-3.48705	-1.25944	-1.49753
C	-1.08845	-1.96879	-0.77573	H	-1.77816	-1.61983	-2.76203
O	1.41449	-0.46854	-1.46985	H	-1.63140	-0.17002	-1.80337
C	2.67192	-0.55972	-1.11697	C	-3.87958	-1.14441	-0.01567
C	3.49085	-1.41149	-2.07435	H	-2.74333	0.70724	0.24411
O	3.16463	-0.05169	-0.10706	H	-3.55423	0.13996	1.68492
C	-1.72791	-0.84022	1.37390	H	-4.92138	-0.81236	0.04659
H	1.17591	-2.21281	0.36730	H	-3.85481	-2.13594	0.45403
H	-0.04371	-2.91764	1.43309	H	-3.90110	-2.19095	-1.90063
C	1.08441	-1.28752	2.30674	H	-3.95577	-0.44680	-2.06468
C	2.32953	-2.06683	2.73886	H	4.55475	-1.29671	-1.86393
H	0.38567	-1.20517	3.14504	H	3.28062	-1.13954	-3.11145
H	1.37936	-0.27321	2.01789	H	3.21247	-2.46290	-1.94675

343 – Bidentate ligand-amine complex

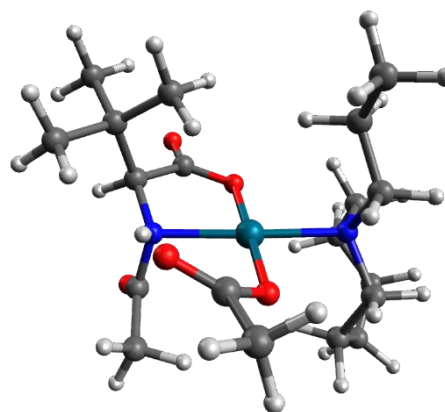
Geometry optimisation:

B3LYP-D3BJ/631G(d,p)/LANL2DZ-IEFPCM(DMF) Energy = -1358.38207928

Thermal correction to Gibbs Free Energy = 0.477667

Single-point energy calculation:

B3LYP-D3BJ/6311+G(2d,p)/SDD-IEFPCM(DMF) Energy = -1359.91888506



Pd	-1.22644	0.35872	-0.15032	H	0.01668	0.44031	-4.36114
O	-0.78344	-1.47716	0.57208	C	-4.19579	0.21888	-1.51319
N	0.67653	0.11168	-1.05326	C	-5.17306	-0.96585	-1.55952
O	-1.58300	2.26757	-0.82770	C	-5.22540	-1.80241	-0.27042
N	-3.13378	0.48889	0.79512	H	0.98944	-0.04799	2.43338
C	0.46031	-1.86514	0.42426	H	1.02110	1.40781	1.41794
O	0.85337	-2.96519	0.80116	H	2.34652	1.08035	2.53882
C	1.43866	-0.87433	-0.23544	H	-1.79555	4.56165	-2.00815
C	2.40147	-0.16990	0.76938	H	-0.23499	5.19330	-1.40073
C	1.63644	0.61311	1.84920	H	-1.60194	4.90895	-0.29037
C	3.32745	0.78665	-0.00895	C	-2.03854	1.17636	2.99683
C	3.27631	-1.24227	1.44375	C	-1.67232	2.42361	3.80522
H	2.67646	-1.94915	2.01816	H	-1.13104	0.73760	2.57220
H	3.98829	-0.75599	2.11773	H	-2.47792	0.42281	3.65776
H	3.84635	-1.80948	0.70046	H	-1.16156	3.16000	3.17522
H	2.79631	1.65265	-0.41210	H	-1.00618	2.16867	4.63422
H	3.82489	0.26708	-0.83478	H	-2.56315	2.90262	4.22587
H	4.10186	1.16897	0.66304	H	-4.00752	1.71893	2.27727
C	0.40679	-0.28608	-2.40266	H	-2.67112	2.43806	1.36511
H	2.05101	-1.46260	-0.92239	H	-3.85372	2.02515	-0.39876
C	0.03908	0.83129	-3.34474	H	-5.12157	1.00912	0.30127
O	0.47264	-1.45816	-2.72032	H	-3.18175	-0.12216	-1.74768
H	0.96165	1.10644	-0.97821	H	-4.45765	0.92827	-2.30535
C	-0.61218	3.12163	-0.93383	H	-4.88511	-1.60696	-2.40094
O	0.60156	2.85523	-0.84998	H	-6.18206	-0.60144	-1.78527
C	-1.08142	4.54261	-1.18091	H	-5.62216	-2.79423	-0.51249
C	-4.14286	0.99607	-0.19528	H	-5.94255	-1.35897	0.43210
C	-3.00543	1.52898	1.86891	H	-3.90850	-2.85285	1.07368
C	-3.52438	-0.81809	1.40680	H	-3.05861	-2.11343	-0.26288
C	-3.87621	-1.95474	0.44652	H	-4.38371	-0.62327	2.06455
H	0.75320	1.65489	-3.26755	H	-2.68620	-1.13026	2.02611
H	-0.94486	1.22921	-3.08174				

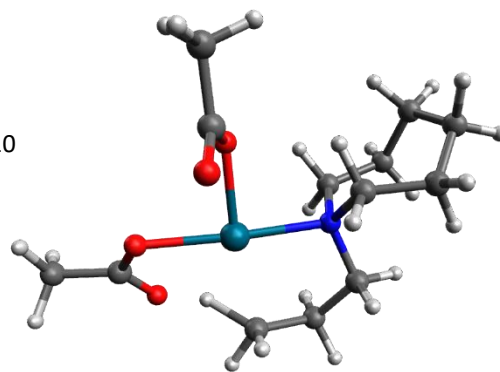
TS₃₇ – Acetate-assisted C–H activation

Geometry optimisation:

B3LYP-D3BJ/631G(d,p)/LANL2DZ-IEFPCM(DMF) Energy = -992.995262810

Thermal correction to Gibbs Free Energy = 0.314402

Imaginary frequency = -1340.2168



Single-point energy calculation:

B3LYP-D3BJ/6311+G(2d,p)/SDD-IEFPCM(DMF) Energy = -994.434851177

O	0.56881	2.59097	-1.49517	H	2.06171	-2.79120	-1.09336
C	0.24669	2.71456	-0.30809	H	2.05560	-1.65419	0.00332
O	2.78760	0.55219	0.02416	H	-0.14834	-3.80639	-1.24010
Pd	0.80453	-0.09276	-0.16260	H	-0.01689	-3.21060	0.40400
O	0.19333	1.74677	0.56223	C	-4.48840	0.30722	0.04451
N	-1.22094	-0.73182	-0.18027	C	-3.93774	0.09147	1.46488
C	-1.29268	-2.04419	-0.89844	H	-0.92893	-1.67272	1.66139
C	-0.05755	-2.89011	-0.64275	H	-1.23881	0.06142	1.74721
C	1.20211	-2.11351	-1.01791	H	-3.01313	-1.42196	2.69229
C	-1.55835	-0.86934	1.27293	H	-3.42419	-1.99934	1.09469
C	-2.04866	0.31116	-0.87601	H	-3.37591	0.97905	1.78247
C	3.54953	-0.33907	0.51134	H	-4.78412	0.01285	2.15569
C	4.96017	0.03892	0.88188	H	-5.39965	-0.28770	-0.08644
O	3.17734	-1.54476	0.68705	H	-4.79407	1.35558	-0.04988
H	-1.35579	-1.81489	-1.96564	H	-3.84703	0.48642	-2.00446
H	-2.20496	-2.57645	-0.61635	H	-3.61270	-1.10718	-1.35279
C	-3.02651	-1.13266	1.63541	H	-1.55517	0.48416	-1.83377
C	-3.52500	-0.04640	-1.10343	H	-1.95113	1.22373	-0.28939
H	5.12295	1.10912	0.76166	C	-0.17741	4.06157	0.26373
H	5.65534	-0.51457	0.24390	H	0.33099	4.25480	1.21188
H	5.15544	-0.25687	1.91575	H	-1.25336	4.04533	0.46795
H	1.12807	-1.66959	-2.01783	H	0.03842	4.86203	-0.44521

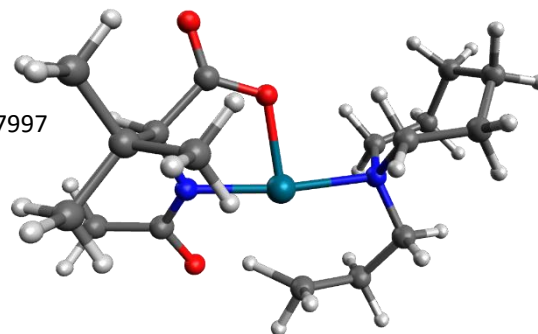
TS₃₈ – Ligand-assisted C–H activation

Geometry optimisation:

B3LYP-D3BJ/631G(d,p)/LANL2DZ-IEFPCM(DMF) Energy = -1129.19977997

Thermal correction to Gibbs Free Energy = 0.419134

Imaginary frequency = -1326.5874



Single-point energy calculation:

B3LYP-D3BJ/6311+G(2d,p)/SDD-IEFPCM(DMF) Energy = -1130.66451483

O	2.64678	-1.56159	-1.65531	H	2.47671	0.56228	2.06294
C	2.38409	-0.51388	-1.06584	H	-1.50393	2.53096	2.07239
C	3.51392	0.40290	-0.54523	H	-2.66854	2.94681	0.81191
H	4.31423	0.38565	-1.29115	C	-3.13477	1.20509	-1.34459
C	4.11569	-0.14457	0.79930	C	-2.82050	0.01111	1.36779
C	4.83894	-1.47331	0.52246	H	5.54380	3.43205	-0.54117
C	5.13442	0.87047	1.34211	H	4.88428	3.72162	-2.15437
C	3.01670	-0.36601	1.85224	H	5.32383	2.07074	-1.65197
N	2.96108	1.74457	-0.40928	H	0.85429	3.28455	1.97567
Pd	0.99240	1.75427	-0.00098	H	1.23500	4.70946	1.07467
O	1.15838	-0.12947	-0.81313	H	1.67169	3.63831	0.02573
N	-1.12346	1.58233	0.24425	H	-1.15449	4.82990	1.31332
C	-1.60712	2.77043	1.01036	H	-0.91194	4.31101	-0.34413
C	-0.77302	4.00460	0.69854	C	-3.66282	-0.72517	0.31125
C	0.70783	3.75064	0.99430	C	-3.43305	-0.28818	-1.14664
C	-1.65555	1.56748	-1.15297	H	-1.45799	2.55942	-1.56610
C	-1.36118	0.30331	0.98776	H	-1.04333	0.85341	-1.70961
C	3.49704	2.88848	-0.77625	H	-3.37141	1.48135	-2.37841
C	4.89801	3.01698	-1.32072	H	-3.78298	1.82493	-0.71407
O	2.82132	3.97233	-0.65436	H	-2.59912	-0.85820	-1.57539
H	5.28685	-1.85145	1.44733	H	-4.31515	-0.56424	-1.73448
H	5.64309	-1.33632	-0.20917	H	-4.71891	-0.58680	0.57063
H	4.15394	-2.22720	0.13103	H	-3.47139	-1.80210	0.38286
H	5.58579	0.48601	2.26241	H	-2.80390	-0.59328	2.28117
H	4.66109	1.82826	1.57449	H	-3.31139	0.94689	1.65165
H	5.94176	1.04839	0.62451	H	-0.75676	0.37947	1.89515
H	3.46322	-0.72010	2.78714	H	-0.93249	-0.49755	0.38159
H	2.28679	-1.11142	1.52286				

TS₃₉ – Acetate-assisted β -H elimination on the heterocycle

Geometry optimisation:

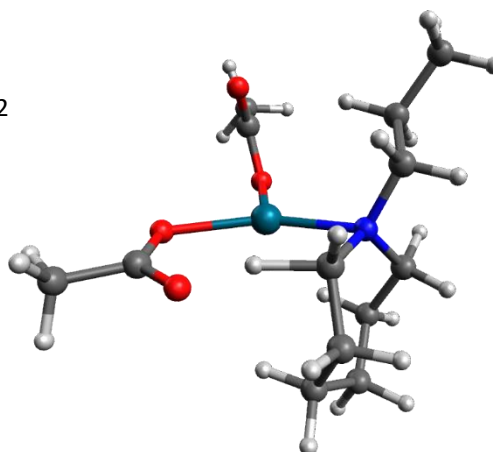
B3LYP-D3BJ/631G(d,p)/LANL2DZ-IEFPCM(DMF) Energy = -993.000456322

Thermal correction to Gibbs Free Energy = 0.310572

Imaginary frequency = -1070.9846

Single-point energy calculation:

B3LYP-D3BJ/6311+G(2d,p)/SDD-IEFPCM(DMF) Energy = -994.443360970



O	-2.32377	2.16448	-0.39306	H	-3.70815	-1.23489	-2.84156
C	-2.22727	1.90958	0.81656	H	-4.85220	-1.23176	-1.49369
O	1.20368	2.21456	0.04513	H	-3.99588	-2.72012	-1.92201
Pd	0.10329	0.41940	0.03627	H	-1.17331	-1.26188	-2.30773
O	-1.31153	1.16735	1.35703	H	-1.47788	-2.84621	-1.58526
N	-0.28978	-1.55614	-0.42657	C	2.75992	-1.78574	0.76397
C	-1.42878	-1.77017	-1.37624	C	0.49664	-2.18893	1.93417
C	0.98220	-1.25909	-1.06411	C	1.98386	-2.53810	1.84572
C	-0.33459	-2.53543	0.69978	H	-0.05131	-3.51596	0.29723
C	2.24814	2.08916	-0.67981	H	-1.38445	-2.59143	0.98441
C	3.17664	3.27763	-0.77857	H	0.05606	-2.75096	2.76504
O	2.55799	1.03245	-1.30754	H	0.35919	-1.12744	2.17295
H	1.51754	0.03421	-1.01517	H	2.08088	-3.61738	1.66690
H	3.37181	3.50163	-1.83022	H	2.44703	-2.34344	2.81945
H	4.13309	3.01878	-0.31458	H	2.75583	-0.70875	0.97244
H	2.75511	4.15071	-0.28176	H	3.80741	-2.10405	0.79879
C	-2.77048	-1.24687	-0.87215	H	3.00723	-1.70259	-1.37351
C	2.24084	-2.01659	-0.65965	H	2.07273	-3.08682	-0.83989
H	0.85117	-1.25123	-2.14621	C	-3.24841	2.44380	1.81449
C	-3.89494	-1.63274	-1.83812	H	-2.74649	2.88282	2.68059
H	-2.71066	-0.15900	-0.78171	H	-3.86505	1.61549	2.17914
H	-2.99270	-1.64492	0.12359	H	-3.89321	3.18579	1.34159

TS₄₀ – Ligand-assisted β -H elimination on the heterocycle

Geometry optimisation:

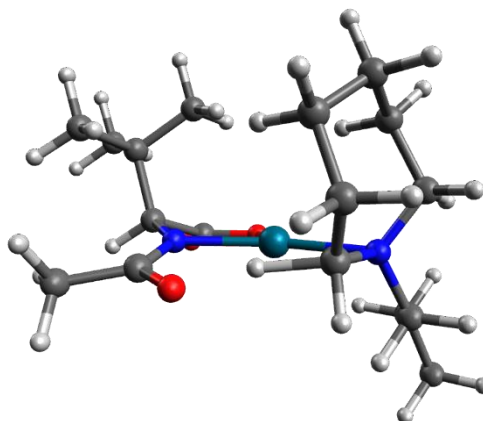
B3LYP-D3BJ/631G(d,p)/LANL2DZ-IEFPCM(DMF) Energy = -1129.19740067

Thermal correction to Gibbs Free Energy = 0.415607

Imaginary frequency = -1076.3291

Single-point energy calculation:

B3LYP-D3BJ/6311+G(2d,p)/SDD-IEFPCM(DMF) Energy = -1130.66546122



O	2.38763	3.05554	-0.69614	H	2.55571	-0.60844	3.89143
C	1.76412	2.02528	-0.43820	H	3.57615	-0.06141	2.53869
C	2.48346	0.81767	0.21501	H	3.21507	-1.78419	2.75186
H	3.23483	1.21444	0.90651	H	-2.34460	-0.89925	1.96714
C	3.24037	-0.02471	-0.88048	C	-1.93761	-2.59879	0.68175
C	4.37076	0.82888	-1.48039	C	-1.06696	-3.06950	-0.48812
C	3.86021	-1.27477	-0.23639	C	-1.97145	-1.34725	-2.19008
C	2.28278	-0.47338	-1.99748	C	-3.19105	2.25770	-0.09383
N	1.46811	0.05492	0.92087	C	-4.03247	3.32584	0.61014
Pd	-0.39206	0.24801	0.20916	H	-3.02675	1.02093	1.65290
O	0.49932	1.86573	-0.73431	H	-4.36092	0.55273	0.58885
N	-2.45099	-0.14963	0.01718	H	-3.50337	2.18017	-1.14069
C	-2.98479	-0.65705	-1.27653	H	-2.13409	2.54690	-0.09842
C	-1.91803	-1.10693	0.98423	H	-5.09448	3.05820	0.61263
C	-3.32222	0.90773	0.60755	H	-3.93152	4.29149	0.10723
C	1.54092	-0.66575	2.02736	H	-3.71636	3.45446	1.65101
C	2.80881	-0.77309	2.84172	C	-1.67843	-2.81469	-1.86721
O	0.51290	-1.28863	2.46393	H	-1.59014	-3.08098	1.60029
H	4.92828	0.24024	-2.21644	H	-2.97849	-2.91862	0.54119
H	5.07423	1.14937	-0.70380	H	-3.83634	-1.31645	-1.06373
H	3.98229	1.72329	-1.97006	H	-3.37644	0.22018	-1.79022
H	4.40615	-1.84571	-0.99444	H	-1.04487	-0.76069	-2.20039
H	3.09473	-1.93144	0.18536	H	-2.38135	-1.29202	-3.20472
H	4.56852	-1.01136	0.55491	H	-0.89457	-4.14547	-0.37612
H	2.82755	-1.07279	-2.73425	H	-0.08410	-2.58698	-0.41079
H	1.83546	0.37879	-2.51613	H	-2.61410	-3.38420	-1.94823
H	1.47103	-1.08679	-1.59596	H	-1.00696	-3.21360	-2.63595
H	-0.62478	-0.98049	1.48081				

A_{T559} – Acetate-assisted β–H elimination on the propyl substituent

Geometry optimisation:

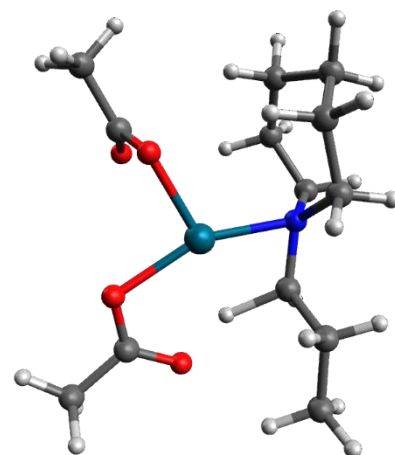
B3LYP-D3BJ/631G(d,p)/LANL2DZ-IEFPCM(DMF) Energy = -992.993539533

Thermal correction to Gibbs Free Energy = 0.311428

Imaginary frequency = -1130.8091

Single-point energy calculation:

B3LYP-D3BJ/6311+G(2d,p)/SDD-IEFPCM(DMF) Energy = -994.435265199



O	-1.00911	2.61974	1.09916	H	3.69780	-2.08046	-0.10523
C	-1.38307	2.53923	-0.07980	H	1.65689	-2.27501	-1.56779
O	1.96904	1.65562	-0.42510	H	1.08886	-3.62810	-0.59195
Pd	0.38392	0.28370	-0.19006	H	1.15248	-1.98554	1.44893
O	-1.00321	1.63606	-0.93110	C	-3.42177	-0.30994	0.65156
N	-0.49957	-1.52642	0.24234	C	-3.60198	-1.45875	-0.34717
C	-1.16748	-2.21023	-0.90195	H	-1.75908	-2.59188	1.53074
C	0.93485	-1.74464	0.40662	H	-0.58074	-1.55910	2.33590
C	-1.29354	-1.60058	1.51131	H	-1.79600	0.45097	1.86620
C	3.01826	1.19261	0.13390	H	-2.79139	-0.74270	2.68607
C	4.26968	2.03839	0.09272	H	-3.19910	0.58873	0.06982
O	3.07799	0.06174	0.70614	H	-4.37390	-0.12085	1.15845
H	1.80214	-0.62390	0.46834	H	-2.78792	-2.13823	-2.23186
H	5.00288	1.54981	-0.55646	H	-2.22682	-0.54255	-1.73693
H	4.70503	2.09939	1.09286	H	-1.35466	-3.24781	-0.59643
H	4.05895	3.03749	-0.28708	H	-0.46590	-2.22295	-1.73328
C	-2.45907	-1.54819	-1.36864	H	-4.53170	-1.28392	-0.89992
C	-2.32502	-0.49593	1.72475	H	-3.73302	-2.41954	0.16792
C	1.65254	-2.68823	-0.55525	C	-2.41319	3.51669	-0.63442
C	3.08851	-2.98593	-0.11343	H	-3.41529	3.11292	-0.45088
H	3.54432	-3.70742	-0.79667	H	-2.29705	3.65414	-1.71095
H	3.10646	-3.41759	0.89287	H	-2.33644	4.47664	-0.12025

A_{TS60} – Ligand-assisted β–H elimination on the propyl substituent

Geometry optimisation:

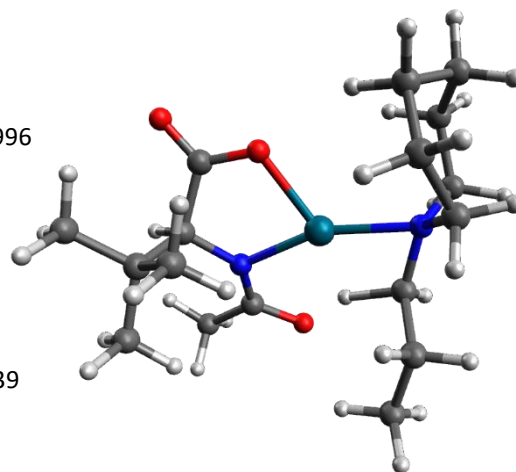
B3LYP-D3BJ/631G(d,p)/LANL2DZ-IEFPCM(DMF) Energy = -1129.19117996

Thermal correction to Gibbs Free Energy = 0.416867

Imaginary frequency = -1163.6279

Single-point energy calculation:

B3LYP-D3BJ/6311+G(2d,p)/SDD-IEFPCM(DMF) Energy = -1130.65849139



O	2.05807	-3.06010	-1.07356	H	3.05747	2.47937	-2.69919
C	1.55729	-1.98960	-0.72660	H	3.86730	1.13268	-1.86145
C	2.45091	-0.74371	-0.50016	H	3.67697	2.70254	-1.06094
H	3.24546	-0.76410	-1.25398	C	-2.71832	-1.32043	1.69876
C	3.13383	-0.80583	0.91707	C	-3.44824	-1.00280	-1.54161
C	4.12702	-1.97964	0.94841	C	-1.40988	2.61530	1.39157
C	3.90545	0.49880	1.17118	C	-0.57800	3.88867	1.20985
C	2.08582	-0.98586	2.02890	H	-0.50224	4.42271	2.16063
N	1.59857	0.42028	-0.66203	H	-1.04307	4.56099	0.48126
Pd	-0.34058	0.12139	-0.26104	H	0.42803	3.65727	0.85445
O	0.27965	-1.84493	-0.48717	H	-0.93649	1.97503	2.14165
N	-2.35660	0.60614	0.08746	H	-2.40266	2.88669	1.77201
C	-2.99977	0.14089	1.34846	H	-1.95220	2.50805	-0.71478
C	-1.59058	1.85546	0.08432	C	-3.96837	-1.99218	-0.48763
C	-3.24788	0.44267	-1.09668	C	-2.91740	-2.35462	0.57264
C	1.84705	1.60764	-1.18360	H	-4.07582	0.31262	1.24026
C	3.20076	1.98558	-1.73573	H	-2.65967	0.76483	2.17070
O	0.92296	2.49240	-1.24020	H	-1.69422	-1.39902	2.08015
H	4.62821	-2.01599	1.92139	H	-3.38258	-1.55091	2.54042
H	4.89705	-1.86129	0.17783	H	-1.96158	-2.51770	0.06524
H	3.62488	-2.93314	0.77687	H	-3.18572	-3.30973	1.03757
H	4.40458	0.44826	2.14433	H	-4.25813	-2.90834	-1.01389
H	3.23790	1.36456	1.18353	H	-4.88533	-1.60915	-0.02031
H	4.67520	0.66431	0.41107	H	-2.49843	-1.38066	-1.93904
H	2.57887	-0.99330	3.00653	H	-4.14902	-0.96303	-2.38388
H	1.53622	-1.92495	1.91891	H	-4.21039	0.91036	-0.85134
H	1.35784	-0.16840	2.02129	H	-2.80075	1.00553	-1.91843
H	-0.30832	1.87409	-0.54631				

III.V. Nuclear coordinates for complexes containing *tert*-butyl 4-propyl-1,4-diazepane-1-carboxylate334 – *tert*-Butyl 4-propyl-1,4-diazepane-1-carboxylate

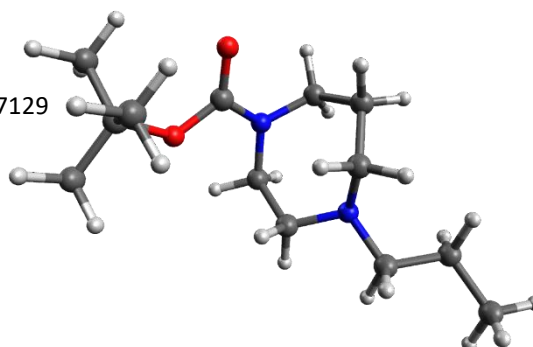
Geometry optimisation:

B3LYP-D3BJ/631G(d,p)/LANL2DZ-IEFPCM(DMF) Energy = -771.136187129

Thermal correction to Gibbs Free Energy = 0.335100

Single-point energy calculation:

B3LYP-D3BJ/6311+G(2d,p)-IEFPCM(DMF) Energy = -771.333420855



C	0.41530	2.17027	-0.60740	C	-3.36289	-0.76654	0.27665
C	1.24834	1.95707	0.66922	C	-4.52417	0.19150	0.00936
H	-0.20071	3.06636	-0.51231	C	-3.04078	-0.89782	1.76587
N	-0.45113	1.03714	-0.93650	C	-3.63982	-2.13779	-0.33797
H	1.07848	2.30586	-1.46376	H	-3.82205	-2.04787	-1.41248
H	2.15174	2.57300	0.59589	H	-4.52229	-2.58400	0.12823
H	0.68558	2.30587	1.54126	H	-2.78853	-2.80665	-0.18343
C	1.63329	0.49303	0.91095	H	-2.82956	0.07573	2.20694
C	0.13981	-0.02849	-1.74801	H	-2.17210	-1.54832	1.90637
N	2.15017	-0.19893	-0.28320	H	-3.89247	-1.34685	2.28520
H	2.38966	0.46419	1.69973	H	-4.32214	1.17531	0.43156
H	0.76107	-0.05157	1.30910	H	-5.43792	-0.20886	0.45853
C	1.09111	-0.94151	-0.97066	H	-4.68862	0.29262	-1.06761
H	-0.65997	-0.62395	-2.18783	H	4.43552	0.49263	1.07530
H	0.68993	0.45661	-2.55968	H	4.76165	0.40522	-0.64746
H	0.50156	-1.55655	-0.26581	C	5.80359	-1.08702	0.53688
H	1.55045	-1.62532	-1.69167	H	3.14208	-1.69079	0.89082
C	3.31858	-1.03334	0.01790	H	3.48825	-1.69558	-0.83809
C	4.58617	-0.20742	0.24471	H	5.64892	-1.68870	1.43941
C	-1.57066	0.85621	-0.17736	H	6.70279	-0.48260	0.68914
O	-1.97517	1.68207	0.63804	H	6.00107	-1.77712	-0.29107
O	-2.16644	-0.32645	-0.45543				

TS₄₁ – Acetate-assisted C–H activation

Geometry optimisation:

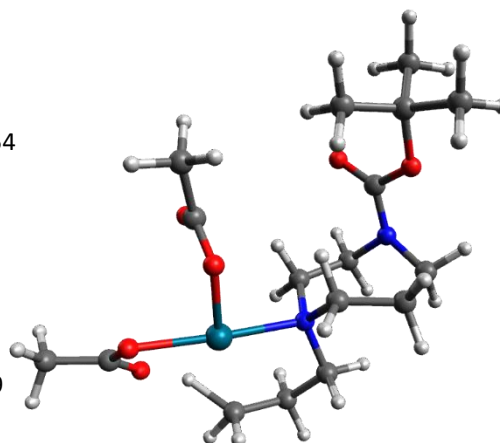
B3LYP-D3BJ/631G(d,p)/LANL2DZ-IEFPCM(DMF) Energy = -1354.90602854

Thermal correction to Gibbs Free Energy = 0.419716

Imaginary frequency = -1344.8427

Single-point energy calculation:

B3LYP-D3BJ/6311+G(2d,p)/SDD-IEFPCM(DMF) Energy = -1356.45281139



O	0.79498	2.17224	1.21885	H	-0.27355	-0.00738	1.26101
C	0.48144	2.33691	0.03275	H	-1.48796	-1.48152	2.73857
O	3.60922	1.28009	-0.58186	H	-1.10114	-2.91805	1.79339
Pd	2.00823	-0.05631	-0.45909	H	-2.47051	-1.53026	-2.19219
O	0.75711	1.52044	-0.94112	H	-1.40761	-2.91012	-2.01005
N	0.36005	-1.36631	-0.19708	H	-0.15730	-0.85121	-2.15682
C	0.86306	-2.76080	-0.38329	H	-1.09882	-0.05777	-0.91605
C	2.22125	-2.94533	0.27109	C	-0.27283	3.58386	-0.41240
C	3.21685	-1.92684	-0.28040	H	-0.82881	4.00759	0.42564
C	-0.07268	-1.07667	1.20920	H	-0.94932	3.36384	-1.24015
C	-0.68650	-1.01911	-1.21636	H	0.45093	4.32952	-0.75974
C	4.47706	1.06284	0.32039	H	-2.29315	-3.50395	0.04971
C	5.58300	2.06655	0.51661	H	-3.67451	-2.58446	-0.52129
O	4.45627	0.02759	1.06283	C	-3.09902	-0.42616	0.99184
H	0.95987	-2.91552	-1.46134	O	-2.85042	0.39844	1.86680
H	0.12928	-3.48079	-0.00884	O	-3.99307	-0.27357	-0.00616
C	-1.29066	-1.84445	1.72819	C	-4.68934	1.00788	-0.21342
C	-1.80440	-2.03580	-1.48586	C	-5.53096	0.72805	-1.45721
H	5.55719	2.43044	1.54740	C	-3.66125	2.10572	-0.48944
H	5.47996	2.90272	-0.17354	C	-5.58048	1.32392	0.98781
H	6.54704	1.57325	0.36574	H	-6.25347	0.48496	1.18877
H	3.26654	-1.95969	-1.37534	H	-6.18972	2.20515	0.76577
H	4.23422	-2.18155	0.04128	H	-4.98230	1.52063	1.87685
H	3.60577	-0.79522	0.47416	H	-3.02429	1.82125	-1.33267
H	2.56008	-3.96892	0.06786	H	-3.03434	2.28500	0.38355
H	2.14294	-2.86116	1.36012	H	-4.17756	3.03402	-0.75041
C	-2.61933	-2.50839	-0.26095	H	-4.89041	0.45448	-2.30044
N	-2.48367	-1.64831	0.91231	H	-6.10132	1.62041	-1.72849
H	0.77722	-1.27774	1.86422	H	-6.23226	-0.09023	-1.27128

TS₄₂ – Ligand-assisted C–H activation

Geometry optimisation:

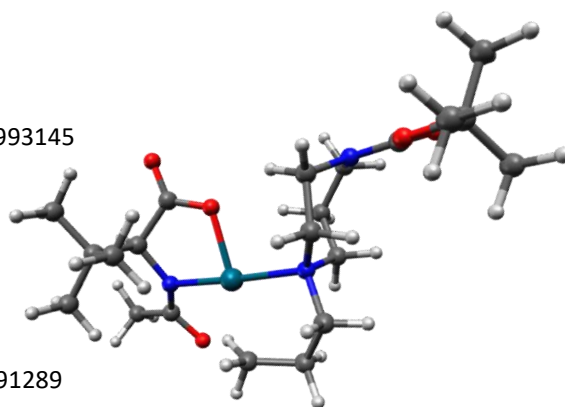
B3LYP-D3BJ/631G(d,p)/LANL2DZ-IEFPCM(DMF) Energy = -1491.10993145

Thermal correction to Gibbs Free Energy = 0.522442

Imaginary frequency = -1320.1835

Single-point energy calculation:

B3LYP-D3BJ/6311+G(2d,p)/SDD-IEFPCM(DMF) Energy = -1492.68191289



O	2.13832	2.92325	1.61411	H	6.18541	-1.13175	0.37761
C	2.14697	1.84634	1.02067	H	1.80823	-1.89857	-2.20223
C	3.45573	1.26841	0.44255	H	2.56451	-3.26259	-1.45955
H	4.24626	1.47226	1.17051	H	2.53230	-2.30768	-0.22296
C	3.85864	1.98413	-0.89639	H	0.33703	-4.01210	-2.06706
C	4.25887	3.43616	-0.58539	H	0.34419	-3.86627	-0.32143
C	5.06564	1.25507	-1.50809	C	-2.33889	-0.05869	2.43897
C	2.69890	1.97581	-1.90658	N	-2.88306	0.48833	1.19855
N	3.26158	-0.16549	0.28127	H	-2.08250	0.75263	3.13201
Pd	1.35739	-0.69380	-0.09379	H	-3.13453	-0.64592	2.89722
O	1.06194	1.14223	0.81506	H	-0.20721	-0.30518	2.09120
N	-0.71843	-1.24841	-0.32655	H	-0.94602	-1.55721	3.06722
C	-0.74520	-2.31573	-1.38026	H	-2.25901	-2.15641	0.81023
C	0.41537	-3.28666	-1.24756	H	-0.62407	-2.73865	1.12547
C	1.74781	-2.54413	-1.31859	H	-2.39471	1.77663	-0.37064
C	-1.21729	-1.83967	0.95974	H	-1.04926	1.33765	0.68112
C	-1.57351	-0.12712	-0.82794	H	-1.03212	0.32770	-1.66127
C	4.07298	-1.13823	0.64138	H	-2.50429	-0.55397	-1.22204
C	5.46642	-0.90701	1.17117	C	-4.21853	0.34828	0.94403
O	3.69659	-2.35793	0.51654	O	-4.51500	0.78553	-0.30172
H	4.56039	3.94400	-1.50743	O	-5.02928	-0.11015	1.74536
H	5.10612	3.46819	0.10877	C	-5.88760	0.72858	-0.82529
H	3.43332	3.98882	-0.13385	C	-5.72820	1.30826	-2.23030
H	5.38327	1.76651	-2.42240	C	-6.80945	1.60683	0.02175
H	4.81999	0.22173	-1.76756	C	-6.35905	-0.72486	-0.89041
H	5.91649	1.24531	-0.81925	H	-5.34588	2.33181	-2.18305
H	3.01238	2.46245	-2.83589	H	-6.69545	1.32127	-2.73979
H	1.82607	2.51306	-1.52341	H	-5.03288	0.70301	-2.81895
H	2.38734	0.95510	-2.14783	H	-5.64765	-1.32618	-1.46491
H	-0.67022	-1.80803	-2.34580	H	-7.32984	-0.77116	-1.39285
H	-1.71665	-2.82467	-1.34534	H	-6.45628	-1.14827	0.10885
C	-1.09920	-0.92770	2.18482	H	-6.40783	2.62265	0.08586
C	-1.94063	0.95571	0.18506	H	-6.91672	1.20310	1.02807
H	5.64612	-1.60238	1.99308	H	-7.79602	1.65820	-0.44844
H	5.63983	0.11234	1.51313				

TS₄₃ – Acetate-assisted β -H elimination on the heterocycle

Geometry optimisation:

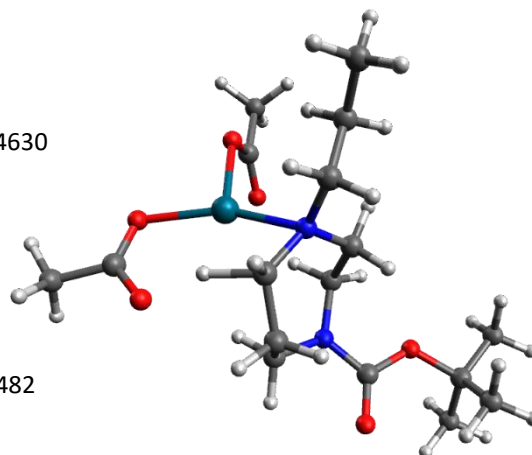
B3LYP-D3BJ/631G(d,p)/LANL2DZ-IEFPCM(DMF) Energy = -1354.90554630

Thermal correction to Gibbs Free Energy = 0.414297

Imaginary frequency = -1072.6440

Single-point energy calculation:

B3LYP-D3BJ/6311+G(2d,p)/SDD-IEFPCM(DMF) Energy = -1356.45607482



O	1.39733	0.90604	2.70420	N	-1.85509	-1.03272	0.51098
C	2.29578	1.60891	2.22056	H	-1.68091	1.09103	-1.11418
O	3.40842	-1.47601	0.54510	H	-0.64123	2.08029	-0.08291
Pd	1.98442	-0.06750	-0.09243	H	-1.85027	0.82769	1.43198
O	2.82274	1.45170	1.04375	H	-0.28439	0.03144	1.40280
N	0.38141	0.65140	-1.17281	H	-0.15926	-2.24433	0.58047
C	0.77271	1.67898	-2.19114	H	-1.61606	-2.99900	-0.08517
C	0.55340	-0.72374	-1.61958	H	-0.19247	-2.65969	-1.95931
C	-0.83636	1.06192	-0.41579	H	-1.42822	-1.41661	-2.08379
C	3.19678	-2.59740	-0.03122	C	2.87513	2.78758	2.99313
C	4.09182	-3.75366	0.34973	C	-3.20178	-1.08168	0.23413
O	2.27540	-2.80167	-0.87689	O	-3.75921	-2.06695	-0.23907
H	1.55147	-1.52805	-1.05107	O	-3.80760	0.07654	0.56471
H	3.53288	-4.42214	1.01265	C	-5.25458	0.26755	0.36395
H	4.98483	-3.40562	0.86813	C	-5.46885	1.69602	0.86204
H	4.36509	-4.32217	-0.54135	C	-6.03734	-0.72959	1.21845
C	1.21254	3.01126	-1.58743	C	-5.58862	0.15670	-1.12415
C	-0.56864	-1.74722	-1.48864	H	-4.96837	0.84876	-1.70202
H	0.96394	-0.72230	-2.62900	H	-6.63745	0.42476	-1.28171
C	1.86372	3.89475	-2.65608	H	-5.42397	-0.85705	-1.48818
H	1.91725	2.81559	-0.77227	H	-5.72801	-0.65393	2.26519
H	0.35670	3.54146	-1.15785	H	-5.87732	-1.75061	0.87315
H	2.76159	3.42017	-3.06610	H	-7.10490	-0.49770	1.15976
H	2.15665	4.85901	-2.23194	H	-5.18492	1.78334	1.91450
H	1.17691	4.08913	-3.48682	H	-6.52243	1.97021	0.76190
H	1.59995	1.25090	-2.76070	H	-4.86887	2.40022	0.27874
H	-0.07516	1.81265	-2.87473	H	2.60306	3.72103	2.48971
C	-1.02714	-2.08365	-0.06652	H	3.96695	2.73308	3.00981
C	-1.18630	0.22537	0.81480	H	2.48901	2.80309	4.01303

TS₄₄ – Ligand-assisted β -H elimination on the heterocycle

Geometry optimisation:

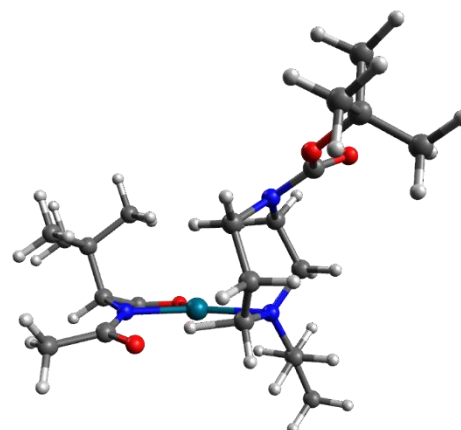
B3LYP-D3BJ/631G(d,p)/LANL2DZ-IEFPCM(DMF) Energy = -1491.10058784

Thermal correction to Gibbs Free Energy = 0.518445

Imaginary frequency = -1059.1942

Single-point energy calculation:

B3LYP-D3BJ/6311+G(2d,p)/SDD-IEFPCM(DMF) Energy = -1492.67732136



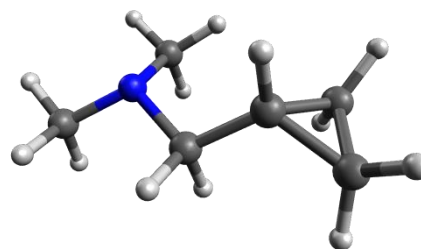
O	4.91909	0.25643	-1.62534	C	0.84284	4.07775	-0.45877
C	3.84667	0.10274	-1.04102	C	1.25411	5.48069	-0.00259
C	3.62363	-1.12159	-0.11806	H	0.56795	3.36699	1.54632
H	4.57170	-1.33166	0.38887	H	-0.93205	3.92870	0.79325
C	3.24856	-2.38862	-0.97648	H	0.28782	4.15212	-1.39965
C	4.45399	-2.78105	-1.84769	H	1.73121	3.46815	-0.65810
C	2.91261	-3.56566	-0.04734	H	0.37813	6.10844	0.19225
C	2.03043	-2.10978	-1.87301	H	1.85669	5.97502	-0.76936
N	2.58988	-0.74862	0.83288	H	1.84818	5.43819	0.91663
Pd	1.33818	0.68338	0.21674	N	-2.35844	-0.41299	-0.68893
O	2.83065	0.91450	-1.19577	H	-1.41655	-0.38194	2.57557
N	-0.33304	1.96677	0.28065	H	-2.52476	0.69246	1.73507
C	-1.35731	1.88169	-0.79317	H	-2.31860	2.23448	-0.40044
C	-0.42591	1.08437	1.44755	H	-1.03671	2.58381	-1.56243
C	0.00363	3.38408	0.61152	H	-0.55887	0.05028	-1.63478
C	2.39994	-1.11220	2.09084	H	-2.02107	0.67140	-2.41183
C	3.35705	-2.02366	2.82254	H	-2.43833	-1.72876	0.91493
O	1.39324	-0.67620	2.74703	H	-0.81898	-1.40962	0.29768
H	4.21530	-3.67885	-2.42734	C	-3.71849	-0.33237	-0.88126
H	5.32903	-3.00441	-1.22711	O	-4.23211	0.31510	-1.78861
H	4.72806	-1.98137	-2.53761	O	-4.38500	-1.06217	0.03342
H	2.67672	-4.45026	-0.64768	C	-5.85666	-1.13922	0.02581
H	2.04316	-3.34900	0.57895	C	-6.14305	-2.04915	1.21933
H	3.75571	-3.82029	0.60172	C	-6.33912	-1.78145	-1.27501
H	1.77111	-3.01080	-2.43830	C	-6.44855	0.25264	0.25043
H	2.22588	-1.30515	-2.58693	H	-5.84895	-2.74843	-1.42267
H	1.16090	-1.82472	-1.27354	H	-6.12658	-1.14063	-2.13027
H	0.62134	0.24978	1.79320	H	-7.41843	-1.95076	-1.21718
H	3.56981	-1.58169	3.79844	H	-6.03569	0.69482	1.16226
H	4.29202	-2.18556	2.28714	H	-7.53278	0.17088	0.37078
H	2.87945	-2.99235	2.99253	H	-6.23485	0.91007	-0.59184
H	-0.28910	1.67873	2.35227	H	-5.67849	-3.02881	1.07643
C	-1.59503	0.12230	1.62086	H	-7.22175	-2.18854	1.32958
C	-1.78171	-0.94738	0.54049	H	-5.75286	-1.60845	2.14103
C	-1.53378	0.51165	-1.45094				

III.VI. Nuclear coordinates for complexes containing 1-cyclopropyl-*N,N*-dimethylmethanamine**362 – 1-Cyclopropyl-*N,N*-dimethylmethanamine**

Geometry optimisation:

B3LYP-D3BJ/631G(d,p)/LANL2DZ-IEFPCM(DMF) Energy = -291.218432290

Thermal correction to Gibbs Free Energy = 0.147942



Single-point energy calculation:

B3LYP-D3BJ/6311+G(2d,p)-IEFPCM(DMF) Energy = -291.289862396

N	1.29601	-0.03121	-0.35473	C	-1.17904	-0.23407	-0.49624
C	0.10533	-0.73460	0.12488	C	-2.49370	-0.60752	0.14215
C	2.50751	-0.69607	0.10922	H	0.01686	-0.67930	1.22995
C	1.30219	1.37489	0.03345	H	0.23356	-1.79558	-0.12366
H	2.60485	-0.69842	1.21199	C	-2.01384	0.82136	0.18947
H	3.38752	-0.19295	-0.30321	H	-1.16123	-0.20490	-1.58342
H	2.51578	-1.73611	-0.23149	H	-2.52072	1.55809	-0.42600
H	1.29208	1.51566	1.13183	H	-1.65583	1.20172	1.14196
H	0.43000	1.88454	-0.37918	H	-2.45948	-1.18302	1.06329
H	2.20208	1.85764	-0.35967	H	-3.32826	-0.85279	-0.50690

A₈ – Bisamine complex

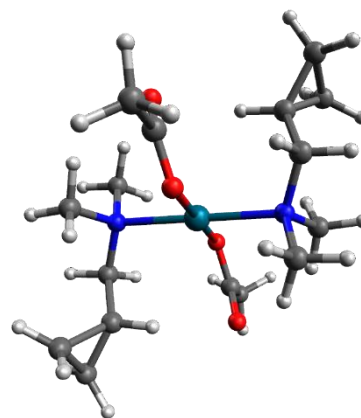
Geometry optimisation:

B3LYP-D3BJ/631G(d,p)/LANL2DZ-IEFPCM(DMF) Energy = -1166.29742074

Thermal correction to Gibbs Free Energy = 0.408852

Single-point energy calculation:

B3LYP-D3BJ/6311+G(2d,p)/SDD-IEFPCM(DMF) Energy = -1167.77935393



Pd	0.00000	0.00000	0.00000	O	1.61324	2.45338	-0.99192
O	0.62232	1.73425	0.90504	C	-3.28302	0.31713	0.54905
N	1.53885	-0.99088	1.13591	H	-2.78374	-0.67884	-1.28183
O	-0.62232	-1.73425	-0.90504	H	-3.61214	0.86839	-1.50356
N	-1.53885	0.99088	-1.13591	C	-4.74679	0.12912	0.86719
C	1.15410	-0.81210	2.55885	H	-0.19082	1.29691	-2.71767
H	0.19082	-1.29691	2.71767	H	-1.90934	1.26461	-3.21464
H	1.07304	0.25401	2.76847	H	-1.07304	-0.25401	-2.76847
H	1.90934	-1.26461	3.21464	C	3.28302	-0.31713	-0.54905
C	2.86338	-0.33797	0.89745	H	0.71805	-2.92536	1.16489
C	1.63643	-2.44178	0.84270	H	2.48509	-2.86571	1.39358
C	-1.63643	2.44178	-0.84270	H	1.77965	-2.59480	-0.22347
H	-0.71805	2.92536	-1.16489	C	4.74679	-0.12912	-0.86720
H	-1.77965	2.59480	0.22347	H	2.78374	0.67884	1.28183
H	-2.48509	2.86571	-1.39358	H	3.61214	-0.86839	1.50355
C	-2.86337	0.33797	-0.89745	C	4.07749	-1.44941	-1.15384
C	-1.15410	0.81210	-2.55885	H	3.87735	-1.71592	-2.18707
C	-1.32318	-2.57881	-0.20486	H	4.33376	-2.28994	-0.51591
O	-1.61324	-2.45338	0.99192	H	5.44581	-0.08821	-0.03634
C	-1.74341	-3.80830	-0.99617	H	5.00408	0.51615	-1.70096
H	-2.49902	-4.37366	-0.44938	H	2.58654	0.20679	-1.19638
H	-0.86741	-4.44642	-1.15536	C	-4.07749	1.44941	1.15384
H	-2.12421	-3.52358	-1.98016	H	-5.00408	-0.51615	1.70096
C	1.32318	2.57881	0.20486	H	-5.44581	0.08821	0.03633
C	1.74341	3.80831	0.99617	H	-3.87736	1.71592	2.18707
H	0.86741	4.44642	1.15536	H	-4.33376	2.28994	0.51591
H	2.49902	4.37366	0.44938	H	-2.58654	-0.20679	1.19638
H	2.12421	3.52358	1.98016				

A₉ – Bidentate ligand-amine complex

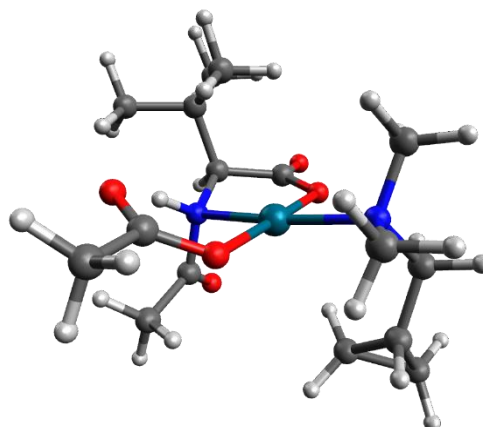
Geometry optimisation:

B3LYP-D3BJ/631G(d,p)/LANL2DZ-IEFPCM(DMF) Energy = -1240.38012218

Thermal correction to Gibbs Free Energy = 0.392495

Single-point energy calculation:

B3LYP-D3BJ/6311+G(2d,p)/SDD-IEFPCM(DMF) Energy = -1241.89098060



Pd	0.45351	0.14002	-0.23047	O	-1.24310	2.79868	0.03997
O	-0.04594	-1.81789	-0.34233	C	0.49146	4.45590	-0.07751
N	-1.32957	0.20464	0.91840	H	1.32995	4.55503	-0.76976
O	0.91658	2.13483	-0.09526	H	0.85170	4.71657	0.92357
N	2.14199	-0.21830	-1.45079	H	-0.31149	5.14171	-0.34977
C	-1.26978	-2.10705	0.03428	C	2.96456	-1.29360	-0.80342
O	-1.69947	-3.25564	0.05212	C	2.95463	0.99693	-1.69161
C	-2.17452	-0.92728	0.43977	C	1.62134	-0.72607	-2.74784
C	-3.16317	-0.48005	-0.68059	H	0.99953	-1.60050	-2.56074
C	-2.43328	-0.01225	-1.95187	H	2.45610	-0.99520	-3.40627
C	-4.04605	0.66330	-0.14114	H	1.02325	0.05302	-3.22159
C	-4.07527	-1.67094	-1.02782	H	-1.11592	2.23922	2.66797
H	-3.50972	-2.50595	-1.44396	H	0.54022	1.67888	2.45825
H	-4.82012	-1.35245	-1.76346	H	-0.32639	1.28694	3.96609
H	-4.60667	-2.03320	-0.14171	H	3.82705	0.73507	-2.30182
H	-1.83784	0.88655	-1.76902	H	3.27562	1.42488	-0.74547
H	-3.16800	0.22910	-2.72677	H	2.34618	1.73478	-2.21136
H	-1.77306	-0.79088	-2.34519	C	3.47711	-0.94919	0.57119
H	-3.48237	1.58405	0.03008	C	3.84954	-2.08688	1.49197
H	-4.53531	0.37437	0.79505	H	3.80180	-1.51262	-1.48108
H	-4.82729	0.89531	-0.87152	H	2.32780	-2.17837	-0.74921
C	-0.92159	0.12686	2.28714	C	2.64067	-1.24028	1.79693
H	-2.76982	-1.27499	1.28699	H	4.12521	-0.07952	0.62581
C	-0.43029	1.41797	2.88978	H	1.66484	-1.68795	1.64227
O	-0.96769	-0.93419	2.88047	H	2.69168	-0.53841	2.62309
H	-1.61124	1.16191	0.63161	H	4.73736	-1.97050	2.10489
C	-0.02076	3.02774	-0.05356	H	3.67784	-3.09926	1.13742

TS₄₇ – Ligand-assisted C–H activation (major enantiomer)

Geometry optimisation:

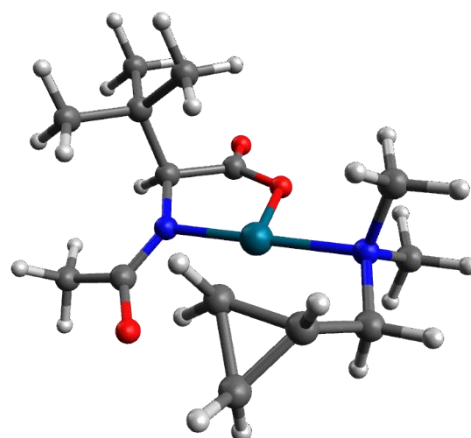
B3LYP-D3BJ/631G(d,p)/LANL2DZ-IEFPCM(DMF) Energy = -1011.20942385

Thermal correction to Gibbs Free Energy = 0.334309

Imaginary frequency = -940.7264

Single-point energy calculation:

B3LYP-D3BJ/6311+G(2d,p)/SDD-IEFPCM(DMF) Energy = -1012.64713405



O	2.45186	-2.26693	-1.55257	H	3.72139	0.88865	2.51472
C	1.67646	-1.45984	-1.04034	H	2.33406	1.64008	1.71398
C	2.19833	-0.12646	-0.45878	H	3.90961	1.58058	0.89900
H	2.97960	0.23296	-1.13474	H	2.39071	-1.18824	2.88992
C	2.86437	-0.34135	0.94909	H	1.66195	-2.07498	1.54200
C	4.15445	-1.16033	0.77491	H	0.98137	-0.52163	2.04733
C	3.22439	1.02739	1.54914	H	3.13797	2.15862	-1.50389
C	1.91482	-1.07614	1.91021	H	2.64173	3.47127	-0.42424
N	1.07827	0.80678	-0.41581	H	2.04612	3.43816	-2.08656
Pd	-0.68580	-0.11953	-0.15634	H	-1.32796	1.79517	1.78726
O	0.39197	-1.68561	-0.92799	H	-0.97156	1.97320	-0.09335
N	-2.51825	-1.17455	-0.00590	H	-3.57177	0.89043	1.91279
C	-3.56255	-0.10571	-0.05794	C	-2.99184	2.38661	0.42682
C	-3.20075	1.00288	0.89841	H	-3.11195	2.59458	-0.63262
C	-1.75557	1.53822	0.82138	H	-3.24486	3.20988	1.08673
C	-2.69066	-2.12924	-1.12223	H	-4.54813	-0.53712	0.16313
C	-2.55589	-1.90027	1.28502	H	-3.57563	0.26775	-1.08458
C	1.07105	2.07397	-0.78075	H	-1.75741	-2.64320	1.29545
C	2.31036	2.81216	-1.23212	H	-3.52366	-2.40328	1.41057
O	-0.01313	2.75457	-0.74517	H	-2.40095	-1.20098	2.10594
H	4.64053	-1.29858	1.74637	H	-1.86683	-2.84218	-1.10566
H	4.86058	-0.64234	0.11621	H	-2.66791	-1.58378	-2.06665
H	3.94895	-2.14072	0.34216	H	-3.64688	-2.65906	-1.02894

TS₄₈ – Ligand-assisted C–H activation (major enantiomer)

Geometry optimisation:

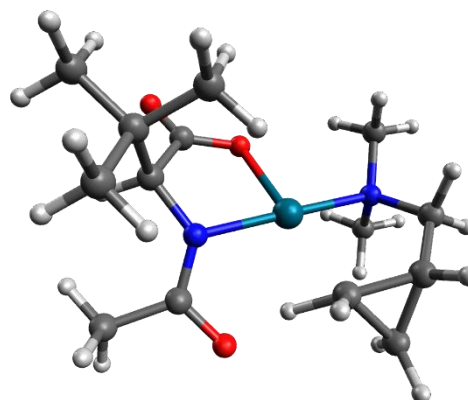
B3LYP-D3BJ/631G(d,p)/LANL2DZ-IEFPCM(DMF) Energy = -1011.19988749

Thermal correction to Gibbs Free Energy = 0.333709

Imaginary frequency = -935.8338

Single-point energy calculation:

B3LYP-D3BJ/6311+G(2d,p)/SDD-IEFPCM(DMF) Energy = -1012.63840447



O	2.44595	-2.29791	-1.49834	H	3.75248	0.94375	2.49110
C	1.67488	-1.47518	-1.00508	H	2.35667	1.67236	1.68094
C	2.20678	-0.13597	-0.44244	H	3.92573	1.59579	0.85649
H	2.98175	0.21242	-1.13130	H	2.42394	-1.13439	2.92185
C	2.88423	-0.32527	0.96113	H	1.68687	-2.04668	1.59577
C	4.17248	-1.14810	0.79336	H	1.00886	-0.48384	2.07631
C	3.24733	1.05746	1.52646	H	-3.14037	-1.09127	1.93672
C	1.94162	-1.04073	1.94332	H	-4.42640	-0.61591	0.82623
N	1.08895	0.79890	-0.40426	H	-2.57871	-1.30784	-2.16455
Pd	-0.67490	-0.10980	-0.12084	H	-3.32836	0.18530	-1.56928
O	0.38664	-1.68505	-0.90218	H	-4.19171	-1.36281	-1.39956
N	-2.55453	-1.09725	-0.06631	H	-1.87410	-2.71672	1.10212
C	-3.35649	-0.50062	1.04426	H	-1.76458	-2.95782	-0.65040
C	-2.99005	0.93403	1.36159	H	-3.35725	-3.05602	0.16350
C	-1.68566	1.57947	0.85999	H	3.12229	2.12133	-1.57177
C	-3.20631	-0.87996	-1.38201	H	2.58598	3.47511	-0.56665
C	-2.38199	-2.55396	0.15110	H	2.01725	3.34976	-2.23499
C	1.04743	2.03367	-0.87257	H	-1.15064	2.12187	1.63539
C	2.27831	2.77191	-1.34665	H	-1.01119	1.87718	-0.17610
O	-0.05682	2.67783	-0.90719	H	-3.16957	1.15475	2.41100
H	4.66654	-1.26693	1.76338	C	-3.08441	2.12091	0.48244
H	4.87339	-0.64411	0.11841	H	-3.36781	2.00380	-0.55840
H	3.96261	-2.13690	0.38228	H	-3.39405	3.06215	0.92624

TS₄₉ – Ligand-assisted C–H activation (minor enantiomer)

Geometry optimisation:

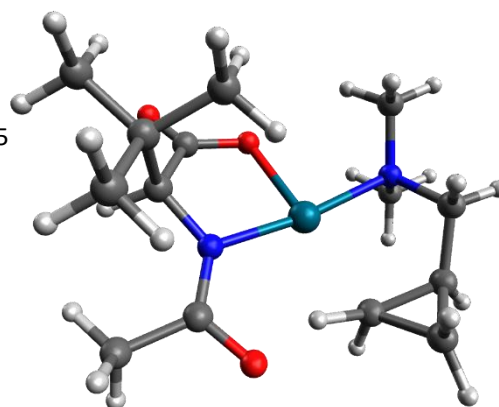
B3LYP-D3BJ/631G(d,p)/LANL2DZ-IEFPCM(DMF) Energy = -1011.20061195

Thermal correction to Gibbs Free Energy = 0.334976

Imaginary frequency = -947.0548

Single-point energy calculation:

B3LYP-D3BJ/6311+G(2d,p)/SDD-IEFPCM(DMF) Energy = -1012.63836876



O	2.35797	-2.31980	-1.61048	H	3.76744	0.77512	2.47450
C	1.63484	-1.50553	-1.03876	H	2.48064	1.65214	1.64728
C	2.18910	-0.16958	-0.51419	H	4.05556	1.42152	0.85679
H	2.99627	0.14170	-1.18443	H	2.26516	-1.11332	2.88319
C	2.82082	-0.38814	0.91804	H	1.46135	-1.98426	1.56601
C	4.03540	-1.32408	0.78464	H	0.92396	-0.35841	2.00436
C	3.30522	0.95025	1.49771	H	-2.67321	-2.12229	-1.70138
C	1.80383	-1.00062	1.89664	H	-3.49750	-0.55631	-1.56272
N	1.09319	0.79897	-0.52579	H	-4.19233	-1.99861	-0.77079
Pd	-0.71630	-0.07611	-0.29339	H	-1.52619	-2.23122	1.74512
O	0.37142	-1.73797	-0.77972	H	-1.48986	-3.05371	0.17450
N	-2.46431	-1.19090	0.17069	H	-3.00906	-3.01047	1.12362
C	-3.19582	-0.28617	1.10987	H	3.27763	2.14249	-1.30512
C	-3.35182	1.06337	0.46200	H	2.83757	3.43942	-0.17523
C	-2.11236	1.68093	-0.21114	H	2.23354	3.48142	-1.83173
C	-3.26175	-1.48323	-1.04210	H	-2.34764	2.14647	-1.16604
C	-2.10346	-2.45634	0.84740	H	-0.90350	2.01176	-0.07085
C	1.20449	2.11427	-0.58955	C	-2.78753	2.31248	1.02227
C	2.48033	2.81741	-0.99918	H	-4.25309	1.18491	-0.13201
O	0.20070	2.86386	-0.35316	H	-2.58868	-0.21538	2.01568
H	4.50997	-1.45490	1.76258	H	-4.16370	-0.73135	1.37744
H	4.78200	-0.90258	0.10241	H	-2.22149	2.24805	1.94731
H	3.74932	-2.30552	0.40288	H	-3.33516	3.23922	0.88333

TS₅₀ – Ligand-assisted C–H activation (minor enantiomer)

Geometry optimisation:

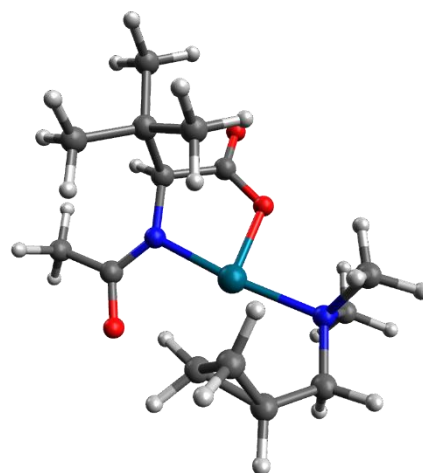
B3LYP-D3BJ/631G(d,p)/LANL2DZ-IEFPCM(DMF) Energy = -1011.18927119

Thermal correction to Gibbs Free Energy = 0.333940

Imaginary frequency = -1247.7196

Single-point energy calculation:

B3LYP-D3BJ/6311+G(2d,p)/SDD-IEFPCM(DMF) Energy = -1012.62775810



O	2.22742	-2.52190	-1.33923	H	3.75348	0.84673	2.46046
C	1.53561	-1.59962	-0.91474	H	2.47244	1.66537	1.55707
C	2.17241	-0.27391	-0.44373	H	4.04579	1.35810	0.79384
H	2.99144	-0.04442	-1.13242	H	2.20019	-1.03385	2.98927
C	2.79323	-0.42550	0.99283	H	1.39134	-1.95123	1.70935
C	3.98930	-1.39014	0.92629	H	0.88888	-0.29071	2.05817
C	3.29210	0.94686	1.47280	H	3.31965	1.89504	-1.57814
C	1.75323	-0.95841	1.99272	H	2.87366	3.31088	-0.61205
N	1.13923	0.75108	-0.50700	H	2.34054	3.19952	-2.29261
Pd	-0.71556	0.02848	-0.26062	H	-0.83076	1.96633	-0.33168
O	0.23077	-1.69365	-0.80083	H	-4.00120	2.03432	0.88374
N	-2.59563	-0.95619	-0.11941	C	-2.19157	1.33585	1.93513
C	-3.68330	0.04147	0.12634	H	-1.74880	0.41573	2.29766
C	-3.20468	1.29593	0.81288	H	-2.34815	2.07374	2.71741
C	-1.82219	1.84776	0.55222	H	-1.64982	-2.59507	0.80273
C	-2.82834	-1.66687	-1.40267	H	-3.42951	-2.57498	0.97891
C	-2.52050	-1.96090	0.97141	H	-2.42537	-1.46142	1.93369
C	1.23156	1.99212	-0.94151	H	-2.83707	-0.94265	-2.21787
C	2.52932	2.61979	-1.38697	H	-3.78759	-2.19837	-1.37347
O	0.18263	2.72344	-0.97985	H	-2.01584	-2.37567	-1.56039
H	4.44835	-1.47921	1.91634	H	-4.49278	-0.44580	0.68436
H	4.75303	-1.01917	0.23364	H	-4.08653	0.32811	-0.84870
H	3.68562	-2.38296	0.59057	H	-1.80402	2.93757	0.51511

TS₅₁ – Ligand-assisted *trans*-C–H activation

Geometry optimisation:

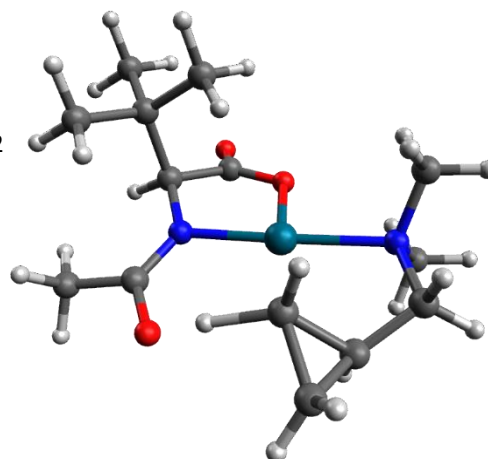
B3LYP-D3BJ/631G(d,p)/LANL2DZ-IEFPCM(DMF) Energy = -1011.18899242

Thermal correction to Gibbs Free Energy = 0.334786

Imaginary frequency = -997.2578

Single-point energy calculation:

B3LYP-D3BJ/6311+G(2d,p)/SDD-IEFPCM(DMF) Energy = -1012.62528071



O	2.33918	-2.22421	-1.72112	H	3.89377	0.72072	2.40807
C	1.60736	-1.45396	-1.09851	H	2.52192	1.57700	1.70045
C	2.17741	-0.13989	-0.51880	H	4.05267	1.44931	0.80724
H	2.93517	0.22075	-1.21948	H	2.48490	-1.27166	2.80198
C	2.89810	-0.41132	0.85578	H	1.63780	-2.09263	1.48050
C	4.13509	-1.29032	0.60065	H	1.06819	-0.51834	2.04877
C	3.36381	0.91830	1.47090	H	-3.80413	-0.13544	1.52952
C	1.96273	-1.11714	1.85217	H	-4.60534	-0.52609	-0.00566
N	1.07947	0.82320	-0.39993	H	-1.97860	-2.49664	-1.39466
Pd	-0.69507	-0.09036	-0.11049	H	-2.99266	-1.14035	-1.92620
O	0.35092	-1.70583	-0.84777	H	-3.73897	-2.50973	-1.06109
N	-2.57478	-1.19308	0.14370	H	-2.18164	-1.67194	2.15736
C	-3.66797	-0.18635	0.44747	H	-1.60662	-2.86407	0.97002
C	-3.13176	1.10794	-0.09057	H	-3.34647	-2.76596	1.35921
C	-1.85648	1.53590	0.67337	H	3.17785	2.17584	-1.41466
C	-2.84221	-1.88205	-1.14003	H	2.79572	3.44398	-0.23450
C	-2.42319	-2.18722	1.22647	H	2.09923	3.52099	-1.85407
C	1.16266	2.11555	-0.57843	H	-1.87652	1.19652	1.71143
C	2.39558	2.83993	-1.05309	H	-0.72680	2.27615	0.10344
O	0.14175	2.88993	-0.35992	H	-3.00435	1.08660	-1.17206
H	4.66431	-1.46414	1.54320	C	-3.07435	2.46930	0.47371
H	4.82968	-0.79893	-0.08965	H	-3.01213	3.29341	-0.23236
H	3.86053	-2.25459	0.17023	H	-3.60259	2.70385	1.39320

TS₅₂ – Ligand-assisted *trans*-C–H activation

Geometry optimisation:

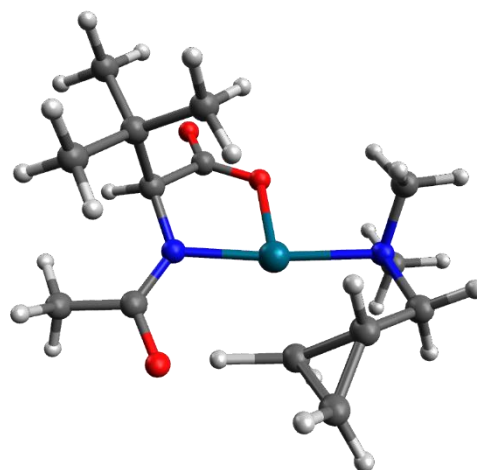
B3LYP-D3BJ/631G(d,p)/LANL2DZ-IEFPCM(DMF) Energy = -1011.18839971

Thermal correction to Gibbs Free Energy = 0.334468

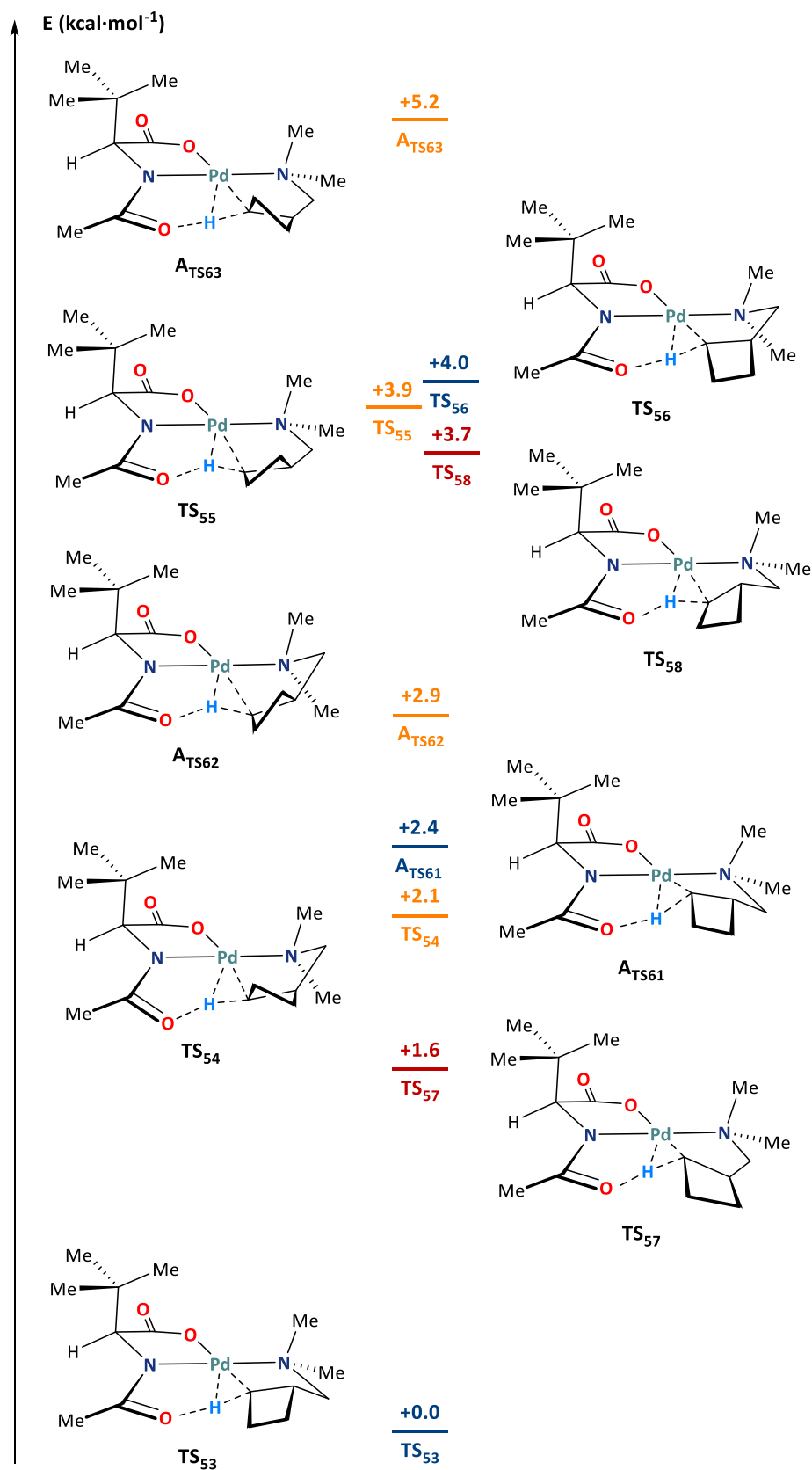
Imaginary frequency = -1047.0840

Single-point energy calculation:

B3LYP-D3BJ/6311+G(2d,p)/SDD-IEFPCM(DMF) Energy = -1012.62475225



O	2.35532	-2.38802	-1.52122	H	3.65686	0.76094	2.55379
C	1.60699	-1.55855	-1.00300	H	2.40008	1.62486	1.66583
C	2.17506	-0.22862	-0.46103	H	3.99820	1.37020	0.93188
H	3.00851	0.05587	-1.10861	H	2.13008	-1.13905	2.94239
C	2.75387	-0.43180	0.99114	H	1.35944	-2.00857	1.60469
C	3.96550	-1.37722	0.91180	H	0.82376	-0.37593	2.01882
C	3.22587	0.91623	1.55967	H	3.35852	1.98479	-1.37343
C	1.70056	-1.02626	1.94164	H	2.91896	3.34896	-0.32781
N	1.11049	0.77822	-0.50987	H	2.38259	3.32964	-2.00852
Pd	-0.71263	-0.06054	-0.29393	H	-2.54648	1.56243	-0.96086
O	0.32792	-1.75643	-0.82962	H	-0.69269	2.32673	-0.30856
N	-2.61277	-1.10120	0.04981	C	-2.79279	2.47520	0.96539
C	-3.57597	-0.10036	0.66276	H	-2.05378	0.71851	1.97797
C	-2.69832	1.01640	1.15316	H	-3.69364	2.91180	0.54384
C	-1.95382	1.66968	-0.04853	H	-2.29046	3.09905	1.69988
C	-3.13686	-1.67791	-1.20577	H	-2.39138	-2.36130	-1.61528
C	-2.29978	-2.18183	1.01343	H	-3.31914	-0.87571	-1.92251
C	1.27006	2.05685	-0.73607	H	-4.07172	-2.22422	-1.02598
C	2.57364	2.69977	-1.13654	H	-1.51361	-2.81036	0.59451
O	0.27655	2.88742	-0.64557	H	-3.19240	-2.78648	1.21869
H	4.40205	-1.50078	1.90818	H	-1.94143	-1.74314	1.94625
H	4.73984	-0.96821	0.25343	H	-4.16438	-0.59817	1.44014
H	3.68484	-2.35978	0.52923	H	-4.25820	0.25034	-0.11384

III.VII. Nuclear coordinates for complexes containing 1-cyclobutyl-*N,N*-dimethylmethanamine

Scheme 74: Transition states leading to an asymmetric C(sp³)-H activation of cyclobutane rings in amine **442** and using acetyl-*tert*-leucine as ligand. Energy values in kcal·mol⁻¹.

442 – 1-Cyclobutyl-*N,N*-dimethylmethanamine

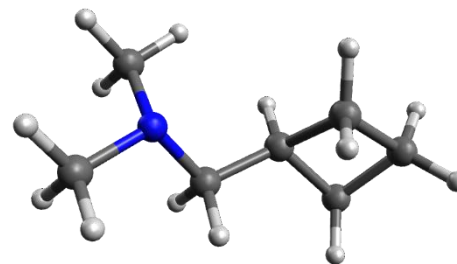
Geometry optimisation:

B3LYP-D3BJ/631G(d,p)/LANL2DZ-IEFPCM(DMF) Energy = -330.543622002

Thermal correction to Gibbs Free Energy = 0.175037

Single-point energy calculation:

B3LYP-D3BJ/6311+G(2d,p)-IEFPCM(DMF) Energy = -330.622506653



N	-1.57626	0.08218	0.27400	H	-0.74639	-1.04764	-1.33865
C	-0.47693	-0.67619	-0.32789	H	-0.31270	-1.56263	0.29746
C	-2.71950	-0.78618	0.52868	C	2.85983	0.19430	0.34208
C	-1.97581	1.22134	-0.54462	H	2.50320	-0.69398	-1.72776
H	-3.14497	-1.22388	-0.39486	H	2.04587	-1.73087	-0.35747
H	-3.51225	-0.21966	1.02710	C	1.47476	0.58350	0.92238
H	-2.42173	-1.60973	1.18495	H	0.74376	0.93631	-1.10554
H	-2.31230	0.92567	-1.55717	H	3.35380	1.04791	-0.13221
H	-1.14712	1.92445	-0.65512	H	3.57393	-0.29331	1.01151
H	-2.80052	1.74948	-0.05680	H	1.18612	-0.06596	1.75565
C	0.82700	0.10093	-0.40196	H	1.31523	1.62349	1.22007
C	2.12896	-0.69351	-0.70020				

A₁₀ – Bisamine complex

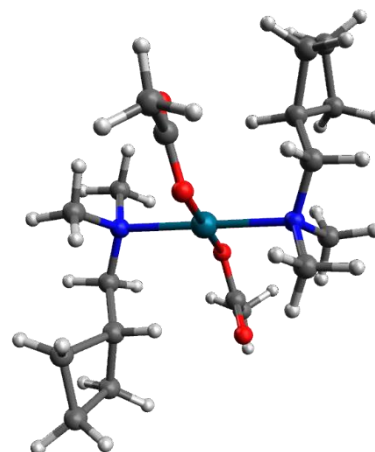
Geometry optimisation:

B3LYP-D3BJ/631G(d,p)/LANL2DZ-IEFPCM(DMF) Energy = -1244.94845792

Thermal correction to Gibbs Free Energy = 0.463466

Single-point energy calculation:

B3LYP-D3BJ/6311+G(2d,p)/SDD-IEFPCM(DMF) Energy = -1246.44596411



Pd	0.00002	0.00001	0.00003	H	-3.38393	0.86969	-1.96235
O	0.55148	1.74772	0.92792	C	-4.66176	-0.46668	0.27391
N	1.37491	-0.98460	1.33504	H	0.16542	1.25127	-2.73922
O	-0.55145	-1.74771	-0.92783	H	-1.47855	1.23254	-3.44717
N	-1.37485	0.98464	-1.33498	H	-0.72564	-0.28881	-2.87975
C	0.81728	-0.78112	2.69623	C	3.34457	-0.33991	-0.13069
H	-0.16528	-1.25112	2.73938	H	0.54184	-2.91489	1.29745
H	0.72582	0.28895	2.87977	H	2.27277	-2.86123	1.72399
H	1.47873	-1.23238	3.44723	H	1.75157	-2.61239	0.03436
C	2.72325	-0.34856	1.25372	C	4.66171	0.46659	-0.27420
C	1.49424	-2.44036	1.07615	H	2.60703	0.67732	1.60326
C	-1.49424	2.44037	-1.07601	H	3.38405	-0.86973	1.96224
H	-0.54187	2.91496	-1.29729	C	-4.09645	1.57868	0.69451
H	-1.75157	2.61234	-0.03422	C	-5.16865	0.61428	1.26421
H	-2.27280	2.86124	-1.72382	H	-4.50101	2.20035	-0.11139
C	-2.72317	0.34854	-1.25378	H	-3.56319	2.22225	1.40004
C	-0.81713	0.78125	-2.69615	H	-6.21603	0.91925	1.19190
C	-1.34802	-2.55945	-0.29363	H	-4.95323	0.34106	2.30167
O	-1.74986	-2.41096	0.86733	H	-4.56900	-1.49720	0.62513
C	-1.74193	-3.77552	-1.11901	H	-5.23848	-0.45785	-0.65798
H	-2.50633	-4.35622	-0.60153	H	-2.61288	-0.03522	0.85136
H	-0.86004	-4.40376	-1.28185	C	5.16847	-0.61442	-1.26453
H	-2.10814	-3.46773	-2.10225	H	5.23855	0.45781	0.65761
C	1.34804	2.55950	0.29375	H	4.56892	1.49709	-0.62546
C	1.74193	3.77553	1.11920	C	4.09629	-1.57877	-0.69471
H	0.86001	4.40370	1.28215	H	2.61276	0.03516	-0.85139
H	2.50626	4.35632	0.60170	H	3.56291	-2.22231	-1.40019
H	2.10823	3.46769	2.10238	H	4.50088	-2.20048	0.11115
O	1.74988	2.41107	-0.86721	H	6.21585	-0.91942	-1.19232
C	-3.34462	0.33985	0.13057	H	4.95296	-0.34122	-2.30199
H	-2.60687	-0.67734	-1.60333				

A11 – Bidentate ligand-amine complex

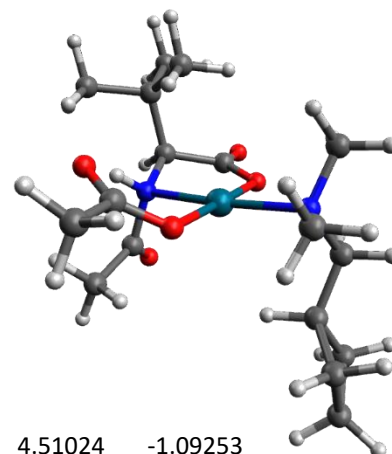
Geometry optimisation:

B3LYP-D3BJ/631G(d,p)/LANL2DZ-IEFPCM(DMF) Energy = -1279.70329417

Thermal correction to Gibbs Free Energy = 0.418068

Single-point energy calculation:

B3LYP-D3BJ/6311+G(2d,p)/SDD-IEFPCM(DMF) Energy = -1281.22316021



Pd	0.16285	0.10590	-0.26847	H	0.89016	4.51024	-1.09253
O	-0.31252	-1.85927	-0.26797	H	0.63833	4.71407	0.64321
N	-1.53142	0.19807	0.99945	H	-0.68671	5.10056	-0.47787
O	0.60335	2.11212	-0.24180	C	2.67318	-1.26084	-0.94072
N	1.76624	-0.26958	-1.59890	C	2.50150	0.95669	-1.98721
C	-1.50367	-2.14601	0.20326	C	1.16683	-0.88728	-2.81097
O	-1.91755	-3.29702	0.29307	H	0.60253	-1.77064	-2.51600
C	-2.39315	-0.96014	0.62427	H	1.95769	-1.16681	-3.51730
C	-3.45787	-0.56543	-0.44486	H	0.49749	-0.16748	-3.28346
C	-2.81616	-0.13982	-1.77716	H	-1.23993	2.30243	2.65788
C	-4.31756	0.58917	0.10787	H	0.40786	1.76570	2.34734
C	-4.37653	-1.77697	-0.68702	H	-0.33901	1.41361	3.92763
H	-3.82882	-2.62325	-1.10419	H	3.33831	0.68582	-2.64131
H	-5.16934	-1.49454	-1.38638	H	2.86987	1.46556	-1.10167
H	-4.84762	-2.10759	0.24445	H	1.82260	1.62628	-2.51284
H	-2.21448	0.76667	-1.66601	C	3.30409	-0.79693	0.36097
H	-3.60183	0.07227	-2.50947	H	3.45658	-1.53266	-1.66266
H	-2.17947	-0.92975	-2.18630	H	2.06501	-2.14763	-0.74893
H	-3.75605	1.52177	0.20572	C	4.11319	-1.87534	1.13227
H	-4.74004	0.33194	1.08496	C	4.57766	0.09685	0.37328
H	-5.14838	0.78415	-0.57720	C	5.12809	-0.77327	1.53201
C	-1.03250	0.18151	2.34067	H	2.53586	-0.37088	1.01630
H	-2.92682	-1.27935	1.52222	H	4.44766	1.16661	0.55845
C	-0.52288	1.50255	2.85771	H	5.16162	-0.03306	-0.54386
O	-1.02958	-0.85310	2.97991	H	4.55930	-2.60051	0.44296
H	-1.84696	1.13991	0.69650	H	3.59442	-2.41876	1.92653
C	-0.34106	2.99568	-0.17032	H	4.88891	-0.34141	2.50833
O	-1.55023	2.75705	0.01902	H	6.18988	-1.03149	1.51210
C	0.15000	4.42613	-0.29385				

TS₅₃ – Ligand-assisted C–H activation (major enantiomer)

Geometry optimisation:

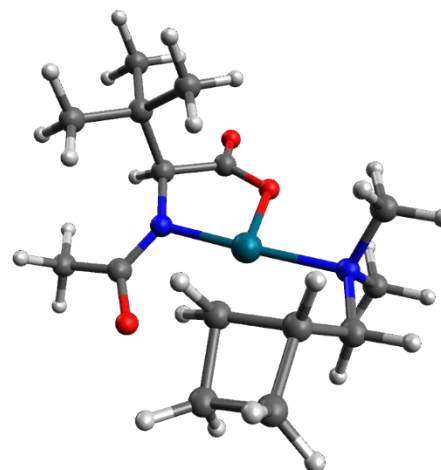
B3LYP-D3BJ/631G(d,p)/LANL2DZ-IEFPCM(DMF) Energy = -1050.52662338

Thermal correction to Gibbs Free Energy = 0.361992

Imaginary frequency = -1237.6546

Single-point energy calculation:

B3LYP-D3BJ/6311+G(2d,p)/SDD-IEFPCM(DMF) Energy = -1051.97327000



O	2.88521	-2.19742	-1.28350	H	3.89357	1.98144	0.79995
C	2.01351	-1.43519	-0.86770	H	2.56295	-0.70003	3.03467
C	2.37647	-0.00318	-0.40693	H	1.94334	-1.77214	1.76915
H	3.13392	0.37477	-1.10055	H	1.12780	-0.23754	2.10417
C	3.01749	-0.01122	1.02808	H	2.35729	3.65178	-0.66131
C	4.37990	-0.72235	0.96972	H	1.86991	3.38341	-2.33784
C	3.23688	1.43927	1.48777	H	3.08373	2.32342	-1.58023
C	2.10556	-0.72466	2.04019	H	-1.34282	1.73372	1.49797
N	1.16387	0.80206	-0.47543	H	-0.98619	1.61382	-0.36065
Pd	-0.51623	-0.26483	-0.22616	H	-2.97864	0.04918	2.08127
O	0.75684	-1.78830	-0.75882	C	-2.90934	2.38790	0.09443
N	-2.21199	-1.53429	-0.10097	C	-4.00194	1.69189	0.93880
C	-3.39670	-0.64675	0.08018	H	-4.97477	1.53256	0.46356
C	-3.07764	0.45463	1.07111	H	-4.15692	2.18354	1.90209
C	-1.86306	1.34016	0.62083	H	-1.11787	-3.02705	0.89466
C	-2.33732	-2.33341	-1.34118	H	-2.88624	-3.12412	1.14251
C	-2.02731	-2.44665	1.05255	H	-1.92433	-1.87012	1.97113
C	1.01437	2.02222	-0.94798	H	-4.26650	-1.24235	0.38907
C	2.16342	2.88164	-1.41373	H	-3.61699	-0.21110	-0.89842
O	-0.15796	2.53792	-1.00898	H	-1.42866	-2.92106	-1.47191
H	4.84927	-0.70494	1.95887	H	-2.45457	-1.66009	-2.19137
H	5.05462	-0.21874	0.26840	H	-3.20666	-3.00047	-1.28059
H	4.27622	-1.76005	0.64881	H	-2.68358	3.43458	0.30840
H	3.71026	1.44664	2.47484	H	-3.08463	2.28243	-0.97954
H	2.29155	1.98306	1.56475				

TS₅₄ – Ligand-assisted C–H activation (minor enantiomer)

Geometry optimisation:

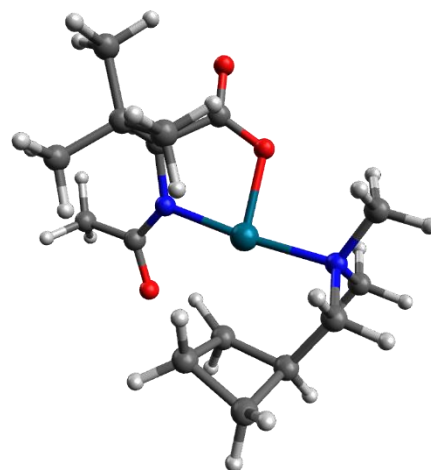
B3LYP-D3BJ/631G(d,p)/LANL2DZ-IEFPCM(DMF) Energy = -1050.52273402

Thermal correction to Gibbs Free Energy = 0.361915

Imaginary frequency = -1247.2650

Single-point energy calculation:

B3LYP-D3BJ/6311+G(2d,p)/SDD-IEFPCM(DMF) Energy = -1051.96992113



O	2.71878	-2.57379	-0.81692	H	3.86360	1.81933	0.73849
C	1.89071	-1.68779	-0.60966	H	2.09014	-0.38804	3.16657
C	2.33405	-0.23385	-0.34008	H	1.53146	-1.61118	2.01446
H	3.19286	-0.02920	-0.98666	H	0.80490	0.00188	2.01126
C	2.81246	-0.05672	1.14775	H	-2.51061	-0.57031	1.84998
C	4.11064	-0.85525	1.35375	H	-4.08216	-0.97679	1.13771
C	3.09641	1.42998	1.41501	H	-2.56154	-2.05288	-2.04894
C	1.74376	-0.54545	2.13997	H	-3.29168	-0.45936	-1.77773
N	1.21115	0.62859	-0.68105	H	-4.10614	-1.92393	-1.16264
Pd	-0.57716	-0.24733	-0.40560	H	-1.54172	-2.59312	1.38928
O	0.60218	-1.91919	-0.56648	H	-1.48881	-3.23620	-0.25983
N	-2.37280	-1.33286	-0.08062	H	-3.03893	-3.21628	0.63865
C	-3.10291	-0.52177	0.93192	H	3.36862	1.82633	-1.74245
C	-3.24362	0.91656	0.46841	H	2.68323	3.32697	-1.09690
C	-1.91120	1.56908	-0.04968	H	2.34121	2.85972	-2.76546
C	-3.13455	-1.44686	-1.34618	H	-2.24052	2.34924	-0.74873
C	-2.09708	-2.68470	0.45531	H	-0.86142	1.59573	-0.88580
C	1.22607	1.78554	-1.31074	C	-1.70680	2.21209	1.34444
C	2.49315	2.47431	-1.75526	C	-3.20772	1.94311	1.63689
O	0.12035	2.37924	-1.55747	H	-3.46537	1.56018	2.62890
H	4.46873	-0.72394	2.38013	H	-3.82969	2.81547	1.42214
H	4.89715	-0.50538	0.67575	H	-1.36508	3.25020	1.36510
H	3.95768	-1.91995	1.16939	H	-1.05257	1.61763	1.98719
H	3.46090	1.55747	2.43942	H	-4.08843	1.01639	-0.21691
H	2.19416	2.03709	1.30250				

TS₅₅ – Ligand-assisted C–H activation (minor enantiomer)

Geometry optimisation:

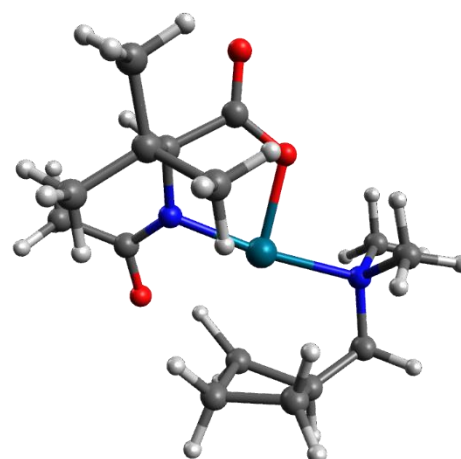
B3LYP-D3BJ/631G(d,p)/LANL2DZ-IEFPCM(DMF) Energy = -1050.52153746

Thermal correction to Gibbs Free Energy = 0.362753

Imaginary frequency = -1259.5042

Single-point energy calculation:

B3LYP-D3BJ/6311+G(2d,p)/SDD-IEFPCM(DMF) Energy = -1051.96787617



O	2.40364	-2.72878	-0.89708	H	3.99571	1.48813	0.70418
C	1.66074	-1.77522	-0.67193	H	2.03140	-0.56295	3.12793
C	2.23778	-0.37237	-0.37905	H	1.31530	-1.68604	1.96138
H	3.10284	-0.23581	-1.03531	H	0.78160	0.00019	2.00772
C	2.75295	-0.26931	1.10342	H	-4.33837	-0.57434	0.78993
C	3.96298	-1.20185	1.28186	H	-4.05051	0.11978	-0.80828
C	3.19755	1.17503	1.38449	H	-2.00225	-2.60662	-1.55370
C	1.65177	-0.65515	2.10515	H	-2.88469	-1.21160	-2.21774
N	1.19668	0.59990	-0.68497	H	-3.75818	-2.44212	-1.26080
Pd	-0.66158	-0.12059	-0.42388	H	-2.19633	-1.54183	1.91442
O	0.35513	-1.89005	-0.63119	H	-1.48321	-2.71893	0.79033
N	-2.50576	-1.13221	-0.14157	H	-3.25097	-2.70486	1.07733
C	-3.57334	-0.12454	0.14488	H	2.90469	3.16170	-1.07634
C	-3.01141	1.15525	0.72208	H	2.50473	2.75227	-2.74717
C	-1.80143	1.83891	0.00650	H	3.44515	1.61535	-1.75065
C	-2.81176	-1.89857	-1.37383	H	-2.13199	2.61106	-0.69927
C	-2.34921	-2.08668	0.98506	H	-0.77249	1.76513	-0.84976
C	1.31248	1.76132	-1.29529	H	-3.83612	1.87905	0.74672
C	2.63174	2.33959	-1.74432	C	-1.33769	2.34603	1.39822
O	0.26308	2.45872	-1.51866	C	-2.23721	1.27004	2.06480
H	4.35151	-1.11297	2.30168	H	-1.68993	3.36260	1.60252
H	4.76939	-0.93363	0.59017	H	-0.26732	2.29530	1.61062
H	3.69616	-2.24381	1.09812	H	-1.65913	0.37538	2.30617
H	3.58297	1.25003	2.40635	H	-2.81940	1.56137	2.94256
H	2.36543	1.87764	1.28863				

TS₅₆ – Ligand-assisted C–H activation (major enantiomer)

Geometry optimisation:

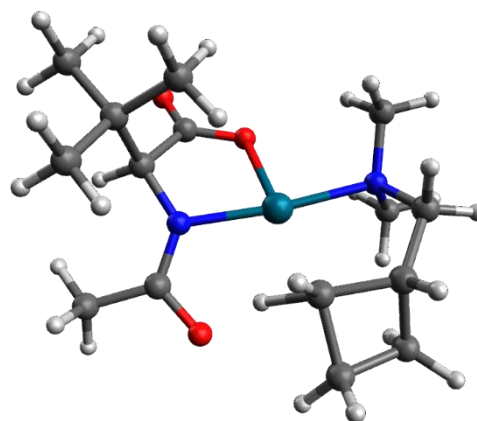
B3LYP-D3BJ/631G(d,p)/LANL2DZ-IEFPCM(DMF) Energy = -1050.52038307

Thermal correction to Gibbs Free Energy = 0.361667

Imaginary frequency = -1297.2184

Single-point energy calculation:

B3LYP-D3BJ/6311+G(2d,p)/SDD-IEFPCM(DMF) Energy = -1051.96658591



O	2.78206	-2.08508	-1.57346	H	3.91515	1.85641	0.90212
C	1.94602	-1.35175	-1.04733	H	2.61737	-1.03098	2.88547
C	2.35027	0.01814	-0.46160	H	1.95496	-1.96357	1.53390
H	3.09791	0.45023	-1.13349	H	1.16097	-0.46832	2.04774
C	3.02486	-0.14220	0.94884	H	-2.70741	-1.30934	2.01140
C	4.37684	-0.85569	0.77933	H	-4.10304	-1.41678	0.93280
C	3.27165	1.25133	1.54876	H	-2.12146	-2.07946	-2.02162
C	2.13333	-0.95057	1.90669	H	-3.18881	-0.70998	-1.66318
N	1.15002	0.84322	-0.42400	H	-3.70024	-2.36221	-1.23682
Pd	-0.53705	-0.21949	-0.16558	H	-1.19292	-2.78807	1.39663
O	0.68739	-1.68958	-0.91897	H	-1.01300	-3.26215	-0.30217
N	-2.18679	-1.54098	0.01150	H	-2.56088	-3.56435	0.54945
C	-3.10183	-0.97884	1.04730	H	2.41099	3.66651	-0.37536
C	-3.14761	0.53471	1.05526	H	1.85693	3.58062	-2.05060
C	-1.84458	1.37707	0.83609	H	3.07048	2.42363	-1.45098
C	-2.84460	-1.67853	-1.31031	H	-1.28657	1.63173	1.74098
C	-1.71045	-2.87978	0.44114	H	-0.97592	1.70756	-0.15098
C	1.01855	2.10407	-0.77306	H	-3.54446	0.82194	2.03768
C	2.17105	2.98138	-1.19384	C	-2.82050	2.49850	0.29550
O	-0.14226	2.64564	-0.74221	C	-3.87566	1.41071	0.01217
H	4.87114	-0.94969	1.75184	H	-2.47868	3.10739	-0.54095
H	5.03999	-0.28608	0.11868	H	-3.12002	3.15438	1.11925
H	4.25237	-1.85208	0.35200	H	-4.92669	1.64390	0.20101
H	3.77152	1.15356	2.51781	H	-3.77409	1.03561	-1.00826
H	2.33442	1.79156	1.70723				

TS₅₇ – Ligand-assisted *trans*-C–H activation

Geometry optimisation:

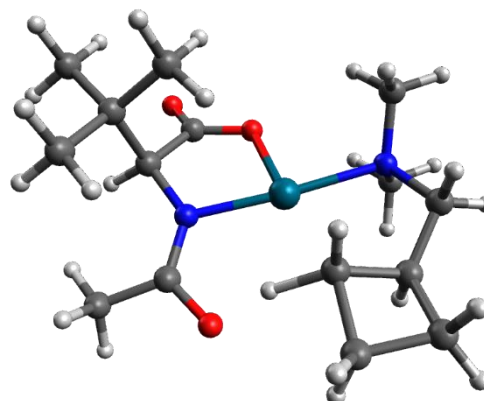
B3LYP-D3BJ/631G(d,p)/LANL2DZ-IEFPCM(DMF) Energy = -1050.52560121

Thermal correction to Gibbs Free Energy = 0.362104

Imaginary frequency = -1276.0922

Single-point energy calculation:

B3LYP-D3BJ/6311+G(2d,p)/SDD-IEFPCM(DMF) Energy = -1051.97091453



O	2.84475	-2.13656	-1.43193	H	3.95368	1.97025	0.74153
C	1.99423	-1.40260	-0.92951	H	2.69787	-0.75341	2.95884
C	2.36635	0.02163	-0.45798	H	2.00658	-1.78835	1.69884
H	3.09442	0.41833	-1.17182	H	1.22486	-0.25551	2.10964
C	3.06460	-0.01940	0.95160	H	2.37916	3.68133	-0.54068
C	4.41856	-0.73761	0.81925	H	1.80381	3.48818	-2.19884
C	3.31636	1.41684	1.43807	H	3.04302	2.38595	-1.55169
C	2.19325	-0.75000	1.98717	H	-1.80318	1.00231	1.57328
N	1.14646	0.82343	-0.46295	H	-0.98053	1.76425	-0.22869
Pd	-0.51462	-0.26494	-0.15729	H	-3.38219	0.57486	-1.02920
O	0.75846	-1.78178	-0.72588	C	-2.82780	2.58116	0.52483
N	-2.18608	-1.61840	0.04444	C	-4.10784	1.71349	0.66610
C	-3.39138	-0.88657	0.55316	H	-2.59013	3.29740	1.31411
C	-3.30093	0.54107	0.06335	H	-2.78768	3.08523	-0.44424
C	-2.00220	1.23921	0.52090	H	-5.00845	2.04185	0.13983
C	-2.43391	-2.16191	-1.31338	H	-4.34781	1.53161	1.71864
C	-1.80265	-2.72167	0.95426	H	-3.35188	-0.90056	1.64579
C	1.00500	2.07676	-0.83015	H	-4.30071	-1.41108	0.23655
C	2.13974	2.94508	-1.31313	H	-1.51072	-2.60569	-1.68645
O	-0.15396	2.63285	-0.78536	H	-2.73901	-1.35591	-1.98164
H	4.93086	-0.74143	1.78694	H	-3.22449	-2.92237	-1.28043
H	5.06524	-0.22525	0.09824	H	-0.90368	-3.19894	0.56364
H	4.29486	-1.76888	0.48489	H	-2.61190	-3.45914	1.02849
H	3.82582	1.39292	2.40670	H	-1.59176	-2.31326	1.94360
H	2.38129	1.96846	1.56692				

TS₅₈ – Ligand-assisted *trans*-C–H activation

Geometry optimisation:

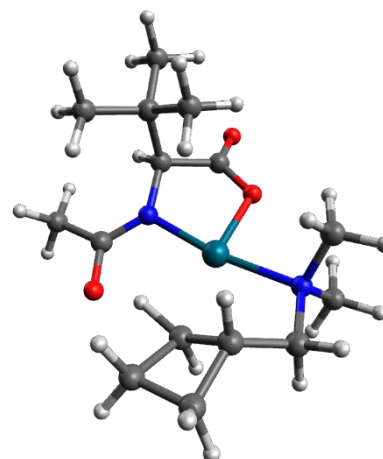
B3LYP-D3BJ/631G(d,p)/LANL2DZ-IEFPCM(DMF) Energy = -1050.52278518

Thermal correction to Gibbs Free Energy = 0.362785

Imaginary frequency = -1213.2752

Single-point energy calculation:

B3LYP-D3BJ/6311+G(2d,p)/SDD-IEFPCM(DMF) Energy = -1051.96820268



O	2.85095	-2.24022	-1.28230	H	3.89662	1.89398	0.89934
C	1.99117	-1.46662	-0.86283	H	2.32375	-0.70381	3.04456
C	2.36248	-0.03816	-0.41351	H	1.73926	-1.77242	1.75836
H	3.16946	0.31276	-1.06383	H	0.96100	-0.20789	2.02505
C	2.91806	-0.05891	1.06179	H	3.21801	2.30099	-1.43115
C	4.25106	-0.82712	1.08003	H	2.53123	3.62768	-0.47463
C	3.17639	1.37831	1.54136	H	2.07357	3.44649	-2.16942
C	1.92373	-0.72851	2.02568	H	-2.62005	1.19353	-1.14759
N	1.17308	0.79572	-0.56442	H	-0.91912	1.79505	-0.42794
Pd	-0.53999	-0.23888	-0.35280	C	-2.71883	2.61653	0.48902
O	0.73551	-1.80876	-0.72027	C	-3.90124	1.76179	1.01944
N	-2.19948	-1.58759	-0.00124	H	-4.30117	1.99485	2.00996
C	-3.43338	-0.81098	0.34865	H	-4.72168	1.72917	0.29538
C	-2.97978	0.52977	0.88209	H	-2.93385	3.44957	-0.18358
C	-2.14396	1.31189	-0.16594	H	-2.07944	2.96643	1.30448
C	-2.41192	-2.45280	-1.18256	H	-2.41368	0.39735	1.81066
C	-1.76535	-2.41669	1.15050	H	-4.04652	-1.38714	1.05065
C	1.11851	2.07443	-0.86762	H	-4.01287	-0.66327	-0.56638
C	2.32252	2.89590	-1.25937	H	-1.47801	-2.96823	-1.40851
O	-0.00812	2.68779	-0.85960	H	-2.69727	-1.83391	-2.03440
H	4.66443	-0.82563	2.09390	H	-3.20176	-3.18880	-0.98542
H	4.98463	-0.35485	0.41717	H	-0.80899	-2.88049	0.90997
H	4.12340	-1.86131	0.75623	H	-2.51363	-3.19058	1.36324
H	3.59177	1.35584	2.55391	H	-1.64355	-1.78321	2.03017
H	2.25520	1.96611	1.57527				

A_{TS61} – Ligand-assisted C–H activation (major enantiomer)

Geometry optimisation:

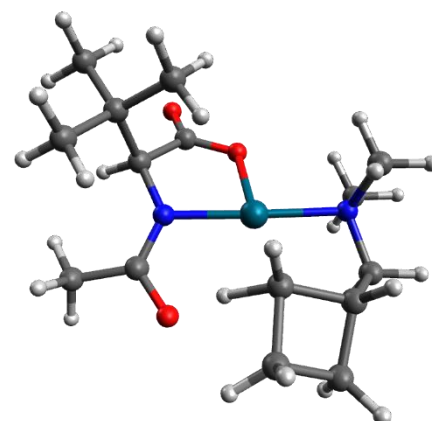
B3LYP-D3BJ/631G(d,p)/LANL2DZ-IEFPCM(DMF) Energy = -1050.52413194

Thermal correction to Gibbs Free Energy = 0.362303

Imaginary frequency = -1356.0791

Single-point energy calculation:

B3LYP-D3BJ/6311+G(2d,p)/SDD-IEFPCM(DMF) Energy = -1051.96979036



O	2.88126	-2.14506	-1.39508	H	3.87703	2.02509	0.71893
C	2.01093	-1.40871	-0.93142	H	2.71978	-0.73482	2.95275
C	2.36063	0.02226	-0.46279	H	2.07298	-1.79913	1.69469
H	3.07734	0.43120	-1.18161	H	1.23178	-0.29492	2.09792
C	3.06416	0.00532	0.94292	H	2.25245	3.68266	-0.63249
C	4.44105	-0.66677	0.80870	H	1.68613	3.43485	-2.28690
C	3.26624	1.45155	1.42328	H	2.96228	2.39026	-1.61484
C	2.21834	-0.75289	1.97961	H	-1.41706	1.09253	1.75633
N	1.12619	0.79676	-0.46483	H	-1.03376	1.66193	-0.22033
Pd	-0.52378	-0.30924	-0.16781	C	-2.67274	2.58916	0.66687
O	0.76874	-1.79018	-0.77661	C	-3.89302	1.84057	0.09461
N	-2.20300	-1.59324	0.00721	H	-2.86182	2.98664	1.66866
C	-3.38511	-0.71637	-0.22873	H	-2.22826	3.37357	0.05496
C	-3.30438	0.52141	0.64421	H	-3.88976	1.84798	-1.00047
C	-1.90369	1.20928	0.78397	H	-4.88345	2.13797	0.44786
C	-2.15172	-2.67386	-1.00276	H	-3.70814	0.31621	1.64153
C	-2.22544	-2.18513	1.36492	H	-4.30856	-1.28956	-0.06254
C	0.93776	2.02579	-0.88556	H	-3.34785	-0.42727	-1.28252
C	2.03933	2.92255	-1.38972	H	-1.33781	-2.80580	1.49351
O	-0.24620	2.52777	-0.86560	H	-3.12354	-2.80301	1.49548
H	4.95315	-0.65793	1.77652	H	-2.21801	-1.39663	2.11641
H	5.07032	-0.12963	0.09023	H	-1.23183	-3.24133	-0.86758
H	4.35037	-1.69957	0.46877	H	-2.15070	-2.23160	-1.99975
H	3.78369	1.45104	2.38798	H	-3.02160	-3.33394	-0.89661
H	2.31199	1.96849	1.55534				

A_{TS62} – Ligand-assisted C–H activation (minor enantiomer)

Geometry optimisation:

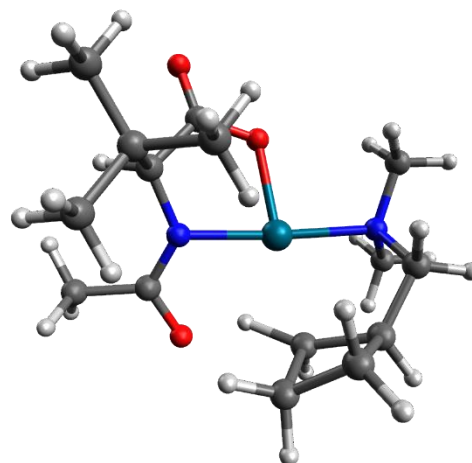
B3LYP-D3BJ/631G(d,p)/LANL2DZ-IEFPCM(DMF) Energy = -1050.52152865

Thermal correction to Gibbs Free Energy = 0.362015

Imaginary frequency = -1194.1235

Single-point energy calculation:

B3LYP-D3BJ/6311+G(2d,p)/SDD-IEFPCM(DMF) Energy = -1051.96861621



O	2.55643	-2.70599	-0.80310	H	3.87396	1.66121	0.66750
C	1.76143	-1.78560	-0.61696	H	2.00655	-0.41715	3.13946
C	2.26167	-0.34558	-0.36762	H	1.40907	-1.64708	2.01422
H	3.12610	-0.18355	-1.01889	H	0.74208	-0.00935	1.96656
C	2.74882	-0.16217	1.11605	H	-2.36854	-0.85204	1.97663
C	4.01265	-1.00963	1.33828	H	-4.02666	-0.80869	1.35643
C	3.09466	1.31640	1.35443	H	-3.02005	-1.47502	-2.09645
C	1.65957	-0.58692	2.11504	H	-3.56853	0.06291	-1.39970
N	1.17196	0.55405	-0.71746	H	-4.41175	-1.44889	-0.97706
Pd	-0.64570	-0.24603	-0.42446	H	-1.63289	-2.79221	0.99916
O	0.46433	-1.96662	-0.58344	H	-1.96292	-3.13240	-0.70655
N	-2.50614	-1.19959	-0.07136	H	-3.31427	-3.08794	0.46398
C	-2.99200	-0.50136	1.15033	H	3.36006	1.64529	-1.83031
C	-2.85551	1.01402	1.00321	H	2.73708	3.17942	-1.20091
C	-1.91704	1.63705	-0.10537	H	2.36423	2.70282	-2.86040
C	-3.43668	-1.00057	-1.20705	H	-2.49095	2.03990	-0.94744
C	-2.34787	-2.64730	0.18988	H	-0.84850	1.58971	-0.89137
C	1.22181	1.69209	-1.38072	C	-1.45890	2.67865	0.95836
C	2.50966	2.32580	-1.84620	C	-2.05290	1.79083	2.07457
O	0.13520	2.31634	-1.63743	H	-3.84344	1.46801	0.87718
H	4.37553	-0.87371	2.36239	H	-1.98434	3.63207	0.84669
H	4.81309	-0.70530	0.65460	H	-0.38580	2.87479	1.00581
H	3.81567	-2.07029	1.17382	H	-1.28867	1.15324	2.53040
H	3.46836	1.44834	2.37492	H	-2.62488	2.28000	2.86683
H	2.21771	1.95807	1.23344				

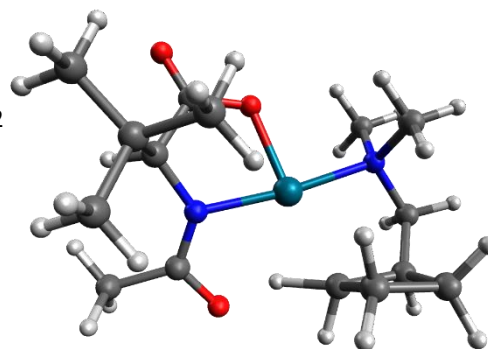
AT₅₆₃ – Ligand-assisted C–H activation (minor enantiomer)

Geometry optimisation:

B3LYP-D3BJ/631G(d,p)/LANL2DZ-IEFPCM(DMF) Energy = -1050.51867732

Thermal correction to Gibbs Free Energy = 0.362473

Imaginary frequency = -1303.9832



Single-point energy calculation:

B3LYP-D3BJ/6311+G(2d,p)/SDD-IEFPCM(DMF) Energy = -1051.96544161

O	2.60023	-2.57897	-0.94197	H	4.01929	1.67267	0.73579
C	1.81668	-1.66710	-0.68214	H	2.24225	-0.56787	3.13892
C	2.33379	-0.24693	-0.36257	H	1.55285	-1.68558	1.95140
H	3.17228	-0.04990	-1.03775	H	0.93288	-0.03254	2.07476
C	2.88682	-0.16347	1.10720	H	3.41345	1.83070	-1.70074
C	4.15124	-1.03186	1.22046	H	2.81363	3.33223	-0.97757
C	3.25861	1.29367	1.42550	H	2.39773	2.94357	-2.64945
C	1.83828	-0.64372	2.12416	H	-0.79781	1.77656	-0.71039
N	1.24016	0.68313	-0.61136	H	-3.99625	1.80036	-0.36804
Pd	-0.58321	-0.13410	-0.37658	H	-1.59828	-2.51623	1.23178
O	0.51957	-1.84444	-0.62621	H	-3.37956	-2.38722	1.28207
N	-2.40738	-1.20289	-0.19508	H	-2.35986	-1.07572	1.92472
C	-3.53668	-0.24996	-0.41827	H	-2.39785	-1.83256	-2.21089
C	-3.30974	1.13440	0.16368	H	-3.38684	-2.84815	-1.12392
C	-1.83305	1.66248	0.17267	H	-1.59788	-2.93590	-1.07314
C	-2.45397	-2.27821	-1.21723	H	-4.46854	-0.69946	-0.04778
C	-2.44289	-1.83144	1.14804	H	-3.62771	-0.14713	-1.50227
C	1.28626	1.86147	-1.19835	H	-1.86993	2.71172	-0.14351
C	2.56614	2.51385	-1.65992	C	-1.82460	1.64129	1.73166
O	0.19979	2.51234	-1.38541	C	-3.35144	1.35278	1.70572
H	4.56360	-0.95509	2.23194	H	-1.51985	2.57524	2.21130
H	4.92125	-0.69584	0.51698	H	-1.24089	0.83207	2.17624
H	3.93682	-2.08028	1.00754	H	-3.70143	0.51088	2.30857
H	3.66783	1.35701	2.43891	H	-3.94894	2.22773	1.97260
H	2.38629	1.95074	1.37476				

Appendix IV – Published work

ARTICLES

<https://doi.org/10.1038/s41557-019-0393-8>nature
chemistryCatalytic C(sp³)-H bond activation in tertiary alkylaminesJesus Rodrialvarez, Manuel Nappi , Hiroki Azuma, Nils J. Flodén, Matthew E. Burns and Matthew J. Gaunt *

The development of robust catalytic methods to assemble tertiary alkylamines provides a continual challenge to chemical synthesis. In this regard, transformation of a traditionally unreactive C-H bond, proximal to the nitrogen atom, into a versatile chemical entity would be a powerful strategy for introducing functional complexity to tertiary alkylamines. A practical and selective metal-catalysed C(sp³)-H activation facilitated by the tertiary alkylamine functionality, however, remains an unsolved problem. Here, we report a Pd(II)-catalysed protocol that appends arene feedstocks to tertiary alkylamines via C(sp³)-H functionalization. A simple ligand for Pd(II) orchestrates the C-H activation step in favour of deleterious pathways. The reaction can use both simple and complex starting materials to produce a range of multifaceted γ -aryl tertiary alkylamines and can be rendered enantioselective. The enabling features of this transformation should be attractive to practitioners of synthetic and medicinal chemistry as well as in other areas that use biologically active alkylamines.

The development of methods catalysed by transition metals for converting C(sp³)-H bonds into a new chemical functionality is an emerging technology that has the potential to streamline chemical synthesis^{1–3}. An important feature of many C(sp³)-H functionalization strategies is the use of coordinating groups, which locate a metal catalyst in proximity to a particular C-H bond, thereby enabling reactivity and ensuring selectivity. In an ideal situation, a native functionality present in the molecule would be capable of steering the C(sp³)-H activation via cyclometallation. Among a limited number of examples, carboxylic acids^{4,5} as well as primary and secondary amines⁶ have been most successfully deployed in combination with Pd(II) catalysts to affect C(sp³)-H functionalization reactions. However, it is more common that the native functional group needs to be modified with an additional directing auxiliary to modulate its coordinating ability, which has led to a diverse range of Pd(II)-catalysed C(sp³)-H activation processes^{7,8}. Despite the efficacy of auxiliary-augmented C(sp³)-H activation strategies, a number of practical drawbacks of this approach exist. First, the auxiliary must be incorporated into the substrate prior to, and removed after, the C-H transformation. Second, their removal sometimes requires harsh conditions that can be incompatible with delicate molecular architectures. A third, and arguably the most compelling, limitation is that auxiliary-augmented C(sp³)-H activation is not possible if there is no functionality in the substrate to which a directing motif can be appended. This problem is especially pertinent when considering C(sp³)-H activation in tertiary alkylamines; there is no simple way to attach and remove a directing auxiliary within a tertiary alkylamine motif^{9–14}.

With an estimated 26% of all drugs and agrochemicals featuring a tertiary alkylamine^{17,18}, the development of robust catalytic methods to assemble and modify the structure of these important molecular features provides a continual challenge to chemical synthesis^{19–23}. A selective single-step transformation of a traditionally unreactive C-H bond, proximal to the nitrogen atom, into a versatile chemical entity would be a particularly powerful strategy for introducing functional complexity to tertiary alkylamines. Despite the apparent efficacy of this ideal, practical and selective

metal-catalysed C(sp³)-H activation facilitated by tertiary alkylamine scaffolds remains an elusive transformation (Fig. 1a). A possible reason for this methodological deficiency is the ease with which the electron-rich nitrogen atom in tertiary alkylamines can undergo decomposition reactions in the presence of many transition metal salts and commonly used oxidants, thus precluding the desired C-H activation pathway (Fig. 1b)²⁰. Using alternative strategies, Hartwig has reported steric-controlled Rh- (ref. 30), Ru- (ref. 31) and Ir-catalysed²¹ C(sp³)-H borylation at methyl groups within simple tertiary alkylamines, in some cases with selectivity at the β -position. Remote C(sp³)-H oxidations using Pt (ref. 33), Ru (ref. 34), Fe²⁵ and W (ref. 36) catalysts under strongly acidic conditions, wherein the transformation is guided by the C-H bond reactivity rather than the directing effect of the amine, have also been described. However, no examples of catalytic C(sp³)-H functionalization directed by tertiary alkylamines have been reported (Fig. 1a,b). Given the ubiquity of tertiary alkylamines in biologically important molecules and the potential efficacy of a method that introduces aryl entities proximal to the nitrogen motif²⁷, the development of strategies involving catalytic C(sp³)-H activation directed by tertiary alkylamines to guide building block functionalization, fragment coupling and late-stage functionalization of biologically relevant molecules is an unmet synthetic need (Fig. 1c).

Results and discussion

We reasoned that a successful Pd(II)-catalysed tertiary-alkylamine-directed C(sp³)-H arylation strategy would depend on the effective coordination of the substrate to the metal. The nitrogen atom is nucleophilic but often sterically hindered; however, based on Ryabov's cyclopalladation studies with benzylamines²⁸, we proposed that the opposing steric and electronic characteristics inherent to tertiary alkylamines might synergistically combine to promote formation of the mono-amine Pd(II) complex required for C-H activation (Fig. 1b). However, the Pd(II)-ligated nitrogen motif in tertiary alkylamines will often be surrounded by a number of C-H bonds that can undergo deleterious β -hydride elimination reactions. Initial investigations revealed that a reaction between amine 1a

Department of Chemistry, University of Cambridge, Cambridge, UK. *e-mail: mjg32@cam.ac.uk

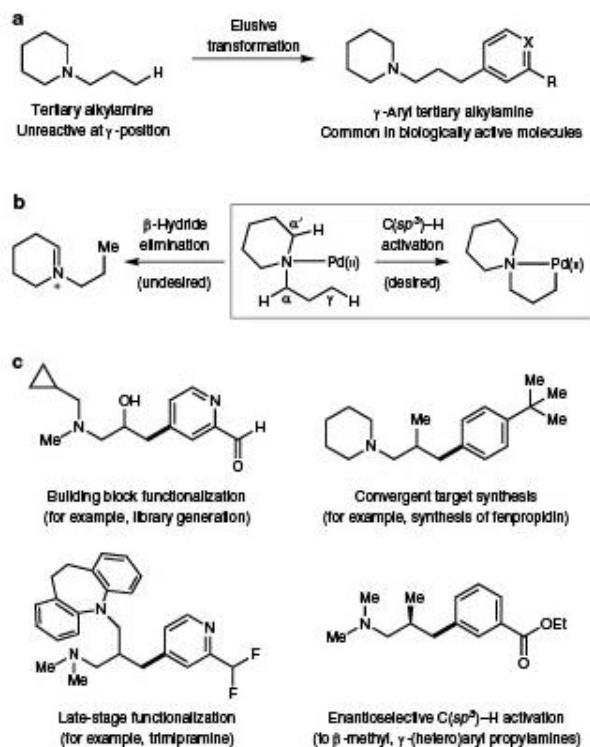


Fig. 1 | Design plan towards γ - $C(sp^3)$ -H arylation of tertiary alkylamines. **a**, Direct methods to selectively arylate tertiary alkylamines at the γ -position do not exist. **b**, Directed $C(sp^3)$ -H activation is a potential solution to the functionalization of tertiary alkylamines; however, the presence of C-H bonds adjacent to the nitrogen atom could lead to undesired β -hydride elimination. **c**, Applications for a Pd(II)-catalysed γ - $C(sp^3)$ -H arylation of tertiary alkylamines, which include the functionalization of available tertiary-alkylamine building blocks, a convergent strategy for target synthesis, late-stage functionalization and enantioselective synthesis of tertiary alkylamines.

and phenylboronic acid **2a** under commonly used Pd(II)-catalysis conditions led to significant amine decomposition and no arylation (see Supplementary Fig. 1)⁸. Computational analysis revealed a lower energy pathway for an acetate-assisted β -hydride elimination (Ts2) (Fig. 2a) than the desired $C(sp^3)$ -H activation (Ts1), supporting the experimental observations. Interestingly, inner-sphere acetate-assisted β -hydride elimination (Ts2) is rarely considered for this common decomposition reaction³⁹, yet all of our calculations converged on this pathway. We considered whether the introduction of a ligand would modulate the energetic preference for these competing pathways. While a number of directing functional groups are capable of intrinsically switching between neutral and anionic coordination to the Pd(II) catalyst, thereby supporting the use of ligands with diverse binding modes⁴⁰, the neutral coordinating nitrogen atom in tertiary alkylamines restricts the type of ligand that can be deployed for $C(sp^3)$ -H activation. We speculated that $C(sp^3)$ -H activation in tertiary alkylamines would be matched to the coordination properties of *N*-acetyl α -amino acid ligands^{11,41,42}, permitting the Pd(II) centre to accommodate the bisanionic ligand (which contains the basic acetamide needed for C-H bond cleavage), the neutral amine and the vacant coordination site required for C-H activation. Yu and co-workers have previously developed a Pd(II)-catalysed method for arylation of $C(sp^3)$ -H bonds in *N*-alkyl sulfonamides with derivatives of aryl-boronic esters¹¹. In their

studies, they reported that an *N*-acetyl amino acid ligand was crucial for reactivity, with no reaction in its absence.

Interestingly, we found that including *N*-acetyl *tert*-leucine **4a** as a ligand lowered the energy of the $C(sp^3)$ -H activation step (Ts3) relative to the corresponding ligand-assisted β -hydride elimination. We believe that the ligand distorts the co-planar geometry empirically required for β -hydride elimination (Ts4), making base-assisted C-H activation the more favoured pathway (see Supplementary Table 5), and represents an extension to the reactivity-inducing capacity of this class of ligand. Our calculations were validated by a reaction employing 25 mol.% of ligand **4a**, which produced a moderate yield of the γ -aryl alkylamine **3a**. An extensive assessment of reaction parameters revealed optimal conditions, which involved the treatment of 2.5 equiv. amine **1a** and phenylboronic acid **2a** with 10 mol.% Pd(OAc)₂, 25 mol.% *N*-acetyl *tert*-leucine **4a**, 2.5 equiv. Ag₂CO₃ and 2 equiv. 1,4-benzoquinone in a solution of *N*-methyl-2-pyrrolidone (NMP) at 50 °C for 15 h to afford **3a** in an 81% yield (Fig. 2b).

An initial proposal for the reaction mechanism of the $C(sp^3)$ -H arylation directed by tertiary alkylamine begins with coordination of amine **1a** to the Pd(II)-ligand catalyst to form Int-I. Cyclopalladation via ligand-assisted concerted metallation deprotonation affords palladacycle Int-II, which undergoes transmetalation with **2a** to Int-III; reductive elimination of the $C(sp^3)$ - $C(sp^2)$ groups, possibly facilitated by benzoquinone⁴³, generates amine **3a** and Pd(0), which reforms the catalytically active Pd(II)-ligand species upon oxidation with Ag(I).

Having established optimal conditions for γ - $C(sp^3)$ -H arylation, we next explored the scope of the amine component (Table 1). The *N*-propyl piperidine scaffolds bearing different functionalities on the heterocycle underwent efficient $C(sp^3)$ -H arylation to the desired products **3a–m** in generally good yields. The yields of product were slightly reduced in the presence of electron-withdrawing substituents on the heterocycle (**3e,f**), which may reflect the attenuated binding of the amine to the Pd(II) catalyst brought about by the inductive effect of the remote functionality. Substrates displaying Lewis-basic aromatic heterocycles were compatible with the reaction conditions, delivering γ -arylated products adorned with the functionality commonly found in pharmaceutical and agrochemical intermediates (**3h–j**). The reacting $C(sp^3)$ -H bond can also be located in a 2-ethyl substituent on the piperidine ring, producing amine **3n** in useful yield. Interestingly, a substrate with the targeted C-H bond in a 3-methyl substituent on the heterocycle undergoes arylation to the 3-benzyl-piperidine derivative **3o**. This means that cyclopalladation must have involved the Pd(II) catalyst binding to the axial lone pair of the piperidine nitrogen, with the reacting methyl group also projected in the axial position. Other saturated heterocycles, including protected piperazines, morpholines and diazepanes, were compatible with the γ - $C(sp^3)$ -H arylation (**3p–s**); the lower yield of pyrrolidine **3t** is due to competing β -hydride elimination. Acyclic scaffolds were also compatible with the arylation process. The *N,N*-dimethyl-derived tertiary alkylamines, for example, are one of the most common classes of amines featured in pharmaceutical and agrochemical agents, and a method to elaborate their structures would represent an attractive transformation. However, these substrates can contain up to eight C-H bonds adjacent to nitrogen, which means they are especially prone to β -hydride elimination on complexation with Pd(II) salts. Therefore, we were pleased to find that a range of *N,N*-dialkylamine derivatives smoothly reacted to form amines **3u–ac** in good yield, reinforcing the ligand effect in facilitating $C(sp^3)$ -H activation over β -hydride elimination. Acyclic tertiary alkylamines displaying a variety of α - and β -substituents along the reacting alkyl chain also undergo γ - $C(sp^3)$ -H arylation (**3v–y**), and useful functionality could also be incorporated into the non-reacting alkyl substituents without affecting the success of the reaction (**3ac**). In a case where

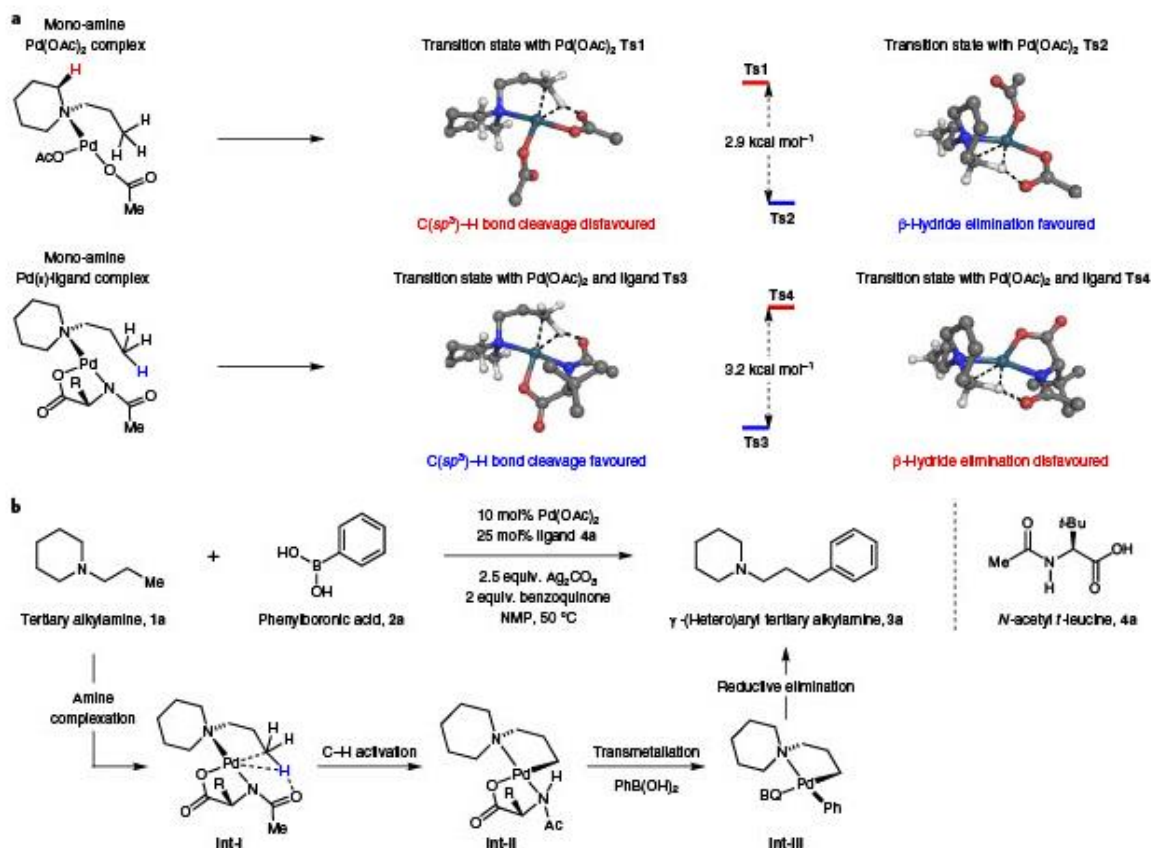


Fig. 2 | The γ -C(sp^3)-H arylation of tertiary alkylamines. **a**, Computational study of ligand-enabled γ -C(sp^3)-H activation. The γ -C-H activation in the amino-alkyl Pd(II) complex was found to require a higher-energy transition state (Ts1) than did the corresponding β -hydride elimination (Ts2). By contrast, with the amino acid ligand bound to the Pd(II) complex, the corresponding intermediate presented a lower-energy transition state (Ts3) for ligand-assisted γ -C-H activation in comparison to Ts4 (for ligand-assisted β -hydride elimination). Calculations were conducted using B3LYP-D3(BJ)/[6-311+G(2d,p)/SDD(Pd)] IEFPCM with DMF as solvent, $T = 323.15$ K. **b**, Optimized reaction and proposed mechanism of γ -C(sp^3)-H arylation. The Pd(OAc)₂, the ligand **4a** and benzoquinone (BQ) are all essential for the observed reactivity. The reaction goes through one turnover in the absence of the Ag₂CO₃. While other amino acid ligands also work, **4a** gave superior yields. Ligands containing the N-Ac motif were superior to other amide and carbamate derivatives.

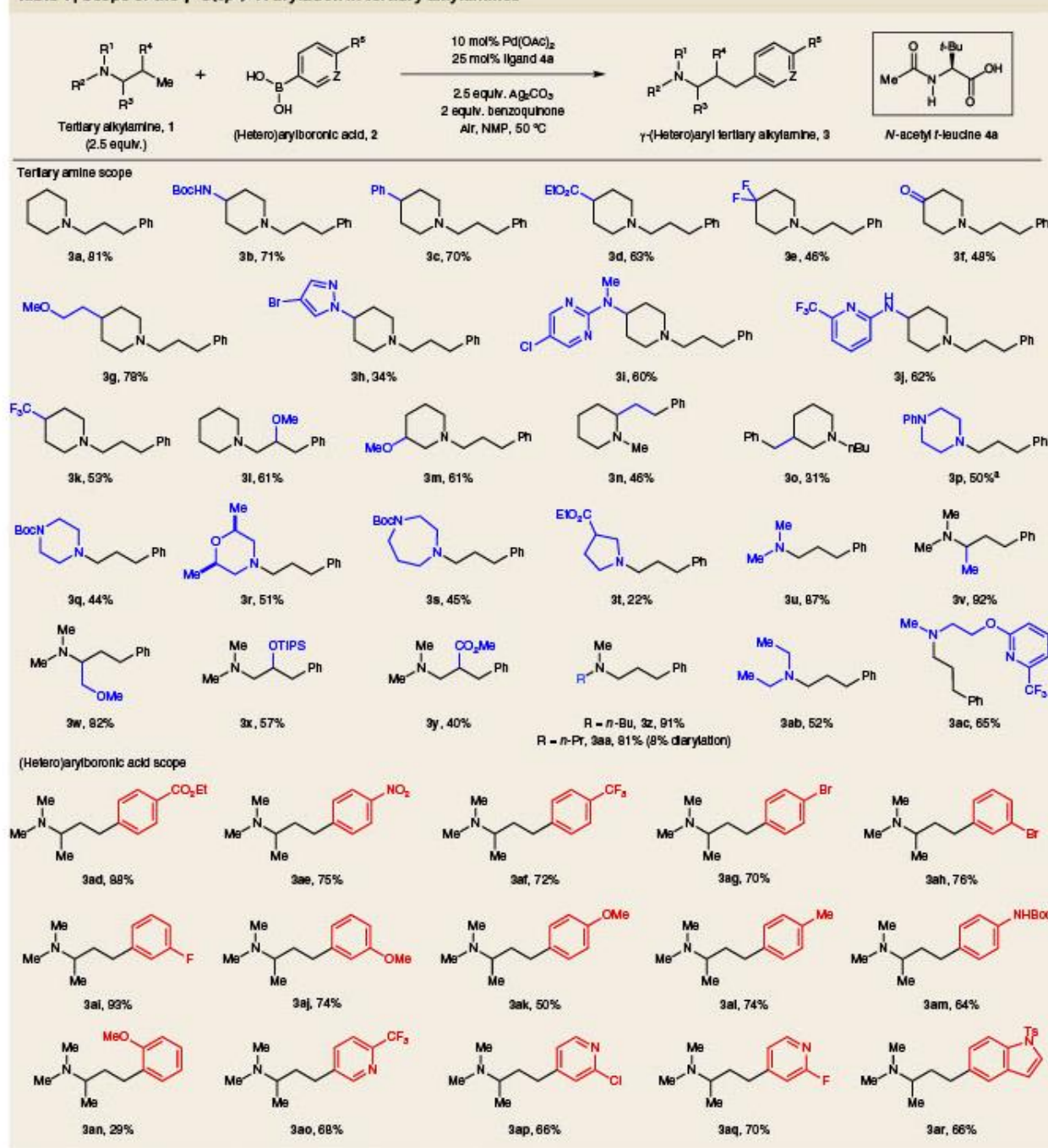
two equivalent propyl groups are present, 81% of the mono-arylated **3aa** product is isolated with only trace amounts (8%) of the competitive diarylation product observed.

Next, we evaluated the scope of the aryl-boronic acid coupling partner. Aryl groups with electron-donating and -withdrawing substituents at the *para*- and *meta*-positions were incorporated with good yields to form the γ -aryl alkylamine products (**3ad-am**); unfortunately, *ortho*-substituted aryl-boronic acids resulted in a lower yield (**3an**). Palladium-sensitive functionalities such as aryl bromides (**3ag,ah**) were tolerated under the mild reaction conditions. Heteroaryl-boronic acids, such as those containing functionalized pyridines and indoles, were successfully introduced into the tertiary amine framework (**3ao-ar**), offering opportunities for downstream structure modification.

Fenpropimorph **5**, a marketed fungicide, can be synthesized in a single step from readily available materials (**1ad** and **2p**), demonstrating a convergent coupling application to target synthesis (Fig. 3a). Such a strategy would be particularly appealing for the synthesis of fenpropimorph analogues, wherein assembly via classical reductive amination or alkylation strategies may be limited by the availability of the corresponding substituted α -methyl hydrocin-namaldehyde or C3-3-aryl-1-halo-2-methylpropanes, respectively; readily available *N*-propyl amines could be directly combined with

the vast array of commercial aryl-boronic acids, providing immediate access to a library of analogues. We found that *N*-propyl analogues of donepezil, ciprofloxacin and fluoxetine underwent γ -C(sp^3)-H arylation without affecting the functionality in these molecules. (**6-8**, Fig. 3b). The tricyclic antidepressant trimipramine, which is used to treat major depressive disorders, was also an excellent substrate for the arylation process, affording γ -(hetero) aryl tertiary alkylamine derivatives **9a-c** in excellent yield (Fig. 3c); 90% of the unreacted excess amine starting material can be recovered, further demonstrating the role of ligand **4a** in controlling the selectivity between potentially competing pathways. The success of this transformation demonstrates the potential of its application as a tool for late-stage functionalization of pharmaceutical agents; many different aryl groups could be transferred to already biologically active molecules, producing previously unexplored candidates that would require multistep syntheses to prepare by traditional means.

Given that the γ -C(sp^3)-H arylation process requires the presence of ligand **4a**, we questioned whether an enantioselective transformation might be possible when using prochiral *N*-isobutyl tertiary alkylamines (**1ae-ag**), thereby generating non-racemic β -methyl γ -aryl propylamines that would be difficult to synthesize directly by other methods. Enantioselective desymmetrization of isobutyl groups is challenging because the catalyst must

Table 1 | Scope of the γ -C(sp^3)-H arylation in tertiary alkylamines

sterically discriminate between an β -hydrogen atom and a relatively small β -methyl group. Furthermore, the prochiral centre is distant from the chirality in the Pd(II) catalyst, making enantioselective control more challenging^{44,45}. On the basis of computational studies, we noted a distinction between two chair-like transition states that orient the non-reacting methyl group in either an equatorial (Ts5) or axial (Ts6) position; the latter transition state appears to be destabilized by pseudo-1,3-diaxial interactions between the axial

N-Me and the non-reacting methyl group and carries an energetic cost of 2.1 kcal mol⁻¹ (Fig. 3d). Under the previously optimal conditions, **1ae** (R = Me) was converted to **3as** with an e.e. of 81%; conducting the reaction in dimethylformamide (DMF) at 40 °C increased the e.e. to 90%. Interestingly, comparable enantioselectivity was observed with the *N*-acetyl alanine as ligand (86% e.e.), suggesting that steric parameters alone are not responsible for the asymmetric induction. Computational analysis suggested that the

ARTICLES

NATURE CHEMISTRY

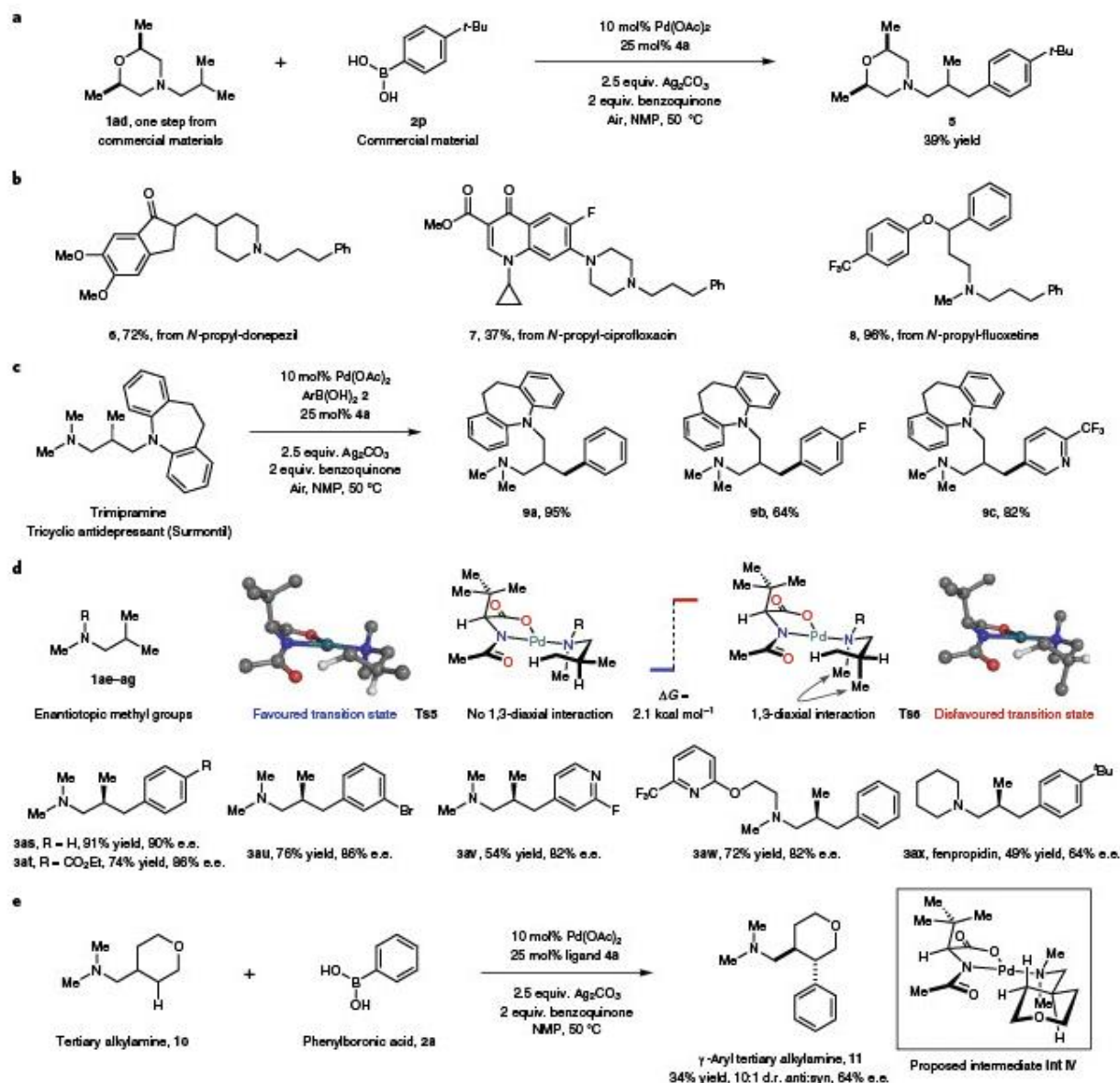


Fig. 3 | Applications and further advances of the γ -C-H arylation of tertiary alkylamines. **a**, Direct synthesis of the fungicide fenpropimorph from readily available materials. **b**, The γ -C(sp^3)-H arylation reaction in substrates containing pharmaceutically relevant amine fragments. **c**, Late-stage arylation of trimipramine. A range of aryl groups can be added directly to trimipramine, generating a range of previously unknown analogues in a single synthetic step. **d**, Enantioselective γ -C(sp^3)-H arylation of tertiary alkylamines. Using substrates containing reacting enantiotopic β -methyl groups, an enantioselective desymmetrizing arylation generates non-racemic β -methyl- γ -aryl tertiary alkylamine products. **e**, Preliminary investigations into methylene C-H activation of tertiary alkylamines show selectivity for the *trans* isomer on cyclic systems.

α -substituent on the ligand projects the amide moiety below the square-plane of the palladium(π) complex, which relays the chiral information to the ligated substrate and controls its conformation. The calculated e.e. (88% for 4a, 83% for *N*-acetyl alanine) agreed with experimental values. A range of aryl-boronic acids and acyclic tertiary alkylamines exhibited good yields and e.e. values (3as–aw), showing only minimal erosion of the enantioselectivity compared to the parent reaction. Despite the lower levels of asymmetric induction, this enantioselective γ -C(sp^3)-H arylation methodology can be used to synthesize the fungicide fenpropidin (3ax) directly from readily available materials in 49% yield and with an e.e. of 64%.

To the best of our knowledge, the only enantioselective synthesis of this compound has been described as requiring six chemical steps; the synthesis of non-racemic substituted-aryl analogues of these fungicides would also be directly accessible through this method (*vide supra*)¹⁶. Finally, we also demonstrated that the process of γ -arylation directed by tertiary alkylamines can be applied to methylene C-H bonds (Fig. 3e). On treatment with the standard conditions, the cyclic dimethylamine derivative 10 underwent methylene C-H arylation to form 11 in a modest, but encouraging, 34% yield. Notably, 11 was produced mainly as the *trans* isomer, reflecting a proposed intermediate (Int-IV) prior to C-H activation that must

proceed through to a 5,6-*trans*-fused palladacycle; the e.e. of the arylation was also found to be a promising 64% (ref. 47).

In summary, we have developed a ligand-enabled Pd(II)-catalysed γ -C(sp³)-H arylation process capable of selectively functionalizing a range of tertiary alkylamines with aryl-boronic acids. As well as having abilities to functionalize building-block-type amines, synthesize biologically active molecules and be applied as a late-stage functionalization tool, this reaction can also be performed enantioselectively.

Online content

Any Nature Research reporting summaries, source data, extended data, supplementary information, acknowledgements, peer review information; details of author contributions and competing interests; and statements of data and code availability are available at <https://doi.org/10.1038/s41557-019-0393-8>.

Received: 2 May 2019; Accepted: 14 November 2019;

Published online: 20 December 2019

References

- He, J., Wasa, M., Chan, K. S. L., Shao, Q. & Yu, J.-Q. Palladium-catalyzed transformations of alkyl C-H bonds. *Chem. Rev.* 117, 8754–8786 (2017).
- Davies, H. M. L. & Morton, D. Guiding principles for site selective and stereoselective intermolecular C-H functionalization by donor/acceptor rhodium carbenes. *Chem. Soc. Rev.* 40, 1857–1869 (2011).
- Capaldo, L. & Ravelli, D. Hydrogen atom transfer (HAT): a versatile strategy for substrate activation in photocatalyzed organic synthesis. *Eur. J. Org. Chem.* 15, 2056–2071 (2017).
- Giri, R. et al. Palladium-catalyzed methylation and arylation of sp² and sp³ C-H bonds in simple carboxylic acids. *J. Am. Chem. Soc.* 129, 3510–3511 (2007).
- Chen, G. et al. Ligand-enabled β -C-H arylation of α -amino acids without installing exogenous directing groups. *Angew. Chem. Int. Ed.* 56, 1506–1509 (2017).
- He, C., Whitehurst, W. G. & Gaunt, M. J. Palladium-catalyzed C(sp³)-H bond functionalization of aliphatic amines. *Chem* 5, 1031–1058 (2019).
- Lyons, T. W. & Sanford, M. S. Palladium-catalyzed ligand-directed C-H functionalization reactions. *Chem. Rev.* 110, 1147–1169 (2010).
- Rouquet, G. & Chatani, N. Catalytic functionalization of C(sp³)-H and C(sp²)-H bonds by using bidentate directing groups. *Angew. Chem. Int. Ed.* 52, 11726–11743 (2013).
- Zaitsev, V. G., Shabashov, D. & Daugulis, O. Highly regioselective arylation of sp³ C-H bonds catalyzed by palladium acetate. *J. Am. Chem. Soc.* 127, 13154–13155 (2005).
- He, G. & Chen, G. A practical strategy for the structural diversification of aliphatic scaffolds through the palladium-catalyzed picolinamide-directed remote functionalization of unactivated C(sp³)-H bonds. *Angew. Chem. Int. Ed.* 50, 5192–5196 (2011).
- Chan, K. S. L. et al. Ligand-enabled cross-coupling of C(sp³)-H bonds with arylboron reagents via Pd(II)/Pd(0) catalysis. *Nat. Chem.* 6, 146–150 (2014).
- Topczewski, J. J., Cabrera, P. J., Saper, N. I. & Sanford, M. S. Palladium-catalyzed transannular C-H functionalization of alicyclic amines. *Nature* 531, 220–224 (2016).
- Wu, Y., Chen, Y.-Q., Liu, T., Eastgate, M. D. & Yu, J.-Q. Pd-catalyzed γ -C(sp³)-H arylation of free amines using a transient directing group. *J. Am. Chem. Soc.* 138, 14554–14557 (2016).
- Xu, Y., Young, M. C., Wang, C., Magness, D. M. & Dong, G. Catalytic C(sp³)-H arylation of free primary amines with an *exo* directing group generated in situ. *Angew. Chem. Int. Ed.* 55, 9084–9087 (2016).
- Liu, Y. & Ge, H. Site-selective C-H arylation of primary aliphatic amines enabled by a catalytic transient directing group. *Nat. Chem.* 9, 26–32 (2017).
- Kapoor, M., Liu, D. & Young, M. C. Carbon dioxide-mediated C(sp³)-H arylation of amine substrates. *J. Am. Chem. Soc.* 140, 6818–6822 (2018).
- Roughley, S. D. & Jordan, A. M. The medicinal chemist's toolbox: an analysis of reactions used in the pursuit of drug candidates. *J. Med. Chem.* 54, 3451–3479 (2011).
- Cernak, T., Dykstra, K. D., Tyagarajan, S., Vachal, P. & Krska, S. W. The medicinal chemist's toolbox for late stage functionalization of drug-like molecules. *Chem. Soc. Rev.* 45, 546–576 (2016).
- Huang, L., Arndt, M., Gooßen, K., Heydt, H. & Gooßen, L. J. Late transition metal-catalyzed hydroamination and hydroamidation. *Chem. Rev.* 115, 2596–2697 (2015).
- Musacchio, A. J. et al. Catalytic intermolecular hydroaminations of unactivated olefins with secondary alkyl amines. *Science* 355, 727–730 (2017).
- Pirnot, M. T., Wang, Y.-M. & Buchwald, S. L. Copper hydride catalyzed hydroamination of alkenes and alkynes. *Angew. Chem. Int. Ed.* 55, 48–57 (2016).
- Perez, F., Oda, S., Geary, L. M. & Krische, M. J. Ruthenium-catalyzed transfer hydrogenation for C-C bond formation: hydrohydroxyalkylation and hydroaminoalkylation via reactant redox pairs. *Top. Curr. Chem.* 374, 35 (2016).
- Matier, C. D., Schwaben, J., Peters, J. C. & Fu, G. C. Copper-catalyzed alkylation of aliphatic amines induced by visible light. *J. Am. Chem. Soc.* 139, 17707–17710 (2017).
- Hanna, S., Holder, J. C. & Hartwig, J. F. A multicatalytic approach to the hydroaminomethylation of α -olefins. *Angew. Chem. Int. Ed.* 58, 3368–3372 (2019).
- Trowbridge, A., Reich, D. & Gaunt, M. J. Multicomponent synthesis of tertiary alkylamines by photocatalytic olefin-hydroaminosylation. *Nature* 561, 522–527 (2018).
- Hsieh, S.-Y. & Bode, J. W. Lewis acid induced toggle from Ir(II) to Ir(IV) pathways in photocatalytic reactions: synthesis of thiomorpholines and thiazepanes from aldehydes and SLAP reagents. *ACS Cent. Sci.* 3, 66–72 (2017).
- Xie, L.-G. & Dixon, D. J. Tertiary amine synthesis via reductive coupling of amides with Grignard reagents. *Chem. Sci.* 8, 7492–7497 (2017).
- Grogan, G. Synthesis of chiral amines using redox biocatalysis. *Curr. Opin. Chem. Biol.* 43, 15–22 (2018).
- Ouyang, K., Hao, W., Zhang, W.-X. & Xi, Z. Transition-metal-catalyzed cleavage of C-N single bonds. *Chem. Rev.* 115, 12045–12090 (2015).
- Lawrence, J. D., Takahashi, M., Bao, C. & Hartwig, J. F. Regioselective functionalization of methyl C-H bonds of alkyl groups in reagents with heteroatom functionality. *J. Am. Chem. Soc.* 126, 15334–15335 (2004).
- Murphy, J. M., Lawrence, J. D., Kawamura, K., Incarvito, C. & Hartwig, J. F. Ruthenium-catalyzed regioselective borylation of methyl C-H bonds. *J. Am. Chem. Soc.* 128, 13684–13685 (2006).
- Li, Q., Liske, C. W. & Hartwig, J. F. Regioselective borylation of the C-H bonds in alkylamines and alkyl ethers. Observation and origin of high reactivity of primary C-H bonds beta to nitrogen and oxygen. *J. Am. Chem. Soc.* 136, 8755–8765 (2014).
- Lee, M. & Sanford, M. S. Platinum-catalyzed, terminal-selective C(sp³)-H oxidation of aliphatic amines. *J. Am. Chem. Soc.* 137, 12796–12799 (2015).
- Mack, J. B. C., Gipson, J. D., Du Bois, J. & Sigman, M. S. Ruthenium-catalyzed C-H hydroxylation in aqueous acid enables selective functionalization of amine derivatives. *J. Am. Chem. Soc.* 139, 9503–9506 (2017).
- Howell, J. M., Feng, K., Clark, J. R., Trzepakowski, L. J. & White, M. C. Remote oxidation of aliphatic C-H bonds in nitrogen-containing molecules. *J. Am. Chem. Soc.* 137, 14590–14593 (2015).
- Schultz, D. M. et al. Oxyfunctionalization of the remote C-H bonds of aliphatic amines by decatungstate photocatalysis. *Angew. Chem. Int. Ed.* 56, 15274–15278 (2017).
- Ghose, A. K., Herberich, T., Hudkins, R. L., Dorsey, B. D. & Mallamo, J. P. Knowledge-based central nervous system (CNS) lead selection and lead optimization for CNS drug discovery. *ACS Chem. Neurosci.* 3, 50–68 (2012).
- Ryabov, A. D., Sakodinskaya, I. & Yatsimirsky, A. Kinetics and mechanism of ortho-palladation of ring-substituted N,N-dimethylbenzylamines. *J. Chem. Soc. Dalton Trans.* 12, 2629–2638 (1985).
- Nielsen, R. J. & Goddard, W. A. III Mechanism of the aerobic oxidation of alcohols by palladium complexes of N-heterocyclic carbenes. *J. Am. Chem. Soc.* 128, 9651–9660 (2006).
- Yang, Y.-F., Hong, X., Yu, J.-Q. & Houk, K. N. Experimental-computational synergy for selective Pd(II)-catalyzed C-H activation of aryl and alkyl groups. *Acc. Chem. Res.* 50, 2853–2860 (2017).
- Cheng, G.-J. et al. Role of N-acyl amino acid ligands in Pd(II)-catalyzed remote C-H activation of tethered arenes. *J. Am. Chem. Soc.* 136, 894–897 (2014).
- Haines, B. E., Yu, J.-Q. & Musaev, D. G. Enantioselectivity model for Pd-catalyzed C-H functionalization mediated by the mono-N-protected amino acid (MPAA) family of ligands. *ACS Catal.* 7, 4344–4354 (2017).
- Vasseur, A., Muzart, J. & Le Bras, J. Ubiquitous benzoquinones, multitasking compounds for palladium-catalyzed oxidative reactions. *Eur. J. Org. Chem.* 2015, 4053–4069 (2015).
- Wu, Q. F. et al. Formation of α -chiral centers by asymmetric β -C(sp³)-H arylation, alkenylation, and alkyenylation. *Science* 355, 499–503 (2017).
- Saint-Denis, T. G., Zhu, R.-Y., Chen, G., Wu, Q.-F. & Yu, J.-Q. Enantioselective C(sp³)-H bond activation by chiral transition metal catalysts. *Science* 359, 747–759 (2018).
- Mlynarski, S. N., Schuster, C. H. & Morken, J. P. Asymmetric synthesis from terminal alkenes by cascades of diboration and cross-coupling. *Nature* 505, 386–390 (2014).
- Chen, G. et al. Ligand-accelerated enantioselective methylene C(sp³)-H bond activation. *Science* 353, 1023–1027 (2016).

Publisher's note Springer Nature remains neutral with regard to jurisdictional claims in published maps and institutional affiliations.

© The Author(s), under exclusive licence to Springer Nature Limited 2019

Data availability

The data that support the findings of this study are available within the paper and its supplementary information files. Raw data are available from the corresponding author on reasonable request.

Acknowledgements

We are grateful to the EPSRC UK National Mass Spectrometry Facility at Swansea University for HRMS analysis. We thank I. Michaelides (AstraZeneca) and M. Grayson (University of Bath) for useful discussion. We are grateful to La Caixa Foundation and the Cambridge European Trust (J.R.) and the Gates Cambridge Trust (N.J.E.) for scholarships, the EPSRC (EP/N031792/1), the Leverhulme Trust (RPG-2016-370 to M.N.), Mitsubishi (H.A.), H2020 Marie Curie Actions (702462 to M.N. and 656455 to M.E.B.) and the Royal Society for a Wolfson Merit Award (to M.J.G.)

Author contributions

J.R., M.N. and M.J.G. conceived the project. J.R., M.N., H.A. and M.E.B. designed and performed the synthetic experiments. J.R. and N.J.E. designed and performed the computational studies. J.R., M.N., H.A., N.J.E. and M.J.G. prepared the manuscript.

Competing Interests

The authors declare no competing interests.

Additional Information

Supplementary information is available for this paper at <https://doi.org/10.1038/s41557-019-0393-8>.

Correspondence and requests for materials should be addressed to M.J.G.

Reprints and permissions information is available at www.nature.com/reprints.

